Grossman's Cardiac Catheterization, Angiography, and Intervention 6th edition (September 2000): by Donald S. Baim (Editor), William, M.D. Grossman (Editor)
By Lippincott Williams & Wilkins Publishers

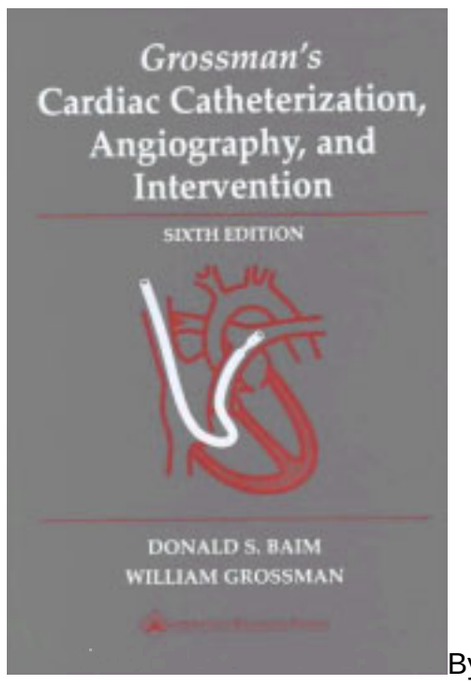

By OkDoKeY

Grossman's Cardiac Catheterization, Angiography, and Intervention

Contents

Section VIII: Profiles of Specific Disorders

Edited by

Donald S. Baim, M.D.
Professor of Medicine
Harvard Medical School;
Director, Center for Innovative Minimally Invasive Therapy
Brigham and Women's Hospital
Boston, Massachusetts

William Grossman, M.D.
Meyer Friedman Distinguished Professor of Medicine
University of California, San Francisco, School of Medicine;
Chief, Division of Cardiology
University of California, San Francisco Medical Center
San Francisco, California

To my wife, Caryn,
and my children, Chris, Adam, Samantha, and Jen

—D.S. Baim

To my wife, Melanie,
and my children, Jennifer, Edward, and Jessica

—W. Grossman

Preface

The cardiac catheter is an important tool, whose use over the latter half of the twentieth century has provided unprecedented improvements in the clinical care of patients with heart disease while extending our understanding of circulatory physiology and vascular pathobiology. In the process, it has defined two new areas of special expertise within our broader parent specialty: invasive and interventional cardiology.

Initially, use of the cardiac catheter was limited to the *measurement of pressures and blood flow* within the various chambers, elucidating both normal physiology and the pathophysiology of various disease states. With the advent of *selective coronary angiography* in the 1960s, the main emphasis of cardiac catheterization began to shift from hemodynamic measurements to the evaluation of coronary anatomy before bypass surgery, prompting the emergence of a cadre of “invasive” cardiologists who were skilled in the performance of such procedures.

Although Forssmann's original goal in 1929 to improve treatment of circulatory collapse through catheterization and limited therapeutic techniques had been developed in pediatric cardiology, it was not until 1977 (when Gruentzig introduced his concept of *percutaneous transluminal coronary angioplasty*) that the field of “interventional cardiology” was launched in earnest. By the mid-1980s, use of coronary angioplasty had grown to 300,000 procedures per year, equaling the number of bypass surgeries. Its scope broadened further in the late 1980s, with the introduction of several *new therapeutic modalities* (valvuloplasty, stent, atherectomy, and laser procedures), whose use in the 1990s grew to dominate coronary intervention. This has allowed progressive improvements in the success, safety, and durability of intervention (as demonstrated in an unprecedented series of clinical trials) and has boosted the annual interventional volume beyond 700,000 procedures. In 1999, the unique and substantial body of knowledge subsumed by this new discipline was further recognized by the creation of separate fellowships and a Certificate of Additional Qualification in the field of Interventional Cardiology.

To those who have entered the fields of invasive and interventional cardiology within the last several years, the incremental (layer upon layer) flavor of these developments tends to be lost, making cardiac catheterization appear as a seamless and unchanging discipline. The editors believe, however, that it is beneficial for physicians and support staff who perform these procedures to understand both the developmental history (including approaches that were tried and abandoned) and the current technical underpinnings of this field. Toward that end, this sixth edition of *Cardiac Catheterization, Angiography, and Intervention* has retained the basic structure of its forerunners. But to capture a rapidly evolving field, all sections—including those relating to general principles, basic techniques, hemodynamic principles, angiographic techniques, evaluation of cardiac function, special catheter techniques, interventional techniques, and profiles of specific disease states—have been updated extensively. Coverage of peripheral vascular disease has been expanded with three new chapters (diagnostic angiography, peripheral intervention, and profiles), and the chapters on implantable electrophysiologic devices and the brachial approach have been enlarged to include newer technical approaches. To avoid unwieldy growth of the book as a result, the chapters on the separate discipline of invasive electrophysiology and ablation have been eliminated, and several chapters from the fifth and previous editions have been combined into single chapters in the sixth edition. For the first time, the entire book is also being distributed on CD-ROM, with inclusion of more than 50 cine case examples and other teaching tools.

With this sixth edition, this textbook has reached it 25th anniversary as the leading text of invasive cardiology. In recognition of the pioneering efforts and continued contributions of Dr. William Grossman, the title of the book (which he began in 1974 as *Cardiac Catheterization and Angiography*, and which was changed to *Cardiac Catheterization, Angiography, and Intervention* in the fourth edition) has been changed again—to *Grossman's Cardiac Catheterization, Angiography, and Intervention*. Dr. Donald S. Baim, who has contributed importantly to the expansion of the scope of the book over the last 16 years, continues as its senior editor. Throughout its history and despite the continued evolution of its content to capture a rapidly changing field, the emphasis of *Grossman's* remains on complete, scientifically accurate, and lucid explanations of underlying principles, concepts, and techniques. Although we realize that the approaches we describe are not the only ones possible, we put them forward as methods that are generally successful and practical and whose strengths and weaknesses are well characterized.

We hope that this sixth edition will continue to serve as a valuable textbook for the training of cardiology fellows and support staff, as well as an important reference resource for those actively participating in this field. If successful, the efforts of ourselves and our contributing authors will be reflected in better patient outcomes that stem from an improved understanding on the part of those who perform and interpret cardiac catheterization procedures. Beyond the list of contributing authors, however, we wish to thank our many colleagues across the country and throughout the world whose shared experiences have been woven into much of the material contained in the book, and several generations of our Cardiology Fellows for their questions and research efforts that have led to many of the principles and techniques described.

Donald S. Baim, Boston, MA
William Grossman, San Francisco, CA

Contributing Authors

Julian Max Aroesty, M.D.
Associate Clinical Professor of Medicine
Harvard Medical School;
Associate Chief for Clinical Affairs
Beth Israel Deaconess Medical Center
330 Longwood Avenue
Boston, Massachusetts 02115

Donald S. Baim, M.D.
Professor of Medicine
Harvard Medical School;
Director, Center for Innovative Minimally Invasive Therapy
Brigham and Women's Hospital
75 Francis Street
Boston, Massachusetts 02115

Ronald P. Caputo, M.D.
Assistant Clinical Professor of Medicine
SUNY Health Science Center;
Attending Invasive Cardiologist
Department of Medicine
St. Joseph's Hospital Health Center
301 Prospect Avenue
Syracuse, New York 13203

Blase A. Carabello, M.D.
Professor of Medicine
Baylor College of Medicine;
Chief, Department of Medicine
Houston Veterans Affairs Medical Center
2002 Holcombe Boulevard
Houston, Texas 77030

Joseph P. Carrozza, Jr., M.D.
Assistant Professor of Medicine
Harvard Medical School;
Invasive Cardiology Section
Beth Israel Hospital
330 Brookline Avenue
Boston, Massachusetts 02115

Jane Chen, M.D.
Assistant Professor
Department of Cardiology
Washington University School of Medicine;
Electrophysiologist, Department of Cardiology
Barnes-Jewish Hospital
One Barnes Hospital Plaza
St. Louis, MO 63110

Tony M. Chou, M.D.
Associate Clinical Professor
Department of Medicine
University of California, San Francisco, School of Medicine
505 Parnassus Avenue, Box 0130
San Francisco, California 94143

Laurence M. Epstein, M.D.
Associate Professor
Department of Medicine
Medical School;
Chief, Arrhythmia Service
Director, Electrophysiology and Pacing Laboratory
Brigham and Women's Hospital
75 Francis Street
Boston, Massachusetts 02115

Michael A. Fifer, M.D.
Associate Professor of Medicine
Harvard Medical School;
Director, Coronary Care Unit
Massachusetts General Hospital
WACC-4, Suite 478
15 Parkman Street
Boston, Massachusetts 02114

Peter J. Fitzgerald, M.D., Ph.D.
Associate Professor of Medicine
Division of Cardiology
Co-Director, Center for Research in Cardiovascular Interventions
Stanford University
300 Pasteur Drive
Stanford, California 94305

C. Michael Gibson, M.S., M.D. F.A.C.C.
Associate Professor of Medicine
Chief of Interventional Cardiology
University of California, San Francisco, School of Medicine
UCSF Medical Center

505 Parnassus Avenue
San Francisco, California 94143

Samuel Z. Goldhaber, M.D.
Associate Professor of Medicine
Harvard Medical School;
Staff Cardiologist
Division of Cardiovascular Medicine
Brigham and Women's Hospital
75 Francis Street
Boston, Massachusetts 02115

William Grossman, M.D.
Meyer Friedman Distinguished Professor of Medicine
University of California, San Francisco, School of Medicine;
Chief, Division of Cardiology
UCSF Medical Center
505 Parnassus Avenue, Box 0124
San Francisco, California 94143

L. David Hillis, M.D.
Vice Chairman, Department of Medicine
James M. Wooten Chair in Cardiology
University of Texas Southwestern Medical Center
Dallas, Texas 75390

Micheal R. Jaff, D.O., R.V.T.
Medical Director, Center for Vascular Care
Co-Director, Vascular Diagnostic Laboratory
Department of Vascular Medicine
Washington Hospital Center
110 Irving Street, NW, Suite 4B-1
Washington, D.C. 20010

John F. Keane, M.D.
Professor of Pediatrics
Harvard Medical School;
Senior Associate
Department of Cardiology
Children's Hospital
300 Longwood Avenue
Boston, Massachusetts 02115

Morton J. Kern, M.D.
Professor of Medicine
Saint Louis University School of Medicine;
Director, Cardiac Catheterization Laboratory
Department of Cardiology
St. Louis University Hospital
3635 Vista Avenue at Grand Boulevard
St. Louis, Missouri 63110

Richard E. Kuntz, M.D.
Associate Professor of Medicine
Harvard Medical School;
Chief, Division of Clinical Biometry
Brigham and Women's Hospital
75 Francis Street
Boston, Massachusetts 02115

James E. Lock, M.D.
Alexander S. Nadas Professor
Department of Pediatrics
Harvard Medical School;
Chairman, Department of Cardiology
Children's Hospital
300 Longwood Avenue
Boston, Massachusetts 02115

Beverly H. Lorell, M.D.
Professor of Medicine
Harvard Medical School;
Director, Hemodynamic Research Laboratory
Beth Israel Deaconess Medical Center
330 Brookline Avenue
Boston, Massachusetts 02215

Stanton B. Perry, M.D.
Associate Professor of Pediatrics
Harvard Medical School;
Chief, Invasive Cardiology
Department of Cardiology
Children's Hospital
300 Longwood Avenue
Boston, Massachusetts 02115

Thomas A. Ports, M.D.
Professor of Medicine
University of California, San Francisco, School of Medicine
505 Parnassus Avenue, Box 0124
San Francisco, California 94143

Stephen R. Ramee, M.D.
Cardiology, Section Head
Department of Cardiology
Ochsner Clinic;
Director, Cardiac Catheterization Laboratory
Alton Ochsner Medical Institution
1514 Jefferson Highway
New Orleans, Louisiana 70121

Kenneth Rosenfield, M.D.
Assistant Professor of Medicine
Tufts University School of Medicine;
Director of Vascular Interventional Suite
Departments of Vascular Medicine and Cardiology
St. Elizabeth's Medical Center
736 Cambridge Street
Boston, Massachusetts 02135

Robert M. Schainfeld, D.O.
Assistant Professor of Medicine
Tufts University School of Medicine;
Director, Non-Invasive Vascular Laboratory
St. Elizabeth's Medical Center
736 Cambridge Street
Boston, Massachusetts 02135

Jose A. Silva, M.D.
Staff, Interventional Cardiologist
Ochsner Clinic, Slidell, Louisiana;
Staff, Interventional Cardiologist
Alton Ochsner Medical Foundation
1514 Jefferson Highway
New Orleans, Louisiana 70121

Lorraine K. Skibo, M.D.
Interventional Radiologist
Saratoga Springs, New York 12866

Timothy W. Smith, D.Phil., M.D.
Assistant Professor of Medicine
Boston University School of Medicine;
Director, Cardiac Device Clinic
Section of Cardiology
Boston Medical Center
88 East Newton Street
Boston, Massachusetts 02118

Lewis Wexler, M.D.
Professor Emeritus of Radiology
Stanford University Medical School
300 Pasteur Drive
Stanford, California 94305

Christopher J. White, M.D.
Chairman, Department of Cardiology
Oschner Clinic
1514 Jefferson Highway
New Orleans, Louisiana 70121

Paul G. Yock, M.D.
Martha Meier Weiland Professor of Medicine
Stanford University;
Director, Center for Research in Cardiovascular Interventions
Stanford University Medical Center
300 Pasteur Drive, H3554
Stanford, California 94305

Christian Zellner, M.D.
Research Fellow
Division of Cardiology
Cardiovascular Research Institute
University of California, San Francisco, School of Medicine
505 Parnassus Avenue
San Francisco, California 94143

1
Historical Perspective and Present Practice of Cardiac Catheterization

William Grossman

University of California, San Francisco, School of Medicine; Division of Cardiology, University of California, San Francisco Medical Center, San Francisco, California 94143

It is difficult to imagine what our concepts of heart disease might be like today if we had to construct them without the enormous reservoir of physiologic and anatomic knowledge derived from the past 60 years' experience in the cardiac catheterization laboratory. As Andre Cournand remarked in his Nobel lecture of December 11, 1956, “the cardiac catheter was. . . the key in the lock” (1). By turning this key, Cournand and his colleagues led us into a new era in the understanding of normal and disordered cardiac function in humans.

According to Cournand (2), cardiac catheterization was first performed (and so named) by Claude Bernard in 1844. The subject was a horse, and both the right and left ventricles were entered by a retrograde approach from the jugular vein and carotid artery. In an excellent review of the history of cardiac catheterization, angiography, and interventional cardiology, Mueller and Sanborn (3) describe and cite references for experiments by Stephen Hales and others whose work antedates that of Claude Bernard, and the interested reader is referred to their review for details (3). Although he may not have been the first to perform cardiac catheterization, Claude Bernard's careful application of scientific method to the study of cardiac physiology using the cardiac catheter demonstrated the enormous value of this technical innovation. An era of investigation of cardiovascular physiology in animals then followed, resulting in the development of many important techniques and principles (e.g., pressure manometry, the Fick cardiac output method) which awaited direct application to the patient with heart disease.

Werner Forssmann usually is credited with being the first person to pass a catheter into the heart of a living person—himself (4). At age 25, while receiving clinical instruction in surgery at Eberswalde, near Berlin, he passed a catheter 65 cm through one of his left antecubital veins, guiding it by fluoroscopy until it entered his right atrium. He then walked to the radiology department (which was on a different level, requiring that he climb stairs), where the catheter position was documented by a chest roentgenogram (Fig. 1.1). During the next 2 years, Forssmann continued to perform catheterization studies, including six additional attempts to catheterize himself. Bitter criticism, based on an unsubstantiated belief in the danger of his experiments, caused Forssmann to turn his attention to other concerns, and he eventually pursued a career as a urologist (5). Nevertheless, for his contribution and foresight he shared the Nobel Prize in Medicine with Andre Cournand and Dickinson Richards in 1956.

FIG. 1.1. The first documented cardiac catheterization. At age 25, while receiving clinical instruction in surgery at Eberswalde, Werner Forssmann passed a catheter 65 cm through one of his left antecubital veins until its tip entered the right atrium. He than walked to the radiology department where this roentgenogram was taken. (Forssmann W. Die Sondierung des rechten Herzens. *Klin Wochenschr* 1929;8:2085, with permission of Springer-Verlag, Berlin.)

Forssmann's primary goal in his catheterization studies was to develop a therapeutic technique for the direct delivery of drugs into the heart. He wrote (4):

> If cardiac action ceases suddenly, as is seen in acute shock or in heart disease, or during anesthesia or poisoning, one is forced to deliver drugs locally. In such cases the intracardiac injection of drugs may be life saving. However, this may be a dangerous procedure because of many incidents of laceration of coronary arteries and their branches leading to cardiac tamponade, and death. . . . Because of such incidents, one often waits until the very last moment and valuable time is wasted. Therefore I started to look for a new way to approach the heart, and I catheterized the right side of the heart through the venous system.

Others appreciated the potential of Forssmann's technique as a diagnostic tool. In 1930, Klein reported 11 right-sided heart catheterizations, including passage to the right ventricle and measurement of cardiac output using the Fick principle (6). The cardiac outputs were 4.5 and 5.6 L/min in two patients without heart disease. In 1932, Padillo and coworkers reported right heart catheterization and measurement of cardiac output in two subjects (2). Except for these few studies, application of cardiac catheterization to study the circulation in normal and disease states was fragmentary until the work of Andre Cournand and Dickinson Richards, who separately and in collaboration produced a remarkable series of investigations of right heart physiology in humans (7,8 and 9). In 1947, Dexter reported his studies on congenital heart disease (10). He went further than his predecessors by passing the catheter to the distal pulmonary artery, observing “the oxygen saturation and source of pulmonary capillary blood” obtained from the pulmonary artery “wedge” position (10). Subsequent studies from Dexter's laboratory (11) and by Werkö (12) elaborated on this pulmonary artery wedge position, and pressure measured at this position was reported to be a good estimate of pulmonary venous and left atrial pressure. During this exciting early period, catheterization was used to investigate problems in cardiovascular physiology by McMichael in England (13), Lenègre in Paris (14), and Warren, Stead, Bing, Dexter, Cournand, and others in the United States (15,16,17,18,19,20,21,22 and 23).

Further developments came rapidly, and highlights include the following:

Retrograde left-sided heart catheterization was first reported by Zimmerman (24) and by Limon-Lason (25) in 1950.

The percutaneous technique developed by Seldinger in 1953 was soon applied to cardiac catheterization of both the left and right heart chambers (26).

Transseptal catheterization was first developed in 1959 by Ross (27) and Cope (28) and quickly became accepted as a standard technique.

Selective coronary arteriography was reported by Sones in 1959 and was perfected to a remarkable excellence over the ensuing years (29,30). This technique was modified for a percutaneous approach by Ricketts and Abrams (31) in 1962 and Judkins (32) in 1967.

In 1970, Swan and Ganz introduced a practical balloon-tipped, flow-guided catheter technique that enabled the application of catheterization outside the laboratory (33).

INTERVENTIONAL CARDIOLOGY

In the last 25 years, investigators have focused once again on the therapeutic potential of the cardiac catheter. In 1977, Grüntzig introduced the technique of percutaneous transluminal coronary angioplasty (PTCA) (34,35). In the ensuing years, catheter-based coronary revascularization has been applied widely. With rapidly evolving technology and expanding indications, PTCA and its “offspring” (e.g., stents, atherectomy) first rivaled and have now surpassed coronary bypass surgery as the dominant therapeutic modality for coronary artery disease. The development of percutaneous coronary intervention stimulated other innovations such as balloon valvuloplasty and devices to close intracardiac shunts, which together have made “interventional cardiology” a new field in cardiovascular medicine. The history of interventional cardiology has been summarized by Spencer King in an excellent review (36), and the interested reader is referred there for further details. In a sense, cardiac catheterization has returned to its roots, because, as mentioned earlier, Werner Forssmann's original intention had been to use the catheter as a tool for therapy, not diagnosis.

At approximately the same time that Grüntzig was developing balloon angioplasty in Zurich, investigators in Germany and Los Angeles were administering the thrombolytic agent streptokinase through catheters placed selectively in the coronary arteries of patients early in the acute phase of transmural myocardial infarction. This new catheter-based therapy, which was viewed as radical at the time, produced angiographic findings that confirmed beyond any doubt the role of acute coronary thrombosis in the genesis of myocardial infarction. When investigators found that similar therapeutic benefit could be achieved by intravenous administration of the thrombolytic agent, the intracoronary direct-infusion technique all but died out except for a few special indications. However, catheter-based therapy for acute coronary thrombosis has undergone a renaissance in the last 10 years with the demonstration that PTCA/stenting in this setting produces results that are comparable or superior to those achieved with thrombolytic therapy (37,38).

It is clear as we enter the 21st century that interventional cardiology—by virtue of its new technologies, potent adjunctive drug therapies (e.g., blockers of the platelet IIb/IIIa receptor), expanding indications, and improving results—has blossomed. In many ways, interventional cardiology, rather than purely diagnostic techniques, has become the dominant discipline within the broad field of cardiac catheterization. Although the emphasis in the field (and in this textbook) is now appropriately on the dynamic field of catheter-based intervention, the basic principles of catheter insertion, hemodynamic measurement, high-quality angiography, and integration of catheterization findings with both the clinical scenario and the findings of noninvasive tests are not just historical curiosities: they are the foundations on which all current interventional techniques are built, and from which future evolution of cardiac catheterization will proceed.

INDICATIONS FOR CARDIAC CATHETERIZATION

As performed today, cardiac catheterization is a combined hemodynamic and angiographic procedure undertaken for diagnostic and often therapeutic purposes. As with any invasive procedure, the decision to perform cardiac catheterization must be based on a careful balance of the risk of the procedure against the anticipated benefit to the patient. A summary of the indications for cardiac catheterization is given in Table 1.1 and discussed in the following paragraphs.

TABLE 1.1. *Indications for cardiac catheterization*

Cardiac catheterization usually is recommended to confirm the presence of a clinically suspected condition, define its anatomic and physiologic severity, and determine the presence or absence of associated conditions when a therapeutic intervention is planned in a symptomatic patient. The most common indication for cardiac catheterization today arises in the patient with an acute coronary ischemic syndrome in whom an invasive therapeutic intervention (PTCA, stent, or coronary artery bypass graft surgery) is contemplated. The patient with an acute coronary ischemic syndrome has most commonly experienced recent rupture of an atherosclerotic plaque within a coronary artery. Exposure of plaque contents to flowing blood leads to platelet deposition and coronary thrombosis, which, in turn, leads to transmural ischemia if the thrombus is completely obstructing, or to unstable angina if it causes only partial or intermittent occlusion. The goal of cardiac catheterization in such patients is to identify the culprit artery and restore vessel patency by PTCA/stent placement. The diagnostic part of the catheterization procedure may reveal other features (e.g., multivessel or left main coronary artery disease, severe associated valvular disease) that provide critical information for the decision to proceed with open-heart surgery.

Is cardiac catheterization necessary in all patients being considered for cardiac surgery? Although few would disagree that consideration of heart surgery is an adequate reason for the performance of catheterization, clinicians differ about whether all patients being considered for heart surgery should undergo preoperative cardiac catheterization. In this regard, it should be emphasized that the risks of catheterization are small compared with those of embarking upon cardiac surgery in a patient for whom an incorrect clinical diagnosis or the presence of an unsuspected additional condition greatly prolongs and complicates the planned surgical approach. The operating room is not a good place for surprises; by providing the surgical team with a precise and complete road map of the course ahead, cardiac catheterization can permit a carefully reasoned and maximally efficient operative procedure. Furthermore, information obtained by cardiac catheterization may be invaluable in the assessment of crucial determinants of prognosis, such as left ventricular function, status of the pulmonary vasculature, and patency of the coronary arteries. For these reasons, my colleagues and I recommend cardiac catheterization for almost all patients for whom heart surgery is contemplated.

Other major therapeutic considerations besides heart surgery may depend on the information afforded by cardiac catheterization and angiography. For example, the decision for pharmacologic intervention with heparin and/or a thrombolytic agent in suspected acute pulmonary embolism, or with high doses of a b-blocker and/or calcium antagonists in suspected hypertrophic subaortic stenosis, might well be considered of sufficient magnitude to warrant confirmation of the diagnoses by angiographic and hemodynamic investigation before the initiation of therapy. A clinical diagnosis of primary pulmonary hypertension made by echocardiography usually requires cardiac catheterization (a) to confirm the diagnosis and (b) to assess potential responsiveness to pharmacologic agents, such as epoprostenol (39).

A second broad indication for performing cardiac catheterization is diagnosis of obscure or confusing problems in heart disease, even when a major therapeutic decision is not imminent. A common instance of this indication is presented by the patient with chest pain of uncertain cause, about whom there is confusion regarding the presence of obstructive coronary artery disease. Both management and prognosis of this difficult problem are greatly simplified when it is known, for example, that the coronary arteries are widely patent. Another example within this category might be the symptomatic patient with a suspected diagnosis of cardiomyopathy. Although some may feel satisfied with a clinical diagnosis of this condition, the implications of such a diagnosis in terms of prognosis and therapy (e.g., long-term bed rest, chronic anticoagulant therapy) are so important that I believe it is worthwhile to be aggressive in ruling out potentially correctable conditions (e.g.,

hemochromatosis, pericardial effusive-constrictive disease) with certainty, even though the likelihood of their presence may appear to be remote on clinical grounds.

Research

On occasion, cardiac catheterization is performed primarily as a research procedure. Although research is conducted to some degree in many of the diagnostic and therapeutic studies performed at major medical centers, this is quite different from catheterization for the sole purpose of a research investigation. Such studies should be carried out only under the direct supervision of an experienced investigator who is an expert in cardiac catheterization, using a protocol that has been carefully scrutinized and approved by the Committee on Human Research at the investigator's institution, and after a thorough explanation has been made to the patient detailing the risks of the procedure and the fact that the purpose of the investigation is to gather research information.

Contraindications

If it is important to carefully consider the indications for cardiac catheterization in each patient, it is equally important to discover any contraindications. Over the years, the concept of contraindications has been modified by the fact that patients with acute myocardial infarction, cardiogenic shock, intractable ventricular tachycardia, and other extreme conditions have tolerated catheterization and coronary angiography surprisingly well. At present the only absolute contraindication to cardiac catheterization is the refusal of a mentally competent patient to consent to the procedure.

A long list of relative contraindications must be kept in mind, however, and these include all intercurrent conditions that can be corrected and whose correction would improve the safety of the procedure. Table 1.2 lists these relative contraindications. For example, ventricular irritability can increase the risk and difficulty of left heart catheterization and can greatly interfere with interpretation of ventriculography (see Chapter 12); if possible, ventricular irritability should be suppressed medically before or during catheterization. Hypertension increases predisposition to ischemia and/or pulmonary edema and should be controlled before and during catheterization. Other conditions that should be controlled before elective catheterization include intercurrent febrile illness, decompensated left-sided heart failure, correctable anemia, digitalis toxicity, and hypokalemia. Allergy to a radiographic contrast agent is a relative contraindication to cardiac angiography, but proper premedication can substantially reduce the risks of a major adverse reaction, as discussed in Chapter 3.

1. Uncontrolled ventricular irritability: the risk of ventricular tachycardia/fibrillation during catheterization is increased if ventricular irritability is uncontrolled
2. Uncorrected hypokalemia or digitalis toxicity
3. Uncorrected hypertension: predisposes to myocardial ischemia and/or heart failure during angiography
4. Intercurrent febrile illness
5. Decompensated heart failure: especially acute pulmonary edema, unless catheterization can be done with the patient sitting up
6. Anticoagulated state: prothrombin time longer than 18 seconds
7. Severe allergy to radiographic contrast agent
8. Severe renal insufficiency and/or anuria: unless dialysis is planned to remove fluid and radiographic contrast load

TABLE 1.2. *Relative contraindications to cardiac catheterization and angiography*

Anticoagulant therapy is more controversial as a contraindication. As pointed out in Chapter 4 and Chapter 11, heparin may lower the incidence of thromboembolic complications during coronary angiography (40). It is important to distinguish anticoagulation with oral anticoagulants (e.g., warfarin) from that with heparin. Heparin anticoagulation can be reversed rapidly during catheterization if necessary (e.g., in the case of perforation of the heart or great vessels or uncontrolled bleeding from femoral or brachial sites). Reversal of the prolonged prothrombin time of oral anticoagulation before or during cardiac catheterization represents a more complex problem. I strongly oppose acute reversal of oral anticoagulation with parenteral vitamin K because of the occasional induction of a hypercoagulable state, which has been known to result in thrombosis of prosthetic valves or thrombus formation within cardiac chambers, arteries, or veins. If reversal of oral anticoagulation is required, we favor administration of fresh-frozen plasma. For patients chronically anticoagulated with an oral agent, we routinely recommend discontinuation of the oral anticoagulants 48 hours before cardiac catheterization, with heparin given during these 48 hours for patients who have a strong indication for continuous anticoagulation (e.g., mechanical cardiac valve prosthesis). I prefer to have the international normalized ratio (INR) less than 2.0, or the prothrombin time less than 18 seconds, and no heparin administration for 4 hours before the catheterization. If anticoagulant therapy cannot be interrupted at all, we prefer heparin for the reasons just mentioned.

FACTORS INFLUENCING CHOICE OF APPROACH

Of the various approaches to cardiac catheterization, certain ones have only historical interest (transbronchial approach, posterior transthoracic left atrial puncture, and suprasternal puncture of the left atrium). In this book only the following are discussed in detail: (a) catheterization by percutaneous approach from various sites (including femoral or radial arteries, transseptal catheterization, and apical left ventricular puncture) and (b) catheterization by direct surgical exposure of the brachial artery and vein.

The great vessels and all cardiac chambers can be entered in almost all cases by either the direct exposure or percutaneous approaches (or a combination of both). Each method has its advantages and disadvantages, its adherents and detractors. In reality, the methods are not mutually exclusive but rather complementary; ideally, the physician performing cardiac catheterization should be well versed in both methods.

Advantages of the Percutaneous Femoral Approach

The percutaneous femoral approach is clearly the dominant technique in cardiac catheterization today, presenting a broad set of advantages and indications. The femoral approach does not require arteriotomy and arterial repair and can be performed repeatedly in the same patient at intervals, whereas the brachial arteriotomy approach can rarely be repeated safely more than two or three times; infection and thrombophlebitis at the catheterization site are rare; surgical (suture) closure of the skin is not necessary; and the approach is readily adaptable to a variety of other entry vessels (e.g., internal jugular vein, axillary artery, radial artery). Larger-caliber devices (i.e., valvuloplasty balloons or intraaortic counterpulsation catheters) can be introduced into the femoral artery but not usually into the smaller brachial artery. The femoral approach is clearly the method of choice in a patient with absent or diminished radial and brachial pulsations or when the direct brachial approach has been unsuccessful. In the occasional patient with tight aortic stenosis in whom retrograde catheterization has proved impossible, percutaneous transseptal catheterization of the left atrium and ventricle is helpful; in the rare instance in which retrograde arterial and transseptal catheterization have not succeeded in gaining entry into the left ventricle (or are contraindicated by the presence of disc mitral and/or aortic prostheses or left atrial thrombus), percutaneous transthoracic puncture of the left ventricle may be considered (see Chapter 4).

Advantages of the Percutaneous Radial Approach

In recent years, percutaneous technique using the radial, brachial, or ulnar arteries as entry sites (41,42,43,44,45 and 46) has been applied to retrograde left heart catheterization, coronary angiography, PTCA, and even stent placement. This approach is becoming increasingly popular and has been demonstrated to have advantages of cost and patient comfort. A study by Mann and colleagues (41) reported on the use of percutaneous transradial catheterization for stent placement in patients with acute coronary syndromes. A total of 144 patients with acute coronary syndromes were randomly assigned to either a femoral or a radial approach. Stenting from the radial approach allowed earlier hospital discharge and was associated with decreased hospital charges and fewer bleeding complications. Not all patients assigned to the radial approach strategy were able to have radial artery catheterization. Six of the 74 had a negative Allen test or Doppler examination, or both, suggesting an incomplete palmar arch, so that radial catheterization was thought to be contraindicated; accordingly, they were included in the femoral approach group. In three additional patients, the radial artery was not successfully cannulated, and these patients also crossed over to the femoral approach group.

Advantages of the Brachial Approach

Much less common today, the direct exposure approach usually utilizes cutdown on the brachial artery and basilic vein at the elbow (see Chapter 5). In general, the percutaneous radial approach has all the advantages of the direct brachial approach and few of its disadvantages. Nevertheless, the brachial cutdown approach is still used by a few centers and is worthy of some comment. The brachial approach may have advantages in a patient with severe peripheral vascular disease involving the abdominal aorta, iliac, or femoral arteries; suspected femoral vein or inferior vena caval thrombosis; or coarctation of the aorta. The brachial or radial approach may also have advantages in the very obese patient, in whom the percutaneous femoral technique may be technically difficult and where hard to control breathing occurs after catheter removal. Another advantage occasionally cited for the direct brachial approach is use of a single left heart catheter (Sones catheter) for left ventriculography and coronary angiography.

DESIGN OF THE CATHETERIZATION PROTOCOL

Every cardiac catheterization should have a protocol—a carefully reasoned, sequential plan designed specifically for the individual patient. Although this protocol may exist only in the mind of the operator, it is often helpful to prepare a written protocol and post it in the catheterization suite so that all personnel in the laboratory understand exactly what is planned and can anticipate the needs of the operator.

Certain general principles should be considered in the design of a protocol. First, hemodynamic measurements should precede angiographic studies whenever possible, so that crucial pressure and flow measurements may be made as close as possible to the basal state. A separate arterial monitor line (which may be just the sidearm of the arterial sheath) can be helpful; when complications develop (and they do, no matter how skilled the operator), this second transducer allows continuous monitoring of arterial pressure. Second, pressures and selected oxygen saturation values should be measured and recorded in each chamber “on the way in,” that is, immediately after the catheter enters and before it is directed toward the next chamber. If problems should develop during the later stages of a catheterization procedure (atrial fibrillation or other arrhythmia, pyrogen reaction, hypotension, or reaction to contrast material), the investigator will be glad to have measured pressures and saturations this way, rather than waiting until the time of catheter pullback. Third, measurements of pressure and cardiac output should be made as simultaneously as possible. A simple routine for recording pressure during the cardiac output measurement can be learned by the laboratory personnel and performed efficiently in every case.

Beyond these general guidelines, the protocol reflects individual patient differences. With regard to angiography, it is important to keep in mind Sutton's law (when asked why he robbed banks, Willie Sutton is reported to have replied, “Because that's where the money is”) and order the contrast injections in relation to the most important diagnostic considerations in a given patient.

PREPARATION AND PREMEDICATION OF THE PATIENT

It goes without saying that the emotional as well as the “medical” preparation of the patient for cardiac catheterization is the responsibility of the operator. It is our firm obligation to fully explain the proposed procedure in such terms that the patient can give truly informed consent. We always tell the patient and his or her family that there is risk involved and the extent of the risk, depending on the specific procedure and the patient's clinical situation. If appropriate, we reassure patient and family that we do not anticipate any special problems. Our consent form lists the specific risks and informs the patient that “There is a less than 1% risk of serious complications (stroke, heart attack, or death).” If the patient and family want to know more about these risks, they will ask for details. We do not understate the discomfort involved or the duration of the procedure—doing so risks one's credibility. We have been satisfied with this overall approach and can heartily recommend it. A study of psychologic preparation for cardiac catheterization (47) found that patients who received careful psychologic preparation had lower levels of autonomic arousal both during and after cardiac catheterization than did control subjects.

Once the question of indications and contraindications has been dealt with and the patient's consent obtained, attention can be directed toward the matter of medications. As mentioned earlier, we prefer to have the INR less than 2.0 (prothrombin time less than 18 seconds) and no heparin administered for 4 hours. One exception is the patient with unstable angina, in whom a therapeutic heparin infusion may be continued until arterial entry and then supplemented by 3,000 to 5,000 additional units. For these patients, “front-wall” arterial puncture is particularly important, as discussed in Chapter 4. For patients receiving chronic anticoagulation therapy, we discontinue oral anticoagulants the day before hospitalization (or 48 hours before study for outpatient catheterizations), and on admission we begin intravenous heparin, which is stopped within 4 hours of the catheterization. Heparin and oral anticoagulants are reinstituted after the catheterization, and heparin is stopped once adequate prolongation of prothrombin time has been achieved.

The question of administering antibiotics prophylactically is raised occasionally, and some laboratories administer them routinely before catheterization. We do not administer antibiotics prophylactically before cardiac catheterization, and we know of no controlled studies to support their use.

A wide variety of sedatives has been employed for premedication. We no longer routinely order premedication to be given before the patient is sent to the catheterization laboratory. Instead, we assess the patient's state of alertness and need for sedation once he or she is on the catheterization table. At that time, we usually administer midazolam (Versed, Roche Laboratories, Nutley, NJ) 1 mg IV and/or fentanyl 25 to 50 mg IV.

It is our practice to have the patient fasting (except for oral medications) after midnight, but some laboratories allow a light tea and toast breakfast without ill effects. Complete vital signs should be recorded before the patient leaves the floor (for inpatients), or shortly after arrival at the ambulatory center (for outpatients), so that the procedure may be aborted if a change has occurred since the patient was last seen.

For a typical inpatient, our precatheterization orders might be the following:

1. To Cardiac Catheterization Laboratory at 7:30 a.m. tomorrow by stretcher; patient to be in hospital gown.
2. Fasting after midnight except for regularly scheduled oral medications.
3. Have patient urinate before leaving for Cardiac Catheterization Laboratory.
4. Record complete vital signs before patient leaves for Cardiac Catheterization Laboratory.

This list is only a general procedure guide and obviously would be modified as the details of specific situations require.

THE CARDIAC CATHETERIZATION FACILITY

A modern cardiac catheterization laboratory requires an area of 500 to 700 ft ^{2}, within which is housed a conglomeration of highly sophisticated electronic and radiographic equipment. Reports of the Inter-Society Commission for Heart Disease Resources on optimal resources for cardiac catheterization facilities appeared in 1971, 1976, and 1983. The most recent American College of Cardiology/American Heart Association (ACC/AHA) Guidelines for Cardiac Catheterization Laboratories (48) were published in 1991. In this report, a variety of issues were dealt with, including the following:

1. Traditional versus nontraditional settings for a cardiac catheterization laboratory; location within a hospital versus a freestanding facility
2. Ambulatory cardiac catheterization: indications and contraindications
3. Ethical issues related to self-ownership of laboratories, self-referral of patients, and advertising
4. Optimal annual caseload for physicians and for the laboratory
5. Safety issues during conduct of the procedure (e.g., sterile technique, heparin)
6. Physical arrangements and space requirements
7. Radiation safety and radiologic techniques.

The report (48) provides detailed discussion of these issues. Certain points, however, are worth discussing here.

Location Within a Hospital Versus a Freestanding Facility

The issue of whether cardiac catheterization laboratories should be hospital-based, freestanding, or mobile has been the subject of much debate (48,49 and 50). There are many potential concerns about performance of cardiac catheterization in a freestanding facility, and the available data from such facilities are limited. Mobile cardiac catheterization laboratories may be either freestanding or hospital-based (as is the case for mobile magnetic resonance imaging and other mobile

diagnostic units), so mobile and freestanding units should not be equated automatically. In its 1991 report, the ACC/AHA Task Force “generally found that in freestanding catheterization laboratories, access to emergency hospitalization may be delayed, and appropriate oversight may be lacking. Additionally, opportunities for self-referral may be fostered and the perception of commercialism and entrepreneurial excess in practice created” (48). The report concluded that “in view of the lack of appropriately controlled safety and need data for hospital-based, mobile or freestanding laboratories operating without on-site (accessible by gurney) cardiac surgical facilities, the Task Force reaffirms the position that further development of these facilities cannot be endorsed at this time” (48).

Outpatient Cardiac Catheterization

Outpatient cardiac catheterization has been demonstrated by a variety of groups to be safe, practical, and highly cost-efficient, and it is widely practiced throughout the world. Outpatient catheterization can be accomplished by the radial or brachial approach, which allows the patient to be ambulatory within minutes after completion of the catheterization study (42,44,45 and 46,51). However, outpatient catheterization also can be accomplished safely by the percutaneous femoral technique (52,53 and 54). In one study (52), 2,207 patients underwent elective outpatient cardiac catheterization at the Kaiser Permamente Regional Cardiac Catheterization Laboratory in Los Angeles, California. Ninety-seven percent of the procedures were done by the percutaneous femoral approach, using 7F catheters without sheaths. Heparin was given intraarterially in a relatively low dose (2,000 to 3,000 units) and was not reversed with protamine at the end of the procedure. Hemostasis was obtained by manual compression for 10 minutes over the femoral artery, followed by placement of a pressure dressing and sandbag for 4 hours. Patients were checked at 15-minute intervals during the 4-hour surveillance period and discharged after they had become ambulatory. Each patient was contacted at home by telephone on the following day by a nurse from the outpatient observation area, and patients were seen after 1 to 2 weeks by their referring cardiologist for follow-up consultation and discussion of results. Complication rates were extremely low, lower than rates generally reported for inpatient diagnostic catheterization (see Chapter 3). More recently, 5F catheters (55,56) and radial artery catheterization techniques (42,44,45 and 46) have been used for outpatient cardiac catheterization, substantially reducing the potential risks.

On-site Cardiac Surgery

Another issue addressed in the ACC/AHA Guidelines is the question of proximity and availability of cardiac surgical facilities. The report emphasized that laboratories without in-house cardiovascular surgery must have formal arrangements with a hospital that has on-site cardiovascular surgery facilities and that regulatory and third-party reimbursement agencies should review these arrangements on a regular basis (48). Immediately available cardiac surgical backup is particularly critical for laboratories performing diagnostic catheterization on unstable, acutely ill, or high-risk patients and for those performing coronary angioplasty, endomyocardial biopsy, or transseptal catheterization.

Physician and Laboratory Caseload

Utilization levels and optimal physician caseload represent a third issue of general interest addressed in the ACC/AHA Guidelines (48). The report recommended certain levels of utilization for cost-effectiveness and maintenance of skills (Table 1.3). Note that the optimal caseload has an upper limit as well as a lower limit. A cardiologist should not have such an excessive caseload that it interferes with proper precatheterization evaluation of the patient or with adequate postcatheterization interpretation of the data, report preparation, patient follow-up, and continuing medical education.

Category	Cases per year
Adult catheterization laboratories	300
Pediatric catheterization laboratories	150
Physician caseload*	
Adult diagnostic catheterizations	≥150 but ≤1,000
Adult PTCA procedures	75
Pediatric catheterizations	50
Electrophysiology procedures	100

* The report indicates that physicians with extensive experience (e.g., more than 1,000 independently performed catheterizations) can perform fewer catheterizations to maintain their skill levels.

Pepine CJ, Allen HD, Bashore TM, et al. ACC/AHA Guidelines for Cardiac Catheterization and Cardiac Catheterization Laboratories. American College of Cardiology/American Heart Association Ad Hoc Task Force on Cardiac Catheterization. *Circulation* 1991;84:2213, and updated in 1999.

TABLE 1.3. *ACC/AHA task force guidelines for catheterization laboratory and physician caseloads*

Performing the Procedure

Having carefully considered indications and contraindications, chosen a method of approach, designed the catheterization protocol, and prepared the patient, the physician's next step is to perform the cardiac catheterization itself and thereby gain the anatomic and physiologic information needed in the individual case. The individual cardiac catheterization selectively draws on the procedures that are described throughout this text. Detailed descriptions of catheter insertion and hemodynamic measurements are contained in Section II (Chapter 4, Chapter 5 and Chapter 6) and Section III (Chapter 7, Chapter 8, Chapter 9 and Chapter 10), respectively. Descriptions of angiographic and interventional techniques are given in Section IV (Chapter 11, Chapter 12, Chapter 13 and Chapter 14) and Section VII (Chapter 23, Chapter 24, Chapter 25, Chapter 26, Chapter 27 and Chapter 28). Methods for evaluation of cardiac function and special techniques used only in selected situations are described in Section V (Chapter 15, Chapter 16 and Chapter 17) and Section VI (Chapter 18, Chapter 19, Chapter 20, Chapter 21 and Chapter 22).

These descriptions are not proposed as the only correct approaches to cardiac catheterization (many laboratories and operators take different approaches, and yet obtain excellent results). Rather, they are the methods that we have consistently found to be safe, successful, and practical. Their strengths and weaknesses are well characterized, and I believe that they constitute an excellent point of reference as one's practice continues to evolve based on new data and personal preference.

CHAPTER REFERENCES

1. Cournand AF. Nobel lecture, December 11, 1956. In: Nobel Lectures, Physiology and Medicine 1942–1962. Amsterdam: Elsevier, 1964:529.
2. Cournand A. Cardiac catheterization: development of the technique, its contributions to experimental medicine, and its initial application in man. *Acta Med Scand Suppl* 1975;579:1.
3. Mueller RL, Sanborn TA. The history of interventional cardiology: cardiac catheterization, angioplasty, and related interventions. *Am Heart J* 1995;129:146.
4. Forssmann W. Die Sondierung des rechten Herzens. *Klin Wochenschr* 1929;8:2085.
5. Forssmann W. *Experiments on myself: memoirs of a surgeon in Germany.* New York: St. Martin's Press, 1974.
6. Klein O. Zur Bestimmung des zerkulatorischen minutens Volumen nach dem Fickschen Prinzip. *Munch Med Wochenschr* 1930;77:1311.
7. Cournand AF, Ranges HS. Catheterization of the right auricle in man. *Proc Soc Exp Biol Med* 1941;46:462.
8. Richards DW. Cardiac output by the catheterization technique in various clinical conditions. *Fed Proc* 1945;4:215.
9. Cournand AF, et al. Measurement of cardiac output in man using the technique of catheterization of the right auricle or ventricle. *J Clin Invest* 1945;24:106.
10. Dexter L, et al. Studies of congenital heart disease: II. The pressure and oxygen content of blood in the right auricle, right ventricle, and pulmonary artery in control patients, with observations on the oxygen saturation and source of pulmonary “capillary” blood. *J Clin Invest* 1947;26:554.
11. Hellems HK, Haynes FW, Dexter L. Pulmonary “capillary” pressure in man. *J Appl Physiol* 1949;2:24.
12. Lagerlöf H, Werkö L. Studies on circulation of blood in man. *Scand J Clin Lab Invest* 1949;7:147.
13. McMichael J, Sharpey-Schafer EP. The action of intravenous digoxin in man. *Q J Med* 1944;13:1123.
14. Lenègre J, Maurice P. Premiers recherches sur la pression ventriculaire droits. *Bull Mem Soc Med d'Hôp Paris* 1944;80:239.
15. Stead EA Jr, Warren JV. Cardiac output in man: analysis of mechanisms varying cardiac output based on recent clinical studies. *Arch Intern Med* 1947;80:237.
16. Stead EA Jr, Warren JV, Brannon ES. Cardiac output in congestive heart failure: analysis of reasons for lack of close correlation between symptoms of heart failure and resting cardiac output. *Am Heart J* 1948;35:529.
17. Bing RJ, et al. Catheterization of coronary sinus and middle cardiac vein in man. *Proc Soc Exp Biol Med* 1947;66:239.
18. Bing RJ, et al. Measurement of coronary blood flow, oxygen consumption, and efficiency of the left ventricle in man. *Am Heart J* 1949;38:1.
19. Bing RJ, Vandam LD, Gray FD Jr. Physiological studies in congenital heart disease: I. Procedures. *Bull Johns Hopkins Hosp* 1947;80:107.
20. Burchell HB. Cardiac catheterization in diagnosis of various cardiac malformations and diseases. *Proc Mayo Clin* 1948;23:481.
21. Wood EH, et al. General and special techniques in cardiac catheterization. *Proc Mayo Clin* 1948;23:494.
22. Burwell CS, Dexter L. Beri-beri heart disease. *Trans Assoc Am Physicians* 1947;60:59.
23. Harvey RM, et al. Some effects of digoxin upon heart and circulation in man: digoxin in left ventricular failure. *Am J Med* 1949;7:439.

24. Zimmerman HA, Scott RW, Becker ND. Catheterization of the left side of the heart in man. *Circulation* 1950;1:357.
25. Limon-Lason R, Bouchard A. El cateterismo intracardico: cateterizacion de las cavidades izquierdas en el hombre. Registro simultaneo de presion y electrocadiograma intracavetarios. *Arch Inst Cardiol Mex* 1950;21:271.
26. Seldinger SI. Catheter replacement of the needle in percutaneous arteriography: a new technique. *Acta Radiol* 1953;39:368.
27. Ross J Jr. Transseptal left heart catheterization: a new method of left atrial puncture. *Ann Surg* 1959;149:395.
28. Cope C. Technique for transseptal catheterization of the left atrium: preliminary report. *J Thorac Surg* 1959;37:482.
29. Sones FM Jr, Shirey EK, Prondfit WL, et al. Cinecoronary arteriography. *Circulation* 1959;20:773(abst).
30. Sones FM Jr. Cine coronary arteriography. In: Hurst JW, Logue RB, eds. *The Heart,* 2nd ed. New York: McGraw-Hill, 1970:377.
31. Ricketts JH, Abrams HL. Percutaneous selective coronary cine arteriography. *JAMA* 1962;181:620.
32. Judkins MP. Selective coronary arteriography: a percutaneous transfemoral technique. *Radiology* 1967;89:815.
33. Swan HJC, Ganz W, Forrester J, et al. Catheterization of the heart in man with use of a flow directed balloon-tipped catheter. *N Engl J Med* 1970;283:447.
34. Grüntzig A, et al. Coronary transluminal angioplasty. *Circulation* 1977;56[Suppl II]:319(abst).
35. Grüntzig A, Senning A, Siegenthaler WE. Nonoperative dilatation of coronary artery stenoses: percutaneous transluminal coronary angioplasty. *N Engl J Med* 1979;301:61.
36. King SB III. The development of interventional cardiology. *J Am Coll Cardiol* 1998;31:64B.
37. Grines CL, Browne KF, Marco J, et al. A comparison of immediate angioplasty with thrombolytic therapy for acute myocardial infarction. *N Engl J Med* 1993;328:673.
38. Tiefenbrunn AJ, Chandra NC, French WJ, et al. Clinical experience with primary percutaneous transluminal coronary angioplasty compared with alteplase (recombinant tissue-type plasminogen activator) in patients with acute myocardial infarction: a report from the Second National Registry of Myocardial Infarction (NRMI-2). *J Am Coll Cardiol* 1998;31:1240.
39. Shapiro SM, Oudiz RJ, Cao T, et al. Primary pulmonary hypertension: improved long-term effects and survival with continuous intravenous epoprostenol infusion. *J Am Coll Cardiol* 1997;30:343.
40. Green GS, McKinnon CM, Rosch J, et al. Complications of selective percutaneous transfemoral coronary arteriography and their prevention. *Circulation* 1972;45:552.
41. Mann T, Cubeddu G, Bowen J, et al. Stenting in acute coronary syndromes: a comparison of radial versus femoral access sites. *J Am Coll Cardiol* 1998;32:572.
42. Lotan Ç, Hasin Y, Mosseri M, et al. Transradial approach for coronary angiography and angioplasty. *Am J Cardiol* 1995;76:164.
43. Feldman T. Ulnar and radial coronary interventions: distal reaches of arterial access. *Cathet Cardiovasc Diagn* 1997;41:131.
44. Kiemeneij F, Laarman GH, Odekerken D, et al. A randomized comparison of percutaneous transluminal coronary angioplasty by the radial, brachial and femoral approaches: the ACCESS study. *J Am Coll Cardiol* 1997;29;1269.
45. Wu C-J, Lo P-H, Chang K-C, et al. Transradial coronary angiography and angioplasty in Chinese patients. *Cathet Cardiovasc Diagn* 1997;40:159.
46. Schneider JE, Mann T, Cubeddu MG, et al. Transradial coronary stenting: a United States experience. *J Invasive Cardiol* 1997;9:569.
47. Anderson KO, Masur FT. Psychological preparation for cardiac catheterization. *Heart Lung* 1989;18:154.
48. Pepine CJ, Allen HD, Bashore TM, et al. ACC/AHA Guidelines for Cardiac Catheterization and Cardiac Catheterization Laboratories. American College of Cardiology/American Heart Association Ad Hoc Task Force on Cardiac Catheterization. *Circulation* 1991;84:2213.
49. Conti CR. Cardiac catheterization laboratories: hospital-based, free-standing or mobile? [President's page]. *J Am Coll Cardiol* 1990;15:748.
50. Elliott CM, Bersin RM, Elliott AV, et al. Mobile cardiac catheterization laboratory. *Cathet Cardiovasc Diagn* 1994;31:8.
51. Fierens E: Outpatient coronary arteriography: a report on 12,719 studies. *Cathet Cardiovasc Diagn* 1984;10:27.
52. Mahrer PR, Young C, Magnusson PT. Efficacy and safety of outpatient catheterization. *Cathet Cardiovasc Diagn* 1987;13:304.
53. Pink S, Fiutowski L, Gianelly RE. Outpatient cardiac catheterizations: analysis of patients requiring admission. *Clin Cardiol* 1989;12:375.
54. Block PC, Ockene I, Goldberg RJ, et al. A prospective randomized trial of outpatient versus inpatient cardiac catheterization. *N Engl J Med* 1988;319:1251.
55. Kern MJ, Cohn M, Talley JD, et al. Early ambulation after 5 French diagnostic cardiac catheterization: results of a multi-center trial. *J Am Coll Cardiol* 1990;15:1475.
56. Slack JD, Higgins B, Pinto R. Use of 5 French catheters for elective outpatient cardiac catheterization: minimal early and late access site bleeding despite early ambulation protocol. *Circulation* 1994;90:I-488(abst).

2
Proper Use of Cineangiographic Equipment and Contrast Agents

Donald S. Baim

Harvard Medical School; Center for Innovative Minimally Invasive Therapy, Brigham and Women's Hospital, Boston, Massachusetts 02115

Although the training for performing cardiac catheterization procedures includes detailed study of cardiac anatomy, physiology, and pathophysiology, such training usually does not include formal instruction concerning radiologic equipment, radiation safety, or the optimal use of contrast agents. As a result, most operators take a "learn as you go" approach to understanding these increasingly complex areas. Crises may develop when it becomes necessary to select new equipment or to describe malfunctions of existing equipment to service personnel. Even between crises, laboratories run by such operators typically devote little attention either to maintaining optimal image quality or to ensuring the radiation safety of their patients and personnel. Accordingly, this chapter attempts to heighten awareness about the equipment used for cardiac angiography, radiographic principles, programs for radiographic quality assurance, radiation protection, and the characteristics of various intravascular contrast agents. Those seeking more detailed technical information are referred to the 1991 American College of Cardiology/American Heart Association Guidelines for Cardiac Catheterization and Cardiac Catheterization Laboratories (1) and Radiation Safety (2), as well as the excellent text of Moore (3).

THE ANGIOGRAPHY ROOM

The modern cardiac catheterization laboratory (Fig. 2.1 and Fig. 2.2) consists of a patient support table, equipment for monitoring intracardiac pressures and electrocardiographic activity, and a floor or ceiling-suspended gantry that allows variable angulation of the x-ray beam through the patient. The patient support consists of an adjustable-height, flat-top table whose locks can be released to allow the table top to "pan" freely (i.e., move the patient's body horizontally toward the head or foot, left or right) within the x-ray beam. The reliance on the gantry to perform all beam angulation represents a distinct improvement (in terms of both patient comfort and maximum achievable angulation) over the cradle systems used in the 1970s. In these earlier systems, the image chain remained stationary while the patient was rolled from side to side to provide views of the heart in different projections. Regardless of its design, the only purpose of the support equipment is to allow precise positioning of the radiographic imaging chain relative to the patient, in terms of both *rotation* (left or right anterior oblique) and *skew* (cranial or caudal) angulation (Fig. 2.3). In some laboratories, a second complete imaging chain may be used to provide simultaneous viewing of cardiac structures from a separate angle. Such "biplane" imaging systems are significantly more expensive than "single plane" systems, and are generally preferred only by laboratories that study a high percentage of congenital cases or whose operators believe that biplane imaging is of value in certain procedures (e.g., transseptal puncture, electrophysiology ablations).

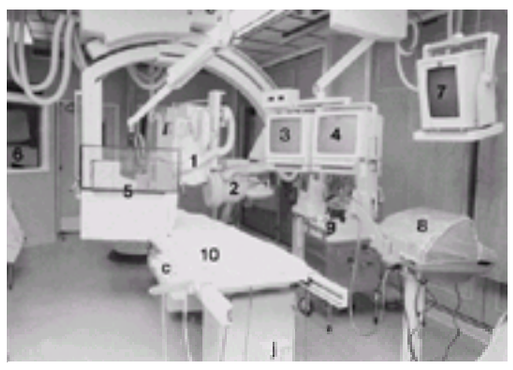

FIG. 2.1. Biplane cineangiography room showing (1) anteroposterior (AP) plane image intensifier, cine camera, television camera, and x-ray tube (partially hidden below table), attached to a floor-mounted parallelogram gantry to allow complex angulation; (2) lateral plane image chain attached to a ceiling-suspended gantry that can be moved into place when biplane imaging is desired; (3) and (4) television monitors for AP and lateral image chains; (5) movable radiation shield to protect operators from scatter dose to eyes and thyroid; (6) physiologic pressure recorder located behind lead-glass window to protect the cardiovascular technician from scatter radiation; (7) remote display of physiologic data; (8) power injector for contrast delivery during ventriculography; (9) emergency cart containing defibrillator, airway management, and drug supplies; and (10) patient support table with (c) control box for table and gantry movement, magnification mode, and beam-restricting "cones" and (j) junction box for connection of pressure transducers to physiologic recorder. The generator and image chain electronics are concealed behind the louvered doors seen along the right wall of the room.

FIG. 2.2. The L/C stand (General Electric, Milwaukee, WI) is a commonly installed alternative to the parallelogram for complex angulation.

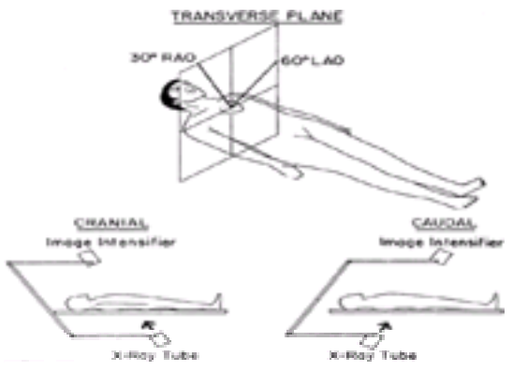

FIG. 2.3. Angulations used in cardiac angiography include both rotation and skew. Rotation is shown here for the classic positions in which the image intensifier is at 60° left anterior oblique (LAO) and 30° right anterior oblique (RAO), relative to the vertical, in the transverse plane. Skew is shown here for the caudocranial (now called cranial) angulation, in which the image intensifier is positioned closer to the patient's head, and the craniocaudal (now called caudal) angulation, in which the image intensifier is positioned closer to the patient's feet. Complex angulations are specified by giving both the rotation and the skew (e.g., “60° LAO, 35° cranial”).

The classic image chain consists of a generator and cine pulse system, an x-ray tube, an image intensifier, an optical distributor, a 35-mm cine camera, and a television camera and monitor. As such, the image chain can provide both “live” *fluoroscopy* to facilitate placement of cardiac catheters and *cineangiography* to permanently capture details about the anatomic and functional state of cardiac chambers, great vessels, and the coronary circulation. Although 35-mm film was the original medium for recording cineangiographic images, since 1998 virtually all newer installations are based on “filmless” technology in which the 35-mm camera is eliminated and the images viewed by the television camera are permanently recorded by digital encoding (see later discussion).

To house this bulky and expensive equipment and the support personnel required to operate it, the room should have a floor area of at least 500 ft ^{2} (47 m^2) with a ceiling height of at least 10 ft (3 m) (1). The walls should be shielded with 1 mm of lead up to a height of 7 ft to provide radiation protection for personnel in surrounding work areas, and any observation windows into the room should be made of lead-treated glass or plastic that provides a similar level of radiation shielding. Although the control and recording equipment was once situated within the room itself, current room design segregates this equipment and operating personnel within a “control area” that provides a similar degree of lead shielding without sacrificing excellent verbal communication or rapid access to the procedure room itself. The bulky components that constitute the generator and its associated electronics (i.e., the “racks”) may be placed in ventilated closets along the walls of the room but must be positioned so that the high-voltage cable runs are short (less than 40 ft [13 m]) and the racks themselves are easily accessible to service personnel for diagnostic and repair activities.

The Generator

The generator is basically a step-up transformer that converts three-phase 480-V line current into the high voltage (70 to 120 kV) and current (300 to 800 mA) needed to power the x-ray tube for the generation of an x-ray beam (4). The transformer is submerged in a large tank of oil for cooling and insulation. The alternating current (AC) output of this transformer is then converted into direct current (DC) by rectifier circuits.

To be useful in a cardiac study, the DC output of the generator must be combined with a cine pulse system, which chops the generator output into the brief (4- to 6-msec) pulses that are required to “freeze” motion-induced blurring of the rapidly moving coronary arteries. Such pulsing is best performed in the secondary or high-voltage side of the system, using either solid-state or vacuum switching tubes (triodes or tetrodes) or a grid-controlled x-ray tube to transiently interrupt the generator current. The cine pulse system must be capable of handling the 60- to 100-kW power output of the generator and delivering it to the x-ray tube. The generator must also contain automatic brightness control (ABC) circuitry, which allows it to compensate for changes in the transmission of x-rays to the image intensifier that occur as the beam is “panned” through structures of differing attenuation. This is accomplished through the use of a photocell (located at the output of the image intensifier) that detects a drop in light and triggers the ABC to increase the generator output so as to return the number of x-rays striking the photocell (and thus the image intensifier) to the level that is optimal for image production. This increase in generator output may be accomplished by increasing one of three factors: *kV or kilovolts*, the energy of the x-ray photons (which increases their penetrating power); *mA or milliampere*s, the electrical current flowing through the x-ray tube (which increases the number of x-ray photons generated); *msec or millisecond*s, the duration of each x-ray pulse (which increases the amount of time the x-ray beam is on and therefore the total number of photons passing through the patient). How these factors are changed is determined by “regulation curves” programmed into the ABC by the manufacturer.

In a steeply angulated view, the ABC system usually relies on increases in kV, because a comparatively small (6 to 8 kV) rise in kV will augment x-ray penetration, as much as doubling the mA or msec. Although doubling the mA would provide the same increase in film blackening, this might well exceed the power-handling capacity of the cine pulse system or x-ray tube (power = kV × mA) and would double patient dose. Widening the pulse width would also increase film blackening, but doubling the msec would cause significant motion blurring and would also double patient dose. So alteration in the kV is the primary change made by the automatic exposure system in its effort to maintain optimal film blackening. But increasing kV is not without its price, because imaging of iodine-based contrast agents is best achieved with relatively low tube voltages (70 to 80 kV). The x-rays generated at these low voltages have energies that are only slightly grater than the 33-keV binding energy of K-shell electrons in the iodine atoms, so x-ray absorption is very intense. This maximizes the differential absorption by iodine versus water (and therefore the imaging contrast). An underpowered generator or cine pulse system—one that can achieve adequate penetration only by using higher (100 to 120) kV energies well above the K-shell binding energy—tends to produce grainy, low-contrast angiographic images in which both water and iodine look gray.

The X-Ray Tube

The x-ray tube converts the electrical energy produced by the generator into a stream of x-rays, much as a light bulb converts electrical energy to visible light. The x-ray tube consists of an evacuated glass or metal housing that contains a tungsten filament (housed in a cathodal focusing cup) and an anode disc (tungsten alloy, 100 to 120 mm in diameter) that rotates at more than 10,000 rpm during cineangiography (Fig. 2.4). Electrons boil off the filament by thermionic emission, in proportion to filament temperature. These electrons accelerate toward the anode under the influence of the electric field (approximately 100 kV) supplied by the generator. Their sudden decelerative interaction with the tungsten atoms in the anode results in the emission of x-ray photons by the Bremsstrallung (braking) reaction. The resulting x-ray photons are emitted at a right angle to the direction of electron travel, and they exit the x-ray tube through a “beam port” in its lead housing. For sharpest imaging, this beam should be as narrow as possible, as though it were coming from a single point source.

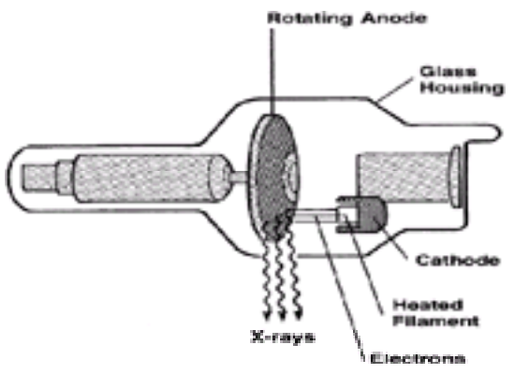

FIG. 2.4. X-ray tube construction. Electrons liberated from the heated filament of the cathode are accelerated toward the slanted surface of the rapidly rotating anode. On impact with the anode, sudden deceleration of the electrons generates x-ray photons, which leave the tube housing through a side-positioned window.

Practically speaking, it is difficult to obtain a true point source of radiation, because concentrating the high-power electron beam on a single point would melt the tungsten anode (3,370°C). To reduce the amount of local heating, the anode is rotated rapidly (10,000 rpm), so that the beam impact point is spread along a track around the anode surface. The impact zone is broadened further by beveling the anode so that it faces the electron beam at a slight angle (Fig. 2.5). The amount of "target angle" is critical: too flat a target angle (less than 8° to 10°) provides little extra area for beam impact and also causes a "heel effect," whereby the anode itself absorbs part of the generated x-ray beam, so that it fails to illuminate the full surface of a 9-inch field. Too steep a target angle avoids these limitations but causes undesirable broadening of the x-ray beam, with resultant loss of image sharpness. Within the range of acceptable heel angles, the apparent size of the focal spot as seen from the image intensifier is referred to as the "effective focal spot"; it is influenced by both filament geometry and the target angle. Most catheterization laboratory x-ray tubes include two different focal spots. The *small focal spot* (usually 0.6 mm) more closely resembles a point source and thus minimizes geometric unsharpness of the image, but it is quite limited in terms of its power-handling capacity (35 kW). This forces the ABC control to resort to a low mA–high kV technique, which provides adequate film blackening only at the expense of poor image contrast. The small focal spot therefore usually is used only for fluoroscopy or for cineangiography in pediatric patients. In adult patients, routine cineangiography uses the *large focal spot* (usually 1.0 mm). Although there is some loss of image sharpness, the fact that the electron beam is spread out over a larger area of the anode gives the large focal spot a higher (100 kW) power-handling capacity, which allows use of a lower-kV technique with better image quality.

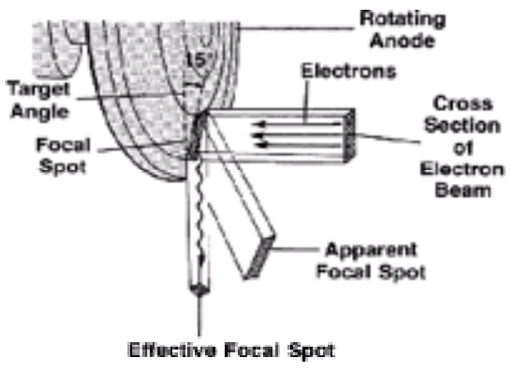

FIG. 2.5. Focal spot geometry. To reduce local heating, the intensity of the electron beam at the anode is decreased by rapid rotation of the anode, which spreads the electron beam into a rectangular shape by beveling the anode surface where the beam hits (target angle). The effective focal spot is defined in the direction perpendicular to the electron beam (out the tube window) and represents the size of the x-ray source as seen from the image intensifier (typically 0.6 or 1 mm). Too much bevel widens one dimension of the effective focal spot excessively, and too little bevel (target angles less than about 10°) causes the anode itself to absorb part of the beam (heel effect), making it impossible to illuminate the full surface of a 9-inch image intensifier.

In addition to the problem of instantaneous power loading of the focal spot (kW), x-ray tubes must be able to absorb a large cumulative heat load. Less than 1% of the electrical energy delivered to the tube is converted to x-rays; the rest is retained as heat. The heat is transmitted to the underlying (usually graphite or molybdenum) anode disk, and from there into the body of the x-ray tube. The heat load can be expressed in terms of heat units (HU = 1.35 × kV × mA × sec), and dissipation of this heat load is one of the biggest challenges of x-ray tube design. A typical single-frame cine exposure delivers roughly 300 HU, and a 10-second run of such exposures at 30 frames per second (fps) delivers 90,000 HU. Most x-ray tubes can absorb only 400,000 HU before their support bearings seize and the tube self-destructs, although some modern tubes that use liquid metal bearings can absorb more than twice that amount before failing. To permit more prolonged studies, the heat input to the anode must be counterbalanced by heat transfer to the oil-filled tube housing, which can absorb roughly 1.5 million HU before reaching a sufficient temperature to rupture its oil seals. This margin can be extended by using more conductive liquid-metal lubrication or by circulating air, water, or oil around the housing to conduct heat away from it more rapidly. Although "waiting for heat units" used to cause delays in laboratories when rapid sequences of cine runs were performed, these improvements in x-ray tube design have largely eliminated this problem.

Although not part of the x-ray tube per se, *beam filtration* and *collimation* are important aspects of the radiation beam. The energies of the photons in an x-ray beam are not uniform but are distributed over a range extending up to the generator kV. The lowest energies in this distribution (those less than 20 keV) are too weak to make it through the patient's body and therefore contribute only to increasing the entry skin dose (and not to image formation). Before it leaves the x-ray tube housing, the beam is passed through a material (usually 2.5- to 3.0-mm thick aluminum) that "hardens" the beam by selectively removing low-energy x-rays. The x-ray beam must also be limited *spatially* so that only the area seen by the image chain is illuminated. Failure to do so unnecessarily increases both patient x-ray dose and the scatter radiation received by in-room personnel. It also degrades image quality by increasing the number of x-ray photons that strike outside of the image field and are then "scattered" back so that they strike the image intensifier. The beam is therefore "collimated" by positioning thick lead sheets within the tube housing to restrict the beam to the appropriate field size. Further limitation of the beam can be achieved by using moveable lead "cones," so that only the area captured on the cine frame is illuminated. Finally, many systems include a moveable "gradient" or "wedge" filter that can be positioned over the lung field so as to attenuate the radiation that would otherwise cause excessive brightness there that might interfere with imaging of the adjacent cardiac structures.

The Image Intensifier

Even a precisely generated x-ray beam is useless unless the pattern created as the beam passes through the patient results in a highly detailed "shadow" that the operator can view. In the beginning of the 20th century, this was done by allowing the x-rays to strike a fluorescent screen (zinc cadmium sulfide), where they produced a glow so faint that it could be seen only if the operator's eyes had been dark-adapted by donning red goggles for 30 minutes before viewing. In the 1950s, this situation improved considerably with the development of image intensifiers (evacuated glass bottles coated internally with a fluorescent phosphor at each end) that increase the brightness of the image more than 1,000-fold (5). Figure 2.6 shows the image intensifier in cross-sectional view. X-rays that have passed through the patient strike the input phosphor (usually cesium iodide), which then emits light. Because the input phosphor is in contact with a photocathode, this light causes the release of low-energy electrons into the interior of the image intensifier. These electrons are accelerated toward the anode by a high-voltage (25- to 35-kV) electric field, until they ultimately strike the small-diameter output phosphor. The impressive gain in image brightness results from a combination of *minification* (the output phosphor surface area is smaller than that of the input phosphor) and *electron amplification* (electrons that come from the photocathode are accelerated so that they strike the output phosphor with enough energy to generate thousands of visible photons for each high-energy electron).

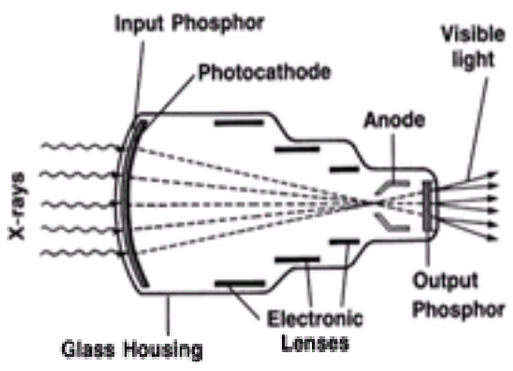

FIG. 2.6. Image intensifier in cross-sectional view. The x-rays that have passed through the patient strike the input phosphor and release electrons from the photocathode. These electrons are focused by an electrostatic lens as they are accelerated toward the anode by a high-voltage electric field, ultimately striking the small-diameter output phosphor.

The image intensifier also contains an electrostatic lens that focuses the electrons during their flight. Although single-mode image intensifiers are still available, cardiac catheterization imaging systems can vary the focus potential to change the image magnification (dual- and triple-mode image intensifiers). A 9-inch (23-cm)

mode uses virtually the entire input phosphor area and is well suited to studies such as left ventriculography that require imaging of a large area with only a modest degree of spatial resolution. A 6- or 7-inch (15- or 17-cm) mode displays a magnified image of the central portion of the input phosphor and provides optimal coverage area and spatial resolution for coronary angiography. In a triple-mode tube, the 4.5- or 5-inch (11- or 12-cm) mode provides still greater magnification for special procedures such as percutaneous transluminal coronary angioplasty (PTCA). Use of this “mag” mode for routine cineangiography is not advised, because it overtaxes the generator and tube capacity and requires careful panning by the operator if the whole coronary tree is to be imaged during a single contrast injection. The need to maintain light output from a small field of view causes the ABC to call for more radiation, so that although the *total* patient dose (reflected by the product of dose × area) is not increased in the “mag” mode, the dose to an individual square centimeter of patient skin may approach the threshold for radiation injury during prolonged imaging. Larger field image intensifiers (i.e., 12 or 14 inches) are not needed for cardiac procedures and may limit extreme gantry angulation, but they are used in some laboratories where peripheral angiography is performed so that the vasculature of both legs can be visualized simultaneously.

The qualities of the image intensifier are central to the performance of the image chain. Certain desirable characteristics, such as gain, quantum detection efficiency, spatial resolution, and contrast, tend to be mutually exclusive, and all available image intensifiers involve some performance tradeoffs. Moreover, an image intensifier's performance degrades rapidly, so that its useful life is only 3 to 5 years in a busy laboratory before loss of gain and contrast necessitate replacement. Despite these limitations, image intensifiers are currently available with on-line resolution in excess of 4 line pairs per millimeter in the 6- to 7-inch mode, and excellent balances of desirable characteristics.

The Television Chain

Real-time viewing of the x-ray image is essential to position catheters, monitor injections, move the patient appropriately during each imaging run, and perform interventional procedures. Since the 1960s, this has been accomplished by placing a television camera so that it can also (along with the 35-mm cine camera) view the output phosphor of the image intensifier (6). When the intent of imaging is only to position a catheter or device or to perform a test injection, the cine camera does not operate, and the generator provides a low dose of radiation that is adequate to create a television image. Although so-called *fluoroscopy* therefore involves less than 1/100 of the x-ray beam intensity that is used for permanent, high-resolution image recording (*cineangiography*), prolonged fluoroscopy times (up to 30 minutes in some interventional procedures) can contribute total patient and operator x-ray doses as great as those of shorter but higher-dose cineangiographic runs. When the intent is to record an image of the highest possible resolution on 35-mm film or electronic media, cineangiography is performed, using the higher x-ray doses needed for optimal image definition. To avoid “blinding” the television camera at this significantly higher level of light from the output phosphor of the image intensifier, the output light is split by a partially silvered mirror—typically 80% to 90% to the film camera and 10% to 20% to the television camera. Even during cineangiographic runs, however, it is important to collect television images that can be viewed by the operator in real time, so that the diagnostic and therapeutic decisions required during the course of an interventional procedure can be made even before the cine film is developed. In newer filmless systems, these television images are even used for the permanent archive of the procedure. High-quality on-line television images are therefore central in both fluoroscopy and cineangiography. Understandably, the performance of the television chain has become paramount to modern cardiac catheterization.

The type of image tube used varies in different television systems. In contrast to the standardvidicon (which uses an antimony trisulfide target), most catheterization systems use a plumbicon (lead monoxide target), saticon (selenium arsenic tellurium target), or primicon (selenium tellurium arsenic target) to maximize image contrast and minimize image carryover or “lag” so that less than 10% of the image signal carries over into the third video field. Solid-state (charge-coupled device, or CCD) television pickups are now entering service; they have the advantage of one-to-one mapping of each element in the camera to a “pixel” in a digital television image.

Another important variable is the scanning format. Interlaced scan systems (like broadcast television) alternately sweep the even- and odd-numbered lines from the overall raster. This may result in degradation of the television image during 30-fps cineangiography, due to misregistration of anatomic details between the odd and even scan lines, as well as “flicker” caused by collection of one set of lines when the x-ray beam is on and another set when it is off. Use of a progressive scanning television format can overcome these limitations so that all scan lines are acquired in numerical sequence each time the x-ray tube is pulsed (1,6,7). A scan converter then picks off the even- and odd-numbered scan lines for display on a standard interlaced monitor.

The other scan variable is the number of scan lines that make up the image. High-line systems (1,023 or 1,049 horizontal lines, compared with the standard 525-line system) can theoretically improve vertical resolution on the television monitor, but they also increase amplifier bandwidth and therefore can introduce more electronic noise into the displayed image. These limitations of “analog” television were largely overcome by the introduction of “digital” systems in the early 1990s. These systems use high-speed computers to perform on-line processing of the television image (improving image contrast, noise, and edge definition). In addition, digital systems store the images obtained in all cineangiographic runs and allow their playback at variable speed, magnification, and level of contrast enhancement. These resulting images can then be retained as a “road map” to facilitate the positioning of interventional devices, to compare anatomy before and after intervention, and (most recently) to perform on-line measurement of stenosis severity (8). Because they provide such substantial improvements in the quality and accessibility of television images that can be studied by the operator in the laboratory, these digital systems have replaced the combinations of videotape recorders and “frame grabbers” that were used in the late 1980s for in-lab review of angiographic runs.

Even newer developments in optical electronics may eventually lead to further improvements in system integration and performance. One such example is flat-panel technology (now being explored for radiography and computed tomographic scanning), which has the potential to replace both the image intensifier and the television chain. This technology uses a cesium iodide layer to turn x-ray photons into light, but then passes these photons on directly to a matrix of millions of tiny photodiodes. The analog electrical output of each photodiode is digitized, processed, and permanently recorded in digital form.

Cine Camera and Associated Optics

Although in-lab assessment of coronary images has become central to the performance of cardiac catheterization, permanent recording of these images is required for postprocedure *review* (as by cardiac surgeons), long-term *archiving* (to compare serial studies in a given patient), and *transfer* (sending images to another site to guide subsequent care there). Although our laboratory has recently been able to fulfill all of these functions with electronic imaging, the long-term standard for permanent recording has been the recording of angiographic images on 35-mm movie film, at a speed of 30 fps. Faster speeds (e.g., 60 fps) were once used to perform left ventriculography (thus capturing more time points during systolic emptying) but were abandoned because they entailed a 2-fold higher radiation dose. Some laboratories have recorded coronary images at speeds as low as 15 fps to reduce patient and operator radiation dose. Because many catheterization laboratories still use 35-mm film, this section reviews some of the unique considerations associated with this archival medium.

The heart of the 35-mm cine system is the camera. Derived from similar cameras used in the movie industry, the cine camera must provide smooth, accurate, and reliable film advancement. The advancement of each frame of film actually triggers the generator to produce each cineangiographic x-ray pulse, so that smooth and reliable camera operation is essential. The cine camera views the output phosphor of the image intensifier through an optical system consisting of matched collimator and camera lenses that maximize light transmission and spatial resolution while minimizing image unsharpness caused by veiling glare. The lens is also equipped with an adjustable f-stop and an interchangeable system of different-sized apertures used to restrict light transmission to balance intensifier output, film characteristics, and processing parameters. The focal length of the optical system determines the framing mode—the way in which the round output phosphor is represented on the rectangular cine frame (Fig 2.7). It is most common to employ maximal horizontal overframing, in which the full width of the output phosphor is recorded on the cine frame. The adjustable cones are used to block out any portion of the image intensifier circle that falls above or below the rectangular cine frame. For convenience in positioning the cones, the television monitor is marked with lines that represent the edges of what will be captured on the cine frame. Positioning of the cones is even more important when the optics are set up for total overframing.

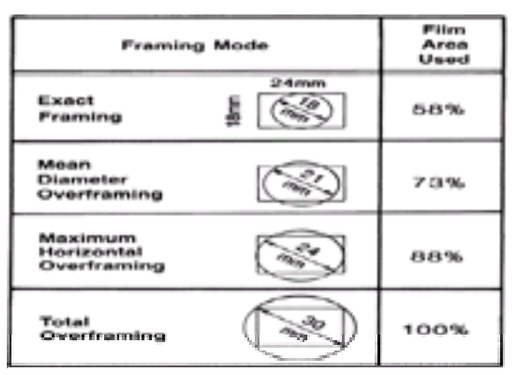

FIG. 2.7. Effect of camera optics on framing mode. A low-power lens system on the cine camera allows the film to record the entire surface of the output phosphor but provides a small image that uses only 58% of the film frame. Higher-power lens systems give a larger image that uses more of the film frame but cuts off either the top and bottom or all four edges of the output phosphor (maximal horizontal overframing and total overframing, respectively). (Modified from Friesinger GC, et al. Report of Inter-Society Commission for Heart Disease Resources. *Circulation* 1983;68:893A.)

Cine Film Selection, Processing, and Viewing

In film-based systems, the ultimate quality of the recorded image depends almost as much on the selection of the cine film and its processing parameters as on the other elements within the image chain. Cine film emulsions are generally slower than those of standard photographic films, but virtually any cine film can be used in a given system if f-stop, aperture, and processing parameters are selected correctly. The choice of a particular cine film therefore depends more on other important features such as contrast, latitude, and grain size, as well as the price and service support provided by the film distributor.

Film characteristics are best explored by plotting the characteristic curve (called the H and D curve, after Hurter and Driffield), using a sensitometer to perform calibrated test-strip exposures and a densitometer to measure the resulting film optical density (OD) (Fig. 2.8). Relevant parameters include the base-plus-fog (the OD of the film at step 0, before exposure to light) and the relative speed index (the sensitometer step that produces a specified increment in OD above base-plus-fog). Two indices of film contrast are also measured—the gamma and the average gradient—which have to do with how steeply the OD rises with increasing exposure. In general, films with lower contrast can recover more diagnostic information because their greater latitude allows distinction of more shades of gray and hence more anatomic detail between the extremes of black and white. Appropriate latitude is obtainable with an average gradient of 1.2 to 1.6, which is preferable to the steep edge gradients produced by some higher-contrast films.

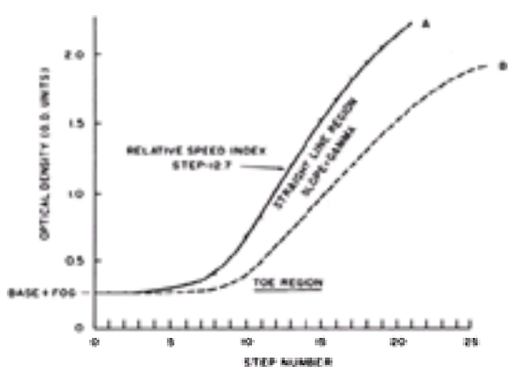

FIG. 2.8. Film characteristic curves (H and D curves), showing the relationship between light exposure (increasing step number on the horizontal axis) and film blackening (increasing optical density on the vertical axis). Measurements are shown for two different films, A and B, including base-plus-fog, relative speed index, and gamma (see text). Film B is less sensitive to light but has a lower contrast and wider latitude.

Note that the characteristics described depend not only on the cine film itself but also on how the film is processed. Important variables include the precise chemistry, temperature, agitation, and immersion time used in the automatic processor. When a new film is brought into the laboratory, all processing and image chain variables (e.g., cine dose, cine camera aperture) must be matched carefully by the technical representatives of the x-ray equipment and film-supplying company. Laboratory personnel must then ensure that these parameters remain stable from day to day, by performing routine sensitometry and limited densitometry. Measurements should include the base-plus-fog, the OD of a “speed step” (whose OD is known to be near 1.0), and the “contrast index” (the OD difference between the speed step and the next-higher-numbered step). Base-plus-fog should not vary more than 0.02, and speed and contrast index should not vary by more than 0.1 from the initial values. Even slight variations beyond these levels should alert personnel to a potential problem with the processor that must be corrected before clinical films are run, if adequate film quality is to be ensured.

Documented stability of film and processing characteristics allow daily checks on the x-ray equipment itself. If a known attenuator (2.3 mm of copper) is filmed using a consistent geometry and exposure mode (selected magnification, focal spot, pulse width, and camera speed), system stability is confirmed by day-to-day reproducibility of the OD at the center of the frame of the resulting film (which averages 0.90 OD units in most laboratories). By recording, in addition, the kV and mA used by the automatic exposure system during these test exposures, the stability of the generator, x-ray tube, and image intensifier can also be verified. The daily quality control routine may also involve imaging a resolution phantom to monitor image intensifier and camera focus. More detailed assessment of system function should be performed by technical representatives at least twice a year, with correction of adjustments (aperture, processing parameters) and any equipment defects (e.g., dose, image intensifier focus, contrast) by appropriate service personnel. Without these routine surveillance measures, significant deterioration may occur in imaging performance before it becomes apparent to the operators (9).

Perceived film quality also depends to some extent on the system used to view films. Suitable systems are available for private viewing or projection of an image on a conventional movie screen in a moderately darkened room (i.e., during conferences). The larger format requires use of a high-output illumination system (arc lamp or halogen bulb). Either claw-advance or rotating-prism systems can provide a high-resolution, flicker-free image of film during forward or backward transport at frame rates up to 60 fps. Like all elements of the image chain, film projectors require regular maintenance and cleaning to deliver optimal performance. And of course it is vital to have ready access to both current and previous studies on patients. This means that a cine file room, equipped with a bank of film viewers and housing at least the previous 6 to 8 months of films produced by the institution, must be available close to the cardiac catheterization laboratory. Older films back to 5 years should be housed in either an on-site archive or an off-site storage facility, so that an old film can be located and brought to the in-house file room within 24 to 48 hours.

The “Filmless” System

Given the rapid developments in the television chain, digital image processing to improve noise and contrast, and digital image recording, it was only a matter of time before “filmless” imaging achieved adequate quality to replace cine film as the review, archiving, and transfer medium for cardiac catheterization studies. Even after sufficient image quality was achieved in the mid-1990s, there was a significant “tower of Babel” problem in which each x-ray equipment vendor was theoretically free to design its own format for encoding and recording the resulting images. Although this might satisfy the review function within a single laboratory, it was less satisfactory for archiving (where standards might change over time, and make old studies unreadable) or for interchange (where the originating and receiving laboratory might use different and incompatible recording standards). It was therefore critically important that a single worldwide standard be developed for at least the interchange function.

The Digital Imaging and Communications in Medicine (DICOM) committee was jointly formed by the American College of Cardiology, the American College of Radiology, and the National Electrical Manufacturers Association to set standards for storing and retrieving these digital images as a replacement for 35-mm cineangiographic film. Their 1995 guidelines (10) addressed two issues: (a) the logical format in which digital information should be recorded (now known as DICOM format) and (b) the physical medium on which recording should take place for interchange with other facilities. Although each manufacturer is free to set internal standards relating to storage format and medium, each must be able to produce a copy of the study on a recordable compact disk (CD-R) with 2:1 lossless compression.

Although the DICOM standards made it possible to set up filmless laboratories, the solution of having a file room filled with CD-R boxes instead of cans of cine film offers only partial relief. It is still possible to have a study lost, misfiled, damaged, or simply in use by another physician when it is needed. One key to the long-term success of the filmless revolution will be the development of networks linking the individual catheterization laboratories and review stations to deep digital archives that can store 5 years' worth of studies and retrieve them quickly and reliably (11). Studies should be available quickly, at any of several viewing stations on a network, and may even be sent over high-bandwidth connections to other institutions. Of course, all such systems currently retain the ability to “burn” a single-patient

DICOM-compatible CD-R for physical transfer to an outside viewer who has a personal computer with the needed viewing software.

Even at the lowest acceptable resolution standards of 512 × 512 pixels with 8 bits/pixel (256 levels of gray), a single cine frame consists of 256 kilobytes (KB) of data. At 30 fps, a moderately “long” angiographic study of 160 seconds (4,800 frames) would consume 1.2 gigabytes (GB) of uncompressed data. With 2:1 lossless compression, one study would fill a current CD-R disc, and even a small laboratory that performed 1,000 studies per year would require truly huge amounts of digital storage—700 GB, or almost 1 terabyte (TB), to store a year's worth of cases. The problem would be exacerbated further by the use of high-resolution imaging (1,024 × 1,024 pixels at 10 bits/pixel), which increases storage requirements by 16-fold. Although storage jukeboxes of digital tape are being developed that can hold hundreds of terabytes, the other solution is to accept higher levels of data compression. In fact, excellent clinical images can be reconstructed even after “lossy” compression up to 15:1 (12). Although the majority of catheterization laboratories that have been installed since 1998 have been filmless, many of these issues still need to be addressed to solidify the ability of this technology to completely replace all of the functions of cine film.

RADIATION SAFETY

Cardiac catheterization delivers one of the highest levels of patient and operator radiation dose of all current diagnostic procedures. Although it remains the gold standard for obtaining diagnostic images of and performing catheter-based interventional procedures on the human heart, the potential hazards of radiation should never be far from the operator's mind (2,13,14). This includes both the risks to the patient and the risks to the operator and support staff. Although the patient receives the bulk of the radiation dose, most patients undergo only a few catheterization studies in their lifetime. The operators, however, have daily exposure with cumulative annual doses that are more than 20 times the normal environmental radiation exposure. Although the magnitude of risk from these levels of exposure is comparatively small, it is fair to say that no level of radiation exposure is completely “safe.” Everyone working in the cardiac catheterization laboratory should therefore become familiar with the units in which radiation exposure are measured, the biologic effects of radiation, and proper use of monitoring and shielding equipment.

Units of Measurement

The primary unit of radiation exposure is the roentgen (R), which is defined in terms of the amount of ionization that the beam produces in air. In the newer International System of Units (SI), 1 R is equivalent to 2.58×10^{-4} coulombs (C) per kilogram of air. To quantitate tissue effects, the more relevant unit is the absorbed dose (rad, or radiation absorbed dose), which measures how much heating the radiation beam produces in each gram of water (1 rad = 100 ergs/g). In SI units, the rad has been supplanted by the term Gray (Gy): 1 Gy = 1 joule (J) per kilogram = 100 rad. But different tissues absorb different amounts of radiation—the principle behind x-ray imaging! For soft tissues, the absorbed dose generally equals 0.9 rad for every 1 R of exposure; denser tissues such as bone absorb 4 rad for every 1 R. In theory, different types of radiation may produce different degrees of damage (i.e., alpha particles versus x-rays); this is taken into account by an absorbed dose equivalent (rem, or radiation equivalent in man), which is expressed in SI units of Sievert (1 Sv = 100 rem). Although this distinction is important for certain types of radiation, the distinction between rads and rems is largely semantic, because they are essentially equivalent for diagnostic x-rays. In 1987, the National Council on Radiation Protection (NCRP) introduced a new term, the effective dose equivalent (EDE, also measured in rem or Sv), which is a weighted average that takes into account the physical distribution of radiation and the relative radiosensitivity of different organs.

Biologic Effects of Radiation

The average person receives approximately 200 mrem of radiation per year, about half from natural and half from human-made sources including medical x-rays. In the 1950s, various regulatory bodies (concerned mostly with the safety of workers in the nuclear industry) set the maximal annual occupational dose at 5,000 mrem (5 rem, or 50 mSv). It has been suggested more recently that the maximal annual dose should be reduced to 2,000 mrem and that the cumulative lifetime dose limit should not exceed 1,000 mrem per year of life. Although these figures represent the upper limits of acceptable occupational exposure, the better approach is known as ALARA (As Low As Reasonably Achievable). This is because some radiation risks (e.g., genetic defects, cancer) are *stochastic*—that is, the severity of the problem stays the same and only the probability of developing the problem increases with increasing radiation dose. These stochastic problems may be caused by even relatively small radiation exposures, although at a very low incidence.

Genetic damage (i.e., mutations that are transmitted to the offspring of an exposed individual) is one of the well-known stochastic risks of radiation. In evaluating the risk, one must bear in mind that such mutations occur spontaneously and cause birth defects in roughly 5% of births. Laboratory studies and analysis of survivors of the Hiroshima and Nagasaki atomic bombings suggest that very large exposures (almost 100 rad, or 100,000 mrem) are required to double the baseline risk of mutation (2,14). Assuming the routine use of appropriate gonadal shielding, a gonadal dose of 200 mrem (2 mSv) per year under a lead apron would translate to 4 rem over a period of 20 years, which would add only 0.1% (to the 5% baseline) risk of such a birth defect. A similar analysis applies to the risk of occupation-related neoplasm related to radiation exposure. Again, based on data from atomic bomb survivors, the risk of fatal cancer is estimated at 0.04% per rem of exposure. Even without considering the effect of appropriate shielding, the allowable occupational dose of 5 rem per year would add only a 0.2% per year increment (to the background 20% spontaneous incidence) of developing a fatal neoplasm.

Unlike these stochastic risks, the major risks of radiation exposure are *deterministic* (i.e., their onset requires a certain cumulative absorbed dose, modified to some extent by the rate of dose accumulation). The lens of the eye, like most exposed organs, is fairly resistant to direct injury, but at a threshold dose of 250 to 500 rem it may undergo cataract formation. Even assuming no eye protection, this would amount to more than a 30-year accumulation at the current maximal operator doses of 15 rem/yr to the eye. The skin is even more radioresistant, requiring 200 rem in a single dose to produce redness and 300 rem to produce temporary hair loss. Absent placing one's hands in the primary radiation beam, it is hard to see how even modestly prudent occupational exposure to radiation in the cardiac catheterization laboratory would approach these thresholds for deterministic (nonstochastic) injury.

Measuring Radiation Exposure

The most important factor controlling radiation exposure is the imaging dose. Cineangiographic systems are usually set to deliver 30 µR per cine frame to the face of the image intensifier in the 6- to 7-inch mode frame. This corresponds to a table-top dose of roughly 40 R/min of cine for the average-sized patient (14). During fluoroscopy, the table-top dose is roughly 10 times lower (2 to 4 R/min). The patient's dose comes from his or her position within the direct radiation beam, and the patient's body absorbs most of the incident radiation beam. Less than 1% of the beam actually passes through the patient to strike the image intensifier. Total skin dose to the patient's back can approach 50 R (roughly 50,000 mrem) during the typical examination—the equivalent of 100 to 250 chest x-ray exposures. Measurements suggest that patient exposures can be substantially higher (approximately 300 R) during complex interventional procedures (15). However, because this dose is distributed among multiple beam entry points as angulation is changed during the procedure, it is tolerable for maximal local skin entry doses not to be exceeded. Prolonged fluoroscopy (i.e., 1.7 hours of continuous fluoroscopy) *in a single-beam position* at a table-top dose of 2 R/min can approach the threshold for skin erythema (2 Gy, or 200 R) (16,17). Episodes of erythema or delayed skin necrosis have been reported in rare instances when prolonged fluoroscopic examinations were performed using a single-beam entry angle and position. In younger patients, there may also be concern about neoplasm or gonadal injury. Dose measurements made during prolonged electrophysiologic ablations suggest a roughly 0.03% increase of lifetime risk of a fatal malignancy associated with undergoing such a procedure. Gonadal dose from secondary scatter is minimal but should be decreased further by avoidance of imaging over the pelvis and use of a pelvic or gonadal shield in younger patients.

Although patient dose is clearly an issue, patients rarely undergo more than a few invasive procedures per year. On the other hand, most operators and support staff perform hundreds of procedures per year. Their main hazard derives not from the portion of the beam that passes to the image intensifier, nor the portion absorbed by the patient, but the remaining portion of the incident beam that is scattered back into the procedure room. At 1 m from the point at which the beam strikes the patient, the scatter exposure is roughly 1/1000 of the patient's skin exposure (i.e., 2 to 4 mrem/min during fluoroscopy and 40 mrem/min during cineangiography). Because scatter is highly asymmetric (with greatest scatter back toward the x-ray tube from the point at which the beam enters the patient), this is at best a rough estimate. In fact, operator exposure is several times higher for imaging performed in the left anterior oblique or left lateral view, compared with the straight anteroposterior (AP) projection (18). During a standard catheterization, the head of the primary operator would (without other shielding) receive a dose of approximately 20 mrem, about half from fluoroscopy and half from cineangiography (2,14). At that rate, an operator could perform no more than 250 procedures per year without exceeding the federal guideline of 5,000 mrem/yr. Performance of more complex procedures (e.g., PTCA) or newer device interventions involve greater fluoros-copy time (roughly 25 minutes) (15,19) and greater operator radiation dose (50 to 100 mrem), which would further reduce the number of procedures that a single operator could perform each year. It should be noted that these doses apply to the first operator, who is standing nearest to the x-ray beam. For assistants who stand further from the beam entry point than the primary operator, radiation exposures are only 0.5 mrem per procedure, or 10% to 30% of the primary operator exposure. For nursing or technical personnel who stand only a few feet further from the patient, doses are even lower, at 2% to 11% than received by the primary operator (2). These doses can be reduced even further by maintaining greater distance when not performing clinically necessary activities that require closer approach or by using portable shielding.

Because the operator dose may be close to the maximal allowable limit and because the dose varies so much depending on geometry, procedure time, and other variables, there is no substitute for having each operator measure his or her own exposure (20). The most common way to do this is by means of a film badge (a small piece of unexposed film in a plastic holder), which must be worn at all times when working in the cardiac catheterization laboratory. The amount of film darkening revealed when the badge is developed reflects the cumulative radiation dose received, with a sensitivity of 10 mrem. If a single “collar” badge is worn, it should be worn on the left shirt collar outside the lead apron, to give an estimate of maximal head and neck exposure. Current recommendations also call for a second “waist” badge, which is worn on the operator's belt just beneath the lead apron. This typically records a dose of only 1 to 2 mrem per procedure, reflecting the lower level of whole-body and gonadal radiation exposure. These two badges should be of different colors (e.g., red for the collar and green for the waist) so that they can be used together to calculate the EDE received, which is equal to 0.3 times the collar badge dose (when worn alone) or to 1.5 times the waist badge dose plus 0.04 times the collar badge dose (when both badges are worn). Each month, these badges should be turned in for processing and replaced with a fresh film packet. Each individual (and the laboratory director) should then confirm that no worker's collar badge dose exceeded 100 mrem/mo without further investigation. The ease of use of film badges has made them the preferred method of monitoring dose, although other techniques (e.g., electronic dosimeters, thermoluminescent salt dosimeters) can be used. The most important issue is that all laboratory personnel must wear their monitoring devices consistently and that their recorded doses must be studied regularly to ensure that occupational exposures are remaining within the prescribed limits.

Reducing Exposure Dose

The operator can use several methods to reduce scatter dose (2,14). The most important of these is minimizing the patient dose, which the ultimate source of scatter to the operator. This means having the x-ray equipment doses calibrated within national standards and as low as possible without degrading the quality of the fluoroscopic and film images. The temptation to use “high-dose” fluoroscopy (more than 10 R/min table-top dose) should be avoided in all but certain angioplasty settings, when it takes the place of even higher-dose cineangiographic runs. If “pulsed fluoroscopy” is available (in which the x-ray tube current is pulsed during fluoroscopy, as is done routinely during cineangiography), it may improve image quality while reducing patient and operator dose by up to 60%. The operator must also remember to keep the face of the image intensifier in near contact with the patient's chest. Raising the image intensifier off the chest is the equivalent of switching to a higher magnification mode; it increases the radiation output required to provide adequate light output from the image intensifier. It also decreases the ability of the image intensifier housing to screen radiation scattered by the patient before it strikes the operator.

One of the most important means of reducing radiation exposure is reducing the amount of fluoroscopy time to the minimum required to position catheters. The total fluoroscopy time should be recorded in each instance and should be well under 10 minutes for a diagnostic procedure. If a trainee experiences difficulty in accomplishing some task (e.g., advancing the right heart catheter), a more experienced operator should take over rather than allowing fluoroscopic time to escalate. It is also important to avoid the “lead foot” syndrome: the operator must learn to depress the fluoroscopy pedal briefly when it is necessary to confirm a catheter position, and to reflexively release the pedal when looking away from the television monitor. Similarly, cineangiographic runs should be selected carefully to show important findings, and each run should be terminated as soon as the necessary information is recorded. Every effort should be made to confine the area irradiated to that imaged, by closure of the adjustable cones to the edges of the cine frame.

The other cardinal measures used to reduce operator x-ray dose are increasing distance and using shielding. The operator should stand as far from the beam as possible to take advantage of the inverse square law—one or two steps further away from the x-ray tube may cut the dose in half. This is particularly important during angulated shots such as the left lateral or LAO cranial projections, which place the operator in close proximity to the beam entry point (Fig. 2.9). Keeping one's distance is easier with the femoral than the brachial approach; the latter carries about twice the exposure to the operator's head.

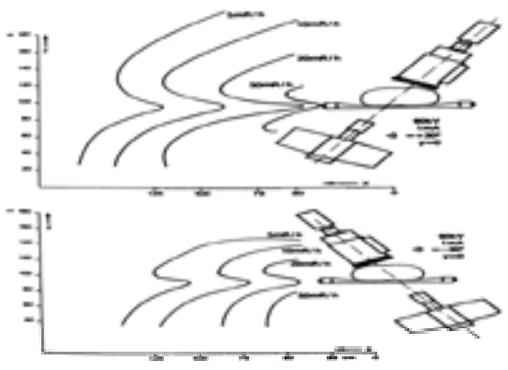

FIG. 2.9. Isoexposure curves of operator radiation exposure during cardiac catheterization for U-arm and C-arm systems. The upper panel represents a 30° LAO view; the lower panel shows a 30° RAO view. The operator is standing to the patient's right, and the patient's feet are toward the reader. Radiation is highest at the level of the table and patient, owing to radiation scatter. (Balter S, Sones FM Jr, Brancato R. Radiation exposure to the operator performing cardiac angiography with U-arm systems. *Circulation* 1978;58:925, with permission.)

It is also advisable to use additional shielding to reduce exposure of radiation-sensitive areas, analogous to the use of a lead apron to shield the torso. Shielding equivalent to 0.5 mm of lead attenuates exposure by a factor of almost 30 (i.e., to less than 1 mrem per procedure). If the operator has occasion to turn away from the patient, a wrap-around apron should be used to provide protection from that direction. Improvements in two-piece (skirt and vest) and one-piece aprons (with elastic belts to distribute much of the weight to the operator's waist) have made wearing adequate shielding more tolerable. Additional radiation protection can be gained from wearing separate thyroid collars and wrap-around leaded eyeglasses. Our preference, however, has been for a movable rectangular lead-acrylic shield (0.5 mm lead-equivalent, available from a variety of manufacturers) that can be positioned between the point at which the x-ray beam enters the patient's body and the operator's head (Fig. 2.1). This shield protects both thyroid and eye as effectively as separate shields, is less cumbersome, and can be covered with a sterile plastic bag to allow placement within the sterile field. Since we began to use such a shield routinely in 1987, not even our busiest operators have exceeded a collar badge reading of 100 mrem/mo.

INTRAVASCULAR CONTRAST AGENTS

Shortly after the classic papers by Roentgen in the 1890s, the search began for effective and nontoxic contrast agents to define vascular anatomy. Although early experimentation involved a number of heavy metals (bismuth, barium, thorium), all modern contrast agents are based exclusively on iodine, which by virtue of its high atomic number and chemical versatility has proved to be an excellent agent for intravascular opacification. Because inorganic iodine (sodium iodide) causes marked toxic reactions, experiments were performed in 1929 using an organic iodide preparation (Selectan) that contained one iodine atom per benzoic acid ring. In the 1950s, a series of substituted triiodobenzoic acid derivatives were developed, which contain three iodine atoms per ring. These agents differ from each other in terms of the specific side chains used in positions 1, 3, and 5 (Fig. 2.10), which influence both solubility and toxicity.

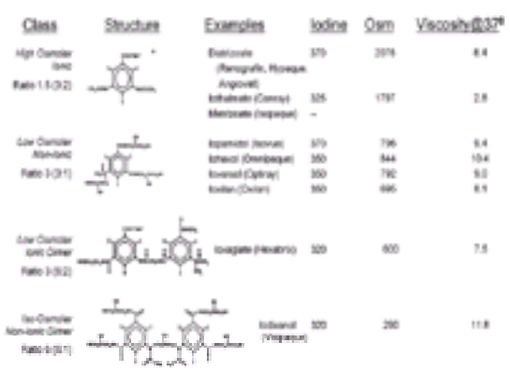

FIG. 2.10. Sample structures and properties of currently available contrast agents. The traditional high-osmolar ionic (HOCM or ratio-1.5) contrast media are sodium

(Na^+)/meglumine salts of substituted triiodobenzoic acid that have three iodine atoms per anion-cation pair, with six times the osmolality of blood. Two types of low-osmolality (LOCM or ratio-3) contrast media are also shown: the true nonionic agents and the Na^+/meglumine salt of an ionic dimer, which have three iodine atoms per nonionic molecule or six iodine atoms per anion-cation pair, with an osmolality two to three times that of blood. The newest class of isoosmolar (IOCM or ratio-6) contrast medium is a nonionic dimer with six iodine atoms per molecule and an osmolality equal to that of blood. Also included are the iodine contents (in mgI/mL), the osmolality (in mOsm/kg-H_2O), and the viscosity at 37°C. The asterisk (*) indicates a mixed sodium and meglumine salt. See text for details.

Ratio-1.5 ionic compounds are substituted ionic triiodobenzoic acid derivatives that contain three atoms of iodine for every two ions (i.e., the substituted benzoic acid ring and accompanying cation). Included in this family are widely used contrast agents such as Renografin (Bracco), Hypaque (Nycomed), and Angiovist (Berlex), which are mixtures of the meglumine and sodium salts of diatrizoic acid. Functionally similar agents are based on iothalmic acid (Conray, Mallinckrodt) or metrizoic acid (Isopaque). These agents have a sodium concentration roughly equal to that of blood, pH titrated between 6.0 and 7.0, and a low concentration (0.1 to 0.2 mg/mL) of calcium disodium ethylenediamine tetraacetic acid (EDTA). Higher or lower sodium concentrations may contribute to ventricular arrhythmias during coronary injection. Some suggest that calcium binding by sodium citrate can cause greater myocardial depression (21). To have an iodine concentration of 320 to 370 mgI/mL, as is required for left ventricular and coronary contrast injections, solutions of these agents are markedly hypertonic (with an osmolality exceeding 1,500 mOsm/kg, roughly six times that of blood).

One modification of ionic contrast came in the mid-1980s with the introduction of ratio-3 low-osmolar contrast materials (LOCM). Although it is still ionic (as a mixture of meglumine and sodium salts), ioxglate (Hexabrix, Mallinckrodt) is a ratio-3 agent by virtue of its unique dimeric structure, which includes six molecules of iodine (three atoms of iodine for every one ion). To achieve an iodine concentration of 320 mgI/mL, Hexabrix has an osmolality roughly twice that of blood. This significantly reduces the undesirable side effects related to hypertonicity (22).

A more significant modification in the late 1980s was the introduction of true nonionic, ratio-3 contrast agents. These LOCMs are water soluble in a noncharged form, without an associated cation. Examples include iopamidol (Isovue, Bracco), iohexol (Omnipaque, Nycomed), metrizamide (Amipaque, Winthrop), ioversol (Optiray, Mallinckrodt), and ioxilan (Oxilan, Cook), each of which contain three atoms of iodine for every molecule (23). With calcium disodium EDTA as a stabilizer and tromethamine (1.2 to 3.6 mg/mL) as a buffer, an iodine content of 320 to 370 mgI/mL can be achieved with an osmolality of 600 to 700 mOsm/kg, between twice and three times that of blood. The viscosity of these agents (which influences ease of injection through small-lumen catheters) is roughly six to ten times that of water. More recently, a nonionic dimeric compound (iodixanol [Visipaque, Nycomed]) has been released. This ratio-6 agent actually requires the addition of sodium and calcium chloride to bring its osmolality up to that of blood (290 mOsm/kg) (24).

The ratio-3 LOCMs definitely are better tolerated by patients undergoing coronary angiography (Table 2.1). They produce fewer episodes of bradycardia and hypotension, precipitate less angina, and cause less nausea and sensation of heat than traditional high-osmolar contrast agents (25,26 and 27). There is also evidence that the nonionic ratio-3 agents produce fewer allergic side effects and may be less nephrotoxic in animal studies (23), although this has been difficult to confirm in human studies (28). For all of these reasons, more than 80% of coronary angiography studies during the 1990s were performed with an LOCM. Some early studies, however, suggested that the true nonionic agents might predispose patients to thrombotic events (29). This has been one of the strongest marketing claims for Hexabrix, the only *ionic* LOCM. It is likely that any prothrombotic effects of the nonionic contrast agents reflect more the absence of the antithrombotic properties seen with the ionic agents. In our laboratory, we have not seen practical clinical problems that related to use of nonionic contrast agents. This is consistent with more recent studies (30), which have failed to confirm any increase in deleterious thrombotic complications.

Effects related to hypertonicity (virtually eliminated by use of LOCMs)	Other adverse effects (only partially reduced by use of LOCMs)
Arteriolar vasodilatation (hypotension, sensation of heat)	Anaphylaxis
Increased intravascular volume	Myocardial ischemia
Electrophysiologic changes (ST-T wave alterations, bradycardia, prolonged PR/QT interval)	Renal toxicity
Nausea and vomiting	
Depression of myocardial function	

LOCM, low-osmolarity contrast material.

TABLE 2.1. *Side effects of contrast agents*

This leaves expense as the major factor that limits the universal use of these agents. Until recently, the 200 mL of contrast material consumed in the average diagnostic catheterization would have cost $150 to $200 for a nonionic agent, compared with roughly $20 for the same amount of an ionic contrast agent. Total conversion to LOCMs therefore would have added $100 to 200 million to the U.S. health care budget. Although randomized trials comparing high- and low-osmolar agents in routine angiography have shown a clear reduction in *minor* side effects, they have failed to show any significant net clinical benefit in terms of serious side effects that would justify across-the-board use of a more expensive agent. It therefore has been suggested that most of the benefit of these agents could be secured if their use were confined to those patients who most need their benefits—the roughly 25% of patients who have two or more of the following characteristics: age greater than 65 years, left ventricular end-diastolic pressure greater than 15 mm Hg, New York Heart Association class IV symptoms, or a history of previous reaction to contrast material (25). This is consistent with the practice in our laboratory, where we have used Renografin as our routine contrast agent but have resorted to a nonionic LOCM in roughly 35% of cases based on specific indications: severe hemodynamic dysfunction not responding to pharmacotherapy, history of prior allergic reaction to ionic contrast, internal mammary injection, or baseline renal insufficiency with a creatinine concentration higher than 2.5 mg/dL. With this strategy, the incidence of severe contrast reaction (wheezing, prolonged hypotension, or frank anaphylactoid reaction) remains well below 0.05%.

With the increasing competition among nonionic contrast agents, there has been a marked reduction in price, so that 200 mL of some nonionic LOCMs now costs as little as $36 (two to three times more than a high-osmolar ionic agent). At such a low incremental cost, the clear reduction in minor side effects may be sufficient to justify more liberal use of nonionic LOCMs.

CHAPTER REFERENCES

1. Pepine CJ. ACC/AHA Guidelines for Cardiac Catheterization and Cardiac Catheterization Laboratories. *J Am Coll Cardiol* 1991;18:1149.
2. Limacher MC, Douglas PS, Germano G, et al. Radiation Safety in the Practice of Cardiology (ACC Expert Consensus Document). *J Am Coll Cardiol* 1998;31:892.
3. Moore RJ. *Imaging Principles of Cardiac Angiography.* Bethesda, MD: Aspen, 1990.
4. Balter S. X-ray generation and control. *Cathet Cardiovasc Diagn* 1999;46:92.
5. Balter S. X-ray image intensifier. *Cathet Cardiovasc Diagn* 1999;46:238.
6. Balter S. Fluoroscopic and fluorographic cameras. *Cathet Cardiovasc Diagn* 1999;46:368.
7. Holmes DR, Bove AA, Wondrow MA, et al. Video x-ray progressive scanning: new technique for decreasing x-ray exposure without decreasing image quality during cardiac catheterization. *Mayo Clin Proc* 1986;61:321.
8. Reiber JHC, van der Zwet PM, Koning G, et al. Accuracy and precision of quantitative digital coronary angiography: observer, short, and medium term variables. *Cathet Cardiovasc Diagn* 1993;28:187.
9. Levin DC, Dunham LR, Stueve R. Causes of cine image quality deterioration in cardiac catheterization laboratories. *Am J Cardiol* 1983;52:881.
10. ACC/ACR/NEMA Ad Hoc Group. American College of Cardiology, American College of Radiology and industry develop standard for digital transfer of angiographic images. *J Am Coll Cardiol* 1995;25:800.
11. Holmes DR, Wondrow MA, Bell MR, et al. Cine film replacement: digital archival requirements and remaining obstacles. *Cathet Cardiovasc Diagn* 1998;44:346.
12. Baker WA, Hearne SE, Spero LA, et al. Lossy (15:1) JPEG compression of digital coronary angiograms does not limit detection of subtle morphological features. *Circulation* 1997;96:1157.
13. Miller SW, Castronovo FP. Radiation exposure and protection in cardiac catheterization laboratories. *Am J Cardiol* 1985;55:171.
14. Johnson LW, Moore RJ, Balter S. Review of radiation safety in the cardiac catheterization laboratory. *Cathet Cardiovasc Diagn* 1992;25:186.
15. Cusma JT, Bell MR, Wondrow MA, et al. Real-time measurement of radiation exposure to patients during diagnostic coronary angiography and percutaneous interventional procedures. *J Am Coll Cardiol* 1999;33:427.

16. Kovoor P, Richardello M, Collins L, et al. Risk to patients from radiation associated with radiofrequency ablation for supraventricular tachycardia. *Circulation* 1998;98:1534.
17. Pitney MR, Allan RM, Giles RW, et al. Modifying fluoroscopic views reduces operator radiation exposure during coronary angioplasty. *J Am Coll Cardiol* 1994;24:1660.

19. Federman J, Bell MR, Wondrow MA, et al. Does the use of new intracoronary interventional devices prolong radiation exposure in the cardiac catheterization laboratory? *J Am Coll Cardiol* 1994;23:347.
20. Balter S. Guidelines for personnel radiation monitoring in the cardiac catheterization laboratory. *Cathet Cardiovasc Diagn* 1993;30:277.
21. Zuckerman LS, Frichling TD, Wolf NM, et al. Effect of calcium binding additives on ventricular fibrillation and repolarization changes during coronary angiography. *J Am Coll Cardiol* 1987;10:1249.
22. Piao ZE, Murdock DK, Hwang MH, et al. Hemodynamic abnormalities during coronary angiography: comparison of Hypaque-76, Hexabrix, and Omnipaque-350. *Cathet Cardiovasc Diagn* 1989;16:149.
23. Ritchie JL, Nissen SE, Douglas JS Jr, et al. Use of non-ionic or low osmolar contrast agents in cardiovascular procedures (ACC Position Statement). *J Am Coll Cardiol* 1993;21:269.
24. Hill JA, Cohen MB, Kou WH, et al. Iodixanol, a new isosmotic nonionic contrast agent compared with iohexol in cardiac angiography. *Am J Cardiol* 1994;74:57.
25. Matthai WH, Kussmaul WG 3rd, Krol J, et al. A comparison of low- with high-osmolality contrast agents in cardiac angiography-identification of criteria for selective use. *Circulation* 1994;89:291.
26. Steinberg EP, Moore RD, Powe NR, et al. Safety and cost effectiveness of high-osmolality as compared with low-osmolality contrast agents in patients undergoing cardiac angiography. *N Engl J Med* 1992;326:425.
27. Barrett BJ, Parfrey PS, Vavasour HM, et al. A comparison of nonionic, low-osmolality radiocontrast agents with ionic, high-osmolality agents during cardiac catheterization. *N Engl J Med* 1992;326:431.
28. Schwab SJ, Hlatkey MA, Pieper KS, et al. Contrast nephrotoxicity: a randomized controlled trial of a nonionic and an ionic radiographic contrast agent. *N Engl J Med* 1989;320:149.
29. Piessens JH, Stammen F, Vrolix MC, et al. Effects of an ionic versus a nonionic low osmolar contrast agent on the thrombotic complications of coronary angioplasty. *Cathet Cardiovasc Diagn* 1993;28:99.
30. Schrader R, Esch I, Ensslen R, et al. A randomized trial comparing the impact of a non-ionic (Iomeprol) versus an ionic (Ioxaglate) low osmolar contrast medium on abrupt vessel closure and ischemic complications after coronary angioplasty. *J Am Coll Cardiol* 1999;33:

3
Complications Of Cardiac Catheterization

Donald S. Baim and William Grossman

DSB: Harvard Medical School; Center for Innovative Minimally Invasive Therapy, Brigham and Women's Hospital, Boston, Massachusetts 02115
WG: University of California, San Francisco, School of Medicine; Division of Cardiology, University of California, San Francisco Medical Center, San Francisco, California 94143

Because all cardiac catheterizations involve the insertion of foreign objects (i.e., cardiac catheters) into the circulatory system, it should not be surprising that a variety of adverse events (complications) can ensue. These complications range from minor problems with no long-term sequelae (e.g., transient bradycardia during coronary contrast injection) to major problems [e.g., cardiac perforation, abrupt closure of a coronary artery during percutaneous transluminal coronary angioplasty (PTCA)] that may require immediate surgical attention or cause irreversible damage (e.g., stroke, myocardial infarction, renal failure, or even death).

Fortunately, the risk of producing a major complication during most procedure types in current practice is generally less than 1%, a level at which the risk-benefit ratio still favors performing cardiac catheterization as part of the investigation or treatment of cardiac disorders that are themselves life-threatening or symptom-limiting. For the individual patient, the risk of sustaining a complication varies widely, depending on demographics (age, gender), the cardiac anatomy (left main coronary artery disease, severe aortic stenosis, diminished left ventricular function), the clinical situation (unstable angina, acute myocardial infarction, cardiogenic shock), and the type of procedure being performed (diagnostic catheterization, angioplasty, and so on). By considering all these factors, however, the physicians and support staff can arrive at a fairly accurate estimate of what level of risk is entailed in any given procedure. Familiarity with those risks can be of immeasurable value in the following: (a) anticipating increased risk of complication, (b) taking extra precautions to avoid them (e.g., placing a prophylactic pacemaker in a patient prior to rotational atherectomy of a right coronary artery lesion), (c) promptly recognizing complications when they occur (e.g., perforation of the right atrium during a transseptal puncture), and (d) taking corrective and potentially life-saving action (e.g., pericardiocentesis for perforation-induced tamponade).

With this knowledge, the details of the planned procedure and its anticipated risks should be discussed candidly with the patient and family. This discussion should include what procedures are planned, what benefits are hoped for, the attendant risks and their probabilities, and how the risks and benefits of the planned procedure compare with those of any possible alternatives (e.g., bypass surgery instead of coronary angioplasty). By covering these cornerstones of “informed consent” clearly and candidly, the patient and family will be realistically prepared should a complication occur. Such a discussion should be documented in the patient's chart, and that documentation should specify the type of procedure that is planned, the potential major complications, and their estimated risk of occurrence (e.g., “death, MI, or stroke < 1%, vascular injury requiring transfusion or surgical repair < 1%”).

If a significant major complication does occur, the patient and family should be told about it as soon as the procedure has been completed (or when a delayed complication occurs, as soon as it is recognized). This discussion should describe the nature of the complication (without placing blame on anyone), indicate whether any long-term consequences are expected, and outline what corrective actions have been and will be pursued. The catheterizing physician also must continue daily inpatient follow-up visits to any patient who has sustained a significant complication, since a patient's feeling abandoned by an uncaring physician tends to foster a desire for retribution (i.e., a malpractice suit).

For these reasons, all individuals performing cardiac catheterization should be intimately knowledgeable about the potential complications of the procedures they perform, as detailed in this chapter. In addition, the catheterization laboratory director should collect information about the frequency of these complications on at least a yearly basis and should review those data with the physician staff to identify where the laboratory as a whole (or an individual operator) is performing below expected standards. We have done this yearly in our laboratory since 1987 (1) following the template shown in Table 3.1, and we have used this analysis to guide the progressive evolution of our practice toward optimizing procedural outcome. This type of data collection, analysis (including breakdown by procedure type and by individual operator), reporting, and adjustment in laboratory policy and procedures is one of the most important jobs of any catheterization laboratory director.

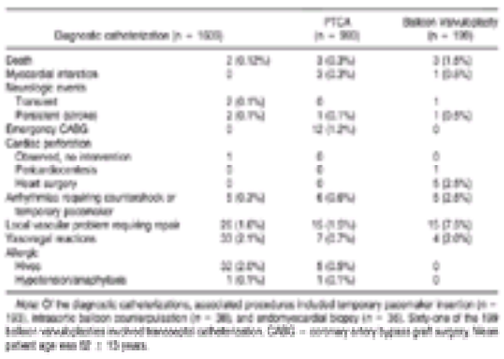

Diagnostic catheterization (n = 1939)		PTCA (n = 960)	Balloon valvuloplasty (n = 196)
Death	2 (0.12%)	3 (0.3%)	3 (1.5%)
Myocardial infarction	0	3 (0.3%)	1 (0.5%)
Neurologic events			
Transient	2 (0.1%)	6	1
Persistent sequelae	2 (0.1%)	1 (0.1%)	1 (0.5%)
Emergency CABG	0	12 (1.2%)	0
Cardiac perforation			
Observed, no intervention	1	6	0
Pericardiocentesis	0	6	1
Heart surgery	0	6	5 (2.6%)
Arrhythmias requiring countershock or temporary pacemaker	5 (0.2%)	6 (0.6%)	5 (2.6%)
Local vascular problem requiring repair	35 (1.8%)	15 (1.5%)	15 (7.5%)
Vasovagal reactions	33 (2.1%)	7 (0.7%)	4 (2.0%)
Allergic			
Hives	32 (2.0%)	8 (0.8%)	0
Hypotension/anaphylaxis	1 (0.1%)	1 (0.1%)	0

Note: Of the diagnostic catheterizations, associated procedures included temporary pacemaker insertion (n = 193), intracoronary balloon counterpulsation (n = 36), and endomyocardial biopsy (n = 34). Sixty-one of the 196 balloon valvuloplasties involved transseptal catheterization. CABG = coronary artery bypass graft surgery. Mean patient age was 62 ± 15 years.

TABLE 3.1. *Complications of cardiac catheterization in 2801 cases (1)*

SPECIFIC COMPLICATIONS

Death

Diagnostic Catheterization

Death as a complication of diagnostic catheterization has declined progressively over the last 30 years. Compared with the 1% mortality seen with diagnostic catheterization in the 1960s (2), the first Society for Cardiac Angiography registry of 53,581 diagnostic catheterizations performed from 1979 to 1981 showed a 0.14% procedure-related mortality (3). By the second registry of 222,553 patients catheterized from 1984 to 1987 (4), procedure-related mortality had fallen slightly more to 0.1%. The small size of this reduction in mortality, however, belies the fact that the second registry included many more patients at higher risk for the procedure. If a “high-risk subgroup” is characterized using the variables identified by analyzing the 218 deaths in the second registry [age > 60, New York Heart Association (NYHA) functional class IV, left ventricular ejection fraction < 30%, or left main disease], the mortality for such patients was cut in half between the first and second registry (5). A third registry of 58,332 patients studied in 1990 showed an even lower overall mortality of 0.08%, with a 1.5% incidence of any major complication (6). A number of

baseline variables (including NYHA class, multivessel disease, congestive heart failure, and renal insufficiency) were identified in this registry, whose presence predicted an up to eight-fold increase in major complication rates (from 0.3 in patients with none of these factors to 2.5%) (7).

Although a progressive reduction in the overall mortality of diagnostic cardiac catheterization has occurred over the last 25 years, certain patient groups remain at increased risk. Table 3.2 lists some of the most important risk factors. Patients with left main coronary disease in the 1976 report by Bourassa had a 6% mortality (8). This same pattern was seen with a mortality of 2.8% for patients with severe left main disease (compared with a mortality of 0.13% in patients without such disease) in the study by Hillis and colleagues of catheterizations performed between 1978 and 1992 (9). Although the mortality of such patients had fallen to 0.86% in the first Society for Cardiac Angiography registry, this was still more than 20 times higher than the 0.03% mortality seen in patients with single-vessel disease (3). Since roughly 7% of patients undergoing coronary angiography in our institution have significant left main disease, the protocol used for coronary angiography (Chapter 11) begins with careful entry into the left coronary ostium to detect early recognition of left main disease through catheter pressure damping or performance of a test "puff" immediately after engagement. Even without these early warnings of left main disease, we routinely perform the first injection in the right anterior oblique (RAO) projection with caudal angulation to screen for left main disease and get the maximal anatomic information on the first injection. If ostial left main stenosis is suspected, a straight anterior (AP) injection may be performed. If severe left main disease is present, the only other injection that is needed is an RAO projection with cranial angulation (to see the left anterior descending and its diagonal branches). Performing a large number of superfluous contrast injections in a patient with a critical left main disease offers little more in the way of important anatomic information and increases the risk of triggering the vicious cycle of ischemia—hypotension—more ischemia, which may lead to irreversible collapse. Careful attention to all other aspects of technique is essential, since even an otherwise minor complication (e.g., a vasovagal reaction or arrhythmia) may have fatal consequences in such patients. If a patient with severe left main disease exhibits any significant instability during the procedure, we tend to place an intraaortic balloon pump (Chapter 21) and arrange for prompt bypass surgery. Similar considerations apply to any patient with an unstable ischemic syndrome or acute myocardial infarction who behaves in a brittle fashion under the stresses of catheter placement and contrast injection.

1. *Age:* Infants (<1 year old) and the elderly (>60 years old) are at increased risk of death during cardiac catheterization.
2. *Functional class:* Mortality in class IV patients is more than 10 times greater than in class I–II patients.
3. *Severity of coronary obstruction:* Mortality for patients with left main coronary artery disease is more than 10 times greater than for patients with single-vessel disease.
4. *Valvular heart disease:* Especially when combined with coronary disease, is associated with a higher risk of death at cardiac catheterization than coronary artery disease alone.
5. *Left ventricular dysfunction:* Mortality for patients with LV ejection <30% is more than 10 times greater than if ejection fraction is >50%.
6. *Severe noncardiac disease:* Patients with renal insufficiency, insulin-requiring diabetes, advanced cerebrovascular and/or peripheral vascular disease, and severe pulmonary insufficiency appear to have an increased incidence of death and other major complications from cardiac catheterization.

TABLE 3.2. *Patient characteristics associated with increased mortality from cardiac catheterization*

Patients with severe baseline left ventricular dysfunction (ejection fraction < 30%) also have a several-fold increased risk of procedural mortality (5), particularly when reduction in ejection fraction is associated with a baseline pulmonary capillary wedge pressure of more than 25 mm Hg and a systolic arterial pressure of less than 100 mm Hg. An effort should generally be made to bring such congestive heart failure under control before cardiac catheterization is attempted. Right-sided heart catheterization should always be performed before angiography in a patient with poor ejection fraction, because the catheterization provides valuable data about baseline hemodynamic status and gives an early warning about hemodynamic decompensation before frank pulmonary edema ensues. If the baseline pulmonary capillary wedge pressure is greater than 30 mm Hg, every effort should be made to improve hemodynamic status before angiography is attempted. This may entail administration of a potent intravenous diuretic (furosemide, Bumex), supplemental oxygen, a vasodilator (intravenous nitroglycerine or sodium nitroprusside) when the mean arterial pressure is greater than 65 mm Hg, or a positive inotrope (dopamine, dobutamine, milrinone) when the mean arterial pressure is less than 65 mm Hg or when severe congestive heart failure hemodynamics persist despite vasodilator treatment. When frank cardiogenic shock is present or develops during a cardiac catheterization, prompt placement of an intraaortic balloon pump in the contralateral groin may be required to get the patient safely though the procedure. More recently, percutaneous cardiopulmonary bypass (CPS) has become available for complete temporary support of the circulation in patients who experience hemodynamic collapse in the cardiac catheterization laboratory (10). The ability to perform necessary angiography without precipitating hemodynamic decompensation in such unstable patients, however, has been greatly aided by the availability of low osmolar contrast agents that produce less myocardial depression than traditional high-osmolar agents (Chapter 2).

Despite the preponderance of coronary artery disease as the indication for diagnostic cardiac catheterization in the 1990s, patients with *severe valvular heart disease* are also at increased risk for dying during cardiac catheterization. The VA Cooperative Study on Valvular Heart Disease (11) thus showed a 0.2% mortality among 1,559 preoperative catheterizations performed in patients with valvular heart disease, with one death in a patient with mitral regurgitation and two deaths in patients with aortic stenosis. Patients who have previously undergone *coronary bypass surgery* make up a growing subgroup (up to 20% in our laboratory) of diagnostic and interventional catheterizations. They are typically 5 years older, have more diffuse coronary and generalized atherosclerosis, have worse left ventricular function, and require a more lengthy and complex procedure to image both native coronary arteries and all grafts. Despite these adverse risk factors, the Post CABG Trial (12) looked at 2,635 diagnostic angiograms performed in stable patients and found no mortality, and major complications in 0.7% (myocardial infarction 0.08%, stroke 0.19%, vascular trauma requiring transfusion or surgery 0.4%). *Pediatric patients* may be at higher risk (Chapter 6). One review of 4,952 patients (median age 2.9 years) studied at the Hospital for Sick Children in Toronto (13) found a mortality of 1.2% confined to patients under age 5 (half in critically ill neonates less than 30 days of age). Although the risk was lower for diagnostic than for electrophysiologic or interventional procedures, there were three deaths (0.1%) among the 3,149 diagnostic procedures.

There are many potential explanations for this progressive decline in the mortality of diagnostic catheterization, including improvement in catheter design (less traumatic "soft" tips), imaging systems, contrast agents, and high annual procedure volume (>1.5 million/year) and shorter procedure duration. It is less clear whether the use of heparin anticoagulation during diagnostic catheterization makes any further contribution. This was probably the case in the 1970s, when crude catheter designs and long procedure times using the femoral approach led to a higher mortality than the brachial approach (14,15). Subsequent studies, performed 15 years later after the routine adoption of systemic heparinization, showed that the mortality was no higher for the femoral approach (4,6,7). Some laboratories continue to use systemic heparinization routinely for diagnostic procedures, based on this circumstantial evidence. On the other hand, many laboratories currently omit heparin for femoral procedures (16) and report comparably low incidences of major complications. It is unlikely that this issue will be resolved by a clinical trial, since finding even a 50% treatment effect (mortality 0.2% to 0.1%) would require randomization of more than 100,000 patients. With or without heparin, however, the speed, the potential for going on to perform a broad range of interventional procedures (angioplasty, stent placement, atherectomy), and the possibility of circulatory assist (e.g., intraaortic balloon) have made the femoral approach the one preferred for cardiac catheterization in high-risk or unstable patients. The 1990 Society of Cardiac Angiography and Intervention (SCA&I) registry thus showed that 83% of diagnostic and 96% of interventional procedures were performed by the femoral approach (6).

Interventional Procedures

Because they involve the use of more aggressive catheters, superselective cannulation of diseased coronary arteries, brief interruption of coronary or even systemic flow (e.g, balloon valvuloplasty, Chapter 26), interventional procedures tend to carry higher mortality than purely diagnostic catheterizations (1). In the first 1,500-patient coronary angioplasty registry sponsored by the National Heart, Lung, and Blood Institute (NHLBI) from 1979 to 1982, the mortality of elective angioplasty was 1.1% (17). This was relatively unchanged at 1.0% in the second NHLBI registry of 1,802 patients treated at 15 centers between 1984 and 1987, largely because the second registry included larger numbers of patients with adverse features (advanced age, poor ventricular function, multivessel disease, prior bypass surgery, and so on) (18). In fact, the mortality for single-vessel procedures fell from 1.3% to 0.2% between the first and second registry. This mortality estimate is supported by contemporaneous data from our own laboratory, showing a 0.3% overall mortality for angioplasty (1), and data from Emory showing a 0.1% mortality in 3,500 patients undergoing elective coronary angioplasty in the mid-1980s (19). With the introduction of newer devices (e.g., stents, atherectomy, laser) to treat high-risk lesions preemptively or reverse abrupt closure following attempted conventional balloon angioplasty, the overall mortality for elective coronary intervention has fallen further (Chapter 23), but the extension of intervention to other high-risk subsets including patients with recent (<30 days) or acute myocardial infarction may be associated with a significantly higher mortality risk than is seen in elective interventions. This has been incorporated in a multivariable model that predicts procedural mortality (range 0% to 35%) based on age, ejection fraction, treatment for AMI/shock, urgent/emergent priority, etc. (20). Other specialized interventional

procedures such as balloon valvuloplasty carry a risk (1% to 2% mortality) similar to that of high-risk coronary angioplasty.

Thus, although it is fair to say that the mortality of catheter-based interventional procedures is roughly 10-fold higher than purely diagnostic catheterization (i.e., 1% vs. 0.1%), there is such a wide variation in risk based on patient comorbidities, clinical indication, and procedure type that these “average” risks should only be quoted to “average” patients. Patients with one or more adverse risk factors should be told candidly during the “informed” consent process that their expected risks are somewhat higher than these averages.

Myocardial Infarction

Diagnostic Catheterization

Although transient myocardial *ischemia* is relatively common during diagnostic catheterization and occurs routinely during coronary intervention, such ischemic episodes usually respond promptly to drug therapy (intravenous or intracoronary nitroglycerine) or deflation of the angioplasty balloon. In contrast, myocardial *infarction* is an uncommon but important complication of diagnostic cardiac catheterization. In the late 1970s, data from the Coronary Artery Surgery Study showed a myocardial infarction rate of 0.25% for coronary angiography (21). In the first, second, and third registries conducted by the Society for Cardiac Angiography (3,4,6), the risk of myocardial infarction fell progressively, from 0.07% and 0.06% to 0.05%. This reduction relative to experience during the 1970s likely reflects greater attention to catheter flushing, pressure damping—all nuances that are now considered integral parts of coronary angiography (Chapter 11), as well as the possible benefits associated with the widespread interval adoption of systemic heparinization for coronary angiography (22).

However, the risk of precipitating myocardial infarction during diagnostic catheterization is clearly influenced by patient-related (as well as technique-related) factors that include the extent of coronary disease (0.06% for single-vessel disease, 0.08% for triple-vessel disease, and 0.17% for left main disease) (4), the clinical indication (e.g., unstable angina or recent subendocardial infarction), and the presence of insulin-dependent diabetes. In such higher-risk patients, avoidance of myocardial infarction again requires adequate patient preparation (e.g., institution of beta blockade, calcium channel blockers, aspirin, heparin, and supplemental oxygen) as well as meticulous attention to technical issues.

When critical lesions are identified in such unstable patients, current practice has evolved toward performing the diagnostic catheterization with “angioplasty stand-by.” If the diagnostic angiogram shows a severe coronary lesion for which a catheter intervention (e.g., angioplasty, atherectomy, stenting) is appropriate, the interventional procedure is then performed in the same sitting. This is true particularly if the patient exhibits clinical instability (including prolonged ischemia with reduced flow or occlusion of a coronary artery) that might signal the transition to myocardial infarction. On the other hand, if angiography reveals anatomy that is better suited for bypass surgery, patients with severe unstable angina should have an intraaortic balloon placed or should at least remain on intravenous heparin (sometimes leaving the vascular sheaths in place) while awaiting surgery. In particular, unstable patients should not have their heparinization reversed by protamine (which may trigger ischemia or frank infarction in an unstable patient), absent a life-threatening bleeding complication. If sheath removal is desired, the heparin infusion can be reduced or interrupted for several hours (until the Activated Clotting Time [ACT] falls below 160 seconds), and then restarted 2 hours later.

Although myocardial infarction may occur in the hours following catheterization (particularly in unstable patients whose lesions and anticoagulant status are not managed aggressively), postprocedure myocardial infarction is rare in elective patients who complete their catheterization procedure without demonstrating signs of instability (e.g., severe or prolonged angina). Elective diagnostic procedures in such individuals are thus now routinely performed on an outpatient basis (23), although roughly one-third of patients preselected for the outpatient approach will require hospital admission based on their anatomic findings, clinical instability, or complications that develop during or following the procedure. For unstable patients (or those who are hospitalized based on anatomic findings or instability during what had been planned as an outpatient procedure), we recommend serial electrocardiogram (ECG) and creatine phosphokinase (CPK) surveillance (immediately after the procedure and again on the following morning). Since CPK may leak from skeletal sources following catheterization and groin compression, measurement of the cardiospecific MB fraction (CK-MB) is also advisable (24).

Should severe ischemic instability develop after the patient leaves the catheterization laboratory, aggressive therapy is indicated. Since the coronary anatomy is known, physicians should consider bringing the patient back to the laboratory for either coronary angioplasty or intraaortic balloon pump placement followed by urgent bypass surgery. It is usually appropriate to reinstitute heparinization, maximize medical therapy (including intravenous nitroglycerine), and administer narcotics to relieve pain and attenuate the consequent sympathetic nervous system response. If urgent catheter-based intervention (rather than bypass surgery) is chosen, consideration should also be given to administration of one of the IIb/IIIa receptor blocker antiplatelet agents (see later) to help facilitate restoration of adequate perfusion and enhance the safety of the planned urgent intervention. We prefer the IIb/IIIa blockers (particularly short-acting small molecules such as Integrilin and Aggrastat) to intravenous thrombolytic therapy for this indication, although the thrombolytic approach may still be appropriate if the patient has ongoing ST-segment elevation, the hospital does not perform coronary intervention, and transfer to a neighboring hospital with that capability is expected to take more 90 minutes.

Interventional Procedures

Coronary interventions may produce myocardial infarction by a variety of mechanisms that include dissection, abrupt vessel closure, “snow-plow” occlusion of side branches, spasm of the epicardial or arteriolar vessels (“no-reflow”), thrombosis, or distal embolization (Chapter 23). In the initial angioplasty experience, myocardial infarction was seen in about half of the 6% of patients who were sent to emergency bypass surgery for abrupt vessel closure (17). Q-wave myocardial infarctions were thus reported in 4.8% of patients in the first NHLBI registry and in 3.6% in the second NHLBI registry (18). The current experience with balloon angioplasty and newer devices suggests that emergency bypass surgery and Q-wave infarction rates have each fallen to roughly 1% (Chapter 23).

Although infarction due to emergency surgery has decreased, the higher proportion of complex lesions (including saphenous vein grafts), treatment of patients with unstable syndromes, and use of more aggressive stent and atherectomy devices has made it clear that at least 20% of patients experience some increase in CK-MB fraction after an otherwise successful intervention. Some elevation of CPK and CPK-MB (generally without associated ST- or T-wave electrocardiographic changes) may be seen in 5% to 10% of otherwise successful balloon angioplasties (25) and as many as 15% to 20% of procedures performed with new devices (particularly directional, rotational, or laser atherectomy) (26). Patients with these low-level enzyme elevations are more likely to have some degree of chest discomfort, although this finding is common also in patients without enzyme elevation, where it presumably represents stimulation of adventitial pain receptors by local stretching at the treatment site (27). Careful review of the cineangiograms sometimes shows compromise of a small side branch originating in the area of a treated lesion.

Considerable debate exists about the meaning of such CK elevations in patients who have had otherwise successful interventional procedures. Our initial observations suggested that low order (one to three times the upper limit of normal) appears to have no short- or long-term consequences and that only elevation above five times normal (i.e., CK-MB > 50 IU/L in a laboratory with an upper limit of normal of 10 IU/L) tends to adversely impact late survival (26). We therefore suggested that only these larger elevations of enzymes should be viewed as a major complication of coronary intervention, equivalent to Q-wave myocardial infarction. This analysis has been challenged by long-term follow-up of patients from other centers and trials (28), where patients with even low-level elevation of postprocedural CK have been found to have greater incidences of long-term (3- to 5-year) adverse outcomes, which (varying from study to study) may include late death, late myocardial infarction, or late repeat revascularization. The question of whether any such relationship is “cause-and-effect” or simply an association of both periprocedural CK elevation and late events with a common “confounding variable” (such as the diffuse underlying atherosclerosis) is still being debated (29). If the relationship were cause-and-effect, randomized trials comparing procedures such as atherectomy (that have substantially higher incidences of CK elevation to conventional balloon angioplasty) *should* show worse late outcomes concentrated among the patients with CK elevation, whereas randomized trials comparing agents such as the IIb/IIIa blockers (which are effective in lowering the incidence of periprocedural CK elevation) should show consistent reductions in these late outcomes. Neither has yet been demonstrated (30,31). Absent finding differential mortality which parallels the frequency of CK elevations in such randomized trials (that match the groups for all other variables, including the diffuseness of atherosclerosis), a more likely explanation is that postprocedural CK elevation is a surrogate marker for diffuse atherosclerosis, not the proximate cause of subsequent adverse events. The answer about causality is important since the main effect of IIb/IIIa receptor blockers on the composite endpoint (death, any infarction, repeat revascularization) has been on non—Q-wave infarction. Until conclusive data are available, we tend to use these agents to prevent closure in vessels with an imperfect mechanical result from intervention or intraprocedural thrombus, rather than as an across-the-board way to reduce the incidence of (non—Q-wave) myocardial infarction. Of course other potent oral antiplatelet agents (e.g., ticlopidine, clopidogrel) work indirectly through the ADP receptor to decrease IIb/IIIa receptor expression on the platelet surface and have many similar effects. They have become part of the standard adjunctive therapy in coronary stent placement and may play an increasing role in all coronary interventions.

Cerebrovascular Complications

Cerebrovascular accidents (strokes) are uncommon but potentially devastating complications of diagnostic cardiac catheterization. Early experience showed an

incidence as high as 0.23% in the 1973 study of Adams (15), compared with the 0.07% incidence for the more recent diagnostic catheterizations included in the Society for Cardiac Angiography registries (3,4). Although their incidence has decreased, strokes are potentially one of the most devastating complications of cardiac catheterization, and every operator should be familiar with potential etiologies, preventive strategies, and treatments for catheterization-related stroke. It is also a good idea to speak with the patient directly at the end of the procedure and to have a low threshold for performing a screening neurologic exam if the patient is less alert, has slurred speech, and has either visual, sensory, or motor symptoms during or after a left heart procedure.

Catheterization-related strokes are almost always embolic in origin. There is come evidence that many such emboli are dislodged from unsuspected aortic plaque or diffuse atherosclerosis, given the observation that atherosclerotic debris is liberated from the wall of the aorta in 40% to 60% of cases during advancement of large-lumen guiding catheters over a 0.035-inch guidewire. This supports the observation that most strokes and neuroophthalmologic complications (i.e., retinal artery embolization) appear to be caused by emboli released by disruption of unrecognized plaques on the walls of the aorta, liberating cholesterol crystals, calcified material, or platelet-fibrin thrombus into the aortic root (32,33 and 34). End-hole (i.e., coronary angiographic or particularly guiding) catheters should thus be introduced over a guidewire to the level of the tracheal carina (descending aorta) and flushed carefully (35). The catheters should then be advanced around the aortic arch smoothly without excessive “catching” in surface features that may suggest the presence of such friable plaques. If any such problems are noted during catheter advancement, the catheter should be pulled back into the descending aorta, double-flushed, and then readvanced around the arch over a leading J-tip guidewire. In fact, many operators now routinely take the left Judkins catheter around the arch over the guidewire before flushing and clearing with contrast (Chapter 4). It is still not clear whether the benefit of advancement over a guidewire completely offsets the risk of introducing debris, clot, or air into the aortic root while performing the first catheter flush there rather than in the descending aorta.

While many or even most cerebral emboli during left heart catheterization appear to come from unintentional trauma to preexisting atherosclerotic aortic plaques, the operator needs to take into account the potential to cause similar central nervous system (CNS) embolic problems by technical errors. These may involve sloppy catheter flushing, introduction of air bubbles during contrast injection, inadvertent placement of wires and catheters into the arch vessels, prolonged (>3-minute) “wire dwell times” during attempts to cross a stenotic aortic valve, and failure to carefully wipe and immerse guidewires in heparinized saline before their reintroduction during left-sided heart catheterization. Avoidance of the arch vessels is probably even more important in patients with known cerebrovascular disease or bruits over the carotid or subclavian arteries. Even in patients without carotid bruit or previous stroke, any carotid manipulation (including *external* carotid sinus massage) carries a risk of precipitating a neurologic complication.

Embolic material may also originate in the cardiac chambers, thrombotic coronary arteries, or surface of cardiac valves. One should thus avoid placing the pigtail catheter fully out to the left ventricular apex in patients with suspected aneurysm or recent myocardial infarction, since either condition may be associated with potentially dislodgeable mural thrombus. Cases have also been reported wherein clot contained in an occluded native coronary artery or vein graft was inadvertently withdrawn or propelled out of that vessel, and into the aortic root during attempted coronary intervention or forceful injection of contrast through a distal superselective catheter (36). Care must also be taken to avoid transseptal catheterization or mitral valvuloplasty in patients with left atrial thrombus, which may increase the incidence of clinical stroke. One study that showed an unexpectedly high incidence of new hyperintense brain lesions by magnetic resonance imaging (MRI) after percutaneous balloon mitral valvuloplasty (37), suggests that small subclinical emboli may occur more commonly than previously suspected. In patients with right-to-left shunting (including atrial septal defects with Eisenmenger physiology, but also patients with right ventricular infarction and a patent foramen ovale), paradoxical embolization may also lead to stroke. In such patients, the same level of care regarding flushing catheters and sheaths that is routine during left heart procedures should also be extended to right heart procedures.

The question of embolic risk also invariably comes up when it is necessary to perform catheterization on patients with endocarditis of left-sided (aortic and mitral) heart valves. On the one hand, the associated vegetations look friable and can embolize spontaneously. On the other hand, they have already withstood repeated trauma from opening and closing of the affected valves without dislodgment. In a series of 35 patients with active endocarditis who underwent left-sided cardiac catheterization (five of whom had prior spontaneous systemic emboli), not one had a catheterization-induced embolic event (38). This supports the view that left-sided cardiac catheterization can be performed safely in patients with active endocarditis for whom surgical intervention is being considered.

Other than cerebrovascular emboli from intracardiac, arterial, or catheter sources, patients receiving aggressive anticoagulation, antiplatelet, or thrombolytic therapy are also prone to spontaneous intracerebral bleeding as a potential cause for postprocedure neurologic complications. If any doubt exists, and particularly if thrombolytic therapy or intensive anticoagulation are being considered as treatment for a presumptive cerebrovascular embolus, neurologic consultation and computerized tomography (CT) or MRI scanning are advisable. The distinction is critical, since there have been reported cases of resolution of embolic strokes that occurred during cardiac catheterization after selective infusion of a thrombolytic into the occluded cerebral vessel (36), and successful treatment of patients with posterior fossa bleeds as the result of prompt recognition and neurosurgical evacuation. If no embolic or hemorrhagic etiology is apparent, it is helpful to recall that transient neurologic deficits have also been reported following the injection of high-osmolar-contrast agents into the carotid or vertebral arteries. Use of low-osmolar agents (Chapter 2) is thus required for internal mammary angiography, both to avoid cerebral contrast toxicity and to minimize the intense pain associated with the injection of high-osmolar contrast into the internal mammary artery.

Local Vascular Complications

Local complications at the catheter introduction site are among the most common problems seen after cardiac catheterization procedures, and probably the single greatest source of procedure-related morbidity. These problems include vessel thrombosis, distal embolization, dissection, or poorly controlled bleeding at the puncture site. Ongoing bleeding may be due to a poorly placed puncture, vessel laceration, excessive anticoagulation, or poor technique in either suture closure (brachial approach) or groin compression (femoral approach). In the femoral approach, poorly controlled bleeding may present as free hemorrhage, femoral or retroperitoneal hematoma, false aneurysm, or arteriovenous fistula. Hemorrhage and hematoma are generally evident within 12 hours of the procedure, but the diagnosis of false aneurysm may not be evident for days or even weeks after the procedure. Given the common and troublesome nature of postprocedure vascular complications, all cardiac catheterization operators must understand vascular access and closure techniques completely, to recognize and treat each type of complication.

Diagnostic Catheterization

In the early experience with brachial cutdown, Machleder reported a 5.4% incidence of brachial reexploration, predominantly for loss of the distal radial arterial pulse following the procedure (39). Early experience with the femoral approach by Judkins reported a 3.6% local complication rate (40). In contrast, the more recent Society for Cardiac Angiography registries reported a 0.5% to 0.6% incidence of vascular complication for diagnostic catheterization, which was similar for the brachial and femoral approaches (6). In keeping with these early experiences, however, brachial complications still tend to be thrombotic, and femoral complications are more likely to be hemorrhagic. Because they are fundamentally different, the vascular complications of these two approaches will be discussed separately.

Brachial Approach

With the brachial approach, arterial thrombosis accounts for the great majority of local complications (Chapter 5). These complications often relate to formation of a thrombus in the proximal arterial segment during the catheterization procedure and failure to effectively remove this thrombus prior to arterial repair. This can usually be accomplished by allowing brief brisk bleeding from each end of the incised brachial artery in turn. Although most operators reserve use of a Fogarty balloon embolectomy catheter to patients in whom such bleeding fails to occur or in whom a weak pulse is still present after arteriotomy repair, another approach is to routinely pass the Fogarty catheter and instill a heparin solution into the proximal and distal arterial segments to prevent thrombus formation just prior to arterial repair (41) to effectively prevent this complication. Brachial arterial thrombosis may also develop secondary to an intimal flap within the arterial lumen that has not been properly “tacked down” or removed at the time of arterial repair, creating a pocket of stasis where thrombus can accumulate. Occasionally, local arterial spasm may develop in the hours immediately following catheterization and successful arterial repair, resulting in secondary arterial thrombosis that can convert an initially bounding radial pulse into one that is weak or absent 6 hours after catheterization.

Prevention of brachial artery thrombosis can best be accomplished by meticulous attention to the details of arterial repair, which are discussed in Chapter 5. Adequate heparinization includes systemic administration of heparin (5,000 units intravenously) shortly after initial arterial entry and local administration of heparin (1,000 to 1,500 units into both proximal and distal arterial segments) at the time of arterial repair. Inspection of the arteriotomy site, trimming of any free intimal flaps, and avoidance of arterial narrowing (as frequently occurs with a purse-string closure) will minimize arterial thrombosis. Anticoagulation is not reversed with protamine at the end of a brachial catheterization; if the arterial repair has been done properly, no local bleeding should occur.

Correction of brachial arterial thrombosis requires reexploration of the arm incision with repeat brachial arteriotomy, Fogarty catheter thrombectomy, and arterial repair (42). Although a vascular surgeon usually performs this procedure in the operating room, cardiologists experienced with the brachial approach may carry out

such corrective procedures in the catheterization laboratory. Successful treatment of brachial artery thrombosis by percutaneous transluminal angioplasty from the femoral artery has also been described.

Other potential local complications of brachial arterial catheterization include injury to the median nerve during cutdown and isolation of the artery, delayed dehiscence of arterial sutures with late arterial bleeding, bacterial arteritis, and local cellulitis-phlebitis associated with the cutdown itself. Injury to the median nerve is rare and should not occur if the dissection is careful. Rarely, postcatheterization bleeding within the brachial wound may lead to hematoma formation and compression of the nerve. This responds to prompt evacuation of the hematoma. Mild injury to the median nerve results in numbness and weakness of the thenar aspect of the hand, which almost always returns to normal within 3 to 4 weeks, although occasionally some neurologic symptoms may require up to 6 months for complete resolution. Local cellulitis-phlebitis is most likely to occur if (a) extensive soft tissue is dissected during the brachial cutdown; (b) large veins are used and tied off; (c) the catheterization procedure is long; (d) seroma or hematoma forms in the incision; (e) nonviable tissue (e.g., fat deprived of its blood supply) is left in the incision; and (f) poor surgical technique or violation of sterile procedure occurs. The routine use of a potent germicidal agent (e.g., 1% povidone-iodine solution) for wound irrigation prior to skin closure substantially reduces the incidence of infection. Routine cases do not require prophylactic antibiotics, but antibiotics should be used any time a high probability of wound infection exists (e.g., a long procedure in which a known breach of sterile technique occurred). In such instances, oxacillin 500 mg by mouth (PO) every 6 hours for 5 days beginning at the time of wound closure (initial loading dose given intravenously) is generally adequate.

Femoral Approach

Femoral artery thrombosis is extremely rare, except in patients with a small common femoral artery lumen (peripheral vascular disease, diabetes, female gender), in whom a large-diameter catheter or sheath (e.g., an intraaortic balloon pump) has been placed, particularly when the catheter dwell time is long. Such patients may complain of leg pain or numbness and have diminished distal pulses during the catheterization procedure, if the diagnostic sheath itself obstructs antegrade flow and adequate collaterals are not present. This type of obstructive limb ischemia generally resolves and distal pulses return promptly when the sheath is removed at the end of the procedure. Patients who have ongoing complaints and diminished or absent distal pulses that fail to resolve with catheter removal (or who develop such findings in the hours after catheterization) may have flow-obstructing dissection or thrombus at the femoral artery puncture site, or a distal arterial embolus. This requires urgent vascular surgery consultation with exploration for local dissection or plaque avulsion, and Fogarty embolectomy of the distal vessel as needed to restore distal pulses. Failure to do so promptly (generally within 2 to 6 hours) may result in extension of thrombosis into smaller distal branches, with attendant muscle necrosis that may necessitate fasciotomy or even amputation.

Femoral venous thrombosis or *pulmonary embolism* are rare complications of diagnostic femoral catheterization. A small number of clinical cases have been reported, however, particularly in the setting of venous compression by a large arterial hematoma, or prolonged procedures with multiple venous lines (e.g., electrophysiologic studies) (43). The actual incidence of thrombotic and pulmonary embolic complications may, however, be substantially underreported, since most are not evident clinically. Asymptomatic lung scan abnormalities have thus been described in up to 10% of patients after diagnostic catheterization (44). One series of endomyocardial biopsy procedures reported a similarly high incidence of echocardiographic detection of thrombi passing through the right-sided heart chambers, particularly when the venous sheath was not aspirated and flushed between insertions of the bioptome (45). To avoid this problem, we attach a continuous drip of heparinized saline to the venous sidearm throughout the catheterization procedure to reduce the chance of clot formation within (and embolization from) the lumen of the venous sheath.

A more common problem after cardiac catheterization by the femoral approach relates to poorly controlled bleeding from the arterial puncture site (46). Uncontrollable free bleeding around the sheath suggests *laceration* of the femoral artery. If such free bleeding does not respond to replacement with the next-larger-diameter sheath, the bleeding should be restricted by manual compression around the sheath until the procedure is completed. Heparin should then be reversed, and an attempt may be made to remove the sheath and control bleeding with prolonged (30- to 60-min) compression, either manually or with a compression device (see Chapter 4). Blood for transfusion should be typed and cross-matched, and the vascular surgeons should be consulted regarding operative repair should the bleeding continue.

More common than free bleeding is the formation of a *hematoma*— collection of blood within the soft tissues of the upper thigh that causes a tender baseball- or softball-sized mass. If ongoing bleeding stops with manual compression, the hematoma will usually resolve over 1 to 2 weeks as the blood gradually spreads and is reabsorbed from the soft tissues. Instances of femoral nerve compression from groin hematomas, however, may lead to quadriceps weakness that may take weeks or even months to resolve. Larger hematomas may require transfusion, but surgical repair for hematoma (as opposed to false aneurysm) is generally not required. Given the discomfort caused by large hematoma and the potential of such hematoma to evolve into false aneurysms, accurate puncture and puncture site compression technique to minimize hematoma formation are essential parts of good catheterization technique.

If the arterial front (or back) wall puncture was made above the inguinal ligament, a hematoma may extend into the retroperitoneal space. Such bleeding is not evident from the surface, but should be considered whenever a patient develops unexplained hypotension (particularly if it responds only briefly to aggressive volume loading), fall in hematocrit, or ipsilateral flank pain following a femoral catheterization procedure. The diagnosis may be confirmed by CT scanning or abdominal ultrasound, but the treatment is usually expectant (transfusion, bedrest) rather than surgical. The best prevention for retroperitoneal bleeding is careful identification of the puncture site, to avoid entry of the common femoral near or above the inguinal ligament. Effective catheter-based interventions have yet to be developed, but localization and occlusion of a retroperitoneal bleeding site using a peripheral angioplasty balloon have been reported (47).

If a hematoma remains in continuity with the arterial lumen (due to dissolution of the clot plugging the arterial puncture site), a *pseudoaneurysm may develop* (Fig. 3.1). Blood may flow in and out of the arterial puncture, expanding the hematoma cavity during systole and decompressing back into the arterial lumen in diastole. Since the hematoma cavity contains no normal arterial wall structures (i.e., media or adventitia), this condition is referred to as false or pseudoaneurysm. On physical examination, it can be distinguished from a simple hematoma by the presence of pulsation and an audible bruit over the site. Duplex ultrasound scanning is confirmatory (48). Since all but the smallest (< 2 cm in diameter) false aneurysms tend to enlarge and ultimately rupture, we usually have the vascular surgeons repair them (generally under local anesthesia) when they are detected (46). Repair is almost certain to be required if the patient needs to take oral anticoagulant medication (i.e., warfarin) after the procedure. More recent alternatives to vascular surgical repair include the use of an ultrasound transducer to compress the narrow “neck” through which blood exits the femoral artery for 30 to 60 minutes, which may permanently close the track and eliminate the need for surgery (49). It may also be possible to inject the false aneurysm cavity with procoagulant solutions or embolization coils during ultrasound-guided occlusion of the aneurysm neck. False aneurysms smaller than 2 cm in diameter may be followed expectantly, with up to half closing before a 2-week follow-up ultrasound (50). Those that persist or cause symptoms should probably be repaired surgically.

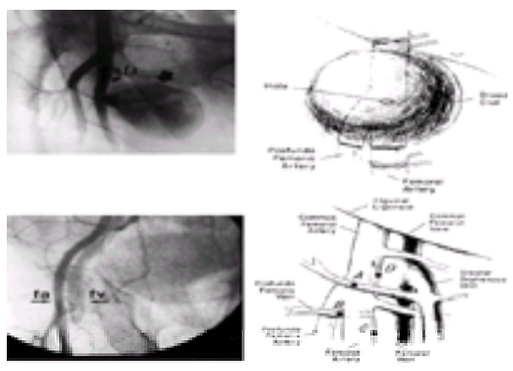

FIG. 3.1. Common significant femoral vascular complications. **Top left:** Angiographic appearance of a false aneurysm of right femoral artery *(arrow)* that developed 4 to 5 days after percutaneous retrograde femoral arterial catheterization complicated by a significant local hematoma after groin compression. Note that the arterial puncture had been made in the superficial (rather than common) femoral artery. **Top right:** Schematic diagram showing the surgical approach to the false aneurysm cavity and the underlying puncture. **Bottom left:** Angiographic appearance of an arteriovenous fistula with simultaneous filling of the femoral artery (left) and vein (right). **Bottom right:** Diagram showing the potential anatomic situations (overlying arterial and venous branches) that may underlie fistula formation after femoral puncture. (From Skillman JJ, Kim D, Baim DS. Vascular complications of percutaneous femoral cardiac interventions. *Arch Surg* 1988;123:1207).

The keys to avoiding pseudoaneurysm formation are accurate puncture of the common femoral artery and effective initial control of bleeding after sheath removal. Although not confirmed in all studies, our experience suggests that punctures of the superficial femoral or profunda artery (i.e., puncture below the bifurcation of the

common femoral) are significantly more likely to lead to false aneurysm formation because of the smaller caliber of the artery and the lack of a bony structure against which to compress after sheath removal (51). Fluoroscopic localization of the skin nick to overlie the inferior border of the femoral head effectively avoids this error (see Chapter 4). Effective initial control is also essential, since allowing a hematoma to form makes effective control more difficult and initiates natural thrombolytic activity in the hematoma that may dissolve the early fibrin plug at the puncture site.

Ongoing bleeding from the femoral puncture site may decompress into an adjacent venous puncture site to form an *arteriovenous fistula* (Fig. 3.1). This can be recognized by a to-and-fro continuous bruit over the puncture site. Like pseudoaneurysms, arteriovenous (AV) fistulas may not be clinically evident for days after a femoral catheterization procedure (52). These fistulas tend to enlarge with time, and if they do not close within 2 to 4 weeks, we refer these patients for surgical repair. The most common findings at surgery are a low puncture (i.e., of the superficial femoral or profunda, transecting a small venous branch), emphasizing the importance of careful puncture technique in avoiding this femoral vascular complication.

Interventional Procedures

Interventional procedures are almost invariably performed by the femoral approach (96% of interventional cases in the 1990 SCA&I registry were so performed) (6), with a higher level of anticoagulant and antiplatelet therapy, and hence are susceptible to the predominantly hemorrhagic complications described earlier for transfemoral diagnostic catheterization. All reports thus suggest a significantly higher incidence of significant local vascular complications (those requiring surgery or transfusion, 2% to 5%) for interventional procedures than for purely diagnostic catheterization (1,53). During the era when uninterrupted transition from intravenous heparin to oral warfarin was used for stenting (1990 to 1996), vascular complications after stenting were as high 10% (see Chapter 25). There were several contributors, including the use of a larger (9F) sheath, the intensity and duration of anticoagulation, and removal of the sheaths only after an overnight dwell (54). Vascular complications were also greater in women and the elderly. In addition to issues relating to puncture technique, sheath size, level of anticoagulation, and patient-related factors, the incidence of femoral vascular complications clearly depends on the timing and the technique used for sheath removal. Thus even before the switch to less aggressive anticoagulant protocols (aspirin and ticlopidine) and second-generation stents that permit use of smaller sheath size, withholding postprocedure heparin until same-day sheath removal (guided by fall in the ACT to less than 160 seconds), reduced the incidence of hemorrhagic access site complications after stenting to 1% to 2%.

Although the mainstay of sheath removal has been manual compression until hemostasis is achieved, the rapid increase in interventional procedure volume has made less labor-intensive approaches essential. Demonstrating that they produce fewer major complications than manual compression has been difficult. One exception may be mechanical or hydraulic devices that can apply local pressure that simulates mechanical compression. In one 778-patient randomized trial (55) comparing a clamp device with manual compression after catheter-based intervention (predominantly 8F sheath size), the incidence of potential complications by physical exam was equal (mostly ecchymoses or small hematomas). When subjected to ultrasound examination, the incidence of larger hematoma (2% vs. 4%), pseudoaneurysm (1% vs. 3%), and arteriovenous fistula (0 vs. 1%) tended to be lower with the mechanical compression. We tend to use mechanical compression devices for removal of most postinterventional sheaths, with the caveat that they must be applied correctly (so as to control the puncture site without prolonged [>3 minutes] occlusion of distal flow) and monitored continuously until control is obtained. They should also be avoided in patients at higher risk of femoral thrombosis due to severe peripheral vascular disease, or prior aorto-femoral or fempopliteal bypass surgery. Nor do we use mechanical compression devices in patients having diagnostic or interventional procedures with smaller (e.g., 6F) sheaths, where 15 minutes of manual compression is usually adequate.

Given the ongoing incidence of complications relating to management of the arterial entry site, alternative management strategies continue to be investigated. Various approaches for collagen plugging or percutaneous suture-mediated closure of the femoral arterial puncture site have been introduced in the last several years (see Chapter 4). Although these devices avoid the discomfort of prolonged manual or mechanical compression and allow earlier or even immediate ambulation, clinical trials have failed to demonstrate significant reduction of major vascular complications compared with compression. Ultimately, it is likely that this class of devices will improve sufficiently to make closure of the femoral artery puncture site so reliable as to eliminate the 1% to 2% incidence of complication. Until then, problems must be repaired when they occur, or operators must be prepared to work from other access sites such as the radial artery (where hemorrhagic complications are unheard of, and thrombosis [with a negative Allen test] is usually inconsequential) (56).

Arrhythmias or Conduction Disturbance

A variety of cardiac arrhythmias (tachy- or bradycardia) or conduction disturbance may occur during the course of diagnostic or therapeutic cardiac catheterization. Most, like ventricular premature beats (VPBs) during catheter entry into the right or left ventricle, are devoid of clinical consequence. Others, like asystole or ventricular fibrillation, pose immediate risk. Finally, some rhythm disturbances (like atrial fibrillation) are well tolerated in most patients but may trigger profound hemodynamic decompensation in patients with severe coronary disease, aortic stenosis, or hypertrophic cardiomyopathy by excessively increasing heart rate or eliminating the atrial “kick” needed to maintain diastolic filling of a stiff left ventricle.

An important part of safe cardiac catheterization is thus for the operator and the nurses/technicians to monitor the surface electrocardiogram on the same physiologic monitor used to display the pressure tracings. The monitoring equipment should also generate an audible beep with each QRS complex, to serve as another channel of information while the operator is intent on watching the fluoroscopic image. In our laboratory, the technicians are trained to call out any disturbance in rhythm such as ventricular premature beats (“Vs, running Vs, change in complex”) that may otherwise escape the operator's attention. The tools to treat these rhythm disorders—including a defibrillator capable of synchronized or asynchronous countershock, temporary transvenous pacing leads and pacemaker generator, and full array of antiarrhythmic drugs—must be immediately accessible in any cardiac catheterization laboratory (57). Promptly recognizing and reversing major rhythm disturbances (e.g., by promptly countershocking ventricular fibrillation, sometimes even before the patient fully loses consciousness) can avoid progression to full cardiopulmonary arrest that would require the institution of cardiopulmonary resuscitation (CPR). All cardiac catheterization personnel, however, must be fully certified in Advanced Cardiac Life Support (ACLS) and should be prepared to institute ventilatory and circulatory support without delay when necessary.

Ventricular Fibrillation

Ventricular ectopy or even brief (three- to five-beat) runs of ventricular tachycardia are not uncommon during passage of catheters into the right or left ventricle. Even balloon-flotation right heart catheterization may cause such brief runs of ventricular tachycardia in up to 30% of patients, with sustained ventricular tachycardia in 3% and ventricular fibrillation in 0.7% of cases (58). This emphasizes the importance of controlling the catheter position in the right ventricle, and smooth passage through the right ventricular outflow tract; similar issues relate to careful positioning of the pigtail catheter free in the mid-portion of the left ventricle (see Chapter 12). If a sudden increase in ectopic activity is noted or if a run of ventricular tachycardia is initiated, the offending catheter must be repositioned immediately so that baseline cardiac rhythm is restored. The same holds true for ventricular ectopy precipitated when the tip of a guidewire is placed into a small intramyocardial branch (usually a septal branch of the left anterior descending) during coronary intervention. The guidewire should be withdrawn slightly and repositioned in the main vessel. Other than these mechanical stimuli, ventricular fibrillation can also be induced by catheter transmission of “leakage” electrical currents into the heart (57,59). This problem has been effectively eliminated, however, by the adoption of standards for grounding systems in the cardiac catheterization laboratory that ensure a maximum leakage current of 20 μA between any two exposed conductive sources.

Although ventricular tachycardia and ventricular fibrillation may result from excess catheter manipulation, they more commonly result from intracoronary contrast injection. This is seen most commonly with injection of ionic (high-osmolar) contrast agents into the right coronary artery, particularly if the injection is prolonged or the catheter pressure is partially damped (see Chapter 11). Changes in injection technique and the formulation of contrast agents used for coronary angiography have progressively reduced the incidence of this complication from 1.28% in the 1973 publication of Adams (15) to 0.77% in the 1970 to 1974 series from the Montreal Heart Institute (8), to less than 0.4% in the Society for Cardiac Angiography registry (6). The incidence of ventricular fibrillation may be somewhat higher in patients with baseline prolongation of the QT interval (60). Some reduction in fibrillation has been reported with use of atropine pretreatment (61), but we do not routinely pretreat with atropine to avoid precipitating sinus tachycardia and ischemia in our predominant unstable angina patient population.

Some of the most refractory ventricular ectopy is seen in the setting of profound transmural ischemia or early myocardial infarction. Such ectopy may respond to loading with intravenous lidocaine (1.5 mg/kg over 1 minute, with a second bolus of 0.75 mg/kg 7 minutes later) or procainamide (15 mg/kg over 20 minutes, watching for fall in blood pressure or broadening of QT or prolongation of QRS intervals). If ectopy progresses to ventricular fibrillation, or particularly if it recurs shortly after defibrillation, intravenous amiodarone, 5 mg/kg over 20 minutes, followed by a drip of 1 g/24 hours, and additional boluses of 150 mg over 10 minutes for breakthrough ectopy may be life-saving. Amiodarone is so lipid soluble that it must be combined with a detergent (Tween-80), which may cause arterial hypotension (62). The administration rates of amiodarone may thus need to be reduced or the infusion suspended if the blood pressure drops below desirable levels.

Atrial Arrhythmias

Atrial extrasystoles are common during catheter advancement from the right atrium to the superior vena cava, or during looping of the catheter in the right atrium to facilitate passage in a patient with enlargement of the right-sided heart chambers. These extrasystoles usually subside once the catheter is repositioned but may go on to atrial flutter or fibrillation in sensitive patients. Both rhythms tend to revert spontaneously over a period of minutes to hours but may require additional therapy if they produce ischemia or hemodynamic instability. Atrial flutter can be treated by a brief (15-second) but rapid (300- to 400-beats-per-minute) burst of right atrial pacing, following which reversion to sinus rhythm or onset of atrial fibrillation (with a more controlled ventricular response) can be expected (63). Care must be taken, however, to ensure a stable atrial pacing location, since catheter migration into the ventricle during burst pacing may trigger ventricular fibrillation.

Atrial fibrillation is generally benign during catheterization but may cause clinical sequelae if the ventricular response is rapid (>100) or if the loss of the atrial kick causes hypotension in a patient with mitral stenosis, hypertrophic cardiomyopathy, or diastolic left ventricular dysfunction. If tolerated poorly in such individuals, atrial fibrillation or flutter may require DC cardioversion. If no significant hemodynamic dysfunction occurs, intravenous beta blockers [propranolol (Inderal, Wyeth-Ayerst, Philadelphia, PA)] 1 mg or esmolol (64) [Brevibloc (Baxter, New Providence, NJ)] at a loading dose of 500 µg/kg per minute for 30 seconds, followed by an infusion of 50 to 250 µg/kg per minute), or a calcium channel blocker (verapamil 5 mg) may be given and up-titrated until adequate control of the ventricular response is achieved. Once the ventricular response is controlled, chemical conversion to normal sinus rhythm can usually be accomplished by administration of intravenous procainamide (15 mg/kg over 20 minutes). Alternatively, the new class III antiarrhythmic drug ibutilide (65) can provide prompt conversion of new-onset atrial fibrillation or flutter. Because it may cause QT prolongation and torsade, it should not be given to patients who are on other QT-prolonging drugs or have reduced potassium or magnesium concentrations, bradycardia, or baseline QTc intervals exceeding 440 msec. In patients weighing more than 60 kg it is given as one vial (1 mg) over 10 minutes, monitoring for conversion or adverse effects (QT prolongation of ventricular ectopy). The patient should be monitored and no other type III agents should be given for 4 hours if ibutilide is administered. If there is significant hemodynamic instability from either atrial flutter or atrial fibrillation, however, the most rapid and reliable therapy is synchronized cardioversion (starting at 35 to 50 W-sec, after appropriate intravenous sedation). In patients with a history of atrial arrhythmia (frequent atrial premature contractions, paroxysmal atrial fibrillation) a single dose of quinidine or procainamide 1 to 2 hours before the procedure may help prevent atrial fibrillation.

Bradyarrhythmias

Transient slowing of the heart rate occurs commonly during coronary angiography, particularly at the end of a right coronary artery injection performed using ionic (high-osmolar) contrast agents. Since forceful coughing helps to clear contrast from the coronaries, support aortic pressure and cerebral perfusion during asystole, and restore normal cardiac rhythm, patients should be warned at the beginning of the procedure that they may be asked to cough forcefully and that they must do so without hesitation when asked. Having the nurses, technicians, and physicians all simultaneously yell “cough” when asystole develops at the end of a coronary injection is one of the most reassuring evidences of a well-trained and alert catheterization laboratory staff!

When bradycardia is more prolonged, other etiologies must be suspected. Vasovagal reaction, in which bradycardia is associated with hypotension, nausea, yawning, and sweating, is one of the more common complications (with a roughly 3% incidence) seen in the cardiac catheterization laboratory (1). It is triggered by pain and anxiety, particularly in the setting of hypovolemia. Some elderly patients may exhibit all the findings of a vasovagal reaction without the hallmark finding of bradycardia (66). In the study by Landau et al. (67), more than 80% of such reactions occurred as vascular access was being obtained, with 16% occurring during sheath removal. This points to the importance of adequate preprocedure sedation and adequate administration of local anesthetic before catheter insertion is attempted. The treatment for vasovagal reaction consists of (a) cessation of the painful stimulus, (b) rapid volume administration (elevation of the legs on a linen pack and hand pumping of saline through the sidearm of the venous sheath), and (c) atropine (0.6 to 1 mg intravenously). If hypotension persists, additional pressor support (Levophed or Neosynephrine) may be needed. Although the vasovagal episode itself tends to be benign, patients with critical valvular heart disease may undergo severe and even irreversible decompensation if they are allowed to remain hypotensive from an indolently treated vasovagal reaction. When the vasovagal constellation occurs during catheter manipulation (instead of sheath insertion or removal), it should still be treated as outlined earlier, but the operator should be aware that vagal stimulation is one of the earliest findings in cardiac perforation (see later) when the pericardium is irritated by blood.

Conduction disturbances (bundle branch block or complete AV block) are an uncommon but potentially serious cause of bradycardia during cardiac catheterization (68,69). They may be precipitated when the catheter impacts the area of the right bundle during right-sided heart catheterization. This may cause a transient change in complex on the monitor electrocardiogram (ECG) but requires no treatment except in the patient with preexisting left bundle branch block. In the case of right bundle branch block superimposed on preexisting left bundle branch block, asystole and cardiovascular collapse may ensue unless an adequate escape rhythm (i.e., a junctional escape) takes over. The same scenario may be seen when left bundle branch block is produced as the aortic valve is crossed in a patient with preexisting right bundle. Complete heart block may also be produced during use of rotational atherectomy, particularly in the right or circumflex coronary arteries (see Chapter 24); coronary thrombectomy in those vessels (or the grafts supplying them); or aortic valvuloplasty (see Chapter 26).

When complete heart block develops, atropine is rarely helpful in the setting of inadequate junctional escape and hemodynamic deterioration but should be given anyway, since it has few adverse effects. Coughing may help support the circulation and maintain consciousness while the right heart catheter is removed and a temporary pacing catheter is inserted. [We use the 7F balloon-tip Baim-Turi pacing catheter (USCI, Billerica, MA) for this purpose.] At one time, we placed such catheters prophylactically in patients with bundle branch block or planned right coronary intervention, but we abandoned this practice after retrospective review showed that frank asystole was rare and that there is generally time for insertion of a pacing catheter through the indwelling venous sheath (70). The only procedures for which we place prophylactic right-sided pacing catheters now are balloon valvuloplasties and rotational atherectomy, particularly in the right and circumflex coronary arteries.

Perforation of the Heart or Great Vessels

Perforation of the cardiac chambers, coronary arteries, or intrathoracic great vessels is a rare event in diagnostic catheterization. In the cooperative study from 1968 (2), 100 patients (0.8%) had perforation during diagnostic catheterization. Most involved the cardiac chambers, particularly the right atrium (33 cases), right ventricle (21 cases), left atrium (10 cases), and left ventricle (10 cases). Thirty of the 33 right atrial perforations involved transseptal catheterization, making the right ventricle the most common site for perforation in the remaining (nontransseptal) diagnostic procedures. The incidence of perforation is clearly related to the performance of procedures that use stiffer catheters (transseptal catheterization, endomyocardial biopsy, balloon valvuloplasty, needle pericardiocentesis, and placement of NIH or temporary pacing catheters). Elderly women (>65 years of age) seem particularly susceptible, since the walls of the right-sided heart chambers may be thinner. Higher-risk procedures involving stiff catheters should thus be performed only by individuals with greater catheterization experience who can exert all due care to avoid this problem.

When cardiac perforation does occur, it is usually heralded by bradycardia and hypotension due to vagal stimulation (see the preceding discussion of vasovagal reaction on p. 51) (71). As blood accumulates in the pericardium, the cardiac silhouette may enlarge and the normal pulsation of the heart borders on fluoroscopy may become blunted. Hemodynamic findings of tamponade may develop in the form of arterial paradox and elevation of the right atrial pressure with loss of the *y* descent. If the patient is hemodynamically stable, a portable transthoracic echocardiogram may help document the presence of blood in the pericardial space. If hemodynamic compromise is severe or progressive, however, immediate pericardiocentesis should be performed via the subxyphoid approach. We use a disposable kit containing an 18-gauge needle, a J-tip guidewire, and a tapered catheter with multiple side holes, which is immediately available in the catheterization laboratory. We generally try to remove most of the free blood before reversing systemic heparinization with protamine, since early administration of protamine may cause blood in the pericardial space to “gel” and make aspiration impossible. Once pericardiocentesis has stabilized the situation and protamine has been administered, the operator must decide whether emergency surgery will be needed to oversew the site of perforation. This decision rests on the anatomic location of the perforation and the pace of ongoing bleeding (manifest as the rate of blood aspiration). Most perforations, in fact, will seal so that surgery is unnecessary. This is illustrated in an 18-year review from the Mayo Clinic (72), during which time 92 patients (0.08% of invasive procedures) developed tamponade. This included 1.9% of valvuloplasties, 0.23% of electrophysiology studies, 0.08% of coronary angioplasties, and 0.006% of diagnostic catheterizations. The majority (57%) of patients were in frank hemodynamic collapse (systolic pressure < 60 mm Hg) at the time of pericardiocentesis. Echo-guided pericardiocentesis was successful in 91 cases, and was the only definitive therapy in 82% of cases (the remaining 18% requiring surgical intervention). There were no procedural deaths in this series, but there were three major complications (pneumothorax, intercostal artery injury, and right ventricular laceration), and seven patients (8%) died within 30 days of the procedure.

Perforation of the great vessels is extremely rare. The aorta is sufficiently elastic to resist perforation, except in the case of weakening by ascending aortic dissection or aneurysm. Aortic puncture may occur, however, during attempted transseptal puncture with too anterior a needle orientation (see Chapter 4). Rupture of the pulmonary artery is also rare, although care must be taken not to use stiff-tip guidewires in these thinner-walled vessels. Perforation of the branch pulmonary arteries has been reported when balloon flotation catheters are inflated while positioned in a distal branch (rather than in the left or right main pulmonary artery) (73,74).

Patients typically develop massive hemoptysis of bright red blood and require tamponade of the proximal pulmonary artery, embolization of the bleeding branch, double-lumen endotracheal intubation to protect the noninjured lung, or even emergency lobectomy or pneumonectomy. Inflation of a balloon-tip catheter at the bedside should thus be performed only after a clear pulmonary artery trace is documented, in a slow, gradual fashion just until the shape of the waveform changes (i.e., from pulmonary artery to pulmonary capillary wedge). This is generally not an issue in the catheterization laboratory (where the position of the catheter tip can be confirmed fluoroscopically before it is inflated), but pulmonary artery rupture can still occur with lack of attention to balloon inflation combined with aggressive thrombolytic, antithrombotic, or antiplatelet therapy.

Perforation of a coronary artery was unheard of in the era of diagnostic catheterization and was a reportedly rare complication with conventional balloon coronary angioplasty (75). With the advent of more aggressive new technologies for coronary intervention (in particular, directional atherectomy, rotational atherectomy, transluminal extraction atherectomy, and excimer laser angioplasty) the incidence of coronary perforation in these procedures has risen to 1% (76). Many of these perforations, particularly those caused by distal positioning of a stiff or hydrophilic-coated guidewire, are limited to deep injury to the vessel wall with localized perivascular contrast staining. Free perforations may also occur, however, and the presence of systemic arterial driving pressure may lead to the development of frank tamponade within seconds to minutes (Fig. 3.2), particularly when the patient is well anticoagulated or has received a IIb/IIIa blocker (77,78). The first countermeasure is to seal the site of leakage by inflation of a balloon catheter that spans the perforated segment. If a perfusion balloon catheter is used, antegrade flow to the myocardium can be maintained while the site of perforation is still effectively sealed. Pericardiocentesis may also be necessary if hemodynamic embarrassment is present. Many localized coronary perforations will seal with prolonged balloon inflation and reversal of heparinization by protamine. Other nonsurgical options include coil embolization if the bleeding site is in a small distal branch, or placement of a covered stent (see Chapter 25) to seal the perforation site in a larger proximal vessel. A free perforation with ongoing leakage is a strong indication for emergent surgical repair (76).

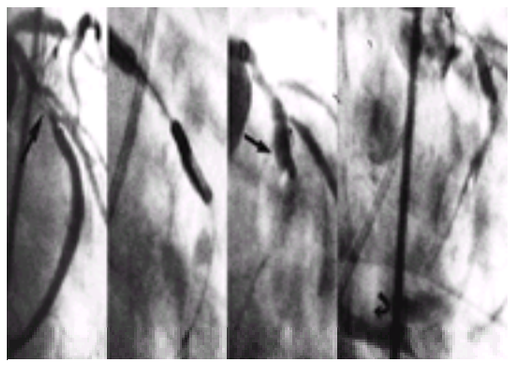

FIG. 3.2. Coronary perforation during directional atherectomy. **Left:** Eccentric stenosis of the mid-circumflex *(bold arrow)* just before small marginal branch *(small arrow)*. **Left center:** Directional atherectomy device. **Right center:** Aneurysmal dilation of circumflex, indicating that atherectomy cuts had been made too distally (note location beyond small marginal branch). **Right:** Free leakage of contrast into the pericardial space, requiring use of a perfusion balloon to stop ongoing leakage, although pericardiocentesis and emergency bypass surgery were required.

Although they are extracardiac, dissection and perforation of vessels used as a route for advancing a cardiac catheter to the heart are also discussed in this section. Mediastinal and retropharyngeal hemorrhage has been reported as a complication of brachial left-sided heart catheterization in two patients, both of whom were excessively anticoagulated with warfarin (prothrombin times 42 and 23 seconds) and presented difficulty in catheter advancement from the brachiocephalic artery into the ascending aorta (79). Supportive measures, including maintenance of the airway to avoid tracheal compression, normalization of clotting status, and blood replacement, were successful. Similar problems with the femoral approach have been reported with dissection or frank laceration of the iliac arteries. Iliac dissections produced with the guidewire may produce pain and may prompt switching to the contralateral femoral artery or the brachial approach but rarely progress to obstruction, since the direction of dissection is opposite that of antegrade blood flow. Cross-femoral access may then be used to dilate or stent the dissected iliac, if needed. In contrast, iliac *laceration* caused by a catheter or introducer sheath has the potential of causing brisk retroperitoneal bleeding. This is rarely controlled without surgical repair, although one instance has been reported in which a small leak was successfully sealed during occlusion by a 20-minute inflation of a peripheral angioplasty balloon (47). When covered stents become available, they would also have the potential to repair iliac leaks from the percutaneous (rather than surgical) approach. The potential for iliac artery laceration underscores the need for careful wire and catheter advancement, and the benefits of performing all catheter exchanges over a guidewire at the level of the diaphragm, even if an arterial sheath is used.

Infections and Pyrogen Reactions

Since cardiac catheterization is an inherently sterile procedure, infection is extremely unusual. In fact, endocarditis prophylaxis is not even recommended when cardiac catheterization is performed with usual sterile precautions (80). Recommended technique includes shaving and cleaning the catheter introduction site with povidone-iodine [Betadine (Purdue Frederick, Norwalk, CT)], use of a nonporous drape, and adequate operator clothing (including a scrub suit, gown, and sterile gloves) (81). Although antibiotics are not needed routinely, we still give a cephalosporin [Kefzol (Eli Lilly, Indianapolis, IN) 1 g on call and every 8 hours for 48 hours] whenever we perform a delayed intervention by exchanging sheaths that were placed in an earlier diagnostic procedure or when any break in sterile technique is suspected. When we must perform a repeat procedure within 2 weeks of an initial diagnostic procedure, we use the contralateral groin, since an increased infection rate has been reported with early reuse of the same groin site (82). Special care should also be taken when performing catheterization through a femoral graft, since such grafts appear more prone to infection with potentially disastrous consequences (83).

The most recent American College of Cardiology/American Heart Association task force does not insist that the operator perform a surgical scrub or wear a surgical cap and mask during femoral procedures (57). These precautions are, however, recommended for catheterization by the brachial approach, where the risk of infection is ten times higher than the femoral approach (0.62% vs. 0.06%). Full sterile precautions (hand scrub, cap, and mask, including a splash shield) are also strongly recommended for the femoral approach when the procedure is prolonged, when the sheath will remain in place for any period, when a stent or permanent pacemaker is being implanted, or when a vascular graft is punctured. Those who have evolved to less stringent sterile precautions should be reminded that there have now been reports of life-threatening stent infections (84), presumably seeded in the cardiac catheterization laboratory. Although some might accuse us of overkill, we have elected to use these precautions on *all* catheterization procedures in our laboratory, partially to protect the patient and partially to protect the operator from blood contamination, as recommended under the universal precaution guidelines of the Occupational Safety and Health Administration (OSHA).

Even with these precautions, exposure to blood through splashes, glove punctures, and needle sticks is one of the risks of working in the cardiac catheterization environment. Vaccination for hepatitis B is encouraged for all laboratory personnel, and anyone who suffers a puncture or laceration should report the event to the laboratory director and employee health personnel, who should give them the option to implement anti-HIV therapy. Retrospective analysis shows that prophylactic zidovudine (AZT) therapy may reduce the risk of infection after being stuck by a needle tainted with blood from an HIV-positive patient (85).

To eliminate the risk of patient-to-patient contamination, we also avoid the multiuse drug vials and clean the room thoroughly between procedures.

With the preceding precautions, it is relatively unlikely that infection is the cause of a postprocedure fever. Although the patient should undergo the usual fever evaluation (chest x-ray, urinalysis, complete blood count, blood cultures), two other etiologies should be considered. Phlebitis may develop after brachial catheterization, with low-grade fever and a warm tender cord overlying the affected vein. Pyrogen reactions may present with shaking chills during or within the first hour after a catheterization, with a brief fever spike as high as 102°F. These reactions are caused by the presence of contaminating materials that may remain on incompletely cleaned catheter surfaces (86). This was a common problem when cardiac catheters were washed and resterilized for repeat use in the 1970s, but has been virtually eliminated by the switch to disposable single-use commercial catheters that are certified as sterile and pyrogen-free. When a pyrogen reaction does occur, small doses of morphine (2 to 4 mg) seem to help alleviate the symptoms. Several countries, however, are now considering the resterilization and reuse of angioplasty balloon catheters as a cost-saving measure, again raising issues about residual ethylene oxide contamination from sterilization, the possibility of pyrogen reactions, and increased complications triggered by reduced performance of resterilized catheters. With progressive falls in the prices of new angioplasty balloons, the cost of reprocessing, medicolegal liability, and the dominant role played by the cost of (nonreusable!) stents, there has been little interest in pursuing reuse strategies for cardiac catheters in recent years.

Allergic and Anaphylactoid Reactions

Cardiac catheterization may precipitate allergic or anaphylactoid reactions to three materials: (a) local anesthetic, (b) iodinated contrast agent, or (c) protamine sulfate. True allergies to local anesthetic do occur but are more common with older ester agents (e.g., procaine) than with newer amide agents (lidocaine, bupivacaine) (87). Some purported allergic reactions to these agents are actually vasovagal episodes or reactions to preservatives. For patients who claim this history, however, use of preservative-free anesthetic (bupivacaine or mepivicaine) represents a practical alternative to performing the procedure without local anesthetic. Skin testing with the intended agent at 1:1,000 dilution can be performed before the procedure to verify absence of a reaction, if desired.

The most common allergic reactions (up to 1% of procedures) are triggered by iodinated contrast agents. In contrast to true anaphylactic reactions [which are mediated by immunoglobulin E (IgE)], reactions to contrast appear to involve degranulation of circulating basophils and tissue mast cells by direct complement activation (i.e., an anaphylactoid reaction) (88). Release of histamine and other agents causes the clinical manifestations (sneezing, urticaria, angioedema of lips and eyelids, bronchospasm, or in extreme cases, shock with warm extremities due to profound systemic vasodilation). Risk of such reactions is increased in patients with other atopic disorders, allergy to penicillin, or allergy to seafood (which contains organic iodine) and may be as high as 15% to 35% in patients who have had a prior reaction to contrast. Premedication of patients with a seafood allergy or prior contrast reaction using the combination of prednisone [20 mg three times daily (tid) for 24 to 48 hours], an H_1 antihistamine (diphenhydramine 25 mg tid), and an H_2 blocker (cimetidine or ranitadine) can reduce the incidence of a second reaction to 5% to 10% and that of severe reactions (bronchospasm or shock) to below 1%. The recent availability of nonionic contrast agents (see Chapter 2), however, adds a further margin of safety, since the rate of severe cross-reactions in patients with prior reaction to an ionic contrast agent is also less than 1% (89,90). For this indication, the true nonionic agents are preferable to an ionic low-osmolar agent such as Hexabrix to which cross-reactions may still occur. Although not absolutely necessary, use of a nonionic contrast agent can be combined with steroid and antihistamine premedication, if extra protection is desired for a patient with a severe prior reaction to contrast.

When a patient with a well-documented prior severe contrast reaction needs to undergo repeat catheterization, aortic pressure should be recorded before the catheter is cleared with contrast, since even this small amount of contrast can cause significant histamine release. The “money shots” of the coronaries should be obtained first, since a severe contrast reaction to the left ventriculogram may preclude further angiography. If a severe reaction occurs, it can be reversed with an intravenous injection of dilute epinephrine (91): One mL of 1:10,000 epinephrine (i.e., 0.1 mg of epinephrine per milliliter) is drawn up from the syringe on the crash cart, diluted further to a total volume of 10 mL (10 mg/mL), and labeled so that it is not mistaken for flush. The epinephrine is administered into the right-sided heart catheter in boluses of 1 mL (or 10 µg) every minute, until arterial pressure is restored. It is rare to have to give more than 10 mL (100 µg) in total, and excessive doses should be avoided, since they may precipitate life-threatening hypertension, tachycardia, or even ventricular fibrillation.

Although reactions to contrast are the most common allergic reaction in the cardiac catheterization laboratory, reactions to protamine sulfate, a biologic product derived from salmon eggs, can also occur. These reactions seem to be more common in insulin-dependent diabetics, who have received NPH insulin (which contains protamine) (92). Although this observation has not been confirmed in another study (93), we tend to omit heparin for diagnostic procedures in such patients, or allow it to wear off before sheath removal rather than take a chance by administering protamine. If a severe anaphylactic reaction occurs, it can be treated as outlined earlier. When giving protamine, administer it slowly (over 5 minutes), since more rapid administration can provoke severe back pain of unknown etiology.

Another allergic reaction that should be considered—even though it is rarely seen in the cardiac catheterization laboratory itself—is heparin-induced thrombocytopenia (HIT) (94). This is defined as a fall in platelet count by at least 50% when accompanied by a positive serologic test for the responsible (usually IgG) antibody. This antibody binds to platelet factor 4 and the PF-4/antibody complex binds to the platelet Fc receptor to cause platelet activation. It seems to be more common with bovine-derived than with porcine-derived heparin. Although onset is typically 7 to 10 days, earlier onset (as early as the first or second day) may be seen in previously sensitized patients. This requires that further heparin administration be curtailed and that any indications for ongoing anticoagulation [including the Heparin-Induced Thrombocytopenia and Thrombosis (HITT) syndrome of aggressive arterial and venous thrombosis] be addressed using an alternative anticoagulant. Options include one of the low-molecular-weight heparin preparations (95), although they frequently cross-react with heparin antibodies, the heparinoid (Organan, danaproid) (96), or one of the direct antithrombin compounds (hirudin, hirulog, or argatroban) (97). Obviously, the same considerations apply if a patient with a history of HIT requires a repeat interventional procedure. If thrombocytopenia develops after a coronary interventional procedure, the assay for heparin antibodies is particularly important, since thrombocytopenia has also been reported in 3.9% of patients within 2 to 12 hours after being treated with the IIb/IIIa receptor blocker abciximab (ReoPro, Eli Lilly, Indianapolis, IN) (98). In 0.9%, severe thrombocytopenia (platelet counts < 50,000) develops. Other potent IIb/IIIa receptor blockers have also been associated with approximately 1% incidence of thrombocytopenia.

Renal Dysfunction

Temporary or permanent renal dysfunction is a serious potential complication of cardiac angiography. The precise mechanism of contrast-induced renal dysfunction (vasomotor instability, increased glomerular permeability to protein, direct tubular injury, or tubular obstruction) has not been established, but at least 5% of patients experience a transient rise in serum creatinine greater than 1 mg/dL following cardiac angiography (99). Patients with diabetes, multiple myeloma, volume depletion, or preexisting renal dysfunction, or who are receiving certain drugs [e.g., gentamycin, angiotensin-converting enzyme inhibitors, nonsteroidal antiinflammatory agents (NSAIDS)] are at increased risk (up to 50%) of this complication. Most such elevations in creatinine are nonoliguric, peak within 1 to 2 days, and then return to baseline by 7 days. Fewer than 1% of patients who develop contrast-induced renal dysfunction go on to require chronic dialysis. Although animal data suggest that low-osmolar contrast agents may have lower renal toxicity, prospective trials comparing high- and low-osmolar contrast agents have failed to show consistent benefit (100,101). In our laboratory, however, we use the smallest possible volumes of low-osmolar agents and aggressive prehydration (see later) when studying patients with a baseline serum creatinine of more than 2.5 mg/dL.

The main defense against contrast-induced nephropathy is limitation of total contrast volume to 3 mL/kg (or 5 mL/kg divided by serum creatinine, in patients with elevated baseline creatinine). In the 1990 SCA&I registry, the mean volume of contrast administered during diagnostic cardiac catheterization was 130 mL for diagnostic procedures and 191 mL for angioplasty procedures, indicating that staying within 3 mL/kg limit for patients with normal renal function (6) usually is possible. In patients with reduced renal function, extra attention must be paid to limiting unnecessary angiographic views and multiple contrast “puffs” during interventional wire and device placement, which may drive up the total contrast volume. Adequate prehydration is also critically important in any patient with impaired baseline renal function. In a classic study (102), 26% of patients with a mean baseline serum creatinine of 2.1 mL/dL had a rise in serum creatinine of more than 0.5 mg/dL. Hydration with half the normal saline for 12 hours before and after the contrast procedure provided the best protection against creatinine rise (which then occurred in 11%, as compared with 26% to 28% of patients who received hydration in combination with either furosemide or mannitol). In a more recent single-center study (103), 98 patients with a baseline creatinine of more than 1.8 mg/dL (mean 2.5 mg/dL) who received a mean of 160 mL of contrast had a mean change in creatinine of 0.6 mg/dL, but 15% developed a peak creatinine of more than 5 mg/dL at 48 hours and 7% went on to dialysis. If postprocedure hourly urinary flow rate could be maintained at a rate of more than 150 mL/hr by the use of fluid loading, low-dose dopamine, and furosemide (as needed), the incidence of severe renal failure (peak creatinine of more than 5 mg/dL at 48 hours, or dialysis) was reduced by half (from 19.7% to 8.1%). Another cause of renal failure following cardiac catheterization is systemic cholesterol embolization (104,105). This syndrome is diagnosed clinically in roughly 0.15% of catheterizations, although cholesterol emboli can be identified pathologically in a far greater number of patients. Patients at greatest risk are those with diffuse atherosclerosis, in whom insertion of a guiding catheter will frequently produce a shower of glistening particles on the table drape. The hallmarks of cholesterol embolization are evidence of peripheral embolization (including livido reticularis, abdominal or foot pain, and purple toes). Episodic hypertension or systemic eosinophilia may be apparent well before the other manifestations develop. Renal failure due to cholesterol embolization tends to develop slowly (over weeks to months, rather than over 1 to 2 days as is seen with contrast nephropathy). Half of the patients with this syndrome progress to frank renal failure. Renal biopsy can confirm the presence of cholesterol clefts but is seldom necessary for diagnosis. Treatment is purely supportive.

Other Complications

Hypotension

Reduction in arterial blood pressure is one of the most common problems seen during catheterization. This reduction represents the final common manifestation of a variety of conditions including: (a) *hypovolemia,* due to inadequate prehydration, blood loss, or excessive contrast-induced diuresis; (b) *reduction in cardiac output,* due to ischemia, tamponade, arrhythmia, or valvular regurgitation; or (c) *inappropriate systemic arteriolar vasodilation,* due to vasovagal, excessive nitrate administration, or vasodilator response to contrast or mixed inotrope-vasodilator drugs such as dopamine or dobutamine. Few places, however, are as well equipped as the cardiac catheterization laboratory, to recognize, diagnose, and treat hypotension. We perform right-sided heart catheterization in only selected diagnostic procedures but in most interventional procedures (where we prefer to leave the right-sided heart catheter in the pulmonary artery for the duration of the case). If

routine right heart catheterization is not done, evolving hypotension is certainly an adequate reason to insert such a catheter.

Low filling pressures mandate rapid volume administration through the peripheral intravenous line and the sidearm of the venous sheath (500 to 1,000 mL of normal saline can be given in 5 minutes by this route) and consideration of potential sites of blood loss (expanding thigh hematoma, retroperitoneal bleeding). If low filling pressures are combined with inappropriate bradycardia, atropine should be given for a potential vasovagal reaction. High filling pressures, however, suggest primary cardiac dysfunction and should prompt consideration of ischemia, tamponade, or sudden onset of valvular regurgitation. Such patients should be supported empirically by inotropic agents (dopamine, dobutamine, milrinone), vasopressors (levophed or neosynephrine), or circulatory support devices [intraaortic balloon counterpulsation, cardiopulmonary support (CPS)] while a more precise etiology is uncovered and treated. The operator also must decide whether the precipitating problem will require surgical intervention, and whether that intervention should be performed immediately after an initial attempt at stabilization in the cardiac catheterization laboratory. If bradycardia is present and does not respond to atropine, consideration should be given to atrial (or AV) sequential pacing to preserve the atrial kick in such patients. One of the most common oversights in managing hypotension, is the failure to assess the cardiac output through thermodilution or measurement of pulmonary arterial oxygen saturation. On several occasions, high pulmonary arterial saturation in a hypotensive patient has signaled coexistent sepsis, contrast reaction, or an idiosyncratic vasodilator reaction to dopamine infusion.

The essential importance of initial empirical and then definitive correction of hypotension and its causes—before hypotension leads to secondary ischemia and an irreversible spiral of left ventricular dysfunction—cannot be overemphasized in providing salvage treatment for patients who might otherwise go on to have major complications.

Volume Overload

Patients in the cardiac catheterization are prone to volume overload due to the administration of hypertonic contrast agents, myocardial depression, or ischemia induced by contrast, poor baseline left ventricular function, as well as their supine position and attempts to volume-load patients at risk for contrast-induced renal dysfunction. The best treatments are prevention by optimizing volume status before or early in the procedure and by use of low-osmolar contrast agents. The support measures described earlier (inotropes, diuretics, vasodilators, balloon pumping) should also be applied in a progressive manner before the patient goes into frank pulmonary edema with the resultant agitation and desaturation. Once pulmonary edema develops, even more aggressive treatment is warranted. Allowing the patient to sit up partially while morphine and nitroprusside are administered to bring filling pressures down may be necessary. If respiratory failure seems imminent, anesthesia support should be requested early enough to allow intubation before a full arrest develops.

Anxiety/Pain

Cardiac catheterization procedures should be well tolerated with oral sedative pretreatment [diazepam (Valium) 5 to 10 mg, and diphenhydramine (Benadryl) 25 to 50 mg] and liberal use of local anesthetic at the catheter insertion site. However, patients' amount of discomfort, level of anxiety, and tolerance for either vary widely. The first effort should be to understand why the patient is having pain (vascular complication, perforation, coronary occlusion, ischemia) and whether anything can be done to reverse the problem. In the meantime, the catecholamine surge associated with pain and anxiety may worsen the condition of a patient who came to the cardiac catheterization laboratory with unstable angina, aortic stenosis, congestive heart failure, or hypertrophic myopathy. It is common practice in our laboratory, therefore, also to manage such complaints symptomatically with small intravenous doses of morphine (2 to 4 mg), fentanyl (25 to 50 mg), and midazolam (Versed, Roche Laboratories, Nutley, NJ; 0.5 to 1 mg). This policy makes the procedure more tolerable for both the patient and the staff, as long as care is taken not to oversedate the patient or overlook an important and treatable etiology for patient complaints. Guidelines for monitoring conscious sedation require monitoring of blood pressure, respiratory rate, and pulse oximetry for 30 minutes after such medications are administered. The antagonist drugs—naloxone (Narcan) for opiates and flumazenil (Mazicon) for benzodiazepines—should also be stocked wherever the agonist drugs are used for conscious sedation.

Respiratory Insufficiency

Problems with adequate ventilation or oxygenation are not uncommon in a cardiac catheterization that deals predominantly with unstable patients. This may result from pulmonary edema, baseline lung disease, allergic reaction, or oversedation. As a screening measure, we routinely send the first arterial sample after sheath insertion to the blood gas laboratory for measurement of pH, P_{CO_2}, as well as P_{O_2}. Patients are then monitored throughout the procedure with a finger pulse oximeter to detect progressive desaturation. Data from such monitoring show that low-flow supplemental oxygen (2 L/min via nasal prongs) helps avoid episodes of desaturation (saturation < 90%) that otherwise occur with surprising frequency during cardiac catheterization (34%) or coronary angioplasty (56%) (106). If oxygen consumption is to be measured as part of a calculation of cardiac output by the Fick method, however, supplemental oxygen administration should not be begun until after that measurement (or should be interrupted for a least 10 minutes before the oxygen consumption is measured).

Retained Equipment

Although diagnostic and therapeutic cardiac catheters have a high degree of reliability, failures can and do occur whereby devices knot (107), become entrapped (108), or leave fragments in the circulation (109,110). Most of these events are precipitated when such devices are stressed beyond their design parameters (e.g., when a coronary angioplasty guidewire is rotated multiple times in a single direction while its tip is entrapped in a total occlusion, or when a bare-mounted coronary stent cannot be advanced across a lesion and strips off the delivery balloon during attempted withdrawal). Operators should thus be familiar with device performance limits and avoid placing devices into situations that promote failure. Operators should also be familiar with the use of vascular snares, bioptomes, baskets, and other devices and techniques that can be used to recover the errant fragments (111) when devices do fail.

OTHER IMPORTANT ASPECTS OF PROCEDURAL COMPLICATION

Caseload

Although many complications are unavoidable, several studies have demonstrated a clear inverse correlation between the caseload of a cardiac catheterization laboratory and each operator, and their incidence of major complications. For coronary angiography, the mortality rate in institutions performing fewer than 100 diagnostic procedures per year was eight times higher than that in institutions performing more than 400 procedures per year. These data were interpreted to mean that greater caseload leads to greater skill and technical proficiency and fewer complications, and are reflected in the most recent ACC/AHA Guidelines (57), which support a minimum of 300 cases per year for an adult catheterization laboratory and a minimum of 150 cases per physician each year. Lower annual caseloads may be permitted for physicians who have demonstrated skills or who limit themselves to lower-risk patient populations. One study of eight cardiac catheterization laboratories in the state of Washington thus had an extremely low rate of major complications in association with coronary angiography, even though the caseload per laboratory (average 50 to 250 cases per year) and caseload per angiographer (average 65 cases per year) were low (112).

For coronary intervention, several studies have shown a similar relationship between higher institutional and operator volumes, and lower rates of major complications. Medicare data regarding coronary angioplasty thus show that institutions performing fewer than 200 such procedures per year, and operators performing fewer than 75 interventions per year, have more than twice the mortality and emergency surgery rates of higher-volume institutions (113). Ellis et al. (114) reported similar findings in high-volume institutions, and Kastrati et al., have shown this pattern persisting even in the era of stenting (115). These data support the recommendations made by the American College of Cardiology regarding maintaining proficiency in interventional procedures (116). The data seem relatively clear: “Practice makes perfect” for both the institution and the individual operator performing invasive cardiac procedures.

Speed

The speed with which a catheterization procedure is accomplished is also widely regarded as one factor that determines the risk of complication. Unfortunately, few data are available on this subject. The Cooperative Study, which analyzed the duration of diagnostic cardiac catheterization procedures in 16 participating laboratories in the late 1960s (2), found that there was a bell-shaped curve, with the most common duration being 2.0 to 3.0 hours (5,022 cases, 41% of total procedures; median, 2.5 hours), with 4,207 procedures (34%) lasting 1.0 to 2.0 hours and 2,054 procedures (17%) lasting between 3 and 4 hours. It was rare for a procedure to last less than 1 hour (1.9%) or longer than 5 hours (2.8%).

Data compiled in our laboratory in the early 1990s show that the average time required (from the administration of xylocaine to that of protamine, using the femoral approach) for a procedure—including right-sided and left-sided heart catheterization, left ventricular angiography, and coronary angiography—is 45 to 60 minutes. This shorter time has been accomplished despite the need for angiography of saphenous vein and internal mammary grafts in the substantial fraction of the diagnostic

catheterization population who have now undergone prior coronary bypass surgery. This shorter time also is consistent with the average arterial times of 33 minutes for diagnostic procedures in the 1990 SCA&I registry (6). Even for procedures involving coronary intervention, the average procedure time is only 70 to 90 minutes, consistent with the 68-minute arterial time for interventional procedures in the 1990 SCA&I registry.

Whereas shorter procedure times have correlated with decreased overall risk, slow speed of performing a procedure does not necessarily carry an increased risk of a complication, unless the slow speed reflects lack of operator skill. Instead, many longer cardiac catheterization procedures are the consequence of factors that themselves tend to be associated with a high risk of complication. For example, the elderly patient with extensive atherosclerosis and arterial tortuosity may have a long procedure because of technical difficulties associated with catheter passage. Patients who frequently have more extensive disease and diminished reserve may also have an increased risk of complications. In this instance, the high risk is not necessarily caused by the increased duration of the procedure: The two are “true, true; unrelated.” Similarly, a young patient with normal vessels and minimal cardiac disease may have a rapid catheterization procedure, but speed of the procedure in this instance cannot fairly be credited with the observed low risk. Thus duration of the procedure should be considered as an important “independent” risk factor, only when it can clearly be related to lack of skill or experience on the part of the operator, or when it leads to severe cardiac decompensation in a critically ill patient poorly prepared to spend more than the minimal time in the supine position.

Pseudocomplications

Finally, a word relevant to “pseudocomplications” of cardiac catheterization is in order. Patients suffering from serious cardiac disease experience major cardiac events (myocardial infarction, ventricular arrhythmia, systemic embolus) as part of the natural history of their disease. If one of these events happens to occur during or within 24 hours after a cardiac catheterization, is it fair to regard it always as a complication of the procedure? Hildner and coworkers examined events that occurred from 24 hours before to 72 hours after scheduled catheterizations (117,118). The incidence of pseudocomplications or events occurring in the 24 hours before scheduled catheterization was 0.81%, including 0.24% deaths. The same period after catheterization saw a 0.81% incidence of catheterization procedure-related complications with no deaths. It is thus clear that the incidence of complications after cardiac catheterization also includes the occurrence of some unexpected major cardiac events that are driven by natural history of the patient's underlying cardiac disease.

Although it is unlikely that anything we do in the catheterization laboratory will completely eliminate these disease-related problems, we each have an obligation to understand how each of the true procedure-related complications described here arises, how to avoid it whenever possible, how to recognize it when it occurs, and how to treat it appropriately to mitigate as much as possible any long-term sequelae. To achieve this goal requires close tracking by the lab director, periodic public review of complication data (as well as timely evaluation of clusters of unusual problems), and ongoing refinement of the laboratory policies and procedures coupled with continuing staff education regarding those policies.

CHAPTER REFERENCES

1. Wyman RM, Safian RD, Portway V, et al. Current complications of diagnostic and therapeutic cardiac catheterization. *J Am Coll Cardiol* 1988;12:1400.
2. Braunwald E, Swan HJC, Gorlin R, McIntosh HD. Cooperative study on cardiac catheterization. *Circulation* 1968;37[suppl III]:1.
3. Kennedy JW. Complications associated with cardiac catheterization and angiography. *Cathet Cardiovasc Diagn* 1982;8:5.
4. Johnson LW, Lozner EC, Johnson S, et al. Coronary angiography 1984–1987: a report of the registry of the Society for Cardiac Angiography and Interventions. I. Results and complications. *Cathet Cardiovasc Diagn* 1989;17:5.
5. Lozner E, Johnson LW, Johnson S, et al. Coronary arteriography 1984–1987: a report of the registry of the Society for Cardiac Angiography and Interventions. 2. An analysis of 218 deaths related to coronary angiography. *Cathet Cardiovasc Diagn* 1989;17:11.
6. Noto TJ, Johnson LW, Krone R, et al. Cardiac catheterization 1990: a report of the registry of the Society for Cardiac Angiography and Interventions. *Cathet Cardiovasc Diagn* 1991;24:75.
7. Lasky W, Boyle J, Johnson LW, and the Registry Committee of the Society for Cardiac Angiography and Intervention. Multivariable model for prediction of risk of significant complication during diagnostic cardiac catheterization. *Cathet Cardiovasc Diagn* 1993;30:185.
8. Bourassa MG, Noble J. Complication rate of coronary arteriography: a review of 5250 cases studied by percutaneous femoral technique. *Circulation* 1976;53:106.
9. Boehrer JD, Lange RA, Willard JE, Hillis LD. Markedly increased periprocedure mortality of cardiac catheterization in patients with severe narrowing of the left main coronary artery. *Am J Cardiol* 1992;70:1388.
10. Guarneri EM, Califano JR, Schatz RA, Morris NB, Teirstein PS. Utility of standby cardiopulmonary support for elective coronary interventions. *Cathet Cardiovasc Diagn* 1999;4:32.
11. Folland ED, Oprian C, Giacomini J, et al. Complications of cardiac catheterization and angiography in patients with valvular heart disease. *Cathet Cardiovasc Diagn* 1989;17:15.
12. Gobel FL, Steward WJ, Campeau L, et al. Safety of coronary angiography in clinically stable patients following coronary bypass surgery. *Cathet Cardiovasc Diagn* 1998;45:376.
13. Vitiello R, McCrindle BW, Nykanen D, Freedom RM, Benson LN. Complications associated with pediatric cardiac catheterization. *J Am Coll Cardiol* 1998;32:1433.
14. Takaro T, Hultgren HN, Littman D, Wright EC. An analysis of deaths occurring in association with coronary arteriography. *Am Heart J* 1973;86:587.
15. Adams DF, Fraser DB, Abrams HL. The complications of coronary arteriography. *Circulation* 1973;48:609.
16. Pepine CJ. ACC/AHA guidelines for cardiac catheterization and cardiac catheterization laboratories. *J Am Coll Cardiol* 1991;18:1149.
17. Dorros G, Cowley MJ, Simpson J, et al. Percutaneous transluminal coronary angioplasty. Report of complications from the National Heart, Lung, and Blood Institute PTCA registry. *Circulation* 1983;67:723.
18. Detre K, Holubkov R, Kelsey S, et al. Percutaneous transluminal angioplasty in the 1985–86 and 1977–81 National Heart, Lung and Blood Institute registry. *N Engl J Med* 1988;318:265.
19. Bredlow CE, Roubin GS, Leimgruber PP, et al. In-hospital morbidity and mortality in patients undergoing elective coronary angioplasty. *Circulation* 1985;72:1044.
20. O'Connor GT, Malenka DJ, Quinton H, et al. Multivariate prediction of in-hospital mortality after percutaneous coronary intervention in 1994–1996. *J Am Coll Cardiol* 1999;34:681.
21. Davis K, Kennedy JW, Kemp HJ, et al. Complications of coronary angiography from the collaborative study of coronary artery surgery (CASS). *Circulation* 1979;59:1105.
22. Judkins MP, Gander MP. Prevention of complications of coronary arteriography. *Circulation* 1974;49:599.
23. Mahrer PR, Young C, Magnusson PT. Efficacy and safety of outpatient cardiac catheterization. *Cathet Cardiovasc Diagn* 1987;13:304.
24. Roberts R, Ludbrook PA, Weiss ES, Sobel BE. Serum CPK isoenzymes after cardiac catheterization. *Br Heart J* 1975;37:144.
25. Klein LW, Kramer BL, Howard E, Lesch M. Incidence and clinical significance of transient creatine kinase elevations and the diagnosis of non—Q wave myocardial infarction associated with coronary angioplasty. *J Am Coll Cardiol* 1991;17:621.
26. Kugelmass AD, Cohen DJ, Moscucci M, et al. Elevation of the creatine kinase myocardial isoform following otherwise successful directional coronary atherectomy and stenting. *Am J Cardiol* 1994;74:748.
27. Jeremias A, Kutscher S, Haude M, et al. Nonischemic chest pain induced by coronary interventions—a prospective study comparing coronary angioplasty and stent implantation. *Circulation* 1998;98:2656.
28. Abdelmeguid AE, Topol EJ. The myth of the myocardial “infarctlet” during percutaneous coronary revascularization procedures. *Circulation* 1996;94:3369.
29. Reeder GS. Elevation of creatine kinase, MB fraction after elective coronary intervention—a valid surrogate end point of poor late outcome? *J Am Coll Cardiol* 1999;34:670.
30. Baim DS, Cutlip DE, Sharma SK, et al. Final results of the Balloon vs. Optimal Atherectomy Trial (BOAT). *Circulation* 1998;97:322.
31. Kong DF, Califf RM, Miller DP, et al. Clinical outcomes of therapeutic agents that block the platelet IIb/IIIa integrin in ischemic heart disease. *Circulation* 1998;98:2829.
32. Tunick PA, Rosenzweig BP, Katz ES, et al. High risk for vascular events in patients with protruding aortic artheromas: a prospective study. *J Am Coll Cardiol* 1994;23:1085.
33. Kosmorsky G, Hanson MR, Tomsak RL. Neuro-ophthalmologic complications of cardiac catheterization. *Neurology* 1988;38:483.
34. Khatibzadeh M, Mitush R, Stierle U, et al. Aortic atherosclerotic plaque as a source of systemic emboli. *J Am Coll Cardiol* 1996;27:664.
35. Keeley EC, Grines CL. Scraping of aortic debris by coronary guiding catheters—a prospective evaluation of 1,000 cases. *J Am Coll Cardiol* 1998;32:1861.
36. Sandoval AE, Laufer N. Thromboembolic stroke complicating coronary intervention—acute evaluation and management in the cardiac catheterization laboratory. *Cathet Cardiovasc Diagn* 1998;44:412.
37. Rocha P, Mulot R, Lacombe P, et al. Brain magnetic resonance imaging before and after percutaneous mitral balloon commissurotomy. *Am J Cardiol* 1994;74:955.
38. Welton DE, Young JB, Raizner AE, et al. Value and safety of cardiac catheterization during active infective endocarditis. *Am J Cardiol* 1979;44:1306.
39. Machleder HI, Sweeney JP, Barker JF. Pulseless arm after brachial artery catheterization. *Lancet* 1972;1:407.
40. Green GS, McKinnon CM, Rosch J, Judkins MP. Complications of selective percutaneous transfemoral coronary arteriography and their prevention. *Circulation* 1972;45:552.
41. Baker LD, Leshin SJ, Mathur VS, Messer JV. Routine Fogarty thrombectomy in arterial catheterization. *N Engl J Med* 1968;279:1203.
42. Nicholas GG, DeMuth WE. Long term results of brachial thrombectomy following cardiac catheterization. *Ann Surg* 1976;183:436.
43. Shammas RL, Reeves WC, Mehta PM. Deep venous thrombosis and pulmonary embolism following cardiac catheterization. *Cathet Cardiovasc Diagn* 1993;30:223.
44. Gowda S, Bollis AM, Haikal AM, Salem BI. Incidence of new focal pulmonary emboli after routine cardiac catheterization comparing the brachial to the femoral approach. *Cathet Cardiovasc Diagn* 1984;10:157.
45. Kreher SK, Ulstad VK, Dick CD, et al. Frequent occurrence of occult pulmonary embolism from venous sheaths during endomyocardial biopsy. *J Am Coll Cardiol* 1992;19:581.
46. Skillman JJ, Kim D, Baim DS. Vascular complications of percutaneous femoral cardiac interventions. *Arch Surg* 1988;123:1207.
47. Mak GYK, Daly B, Chan W, et al. Percutaneous treatment of post catheterization massive retroperitoneal hemorrhage. *Cathet Cardiovasc Diagn* 1993;29:40.
48. Sheikh KH, Adams DB, McCann R, et al. Utility of color flow imaging for identification of femoral arterial complications of cardiac catheterization. *Am Heart J* 1989;117:623.
49. Agarwal R, Agrawal SK, Roubin GS, et al. Clinically guided closure of femoral arterial pseudoaneurysms complicating cardiac catheterization and coronary angioplasty. *Cathet Cardiovasc Diagn* 1993;30:96.
50. Kent KC, McArdle CR, Kennedy B, et al. A prospective study of the clinical outcome of femoral pseudoaneurysms and arteriovenous fistulas induced by arterial puncture. *J Vasc Surg* 1993;17:125.
51. Kim D, Orron DE, Skillman JJ, et al. Role of superficial femoral artery puncture in the development of pseudoaneurysm and arteriovenous fistula complicating percutaneous transfemoral cardiac catheterization. *Cathet Cardiovasc Diagn* 1992;25:91.
52. Smith SM, Galland RB. Late presentation of femoral artery complications following percutaneous cannulation for cardiac angiography or angioplasty. *J Cardiovasc Surg* 1992;33:437.
53. Oweida SW, Roubin GS, Smith RB, Salam AA. Postcatheterization vascular complications associated with percutaneous transluminal coronary angioplasty. *J Vasc Surg* 1990;12:310.
54. Moscucci M, Mansour KA, Kuntz RE, et al. Peripheral vascular complications of directional coronary atherectomy and stenting-predictors, management, and outcome. *Am J Cardiol* 1994;74:448.
55. Pracyk JB, Wall TC, Longabaugh P, et al. A randomized trial of vascular hemostasis techniques to reduce femoral vascular complications after coronary intervention. *Am J Cardiol* 1998;81:970.
56. Kiemeneij F, Laarman GJ, Odekerken D, Slagboom T, Wieken R. A randomized comparison of percutaneous transluminal coronary angioplasty by the radial, brachial and femoral approaches—the Access Study. *J Am Coll Cardiol* 1997;29:1269.
57. Pepine CJ. ACC/AHA guidelines for cardiac catheterization and cardiac catheterization laboratories. *J Am Coll Cardiol* 1991;18:1149.

58. Sprung CL, Pozen RG, Rozanski JJ, et al. Advanced ventricular arrhythmias during bedside pulmonary artery catheterizations. *Am J Med* 1982;72:203.
59. Starmer CF, McIntosh HD, Whalen RE. Electrical hazards and cardiovascular function. *N Engl J Med* 1971;284:181.
60. Arrowood JA, Mullan DF, Kline RA, Engel TR, Kowey PR. Ventricular fibrillation during coronary angiography: the precatheterization QT interval. *J Electrocardiol* 1987;20:255.
61. Lehmann KG, Chen YC. Reduction of ventricular arrhythmias by atropine during coronary angiography. *Am J Cardiol* 1989;63:447.
62. Kowey PR, Marinchak RA, Rials JJ, Filert RA. Intravenous amiodarone. *J Am Coll Cardiol* 1997;29:1190.
63. Greenberg ML, Kelley TA, Lerman BB, et al. Atrial pacing for conversion of atrial flutter. *Am J Cardiol* 1986;58:95.
64. Kirshenbaum JM, Kloner RF, McGowan N, Antman EM. Use of an ultrashort-acting beta-receptor blocker (Esmolol) in patients with acute myocardial ischemia and relative contraindications to beta-blockade therapy. *J Am Coll Cardiol* 1988;12:773.
65. Murray KT. Ibutilide. *Circulation* 1998;97:493.
66. Weissler AM, Warren JV. Vasodepressor syncope. *Am Heart J* 1959;57:786.
67. Landau C, Lange RA, Glamann DB, Willard JE, Hillis LD. Vasovagal reactions in the cardiac catheterization laboratory. *Am J Cardiol* 1993;73:95.
68. Gupta PK, Haft JI. Complete heart block complicating cardiac catheterization. *Chest* 1972;61:185.
69. Sprung CL, Elser B, Schein RM, et al. Risk of right bundle branch block and complete heart block during pulmonary artery catheterization. *Crit Care Med* 1989;17:1.
70. Harvey JR, Wyman RM, McKay RG, Baim DS. Use of balloon flotation pacing catheters for prophylactic temporary pacing during diagnostic and therapeutic catheterization procedures. *Am J Cardiol* 1988;62:941.
71. Friedrich SP, Berman AD, Baim DS, Diver DJ. Myocardial perforation in the cardiac catheterization laboratory-incidence, presentation, diagnosis, and management. *Cathet Cardiovasc Diagn* 1994;32:99.
72. Tsang TM, Freeman WK, Barnes ME, Reeder GS, Packer DL, Seward JB. Rescue echocardiographically guided pericardiocentesis for cardiac perforation complicating catheter-based procedures—the Mayo Clinic experience. *J Am Coll Cardiol* 1998;32:1345.
73. Chun CHM, Ellestad MH. Perforation of the pulmonary artery by a Swan-Ganz catheter. *N Engl J Med* 1971;284:1041.
74. Foote GA, Schabel SI, Hodges M. Pulmonary complications of the flow-directed balloon-tipped catheter. *N Engl J Med* 1974;290:927.
75. Saffitz JE, Rose TE, Oaks JB, et al. Coronary artery rupture during coronary angioplasty. *Am J Cardiol* 1983;51:902.
76. Ellis SG, Ajluni S, Arnold AZ, et al. Increased coronary perforation in the new device era—incidence, classification, management, and outcome. *Circulation* 1994;90:2725.
77. Wong CM, Mak GYK, Chung DTW. Distal coronary artery perforation resulting from the use of hydrophilic coated guidewire in tortuous vessels. *Cathet Cardiovasc Diagn* 1998;44:93.
78. Chadow HL, Gaba MK, Safi A, Afflu E, Feit A. Rescue PTCA complicated by pulmonary artery rupture after tPA and abciximab. *Cathet Cardiovasc Diagn* 1999;46:89.
79. Eshaghy B, Loeb HS, Miller SE, et al. Mediastinal and retropharyngeal hemorrhage: A complication of cardiac catheterization. *JAMA* 1973;226:427.
80. Dajani AS. Prevention of bacterial endocarditis (AHA Medical/scientific statement). *Circulation* 1991;83:1174.
81. Heupler FA, Heisler M, Keys TF, et al. Infection prevention guidelines for cardiac catheterization laboratories. *Cathet Cardiovasc Diagn* 1992;25:260.
82. Wiener RS, Ong LS. Local infection after percutaneous transluminal coronary angioplasty—relationship to early repuncture of ipsilateral femoral artery. *Cathet Caridovasc Diagn* 1989;16:180.
83. McCready RA, Siderys H, Pittman JN, et al. Septic complications after cardiac catheterization and percutaneous transluminal coronary angioplasty. *J Vasc Surg* 1991;14:170.
84. Leroy O, Martin E, Prat A, et al. Fatal infection of coronary stent implantation. *Cathet Cardiovasc Diagn* 1996;39:168.
85. Cardo DM, Culver DH, Ciesielski CA, et al. A case-control study of HIV seroconversion in health care workers after percutaneous exposure. Centers for Disease Control and Prevention Needlestick Surveillance Group. *N Engl J Med* 1997;337:1485.
86. Reyes MP, Ganguly S, Fowler M, et al. Pyrogenic reactions after inadvertent infusion of endotoxin during cardiac catheterizations. *Ann Intern Med* 1980;93:32.
87. Feldman T, Moss J, Teplinsky K, Carroll JD. Cardiac catheterization in the patient with a history of allergy to local anesthetics. *Cathet Cardiovasc Diagn* 1990;20:165.
88. Wittbrodt ET, Spinler SA. Prevention of anaphylactoid reactions in high-risk patients receiving radiographic contrast media. *Ann Pharmacother* 1994;28:236.
89. Matthai WH, Kussmal WG, Krol J, Goin JE, Schwartz JS, Hirshfeld JW. A comparison of low- with high-osmolar contrast agents in cardiac angiography-identification of criteria for selective use. *Circulation* 1994;89:291.
90. Ritchie JL, Nissen SE, Douglas JS Jr, et al. Use of nonionic or low osmolar contrast agents in cardiovascular procedures. *J Am Coll Cardiol* 1993;21:269.
91. Goss, JE, Chambers CE, Heupler FA, et al. Systematic anaphylactoid reactions to iodinated contrast media during cardiac catheterization procedures--guidelines for prevention, diagnosis, and treatment. *Cathet Cardiovasc Diagn* 1995;34:99.
92. Stewart WJ, McSweeney SM, Kellet MA, Faxon DB, Ryan TJ. Increased risk of severe protamine reactions in NPH insulin dependent diabetics undergoing cardiac catheterization. *Circulation* 1984;70:788.
93. Reed DC, Gascho JA. The safety of protamine sulfate in diabetics undergoing cardiac catheterization. *Cathet Cardiovasc Diagn* 1988;14:19.
94. Brieger DB, Mak KH, Kottke-Marchant K, Topol EJ. Heparin-induced thrombocytopenia. *J Am Coll Cardiol* 1998;31:1449.
95. Weitz AJJ. Low-molecular weight heparins. *N Engl J Med* 1997;337:688.
96. Hale LP, Smith K, Braden GA, Owen J. Organan during rotation atherectomy in the setting of heparin-induced thrombocytopenia. *Cathet Cardiovasc Diagn* 1998;45:318.
97. Burchenal JEB, Marks DS, Mann JT, et al. Effect of the direct thrombin inhibition with bivalirudin (Hirulog) on restenosis after coronary angioplasty. *Am J Cardiol* 1998;82:511.
98. Berkowitz SD, Sane DC, Sigmon KN, et al. Occurrence and clinical significance of thrombocytopenia in a population undergoing high-risk percutaneous coroanry revascularization. *J Am Coll Cardiol* 1998;32:311.
99. Tommaso CL. Contrast-induced nephrotoxicity in patients undergoing cardiac catheterization. *Cathet Cardiovasc Diagn* 1994;31:316.
100. Steinberg EP, Moore RD, Powe NR, et al. Safety and cost effectiveness of high-osmolality as compared with low-osmolality contrast material in patients undergoing cardiac angiography. *N Engl J Med* 1992;326:425.
101. Rudnick MR, Goldfarb S, Wexler L, et al. Nephrotoxicity of ionic and non-ionic contrast media in 1196 patients—a randomized trial (the Iohexol Cooperative Study). *Kidney Int* 1995;47:254.
102. Solomon R, Werner C, Mann D, et al. Effects of saline, mannitol, and furosemide on acute decreases in renal function induced by radiocontrast agents. *N Engl J Med* 1994;331:1416.
103. Stevens MA, McCullough PA, Tobin KJ, et al. A prospective randomized trial of prevention measures in patients at high risk for contrast nephropathy. *J Am Coll Cardiol* 1999;33:403.
104. Gaines DA, Cumberland DC, Kennedy A. Cholesterol embolization: a lethal complication of vascular catheterization. *Lancet* 1988;1:168.
105. Rosman HS, Davis TP, Reddy D, Goldstein S. Cholesterol embolization—clinical findings and implications. *J Am Coll Cardiol* 1990;15:1296.
106. Amar D, Greenberg MA, Menegus MA, Breitbart S. Should all patients undergoing cardiac catheterization or percutaneous transluminal coronary angioplasty receive oxygen? *Chest* 1994;105:727.
107. Lipp H, O'Donoghue K, Resnekov L. Intracardiac knotting of a flow-directed balloon-tipped catheter. *N Engl J Med* 1972;284:220.
108. Kober G, Hilgermann R. Catheter entrapment in a Bjork-Shiley prosthesis in aortic position. *Cathet Cardiovasc Diagn* 1987;13:262.
109. Hartzler GO, Rutherford BD, McConahay DR. Retained percutaneous transluminal coronary angioplasty equipment components and their management. *Am J Cardiol* 1987;60:1260.
110. Grabenwoeger F, Bardach G, Dock W, et al. Percutaneous extraction of centrally embolized foreign bodies—a report of 16 cases. *Br J Radiol* 1988;61:1014.
111. Veldhuijzen FLMJ, Bonnier HJ, Michels HR, et al. Retrieval of undeployed stents from the right coronary artery—report of 2 cases. *Cathet Cardiovasc Diagn* 1993;30:245.
112. Hansing CE, Hammermeister K, Prindle K, et al. Cardiac catheterization experience in hospitals without cardiovascular surgery programs. *Cathet Cardiovasc Diagn* 1977;3:207.
113. Jollis JG, Peterson ED, Nelson CL, et al. Relationship between physician and hospital coronary angioplasty volume and outcome in elderly patients. *Circulation* 1997;95:2485.
114. Ellis SG, Weintraub W, Holmes D, Shaw R, Block PC, King SB. Relation of operator volume and experience to procedural outcome of percutaneous coronary revascularization at hospitals with high interventional volumes. *Circulation* 1997;96:2479.
115. Kastrati A, Neuman FJ, Schomig A. Operator volume and outcome of patients undergoing coronary stent placement. *J Am Coll Cardiol* 1998;32:970.
116. Hirshfeld JW, Ellis SG, Faxon DP, et al. Recommendations for the assessment and maintenance of proficiency in coronary interventional procedures—statement of the American College of Cardiology. *J Am Coll Cardiol* 1998;31:722.
117. Hildner FJ, Javier RP, Ramaswamy K. Pseudocomplications of cardiac catheterization. *Chest* 1973;63:15.
118. Hildner FJ, Javier RP, Tolentino A, Samet P. Pseudocomplications of cardiac catheterization: update. *Cathet Cardiovasc Diagn* 1982;8:43.

4
Percutaneous Approach, Including Transseptal and Apical Puncture

Donald S. Baim

Harvard Medical School; Center for Innovative Minimally Invasive Therapy, Brigham and Women's Hospital, Boston, Massachusetts 02115

In contrast with the direct brachial technique (see Chapter 5), the percutaneous approach to left and right heart catheterization achieves vascular access by needle puncture (1), and thus obviates surgical isolation of the vessel during either the insertion or the subsequent withdrawal of the cardiac catheter. Once the needle has been positioned within the vessel lumen, a flexible guidewire is advanced through the needle and well into the vessel being accessed (2). This guidewire remains in an intravascular position as the needle is withdrawn and provides the means for introducing the desired catheter. Although most operators once inserted end-hole catheters directly over the guidewire, current practice is to first place an introducing sheath over the guidewire, and then to advance the catheter through this sheath (3,4). This modification reduces patient discomfort and eliminates repetitive local arterial trauma during catheter exchanges, although it does increase the size of the puncture slightly (the outer diameter of the sheath is 1F size or 0.33 mm larger than the corresponding bare catheter). At the termination of the percutaneous catheterization procedure, the catheters and introducing sheaths are withdrawn, and bleeding from the puncture sites is controlled by the application of direct pressure.

Percutaneous entry via the femoral approach has become the dominant approach to cardiac catheterization. More than 85% of the procedures contained in the 1990 registry of the Society for Cardiac Angiography and Intervention were performed via this route (5). With appropriate skill and knowledge of regional anatomy, moreover, the same percutaneous techniques used for femoral artery and vein cannulation can be adapted to allow catheter insertion from a variety of other entry sites. Venous catheterization can thus be performed via the internal jugular, subclavian, or median antecubital vein, whereas arterial catheterization can be performed via the brachial, axillary, or radial arteries, or even the lumbar aorta.

CATHETERIZATION VIA THE FEMORAL ARTERY AND VEIN

Patient Preparation

After palpation of the femoral arterial pulse within the inguinal skin crease, a safety razor is used to shave an area approximately 10 cm in diameter surrounding this point. Although most catheterizations can be performed quickly and easily from a single groin, we have found it expedient to prepare both groins routinely. The right groin is generally used, since it is more easily accessed by the operator standing on that side of the table. If difficulties in catheter advancement force a switch to the other groin once the procedure has begun, however, having the left groin already prepared saves time and inconvenience. The shaved areas are scrubbed with a povidone-iodine/detergent mixture and then painted with povidone-iodine solution. The latter is blotted dry using a sterile towel and the patient is draped from clavicles to below the feet, leaving exposed only the sterile prepared groin areas. Most laboratories now use disposable paper drapes with adhesive-bordered apertures for this purpose, frequently packaged together with other disposable supplies (syringes, needles, bowls, and so on) in a custom kit available from any of several vendors.

Selection of Puncture Site

The adjacent femoral artery and vein (Fig. 4.1*A*, Fig. 4.1*B*) are the most commonly used vessels for percutaneous diagnostic cardiac catheterization (5). It is important to perform the punctures at the correct level (1 or 2 cm below the inguinal ligament) to facilitate vessel entry and avoid local vascular complications. To do so, some operators rely on the location of the inguinal skin crease to position the skin nicks through which puncture will be attempted (see later). We prefer locating the skin nicks in reference to the inguinal *ligament* (which runs from the anterior superior iliac spine to the pubic tubercle), since the position of the skin crease can be misleading in obese patients. More recently, we have begun to confirm the appropriate localization of the skin nick by fluoroscopy, which should show the nick to overlie the inferior border of the femoral head (6) (Fig. 4.1*C*, Fig. 4.1*D*). Making the skin nicks at this level increases the chance that needle puncture will take place in the common femoral segment, rather than too high (above the inguinal ligament) or too low (in the superficial femoral or profunda branches of the common femoral artery). The femoral artery should be easily palpable over a several-centimeter span above and below the skin nick site. The femoral vein will lie approximately one fingerbreadth medial to the artery, along a parallel course.

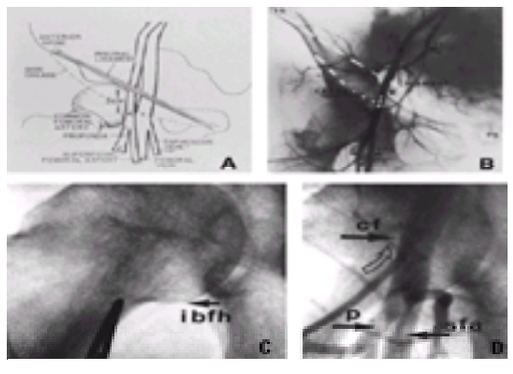

FIG. 4.1. Regional anatomy relevant to percutaneous femoral arterial and venous catheterization. **A:** Schematic diagram showing the right femoral artery and vein coursing underneath the inguinal ligament, which runs from the anterior superior iliac spine to the pubic tubercle. The arterial skin nick (indicated by X) should be placed approximately 3 cm below the ligament and directly over the femoral arterial pulsation, and the venous skin nick should be placed at the same level but approximately one fingerbreadth more medial. Although this level corresponds roughly to the skin crease in most patients, anatomic localization relative to the inguinal ligament provides a more constant landmark (see text for details). **B:** Corresponding radiographic anatomy as seen during abdominal aortography. **C:** Fluoroscopic localization of skin nick (marked by clamp tip) to the inferior border of the femoral head (ibfh). **D:** Catheter *(open arrow)* inserted via this skin nick has entered the common femoral artery (cf), safely above its bifurcation into the superficial femoral (sfa) and profunda branches. (For further details see Kim D, Orron DE, Skillman JJ, et al. Role of superficial femoral artery puncture in the development of pseudoaneurysm and arteriovenous fistula complicating percutaneous transfemoral cardiac catheterization. *Cathet Cardiovasc Diagn* 1992;25:91.)

Most difficulties in entering the femoral artery and vein—and most vascular complications—arise as the result of inadequate identification of these landmarks prior to attempted vessel puncture. Puncture of the artery at or above the inguinal ligament makes catheter advancement difficult and predisposes to inadequate compression, hematoma formation, and/or retroperitoneal bleeding following catheter removal. Puncture of the artery more than 3 cm below the inguinal ligament increases the chance that the femoral artery will have divided into its profunda and superficial femoral branches. Puncture in the crotch between these two branches fails to enter the arterial lumen, while puncture of either one of the branches increases the risk of false aneurysm formation or thrombotic occlusion due to smaller vessel caliber. Because the superficial femoral artery frequently overlies the femoral vein, low venous punctures may pass inadvertently through the superficial femoral artery, leading to excessive bleeding and possible arteriovenous fistula formation (6) (see Chapter 3).

Local Anesthesia

Adequate local anesthesia is essential for a successful catheterization. Inadequate anesthesia leads to poor patient cooperation and makes the time in the catheterization laboratory unpleasant for both patient and operator. Once the inguinal ligament and femoral artery have been identified, the femoral artery is palpated along its course using the three middle fingers of the left hand, with the uppermost finger positioned just below the inguinal ligament. Without moving the left hand, a linear intradermal wheal of 1% or 2% lidocaine is raised slowly by tangential insertion of a 25- or 27-gauge needle along a course overlying both the femoral artery and vein at the desired level of entry.

With the left hand remaining in place, transverse skin punctures are made over the femoral artery and vein, using the tip of a No. 11 scalpel blade. The smaller needle is then replaced by a 22-gauge 1.5-inch needle, which is used to infiltrate the deeper tissues along the intended trajectory for arterial and venous entry. As this needle is advanced, small additional volumes of lidocaine are infiltrated by slow injection. Each incremental infiltration should be preceded by aspiration so that intravascular boluses can be avoided. If the anesthetic track passes through the artery or vein, infiltration should be suspended until the tip of the needle has passed out of the back wall of the vessel and then continued to the full length of the needle or to the point where the needle tip contacts the periosteum. Approximately 10 to 15 mL of 1% xylocaine administered in this fashion usually provides adequate local anesthesia. The patient should be warned that he may experience some burning as the anesthetic is injected, but that the medication will abolish any subsequent sharp sensations.

Once local anesthesia has been achieved, the small skin nicks can be enlarged and deepened, using the tips of a curved “mosquito” forceps. This procedure decreases the resistance that is encountered during subsequent advancement of the needle and subsequent vascular sheath, and increases the likelihood that any vascular bleeding will become manifest as oozing through the puncture rather than hidden in the formation of a deep hematoma.

Femoral Vein Puncture

If right heart catheterization is to be performed or secure venous access is desired (for administration of fluids and medications, or rapid placement of a temporary pacing catheter), the femoral venous puncture is usually performed prior to arterial puncture. With the left hand palpating the femoral artery along its course below the inguinal ligament, the needle is introduced through the more medial skin nick. Classically, the 18-gauge thin-walled Seldinger needle, which consists of a blunt, tapered external cannula through which a sharp solid obturator projects (Fig. 4.2) was used for both arterial and venous access. The needle should be grasped so that the index and middle fingers lie below the lateral flanges of the needle and the thumb rests on the top of the solid obturator as the needle is advanced along the sagittal plane angled approximately 45° cephalad. Although this needle can occasionally be advanced up to its hub, the tip of the needle will usually stop more superficially as it encounters the periosteum of the underlying pelvic bones. The periosteum is well innervated and may be quite tender if the initial lidocaine infiltration failed to reach this level. Accordingly, forceful contact with the periosteum is neither necessary nor desirable. If the patient experiences significant discomfort, some operators will remove the obturator from the Seldinger needle and infiltrate additional lidocaine into the deep tissues through the outer cannula.

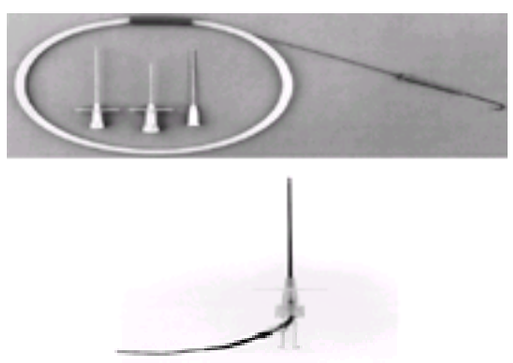

FIG. 4.2. Percutaneous needles and guidewire. **Top panel** shows a Seldinger needle (left) with its sharp solid obturator in place, a Potts-Cournand needle (center), which differs in the fact that its obturator is hollow and therefore allows the operator to see blood flashback as the artery is punctured, and an 18-gauge thin-wall needle (right) used for internal jugular vein puncture and now frequently also for arterial entry. These percutaneous needles are surrounded by an 0.038-inch, 145-cm J guidewire. **Bottom panel:** A Doppler-guided Smart Needle.

At this point, it is hoped that the Seldinger needle has transfixed the femoral vein. The obturator is removed, and a 10-mL syringe is attached to the hub of the cannula. The syringe and cannula are then depressed so that the syringe lies closer to the anterior surface of the thigh (Fig. 4.3) and the needle is more parallel (rather than perpendicular) to the vein. Gentle suction is applied to the syringe, and the whole assembly is slowly withdrawn toward the skin surface. In doing so, it is helpful to control the needle with both the left hand (which also rests on the patient's leg for support) and the right hand (which also controls the aspirating syringe). As the tip of the cannula is withdrawn into the lumen, venous blood will flow freely into the syringe.

FIG. 4.3. Seldinger technique for venous puncture. A skin nick has been created overlying the desired vein, which is punctured through and through by a Seldinger needle with its solid obturator in place. In the center panel, the obturator is removed and the needle cannula is attached to a syringe. Depression of the syringe toward the surface of the skin tents the vessel slightly and facilitates axial alignment of the cannula at the moment that slow withdrawal brings the tip of the cannula back into the vessel lumen. This is recognized by the sudden ability to withdraw venous blood freely into the syringe, which is then removed from the needle cannula to permit advancement of the J guidewire (shown here with a plastic straightener in place). Once the guidewire has been advanced safely into the vessel, the needle cannula can be removed.

We and most laboratories, however, have switched away from the Seldinger needle, in favor of an 18-gauge “single-wall-puncture” needle that has a sharpened tip

and lacks the inner obturator. Placement of a fluid-filled syringe on the needle's hub allows direct entry into the lumen of the vein, without the need to first exit the back wall and then pull back. Otherwise, the technique used after entry of the venous lumen has been achieved is identical. With the left hand stabilizing the needle, the right hand is used to remove the syringe and to advance a 0.035- or 0.038-inch J guidewire into the hub of the needle. The wire tip may be straightened by hyperextension of the wire shaft in the right hand or by leaving the tip of the wire within the plastic introducer supplied by the manufacturer. The wire should slide through the needle and 30 cm into the vessel with no perceptible resistance. Fluoroscopy should then show the tip of the guidewire just to the left (patient's right) of the spine.

If difficulty is encountered in advancing the guidewire, it should never be overcome by force. Fluoroscopy may simply reveal that the tip of the wire has lodged in a small lumbar branch; it can be drawn back slightly and redirected or gently prolapsed up the iliac vein. When resistance to advancement is encountered at or just beyond the tip of the needle, however, even greater care is required. This resistance may simply be caused by apposition of the tip of the needle to the back wall of the vein, which can be corrected by further depression of the needle hub, with or without slight withdrawal of the needle shaft. If this maneuver fails to allow free advancement of the wire, however, the wire should be removed, and the syringe should be reattached to the needle hub to ensure that free flow of venous blood is still present before additional wire manipulation is attempted; the wire should not be reintroduced unless free flow is obtained. If it is necessary to withdraw the wire, this should always be done gently, since it is theoretically possible for the wire to “snag” on the tip of the needle. Were this to occur, the needle and wire should be removed as a unit. If the wire still cannot be advanced after these manuevers, the needle should be withdrawn, and the puncture site should be compressed for 1 to 3 minutes. The anatomic landmarks should be reconfirmed and puncture reattempted. In some cases, puncturing the vein during a Valsalva maneuver may help by distending the femoral vein and making clean puncture more likely.

After the wire has freely entered the vein, the needle is removed, leaving the wire well within the vein and secured at the skin entry site by the left hand. The protruding wire is wiped with a moistened gauze pad, and its free end is threaded into the lumen of a sheath and dilator combination adequate to accept the intended right-sided heart catheter. All current sheaths are equipped with a backbleed valve and sidearm connector (Fig. 4.4) to control bleeding around the catheter shaft and to provide a means of administering drugs or extra intravenous fluids during the right-sided heart catheterization. The operator must make sure that he has control of the proximal end of the guidewire and that it is held in a fixed position as the sheath and dilator are introduced through the skin. Insertion is eased if the sheath and dilator are rotated as a unit while they are advanced progressively through the soft tissues. If excessive resistance is encountered, it may be necessary to remove the dilator from the sheath and to introduce the dilator alone before attempting to introduce the combination. If inspection shows that initial attempts have created significant burring at the end of the sheath, a new sheath should be obtained.

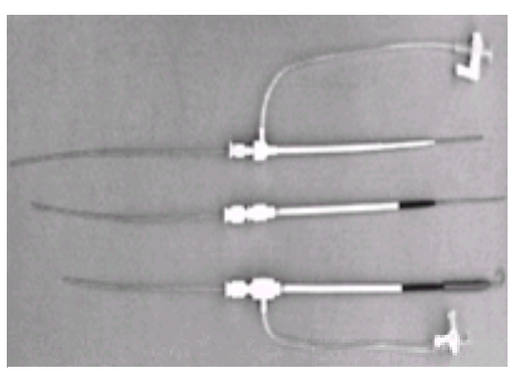

FIG. 4.4. Vascular sheaths. **Center:** An original sheath and dilator assembly (USCI “888”). In contrast to the original design, modern arteriovenous introducers are equipped with backbleed valves and sidearm attachment. **Top:** A Cordis sheath. **Bottom:** A USCI Hemaquet. Each device is inserted over a conventional guidewire as a unit, following which the inner Teflon dilator is removed to permit catheter introduction. The sidearm sheaths also permit fluid infusion and an additional site for pressure monitoring with the catheter in place.

Once the sheath is in place, the wire and dilator are removed, and the sheath is flushed by withdrawal of blood and injection of heparinized saline solution. In our laboratory we usually infuse the sidearm of the venous sheath from a 1-L bag of normal saline solution, connected via a sterile length of intravenous extension tubing, to maintain sheath patency and provide a carrier for drug administration by the nurse. Although drug administration can also take place via a peripheral intravenous line, the side arm of the sheath avoids any concerns about how quickly volume can be administered or whether infiltration of the peripheral line might jeopardize drug delivery in an emergency. Even if right heart catheterization is not planned, the femoral sheath makes it easy to place a right heart catheter or a temporary transvenous pacemaker lead if hemodynamic instability or bradyarrhythmia ensue.

Catheterizing the Right Heart from the Femoral Vein

A right (as well as a left) heart catheterization is needed to obtain a “full” profile of the hemodynamic state. Only the right heart catheterization can provide data regarding mean left heart filling pressure (the pulmonary capillary wedge, rather than just the post-a wave left ventricular end-diastolic pressure), detect pulmonary arterial hypertension, measure the cardiac output, and detect left-to-right intracardiac shunts. Leaving the right heart catheter in the pulmonary artery during the procedure also gives an ongoing measure of changes in the hemodynamic state as fluid and contrast loading take place, various medications (nitrates, diuretics, etc.) are given, and episodes of ischemia develop and are treated. For these reasons, our practice was once to perform a right heart catheterization in every patient who came to the cardiac catheterization laboratory.

In contrast, the 1990 Society for Cardiac Angiography and Intervention (SCA&I) survey showed that the practice was to perform right heart catheterization in only 28% of procedures (5). This practice has likely fallen further, after several standard-setting and regulatory agencies ruled that a left heart catheterization alone is adequate for most patients undergoing evaluation for coronary artery disease. The time (<5 minutes), added expense (<$100), and added risk (<1/10,000) of right heart catheterization are small, but so is the added information. We now skip the right heart catheterization in patients with a primary diagnosis of coronary artery disease, unless they have symptoms of congestive heart failure, noninvasive evidence of depressed left ventricular function or associated valvular disease, or recent myocardial infarction. In such patients, however, we still believe that the quantitation of overall hemodynamic function provided by right heart catheterization justifies performance of this low-risk adjunctive part of the overall catheterization evaluation.

If right heart catheterization *is* to be performed, the desired right heart catheter (Fig. 4.5) is flushed, attached to the venous manifold, introduced into the sheath, and advanced up the inferior vena cava. Although conventional woven Dacron (Goodale-Lubin or Cournand) catheters provide excellent torque control, their inherent stiffness makes them poorly suited for routine use in a training laboratory. We therefore for a time used 7F Swan-Ganz catheters to exploit their ease of passage, low risk of injury to the right-sided heart chambers, and ability to perform thermodilution measurements of cardiac output. Unfortunately, such soft catheters have poor frequency response (see Chapter 7), do not adequately transmit the torque required for easy catheterization of the right-sided heart from the femoral approach, and accept only 0.021-inch guidewires. To bridge this gap, we have begun using a stiffer, balloon-tipped catheter [PWP monitoring catheter (USCI, Billerica, MA)] that combines the safety of the Swan-Ganz catheter with the catheter control and frequency response previously found only in the woven Dacron catheters. The larger lumen diameter and stiffer wall of this catheter (compared with the traditional Swan-Ganz design) improve frequency response and allow the passage of conventional 0.035- and 0.038-inch-diameter guidewires when necessary. When temporary pacing is desired, this catheter is also available with bipolar pacing capacity (Baim-Turi, USCI).

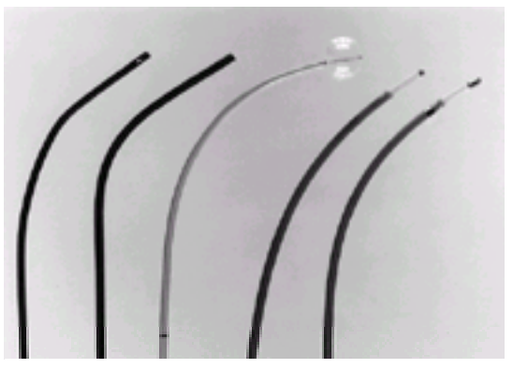

FIG. 4.5. Right-sided heart catheters used from the femoral approach. **Left:** Woven Dacron Goodale-Lubin, Cournand catheters. **Center:** Swan-Ganz catheter. **Right:** Newer balloon catheters, including the PWP pressure measurement catheter and the Baim-Turi catheter with bipolar pacing electrodes (USCI).

Deviation of the catheter tip from its paraspinous position during advancement from the leg suggests entry into a renal or hepatic vein, which can be corrected by slight withdrawal and rotation of the catheter. Once the catheter is above the diaphragm and within the right atrium, it is rotated counterclockwise to face the lateral wall of the right atrium (Fig. 4.6). Additional counterclockwise rotation and gentle advancement allow passage of the catheter tip into the superior vena cava, which is contiguous with the posterolateral wall of the right atrium. In contrast, anterior orientation of the catheter tip at this point may result in its entrapment in the right atrial appendage and inability to reach the superior vena cava. Alternatively, the tip of the catheter can be withdrawn to the inferior vena cava, and a 0.035-inch J guidewire can be introduced to bridge the straight line path from the inferior to the superior vena cava, along the back wall of the right atrium. Once in position, a baseline superior vena caval blood sample is obtained for measurement of oxygen saturation and comparison with the subsequently measured pulmonary arterial blood oxygen saturation, to screen for unsuspected left-to-right shunts. The catheter is then flushed with heparinized saline solution and withdrawn to the right atrium for pressure measurement.

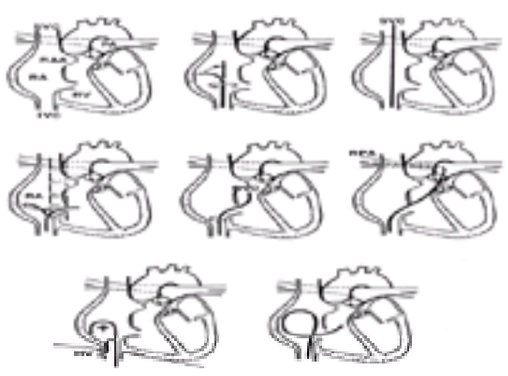

FIG. 4.6. Right heart catheterization from the femoral vein, shown in cartoon form. **Top Row:** The right heart catheter is initially placed in the right atrium (RA) aimed at the lateral atrial wall. Counterclockwise rotation aims the catheter posteriorly and allows advancement into the superior vena cava (SVC). Although not evident in the figure, clockwise catheter rotation into an anterior orientation would lead to advancement into the right atrial appendage (RAA), precluding SVC catheterization. **Center row:** The catheter is then withdrawn back into the right atrium and aimed laterally. Clockwise rotation causes the catheter tip to sweep anteromedially and cross the tricuspid valve. With the catheter tip in a horizontal orientation just beyond the spine, it is positioned below the right ventricular outflow (RVO) tract. Additional clockwise rotation causes the catheter to point straight up, allowing for advancement into the main pulmonary artery and from there into the right pulmonary artery (RPA). **Bottom row:** Two maneuvers useful in catheterization of a dilated right heart. A larger loop with a downward-directed tip may be required to reach the tricuspid valve and can be formed by catching the catheter tip in the hepatic vein (HV) and advancing the catheter quickly into the right atrium. The reverse loop technique (bottom right) gives the catheter tip an upward direction, aimed toward the outflow tract.

To advance a catheter from the femoral vein to the pulmonary artery, the tip of the catheter is positioned in the lower portion of the right atrium, directed toward its lateral border. If a balloon flotation catheter is being used, the balloon is inflated at this point. Clockwise rotation is applied, which causes the catheter tip to sweep the anterior and anteromedial wall of the right atrium, along which the tricuspid valve is located (see Fig. 4.6). As the catheter tip passes over the tricuspid orifice, slight advancement causes it to enter the right ventricle, where pressure is again recorded. If the right atrium is enlarged, greater curvature of the catheter may be necessary (i.e., a large J loop). Such a loop may be formed by bending the tip of the catheter against the lateral right atrial wall or by engaging in the ostium of the hepatic vein (just below the diaphragm). This larger loop can then be rotated clockwise in the atrium as described earlier, causing the tip of the catheter to enter the right ventricle. Right ventricular pressure is then recorded.

Simple advancement of the catheter in the right ventricle causes the tip to move toward the apex of that chamber and usually does not result in catheterization of the pulmonary artery. To achieve this latter end, the catheter must be withdrawn slightly so that its tip lies horizontally and just to the right (patient's left) of the spine. In this position, clockwise rotation causes the tip of the catheter to point upward (and slightly posteriorly) in the direction of the right ventricular outflow tract (Fig. 4.6). The catheter should be advanced only when it is in this orientation to minimize the risk of ventricular arrhythmias or injury to the right ventricle. Advancement may be facilitated if performed as the patient takes a deep breath. If these maneuvers fail to achieve access to the pulmonary artery due to enlargement of the right atrial and ventricular chambers, the catheter may be withdrawn to the right atrium and formed into a large “reverse loop,” which allows the tip of the catheter to cross the tricuspid valve in an upward orientation more likely to enter the outflow tract (Fig. 4.6, bottom right). When manipulated appropriately, the catheter tip should cross the pulmonic valve and advance to a wedge position without difficulty. Having the patient take a deep breath and cough during advancement is often of assistance in achieving a wedge position. Alternatively, a small amount of air may be released from the balloon to decrease its size and facilitate wedging in a smaller, more distal branch of the pulmonary artery. Catheters advanced from the leg are more likely to seek the left pulmonary artery, whereas catheters advanced from above tend to seek the right pulmonary artery as they make a continuous counterclockwise curve through the right heart chambers. If needed, either pulmonary artery can be catheterized by appropriate manipulation or careful introduction of a curved J guidewire, although we generally do not like to extend guidewires into the thin-walled pulmonary arteries unless absolutely necessary. Following measurement of the wedge pressure, the balloon (if a balloon-tip catheter is being used) is deflated, and the catheter is withdrawn into the more proximal left or right pulmonary artery. There, pulmonary arterial pressure is measured and another blood sample for measurement of oxygen saturation is obtained. If a more simultaneous “snapshot” of the hemodynamic state is desired, these “entry” pressures can be rerecorded during a right-sided heart pullback. For practical reasons, we now tend to rerecord only the wedge pressure (simultaneous with the left ventricular pressure) and pulmonary artery pressure, coincident with the measurement of the cardiac output. We then leave the right heart catheter in the proximal pulmonary artery for the duration of the case, allowing continuous monitoring of the pulmonary artery diastolic pressure as an index of volume status and ischemic left ventricular dysfunction.

Attempts to perform right heart catheterization occasionally result in entry into other structures. If a woven Dacron catheter is advanced in the right atrium with a posteromedial orientation, it may cross a patent foramen ovale and enter the left atrium. This is sometimes hard to detect by catheter position alone because the catheter appearance in the left atrium or ventricle may be indistinguishable (in the anteroposterior view) from its course during usual right heart catheterization. It can, however, be recognized by a change in the pressure waveform, position of the catheter tip across the spine, and ability to withdraw fully oxygenated blood from the catheter tip. Although more unusual, a woven Dacron catheter can also enter the ostium of the coronary sinus, located inferiorly and posteriorly to the tricuspid orifice. There will be continued presence of a right atrial waveform, but blood sampling will disclose a far lower oxygen saturation (20% to 30%) than was present in the superior vena cava. Anatomic abnormalities can also be suspected when the catheter takes an unusual position or course during attempted right heart catheterization. Figure 4.7 depicts the appearance of the right-sided heart catheter course in three such congenital abnormalities (persistent left superior vena cava, patent ductus arteriosus, and anomalous pulmonary venous return). The most important points about these side trips off the beaten path to the right ventricle are that the operator should recognize that the tip of the catheter is not in the right ventricle (i.e., one should not attempt to get to the pulmonary artery) and should decide where the catheter is (by pressure monitoring, saturation analysis, or hand injection of a small amount of contrast agent) before withdrawing the catheter to the right atrium and proceeding with the right heart catheterization.

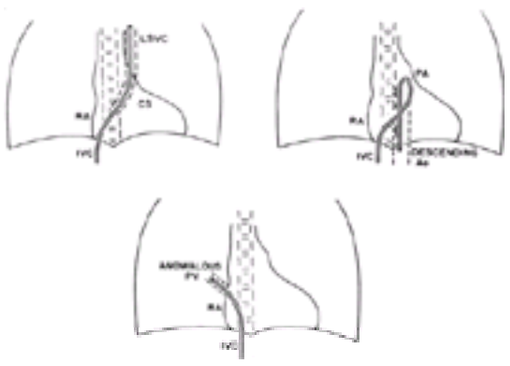

FIG. 4.7. Unsuspected anatomic abnormalities frequently can be detected by an unusual catheter course or position. **Upper left panel:** The course of a catheter passed from the femoral vein to the inferior vena cava (IVC), right atrium (RA), coronary sinus (CS), and up into an anomalous left superior vena cava (LSVC). **Upper right panel:** The catheter crossing from the pulmonary artery (PA) to the descending aorta (Ao) by way of a patent ductus arteriosus. **Bottom panel:** The catheter entering an anomalous pulmonary vein draining into the right atrium.

In patients with elevated right heart pressures, prior placement of an inferior vena caval filter or umbrella, those undergoing specialized procedures (endomyocardial biopsy, coronary sinus catheterization), or those in whom prolonged postprocedure monitoring with a balloon-flotation catheter is desired, the *right internal jugular vein* offers an excellent alternative to the femoral vein. The technique for jugular puncture is described in Chapter 20, and the method of advancing the right-sided heart catheter to the pulmonary artery is identical to that described for the brachial approach in Chapter 5. On occasion, percutaneous right heart catheterization is performed from the subclavian or median basilic vein using a similar technique.

Femoral Artery Puncture

The common femoral artery is punctured by inserting the Seldinger or single-wall-puncture needle through the more lateral skin nick. Again, the needle is inserted at approximately 45° along the axis of the femoral artery as palpated by the three middle fingers of the left hand. The experienced operator may feel the transmitted pulsations as the tip of the needle contacts the wall of the femoral artery. With the Seldinger needle it is customary to advance the needle completely through the artery until the periosteum is encountered. The obturator is then removed, and the hub of the needle is depressed slightly toward the anterior surface of the thigh. Arterial pressure makes it unnecessary to attach a syringe to the cannula, so that both hands can be used to stabilize the needle as it is slowly withdrawn. When the needle comes back into the lumen of the femoral artery as evidenced by vigorous pulsatile flow of arterial blood, a 0.035- or 0.038-inch J guidewire should then be advanced carefully into the needle.

If a single wall puncture is desired, the operator may prefer a Potts-Cournand needle (Fig. 4.2), in which the obturator has a small lumen that transmits a flashback of arterial blood as the vessel is entered, or the same single-wall-puncture needle described for venous entry. When the femoral pulse is difficult to palpate or numerous needle insertions have been fruitless, it may be easiest to utilize the 18-gauge SmartNeedle (CardioVascular Dynamics, Irvine CA; see Fig. 4.2, bottom panel). The obturator of this device contains a Doppler crystal that helps aim the needle tip toward the center of the arterial lumen. Pulsatile arterial flow has auditory characteristics that distinguish it clearly from the more continuous venous flow signals detected from the adjacent femoral vein.

Whichever needle is used to enter the arterial lumen, the guidewire introduced through the needle should move freely up the aorta [located to the right (patient's left) side of the spine on fluoroscopy] up to the level of the diaphragm. When difficulty in advancing the guidewire is encountered at or just beyond the tip of the needle and is not corrected by slight depression or slight withdrawal of the needle, the guidewire should be withdrawn to ensure that vigorous arterial flow is still present before any further wire manipulation is attempted. If flow is not brisk or if the wire still cannot be advanced, the needle should be removed and the groin should be compressed for 5 minutes. The operator should verify the correctness of the anatomic landmarks and attempt repuncture of the femoral artery. If the second attempt is unsuccessful in allowing wire advancement, a third attempt on the same vessel is unwise, and an alternative access site should generally be selected.

If wire motion is initially free but resistance is encountered after several centimeters (particularly if the patient complains of any discomfort during wire advancement), extensive iliac disease or subintimal position of the wire is possible. The wire should be pulled back slightly under fluoroscopic control and the needle should be removed as the left hand is used to stabilize the wire and control arterial bleeding. After the wire is wiped with a moist gauze pad, a small (5F) dilator can be cautiously introduced to a point just below where wire movement became difficult. The wire is then withdrawn from the dilator, which is aspirated to ensure free flow of blood and flushed carefully. A small bolus of contrast medium (either a low-osmolar agent or ionic contrast diluted to half strength, to avoid local discomfort) is then injected gently under fluoroscopic monitoring. This should disclose the anatomic reason for difficult wire advancement—generally either iliac tortuosity, stenosis, or dissection. Problems advancing the wire above the aortic bifurcation may also suggest the presence of an abdominal aortic aneurysm (7), which warrants use of soft-tip guidewires and extreme care to avoid perforation or dislodgment of cavitary thrombus or debris. If contrast injection through the small dilator reveals that subintimal wire passage has occurred, retrograde left heart catheterization should be relocated to the other femoral artery or to the brachial or radial artery and the patient should be observed for signs of progressive dissection or arterial compromise, both of which are fortunately rare with retrograde guidewire dissections. If the problem turns out to be more tortuosity or stenosis (Fig. 4.8*A*), a more specialized guidewire (e.g., a steerable peripheral guidewire such as a Wholey, or a hydrophyllic-coated guidewire such as the Terumo Glidewire) may be carefully reintroduced through the dilator in an attempt to reach the descending aorta. In an era when the obstructing lesion can be quickly and effectively treated by angioplasty or stent placement (see Chapter 27), iliac stenosis is no longer a firm indication to abandon retrograde left heart catheterization

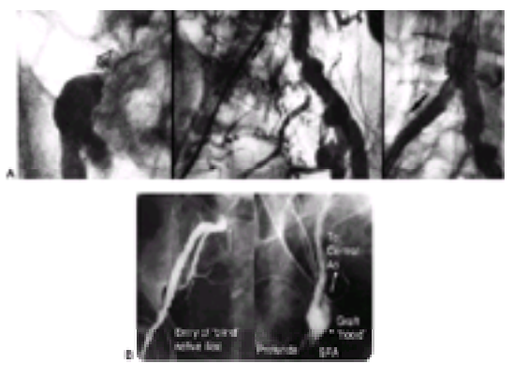

FIG. 4.8. A: Entry of the right femoral artery was straightforward, but guidewire advancement stopped in the iliac system. **Left:** Contrast injection through a 5F dilator shows severe iliac stenosis with extensive cross-pelvic collaterals. This was crossed with a Terumo Glidewire to allow completion of the diagnostic angiography and a right coronary artery angioplasty (not shown). **Center:** Injection in the abdominal aorta shows the proximal extent of the iliac stenosis. **Right:** Iliac stenosis then dilated and treated by placement of a Palmaz-Schatz iliac stent, with restored antegrade iliac flow. **B:** Retrograde left heart catheterization in a patient with previous aortic-bifemoral grafting (left) entry of the graft hood has resulted in passage of the wire into the “blind” native iliac. In a RAO projection, the more anterior pathway to the central aorta (Ao) via the graft can be seen overlying the native iliac, with the bifurcation of the common femoral artery into the profunda and superficial femoral artery (SFA) just below.

In an aging population with diffuse atherosclerotic disease, the question of performing left heart catheterization via a prosthetic (e.g., aortobifemoral) graft arises frequently (8,9). This is not an ideal approach because the graft wall is tough (making sheath insertion difficult), such grafts may contain diffuse atherosclerotic or thrombotic debris, and graft closure or serious graft infection may occur. The graft should be identified as a separate structure from the adjacent native femoral artery and punctured using a front-wall approach. Even if the graft hood is punctured correctly, the guidewire may pass through the anastomosis and into the native femoral artery rather than proximally up the graft (8). In that event, contrast injections through a small dilator in a right anterior oblique (RAO) projection (right leg) and the use

of special steerable guidewires may be required to remain within or cross into the graft lumen, and thereby reach the descending aorta (Fig. 4.8*B*). A vascular introducing sheath should always be used to avoid excessive friction during catheter movement, or excessive traction on catheter tips during withdrawal, but may require the use of serial dilators for passage of the sheath through the tough graft wall. This approach via a vascular graft can thus be used with care, particularly when other alternatives (e.g., brachial, axillary, or radial artery) are themselves less than desirable. Some operators choose to administer prophylactic antibiotics [Kefzol (Eli Lilly, Indianapolis, IN) 1 g every 8 hours for 24 hours] when accessing a prosthetic graft.

Catheterizing the Left Heart from the Femoral Artery

Once the guidewire has been advanced to the level of the diaphragm and the needle has been removed, the operator's left hand is used to stabilize the wire and control arterial bleeding while the wire is wiped with a moistened gauze pad to remove any adherent blood. If the catheter is to be introduced directly into the artery, the soft tissues are predilated by brief introduction of a Teflon arterial dilator one F-size smaller than the intended catheter, before inserting the left heart catheter itself. Essentially all left heart catheterizations from the femoral approach, however, are now performed using an appropriate-sized vascular sheath (e.g., a 7F sheath for a 7F catheter) that is equipped with a backbleed valve and sidearm tubing as described earlier. The 15-cm length sheath is commonly used for diagnostic catheterization but can only reach the mid-iliac. In the presence of severe tortuosity, it may be preferable to use the 23-cm-length sheath designed for interventional procedures, which is sufficiently long to enter the distal aorta above the bifurcation. This helps to improve the torque responsiveness of diagnostic catheters under those circumstances.

The chosen sheath is introduced over the guidewire (the proximal end of which is held in a straightened, fixed position) with a rotational motion, following which the guidewire and dilator are removed and the sheath is aspirated, flushed, and connected to a pressurized flush system [Intraflo II (30 mL/hr), Abbot Critical Care, North Chicago, IL] to avoid clot formation in the sheath. Alternatively, this sidearm can be connected to a manifold for monitoring arterial pressure at a separate site (e.g., during passage of a pigtail catheter across a stenotic aortic valve). This sheath should be “power” flushed immediately after each catheter is introduced or withdrawn, by briefly activating the Intraflow device.

Classically, once the sheath had been inserted, the guidewire was removed. The desired left heart catheter was then flushed and loaded with a 145-cm J guidewire and its nose was introduced into the backbleed valve of the sheath. The soft end of the guidewire was then advanced carefully through the catheter, out the end of the sheath, and to the level of the diaphragm before the catheter itself was advanced. One concern, however, is that readvancement of the guidewire out the end of the sheath can cause vascular injury if severe iliac tortuosity or disease is present. We therefore adopted a modified technique in which a short-exchange length (175 cm) Newton J (Cook, Bloomington, IN) is placed through the access needle and its tip is left at the diaphragm as the dilator is removed from the sheath and the left heart catheter is inserted. This obviates the need to renegotiate complex iliofemoral anatomy with the guidewire.

Once the catheter has been advanced to the desired level (either above the diaphragm or into the ascending aorta), the guidewire is removed, so that the catheter can be connected to the arterial manifold and double-flushed (withdrawal and discarding of 10 mL of blood, followed by injection of heparinized saline solution). All subsequent left heart catheters are then introduced by reinserting this wire to the level of the diaphragm (allowing one catheter to be removed and the second to be reintroduced safely), rather than withdrawing the first catheter completely and then inserting the second catheter and wire through the sheath *de novo.* Of course if the left heart catheterization is being performed without the aid of a sheath, the operator must leave the tip of the wire in the abdominal aorta during the removal of the first catheter and the introduction of a second catheter to retain access to the vessel. These “over-the- wire” catheter exchanges are facilitated by extending the back end of the wire straight down the patient's leg and holding it fixed there to ensure that the wire remains in constant position within the aorta as the newer catheter is advanced.

A Word About Heparin

As described in Chapter 3, early catheterizations from the femoral artery had a higher incidence of major complications than catheterization from the brachial artery. One difference was that brachial catheterization utilized systemic heparinization to avoid thrombosis in the smaller brachial artery with a potentially occlusive catheter in its lumen. When systemic heparinization was adopted in femoral procedures, the rates of complications became equivalent. On this basis, the practice of full intravenous heparinization (5,000 U) immediately after the left-sided sheath was inserted, became a standard way to provide therapeutic anticoagulation that lasted at least 40 minutes in most patients. Lesser amounts of heparin (2,500 to 3,000) may also be used, particularly in smaller patients. If it is decided to perform catheter-based coronary intervention, larger heparin doses (usually 10,000 U, or 70 to 100 U/kg) are required, which will require further supplementation if a smaller heparin dose has been administered for the immediately preceding diagnostic procedure. This type of higher heparin dosing is routinely monitored by an activated clotting time (ACT) machine in the cardiac catheterization laboratory, and titrated to an ACT of roughly 300 seconds (10). If it is planned to use an intravenous IIb/IIIa receptor blocker, lower levels of heparin anticoagulation (ACT 250 to 275) may be desired to prevent excessive bleeding risk. Given the limitations of heparin (see Chapter 3), other anticoagulant agents, including low-molecular-weight heparins and other direct-acting thrombin antagonists, are being explored for cardiac catheterization procedures.

While the use of heparin is mandatory for interventional or prolonged diagnostic procedures, many laboratories have abandoned the use of systemic heparinization for simple diagnostic catheterizations, where the complications are extremely low with or without heparin (11). For this issue to be decided scientifically, more than 100,000 patients would have to be randomized to undergo diagnostic catheterization with and without systemic heparinization. Absent such trial data, we are now less likely to use systemic heparinization for simple procedures but still feel that systemic heparinization is appropriate for more prolonged or complex diagnostic catheterizations, cases where a guidewire will be required to cross a stenotic aortic valve, and (absolutely) for all percutaneous coronary interventions.

If systemic heparinization is used, its effects must be reversed at the termination of the left heart catheterization and associated angiography. This is usually accomplished by the administration of protamine (1 mL = 10 mg of protamine for every 1,000 IU of heparin) (12). The operator should be watchful for potential adverse reactions to protamine, characterized by hypotension and vascular collapse, as discussed in Chapter 3. Protamine reactions appear to be more common in insulin-dependent diabetics and patients with previous protamine exposure, who are more likely to have elevated levels of IgG or IgE antiprotamine antibodies (13). Although severe protamine reactions in these patients are uncommon, we prefer delaying sheath removal for approximately 1 hour in insulin-dependent diabetics to allow heparin to wear off without protamine administration. This is also our practice in patients with unstable symptoms, threatening anatomy, where there is a concern that abrupt reversal of the heparin effect may trigger thrombosis.

Catheter Selection

The initial left heart catheter in most cases is a pigtail catheter with multiple side holes (Fig. 4.9). This catheter usually can be flushed in the descending aorta and then advanced to the ascending aorta without difficulty. If left ventricular and femoral arterial (sheath side arm) pressures are being monitored (as in catheterization to evaluate aortic stenosis), the rough equality of central aortic and femoral arterial pressure should be confirmed at this time (Fig. 4.10) (3,4,14). The systolic peak in the femoral waveform may be slightly delayed and accentuated compared with the ascending aortic pressure trace, but the diastolic and mean pressures should be virtually identical. A greater difference in mean pressure between the catheter and the sheath may be seen in a patient with an extensively diseased iliac artery and may require the use of a longer sheath, as described earlier. For the highest-pressure fidelity, the sheath size should be one F larger than the intended left heart catheter (e.g., a 6F pigtail advanced through a 7F sheath). Alternatively, catheters can be advanced from separate arterial entry sites to record left ventricular and ascending aortic pressure, or a specially designed 8F pigtail with separate end lumens and a side-hole lumen may be used to perform such pressure recordings (15).

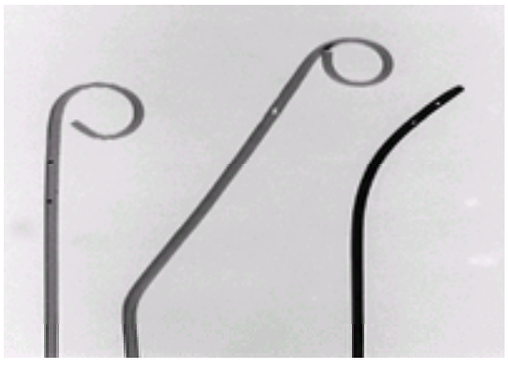

FIG. 4.9. Left heart catheters used from the femoral approach. **Left to right:** Pigtail, 145° angled pigtail, and Teflon Gensini catheter (no longer in common use). All three catheters have an end hole to allow placement over a guidewire and multiple side holes to minimize the tendency for catheter whipping or intramyocardial

injection during power injection of contrast.

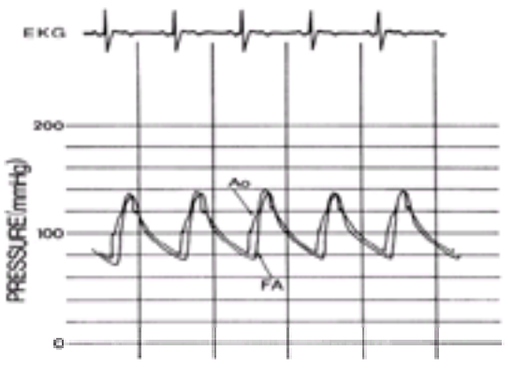

FIG. 4.10. Central aortic pressure (Ao) measured through a 7.3F pigtail catheter (Cook) and femoral artery (FA) pressure measured from the sidearm of an 8F arterial sheath (Cordis, Miami Lakes, FL). Only minimal damping of the femoral artery pressure is seen, blunting its systolic overshoot, which frequently exceeds central aortic systolic pressure (see Chapter 9). With larger (7.5F and 8F) catheters, more damping may occur in the sidearm pressure. Catheter and sidearm are connected to small-volume-displacement transducers without intervening tubing.

Crossing the Aortic Valve

After measurement of the ascending aortic pressure, the pigtail catheter is advanced across the aortic valve and into the left ventricle. If the aortic valve is normal and the pigtail is oriented correctly, it will usually cross the valve directly. In many cases, however, it may be necessary to advance the pigtail down into one of the sinuses of Valsalva to form a secondary loop (Fig. 4.11). As the catheter is withdrawn slowly, this loop will open to span the full diameter of the aorta, at which point a very subtle further withdrawal will often cause the pigtail to fall across the valve.

FIG. 4.11. Crossing the aortic valve with a pigtail catheter. **Top row, left:** Although a correctly oriented pigtail catheter will frequently cross a normal aortic valve directly, it may also come to rest in the right or noncoronary sinus of Valsalva. **Top row, center:** Further advancement of the catheter enlarges the loop to span the aortic root and positions the catheter. **Top row, right:** Slow withdrawal causes the catheter to sweep across the aortic orifice and fall into the left ventricle. **Bottom row, left:** To cross a stenotic aortic valve, the pigtail catheter must be led by a segment of straight guidewire. Increasing the length of protruding guidewire straightens the catheter curve and causes the wire to point more toward the right coronary ostium; reducing the length of protruding wire restores the catheter curve and causes the wire to point more toward the left coronary. Once the correct length of wire and the correct rotational orientation of the pigtail catheter have been found, repeated advancement and withdrawal of both the catheter and guidewire as a unit will allow the wire to cross the valve. **Bottom row, center:** In a dilated aortic root, an angled pigtail provides more favorable wire positions. **Bottom row, right:** In a small aortic root, a Judkins right coronary catheter may be preferable.

If significant aortic stenosis is present, the pigtail must be advanced across the valve with the aid of a straight 0.038-inch guidewire. Approximately 6 cm of the guidewire is advanced beyond the end of the pigtail catheter, and the catheter is withdrawn slightly until the tip of the guidewire is leading (Fig. 4.11). The position of the tip of the guidewire within the aortic root can then be controlled by rotation of the pigtail catheter and adjustment of the amount of wire that protrudes. Less wire protruding directs the wire tip more toward the left coronary ostium, whereas more wire protruding directs the wire more toward the right coronary ostium. With the wire tip positioned so that it is directed toward the aortic orifice, the tip of the wire usually quivers in the systolic jet. Wire and catheter are then advanced as a unit until the wire crosses into the left ventricle. If the wire buckles in the sinus of Valsalva instead of crossing the valve, the catheter-wire system is withdrawn slightly and readvanced with or without subtle change in the length of protruding wire or the orientation of the pigtail catheter. Alternatively, some operators prefer to leave the pigtail catheter fixed and move the guidewire independently in attempts to cross stenotic aortic valves. In either case, the wire should be withdrawn and cleaned and the catheter should be double-flushed vigorously every 3 minutes despite systemic heparinization. If promising wire positions are not obtained, the process should be repeated using a different catheter: an angled pigtail or left Amplatz catheter if the aortic root is dilated or a Judkins right coronary catheter if the aortic root is unusually narrow (16). Other catheters have been proposed for this purpose (17), but we have found these standard catheters to suffice in virtually all cases.

When the tip of the guidewire is across the aortic valve, additional wire should be inserted before any attempt is made to advance the catheter itself. Otherwise the catheter may be diverted into a sinus of Valsalva, causing the wire to flip out of the left ventricle. The straight wire should be advanced carefully, since there is a potential (admittedly small in the hypertrophic left ventricle of a patient with aortic stenosis) to perforate the left ventricular wall if the guidewire is advanced further when it has become trapped in an endocardial surface feature. Once the catheter is in the left ventricle, the wire is immediately withdrawn and the catheter is aspirated vigorously, flushed, and hooked up for pressure monitoring, so that a gradient can be measured even if the catheter is rapidly ejected from the left ventricle or must be withdrawn because of arrhythmia. When using a left Amplatz catheter to cross a stenotic valve, however, we prefer to cross the valve with a full-exchange-length (260-cm) guidewire. Once the tip of this wire has entered the left ventricle, it is left in position as the Amplatz catheter is removed, and a conventional pigtail catheter is substituted before an attempt is made to measure left ventricular (LV) pressure.

The same approach applies to retrograde catheterization across a porcine aortic valve prosthesis, although it is more common to use a J-tip guidewire to help avoid the area between the support struts and the aortic wall. Ball valves (Starr-Edwards, Baxter-Healthcare, Santa Ana, CA) can be crossed retrograde with this approach, but use of a small (4F or 5F) catheter will minimize the amount of aortic regurgitation resulting from catheter interference with diastolic ball seating. Tilting disc valves (Bjork-Shiley, Shiley, Inc., Irvine, CA; St. Jude Medical, St. Paul, MN; Sulzer Carbomedics, Austin, TX), however, should not be crossed retrograde because of the potential for producing torrential aortic regurgitation, catheter entrapment, or even disc dislodgement, if the catheter passes across the smaller (minor) orifice. Although safe passage through the major orifice may be possible under careful fluoroscopic control (18), we still prefer a transseptal or even apical puncture approach (see later) when it is necessary to enter the left ventricle in a patient who has a tilting disc valve in the aortic position.

Control of the Puncture Site Following Sheath Removal

After the effect of heparin (if used) has been reversed by Protamine or has been allowed to wear off (to an ACT < 160 seconds), the arterial catheter and sheath are removed. The standard way to control the puncture site and promote the formation of a hemostatic plug is to apply firm manual pressure. This is best done using three fingers of the left hand that are positioned sequentially up the femoral artery beginning at the skin puncture. With the fingers in this position, there should be no ongoing bleeding into the soft tissues or through the skin puncture. It should be possible to apply sufficient pressure to obliterate the pedal pulses and then release just enough pressure to allow them to barely return. This pressure is then gradually reduced over the next 10 to 15 minutes, at the end of which time pressure is

removed completely. The venous sheath is usually removed 5 minutes after compression of the arterial puncture has begun, with gentle pressure applied over the venous puncture using the right hand. To avoid tying up the catheterization laboratory during this period, the patient is usually taken to a special “holding room” in the catheterization laboratory or back to his hospital bed before the sheaths are removed. If such relocation is to be performed prior to sheath removal, it is important that the sheaths be secured in place (suture, or at least tape) to prevent them from being pulled out during transport.

After procedures using larger arterial sheaths (i.e., PTCA or balloon valvuloplasty), or performed in the setting of thrombolytic agents or IIb/IIIa receptor blockers, more prolonged compression (30 to 45 minutes) is typically required. To avoid fatigue of the operator or other laboratory personnel performing compression, we typically use a mechanical device such as the Compressar (Instromedix, Beaverton, OR) or FemoStop (USCI, Billerica, MA)] to apply similar local pressure. These devices can be equally or even more effective in prolonged holds (19), but we still prefer manual compression for removal of smaller (6F and 7F) sheaths or in patients with peripheral vascular disease or prior peripheral grafting surgery that makes it important to avoid compressive occlusion or flow restriction that may cause arterial occlusion. In every case, however, it should be emphasized that a trained person must be in attendance throughout the compression to ensure that the device is providing adequate control of puncture site bleeding and is not compromising distal perfusion.

After compression has been completed, the puncture site and surrounding area are inspected for hematoma formation and active oozing, and the quality of the distal pulse is assessed before application of a bandage.

It is our policy to keep the patient at bedrest with the leg straight for 4 to 6 hours following percutaneous femoral catheterization (20), with a sandbag in place over the puncture site for the first few hours after catheter removal. In patients at higher risk for rebleeding (those with hypertension, obesity, or aortic regurgitation), application of a pressure bandage in addition to the sandbag may be of value. Although the patient should be instructed not to move the leg for several hours following the catheterization procedure, the patient does not have to lie flat during this time. Elevation of the head and chest to 30° to 45° by the electrical or manual bed control, without muscular effort by the patient, will greatly increase the patient's comfort and will not increase the risk of local bleeding. The only reason to insist that the patient lie completely flat is if there is significant orthostatic hypotension. Before ambulation and again before discharge, the puncture site should be reinspected for recurrent bleeding, hematoma formation, development of a bruit suggestive of pseudoaneurysm or A-V fistula formation, or loss of distal pulses.

Puncture Closure Devices

The technique described earlier relies on manual or mechanical pressure for initial control of arterial bleeding and then on local hemostasis for ongoing plugging of the arterial puncture site. The potential for ongoing bleeding (with formation of hematoma, false aneurysm, or arteriovenous fistula) has already been described in Chapter 2 and tends to be more common with interventional procedures that require larger sheath size or more aggressive postprocedure antithrombotic therapy. This has prompted the development of a variety of new devices that seek to provide more positive closure of the arterial puncture site (Fig. 4.12). The simplest device (Vasoseal, Datascope, Paramus, NJ) applies a collagen plug in the skin track apposed to outer wall of the femoral artery (21). In randomized trials, this device shortens the time to hemostasis (from 17 to 4 minutes) and ambulation (from 19 to 13 hours), without clear benefit in terms of hematoma formation or the need for vascular surgery compared with manual compression. In diagnostic catheterization, it can also accelerate time to ambulation to 1 to 2 hours (22). Next in complexity is the AngioSeal hemostatic punc- ture closure device (Sherwood, Davis & Geck), which positions a rectangular absorbable “anchor” made of absorbable suture material against the inside wall of the artery and uses an attached suture to winch a small collagen plug down against the outside of the artery (23). In a randomized trial of mostly diagnostic procedures (24), the AngioSeal reduced the time to hemostasis (2.6 versus 15.3 minutes) and ambulation (1 hour versus 4 to 6 hours) compared with manual compression, with a modest decrease in hematoma formation. The Duett device (25) differs in that it uses a liquid procoagulant mixture (thrombin and collagen) that is injected into the soft-tissue track leading from the outside of the artery to the skin. A compliant balloon-on-a-wire is first positioned and inflated within the artery, pulled into contact with the end of the same sheath that was used for the catheterization, and pulled back against the inside of the puncture site to tamponade bleeding. The sheath is then withdrawn roughly 1 cm further so that its end lies outside the vessel lumen, and the sheath sidearm is used to inject the procoagulant into the soft-tissue tract leading to the outside of the artery. While each of these devices places a great deal of faith in the pro-coagulant properties of its collagen component, the approach of Perclose (Redwood City, CA) relies on the use of a sheathlike device to perform suture-mediated closure of the arterial puncture site. This device has undergone several design changes to improve the ease of delivery, but it still relies on the passage of fine nitinol needles through the margins of the arterial puncture and out through the skin tunnel, where they can be tied to provide surgical hemostasis (26). It shortens the time from the end of the procedure to hemostasis (19 minutes versus 243 minutes) and ambulation (106 minutes for diagnostic and 232 minutes for interventional procedures, versus 4 to 6 hours and 6 to 12 hours, respectively), with a comparably low incidence of major complications (27). If no venous sheath has been placed, some laboratories even allow immediate ambulation after a successful suture-mediated closure.

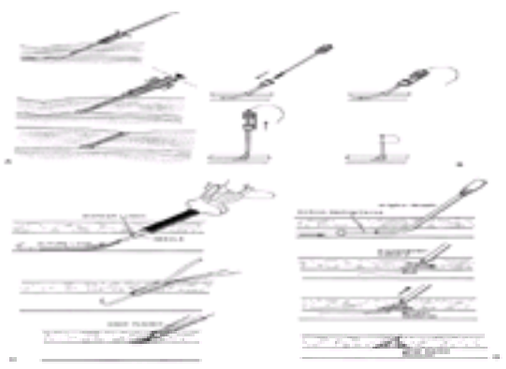

FIG. 4.12. Schematic diagrams of various new devices for the closure of femoral arterial punctures. **A:** The Vasoseal. **B:** The AngioSeal (Kensey-Nash) device. **C:** The Prostar suture device. **D:** The Duet device. (See the text for details.)

Given this array of new devices, groin closure devices are being used in most cases in some laboratories. Others, under less pressure to provide early ambulation and same-day discharge, restrict it to patients with an increased risk of bleeding with manual compression or other conditions (back pain, trouble voiding) that make prolonged bedrest undesirable. As these devices continue to evolve and the demand for early ambulation offsets the moderate cost ($100 to $300) of a closure device, they may ultimately replace prolonged local manual or mechanical pressure in the control of postprocedure bleeding from the femoral artery. The conversion to puncture-sealing devices will be accelerated if they can consistently reduce the 1% to 2% incidence of hemorrhagic complications at the arterial puncture site that constitute one of the most common morbidities associated with catheterization from this route. Of course, the success of these puncture-sealing approaches rests on the premise that a single, accurate, front-wall puncture of the common femoral artery has been performed and that favorable conditions prevail within the vessel and the surrounding soft tissue. Each also requires a modest level of skill and training on the part of the operator, and the realization that difficulties encountered in performing a clean closure once the sheath has been removed and wire access has been given up, may increase rather than decrease the incidence of complications requiring vascular surgery or transfusion. In an era of increasingly sophisticated catheter-based therapies, it seems likely that an effective device for definitive closure of the femoral artery puncture site will replace the 50-year-old practice of pressing on the puncture site until the bleeding stops!

Contraindications to Femoral Approach to Left Heart Catheterization

As discussed in Chapter 1, the choice of catheterization approach (femoral or brachial) is usually a function of operator, institution, and patient preference. Because of technical ease, however, data from the 1990 SCA&I registry shows that 83% of diagnostic (and 96% of interventional) catheterizations are performed via the femoral approach (5). In patients with peripheral vascular disease (femoral bruits or diminished lower extremity pulses), abdominal aortic aneurysm, marked iliac tortuosity, prior femoral arterial graft surgery, or gross obesity, however, catheter insertion and manipulation may present technical challenges even for experienced operators. Recognition of these relative contraindications may favor the use of the percutaneous axillary, brachial, radial, or even translumbar aortic approaches (see later). Each laboratory should thus have one or more operators skilled in these alternative percutaneous routes, particularly if no operators skilled in the brachial cutdown approach (see Chapter 5) are available.

Beyond the limitations of access to the central arterial circulation, one important parameter in the selection of a percutaneous access site is the ability to obtain hemostasis after catheter removal. In the femoral arterial entry technique, this is usually obtained easily after removal of a percutaneous arterial catheter, but patients with a wide pulse pressure (e.g., severe aortic incompetence or systemic hypertension), gross obesity, or ongoing anticoagulation have more problems with bleeding after femoral catheterization than do patients without these factors, particularly if a groin closure device is not used. The vascular complications of percutaneous

retrograde arterial catheterization are usually not life-threatening (28,29,30 and 31) and have already been discussed in Chapter 3. In the final analysis, however, there are relatively few patients who absolutely cannot be catheterized from the femoral approach.

ALTERNATIVE SITES FOR LEFT HEART CATHETERIZATION

The techniques described earlier for percutaneous insertion of a femoral catheter also can be used successfully from the axillary, brachial, or radial arteries, or even the lumbar aorta, with the use of an introducing sheath. In certain cases, access to the left heart may be gained by transseptal puncture from the right atrium to the left atrium, or even by direct percutaneous entry via the left ventricular apex. Although these other access sites may utilize the similar needle puncture, guidewire advancement, and sheath insertion skills outlined earlier for the femoral approach, the operator wishing to use one of the alternative percutaneous routes must master the local anatomy, details of maximal allowable catheter size, limitations on catheter selection, techniques for achieving postprocedure hemostasis, and range of complications that may ensue from bleeding or thrombosis at that anatomic location. Individuals interested in mastering one or more of these approaches are referred to the growing body of literature.

Percutaneous Entry of the Axillary, Brachial, Radial Arteries, and Lumbar Aorta

Axillary puncture has long been used as an alternative to femoral entry by the vascular radiologist (32). The patient's hand is brought behind his or her head to expose the axillary fossa, in which the artery can be felt to course. Using local anesthesia and needle puncture and guidewire techniques like those described earlier, the axillary artery is entered over the head of the humerus. The left axillary artery is generally preferred to allow use of preformed Judkins catheters and avoid the brachiocephalic trunk. Effective control of the puncture site after catheter removal is critical, since accumulation of even modest amounts of hematoma around the artery can cause nerve compression (33).

The *brachial* artery is, of course, readily approached by surgical cutdown (see Chapter 5) but may also be approached using percutaneous (needle and guidewire) techniques (34). The antecubital fossa is prepared and anesthetized as for the cutdown approach. A 21-gauge arterial needle, a special 0.021 heavy-duty guidewire, and a 5F or 6F sheath (MicroPuncture set, Cook) can be used to gain access, after which traditional percutaneous catheter techniques are used. Working from the right brachial artery, Amplatz coronary curves are preferred (see Chapter 11). At the end of the procedure, the sheath is removed, and the area is compressed manually. Alternatively, proximal occlusion can be obtained by inflation of a blood pressure cuff, while a gauze pad and a clear intravenous infusion pressure bag is inflated to above systolic pressure over the puncture site (35). Pressure is then released gradually over 20 to 25 minutes. Comparisons of this percutaneous brachial technique to brachial cut-down show a shorter procedure time (without the need for dissection or repair) and no increase in complications, although surgical repair may be needed occasionally (36). This represents a viable approach for outpatient catheterization or an excellent alternative for access in a patient with difficult femoral or iliac anatomy when a Sones-trained angiographer is not available.

The *radial* artery was previously viewed as a site for placement of monitoring lines in the coronary care unit, rather than an access route for cardiac catheterization. Largely through the efforts of champions like Kiemeneij, however, this has been adapted to the performance of diagnostic angiography and many types of percutaneous coronary intervention (including stent placement!) (37,38). The small caliber of this vessel makes the use of small (5F or 6F) catheters mandatory in most patients. In some patients (mostly males) who have larger-caliber radial arteries, 7F or 8F sheaths can be used (39). Liberal use of lidocaine, nitroglycerin, or a calcium channel blocker through the sheath sidearm may be required to control local spasm that might render the procedure painful and catheter manipulation difficult. Controlling bleeding from the catheterization site at the end of the procedure usually is not difficult, and several “wrist-band” compression devices are available. Obviously, patients can get up and walk immediately after a radial arterial procedure. Although bleeding is not a problem, radial artery thrombosis occurs in roughly 5%, usually without clinical sequelae in patients for whom a preprocedure Allen test has confirmed adequate perfusion of the hand from the ulnar artery even while the radial artery is compressed firmly. The rapid (immediate) ambulation, availability of stents and other devices that can be used through current large-lumen guiding catheters, and paucity of entry-site complications (40) have made the percutaneous radial the preferred (or the preferred alternative to the femoral artery) approach in many laboratories.

Percutaneous puncture of the lumbar aorta is a technique that has been used by radiologists to study patients with extensive peripheral vascular disease since the early 1980s and was then adapted to the performance of coronary angiography (41). More recently, this approach has even been used for coronary stent placement (42), although the fact that the procedure must be done with the patient prone complicates angiographic views and limits resuscitative efforts. The inability to apply direct pressure over the arterial entry site (the posterior wall of the aorta) also limits aggressive anticoagulation. Because of these negative factors, direct aortic puncture should be considered a last resort for vascular entry.

Transseptal Puncture

With refinements and improvements in techniques for retrograde left heart catheterization, the use of transseptal puncture for access to the left atrium and left ventricle (43,44) had become an infrequent procedure in most adult cardiac catheterization laboratories (45). In these laboratories, transseptal puncture was reserved for situations in which direct left atrial pressure recording was desired (pulmonary venous disease), in which it was important to distinguish true idiopathic hypertrophic subaortic stenosis (IHSS) from catheter entrapment, and in which retrograde left-sided heart catheterization had failed (e.g., due to severe peripheral arterial disease or aortic stenosis) or was dangerous because of the presence of a certain type of mechanical prosthetic valve (e.g., Bjork-Shiley or St. Jude valves). The infrequency with which the procedure was performed made it difficult for most laboratories to maintain operator expertise and to train cardiovascular fellows in transseptal puncture and gave the procedure an aura of danger and intrigue. With the advent of percutaneous mitral valvuloplasty (Chapter 26) and the availability of improved equipment, however, transseptal catheterization has again become a relatively common procedure (46).

The goal of transseptal catheterization is to cross from the right atrium to the left atrium through the fossa ovalis. In approximately 10% of patients, this maneuver is performed inadvertently during right heart catheterization with a woven Dacron catheter because of the presence of a probe-patent foramen ovale, but in the remainder, mechanical puncture of this area with a needle and catheter combination is required to enter the left atrium. Although puncture of the fossa ovalis itself is quite safe, the danger of the transseptal approach lies in the possibility that the needle and catheter will puncture an adjacent structure (i.e., the posterior wall of the right atrium, the coronary sinus, or the aortic root). To minimize this risk, the operator must have a detailed familiarity with the regional anatomy of the atrial septum (Fig. 4.13). As viewed from the feet with the patient lying supine, the plane of the atrial septum runs from 1 o'clock to 7 o'clock. The fossa ovalis is posterior and caudal to the aortic root and anterior to the free wall of the right atrium. The fossa ovalis is located superiorly and posteriorly to the ostium of the coronary sinus and well posterior of the tricuspid annulus and right atrial appendage. The fossa ovalis itself is approximately 2 cm in diameter and is bounded superiorly by a ridge—the limbus.

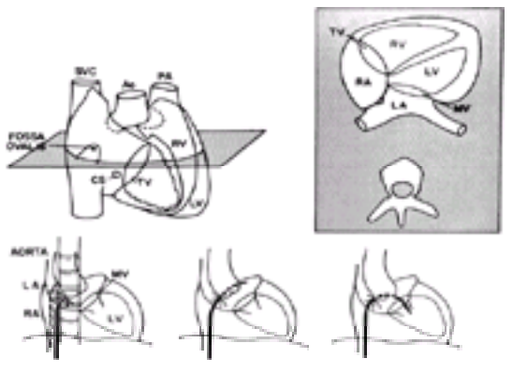

FIG. 4.13. Regional anatomy for transseptal puncture. **Upper left:** The position of the fossa ovalis is shown relative to the superior vena cava (SVC), aortic root (Ao), coronary sinus (CS), and tricuspid valve (TV). **Upper right:** A cross-section through the fossa (looking up from the feet) demonstrating the posteromedial direction of the interatrial septum (bold line) and the proximity of the lateral free wall of the right atrium. **Bottom row:** The appearance of the transseptal catheter as it is withdrawn from the SVC in a posteromedial orientation. As the catheter tip slides over the aortic root (bottom left, dotted position) it appears to move rightward on to the spine. Slight further withdrawal leads to more rightward movement into the fossa (solid position). **Bottom row, center:** Puncture of the fossa with advancement of the catheter into the left atrium. **Right:** Advancement into the left ventricle with the aid of a curved tip occluder. (Redrawn from Ross J Jr. Considerations regarding the technique for transseptal left heart catheterization. *Circulation* 1966;34:391.)

This anatomy can be distorted somewhat by the presence of aortic or mitral valve disease (47). In aortic stenosis, the plane of the septum becomes more vertical, and the fossa may be located slightly more anteriorly. In mitral stenosis, the intraatrial septum becomes flatter with a more horizontal orientation, and the fossa tends to lie lower. Combined with the fact that the septum (and fossa) may then bulge into the right atrium, this makes detailed familiarity with the anatomy even more important when transseptal catheterization is attempted in patients with advanced valvular heart disease. In such patients, intraprocedural transthoracic (48), transesophageal (49), or intracardiac (50) ultrasound may aid in identifying the optimal location for puncture of the intraatrial septum. Alternatively, several algorithms using fluoroscopic landmarks determined by right and left atrial angiography, or the position of a pigtail catheter in posterior (noncoronary) aortic sinus of Valsalva, have been developed to aid localization of the best site for transseptal puncture (51,52) (Fig. 4.14).

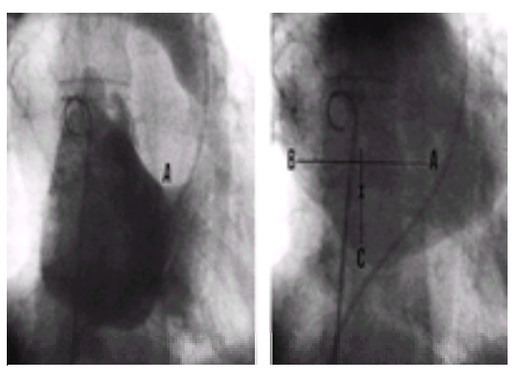

FIG. 4.14. Fluoroscopic landmarks for localizing the fossa ovalis. **Left panel:** As described by Inoue, right atrial injection can be used to locate the upper corner of the tricuspid valve (point *A*), which is marked on the TV monitor. **Right panel:** Continued filming during the levophase fills the left atrium. A horizontal line is drawn from point *A* to the back wall of the left atrium, defining point *B*. That line is divided in half, and a vertical line is dropped to the floor of the left atrium, defining point *C*. The location of the fossa (*x*) is along this vertical line, approximately one vertebral body height above point *C*. When the borders of the left atrium are visible fluorscopically, the position of a pigtail catheter in the noncoronary sinus of Valsalva can be substituted for point *A*, allowing localization of the ideal puncture site without contrast injection (see reference 40). A similar localization scheme (not shown) has been proposed in the 40° RAO projection by Croft and associates (reference 39), using the aortic pigtail and the posterior border of the left atrium. Puncture is made 1 to 3 cm below the midpoint of a line connecting the posterior wall of the aorta to the back wall of the left atrium.

Transseptal catheterization is performed only from the right femoral vein. We use a 70-cm curved Brockenbrough needle (USCI, Billerica, MA) that tapers from 18 gauge to 21 gauge at the tip (Fig. 4.15). The needle is introduced via a matching Brockenbrough catheter or 8F Mullins sheath and dilator combination (53) (USCI) that has been inserted to the superior vena cava over a flexible 0.032-inch, 145-cm J guidewire. Once the wire has been removed and the catheter has been flushed, the Brockenbrough needle is advanced through the catheter, with an obturator (Bing stylet) protruding slightly beyond the tip of the needle to avoid abrasion or puncture of the catheter wall during needle advancement. As the needle and its stylet are advanced through the catheter, the patient may experience a slight pressure sensation due to distortion of the venous structures by the rigid needle. During needle advancement, it is thus essential to allow the needle and its direction indicator to rotate freely so that it may follow the curves of the catheter and venous structures; the hub of the needle should never be grasped and rotated at this point. The progress of the needle tip should be monitored fluoroscopically, looking for any sign of perforation of the catheter by the needle. The stylet is then removed at the diaphragm and the needle hub is connected to a pressure manifold using a stop-cock with a short length of tubing and is carefully flushed. The needle is then advanced to lie just inside the tip of the catheter or sheath, as indicated by measurements made by comparing the distance between the needle flange and the catheter hub, with similar measurements made with a sterile ruler before insertion (Fig. 4.16). Alternatively, current high-quality fluoroscopy can be used to visually monitor advancement of the needle to the catheter tip.

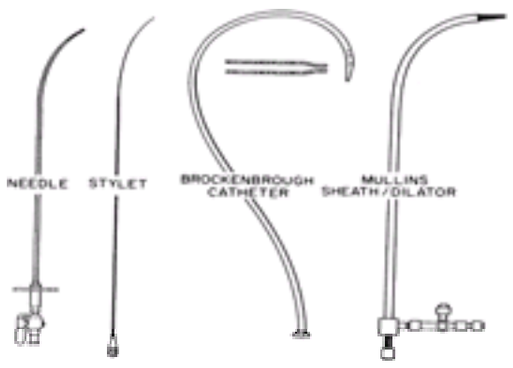

FIG. 4.15. Equipment for transseptal puncture. **Left:** The Brockenbrough needle. **Left center:** Bing stylet. These can be used in conjunction with the following. **Right center:** Traditional Brockenbrough catheter. **Right:** Mullins sheath/dilator system.

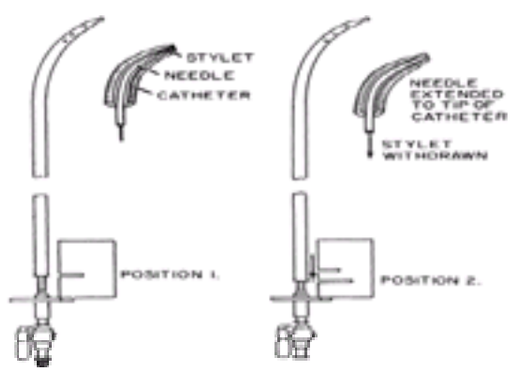

FIG. 4.16. The Brockenbrough system with the needle and stylet inserted into the catheter. Ruler measurement of the distance from the catheter hub to the needle flange is shown with the tip of the stylet at the tip of the catheter (position 1) and with the stylet withdrawn and the needle tip extended to the tip of the catheter (position 2). (Redrawn from Ross J Jr. Considerations regarding the technique for transseptal left heart catheterization. *Circulation* 1966;34:391.)

The superior vena caval pressure should then be recorded through the needle, with the needle rotated so that the direction indicator points anteriorly. Under continuous fluoroscopic and pressure monitoring, the needle and catheter are then held in constant relationship as they are withdrawn slowly, using both hands. The direction indicator is firmly controlled with the right hand and used to rotate the needle clockwise during this withdrawal from the superior vena cava, until the arrow is oriented posteromedially (4 o'clock when looking from below). As the tip of the catheter enters the right atrium, it moves slightly rightward (toward the patient's left). The needle and catheter are maintained in their posteromedial orientation, and they continue to be withdrawn slowly. As the catheter tip slips over the bulge of the ascending aorta, it again moves rightward to overlie the vertebrae in the anterior projection. Further slow withdrawal maintaining the 4 o'clock orientation will be associated with a third rightward movement as the catheter tip “snaps” into the fossa ovalis. This is confirmed by the fact that advancement will cause the catheter tip to flex slightly (rather than move back up the atrial septum) if its tip is lodged in the fossa. Clear fluoroscopic evidence of fossa engagement is thus essential to

successful transseptal puncture.

If the foramen is patent, the catheter may actually cross into the left atrium spontaneously at this point, as indicated by a change in atrial pressure waveform and the ability to withdraw oxygenated blood from the needle. Otherwise, the catheter is advanced slightly to flex its tip against the limbus at the superior portion of the foramen ovale. Once the operator is satisfied with this position, she or he advances the Brockenbrough needle smartly so that its point emerges from the tip of the catheter and perforates the atrial septum. Successful entry into the left atrium should be confirmed by both the recording of a left atrial pressure waveform and the withdrawal of oxygenated blood or the demonstration of the typical fluoroscopic appearance of the left atrium during a contrast puff through the needle. Once the operator is confident that the needle tip is across the interatrial septum, the needle and catheter are advanced as a unit, a short distance into the left atrium, taking care to control their motion so that the protruding needle does not injure left atrial structures. When the catheter is across the atrial septum, the needle is withdrawn, and the catheter is double-flushed vigorously and connected to a manifold for pressure recording.

The main risk during transseptal catheterization is inadvertent puncture of adjacent structures (the aortic root, coronary sinus, or posterior free wall of the right atrium) rather than the fossa ovalis. As long as the patient is not anticoagulated and perforation is limited to the 21-gauge tip of the Brockenbrough needle (i.e., perforation is recognized and the catheter itself is not advanced), this is usually benign. However, if the 8F catheter itself is advanced into the pericardium or aortic root, potentially fatal complications may occur, underscoring the need for the operator to monitor closely the location of the transseptal apparatus by fluoroscopic, pressure, and oxygen saturation at each stage of the procedure. Damped pressure waveform during attempted septal puncture may indicate puncture into the pericardium or simply incomplete penetration of a thickened interatrial septum. Injection of a small amount of contrast through the needle can be useful in this case by staining the atrial septum, and allowing confirmation of an appropriate position in the left anterior oblique (LAO) and RAO projection before more forceful needle advancement is attempted. If the initial attempt at transseptal puncture is unsuccessful, the operator may wish to repeat the catheter positioning procedure by removing the transseptal needle from the catheter, withdrawing the catheter slightly, and reinserting the 0.032-inch guidewire into the superior vena cava. In general, one should never attempt to reposition the catheter-needle combination in the superior vena cava in any other way, since perforation of the right atrium or atrial appendage is a distinct possibility during such maneuvers.

Once the catheter is safely in the left atrium, additional manipulation may be required to enter the left ventricle. If the tip of the catheter has entered an inferior pulmonary vein (as evident by its projection outside the posterior heart border in the right anterior oblique projection), the left ventricle can be approached by torquing the catheter 180° in a counterclockwise direction so that its tip moves anteriorly as it is withdrawn slightly. As the catheter tip moves anteriorly and downward, further advancement will usually allow it to cross the mitral valve and enter the left ventricle. If not, it may be necessary to insert a curved-tip occluder into the catheter through an O-ring sidearm adapter to tighten the tip curve and facilitate advancement into the ventricle. By converting the Brockenbrough catheter from an end-and-side-hole to a side-hole-only device, the tip occluder also minimizes the chance for left ventricular staining and perforation during contrast ventriculography. However, contrast angiography at 8 to 10 mL/sec for 40 to 50 mL total injection (as with the Sones catheter) can usually be accomplished safely without a tip occluder, if desired. Following the completion of hemodynamic and angiographic evaluation, the Brockenbrough catheter is withdrawn in the usual manner during continuous pressure recording.

The technique for transseptal catheterization using the Mullins sheath (53) is similar, except that care must be taken to advance both the dilator and the 8F sheath into the left atrium without injuring the opposite left atrial wall. Slight counterclockwise rotation and repeated puffs of contrast to define location of the catheter tip may be helpful in this regard. Once the sheath is secure in the left atrium, the needle and dilator are withdrawn and the sheath is flushed carefully. Either a specially curved pigtail catheter (in patients with a normal mitral valve) or a CO_2-inflated balloon flotation catheter (in patients with mitral stenosis) may then be inserted through the sheath and passed into the left ventricle. The current Mullins sheath designs have a sidearm connection and backbleed valve, allowing ongoing measurement of left atrial pressure around the left ventricular catheter.

Complications of transseptal catheterization are generally infrequent (“needle tip” perforation, less than 3%; tamponade, less than 1%; and death, less than 0.5%) in experienced hands. This is supported by experience in 1,279 cases from the Massachusetts General Hospital (54), 597 cases from Los Angeles (47), and 500 cases from Taiwan (52). The excellent results in these large series indicate that the technique for transseptal puncture has not been lost (or may even have improved) since its first wave of popularity in the 1960s and 1970s! Because serious complications can occur and are significantly more common early in an operator's experience or in high-risk patients, however, performance of this procedure should be limited to a few operators at each site who can do enough annual procedures to perfect their technique. This is particularly true in patients with distorted anatomy due to congenital heart disease, marked left or right atrial enlargement, significant chest or spine deformity, inability to lie flat, ongoing anticoagulation, or left atrial thrombus/tumor, in whom the technique should generally be avoided.

Apical Left Ventricular Puncture

Historically, a variety of direct puncture techniques were used to enter the cardiac chambers before the introduction of percutaneous left and right heart catheterization. These techniques included transbronchial (55) and transthoracic (56) approaches to the left atrium, the suprasternal puncture technique of Radner (57), and apical left ventricular puncture (58,59). Of these, only the last has survived, albeit as an infrequent (roughly one per year in our laboratory) way to measure left ventricular pressure in a patient where retrograde and transseptal catheterization of the LV are precluded by the presence of mechanical aortic and mitral prostheses.

The site of the apical impulse is located by palpation and confirmed by fluoroscopy of a hemostatic clamp placed at the intended puncture site. Alternatively, the true left ventricular apex can be located using echocardiography (60) and may be found to lie significantly more lateral than the palpated “apical” impulse in patients with right ventricular enlargement. After liberal local anesthesia, an 18-gauge needle (like that used for internal jugular puncture) is introduced at the apex and directed along the long axis of the left ventricle. This is accomplished by aiming the needle tip roughly toward the back of the right shoulder. Contact with the left ventricular wall can usually be felt as a distinct impulse (and the onset of ventricular premature beats). Sharp advancement of the needle at this point will cause its tip to enter the left ventricular cavity, with pulsatile ejection of blood.

In the technique of Semple (59), an outer Teflon catheter was then advanced over the puncture needle and into the left ventricle (sometimes out through the aortic valve as well). We, however, have preferred the technique in which a 0.035-inch 65-cm-long J guidewire is advanced through the needle and into the left ventricle under fluoroscopic guidance. This allows the advancement of a 4F dilator followed by a 4F pigtail catheter to allow pressure measurement and/or left ventricular angiography (Fig. 4.17).

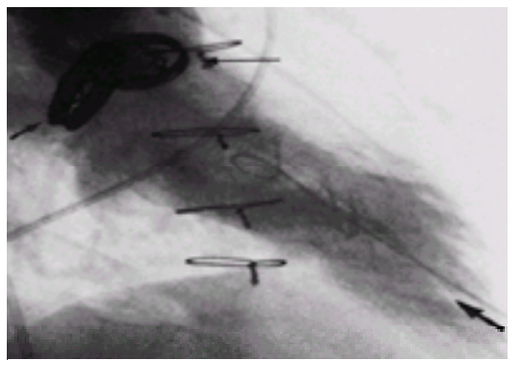

FIG. 4.17. Apical left ventricular puncture. In this patient with Björk-Shiley aortic and mitral valve prostheses *(arrow, upper left),* percutaneous puncture of the left ventricular apex was performed to allow left ventricular pressure measurement and contrast ventriculography using a 4F angiographic pigtail catheter shown entering the LV apex *(arrow, lower right)*. This catheter was advanced into the left ventricle over a 0.035-inch guidewire, following apical puncture with an 18-gauge thin-wall needle. (See the text for details.)

One series describes excellent results of apical puncture in 102 patients (61). Major complications (tamponade or pneumothorax) occurred in 3%, although tamponade was not seen at all in postoperative patients (who have adhesive pericardium). Other complications of apical puncture can include hemothorax, intramyocardial injection, ventricular fibrillation, as well as pleuritic chest discomfort (approximately 10%) and reflex hypotension due to vagal stimulation

(approximately 5%). We thus reserve this technique for patients in whom it is essential to enter the left ventricle and in whom neither retrograde nor anterograde (transseptal) entry of the left ventricle is feasible.

CHAPTER REFERENCES

1. Seldinger SI. Catheter replacement of the needle in percutaneous arteriography, a new technique. *Acta Radiol* 1953;39:368.
2. Judkins MP, Kidd HJ, Frische LH, Dotter CT. Lumen-following safety J-guide for catheterization of tortuous vessels. *Radiology* 1967;88:1127.
3. Barry WH, Levin DC, Green LH, et al. Left heart catheterization and angiography via the percutaneous femoral approach using an arterial sheath. *Cathet Cardiovasc Diagn* 1979;5:401.
4. Hillis LD. Percutaneous left heart catheterization and coronary arteriography using a femoral artery sheath. *Cathet Cardiovasc Diagn* 1979;5:393.
5. Noto TJ, Johnson LW, Krone R, et al. Cardiac catheterization 1990: a report of the registry of the Society for Cardiac Angiography and Interventions. *Cathet Cardiovasc Diagn* 1991;24:75.
6. Kim D, Orron DE, Skillman JJ, et al. Role of superficial femoral artery puncture in the development of pseudoaneurysm and arteriovenous fistula complicating percutaneous transfemoral cardiac catheterization. *Cathet Cardiovasc Diagn* 1992;25:91.
7. Ernst CB. Abdominal aortic aneurysm. *N Engl J Med* 1993;328:1167.
8. Smith DC, Willis WH. Transfemoral coronary arteriography via a prosthetic aortic bifurcation graft. *Cathet Cardiovasc Diagn* 1988;14:121.
9. Lesnefsky EJ, Carrea EP, Groves BM. Safety of cardiac catheterization via peripheral vascular grafts. *Cathet Cardiovasc Diagn* 1993;29:113.
10. Ferguson JJ, Dougherty KG, Gaos CM, Bush HD, Marsh KC, Leachman DR. Relationship between procedural activated clotting time and outcome after percutaneous transluminal coronary angioplasty. *J Am Coll Cardiol* 1994;23:1061.
11. Pepine CJ. ACC/AHA guidelines for cardiac catheterization and cardiac catheterization laboratories. *J Am Coll Cardiol* 1991;18:1149.
12. Dehmer GJ, Haagen D, Malloy CR, et al. Anticoagulation with heparin during cardiac catheterization and its reversal by protamine. *Cathet Cardiovasc Diagn* 1987;13:16.
13. Weiss ME, Nyhan D, Peng ZK, et al. Association of protamine IgE and IgG antibodies with life-threatening reactions to intravenous protamine. *N Engl J Med* 1989;320:886.
14. Krueger SK, Orme EC, King CS, Barry WH. Accurate determination of the transaortic valve gradient using simultaneous left ventricular and femoral artery pressures. *Cathet Cardiovasc Diagn* 1990;16:202.
15. Jayne JE, Catherwood E, Niles NW, Friedman BJ. Double-lumen catheter assessment of aortic stenosis—comparison with separate catheter techniques. *Cathet Cardiovasc Diagn* 1993;29:157.
16. Harrison JK, Davidson CJ, Phillips HR, et al. A rapid, effective technique for retrograde crossing of valvular aortic stenosis using standard coronary catheters. *Cathet Cardiovasc Diagn* 1990;21:51.
17. Feldman T, Carroll JD, Chiu YC. An improved catheter design for crossing stenosed aortic valves. *Cathet Cardiovasc Diagn* 1989;16:279.
18. MacDonald RG, Feldman RL, Pepine CJ. Retrograde catheteriation of the left ventricle through tilting disc valves using a modified catheter system. *Am J Cardiol* 1984;54:1373.
19. Pracyk JB, Wall TC, Longabaugh P, et al. A randomized trial of vascular hemostasis techniques to reduce femoral vascular complications after coronary intervention. *Am J Cardiol* 1998;81:970.
20. Lau KW, Tan A, Kob TH, et al. Early ambulation following diagnostic 7-French cardiac catheterization—a prospective randomized trial. *Cathet Cardiovasc Diagn* 1993;28:34.
21. Sanborn TA, Gibbs HH, Brinker JA, et al. A multicenter randomized trial comparing a percutaneous collagen hemostasis device with manual compression after diagnostic angiography and angioplasty. *J Am Coll Cardiol* 1993;22:1273.
22. Brachmann J, Ansah M, Kosinski E, Schuler G. Improved clinical effectiveness with a collagen vascular hemostasis device for shortened immobilization time following diagnostic angiography and percutaneous transluminal coronary angioplasty. *Am J Cardiol* 1998;81:1502.
23. Aker UT, Kensey KR, Heuser RR, et al. Immediate arterial hemostasis after cardiac catheterization—initial experience with a new puncture closure device. *Cathet Cardiovasc Diagn* 1994;31:228.
24. Kussmaul WG, Buchbinder M, Whitlow P, et al. Rapid arterial hemostasis after cardiac catheterization and percutaneous transluminal angiolasty—results of a randomized trial of a novel homeostatic device. *J Am Coll Cardiol* 1995;25;1685.
25. Silber S, Gershony G, Schoen N, et al. A novel vascular sealing device for closure of percutaneous arterial access sites. *Am J Cardiol* 1999;83:1248.
26. Carere RG, Webb JG, et al. Initial experience with Prostar, a new device for percutaneous suture-mediated closure of the arterial puncture site. *Cathet Cardiovasc Diagn* 1996;37;367.
27. Baim DS, Knopf WDD, Hinohara T, et al. Suture-mediated closure of the femoral access site after cardiac catheterization. *Am J Cardiol* 2000;85:864.
28. Skillman JJ, Kim D, Baim DS. Vascular complications of percutaneous femoral cardiac interventions—incidence and operative repair. *Arch Surg* 1988;123:1207.
29. Mills JL, Wiedeman JE, Robison JG, Hallet JW. Minimizing mortality and morbidity from iatrogenic arterial injuries—the need for early recognition and prompt repair. *J Vasc Surg* 1986;4:22.
30. Kent KC, McArdle CR, Kennedy B, et al. A prospective study of the clinical outcome of femoral pseudoaneurysms and arteriovenous fistulas induced by arterial puncture. *J Vasc Surg* 1993;17:125.
31. Lumsden AB, Miller JM, Kosinski AS, et al. A prospective evaluation of surgically treated groin complications following percutaneous cardiac procedures. *Am Surg* 1994;60:132.
32. Valeix B, Labrunie P, Jahjah F, et al. Selective coronary arteriography by percutaneous transaxillary approach. *Cathet Cardiovasc Diagn* 1984;10:403.
33. Molnar W, Paul DJ. Complication of axillary arteriotomies—analysis of 1762 consecutive studies. *Radiology* 1972;104:269.
34. Fergusson DJG, Kamada RO. Percutaneous entry of the brachial artery for left heart catheterization using a sheath: further experience. *Cathet Cardiovasc Diagn* 1986;12:209.
35. Cardenas JAR, Yellayi S, Schatz RA, Franklin M. A new method for brachial artery hemostasis following coronary angiography. *J Invasive Cardiol* 1994;6:285.
36. Cohen M, Rentrop P, Cohen BM, Holt J. Safety and efficacy of percutaneous entry of the brachial artery versus cutdown arteriotomy for left-sided cardiac cathetrization. *Am J Cardiol* 1986;57:682.
37. Campeau L. Percutaneous radial artery approach for coronary angiography. *Cathet Cardiovasc Diagn* 1989;16:3.
38. Kiemeneij F, Laarman GJ. Percutaneous transradial approach for coronary Palmaz-Schatz stent implantation. *Am Heart J* 1994;128:167.
39. Saito S, Ikei H, Tanaka S. Influence of the ratio between radial artery inner diameter and sheath outer diameter on radial artery flow after transradial coronary intervention. *Cathet Cardiovasc Diagn* 1999;46:173.
40. Kiemeneij F, Laarman GJ, Odekerken D, Slagbloom T, Wieken R. A randomized comparison of percutaneous trasluminal coronary angiolasty by the radial, brachial and femoral aproaches—the Acces study. *J Am Coll Cardiol* 1997;29:1269.
41. Nath PH, Soto B, Holt JH, Satler LF. Selective coronary angiography by translumbar aortic puncture. *Am J Cardiol* 1983;52;425.
42. Henry GA, Williams B, Pollak J, Pfau S. Placement of an intracoronary stent via translumbar puncture. *Cathet Cardiovasc Diagn* 1999;46;340.
43. Ross J Jr. Considerations regarding the technique for transseptal left heart catheterization. *Circulation* 1966;34:391.
44. Brockenbrough EC, Braunwald E. A new technique for left ventricular angiocardiography and transseptal left heart catheterization. *Am J Cardiol* 1960;6:1062.
45. Schoonmaker FW, Vijay NK, Jantz RD. Left atrial and ventricular transseptal catheterization review: Losing skills? *Cathet Cardiovasc Diagn* 1987;13:233.
46. O'Keefe JH, Vlietstra RE, Hanley PC, et al. Revival of the transseptal approach for catheterization of the left atrium and ventricle. *Mayo Clin Proc* 1985;60:790.
47. Clugston R, Lau FYK, Ruiz C. Transseptal catheterization update 1992. *Cathet Cardiovasc Diagn* 1992;26:266.
48. Kronzon I, Glassman E, Cohen M, et al. Use of two-dimensional echocardiography during transseptal cardiac catheterization. *J Am Coll Cardiol* 1984;4:425.
49. Ballal RS, Mahan EF 3rd, Nanda NC, et al. Utility of transesophageal echocardiography in interatrial septal puncture during percutaneous mitral balloon commissurotomy. *Am J Cardiol* 1990;66:230.
50. Hung JS, Fu M, Yeh KH, et al. Usefulness of intracardiac echocardiography in transseptal puncture during percutaneous transvenous mitral commissurotomy. *Am J Cardiol* 1993;72:853.
51. Croft CH, Lipscomb K. Modified technique of transseptal left heart catheterization. *J Am Coll Cardiol* 1985;5:904.
52. Hung JS. Atrial puncture technique in percutaneous transvenous mitral commissurotomy, mitral valvuloplasty using the Inoue balloon catheter technique. *Cathet Cardiovasc Diagn* 1992;26:275.
53. Mullins CE. Transseptal left heart catheterization: experience with a new technique in 520 pediatric and adult patients. *Pediatr Cardiol* 1983;4:239.
54. Roelke M, Smith AJC, Palacios IF. The technique and safety of transseptal left heart catheterization—the Massachusetts General Hospital experience with 1279 procedures. *Cathet Cardiovasc Diagn* 1994;32:332.
55. Morrow AG, Braunwald E, Lanenbaum HL. Transbronchial left heart catheterization: modified technique and its physiologic evaluation. *Surg Forum* 1958;8:390.
56. Bjork VD. Direct pressure measurement in the left atrium, the left ventricle and the aorta. *Acta Chir Scand* 1954;107:466.
57. Radner S. Extended suprasternal puncture technique. *Acta Med Scand* 1955;151:223.
58. Brock R, Milstein BB, Ross DN. Percutaneous left ventricular puncture in the assessment of aortic stenosis. *Thorax* 1956;11:163.
59. Semple T, McGuiness JB, Gardner H. Left heart catherization by direct ventricular puncture. *Br Heart J* 1968;30:402.
60. Vignola PA, Swaye PS, Gosselin AJ. Safe transthoracic left ventricular puncture performed with echocardiographic guidance. *Cathet Cardiovasc Diagn* 1980;6:317.
61. Morgan JM, Gray HH, Gelder C, et al. Left heart catheterization by direct ventricular puncture: withstanding the test of time. *Cathet Cardiovasc Diagn* 1989;16: 87.

5
Brachial Cutdown Approach

Ronald P. Caputo and William Grossman

RPC: Interventional Research Cardiovascular Laboratory, SUNY Health Science Center, St. Joseph's Hospital Health Center, Syracuse, New York 13203.
WG: Division of Cardiology, University of California, San Francisco Medical Center, San Francisco, California 94143.

Although it was once the dominant technical approach used for cardiac catheterization and angiography, the popularity of the brachial cutdown approach has diminished progressively over the past 25 years, as a result of the rise and dominance of the percutaneous femoral, brachial, and (more recently) radial approaches described in Chapter 4. Although the brachial cutdown approach is now used in only a small minority (fewer than 10%) of cardiac catheterization procedures, and the skills required for brachial arterial and venous cutdown and vascular repair are vanishing in the general cardiology community, this approach may still be of great utility in selected patients. Accordingly, this chapter is written (a) as a guide for those learning to perform the brachial cutdown approach in a center where the approach is still used and where experienced, senior physicians are available to help if problems develop, and (b) as a refresher for those previously trained in the brachial approach who may need to use this technique on occasion in a particular patient. However, the brachial cutdown approach should not be used by an inexperienced operator, unless backup is provided by a vascular surgeon or a cardiologist with expertise in this technique. Although the method described in earlier editions of this text is well characterized and successful (Dr. Grossman's method), we have now added an alternative and somewhat simplified method for brachial catheterization as is currently practiced in the Cardiac Catheterization Laboratory at St. Joseph's Hospital in Syracuse, New York. Physicians learning this approach are well advised to study the details of both techniques and adopt helpful elements from each as their own personal technique develops.

DR. GROSSMAN'S METHOD

Incision, Isolation of Vessels, and Catheter Insertion

With the direct brachial approach, a single cutdown is made in the right antecubital fossa, through which both the brachial artery and vein can be isolated and used to perform left- and right-sided heart catheterization, respectively. With the patient's arm fully extended flat on the armboard and the hand supinated, the brachial artery (Fig. 5.1) is identified by palpation, and local anesthesia is induced in the overlying soft tissues with the use of 1% to 2% lidocaine. This is first injected intradermally through a short 25- or 27-gauge needle to raise a bleb, and then deeper with a long (1.5-inch) 22-gauge needle to infiltrate the subcutaneous, deep fascial, and periosteal tissues. Liberal amounts of lidocaine are commonly used—5 to 15 mL initially, and repeating frequently so that 10 to 20 mL may be administered in the course of a catheterization. If anesthetization is done properly, the catheter insertion site ought to be virtually painless throughout the procedure.

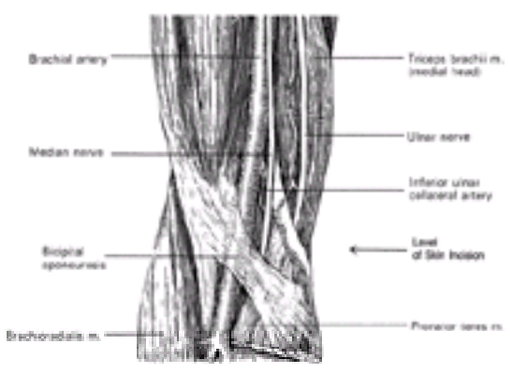

FIG. 5.1. Anatomy of antecubital fossa illustrating course of the brachial artery. The artery is best sought at or slightly above the antecubital skin crease, medial to the bicipital aponeurosis. Care must be taken not to disturb the median nerve, which usually lies medial to the brachial artery. (Clemente C. *Gray's Anatomy of the Human Body,* 30th American ed. Philadelphia, Lea & Febiger, 1985.)

Next, a transverse incision is made with a no. 15 surgical blade just proximal to (i.e., approximately 2 cm above) the flexor crease. If both right and left heart catheterizations are contemplated, the incision is wide and made over the palpable brachial artery; if right heart study alone is planned, the incision is narrow and made directly over a previously identified medial vein. Those who ignore this latter dictum soon learn that the large, plump veins of the lateral antecubital fossae usually drain into the cephalic system, through which it may be difficult to navigate the catheter into the right atrium, whereas the medial veins drain into either the basilic or the brachial venous systems, which join the axillary vein by direct continuation and thus provide the easiest routes to the superior vena cava (SVC) and right atrium (Fig. 5.2).

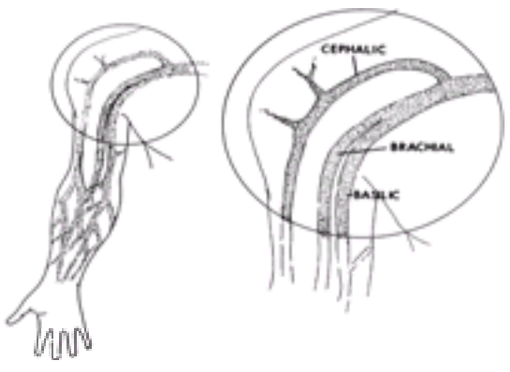

FIG. 5.2. Venous anatomy of the arm. Brachial and basilic veins are medial to the cephalic vein within the antecubital fossa. Note that the brachial and basilic veins continue directly into the axillary and subclavian system, whereas the cephalic system frequently joins the subclavian vein at a right angle. Passage of a catheter from

the cephalic system to the right atrium may be quite difficult; the medial veins provide the straightest pathway.

During the cutdown, the operator should stand between the patient's arm and chest, so that the operator's line of vision into the incision is angled from medial to lateral. This is important because the brachial artery usually lies below the bicipital aponeurosis and can be visualized only as the aponeurosis is lifted and retracted laterally. If one is instead standing at the outside (lateral aspect) of the arm, it is more likely that the first structure seen and isolated by the operator will be the median nerve (which must be avoided) rather than the desired brachial artery.

The tissues are separated by blunt dissection with a curved Kelly forceps (this and the other instruments useful in a brachial catheterization are shown in Fig. 5.3), and an appropriate vein is brought to the surface, separated from adjacent nerves and fascia, and tagged proximally and distally with a loop of 3–0 or 4–0 silk suture material. The brachial artery is similarly brought to the surface with a curved Kelly forceps, isolated from adjacent nerves, veins, and fascia, and tagged proximally and distally with moistened umbilical tape or silicone elastomer surgical tape (Fig. 5.4). After isolation of the brachial artery and basilic or brachial vein, it is time to proceed with the right heart catheterization. An appropriate catheter is selected (see later discussion), such as a Swan-Ganz balloon-flotation catheter, Goodale-Lubin, or Cournand, and flushed vigorously with heparinized solution (3,000 IU heparin per liter of 5% dextrose in water or normal saline solution). A transverse incision is made in the vein with small scissors, and the catheter is introduced with the aid of either curved tissue forceps without teeth or a small plastic catheter introducer (Becton-Dickinson, Rutherford, NJ). Alternatively, the vein may be placed over a “bridge” formed by straight forceps to enable better control and to diminish oozing during passage of the catheter (Fig. 5.4*A*). Once the catheter has been introduced and passed a short distance, blood is aspirated, and the catheter is again flushed with heparinized solution. The catheter may then be connected either directly or by means of flexible plastic tubing to the side port of a manifold with an appropriate pressure transducer (see Chapter 7). The manifold allows entry of heparinized flush solution, and by turning the stopcock the operator can have either pressure monitoring or catheter flush; the presence of the transducer on the manifold offers excellent frequency-response characteristics for high-fidelity pressure tracings.

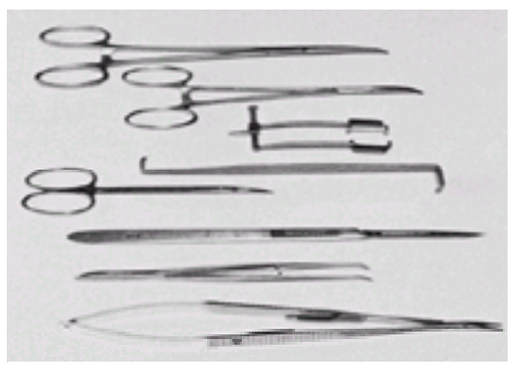

FIG. 5.3. Instruments that are useful in cardiac catheterization by the brachial approach (from top to bottom): curved Kelly forceps (V. Mueller, SU 2722); curved mosquito forceps; ophthalmic retractor (V. Mueller, OP-160, XSAQ), used to hold skin margins open; handheld retractor (V. Mueller, SU 3720); iris scissors (V. Mueller, OP 5005); plastic introducer (Becton-Dickinson); scalpel (no. 11 blade for arteriotomy, no. 15 for skin); and, for use in arterial repair, small curved forceps without teeth (Miltex, 18–784) and Castro-Viejo needle holder (V. Mueller, XHMQ, OP-7380).

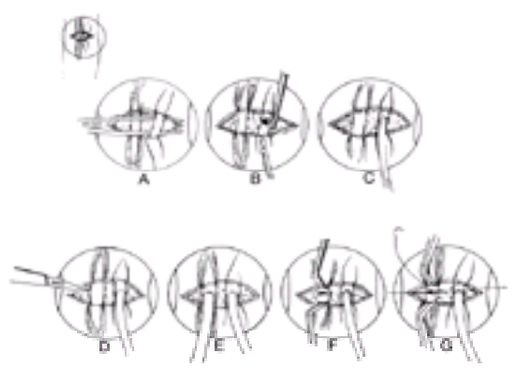

FIG. 5.4. Catheterization by direct exposure of brachial artery and vein. **A:** Artery and vein have been isolated. Both are tagged proximally and distally, the artery with moist umbilical or silicone-elastomer tape, the vein with 3–0 silk. The vein has been placed over a “bridge” formed by a straight forceps to enable better control. **B:** The vein has been incised with a small scissors, and the catheter is about to be inserted with the aid of a plastic catheter introducer (see text). **C:** Passage of the right heart catheter. **D:** Incision of the brachial artery with a no. 11 surgical blade. The cutting edge of the blade is facing upward, and the point approaches the artery from the side and at an angle of 10° to 20° to the horizontal to avoid perforating the posterior wall. **E:** Passage of the left heart catheter. **F:** In preparation for arterial repair, concentrated heparinized saline solution is “locked” in the vessel by placing bulldog clamps as far above and below the arteriotomy as possible (see text). **G:** Closure of the arteriotomy by continuous or running stitch. Stay sutures are placed at each end of the arteriotomy (see text).

After passage of the right heart catheter (discussed later), the brachial artery is cleaned and incised transversely by making a small (2-mm) nick in its anterior surface with a no. 11 surgical blade (Fig. 5.4*D*). An appropriately selected left heart catheter (see the following section) is flushed, inserted into the arteriotomy, and passed retrograde a short distance. It is then connected to the left heart manifold and aspirated and cleared with heparinized solution. When the catheter is flushed manually, the barrel of the flush syringe should always be vertical, with the hub facing downward, to minimize the chance of air embolism. The catheter should be aspirated first until there is a free return of blood, and only 2 to 3 mL of flush solution need be injected, although the syringe should contain more than this. Many laboratories administer heparin solution (e.g., 3,000 to 5,000 IU heparin) into the distal brachial artery routinely; this may reduce the incidence of arterial thrombosis, but intravenous administration of 5,000 IU of heparin after the arterial catheter has reached the central aorta achieves the same effect.

Catheter Selection

Right Heart Catheters

When right heart catheterization is being performed only for measurement of right atrial, right ventricular, pulmonary artery, and pulmonary capillary wedge pressures, any of the end-hole catheters is adequate (although some of the woven Dacron catheters also have side-holes in close proximity to the tip to facilitate aspiration of blood). The Goodale-Lubin and Cournand catheters (USCI Division, Bard Inc., Billerica, MA) are classic woven Dacron right heart catheters, although most laboratories now prefer a flow-directed balloon-flotation catheter (e.g., Swan-Ganz catheter) for routine right heart catheterization.

Passage of the right heart catheter may occasionally produce transient right bundle branch block. Should this occur in a patient with preexisting left bundle branch block, bilateral or complete heart block will develop and may require emergency ventricular pacing. A Swan-Ganz or other flotation balloon-tipped catheter is preferable in patients with left bundle branch block, because it is less likely to cause trauma to the right bundle. Alternatively, a pacing catheter may be used so that immediate ventricular pacing can be instituted should complete heart block develop.

For right-sided angiography, a closed-end catheter that has multiple side-holes and is easy to pass to the pulmonary artery should be chosen. For this purpose the Eppendorf catheter (USCI) and the Berman angiographic catheter (Arrow International, Reading, PA) are excellent choices.

Left Heart Catheters

When the direct brachial approach is employed, potential catheters include both open-end and closed-end, multiple-side-hole designs, which are used for both pressure measurement and angiography. The Sones catheter is commonly used as a left heart catheter, and it can be most helpful at times in crossing a tight aortic valve when other catheters have failed. The Sones has a tendency to recoil during ventriculography, and it may produce myocardial staining when used by an inexperienced operator. However, with proper positioning and a low injection rate (i.e., 7 to 10 mL/sec), excellent left ventriculograms can be obtained routinely.

The polyurethane Sones catheter (80-cm Cordis SON-II, Sones Technique), marketed by Cordis Corporation (Miami, FL), is particularly easy to manipulate into the ascending aorta, coronary arteries, and left ventricle. This catheter has a variety of curves, of which the type I is standard. The 7F or 8F shaft tapers to a 5F external diameter near its tip. It has an end-hole and four side-holes within 7 mm of the tip. The catheter accepts a 0.035-inch guidewire, which is often helpful in navigating through a tortuous subclavian artery into the ascending aorta. It is an excellent catheter for crossing a tight aortic valve, with or without the added help of a straight guidewire.

Some operators prefer a closed-end, multiple-side-hole catheter for left ventriculography and initial hemodynamic measurements. In this regard, the polyurethane 7F or 8F NIH catheter made by Cordis Corporation is easy to use and to advance into the left ventricle. The Eppendorf catheter (USCI) is similar to the NIH catheter and may be used for ventriculography. Some operators prefer to use a pigtail catheter from the brachial approach, inserting it over a protruding J-tipped guidewire to straighten its tip during arterial entry. Two catheters frequently used for right and left heart catheterization from the brachial approach are shown in Fig. 5.5.

FIG. 5.5. Useful catheters for right and left heart catheterization. The Goodale-Lubin catheter **(left)** has an end-hole and two side-holes and is ideal for right heart catheterization, including measurement of pulmonary capillary wedge pressure. The polyurethane Sones catheter **(right)** tapers to a 5F tip with an end-hole and four side-holes; it is useful for coronary angiography and for left ventriculography (at low flow rates).

When high-fidelity artifact-free tracings are needed, a micromanometer-tipped catheter may be chosen, such as the Mikro-tip (Millar Instruments, Houston, TX) (see Chapter 7). The Mikro-tip catheter is available in modifications with multiple side-holes through which angiography can be performed. It is also available with a pigtail end for percutaneous placement.

Other left heart catheters include the Gensini (usually employed with percutaneous technique—see Chapter 4), the Lehman ventriculography catheter, the Rodriguez-Alvarez catheter, and the Shirey catheter (which may be used for a retrograde approach to the left atrium); all of these are made by USCI.

Advancing the Right Heart Catheter

The right heart catheter is advanced under fluoroscopic control to the SVC. If there is difficulty entering the SVC, it is sometimes helpful to try the following maneuvers: have the patient take a deep breath; raise the patient's right arm and shoulder toward the head (ask the patient to shrug his or her right shoulder); turn the patient's head to the extreme left; remove the patient's pillow. If the catheter tip consistently points in a cephalad direction, try to gently form a loop proximal to the tip, which then may buckle and prolapse into the SVC. In the last suggestion, the word *gently* must be emphasized; a catheter should never be forcibly advanced against a resistance. On occasion, a guidewire may be helpful in passing from the subclavian vein into the SVC. If these maneuvers do not meet with prompt success, try a different catheter. Each catheter has a slightly different bend, and usually one will be just right for a given patient.

A word of caution is offered here concerning venous spasm, which may develop in any patient but is especially common in women. If spasm develops, do not try to advance the catheter, but instead withdraw it for a distance of 10 to 20 cm and then briskly move it to-and-fro in short (approximately 5-cm) strokes. This will commonly “break” the spasm, and the catheter may then be freely advanced to the right side of the heart. The same approach applies equally to arterial spasm. If spasm persists, a smaller catheter must be used. Right heart catheterization in adults can be accomplished successfully with 5F or 6F catheters; if this is not successful, a percutaneous femoral venous approach can be used. Persistent attempts to advance or manipulate the catheter in the presence of spasm produces pain, vagal reactions, and hypotension, and a minor problem may thus be converted into a catastrophe.

When the catheter tip has been advanced to the SVC, the operator should draw a blood sample for oximetry. If the SVC blood oxygen saturation is substantially lower than the subsequently measured pulmonary artery oxygen saturation, a full oximetry run should be done (see Chapter 9). Such an oxygen “step-up” may be the only clue to unsuspected atrial septal defect. To accomplish all these tasks successfully requires 1 to 2 minutes. The catheter tip is next advanced to the right atrium, where pressure is recorded before the catheter is advanced to the pulmonary artery.

Advancing from Right Atrium to Pulmonary Artery

In navigating from the right atrium to right ventricle and pulmonary artery with either a Cournand or a Goodale-Lubin catheter, the J loop technique should be tried first. The catheter is advanced so that its tip catches on the lateral right atrial wall and the catheter looks like the letter J on fluoroscopy (Fig. 5.6). Next, the catheter is rotated counterclockwise so that the tip of the J sweeps the anterior right atrial wall (thus avoiding the coronary sinus, whose ostium lies posterior to the tricuspid valve) and jumps across the tricuspid valve into the right ventricle. At this point, the technician monitoring the patient's electrocardiogram frequently notes extrasystoles and calls these off to the operator; this is a sign that the catheter has entered the right ventricle. Because the catheter usually still retains its J curve (woven Dacron catheters have a “memory” and retain an imposed shape for a short time after the imposing force has been removed), its tip will now be pointing toward the right ventricular outflow tract and can easily be advanced into the pulmonary artery. Right ventricular pressure may be recorded during the transit or subsequently during the catheter pullback.

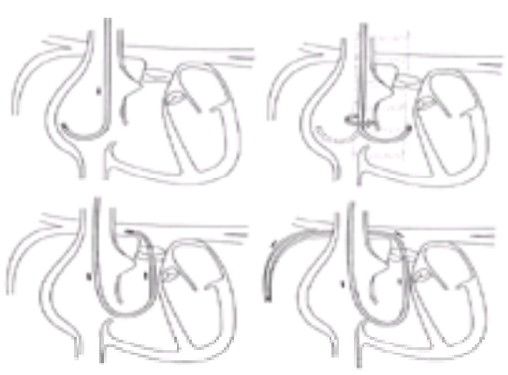

FIG. 5.6. Advancing the right heart catheter. In navigating from right atrium to pulmonary artery, the J loop technique should be tried first. **Upper left:** The catheter is advanced so that its tip catches on the lateral right atrial wall and forms the letter J. **Upper right:** It is then rotated counterclockwise so that the catheter tip sweeps

the anterior right atrial wall (thus avoiding the coronary sinus) and jumps across the tricuspid valve into the right ventricle. **Lower left:** The catheter tip, pointing toward the right ventricular outflow tract, can be easily advanced into the pulmonary artery. **Lower right:** The patient takes a deep breath, and the catheter is advanced to the "wedge" position (see text).

If the catheter tip meets any resistance during its transit through the right ventricular outflow tract, do not advance it. Pull back until the tip is free, and again gently try to advance to the pulmonary artery. It is easy to perforate the right ventricular outflow tract and end up in the pericardial space. Older women (e.g., more than 65 years old) seem particularly susceptible to this complication, and it is advisable to use 7F (or smaller) catheters routinely in these patients.

With the catheter now in the pulmonary artery, pressure is again measured and blood is sampled for oximetry.

Advancing to Pulmonary Capillary Wedge Position

Next, the catheter is advanced to the "wedge" position. This can be done simply by having the patient take a deep breath and hold it while the catheter is advanced until its tip will go no farther (Fig. 5.6) and does not pulsate with the heart. Having the patient cough at this time will frequently advance the catheter tip into a true "wedge" position. The catheter loop may need to be pulled back slightly at this point to avoid coiling up in the right ventricle and atrium.

The pressure waveform is examined, and if it has the appearance of a true wedge pressure (Fig. 5.7), it is recorded. If there is any doubt that a true wedge position has been achieved, blood is sampled from the catheter. The pressure is confirmed as a true wedge pressure only if blood that is completely (95% or more) saturated with oxygen can be aspirated gently from the catheter (1). In patients who are hypoxemic, a wedge blood oxygen saturation of 90% or more may be accepted, especially if the oxygen saturation of pulmonary artery blood is much lower (e.g., 70% or less). When mitral stenosis is not expected to be present, the wedge pressure may be "confirmed" simply by its typical waveform and by its match against simultaneous left ventricular diastolic pressure. If an unexpected diastolic gradient is detected between left ventricular and pulmonary wedge pressures, the wedge position should be confirmed by blood sampling. As mentioned, oxygen saturation of blood aspirated from a true wedge position should be 95% or more, unless the catheter is wedged in a lung segment with poor aeration (e.g., atelectatic lobe, pneumonia, pulmonary edema). If a Swan-Ganz catheter is used to obtain pulmonary capillary wedge pressure, it is often necessary to aspirate and discard the 5 to 15 mL of pulmonary artery blood that lies between the balloon and the pulmonary capillary bed before bright red pulmonary capillary blood can be sampled.

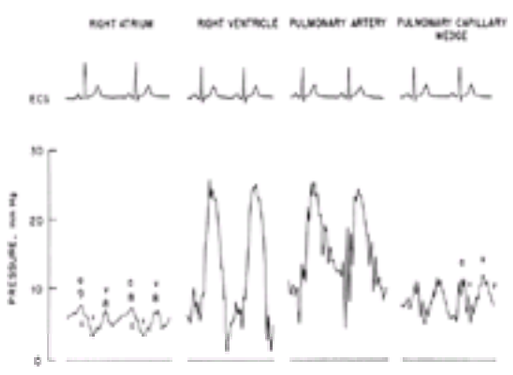

FIG. 5.7. Normal right heart pressures as measured through a 7F Goodale-Lubin catheter in a patient with moderate coronary artery disease, normal left ventricular function, and normal cardiac output. Both right atrial and pulmonary capillary wedge pressures show distinct a and v waves. (See text for details.)

Over the years, debate has continued about the validity and usefulness of pulmonary capillary wedge pressure (sometimes called pulmonary artery wedge pressure) as a measure of pulmonary venous and left atrial pressure (2,3,4,5,6,7,8,9 and 10). Most studies (2,3,4,5,6 and 7,10) have reported excellent agreement between mean left atrial and pulmonary capillary wedge pressure. The phasic pressure waveform of the wedge pressure is commonly somewhat damped compared with a matched left atrial waveform, with a and v wave peaks being smaller in the wedge tracing. The timing of a and v waves is delayed in the wedge tracing, compared with left atrial pressure (Fig. 5.8). Lange and associates (10) found this delay to average 70±15 msec (mean±SD) and reported a significant improvement in accuracy of mitral valve gradient and valve area calculations when appropriate adjustment was made for this delay (see Chapter 10 for details). In Lange's study, wedge pressure was measured with an 8F Goodale-Lubin catheter, which almost certainly maximized the fidelity of waveform transmission from the left atrium. Use of smaller-lumen balloon-tipped catheters increases somewhat the likelihood of excessive damping of the waveform and longer transmission time delay. In both of the studies (8,9) that found wedge pressure unreliable compared with left atrial pressure for the accurate assessment of transmitral gradient, the wedge pressure was measured with smaller-lumen balloon-tipped catheters, without oximetric confirmation. *Pulmonary capillary wedge pressure provides an accurate estimate of left atrial pressure, whether measured with Cournand, Goodale-Lubin, or balloon-tipped catheters, if appropriate attention is paid to (a) accurate assessment of pressure waveform, (b) oximetric confirmation, and (c) correction for time delay.*

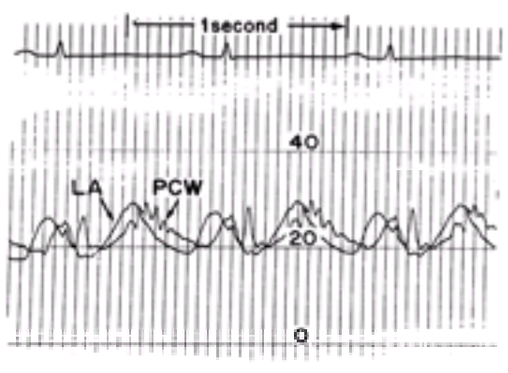

FIG. 5.8. Simultaneous left atrial (LA) and pulmonary capillary wedge (PCW) pressures in a patient undergoing transseptal catheterization. Note that the a and v waves are delayed by 50 to 70 msec in the PCW tracing compared with the LA tracing. (See text for details.) (Modified from Lange RA, Moore DM Jr, Cigarroa RG, et al. Use of pulmonary capillary wedge pressure to assess severity of mitral stenosis: is true left atrial pressure needed in this condition? *J Am Coll Cardiol* 1989;13:825, with permission.)

Accurate assessment of pressure waveform requires a proper pressure measurement technique with high natural frequency and optimal damping, as discussed in Chapter 7. With regard to the pressure measurement technique, a trick that is sometimes helpful is a maneuver called "developing" the wedge pressure. Many operators have noticed that the wedge pressure waveform often appears damped at first but improves immediately after a slow, gentle saline flush or brief infusion through the lumen of the wedged catheter. This may, in some instances, be related to clearing the catheter of blood, platelet aggregates, or microthrombi that are causing damping of the pressure waveform, but it seems equally likely that vasodilatation of the pulmonary capillary bed is playing a role. Similar improvement in pulmonary capillary wedge waveform may also be seen after sublingual or intravenous administration of nitroglycerin.

When using a Cournand or Goodale-Lubin catheter to obtain a wedge pressure, it is safe to leave the catheter in the wedge position, flushing intermittently at 3-minute intervals (continuous flushing in the wedge position frequently causes the patient to develop violent coughing), and proceed with the left heart catheterization. We perform cardiac output determinations with right heart catheter pullback to the pulmonary artery, only after simultaneous pulmonary capillary wedge and left ventricular pressures have been recorded. A different practice must be followed when the Swan-Ganz or other balloon catheter is used as a right heart

catheter. These catheters must never be left in the wedge (balloon-inflated) position for any significant period. *Failure to observe this rule may cause pulmonary infarction or rupture of the pulmonary artery, or both.*

The Cournand catheter is somewhat stiffer than the Goodale-Lubin and may be easier to control in the right heart and to advance to wedge position. Stiffer right heart catheters (e.g., Cournand, Gorlin) may also be more dangerous, particularly in elderly women, in whom perforation of the heart can easily occur. One way of temporarily stiffening a Goodale-Lubin or other catheter is to advance a 0.038- or 0.045-inch guidewire (soft end first) to within 2 to 3 inches of the catheter's tip. This maneuver commonly gives the added stiffness necessary to get from the pulmonary artery to the wedge position. The guidewire should not remain in the catheter for more than 2 to 3 minutes, after which it is removed and the catheter is carefully aspirated and flushed. This maneuver should not be used in attempting to manipulate the catheter from the right atrium to the right ventricle and pulmonary artery, because it increases the risk of cardiac perforation.

Advancing the Left Heart Catheter

After the right heart catheter has been advanced to the pulmonary artery or wedge position, an appropriately selected left heart catheter is inserted into the brachial artery as described previously. This catheter is then advanced into the ascending aorta just above the aortic valve. If there is difficulty navigating from the subclavian or innominate (brachiocephalic) artery into the ascending aorta, the operator may try all the maneuvers suggested for guiding the right heart catheter into the SVC. These include having the patient take a deep breath, shrug the right shoulder, turn the head to the extreme left, remove the pillow, and extend the right arm by manual traction on the wrist.

As with right heart catheterization, if the catheter does not pass easily after a relatively brief attempt at manipulation, resist the temptation to become more vigorous. When using an end-hole catheter (e.g., the Sones catheter) a soft J-tipped spring guidewire may be advanced through the catheter tip to lead the way. The 0.035-inch-diameter guidewire can be used with the Cordis Sones catheter, and larger sizes with the pigtail or Gensini catheters. If the ascending aorta cannot be entered easily with a standard J-tipped guidewire, a Wholey wire may be useful for negotiating tortuous arterial systems. On rare occasions, the ascending aorta cannot be entered by way of the right brachial artery, necessitating a percutaneous femoral or left brachial artery approach.

Once the catheter is in the ascending aorta, central aortic pressure is measured and recorded simultaneously with arterial monitor pressure. The catheter is then advanced across the aortic valve into the left ventricle. Usually this can be accomplished by producing to-and-fro excursions of the catheter while gradually rotating it through 360° so that the catheter tip moves up and down on the aortic valve over its entire plane.

As mentioned previously, the Cordis polyurethane Sones catheter is used widely as a left heart catheter when the brachial approach is employed. This soft-tipped catheter may be advanced directly (tip first) into the left ventricle, or it may be prolapsed across the aortic valve, loop first, as illustrated in Fig. 5.9.

FIG. 5.9. Illustration of technique for retrograde catheterization of the left ventricle using the Sones catheter. The catheter is advanced **(upper left)** to touch the aortic valve. Further advancement usually produces a loop **(upper right)** in the ascending aorta, which prolapses readily **(lower left)** into the left ventricle. The catheter is then withdrawn **(lower right)** to eliminate the loop and obtain a proper axial orientation for left ventriculography.

On occasion, entering the left ventricle may be difficult, particularly in a patient with severe aortic stenosis. In this circumstance, catheters of different shapes may help, although good results are obtained with the Sones catheter, which often passes a tight aortic valve easily. A straight-tipped guidewire should be used to probe the valve before abandoning the attempt. When crossing a stenotic aortic valve retrograde, it is often helpful to view the aortic root and valve in left anterior oblique projection. This view shows the calcified leaflets well and may demonstrate the location of the orifice that provides a target for repeated to-and-fro excursions of the catheter tip or straight-tipped guidewire. If a guidewire is used, the catheter is advanced over the guidewire into the ventricular chamber; after removal of the guidewire, the catheter is then aspirated vigorously and flushed. With a guidewire-facilitated entrance into the left ventricle, there is a danger that the guidewire tip may pass under endocardial trabeculations or chordae tendineae, so that when the catheter is subsequently advanced over the guidewire, it is not free in the ventricular chamber. This can lead to serious myocardial staining during power injection of contrast material but should be detectable from appearance of the catheter tip and from the washout of contrast medium after a test injection. Success in crossing a tight aortic valve depends on experience, luck, and sheer determination.

A special-purpose left heart catheter was developed by Dr. Earl Shirey for retrograde catheterization of the left atrium. The Shirey catheter is a tapered, multiple-side-hole, woven Dacron catheter that resembles the Sones catheter. It can be prolapsed loop-first into the left ventricle, so that its tip faces the mitral valve (Fig. 5.10) rather than the left ventricular apex. Withdrawal of the redundant loop frequently guides the catheter tip into the left atrium.

FIG. 5.10. Diagrammatic illustration of retrograde catheterization of the left atrium using the Shirey catheter. It can be prolapsed loop-first into the left ventricle **(upper left)**, so that its tip faces the aortic and mitral valves **(upper right)** rather than the left ventricular apex. Withdrawal of the redundant loop frequently guides the catheter tip into the left atrium **(lower panel)**.

Once the left ventricle has been entered and a stable position found, immediately obtain simultaneous recordings of critical pressures, such as left ventricular, peripheral arterial (through the arterial monitor line), and pulmonary capillary wedge pressures. Although these pressures will be recorded again during the cardiac output determination, arrhythmias or other unanticipated problems may develop, substantially altering the basal physiologic state and possibly requiring catheter withdrawal. In such circumstances, the operator will sorely regret not having measured the pressures earlier.

After completion of hemodynamic and cardiac output measurements (see Chapter 8), most cardiac catheterization procedures today proceed to left ventriculography and coronary angiography. The details of these techniques as applied to both brachial and femoral approaches are discussed in Chapter 11 and Chapter 12.

Repair of Vessels and Aftercare

After the completion of diagnostic studies, the left heart catheter is removed and the brachial arteriotomy is repaired. Repair may be done in many ways (pursestring, interrupted, continuous), but only the approach that worked well for Dr. Grossman over the years is described here. The approach used at St. Joseph's Hospital is described later in this chapter.

The proximal and distal portions of the artery are checked for vigorous and free bleeding, and an arterial (Fogarty) embolectomy catheter (3F, 40 cm, Shiley Laboratories, Irvine, CA) is employed (11). The use of a Fogarty catheter routinely in all brachial catheterizations has resulted in a low incidence of diminished radial pulse and arterial insufficiency. Although the procedure may be performed routinely, other brachial operators reserve it for instances in which proximal flow or distal pulsation (after repair) are impaired.

When good proximal flow has been established, 10 to 15 mL of a concentrated solution of heparinized saline (3,000 IU of heparin in 30 mL normal saline) is infused into the proximal artery through the Sones catheter; this solution is “locked” in the vessel by immediately placing a vascular bulldog-type clamp (DeBakey peripheral vascular bulldog clamps with angled jaws, V. Mueller, Chicago, IL) as far above the arteriotomy as possible (Fig. 5.4*F*). The same procedure is then repeated for the distal segment (i.e., use of Fogarty catheter, administration of heparin, placement of bulldog clamp). At this point, a stay suture is placed at each end of the arteriotomy, which is then closed using a continuous or running stitch (Fig. 5.4*G*) with fine nonwettable suture material such as 6–0 Tevdek (Deknatel Company). The stay suture at one end of the incision is the start of the running stitch, and the stitch is completed by tying to the other stay suture. The advantage of a continuous suture is that it tightens as the artery expands after the clamps are removed.

A special needle holder (Castro-Viejo type), with a delicate hold and release mechanism, is quite useful when doing the arterial repair. Needle holders of this type (Fig. 5.3) are commonly used in ophthalmologic and vascular surgery and aid in the fine control of suture placement.

After suture of the artery, the distal bulldog clamp is removed first, and the forearm is massaged gently from the wrist toward the elbow, to milk out any air within the lumen of the artery before releasing the proximal bulldog clamp. The proximal clamp is then removed, and any minor leaks are controlled by direct finger pressure, which must be sufficiently gentle that the radial pulse can be palpated. If leaking does not stop within a few minutes of such finger pressure, an additional suture or two may be required. The radial pulse must be palpable and essentially of the same amplitude as before the arteriotomy. If the pulse is absent or greatly diminished, the artery should be reopened and a Fogarty catheter again passed proximally and distally. If this is unsuccessful, prompt consultation should be obtained with an experienced vascular surgeon (if possible while the wound is still open), who usually will be able to identify and correct the problem. The operator should carefully watch the vascular surgeon and learn exactly what the problem was, how it was corrected, and how it might have been prevented.

After successful repair of the arteriotomy, the vein utilized in the right heart catheterization may be tied off or repaired (a purse-string repair is usually adequate), depending on the needs of the individual case. The wound is then flushed out with copious quantities of fresh sterile saline solution followed by 10% povidone-iodine solution. The skin is closed using a subcuticular stitch of an absorbable suture (4–0 Dexon Plus, Davis and Geck, Inc., on a cutting needle), thereby avoiding the need for suture removal. Alternatively, the skin may be closed with interrupted mattress sutures of 4–0 nylon; these sutures must be removed 7 to 10 days later. Antibiotic ointment is placed on the suture line and covered with a firm dressing (although not so firm that it diminishes the radial pulse).

Brachial artery catheterization is well suited to performance on an outpatient basis, in which case the patient can usually be discharged to home after 4 to 6 hours of observation if stable. There is no need for the patient to be kept flat or motionless in bed after the procedure. The patient may sit up, eat, and (if no groin procedure has been done) get out of bed (with assistance) to go to the bathroom. The operator should see the patient later in the afternoon to check the dressing, the peripheral pulses, and the general condition of the patient. This may also be a suitable time to discuss with the patient and family the results of the investigation and recommendations for further treatment (e.g., surgical procedures), if any. If the catheterization was done as an outpatient procedure, the patient may be discharged to home after a check of the radial pulse and antecubital fossa incision.

In fewer than 2% of cases, in our experience, a radial pulse is absent by the time the patient is seen on late afternoon rounds. In such cases, a successful strategy has been to administer one aspirin and watch the patient overnight, with a plan to bring the patient to the catheterization laboratory (or operating room) the next morning for reexploration by the original operator, if he or she is an expert in brachial catheterization, or by a vascular surgeon. In about one third of the cases there is a strong pulse the next morning, and the absence of a pulse on evening rounds is attributed to spasm or a transient thrombus. In two thirds of the cases, the radial pulse is still weak or absent, and these patients come to the laboratory or operating room where, under local (1% to 2% lidocaine) anesthesia, the incision is reopened, the arterial repair is taken down, and a Fogarty catheter is passed in both directions (usually extracting a sizeable thrombus). Any intimal fronds or flaps that are visible are trimmed with a fine scissors. Heparin is administered systemically (5,000 IU) and locally into the proximal and distal segments of the artery, and the artery is repaired with 6–0 Tevdek in a continuous suture, as before. This approach is recommended only for operators who have extensive experience with the brachial approach and use of the Fogarty catheter. For those with limited brachial experience, or when the initial arterial repair was difficult, prompt consultation with an experienced vascular surgeon is indicated. The word *prompt* is worth emphasizing, because patients with a weak or absent radial pulse 18 to 24 hours after brachial catheterization almost always have a localized thrombus. These thrombi propagate over the ensuing days and weeks, often eventuating in severe claudication. If the patient is seen late (e.g., more than 1 week after catheterization), these thrombi may be impossible to remove, necessitating venous bypass surgery to relieve arm ischemia.

It is important to emphasize that the complications of a catheterization should be managed whenever possible by the physicians who have done the catheterization. They are most likely to understand the genesis of a specific problem, and this is clearly the best method of continuing education to ensure the prevention of future complications.

THE ST. JOSEPH'S HOSPITAL (SYRACUSE) APPROACH

Although Dr. Grossman's technique is quite dependable, we at St. Joseph's Hospital have adopted a somewhat different technique based on the high volume of brachial procedures we perform. This technique has been used in more than 16,000 brachial catheterizations since 1978, with a success rate of 99% and complication rate of 0.6%, for both diagnostic and interventional procedures. Adherence to this standard technique allows an operator to achieve satisfactory results after adequate experience with arterial cutdown and repair; we believe that roughly 100 cases must be done to attain the necessary expertise.

Indications

We choose the brachial approach for patients with several conditions: (a) severe peripheral vascular disease, making upper extremity vascular access preferable; (b) urgent or emergent cardiac catheterization with an increased risk for bleeding (due to chronic oral anticoagulation or recent thrombolytic therapy); (c) a need for early ambulation or mobility (e.g., outpatient procedures, severe back pain).

Although percutaneous radial artery catheterization can also be useful for such patients, the brachial cutdown approach can provide additional advantages, including:

1. The ability to perform concomitant *right* heart catheterization—for assessing patients with suspected or known valvular heart disease, congestive heart failure, intracardiac shunt, or other conditions
2. Reliable arterial access with catheter sizes of 7F or greater, often needed for percutaneous coronary interventions, or special catheters
3. Venous access to allow for foreign body retrieval (from the superior and inferior vena cava, right ventricle, or pulmonary artery), measurement of hepatic vein wedge pressure, and other procedures.

Relative contraindications to brachial artery cutdown are few but include absence of a brachial pulse, presence of an arteriovenous fistula, overlying soft tissue infection, severe ipsilateral axillary or subclavian vascular disease, and inability to extend the arm at the elbow or supinate the hand.

Preprocedure Evaluation

Proper preprocedure patient evaluation is critical for a successful brachial catheterization. Inspection and identification of the antecubital folds, biceps tendon, and medial and lateral epicondyles of the humerus is important and takes only a few seconds. This inspection should be performed with the patient's arm extended and the hand supinated to assess for the ability to properly position the arm for the procedure. The general location for arterial cutdown is approximately 2 to 3 cm above

the antecubital skin fold, slightly superior to the level of the humeral epicondyles, and medial to the biceps tendon. A cutdown below this level is not recommended, because the artery subsequently courses under the biceps tendon and bifurcates. A cutdown performed above this level is feasible but may be awkward owing to the medial course of the artery. Brachial pulses should be carefully palpated bilaterally. A weak unilateral pulse usually indicates proximal vascular occlusive disease. Auscultation should be performed over the brachial, axillary, and subclavian areas to assess for bruits. A diminished pulse and/or bruits should lead the operator to anticipate proximal vascular occlusive disease and plan accordingly, with consideration for a contralateral procedure, femoral access, or the use of soft and steerable guidewires. If a prior cutdown has been performed, the brachial pulse should be assessed 1 to 2 cm from the old scar (to avoid the need to dissect through scar tissue with potential adhesions to the pervious arteriotomy site), with the new cutdown preferably performed proximally to the previous one.

Technique

Cutdown

Before starting the procedure, selection of the proper instruments is necessary. We have found that a set which includes a no. 15 blade with handle, a no. 11 blade without a handle (or with a short handle) for improved control during arteriotomy, two or three curved hemostats, two straight hemostats, one self-retaining retractor, two soft tissue retractors, one small scissors, one needle holder, one toothless forceps, one small forceps, two segments of umbilical tape or vascular loops, 6.0 Prolene suture on a $^{3}/_{8}$-inch needle, 3–0 absorbable suture with a curved needle, silk or chromic ties, and a vein lifter is sufficient for almost all cases (Fig. 5.11).

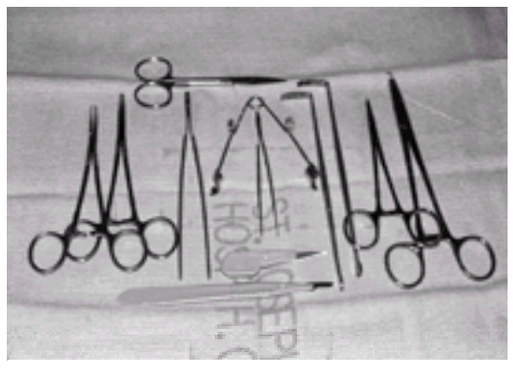

FIG. 5.11. Instruments used for brachial cutdown via the Syracuse approach: two curved Halstead curved mosquito 5-inch hemostats, one Halstead straight mosquito 5-inch hemostat, one thumb dressing 6-inch forceps without teeth, one straight iris forceps without teeth, one short-handled scalpel (no. 11 blade), one long-handled scalpel (no. 15 blade), one Grieshaber wire self-retaining retractor, two Davis double-end soft tissue retractors, one straight 4-inch iris scissors, and one Halsey 5-inch needle holder. All except the scalpels are from Pilling Instruments, Washington, PA.

With the patient supine, the arm is placed in the supine and extended position on an armboard and abducted to 45° to 90°. We prefer an armboard that has the capacity to swivel in the horizontal plane so that the arm may be repositioned closer to the body during the procedure. After sterile preparation and draping of the surgical field, the operator positions himself *lateral* to the arm with the assistant positioned between the armboard and the patient. Although this is contrary to the technique described by Dr. Grossman, we favor this positioning because it gives the operator a direct and unhindered view of the median nerve as it gradually appears during blunt dissection, decreasing the chance of its injury. Local anesthesia is administered by subcutaneous injection of 2% lidocaine delivered through a 5- to 10-mL syringe with a 25-mm long, 25-gauge needle. During the procedure, further anesthesia is usually applied by direct topical application (often by pouring 3- to 4-mL aliquots directly onto the site) rather than reinjection. This seems to have a satisfactory effect and avoids further tissue trauma.

As mentioned previously, the ideal location for a cutdown is approximately *2 cm above* the medial portion of the antecubital (flexor) crease. A 2-cm transverse incision with a no. 15 blade is made through the dermis. The operator performs blunt dissection through the subcutaneous fat with a curved hemostat, simultaneously performing lateral retraction, while the assistant retracts medially. As the handheld retractors are applied to the lateral ends of the incision, the self-retaining retractor is applied superoinferiorly. This provides optimal exposure, particularly when substantial amounts of adipose tissue are present. After the fascia overlying the brachial artery is exposed, the artery is palpated again, and longitudinal dissection through the fascia is then performed parallel and *lateral* to the artery. This further decreases the chance for median nerve injury. When the artery is partially exposed, longitudinal dissection is continued to separate the artery from adjacent veins and other structures. At this point, the artery is easily recognized by its pulsation and characteristic silvery-white color. Veins, in contrast, are nonpulsatile, much darker, and usually of smaller caliber. The median nerve is yellowish with a slightly corrugated surface, and should not be manipulated! A few patients have an accessory brachial artery, which is smaller and usually not suitable for catheterization. This vessel has a more superficial course and generally is not surrounded by veins. Deeper palpation often reveals the location of the true brachial artery.

After isolation, the brachial artery is lifted with a curved hemostat (Fig. 5.12). Two segments of umbilical tape (about 20 cm long and moistened with lidocaine) are looped around the artery and secured with curved hemostats to provide complete control of the vessel. Elastic vascular loops may be used instead of umbilical tape. Superficial antecubital veins in the medial aspect of the antecubital fossa or veins running along with the brachial artery drain into the basilic system and are most suitable for catheterization, as pointed out earlier. After dissection, a segment of vein is lifted with a curved hemostat and ligated distally with a strand of silk or chromic. A second strand of suture is looped around the vein proximally. Both sutures are then secured with curved hemostats (Fig. 5.13).

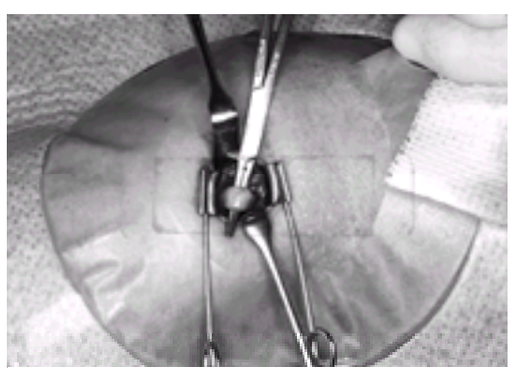

FIG. 5.12. Isolation of the brachial artery in the Syracuse approach. The incision is held open supero-chinferiorly by the self-retaining retractor and laterally by the manual retractors while a curved hemostat is manipulated underneath the artery.

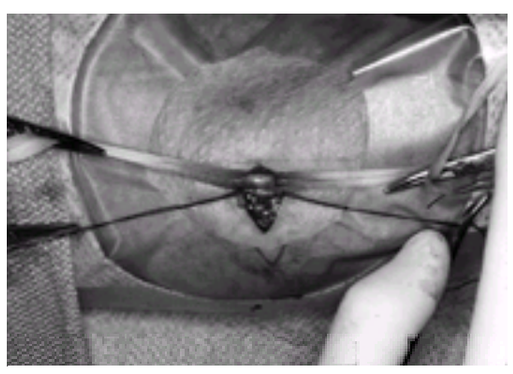

FIG. 5.13. Isolation and securing of the brachial artery and adjacent vein in the Syracuse approach. The brachial artery is secured superiorly and inferiorly with moistened umbilical tapes fixed with curved hemostats. The isolated segment of vein is secured in similar fashion with 4–0 suture.

Venous Access

To insert the venous catheter, extend the vein by applying longitudinal pressure on the hemostats as described previously, and carefully make a 1- to 2-mm *longitudinal* incision using the no. 11 surgical blade. This must be done gently, because the thin-walled vein is prone to tearing and perforation. The superior margin of the incision is elevated with a vein lifter or small forceps as the catheter tip is inserted. The catheter can usually be advanced blindly to the shoulder, again being cognizant to stop advancement at any point of resistance. The catheter should be advanced into the right atrium under fluoroscopy. Owing to the small size of more peripheral veins, it usually is not advisable to inflate balloon-tipped catheters until the thoracic cavity (subclavian vein) has been reached. Tortuosity may require the use of guidewires to facilitate catheter passage. We recommend an 0.018-inch intracoronary guidewire for balloon-tip catheters and an 0.032 J-tipped wire in conjunction with larger end-hole catheters.

Arterial Access

Before arteriotomy, the artery is positioned by applying gentle pressure on the hemostats or umbilical tapes using the thumb and index finger to stretch the artery longitudinally. This maneuver is critical because it allows for arterial positioning, stabilization, and (with adequate tension) excellent hemostatic control. A *longitudinal* arteriotomy is then made with the no. 11 surgical blade held at a 30° angle to the artery with the sharp edge facing upward (toward the ceiling) to minimize risk of injury to the posterior wall. The tip of the blade should penetrate 2 to 3 mm, making an incision approximately 2 mm in length. In our experience, performing the arteriotomy in a longitudinal direction is associated with a lower risk for arterial transection, although repair must be done cautiously to avoid narrowing the lumen. Small forceps may be used to probe or slightly expand the arteriotomy. At this point a sheath or catheter may be introduced (Fig. 5.14). Tapered-tip catheters, such as the Sones or multipurpose catheters, can be inserted without a sheath. A sheath may be preferable, however, when multiple catheter exchanges are planned and when catheters with a nontapered tip are used, such as guiding catheters for percutaneous coronary interventions. To minimize the risk for arterial dissection during insertion of a relatively rigid arterial sheath, we recommend that all sheaths be introduced over a wire. Sheaths and catheters must be carefully aspirated and flushed after insertion.

FIG. 5.14. Insertion of an 8F Sones I catheter (Cordis Company, Miami, FL) into the brachial arteriotomy in the Syracuse approach. A 7F balloon-tipped Swan-Ganz catheter (Baxter Healthcare, Irvine CA) has been placed in the adjacent vein immediately above. The umbilical tapes are retracted using pressure exerted by the thumb and index finger to control bleeding.

After successful arterial cannulation, we recommend systemic anticoagulation with heparin (50 IU/kg) to help prevent thromboembolic events in the distal extremity. If given arterially, heparin should be delivered through the catheter only after it has been advanced into the central circulation, in order to prevent a burning discomfort often experienced during more peripheral infusions.

Access to the Ascending Aorta

Sones and multipurpose catheters can generally be advanced without a guidewire, provided the operator is sensitive to immediately discontinuing advancement of the catheter when *any* resistance is encountered. If resistance is met, further catheter movements must be done under fluoroscopy with the image intensifier positioned to show the clavicle superiorly and the left shoulder articulation laterally. If tortuosity of brachial, axillary, subclavian, or innominate vessels prevents access to the ascending aorta, deep and held inspiration, and lifting of the chin with rotation of the head leftward and over the left shoulder may also facilitate catheter passage. Often, small-volume contrast injections to delineate the vascular path and guidewire support are also necessary for successful catheter passage. An 0.032- or 0.035-inch, moveable-core, J-tipped guidewire or, in extreme situations, a 0.35-inch steerable wire (Magic Torque-MediTech) are helpful. Of note, severe proximal vessel tortuosity greatly reduces catheter movement within the aortic root, consequently impairing the ability to cross the aortic valve or engage the coronary ostia. Occasionally such difficulties cause us to reconsider using an alternative vascular approach.

Catheter Selection

For left heart catheterization, the 8F Sones B-curve and 7F Sones Hi-Flow catheters (USCI), both 80 cm long, are optimal for aortic valve crossing, pressure recording, blood sampling, left ventriculography, aortography, and coronary angiography. Flows of up to 8 mL/sec for the Sones 8F and 10 mL/sec for the Sones 7F Hi-Flow are usually possible without resulting in significant recoil. Castillo type 1, 2, or 3 curves are available in 7F and 8F sizes (Cordis) and are very useful for angiography of coronary artery bypass grafts, coronary engagement in patients with large aortic roots, and situations in which more forceful torque must be applied (see later discussion). The Sones A-type curve is useful for patients with a high takeoff of the left coronary artery. Multipurpose type I and type II catheters have applications generally similar to the Sones. Pigtail catheters (7F or 8F) should be used when contrast flows greater than 10 mL/sec are needed. We find that the dual-lumen multipurpose 8F catheter (Cordis) provides accurate measurement of transvalvular gradients and easily crosses the aortic valve. From the right brachial approach, the femoral mammary catheter is adequate for angiography of the right internal mammary artery, whereas the brachial mammary catheter is required for angiography of the left internal mammary (see later discussion).

Right Heart Catheterization

We generally adhere to the techniques described at the beginning of this chapter, adding that, although optimal for accessing the pulmonary arteries, balloon-tipped catheters are often suboptimal for access to the inferior vena cava. In that case, we still find that the 7F and 8F Cournand catheters (USCI) can achieve adequate access to the inferior vena cava, hepatic vein, and renal veins, particularly when used in conjunction with a soft-tipped guidewire.

Arteriotomy Repair

The catheter is removed while gentle longitudinal pressure is exerted on the umbilical tape loops to control bleeding. Pressure on the *proximal* loop should be released briefly to allow generous antegrade bleeding and flush out possible thrombi that have formed around the catheter. The proximal bleeding is then controlled, and pressure on the distal umbilical tape is released to allow for retrograde (collateral-fed) bleeding to ensure patency of the distal artery. If there is brisk back-bleeding, we believe that no further maneuvers are indicated and arterial closure can commence. If no back-bleeding is present, our next recourse is to manually “milk” or massage the area overlying the radial and distal brachial artery, in distal to proximal fashion, in order to dislodge and remove any possible thromboemboli. If there is still no retrograde flow, we insert a Sones or multipurpose catheter distally through the arteriotomy and carefully advance it until resistance is met. The catheter is then slowly withdrawn while gentle suction is applied to its lumen with a syringe. Only if these maneuvers fail to restore back-bleeding do we believe a

Fogarty embolectomy procedure is warranted.

To repair the arteriotomy, the artery is stabilized by applying pressure with the umbilical tapes or placing a large forceps transversely beneath the artery. A stay suture is placed approximately 1 mm above the proximal end of the arteriotomy, and a continuous lockstitch is performed with sutures evenly spaced at 0.5-mm intervals (Fig. 5.15). The lockstitch is closed with a second stay suture located 1 to 2 mm distal to the incision (Fig. 5.16). Minor bleeding around the sutures can often be controlled with gentle manual pressure or temporary application of a small Gelfoam pad, or both. Once the assistant has confirmed the presence of an adequate radial pulse, the skin and subcutaneous tissues are closed using absorbable suture material and the subcutaneous technique. Two or three ¼-inch Steri-Strips are then applied in transverse fashion across the incision. A small Telfa pad coated with an antibacterial ointment is applied directly over the site and covered with a small stack of 4 × 4 gauze pads, which are then wrapped in firm fashion with a 3-inch wide Ace bandage.

FIG. 5.15. Suture repair of the brachial arteriotomy in the Syracuse approach. The artery is stabilized by placing a large forceps underneath it in transverse orientation. A stay suture has been placed above the superior margin of the longitudinal incision. Lockstitch running sutures will be placed beyond the inferior margin of the incision to close the arteriotomy.

FIG. 5.16. Completed repair of a brachial arteriotomy.

Postprocedure Care

The patient may ambulate with assistance from the catheterization table to a wheelchair. We recommend that the patient then rest in a chair or bed for 2 hours with the arm held straight. Diet and medications can be resumed. Vital signs should be determined every 15 minutes for 2 hours. Blood pressure measurements should not be performed on the arm used for the catheterization for 24 hours after cutdown. Concomitant with vital signs, the catheterization site should be checked for bleeding or swelling. Distal pulses, sensation, and motor function should also be assessed, without unwrapping the Ace bandage. The Ace bandage is first released 2 hours after the procedure to reassess the surgical site. The arm is then rewrapped firmly but comfortably. The Ace bandage should then remain in place for 48 hours. The incision should be kept dry for at least 3 days, with the Steri-Strips removed after 1 week.

Special Techniques

Coronary Bypass Grafts

Aortocoronary vein grafts have a high takeoff compared with coronary arteries; therefore, when using Sones or multipurpose catheters, a longer curve is preferable, such as a Sones A or MP2. Engagement techniques are similar to those used with native coronary arteries. If no graft markers are present, the left anterior oblique projection is preferred for right coronary bypass grafts, which are generally located above the takeoff of the right coronary artery. For left coronary bypass grafts, the right anterior oblique projection offers optimal spatial orientation. The ostia of these bypass grafts are usually “stacked” above the takeoff of the left main coronary artery. When proximal vessel tortuosity limits maneuverability, the aorta is dilated, or the graft ostia are outside their usual locations, a preshaped catheter such as the Castillo or Amplatz is preferable, generally with a type 2 or 3 curve.

Internal Mammary Arteries

The mammary arteries usually originate from the subclavian arteries with inferior takeoffs opposite to the origin of the vertebral arteries. Although the internal mammary artery is best engaged from an ipsilateral brachial approach using preformed femoral catheters, it is usually possible to engage the left mammary from the right brachial approach using one of two techniques. An Amplatz catheter (usually an AR2 or AL0.75) is advanced to the aortic arch and engaged into the left subclavian artery through clockwise rotation. An exchange length wire is passed through this catheter into the subclavian artery and used to exchange the Amplatz for a femoral mammary catheter. Alternatively, a 6F or 7F Giambartolomei brachial-mammary catheter (Cordis) is advanced over a wire into the ascending aorta. The length of the secondary curve of this catheter should be chosen in relation to the width of the aorta. The catheter is advanced against the aortic root, causing prolapse of the secondary curve and formation of a loop within the ascending aorta. While rotating clockwise, the catheter is withdrawn so that the tip is directed into the left subclavian artery. With the catheter tip in the left subclavian, further gentle catheter withdrawal straightens the secondary curve, causing advancement of the tip toward the origin of the left mammary, which can be engaged with further minor manipulations. If the left subclavian artery cannot be engaged with this approach, an alternative is to repeat this maneuver by creating a loop in the secondary curve of the catheter within the *descending* aorta. Similar manipulations are then performed. If these methods are unsuccessful, a left brachial or femoral approach is recommended.

Hepatic Wedge

Indications for measurement of hepatic wedge pressure include the definitive diagnosis of portal hypertension and localization of the lesion resulting in portal hypertension. Posthepatic causes of portal hypertension (e.g., right-sided heart failure, Budd Chiari syndrome, extrinsic obstruction of the upper portion of the SVC) can be readily delineated from intrahepatic or prehepatic causes. Suprahepatic veins join the inferior vena cava at an acute angle and cannot be easily engaged from the femoral approach. Balloon-tipped catheters are often unsuitable because of poor steerability. Open-ended, untapered catheters without side-holes, such as the Cournand, are usually adequate. The catheter is first maneuvered into the right atrium, where the tip is rotated inferiorly, entering the inferior vena cava. Clockwise torque will provide access to the suprahepatic veins. This is indicated by a sharp deviation of the catheter tip from the midline. The catheter is then advanced gently to the wedge position, which is reached when the wave form changes from a right atrial pattern to a straight line and there is no bleed-back. Pressures are recorded in the wedge, intrahepatic, suprahepatic, inferior vena caval, and right atrial positions. A significant gradient (more than 6 mm Hg) between right atrial and hepatic wedge pressures indicates a posthepatic cause of portal hypertension.

Anomalous Coronary Takeoff

Preshaped catheters with Castillo or Amplatz curves are preferable. Some catheter recommendations for specific situations follow:

1. Right coronary artery with inferior takeoff or horizontal heart—AR2, Castillo 1
2. Right coronary artery with anterior takeoff—Castillo 1 or 2
3. Left coronary artery with a high takeoff—Castillo 3, Sones A, MP1
4. Left circumflex coronary originating from the right coronary, if the Sones catheter "overshoots" the origin of the circumflex because it either is very proximal or is immediately adjacent to the right coronary ostium—AR2, Castillo 1
5. Right coronary artery with anomalous takeoff from the left sinus of Valsalva or left coronary artery arising from the right sinus of Valsalva—Castillo 2 or 3, to "scan" the aortic wall seeking the ostium.

Percutaneous Coronary Interventions

A sheath should always be inserted into the brachial artery for these procedures, because guiding catheters are nontapered and difficult to insert without causing arterial trauma. The sheath can be secured to the skin with a suture or by wrapping the umbilical tape loops around the hub. This helps to stabilize the sheath during catheter manipulations. Guiding catheters must always be inserted over a wire because of their reduced flexibility and sharp edges. The 6F or 7F catheter sizes are often useful for percutaneous transluminal coronary angioplasty and stenting (see Chapter 23 and Chapter 25). The 8F catheters are preferred for rotational atherectomy, kissing balloons, large-profile stents (biliary), or when extra support is needed. Visual assessment of brachial artery size allows the operator to assess its suitability for the 10F catheter, which is often required for directional coronary atherectomy.

We suggest the following guiding catheter shapes.

Right Coronary. The secondary curve of guiding catheters advanced from the right brachial position necessarily lies against the left wall of the aorta, yielding superior "backup" support when compared to catheters advanced from the femoral position. Therefore, we often prefer the right brachial approach in cases of severe right coronary tortuosity, calcification, and so on. The hockey-stick design is usually optimal; however, in patients with a small aorta an AR2 may be needed. When deep seating of the catheter is required, the AL 0.75, type 1 or 2 curve is useful.

Left Coronary. Amplatz shapes AL0.75 through AL3 are excellent, especially when engaging a left main coronary artery with a superior takeoff or when approaching a left anterior descending coronary with superior angulation. Other useful curves include the JCL or Q, Voda or XB, and Kimny (6F). From the left brachial approach, standard femoral guiding catheter shapes can be used.

Bypass Grafts. Amplatz types 1, 2, 3, hockey-stick, and multipurpose shapes are usually adequate.

Troubleshooting

Tortuosity of Brachial and Proximal Intrathoracic Vessels

The angle between the innominate (brachiocephalic) and axillary arteries is usually between 90° and 120° and can be negotiated easily with the techniques described earlier (deep inspiration, leftward rotation of the head, and upward chin tilt). These maneuvers may be unsuccessful in cases where severe tortuosity is combined with arterial fibrosis or calcification. In such patients, we first employ a 0.032- or 0.035-inch, moveable-core J-tipped wire, softening a portion of the distal tip in order to negotiate the tortuosity. If this maneuver fails, the tip of a steerable wire is curved between 30° and 90° along a 2- to 4-cm length and is then gently advanced while rotating. Breathing maneuvers are often simultaneously employed. When the axillary artery originates anomalously as a separate fourth branch of the aortic arch, access to the ascending aorta is very difficult and catheter maneuverability very limited. An alternative to the right brachial approach is advisable in this situation.

Attempting catheter passage through calcified and tortuous axillary and innominate arteries may cause vessel wall damage. This occurs more frequently when a guidewire is not used and must be suspected whenever there is resistance to catheter advancement. Injection of a small amount of nonionic or diluted contrast material through the catheter may uncover the presence of a dissection, which does not *necessarily* preclude completion of the procedure. If a steerable guidewire can be advanced carefully beyond the dissection and all further catheter advancement performed over a wire, the procedure can be successfully completed and further injury avoided. Such dissections against the direction of blood flow are usually self-sealing, but in situations in which there is evidence of neurovascular compromise after catheter removal, consultation with a vascular surgeon is advised. Of course, if the tip of a steerable guidewire continues to enter the dissection rather than the proximal true lumen, alternative vascular access must be sought.

Spasm

Brachial and/or axillary artery spasm is more prevalent in younger patients, particularly women, and when the catheter is of large caliber compared with the artery. Exchanging it for a smaller catheter is usually beneficial. Vasodilators such as nitroglycerin or injectable calcium channel blockers have been of limited value, in our experience. We find that that *intravenous* papaverine (30 to 60 mg) is often more efficacious. It should be noted that papaverine is quite painful when administered *intraarterially* and may actually exacerbate spasm.

Loss of Radial Pulse

The most frequent causes of an absent or diminished radial pulse after a brachial procedure are thrombosis at the arteriotomy site, embolization to the radial artery, dissection at the arteriotomy site, inappropriate suturing, and spasm. If arterial spasm was not a factor during catheter manipulation, it is unlikely to develop after arteriotomy repair and, therefore, should not be assumed to be responsible for a poor radial pulse.

When the radial pulse is absent, the artery should be reisolated and secured with umbilical tapes and curved hemostats. The arteriotomy sutures are then carefully removed and antegrade and retrograde bleeding reassessed. If blood flow is normal, a problem with the initial arterial closure should be suspected (e.g., suturing through the posterior wall of the artery, creation of a significant cross-sectional narrowing of the arterial lumen). The arteriotomy should then be carefully resutured to avoid such problems.

When blood flow remains diminished from either direction, further massaging or "milking" of the artery is performed, as described previously, to dislodge and flush out any thrombi. The arteriotomy can be inspected proximally and distally to assess for a dissection flap by inserting a small forceps. If a dissection is evident, the true arterial lumen should be located with the small forceps and a soft-tipped catheter (Sones) carefully inserted a short distance. The catheter acts as a stent to appose all layers of the arterial wall. While the catheter is in place, two or three interrupted sutures are used to bind the layers of the arterial wall together. The arteriotomy is then repaired. When dissection is not evident, the catheter aspiration maneuver described earlier should be performed. If poor retrograde blood flow persists, a no. 3 Fogarty catheter should then be inserted distally and embolectomy attempted using standard techniques. After embolectomy the arteriotomy is resutured, slightly extending the length and depth of the suture line so as to "tack down" any possible intimal disruptions (flaps).

Following these maneuvers, the radial pulse is often reestablished but diminished due to resulting arterial spasm. Administration of oral nifedipine (10 mg) or intravenous papavarine (30 mg) is frequently beneficial. Consultation with a vascular surgeon should be obtained if a radial pulse is not reestablished, particularly if signs of neurovascular compromise are present.

Hand Numbness

Hand numbness may result from impaired circulation or median nerve compromise. If the brachial dressing is not overly tight and the radial pulse is palpable, the cause of numbness is unlikely to be circulatory. Severe median nerve injury during cutdown is usually apparent immediately because the patient experiences a striking and characteristic discomfort (electric shock sensation). The most common cause of later median nerve injury is compression induced by hematoma formation after skin closure. This usually develops gradually over the course of several hours after the procedure. The hematoma should be evacuated promptly, to avoid

potentially irreversible damage from long-standing median nerve compression.

ACKNOWLEDGMENT

The authors acknowledge the input and assistance provided by Alessandro Giambartolomei, Paolo Esente in the preparation of this chapter.

CHAPTER REFERENCES

1. Rapaport E, Dexter L. Pulmonary “capillary” pressure. In: *Methods in Medical Research,* vol 7. Year Book, 1958:85.
2. Dexter L, Burwell CS, Haynes FW, et al. Oxygen content of pulmonary “capillary” blood in unanesthetized human beings. *J Clin Invest* 1946;25:913.
3. Dexter L, et al. Studies of congenital heart disease: II. The pressure and oxygen content of blood in the right auricle, right ventricle and pulmonary artery in control patients, with observations on the oxygen saturation and source of pulmonary “capillary” blood. *J Clin Invest* 1947;26:554.
4. Hellens HK, Haynes FW, Dexter L. Pulmonary “capillary” pressure in man. *J Appl Physiol* 1949;2:24.
5. Werko L, Varnauskas E, Eliasch H, et al. Further evidence that the pulmonary capillary venous pressure pulse in man reflects cyclic changes in the left atrium. *Circ Res* 1953;1:337.
6. Connolly DC, Kirklin JW, Wood EH. The relationship between pulmonary artery wedge pressure and left atrial pressure in man. *Circ Res* 1954;2:434.
7. Batson GA, Chandrasekhar KP, Payas Y, et al. Measurement of pulmonary wedge pressure by the flow directed Swan-Ganz catheter. *Cardiovasc Res* 1972;6:748.
8. Schoenfeld MH, Palacios IF, Hutter AM, et al. Underestimation of prosthetic mitral valve areas: role of transseptal catheterization in avoiding unnecessary repeat mitral valve surgery. *J Am Coll Cardiol* 1985;5:1387.
9. Hosenpud JD, McAnulty JH, Morton MJ. Overestimation of mitral valve gradients obtained by phasic pulmonary capillary wedge pressure. *Cathet Cardiovasc Diagn* 1983;9:283.
10. Lange RA, Moore DM Jr, Cigarroa RG, et al. Use of pulmonary capillary wedge pressure to assess severity of mitral stenosis: is true left atrial pressure needed in this condition? *J Am Coll Cardiol* 1989;13:825.
11. Baker LD, Leshin SJ, Mathur VS, et al. Routine Fogarty thrombectomy in arterial catheterization. *N Engl J Med* 1968;279:1203.

6
Diagnostic Catheterization In Infants And Children

John F. Keane, James E. Lock, and Stanton B. Perry

Department of Cardiology, Harvard Medical School, Children's Hospital, Boston, Massachusetts 02115

The mission of the pediatric catheterization laboratory continues to evolve. Although the total number of patients catheterized per year has not changed a great deal in the past several years, the proportion undergoing an interventional procedure continues to increase, from 6% in 1984 to 68% in 1997 (Fig. 6.1).

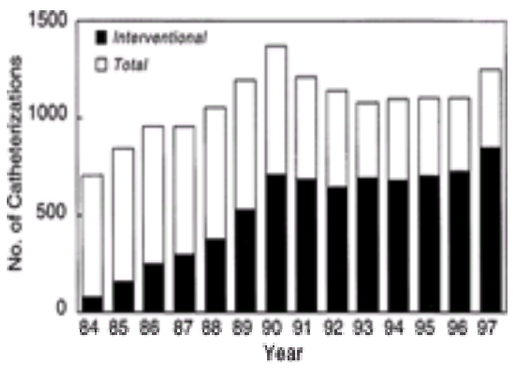

FIG. 6.1. Number of cardiac catheterizations per year, 1984 through 1997, at Children's Hospital, Boston, with the increasing proportion of interventional procedures indicated by the shaded areas.

Echocardiography has greatly influenced the catheterization laboratory patient profile. The remarkable diagnostic precision of this tool has essentially eliminated the need for preoperative diagnostic catheterization in many of the common congenital lesions, such as tetralogy of Fallot, total anomalous pulmonary venous return, and endocardial cushion defects (1,2). On the other hand, echocardiography identifies lesions, formerly undetected by other noninvasive means, that may be now therapeutically managed in the laboratory, such as a “silent” patent ductus arteriosus (PDA) and a small atrial septal defect (ASD). In addition, it is being used more frequently, particularly in the transesophageal mode, during interventional procedures such as septal device placement (3).

Although obtaining hemodynamic and/or diagnostic data was the sole reason for study in some 400 patients (approximately one third of our total catheterizations), these data remained “part and parcel” of most of the other studies as well, being used for example to accurately quantitate results of interventions. This chapter presents our current catheterization methodology, including information on sedation, anesthesia, and vessel access. In addition a few specialized procedures such as ASD creation, transseptal puncture, endomyocardial biopsy, coronary angiography, and pulmonary vein wedge angiography are described. Details of interventional techniques for management of lesions such as ASD, ventricular septal defect (VSD), PDA, stenotic valves, and collateral vessels are presented in Chapter 28 and Chapter 34.

CATHETERIZATION PROTOCOL

General

Patient Population

At least 80% of our population come as outpatients, fasting, for their studies, all necessary precatheterization tests having been completed in the preceding days. Older patients are given nothing by mouth after midnight, and infants are given clear liquids up to 3 hours before the procedure. Patients with a hematocrit greater than 50% are admitted the preceding day and adequate hydration is maintained via intravenous fluids. All patients have an intravenous line placed on arrival. Because of the very high incidence of interventional procedures, each patient has an assigned nurse throughout the study. Anesthesiologists provide general anesthesia for some 25% of the studies and medication advice and supervision for many of the others. At the conclusion of the study, many of the patients are discharged the same day, including all noninterventional cases except for PDA occlusion (4) and a few older pulmonary stenosis balloon valvotomy patients. All available patient information is discussed in some detail by the catheterizing physicians, including the anesthesiologist, immediately before the study, and procedure plans are then formulated.

Sedation and Anesthesia

Significant changes have occurred over the past decade, and continue to be made, in sedation and anesthesia administration, largely because of the increasing proportion of interventional studies. Approximately 80% of patients are studied using “conscious” sedation; the remainder are intubated and receive general anesthesia from the outset. There are some in whom sedation alone is insufficient during the procedure, who then require general anesthesia.

Sedation

This modality is used for all noninterventional studies; for balloon dilation of pulmonary and aortic valvar stenosis, coarctation, most pulmonary artery stenoses, and most stent placements; and for coil occlusion of aortopulmonary collaterals and PDAs. For those patients weighing 10 kg or less, intravenous morphine (0.025 to 0.05 mg/kg) and midazolam (0.025 to 0.05 mg/kg) are given, and additional doses may be given during the procedure to a maximum total for each of 0.4 mg/kg. In patients weighing 10 to 25 kg, demerol compound (thorazine 6.25 mg/mL, phenergan 6.25 mg/mL, and demerol 25 mg/mL) is given subcutaneously for premedication to a maximum of 2 mL, the dose based on weight and arterial oxygen saturation (5,6). During the procedure if additional sedation is necessary, midazolam and morphine (each 0.025 to 0.05 mg/kg IV) may be given to a maximum total for each of 0.3 mg/kg. If Demerol compound premedication is not used initially, then midazolam alternating with morphine using the above dosages may be given to a total for each of 0.4 mg/kg. For those patients weighing more than 25 kg, midazolam may be

used for premedication and, alternating with morphine, during the study at the above dosage levels. If these are unsatisfactory, droperidol, 0.025 mg/kg IV over 15 to 30 minutes, may be given twice.

Anesthesia

Although this sedation technique is referred to as “conscious sedation” in adults, in our experience most of the patients are in fact “unconscious”—that is, they often exhibit no response on needle insertion for local anesthesia. Respiratory depression is not uncommon, and frequent blood gas monitoring is mandatory. General anesthesia from the outset of the procedure is undertaken in all those in whom placement of a septal double-umbrella device is planned (7,8). It is also used for those with bilateral peripheral pulmonary stenosis with right ventricular systolic pressure at or above systemic arterial level when balloon dilation is planned, particularly if concomitant left-sided heart obstruction is present, and in patients with severe congenital mitral stenosis. In addition, all those to undergo mapping and ablation electrophysiologic procedures receive general anesthesia.

This is a very complex and complicated technique. It requires management by an experienced anesthesiologist and is beyond the scope of this text. In brief, drugs such as morphine and fentanyl (analgesics) or thiopental and propofol (anesthetics) are used for induction, and inhaled nitrous oxide, oxygen, and isoflurane are used throughout the study together with a muscle relaxant such as pancuronium. Many of these agents have hemodynamic ill effects, although some, such as remifentanil, are considered free of these (9).

Catheterization Study

Although most lesions today have been correctly identified by physical examination and noninvasive techniques before the study begins, setting out with an open mind rather than simply trying to prove the existence of what one already thinks is present is extremely important. Physicians who catheterize “with blinders on” miss important diagnoses.

Catheters are introduced percutaneously into the femoral vessels in the great majority of cases at the level of the superior ramus of the pubis, using the smallest catheters that are adequate to obtain the necessary information. Before the infusion of any heparin or heparinized flush solution, an activated clotting time (ACT) is measured and heparin (100 IU/kg) is then administered intravenously to a maximum of 5,000 IU, with additional doses to maintain the ACT at greater than 200 seconds throughout the study. The initial phase of the procedure is aimed at gathering physiologic data. A right-sided heart catheterization is performed, measuring oxygen saturation in the superior vena cava and recording pressures and saturations in the midlateral right atrium (RA); inflow and outflow portions of the right ventricle (RV); main, right and left pulmonary arteries (PA); and pulmonary capillary wedge positions. The atrial septum is explored and, if traversed, pressures and saturations are recorded in the left atrium (LA) at least one pulmonary vein, and left ventricle (LV). The catheter is then repositioned in a distal PA branch. An arterial catheter, placed in most cases, is used to record pressure, oxygen saturation, and blood gas values in the descending and then ascending aorta. The arterial catheter is advanced to the LV, oxygen saturation is measured, and pressure is recorded simultaneously with pulmonary capillary wedge pressure. Oxygen consumption is measured using a flow-through metabolic rate meter (Waters Inc., Rochester, MN), as right and left heart chamber pressures and saturations are recorded during catheter withdrawal for use in computation of pulmonary and systemic flow and resistance values. In the absence of intracardiac shunting, cardiac output may also be assessed by thermodilution (10).

The next phase of the study consists of angiography with particular emphasis on appropriate patient positioning for optimum visualization of specific cardiac anatomy. If no other data collection or procedures are contemplated, the renal shadows are viewed under fluoroscopy (11), the catheters are removed, and bleeding at the entry sites is controlled with a minimum of 15 minutes of local pressure. In our experience, protamine sulphate administration has rarely been necessary, at most once per year. We have, however, encountered rare episodes of pelvic bleeding due to arterial catheter entry proximal to the pubic ramus, some of which have required surgical intervention, manual vessel compression after catheter removal being ineffective in such a setting.

Other Vascular Entry Sites

Umbilical Vessels

In the neonate, venous access is feasible for some 3 days after birth. Anatomically, the umbilical vein enters at the bifurcation of the portal vein, opposite to which the ductus venosus arises, the latter then coursing posteriorly to open into the inferior vena cava. This is a tortuous course, approximately 180° in the lateral view, and catheter passage is more safely accomplished in the laboratory where angiographic delineation aids catheter entry (Fig. 6.2). Use of a tip deflector system (Cook, Bloomington, IN) facilitates catheter negotiation to the heart and also from RA to RV. At our own institution, a survey several years ago involving multiple operators revealed successful entry for 70% of neonates in the first day of life, 56% in the second, and 43% in the third. Although catheterization of right heart structures is more difficult with this technique than from a femoral venous approach, access to left heart structures, including the aorta, is relatively easy. The umbilical vein is commonly used for balloon atrial septostomy (see later discussion). The umbilical artery is traversible longer than the umbilical vein, occasionally to age 10 days. Anatomically, this vessel turns acutely posteriorly and distally to join the iliac artery, and a further 90° turn by the catheter is then necessary to reach the descending aorta. Nevertheless, passage is surprisingly easy, and this route has provided a means for arterial pressure and saturation monitoring, aortography, and even balloon dilation of critical valvar aortic stenosis (12).

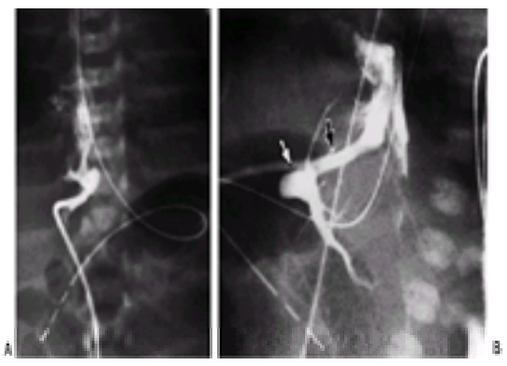

FIG. 6.2. Posteroanterior **(A)** and lateral **(B)** views outlining contrast course via umbilical vein to portal vein *(open arrow)*, then via ductus venosus *(closed arrow)* to inferior vena cava.

Transhepatic Venous Route

In patients in whom femoral venous channels are occluded and those with congenital inferior vena cava interruption, a transhepatic venous approach has been increasingly used both for diagnostic and interventional procedures (13,14 and 15). We use the expertise of our radiology colleagues to help place these lines. After local anesthesia, a long 22-gauge needle is inserted in the midaxillary line, approximately halfway between the diaphragm and the inferior liver edge, and advanced with the use of ultrasound guidance and contrast injections into a large central hepatic vein. A sheath and dilator are then advanced over a guidewire to the RA. In addition to acquiring diagnostic data, this route has been used for interventional procedures such as transseptal studies and placement of double-umbrella devices in atrial defects using sheaths as large as 11F even in children. At the conclusion of the procedure, the hepatic tissue channel is occluded with coils during final catheter withdrawal. This procedure has been surprisingly uncomplicated, the most frequent problem being transient abdominal discomfort, presumably due to peritoneal irritation.

Internal Jugular Vein

This vessel, usually the right, large even in infants, is frequently used for RV biopsies, in double-umbrella device closure of apical muscular VSDs, in patients with bidirectional Glenn shunts, and in electrophysiologic studies. The ipsilateral arm is placed at the patient's side, and the head is turned to the opposite shoulder. A catheter in the vessel from a femoral venous approach, if available, provides an excellent guide for needle entry. The percutaneous needle, after local anesthesia, is

advanced in the depression between the two heads of the sternomastoid, above the medial end of the clavicle, in a direction posterior to the latter, while gently aspirating. A wire, sheath, and dilator are then introduced. Complications have been surprisingly few, consisting mainly of local hematomas or inadvertent entry of the more medially located carotid artery.

Subclavian Vein

This vessel is commonly used in patients of all ages, even in babies weighing 3 kg (16). It is necessary where thrombosis of iliac veins or infrarenal inferior vena cava has occurred after prior catheterization. In addition, palliative surgical procedures, such as the bidirectional Glenn procedure, which consists of anastomosis of the cephalad end of the superior vena cava with the PA, make this approach necessary to reach the PA. We prefer the left subclavian vein, largely because later catheter manipulation seems easier. The patient is first placed in a slight Trendelenburg position, a small rolled-up towel is placed lengthwise under the thoracic spine, and the patient's left arm is positioned at the side. Lidocaine is injected down to the periosteum at the junction of the clavicle and first rib. A 19-gauge, short, bevelled, thin-walled needle is used to enter the skin at the junction of the medial and middle thirds of the clavicle in adults, or 1 to 2 cm lateral to that point in infants and children (17). The needle is advanced toward the suprasternal notch, while maintaining an orientation that is both perpendicular to the spine and parallel to the floor as the needle tip passes between the clavicle and first rib, with continual aspiration of the syringe. Once venous blood returns freely, a preformed guidewire is inserted and advanced to the superior vena cava, and an appropriate-sized sheath with a backbleed valve is then inserted. At the conclusion of the study, the sheath is removed and bleeding is controlled with at least 15 minutes of gentle pressure on the first rib. Outlining the vessel by prior contrast injection in the left hand is particularly helpful. In addition to acquisition of hemodynamic and angiographic data, this approach has been of considerable value in reaching distal PAs when the RV is large and in placement of PA stents.

EQUIPMENT USED IN CATHETERIZATION

Catheters

Based on issues of patient safety, teaching responsibilities, and cost, balloon-tipped flow-directed transvenous catheters are used initially in all age groups. These may be either end-hole or side-hole (angiographic) in type and range from 4F to 7F in diameter. Acute bends may be shaped by hand just before insertion, especially with the smaller catheters. Deflector wires may be used within these catheters to help attain access to desired sites (e.g., LV from LA, aorta from LV). For arterial studies, ultrathin-walled white Teflon pigtail catheters ranging from 3.2F to 7F are used (18,19); they provide satisfactory contrast flow rates (e.g., up to 35 mL at 35 mL/sec through a 6F, 80-cm catheter). Using a Y adapter (USCI, Billerica, MA), satisfactory pressures and angiograms (up to 20 mL at 20 mL/sec) are obtainable even with a 0.035-inch guidewire in place through a 7F pigtail catheter (20).

Contrast Material

Currently only the osmolar (nonionic or dimeric) contrast materials are used, their cost having decreased substantially in recent years. We make every effort not to exceed a total dose of 5 mL/kg for the entire study.

Radiographic Equipment

Because of contrast agent constraints and the necessity of acquiring as much anatomic information as possible from each injection, biplane equipment is essential for pediatric catheterization. Given the broad range in patient age and size, a wide range of image intensifier modes is necessary, from 5 inches for neonates to 12 to 14 inches for older patients in whom it is necessary to image the PAs and larger cardiac chambers. Precise patient positioning is essential to provide optimum visualization of anatomy (21,22). The most common views used are the long axial oblique (for VSD, Fig. 6.3), the right anterior oblique (for subaortic stenosis, Fig. 6.4), the four-chamber or hepatoclavicular (for endocardial cushion defect, Fig. 6.5), and the sitting up or cranial angled view (for central PA anatomy, Fig. 6.6). All cineangiograms in our institution are now recorded with the use of digital enhancement and stored in a RAID (Redundant Array of Independent Discs) system and on individual compact disks.

FIG. 6.3. Long axial oblique (analogous to 30° left anterior oblique, 30° cranial) view of left ventricular cineangiogram in an infant with a membranous ventricular septal defect *(arrow)*.

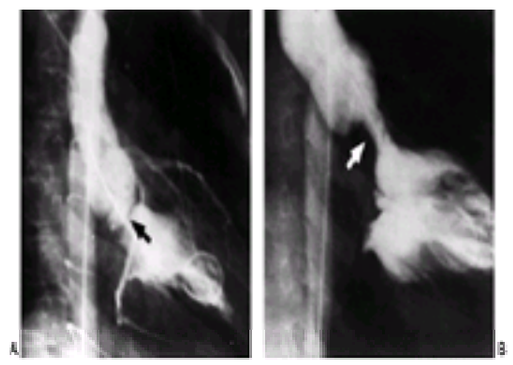

FIG. 6.4. Subaortic stenosis, right anterior oblique view, discrete (**A**, *arrow*) and diffuse muscular (**B**, *arrow*).

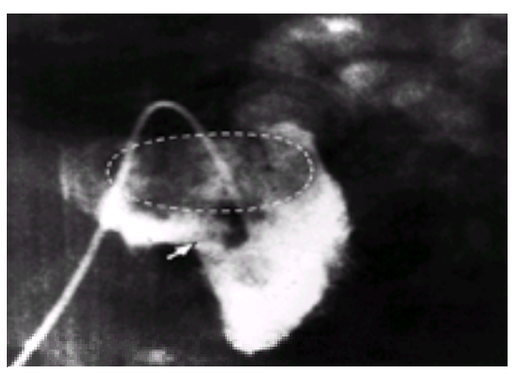

FIG. 6.5. Four-chamber or hepatoclavicular view of endocardial cushion defect with common atrioventricular valve *(dashed line)* in atrial systole and ventricular septal

defect *(arrow)* in an infant.

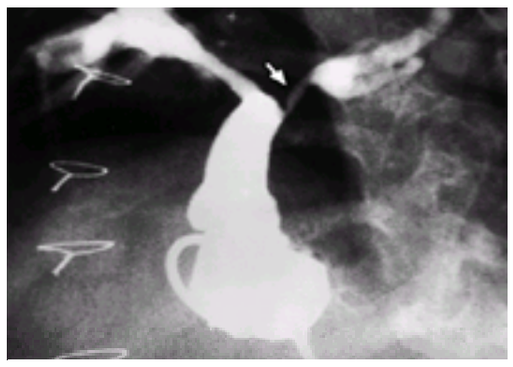

FIG. 6.6. MPA cine, with cranial angulation (“sitting up” view) with (L) anterior oblique, in postoperative patient with tetralogy of Fallot showing bilateral pulmonary artery stenosis, severe *(arrow)*, at the original of the left pulmonary artery.

SPECIAL PROCEDURES

Atrial Septostomy

Since the introduction of balloon atrial septostomy (BAS) by Rashkind and Miller in 1966 (23), this procedure has been the standard initial therapy for infants with d-transposition of the great arteries. This congenital anomaly, in which the pulmonary and systemic circuits are in parallel rather than in series, often results in severe hypoxia and acidosis immediately after birth. In this setting, BAS improves bidirectional mixing at the atrial level, resulting in an immediate rise in arterial oxygen saturation with alleviation of acidosis. This procedure is also of value in neonates with left atrial outflow obstruction (e.g., mitral atresia), because an initial atrial septal opening frequently narrows within weeks of birth.

Vascular entry is obtained either by way of the umbilical vein or percutaneously from a femoral vein. The septostomy catheter we most commonly use is the 5F Miller-Edwards catheter (American Edwards Laboratories, Santa Ana, CA), which requires a 7F sheath for insertion to allow passage of the unrecessed balloon. For the umbilical venous approach, we use a sheath with a valve (back-flow adapter) to avoid air embolism. The catheter tip is advanced to the middle LA, using biplane fluoroscopy. The balloon is held against the atrial septum and inflated rapidly (to a maximum of 4 cc). The catheter is then advanced 1 or 2 mm before being pulled briskly to the junction of the inferior vena cava and RA, advanced to the RA, and then rapidly deflated. This sequence is usually repeated at least twice to ensure that an adequate atrial septal opening has been created. It results in a rapid rise in arterial blood oxygen saturation, evidence of bidirectional shunting at the atrial level, and abolition of the interatrial pressure gradient. Alternatively, this procedure can be carried out at the bedside under two-dimensional echocardiographic guidance. Complications are extremely rare, but tears of pulmonary veins and atrial walls have occurred.

The BAS technique just described is usually ineffective after 1 month of age and in those neonates with very thick atrial septa. In such patients, the atrial septum is crossed in a location other than the patent foramen with a transseptal needle and sheath. Then, via the sheath a guidewire is passed, preferably to a left pulmonary vein, after which a succession of angioplasty balloon catheters of increasing size are inflated in the newly created atrial hole. An alternative method, now uncommonly used, consists of placing a catheter with a retractable blade (24) via a sheath into the LA. Blade lengths of 9.4, 13.4, and 20 mm are available (Cook). The blade is opened carefully in the LA under biplane fluoroscopic monitoring and then withdrawn slowly across the atrial septum. This procedure is followed by a balloon septostomy to further enlarge the resulting opening. If oxygen saturation rise and pressure gradient reduction are inadequate, the procedure is repeated using a larger blade and/or balloon catheters until the mean residual left-to-right atrial gradient is less than or equal to 3 mm Hg (25).

Transseptal Left-Sided Heart Catheterization

The availability of biplane fluoroscopy has significantly reduced the complication rate associated with this technique. In addition, introduction of the long Mullins sheath (USCI) has made transseptal catheterization easier and has broadened the indications for this procedure (26). Current indications include LA access for balloon valvotomy of mitral stenosis, LV catheterization in the presence of an aortic valve prosthesis, and device closure of VSD. We have not encountered any fatal complications related directly to this procedure.

Available equipment includes 6F and 7F long sheaths and needles of appropriate size. The sheath is introduced percutaneously by way of the right femoral vein, although we have used the left femoral vein after additional prebending of the distal needle shaft. We prefer to attach the needle lumen to a syringe filled with contrast material rather than a pressure transducer, to allow precise location of the needle tip after its initial extrusion. Pressure measurement alone via the needle tip can give misleading information about tip location. Availability of two-dimensional echocardiographic visualization during the procedure is also helpful when the atrial septal location is unusual.

Selective Coronary Arteriography

In general, ventriculography and aortography are sufficient to identify the major proximal coronary arteries in such conditions as tetralogy of Fallot, d-transposition of the great vessels, or double-outlet right ventricle. However, selective coronary injections are necessary in a variety of anomalies, including Kawasaki disease, coronary artery fistulae, and pulmonary atresia with intact ventricular septum, and frequently when origin of the left anterior descending artery from the right coronary artery is suspected. Borrowing from the enormous experience of our colleagues with adult patients, miniaturized catheters for use in pediatric patients, including infants, have been developed. We use a variety of such catheters, ranging from 4.5F to 7.3F, in Judkins or Amplatz configurations (Cook) with varying secondary loop sizes. We use standard techniques and angiographic views (see Chapter 11) and appropriately smaller doses of contrast material.

Pulmonary Vein Wedge Angiography

Some patients, as a result of a congenital defect or prior cardiac surgery, have complete occlusion of a proximal pulmonary artery, usually the left. Although an injection in the aorta or even in a collateral vessel may outline the size and location of the isolated PA, it is essential before any surgical reanastomosis is undertaken to identify unequivocally the presence and size of that PA. A balloon-tipped end-hole catheter is placed across the atrial septum and into a pulmonary vein in the appropriate lung. With the balloon inflated, up to 0.3 mL/kg of nonionic contrast agent (which causes less coughing than high-osmolar ionic agents) is injected, followed immediately by an equal volume of saline. The parenchymal vessels are usually well outlined by this method, with back-filling, if present, of the mediastinal segment. On occasion, the main and contralateral PA may also fill if they are in continuity. It is important to use biplane cineangiography for these injections to identify accurately the degree of proximal extension of the vessel relative to the bronchus on that side.

Endomyocardial Biopsy

The technique of endomyocardial biopsy has improved considerably in recent years (see Chapter 20). Many bioptomes, some as small as 3F, are now available, and together with preformed long sheaths they have made biopsy a rather safe procedure, even in newborns. The number of biopsies at our institution has increased markedly, mostly because of cardiac transplantation. The great majority of procedures involve right ventricular biopsy, although left-sided specimens can be obtained if necessary. Because the procedure is repeated frequently in patients with a cardiac transplant, a different venous percutaneous access site is usually used with each procedure. The vessels used are the internal jugular, subclavian, and femoral veins for right-sided biopsies. If left ventricular samples are required, the approach is transseptal in infants and retrograde from a femoral artery in older patients.

SPECIAL CATHETER TECHNIQUES

With continued widespread use of homografts to bypass stenotic or atretic lesions, particularly in the right side of the heart, obstruction over time is increasingly encountered. With the advent of balloon dilation and stents (27), localization of the exact sites of obstruction to make use of these therapeutic modalities is important. To this end, a very useful double-lumen balloon catheter (Fig. 6.7 and Fig. 6.8) is available with the ports 3 cm apart in the 7F size and 2 cm in the 6F size (28).

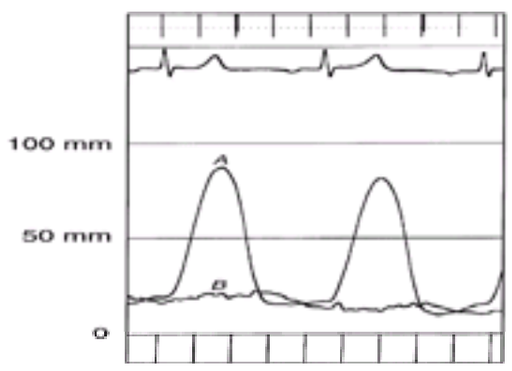

FIG. 6.7. Simultaneous pressure tracings proximal **(A)** and distal **(B)** to obstructed valve in right ventricle to pulmonary artery homograft recorded using double-lumen 7F catheter.

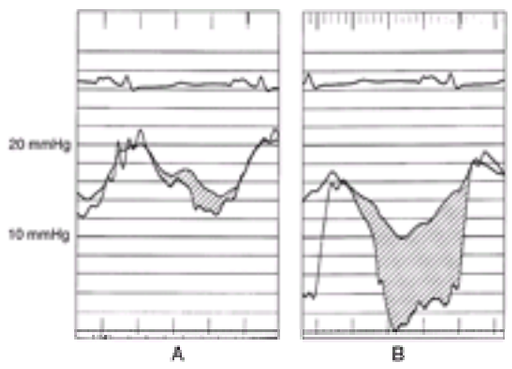

FIG. 6.8. Simultaneous pressure tracings in a 21-year-old patient with tricuspid atresia with right atrium–nright ventricle valved conduit. **A:** No obstruction present at valve. **B:** Significant obstruction *(shaded)* evident between distal conduit and right ventricle.

A number of lesions amenable to balloon dilation, such as peripheral pulmonary stenosis and aortic coarctation, require measurement of pressures across the dilated areas together with angiography to assess the results of such therapy. To facilitate such studies safely, cutoff pigtail catheters with Y adapters are used over guidewires. A review of 737 such procedures found that satisfactory data were obtained with only one instance of wire dislodgment. Contrast volume and flow rates were determined using a variety of catheter and wire combinations (20).

Older patients with tetralogy of Fallot who had a transannular right ventricular outflow patch placed as part of their surgical repair frequently have right and/or left PA origin stenosis, very dilated RA and RV chambers, and both tricuspid and pulmonary regurgitation. From a femoral venous approach, it is often difficult to reach the distal PA branches for balloon/stent therapy. In many, an approach from the left subclavian vein provides a more stable catheter course. In addition, use of a large guiding sheath with its tip just proximal to the PA origins allows easier passage of dilating balloons and stents. Use of Amplatz coronary artery catheters also allows easier access to these PAs, especially the left.

SUMMARY

The past 15 years have seen substantial changes in the cardiac catheterization of infants and children, both as a diagnostic tool and particularly as an important therapeutic modality. The diagnoses (e.g., complex congenital heart disease), techniques (e.g., umbilical artery and vein access), patient management (e.g., deep sedation or even general anesthesia), and specific procedures (e.g., atrial septostomy) in this population are not part of the day-to-day world of the adult cardiac catheterization specialist. We hope that this overview of pediatric catheterization and the companion chapter on pediatric intervention (Chapter 28) will contribute to a more rounded overview of invasive cardiology.

CHAPTER REFERENCES

1. Lipshultz SE, Sanders SP, Mayer JE, et al. Are routine preoperative cardiac catheterization and angiography necessary before repair of ostium primum atrial septal defect? *J Am Coll Cardiol* 1988;11:373.
2. Huhta JC, Glasgow P, Murphy DJ Jr, et al. Surgery without catheterization for congenital heart defects: management of 100 patients. *J Am Coll Cardiol* 1987;9:823.
3. van der Velde ME, Perry SB. Transesophageal echocardiography during interventional catheterization in congenital heart disease. *Echocardiography* 1997;14:513.
4. Wessel DL, Keane JF, Parness I, et al. Outpatient closure of patent ductus arteriosus. *Circulation* 1988;77:1068.
5. Lock JE. Evaluation and management prior to catheterization. In: Lock JE, Keane JF, Fellows KE. *Diagnostic and Interventional Catheterization in Congenital Heart Disease.* Boston, Martinus Nijhoff, 1987:1.
6. Ruckman RN, Keane JF, Freed MD, et al. Sedation for cardiac catheterization: a controlled study. *Pediatr Cardiol* 1980;1:263.
7. Hickey PR, Wessel DL, Streitz SL, et al. Transcatheter closure of atrial septal defects: hemodynamic complications and anesthetic management. *Anesth Analg* 1992;74:44.
8. Laussen PC, Hansen DD, Perry SB, et al. Transcatheter closure of ventricular septal defect: hemodynamic instability and anesthetic management. *Anesth Analg* 1995;80:1076.
9. Lynn AM. Remifentanil: the paediatric anaesthetist's opiate? [Editorial]. *Paediatr Anaesth* 1996;6:433.
10. Freed MD, Keane JF. Cardiac output by thermodilution in infants and children. *J Pediatr* 1978, 92:39.
11. Nussbaum AR, Newman B, Freed MD, et al. Nonutility of cineurograms in children with congenital heart disease. *Am J Cardiol* 1987;60:684.
12. Egito ET, Moore P, O'Sullivan J, et al. Transvascular balloon dilation for neonatal critical aortic stenosis: early and midterm results. *J Am Coll Cardiol* 1997;29:442.
13. Wallace MJ, Hovsepian DM, Balzer DT. Transhepatic venous access for diagnostic and interventional cardiovascular procedures. *J Vasc Interv Radiol* 1996;74:57.
14. Shim D, Lloyd TR, Cho KJ, et al. Transhepatic cardiac catheterization in children: evaluation of efficacy and safety. *Circulation* 1995;92:1526.
15. Johnson JL, Fellows KE, Murphy JD. Transhepatic central venous access for cardiac catheterization and radiologic intervention. *Cathet Cardiovasc Diagn* 1995;35:168.
16. Linos DA. Subclavian vein: a golden route. *Mayo Clin Proc* 1980;55:315.
17. Keane JF, Lock JE. Vessel entry and catheter manipulation. In: Lock JE, Keane JF, Fellows KE. *Diagnostic and Interventional Catheterization in Congenital Heart Disease.* Boston, Martinus Nijhoff, 1987:14.
18. Keane JF, Fellows JE, Lang P, et al. Pediatric arterial catheterization using a 3.2 French catheter. *Cathet Cardiovasc Diagn* 1982;8:201.
19. Keane JF, Freed MD, Fellow KE, et al. Pediatric cardiac angiography using a 4 French catheter. *Cathet Cardiovasc Diagn* 1977;3:313.
20. Verma R, Keane JF. Use of cut-off pigtail catheters with intra-luminal guide wires in interventional procedures in congenital heart disease. *Cathet Cardiovasc Diagn* 1994;33:85.
21. Elliot LP, Bargeron LM Jr, Bream PR, et al. Axial cineangiography of congenital heart disease: section II. Specific lesions. *Circulation* 1977;56:1084.
22. Fellows KE, Keane JF, Freed MD. Angled views in cineangiography of congenital heart disease. *Circulation* 1977;56:485.
23. Rashkind WJ, Miller WW. Creation of an atrial septal defect without thoracotomy: a palliative approach to complete transposition of the great arteries. *JAMA* 1966;196:991.
24. Park SC, Neches WH, Zuberbuhler Jr, et al. Clinical use of blade atrial septostomy. *Circulation* 1978;58:600.
25. Perry SB, Lang P, Keane JF, et al. Creation and maintenance of an adequate interatrial communication in patients with left atrioventricular valve atresia or stenosis. *Am J Cardiol* 1986;58:622.
26. Mullins CE. Transseptal left heart catheterization: experience with a new technique in pediatric and adult patients. *Pediatr Cardiol* 1983;4:239.
27. Powell AJ, Lock JE, Keane JF, et al. Prolongation of RV-PA conduit life span by percutaneous stent implantation. *Circulation* 1995;92:3282.
28. Zeevi B, Rome JJ, Keane JF. A newly designed double pressure balloon catheter: clinical use in congenital heart disease. *J Invest Cardiol* 1989;1:129.

7
Pressure Measurement

William Grossman

University of California, San Francisco, School of Medicine; Division of Cardiology, University of California, San Francisco Medical Center, San Francisco, California 94143

The measurement of dynamic blood pressure has been of interest to physiologists and physicians since 1732, when Reverend Stephen Hales measured the blood pressure of a horse by using a vertical glass tube (1). Methodology has advanced impressively since Reverend Hales's day, but with increased technical capability has come greater complexity of instrumentation, so that few physicians today have a firm understanding of the instruments on which they rely.

THE INPUT SIGNAL: WHAT IS A PRESSURE WAVE?

Force is transmitted through a fluid medium as a pressure wave, and an important objective of the cardiac catheterization procedure is to assess accurately the forces and therefore the pressure waves generated by various cardiac chambers. For example, a ventricular pressure wave may be considered a *complex periodic fluctuation in force per unit area*, with one cycle consisting of the time interval from the onset of one systole to the onset of the subsequent systole. The number of times the cycle occurs in 1 second is termed the *fundamental frequency* of cardiac pressure generation. Thus, a fundamental frequency of two corresponds to a heart rate of 120 bpm. Definitions of terms relevant to the theory and practice of pressure measurement are listed in Table 7.1.

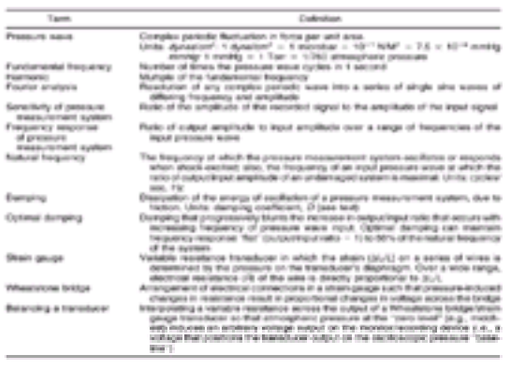

Term	Definition
Pressure wave	Complex periodic fluctuation in force per unit area. Units: dyne/cm² × 1 dyne/cm² = 1 microbar = 10⁻³ N/M² = 2.5 × 10⁻⁴ mmHg; mmHg × mmHg = 1 Torr = 1/760 atmosphere pressure
Fundamental frequency	Number of times the pressure wave cycles in 1 second
Harmonic	Multiple of the fundamental frequency
Fourier analysis	Resolution of any complex periodic wave into a series of single sine waves of differing frequency and amplitude
Sensitivity of pressure measurement system	Ratio of the amplitude of the recorded signal to the amplitude of the input signal
Frequency response of pressure measurement system	Ratio of output amplitude to input amplitude over a range of frequencies of the input pressure wave
Natural frequency	The frequency at which the pressure measurement system oscillates or responds when shock-excited; also, the frequency of an input pressure wave at which the ratio of output/input amplitude of an underdamped system is maximal. Units: cycles/sec, Hz
Damping	Dissipation of the energy of oscillation of a pressure measurement system, due to friction. Units: damping coefficient, D (see text)
Optimal damping	Damping that progressively blunts the increase in output/input ratio that occurs with increasing frequency of pressure wave input. Optimal damping can maintain frequency-response "flat" (output/input ratio = 1) to 58% of the natural frequency of the system
Strain gauge	Variable resistance transducer in which the strain ($\Delta L/L$) on a series of wires is determined by the pressure on the transducer's diaphragm. Over a wide range, electrical resistance (R) of the wire is directly proportional to $\Delta L/L$
Wheatstone bridge	Arrangement of electrical connections in a strain-gauge such that pressure-induced changes in resistance result in proportional changes in voltage across the bridge
Balancing a transducer	Interpositing a variable resistance across the output of a Wheatstone bridge strain-gauge transducer so that atmospheric pressure at the "zero level" (e.g., midchest) induces an arbitrary voltage output on the monitor/recording device (i.e., a voltage that positions the transducer output on the electroscope/pressure "baseline")

TABLE 7.1. *Definitions of terms relevant to the theory and practice of pressure measurement*

Considered as a complex periodic waveform, the pressure wave may be subjected to a type of analysis developed by the French physicist Fourier, whereby any complex wave form may be considered the mathematical summation of a series of simple sine waves of differing amplitude and frequency (Fig. 7.1). Even the most complex waveform can be represented by its own Fourier series, in which the sine wave frequencies are usually expressed as *harmonics*, or multiples of the fundamental frequency. For example, at a heart rate of 120 bpm, the fundamental frequency is 2 cycles per second (Hz) and the first five harmonics are sine waves whose frequencies are 2, 4, 6, 8, and 10 Hz. The practical consequence of this analysis is that, to record pressure accurately, a system must respond with equal amplitude for a given input throughout the range of frequencies contained within the pressure wave. If components in a particular frequency range are either suppressed or exaggerated by the transducer system, the recorded signal will be a grossly distorted version of the original physiologic waveform. For example, the dicrotic notch of the aortic pressure wave contains frequencies above 10 Hz. If the pressure measurement system were unable to respond to frequencies greater than 10 Hz, the notch would be slurred or absent.

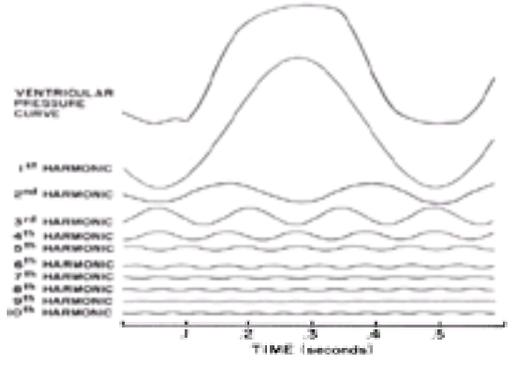

FIG. 7.1. Resolution of a normal ventricular pressure curve (top) into its first 10 harmonics by Fourier analysis. If components in a particular frequency range (e.g., the third harmonic, which in this case is 7 Hz) were either suppressed or exaggerated by the transducer system, the recorded signal would be a grossly distorted version of the original physiologic signal. (Adapted from Wiggers CJ. *The Pressure Pulses in the Cardiovascular System.* London: Longmans, Green, 1928:1.)

PRESSURE MEASURING DEVICES

The manometer used by Starling, Wiggers (2), and others was a modification of that devised by Hürthle (3) in 1898 and is illustrated in Fig. 7.2 A rubber tambour was

coupled with a writing lever that recorded change in pressure on a rotating smoked drum. The system had a high inertia and a low elasticity, giving it a narrow range of usefulness. However, consideration of the mechanics of this primitive system helps give a tangible meaning to key concepts applicable to modern pressure measurement devices.

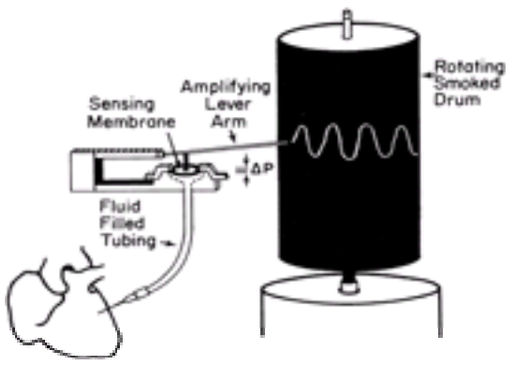

FIG. 7.2. Schematic illustration of the Hürthle manometer. A rubber tambour serves as the sensing membrane and is coupled with an amplifying lever arm that records changes in pressure (DP) on a rotating smoked drum. Pressure is transmitted from the heart *(lower left corner)* to the sensing membrane by fluid-filled tubing.

Sensitivity

The sensitivity of such a measurement system may be defined as the ratio of the amplitude of the recorded signal to the amplitude of the input signal. With the Hürthle manometer illustrated in Fig. 7.2, the more rigid the sensing membrane, the lower the sensitivity; conversely, the more flaccid the membrane, the higher the sensitivity. This general principle applies to manometers currently in use.

Frequency Response

A second crucial property of any pressure measurement system is its frequency response. The frequency response of a pressure measurement system may be defined as the ratio of output amplitude to input amplitude over a range of frequencies of the input pressure wave. To accurately measure pressure, the frequency response (amplitude ratio) must be constant over a broad range of frequency variation. Otherwise, the amplitude of major frequency components of the pressure waveform may be attenuated while minor components are amplified, so that the recorded waveform becomes a distorted caricature of the physiologic event. Referring again to the Hürthle manometer in Fig. 7.2, the range of good frequency response is improved by stiffening the membrane, and it is narrowed by making the membrane more flaccid, because the flaccid membrane cannot respond well to higher frequencies. Thus, *frequency response* and *sensitivity* are related reciprocally, and one can be obtained only by sacrificing the other.

Natural Frequency and Damping

A third important concept is the *natural frequency* of a sensing membrane and how it determines the degree of damping required for optimal recording. If the sensing membrane were to be shock-excited (like a gong) in the absence of friction, it would oscillate for an indefinite period in simple harmonic motion. The frequency of this motion would be the natural frequency of the system. Any means of dissipating the energy of this oscillation, such as friction, is called *damping*. The dynamic response characteristics of such a system are determined largely by the natural frequency and the degree of damping that the system possesses (4).

The significance of the natural frequency and the importance of proper damping are illustrated in Fig. 7.3. The amplitude of an output signal tends to be augmented as the frequency of the input signal approaches the natural frequency of the sensing membrane. The physical counterpart of this augmentation is that the sensing membrane of the pressure transducer vibrates with increasing energy and violence. The same mechanism underlies the fracture of a crystal glass when an opera singer vocalizes the appropriate “input” frequency. Damping dissipates the energy of the oscillating sensing membrane, and optimal damping dissipates the energy gradually, thereby maintaining the frequency response curve nearly flat (constant output/input ratio) as it approaches the region of the pressure measurement system's natural frequency.

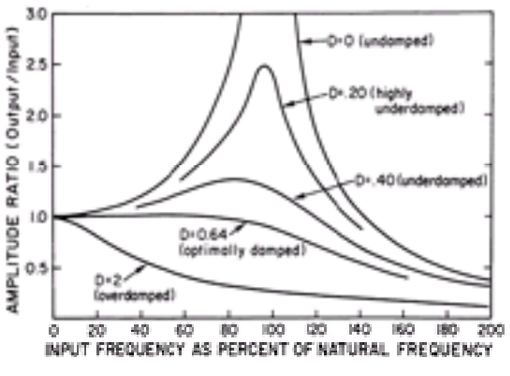

FIG. 7.3. Frequency response curves of a pressure measurement system, illustrating the importance of optimal damping. The amplitude of an input signal tends to be augmented as the frequency of that signal approaches the natural frequency of the sensing membrane. Optimal damping dissipates the energy of the oscillating sensing membrane gradually, and thereby maintains a nearly flat natural frequency curve (constant output/input ratio) as it approaches the region of the pressure measurement system's natural frequency (see text). D, damping coefficient.

As an analogy to further help the reader understand the significance of damping, consider the simple case of a weight suspended from a spring. If the weight is displaced and then released, the stretched spring recoils so that the weight moves past its original position and then oscillates up and down. In the absence of frictional forces (damping), the oscillation would continue indefinitely at a frequency determined by the stiffness of the spring and an amplitude determined by the mass of the weight. In practice there is always some damping, and this has two effects: (a) the amplitude of the oscillations gradually diminishes, and (b) the frequency of oscillation is reduced. This second important consequence of damping—reduction of the natural frequency of a system—is not widely appreciated. If we continue with our analogy, imagine that the spring and its weight are suspended in a jar of syrup or honey; the spring will clearly vibrate with lesser amplitude of vibration and lesser frequency than before. The effect of the viscous medium is to further damp the oscillations. If the medium's viscosity is high enough, it prevents any overshoot or oscillation: The weight returns to its original position regardless of its initial displacement. Further damping at this point simply slows the return of the weight to its equilibrium position, thereby depressing the frequency response characteristics of the system. Therefore, damping helps to prevent overshoot artifacts resulting from resonance of the system, but at the cost of diminished frequency response.

WHAT FREQUENCY RESPONSE IS DESIRABLE?

Wiggers (2) suggested that the shortest “significant” vibrations contained within physiologic pressure waves have one-tenth the period of the entire pressure curve—that is, the essential physiologic information is contained within the first 10 harmonics of the pressure wave's Fourier series. At a heart rate of 120 bpm, the fundamental frequency is 2 Hz and the tenth harmonic is 20 Hz. Therefore, a pressure measurement system with a frequency response range that is flat to 20 Hz should be adequate in such a circumstance, and support for this hypothesis has come from experimental work comparing high frequency-response systems with conventional catheter systems (5).

The useful frequency response range of commonly used pressure measurement systems is usually less than 20 Hz unless special care is taken. Wood and colleagues (6) and Gleason and Braunwald (7) found that frequency response was flat to less than 10 Hz with small-bore (6F) catheters attached to standard strain gauge manometers.

To ensure a high frequency-response range, the pressure measurement system must be set up in such a way that it has the highest possible *natural frequency* as well as *optimal damping*. The natural frequency is directly proportional to the lumen radius of the catheter system. It is inversely proportional to the length of the catheter and associated tubing and to the square root of the catheter and tubing compliance and the density of fluid filling the system. The highest natural frequency is obtained by using a short, wide-bore, stiff catheter connected to its transducer without intervening tubing or stopcocks and filled with a low-density liquid from which small air bubbles, which increase compliance, have been excluded (e.g., boiled saline solution). Such a system is impractical for routine use, but deviation from it occurs only at a significant sacrifice.

If such a system is constructed, it will be found to be grossly underdamped (Fig. 7.3). Accordingly, it is important to introduce damping into the system to keep the frequency response flat as the frequency of the input signal approaches the natural frequency of the pressure measurement system. With optimal damping, the frequency response can be maintained flat (±5%) to within 88% of the natural frequency, according to Fry (4), although it is unusual to achieve more than 50% in most laboratories. Damping may be introduced by interposing a “damping needle” between the catheter and manometer (6) and gradually shortening it until optimal damping is obtained; by filling the manometer or tubing with a viscous medium, such as Renografin (a radiographic contrast agent); or by any of several other methods.

EVALUATION OF FREQUENCY RESPONSE CHARACTERISTICS

Ideally, the frequency response characteristics of a pressure measurement system should be evaluated using a sine wave pressure generator to construct curves similar to those seen in Fig. 7.3. By altering the characteristics of the system discussed in the previous section, a reasonable compromise between frequency response, damping, and practicality can be achieved for each laboratory. Such a sine wave pressure generator is commercially available (Millar Instruments, Houston, TX). An example of the use of this device in estimating frequency response of a pressure measurement system is provided in Fig. 7.4.

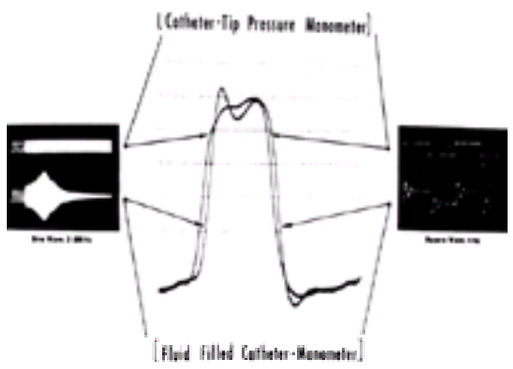

FIG. 7.4. Left ventricular pressure *(center panel)* measured with the use of a fluid-filled standard catheter and micromanometer (catheter-tip pressure manometer) in a patient undergoing cardiac catheterization. Left and right panels show *in vitro* comparisons of frequency response for micromanometer *(upper)* and fluid-filled *(lower)* systems. The left panel recordings were obtained by continuously increasing the input frequency of a sine-wave pressure waveform from 2 to 200 Hz. The fluid-filled system resonated (natural frequency) at 37 Hz but was “flat” (±5%) only to 12 Hz. Therefore its useful range is only to approximately 12 Hz. The right panel shows the response of each system to a square-wave pressure input signal. (From Nichols WW, Pepine CJ, Millar HD, et al: Percutaneous left ventricular catheterization with an ultraminiature catheter-tip pressure transducer. *Cardiovasc Res* 1978;12:566, with permission.)

Another method, which does not require the use of such a pressure waveform generator, is described here. This technique may be used for measuring the dynamic response characteristics of a pressure measurement system.

The catheter to be studied is connected by means of a three-way stopcock with or without intervening tubing to one arm of a strain gauge transducer (Fig. 7.5). The transducer used should be of the low-volume-displacement type (small chamber capacity) to enhance frequency response. The tip of the catheter is snugly projected through a hole in a no. 6 rubber stopper, which is tightly inserted into the cutoff barrel of a 60-mL plastic syringe. The syringe plunger is removed, and the barrel is fixed in a vertical position, pointing downward, so that the catheter enters from below. The manometer and catheter are filled with saline solution, care being taken to avoid even small air bubbles, and the catheter is flushed until the catheter tip and holes are submerged in approximately 30 mL of saline solution. The plunger is slowly inserted into the syringe, producing an upward deflection of the pressure trace on the oscilloscope of the recording apparatus. When the trace comes to rest at the top of the oscilloscope, the recorder is turned on at rapid paper speed and the plunger is suddenly withdrawn. This method, modified from Hansen (8), produces shock excitation vibrations of the type seen in Fig. 7.6. The mathematical foundation for analysis of such a shock excitation has been described by Wiggers (2) and Fry (4) and may be summarized as follows.

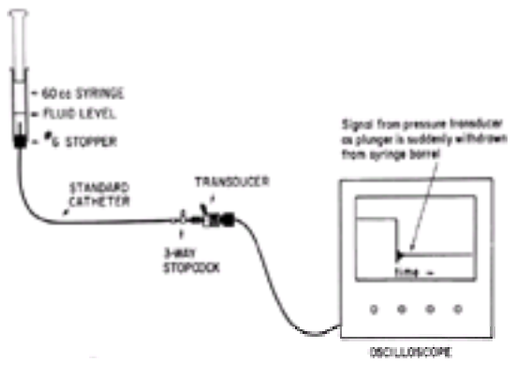

FIG. 7.5. Practical evaluation of dynamic response characteristics of a catheter-transducer system. The catheter hub is connected by means of a three-way stopcock to one arm of a low-volume-displacement pressure transducer. The tip of the catheter is snugly projected through a hole in a no. 6 rubber stopper, which is tightly inserted into the cutoff barrel of a 60-mL plastic syringe. The manometer and catheter are filled with saline solution, care being taken to avoid even small air bubbles, and the catheter is flushed until the catheter tip and holes are submerged in approximately 30 mL of saline solution. Next, the plunger is slowly inserted into the syringe, producing an upward deflection of the pressure trace on the oscilloscope of the recording apparatus. When the pressure trace comes to rest at the top of the oscilloscope screen, the recorder is turned on and the plunger is suddenly withdrawn from the syringe barrel. Dynamic response characteristics are then calculated as shown in Fig. 7.6.

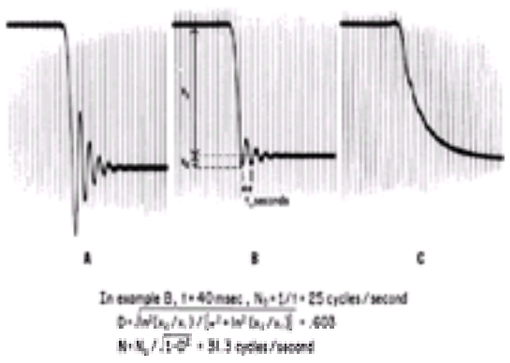

FIG. 7.6. Records of dynamic frequency response characteristics obtained from the system illustrated in Fig. 7.5. Panels **A, B**, and **C** represent progressive increases in damping produced by introducing increasing amounts of a viscous radiographic contrast agent (Renografin-76) into the catheter-transducer system. The catheter was 80 cm long, and its diameter was 8F. **A,** Underdamped. **B,** almost optimally damped. **C,** Overdamped. The percent overshoot (X_2/X_1) is used in the calculation of the damping coefficient, D. The undamped natural frequency, N, is calculated from D and the damped natural frequency, N_D. Time lines are 20 msec. Using the curves illustrated in Fig. 7.3 for various values of D, the frequency response of the system in panel **B** can probably be considered flat (±5%) to 0.88N = 27.5 Hz.

The frequency of the after-vibrations produced by shock excitation is the damped natural frequency of the system. This is obtained by measuring the time, t, between two successive vibrations and obtaining the damped natural frequency, N_D as 1/t. In the example in Fig. 7.6, $N_D = 1/0.04 = 25$ Hz. Next, the damping coefficient, D, is calculated as a function of the ratio by which successive single vibrations decrease. In Fig. 7.6, this may be calculated from the ratio of X_2 to X_1, the percent overshoot:

$$D = \sqrt{\ln^2(x_2/x_1)/[\pi^2 + \ln^2(x_2/x_1)]} \qquad \textbf{(7.1)}$$

where $\ln(X_2/X_1)$ is the natural logarithm of the percent overshoot. In our example, $X_2/X_1 = 0.093$, $\ln(X_2/X_1) = -2.379$, and D = 0.603. From the damping coefficient D and the damped natural frequency N_D, we may determine the undamped natural frequency N as

$$N = N_D/\sqrt{1 - D^2} \qquad \textbf{(7.2)}$$

A simple practical goal is to try to regulate the damping of an actual pressure measurement system so that its damping coefficient is as close to 0.64 (so-called optimal damping) as possible. At this value, the pressure measurement system shows uniform frequency response (±5%) to about 88% of its natural frequency, according to Fry (2). If such optimal damping is achieved for the system illustrated in Fig. 7.6, its frequency response could be considered flat to 0.88N = 27.5 Hz. Improperly damped systems with low natural frequencies (because of small air bubbles or excessively compliant tubing) may achieve uniform frequency response to less than 10 Hz.

TRANSFORMING PRESSURE WAVES INTO ELECTRICAL SIGNALS: THE ELECTRICAL STRAIN GAUGE

Pressure measurement systems today generally use electrical strain gauges and employ the principle of the Wheatstone bridge. In its simplest form, the strain gauge is a variable-resistance transducer whose operation depends on the fact that when an electrical wire is stretched, its resistance to the flow of current increases. As long as the strain remains well below the elastic limit of the wire, there is a wide range within which the increase in resistance is accurately proportional to the increase in length.

Figure 7.7 illustrates how the Wheatstone bridge employs this principle in converting a pressure signal into an electrical signal. In this schematic representation of a pressure transducer, pressure is transmitted through port P and acts on diaphragm D, which is vented to atmospheric pressure on its opposite side. In the illustration, the diaphragm is attached on its undersurface to a plunger, which in turn is attached to four wires, G_1 through G_4, as illustrated. The manner of attachment is such that increased pressure on the diaphragm stretches and therefore increases the electrical resistance of G_1 and G_2 and has the opposite effect on G_3 and G_4. In the Wheatstone bridge, G_1, G_2, G_3, and G_4 are connected electrically, as in Fig. 7.8, and are attached to a voltage source B. If all four resistances are equal, then exactly half the voltage of battery B exists at the junction of G_1 and G_4 and half at the junction of G_2 and G_3; therefore, no current flows between the output terminals. However, when pressure is applied to the diaphragm (Fig. 7.7), the resistances are unbalanced, so that the junction of G_1 and G_4 becomes negative, and a current flows across the output terminals.

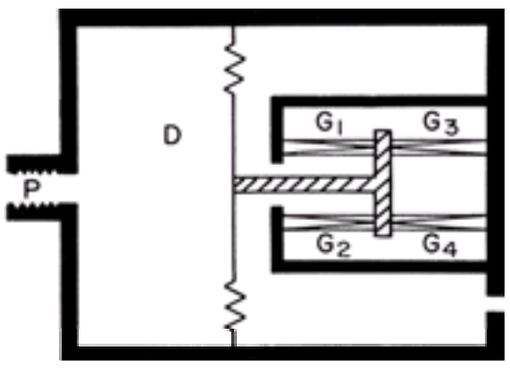

FIG. 7.7. Schematic representation of a strain-gauge pressure transducer. Pressure is transmitted through port P and acts on diaphragm D, which is vented to atmospheric pressure on its opposite side. Pressure on the diaphragm stretches and therefore increases the resistance of wires G_1 and G_2, while having the opposite effect on G_3 and G_4. The wires are electrically connected as shown in Fig. 7.8.

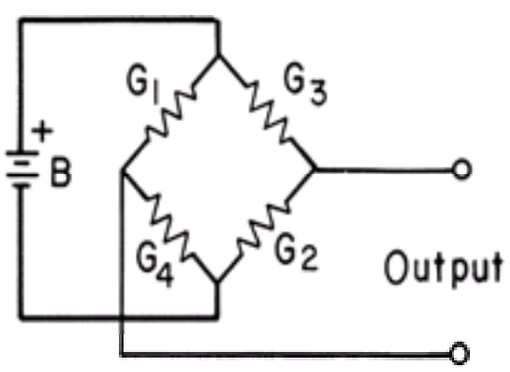

FIG. 7.8. Strain-gauge connection of the Wheat stone bridge. In this arrangement, if all resistances are equal, then exactly half the voltage of battery B exists at the junction of G_1 and G_4 and half at the junction of G_2 and G_3; therefore, no current will flow between the output terminals. However, when pressure is applied to the diaphragm (see Fig. 7.7), the resistances are unbalanced, so that the junction of G_1 and G_4 becomes negative, and a current flows across the output terminals.

Because movement of the diaphragm D in Fig. 7.7 is necessary to produce current flow in the Wheatstone bridge, a certain volume of fluid must actually move through the catheter and connecting tubing to produce a recorded pressure. Therefore, the use of a low-volume-displacement transducer with a small chamber volume improves the frequency-response characteristics of the system.

Balancing a transducer is simply a process whereby a variable resistance (the R balance of most amplifiers) is interpolated into the circuit (Fig. 7.8), so that at an arbitrary baseline pressure, the voltage across the output terminal can be reduced to zero. Some amplifiers use an alternating current (AC) signal in place of the DC current source shown in Fig. 7.8. When these “carrier current” amplifiers are employed, a variable capacitor (the C balance) must be used in addition to the variable resistor to balance the bridge.

PRACTICAL PRESSURE TRANSDUCER SYSTEM FOR THE CATHETERIZATION LABORATORY

Incorporating all the principles discussed so far in this chapter, many laboratories have settled on a practical system in which a fluid-filled catheter is attached by means of a manifold to a small-volume-displacement strain-gauge-type pressure transducer (Fig. 7.9).

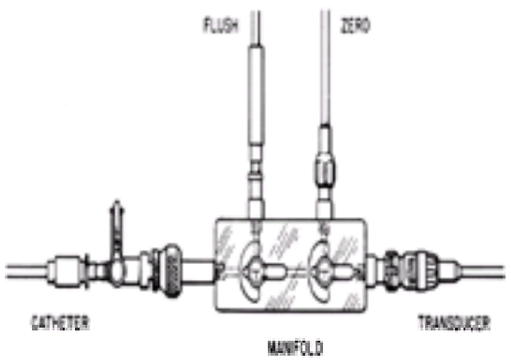

FIG. 7.9. A practical system for pressure measurement with excellent frequency response. The catheter is connected by a stopcock to a manifold, which is connected at its other end to a small-volume fluid-filled pressure transducer. The manifold's two sidearms are connected by fluid-filled tubing to a zero pressure reference level and to a pressurized flush solution.

The system illustrated is used for pressure measurement from the right side of the heart and for arterial monitor lines. The system used for left-sided heart pressure measurement is more complex because it also incorporates ports for radiographic contrast administration and blood discard, as well as a syringe for coronary angiography. Our laboratory at the University of California, San Francisco currently uses relatively inexpensive, sterile, disposable pressure transducers in which a tiny integrated circuit on a thin silicon diaphragm serves as the sensing element. Fluid pressure is transmitted to this element through a gel medium, bending the circuit and altering the resistance of resistors in the silicon diaphragm. The circuit delivers an electrical output proportional to the pressure being applied, as discussed previously.

To the first sidearm of the manifold (Fig. 7.9), a fluid-filled connecting tube is attached, the distal end of which is adjusted to the zero reference level (see above). The second sidearm is connected by a fluid-filled tube to a pressurized flush bag containing heparinized saline solution. The cardiac catheter is connected directly to the front of the manifold through a built-in rotating adapter. By turning the stopcock attached to the flush solution, the operator can flush the catheter intermittently (e.g., every 3 minutes) to clear blood. Turning this stopcock the other way permits filling and flushing of the zero line or the pressure transducer. With this system, a frequency response that flat (±5%) to more than 20 Hz can be achieved routinely. The transducers may be sterilized with gas or Cidex between uses.

The establishment of a zero reference is an important practical undertaking that must be accomplished as a part of each catheterization procedure. Midchest level is used widely as zero reference, because fluoroscopic visualization in a lateral projection confirms that the left ventricle and aorta are generally located midway between the sternum and the table top when the patient is supine. However, the validity of choosing the midchest level for zero reference has been challenged in an excellent study by Courtois et al. (9). They carefully examined the influence of hydrostatic forces (caused by the effects of gravity) and concluded that intracardiac pressures should be referenced to an external fluid-filled transducer aligned with the uppermost blood level in the chamber where pressure is being measured. In practical terms, for measurement of left ventricular and aortic pressure, the zero level should be positioned approximately 5 cm below the left sternal border at the fourth left intercostal space (4th LICS). This eliminates the gravitational/hydrostatic effect of a column of blood above the catheter tip and within the ventricular chamber. Although the right ventricle and left atrium are at different levels in the chest than the left ventricle, Courtois et al. (9) calculated that the error introduced by use of a point 5 cm below the 4th LICS, at the left sternal border, is in the order of ±0.8 mm Hg for chambers other than the left ventricle.

If a decision has been made to use the mid chest level for zero reference, each case should begin with measurement of the patient's anteroposterior (AP) thoracic diameter at the level of the angle of Louis. This is done with the use of a large square chest caliper (Picker Instruments), as illustrated in Fig. 7.10. The patient then lies supine on the catheterization table and is draped and otherwise prepared for catheterization (a 12-lead electrocardiogram is recorded, skin sites are shaved and cleansed), and the zero level is established on an adjustable pole attached to the side of the table. This is accomplished with the use of a yardstick to which a carpenter's level has been taped. One end of the yardstick is placed on the patient's sternum at the angle of Louis and the other end against the adjustable metal pole. As illustrated in Fig. 7.10, the metal pole has a centimeter-ruled tape attached to it, allowing identification of the level of midchest (one half of the patient's AP diameter below the angle of Louis). Alternatively, the yardstick with its “level” can be used to identify the position on the metal pole that is 5 cm below the left sternal border at the 4th LICS. With this technique, a Morse manifold (NAMIC, Medical Products Division, Hudson Falls, NY) or similar device that can be moved up and down the metal pole is set at either the midchest level or 5 cm down from the 4th LICS; one end of the zero line (clear polyethylene tubing) is connected to the manifold, and the other end is connected to the pressure measurement manifold (Fig. 7.9). The zero line, manifold, and pressure transducer are next filled with saline from the flush line, so that the pressure transducer can be connected directly with the zero line by the turn of a stopcock on the pressure manifold. The pressure transducers are calibrated with the use of a mercury manometer attached to a free port on the Morse manifold, 100 mm Hg pressure being transmitted through the fluid-filled zero line to all pressure transducers to be used in a particular case (e.g., left heart, right heart, arterial monitor). Otherwise, the free port of the Morse manifold is left open to air, in communication with the individual zero lines of the various left and right heart manifold systems by way of the series of stopcocks that constitute the Morse manifold, thus referencing all the transducer systems to a common “zero level.”

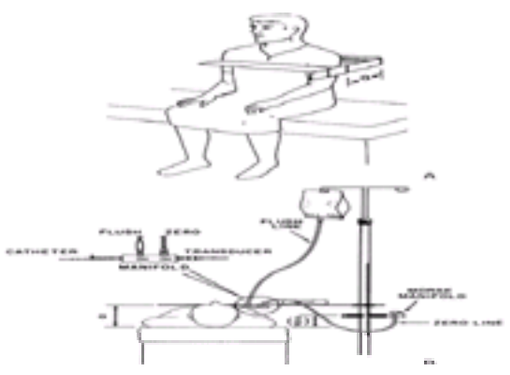

FIG. 7.10. A: Technique for measurement of a patient's anteroposterior diameter (a), using a metal chest caliper. **B:** Establishment of zero level. (See text for detailed explanation.)

PHYSIOLOGIC CHARACTERISTICS OF PRESSURE WAVEFORMS

Reflected Waves

Recognizing the appearance of normal pressure waveforms is a prerequisite to identifying abnormalities that characterize certain cardiovascular disorders. As shown in Fig. 7.11 *forward* pressure and flow waves, as seen in the central aorta, are intrinsically identical in shape and timing. The pressure wave is modified by summation with a *reflected* pressure wave ($P_{backward}$), and the resultant *measured* central aortic pressure wave shows a steady increase throughout ejection (10,11). The flow wave is also modified by summation with a reflected flow wave ($F_{backward}$), but because flow is directional, $F_{backward}$ reduces the magnitude of flow in late ejection, giving the characteristic $F_{measured}$ as is seen with aortic flow meters or Doppler signals.

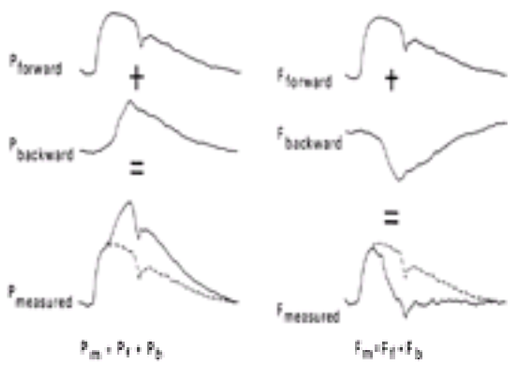

FIG. 7.11. Central aortic pressure (P) and flow (F) measured in a patient during cardiac catheterization. Computer-derived forward and backward pressure and flow components are shown individually: Their sum results in the measured waves. (See text for discussion.) (From Murgo JP, Westerhof N, Giolma JP, et al. Manipulation of ascending aortic pressure and flow wave reflections with Valsalva maneuver: relationship to input impedance. *Circulation* 1981;63:122, with permission.)

The reflections for pressure occur from many sites within the arterial tree, but the major effective reflection site in humans appears to be the region of the terminal abdominal aorta (11). As seen in Fig. 7.12 ascending aortic pressure is increased substantially within one beat after bilateral occlusion of the femoral arteries by external manual compression. High-speed recordings (Fig. 7.12, right panel) show that the major part of the increase in pressure occurs late in systole, consistent with an increase in the magnitude of the reflected pressure.

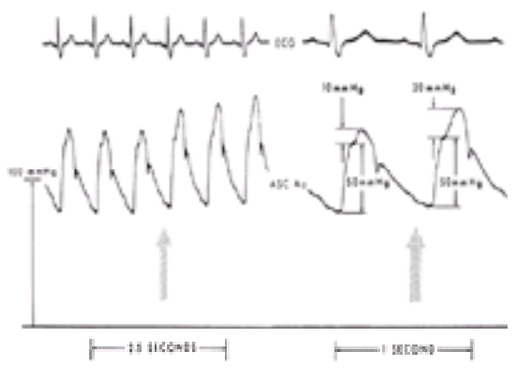

FIG. 7.12. Ascending aortic (ASC Ao) pressure waveform in a patient before and after bilateral occlusion of the femoral arteries by external manual compression *(left arrow)*. On the right, high-speed recordings show that the major portion of the increase in pressure results from augmentation of the late (reflected) wave. ECG, electrocardiogram. (From Murgo JP, Westerhof N, Giolma JP, et al. Aortic input impedance in normal man: relationship to pressure wave forms. *Circulation* 1980;62:105, with permission.)

A variety of factors influence the magnitude of reflected waves (Table 7.2). Pressure reflections are diminished during the strain phase of the Valsalva maneuver (10), with the result that pressure and flow waveforms become similar in appearance (Fig. 7.13). After release of the Valsalva strain, reflected waves return and are exaggerated. Therefore, the commonly noted late-peaking appearance of central aortic and left ventricular pressure tracings in humans (Fig. 7.14), referred to as the type A waveform pattern (10), is a result of strong pressure reflections in late systole. In addition to the Valsalva maneuver, pressure reflections are diminished during hypovolemia, hypotension, and in response to a variety of vasodilator agents (Table 7.2). In these circumstances, the left ventricular and central aortic pressure waves exhibit a type C pattern (Fig. 7.14). However, vasoconstriction and hypertension may be expected to accentuate the normal type A waveform. Because the contribution of reflections to the arterial pressure waveform should move earlier in systole the closer one gets to the source of the reflections, it is not surprising that the pressure peaks earlier as the catheter is withdrawn from the central aorta to the periphery (Fig. 7.15).

Factors that augment pressure wave reflections
Vasoconstriction
Heart failure
Hypertension
Aortic or iliofemoral obstruction
Valsalva maneuver—after release
Factors that diminish pressure wave reflections
Vasodilation
Physiologic (e.g., fever)
Pharmacologic (e.g., nitroglycerin, nitroprusside)
Hypovolemia
Hypotension
Valsalva manuever—strain phase

TABLE 7.2. *Factors that influence the magnitude of reflected waves*

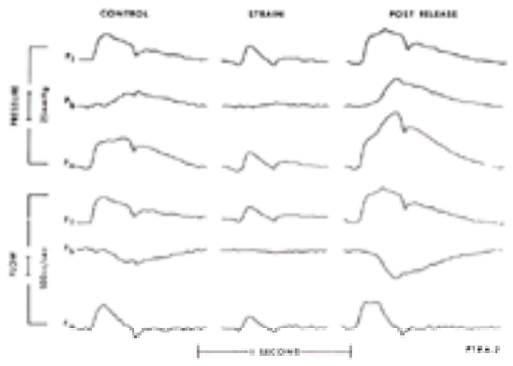

FIG. 7.13. Measurements of central aortic pressure (P_m) and flow (F_m) in a patient performing Valsalva maneuver during cardiac catheterization. Control, Valsalva strain, and post–Valsalva release tracings are shown. P_m is the sum of forward (P_f) and backward or reflected (P_b) pressure waves; F_m is the sum of F_f and F_b. (See text for discussion.) (From Murgo JP, Westerhof N, Giolma JP, et al. Manipulation of ascending aortic pressure and flow wave reflections with Valsalva maneuver: relationship to input impedance. *Circulation* 1981;63:122, with permission.)

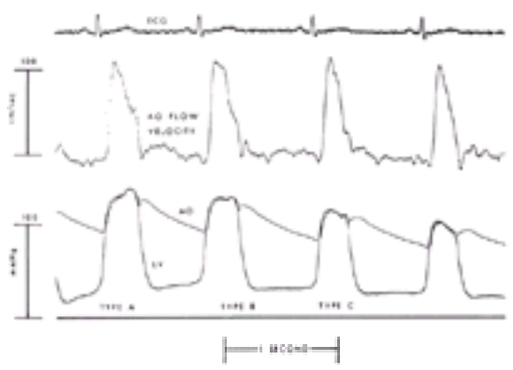

FIG. 7.14. Left ventricular (LV) and central aortic (AO) pressure and aortic flow velocity tracings in a patient at the initiation of the strain phase of a Valsalva maneuver. (See text for details.) (From Murgo JP, Westerhof N, Giolma JP, et al. Manipulation of ascending aortic pressure and flow wave reflections with Valsalva maneuver: relationship to input impedance. *Circulation* 1981;63:122, with permission.)

FIG. 7.15. Pressure waveforms in a patient undergoing cardiac catheterization, as a function of distance from the aortic valve (Ao V). Ao, aorta; ASC, ascending; Hi D, high descending; MID T, midthoracic; DIAP, diaphragmatic; ABD, abdominal; TERM, just above aortic bifurcation; ECG, electrocardiogram. First vertical line marks onset of primary (forward) pressure wave, which occurs progressively later after the QRS complex with increasing distance from the aortic valve. Second vertical line marks onset of secondary pressure rise associated with the backward or reflected pressure wave. See text for discussion. (From Murgo JP, Westerhof N, Giolma JP, et al. Aortic input impedance in normal man: relationship to pressure wave forms. *Circulation* 1980;62:105, with permission.)

Reflected waves can be of substantial magnitude and are increased in the patient with heart failure (12). Laskey and Kussmaul (12) showed that reflected pressure waves were increased in amplitude in 17 patients with heart failure secondary to idiopathic dilated cardiomyopathy, often producing an exaggerated dicrotic wave. The magnitude of these reflections did not decrease consistently during exercise, as is characteristic of the normal circulation. Infusion of sodium nitroprusside intravenously, markedly reduced the magnitude of the reflected pressure waves and delayed their timing; both these changes were deemed beneficial with regard to left ventricular systolic load (12).

Wedge Pressures

A physiologic aspect of pressure measurement that has been of interest for many years is the concept of the “wedge pressure.” Broadly stated, a wedge pressure is obtained when an end-hole catheter is positioned in a designated blood vessel with its open end-hole facing a capillary bed, with no connecting vessels conducting flow into or away from the designated blood vessel between the catheter's tip and the capillary bed. *A true wedge pressure can be measured only in the absence of flow*. In the absence of flow, pressure equilibrates across the capillary bed so that the catheter tip pressure is equal to that on the other side of the capillary bed. If minimal damping occurs between the catheter tip and the opposite side of the capillary bed—that is, if there is a large, relatively dilated capillary bed, if the precapillary arterioles and postcapillary venules are not constricted, and if there is no other source of obstruction, such as the presence of microthrombi–phasic as well as mean pressure may be transmitted to the wedged catheter. Thus, an end-hole catheter wedged in a hepatic vein may be used to measure portal venous pressure; a catheter wedged in a distal pulmonary artery measures pulmonary venous pressure, and if it is wedged in a pulmonary vein it measures pulmonary artery pressure. The details involved in measurement of pulmonary artery wedge pressure, commonly termed *pulmonary capillary wedge pressure*, are discussed in Chapter 5. Properly performed, this determination accurately measures pulmonary venous pressure. In the absence of cor triatriatum or obstruction to pulmonary venous outflow, the pulmonary venous and left atrial pressures are equal, so that pulmonary artery wedge pressure may be used as a substitute for left atrial pressure. Issues of damping and time delay need to be considered when using this pressure to assess a transmitral gradient in a patient with mitral stenosis or prosthetic valve obstruction. These issues have been addressed by Lange et al. (13).

SOURCES OF ERROR AND ARTIFACT

Even when every effort has been made to design a pressure measurement system with high sensitivity, uniform frequency response, and optimal damping, distortions and inaccuracies in the pressure waveform may occur. Some common sources of error and artifact in clinical pressure measurement include deterioration in frequency response, catheter whip artifact, end-pressure artifact, catheter impact artifact, systolic pressure amplification in the periphery, and errors in zero level, balancing, and calibration.

Deterioration in Frequency Response

Although frequency response may be high and damping optimal during setup of the transducers, substantial deterioration in the characteristics can develop during the course of a catheterization study. Air bubbles may be introduced into the catheters, stopcocks, or tubing, or dissolved air may come out of the saline solution used to fill the transducer (just as dissolved air may come out of solution in a glass of water allowed to stand unperturbed for a few hours). Even the smallest air bubbles have

a drastic effect on pressure measurement because they cause excessive damping and lower the natural frequency (by serving as an added compliance). When the natural frequency of the pressure measurement system falls, high-frequency components of the pressure waveform (such as those that occur with intraventricular pressure rise and fall) may set the system in oscillation, producing the ventricular pressure "overshoot" commonly seen in early systole and diastole (Fig. 7.4 and Fig. 7.16). Flushing out the catheter, manifold, and transducer dispels these small air bubbles and restores the frequency response of the pressure measurement system.

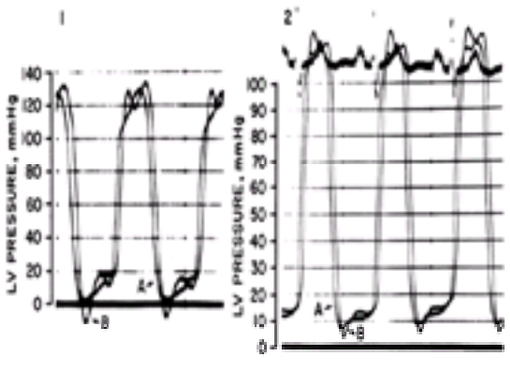

FIG. 7.16. Left ventricular (LV) pressure signals as recorded with a micromanometer and with a system employing long, fluid-filled tubing and several interposed stopcocks between the pressure transducer and the 7F NIH catheter. The micromanometer tracing is labeled A, and the fluid-filled catheter tracing is labeled B. Note both the early diastolic and the early ejection phase overshoots recorded with the fluid-filled catheter, indicating a poor frequency response, especially in panel 1.

Catheter Whip Artifact

Motion of the tip of the catheter within the heart and great vessels accelerates the fluid contained within the catheter. Such catheter whip artifacts may produce superimposed waves of ±10 mm Hg. Catheter whip artifacts are particularly common in tracings from the pulmonary arteries and are difficult to avoid.

End-Pressure Artifact

Flowing blood has a kinetic energy by virtue of its motion, and when this flow suddenly comes to a halt the kinetic energy is converted in part into pressure. Therefore, an end-hole catheter pointing upstream (e.g., radial or femoral arterial pressure monitoring line) records a pressure that is artifactually elevated by the converted kinetic energy. This added pressure may range from 2 to 10 mm Hg.

Catheter Impact Artifact

Catheter impact artifact is similar but not identical to catheter whip artifact. When a fluid-filled catheter is "hit" (e.g., by valves in the act of opening or closing or by the walls of the ventricular chambers), a pressure transient is created. Any frequency component of this transient that coincides with the natural frequency of the catheter-manometer system causes a superimposed oscillation on the recorded pressure wave. Catheter impact artifacts are common with pigtail catheters in the left ventricular chamber, where the terminal pigtail may be hit by the mitral valve leaflets as they open in early diastole.

Systolic Pressure Amplification in the Periphery

When radial, brachial, or femoral arterial pressures are measured and used to represent aortic pressure, it must be remembered that peak systolic pressure in these arteries may be considerably higher (e.g., by 20 to 50 mm Hg) than peak systolic pressure in the central aorta (Fig. 7.17), although mean arterial pressure will be the same or slightly lower. There has been debate concerning the mechanism of this amplification of systolic pressure. McDonald (5) and Murgo (10,11) presented convincing evidence that the change in waveform of arterial pressure as it travels away from the heart is largely a consequence of reflected waves. These waves, presumably reflected from the aortic bifurcation, arterial branch points, and small peripheral vessels, reinforce the peak and trough of the antegrade pressure waveform, causing amplification of the peak systolic and pulse pressures (Fig. 7.17). This phenomenon may mask and distort pressure gradients across the aortic valve or left ventricular outflow tract. Use of a double-lumen catheter (e.g., double-lumen pigtail) allows measurement of left ventricular and central aortic pressures simultaneously, thus avoiding this problem. Another method is the transseptal technique with a second catheter in the central aorta (see Chap. 4). Finally, special attention to performing careful pullback tracings may also help the operator to avoid this particular error.

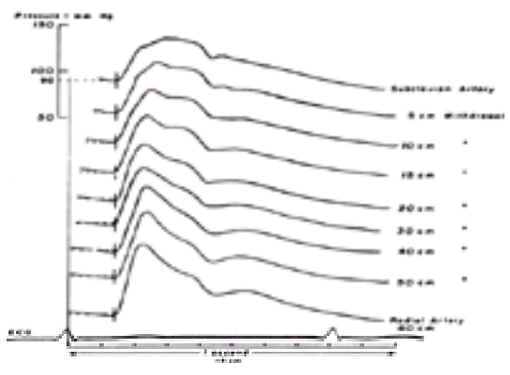

FIG. 7.17. Transformation of arterial pressure waveform with transmission to the periphery in a healthy 30-year-old man. Onsets of pressures are aligned for purposes of comparison. As the pulse wave moves peripherally, the upstroke steepens and increases in magnitude, giving the pressure a "spiky" appearance. The horizontal line intersecting onset of each pulse contour is calibration reference of 90 mm Hg. (From Marshall, HW, et al: Physiologic consequences of congenital heart disease. In: Hamilton WF, Dow P, eds. *Handbook of Physiology: section 2. Circulation,* vol. 1. Washington DC: American Physiologic Society, 1962:417.)

The operator should record central aortic pressure together with peripheral arterial pressure routinely, immediately before entering the left ventricle during retrograde left heart catheterization. If this tracing shows a "reverse gradient" (peak systolic pressure in periphery higher than in central aorta), the amount of this pressure difference must be considered when subsequent comparisons of left ventricular and "systemic arterial" pressure are made for the detection of aortic or subaortic stenosis. The peripheral arterial systolic pressure may commonly appear to be 20 mm Hg higher than the left ventricular systolic pressure as a result of this phenomenon. This pressure amplification in the periphery is particularly marked in the radial artery (Fig. 7.17), especially if there is also some end-pressure artifact, and may mask the presence of aortic stenosis. If any doubt exists concerning the presence of a true pressure gradient, either a double-lumen left heart catheter or a second central aortic catheter should be introduced, to measure accurately the gradient across the aortic valve.

Errors in Zero Level, Balancing, or Calibration

Error in the quantitation of pressures because of improper zero reference is common. As mentioned earlier, in many laboratories the zero reference point is taken at the midchest with the patient supine, although some laboratories use a point 10 cm vertically up from the back or 5 cm vertically down from the sternal angle. All manometers must be zeroed at the same point (Fig. 7.10), and the zero reference point should be changed if the patient's position is changed during the course of the study (e.g., if pillows are placed to prop up the patient). Transducers should be calibrated before each period of use: Electrical calibration signals and "calibration factors" can usually be relied on as a substitute for mercury calibration, but they should be confirmed regularly against a standard mercury reference. Linearity of response should be checked by using mercury inputs of 25, 50, and 100 mm Hg. If possible, all transducers should be exposed to the calibrating system simultaneously to avoid false "gradients" caused by unequal amplification of the same pressure signal. In the system described here (Fig. 7.10), a bubble in the

zero-reference line can result in a false zero level; therefore, in tracking down an unexpected pressure gradient, flushing of the zero line is an important initial step. If the unexpected gradient persists, catheter attachments should be switched between the two involved manifolds. An artifactual gradient reverses direction, whereas a true gradient persists after this maneuver.

Micromanometers

To reduce the mass and inertia of the pressure measurement system, improve the frequency response characteristics, and decrease artifacts associated with overdamping and catheter whip, miniaturized transducers have been developed that fit on the distal tip of standard catheters and therefore may be used as intracardiac manometers (Fig. 7.4 and Fig. 7.16). Several models are commercially available, but many still have major technical shortcomings, such as fragility, electrical drift problems, temperature sensitivity, and inability to withstand the usual catheter sterilization techniques. Particularly reliable catheter-tip manometers are made by Millar Instruments. Available modifications of this catheter have multiple side-holes and therefore permit angiography and high-fidelity pressure measurement through the same catheter. A modification of this catheter has a pigtail tip. The catheter may be subjected to gas sterilization (ethylene oxide) along with other catheters and instruments, and it may be calibrated externally at room temperature because its response characteristics are not appreciably affected by temperature changes over a wide range. In addition, modifications are available with electromagnetic flow velocity sensors and other special capabilities for research applications. Some laboratories have used a disposable high-fidelity transducer catheter and have shown that the pressures measured with these catheters are superior in waveform and accuracy to those measured with standard techniques (14).

For accurate measurement of the rate of ventricular pressure rise (dP/dt) and other parameters of myocardial performance occurring during the first 40 to 50 msec of ventricular systole, high frequency-response characteristics are necessary. Although there is some debate on this subject (15), micromanometer-tipped catheters are generally required in patient studies when myocardial mechanics are being examined. Gersh et al. published a careful study on the physical criteria for measurement of left ventricular pressure and its first derivative (16). They showed that pressure measurement flat to ±5% of the first 20 harmonics of the left ventricular pressure curve is required for accurate reproduction of the amplitude of maximal dP/dt. In their study, accuracy to six harmonics led to a 20% underestimation of peak dP/dt. At a heart rate of 80 bpm, the fundamental frequency is 80/60 = 1.33 Hz, and the 20th harmonic is 26.7 Hz. As seen in Fig. 7.6, this may be possible to achieve with a short, wide-bore catheter attached directly to the pressure transducer, with optimal damping. If the heart rate increases to 100 bpm, however, the 20th harmonic becomes 100/60 × 20 = 33.3 Hz, which exceeds the capacity for even this optimal fluid-filled system. Therefore, to minimize the chance of error, micromanometer catheters should be used exclusively when dP/dt is being measured. Examples of pressure recordings taken with and without micromanometer-tipped catheters may be seen in Fig. 7.4 and Fig. 7.16.

CHAPTER REFERENCES

1. Hales S. In: Willius FA, Keys TE, eds. *Classics in Cardiology.* New York: Dover, 1961:131.
2. Wiggers CJ. *The Pressure Pulses in the Cardiovascular System.* London: Longmans, Green, 1928:1.
3. Hürthle K. Beiträge zur Hämodynamik. *Arch Ges Physiol* 1898;72:566.
4. Fry DL. Physiologic recording by modern instruments with particular reference to pressure recording. *Physiol Rev* 1960;40:753.
5. McDonald DA. *Blood Flow in Arteries,* 2nd ed. Baltimore: Williams & Wilkins, 1974.
6. Wood EH, Leusen IR, Warner HR, et al. Measurement of pressures in man by cardiac catheters. *Circ Res* 1954;2:294.
7. Gleason WL, Braunwald E. Studies on the first derivative of the ventricular pressure pulse in man. *J Clin Invest* 1962;41:80.
8. Hansen AT. Pressure measurement in the human organism. *Acta Physiol Scand* 1949;19[Suppl. 68]:87.
9. Courtois M, Fattal PG, Kovacs SJ, et al. Anatomically and physiologically based reference level of measurement of intracardiac pressures. *Circulation* 1995;92:1994
10. Murgo JP, Westerhof N, Giolma JP, et al. Manipulation of ascending aortic pressure and flow wave reflections with Valsalva maneuver: relationship to input impedance. *Circulation* 1981;63:122.
11. Murgo JP, Westerhof N, Giolma JP, et al. Aortic input impedance in normal man: relationship to pressure wave forms. *Circulation* 1980;62:105.
12. Laskey WK, Kussmaul WG. Arterial wave reflection in heart failure. *Circulation* 1987;75:711.
13. Lange RA, Moore DM Jr, Cigarroa RG, et al. Use of pulmonary capillary wedge pressure to assess severity of mitral stenosis: is true left atrial pressure needed in this condition? *J Am Coll Cardiol* 1989;13:825.
14. Cha SD, Roman CF, Maranhao V. Clinical trial of the disposable transducer catheter. *Cathet Cardiovasc Diagn* 1988;14:63.
15. Falsetti HL, Mates RE, Greene DG, et al. V_{max} as an index of contractile state in man. *Circulation* 1971;43:467.
16. Gersh BJ, Hahn CEW, Prys-Roberts C. Physical criteria for measurement of left ventricular pressure and its first derivative. *Cardiovasc Res* 1971;5:32.

8
Blood Flow Measurement: The Cardiac Output and Vascular Resistance

William Grossman

University of California, San Francisco, School of Medicine; Division of Cardiology, University of California, San Francisco Medical Center, San Francisco, California 94143

The maintenance of blood flow commensurate with the metabolic needs of the body is a fundamental requirement of human life. In the absence of major disease of the vascular tree (e.g., arterial obstruction), the maintenance of appropriate blood flow to the body depends largely on the heart's ability to pump blood in the forward direction. The quantity of blood delivered to the systemic circulation per unit time is termed the cardiac output, generally expressed in liters per minute.

ARTERIOVENOUS DIFFERENCE AND EXTRACTION RESERVE

Because the extraction of nutrients by metabolizing tissues is a function not only of the rate of delivery of those nutrients (the cardiac output) but also of the ability of each tissue to extract those nutrients from the circulation, tissue viability can be maintained despite a fall in cardiac output as long as there is increased extraction of required nutrients. The extraction of a given nutrient (or of any substance) from the circulation by a particular tissue is expressed as the arteriovenous difference across that tissue, and the factor by which the arteriovenous difference can increase at constant flow (due to changes in metabolic demand) may be termed the *extraction reserve.* For example, arterial blood in humans is normally 95% saturated with oxygen; that is, if 1 L of blood has the capacity to carry approximately 200 mL of oxygen when fully saturated, arterial blood will usually be found to contain 190 mL of oxygen per liter (190/200 = 95%). Venous blood returning from the body normally has an average oxygen saturation of 75%; that is, mixed venous blood generally contains 150 mL of oxygen per liter of blood (150/200 = 75%). Thus the normal arteriovenous difference for oxygen is 40 mL/L (190 mL/L – 150 mL/L).

The normal extraction reserve for oxygen is 3, which means that under extreme metabolic demand, the body's tissues can extract up to 120 mL of oxygen (3 × 40 mL) from each liter of blood delivered (1). Thus if arterial saturation remains constant at 95%, full utilization of the extraction reserve will result in a mixed venous oxygen content of 70 mL/L (190 mL/L – 120 mL/L) or a mixed venous oxygen saturation of 35% (70/200 = 35%). This is essentially the value found for mixed venous (i.e., pulmonary artery) oxygen saturation in normal men studied at maximal exercise. The relation between cardiac output and arteriovenous O_2 difference is illustrated in Fig. 8.1.

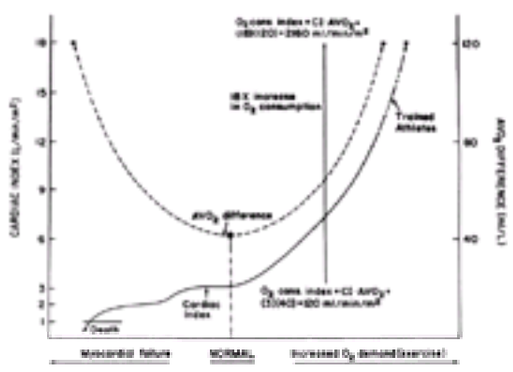

FIG. 8.1. Relationship between arteriovenous oxygen (A-VO_2) difference (broken line) and cardiac index (solid curve) in normal subjects at rest (center) and during exercise (right) and in the patient with progressively worsening myocardial failure (left). (See text for discussion.)

Lower Limit of Cardiac Output

The value of 3 for the oxygen extraction reserve predicts that in progressive cardiac decompensation, meeting the basal oxygen requirements of the body demands that oxygen extraction increase as cardiac output falls, until arteriovenous oxygen difference has tripled and cardiac output has fallen to one-third of its normal value (Fig. 8.1). Because the extraction reserve has now been used fully, further reduction of cardiac output will result in tissue hypoxia, anaerobic metabolism, acidosis, and eventually, circulatory collapse. This prediction appears to be quite accurate; clinical investigators have observed for many years that a fall in resting cardiac output to below one-third of normal (i.e., a cardiac index of £1.0 L/min/m^2) is incompatible with life.

Upper Limit of Cardiac Output

Several studies have indicated that the largest increase in cardiac output that can be achieved by a trained athlete at maximal exercise is 600% of the resting output. If a normal 70-kg man has a cardiac output of 5 L/min or 3.0 L/min/m^2, his maximal cardiac output might be as high as 30 L/min (18 L/min/m^2). Because cardiac output increases approximately 600 mL for each 100-mL increase in oxygen requirements of the body, an increase in cardiac output of 25 L/min with maximal exercise would suggest an increase in total-body oxygen requirements of 4,167 mL/min, which is approximately an 18-fold increase over the normal resting value of 250 mL/min. The 18-fold increase in total-body oxygen requirements is met by the combined sixfold increase in oxygen “delivery” (i.e., cardiac output) and threefold increase in oxygen extraction (extraction reserve). These relations are illustrated in Fig. 8.1.

Factors Influencing Cardiac Output in Normal Subjects

The range of the “normal” cardiac output is difficult to define with precision because it is influenced by several variables. Obviously, body size is important, and the ranges of normal values for cardiac output of 2-year-old children, 10-year-old children, and 50-year-old men are so different that they show only minimal overlap. For this reason, normalization of the cardiac output for differing body size is considered fundamental by all students of this subject, although there is disagreement about the best way to accomplish this normalization. Because cardiac output seems to be predominantly a function of the body's oxygen consumption or metabolic rate (1,2) and because metabolic rate was thought to correlate best with body surface area (3,4), it has become customary to express cardiac output in terms of the cardiac

index [(liters/min)/(body surface area, m^2)]. Body surface area is not measured directly but is instead calculated from one of the experimentally developed formulas, such as that of Dubois (4).

$$\text{Body surface area } (m^2) = 0.007184 \times \text{weight}^{0.425}\ (kg) \times \text{height}^{0.725}\ (cm) \quad \textbf{(8.1)}$$

Despite the shortcomings and weaknesses of this approach to normalization of the cardiac output (1,5), the method has gained nearly universal acceptance by clinicians over the past 40 years and will be employed throughout this book. A chart to aid calculation of body surface area (if weight and height are known) appears in Fig. 8.2.

FIG. 8.2. Nomogram for calculation of body surface area given the weight and height of the patient. From the formula of Dubois (4).

Although expression of cardiac output as the cardiac index greatly narrows the range of normal values among our groups of 2-year-old children, 10-year-old children, and 50-year-old men, it does not completely abolish the differences in these ranges. In fact, the normal cardiac output appears to vary with age, steadily decreasing from approximately 4.5 L/min/m^2 at age 7 years to 2.5 L/min/m^2 at age 70 years (1,6). This is not surprising because it is well known that the body's metabolic rate is affected greatly by age, being highest in childhood and progressively diminishing to old age.

In addition to age, cardiac output is affected by posture, decreasing approximately 10% when rising from a lying to a sitting position and approximately 20% when rising (or being tilted) from a lying to a standing position. Also, body temperature, anxiety, environmental heat and humidity, and a host of other factors influence the normal resting cardiac output (1), and these must be considered in interpreting any value of cardiac output measured in the clinical setting.

Techniques for Determination of Cardiac Output

Of the numerous techniques devised over the years to measure cardiac output, two have won general acceptance in cardiac catheterization laboratories: the Fick oxygen technique and the indicator dilution technique. Both techniques resemble each other in that they are based on the theoretical principle enunciated by Adolph Fick (7) in 1870. The principle, which was never actually applied by Fick, states that the total uptake or release of any substance by an organ is the product of blood flow to the organ and the arteriovenous concentration difference of the substance. For the lungs, the substance released to the blood is oxygen, and the pulmonary blood flow can be determined by knowing the arteriovenous difference of oxygen across the lungs and the oxygen consumption per minute.

Fick's principle is illustrated in Fig. 8.3. In this figure, a train is passing by a hopper that is delivering marbles to the boxcars at a rate of 20 marbles per minute. If the boxcars each contain 16 marbles before passing under the hopper and 20 marbles after passing under the hopper, each boxcar is picking up four marbles and must be taking only 0.20 minute to pass under the hopper, because it would pick up 20 marbles in each full minute under the hopper. If each boxcar takes 0.20 minute to pass by the hopper, the train is moving at a speed sufficient to deliver five boxcars per minute to any point down the line. This could have been calculated as shown in Fig. 8.3:

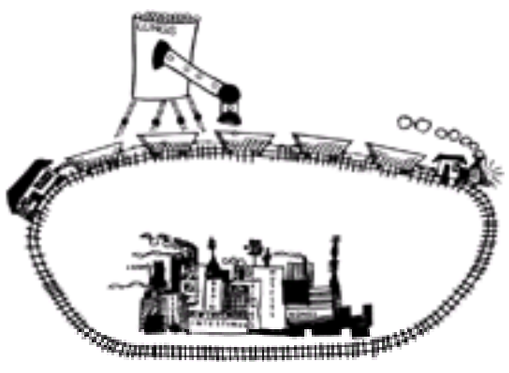

FIG. 8.3. Illustration of Fick's principle. A train, representing the circulation, passes by a hopper (the lungs) that delivers marbles (oxygen) to the train's boxcars at a rate of 20 marbles per minute. Because the boxcars each contain 16 marbles before and 20 marbles after passing under the hopper, each boxcar is picking up 4 marbles and must be taking only 0.20 minute to pass under the hopper, since it would pick up 20 marbles in each full minute under the hopper. If each boxcar takes only 0.20 minute to pass by the hopper, the train is moving at a speed sufficient to deliver 5 boxcars per minute to any point down the line. This could have been calculated as

Train's speed (boxcars/min) = marble delivery rate (marbles/min)/"A-V" marble difference (marble/min)
= (20 marbles/min)/(4 marbles/boxcar)
= 5 boxcars/min

If one boxcar is 1 L of blood and each marble is 10 mL oxygen, then we have an arteriovenous oxygen difference of 40 mL/L, an O_2 consumption of 200 mL/min, and a cardiac output of 5 L/min. (Illustration kindly provided by Jennifer Grossman, age 11.)

Train's speed (boxcars/min)

= marble delivery rate (marbles/min)

÷ “A-V” marble difference(marbles/boxcar)

= (20 marbles/min)/(4 marbles/boxcar)

= 5 boxcars/min

If one boxcar is 1 L of blood and each marble is 10 mL of oxygen, then we have an arteriovenous O_2 difference of 40 mL/L, an oxygen consumption of 200 mL/min,

and a cardiac output of 5 L/min.

Fick Oxygen Method

In the Fick oxygen method, pulmonary blood flow should be determined ideally by measuring the arteriovenous difference of oxygen across the lungs and the rate of oxygen uptake by blood from the lungs. If there is no intracardiac shunt and pulmonary blood flow is equal to systemic blood flow, the Fick oxygen method also measures systemic blood flow. Thus, *cardiac output = oxygen consumption ¸ arteriovenous oxygen difference*.

In actual practice, the rate at which oxygen is taken up from the lungs by blood is not measured, but rather the uptake of oxygen from room air by the lungs is measured, because in a steady state these two measurements are equal. Furthermore, arteriovenous oxygen difference across the lungs is not measured directly. Generally, pulmonary arterial blood (true mixed venous blood) is sampled, but pulmonary venous blood is not sampled. Instead, left ventricular or systemic arterial blood is sampled and assumed to have an oxygen content representative of mixed pulmonary venous blood. Actually, because of bronchial venous and thebesian venous drainage, the oxygen content of systemic arterial blood is commonly 2 to 5 mL/L of blood lower than pulmonary venous blood as it leaves the alveoli.

Oxygen Consumption

Two different methods for measurement of oxygen consumption are widely used today: the polarographic method and the paramagnetic method. The older Douglas bag method is rarely used.

Oxygen consumption may be measured using the metabolic rate meter (MRM) made by Waters Instruments (Rochester, MN) or the Deltatrac II, made by Sensormedics (Yorba Linda, CA). The MRM instrument contains a polarographic oxygen sensor cell (gold and silver/silver chloride electrodes), a hood or face mask, and a blower of variable speed connected to a servocontrol loop with the oxygen sensor (Fig. 8.4). This device is convenient and accurate and represents a significant advance over the older, standard procedure of collecting expired air for 3 minutes in a Douglas bag and measuring volume (Tissot spirometer) and oxygen content. The principle of operation for the MRM involves using a variable-speed blower to maintain a unidirectional flow of air from the room through the hood and via a connecting hose to the polarographic oxygen-sensing cell. As illustrated in Fig. 8.4, room air enters the hood at a rate $\dot{V}_R$ (mL/min), which is determined by the blower's discharge rate $\dot{V}_M$ (mL/min), as well as the patient's ventilatory rate ($\dot{V}_i$, inhaled air in mL/min; $\dot{V}_E$, exhaled air). The blower speed $\dot{V}_M$ is controlled by a servoloop designed to maintain the oxygen content of air flowing past the polarographic cell constant at a predetermined value. In a steady state, the average value of $\dot{V}_M$ together with the oxygen content of room air and of air flowing past the polarographic cell can be used to calculate the patient's oxygen consumption, as follows:

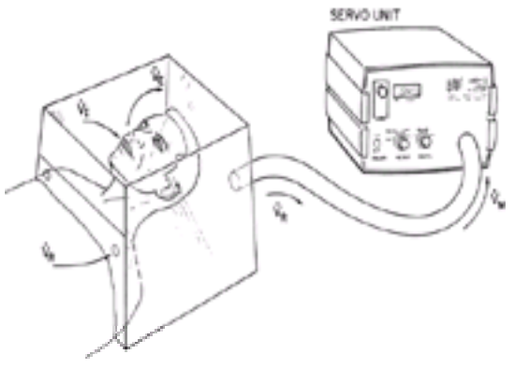

FIG. 8.4. Measurement of O_2 consumption by a polarographic cell technique using the Waters Instruments metabolic rate meter (MRM). A transparent hood fits snugly over the patient's head, resting on his or her pillow. Air enters the hood through holes in a plastic sheet at a flow rate of $\dot{V}_R$. The patient's inspiratory ($\dot{V}_I$) and expiratory ($\dot{V}_E$) flow rates subtract and add to $\dot{V}_R$ to yield $\dot{V}_M$, the flow rate leaving the hood and entering the servounit. A blower motor in the servounit adjusts $\dot{V}_M$ to keep the O_2 sensed by a polarographic cell constant. (See text for details.)

The patient's oxygen consumption $\dot{V}O_2$ is given by

$$\dot{V}_{O_2} = (F_RO_2 \cdot \dot{V}_R) - (F_MO_2 \cdot \dot{V}_M) \quad \textbf{(8.2)}$$

where F_RO_2 and F_MO_2 are the fractional contents of oxygen in room air and in air flowing past the polarographic cell, respectively.

As can be seen from Fig. 8.4,

$$\dot{V}_M = \dot{V}_R - \dot{V}_i + \dot{V}_E \quad \textbf{(8.3)}$$

which can be rewritten as

$$\dot{V}_R = \dot{V}_M + \dot{V}_i - \dot{V}_E \quad \textbf{(8.4)}$$

Substituting this in Eq. (8.2) gives

$$\begin{aligned} \dot{V}_{O_2} &= F_RO_2(\dot{V}_M + \dot{V}_i - \dot{V}_E) - F_MO_2 \cdot \dot{V}_M \quad \textbf{(8.5)} \\ &= F_RO_2(\dot{V}_M) - F_MO_2(\dot{V}_M) + F_RO_2(\dot{V}_i) \\ &\quad - F_RO_2(\dot{V}_E) \\ &= \dot{V}_M(F_RO_2 - F_MO_2) + F_RO_2(\dot{V}_i - \dot{V}_E) \end{aligned}$$

Since the fractional content of oxygen in room air (F_RO_2 is 0.209, oxygen consumption is given by

$$\dot{V}_{O_2} = \dot{V}_M(0.209 - F_MO_2) + 0.209(\dot{V}_i - \dot{V}_E) \quad \textbf{(8.6)}$$

Thus in a steady state (where $\dot{V}_i - \dot{V}_E$ is constant), oxygen consumption can be determined by measuring the volume rate of air moved by the blower motor ($\dot{V}_M$) and the fractional oxygen content of air moving past the polarographic sensor. In the MRM, a servocontrolled system adjusts $\dot{V}_M$ to keep F_MO_2 at a constant predetermined value. In practice, F_MO_2 is set at 0.199 so that Eq. (8.6) becomes

$$\begin{aligned} \dot{V}_{O_2} &= \dot{V}_M(0.209 - 0.199) \quad \textbf{(8.7)} \\ &\quad + 0.209(\dot{V}_i - \dot{V}_E) \\ \dot{V}_{O_2} &= 0.01\ \dot{V}_M + 0.209(\dot{V}_i - \dot{V}_E). \end{aligned}$$

For practical purposes, the respiratory quotient (RQ) is assumed to be 1.0; accordingly, $\dot{V}_i = \dot{V}_E$ and $\dot{V}_{O2} = 0.01\,\dot{V}_M$. If the RQ is actually 0.9 (e.g., the patient releases 0.9 L of CO_2 for each liter of O_2 consumed), the error in $\dot{V}O_2$ resulting from the assumption of an RQ of 1.0 is 1.6%, and if RQ is 0.8, the error would be 3.2%. The MRM O_2 consumption monitor has a calibrated blower motor in addition to the servocontrol polarographic sensor and gives a readout of oxygen consumption in liters per minute by digital scale (MRM-2) or by meter and paper (MRM-1). The MRM-2 model is calibrated to be highly accurate in the oxygen consumption range from 10 to 1,000 mL O_2/min and is thus best suited for measurement of resting O_2 consumption in the catheterization laboratory. The MRM-1 model, which is calibrated in the range of 150 to 5,000 mL O_2/min, is best suited for exercise studies.

The Sensormedics Deltatrac II differs from the Waters Instruments MRM device in several aspects. First, it is more sophisticated than the MRM and measures directly the fractional content of oxygen as well as the concentration of carbon dioxide in expired flow, and thus calculates the RQ of each patient. The Sensormedics device is calibrated prior to each period of use with a cylinder containing a test gas of 95% oxygen and 5% carbon dioxide. The Sensormedics device uses a constant flow rate $\dot{V}_M$ leaving the canopy or hood and entering the metabolic monitor unit. The sensors in this unit measure oxygen (paramagnetic sensor) and carbon dioxide (infrared sensor), and the unit adjusts for temperature and the partial pressure of water vapor, expressing O_2 consumption and CO_2 production at STPD (dry gas at O°C and 760 mm Hg).

Both the Waters Instruments and Sensormedics devices are relatively easy to use, although a fair amount of attention to detail is required to obtain reproducible readings consistently. A study by Lange et al. (8), however, found that values of oxygen consumption measured by metabolic rate meter (MRM-2, Waters Instruments, Rochester, MN) were significantly lower than those measured using the standard Douglas bag technique (see later discussion).

Douglas Bag Method

The older Douglas bag method is rarely used today, and interested readers are referred to earlier editions of this book for details.

Arteriovenous Oxygen Difference

The arteriovenous oxygen difference across the lungs must be measured to calculate cardiac output by Fick's principle, and this can be accomplished by the following method. From appropriately positioned catheters, systemic arterial and mixed venous (pulmonary arterial) blood samples are obtained during the period when O_2 consumption is being measured. The samples are drawn into heparinized syringes and capped quickly. If the patient has received heparin systemically, the syringes for collection of these blood samples need not be heparinized. If the samples will be analyzed immediately by oximetry, plastic syringes may be used. O_2 may diffuse through the walls of plastic syringes, however, and glass syringes are considered preferable by some if there will be a delay in oximetric analysis of the blood. In a test in my laboratory, no appreciable increase in O_2 saturation of venous blood could be detected over 2 hours. (Capped plastic 15-mL syringe filled with venous blood sitting at room temperature was sampled every 15 minutes for oximetry.) The samples should be drawn simultaneously and as close to the midpoint of the oxygen consumption determination as possible. Care must be taken to avoid contamination of the blood samples with air bubbles.

Oxygen content (in milliliters of oxygen per liter of blood) can be determined by a variety of methods, the most classic of which (and the one that serves as a standard for all others) is the manometric technique of Van Slyke and Neill (9). The major drawback of the Van Slyke and Neill technique is that 15 to 30 minutes are required to run a single blood sample. The different devices for oximetry measurement have been studied and compared by Shepherd and McMahan (9). The older Van Slyke methodology is rarely used today, and the Lex-O_2-Con fuel cell technique is no longer available. Devices in widespread use today are of the cooximeter class and either hemolyze the blood sample (by ultrasonic or chemical techniques) or use whole blood; both types of cooximeter depend on spectrophotometric measurement of the percent oxygen saturation of hemoglobin. Several devices in use today have been demonstrated to be accurate (9), including the Radiometer OSM2 and AVOXimeter 1000 (A-Vox Systems, San Antonio, TX) devices. Using these devices, oximetry of heparinized blood samples is simple and quick and measures the percentage of hemoglobin present as oxyhemoglobin. This percentage, multiplied by the theoretical oxygen-carrying capacity of the patient's blood, yields the calculated oxygen content of that sample (Fig. 8.5). A formula for approximating the theoretical oxygen-carrying capacity in humans is

$$\begin{aligned}&\text{Hemoglobin (g/dl)} \\ &\times\ 1.36\ (\text{mL } O_2\text{/g of hemoglobin}) \\ &\times\ 10\ =\ \text{theoretical } O_2 \\ &=\ \text{carrying capacity (ml } O_2\text{/liter of blood)}\end{aligned} \qquad \textbf{(8.8)}$$

Step 1. Theoretic oxygen-carrying capacity:
Hemoglobin (gm/dl) 1.36 [ml of O_2/gm of Hb) 10 _____ ml O_2/l blood

Step 2. Saturation of arterial (BA, FA, Aa) blood _____ %

Step 3. Oxygen content of arterial blood:
Theoretic capacity (step 1) % saturation (step 2) _____ ml/l

Step 4. Saturation of mixed venous (PA) blood _____ %

Step 5. Oxygen content of mixed venous blood:
Theoretic capacity (step 1) % saturation (step 4) _____ ml/l

Step 6. AV O_2 difference:
Arterial O_2 content (step 3) venous O_2 content (step 5) _____ ml/l

FIG. 8.5. Calculation of oxygen content and A-V oxygen difference when using the reflectance oximetry method.

In several textbooks the constant is given as 1.34, but studies on crystalline human hemoglobin suggest that the correct number may be 1.36 (10,11). Whatever its correct value, the formula is only an approximation. Figure 8.5 is a flow sheet that may be used to calculate oxygen content of blood samples and arteriovenous oxygen difference when the spectrophotometric oximeter method is used. Oxygen contents of arterial and mixed venous blood samples are calculated as the percentage of oxyhemoglobin saturation of these samples multiplied by the oxygen-carrying capacity (steps 2 to 5, Fig. 8.5). The arteriovenous oxygen difference (step 3 minus step 5, Fig. 8.5) may then be divided into the oxygen consumption to yield the cardiac output. Current oximeters, such as the AVOXimeter 1000, illuminate a very small sample of heparinized blood (volume 50 mL) with light of multiple wavelengths and record the optical density of each transmitted wavelength. This approach allows estimation of total hemoglobin concentration as well as the concentrations of various components: oxyhemoglobin, methemoglobin, and carboxyhemoglobin. This permits instantaneous calculation of oxygen content, which is displayed on the oximeter's liquid crystal display (LCD) screen. This value can then be entered directly in steps 3, 5, and 6 of Fig. 8.5. Arterial blood may be taken from a systemic artery, the left ventricle, the left atrium, or the pulmonary veins. Theoretically, pulmonary venous blood is preferable to peripheral arterial blood for the arteriovenous oxygen difference calculations. However, except in the presence of a right-to-left intracardiac shunt, pulmonary venous oxygen content may be approximated by systemic arterial oxygen content, ignoring the small amount of venous admixture resulting from bronchial and thebesian venous drainage. If arterial desaturation (e.g., arterial blood oxygen saturation <95%) is present, a central right-to-left shunt should be excluded before accepting systemic arterial oxygen content as representative of pulmonary venous blood. Techniques for detecting and quantifying such shunts are described in Chapter 9.

The most reliable site for obtaining mixed ve- nous blood is the pulmonary artery. Because of streaming and incomplete mixing, using blood from more proximal sites such as the right atrium or vena cavae as representative of mixed venous blood is much less accurate (12,13). Right ventricular blood is closer to true mixed venous blood and may be substituted for pulmonary arterial blood if necessary.

Sources of Error

The techniques described for cardiac output measurement by application of Fick's principle assume that a steady state exists (i.e., that the cardiac output and oxygen consumption are constant during the period of measurement). Therefore strict quiet, calm, and decorum must be maintained in the cardiac catheterization laboratory during this time to encourage the achievement of a steady-state condition. Potential errors in the determination of cardiac output by the Fick oxygen technique may come from a number of sources.

The spectrophotometric determination of blood oxygen saturation may introduce inaccuracies related to carboxyhemoglobin or other abnormal hemoglobins, as discussed previously. This method also may be inaccurate if indocyanine green dye is present in the circulation, although the newer oximeters are not affected by this problem. Reflectance oximetry, as performed on whole blood, is accurate in the range of blood oxygen saturations from 45% to 98% but may not be reliable when blood O_2 saturation is less than 40%, as is the case in pulmonary artery blood from patients with very low cardiac output or during strenuous exercise.

Improper collection of the mixed venous blood sample (e.g., air bubbles) is a common source of error. Partial contamination of pulmonary arterial blood with pulmonary capillary wedge blood may result in a falsely high mixed venous oxygen content. If the mixed venous blood sample is taken from the right atrium, inferior vena cava, coronary sinus, or similar sites, a falsely low or high value for arteriovenous difference may result. Also, care must be taken not to dilute the blood sample with too much heparinized saline solution.

The average error in determining oxygen consumption has been estimated to be approximately 6% (13). The error for arteriovenous oxygen difference has been estimated at 5% (14,15). Narrow arteriovenous oxygen differences are more prone to introduce error than wide arteriovenous oxygen differences. Thus the Fick oxygen method is most accurate in patients with low cardiac output, in whom the arteriovenous oxygen difference is wide. The total error in determination of the cardiac output by the Fick oxygen method has been established to be about 10% (16).

Does oxygen consumption actually need to be measured? To avoid the technical difficulties and expense associated with measurement of oxygen consumption, some laboratories assume that O_2 consumption can be predicted from the body surface area, with or without a correction for age and sex. Thus, some laboratories assume that resting O_2 consumption is 125 mL/m^2, or 110 mL/m^2 for older patients. The validity of such an assumption has been addressed in a study from the University of Texas at Dallas (17). Cardiac output was determined by the indicator dilution technique, and O_2 consumption was calculated by dividing cardiac output by arteriovenous oxygen difference, which was measured directly. In the 108 patients studied, O_2 consumption index averaged 126 ± 26 mL/min/m^2 (mean ± standard deviation), but there was wide variability as indicated by the standard deviation, and the authors concluded that O_2 consumption varies greatly among adults at the time of cardiac catheterization. In another study from Bristol Royal Infirmary in the United Kingdom (18), direct measurement of O_2 consumption was compared with assumed values in 80 patients (aged 38 to 78 years). Large discrepancies were evident, with more than half the values differing by more than ±10% and several by ±25% or more. Thus, assumed values for O_2 consumption are likely to introduce considerable error.

Indicator Dilution Methods

The indicator dilution method is merely a specific application of Fick's general principle. In the Fick oxygen method, the “indicator” is oxygen, the site of injection is the lungs, and the injection procedure is that of continuous infusion. Stewart (19) was the first to use the so-called indicator dilution method for measuring cardiac output; he used the continuous-infusion technique and reported his first studies in 1897.

There are two general types of indicator dilution methods: the continuous-infusion method and the single-injection method. The single-injection method is the most widely used and is discussed here in detail. The fundamental requirements for this method include the following:

A bolus of nontoxic indicator substance, which mixes completely with blood and whose concentration can be measured accurately, is injected.

The indicator substance is neither added to nor subtracted from the blood during passage between injection and sampling sites.

Most of the indicator must pass the site of sampling before recirculation begins.

The indicator substance must go through a portion of the central circulation where all the blood of the body becomes mixed.

For the single-injection method, theoretical considerations may be summarized as follows: An injection of a specified amount of an indicator I into a proximal vessel or chamber (e.g., the vena cava or right atrium for the thermodilution method and the pulmonary artery for the indocyanine green dye method) is followed by continuous measurement of the indicator concentration C in blood as a function of time t at a point downstream from the injection (e.g., pulmonary artery for thermodilution technique and radial or femoral artery for the indocyanine green dye method). Because all the injection indicator I must pass the downstream measurement site,

$$I = Q \int_0^\infty C(t)\, dt \qquad \textbf{(8.9)}$$

where $\dot{Q}$ is the volume flow (in milliliters per minute) between the sites of injection and measurement. Thus $\dot{Q}$ (which is the cardiac output in the methods to be described) may be calculated as

$$Q = \frac{I}{\int_0^\infty C(t)\, dt} \qquad \textbf{(8.10)}$$

Numerous indicators have been used successfully, and the history of this subject is reviewed thoroughly by Guyton et al. (1). Indocyanine green previously had enjoyed long-standing acceptance in clinical practice but is rarely used today for routine measurement of cardiac output. Accordingly, it will not be discussed here and the interested reader is referred to previous editions of this textbook. We will only discuss thermodilution (in which “cold” is the indicator), which is now the dominant technique.

Thermodilution Method

A thermal indicator method for measuring cardiac output was first introduced by Fegler (20) in 1954 but was not applied to the clinical situation until the work of Branthwaite and Bradley (21)) and Ganz et al. (22,23). In the initial report by Ganz et al. (22), two thermistors were used: one in the superior vena cava at the site at which the cold dextrose solution was injected into the bloodstream and a second “downstream” thermistor in the pulmonary artery. These two thermistors allowed accurate measurement of the temperature of the injectate T_I as well as the temperature of blood T_B downstream from the injectate. Using the basic indicator dilution equation, the cardiac output by thermodilution CO^{TD} in milliliters is given as

$$CO_{TD} = \frac{V_I(T_B - T_I)(S_I \cdot C_I / S_B \cdot C_B)60(\text{sec/min})}{\int_0^\infty \Delta T_B(t)\, dt} \qquad \textbf{(8.11)}$$

where V_I = volume of injectate (mL), and S_B, S_I, C_B, and C_I are the specific gravity and specific heat of blood and injectate, respectively. When 5% dextrose is used as an indicator ($S_I \cdot C_I/S_B \cdot C_B$) = 1.08. Most commercially available thermodilution systems use a single thermistor only, placed at the downstream site, and assume that the temperature of the injectate (measured in a bowl before injection) increased by a predictable amount (“catheter warming”) during injection. The calculated cardiac output by the thermodilution equation is multiplied by an empirical correction factor (0.825) to correct for the catheter warming (23). However, a recent report (24) has

demonstrated that improved accuracy and precision can be obtained with the thermodilution technique when cardiac output is measured using a dual thermistor catheter system. These investigators used a specialized dual thermistor right heart catheter, constructed with a second thermistor, positioned to measure temperature at the point where the injectate exits the catheter in the right atrium. This takes into account any warming of the injectate that may take place as it travels from the injectate syringe to the point of exit from the catheter in the right atrium. Using this technique there was substantially less measurement variability, and better agreement with simultaneously measured Fick cardiac output (the latter determined using a 5-minute Douglas bag collection of expired air and paired blood samples from pulmonary and femoral arteries).

The thermodilution method for measuring cardiac output has several advantages over the indocyanine green dye method, and these include the following:

1. It does not require withdrawal of blood.
2. It does not require an arterial puncture.
3. An inert and inexpensive indicator is used.
4. There is virtually no recirculation, making computer analysis of the primary curve simple.

Sources of Error

1. The method is unreliable in the presence of significant tricuspid regurgitation.
2. The baseline temperature of blood in the pulmonary artery usually shows distinct fluctuations associated with respiratory and cardiac cycles. If these fluctuations are large, they may approach the magnitude of the temperature change produced by the “cold” indicator injection.
3. Loss of injected indicator (“cold”) between injection and measuring sites (vena cava and pulmonary artery) is not usually a problem, but in low-flow, low-output states, loss of indicator may occur because of warming of blood by the walls of the cardiac chambers and surrounding tissues. This concern is supported by the study of van Grondelle et al. (25), who found that thermodilution cardiac output measurements overestimated cardiac output consistently in patients with low output (<3.5 L/min), and this overestimation was greatest, averaging 35%, in patients whose cardiac outputs were <2.5 L/min. This is what might be expected from the equation for calculation of cardiac output by thermodilution, since the change in pulmonary artery blood temperature (D T_B) will be reduced if cold is lost by warming of the injectate during slow passage through the vena cava, right atrium, and right ventricle. Because D T_B is the denominator in the equation for cardiac output calculation, reduction in D T_B will result in a rise in calculated cardiac output.
4. The empirical correction factor of 0.825 may be inadequate to correct for deviations in true injectate temperature from the temperature of the injectate bowl or reservoir due to warming in the syringe by the hand of the individual injecting the dextrose solution from the syringe or by catheter warming.

In general, indicator dilution cardiac output determinations have an error of 5% to 10% when performed carefully. The values obtained correlate well with those calculated by the Fick oxygen method.

Clinical Measurement of Vascular Resistance and Assessment of Vasodilator Drugs

Poiseuille's Law

The French physician Jean Léonard Marie Poiseuille (1799–1869) made many important contributions to the study of hemodynamics. At age 18, he introduced the mercury manometer for the measurement of blood pressure, a technical innovation that continues in use to this day. In 1846 he formulated a series of equations describing the flow of fluids through cylindrical tubes. Although Poiseuille was interested in blood flow, he substituted simpler liquids in his measurements of flow through rigid glass tubes. His discoveries, later modified by others, are expressed in what is regarded as Poiseuille's law (26), which may be stated as follows:

$$Q = \frac{\pi (Pi - Po)\, r^4}{8 \eta l} \qquad \textbf{(8.12)}$$

where:

Q = volume flow

$Pi - Po$ = inflow pressure – outflow pressure

r = the radius of the tube

l = the length of the tube

h = viscosity of the fluid

This relationship applies in the specific circumstance of steady-state laminar flow of a homogeneous fluid through a rigid tube. Under these conditions, flow, Q, varies directly as the pressure difference, $Pi - Po$, and the fourth power of the tube's radius, r. It varies inversely as the length, l, of the tube and the viscosity, h of the fluid.

Hydraulic resistance, R, is defined by analogy to Ohm's law as the ratio of mean pressure drop, D P, to flow, Q, across the vascular circuit. The various factors contributing to vascular resistance can be illustrated by rearranging Poiseuille's law as follows:

$$R = \frac{Pi - Po}{Q} = \frac{8 \eta l}{\pi r^4} \qquad \textbf{(8.13)}$$

It is apparent from this equation that, in the condition of steady laminar flow of a homogeneous fluid through a rigid cylindrical tube, resistance to flow depends only on the dimensions of the tube and the viscosity of the fluid. In particular, the resistance is remarkably sensitive to changes in the radius of the tube, varying inversely with its fourth power.

Vascular Resistance and Pressure-Flow Relationships

The applicability of laws derived from steady-state fluid mechanics in assessing vascular resistance is somewhat ambiguous because blood flow is pulsatile, blood is a nonhomogeneous fluid, and the vascular bed is a nonlinear, elastic, frequency-dependent system. In such a system, resistance varies continuously with pressure and flow and is influenced by many factors, such as inertia, reflected waves, and the phase angle between pulse and flow wave velocities (26,27 and 28).

To assess both vessel caliber and elasticity, the resistive and compliant characteristics of the vascular system, the concept of *vascular impedance* has been used (27). Vascular impedance has been defined as the instantaneous ratio of pulsatile pressure to pulsatile flow (28,29). Because impedance may not be the same for all frequencies, its calculation requires resolution of the harmonic components of both pressure and flow pulsations. The *impedance modulus* so calculated is then expressed as a spectrum of impedance versus frequency. Although measurement of impedance is important in research studies, it is rarely included in routine diagnostic cardiac catheterization, and the reader is referred elsewhere (26) for a full discussion.

As a consequence of the foregoing considerations and the many active and passive factors that influence pressure and flow in blood vessels, the concept of vascular resistance in its pure physical sense is limited in application. In the context of the clinical and physiologic setting, however, pulmonary and systemic vascular resistances calculated from hemodynamic measurements made during cardiac catheterization have acquired empiric pathophysiologic meaning and are often important factors in clinical decision making.

Estimation of Vascular Resistance in the Clinical Situation

Calculations of vascular resistance are usually applied to both the pulmonary and systemic circulations. Although many authors refer to systemic or pulmonary

arteriolar resistance, I prefer the term *vascular resistance* because it is less committal concerning the anatomic site of the resistance. As has been mentioned, arteriolar tone is only one determinant of vascular resistance to blood flow. To estimate pulmonary and systemic vascular resistances quantitatively, knowledge of both the driving pressure across the pulmonary and systemic vascular beds and the respective blood flow through them is required.

The formulae generally used are:

$$\text{1. Systemic vascular resistance} = \frac{\overline{Ao} - \overline{RA}}{Q_s} \qquad \textbf{(8.14)}$$

$$\text{2. Total pulmonary resistance} = \frac{\overline{PA}}{Q_p}$$

$$\text{3. Pulmonary vascular resistance} = \frac{\overline{PA} - \overline{LA}}{Q_p}$$

where $\overline{Ao}$ = mean systemic arterial pressure, $\overline{RA}$ = mean right atrial pressure, $\overline{PA}$ = mean pulmonary arterial pressure, $\overline{LA}$ = mean left atrial pressure, Q_s = systemic blood flow, Q_p = pulmonary blood flow.

In many laboratories, the mean pulmonary capillary wedge pressure is used as an approximation of mean left atrial pressure. This should cause no problem because there is ample evidence that pulmonary capillary wedge pressure, properly obtained, closely approximates the level of left atrial pressure (30, 31 and 32). The flows are volume flows (as opposed to velocity flows) and are expressed in liters per minute, and pressures are expressed in millimeters of mercury (mm Hg). These equations yield resistance in arbitrary resistance units (R units) expressed in mm Hg per liter per minute, also called *hybrid resistance units* (HRU). These HRU units are sometimes referred to as Wood units, since they were first introduced by Dr. Paul Wood. They may be converted to metric resistance units expressed in dynes-sec-cm^{-5} by use of the conversion factor 80. In this system, resistance is expressed as:

$$\text{Resistance} = \qquad \textbf{(8.15)}$$

$$\frac{\Delta P\,(\text{mm Hg}) \times 1332\,\text{dynes/cm}^2/\text{mm Hg}}{Q_s \text{ or } Q_p\,(\text{L/min}) \times 1{,}000\,\text{mL/L} \div 60\,\text{sec/min}}$$

$$= \frac{\Delta P}{Q_s \text{ or } Q_p} \times 80 = \text{dynes-sec-cm}^{-5}$$

There is no particular advantage to either system, since both express precisely the same ratio. Most pediatric cardiologists use hybrid resistance units, whereas cardiologists with adult practices generally use metric units.

In pediatric practice it is conventional to normalize vascular resistances for body surface area (BSA), thus giving a resistance index. Although this is not commonly done in adult cardiac catheterization laboratories, the practice makes sense because normal cardiac output and therefore vascular resistance may be substantially different in a 260-lb man and a 110-lb woman. The normalized resistance, however, is not obtained by dividing resistance (as calculated in Eq. 8.14) by body surface area. Rather, normalized resistance is calculated by substituting blood flow index for blood flow in the resistance formula. Thus systemic vascular resistance index (SVRI) is calculated as

$$\text{SVRI} = \frac{(\overline{Ao} - \overline{RA})\,80}{\text{CI}} \qquad \textbf{(8.16)}$$

where CI is the cardiac (or systemic blood flow) index. Therefore, SVRI equals SVR multiplied by BSA.

Cardiac output, usually measured by either the Fick or the thermodilution method, is used as mean blood flow. It is important to realize that in conditions of intracardiac shunts or shunts between the pulmonary and systemic circulations, pulmonary blood flow and systemic flow may not be equal, and the respective flow through each circuit must be measured and used in the appropriate resistance calculation.

Normal values for vascular resistance in adults are given in Table 8.1.

Systemic vascular resistance	1,170 ± 270 dynes-sec-cm^{-5}
Systemic vascular resistance index	2,130 ± 450 dynes-sec-cm^{-5} · M^2
Pulmonary vascular resistance	67 ± 30 dynes-sec-cm^{-5}
Pulmonary vascular resistance index	123 ± 54 dynes-sec-cm^{-5} · M^2

Values are expressed as mean ± standard deviation and are derived from 37 subjects without demonstrable cardiovascular disease [17 males, 20 females, age 47 ± 9 years] who underwent diagnostic cardiac catheterization at the Peter Bent Brigham Hospital between July 1, 1975, and June 30, 1976.

TABLE 8.1. *Normal values for vascular resistance*

Clinical Use of Vascular Resistance

As can be deduced from the Poiseuille equation, changes in systemic or pulmonary vascular resistance may result theoretically from one of three mechanisms. Because changes in length of the vascular beds are uncommon after growth has been completed, changes in vascular resistance reflect either altered viscosity of blood or a change in cross-sectional area (radius) of the vascular bed.

There is ample evidence that changes in blood viscosity alter measured vascular resistances. Nihill (33) has shown that an approximate doubling of pulmonary vascular resistance occurs with increases in hematocrit from 43% to 64%. Similarly, low values for measured vascular resistance are commonly seen in patients with severe chronic anemia, although the low vascular resistance in such cases probably represents more than a viscosity effect alone.

With regard to changes in cross-sectional area of the pulmonary or systemic vascular bed, such changes do not invariably imply altered arteriolar tone. In the normal systemic circulation, mean aortic pressure may be 100 mm Hg, whereas right atrial pressure is only 5 mm Hg. Although the greatest part of this pressure drop occurs at the arteriolar level (approximately 60%), about 15% occurs in the capillaries, 15% in small veins, and 10% in the arterial system proximal to the arterioles (27). Thus although systemic vascular resistance is dominated by the caliber of the arterioles, the other components of the systemic vascular bed are by no means negligible. For example, Read and coworkers (34) studied systemic vascular resistance in dogs with constant (pump-controlled) cardiac output and found that a rise in venous pressure consistently caused a fall in resistance. The magnitude of the fall was proportional to the increment in venous pressure rise and was about 20% for an increase in venous pressure of 20 mm Hg. Other studies show no change in resistance when arterial pressure is so manipulated (in the absence of baroreceptor control). These findings have been interpreted by McDonald (28) to suggest that the decline in systemic vascular resistance with increased venous pressure results from dilation of small venous channels, whereas systemic arterioles do not distend passively with increased pressure. Therefore measurement of vascular resistance

is not a precise tool for assessing the dynamics of individual sections of the vascular bed, and the term *vascular resistance* should not be used as synonymous with arteriolar resistance.

Systemic Vascular Resistance

The minute-to-minute control of vascular resistance, at least in the systemic bed, is an amalgam of autonomic nervous system influences and local metabolic factors. Hypotension or reduced cardiac output generally triggers increased systemic resistance by means of the baroreceptors, alpha-adrenergic neural pathways, and release of humoral vasoconstrictor hormones, but these influences may be opposed by metabolic factors if the hypotension or low cardiac output results in decreased tissue perfusion with local hypoxia and acidosis. This latter circumstance is commonly seen in congestive heart failure or shock.

Knowledge of changes in systemic vascular resistance is also important in evaluating the hemodynamic response to stress tests, such as dynamic or isometric exercise (35). In this regard, there is ample evidence that normally, the systemic vascular resistance falls in response to dynamic exercise, but pulmonary vascular resistance is unchanged (at least with supine bicycle exercise). Transient elevations in systemic vascular resistance have been provoked by infusions of vasopressor drugs in an effort to evaluate the left ventricular response to a sudden increase in afterload (36).

Low systemic vascular resistance may be seen in conditions in which blood flow is abnormally high, such as may occur in patients with arteriovenous fistula, severe anemia, and other high-output states. It is important to realize that in these circumstances there may well be regional differences in vascular resistance (e.g., very low in the arteriovenous fistula but normal or increased in other vascular beds), and calculations based on mean pressure and flow in the entire systemic circulation must be interpreted with caution.

Total Pulmonary Resistance

Calculated as the ratio of mean pulmonary artery pressure to pulmonary blood flow, total pulmonary resistance expresses the resistance to flow in transporting a volume of blood from the pulmonary artery to the left ventricle in diastole, neglecting left ventricular diastolic pressure. This relationship is obviously influenced by alterations in left atrial pressure and will not consistently provide useful information about the condition of the pulmonary vasculature. Although widely used 25 years ago, this parameter is less commonly used today, and in general should be used primarily in the patient where measurement of left atrial or pulmonary capillary wedge pressure is not possible.

Pulmonary Vascular Resistance

Sometimes (inappropriately) called pulmonary arteriolar resistance, pulmonary vascular resistance expresses the pressure drop across the major pulmonary vessels, the precapillary arterioles, and the pulmonary capillary bed, and is more precise in assessing the presence and degree of pulmonary vascular disease than is total pulmonary resistance. Simple calculation of pulmonary vascular resistance provides general information about the pulmonary circulation, but this must be interpreted in the context of the clinical situation and other hemodynamic data obtained during cardiac catheterization. The pulmonary vasculature is a dynamic system and is subject to many mechanical, neural, and biochemical influences.

Measured pulmonary vascular resistance may be *increased* by hypoxia, hypercapnia, increased sympathetic tone, polycythemia, local release of serotonin, mechanical obstruction by multiple pulmonary emboli, precapillary pulmonary edema, or lung compression (pleural effusion, increased intrathoracic pressure via respirator). Pulmonary vascular resistance may be *decreased* by oxygen, adenosine, isoproterenol, alpha antagonists such as phentolamine or tolazoline, inhaled nitric oxide, prostacyclin infusions, and high doses of calcium channel blockers. These vasodilators may be used to test for fixed, irreversible pulmonary hypertension. A practical approach used in many laboratories to test for responsiveness and determine therapeutic dosage, uses intravenous epoprostenol (Flolan, Glaxo Wellcome, Research Triangle Park, NC), starting at 2 ng/kg/min and increasing by increments of 2 ng/kg/min every 15 minutes until dose-limiting pharmacologic effects (such as nausea, headache, or hypotension) are seen.

The tolazoline test for fixed pulmonary hypertension is rarely performed at present, and the interested reader is referred to earlier editions of this textbook for details as to its use. *Oxygen inhalation* may be of value in assessing pulmonary vascular reactivity. Patients with high pulmonary vascular resistance (i.e., greater than or equal to 600 dynes-sec-cm^{-5}) in association with a central shunt (e.g., ventricular septal defect) should be given 100% oxygen by face mask before concluding that the changes are fixed. Older patients with a combination of left heart failure and chronic obstructive lung disease may have considerable pulmonary vasoconstriction due to alveolar hypoventilation and its resultant hypoxia. Inhalation of 100% oxygen in such cases may result in a dramatic fall in pulmonary arterial pressure and vascular resistance.

Most studies demonstrating the usefulness of tolazoline or oxygen inhalation in the assessment of pulmonary vascular disease associated with central shunts were carried out in patients living at high altitudes. The usefulness of such assessment in patients living at sea level is less certain.

Pulmonary Vascular Disease in Patients with Congenital Central Shunts

The decision as to whether a patient with congenital heart disease would profit from corrective surgery often hinges on the calculated pulmonary vascular resistance. Although each case must be evaluated on its own characteristics, many criteria for operability have been proposed (37,38). It has been suggested that the ratio between pulmonary vascular resistance and systemic vascular resistance (resistance ratio, PVR/SVR) be used as a criterion for operability in dealing with congenital heart disease (37). Normally, this ratio is less than or equal to 0.25. Values of 0.25 to 0.50 indicate moderate pulmonary vascular disease, and values greater than 0.75 indicate severe pulmonary vascular disease. When the PVR/SVR resistance ratio equals 1.0 or more, surgical correction of the congenital defect is considered contraindicated because of the severity of the pulmonary vascular disease.

The resistance ratio has the value of factoring in miscellaneous neural, hormonal, and blood viscosity influences that may be affecting both pulmonary and systemic vascular beds and that may be primarily related to the patient's immediate clinical status more than to intrinsic pulmonary vascular changes. Many patients with left ventricular failure and low systemic output (from any cause) have associated high systemic and pulmonary vascular resistance, but the resistance ratio will be normal in the absence of intrinsic vascular pathology.

We have reported (37) three patients with congenital heart disease (two with atrial septal defect and one with patent ductus arteriosus) having cyanosis and pulmonary arterial hypertension at nearly systemic levels. Each of our patients (37) had PVR/SVR ratios of less than 0.50 and net left-to-right shunts, despite severe pulmonary hypertension (e.g., pulmonary artery pressure 110/55 mm Hg). Each patient had progressive improvement in pulmonary vascular resistance toward normal following operative closure of the shunts. These cases illustrate the importance of increased blood viscosity associated with the polycythemia of cyanosis (hematocrits in the 56% to 66% range), which may contribute substantially to the measured increase in pulmonary and systemic vascular resistances. As mentioned earlier, studies in dogs showed that calculated pulmonary vascular resistance doubled when hematocrit was raised from 43% to 64%. Accordingly, elimination of severe cyanosis with return of hematocrit to normal may lead to a 50% reduction in pulmonary vascular resistance. This influence of viscosity, as well as the generalized vasoconstriction often seen in patients with advanced cardiac disease, will be factored out by the ratio of PVR/SVR.

In his classic description of the Eisenmenger syndrome, Wood pointed out that attempted surgical repair of the shunt defect was a major source of death in these patients (38). He stated that in patients with pulmonary blood flow of less than 1.75 times systemic flow or with total pulmonary vascular resistance greater than 12 Wood or “hybrid” units (960 dynes-sec-cm^{-5}), ordinary surgical repair of the defect should not be attempted. Others have suggested similar criteria for special instances or conditions. In my opinion, surgical repair should be limited to patients in whom the net shunt is left-to-right and the pulmonary vascular resistance is less than systemic vascular resistance, preferably with a resistance ratio of less than 0.50.

Pulmonary Vascular Disease in Patients with Mitral Stenosis

Marked elevations in pulmonary vascular resistance may also be seen in acquired heart disease, notably in mitral stenosis. The effect of mitral valve replacement in patients with mitral stenosis and/or regurgitation associated with pulmonary hypertension has been evaluated (39,40). Most patients experience significant reduction in pulmonary vascular resistance following successful repair of the mitral valve lesion. Although some degree of pulmonary hypertension may persist postoperatively, significant palliative benefit usually occurs, and the decision regarding surgery must be made in light of information regarding left and right ventricular function as well as the degree of pulmonary hypertension.

Currently, percutaneous balloon mitral valvuloplasty is used widely as an alternative to surgery for treating patients with advanced mitral stenosis. The procedure results in an immediate improvement in mitral valve area and in pulmonary hypertension. Its effects on pulmonary vascular resistance have been studied in a cohort of 14 patients with critical mitral stenosis and severe pulmonary hypertension (41). Balloon mitral valvuloplasty resulted in an immediate improvement in mitral valve area (0.7 ± 0.2 cm^2 to 1.6 ± 0.7 cm^2, $p < .01$), mean left atrial pressure (26 ± 6 mm Hg to 15 ± 5 mm Hg, $p < .01$), mean pulmonary artery pressure (51 ± 17 mm Hg to 40 ± 14 mm Hg), and pulmonary vascular resistance (630 ± 570 dynes-sec-cm^{-5} to 447 ± 324 dynes-sec-cm^{-5}, $p < .01$). At an average of 7 months follow-up, repeat catheterization showed that pulmonary vascular resistance had declined further and now averaged 280 ± 183 dynes-sec-cm^{-5}. Of note, two patients who showed substantial restenosis to mitral valve areas of less than 1.0 cm^2 exhibited a return of pulmonary vascular resistance to prevalvuloplasty values (41). The decline in pulmonary vascular resistance after balloon valvuloplasty is not offset by the bronchopulmonary stresses associated with thoracotomy and general anesthesia, making mitral balloon valvuloplasty appealing as either an alternative to surgery or a preparatory procedure before surgery in patients with mitral stenosis and advanced pulmonary hypertension.

Assessment of Vasodilator Drugs

Cardiac catheterization provides an ideal opportunity for assessing the potential response of a patient to a change in medical regimen, particularly with regard to vasodilator drugs. In recent years, vasodilator drugs have assumed a major role in the treatment of patients with congestive heart failure. There is, however, great variability among currently used vasodilator agents, and the relative effects of a particular drug on resistance and capacitance vessels is of major importance in predicting its hemodynamic effects (42). This problem may become complex when a particular drug may have different effects, depending on the level of resting tone in resistance and capacitance beds. For example, nitrate preparations are well known to influence venous capacitance; this influence is presumably responsible (at least in part) for the fact that ventricular filling pressures and pulmonary congestion are consistently improved when nitrate therapy is given to patients with congestive heart failure. Despite this consistent effect on preload, the effect of nitrates on forward cardiac output has been variable (43,44 and 45), and studies have reported decreases, increases, or mixed effects on cardiac output in normal subjects and in patients with heart failure. Goldberg and colleagues (46) studied 15 patients with chronic congestive heart failure who were given an oral nitrate (erythrityl tetranitrate) at the time of cardiac catheterization to identify predictors of nitrate effect on cardiac output. There were significant reductions in right atrial, pulmonary capillary wedge, and mean arterial pressure in nearly all patients. Augmentation in cardiac output by ³10% occurred in eight patients (thereby defined as “responders”), but no change or decline occurred in seven patients (“nonresponders”). The level of peripheral vasoconstriction, as reflected by resting systemic vascular resistance, was significantly higher for the responders than for the nonresponders (2,602 ± 251 versus 1,744 ± 193 dynes-sec-cm^{-5}, $p < .02$). Furthermore, a significant reduction in systemic vascular resistance occurred only in responders, and the decline was a linear function of resting resistance (Fig. 8.6).

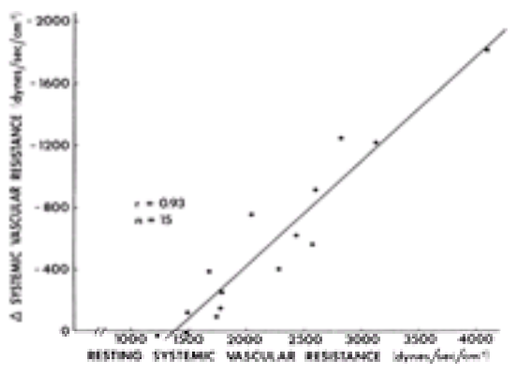

FIG. 8.6. The change (D) in systemic vascular resistance following administration of erythrityl tetranitrate plotted as a function of resting systemic vascular resistance in 15 patients with congestive heart failure. Patients with the greatest degree of vasoconstriction at rest demonstrated the greatest fall in resistance in response to the nitrate. (From Goldberg et al. Nitrate therapy of heart failure in valvular heart disease. *Am J Med* 1978;65:161, with permission.)

Thus, although reductions in arterial pressure and left and right ventricular filling pressures are a constant result of nitrate therapy, significant augmentation in forward cardiac output is likely only in patients with the most intense resting peripheral vasoconstriction. The design of a catheterization protocol in a patient with congestive heart failure can include assessment of vasodilator therapy based on these principles. For example, if the resting cardiac output is low and if right and left ventricular filling pressures as well as systemic vascular resistance are high, a long-acting nitrate or a balanced agent (e.g., sodium nitroprusside or an angiotensin-converting enzyme inhibitor) might be expected to be particularly beneficial and can be tested while the catheters are still in place. On the other hand, if the output is low and resistance is high but filling pressures are near normal, a nitrate might not help because the lowered resistance may be offset by the fall of the already normal preload, with the result being no increase in output. In such a patient, a selective lowering of resistance would be desirable, and hydralazine could be tested before removing the catheters. If the cardiac output is low but resistance is normal, neither a nitrate nor a converting enzyme inhibitor is likely to increase output and should be tested only if filling pressures are high and symptoms of congestion are a prominent part of the clinical picture. In such patients, the combination of an inotropic agent and a nitrate may be particularly helpful and could be tested at the time of catheterization. Finally, if the output is low but filling pressures and systemic vascular resistance are normal, vasodilator drugs will probably do more harm than good, and a therapeutic trial of preload elevation (administration of colloid) with or without an inotropic agent could be tested during the catheterization.

These examples are presented merely to illustrate the principle of using cardiac catheterization parameters (i.e., resistances, flows, and filling pressures) to design a therapeutic regimen and then, while the catheters are still in place, put it to the test. We have found this most useful with regard to the patient with heart failure, and cardiac catheterization in such patients should include full right and left heart catheterization with measurement of cardiac output, left and right heart pressures, and systemic and pulmonary vascular resistances.

CHAPTER REFERENCES

1. Guyton AC, Jones EC, Coleman TG. *Circulatory physiology: cardiac output and its regulation.* Philadelphia: WB Saunders, 1973:4.
2. Dexter L, et al. Effect of exercise on circulatory dynamics of normal individuals. *J Appl Physiol* 1951;3:439.
3. Berkson J, Boothby WB. Studies of metabolism of normal individuals: comparison of estimation of basal metabolism from linear formula and surface area. *Am J Physiol* 1936;116:485.
4. Dubois EF. *Basal metabolism in health and disease.* Philadelphia: Lea & Febiger, 1936.
5. Holt JP, Rhode EA, Kines H. Ventricular volumes and body weight in mammals. *Am J Physiol* 1968;215:704.
6. Brandfonbrener M, Landowne M, Shock NW. Changes in cardiac output with age. *Circulation* 1955;12:556.
7. Fick A. Uber die Messung des Blutquantums in den Herzventrikeln. *Sitz der Physik-Med ges Wurtzberg* 1870:16.
8. Lange RA, Dehmer GJ, Wells PJ, et al. Limitations of the metabolic rate meter for measuring oxygen consumption and cardiac output. *Am J Cardiol* 1989;64:783.
9. Shepherd AP, McMahan CA. Role of oximeter error in the diagnosis of shunts. *Cathet Cardiovasc Diagn* 1996;37:435.
10. Bernhard FW, Skeggs L. The iron content of crystalline human hemoglobin. *J Biol Chem* 1943;147:19.
11. Diem K, ed. *Documenta Geigy-scientific tables,* 6th ed. Ardsley, NY: Geigy Pharmaceuticals, 1962:578.
12. Dexter L, et al. Studies of congenital heart disease: II. The pressure and oxygen content of blood in the right auricle, right ventricle, and pulmonary artery in control patients. *J Clin Invest* 1947;26:554.
13. Barratt-Boyes BG, Wood EH. The oxygen saturation of blood in the venae cavae, right heart chambers, and pulmonary vessels of healthy subjects. *J Lab Clin Med* 1957;50:93.
14. Selzer A, Sudrann RB. Reliability of the determination of cardiac output in man by means of the Fick principle. *Circ Res* 1958;6:485.
15. Thomassen B. Cardiac output in normal subjects under standard conditions: the repeatability of measurements by the Fick method. *Scan J Clin Lab Invest* 1957;9:365.
16. Visscher MB, Johnson JA. The Fick principle: analysis of potential errors in the conventional application. *J Appl Physiol* 1953;5:635.
17. Dehmer GJ, Firth BG, Hillis LD. Oxygen consumption in adult patients during cardiac catheterization. *Clin Cardiol* 1982;5:436.
18. Kendrick AH, West J, Papouchado M, Rozkovec A. Direct Fick cardiac output: are assumed values of oxygen consumption acceptable? *Eur Heart J* 1988;9:337.
19. Stewart GN. Researches on the circulation time and on the influences which affect it: IV. The output of the heart. *J Physiol* 1897;22:159.
20. Fegler G. Measurement of cardiac output in anesthetized animals by a thermodilution method. *Q J Exp Physiol* 1954;39:153.
21. Branthwaite MA, Bradley RD. Measurement of cardiac output by thermodilution in man. *J Appl Physiol* 1968;24:434.
22. Ganz W, et al. A new technique for measurement of cardiac output by thermodilution in man. *Am J Cardiol* 1971;27:392.
23. Forrester JS, et al. Thermodilution cardiac output determination with single flow-directed catheter. *Am Heart J* 1972;83:396.
24. Lehmann KG, Platt MS. Improved accuracy and precision of thermodilution cardiac output measurement using a dual thermistor catheter system. *J Am Coll Cardiol* 1999;33: 883.
25. van Grondelle AV, Ditchey RV, Groves BM, et al. Thermodilution method overestimates low cardiac output in humans. *Am J Physiol* 1983;245:H690.
26. Milnor WR. *Hemodynamics,* 2nd ed. Baltimore: Williams & Wilkins, 1989.
27. O'Rourke MF. *Arterial function in health and disease.* Edinburgh: Churchill Livingstone, 1982.

28. McDonald DA. *Blood flow in arteries,* 2nd ed. Baltimore: Williams & Wilkins, 1974.
29. Murgo JP, Westerhof N, Giolma JP, Altobelli SA. Aortic input impedance in normal man: relationship to pressure wave forms. *Circulation* 1980;62:105.
30. Connolly DC, Kirklin JW, Wood CH. The relationship between pulmonary artery pressure and left atrial pressure in man. *Circ Res* 1954;2:434.
31. Rapaport E, Dexter L. Pulmonary “capillary” pressure. *Methods Med Res* 1958;7:85.
32. Lange RA, Moore DM Jr, Cigarroa RG, Hillis LD. Use of pulmonary capillary wedge pressure to assess severity of mitral stenosis: Is true left atrial pressure needed in this condition? *J Am Coll Cardiol* 1989;13:825.
33. Nihill MR, McNamara DG, Vick RL. The effects of increased blood viscosity on pulmonary vascular resistance. *Am Heart J* 1976;92:65.
34. Read RC, Kuida H, Johnson JA. Venous pressure and total peripheral resistance in the dog. *Am J Physiol* 1958;192:609.
35. Grossman W, et al. Changes in inotropic state of the left ventricle during isometric exercise. *Br Heart J* 1973;35:697.
36. Ross J Jr, Braunwald E. The study of left ventricular function in man by increasing resistance to ventricular ejection with angiotensin. *Circulation* 1964;29:739.
37. DiSesa VJ, Cohn LH, Grossman W. Management of adults with congenital bidirectional shunts, cyanosis, and pulmonary vascular obstruction: successful operative repair in 3 patients. *Am J Cardiol* 1983;51:1495.
38. Wood P. The Eisenmenger syndrome or pulmonary hypertension with reversal central shunt. *Br Med J* 1958;2:701.
39. Braunwald E, Braunwald NS, Ross J Jr, Morrow AG. Effects of mitral-valve replacement on the pulmonary vascular dynamics of patients with pulmonary hypertension. *N Engl J Med* 1965;273:509.
40. Dalen JE, et al. Early reduction of pulmonary vascular resistance after mitral valve replacement. *N Engl J Med* 1967;277:387.
41. Levine MJ, Weinstein JS, Diver DJ, et al. Progressive improvement in pulmonary vascular resistance following percutaneous mitral valvuloplasty. *Circulation* 1989;79:1061.
42. Braunwald E, Colucci WS. Vasodilator therapy of heart failure: Has the promissory note been paid? *N Engl J Med* 1984;310:459.
43. Ferrer MI, et al. Some effects of nitroglycerin upon the splanchnic, pulmonary and systemic circulations. *Circulation* 1966;33:357.
44. Williams JF, Glick G, Braunwald E. Studies on cardiac dimensions in intact unanesthetized man V. Effects of nitroglycerin. *Circulation* 1965;32:767.
45. Gold HK, Leinbach RC, Sanders CA. Use of sublingual nitroglycerin in congestive failure following acute myocardial infarction. *Circulation* 1972;46:389.
46. Goldberg S, Mann T, Grossman W. Nitrate therapy of heart failure in valvular heart disease: importance of resting level of peripheral vascular resistance in determining cardiac output response. *Am J Med* 1978;65:161.

9
Shunt Detection and Quantification†

William Grossman

University of California, San Francisco, School of Medicine; Division of Cardiology, University of California, San Francisco Medical Center, San Francisco, California 94143

Detection, localization, and quantification of intracardiac shunts are an integral part of the hemodynamic evaluation of patients with congenital heart disease. In most cases, an intracardiac shunt is suspected on the basis of the clinical evaluation of the patient before catheterization. There are several circumstances, however, in which data obtained at catheterization should alert the cardiologist to look for a shunt that had not been suspected previously:

1. Unexplained arterial desaturation should immediately raise the suspicion of a right-to-left intracardiac shunt, which may then be assessed by the methods to be discussed. Most commonly, arterial desaturation (i.e., arterial blood oxygen saturation under 95%) detected at the time of cardiac catheterization represents alveolar hypoventilation. The causes for this alveolar hypoventilation and its associated "physiologic" right-to-left shunt include (a) excessive sedation from the premedication, (b) chronic obstructive lung disease or other pulmonary parenchymal disease, and (c) pulmonary congestion/edema secondary to the patient's cardiac disease. Alveolar hypoventilation associated with each of these problems is exacerbated by the supine position of the patient during the catheterization procedure. Helping the patient to assume a more upright posture (head-up tilt, or propping the patient up with a large wedge if tilt mechanism is not available) and encouraging the patient to take deep breaths and to cough will correct or substantially ameliorate arterial hypoxemia in most cases. If arterial desaturation persists, oxygen should be administered by face mask for both therapeutic and diagnostic purposes. If full arterial blood oxygen saturation cannot be achieved by face-mask administration of oxygen (it is best in this regard to use a rebreathing mask that fits snugly), a right-to-left shunt is presumed to be present, and its anatomic site and magnitude should be determined using the methods described later in this chapter.
2. Conversely, when the oxygen content of blood in the pulmonary artery is unexpectedly high (i.e., if the pulmonary artery [PA] blood oxygen saturation is above 80%), the possibility of a left-to-right intracardiac shunt should be considered. It is for these two reasons that arterial and pulmonary artery saturation should be measured routinely *during* cardiac catheterization.
3. When the data obtained at cardiac catheterization do not confirm the presence of a suspected lesion, one should consider the presence of an intracardiac shunt. For example, if left ventricular cineangiography fails to reveal mitral regurgitation in a patient in whom this was judged to be the cause of a systolic murmur, it is prudent to look for evidence of a ventricular septal defect (VSD) with left-to-right shunting.

DETECTION OF LEFT-TO-RIGHT INTRACARDIAC SHUNTS

Many different techniques are available for the detection, localization, and quantification of left-to-right intracardiac shunts. The techniques vary in their sensitivity, in the type of indicator they use, and in the equipment needed to sense and read out the presence of the indicator.

Measurement of Blood Oxygen Saturation and Content in the Right Heart (Oximetry Run)

In the oximetry run, a basic technique for detecting and quantifying left-to-right shunts, the oxygen content or percent saturation is measured in blood samples drawn sequentially from the pulmonary artery, right ventricle (RV), right atrium (RA), superior vena cava (SVC), and inferior vena cava (IVC). A left-to-right shunt may be detected and localized if a significant step-up in blood oxygen saturation or content is found in one of the right heart chambers. A *significant step-up* is defined as an increase in blood oxygen content or saturation that exceeds the normal variability that might be observed if multiple samples were drawn from that cardiac chamber.

The technique of the oximetry run is based on the pioneering studies of Dexter and his associates in 1947 (1). They found that multiple samples drawn from the right atrium could vary in oxygen content by as much as 2 volumes percent (vol%).* This variability has been attributed to the fact that the right atrium receives its blood from three sources of varying oxygen content: the superior vena cava, the inferior vena cava, and the coronary sinus. The maximal normal variation within the right ventricle was found to be 1 vol%. Because of more adequate mixing, a maximal variation within the pulmonary artery of only 0.5 vol% was found by Dexter. Thus, using the Dexter criteria, a significant step-up is present at the atrial level when the highest oxygen content in blood samples drawn from the right atrium exceeds the highest content in the venae cavae by 2 vol%. Similarly, a significant step-up at the ventricular level is present if the highest right ventricular sample is 1 vol% higher than the highest right atrial sample, and a significant step-up at the level of the pulmonary artery is present if the pulmonary artery oxygen content is more than 0.5 vol% greater than the highest right ventricular sample.

Dexter's study described normal variability and gave criteria for a significant oxygen step-up only for measurement of blood oxygen content. This in part reflects the methodology available to him because spectrophotometric oximetry was not used widely at that time. In recent years, nearly all cardiac catheterization laboratories (especially those primarily involved in pediatric catheterization) have moved toward the measurement of percentage oxygen saturation by spectrophotometric oximetry as the routine method for oximetric analysis of blood samples. Oxygen content may then be calculated from knowledge of percentage saturation, the patient's blood hemoglobin concentration, and an assumed constant relationship for oxygen-carrying capacity of hemoglobin, as discussed in Chapter 8 (1.36 mL O_2 hemoglobin). When oxygen content is derived in this manner, rather than by measurement by the Van Slyke or other direct oximetric technique, the value is no more accurate (and probably less so because of the potential presence of carboxyhemoglobin or hemoglobin variants with O_2 capacity other than 1.36) than the percentage oxygen saturation values from which it is calculated.

To clarify this situation, Antman and coworkers studied prospectively the normal variation of both oxygen content and oxygen saturation of blood in the right heart chambers (2). The study population consisted of patients without intracardiac shunts who were undergoing diagnostic cardiac catheterization for evaluation of coronary artery disease, valvular heart disease, cardiomyopathy, or possible pulmonary embolism. Each patient had a complete right heart oximetry run (see later discussion) with sampling of multiple sites in each chamber. Oxygen content was measured directly by an electrochemical fuel-cell method (Lex-O_2-Con, Lexington Instruments, Lexington, MA), a method that had been validated previously against the Van Slyke method. Oxygen saturation was calculated as blood oxygen content divided by oxygen-carrying capacity. The relationship between oxygen content and oxygen saturation obviously depends on the hemoglobin concentration of the patient's blood (e.g., 75% oxygen saturation of pulmonary artery blood will be associated with a substantially lower oxygen content in an anemic patient than in one with normal hemoglobin concentration). Also, systemic blood flow may be an important determinant of oxygen variability in the right heart chambers because high systemic flow tends to equalize the differences across various tissue beds.

In the context of these considerations, I have listed criteria in Table 9.1 for a significant step-up in right heart oxygen content and percentage oxygen saturation associated with various types of left-to-right shunt, based on the study of Antman and coworkers (2) and other investigators (1,3,4). As can be seen from the bottom line (ANY LEVEL) of Table 9.1, the simplest way to screen for a left-to-right shunt is to sample SVC and PA blood and measure the difference, if any, in percentage O_2

saturation. We recommend obtaining blood samples from SVC and PA routinely at the time of right heart catheterization and determining their O_2 saturation by reflectance oximetry. If the DO_2 saturation between these samples is ³8%, a left-to-right shunt may be present at atrial, ventricular, or great vessel level, and a full oximetry run should be done.

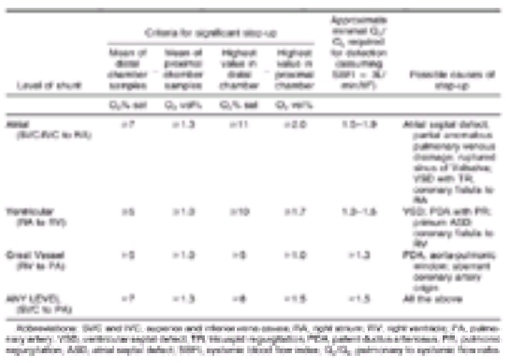

Level of shunt	Criteria for significant step-up: Mean of distal chamber samples	Criteria for significant step-up: Mean of proximal chamber samples	Criteria for significant step-up: Highest value in distal chamber	Criteria for significant step-up: Highest value in proximal chamber	Approximate minimal Q_p/Q_s required for detection (assuming SBFI = 3L/min/M²)	Possible causes of step-up
	O_2% sat	O_2 vol%	O_2% sat	O_2 vol%		
Atrial (SVC/IVC to RA)	>7	>1.3	>11	>2.0	1.3–1.9	Atrial septal defect, partial anomalous pulmonary venous drainage, ruptured sinus of Valsalva, VSD with TR, coronary fistula to RA
Ventricular (RA to RV)	>5	>1.0	>10	>1.7	1.3–1.8	VSD, PDA with PR, untreated ASD, coronary fistula to RV
Great Vessel (RV to PA)	>3	>1.2	>5	>1.0	>1.3	PDA, aortopulmonary window, aberrant coronary artery origin
ANY LEVEL (SVC to PA)	>7	>1.3	>8	>1.5	>1.5	All the above

Abbreviations: SVC and IVC, superior and inferior vena cavae; RA, right atrium; RV, right ventricle; PA, pulmonary artery; VSD, ventricular septal defect; TR, tricuspid regurgitation; PDA, patent ductus arteriosus; PR, pulmonic regurgitation; ASD, atrial septal defect; SBFI, systemic blood flow index; Q_p/Q_s, pulmonary to systemic flow ratio.

TABLE 9.1. *Detection of left-to-right shunt by oximetry*

Oximetry Run

The blood samples needed to localize a step-up in the right heart are obtained by performing what is called an oximetry run. The samples needed and the order in which we recommend they be obtained follow.

Obtain a 2-mL sample from each of the following locations:

1. Left and/or right pulmonary artery
2. Main pulmonary artery*
3. Right ventricle, outflow tract*
4. Right ventricle, mid†
5. Right ventricle, tricuspid valve or apex*,†
6. Right atrium, low or near tricuspid valve
7. Right atrium, mid
8. Right atrium, high
9. Superior vena cava, low (near junction with right atrium)
10. Superior vena cava, high (near junction with innominate vein)
11. Inferior vena cava, high (just at or below diaphragm)
12. Inferior vena cava, low (at L4–L5)
13. Left ventricle
14. Aorta (distal to insertion of ductus)

In performing the oximetry run, an end-hole catheter (e.g., Swan-Ganz balloon-flotation catheter) or one with side holes close to its tip (e.g., a Goodale-Lubin catheter) is positioned in the right or left pulmonary artery. Cardiac output is measured by the Fick method. As soon as the determination of oxygen consumption is completed, the operator begins to obtain 2-mL blood samples from each of the locations indicated. This is done under fluoroscopic control, with catheter tip position further confirmed by pressure measurement at the sites noted. The entire procedure should take less than 7 minutes. If a sample cannot be obtained from a specific site because of ventricular premature beats, that site should be skipped until the rest of the run has been completed.

Oxygen saturation and/or content in each of the samples is determined as discussed previously, and the presence and localization of a significant step-up are determined by applying the criteria listed in Table 9.1.

An alternative method for performing the oximetry run is to withdraw a fiberoptic catheter from the pulmonary artery through the right heart chambers and the inferior and superior venae cavae. This permits a continuous readout of oxygen saturation that allows detection of a step-up in oxygen content.

If the oximetry run reveals that a significant step-up is present, the pulmonary blood flow, systemic blood flow, and magnitude of left-to-right and right-to-left shunts may be calculated according to the following formulas.

Calculation of Pulmonary Blood Flow (Q_p)

Pulmonary blood flow is calculated by the same formula used in the standard Fick equation:

$$\underset{(\text{L/min})}{Q_p} = \frac{\text{O}_2 \text{ consumption (mL/min)}}{\begin{bmatrix}\text{PV O}_2 \\ \text{content} \\ \text{(mL/L)}\end{bmatrix} - \begin{bmatrix}\text{PA O}_2 \\ \text{content} \\ \text{(mL/L)}\end{bmatrix}} \qquad \textbf{(9.1)}$$

If a pulmonary vein (PV) has not been entered, systemic arterial oxygen content may be used in the preceding formula, if systemic arterial oxygen saturation is 95% or more. If systemic oxygen saturation is less than 95%, one must determine whether a right-to-left intracardiac shunt is present. If there is an intracardiac right-to-left shunt, an assumed value for pulmonary venous oxygen content of 98% oxygen capacity should be used in calculating pulmonary blood flow. If arterial desaturation is present and is not due to a right-to-left intracardiac shunt, the observed systemic arterial oxygen saturation should be used to calculate pulmonary blood flow.

Example

Let us suppose that a patient is found to have an atrial septal defect with a left-to-right shunt clearly detected by oximetry run. Furthermore, the catheter crosses the defect and a pulmonary vein is entered, from which a blood sample shows O_2 saturation of 98%. Let us further suppose, however, that systemic arterial blood saturation is 90% and that this is due to chronic pulmonary disease. After ruling out a right-to-left shunt (e.g., inhalation of 100% oxygen, indocyanine green dye injection in inferior vena cava, echocardiogram-bubble study), should we use 98% or 90% for pulmonary venous blood O_2 saturation in the calculation of *Q*? As indicated earlier, because arterial desaturation is not caused by a right-to-left intracardiac shunt, the observed systemic arterial O_2 saturation (90%) should be used because this summates all the pulmonary veins draining both lungs, not just the one with 98% O_2 saturation.

Calculation of Systemic Blood Flow (Q_s)

Use the following equation for systemic blood flow:

$$Q_s\ (\text{L/min}) = \frac{O_2 \text{ consumption (mL/min)}}{\left[\begin{matrix}\text{SA } O_2 \\ \text{content} \\ \text{(mL/L)}\end{matrix}\right] - \left[\begin{matrix}\text{MV } O_2 \\ \text{content} \\ \text{(mL/L)}\end{matrix}\right]} \quad (9.2)$$

The key to the measurement of systemic blood flow in the presence of an intracardiac shunt is that the mixed venous oxygen content must be measured in the chamber immediately proximal to the shunt, as shown in Table 9.2.

Location of shunt as determined by site of O_2 step-up	Mixed venous sample to use in calculating systemic blood flow
1. Pulmonary artery (e.g., patent ductus arteriosus)	Right ventricle, average of samples obtained during oximetry run
2. Right ventricle (e.g., ventricular septal defect)	Right atrium, average of all samples during oximetry run
3. Right atrium (e.g., atrial septal defect)	$\frac{3(\text{SVC } O_2 \text{ content}) + 1(\text{IVC } O_2 \text{ content})}{4}$

TABLE 9.2. *Calculation of systemic blood flow in the presence of left-to-right shunt*

The formula generally used by cardiologists who treat adults for the calculation of venous content in the presence of an atrial septal defect (ASD) was derived by Flamm and coworkers (5). They found that systemic blood flow calculated from mixed venous oxygen content as determined from the formula listed in Table 9.2 most closely approximates systemic blood flow as measured by left ventricular to brachial artery (BA) dye curves in patients with atrial septal defect studied at rest. It should be noted that Flamm's formula "weights" blood returning from the superior vena cava more heavily than might be expected on the basis of relative flows in the superior and inferior cavae. The success of this empirical weighting of the relatively desaturated superior vena cava blood (O_2 saturation is almost always less in blood from the superior as opposed to the inferior vena cava) probably reflects the fact that the third contributor to mixed venous blood—mdesaturated coronary sinus blood—mis not sampled during the oximetry run and therefore cannot be included directly in the formula. The formula (3 SVC O_2 + 1 IVC O_2)/4 was validated by Flamm and associates for mixed venous oxygen content at rest (5). Thus in 18 patients without shunt, this value agreed closely with pulmonary artery blood oxygen content at rest. During supine bicycle exercise, however, a different relationship was found to apply, in which mixed venous (pulmonary artery) oxygen content in patients without shunts was best approximated as (1 SVC O_2 + 2 IVC O_2)/3. This formula was then used for patients with atrial septal defect during exercise, and it reliably predicted systemic blood flow measured by left ventricular to brachial artery dye-dilution curve. Therefore for patients with left-to-right shunt at the atrial level, the formula in Table 9.2 should be used only for calculation of resting mixed venous O_2 content.

Obviously, calculations from the formula in Table 9.2 would be little changed in many cases by ignoring inferior vena cava blood altogether, and this is done in some laboratories (especially those involved in pediatric catheterization). Flamm and associates, however, examined the effects of assuming that superior vena cava O_2 content equaled mixed venous O_2 content, and concluded that this was somewhat less accurate (both in the 18 subjects without shunt and in the 9 patients with atrial septal defect and left-to-right shunt) than the formula given in Table 9.2 (5).

Calculation of Left-to-Right Shunt

If there is no evidence of an associated right-to-left shunt, the left-to-right shunt is calculated by

$$\underset{\text{(L/min)}}{\text{L} \rightarrow \text{R Shunt}} = Q_p - Q_s \quad (9.3)$$

Examples of Left-to-Right Shunt Detection and Quantification

Some examples of oximetry runs are presented to illustrate interpretation.

Atrial Septal Defect

In the example seen in Fig. 9.1, there is a step-up in oxygen saturation in the mid-right atrium. The average or mean value for the vena caval samples in this patient is calculated as [3(SVC) + 1(IVC)] ÷ 4. SVC is the average of SVC samples (i.e., 67.5% in this example), and IVC is the value for the IVC sample taken at the level of the diaphragm only (i.e., 73%). Thus the vena caval mean O_2 saturation for the patient in Fig. 9.1 is [3(67.5) + 1(73)] ÷ 4 = 69%. The right atrial mean O_2 saturation for this patient is (74 + 84 + 79) ÷ 3 = 79%. The 10% step-up in mean O_2 saturation from vena cava to right atrium is higher than the 7% value listed in Table 9.1 as a criterion for a significant step-up at the atrial level. Note that for this example, the highest-to-highest approach (highest right atrial O_2 saturation to highest vena caval O_2 saturation) would barely meet criteria for a significant step-up, because of the high value for IVC saturation (73%) compared with SVC saturation. Thus for the detection of a significant step-up at the atrial level using the highest-to-highest approach, it is best to use the highest RA and SVC samples. In this case, the result would be (84% — 68%) = 16%, which is clearly above the 11% value listed in Table 9.1 for detection of a significant step-up. Also, the screening samples that we recommend for all right heart catheterizations (single sample from SVC and PA) would have strongly indicated a shunt at some level in the right heart, since DO_2 saturation from SVC to PA is 12 to 13%, well above the 8% value for a significant step-up.

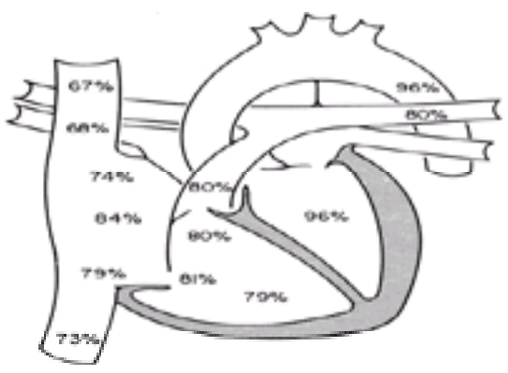

FIG. 9.1. Schematic representation of the results of an oximetry run in a patient with a small to moderate-sized atrial septal defect. Values represent percentage O_2 saturation of blood at multiple locations. (See text for details.)

To calculate pulmonary and systemic blood flows for the example given in Fig. 9.1, we need to know O_2 consumption and blood O_2 capacity. If the patient's O_2

consumption determined by the methods described in Chapter 8 is 240 mL O_2/min and the blood hemoglobin concentration is 14 g%, pulmonary and systemic blood flows may be calculated as follows:

$$Q_p = \frac{O_2 \text{ consumption (mL/min)}}{\left[\begin{matrix}\text{PV } O_2 \\ \text{content} \\ \text{(mL/L)}\end{matrix}\right] - \left[\begin{matrix}\text{PA } O_2 \\ \text{content} \\ \text{(mL/L)}\end{matrix}\right]} \tag{9.4}$$

PV O_2 content was not measured, but left ventricular (LV) and arterial blood O_2 saturation was 96% (effectively ruling out a right-to-left shunt), and therefore it may be assumed that PV blood O_2 saturation was 96%. As described in Chapter 8, oxygen content for PV blood is calculated as follows:

$$0.96\left(\frac{14 \text{ g Hgb}}{100 \text{ mL blood}}\right) \times \left(\frac{1.36 \text{ mL } O_2}{\text{g Hgb}}\right) \tag{9.5}$$

$$= 18.3 \text{ mL } O_2/100 \text{ mL blood}$$

$$= 183 \text{ mL } O_2/\text{liter}$$

Similarly, PA O_2 content is calculated as

$$0.80(14)1.36 \times 10 = 152 \text{ ml } O_2/\text{liter} \tag{9.6}$$

Therefore;

$$Q_p = \frac{240 \text{ mL } O_2/\text{min}}{[183 - 152] \text{ mL } O_2/\text{L}} \tag{9.7}$$

$$= 7.74 \text{ L/min}$$

Systemic blood flow for the patient in Fig. 9.1 is calculated as

$$Q_s = \frac{240 \text{ mL } O_2/\text{min}}{\left[\begin{matrix}\text{systemic} \\ \text{arterial} \\ O_2 \text{ content}\end{matrix}\right] - \left[\begin{matrix}\text{mixed} \\ \text{venous} \\ O_2 \text{ content}\end{matrix}\right]} \tag{9.8}$$

$$= \frac{240}{(0.96 - 0.69)14(1.36)10}$$

$$= 4.6 \text{ L/min}$$

For this calculation, mixed venous O_2 saturation was derived from the formula given in Table 9.2, as 69%. Thus the ratio of Q_p/QO_s in this example is 7.74/4.6 = 1.68, and the magnitude of the left-to-right shunt is 7.7 – 4.7 = 3 L/min. This patient has a small-to-moderate-sized atrial septal defect.

Ventricular Septal Defect

Figure 9.2 shows another example of findings in an oximetry run. In this case, the patient has a large O_2 step-up in the right ventricle, indicating the presence of a ventricular septal defect. If O_2 consumption is 260 mL/min and hemoglobin is 15 g%, then

$$Q_p = \frac{260}{(0.97 - 0.885)15(1.36)10} = 15 \text{ L/min} \tag{9.9}$$

$$Q_s = \frac{260}{(0.97 - 0.66)15(1.36)10} = 4.1 \text{ L/min}$$

$$Q_p/Q_s = 15/4.1 = 3.7$$

$$\text{L} \rightarrow \text{shunt} = 15 - 4.1 = 10.9 \text{ L/min}$$

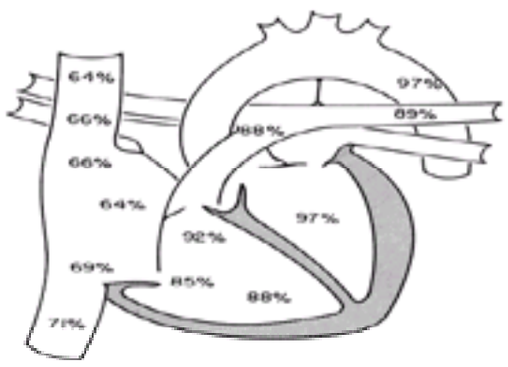

FIG. 9.2. Findings from an oximetry run performed in a patient with a large ventricular septal defect. (See text for details.)

In this case, the O_2 saturation of mixed venous blood is calculated by averaging the right atrial O_2 saturations because the right atrium is the chamber immediately proximal to the O_2 step-up.

Flow Ratio

The ratio Q_p/Q_s gives important physiologic information about the magnitude of a left-to-right shunt. In addition, because it factors out other variables (e.g., O_2 consumption), the ratio can be calculated from knowledge of blood O_2 saturation alone. A Q_p/Q_s ratio of less than 1.5 signifies a small left-to-right shunt and is often felt to argue against operative correction, particularly if the patient has an otherwise uncomplicated atrial or ventricular septal defect. A ratio of ³2.0 indicates a large left-to-right shunt and is generally considered sufficient evidence to recommend surgical repair of the defect, to prevent late pulmonary vascular disease as well as other complications of prolonged circulatory overload. Flow ratios between 1.5 and 2.0 are obviously intermediate in magnitude; surgical correction is generally recommended if operative risk is low.

A flow ratio of less than 1.0 indicates a net right-to-left shunt and is often a sign of the presence of irreversible pulmonary vascular disease.

A *simplified formula* for calculation of flow ratio can be derived by combining the equations for systemic and pulmonary blood flow to obtain

$$\frac{Q_p}{Q_s} = \frac{(SA\ O_2 - MV\ O_2)}{(PV\ O_2 - PA\ O_2)} \quad \textbf{(9.10)}$$

where SA O_2, MV O_2, PV O_2, and PA O_2 are systemic arterial, mixed venous, pulmonary vennous, and pulmonary arterial blood oxygen saturations, respectively. For the patient illustrated in Fig. 9.1, Q_p/Q_s = (96% – 69%)/(96% – 80%) = 1.68.

Calculation of Bidirectional Shunts

If there is evidence of a right-to-left shunt, as well as a left-to-right shunt, the formulas in Eq. (9.11) are used (6).

$$L \rightarrow R = \frac{Q_p\ (MV\ O_2\ content - PA\ O_2\ content)}{(MV\ O_2\ content - PV^*\ O_2\ content)}$$

$$R \rightarrow L = \frac{Q_p\ (PV^*\ O_2\ content - SA\ O_2\ content)(PA\ O_2\ content - PV^*\ O_2\ content)}{(SA\ O_2\ content - MV\ O_2\ content) \times (MV\ O_2\ content - PV^*\ O_2\ content)} \quad \textbf{(9.11)}$$

* If pulmonary vein is not entered, use 98% × O_2 capacity.

This formula for calculation of bidirectional shunts tends to be too complex for easy use during the procedure. A quick approximation can be obtained by using a hypothetic quantity known as the effective blood flow, the flow that would exist in the absence of any left-to-right or right-to-left shunting:

$$Q_{eff} = \frac{O_2\ consumption\ (mL/min)}{\begin{bmatrix} PV\ O_2 \\ content \\ (mL/L) \end{bmatrix} - \begin{bmatrix} MV\ O_2 \\ content \\ (mL/L) \end{bmatrix}} \quad \textbf{(9.12)}$$

The approximate left-to-right shunt then equals $Q_p - Q_{eff}$, and the approximate right-to-left shunt equals $Q_s - Q_{eff}$.

Limitations of Oximetry Method

There are several limitations and potential sources of error in the calculations of blood flow using the data obtained from an oximetry run. A primary source of error may be the absence of a steady state during the collection of blood samples. That is, if the oximetry run is prolonged because of technical difficulties, if the patient is agitated, or if arrhythmias occur during the oximetry run, the data may not be consistent.

An important limitation of the oxygen step-up method for detecting intracardiac shunts is that it lacks sensitivity. Most shunts of a magnitude that would lead to a recommendation for surgical closure of a ventricular septal defect or patent ductus arteriosus are detected by this method. Small shunts, however, are not consistently detected by this technique.

As pointed out by Antman and coworkers (2), the normal variability of blood oxygen saturation in the right heart chambers is strongly influenced by the magnitude of systemic blood flow. High levels of systemic flow tend to equalize the arterial and venous oxygen values across a given vascular bed. Therefore elevated systemic blood flow will cause the mixed venous oxygen saturation to be higher than normal, and interchamber variability due to streaming will be blunted. Even a small increase in right heart oxygen saturation under such conditions might indicate the presence of a significant left-to-right shunt; larger increases would indicate voluminous left-to-right shunting of blood. For a patient with a systemic blood flow index of 3.0 L/min/M^2, minimum shunt sizes that could be detected reliably by oximetry are listed in Table 9.1.

Fundamental to the oximetric method of shunt detection is the fact that left-to-right shunting across an intracardiac defect will cause an increase in blood O_2 saturation in the chamber receiving the shunt proportional to the magnitude of the shunt. The increase in blood O_2 content in the chamber receiving the shunt, however, depends not only on the magnitude of the shunt but also on the O_2-carrying capacity of the blood (i.e., the hemoglobin concentration). As reported by Antman and colleagues (2), the influence of blood hemoglobin concentration may be important when blood O_2 content (rather than O_2 saturation) is used to detect a shunt (Table 9.3.).

Increase in O_2 saturation	Hemoglobin Concentration (g/100 mL) 10	12	15
5%	0.68 vol%	0.82 vol%	1.02 vol%
10%	1.36 vol%	1.63 vol%	2.04 vol%
15%	2.04 vol%	2.45 vol%	3.06 vol%
20%	2.72 vol%	3.26 vol%	4.08 vol%

* Modified from Antman EM, Marsh JD, Green LH, Grossman W. Blood oxygen measurements in the assessment of intracardiac left to right shunts: a critical appraisal of methodology. *Am J Cardiol* 1980;46:265, with permission.

TABLE 9.3. *Expected value of O_2 content (volumes percent) for various levels of O_2 step-up and blood hemoglobin concentration**

Thus, the same shunt giving the same blood O_2 saturation step-up would give markedly different blood O_2 content step-ups if the blood hemoglobin concentration varied significantly. Accordingly, when evaluating oximetric data for shunt detection, it is more precise to exclude the potential influence of blood O_2-carrying capacity and use only O_2 saturation data. This is especially true in pediatric cases (4) where the normal blood O_2-carrying capacity may vary from 20 to 28 vol% in the neonate to 12 to 16 vol% in infancy.

To minimize errors and maximize the physiologic strengths of the oximetry method for shunt detection and quantification, the guidelines listed in Table 9.4 should be followed.

1. Blood samples at multiple sites should be obtained rapidly.
2. Blood O_2 saturation data rather than O_2 content data are preferable to identify the presence and location of a shunt.
3. Comparison of the mean of all values obtained in the respective chambers is preferable to comparison of highest values in each chamber.
4. Because of the important influence of systemic blood flow on shunt detection, exercise should be used in equivocal cases where a low systemic blood flow is present at rest.

* Based on the data of Antman EM, Marsh JD, Green LH, Grossman W. Blood oxygen measurements in the assessment of intracardiac left to right shunts: a critical appraisal of methodology. *Am J Cardiol* 1980;46:265.

TABLE 9.4. *Guidelines for optimum utilization of oximetric method for shunt detection and quantification**

Other Indicators

Many more sensitive techniques are available to detect smaller left-to-right shunts (7,8,9,10,11,12,13,14,15,16,17,18 and 19). These include indocyanine green dye curves, radionuclide techniques, contrast angiography, and echocardiographic methods. Some of these methods (e.g., green dye) were discussed extensively in previous editions of this textbook, and the interested reader is referred there for details. For discussion of other predominantly non–catheter-based methods (e.g., echo, radionuclide) the reader is referred to textbooks devoted to those techniques. We will only give one example here of one of the older methods.

EARLY RECIRCULATION OF AN INDICATOR

Standard indicator dilution curves, performed by injection of indocyanine green into the pulmonary artery with sampling in a systemic artery, are rarely done today, and most laboratories are not even equipped to do them. In the presence of a left-to-right shunt, however, a green dye curve produced by this technique will demonstrate early recirculation on the downslope of the dye curve (7) (Fig. 9.3).

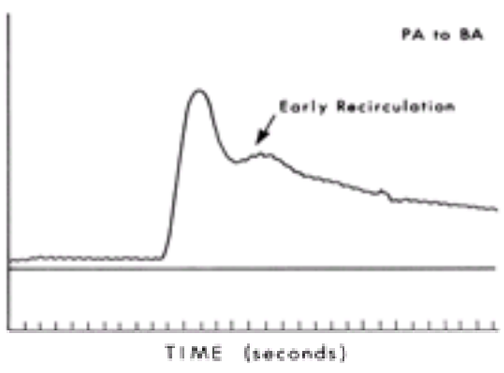

FIG. 9.3. Left-to-right shunt. This indicator dilution curve, performed by injecting indocyanine green into the pulmonary artery with sampling in the brachial artery, demonstrates early recirculation on the downslope, indicating a left-to-right shunt. Injection was at time zero. This technique does not localize the site of the left-to-right shunt.

This technique can detect left-to-right shunts too small to be detected by the oxygen step-up method (8). Thus if there is no evidence of a left-to-right shunt by this method, there is no need to perform an oximetry run. The studies of Castillo and coworkers (9) suggest that left-to-right shunts as small as 25% of the systemic output can be detected by standard pulmonary artery to systemic artery dye curves.

Although a simple pulmonary to systemic artery indocyanine green dye curve may detect the presence of a shunt, it does not localize it. That is, a pulmonary artery to systemic artery dye curve will show evidence of early recirculation in the presence of a left-to-right shunt due to an atrial septal defect, ventricular septal defect, or patent ductus arteriosus.

ANGIOGRAPHY

Selective angiography is effective in visualizing and localizing the site of left-to-right shunts. Angiographic demonstration of anatomy has become a routine part of the preoperative evaluation of patients with congenital or acquired shunts and is useful in localizing the anatomic site of the shunt. Actually, the use of angiography in this fashion should be considered an indicator-dilution method, with the radiographic contrast agent being the indicator and the cinefluoroscopy unit serving as the “densitometer.”

In general, assessment of the patient with a left-to-right shunt virtually always includes a left ventriculogram. If this is performed in the left anterior oblique projection with cranial angulation (or done as a biplane study with both left and right anterior oblique views), excellent visualization of the interventricular septum, sinuses of Valsalva, and ascending and descending thoracic aorta will allow diagnosis and localization of essentially all the causes of left-to-right shunt other than atrial septal defect and anomalous pulmonary venous return.

Complicated lesions (e.g., endocardial cushion defects, coronary artery/right heart fistulas, ruptured aneurysms at the sinus of Valsalva) commonly require angiographic delineation before surgical intervention can be undertaken. Angiography also helps to assess the “routine” cases more completely. For instance, does the patient with secundum atrial septal defect have associated left ventricular dysfunction or mitral valve prolapse? Does the patient with ventricular septal defect have associated aortic regurgitation (caused by prolapse of the medial aortic leaflet) or infundibular pulmonic stenosis?

Angiography, however, cannot replace the important physiologic measurements that allow quantitation of flow and vascular resistance. Without quantitative evaluation of pulmonary and systemic flows (Q_p and Q_s) and their associated resistances (PVR and SVR), appropriate decisions regarding patient management cannot be made, nor can prognosis be assessed.

DETECTION OF RIGHT-TO-LEFT INTRACARDIAC SHUNTS

The primary indication for the use of techniques to detect and localize right-to-left intracardiac shunts is the presence of cyanosis or, more commonly, arterial hypoxemia. The presence of arterial hypoxemia raises two specific questions: first, is the observed hypoxemia due to an intracardiac shunt, or is it due to a ventilation/perfusion imbalance secondary to a variety of forms of intrinsic pulmonary disease? This problem is particularly important in patients with coexistent congenital heart disease and pulmonary disease. Second, if hypoxemia is caused by an intracardiac shunt, what is its site and what is its magnitude?

Attempts to measure right-to-left shunts in patients with cyanotic heart disease date back at least to 1941 (20,21,22 and 23). Prinzmetal (20), in a series of ingenious experiments, expanded the earlier observation of Benenson and Hitzig that ether injected intravenously in patients with cyanotic heart disease will cause a prickly, burning sensation of the face (18). This sensation is caused by the entrance of ether into the systemic circulation of patients with right-to-left shunts. In normal subjects without right-to-left shunts, the ether is eliminated by the lungs and thus does not reach the systemic circulation. Prinzmetal then measured the time necessary for an intravenous injection of a dilute solution of saccharin to be tasted. This time is equal to the transit time from a peripheral vein through the lungs, through the left heart, and then to the systemic circulation. By increasing the concentration of the saccharin, he found that a second, much shorter appearance time

occurred in patients with cyanotic heart disease because of the presence of a right-to-left shunt bypassing the pulmonary circulation. He then estimated the percent right-to-left shunt by the following formula:

$$\% \text{ R} \rightarrow \text{L Shunt} = \frac{A}{A + C} \quad \textbf{(9.13)}$$

where *A* is the smallest concentration of saccharin to be tasted by way of the long circuit and *C* is the smallest concentration of saccharin to be tasted by the short circuit. Our current methods of documenting and quantitating right-to-left shunts may not be as ingenious and certainly are not as sweet, but they are nonetheless effective.

Angiography

With appropriate techniques, angiography may be used to demonstrate right-to-left intracardiac shunts. This method is particularly important in detecting right-to-left shunting due to a pulmonary arteriovenous fistula. In this circumstance, the shunt cannot be detected by indicator dilution curves on the basis of a shortened appearance time. That is, the difference in transit time when the pulmonary capillaries are bypassed is not perceptible by standard indicator dilution techniques. Although angiography may localize right-to-left shunts, it does not permit quantification.

Oximetry

The site of right-to-left shunts may be localized if blood samples can be obtained from a pulmonary vein, the left atrium, left ventricle, and aorta. The pulmonary venous blood of patients with arterial hypoxemia caused by an intracardiac right-to-left shunt is fully saturated with oxygen. Therefore the site of a right-to-left shunt may be localized by noting which left heart chamber is the first to show desaturation (i.e., a step-down in oxygen concentration). Thus if left atrial blood oxygen saturation is normal but desaturation is present in the left ventricle and in the systemic circulation, the right-to-left shunt is across a ventricular septal defect. The only disadvantage of this technique is that a pulmonary vein and the left atrium must be entered. This is not as easy in adults as it is in infants, in whom the left atrium may be entered routinely by way of the foramen ovale.

Echocardiographic methods have proved sensitive for the detection and localization of left-to-right and right-to-left shunts. The so-called echocardiographic contrast or “bubble study” using agitated saline solution with microbubbles or some of the newer specifically designed echo contrast agents can detect small shunts, and the use of two-dimensional echocardiographic techniques can usually localize the site of the shunt to the atrial or ventricular septum. Combined echocardiographic and cardiac catheterization studies allow injection of the echo contrast agent into the right or left heart chambers sequentially, thus permitting localization of the shunt and determination as to whether it is unidirectional or bidirectional. Echo-Doppler techniques can also be used to detect and localize intracardiac shunts. In this regard, color Doppler echocardiography is particularly useful in detecting and localizing small intracardiac shunts without the need for injection of an echo contrast agent. An example of the use of echo-contrast technique for the detection of an atrial septal defect with left-to-right shunting is shown in Fig. 9.4.

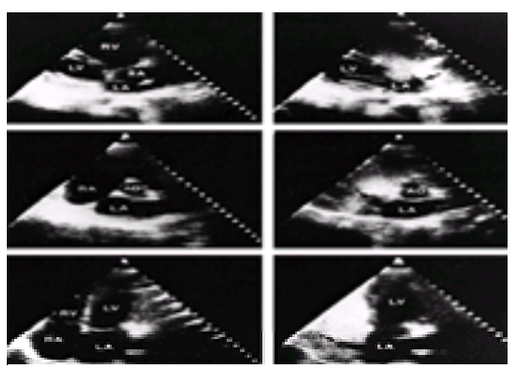

FIG. 9.4. Two-dimensional echo showing right ventricular (RV) inflow tract (upper panels), short axis views at the base (middle panels) and four-chamber apical view (bottom panels) in a patient with an atrial septal defect (ASD) shown at cardiac catheterization to be associated with a Q_p/Q_s of 3.0. The left side of each panel shows the anatomy before echo contrast injection. Following an intravenous injection of agitated saline solution (right side of each panel), a negative contrast effect *(black arrows)* is seen within the right atrium (RA), compatible with entry of unopacified blood from the left atrium (LA) across the ASD into the RA. The ASD is visualized *(white arrow)* as an area of septal dropout. (Reproduced from Come PC, Riley M. Contrast echocardiography. In: Come PC, ed. *Diagnostic cardiology: noninvasive imaging techniques.* Philadelphia: JB Lippincott, 1984:294, with permission.)

† Some material in this chapter has been retained from the first and second editions, to which Dr. James E. Dalen contributed.
* 1 vol% = 1 mL O_2/100 mL blood, or 10 mL O_2/L of blood.

* Confirm location by pressure measurement.
† If frequent extrasystoles occur, do not persist. Obtain samples from three different locations in right ventricle and right atrium.

CHAPTER REFERENCES

1. Dexter L, et al. Studies of congenital heart disease. II. The pressure and oxygen content of blood in the right auricle, right ventricle, and pulmonary artery in control patients, with observations on the oxygen saturation and source of pulmonary capillary blood. *J Clin Invest* 1947;26:554.
2. Antman EM, Marsh JD, Green LH, Grossman W. Blood oxygen measurements in the assessment of intracardiac left to right shunts: a critical appraisal of methodology. *Am J Cardiol* 1980;46:265.
3. Barratt-Boyes BF, Wood EH. The oxygen saturation of blood in the vena cavae, right heart chambers, and pulmonary vessels of healthy subjects. *J Lab Clin Med* 1957;50:93.
4. Freed MD, Miettinen OS, Nadas AS. Oximetric determination of intracardiac left to right shunts. *Br Heart J* 1979;42:690.
5. Flamm MD, Cohn KE, Hancock EW. Measurement of systemic cardiac output at rest and exercise in patients with atrial septal defect. *Am J Cardiol* 1969;23:258.
6. Dexter L, et al. Studies of congenital heart disease. I. Technique of venous catheterization as a diagnostic procedure. *J Clin Invest* 1947;26:547.
7. Swan HJC, Wood EH. Localization of cardiac defects by dye-dilution curves recorded after injection of T-1824 at multiple sites in the heart and great vessels during cardiac catheterization. *Proc Staff Meet Mayo Clin* 1953;28:95.
8. Hyman AL, et al. A comparative study of the detection of cardiovascular shunts by oxygen analysis and indicator dilution methods. *Ann Intern Med* 1962;56:535.
9. Castillo CA, Kyle JC, Gilson WE, Rowe GG. Simulated shunt curves. *Am J Cardiol* 1966;17:691.
10. Braunwald E, Tannenbaum HL, Morrow AG. Localization of left-to-right cardiac shunts by dye-dilution curves following injection into the left side of the heart and into the aorta. *Am J Med* 1958;24:203.
11. Long RTL, Braunwald E, Morrow AG. Intracardiac injection of radioactive krypton: clinical applications of new methods for characterization of circulatory shunts. *Circulation* 1960;21:1126.
12. Levy AM, Monroe RG, Hugenholtz PG, Nadas AS. Clinical use of ascorbic acid as an indicator of right-to-left shunt. *Br Heart J* 1967;29:22.
13. Hugenholtz PG, et al. The clinical usefulness of hydrogen gas as an indicator of left-to-right shunts. *Circulation* 1963;28:542.
14. Amplatz K, et al. The Freon test: a new sensitive technique for the detection of small cardiac shunts. *Circulation* 1969;39:551.
15. Singleton RT, Dembo DH, Scherlis L. Krypton-85 in the detection of intracardiac left-to-right shunts. *Circulation* 1965;32:134.
16. Morrow AG, Sanders RJ, Braunwald E. The nitrous oxide test: an improved method for the detection of left-to-right shunts. *Circulation* 1958;17:284.
17. Long RT, Waldhausen JA, Cornell WP, Sanders RJ. Detection of right-to-left circulatory shunts: a new method utilizing injections of krypton-85. *Proc Soc Exp Biol Med* 1959;102:456.
18. Benenson W, Hitzig LWM. Diagnosis of venous arterial shunt by ether circulation time method. *Proc Soc Exp Biol Med* 1938;38:256.
19. Parker JA, Treves S. Radionuclide detection, localization, and quantitation of intracardiac shunts and shunts between the great arteries. *Prog Cardiovasc Dis* 1977;20:121.
20. Prinzmetal M. Calculation of the venous arterial shunt in congenital heart disease. *J Clin Invest* 1941;20:705.
21. Swan HJC, Zapata-Diaz J, Wood EH. Dye dilution curves in cyanotic congenital heart disease. *Circulation* 1953;8:70.
22. Swan HJC, Burchell HB, Wood EH. The presence of venoarterial shunts in patients with interatrial communications. *Circulation* 1954;10:705.
23. Banas JS, et al. A simple technique for detecting small defects of the atrial septum. *Am J Cardiol* 1971;28:467.

10
Calculation of Stenotic Valve Orifice Area

Blase A. Carabello and William Grossman

BAC: Baylor University, Department of Medicine, Houston Veterans Affairs Medical Center, Houston, Texas 77030.
WG: University of California, San Francisco, School of Medicine; Division of Cardiology,
University of California, San Francisco Medical Center, San Francisco, California 94143.

The normal cardiac valve offers little resistance to blood flow, even when flow velocity across it is high. As valvular stenosis develops, the valve orifice produces progressively greater resistance to flow, resulting in a pressure drop (pressure gradient) across the valve. At any stenotic orifice size, greater flow across the orifice yields a greater pressure gradient. Using this principle together with two fundamental hydraulic formulas, Dr. Richard Gorlin and his father developed a formula for the calculation of cardiac valvular orifices from flow and pressure-gradient data (1).

GORLIN FORMULA

The first hydraulic formula that the Gorlins used was Torricelli's law, which describes flow across a round orifice:

$$F = AVC_C \tag{10.1}$$

where F = flow rate, A = orifice area, V = velocity of flow, and C_c = coefficient of orifice contraction. The constant C_c compensates for the physical phenomenon that, except for a perfect orifice, the area of a stream flowing through an orifice will be less than the true area of the orifice.

Rearranging the terms,

$$A = \frac{F}{VC_C} \tag{10.2}$$

The second hydraulic principle used in the derivation of Gorlin's formula relates pressure gradient and velocity of flow:

$$V^2 = (C_v)^2 \cdot 2gh \quad \text{or} \quad V = (C_v)\sqrt{2gh} \tag{10.3}$$

where V = velocity of flow; C_v = coefficient of velocity, correcting for energy loss as pressure energy is converted to kinetic or velocity energy; g = acceleration due to gravity (980 cm/sec/sec), and h = pressure gradient in cm H_2O.

Combining the two equations,

$$A = \frac{F}{C_v\sqrt{2gh}\cdot C_C} = \frac{F}{C_V C_C\sqrt{2\cdot 980\cdot h}} = \frac{F}{(C)(44.3)\sqrt{h}} \tag{10.4}$$

where C is an empirical constant accounting for C_V and C_C, the expression of h in mm Hg, and correcting calculated valve area to actual valve area measured at surgery or autopsy.

It is obvious that antegrade flow across the mitral and tricuspid valves occur only in diastole, whereas that across the aortic and pulmonic valves occur only in systole. Accordingly, the flow F for Eq. (10.4) is the total cardiac output expressed in terms of the seconds per minute during which there is actually forward flow across the valve. For the mitral and tricuspid valves, this is calculated by multiplying the diastolic filling period (seconds per beat) times the heart rate (beats per minute [bpm]), yielding the number of seconds per minute during which there is diastolic flow. The cardiac output in milliliters per minute (or cm^3/min) is then divided by the seconds per minute during which there is flow, yielding diastolic flow in cubic centimeters per second. For the aortic and pulmonic valves, the systolic ejection period is substituted for the diastolic filling period. The manner in which the diastolic filling period and systolic ejection period are measured is shown in Fig. 10.1. The diastolic filling period begins at mitral valve opening and continues until end-diastole. The systolic ejection period begins with aortic valve opening and proceeds to the dicrotic notch or other evidence of aortic valve closure.

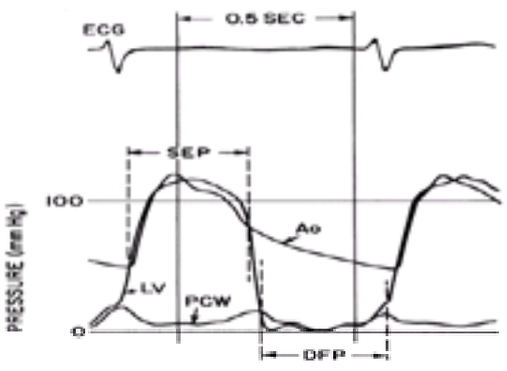

FIG. 10.1. Left ventricular (LV), aortic (Ao), and pulmonary capillary wedge (PCW) pressure tracings from a patient without valvular heart disease, illustrating the definition and measurement of diastolic filling period (DFP) and systolic ejection period (SEP). See text for discussion.

Thus the final equation for the calculation of valve orifice area A (in cm^2) is

$$A = \frac{CO/(DFP \text{ or } SEP)(HR)}{44.3C\sqrt{\Delta P}} \quad \textbf{(10.5)}$$

where CO = cardiac output (cm^3/min), DFP = diastolic filling period (sec/beat), SEP = systolic ejection period (sec/beat), HR = heart rate (beats/min), C = empirical constant, and P = pressure gradient. The DFP is measured directly from left ventricular versus pulmonary capillary wedge or left atrial pressure tracings as shown in Fig. 10.1.

An empirical constant of 0.7 (later adjusted to 0.85) was derived by comparing calculation and actual mitral valve areas (1,2). Using this constant, the maximum deviation of calculated valve area from measured valve area was 0.2 cm^2. The empirical constant for the aortic tricuspid and pulmonic valve was never derived. The constant for these valves has been assumed to be 1.0 (i.e., 1.0 × 44.3 = 44.3) for lack of data comparing actual with calculated valve areas for those valves. Nonetheless, the Gorlin formula remains the “gold standard” for assessing the severity of stenotic cardiac valves.

MITRAL VALVE AREA

By rearranging the terms of Eq. (10.5), one sees that for the mitral valve,

$$\Delta P = \left[\frac{CO/(HR)(DFP)}{(MVA)(44.3)(0.85)}\right]^2 \quad \textbf{(10.6)}$$

where DP = mean transmitral pressure gradient, and MVA = mitral valve area. Thus by doubling cardiac output, one will quadruple the gradient across the valve, if heart rate and diastolic filling period remain constant. The normal mitral orifice in an adult has a cross-sectional area of 4.0 to 5.0 cm^2 when the mitral valve is completely open in diastole. Considerable reduction in this orifice area can occur without symptomatic limitation, but when the area is 1.0 cm^2 or less, a substantial resting gradient will be present across the mitral valve, and any demand for increased cardiac output will be met by increases in left atrial and pulmonary capillary pressure that lead to pulmonary congestion and edema.

Figure 10.2. demonstrates that a cardiac output of 5 L/min can be maintained with only a minimal mitral diastolic gradient as the mitral orifice area contracts from its normal 4.0 to 5.0 cm^2 to a moderately stenotic area of 2.0 cm^2. After that, the gradient rises so that at an orifice area of 1.0 cm^2 a resting gradient of 8 to 10 mm Hg is required to maintain cardiac output at 5 L/min, with a normal resting heart rate of 72 bpm (Fig. 10.2*A*). Note that even at this level of cardiac output, substantial increases in gradient may occur in response to tachycardia (Fig. 10.2*B*, Fig. 10.2*C*), which reduces the total time per minute available for diastolic filling. Thus 1.0 cm^2 is generally viewed as the “critical” mitral valve area because only small increases in cardiac output lead to pulmonary congestion and severe dyspnea. Some allowance, however, needs to be made for the patient's size in assessing critical valve area. Larger patients need greater flows to maintain tissue perfusion than smaller patients and have higher gradients because of higher cardiac output for any given valve orifice area. Thus 1.2 cm^2 could be a critical mitral valve area for a larger patient. Currently, no uniform agreement exists on indexing critical valve area to body size.

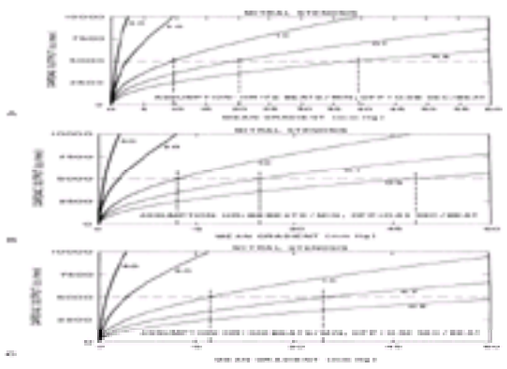

FIG. 10.2. Relationships between cardiac output and mean diastolic pressure gradient in patients with mitral stenosis, calculated using Eq. (10.6), derived from the Gorlin formula. Individual curves represent orifice areas of 4.0, 2.0, 1.0, 0.7, and 0.5 cm^2. **(A), (B)**, and **(C)** represent flow-gradient relations at differing heart rates and diastolic filling periods. (See text for discussion.) (Courtesy of Dr. James J. Ferguson III.)

Example of Valve Area Calculation in Mitral Stenosis

Figure 10.3 shows pulmonary capillary wedge (PCW) and left ventricular (LV) pressure tracings in a 40-year-old woman with rheumatic heart disease and severe mitral stenosis. This woman also had hypertension and significant elevation of her LV diastolic pressure. The valve orifice area is calculated with the aid of a form reproduced as Table 10.1. In this patient, five beats were chosen from the recordings taken closest in time to the Fick cardiac output determination. Planimetry of the area between PCW and LV pressure tracings (Fig. 10.3) was done for these five beats, and these areas were divided by the length of the diastolic filling periods for each beat, giving an average gradient deflection in millimeters. The mean gradient in millimeters of mercury (Table 10.1, part B) was calculated as the average gradient deflection in millimeters multiplied by the scale factor (mm Hg/mm deflection). In this case, the mean gradient was 30 mm Hg. Next, the average diastolic filling period is calculated (Table 10.1, part C) using the average measured length between initial PCW–LV crossover in early diastole and end-diastole (peak of the R wave by ECG). This average length in millimeters is divided by the paper speed (mm/sec) to give the average diastolic filling period, which in this case was 0.40 sec. Heart rate and cardiac output (Table 10.1, parts D and E) are recorded, ideally from data collected simultaneously with the recording of the PCW–LV pressure gradient. Heart rate was 80 bpm and cardiac output was 4,680 cm^3/min in the case illustrated in Fig. 10.3. Note that cardiac output must be expressed in cubic centimeters per minute if valve area is expressed in square centimeters of cross-sectional area.

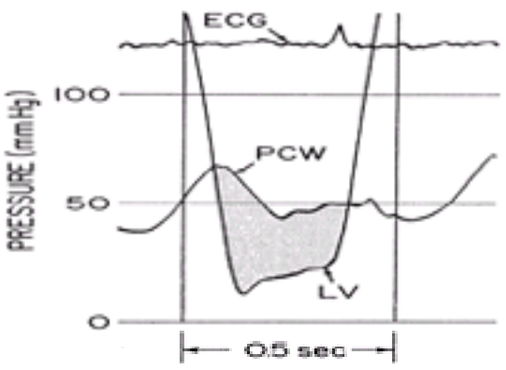

FIG. 10.3. Pulmonary capillary wedge (PCW) and left ventricular (LV) pressure tracings in a 40-year-old woman with severe mitral stenosis. This woman also had systemic arterial hypertension and significant elevation of her LV diastolic pressure. See text for discussion.

Patient _____ Age ____ Unit number _____ Date _____

A. Complex no.	Area of gradient (mm²)	/	Length of diastolic or systolic period (mm)	=	Average gradient (deflection, mm)
1.	_____	/	_____	=	_____
2.	_____	/	_____	=	_____
3.	_____	/	_____	=	_____
4.	_____	/	_____	=	_____
5.	_____	/	_____	=	_____

B. Mean gradient = Average gradient (mm deflection) × scale factor (mm Hg/mm deflection)
= _____ × _____ = _____ mm Hg

C. Average diastolic or systolic period = average length (mm)/paper speed (mm/sec)
= _____ / _____ = _____ sec/beat

D. Heart rate = _____ beats/min

E. Cardiac output (Fick or indicator dilution) = _____ mL/min

F. Valve area = $\frac{\text{cardiac output/heart rate} \times \text{avg. diastolic or systolic period}}{\text{valve constant}^a \times \sqrt{\text{mean gradient}}}$

$= \frac{\text{_____} \times \text{_____}}{\text{_____} \times \sqrt{\text{_____}}} = \text{_____ cm}^2$

G. Valve area index = valve area/body surface area = _____ cm²/m²

[a] Valve constants: for mitral valve use 37.7; for aortic, tricuspid, and pulmonic valves use 44.3.

TABLE 10.1. *Valve orifice area determination*

Entering these values in the formula given in Table 10.1, part F and using a constant of 0.85(44.3) = 37.7 for the mitral valve, we get

$$\text{Mitral orifice area} = \frac{(4{,}680\,\text{cm}^3/\text{min})/(80\,\text{beats/min})(0.40\,\text{sec/beat})}{37.7\sqrt{30\,\text{mm Hg}}} \qquad \textbf{(10.7)}$$

$$\text{Area} = 0.71\,\text{cm}^2$$

Because the accuracy of the method to hundredths of a square centimeter has not been demnonstrated, the resulting valve area is rounded off and expressed as 0.7 cm^2.

Pitfalls

Pulmonary Capillary Wedge Tracing

In most cases, PCW pressure is substituted for left atrial pressure under the assumption that a properly confirmed wedge pressure accurately reflects left atrial pressure. Nishimura et al. (3) found that transmitral gradient was overestimated by 3.3 ± 3.5 mm Hg when a Swan-Ganz catheter was used to measure wedge pressure compared with actual left atrial pressure. However, these “wedge” pressures were not confirmed as true wedge pressures, using the techniques described in Chapter 5. Conversely, Lange et al. (4) measured left atrial pressure directly (transseptal) and compared it with oximetrically confirmed wedge pressure obtained using a stiff woven Dacron catheter. In this study, overestimation of true left atrial pressure was only 1.7 ± 0.6 mm Hg. Thus we and others believe that the weight of evidence (5) and our own experience support the use of the PCW pressure as a satisfactory substitution for left atrial pressure, except in some patients with pulmonary venoocclusive disease or cor triatriatum. Failure to wedge the catheter properly may, however, cause one to compare a damped pulmonary artery pressure with the LV pressure, yielding a falsely high gradient. To ensure that the right heart catheter is properly wedged, one should verify that

1. The mean wedge pressure is lower than the mean pulmonary artery pressure.
2. Blood withdrawn from the wedged catheter is 95% or more saturated with oxygen, or at least equal in saturation to arterial blood.

Alignment Mismatch

Alignment of the PCW and LV pressure tracings does not match alignment of simultaneous left atrial and LV tracings because there is a time delay in the transmission of the left atrial pressure signal back through the pulmonary venous and capillary beds. The resulting pressure mismatch is small when PCW pressure is measured in the distal pulmonary arteries using a 7F or 8F Cournand or Goodale-Lubin catheter, but may be larger when wedge pressure is measured more proximally in the pulmonary arterial tree using a balloon-tipped flow-directed catheter. As illustrated in Fig. 5.8, the A and V waves in an optimally damped PCW tracing are delayed typically by 50 to 70 msec compared with a simultaneous left atrial pressure tracing. Thus, ideally, the wedge pressure should be realigned with the LV pressure (using tracing paper) by shifting it leftward by 50 to 70 msec.

The V wave, which is normally present in the left atrium (where it represents pulmonary venous return), peaks immediately before the downstroke of the LV pressure tracing. With a wedge pressure measured distally using a 7F Goodale-Lubin catheter (Fig. 10.3), the peak of the V wave is bisected by the rapid downstroke of LV pressure decline. Realignment of a wedge tracing so that the V wave peak is bisected by (or slightly to the left of) the downstroke of LV pressure is a practical method for achieving more physiologic realignment.

Calibration Errors

Failure to calibrate pressure transducers properly and adjust them to the same zero reference point may yield an erroneous gradient. A quick way to check the validity of an unsuspected transmitral pressure gradient is to switch left and right heart catheters to opposite transducers, which if calibrated equally yields the same gradient.

Cardiac Output Determination

Cardiac output must be determined accurately using the techniques described in Chapter 8. The cardiac output used in valve area calculation should be the value measured simultaneously with the gradient determination. The measurement used in the valve area formula is usually the forward cardiac output determined by the Fick method or the thermodilution method. If mitral valvular regurgitation exists, the gradient across the valve will reflect not only net forward flow but forward plus regurgitant or total transmitral diastolic flow. Thus using only net forward flow to calculate the valve orifice area will *underestimate* the actual anatomic valve area in cases where regurgitation coexists with stenosis. It is worth noting that many patients with mitral stenosis have coexistent tricuspid regurgitation. As indicated in Chapter 8, tricuspid regurgitation may cause the thermodilution technique of measuring cardiac output to be inaccurate.

Early Diastasis

Even when left atrial and LV pressures equalize (diastasis) before the end of diastole, there will generally still be flow through the mitral valve after the point of diastasis. The diastolic filling period to be used in valve area calculation should include all of nonisovolumic diastole, not just the period during which a gradient is present.

AORTIC VALVE AREA

An aortic valve area of 0.7 cm^2 or less is generally considered severe enough to account for the symptoms of angina, syncope, or heart failure in a patient with aortic stenosis. Since the development of symptoms in patients with aortic stenosis portends an abrupt worsening of prognosis, this valve area is termed “critical.” However, it must be pointed out that no unique “critical” valve area has been established and that an aortic valve area as large as 1.0 cm^2 can cause symptoms and thus be “critical,” especially in a large individual. Conversely, smaller calculated valve orifice areas in a totally asymptomatic patient may not be “critical.” Figure 10.4 illustrates the relationship between cardiac output and aortic pressure gradient over a range of values for aortic valve area at three values for heart rate and systolic ejection period. For the aortic valve, Eq. (10.4) can be rearranged as

$$\Delta P = \left[\frac{\text{CO}/(\text{HR})(\text{SEP})}{44.3\text{AVA}}\right]^2 \qquad \textbf{(10.8)}$$

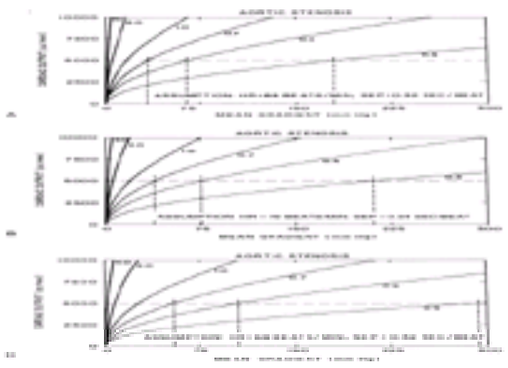

FIG. 10.4. Relationships between cardiac output and mean aortic systolic pressure gradient in patients with aortic stenosis, calculated using Eq. (10.7), derived from the Gorlin equation. Individual curves represent orifice areas of 4.0, 2.0, 1.0, 0.7, 0.5, and 0.3 cm^2. **(A), (B)**, and **(C)** represent flow-gradient relations at differing heart rates and systolic ejection periods. (Courtesy of Dr. James J. Ferguson III.)

As can be seen in Fig. 10.4A, at a normal resting cardiac output of 5.0 L/min, an aortic orifice area of 0.7 cm^2 will result in a gradient of approximately 33 mm Hg across the aortic valve. Doubling of the cardiac output, as might occur with exercise, would increase the gradient by a factor of 4 to 132 mm Hg if the systolic time per minute did not change. This increase in gradient would require a peak LV pressure in excess of 250 mm Hg to maintain a central aortic pressure of 120 mm Hg. Such a major increase in LV pressure obviously increases myocardial oxygen demand and limits ejection performance. These factors contribute to the symptoms of angina and congestive heart failure, respectively (6,7). The limitations in cardiac output imposed by high afterload may contribute to hypotension when peripheral vasodilation occurs during muscular exercise. Actually, the systolic time per minute does not remain constant during the increase in cardiac output associated with exercise. As heart rate increases during exercise, the systolic ejection period tends to become shorter, but the tendency is counteracted by both increased venous return and systemic arteriolar vasodilation, factors that normally help to maintain LV stroke volume constant (or even allow it to increase) during exercise. Thus, heart rate is increasing but systolic ejection period is diminishing only slightly so that their product (systolic ejection time per minute) increases. This is the counterpart of the decreased diastolic filling time per minute during exercise discussed earlier. Examining Eq. 10.8, it can be seen that the increase in cardiac output will be partially offset by the increase in (HR)(SEP) so that the gradient will not quadruple with a doubling of cardiac output during exercise.

Figure 10.4*B* and Figure 10.4*C* show that with decreasing heart rate, the gradient *increases* in aortic stenosis for any value of cardiac output. This is opposite to the effect of heart rate in mitral stenosis and reflects the *opposite effects* of heart rate on systolic and diastolic time per minute. Viewed another way, as the heart rate slows in aortic stenosis, the stroke volume increases if cardiac output remains constant. Thus the flow per beat across the aortic valve increases and so does the pressure gradient.

As with mitral stenosis, some allowance must be made for body size in deciding what is a critical valve area in patients with aortic stenosis; larger patients who require higher output may become symptomatic at somewhat larger valve areas. Thus, a very large man with a body surface area of 2.4 m^2 and a cardiac index of 3.0 L/min/m^2 would have a cardiac output of 7,200 mL/min. At a heart rate of 68 bpm (Fig. 10.4*C*), this man might have a 50-mm Hg aortic valve gradient with an orifice area of 0.9 to 1.0 cm^2. Thus, for him, this might be a critical valve area.

Example

Figure 10.5. demonstrates simultaneous pressure tracings from the left ventricle (LV) and right femoral artery (RFA) in a patient with exertional syncope. Since the pulse wave takes a finite period of time to travel from the left ventricle to the femoral artery, the femoral artery tracing is somewhat delayed (Fig. 10.5*A*). Figure 10.5*B* shows the LV and RFA tracings realigned to correct for the delay in transmission time. This is accomplished by using tracing paper and aligning the arterial upstroke to coincide with the LV upstroke. After such alignment, the mean pressure gradient can now be obtained by planimetry, and the orifice area can be calculated using the form given in Table 10.1. For this example, the average aortic pressure gradient was 40 mm Hg, the systolic ejection period is 0.33 sec, the heart rate is 74 bpm, and the cardiac output is 5,000 mL/min. Using these values together with an aortic valve constant of (1)(44.3) = 44.3 in the equation in Table 10.1 gives

$$\text{Aortic valve area} = \frac{(5{,}000\,cm^3/min)/(74\,beats/min)(0.33\,sec/beat)}{44.3\sqrt{40\,mm\,Hg}} = 0.7\,cm^2 \quad \textbf{(10.9)}$$

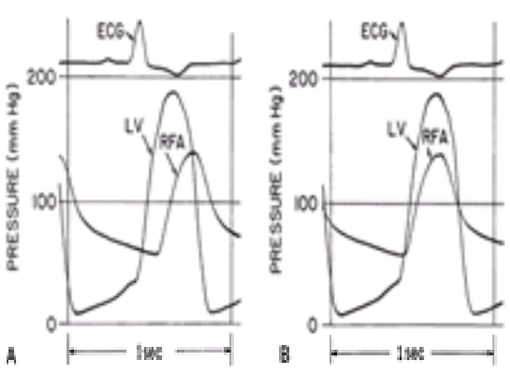

FIG. 10.5. Left ventricular (LV) and right femoral artery (RFA) pressure tracings in a patient who presented with exertional syncope due to aortic stenosis. **A:** The tracings actually recorded, demonstrating the significant time delay for the pressure waveform to reach the RFA. **B:** Realignment using tracing paper. (See text for discussion.)

As discussed in Chapter 7, peripheral arterial pressure waveforms are distorted in ways other than time delay. These distortions include systolic amplification and spreading out (widening) of the pressure waveform. To assess possible errors introduced by the use of peripheral arterial pressure as a substitute for ascending aortic pressure, Folland et al. (8) compared the LV-ascending aortic (LV-Ao) mean gradient in 26 patientswith aortic stenosis with the LV-femoral artery (LV-FA) systolic gradient, with and without realignment (Fig. 10.6). Without realignment, the LV-FA gradient overestimated the LV-Ao gradient by about 9 mm Hg. In contrast, aligned LV-FA gradients underestimated the LV-Ao gradient by about 10 mm Hg, possibly representing the fact that peak systolic arterial pressure is higher in peripheral arterial pressure tracings than in central aortic tracings so that the planimetered gradient will be smaller when using LV-FA. Without realignment, this effect is offset by the fact that much of the arterial systolic waveform is outside and to the right of the LV pressure tracing (Fig. 10.6). A second error in gradient measurement can occur if the LV catheter is placed in the LV outflow tract (9). As shown in Fig. 10.7, a gradient usually exists between the body of the left ventricle and outflow tract, produced as blood accelerates when it enters this relatively narrow portion of the left ventricle. A catheter tip placed in the LV outflow tract will measure a typical LV pressure tracing but can underestimate the true LV-aorta gradient by 30 mm Hg. Assey et al. (10) measured the transaortic valve gradients in 15 patients from eight different combinations of catheter locations using the schema shown in Fig. 10.8. The average mean gradient recorded between positions 1 and 3 was the greatest, while the gradient between positions 1 and 5 using the alignment technique produced the smallest value. In some patients, the differences in gradient among the different measurement sites were as much as 45 mm Hg. In calculating aortic valve area, the gradient between sites 1 and 3, which records gradient before pressure recovery, is probably the most accurate reflection of the pressure drop across the valve. When the aortic catheter is placed at a more distal site, it records the effect of pressure recovery, which reduces gradient as blood flow again becomes laminar. The more proximal aortic position is probably the ideal location for measuring the gradient for the valve area calculation; the more distal positions may better reflect the actual overload on the myocardium. When the transvalvular gradient recorded

from positions 1 and 5a in Fig. 10.8 is larger than 60 mm Hg, these differences are of little clinical importance. When a small transvalvular gradient is present in conjunction with a low cardiac output, however, the differences between aligned and unaligned tracings and between gradients recorded at different catheter locations may affect the decision about whether to replace the valve. In such instances, we recommend that the problem be obviated by placing a second catheter in the proximal ascending aorta without need for alignment (8) (Fig. 10.6*A*). As an alternative, the difference between peak central aortic and peripheral arterial pressure is added to the planimetered gradient measured during the Fick output determination. This compensates for the fact that the planimetered gradient with realignment (Fig. 10.6*C*) underestimates the true gradient (Fig. 10.6*A*). The most accurate approach, however, involves the use of a second catheter positioned in the ascending aorta, as discussed earlier.

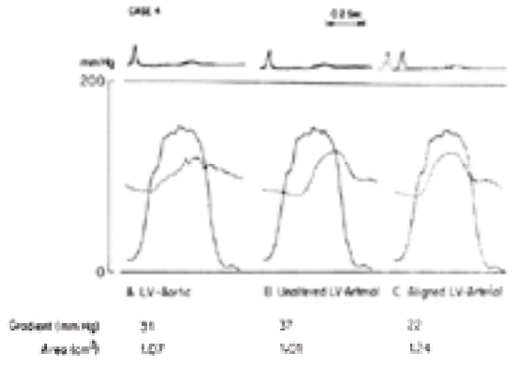

FIG. 10.6. Pressure gradients in aortic stenosis. **A:** The left ventricular (LV)–central aortic gradient. **B:** LV–femoral artery gradient without alignment. **C:** LV–femoral artery gradient with alignment obtained by moving the femoral artery tracing leftward so that its upstroke coincides with the LV pressure upstroke. (Reproduced with permission from Folland ED, Parisi AF, Carbone C. Is peripheral arterial pressure a satisfactory substitute for ascending aortic pressure when measuring aortic valve gradients? *J Am Coll Cardiol* 1984;4:1207.)

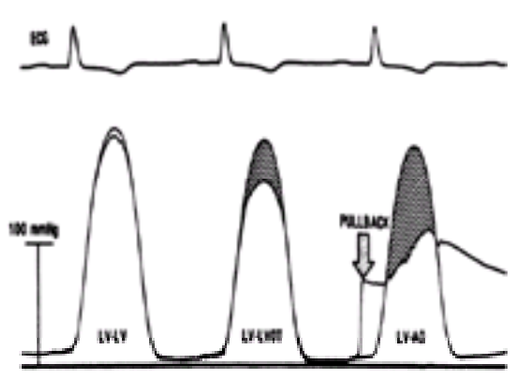

FIG. 10.7. A: Pressure tracings recorded from two catheters placed within the body of the left ventricular chamber. Both are nearly identical. **B:** Pressure recorded by one catheter placed in the body of the left ventricular chamber and by a second catheter placed in the left ventricular outflow tract, proximal to the aortic valve. Both catheters record characteristic left ventricular pressure tracings; however, there is a substantial pressure gradient between the body of the left ventricle and the outflow tract. This is not due to anatomic subvalvular stenosis but rather to acceleration of blood as it enters the relatively narrow outflow tract. **C:** Pressures recorded from the catheter in the body of the left ventricle and from a second catheter in the proximal aorta. These tracings demonstrate the gradient across the aortic valve and outflow tract. (Reproduced from Pasipoularides A. Clinical assessment of ventricular ejection dynamics with and without outflow obstruction. *J Am Coll Cardiol* 1990;15:859, with permission.)

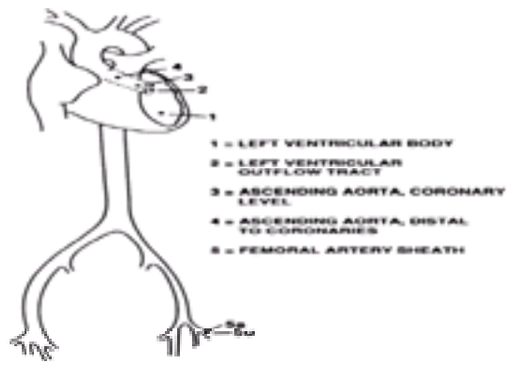

FIG. 10.8. Two sites for recording left ventricular pressure (1 and 2) and three sites for recording distal pressure (3, 4, and 5) are shown. 5u represents the actual femoral artery pressure tracing which is unaligned with the left ventricular pressure tracing. 5a represents the recording obtained from the femoral artery, which is then manually aligned to match the left ventricular pressure tracing in time. The following are the potential recording sites for obtaining the transaortic valve pressure gradient in aortic stenosis: 1–3, 1–4, 1–5a, 1–5u, 2–3, 2–4, 2–5a, and 2–5u. Gradients recorded at these different sites may vary widely in any given patient. (Reproduced with permission from Assey ME, Zile MR, Usher BW, Karavan MP, Carabello BA. Effect of catheter positioning on the variability of measured gradient in aortic stenosis. *Cathet Cardiovasc Diagn* 1993;30:287.)

Another approach to increasing the accuracy of transaortic valve gradient measurement using simultaneous LV and femoral artery pressures has been introduced by Krueger et al. (11) at the University of Utah. As seen in Fig. 10.9, the mean LV systolic pressure during interval A and the mean femoral artery systolic pressure during interval B are determined by planimetry. Their difference was nearly identical to the gradient measured by planimetry of simultaneous LV and central aortic pressures and was more accurate than other techniques commonly used (11).

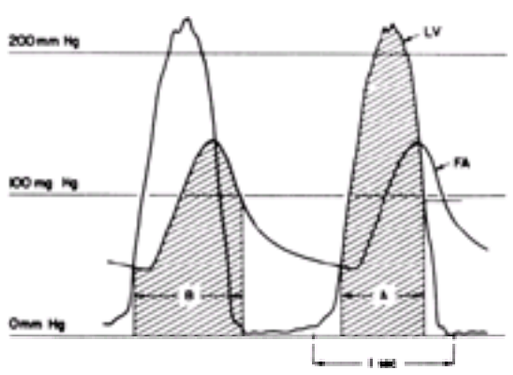

FIG. 10.9. Simultaneous recordings of left ventricular (LV) and femoral artery (FA) pressures in a patient with aortic stenosis. The mean LV systolic pressure during interval A and the mean FA systolic pressure during interval B are determined by planimetry, and the systolic LV-aortic gradient is estimated as the difference between these mean pressures. (Reproduced with permission from Krueger SK, Orme EC, King CS, Barry WH. Accurate determination of the transaortic valve

gradient using simultaneous left ventricular and femoral artery pressures. *Cathet Cardiovasc Diagn* 1989;16:202.)

If a second catheter is not used to obtain simultaneous LV and peripheral pressures, the gradient may be obtained by recording LV pressure and superimposing it on the aortic pressure obtained immediately after the LV catheter is pulled back into the aorta.

Pitfalls

Transducer Calibration

As with calculation of mitral valve area, attention to cardiac output determination and transducer calibration is critical. Assurance that proper transducer calibration has been accomplished can be obtained by comparing the left heart catheter pressure with the peripheral arterial catheter pressure before insertion of the left heart catheter into the left ventricle. Since in the absence of peripheral stenosis mean arterial pressure will be the same throughout the arterial tree, the mean pressure recorded by both catheters should be identical, confirming identical transducer calibration. Further gradient verification is made by comparing the LV pressure with aortic pressure obtained by the left heart catheter during catheter pullback. In this case, both LV and aortic pressures are recorded by the same catheter and transducer, eliminating the second transducer as a source of error.

Pullback Hemodynamics

When the aortic valve area is diminished to 0.6 cm^2 or less, a 7F or 8F catheter placed retrograde across the valve takes up a significant amount of the residual orifice area, and the catheter may actually increase the severity of stenosis. Conversely, removal of the catheter reduces the severity of stenosis. We have observed that a peripheral pressure rise occurs in severe aortic stenosis when the LV catheter is removed from the aortic valve orifice (12). In our experience, an augmentation in peripheral systolic pressure of more than 5 mm Hg at the time of LV catheter pullback indicates that significant aortic stenosis is present. This sign is present in more than 80% of patients with an aortic valve area of 0.5 cm^2 or less, a point that is discussed further in Chapter 29.

AREA OF TRICUSPID AND PULMONIC VALVES

Because of the rarity of tricuspid and pulmonic stenosis in adults, no general agreement exists as to what constitutes a critical orifice area for these valves. In general, a mean gradient of 5 mm Hg across the tricuspid valve is sufficient to cause symptoms of systemic venous hypertension. Gradients across the pulmonic valve of less than 50 mm Hg are usually well tolerated, but gradients of more than 100 mm Hg indicate a need for surgical correction. Between 50 and 100 mm Hg, decisions regarding surgical correction depend on the clinical features in each case.

ALTERNATIVES TO THE GORLIN FORMULA

A simplified valve formula for the calculation of stenotic cardiac valve areas was proposed by Hakki et al. (13) and tested in 100 consecutive patients with either aortic or mitral stenosis. The simplified formula is

$$\text{Valve area} = \frac{\text{cardiac output (liters/min)}}{\sqrt{\text{pressure gradient}}} \qquad \textbf{(10.10)}$$

and is based on their observation that the product of heart rate, SEP or DFP, and the Gorlin equation constant was nearly the same for all patients whose hemodynamics were measured in the resting state, and the value of this product was close to 1.0. For the examples given earlier in this chapter, the simplified formula works reasonably well. Thus for the patient with mitral stenosis (Fig. 10.3) with a cardiac output of 4,680 mL/min and a mitral diastolic gradient of 30 mm Hg, mitral valve area $= 4.68 \div \sqrt{30} = 0.85\ cm^2$ using the simplified formula as opposed to the value of 0.71 cm^2 calculated using the Gorlin formula. For the patient with aortic stenosis whose tracings are shown in Fig. 10.5 (cardiac output 5 L/min, aortic gradient 40 mm Hg), the aortic valve area by the simplified formula is $5 \div \sqrt{40} = 0.79\ cm^2$ as opposed to 0.73 cm^2 by the Gorlin formula. Because the percentage of time per minute spent in diastole or systole changes substantially at higher heart rates, the simplified formula may be less useful in the presence of substantial tachycardia. This point, however, has not been tested adequately.

ASSESSMENT OF AORTIC STENOSIS IN PATIENTS WITH LOW CARDIAC OUTPUT

In the patient with a forward cardiac output of 3 L/min, a mean transvalvular gradient of 20 mm Hg will yield a calculated valve area of 0.7 cm^2, indicating critical aortic stenosis. However, not all such patients actually have severe aortic stenosis. Valve calculations made using the Gorlin formula are flow dependent. That is, as cardiac output increases, calculated area increases, and as cardiac output decreases, calculated area decreases (14,15). Two potential mechanisms exist by which calculated valve orifice area increases with cardiac output: (a) Increased flow through the stenotic aortic valve in conjunction with increased LV pressure physically opens the valve to a greater orifice area, and thus the valve orifice really is wider during increased flow, and (b) inaccuracies in the Gorlin formula cause the calculated area (but not necessarily the actual orifice area) to be flow dependent. The Gorlins themselves noted that they had no data from which to calculate an empirical constant for the aortic valve (1). Indeed, such a constant has never been calculated but has been assumed to be 1.0 by the cardiologic community. The issue remains in doubt, but in all probability both explanations are correct in part. On one hand, Tardif and coworkers have shown that twodimensional transesophageal echocardiographic imaging of the stenotic aortic valve has failed to demonstrate true change in valve orifice areas when increased flow caused calculated area to increase (16). These data suggest calculated area-flow dependence resides within the calculation rather than in representing a true change in area. However, it remains unclear whether the echocardiographic method used is sensitive enough to detect tiny (0.2 to 0.4 cm^2) changes in actual valve area. On the other hand, Voelker and colleagues working *in vitro* concluded that changes in calculated orifice area with changes in flow were probably due to actual changes in valve area (17). Flow dependence of calculated valve orifice area appears less in bicuspid than in tricuspid valves (18) but is greater at lower than at higher flows (19). These problems in assessing stenosis severity have substantial clinical importance. Consider a patient with reduced cardiac output and low LV ejection fraction who has both cardiomyopathy and mild aortic stenosis. Despite a calculated valve area of 0.7 cm^2, such a patient will probably not benefit from aortic valve replacement because aortic stenosis was not the cause of the LV dysfunction. On the other hand, although patients with low aortic valve gradients are generally at higher risk for perioperative death associated with aortic valve replacement (7,20), Brogan et al. (21) have demonstrated that some patients with low gradients may improve substantially following surgery. It is likely that such patients have truly severe aortic stenosis, which is the cause of their hemodynamic decompensation; in these patients, correcting the aortic stenosis is beneficial. Preliminary data from three studies suggest that cautious hemodynamic manipulation in the catheterization laboratory can distinguish between these two different clinical entities (22,23,24 and 25). In patients with mild aortic stenosis, an infusion of nitroprusside or dobutamine increases forward output substantially but may actually decrease the transvalvular gradient. In such cases, the calculated aortic valve area increases dramatically and is no longer within the “critical” range. On the other hand, in patients with truly severe aortic stenosis, infusion of nitroprusside widens the transvalvular gradient and increases the calculated aortic valve area only slightly, if at all. The results of nitroprusside infusion in a patient with mild aortic stenosis are demonstrated in Table 10.2 (24). The patient's initial calculated valve orifice area was 0.6 cm^2, which would indicate a need for surgery. However, following nitroprusside infusion, the gradient actually fell and calculated valve area increased. The patient improved on chronic vasodilator therapy, usually contraindicated in aortic stenosis unless the disease is mild. It must be emphasized that infusion of nitroprusside in patients with aortic stenosis must be performed with great caution, since if true aortic stenosis is present, hypotension may result. If it is known that the patient has normal coronary arteries, dobutamine, which produces similar changes in cardiac output, can be infused instead of nitroprusside. However, dobutamine infusion may be dangerous in patients who also have coronary disease, in whom it may precipitate ischemia.

	Baseline	Nitroprusside (0.5 μg/kg/min)
Cardiac output (liters/min)	3.0	4.5
Left ventricular pressure (mm Hg)	130/30	120/20
Aortic pressure (mm Hg)	90/60	90/50
Aortic valve area (cm^2)	0.6	1.0
Valve resistance (dyn sec cm^{-5})	200	160

From Carabello BA, Ballard WL, Gazes PC. Patient 65. *Cardiology Pearls*. Philadelphia: Hanley & Belfus, 1994: 142.

TABLE 10.2. *Nitroprusside infusion in a patient with mild aortic stenosis*

VALVE RESISTANCE

Valve resistance is simply the mean aortic valve gradient divided by the cardiac output per second of systolic flow. It has the advantage of being calculated from two directly obtained pieces of data (output and gradient) and requires no discharge coefficient (26). A simplified formula for calculating aortic valve resistance is

$$\frac{\left(\begin{matrix}\text{Mean}\\ \text{gradient}\end{matrix}\right)\left(\begin{matrix}\text{Systolic ejection}\\ \text{period}\end{matrix}\right)\left(\begin{matrix}\text{Heart}\\ \text{rate}\end{matrix}\right) \times 1.33}{\text{Cardiac output (liters/min)}} \qquad \textbf{(10.11)}$$

Valve resistance has been shown by Cannon et al. (22) to help separate patients with severe aortic stenosis from those patients who had similarly small calculated aortic valve areas, but who were subsequently demonstrated to have mild disease. Resistance appears less flow dependent than valve area (22,26). Resistance is unlikely to supplant the Gorlin formula in assessing stenosis severity but may be an important adjunct to it in patients with low cardiac output.

Currently, we recommend cautious hemodynamic manipulation with dobutamine or nitroprusside for patients with a cardiac output of less than 4.5 L/min who have a transvalvular gradient of less than 40 mm Hg and a valve resistance of less than 275 dyn-sec-cm $^{-5}$. If patients respond by substantially increasing the measured gradient, they probably have truly severe aortic stenosis and may benefit from aortic valve replacement. However, if cardiac output increases substantially but gradient increases only slightly, or actually declines, the aortic stenosis is mild and the patient is unlikely to benefit from aortic valve replacement.

ACKNOWLEDGMENT

We would like to express our appreciation to Dr. James J. Ferguson, III, who supplied Fig. 10.2, Fig. 10.3 and Fig. 10.4, constructed by him from computer simulation.

CHAPTER REFERENCES

1. Gorlin R, Gorlin G. Hydraulic formula for calculation of area of stenotic mitral valve, other cardiac values and central circulatory shunts. *Am Heart J* 1951;41:1.
2. Cohen MV, Gorlin R. Modified orifice equation for the calculation of mitral valve area. *Am Heart J* 1972;84:839.
3. Nishimura RA, Rihal CS, Tajik AJ, Holmes DR Jr. Accurate measurement of the transmitral gradient in patients with mitral stenosis: a simultaneous catheterization and Doppler echocardiographic study. *J Am Coll Cardiol* 1994;24:152.
4. Lange RA, Moore DM, Cigarroa RG, Hillis LD. Use of pulmonary capillary wedge pressure to assess severity of mitral stenosis: Is true left atrial pressure needed in this condition? *J Am Coll Cardiol* 1989;13:825.
5. Alpert JS. The lessons of history as reflected in the pulmonary capillary wedge pressure. *J Am Coll Cardiol* 1989;13:830.
6. Strauer BE, Burger SB. Systolic stress, coronary hemodynamics and metabolic reserve in experimental and clinical cardiac hypertrophy. *Basic Res Cardiol* 1980;75:234.
7. Carabello BA, et al. Hemodynamic determinants of prognosis of aortic valve replacement in critical aortic stenosis and advanced congestive heart failure. *Circulation* 1980;62:42.
8. Folland ED, Parisi AF, Carbone C. Is peripheral arterial pressure a satisfactory substitute for ascending aortic pressure when measuring aortic valve gradients? *J Am Coll Cardiol* 1984;4:1207.
9. Pasipoularides A. Clinical assessment of ventricular ejection dynamics with and without outflow obstruction. *J Am Coll Cardiol* 1990;15:859.
10. Assey ME, Zile MR, Usher BW, Karavan MP, Carabello BA. Effect of catheter positioning on the variability of measured gradient in aortic stenosis. *Cathet Cardiovasc Diagn* 1993;30:287.
11. Krueger SK, Orme EC, King CS, Barry WH. Accurate determination of the transaortic valve gradient using simultaneous left ventricular and femoral artery pressures. *Cathet Cardiovasc Diagn* 1989;16:202.
12. Carabello BA, Barry WH, Grossman W. Changes in arterial pressure during left heart pullback in patients with aortic stenosis: a sign of severe aortic stenosis. *Am J Cardiol* 1979;44:424.
13. Hakki AH, et al. A simplified valve formula for the calculation of stenotic cardiac valve areas. *Circulation* 1981;63:1050.
14. Burwash IG, Thomas DD, Sadahiro M, et al. Dependence of Gorlin formula and continuity equation valve areas on transvalvular volume flow rate in valvular aortic stenosis. *Circulation* 1994;39:827.
15. Carabello BA. Advances in the hemodynamic assessment of stenotic cardiac valves. *J Am Coll Cardiol* 1987;10:912.
16. Tardif JC, Rodrigues AG, Hardy JF, et al. Simultaneous determination of aortic valve area by the Gorlin formula and by transesophageal echocardiography under different transvalvular flow conditions: evidence that anatomic aortic valve area does not change with variations in flow in aortic stenosis. *J Am Coll Cardiol* 1997;29:1296.
17. Voelker W, Reul H, Nienhaus G, et al. Comparison of valvular resistance, stroke work loss and Gorlin valve area for quantification of aortic stenosis: an *in vitro* study in a pulsatile aortic flow model. *Circulation* 1995;91:1196.
18. Shively BK, Charlton GA, Crawford MH, Chaney RK. Flow dependence of valve area in aortic stenosis: relation to valve morphology. *J Am Coll Cardiol* 1998;31:654.
19. Marcus R, Bednarz J, Abruzzo J, et al. Mechanism underlying flow-dependency of valve orifice area determined by the Gorlin formula in patients with aortic valve obstruction. *Circulation* 1993; 88[Suppl I]:I-103(abst).
20. Lund O. Preoperative risk evaluation and stratification of long-term survival after valve replacement for aortic stenosis: reasons for earlier operative intervention. *Circulation* 1990;82:124.
21. Brogan WC III, Grayburn PA, Lange RA, Hillis LD. Prognosis after valve replacement in patients with severe aortic stenosis and a low transvalvular pressure gradient. *J Am Coll Cardiol* 1993;21:1657.
22. Cannon JD Jr, Zile MR, Crawford FA Jr, Carabello BA. Aortic valve resistance as an adjunct to the Gorlin formula in assessing the severity of aortic stenosis in symptomatic patients. *J Am Coll Cardiol* 1992;20:1517.
23. Casale PN, Palacios IF, Abascal VM, et al. Effects of dobutamine on Gorlin and continuity equation valve areas and valve resistance in valvular aortic stenosis. *Am J Cardiol* 1992;70:1175.
24. DeFilippi CR, Willett DL, Brickner ME, et al. Usefulness of dobutamine echocardiography in distinguishing severe from nonsevere valvular aortic stenosis in patients with depressed left ventricular function and low transvalvular gradients. *Am J Cardiol* 1995;75:191.
25. Carabello BA, Ballard WL, Gazes PC. *Cardiology pearls.* Philadelphia: Hanley & Belfus, 1994:142.
26. Ford LE, Feldman T, Chiu YC, Carroll JD. Hemodynamic resistance as a measure of functional impairment in aortic valvular stenosis. *Circ Res* 1990;66:1.

11
Coronary Angiography

Donald S. Baim and William Grossman

DSB: Harvard Medical School; Center for Innovative Minimally Invasive Therapy, Brigham and Women's Hospital, Boston, Massachusetts 02115.
WG: University of California, San Francisco, School of Medicine, Division of Cardiology, University of California, San Francisco Medical Center, San Francisco, California 94143

Because of progressive evolution in catheterization technique (including better radiographic imaging equipment and better-tolerated contrast media) coupled with the development of effective treatment options for coronary artery disease (i.e., bypass surgery and angioplasty), diagnostic coronary angiography (also called coronary *arterio*graphy) has become one of the primary components of cardiac catheterization. It is estimated that more than 1,200,000 coronary angiographic procedures (roughly 400 per 100,000 population) are performed each year in the United States (1,2) with a procedure-related mortality rate of 0.1%. In each procedure, the objective is to examine the entire coronary tree (both native vessels and any surgically constructed bypass grafts), recording details of coronary anatomy that include the individual pattern of arterial distribution, anatomic or functional pathology (atherosclerosis, thrombosis, congenital anomalies, or focal coronary spasm), and the presence of intercoronary and intracoronary collateral connections. Despite gains in noninvasive techniques such as magnetic resonance angiography (3) and fast computed tomography (fast-CT) (4) as *screening* tests for coronary artery disease (and limited imaging of the proximal coronary arteries in some patients); the use of intravascular ultrasound (see Chapter 19) and angioscopy to define the status of the local vessel wall and luminal surface; and the use of intracoronary pressure and flow measurement technology to assess physiologic significance (see Chapter 18), selective coronary angiography remains the clinical “gold standard” for evaluating coronary anatomy. By performing a series of intracoronary injections of contrast agents in carefully chosen angulated views using current high-resolution x-ray imaging (see Chapter 2), it is possible to define all portions of the coronary arterial circulation down to vessels as small as 0.3 mm, free of any artifacts caused by vessel overlap or foreshortening. The performance of high-quality coronary angiography, safely defining each and every coronary stenosis in an optimal view, is an important measure of an operator's skill in cardiac catheterization and is the foundation on which the operator's ability to perform successful coronary interventional procedures rests.

CURRENT INDICATIONS

There are a variety of indications for coronary angiography, which are summarized comprehensively in the most recent set of American College of Cardiology/American Heart Association (AHA/ACC) guidelines on coronary angiography (2). These indications continue to evolve as new applications of catheter-based therapy are developed, but they are still best summarized by the principle stated by F. Mason Sones: coronary arteriography is indicated when a problem is encountered whose resolution may be aided by the objective demonstration of the coronary anatomy, provided competent personnel and adequate facilities are available and the potential risks are acceptable to the patient and physician.

The most frequent indication is the further evaluation of *patients in whom the diagnosis of coronary atherosclerosis is almost certain*, and in whom anatomic correction by means of coronary artery bypass surgery or transluminal coronary angioplasty is contemplated. Angiographic evaluation of coronary anatomy in such patients provides the crucial information needed to select the most appropriate treatment strategy—catheter intervention (see Chapter 23, Chapter 24 and Chapter 25), bypass surgery, or medical therapy. Included in this category are patients with *stable angina pectoris* refractory to medical therapy. Recent data suggest that *asymptomatic* patients with noninvasive evidence of myocardial ischemia also benefit from revascularization and therefore are candidates for coronary angiography (5). Another target population is comprised of patients with *unstable angina* (new onset, progressive, or rest pain). Whereas intensive drug therapy (b-blocker, calcium channel blocker, nitrate, heparin, aspirin, one of the newer blockers of the platelet IIb/IIIa receptor) alone may be tried in patients with unstable angina, almost two thirds of such patients come to angiography within 6 weeks after presentation because of ongoing clinical symptoms or a positive exercise test (6). Such patients are candidates for early coronary angiography, particularly if they display indicators (rest pain, electrocardiographic [ECG] abnormalities, heart failure) that place them in the category of Braunwald class II or III unstable angina (7) with high risk of progression to myocardial infarction (MI). In such patients, diagnostic catheterization (with the ability to proceed to coronary intervention during the same procedure, if indicated) should be performed after or concurrent with the initiation of multidrug antianginal therapy. Patients with *acute myocardial infarction* may undergo immediate coronary angiography if primary angioplasty is planned (8) or early angiography (hours to days) if they have recurrent spontaneous or exercise-induced angina after thrombolytic therapy (9). The most recent AHA/ACC guidelines for the management of myocardial infarction (8) extend these indications to potentially include patients with post-MI arrhythmias, congestive heart failure, or an ejection fraction less than 40%; all patients after non—nQ wave infarction; and patients in whom ongoing occlusion of the infarct vessel or three-vessel disease is suspected. Coronary angiography is also indicated if clinical evidence of a mechanical defect (ventricular septal defect or papillary muscle rupture) develops in the days after an MI. Routine post-MI coronary angiography in the stable patient without these indications is still advocated by some cardiologists (9), but its value (compared with the conservative strategy outlined here) has not been established.

A second group of indications for coronary angiography concerns patients in whom the *presence or absence of coronary artery disease is unclear* (2). This includes patients with troublesome chest pain syndromes but ambiguous noninvasive test results, patients with unexplained heart failure or ventricular arrhythmias, survivors of out-of-hospital cardiac arrest (10), patients with suspected or proven variant angina (11), and patients with risk factors for coronary artery disease who are being evaluated for major abdominal, thoracic, or vascular surgery (12). This category also includes patients scheduled for correction of congenital or valvular pathology. Patients with congenital defects such as tetralogy of Fallot frequently have anomalies of coronary distribution that may lead to surgical complications if unrecognized (13), whereas patients older than 45 years of age with valvular disease may have advanced coronary atherosclerosis without clinical symptoms. Although younger patients with valvular disease are commonly operated on without prior coronary angiograms, given the extraordinary low risk of diagnostic catheterization and the potential benefit of knowing the coronary anatomy, most surgical centers believe it is best to perform a preoperative diagnostic catheterization to identify (and then

correct) significant coronary lesions, so as to provide the best and safest outcome during concurrent valve replacement (14).

Finally, coronary angiography is frequently performed when a patient develops *recurrent angina after coronary intervention* (to detect and treat restenosis; see Chapter 27) *or after bypass surgery* (to detect vein graft failure, which might require catheter intervention or reoperation). Routine follow-up angiography 6 months after catheter intervention is not indicated clinically but may play an important role in the research evaluation of new technologies or drug therapies targeted at reducing restenosis (15).

GENERAL ISSUES

The initial attempts to perform coronary angiography used nonselective injections of contrast medium into the aortic root to simultaneously opacify both left and right coronary arteries, recording the angiographic images on conventional sheet film (16). To improve contrast delivery into the coronary ostia, some early investigators employed transient circulatory arrest induced by the administration of acetylcholine or by elevation of intrabronchial pressure, followed by occlusion of the ascending aorta by a gas-filled balloon and injection of the contrast bolus. Although nonselective aortic root injection is still used occasionally today to evaluate ostial lesions, anomalous coronary ostia, or coronary bypass grafts, intentional circulatory arrest is no longer practiced, and the nonselective technique has largely been replaced by selective coronary injection using specially designed catheters advanced from either the brachial or the femoral approach.

In most patients, successful coronary angiography can be performed by either the brachial cutdown or the percutaneous approach (from the femoral, brachial, or radial artery), leaving the choice up to physician and patient. Data from the Society for Cardiac Angiography and Intervention in 1990 (17) show that the percutaneous femoral approach was used in 83% of cases. The brachial approach, either by percutaneous (see Chapter 4) or cutdown (see Chapter 5) entry, may offer a selective advantage in patients with severe peripheral vascular disease or known abdominal aortic aneurysm. In either case, it is important for the catheterization team to meet the patient before the actual procedure to evaluate the best approach to catheterization, to gain an appreciation of the clinical questions that need to be answered by coronary angiography, to uncover any history of adverse reaction to medications or organic iodine compounds, and to explain the procedure in detail.

Although coronary angiography was traditionally performed as an inpatient procedure, in the 1990s outpatient protocols were developed for diagnostic catheterization in low-risk patients (2,18,19). This includes younger patients with relatively stable symptoms and few other comorbidities (e.g., heart failure, valve disease, renal insufficiency, peripheral vascular disease) who live within a 1-hour drive from the cardiac catheterization facility. More than half of the patients referred for coronary angiography may be suitable for such a procedure, which in each case may save up to $900 in hospital charges (but only roughly $200 in true costs), compared with inpatient catheterization (20,21). Outpatient procedures are performed identically to the technique described herein, using either the brachial or the femoral approach. After a percutaneous femoral procedure, at least 2 hours of bedrest (4 to 6 hours in many institutions) is required, unless a puncture-sealing device is employed.

In either inpatient or outpatient coronary angiography, preparation for catheterization should include proscription of oral intake except for medications and limited quantities of clear liquids over the 6 to 8 hours before catheterization, a baseline 12-lead ECG, and a suitable sedative premedication (usually diazepam, 5 to 10 mg PO, and diphenhydramine, 50 mg PO) administered on call to the catheterization laboratory. We do not routinely premedicate patients with either atropine or nitroglycerin, although both are immediately on hand if needed.

THE FEMORAL APPROACH

As described in Chapter 4, the femoral approach to left-sided heart catheterization involves insertion of the catheter either directly over a guidewire or through an introducing sheath. Systemic anticoagulation (heparin, 3,000 to 5,000 units at the time of sheath introduction) is used in many laboratories (2), although others now omit heparin in brief diagnostic procedures. A series of preformed catheters are employed, starting with a pigtail catheter for left ventriculography, followed by separate catheters (either Judkins or Amplatz shapes) for cannulation of the left and right coronary arteries. Coronary catheters are available in 5F, 6F, 7F, or 8F end-hole designs that taper further near the tip. They may be constructed of either polyethylene (Cook Inc., Bloomington, IN) or polyurethane (Cordis Corporation, Miami, FL, and USCI, Billerica, MA) and contain either steel braid, nylon, or other reinforcing materials within the catheter wall to provide the excellent torque control needed for coronary cannulation. In the 1970s, 8F catheters predominated, because they provided excellent torque control and permitted rapid contrast delivery. In the 1980s, improvements in the design of 7F catheters allowed for a comparable lumen diameter in standard 8F catheters, making them the standard in most laboratories. Smaller (6F and even 5F) coronary angiographic catheters are now available with technology similar to that used in guiding catheters to provide thinner catheter walls and larger lumens (6F lumens up to 0.064 inches), exceeding the lumen size once available in 8F diagnostic catheters (22). We now use such 6F catheters for all of our routine diagnostic procedures. Coronary catheters used for native coronary injection via the femoral or brachial approach are shown in Fig. 11.1.

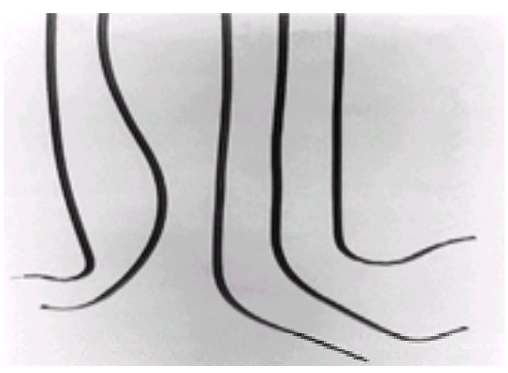

FIG. 11.1. Types of catheters currently in wide use for selective native coronary angiography *(left to right)*: Amplatz right, Judkins right, Sones, Judkins left, and Amplatz left.

Insertion and Flushing of the Coronary Catheter

The desired catheter is inserted into the femoral sheath and advanced to the level of the left mainstem bronchus over the guidewire. Alternatively, the tip of the coronary angiography catheter may be advanced “around the arch” and into the ascending aorta before the guidewire is removed. This may reduce snagging of the catheter tip on aortic wall irregularities, but it places greater emphasis on the initial catheter flushing. After removal of the guidewire, the catheter is attached to a specially designed manifold system which permits the maintenance of a “closed system” during pressure monitoring, catheter flushing, and contrast agent administration (Fig. 11.2). The catheter is immediately double-flushed: blood is withdrawn and discarded, and heparinized saline flush is injected through the catheter lumen. Difficulty in blood withdrawal suggests apposition of the catheter tip to the aortic wall, which can be rectified by slight advancement or rotation of the catheter until free blood withdrawal is possible. The lumen of the introducing sheath should also be flushed immediately before and after each catheter insertion and every 5 minutes thereafter, to prevent the encroachment of blood into the sheath. Alternatively, the sidearm of the sheath may be connected to a 30 mL/hr continuous-flow regulator (Intraflow II, Abbott, King of Prussia, PA). Once the catheter has been flushed with saline solution, tip pressure should be displayed on the physiologic monitor at all times (except during actual contrast injections). Next, the catheter lumen should be gently filled with contrast agent under fluoroscopic visualization, avoiding selective contrast administration into small aortic branches. Filling with contrast results in slight attenuation of high-frequency components in the aortic pressure waveform, whose new shape should be carefully noted. Any alteration in that waveform during coronary angiography (see next section) may signify an ostial coronary stenosis or an unfavorable catheter position within the coronary artery. Once these measures are completed, the coronary angiographic catheter is advanced into the aortic root in preparation for selective engagement of the desired coronary ostium.

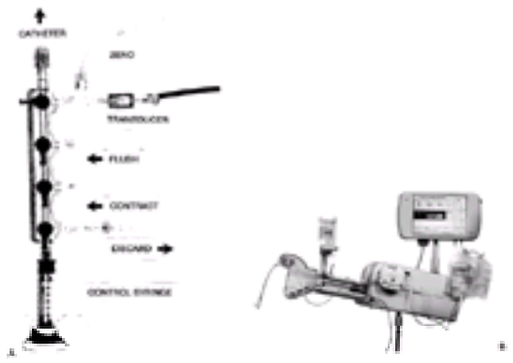

FIG. 11.2. A: Four-port coronary manifold. This manifold provides a closed system with which blood can be withdrawn from the catheter and discarded. The catheter can be filled with either flush solution or contrast medium, and the catheter pressure can be observed, all under the control of a series of stopcocks. The fourth port is connected to an empty plastic bag and is used as a discard port (for blood from the double flush, air bubbles) so that the syringe need not be disconnected from the manifold at any time during the procedure. Attachment of the transducer directly to the manifold allows optimal pressure waveform fidelity (see Chapter 7), and the fluid-filled reference line allows zeroing of the transducer to midchest level. **B:** The Bracco-Squibb Acist device consists of a contrast-filled power injector, controlled by a sterile pneumatic actuator to deliver contrast in amounts and rates up to the limits preprogrammed on the digital panel. A power flushing system and a pressure transducer are also included, duplicating many of the functions of the traditional four-port manifold.

Damping and Ventricularization of the Pressure Waveform

A fall in overall catheter tip pressure (damping) or a fall in diastolic pressure only (ventricularization) during catheter engagement in a coronary ostium indicates restriction of coronary inflow (Fig. 11.3). The catheter tip may have been inserted into a proximal coronary stenosis or may have an adverse catheter lie that places it against the coronary wall. If either of these phenomena is observed, the catheter should be withdrawn into the aortic root immediately until the operator can analyze the situation further. The catheter may be reengaged and a cautious small-volume contrast injection made to further clarify the situation. It may disclose a proximal occlusion of the vessel, against which the tip of the coronary catheter is resting, in which case a cine run should be performed to document this finding. The test injection may also indicate ostial stenosis through absence of reflux into the aortic root or retention of the injected contrast material in the proximal and middle vessel. Along with damping or ventricularization of the pressure waveform, this indicates that the catheter tip is severely restricting or occluding ostial inflow. In this case, a cautious injection may be documented on cine, with immediate removal of the catheter at the end of the cine run to restore antegrade flow. Continuing to inject and film as the catheter is removed from the ostium may capture a single frame or frames that show the ostial lesion clearly. Another approach is to perform a nonselective injection into the sinus of Valsalva in an appropriate view (one that displays the ostium of the vessel in question with no overlap by the sinus of Valsalva) to confirm the presence of an ostial stenosis. On occasion, an end-hole diagnostic catheter may be exchanged for an end-and side-hole angioplasty guiding catheter to overcome damping by preserving antegrade flow into the side-holes, through the lumen of the catheter, and into the coronary artery, even though the catheter tip may be obstructing entry of blood into the ostium itself (see Cannulation of the Right Coronary Ostium). *Vigorous injection despite a damped or ventricularized pressure waveform should be avoided, because it predisposes to ventricular fibrillation or dissection of the proximal coronary artery with major ischemic sequelae.* Such a dissection is manifested by tracking of contrast medium down the vessel over the course of the injection and by failure of contrast to clear on fluoroscopy after the injection is terminated. Prompt consideration of repair by catheter-based intervention or bypass surgery should be considered if creation of such a “dye stain” is associated with impeded antegrade coronary flow and signs of myocardial ischemia.

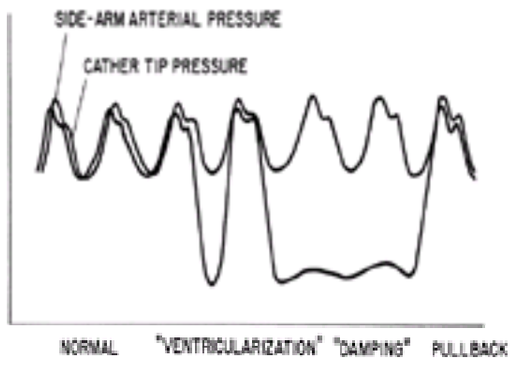

FIG. 11.3. Pressure tracings as recorded during coronary angiography. Except for its earlier phase and slightly lower systolic pressure, catheter tip pressure should resemble the pressure waveform simultaneously monitored by way of the femoral sidearm sheath or other arterial monitor (e.g., radial artery). In the presence of an ostial stenosis or an unfavorable catheter position against the vessel wall, the waveform shows either ventricularization (in which systolic pressure is preserved but diastolic pressure is reduced) or frank damping (in which both systolic and diastolic pressures are reduced). In either case, the best approach is to withdraw the catheter immediately until the waveform returns to normal and to attempt to define the cause of the problem by nonselective injections in the sinus of Valsalva. Alternatively, a catheter equipped with side-holes near the tip may be used to provide ongoing coronary perfusion.

Cannulation of the Left Coronary Ostium

With the Judkins technique it is usually easy to engage the left coronary ostium. As Judkins himself stated, “No points are earned for coronary catheterization—the catheters know where to go if not thwarted by the operator” (23). If a left Judkins catheter with a 4-cm curve (commonly referred to as a JL4) is simply allowed to remain *en face* as it is advanced down into the aortic root, it will engage the left coronary ostium without further manipulation in 80% to 90% of patients (Fig. 11.4). Engagement should take place with the arm of the catheter traversing the ascending aorta at an angle of approximately 45°, the tip of the catheter in a more or less horizontal orientation, and no change in the pressure waveform recorded from the catheter tip.

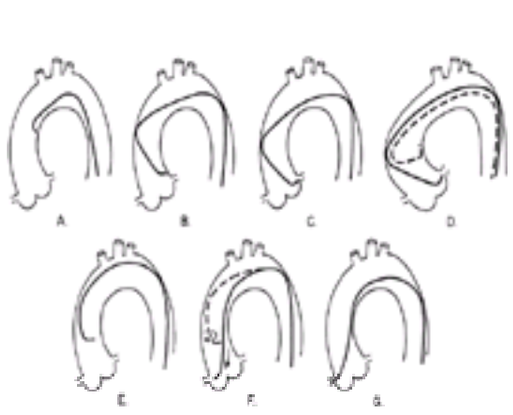

FIG. 11.4. Judkins technique for catheterization of the left and right coronary arteries as viewed in the left anterior oblique (LAO) projection. In a patient with a normal-size aortic arch, simple advancement of the JL4 catheter leads to intubation of the left coronary ostium (**A**, **B**, and **C**). In a patient with an enlarged aortic root **(D)** the arm of the JL4 may be too short, causing the catheter tip to point upward or even flip back into its packaged shape *(dotted line)*. A catheter with an appropriately longer arm (a JL5 or JL6) is required. To catheterize the right coronary ostium, the right Judkins catheter is advanced around the aortic arch with its tip directed leftward, as viewed in the LAO projection, until it reaches a position 2 to 3 cm above the level of the left coronary ostium **(E)**. Clockwise rotation causes the catheter tip to drop into the aortic root and point anteriorly **(F)**. Slight further rotation causes the catheter tip to enter the right coronary ostium **(G)**.

In patients with a widened aortic root due to aortic valve disease or long-standing hypertension, the 4-cm left Judkins curve may be too short to allow successful engagement. In such a case, the catheter arm may lie almost horizontally across the aortic root with the tip pointing vertically against the roof of the left main artery, or it may even refold into its packaged shape during advancement into the aortic root (Fig. 11.4*D*). In this case, a left Judkins catheter with a larger curve (JL4.5, JL5, or even JL6) curve should be selected. In the long run, changing to a larger catheter under these circumstances may save time compared with persevering in trying to make an unsuitable catheter work. In the occasional patient with a short or narrow aortic root (usually a younger female, particularly if of short stature), even the 4-cm Judkins curve may be too long. When brought down into the aortic root, the catheter arm may lie almost vertically with the tip pointing downward, below the left coronary ostium. The left ostium may still be engaged, by pushing the catheter down into the left sinus of Valsalva for approximately 10 seconds to tighten the angle on the catheter tip and then withdrawing the catheter slowly. Having the patient take a deep breath during this maneuver also helps by pulling the heart into a more vertical position to assist in engagement of the left ostium. The most satisfactory approach, however, is to exchange for a JL3.5 catheter with a shorter curve.

On the rare occasions when the left coronary ostium lies “out of plane” (typically high and posterior), limited counterclockwise rotation of the left Judkins catheter in the right anterior oblique (RAO) projection may help orient the catheter's tip posteriorly and facilitate engagement. Too much rotation of this catheter, however, may result in a refolded catheter that requires guidewire reinsertion to straighten. In this case, it may be helpful to step up to the next larger Judkins curve. Alternatively, some operators prefer to switch to a left Amplatz catheter (Fig. 11.1); these are available in progressively larger curves—AL1, AL2, AL3, and AL4. Amplatz catheters (24) are more tolerant of rotational maneuvering and allow easy engagement of left coronary ostia that lie out of the conventional Judkins plane, as well as subselective engagement of the left anterior descending (LAD) and circumflex coronary arteries in patients with short left main coronary segments or separate left coronary ostia. The left Amplatz is advanced around the arch, oriented toward the left coronary ostium (Fig. 11.5). The tip of the catheter usually comes to rest in the sinus of Valsalva below the coronary ostium. As the catheter is advanced further, the Amplatz shape causes the tip of the catheter to ride up the wall of the sinus until it engages the ostium. At that point, slight withdrawal of the catheter causes deeper engagement of the coronary ostium, whereas further slight advancement causes paradoxic retraction of the catheter tip.

FIG. 11.5. Catheterization of the left coronary artery with an Amplatz catheter. The catheter should be advanced into the ascending aorta with its tip pointing downward, so that the terminal catheter configuration resembles a diving duck. As the Amplatz catheter is advanced into the left sinus of Valsalva, its tip initially lies below the left coronary ostium *(left)*. Further advancement causes the tip to ride up the aortic wall and enter the ostium *(center)*. Subsequently, slight withdrawal of the catheter causes the tip to seat more deeply in the ostium *(right)*.

Cannulation of the Right Coronary Ostium

The Judkins technique for engaging the right coronary ostium requires slightly more catheter manipulation than does cannulation of the left coronary ostium (16,23). After being flushed and filled with contrast medium in the descending aorta (with the catheter tip directed anteriorly to avoid injection into the intercostal arteries), the right Judkins catheter with a 4-cm curve (JR4) is brought around the aortic arch with the tip facing inward until it comes to lie against the right side of the aortic root with its tip aimed toward the left coronary ostium (Fig. 11.4). In a left anterior oblique (LAO) projection, the operator slowly and carefully rotates the catheter clockwise by almost 180° to engage the right coronary artery. The tip of the right Judkins catheter tends to drop more deeply into the aortic root when the catheter is rotated toward the right ostium, as the tertiary curve rotates into alignment with the top of the aortic arch. To compensate for this effect, the operator must either begin the rotational maneuver with the tip 2 to 3 cm above the coronary ostium or withdraw the catheter slowly during rotation. Care must be taken to avoid “overrotation” of the catheter, which tends to cause undesirably deep engagement of the right coronary artery. To avoid this common technical error, the operator must not continue to apply clockwise torque when the tip of the catheter is “stuck” in the aortic root, and should be prepared to apply a small amount of counterclockwise torque immediately as the catheter enters the ostium.

Catheters with smaller (3.5-cm) or larger (5- or 6-cm) Judkins curves or right Amplatz catheters (AR1 or AR2) may be of value if aortic root configuration and proximal right coronary anatomy make engagement difficult. One such situation occurs when the right coronary ostium lies high and anterior, usually above the commissure of the left and right aortic valve leaflets but occasionally above the left sinus itself. In that case, a left Amplatz catheter (either AL0.75 or AL1) may be required to make contact with the aortic wall at the location of the ostium. Damping and ventricularization are far more common in the right coronary artery than in the left. It may be caused by (a) the generally smaller caliber of the vessel, (b) ostial spasm around the catheter tip, (c) selective engagement of the conus branch, or (d) true ostial stenosis. These problems in right coronary artery engagement can usually be elucidated by nonselective injections into the right sinus of Valsalva or cautious injections in the damped position with immediate postinjection withdrawal of the catheter. As mentioned earlier, a 6F or 7F angioplasty guiding catheter with side-holes near the tip may be used to allow uninterrupted coronary perfusion between contrast injections, if necessitated by true ostial or proximal right coronary disease.

Cannulation of Saphenous Vein Grafts

Despite the high initial rate of anginal relief after bypass surgery, 3% to 12% of saphenous vein grafts occlude due to thrombosis within the first month. Additional veins occlude between 1 month and 1 year after surgery due to exaggerated neointimal hyperplasia. By far the dominant failure mode of saphenous vein graft failure beyond 1 year—accounting for up to 50% graft closure by 7 years—is diffuse graft atherosclerosis (25). For these reasons, an increasing number of patients develop recurrent angina after prior bypass surgery, accounting for more than 20% of the diagnostic procedures in our laboratory.

The proximal anastomosis is placed on the right or left anterior aortic surface, several centimeters above the sinuses of Valsalva. Because many surgeons resist the practice of placing radiopaque markers on the proximal graft (26), the operator usually must rely on the surgeon's operative report or diagram and knowledge of surgical practice in the institution. The operative report should be obtained before elective angiography on any patient with prior bypass surgery, but is absolutely essential for patients who underwent their operation at another medical center (where local preference may include practices such as anastomosis to the right-*posterior* surface of the aorta; see later discussion). It can be quite frustrating to embark on coronary angiography in such a patient without a detailed graft map or operative note in hand.

Most commonly, *grafts to the left coronary artery* arise from the left anterior surface of the aorta, with grafts to the LAD coronary artery originating somewhat below grafts to the circumflex system. Some surgeons prefer to route grafts to the circumflex through the transverse sinus behind the heart, in which case the circumflex graft may originate from the posterior surface of the aorta. *Grafts to the right coronary artery* (or the distal portions of a dominant circumflex) usually originate from the right anterior surface of the aorta, above and somewhat behind the plane of the native right coronary ostium. We usually use the right Judkins (JR4) or Amplatz (AL1) catheter to engage anterior (i.e., left) coronary grafts. Special left coronary bypass, internal mammary, or hockey-stick catheters may be required for left grafts that originate with an upward trajectory (Fig. 11.6). For downward-pointing right coronary artery grafts, we prefer a soft catheter with no primary curve (a multipurpose, Wexler, or JR3.5 short-tip catheter), which provides better alignment with the proximal portion of the graft and therefore better opacification. The Wexler catheter can also be used for grafts originating from the left or posterior surface of the aorta, because its tip remains in contact with the aortic wall. Once the ostium has been selected, the shaft of this catheter may be rotated or the tip may be flexed to bring it into alignment with the proximal graft.

FIG. 11.6. Catheters used for bypass graft angiography. Although the right Judkins or Amplatz catheters can be used for many anterior takeoff vein grafts, catheters with the following shapes may be useful (left to right): Wexler, multipurpose, hockey-stick shape, and internal mammary.

If no markers have been provided, the catheter tip should be oriented against the appropriate aortic wall and slowly advanced and then withdrawn until its tip "catches" in a graft ostium. The graft is injected in multiple projections that show its origin, shaft, distal anastomosis, and the native vessels beyond the anastomosis. This process must then be repeated until all graft sites have been identified. Grafts should not be written off as occluded unless a clear "stump" is demonstrated. If the myocardial territory supplied by a graft assumed to be occluded is still contracting and there is no evident native or collateral blood supply to that territory, there must be some "visible means of support," which may be a missed graft! It may be valuable to perform an aortogram in an appropriate view to try to demonstrate flow in and locate the origin of such a missed graft. The emergence of effective therapies for focal lesions in vein grafts has placed a premium on being able to find and fix such diseased grafts before they occlude (Fig. 11.7; see Chapter 23, Chapter 24 and Chapter 25).

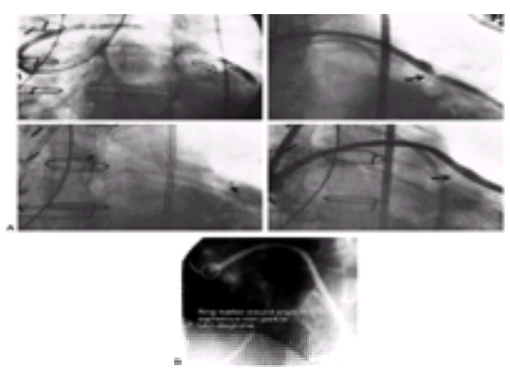

FIG. 11.7. A: Sample of saphenous vein graft angiography, showing an occluded graft to the circumflex, filled with thrombus *(upper left, open arrow)*. A drug-infusion catheter (Tracker, Target Therapeutics) was placed *(lower left, curved arrow)* and used to administer urokinase (50,000 IU/hr) overnight. The following morning *(upper right)*, the thrombus had been dissolved, revealing the underlying ulcerated culprit lesion. This was treated with a single Palmaz-Schatz coronary stent *(lower right)*, reestablishing full patency. **B:** Saphenous vein graft with origin localized by ring marker implanted at the time of surgery.

Internal Mammary Cannulation

Based on their superior demonstrated 10-year patency, the left and right internal mammary (also known as internal *thoracic*) arteries have become the conduits of choice. More than 90% of current elective bypass procedures involve placement of at least one internal mammary graft. Successful cannulation (27) requires knowledge of the left subclavian and brachiocephalic trunk as well as the right subclavian arteries, as shown in Fig. 11.8*A*. It is also important to understand some of the common anatomic variants in the internal mammary artery, including more proximal origin in the vertical portion of the subclavian, or origin as a common vessel with the thyrocervical trunk. Although uncommon, these grafts can develop significant lesions, making it important to evaluate such grafts during any postbypass catheterization. In patients with early recurrence of angina (within the first 6 months after surgery), the most common lesion is located at the distal mammary-coronary anastomosis. It is usually caused by local intimal hyperplasia rather than atherosclerosis and responds well to balloon angioplasty (see Chapter 23). Flow-limiting "kinks" may also be present in the midgraft, and ostial lesions at the origin of the internal mammary from the subclavian may also occur. Years after bypass surgery, significant lesions may develop in the native coronary artery beyond the internal mammary touchdown. In addition to establishing the patency of the internal mammary itself, it may also be important to look for large nonligated side branches that may divert flow from the coronary circulation, and whose occlusion (on occasion) may be required for angina relief (28). It is also important to look for stenoses in the subclavian artery before the takeoff of the internal mammary that may compromise the inflow to the graft and thereby cause myocardial ischemia (Fig. 11.9). Such lesions may require construction of a carotid-to-subclavian graft or catheter intervention (angioplasty, directional atherectomy, or stenting) (29) to restore normal graft flow through the internal mammary artery.

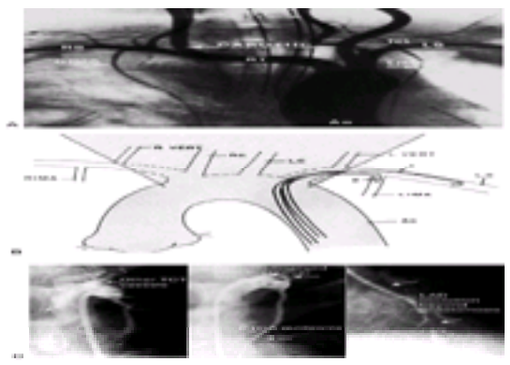

FIG. 11.8. Internal mammary angiography. **A:** Aortic arch injection shows the left internal mammary artery (LIMA) originating from the left subclavian (LS), just opposite the thyrocervical trunk (tct) and distal to the right vertebral artery (VERT). The right internal mammary artery (RIMA) originates from the right subclavian (RS) just distal to the bifurcation of the right carotid from the brachiocephalic trunk (BT). **B:** Schematic diagram shows the corresponding arch vessel origins. Note that the left subclavian artery originates just inside the leftmost edge of the wedge-shaped shadow cast by the upper-mediastinal structures in the left anterior oblique projection. Catheter manipulation in this projection facilitates advancement of a guidewire into the LS (step 1), facilitating selective cannulation of the LIMA during catheter withdrawal and slight counterclockwise rotation (step 2, see text). **C:** Variant in which the internal mammary artery originates in common with the thyrocervical trunk, resulting in poor opacification. An angioplasty guidewire was placed down the internal mammary artery through the 6F diagnostic catheter and used to advance the tip of the diagnostic catheter selectively down the internal mammary artery. From that position, sufficient opacification was obtained to demonstrate occlusion of the distal left anterior descending artery beyond the anastomosis as the cause of the patient's recurrent angina.

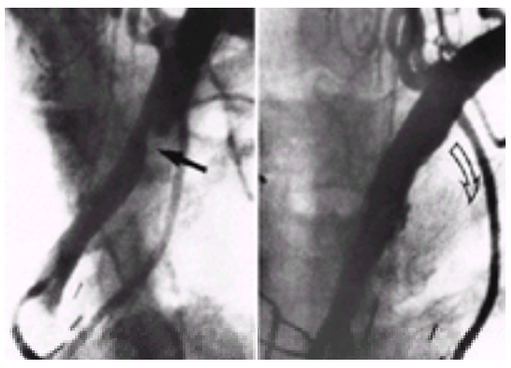

FIG. 11.9. Left subclavian artery stenosis in a patient with recurrent angina in the distribution of the otherwise patent left internal mammary artery *(left panel)*, treated by placement of Palmaz-Schatz biliary stents *(right panel)*.

Although mammary grafts can be studied easily from the ipsilateral brachial approach, we prefer the femoral approach using a soft-tip preformed internal mammary catheter, which resembles a right Judkins catheter except for a tighter primary curve. This used to be a time-consuming process (up to 20 minutes for some operators), but it has been reduced to less than 3 minutes in our laboratory by adoption of a systematic strategy (Fig. 11.8*B*) (27). In the LAO projection, cannulation of the left internal mammary artery begins by advancement of this catheter into the aortic arch, until it lies just inside the left edge of the wedge-like density formed by the shadow of the upper mediastinum against the lung fields. With 1 to 2 cm of J guidewire protruding from its tip, the mammary catheter is rotated counterclockwise until it falls into the subclavian artery origin. From there, the wire can be advanced well out into the axillary artery. The mammary catheter is then advanced over the wire, into the middle subclavian. The guidewire is then removed, and the catheter is flushed and filled with contrast medium. A low-osmolar contrast agent should be used to avoid causing central nervous system toxicity by reflux of hyperosmolar ionic contrast medium up the vertebral arteries. Switching to the straight anteroposterior projection, the catheter is rotated counterclockwise slightly (to make the tip point slightly anteriorly) and is withdrawn slowly until the internal mammary is engaged. Intermittent gentle puffs of contrast material help localize the mammary origin during this withdrawal. Great care should be taken to avoid catheter tip trauma and dissection of the relatively delicate mammary vessel. If selective cannulation is difficult because of tortuosity or anatomic variations, a variety of superselective or nonselective techniques can be used to permit angiographic evaluation. Nonselective injections into the subclavian artery usually allow opacification which is adequate to see that the internal mammary is open but usually not enough to provide detailed information about the distal native vessel. Inflation of a blood pressure cuff on the ipsilateral arm may help reduce runoff through the axillary artery and improve opacification of the internal mammary in cases in which selective cannulation is difficult.

Cannulation of the right internal mammary artery may be slightly more difficult because of the need to avoid the right carotid artery before entering the right subclavian itself. Again in the LAO projection, the upper mediastinal wedge is identified. The mammary catheter with protruding J wire is taken to the right edge of this shadow and rotated counterclockwise until it falls into the brachiocephalic trunk. The wire is then advanced toward the right subclavian artery. Predilection for the wire to advance into the right carotid artery may require removal of the guidewire and a nonselective contrast injection in the brachiocephalic trunk to identify the origin of the subclavian branch. The subclavian can then be cannulated with the use of a steerable (Wholey) guidewire. Once the wire is firmly out the subclavian artery, the mammary catheter is advanced as described previously. For cannulation of the right internal mammary artery, however, the catheter is rotated slightly clockwise during withdrawal to point its tip anteriorly.

Gastroepiploic Graft Cannulation

Taken together, the left and right internal mammary arteries can be used to revascularize most lesions in the LAD, proximal circumflex, and proximal right coronary arteries. Even with sequential distal anastomoses, however, the fact that there are only two internal mammary arteries means that most revascularization procedures still suffer the long-term limitations associated with the use of saphenous veins. Free segments of radial artery have also been used as bypass conduits, either from the ascending aorta (like a saphenous vein) or from the descending thoracic aorta (30) in some patients undergoing repeat bypass surgery. Although the radial artery may have slight benefit over the saphenous vein, it is prone to spasm in the early postoperative period and does not match the long-term patency record of the internal mammary artery (because it does not retain its blood supply and innervation when used as a free graft). The effort to perform “all arterial” bypass has brought back the use of the right gastroepiploic artery (as an arterial pedicle graft) for anastomosis to the posterior descending coronary artery or other vessels on the inferior surface of the heart (31,32). The right gastroepiploic normally supplies the majority of the greater curvature of the stomach but can be dissected free from that organ and tunneled through the diaphragm to reach the inferior wall of the heart. Angiography of this vessel is possible with the use of standard visceral angiographic catheters (e.g., cobra catheter), which are designed to enter visceral arteries such as the celiac axis (33). From there, the catheter can be advanced into the common hepatic artery (as opposed to the splenic artery) and then turned downward into the gastroduodenal artery (Fig. 11.10). A 0.025-inch Glidewire (Terumo) can then be used to cannulate the right gastroepiploic artery (as opposed to the superior pancreatoduodenal artery) if more selective injection is desired.

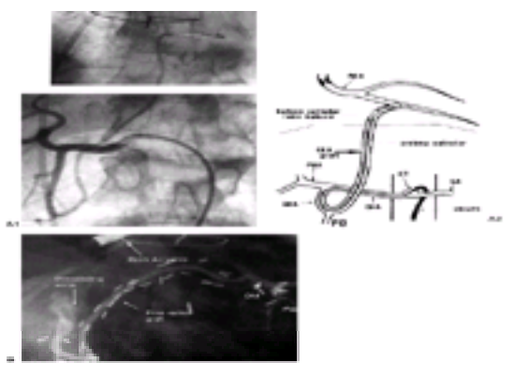

FIG. 11.10. A: Gastroepiploic graft anatomy. The common hepatic artery (CHA) originates with the splenic artery (SA) from the celiac trunk (CT). The gastroduodenal artery (GDA) originates from the CHA, which then becomes the proper hepatic artery (PHA). The terminal branches of the GDA are the pancreatoduodenal (PD) and the right gastroepiploic artery (GEA), shown here undergoing angioplasty of a lesion at its anastomosis to the right coronary artery (RCA). (Diagram from Ishiki T, et al. Percutaneous angioplasty of stenosed gastroepiploic artery grafts. *J Am Coll Cardiol* 1993;21:727, with permission.) **B:** Free radial graft from the descending aorta to an obtuse marginal graft, cannulated with the use of a cobra visceral angiographic catheter. Localization of the graft ostium was aided by the presence of multiple surgical clips, used to ligate small side branches of the radial artery at the time of bypass.

THE BRACHIAL CUTDOWN APPROACH

The technique of performing brachial artery cutdown was the first used for selective coronary angiography, as described in Chapter 5. The original catheter designed by Dr. F. Mason Sones, Jr., was a thin-walled radiopaque woven Dacron catheter with a 2.67-mm (8F) external diameter to its shaft (16,34). The tip is open, and current models also include side-holes that are arranged in opposed pairs within 7 mm of the distal end. The shaft tapers abruptly to 5F external diameter at a point 5 cm from its tip. As Sones stated, this provides a “flexible finger” that may be curved upward into the coronary orifices by pressure of the more rigid shaft against the aortic valve cusps. This enables the Sones catheter to be used for cannulation of both the left and right coronary arteries, as well as entry into the left ventricle for ventriculography. The standard Sones catheter is available in lengths of 80, 100, and 125 cm and in 7F and 8F diameters.

Some operators use a Sones type of coronary catheter constructed of polyurethane and made by Cordis Corporation. This catheter has the same shape and taper as the woven Dacron catheter and has an end-hole with four side-holes within 7 mm of its tip. This catheter traverses a tortuous subclavian system with much greater facility and smoothness than does the woven Dacron catheter, and its enhanced torque control and reduced friction coefficient permit greater ease in engaging the coronary ostia. It can pass an 0.035-inch guidewire and is an excellent catheter for crossing a stenotic aortic valve. See Fig. 11.1 for a variety of coronary catheters

that are also effective from the brachial approach.

When the Sones method is used, catheter-tip pressure should be monitored continuously once the catheter enters the brachial artery. Further passage of the catheter into the subclavian and innominate (brachiocephalic) arteries should be accomplished under both pressure monitoring and fluoroscopic visualization. Occasionally, it may be difficult to pass the catheter from the subclavian artery to the aortic arch, but a simple maneuver by the patient—such as a deep inspiration, shrugging the shoulders, or turning the head to the left—often facilitates passage of the catheter into the ascending aorta. If passage of the catheter from the subclavian artery to the ascending aorta is not accomplished immediately and with complete ease, the operator should stop catheter manipulation and use a soft J-tip 0.035-inch guidewire. Once the catheter is in the ascending aorta, the guidewire is removed and the catheter is aspirated, flushed, and reconnected to the rotating adapter of the manifold, either directly or by a short length of large-bore flexible connecting tubing.

With the Sones technique, selective engagement of the *left coronary artery* is accomplished as follows. In an LAO projection, the sinus of Valsalva containing the ostium of the left coronary artery lies to the left and the sinus containing the ostium of the right coronary artery lies to the right. The noncoronary sinus lies posteriorly. The operator advances the catheter to the aortic valve and then continues to advance the catheter until its tip bends cephalad and points toward the left coronary ostium. When the catheter is properly positioned with its tip bent cephalad, slight advancement or rotation of the catheter usually results in selective engagement of the left coronary ostium, which is verified by a small injection of radiographic contrast agent. Occasionally, a deep breath taken by the patient can facilitate this selective engagement. Once the catheter tip is engaged, it commonly (but not always) appears to be fixed by the coronary orifice. There is more than one way to successfully engage the left coronary artery with the Sones catheter. Our usual approach, illustrated in the upper left panel of Fig. 11.11, involves forming a smooth, shallow loop and gradually "inching up" to the ostium from below. If the distal 2 to 3 mm of the catheter tip bends downward during this inching-up process, the tip may enter the left coronary artery, giving a "cobra head" appearance (Fig. 11.11, upper right panel) similar to that achieved with the left Amplatz catheter (Fig. 11.5). This is a stable position that allows rotation of the patient in a cradle-type table top without disengagement of the catheter. For the high-takeoff left coronary ostium, the catheter may have an appearance in which the catheter tip is lying across the ostium, at right angles to the course of the left main coronary artery (as in Fig. 11.11, bottom). During contrast injection in this instance, coronary blood flow usually carries the contrast agent down the vessel, giving good opacification of the entire left coronary artery.

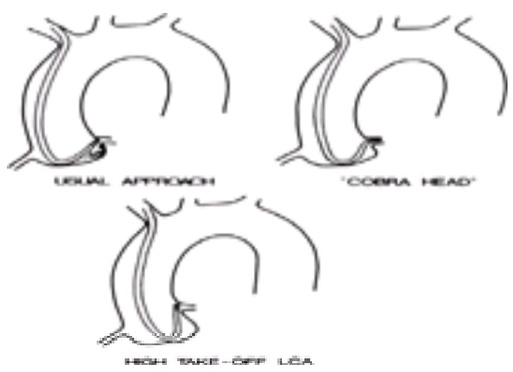

FIG. 11.11. Selective catheterization of the left coronary artery using the Sones catheter. The standard approach involves forming a smooth, shallow loop and gradually "inching up" to the ostium from below. If the distal 2 to 3 mm of the catheter tip bends downward during this inching-up process, the tip may enter the left coronary artery, giving a "cobra-head" appearance *(upper right)*. When the left coronary ostium originates high in the left sinus of Valsalva ("high-takeoff" left coronary artery), the catheter may have the appearance seen in the bottom panel, where the tip is lying across the ostium, at right angles to the course of the left main coronary artery. During coronary injection in this instance, coronary blood flow usually carries the contrast agent down the vessel, giving good opacification of the entire left coronary artery.

Once the catheter tip has engaged the coronary ostium and no damping of pressure from the catheter tip is observed, cineangiography may be performed with selective injection of radiopaque material in a variety of views, as described later.

Selective engagement of the *right coronary* orifice may be accomplished as illustrated in steps 1 through 3 of Fig. 11.12. In the shallow LAO projection, the catheter is curved up toward the left coronary artery (step 1) and clockwise torque is applied. While the operator is gradually applying clockwise torque, a gentle to-and-fro motion of the catheter (excursions of not more than 5 to 10 mm) helps to translate the applied torque to the catheter tip. When the tip starts moving in its clockwise sweep of the anterior wall of the aorta, the operator maintains (but does not increase) a clockwise torque tension on the catheter and simultaneously pulls the catheter back slightly (step 2, Fig. 11.12), because the right coronary ostium is lower than that of the left coronary artery. At this point, the catheter usually makes an abrupt turn into the right coronary ostium, at which time the operator must release all torque to prevent the catheter tip from continuing its sweep past the ostium. On occasion, the Sones catheter literally leaps into the right coronary artery and 4 to 5 cm down its lumen. If this occurs, the catheter should be gently withdrawn until its tip is stable just within the ostium. Another technique for catheterizing the right coronary artery involves a more direct approach by way of the right coronary cusp. With the catheter in the right sinus, the operator should make a small curve on the tip, directed rightward. A small dose of contrast material in the right sinus of Valsalva allows visualization of the right coronary orifice and facilitates selective engagement. Occasionally, a deep inspiration by the patient accompanied by gentle advancement of the catheter to the right of the aortic root, results in selective engagement of the right coronary artery.

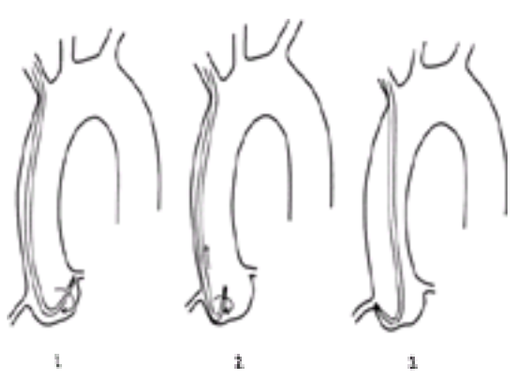

FIG. 11.12. Selective catheterization of the right coronary artery using the Sones catheter. In the shallow left anterior oblique projection, the catheter is curved upward and to the left (1) and clockwise torque is applied. While the operator is gradually applying clockwise torque, a gentle to-and-fro motion of the catheter helps to translate the applied torque to the catheter tip. When the tip starts moving in its clockwise sweep of the anterior wall of the aorta, the operator maintains (but does not increase) a clockwise torque tension on the catheter and simultaneously pulls the catheter back slightly (2), because the right coronary ostium is lower than that of the left coronary artery. At this point the catheter usually makes an abrupt leap into the right coronary ostium (3), at which time the operator must release all torque to prevent the catheter tip from continuing its sweep and passing by the ostium. (See text for details and alternative methods.)

In addition to the Sones catheter, many other catheters may be used for coronary arteriography from the brachial cutdown or percutaneous approach, including the Amplatz (24), Schoonmaker (35), Bourassa, Judkins, and other specially designed catheters. Some of these catheters are illustrated in Fig. 11.1. Although the Amplatz catheters were originally devised for use from the percutaneous femoral approach, we have found these catheters highly useful from the brachial approach in cases in which there was difficulty in seating the Sones catheter. Amplatz catheters come in different shapes for the right and left coronary artery and basically incorporate a preformed curvature that is like that of an already-engaged Sones catheter. We have found the AL2 to be adequate for most patients with normal aortic roots, whereas the AL3 may be necessary for a dilated ascending aorta or in large men. Occasionally an AL4 is needed for pronounced aortic dilatation or for a left coronary artery whose ostium originates very high in the left sinus of Valsalva (high-takeoff left coronary artery). The AR1 right coronary catheter is usually adequate for patients with a normal aortic root, whereas the AR2 may be required for patients with an enlarged aortic root or for engagement of saphenous vein bypass grafts. The Amplatz catheters should be introduced through the subclavian artery over a guidewire and (unlike the Sones catheter) cannot be used safely for

ventriculography. When working from the left brachial approach, it is also possible to use standard Judkins catheters, since the course of the catheter around the arch emulates its path from the femoral approach in that area. We have not had experience with the Bourassa or Schoonmaker catheters from the brachial approach, but large published series using these catheters from the femoral artery approach suggest that they should also be effective from the brachial approach. Of course, all of these considerations about coronary angiography from the brachial cutdown approach also apply to the percutaneous brachial, axillary, or radial approaches (see Chapter 4).

ADVERSE EFFECTS OF CORONARY ANGIOGRAPHY

Once the coronary vessels have been engaged, selective angiography requires transient but nearly complete replacement of blood flow with a radiopaque contrast agent. A wide variety of iodine-containing agents are currently used for coronary angiography and have already been discussed in greater detail in Chapter 2.

Coronary injection of a high-osmolar contrast agent may have potentially deleterious effects (see Chapter 2 and Chapter 3) that include (a) transient (10- to 20-second) hemodynamic depression marked by arterial hypotension and elevation of the left ventricular end-diastolic pressure; (b) ECG effects with T-wave inversion or peaking in the inferior leads (during right and left coronary injection, respectively), sinus slowing or arrest, and prolongation of the PR, QRS, and QT intervals (36,37); (c) significant arrhythmia (asystole or ventricular tachycardia/fibrillation) (38); (d) myocardial ischemia due to interruption of oxygen delivery or inappropriate arteriolar vasodilation (coronary “steal”); (e) allergic reaction (39); and (f) cumulative renal toxicity (40). Some (but not all) of these adverse effects are eliminated by use of a low-osmolar contrast agent, albeit at a modestly increased expense (41).

To recognize, treat, and hopefully prevent these adverse effects, patients undergoing coronary angiography should be monitored continuously in terms of clinical status, surface ECG, and arterial pressure from the catheter tip. In patients with baseline left ventricular dysfunction or marked ischemic nstability, we also like to display pulmonary artery pressure continuously on the same scale as the arterial pressure, because this provides the earliest indication of procedural problems or decompensation. A significant rise in pulmonary artery mean or diastolic pressure should prompt temporary suspension of angiography and initiation of treatment (e.g., intravenous furosemide, nitroglycerin, nitroprusside) before frank pulmonary edema develops.

If right-sided heart catheterization is to be performed, the venous sheath provides a ready route for the rapid administration of fluid or medications through its sidearm and allows rapid insertion of a temporary pacing electrode if needed.

We do not, however, endorse the routine prophylactic placement of temporary pacing electrodes in patients undergoing coronary angiography (42). Most episodes of bradycardia or asystole are brief and are resolved promptly by having the patient give a forceful cough, which elevates central aortic pressure and probably helps wash residual contrast material out of the myocardial capillary bed. True life-threatening bradycardia is very uncommon and can be managed successfully by having the patient cough at 1- to 2-second intervals while a temporary pacing lead is inserted through the indwelling venous sheath and attached to a generator kept at standby at the foot of the catheterization table. Similarly, prophylactic drugs are not given routinely to prevent ventricular tachyarrhythmias, although drugs (e.g., lidocaine, procainamide, atropine, epinephrine), a defibrillator, and airway management equipment are always kept at the ready and can be brought into play within seconds.

One of the most common adverse effects seen during coronary angiography is the provocation of myocardial ischemia, particularly in patients with unstable angina. In such patients, we commonly do not interrupt any precatheterization heparin infusion (and usually give additional heparin during the catheterization itself) and do not reverse heparin at the completion of the procedure. In very unstable patients, we modify our usual practice of performing the left ventriculogram before coronary angiography (lest an adverse reaction to the ventriculogram compromise the more crucial coronary study). When myocardial ischemia does occur during coronary angiography, the best course of action is to remove the catheter from the coronary ostium and temporarily suspend injections until angina resolves. If this takes more than 30 seconds, we typically administer nitroglycerin (200-µg bolus, repeated at 30-second intervals up to a total of 1,000 µg) into either the involved coronary artery or the pulmonary artery catheter. If marked arterial hypertension is present and fails to respond to nitroglycerin, we may administer other vasodilators as needed to bring the blood pressure down. In patients with inappropriate tachycardia in the setting of angina and reasonable systolic left ventricular function, intravenous propranolol (1 mg every minute to a total dose of 0.1 to 0.15 mg/kg) or an infusion of a short-acting b-blocking agent (esmolol) is frequently beneficial. Only rarely (in patients with severe three-vessel disease and/or left main coronary artery disease and those whose ischemia is associated with hypotension) is myocardial ischemia severe enough and refractory to this management program to prompt placement of an intraaortic counterpulsation balloon in the contralateral femoral artery before completion of coronary angiography (see Chapter 21). In any patient with prolonged or refractory ischemia during diagnostic coronary angiography, it may be worthwhile to perform limited reexamination of the coronary vessels to determine whether the angiographic procedure has caused a problem (spasm, dissection, thrombosis) that might require immediate treatment with additional vasodilators, balloon angioplasty, thrombolysis, or emergency bypass surgery.

Severe allergic reactions are uncommon during coronary angiography and are best prevented by 18 to 24 hours of premedication (prednisone, 20 to 40 mg, and cimetidine, 300 mg every 6 hours) (32) and/or use of a nonionic contrast agent in patients with a history of prior allergic reaction to radiographic contrast media (41). When a severe unexpected reaction does occur, it usually responds promptly to the intravenous administration of epinephrine (0.1 mg = 1 mL of the 1:10,000 solution available on most emergency carts, repeated every 2 minutes until the blood pressure and/or wheezing improves). Larger bolus doses of epinephrine are to be avoided, because they may provoke marked tachycardia, hypertension, and arrhythmia.

Renal insufficiency may develop after coronary angiography, particularly in patients who are hypovolemic, who receive large volumes of contrast material (more than 3 mL/kg), or who have had prior renal insufficiency, diabetes, or multiple myeloma (33). In these patients, every effort should be made to give adequate hydration before and after the procedure (see Chapter 2 and Chapter 3). Use of low-osmolar contrast agents may be helpful in this situation, but their real benefit remains controversial (41).

INJECTION TECHNIQUE

As mentioned previously, high-quality coronary angiography requires selective injection of radiographic contrast material at an adequate rate and volume to transiently replace the blood contained in the involved vessel with slight but continuous reflux into the aortic root. Too timid an injection allows intermittent entry of non-opaque blood into the coronary artery (producing streaming, which makes interpretation of lesions difficult) and prevents visualization of the coronary ostium and proximal coronary branches. However, too vigorous an injection can cause coronary dissection or excessive myocardial blushing, and too prolonged an injection may contribute to increased myocardial depression or bradycardia.

We train our fellows to adjust the rate and duration of manual contrast injection to match the observed filling pattern of the particular vessel being injected. Injection velocity is built up gradually during the initial 1 second until the injection rate is adequate to completely replace antegrade blood flow into the coronary ostium (Fig. 11.13). The associated rate and volume required to accomplish this goal have been measured (43) and found to average 7 mL at 2.1 mL/sec in the left and 4.8 mL at 1.7 mL/sec in the right coronary artery. In patients with occlusion, much smaller rates and volumes are required, and in patients with left ventricular hypertrophy (e.g., aortic stenosis, hypertrophic myopathy), much larger volumes and higher rates of injection may be required.

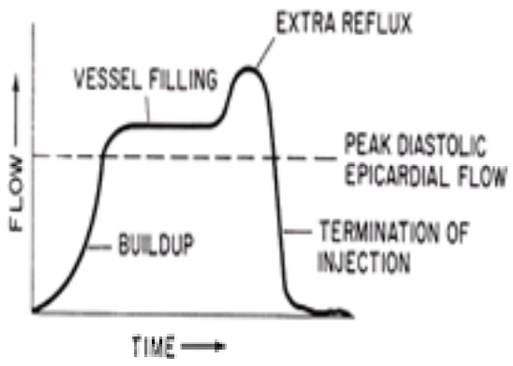

FIG. 11.13. Suggested injection pattern for coronary angiography. To appropriately replace antegrade coronary blood flow with contrast medium throughout the cardiac cycle, the operator should build up the velocity of injection over 1 to 2 seconds until no unopacified blood is seen to enter the ostium and there is reflux of contrast medium into the aorta during systole and diastole. This injection is maintained until the entire coronary artery is filled with contrast medium. If the ostium has not been well seen, a brief extra push should be given to cause adequate reflux into the aortic root, and then the injection is terminated. Prolonged held inspiration

with some degree of Valsalva maneuver is sometimes used during Sones angiography to reduce coronary flow and make it much easier to replace blood flow during manual contrast injection.

The injection is maintained until the entire vessel is opacified. If there is any question as to whether the body of the injection has provided adequate reflux to visualize the coronary ostium, an additional burst of contrast agent (extra reflux) should be given before the injection is terminated. The injection is then terminated abruptly by turning the manifold stopcock back to monitor pressure, although cine filming continues until opacification of distal vessels or late-filling branches is complete. The operator monitors for excessive bradycardia or hypotension, reviews the video playback, and sets the gantry angles for the next injection. To avoid problems, each injection should begin with a completely full (and bubble-free) injection syringe, held with the handle slightly elevated so that any microbubbles will drift up toward the plunger. Recent changes in labeling of contrast agents also suggest that the injection syringe be managed in such a way as to avoid mixtures of blood and contrast material, because such mixtures may promote formation of thrombi (particularly when nonionic contrast agents are used).

Although manual contrast injection is the standard technique in coronary angiography, some operators favor use of a power injector (as used in left ventriculography or aortography) to perform coronary injections (44). The injector is preset for a rate to match the involved vessel (2 to 3 mL/sec for the right and 3 to 4 mL/sec for the left coronary artery) and is activated by a foot switch for a period sufficient to fill the coronary artery with contrast medium (usually 2 to 3 seconds). This approach allows a single operator to perform injections and move the table and has proved safe in thousands of procedures. A new power injector has been introduced (Acist, Bracco Bristol Myers Squib) (Fig. 11.2) that can perform such power injections under rate control by finger pressure on a sterile control handle, reverting automatically to pressure monitoring when the injection is terminated. This may be of value when a single operator must both perform injections and pan the table during diagnostic coronary angiography.

ANATOMY, ANGIOGRAPHIC VIEWS, AND QUANTITATION OF STENOSIS

Coronary Anatomy

The coronary angiographer must develop a detailed familiarity with normal coronary arterial anatomy and its common variants. For those just learning coronary anatomy, the main coronary trunks can be considered to lie in one of two orthogonal planes (Fig. 11.14). The anterior descending and posterior descending coronary arteries lie in the plane of the interventricular septum, whereas the right and circumflex coronary trunks lie in the plane of the atrioventricular valves. In the 60° LAO projection, one is looking down the plane of the interventricular septum, with the plane of the atrioventricular (AV) valves seen *en face*; in the 30° RAO projection, one is looking down the plane of the AV valves, with the plane of the interventricular septum seen *en face*. The major segments and branches have each been assigned a numeric identification in the Bypass Angioplasty Revascularization Investigation (BARI) modification (45) of the Coronary Artery Surgery Study (CASS) nomenclature (Fig. 11.15).

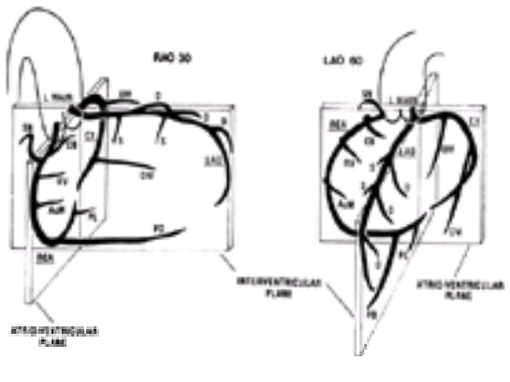

FIG. 11.14. Representation of coronary anatomy in relation to the interventricular and atrioventricular valve planes. Coronary branches are as indicated: L Main, left main; LAD, left anterior descending; D, diagonal; S, septal; CX, circumflex; OM, obtuse marginal; RCA, right coronary; CB, conus branch; SN, sinus node; AcM, acute marginal; PD, posterior descending; PL, posterolateral left ventricular.

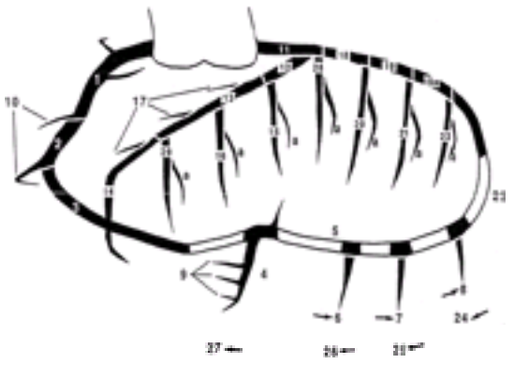

FIG. 11.15. The numeric coding system and official names of the coronary segments, as used in the Bypass Angioplasty Revascularization Investigation (BARI) study. *Right coronary:* 1, proximal; 2, middle; 3, distal; 4, posterior descending; 5, posteroatrioventricular; 6, first posterolateral; 7, second posterolateral; 8, third posterolateral; 9, inferior septals; 10, acute marginals. *Left coronary:* 11, left main; 12, proximal left anterior descending; 13, middle left anterior descending; 14, distal left anterior descending; 15, first diagonal (a, branch of first diagonal); 16, second diagonal; 17, septals (anterior septals); 18, proximal circumflex; 19, middle circumflex; 20, distal circumflex; 21, 22, and 23, first, second, and third obtuse marginals; 23, left atrioventricular; 24, 25, and 26, first, second, and third posterolaterals (in left- or balanced-dominant system); 27, left posterior descending (in left-dominant system); 28, ramus (ramus intermedius); 29, third diagonal. (From The BARI protocol. Protocol for the Bypass Angioplasty Revascularization Investigation. *Circulation* 1991;84:V1, with permission.)

Right-dominant Circulation

The right coronary artery gives rise to the conus branch (which supplies the right ventricular outflow tract) and one or more acute marginal branches (which supply the free wall of the right ventricle), whether or not the circulation is right-dominant. In the 85% of patients who have a right-dominant coronary artery, it goes on to form the AV nodal artery, the posterior descending, and the posterolateral left ventricular branches which supply the inferior aspect of the left ventricle and interventricular septum (Fig. 11.14). The left main trunk branches after a short (but variable) distance into the LAD and the circumflex coronary arteries. The LAD artery gives rise to septal branches, which curve down into the interventricular septum, as well as diagonal branches, which wrap over the anterolateral free wall of the left ventricle. Some patients have a “twin” LAD system, in which one trunk (frequently intramyocardial) supplies the entire septum and the other trunk runs on the surface of the heart, supplying all the diagonal branches. The circumflex artery courses clockwise in the AV groove (viewed from the apex) as it gives rise to one or more obtuse marginal branches which supply the lateral free wall of the left ventricle, but it does not reach the crux in patients with a right-dominant circulation. In some patients, a large intermedius or ramus medianus branch (neither a diagonal nor a marginal) may originate directly from the left main trunk, bisecting the angle between the LAD and circumflex arteries, to create a trifurcation pattern of the left main coronary artery. Regardless of whether the patient is right-or left-dominant, the sinus node originates as a proximal branch of the right coronary in 60% of patients and as a left atrial branch of the circumflex in the remaining 40% of patients.

Left-dominant Circulation

In 8% of patients, the coronary circulation is left-dominant; that is, the posterolateral left ventricular, posterior descending, and AV nodal arteries are all supplied by the terminal portion of the left circumflex coronary artery. In such patients, the right coronary artery is quite small and supplies only the right atrium and right ventricle. It may be important to visualize, as a potential source of right-to-left collaterals, but the small diameter of a nondominant right coronary artery predisposes it to damping and catheter-induced spasm (see later discussion), which make limited injections advisable.

Balanced-dominant Circulation

In about 7% of hearts, there is a codominant or balanced system, in which the right coronary artery gives rise to the posterior descending artery and then terminates, and the circumflex artery gives rise to all the posterior left ventricular branches and perhaps also to a parallel posterior descending branch that supplies part of the interventricular septum. In some patients, the supply to the inferior wall is further fractionated among a short posterior descending branch of the right coronary (which supplies the inferobase), branches of the distal circumflex (which supply the midinferior wall), and branches of the acute marginal (which extend to supply the inferoapex).

Anatomic Variants

Although these basic concepts describe the general pattern of the coronary circulation, it must be noted that there is considerable patient-to-patient variability in the size and position of the various coronary arterial branches (46). In 1% to 2% of patients, these coronary anatomic features are sufficiently divergent to qualify as *coronary anomalies.* Every operator must be thoroughly familiar with these anatomic anomalies and continually vigilant for their occurrence, lest failure to recognize an anomaly result in an incomplete and therefore inadequate examination. In a review of 126,595 cases from the Cleveland Clinic (47), the most common of these anomalies was separate ostia of the LAD and left circumflex arteries (0.41%). When this anomaly is present, the catheter usually sits with its tip in the LAD, although there is generally adequate spillover to opacify the circumflex. If not, separate cannulation of the circumflex may be necessary, using the next-larger size left Judkins catheter (e.g., JL5 instead of JL4) or a left Amplatz catheter. A similar situation may exist in the right coronary artery, where the conus branch may have a separate ostium whose separate cannulation may be necessary to demonstrate important collaterals when reflux during the right coronary injection is not adequate to opacify the conus (Fig. 11.16).

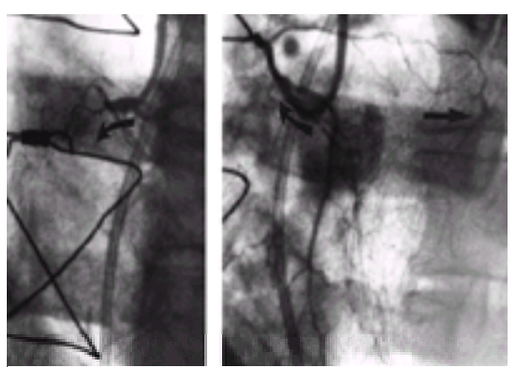

FIG. 11.16. Importance of adequate reflux or separate injection of the conus branch when it is a major source of collaterals. **Left,** Selective injection of the native right coronary artery showing proximal occlusion, with no filling of the conus branch. **Right,** Selective gentle injection into the conus branch shows extensive collaterals to the left anterior descending as well as the distal right coronary artery.

The next most common anomaly is origin of the circumflex from the right coronary artery or right sinus of Valsalva (0.37%). This should be suspected when the left main coronary artery is unusually long and a paucity of vessels to the lateral wall are identified. Careful review of the RAO left ventriculogram may show a “dot” of contrast material just behind the aortic valve when the anomalous circumflex runs posterior to the aorta (48). If an anomalous circumflex is not filled adequately during right coronary injection, it must be cannulated separately (usually with an AL1 catheter). We have seen patients in whom the only coronary lesion was located in such an anomalous circumflex, and failure to identify and opacify this vessel would have led to failure to diagnose and treat the problem. In another common variant, anomalous vessels (particularly the right coronary artery) may originate unusually high in the aortic root or out of the normal coronary plane (38), making them easier to cannulate with left Amplatz rather than right Judkins catheters. The left coronary may originate from the right sinus of Valsalva (Fig. 11.17), either as a separate ostium (49) or as part of a single coronary (50). Origin of a coronary artery from the “noncoronary” sinus of Valsalva is rare but has been reported (47,51). The main effect of these coronary anomalies is to test the patience, knowledge, and resourcefulness of the angiographer. Other anomalies, however, may themselves cause myocardial ischemia (even in the absence of atherosclerotic stenosis); they are described later in the section on nonathereosclerotic coronary artery disease.

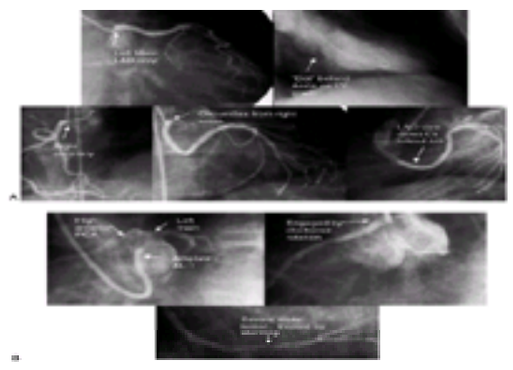

FIG. 11.17. A: Anomalous origin of the circumflex from the right coronary artery (RCA). Note the “long left main” *(upper left)* and absence of a circumflex during injection of the left coronary artery. Review of the right anterior oblique (RAO) left ventriculogram *(upper right)* shows the telltale “dot” behind the aortic root, created by an end-on look at the anomalous circumflex coursing behind the aorta. The right coronary originates normally *(lower left)*, with the anomalous circumflex *(lower center)* originating from the right sinus of Valsalva immediately posterior to the RCA origin, then coursing behind the aorta to reach the lateral wall of the left ventricle. The left anterior oblique (LAO) projection *(lower right)* shows the anomalous circumflex coursing behind the aorta. **B:** Anomalous origin of the right coronary from the left sinus of Valsalva. Nonselective injection through a Amplatz left (AL1) catheter in the left sinus *(upper left)* shows filling of both the left main and the high anterior right (RCA) coronary. The anomalous RCA is engaged by clockwise rotation of the catheter *(upper right)*, allowing successful stenting of the severe distal lesion *(bottom)*.

Angiographic Views

Accurate coronary diagnosis requires coronary injections in multiple views, to be sure that all coronary segments are seen clearly without foreshortening or overlap. The angulation of each view is given in two terms. The first term denotes *rotation.* For example, the term RAO designates a view in which the image intensifier is located over the patient's right anterior chest wall, and LAO refers to a view in which the image intensifier is located over the patient's left anterior chest wall. The second term denotes *skew*—the amount of angulation toward the patient's head (cranial) or foot (caudal). Although the full nomenclature of skew specifies first the source of the beam and then the location of the imaging device—such as “caudocranial,” to denote that the x-ray tube is toward the patient's feet and the image intensifier is located toward the patient's head—in practice this is simplified to give just the location of the imaging device. The term RAO caudocranial is thus stated as RAO-cranial.

When cradle systems were used in the 1970s, these views were usually limited to different degrees of left or right anterior obliquity in the transverse plane, including

the classic 60° LAO and 30° RAO projections (Fig. 11.14). To allow concurrent cranial angulation of the x-ray beam, cradle systems were modified by propping the patient's shoulders up on a foam wedge (hence the name “sit-up view”) to provide compound LAO-cranial projection. In the 1980s, cradle systems were abandoned in favor of systems in which the x-ray tube and image intensifier are mounted on a parallelogram or on a rigid U-arm supported by a rotating pedestal (see Chapter 2) to allow compound beam angulation in any combination of conventional transverse (LAO, RAO) and skew (cranial, caudal) angulation (Fig. 11.18). Although these views place increased demands on the generator and increase the amount of scattered radiation, there is no doubt that they have improved our ability to define coronary anatomy (52,53 and 54).

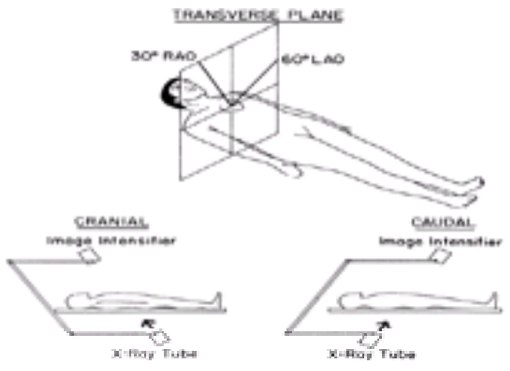

FIG. 11.18. Geometry of angulated views. Conventional coronary angiography was performed with angulation only in the transverse plane *(top)*, as demonstrated by the 60° left anterior oblique (LAO) and 30° right anterior oblique (RAO) views. Improved x-ray equipment now permits simultaneous cranial or caudal angulation in the saggital plane. Each view is named according to the location of the image intensifier, rather than by the older nomenclature, which specified the location of both the x-ray tube and intensifier. For example, “cranial” is equivalent to caudocranial.

Not all potential views are necessary in a given patient to constitute an adequate study. Rather, a series of screening views should be used as the foundation of the study, adjusted or supplemented by one or more additional views selected especially to more completely define suspicious areas. This requires the operator to interpret the coronary anatomy as each injection is made, or at least during in-room review from the digital storage system—rather than simply shooting a series of routine views and hoping that the study will prove adequate when reviewed later. Although some laboratories rely on a technician to set up shots and pan the table during coronary angiography, each operator should know how to do this, in order to develop a good understanding of how changes in gantry angulation influence the projected coronary anatomy. One valuable training tool in this respect is a simple wire model of the coronary anatomy which is viewed as it is moved into different angles (Fig. 11.19) (55). A computer program that simulates the effect of changing angles on the projected coronary anatomy is also available. Although there is no substitution for this type of “hands-on” learning, the discussion below is provided as a rough introduction.

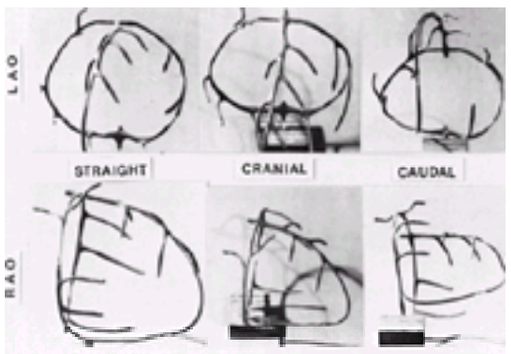

FIG. 11.19. Demonstration of angiographic projections using the author's coronary model. Left anterior oblique (LAO) and right anterior oblique (RAO) projections are photographed straight (i.e., with no cranial or caudal angulation) and with moderate cranial and moderate caudal angulation (see text for details).

Right Anterior Oblique Projections

For historic reasons relating to cradle systems, the screening views used in many laboratories were the straight LAO-RAO angulations. With the availability of more modern gantry systems, it is clear that certain cranial and caudal angulated views offer far better anatomic definition. Therefore, we generally avoid the straight 30° RAO projection of the left coronary artery, because it suffers from overlap and foreshortening of both the LAD and circumflex vessels (Fig. 11.19). Instead, we have made the RAO-caudal projection (0° to 10° RAO and 15° to 20° caudal) our initial view of choice in studying unstable patients, because it provides an excellent view of the left main bifurcation, the proximal LAD artery, and the proximal to middle circumflex artery. The second view we perform is a shallow RAO-cranial projection (0° to 10° RAO and 25° to 40° cranial), which provides a superior view of the middle and distal LAD, with clear visualization of the origins of the septal and diagonal branches. This shallow RAO cranial view is also quite good for examination of the distal right coronary artery or distal circumflex, because it effectively “unstacks” the posterior descending and posterolateral branches and projects them without foreshortening. It seldom, however, provides any useful information about the left main or circumflex coronary artery, because it causes them to be overlapped and foreshortened.

Left Anterior Oblique Projections

The conventional 60° LAO projection is limited by overlap and foreshortening of the left coronary artery, although it is very useful in the evaluation of the proximal and middle right coronary artery. The LAO-cranial view, created by the addition of 15° to 30° of cranial angulation, elongates the left main and proximal LAD arteries while projecting the intermedius or first diagonal branch downward off the proximal circumflex. If radiographic penetration in this view is difficult, reducing the LAO angulation to 30° to 40° usually allows the LAD artery to fall into the lucent wedge between the right hemidiaphragm and the spine. Alternatively, performing the cine run during a sustained maximal inspiration usually pulls the diaphragm down and improves x-ray penetration. The LAO-caudal view (40° to 60° LAO and 10° to 20° caudal) projects the left coronary artery upward from the left main in the appearance of a spider, and it usually offers improved visualization of the left main, proximal LAD, and proximal circumflex arteries. It is particularly valuable in patients whose heart has a horizontal lie (i.e., the origin of the left main artery projects at or below the proximal LAD artery in the standard LAO projection). This “spider view” (LAO-caudal) can often be enhanced by filming during maximal expiration, which accentuates a horizontal cardiac position and allows a better look from below, although it stresses the radiographic capacity of most older installations.

Posteroanterior and Left Lateral Projections

The straight posteroanterior (PA, or “0–0”) and left lateral projections tend to be underutilized in the era of complex angulation. Because the left main coronary artery curves from a more leftward to an almost anterior direction along its length, the *PA projection (sometimes referred to incorrectly as the “AP” projection)* frequently provides the best view of the left main ostium. On the other hand, the shallow RAO-caudal view frequently provides a better look at the more distal left main artery. The *left lateral projection* is particularly useful in examining the proximal circumflex and the proximal and distal LAD arteries, particularly when combined with slight (10° to 15°) cranial angulation. This projection also provides the best look at the anastomosis of a left internal mammary graft to the mid-distal LAD, and it offers an excellent look at the midportion of the right coronary artery, free of the excessive motion seen when this portion of the vessel is viewed in the straight RAO projection. The left lateral projection also has the advantage of allowing easy radiographic penetration in most patients when it is performed with both of the patient's hands positioned behind the head, although it generates the highest degree of backscatter to the operator given the proximity of the beam entry point on the patient's right side.

Over the past several years, operators in our laboratory have adopted a uniform sequence of these views, adjusting the exact angles slightly in each patient as

dictated by test puffs of contrast agent. Beginning with the left coronary artery, these views include

1. RAO-caudal to visualize the left main, proximal LAD, and proximal circumflex
2. RAO-cranial to visualize the middle and distal LAD without overlap of septal or diagonal branches
3. LAO-cranial to visualize the middle and distal LAD in an orthogonal projection
4. LAO-caudal to visualize the left main and proximal circumflex.

One or more supplemental views (PA, lateral-cranial, lateral-caudal) may then be taken to clarify any areas of uncertainty. The right coronary catheter is then placed, after which three screening views are obtained:

1. LAO to visualize the proximal right coronary artery
2. RAO-cranial to visualize the posterior descending and posterolateral branches
3. Lateral to visualize the middle right coronary artery.

Lesion Quantification

To quantify a coronary stenosis accurately, it must be seen in profile, free from artifact related to foreshortening or obfuscation by a crossing vessel. Multiple views are important, because many lesions leave a lumen that is markedly eccentric (elliptic rather than round) (56). When seen across its major axis, the width of the lumen may appear almost normal; the only clue to the severe degree of narrowing may be marked lucency, caused by thinning of the contrast column. Any such suspicious lesions must be examined in a variety of other projections to reveal their true severity and to distinguish the lucency caused by eccentric stenosis from a similar lucency that may be seen adjacent to an area of denser contrast (caused by tortuosity or overlapping vessels in the absence of any true abnormality at the site) through a perceptual artifact known as the Mach effect (57).

The ability of coronary angiography to quantify the degree of stenosis at different points in the coronary circulation is fundamentally limited by the fact that it consists of a “lumen-o-gram,” in which each stenosis can be evaluated only by comparison to an adjacent “reference” segment that is presumed to be free of disease. In fact, both intravascular ultrasound (56) (see Chapter 19) and pathologic examination (58) show that even segments that appear smooth on angiography may harbor substantial plaque. It is therefore important to have a sense of the normal caliber of the major coronary arteries: 4.5 ± 0.5 mm for the left main coronary artery, 3.7 ± 0.4 mm for the LAD, 3.4 ± 0.5 mm for a nondominant versus 4.2 ± 0.6 mm for a dominant circumflex, and 3.9 ± 0.6 mm for a dominant versus 2.8 ± 0.5 mm for a nondominant right coronary artery (59). By comparing the diameter of a presumably disease-free segment of coronary artery to the size of the diagnostic catheter (6F = 2 mm), the operator can identify vessels that fall below these normal size ranges and therefore may be diffusely diseased.

Other than the difficulty in finding a disease-free reference segment, another major problem in the interpretation of a coronary angiogram is deciding on the severity of any given stenosis. Both animal data (60) and human data (61) show that a stenosis that reduces the lumen diameter by 50% (hence reducing the cross-sectional area by 75%) is “hemodynamically significant” in that it reduces the normal three-to four-fold flow reserve of a coronary bed (Fig. 11.20). A 70% diameter stenosis (90% cross-sectional area) eliminates virtually any ability to increase flow above the resting level (see Chapter 18). Stenoses that reduce the lumen diameter by 90%, however, rarely exist without reducing antegrade flow (i.e., grade 1 or 2, rather than grade 3 normal flow, on the TIMI [Thrombolysis in Myocardial Infarction] scale). Other than the subjective TIMI flow grading system, Gibson et al. (62) have created norms for the number of cine frames (at 30 frames per second) required for contrast material to leave the catheter tip and reach standardized distal landmarks in each coronary artery (e.g., the LAD “mustache,” the first posterolateral branch of the right coronary). Contrast medium normally reaches these points in 20 frames for the RCA and 36 frames for the LAD. TIMI 2 (partial) flow corresponding to more than a doubling of those frame counts. Of course, even more precise data about hemodynamic lesion significance can be determined by performance of flow or pressure gradient measurements, at rest and during arteriolar vasodilation (e.g., after adenosine administration) to calculate the coronary flow or fractional flow reserve (63). Lesions that permit a flow increase of more than two-fold or that have a ratio of distal pressure to aortic pressure greater than 0.75 in the setting of peak flow after adenosine injection are generally considered not to be hemodynamically significant, and usually have a diameter stenosis less than 50% by quantitative angiography and no exercise perfusion defect on thallium scintigraphy (see Chapter 18).

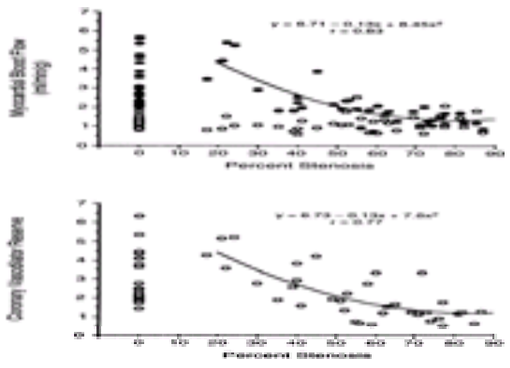

FIG. 11.20. Effect of coronary stenosis on myocardial blood flow and coronary vasodilator reserve. The top panel shows that resting flow *(open circles)* is well maintained at approximately 1 mL/min per gram of myocardium, throughout the range of evaluated diameter stenosis. The ability to increase flow during vasodilator stimulus *(closed circles)*, however, becomes impaired for stenosis greater than 50% and is virtually abolished at more than 70% stenosis. The bottom panel shows the vasodilator reserve (dilated flow/resting flow), which has a normal value of 3 to 4 but is reduced with stenosis greater than 50% and falls to 1 with stenosis greater than 70%. (From Uren NG, et al. Relation between myocardial blood flow and the severity of coronary artery stenosis. *N Engl J Med* 1994;330:1782, with permission).

In clinical practice, however, the degree of lesion stenosis usually is simply estimated visually from the coronary angiogram. The operator must develop a sense of what constitutes a 50%, 70%, or 90% diameter stenosis (Fig. 11.21). Although the process of visually estimating the degree of coronary stenosis may *seem* straightforward, it is subject to significant operator variability (the standard deviation for repeat estimates is up to 18%) (64), as well as a systematic form of “stenosis inflation” that causes operators to estimate a diameter stenosis that is roughly 20% higher than that measured by quantitative coronary angiography (65). A stenosis that measures 50% may typically be called 70%, and one that measures 70% may be called 90%.

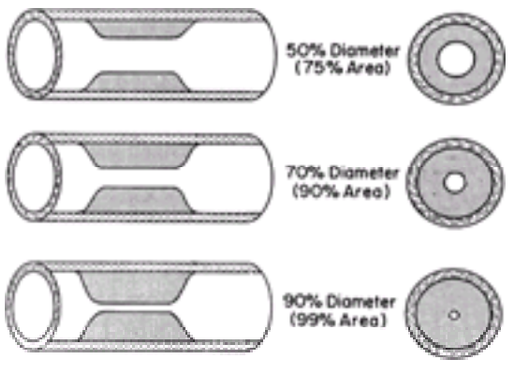

FIG. 11.21. Coronary stenoses of 50%, 70%, and 90% diameter reduction are shown in longitudinal and cross-section. The corresponding reductions in cross-sectional area are indicated in parentheses.

Tools are available to resolve this problem. The simplest is to project the coronary image on a wall-mounted viewing screen and to use inexpensive digital calipers

(available from machinist supply houses) to measure the relative diameters of the stenotic and reference segments (66). Percent stenosis then can be calculated as 100 × [1 – (stenosis diameter/reference diameter)] to provide a more accurate estimate. This technique also reduces the standard deviation for diameter stenosis 6% to 8% (64,66). Even greater precision can be obtained by using computer-assisted algorithms to perform automated edge detection on digitally acquired images to measure the coronary lumen with a standard deviation of less than 5% (67,68). The amount of variation in diameter stenosis readings for one study (69) using these different methods concurrently is shown in Fig. 11.22.

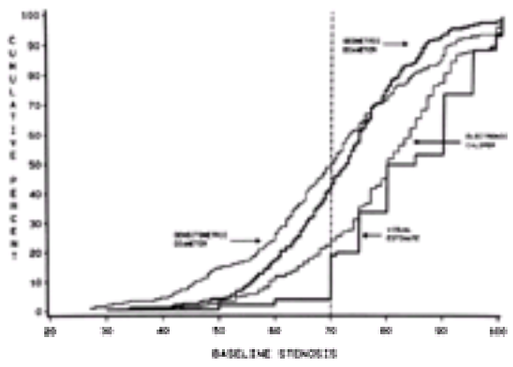

FIG. 11.22. In a series of 227 patients with single-vessel disease, visual estimates (*right curve*, average almost 90%) were consistently higher than either caliper measurements (average approximately 80%) or computer-assisted quantitative angiography by either geometric or densitometric techniques (*left curves*, average approximately 70% diameter stenosis). (From Folland ED, Vogel RA, Hartigan P, et al. Relation between coronary artery stenosis assessed by visual, caliper, and computer methods and exercise capacity in patients with single-vessel coronary artery disease. *Circulation* 1994;89:2005, with permission).

The good news is that angiographers who have trained their eye in actual stenosis quantification (by using digital calipers or computer-assisted quantitative coronary angiography) can then actually give visual estimates much closer to true measurements (70). This allows angiographers to be more uniform in their visual estimates and to move away from reporting physiologically impossible findings such as a 95% stenosis with normal distal flow. Until there is a “stenosis reading reform,” so that those of us who call such lesions accurately (e.g., 70%) will not be accused of intervening on mild lesions, there can be no substitute for “seeing the films yourself” before making any clinical decisions!

It has also become important to evaluate lesion morphology more accurately from the coronary angiogram. Features such as eccentricity, ulceration, and thrombus may be associated with unstable clinical patterns (71,72), and features such as calcification, eccentricity, or thrombus may influence the choice of catheter intervention. Many of these features can be recognized from careful study of high-quality cineangiograms, although angiography is clearly not as sensitive to these features as intravascular ultrasound (73) or angioscopy (for thrombus or dissection) (74). It may also be difficult to predict the physiologic significance of a coronary lesion from angiography alone, in which case it may need to be supplemented by other techniques such as direct flow or distal pressure measurements (63). Finally, the absence of lesions that narrow the coronary lumen by more than 50% does not necessarily confer immunity from subsequent coronary events, because it is frequently a less severe stenotic lesion that has a large lipid core and a thin fibrous cap that predisposes to subsequent plaque rupture and the resulting coronary thrombosis (75). Despite these recognized limitations in quantification and morphology assessment, contrast coronary angiography remains the clinical standard on which lesions are evaluated and decisions are made regarding the need for (and best mode of providing) revascularization in the patient with ischemic heart disease.

Coronary Collaterals

In reviewing the coronary angiogram, one basic principle is that there should be evident blood supply to all portions of the left ventricle. Previously occluded vessel branches are usually manifested as truncated stumps, but no stump may be evident if there has been a flush occlusion at the origin of the involved vessel. These occluded or severely stenotic vessels are seen frequently to fill late in the injection by antegrade (so-called bridging) collaterals or collaterals that originate from the same (intracoronary) or an adjacent (intercoronary) vessel; this phenomenon is reviewed in an excellent paper by Levin (76) and illustrated in Fig. 11.23, Fig. 11.24 and Fig. 11.25. Finally, coronary occlusion may manifest in some patients simply as an angiographically arid area to which there is no evidence of either antegrade or collateral flow and no evident vascular stump. If such an area fails to show regional hypokinesis on the left ventriculogram, however, the operator should search carefully for blood supply by way of anomalous vessels or unopacified collaterals (i.e., a separate origin conus branch that was not opacified during the main right coronary artery injections), because the myocardium cannot continue to function normally with no visible means of support. Functioning collaterals can maintain a coronary wedge pressure that averages almost 40% of mean aortic pressure (77,78), thereby maintaining myocardial viability in the collateral-fed distribution. Along with other measures of retained or augmentable wall motion, redistributing defects on perfusion imaging, and positron emission tomographic (PET) evidence of ongoing glucose metabolism, the angiographic presence of collateral flow to an area in the distribution of an occluded coronary artery is one of the strongest evidences of ongoing myocardial viability and an important factor in determining the best revascularization strategy.

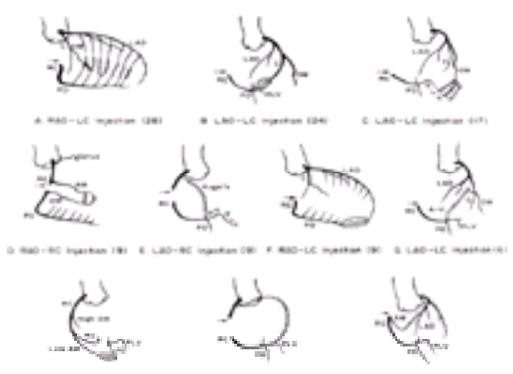

FIG. 11.23. Ten collateral pathways observed in patients with right coronary (RC) obstruction (total occlusion or greater than 90% stenosis). LAD, left anterior descending; C, circumflex; OM, obtuse marginal; PD, posterior descending; PLV, posterior left ventricular branch; AM, acute marginal branch of right coronary artery; A-V, atrioventricular nodal; LC, left coronary. Numbers in parentheses represent numbers of cases in this series. (From Levin DC. Pathways and functional significance of the coronary collateral circulation. *Circulation* 1974;50:831. By permission of the American Heart Association, Inc.)

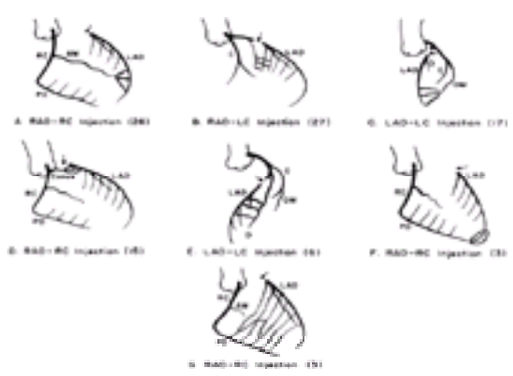

FIG. 11.24. Seven collateral pathways observed in patients with left coronary artery obstruction. Abbreviations and format are the same as in Fig. 11.23. (From Levin DC. Pathways and functional significance of the coronary collateral circulation. *Circulation* 1974;50:831. By permission of the American Heart Association, Inc.)

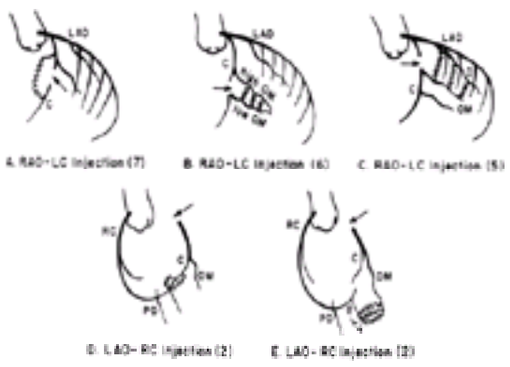

FIG. 11.25. Five collateral pathways observed in patients with circumflex coronary artery obstruction. Abbreviations and format are the same as in Fig. 11.23. (From Levin DC. Pathways and functional significance of the coronary collateral circulation. *Circulation* 1974;50:831. By permission of the American Heart Association, Inc.)

Although it is uncommon, what appears to be a network of collaterals may be the vascular supply to an organized thrombus (in the left ventricle or left atrium) or a cardiac tumor. Those entities should be suspected when filling of an apparent collateral network is seen in the absence of occlusion or severe stenosis of the normal supply to a myocardial territory.

NONATHEROSCLEROTIC CORONARY ARTERY DISEASE

Although atherosclerotic stenosis is by far the most common pathologic process responsible for myocardial ischemia, the angiographer must be aware of a variety of other potential causes (79). These include certain congenital anomalies of coronary origin (46,80,81 and 82), such as an anomalous coronary artery that courses between the aorta and the pulmonary artery, in which flow may be compromised by deformation of the ostium or compression of the proximal vessel, potentially even causing sudden death. Other abnormalities include coronary fistulas (Fig. 11.26), coronary aneurysms (83,84), and muscle bridges (Fig. 11.27) (85,86). *Coronary fistulas*, connections mostly from a coronary artery to the right ventricle, right atrium, pulmonary artery, or coronary sinus, are found in roughly 0.1% of patients coming to cardiac catheterization. When they are large (or in the setting of proximal coronary disease), these fistulas may cause chronic volume overload or myocardial ischemia and must be closed, using surgery or newer catheter techniques (e.g., embolization coils, covered stents) (87). Smaller, asymptomatic fistulas may close spontaneously and can be managed conservatively (88). *Muscle bridges* are sections of a coronary artery (almost always the LAD) that run under a strip of left ventricular muscle, which compresses the lumen during ventricular systole despite a normal appearance during diastole (85,86). Similar systolic compression of the first septal branch (saw-toothing) is also seen in many patients with hypertrophic cardiomyopathy (89). *When one of these congenital anomalies is present in a patient with ischemic symptoms in whom catheterization has failed to demonstrate the expected finding of coronary atherosclerosis, the angiographer should be able to recognize it as a potential cause of ischemia and recommend additional functional testing with an eye toward surgical or catheter-assisted repair (*e.g.*, fistula coil embolization, muscle bridge stent placement).*

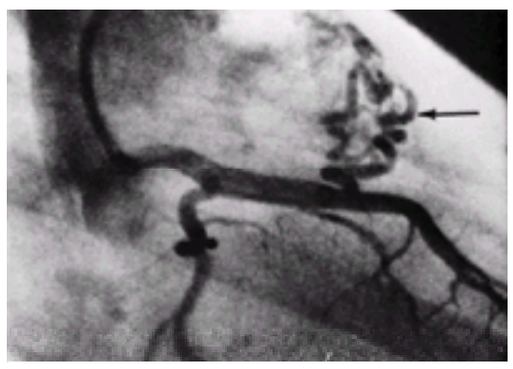

FIG. 11.26. Coronary artery fistula *(arrow)* between the middle left anterior descending coronary artery and the pulmonary artery, shown in the right anterior oblique view.

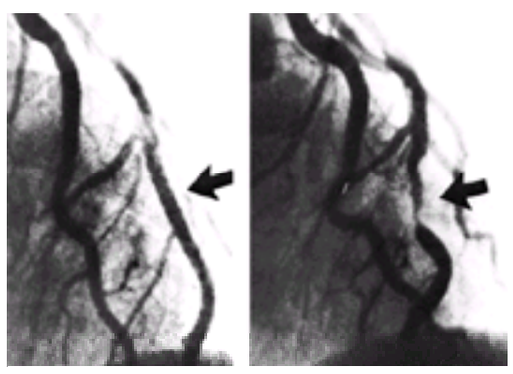

FIG. 11.27. Muscle bridge. Moderately severe muscle bridge of the left anterior descending coronary artery *(arrows)* as seen in diastole *(left)* and systole *(right)*.

The coronary arteries may also be affected by medium-size-vessel *vasculitis* (90), including polyarteritis nodosa and the mucocutaneous lymph node syndrome (Kawasaki disease). The latter is largely a childhood illness, in which coronary arteritis may lead to aneurysm, stenosis, or thrombosis that, before the use of high-dose gamma globulin to treat the acute illness, was often fatal (usually in the first month of the illness). When coronary aneurysms are found in adults, it may be difficult to determine whether they represent atherosclerotic damage to the vessel wall or the remainders of childhood Kawasaki disease (83). However, the treatment for the stenotic lesions (bypass or catheter-based intervention) is the same regardless of the cause. Although not an arteritis, *cardiac allograft vasculopathy* (91) is one of the most troublesome long-term complications of heart transplantation. The mechanism seems to be an immune-mediated diffuse vascular proliferative response involving distal as well as proximal coronary arteries, with superimposed focal lesions of the proximal vessels. The latter may be amenable to catheter-based revascularization. Patients who have received prior mantle radiation therapy for Hodgkin disease may be at risk for *radiation-induced coronary stenosis* (92), particularly of the left and right coronary ostia and the proximal left coronary artery, up to 20 years after completing their course of therapy. The pathology is most commonly fibrotic contraction of the vessel wall, rather than intimal proliferation or plaque formation.

Finally, some patients who come to catheterization have no demonstrable coronary abnormality to account for their clinically suspected ischemic heart disease. Although angina-like pain can be seen in patients with noncoronary cardiac abnormality (e.g., mitral valve prolapse, hypertrophic cardiomyopathy, aortic stenosis, myocarditis) or extracardiac conditions (esophageal dysmotility (93), cholecystitis), one must also consider the possibility of coronary vasospastic disease (94).

Coronary Vasospasm

Vasospasm of an epicardial coronary artery typically presents as variant (Prinzmetal) angina in which episodes of rest pain occur despite well-preserved effort

tolerance at other times (94). An ECG recorded during an episode of spontaneous pain usually shows ST elevation in the territory supplied by the vasospastic artery. Absence of a significant coronary lesion in such a patient confirms the diagnosis of variant angina due to focal coronary spasm (Fig. 11.28). In these patients, coronary angiography is performed mainly to look at the extent of underlying atherosclerosis (95); we generally do not attempt to provoke spasm in such patients as was once done to evaluate drug therapy (96). When the diagnosis of variant angina is uncertain and a patient with troublesome chest pain fails to manifest sufficient disease to explain its origin, however, provocative testing for coronary spasm may be helpful.

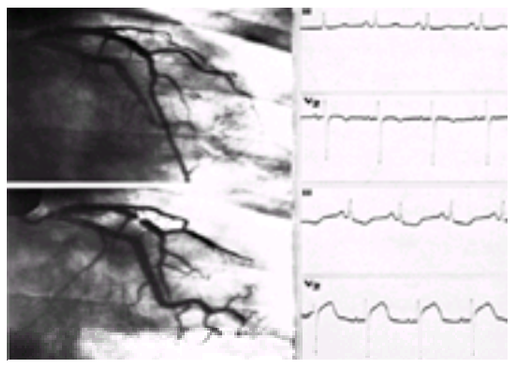

FIG. 11.28. True coronary spasm. Intense focal vasospasm of the left anterior descending coronary artery is shown in right anterior oblique projection in a patient with variant angina. Note the absence of a significant underlying atherosclerotic stenosis in the top panel, the absence of vasoconstriction of other vessel segments, and the marked ST elevation in the anterior leads during the spontaneous vasospastic episode. (From Baim DS, Harrison DC. Nonatherosclerotic coronary heart disease. In: Hurst JW, ed. The Heart, 5th ed. New York: McGraw-Hill, 1985, with permission.)

If provocational testing for coronary spasm is contemplated, the patient should be withdrawn from calcium channel blockers for at least 24 hours and long-acting nitrates for at least 12 hours before the study and should not be premedicated with either atropine or sublingual nitroglycerin. Ongoing therapy with any of these agents may render provocative tests falsely negative (96). Although a variety of provocative tests have been used (methacholine, epinephrine and propranolol, hyperventilation and tris-buffer, cold pressor), the most commonly used provocative agents are ergonovine and methylergonovine maleate (Methergine, Sandoz, East Hanover, NJ) (97,98 and 99), stimulants of the a-adrenergic and serotonin receptors in coronary vascular smooth muscle. Ergonovine is no longer generally available in the United States, and the availability of methylergonovine is limited. If it is not available, one easy alternative provocative test is hyperventilation (100), done vigorously for 6 minutes in the early morning (between 6 and 8 a.m., when spasm is more active). This produces spasm in most patients with variant angina and can obviate the need for further drug testing. Although this finding is 100% specific for coronary spasm, it is only 62% sensitive. If spasm is suspected but has not been elicited by hyperventilation, and if methylergonovine is not available, further testing can be performed using intracoronary acetylcholine (50 to 100 µg injected into the left coronary or 20 to 50 µg injected into the right coronary artery).

Testing for coronary spasm should be performed only after baseline angiographic evaluation of both the left and right coronary arteries. It should not be performed in patients with severe hypertension or severe anatomic cardiac pathology (left ventricular dysfunction, left main or multivessel disease, aortic stenosis). As an example, our protocol for using ergonovine calls for a total of 0.4 mg (400 µg = 2 ampules) of ergonovine maleate to be diluted to a total volume of 8 mL in a 10-mL syringe that is appropriately labeled. The provocative test consists of graded intravenous administration of 1 mL (0.05 mg), 2 mL (0.10 mg), and 5 mL (0.25 mg) of this mixture at 3- to 5-minute intervals. Parenteral nitroglycerin (100 to 200 µg/mL) must be premixed and loaded in a labeled syringe before the testing is begun. At 1 minute before each ergonovine dose, the patient is interrogated about symptoms similar to those of her or his clinical complaint, and a 12-lead ECG is recorded. After each ECG, coronary angiography is performed, looking either at both arteries or only at the artery of highest clinical suspicion for vasospasm. In the absence of clinical symptoms, ECG changes, or focal coronary vasospasm exceeding 70% diameter reduction, the next ergonovine dose is administered, and the cycle is repeated until the total dose of 0.4 mg has been given. Some operators have employed an *intracoronary* methylergonovine administration protocol, in which doses of 5 to 10 µg are given into a coronary artery, and after 3 minutes imaging studies are performed before a second dose is given (maximal total dose 50 µg). This may be advantageous in that it produces less systemic effect (e.g., hypertension, esophageal spasm).

If provocative testing produces *clinical* symptoms, but no ECG changes or angiographic evidence of vasospasm in either coronary artery, an alternative diagnosis such as esophageal dysmotility is suggested (93). Even if there are no symptoms or ECG changes, both coronary arteries should be opacified at the end of the provocative test, and any generalized vasoconstrictor effect should be terminated by administration of nitroglycerin. Coronary artery spasm may occur in two vessels simultaneously (Fig. 11.29), and visualization of only one vessel may fail to adequately assess the magnitude of the vasospastic response. The provocative test should be considered positive only if focal spasm (greater than 70% diameter stenosis) occurs and is associated with clinical symptoms and/or ECG changes. The patient is then treated immediately with parenteral nitroglycerin, 200 µg administered either by vein or, preferably, directly into the spastic coronary artery. The involved artery should then be reopacified 1 minute after nitroglycerin administration, to document the resolution of spasm and the extent of underlying atherosclerotic stenosis. The operator should be prepared to use additional doses of parenteral nitroglycerin, sublingual nifedipine, or sodium nitroprusside to treat refractory spasm or the occasional severe hypertensive reaction that can occur after ergonovine administration. Low doses of intracoronary verapamil (100 to 200 µg) or diltiazem (500 to 1,000 µg) have also proved useful in refractory spasm, although care must be taken to avoid excessive bradycardia or myocardial depression. Temporary pacing and defibrillatory equipment should also be available to treat the bradyarrhythmias or tachyarrhythmias that sometimes accompany coronary spasm. Because finding spasm is so uncommon now that the syndrome is detected clinically in most patients, and because it is treated so effectively by calcium channel blockers, the risk of ergonovine testing to evaluate patients with atypical symptoms and minimal fixed coronary disease is remarkably low. In the Duke study of ergonovine testing in 3,447 patients without significant coronary disease or variant angina, significant complications occurred in only 11 patients (0.03%), including myocardial infarction in 4 patients and ventricular tachycardia/ventricular fibrillation in 7 (101).

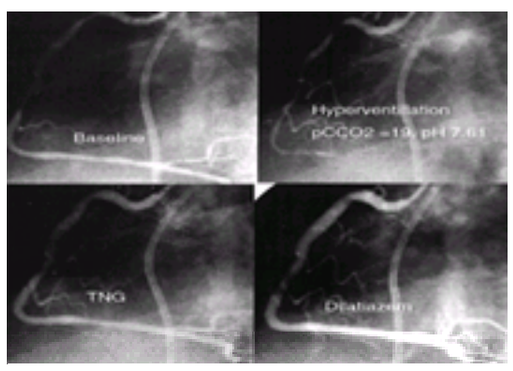

FIG. 11.29. This 37-year-old man was admitted with rest pain and ST-segment elevation in the inferior leads. Emergency catheterization was performed for presumed acute myocardial infarction within 30 minutes after presentation *(upper left)*. It disclosed a dominant right coronary artery with only mild disease at a time when pain had resolved after nitrate and heparin therapy. Hyperventilation (30 breaths per minute for 5 minutes) was performed with reduction of the partial pressure of carbon dioxide (PCO_2) to 19 mm Hg and elevation of the pH to 7.61, resulting in provocation of occlusive focal spasm of the distal right coronary artery with return of chest pain and ST segment elevation *(upper right)*. Relief of vasospasm and marked general dilation of the right coronary artery were produced by intracoronary administration of trinitroglycerin 200 µg *(lower right)* and diltiazem 500 µg *(lower right)*.

Several additional comments about ergonovine are in order. Our group avoids ergonovine testing in patients with severe atherosclerotic stenosis (80% or greater), in whom spasm is not required to explain the clinical symptoms. In these patients, however, we frequently do repeat coronary angiography of the stenotic vessel after the intracoronary administration of 200 mg of nitroglycerin, to exclude the possibility that spontaneous focal vasospasm is contributing to the appearance of severe atherosclerotic stenosis. Second, the operator should be aware that the positivity rate of ergonovine testing depends strongly on which patients are studied; the test is almost always positive in patients with known variant angina (if their disorder is active and medications have been withheld) and is positive in approximately one third

of patients with clinically suspected variant angina, but it is positive in fewer than 5% of patients whose symptoms do not suggest variant angina (99). The Duke group (101) reported an overall positivity rate of 4% in such patients, with two independent predictors of a positive test: mild to moderate disease on the angiogram (spasm often takes place at the point of such disease) and a history of smoking, whose presence increased the positivity rate to 10%. It is also important to distinguish the intense focal spasm seen in patients with variant angina from the normal mild (15% to 20%) diffuse coronary narrowing seen as a pharmacologic response to ergonovine in normal patients (102). True coronary spasm must also be distinguished from spasm induced by mechanical interventions such as rotational atherectomy (see Chapter 28) or catheter tip spasm (Fig. 11.30). Catheter tip spasm is most common in the right coronary artery, is not associated with clinical symptoms or ECG changes, and does not indicate variant angina (103). It should be recognized as such, however, and treated by withdrawal of the catheter, administration of nitroglycerin, and nonselective or cautious repeat selective opacification of the involved vessel, to avoid mistaking catheter-tip spasm for an atherosclerotic lesion. Spasm should also be distinguished from a “pleating” artifact that may occur when a curved artery is straightened out by a stiff guidewire (Fig. 11.31), causing folds of the vessel wall to impinge on the lumen. Pleating is refractory to nitroglycerin but resolves immediately when the stiff guidewire is withdrawn (104).

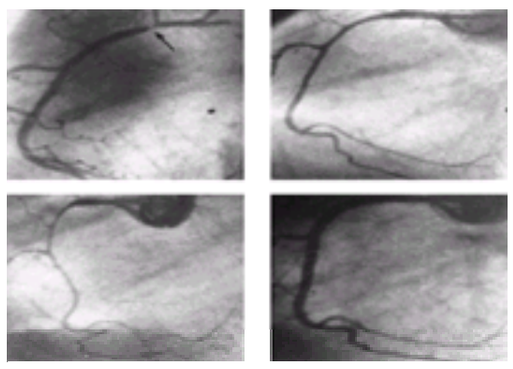

FIG. 11.30. Vasomotor changes not representing true coronary spasm. During right coronary catheterization with a Judkins catheter *(upper left)*, this patient developed severe catheter-tip spasm. Recatheterization 24 hours later with an Amplatz catheter *(upper right)* showed neither catheter-tip spasm nor an atherosclerotic stenosis. After administration of ergonovine 0.4 mg, marked diffuse coronary narrowing was observed *(lower left)*, without angina or electrocardiographic changes. After the intracoronary administration of nitroglycerin 200 µg *(lower right)*, there is marked diffuse vasodilation.

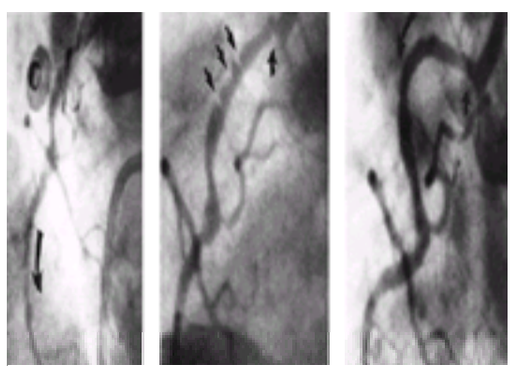

FIG. 11.31. Right coronary artery “pleating” artifact. Baseline injection *(left)* shows diffuse disease in this tortuous right coronary artery selected for rotational atherectomy. Middle panel shows straightening of the proximal vessel by the stiff “type C” wire, creating three areas of infolding of the vessel wall *(arrows)*, as well as the appearance of ostial stenosis *(curved arrow)*. Immediately on withdrawal of the guidewire, the artery returned to its baseline curvature, and these defects resolved *(arrows)*.

Abnormal Coronary Vasodilator Reserve

Evidence has been accumulating that the population of patients with angina and angiographically normal coronary arteries may contain a subgroup of patients who have myocardial ischemia on the basis of abnormal vasodilator reserve. Despite angiographic normality, intravascular ultrasound examination may show normal vessel wall architecture, intimal thickening, or atheromatous plaque (84). In these patients, coronary blood flow (as described in Chapter 18) may fail to rise normally with pacing tachycardia or exercise, and the coronary vascular resistance is increased abnormally (105). Also, many of these patients show an abnormal rise in left ventricular end-diastolic pressure after pacing tachycardia and show less lactate consumption than normal subjects in response to pacing tachycardia (106). A failure of small vessel coronary vasodilation, inappropriate vasoconstriction at the arteriolar level, or functional abnormalities of capillary endothelial cells in releasing endothelium-derived relaxing factor (EDRF) have been postulated to account for these findings. Many patients with so-called syndrome X respond at least partially to treatment with a calcium channel blocker, but other patients show no clear flow or contractile abnormality, so that the primary problem may be simply increased sensitivity to pain (11).

MISTAKES IN INTERPRETATION

An inexperienced operator often produces an incomplete or uninterpretable study, especially if poor equipment is used. Such an operator is also likely to misinterpret the angiographic findings, with potentially serious clinical consequences. The following discussion summarizes some of the most common pitfalls that may lead the inexperienced coronary angiographer to mistaken conclusions.

Inadequate Number of Projections

There is no standard number of projections that will always provide complete information. Each major vessel must be viewed in an isolated fashion as it stands apart from other vessels. Usually, the angulated views discussed earlier in this chapter are necessary to visualize clearly the anatomy of the proximal LAD and circumflex arteries.

Inadequate Injection of Contrast Material

The inexperienced operator or assistant has a tendency to hold back on the volume and force of injection into the coronary circulation. This results in inadequate or intermittent, pulsatile opacification of the coronary arterial tree, because contrast flow fails short of peak coronary flow during diastole. There is inadequate mixing of contrast agent and blood, and pockets of nonradiopaque blood in such inadequate injections may even give the appearance of arterial narrowing.

Superselective Injection

It is not uncommon to catheterize the LAD or circumflex coronary artery superselectively, especially when the left main coronary artery is short and its bifurcation is early. To the inexperienced operator, this may give the impression of total occlusion of the nonvisualized vessel (e.g., if only the circumflex artery is opacified, the operator may conclude that the LAD artery is occluded). If adequate filling of the noncannulated vessel cannot be achieved by reflux, selective cannulation of the LAD may be obtained by counterclockwise rotation or use of a Judkins catheter of the next smaller size (e.g., JL3.5), whereas selective cannulation of the circumflex may be obtained by clockwise rotation or use of the next larger size (e.g., JL5). With the right coronary artery, superselective injection may occur if the catheter tip is too far down the vessel, leading to failure to visualize the conus and sinus node arteries. Because these are important sources of collateralization of the left coronary system, important information may be missed (Fig. 11.13). Injection that is adequate to provide a continuous (nonpulsatile) reflux of contrast agent back into the sinus

of Valsalva helps the operator to recognize vessels that originate proximally to the catheter tip and thereby avoid the interpretation error of superselective injection.

Selective cannulation of a coronary artery may also fail to detect significant ostial stenosis, particularly if the catheter tip lies beyond the lesion and adequate contrast reflux is not produced. If ostial stenosis is suspected (e.g., if there is partial ventricularization or damping), we have found it helpful to perform a final injection during withdrawal of the catheter from the ostium (Fig. 11.32).

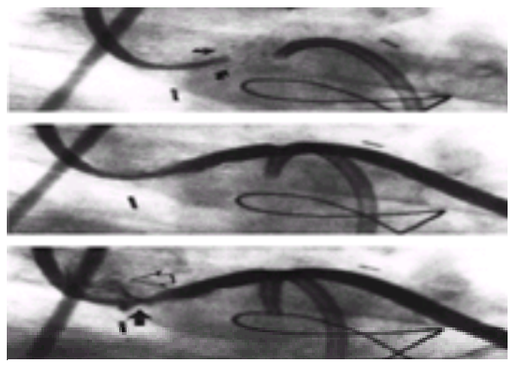

FIG. 11.32. Masking of ostial stenosis during superselective cannulation. Ostial stenosis of previously stented vein graft is not apparent with the tip of the catheter well beyond the stenosis *(top and middle panels)*. Continued injection during catheter withdrawal *(bottom panel)* causes reflux into the aorta *(solid arrow)* and clearly shows significant ostial stenosis.

Catheter-induced Coronary Spasm

Coronary artery spasm may be related to the catheter itself, possibly caused by mechanical irritation and a myogenic reflex (Fig. 11.30). It is seen most commonly when the right coronary artery is engaged selectively, although it may occur rarely in the LAD artery as well. Although catheter-tip spasm can occur with either the brachial or femoral approach, it is probably more common with the right Judkins catheter, especially if the catheter tip enters the right coronary ostium at an angle and produces tenting of the proximal vessel. If coronary narrowing suggests the occurrence of spasm to the operator, sublingual, intravenous, or intracoronary nitroglycerin should be given and the injection repeated.

Congenital Variants of Coronary Origin and Distribution

This topic has been discussed earlier in this chapter, but it bears reemphasis. Variation in origin and distribution of the coronary artery branches may confuse the operator and lead to a mistaken diagnosis of coronary occlusion. For example, a small right coronary artery that terminates in the AV groove well before the crux may be interpreted as an abnormal or occluded artery, whereas it is a normal finding in 7% to 10% of human hearts. Double ostia of the right coronary artery or origin of the circumflex artery from the right coronary artery may be similarly confusing and lead to misdiagnosis.

Myocardial Bridges

As discussed earlier, coronary arteries occasionally dip below the epicardial surface under small strips of myocardium. During systole, the segment of the artery surrounded by myocardium is narrowed and appears as a localized stenosis. These myocardial bridges occur most commonly in the distribution of the LAD artery and its diagonal branches. The key to recognition of these bridges is that the apparent localized stenosis returns to normal during diastole. Studies using the flow wire (see Chapter 18) show clear derangement in phasic flow dynamics in muscle bridge segments, and their normalization by stent placement. Although some severe muscle bridges can therefore cause true myocardial ischemia under certain circumstances, they are seen in at least 5% of normal angiograms obtained in patients with no evidence of ischemia in the LAD territory.

Total Occlusion

If a coronary artery or branch is totally occluded at its origin, it may not be visualized, and the occlusion may be missed. If the occlusion is flush with the parent vessel, no stump will be seen. Such occlusions are recognized primarily by visualization of the distal segment of the occluded vessel by means of collateral channels or by noting the absence of the usual vascularity seen in a particular portion of the heart.

CHAPTER REFERENCES

1. Kennedy RH, Kennedy MA, Frye RL, et al. Cardiac-catheterization and cardiac-surgical facilities: use, trends and future requirements. *N Engl J Med* 1982;307:986.
2. Scanlon PJ, Faxon DP, Audet A, et al. AHA/ACC guidelines or coronary angiography: a report of the ACC/AHA Task Force on Practice Guidelines. *J Am Coll Cardiol* 1999;33:1756.
3. Botnar RM, Stuber M, Danias PG, et al. Improved coronary artery definition with T2-weighted, free-breathing, three dimensional coronary MRA. *Circulation* 1999;99:3139.
4. Achenbach S, Moshage W, Ropers D, et al. Value of electron-beam computed tomography for the noninvasive detection of high-grade coronary-artery stenoses and occlusions. *N Engl J Med* 1998;339:1964.
5. Davies RF, Goldberg AD, Forman S, et al. Asymptomatic Cardiac Ischemia Pilot (ACIP) Study two-year follow-up: outcomes of patients randomized to initial strategies of medical therapy versus revascularization. *Circulation* 1997;95:2037.
6. The TIMI IIIB Investigators. Effects of tissue plasminogen activator and a comparison of early invasive and conservative strategies in unstable angina and non-Q wave myocardial infarction: results of the TIMI IIIB trial (Thrombolysis in Myocardial Ischemia). *Circulation* 1994;89:1545.
7. Miltenberg AJM, et al. Incidence and follow-up of Braunwald subgroups in unstable angina pectoris. *J Am Coll Cardiol* 1995;25:1286.
8. Ryan TJ, Anderson JL, Antman EM, et al. ACC/AHA guidelines for the management of patients with acute myocardial infarction: executive summary. *Circulation* 1996;94:2341.
9. The TIMI Study Group. Comparison of invasive and conservative strategies after treatment with intravenous tissue plasminogen activator in acute myocardial infarction. *N Engl J Med* 1989;320:618.
10. Spaulding CM, Joly L, Rosenberg A, et al. Immediate coronary angiography in survivors of out-of-hospital cardiac arrest. *N Engl J Med* 1997;336:1629.
11. Panza JA, Laurienzo JM, Curiel RV, et al. Investigation of the mechanism of chest pain in patients with angiographically normal coronary arteries using transesophageal dobutamine stress echocardiography. *J Am Coll Cardiol* 1997;29:293.
12. Eagle KA, et al. Guidelines for perioperative cardiovascular evaluation for noncardiac surgery (report of the ACC/AHA Task Force on Practice Guidelines). *J Am Coll Cardiol* 1996;27:910.
13. Neufeld NH, Blieden LC. Coronary artery disease in children. *Prog Cardiol* 1975;4:119.
14. Roberts WC. No cardiac catheterization before cardiac valve replacement: a mistake. *Am Heart J* 1982;103:930.
15. Baim DS, Kuntz RE. Appropriate uses of angiographic follow-up in the evaluation of new technologies for coronary intervention. *Circulation* 1994;90:2560.
16. Conti CR. Coronary arteriography. *Circulation* 1977;55:227.
17. Noto TJ, Johnson LW, Krone R, et al. Cardiac catheterization 1990: 1 report of the registry of the Society for Cardiac Angiography and Interventions. *Cathet Cardiovasc Diagn* 1991;24:75.
18. Fierens E. Outpatient coronary arteriography. *Cathet Cardiovasc Diagn* 1984;10:27.
19. Maher PR, Young C, Magnusson PT. Efficacy and safety of outpatient cardiac catheterization. *Cathet Cardiovasc Diagn* 1987;13:304.
20. Lee JC, et al. Feasibility and cost-saving potential of outpatient cardiac catheterization. *J Am Coll Cardiol* 1990;15:378.
21. Talley JD. The cost of performing diagnostic cardiac catheterization. *J Intervent Cardiol* 1994;7:273.
22. Kohli RS, Vetrovec GW, Lewis SA, et al. Study of the performance of 5 French and 7 French catheters in coronary angiography: a functional comparison. *Cathet Cardiovasc Diagn* 1989;18:131.
23. Judkins MP. Selective coronary arteriography: a percutaneous transfemoral technique. *Radiology* 1967;89:815.
24. Amplatz K, Formanek G, Stanger P, et al. Mechanics of selective coronary artery catheterization via femoral approach. *Radiology* 1967;89:1040.
25. Fizgibbon GM, Kafka HP, Leach AJ, et al. Coronary bypass graft fate and patient outcome: angiographic follow-up of 5,065 grafts related to survival and reoperation in 1,388 patients during 25 years. *J Am Coll Cardiol* 1996;28:616.
26. Eisenhauer TL, Collier E, Cambier PA. Beneficial impact of aorto-coronary graft markers on post-operative angiography. *Cathet Cardiovasc Diagn* 1997;40:249.
27. Kuntz RE, Baim DS. Internal mammary angiography: a review of technical issues and newer methods. *Cathet Cardiovasc Diagn* 1990;20:10.
28. Ayres RW, et al. Transcatheter embolization of an internal mammary artery bypass graft sidebranch causing coronary steal syndrome. *Cathet Cardiovasc Diagn* 1994;31:301.
29. Breal JA, et al. Coronary-subclavian steal: an unusual cause of angina pectoris after successful internal mammary artery bypass grafting. *Cathet Cardiovasc Diagn* 1991;24:274.
30. Bilazarian SD, Shemin RJ, Mills RM. Catheterization of coronary artery bypass graft from the descending aorta. *Cathet Cardiovasc Diagn* 1990;21:103.
31. Mills NL, Everson CT. Right gastroepiploic artery: a third arterial conduit for coronary artery bypass. *Ann Thorac Surg* 1989;47:706.
32. Suma H, et al. The right gastroepiploic artery graft: clinical and angiographic mid-term results in 200 patients. *J Thorac Cardiovasc Surg* 1993;105:615.
33. Tanimoto Y, et al. Angiography of right gastroepiploic artery for coronary artery bypass graft. *Cathet Cardiovasc Diagn* 1989;16:35.
34. Sones FM, Shirey EK. Cine coronary arteriography. *Mod Concepts Cardiovasc Dis* 1962;31:735.
35. Schoonmaker FW, King SB. Coronary arteriography by the single catheter percutaneous femoral technique, experience in 6,800 cases. *Circulation* 1974;50:735.

36. Ovitt T, et al. Electrocardiographic changes in selective coronary arteriography: the importance of ions. *Radiology* 1972;102:705.
37. Tragardh B, Bove AA, Lynch PR. Mechanism of production of cardiac conduction abnormalities due to coronary arteriography in dogs. *Invest Radiol* 1976;11:563.
38. Paulin S, Adams DF. Increased ventricular fibrillation during coronary arteriography with a new contrast medium preparation. *Radiology* 1971;101:45.
39. Lasser EC, et al. Pretreatment with corticosteroids to alleviate reactions to intravenous contrast material. *N Engl J Med* 1987;317:845.
40. Parfrey PS, et al. Contrast material-induced renal failure in patients with diabetes mellitus, renal insufficiency, or both. *N Engl J Med* 1989;329:143.
41. Ritchie JL, et al. Use of nonionic or low osmolar contrast agents in cardiovascular procedures (ACC Position Statement). *J Am Coll Cardiol* 1993;21:269.
42. Harvey JR, et al. Use of balloon flotation pacing catheters for prophylactic temporary pacing during diagnostic and therapeutic catheterization procedures. *Am J Cardiol* 1988;62:941.
43. Dodge JT, Nykiel M, Altmann J, et al. Coronary artery injection technique: a quantitative *in vivo* investigation using modern catheters. *Cathet Cardiovasc Diagn* 1998;44:34.
44. Ireland MA, et al. Safety and convenience of a mechanical injector pump for coronary angiography. *Cathet Cardiovasc Diagn* 1989;16:199.
45. The BARI protocol. Protocol for the Bypass Angioplasty Revascularization Investigation. *Circulation* 1991;84:V1.
46. Angelini P, Villason S, Chan AV, et al. Normal and anomalous coronary arteries in humans. In: Angelini P, ed. Coronary artery anomalies: a comprehensive approach. Philadelphia: Lippincott Williams & Wilkins, 1999:27.
47. Yamanaka O, Hobbs RE. Coronary artery anomalies in 126,595 patients undergoing coronary arteriography. *Cathet Cardiovasc Diagn* 1990;21:28.
48. Serota H, et al. Rapid identification of the course of anomalous coronary arteries in adults: the “dot and eye” method. *Am J Cardiol* 1990;65:891.
49. Ishikawa T, Brandt PWT. Anomalous origin of the left main coronary artery from the right aortic sinus: angiographic definition of anomalous course. *Am J Cardiol* 1985;55:770.
50. Shirani J, Roberts WC. Solitary coronary ostium in the aorta in the absence of other major congenital cardiovascular abnormalities. *J Am Coll Cardiol* 1993;21:137.
51. Cohen DJ, Kim D, Baim DS. Origin of the left main coronary artery from the “non-coronary” sinus of Valsalva. *Cathet Cardiovasc Diagn* 1991;22:190.
52. Aldridge HE. A decade or more of cranial and caudal angled projections in coronary arteriography: another look. *Cathet Cardiovasc Diagn* 1984;10:539.
53. Elliott LP, et al. Advantage of the cranial-right anterior oblique view in diagnosing mid left anterior descending and distal right coronary artery disease. *Am J Cardiol* 1981;48:754.
54. Grover M, Slutsky R, Higgins C, et al. Terminology and anatomy of angulated coronary arteriography. *Clin Cardiol* 1984;7:37.
55. Taylor CR, Wilde P. An easily constructed model of the coronary arteries. *AJR Am J Radiol* 1984;142:389.
56. Mintz GS, Popma JJ, Pichard AD, et al. Limitations of angiography in the assessment of plaque distribution in coronary artery disease: a systematic study of target lesion eccentricity in 1446 lesions. *Circulation* 1996;93:924.
57. Randall PA. Mach bands in cine coronary arteriography. *Radiology* 1978;129:65.
58. Arnett EN, et al. Coronary artery narrowing in coronary heart disease: comparison of cineangiographic and necropsy findings. *Ann Intern Med* 1979;91:350.
59. Dodge JT, Brown BG, Bolson EL, et al. Lumen diameter of normal human coronary arteries: influence of age, sex, anatomic variation, and left ventricular hypertrophy or dilation. *Circulation* 1992;86:232.
60. Gould KL, et al. Physiologic basis for assessing critical coronary stenosis: instantaneous flow response and regional distribution during coronary hyperemia as measures of flow reserve. *Am J Cardiol* 1974;33:87.
61. Uren NG, et al. Relation between myocardial blood flow and the severity of coronary artery stenosis. *N Engl J Med* 1994;330:1782.
62. Gibson CM, Cannon CP, Daley WL, et al. TIMI frame count: a quantitative method of assessing coronary artery flow. *Circulation* 1996;93:879.
63. Pijls NHJ, de Bruyne B, Peels K, et al. Measurement of fractional flow reserve to assess the functional severity of coronary-artery stenoses. *N Engl J Med* 1996;334:1703.
64. Gibson CM, Safian RD. Limitations of cineangiography: impact of new technologies for image processing and quantitation. *Trends Cardiovasc Med* 1992;2:156.
65. Stadius ML, Alderman EL. Coronary artery revascularization: critical need for and consequences of objective angiographic assessment of lesion severity. *Circulation* 1990;82:2231.
66. Scoblionko DP, et al. A new digital electronic caliper for measurement of coronary arterial stenosis: comparison with visual estimates and computer-assisted measurements. *Am J Cardiol* 1984;53:689.
67. Gronenshild E, Jannsen J, Tijdent F. CAAS II: a second generation system for off-line and on-line quantitative coronary angiography. *Cathet Cardiovasc Diagn* 1994;33:61.
68. Escaned J, Baptiwsta J, DiMario C, et al. Significance of automated stenosis detection during quantitative angiography: insights gained from intracoronary ultrasound imaging. *Circulation* 1996;94:966.
69. Folland ED, Vogel RA, Hartigan P, et al. Relation between coronary artery stenosis assessed by visual, caliper, and computer methods and exercise capacity in patients with single-vessel coronary artery disease. *Circulation* 1994;89:2005.
70. Danchin N, Foley D, Serruys PW. Visual versus quantitative assessment of the severity of coronary artery stenoses: can the angiographer's eye be reeducated? *Am Heart J* 1993;126:594.
71. Ambrose JA, Hjemdahl-Monsen CE: Angiographic anatomy and mechanisms of myocardial ischemia in unstable angina. *J Am Coll Cardiol* 1987;9:1397.
72. Dangas G, Mehran R, Wallenstein S, et al. Correlation of angiographic morphology and clinical presentation in unstable angina. *J Am Coll Cardiol* 1997;29:519.
73. Mintz GS, Pichard AD, Popma JJ, et al. Determinants and correlates of lesion calcium in coronary artery disease: a clinical, angiographic and intravascular ultrasound study. *J Am Coll Cardiol* 1997;29:268.
74. Waxman S, Sassower MA, Mittleman MA, et al. Angioscopic predictors of early adverse outcome after coronary angioplasty in patients with unstable angina and non-Q-wave myocardial infarction. *Circulation* 1996;93:2106.
75. Fishbein MC, Siegel RJ. How big are coronary atherosclerotic plaques that rupture? *Circulation* 1996;94:2662.
76. Levin DC. Pathways and functional significance of the coronary collateral circulation. *Circulation* 1974;50:831.
77. Piek JJ, van Liebergen RAM, Koch KT, et al. Clinical, angiographic and hemodynamic predictors of recruitable collateral flow during balloon angioplasty of coronary occlusion. *J Am Coll Cardiol* 1997;29:275.
78. Seiler C, Fleisch M, Garachemani A, et al. Coronary collateral quantitation in patients with coronary artery disease using intravascular flow velocity or pressure measurements. *J Am Coll Cardiol* 1998;32:1272.
79. Razavi M. Unusual forms of coronary artery disease. *Cardiovasc Clin* 1975;7:25.
80. Levin DC, Fellows KE, Abrams HL. Hemodynamically significant primary anomalies of the coronary arteries: angiographic aspects. *Circulation* 1978;58:25.
81. Click RL, et al. Anomalous coronary arteries: location, degree of atherosclerosis and effect on survival. A report from the Coronary Artery Surgery Study. *J Am Coll Cardiol* 1989;13:531.
82. Liberthson RR. Sudden death from cardiac causes in children and young adults. *N Engl J Med* 1996;334:1039.
83. Shapira OM, Shemin RJ. Aneurysmal coronary artery disease: atherosclerotic coronary artery disease or adult mucocutaneous lymph node syndrome (Kawasaki's disease)? *Chest* 1997;111:796.
84. Baretella MB, Bott-Silverman C. Coronary artery aneurysms: an unusual case report and a review of the literature. *Cathet Cardiovasc Diagn* 1993;29:57.
85. Ge J, Erbel R, Rupprecht HJ, et al. Comparison of intravascular ultrasound and angiography in the assessment of myocardial bridging. *Circulation* 1994;89:1725.
86. Klues HG, Schwarz ER, von Dahl J, et al. Disturbed intracoronary hemodynamics in myocardial bridging: early normalization by intracoronary stent placement. *Circulation* 1997;96:2905.
87. Dorros G, Thota V, Ramireddy K, et al. Catheter-based techniques for closure of coronary fistulae. *Cathet Cardiovasc Diagn* 1999;46:143.
88. Sherwood MC, Rockenmacher S, Colan SD, et al. Prognostic significance of clinically silent coronary artery fistulas. *Am J Cardiol* 1999;83:407.
89. Yetman AT, McCrindle BW, MacDonald C, et al. Myocardial bridging in children with hypertrophic cardiomyopathy: a risk factor for sudden death. *N Engl J Med* 1998;339:1201.
90. Jennette JC, Falk RJ. Small-vessel vasculititis. *N Engl J Med* 1997;337:1512.
91. Weis M, von Scheidt W. Cardiac allograft vasculopathy: a review. *Circulation* 1997;96:2069.
92. Om A, Ellaham S, Vetrovec GW. Radiation-induced coronary artery disease. *Am Heart J* 1992;124:1598.
93. Cohen S. Motor disorders of the esophagus. *N Engl J Med* 1979;301:183.
94. Maseri A, Chierchia S. Coronary artery spasm: demonstration, definition, diagnosis, and consequences. *Prog Cardiovasc Dis* 1982;25:169.
95. Mark DB, et al. Clinical characteristics and long-term survival of patients with variant angina. *Circulation* 1984;69:880.
96. Waters DD, Theroux P, Szlachcic J, et al. Provocative testing with ergonovine to assess the efficacy of treatment with nifedipine, diltiazem and verapamil in variant angina. *Am J Cardiol* 1981;48:123.
97. Heupler FA, et al. Ergonovine maleate provocative test for coronary arterial spasm. *Am J Cardiol* 1978;41:631.
98. Raizner AE, et al. Provocation of coronary artery spasm by the cold pressor test. *Circulation* 1980;62:925.
99. Bertrand ME, et al. Frequency of provoked coronary arterial spasm in 1089 consecutive patients undergoing coronary arteriography. *Circulation* 1982;65:1299.
100. Nakao K, Ohgushi M, Yoshimura M, et al. Hyperventilation as a specific test for diagnosis of coronary artery spasm. *Am J Cardiol* 1997;80:545.
101. Harding MB, Leithe ME, Mark DB, et al. Ergonovine maleate testing during cardiac catheterization: a 10 year perspective in 3,447 patients without significant coronary artery disease or Prinzmetal's variant angina. *J Am Coll Cardiol* 1992;20:107.
102. Cipriano PR, et al. The effects of ergonovine maleate on coronary arterial size. *Circulation* 1979;59:82.
103. Friedman AC, Spindola-Franco H, Nivatpumin T. Coronary spasm: Prinzmetal's variant angina vs. catheter-induced spasm; refractory spasm vs. fixed stenosis. *Am J Radiol* 1979;132:897.
104. Hays JT, Stein B, Raizner AE. The crumpled coronary artery: an enigma of arteriopathic pseudopathology and its potential for misinterpretation. *Cathet Cardiovasc Diagn* 1994;31:293.
105. Cannon RO III, Watson RM, Rosing DR, et al. Angina caused by reduced vasodilator reserve of the small coronary arteries. *J Am Coll Cardiol* 1983;1:1359.
106. Cannon RO III, et al. Left ventricular dysfunction in patients with angina pectoris, normal epicardial coronary arteries, and abnormal vasodilator reserve. *Circulation* 1985;72:218.

12
Cardiac Ventriculography

Donald S. Baim and L. David Hillis

DSB: Harvard Medical School; Center for Innovative Minimally Invasive Therapy, Brigham and Women's Hospital, Boston, Massachusetts 02115.
LDH: Department of Medicine, Division of Cardiology, University of Texas Southwestern Medical Center, Dallas, Texas 75235

Cardiac ventriculography is used to define the anatomy and function of the ventricles and related structures in patients with congenital, valvular, coronary, and myopathic heart disease (1,2,3,4 and 5). Specifically, left ventriculography may provide valuable information about global and segmental left ventricular function, mitral valvular incompetence, and the presence, location, and severity of a number of other abnormalities such as ventricular septal defect, hypertrophic cardiomyopathy, or left ventricular mural thrombus. As a result, left ventriculography is a routine part of diagnostic cardiac catheterization in patients being evaluated for coronary artery disease, aortic or mitral valvular disease, unexplained left ventricular failure, or congenital heart disease. Similarly, *right* ventriculography may provide information about global and segmental right ventricular function and can be especially helpful in patients with congenital heart disease. In reality, however, right ventriculography is rarely performed in an adult cardiac catheterization laboratory.

INJECTION CATHETERS

To achieve adequate opacification of the left or right ventricle, it is necessary to deliver a relatively large amount of contrast material in a relatively short time. In adults, a 6F, 7F, or 8F catheter with multiple side-holes allows rapid delivery of contrast material while allowing the catheter to remain in a stable position during injection, thereby producing no disturbance of cardiac rhythm. In contrast, catheters that have only an end-hole (e.g., Cournand, multipurpose) are not well suited for left ventriculography, because the contrast jet out of the single end-hole causes the catheter to recoil during contrast delivery, resulting in ventricular ectopic beats, inadequate ventricular opacification, and myocardial penetration (so-called endocardial staining) or even perforation.

Pigtail Catheter

The pigtail catheter, as developed by Judkins, has several advantages over an end-hole design for left and right ventriculography (Fig. 12.1). Although its end-hole permits insertion of the pigtail catheter over a J-tipped guidewire, so that it can be advanced safely to the left ventricle from the arm or leg even in the patient with brachiocephalic or iliac arterial tortuosity, the loop shape keeps the end-hole away from direct contact with the endocardium. The presence of multiple side-holes on the several centimeters of catheter shaft proximal to the pigtail loop provides numerous simultaneous exit routes for contrast material, thus stabilizing the catheter within the left ventricle during contrast injection and reducing the magnitude of catheter recoil. These characteristics virtually eliminate the possibility of endocardial staining, since the end-hole usually is not positioned adjacent to ventricular trabeculae, and substantially reduces the occurrence of ventricular ectopic beats. The pigtail usually passes easily across a normal aortic valve, either directly or by prolapsing across the valve leaflets, whereas passage across a stenotic aortic valve requires use of a straight leading guidewire (see Chapter 4). It can usually be passed across a porcine aortic valve bioprosthesis, and more easily than straight catheters such as the NIH or Eppendorf, since the pigtail configuration seems to prevent the catheter from sliding down into the lateral sinuses outside the support struts. Pigtail catheters can also be passed retrograde across a ball valve prosthesis (Starr-Edwards), although its interference with seating of the ball during diastole may cause significant aortic regurgitation. Only the smallest diameter (e.g., 4F) catheter should be used for this purpose, dwell time across the valve should be kept to a minimum, and the patient should be monitored carefully for hemodynamic deterioration until the catheter is withdrawn from the left ventricle. Of course, no catheter should ever be passed across a tilting disc aortic valve prosthesis (Bjork-Shiley, Medtronic-Hall, or St. Jude) because of the risk of catheter entrapment if it were to pass through the minor orifice of the valve.

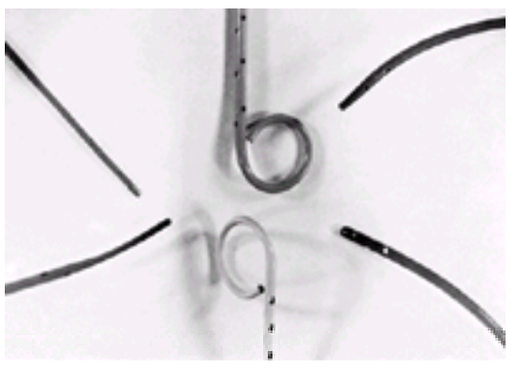

FIG. 12.1. Examples of ventriculographic catheters in current use (clockwise from the top): pigtail, 8F (Cook); Gensini, 7F; NIH, 8F; pigtail; 8F (Cordis); Lehman ventriculographic, 8F; Sones, 7.5F tapering to a 5.5F tip. The advantages and disadvantages of each catheter are discussed in the text. The Gensini and Sones catheters may cause endocardial staining because of the high-pressure jet of contrast material exiting the end-hole; therefore, ventriculography with them should be performed with special attention to catheter position and rate of contrast injection.

The original pigtail design had a straight shaft leading up to the pigtail end. It was designed to sit directly under the aortic valve, and just in from of the mitral inflow, relying on that inflow to distribute contrast to the apex of the left ventricle. The more recently developed “angled” pigtail catheters, which have a 145° to 155° shaft angle at the distal end (just proximal to the side-holes segment) may be helpful in achieving a central position within the left ventricular long axis, particularly in the patient whose left ventricle is positioned horizontally. This may be improved further if the heart is pulled into a somewhat more vertical orientation by having the patient take and maintain a deep breath during the left ventriculographic injection. Although the angle approximates that formed by the intersection of the left ventricular and ascending aortic long axes, the angled pigtail is especially likely to recoil during injection of a relatively large volume of contrast material. Some authors have suggested that catheter manipulation and overall image quality are better with the angled than with the straight pigtail (6), but adequate ventriculography can be achieved with either shape, so the choice of pigtail design remains a matter of operator preference.

Sones Catheter

The Sones catheter is used widely for left ventriculography when catheterization is performed from the brachial approach, although some operators prefer to use a pigtail catheter, as described in the previous section. The polyurethane Sones catheter (80 cm Cordis SON-II, Sones Technique, Cordis Corporation, Miami, FL) is particularly suitable for left ventriculography because it has four side-holes in addition to its end-hole. The catheter comes in 7F and 8F sizes and tapers to a 5F external diameter near its tip. The catheter accepts an 0.035-inch guidewire, which can be useful in crossing a severely stenotic aortic valve. Techniques for traversing a tortuous subclavian artery system and entering the left ventricle with the Sones catheter are discussed in Chapter 5. For left ventriculography, the Sones catheter should be positioned in an axial orientation (parallel to the ventricular long axis), with its tip midway between the aortic valve and left ventricular apex. Low injection rates (see later discussion) usually minimize the extent and forcefulness of catheter recoil. Catheter recoil may still occur, however, with induction of multiple ventricular extrasystoles and potential danger of endocardial staining. Accordingly, the operator should hold the catheter during injection and be prepared to withdraw it if significant recoil develops.

NIH and Eppendorf Catheters

The NIH and Eppendorf catheters have multiple side-holes and no end-hole (Fig. 12.1). They are easily inserted through an arteriotomy (by the brachial approach) or a percutaneously introduced femoral arterial sheath. The 7F NIH catheter prepared by USCI (Bard Inc., Billerica, MA) is made of woven Dacron with nylon reinforcement and is especially stiff. The polyurethane Cordis NIH catheter (Cordis Corporation, Miami, FL) and the polyethylene Cook NIH Torcon blue catheter (Cook, Bloomington, IN) are much softer and less likely to cause dissection or perforation. The Eppendorf catheter (USCI), of woven Dacron construction is less stiff as well, and the tips of both the Cordis NIH and the USCI Eppendorf catheters are sufficiently soft that they can be gently prolapsed across the aortic valve. In our catheterization laboratories, the Eppendorf catheter and polyurethane and polyethylene NIH catheters are sometimes used for left ventriculography by the brachial approach. In some patients, especially those whose left ventricles are small, left ventriculography with an NIH or Eppendorf catheter induces frequent ventricular premature beats. Despite the absence of an end-hole, endocardial staining occasionally occurs with these catheters, usually in patients in whom the end of the catheter is wedged within the ventricular trabeculae. The NIH and Eppendorf catheters are practical and effective for right ventricular angiography, but the standard pigtail catheter or the Grollman catheter (which has a pigtail tip and an angulated shaft) is now preferred for right ventriculography and pulmonary angiography.

Lehman Catheter

The Lehman ventriculographic catheter has a tapered, closed tip that extends beyond multiple side-holes (Fig. 12.1). The tapered tip may assist the operator in manipulating the catheter through tortuous arteries and across a stenotic aortic valve. Once in the left ventricle, the tip lessens the likelihood of endocardial staining, but, in our experience, this tip increases the chance of ventricular ectopy during the injection of contrast material.

INJECTION SITE

The adequate opacification of either ventricle is accomplished only if a large amount of contrast material is delivered in a short time. Satisfactory opacification of the left ventricle can usually be achieved by the injection of contrast material into the left atrium, with cineangiographic acquisition as the left ventricle is filled. Although such a left atrial injection might be advantageous because it seldom causes atrial or ventricular ectopic activity, it requires a transseptal catheterization, does not allow an evaluation of mitral valvular incompetence, and may obscure the basal portion of the left ventricle and the aortic valve. The left ventricle may be opacified by aortography in the patient who has significant aortic regurgitation. Similarly, the right ventricle may be opacified satisfactorily by injection of contrast material into the venae cavae or right atrium. These injection sites, however, do not allow an assessment of tricuspid valvular incompetence, and filming the injection in an obliquity that eliminates overlap of the venae cavae, right atrium, and right ventricle is often difficult.

Ventriculography in the adult therefore is best accomplished by injecting contrast material directly into the ventricular chamber in question. In the left ventricle, the optimal catheter position is the midcavity, provided that ventricular ectopy is not a problem (Fig. 12.2). Such a midcavitary position ensures (a) that adequate contrast material is delivered to the chamber's body and apex; (b) that the catheter does not interfere with mitral valvular function, thereby producing factitious mitral regurgitation; and (c) that the holes through which the contrast material is injected are not wedged within the ventricular trabeculae (possibly causing endocardial staining). In some patients, a midcavitary position induces repetitive ventricular ectopy, especially with an NIH or Eppendorf catheter. In these individuals, the tip of the catheter is best positioned in the left ventricular inflow tract, immediately in front of the posterior leaflet of the mitral valve (Fig. 12.3 and Fig. 12.4). This position usually does not cause ventricular ectopy, but mitral regurgitation may be produced if the catheter is too close to the mitral valve. In occasional patients with vigorous ventricular contraction, no stable midventricular position can be found for the catheter. Intermittent bumping of the catheter into the endocardium may cause enough ventricular ectopy to interfere with meaningful ventriculography. If a pigtail catheter is being used, it is sometimes useful to advance the catheter into continuous contact with the left ventricular apex, assuming that there is no evidence of apical aneurysm or mural thrombus. This may allow measurement of left ventricular pressure during stable rhythm, and left ventriculography may even be performed from this position if the rate of contrast injection is reduced to 10 mL/sec (see later discussion).

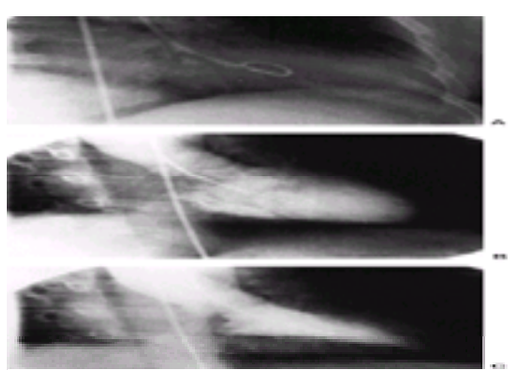

FIG. 12.2. An example of midcavitary catheter position for 30° right anterior oblique left ventriculography using a pigtail catheter: before the injection of contrast material **(A)**, at end-diastole **(B)**, and at end-systole **(C)**.

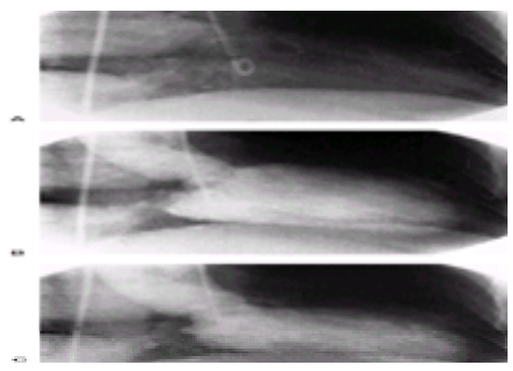

FIG. 12.3. An example of left ventricular inflow tract catheter position for 30° right anterior oblique left ventriculography using a pigtail catheter: before the introduction of contrast material **(A)**, at end-diastole **(B)**, and at end-systole **(C)**. Note that this patient has a large anteroapical aneurysm.

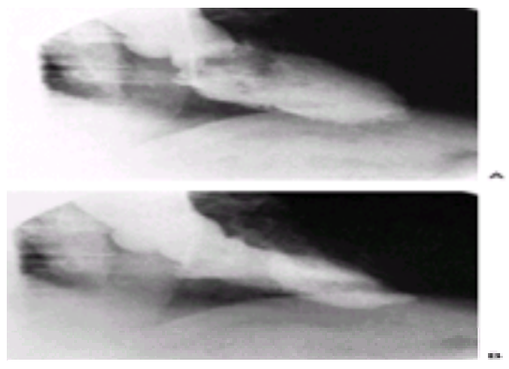

FIG. 12.4. An example of left ventricular inflow tract catheter position for 30° right anterior oblique left ventriculography using an Eppendorf catheter: at end-diastole **(A)** and at end-systole **(B)**.

In the right ventricle, the optimal catheter position is the midcavity, provided that repetitive ventricular ectopy does not occur. If ectopy is uncontrollable, the catheter may be positioned in the outflow tract, below the pulmonic valve. Even here, however, repetitive ventricular ectopy may present a difficult problem. In our experience, right ventriculography is often accompanied by frequent ventricular premature beats regardless of catheter position.

INJECTION RATE AND VOLUME

The rapid delivery of an adequate amount of contrast material requires the use of a power injector. There are two types of power injectors. The *pressure injector* allows one to select the volume of contrast material and its delivery pressure, but the rate of delivery is determined by the lumen size and length of the catheter, the viscosity of the contrast material, and the size of the injector syringe. The rapid delivery of contrast material is facilitated by a large bore and short catheter length, prewarmed contrast material, and an injector syringe of small diameter. The pressure injector is now outmoded and does not have the versatility of the flow injector.

The *flow injector* (most commonly, the device manufactured by Medrad) allows one to select both the volume *and* the rate of delivery of contrast material. A pressure sufficient to deliver a selected volume of injectate in a selected time is automatically developed, although a maximal pressure cutoff will shut the injector down immediately if the pressure required exceeds a preset maximum pressure. In most catheterization laboratories, the maximal pressure cutoff is set at 1,000 psi. Of course, this high pressure is not actually delivered to the catheter tip; instead, most of it is dissipated by frictional losses in the shaft of the catheter.

Some injectors permit synchronization of the injection of contrast material with the R wave of the electrocardiogram, so that a set flow rate is delivered in each of several successive diastolic intervals (7). Although this technique has been said to lessen the incidence of ventricular ectopic beats and to minimize the volume of contrast material required for adequate ventricular opacification, our impression is that it offers no clear advantage over nonsynchronized methods.

Cine left ventriculography is accomplished using an injection rate and volume that depend on (a) the type and size of catheter, (b) the size of the ventricular chamber to be opacified, (c) the approximate ventricular stroke volume, and (d) the preventriculography hemodynamics. A number of years ago, we asked our colleagues in several laboratories to tell us their usual parameters for left ventricular injection using various catheters and either femoral or brachial techniques, and these parameters are listed in Table 12.1. As can be seen, there is a fairly wide spectrum of injection rates and volumes for the pigtail catheter for either a femoral or a brachial approach. For the pigtail, Eppendorf, and NIH catheters, an injection rate of 10 to 16 mL/sec (higher for high cardiac output and large ventricular chamber) and a total volume of 30 to 55 mL (depending on ventricular size) represent average values from Table 12.1. The current injection parameters used most commonly with pigtail catheters are 30 to 36 mL at 10 to 12 mL/sec. If a Sones catheter is used for left ventriculography, the rate of injection of contrast material should not exceed 7 to 12 mL/sec, to minimize the chance of recoil and staining.

	Femoral approach			Brachial approach		
Institution and city	Catheter used	Injection rate (mL/sec)	Volume (mL)	Catheter used	Injection rate (mL/sec)	Volume (mL)
Parkland Hospital Dallas, TX	Pigtail	12–16	40–55	Pigtail	12–16	40–55
Beth Israel Hospital Boston, MA	Pigtail	12–15	30–40	Sones	7–10	30–40
U of Pennsylvania Philadelphia, PA	Pigtail	10–14	40–50	Pigtail, Sones	10–14 8–10	40–50 40–45
Barnes Hospital St. Louis, MO	Pigtail	10–14	30–40	NIH	10–14	30–40
AMI Inst. Heart Bethesda, MD	Pigtail	10–15	30–45	NIH	10–15	30–45
U of Washington Seattle, WA	Pigtail	15–20	40–50	Few catheterizations by this approach		
Baylor University Houston, TX	Pigtail	12–15	35–45	Sones	8–10	33–40
Brown University Providence, RI	Pigtail	15–20	35–50	Pigtail, NIH	15–20	35–50
Yale University New Haven, CT	Pigtail	12–16	35–45	Pigtail, NIH	12	35
Mayo Clinic Rochester, MN	Pigtail	12–16	40–55	NIH, Rodriguez	12–16	40–55
U of Florida Gainesville, FL	Pigtail	8–12	25–35	Sones	8–12	25–35
New York Hospital New York, NY	Pigtail	8–12	30–45	Sones	8–12	30–45
U of Iowa Hospital Iowa City, IA	Pigtail	12–16	45–60	Pigtail	12–16	45–60
U of N Carolina Chapel Hill, NC	Pigtail	10–14	30–40	Pigtail	10–14	30–40

TABLE 12.1. *Catheter type, injection rate, and volume of contrast material used for left ventriculography*

In the patient with hemodynamic evidence of severe left ventricular dysfunction (mean pulmonary capillary wedge pressure higher than 25 mm Hg), left ventriculography should be performed with the use of a low-osmolar contrast agent. Nonionic contrast agents, discussed in Chapter 2, have substantially improved the safety of left ventriculography in patients with depressed myocardial function, severe coronary artery disease, and/or aortic stenosis. Compared with high-osmolar agents (e.g., sodium meglumine diatrizoate), the low-osmolar agents produce only minor decreases in ionized calcium in the coronary circulation and therefore have a minimal myocardial depressant effect (8,9,10 and 11). They should generally be used for performing ventriculography in patients with elevated left ventricular filling pressures due to coronary artery disease, cardiomyopathy, or severe aortic or mitral regurgitation. If filling pressures are markedly elevated, left ventriculography should be performed during the administration of an acutely imposed “protective regimen” of sublingual nitroglycerin or during the intravenous infusion of nitroglycerin or sodium nitroprusside. If the pulmonary capillary wedge pressure is greatly elevated because of mitral stenosis, left ventriculography should be preceded by the intravenous administration of morphine sulfate and furosemide. Failure to take a highly elevated preventriculography pulmonary capillary wedge pressure seriously can lead to disastrous consequences, such as intractable pulmonary edema and even death. In our experience, the left ventricular end-diastolic pressure is not as reliable a predictor of impending pulmonary edema as the wedge pressure because (as discussed elsewhere) the left ventricular end-diastolic and mean pulmonary capillary wedge pressures may be widely disparate. One should always ask the question in a patient with increased risk (left ventricular dysfunction, mural thrombus, renal insufficiency) as to whether noninvasive means of assessing left ventricular function (see later discussion) might not be preferable to contrast ventriculography. But with current radiographic equipment with digital subtraction capability (12), low-osmolar contrast agents, and techniques using smaller amounts of contrast material, it is a rare patient who cannot undergo left ventriculography safely.

Before the power injection of contrast material, one should take appropriate precautions in filling and firing the power injector to prevent air embolism. In our catheterization laboratories, a Medrad Mark IV power injector with a 130-mL translucent syringe is used. These syringes are made of siliconized plastic so that the contrast medium and any air can easily be seen. The injector is loaded with contrast material through a short U-shaped straw while the syringe barrel is pointed upward. With the injector still in the vertical position, a 30-inch length of sterile roentgenography tubing is connected to the syringe and all air is expelled from the syringe and tubing. This is done by holding the load switch in the forward position as the operator taps the syringe and its Luer-Lok connector to discharge all air bubbles. Only then is the injector head inverted, and a “running connection” is made between the roentgenography tubing and the catheter hub. Specifically, a fluid-to-fluid connection is accomplished by touching the meniscus of blood is spurting from the hub of the catheter to the meniscus of contrast material exiting the roentgenography tubing as the technician depresses the forward position of the load switch or manually advances the syringe plunger of the injector. After the connection is made, the injector operator presses the reverse position of the load switch or manually retracts the plunger until the “interface” between contrast material and blood in the roentgenography tubing can be seen and verified to be free of air bubbles. Before the left ventriculographic run, a test injection of a small amount of contrast material is performed under fluoroscopic visualization. This enables the physician to (a) assess catheter and patient position, (b) confirm that ventricular ectopy does not occur, and (c) exclude a reaction to contrast material (if this is the patient's first exposure to it). If the catheter is repositioned, another test

injection is recommended.

The physician performing the catheterization should look closely at the injector syringe to be sure that it is filled with contrast medium, free of air, and oriented in the desired “nose-down” direction. This physician should grasp the catheter at the point of its insertion into the body during the power injection of contrast material, so that it may be pulled back instantaneously if ventricular extrasystoles, myocardial staining, or other untoward events develop during injection. The physician operator must have good visualization of the fluoroscopic screen during ventriculography, and the technician or other individual firing the injector should be prepared to abort the injection on command from the physician operator in the event of an untoward occurrence. In many laboratories, the physician performing the catheterization holds the connection between catheter and roentgenography tubing tightly in one hand during the power injection to prevent uncoupling of this connection.

Proper catheter positioning is important to avoid extrasystoles during ventriculography, as discussed earlier in this chapter. If extrasystoles develop, it is our policy to withdraw the ventriculographic catheter immediately after the first extrasystole, for a distance of approximately 2 to 3 cm. This usually results in a quiet position for the remainder of the 3- to 4-second contrast injection, and it is particularly effective when the Sones catheter is being used for left ventriculography; this technique has not resulted in ventricular staining in a very large experience.

Instructions to the patient regarding respiration during contrast ventriculography vary from laboratory to laboratory. Previously, imaging systems were often inadequate to give good definition of the left ventricular silhouette unless ventriculography was performed during deep inspiration to move the diaphragm out of the radiographic field. With modern imaging systems, excellent definition of the ventricular silhouette can be achieved without performing ventriculography during held deep inspiration. Left ventriculography done during normal quiet breathing allows physiologic interpretation of left ventricular volumes, angiographic stroke volume, and calculated left ventricular regurgitant fraction in cases of valvular regurgitation. In the catheterization laboratory at Parkland Memorial Hospital (Dallas, Texas), most left ventriculograms are performed after the patient simply has stopped breathing (without first inspiring deeply).

FILMING PROJECTION AND TECHNIQUE

As a general rule, biplane ventriculography is preferable to single-plane ventriculography because it allows one to obtain more information at essentially no additional risk to the patient. For example, in the patient with coronary artery disease, biplane left ventriculography is superior to single-plane left ventriculography in providing information on the location and severity of segmental wall motion abnormalities. In the patient with congenital heart disease, biplane right ventriculography allows one to assess accurately the anatomy of the right ventricular outflow tract, the pulmonic valve, and the proximal portions of the pulmonary artery. Biplane ventriculography does have several disadvantages, including (a) the increased expense of biplane cineangiographic equipment, (b) the reduced quality of cineangiographic imaging in each plane that results from the radiation scatter caused by the opposite plane, (c) the additional time required to position the biplane equipment appropriately, especially when the brachial approach is used, and (d) the additional radiation exposure to personnel in the room.

Whether performing biplane or single-plane ventriculography, one should use projections that provide maximal delineation of the structure of interest and minimal overlapping of other structures. Most laboratories doing biplane left ventriculography prefer a 30° right anterior oblique (RAO) and a 60° left anterior oblique (LAO) view. The 30° RAO projection eliminates overlap of the left ventricle and the vertebral column; allows one to assess anterior, apical, and inferior segmental wall motion; and places the mitral valve in profile, thus providing a reliable assessment of the presence and angiographic severity of mitral regurgitation. As seen in Fig. 12.5, the 30° RAO projection allows excellent visualization of the extent of an anterior wall aneurysm of the left ventricle in a patient with isolated proximal occlusion of the left anterior descending artery. The 60° LAO view allows one to assess ventricular septal integrity and motion, lateral and posterior segmental function, and aortic valvular anatomy. To prevent the foreshortening of the left ventricle that commonly occurs with LAO views and visualize the entire length of the interventricular septum in profile, 15° to 20° cranial angulation should be added to the 60° LAO view.

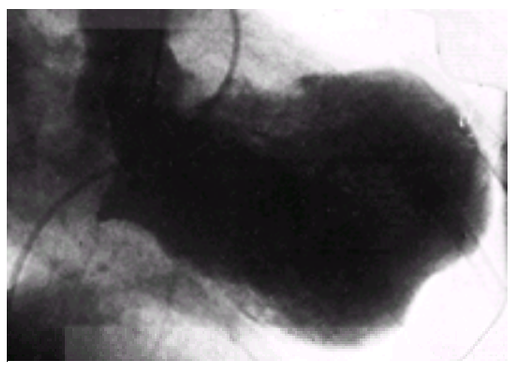

FIG. 12.5. Left ventriculogram in a 30° right anterior oblique projection (end-systolic frame) showing a large anterior wall aneurysm. The patient was a 65-year-old man who had a massive myocardial infarction (peak creatine kinase measurement, 4,460 units) and showed subsequently a progressively enlarged cardiac silhouette on roentgenography. Catheterization 4 weeks after infarction demonstrated a large anterior wall left ventricular (LV) aneurysm, with LV pressure 95/40 mm Hg, pulmonary capillary wedge pressure 34 mm Hg, and occlusion of the left anterior descending artery proximal to the first septal perforator. Ejection fraction was 18%, and the other coronary arteries were normal.

If biplane cineangiographic equipment is not available, the single-plane projection that provides the best delineation of structures of interest should be used. For example, the 30° RAO projection allows a reliable assessment of mitral regurgitation, whereas a 45° to 60° LAO view (with cranial angulation of 15° if possible) provides the opportunity to visualize a ventricular septal defect and the associated left-to-right shunting.

For routine left or right ventriculography, we perform cineangiography at 30 frames per second, using the 9-inch field of view. This allows us to visualize the entire ventricle within the field. In many patients, ventriculography performed with a greater degree of magnification (e.g., 6-inch intensifier) is not adequate for assessment of the entire ventricular silhouette together with the left atrium and ascending aorta.

ANALYSIS OF THE VENTRICULOGRAM

The most common analysis of the left ventriculogram is a qualitative assessment of global and regional systolic function. Analysis should use a normal sinus beat that follows a previous normal sinus beat, and in which the ventricle is well opacified. Use of ectopic beats or postectopic beats will give a false impression of ventricular function. The ejection fraction (see Chapter 16 and Chapter 17) may be estimated as normal (50% to 69%), hyperdynamic (more than 70%), mildly hyopkinetic (35% to 49%), moderately hypokinetic (20% to 24%), or severely hypokinetic (less than 20%). Regional wall motion can also be graded as being normal, hypokinetic, akinetic, or dyskinetic for each of the segments seen in the RAO projection (anterolateral, apical, inferior, and posterobasal segments) and in the LAO projection (basal septal, apical septal, apical lateral, and basal lateral segments). Using the area-length method described in Chapter 16, actual end-diastolic and end-systolic volumes can be calculated, and from them the actual ejection fraction (the percent of blood volume present at end-diastole that is ejected by end-systole).

The degree of mitral regurgitation can be estimated (on a scale of 1+ to 4+) by looking for leakage of contrast material from the left ventricle back into the left atrium and the relative opacification of the left atrium, in the RAO projection (see Chapter 29). Comparison of the angiographic stroke volume (end-diastolic volume minus end-systolic volume) with the forward stroke volume (cardiac output divided by heart rate) in patients with aortic or mitral regurgitation allows calculation of the regurgitant volume and regurgitant fraction (angiographic stroke volume minus forward stroke volume, as a percentage of angiographic stroke volume). Mild (1+) mitral regurgitation is usually associated with a regurgitant fraction of less than 30%; moderate (2+), 30% to 39%; moderately severe (3+), 40% to 49%; and severe, greater than 50% (13).

INTERVENTION VENTRICULOGRAPHY

Segmental dysfunction of the left ventricular wall can be caused by ischemia or infarction. Over the years, several techniques have been described that allow one to determine during left ventriculography whether an asynergic segment of the left ventricle is ischemic or infarcted. With each of these techniques, segments whose abnormal wall motion is caused by ischemia show improvement in systolic motion, whereas segments whose abnormal wall motion is caused by infarction fail to

improve.

First, left ventricular segmental wall motion can be improved substantially by the administration of catecholamines (14). Two left ventriculograms are performed—the first in the resting (baseline) state, and the second during a steady-state infusion of epinephrine (1 to 4 mg/min) or dobutamine (10 to 15 μg/kg per minute). Segments that are ischemic and, as a result, hypokinetic or akinetic on baseline ventriculography improve their contractile pattern during epinephrine infusion; in contrast, segments that are asynergic due to infarction show no alteration in contractility when stimulated by epinephrine.

Second, left ventricular segmental wall dysfunction can be improved by nitroglycerin (15), either by improving collateral blood flow, reducing myocardial oxygen consumption to fall within available supply, or simply reducing the afterload against which the left ventricle must eject. Here, also, two left ventriculograms are performed, one before and the other after sublingual administration of nitroglycerin, when there is evidence of a nitroglycerin-induced fall in systemic arterial pressure. Segments of the left ventricle in which contraction is abnormal on the baseline ventriculogram but improves after nitroglycerin administration are reversibly injured (i.e., ischemic), whereas those in which asynergy is present before nitroglycerin and is not altered by it are most likely irreversibly damaged (i.e., infarcted). Segments in which motion improves with nitroglycerin generally maintain this level of improvement after successful surgical revascularization; in contrast, segments in which contractile function is not influenced by nitroglycerin are not improved by revascularization.

Third, left ventricular segmental wall motion can be influenced by postextrasystolic potentiation (16). A single ventricular premature beat is introduced during left ventriculography and is followed by a compensatory pause and then a potentiated beat. Segmental wall motion during one of the preceding sinus beats is compared with that of the postextrasystolic beat. Left ventricles with asynergic wall motion during a preceding sinus beat that improves on the potentiated beat are ischemic, whereas those in which asynergy is similar on the preceding sinus beat and on the postextrasystolic beat are infarcted. Augmentation ventriculography by this technique offers the advantage that both baseline and potentiated left ventricular wall motion can be characterized on a single ventriculogram. Postextrasystolic potentiation may be provided by introducing a timed stimulus (delivered through a right ventricular pacing catheter) or by pullback of a right ventricular catheter during left ventriculography. It is probably unwise to attempt to induce the ventricular extrasystole by manipulating the left ventriculographic catheter during the injection of contrast material, because such manipulation may cause endocardial staining.

Other types of intervention ventriculography may be of use in the patient with chronic left ventricular volume overload caused by aortic or mitral regurgitation. In the patient with aortic regurgitation and well-preserved left ventricular function, angiotensin in a dose sufficient to increase left ventricular systolic pressure by 20 to 50 mm Hg causes no change in left ventricular ejection fraction (17). In the patient whose aortic regurgitation has caused a loss of left ventricular contractile reserve, a similar amount of angiotensin causes a fall in left ventricular ejection fraction of more than 0.10. Thus, left ventriculography during “afterload stress” may provide additional information about left ventricular functional capability. Alternatively, intervention ventriculography using sodium nitroprusside may be used in patients with mitral regurgitation, aortic regurgitation, or dilated cardiomyopathy to assess the potential benefit of chronic vasodilator therapy.

COMPLICATIONS AND HAZARDS

Although complications of cardiac catheterization and angiography are discussed in detail in Chapter 3, certain specific points relevant to ventriculography are presented here.

Complications of Injection

Arrhythmias

Ventricular extrasystoles occur frequently during ventriculography and are usually caused by mechanical stimulation of the ventricular endocardium by the catheter or a jet of contrast agent. Such extrasystoles can usually be eliminated or at least minimized by repositioning the catheter. Although short runs of ventricular tachycardia occur during an occasional ventriculogram, they almost always cease promptly when the catheter is removed from the ventricle. Rarely, the ventricular tachycardia caused by ventriculography is sustained even after catheter removal. It should be treated quickly with a bolus of intravenous lidocaine and, if necessary, direct current countershock. Ventricular fibrillation has been reported to be induced by an improperly grounded power injector (18).

Intramyocardial Injection(Endocardial Staining)

Deposition of contrast material within the endocardium and myocardium (so-called endocardial staining) is usually caused by improper positioning of the ventriculographic catheter so that it passes under one of the papillary muscles or so that a side-hole lies firmly against the endocardium. Although a small endocardial stain usually causes no problem, a large stain may lead to medically refractory ventricular tachyarrhythmias, including ventricular tachycardia or fibrillation. In the catheterization laboratory at Parkland Memorial Hospital, about 3,500 left ventriculograms have been performed with a pigtail catheter. A very small endocardial stain occurred in only one case, and it was not accompanied by ventricular tachyarrhythmias. Rarely, the power injection of contrast material causes myocardial perforation, with resultant leakage of blood and contrast material into the pericardial space and the development of cardiac tamponade. This must be treated by emergency pericardiocentesis, and immediate consultation must be obtained from a cardiothoracic surgeon.

Fascicular Block

Because of the proximity of the anterior fascicle of the left bundle to the left ventricular outflow tract, transient left anterior fascicular block may occur during retrograde left-sided heart catheterization. In the patient with underlying right bundle branch block and left posterior fascicular block, complete heart block may occur as the catheter is advanced into the left ventricle (19). Although temporary pacing is usually required, catheter-induced fascicular block usually resolves within 12 to 24 hours. Transient complete left bundle branch block is an extremely rare complication of retrograde left heart catheterization (20).

Embolism

The inadvertent injection of air or thrombus probably poses the greatest risk associated with ventriculography. The presence of thrombi on or within the ventriculographic catheter is minimized by (a) frequent flushing of the catheter with a solution containing heparin and (b) systemic heparinization of the patient when the ventriculographic catheter is first introduced. Some operators still administer 5,000 units of heparin intravenously when the first arterial catheter (brachial or femoral) is introduced into the aorta, whereas others omit heparin and substitute careful and frequent catheter flushing and a rapid procedure as ways to reduce the risk of embolism.

Occasionally, a patient is referred for catheterization in whom (from noninvasive testing) a thrombus in the left ventricular apex is suspected. If left ventriculography is required in such a patient, great care should be taken to position the ventriculographic catheter in the left ventricular inflow tract, avoiding the apical portion completely. Partially organized thrombi may be dislodged from the left ventricular cavity by the catheter tip or by the force of a power injection. Accordingly, the ventricular angiographic catheter should not be advanced to the left ventricular apex except under exceptional circumstances (e.g., suspicion of idiopathic hypertrophic subaortic stenosis).

Complications of Contrast Material

For 20 to 30 seconds after ventriculography with a high-osmolar agent, the patient will experience a “hot flash” owing to the powerful vasodilation caused by the contrast material as it distributes throughout the arterial tree (see Chapter 2). Transient nausea and vomiting may also occur in 20% to 30% of patients. With low-osmolar contrast agents, these complications are uncommon. The immediate but short-lived hemodynamic effects of ventriculography with ionic contrast agents include a modest fall in systemic arterial pressure, a reflex increase in heart rate, and a transient depression of left ventricular contractility; these resolve within 1 to 2 minutes.

ALTERNATIVES TO CONTRAST VENTRICULOGRAPY

Echocardiographic Visualization of the Left Ventricle

Two-dimensional echocardiography may be used as an alternative to contrast ventriculography to assess global and regional left ventricular performance.

Echocardiography is noninvasive, does not require exposure to radiation, and does not add to the contrast load of coronary angiography in patients at high risk for contrast-induced renal dysfunction. In a minority of subjects, echocardiography fails to provide adequate images owing to extreme obesity or an increased anteroposterior chest dimension. In most, however, adequate images of the left ventricle can be acquired in multiple short- and long-axis planes to evaluate segmental and global left ventricular function as well as the degree of mitral regurgitation. Two-dimensional echocardiographic imaging also allows determination of left ventricular volumes using a modification of Simpson's rule, based on analysis of orthogonal long-axis views. If only a single view is available, the area-length method may be applied to the end-diastolic and end-systolic images. The left ventricular volumes provided by echocardiography are somewhat smaller and the estimates of mitral regurgitation somewhat higher than those obtained with contrast ventriculography (13,21). Because two-dimensional echocardiography can be used to determine left ventricular wall thickness, it is an excellent method for quantitating left ventricular mass.

Magnetic Resonance Imaging Ventriculography

In preliminary assessments, magnetic resonance imaging (MRI) has also appeared to be a reliable alternative technique for measuring ventricular dimensions and evaluating regional wall motion. MRI images are acquired in a gated fashion throughout the cardiac cycle, and end-diastolic and end-systolic frames are identified. Because these images are acquired in multiple planes, a detailed assessment of regional wall motion can be accomplished in almost all subjects regardless of body shape or size. Left ventricular volumes are calculated using Simpson's rule (i.e., volume = S area × slice thickness), with each area determined from consecutive short-axis slices through the ventricle. Alternatively, ventricular volumes may be determined by acquiring a single long-axis image and applying the area-length method (as with contrast ventriculography). The use of Simpson's rule requires lengthy image acquisition, whereas the area-length method relies on geometric assumptions that may be invalid in some subjects. In general, MRI provides values for left ventricular volumes that are similar to those obtained with contrast ventriculography (22,23). As with two-dimensional echocardiography, MRI provides an accurate quantitation of left ventricular wall thickness, from which mass is easily calculated, and it may be particularly valuable when a high degree of anatomic localization is required (24).

Electromechanical Mapping

Originally developed for electrophysiology, the Biosense electromechanical mapping catheter (Biosense-Webster, Diamond Bar, CA) uses tip sensors to measure the relative strength of electromagnetic fields emitted by three coils positioned under the patient support, and thereby calculate the exact position of the catheter tip in three dimensions (25,26). When the catheter is placed in contact with the left ventricular endocardium, the unipolar electrogram can be recorded from multiple locations within the left ventricle. Recording the motion of the catheter over the cardiac cycle allows calculation of cardiac volumes (including those at end-diastole and end-systole), local wall motion, and wall shortening. Areas of myocardial infarction show poor local shortening with low unipolar voltage. In contrast, areas with severe ischemia show reduced local shortening with retained unipolar voltage. Although more time-consuming than contrast ventriculography, electromechanical mapping may provide more detailed assessment of ventricular function and a highly accurate way to deliver local therapies (direct myocardial revascularization, local drug injection) to ischemic areas of the left ventricle.

ACKNOWLEDGMENT

Charles Landau, M.D., of the University of Texas, Dallas, contributed to this chapter in the previous edition.

CHAPTER REFERENCES

1. Hildner FJ, et al. New principles for optimum left ventriculography. *Cathet Cardiovasc Diagn* 1986;12:266.
2. Grossman W. Assessment of regional myocardial function. *J Am Coll Cardiol* 1986;7:327.
3. Herman MV, Gorlin R. Implication of left ventricular asynergy. *Am J Cardiol* 1969;23:538.
4. Bruschke AVG, Proudfit WL, Sones FM Jr. Progress study of 590 consecutive nonsurgical cases of coronary disease followed 5–9 years: II. Ventriculographic and other correlations. *Circulation* 1973;47:1154.
5. Rackley CE, Hood WP Jr. Quantitative angiographic evaluation and pathophysiologic mechanisms in valvular heart disease. *Prog Cardiovasc Dis* 1973;15:427.
6. Lehmann KG, Yang JC, Doria RJ, et al. Catheter optimization during contrast ventriculography: a prospective randomized trial. *Am Heart J* 1992;123:1273.
7. Schad N, et al. The intermittent phased injection of contrast material into the heart. *AJR Am J Roentgenol* 1968;104:464.
8. Bourdillon PD, et al. Effects of a new nonionic and a conventional ionic contrast agent on coronary sinus ionized calcium and left ventricular hemodynamics. *J Am Coll Cardiol* 1985;6:845.
9. Salem DN, Konstam MA, Isner JM, et al. Comparison of the electrocardiographic and hemodynamic response to ionic and nonionic radiocontrast media during left ventriculography: a randomized double-blind study. *Am Heart J* 1986;111:533.
10. Benotti JR. The comparative effects of ionic versus nonionic agents in cardiac catheterization. *Invest Radiol* 1988;23[Suppl 2]:5366.
11. Wisneski JA, Gertz EW, Dahlgren M, et al. Comparison of low osmolality ionic (ioxaglate) versus nonionic (iopamidol) contrast media in cardiac angiography. *Am J Cardiol* 1989;63:489.
12. Mancini GB, et al. Quantitative assessment of global and regional left ventricular function with low-contrast dose digital subtraction ventriculography. *Chest* 1985;87:598.
13. Dujardin KS, Enriques-Sarano M, Bailey KR, et al. Grading of mitral regurgitation by quantitative Doppler echocardiography: calibration by left ventricular angiography in routine clinical practice. *Circulation* 1997;96:3409.
14. Horn HR, et al. Augmentation of left ventricular contraction pattern in coronary artery disease by an inotropic catecholamine: the epinephrine ventriculogram. *Circulation* 1974;49:1063.
15. Helfant RH, et al. Nitroglycerin to unmask reversible asynergy: correlation with post coronary bypass ventriculography. *Circulation* 1974;50:108.
16. Dyke SH, Cohn PF, Gorlin R, et al. Detection of residual myocardial function in coronary artery disease using postextrasystolic potentiation. *Circulation* 1974;50:694.
17. Bolen JL, et al. Evaluation of left ventricular function in patients with aortic regurgitation using afterload stress. *Circulation* 1976;53:132.
18. Rowe GG, Zarnstorff WC. Ventricular fibrillation during selective angiography. *JAMA* 1965;192:947.
19. McBride W, Hillis LD, Lange RA. Complete heart block during retrograde left-sided cardiac catheterization. *Am J Cardiol* 1989;63:375.
20. Shammas NW, Lee JK, Daubert JP, et al. Complete heart block complicating retrograde left ventricular catheterization: case report and review. *Cathet Cardiovasc Diagn* 1994;31:122.
21. Schiller NB, Shah PM, Crawford M, et al. Recommendations for quantitation of the left ventricle by two-dimensional echocardiography. *J Am Soc Echo* 1989;2:358.
22. Cranney GB, Lotan CS, Dean L, et al. Left ventricular volume measurement using cardiac axis nuclear magnetic resonance imaging: validation by calibrated ventricular angiography. *Circulation* 1990;82:154.
23. Yang PC, Kerr AB, Liu AC, et al. New real-time interactive cardiac magnetic resonance imaging system complements echocardiography. *J Am Coll Cardiol* 1998;32:2049.
24. Woods T, Grist T, Rahko P. Leaking left ventricular pseudoaneurysm. *Circulation* 1999;100:329.
25. Gepstein L, Hayam G, Shpun S, et al. Hemodynamic evaluation of the heart with a nonfluoroscopic electromechanical mapping technique. *Circulation* 1997;96:3672.
26. Gepstein L, Goldin A, Lessick J, et al. Electromechanical characterization of chronic myocardial infarction in the canine coronary occlusion model. *Circulation* 1998;98:2055.

13
Pulmonary Angiography

Lorraine K. Skibo and Lewis Wexler

LKS: Interventional Radiologist, Saratoga Springs, NY 12866.
LW: Department of Radiology, Stanford University Hospital, Stanford, CA 94305.

Angiographic opacification of the main and branch pulmonary arteries is an infrequent but important procedure in the cardiac catheterization laboratory. The procedure was first reported by Robb and Steinberg in 1938 (1). Though the basic objective is unchanged, virtually unlimited catheter designs are available, iodinated contrast safety has increased by generations, and radiographic images can resolve seventh-order pulmonary arteries. Alternative technologies for capturing an angiographic image have also evolved, including computed tomography (CT), and magnetic resonance (MR) imaging. With the use of CT and MR angiography in the workup of suspected pulmonary embolism, fewer diagnostic pulmonary angiograms are being performed, but increasingly, more therapeutic options are catheter directed (2). Maintenance of technical skills in pulmonary arterial catheterization is therefore vital. The principles of pulmonary angiography should be part of the basic knowledge of all physicians performing catheterizations.

THE CHANGING ROLE OF CATHETER PULMONARY ANGIOGRAPHY

Indications

The basic indications for pulmonary angiography are summarized in the guidelines developed by the American College of Radiology and the Society of Cardiovascular and Interventional Radiology (Table 13.1) (3). The most common indication for pulmonary angiography probably remains pulmonary embolism. The patient may arrive for pulmonary angiography from the emergency room, after scintigraphy, or after CT or MR angiography. It is important for the conventional angiographer to understand the limitations of each imaging technique (CT and MR), to tailor the catheter angiographic study to achieve a diagnosis expeditiously and with the least risk to the patient.

Suspected pulmonary embolus when lung scintigraphy cannot be performed
High-probability lung scan when there is a contraindication to anticoagulation
Indeterminate lung scan in a patient suspected of having pulmonary embolus
Low-probability ventilation—perfusion scan in a patient with a high clinical suspicion of pulmonary embolus
Diagnosis and evaluation of suspected chronic pulmonary embolus
Diagnosis and evaluation of other suspected pulmonary abnormalities such as vasculitis, congenital and acquired anomalies, tumor encasement, and vascular malformation

TABLE 13.1. *Indications for pulmonary angiography (3)*

CT and MR Pulmonary Angiographic Limitations

Reduced image acquisition time for both CT and MR scanners has allowed images of the pulmonary arteries to be obtained during a single breath-hold while maintaining resolution. CT images can be obtained fast enough to eliminate significant image degradation from adjacent cardiac motion, and MR images can be sampled from the same phase in the cardiac cycle to freeze heart and vessel motion. Peripheral intravenous injection of iodinated (CT) or chelated gadolinium (MR) contrast material increases contrast between flowing blood and stationary tissue, producing an angiographic effect. With both modalities, cross-sectional or reconstructed three-dimensional images can be manipulated on monitors to detect subtle nonocclusive emboli.

Contrast-enhanced helical CT of the pulmonary arteries has been reported to have 90% sensitivity and 96% specificity for detection of emboli within the central pulmonary arteries (4). When Goodman et al. included subsegmental vessels, sensitivity and specificity dropped to 63% and 89%, respectively (5). Drucker and colleagues had similar findings, including subsegmental vessels, with a sensitivity of 60% and specificity of 81% (6). The CT scanners in these studies probably excluded most subsegmental vessels, as only 15 cm of the chest were scanned, starting at the top of the aortic arch. With multi-row detector CT equipment today, thin sections of the whole lung can be obtained in a single breath-hold, but subsegmental emboli may not be visualized because of limitations of spatial resolution. Partial volume effects lower contrast resolution in the right middle lobe and lingular vessels.

From a clinical perspective, failure to detect subsegmental emboli may be a major limitation of CT. For example, using the PIOPED data, Stein et al. found that 6% of patients with pulmonary embolism had emboli limited to the subsegmental vessels (7). In the subgroup of patients with low-probability perfusion scans and no

cardiopulmonary disease, patients with emboli limited to subsegmental vessels increased to 30%. In a retrospective review of patients with pulmonary embolism, Oser et al. found 30% of emboli limited to subsegmental vessels in 88 patients with positive pulmonary angiogram (8). Two patients had segmental emboli limited to the lingular or right middle lobe vessels. Although these peripheral emboli in themselves may not be immediately life-threatening, failure to detect them may lead to failure to treat the underlying condition and thus expose the patient to the risk of recurrent and potentially fatal emboli.

MR pulmonary angiography is at an earlier stage of development than CT angiography. Pulmonary MR vascular imaging is difficult because of artifacts created by motion and the air–vessel interface. Results of recent clinical studies are encouraging. Meaney et al. found sensitivities of 100%, 87%, and 75% in three independent readers of scans for suspected pulmonary embolism (9). As the technical limitations of MR pulmonary angiography are overcome, the technique may rival or surpass CT as the preferred noninvasive pulmonary angiographic technique.

Implication for Catheter Angiography After Cross-sectional Imaging

Because of the limited ability of CT and MR angiography in detecting subsegmental emboli, the patient presenting for diagnostic pulmonary angiography after a negative or nondiagnostic CT or MR study will require meticulous examination of the subsegmental vessels. Superselective injections with or without magnification may be indicated. Another reason to prefer superselective angiography is that iodinated contrast will have been given in CT, which will reduce the acceptable contrast dose available for same-day diagnostic or therapeutic pulmonary angiography.

TECHNICAL REQUIREMENTS

Digital Versus Cut-Film Angiography

For diagnostic pulmonary angiography, the American College of Radiology recommends at least a high-resolution image intensifier and television chain, plus a standard 14-inch serial film changer (3). Conventional film (with two views of each lung) is the only imaging modality that has been validated against clinical outcome (in pulmonary embolism) in a large trial (10). Recently, Hagspiel et al. found digital pulmonary angiography with selective pulmonary arterial injections equivalent to conventional cut-film angiography in diagnostic performance and image quality in the diagnosis of pulmonary embolism (11). In a prospective trial in 80 patients, Johnson et al. found digital subtraction pulmonary angiography allowed more confident detection of pulmonary emboli than did conventional cut film, without loss of accuracy (12). Though not included in the statistical analysis, Johnson et al. found more emboli with digital subtraction than cut film and with better interobserver agreement. Forauer and colleagues followed 54 patients for a mean of 12.1 months after a negative digital study for pulmonary embolism and found no documented pulmonary embolism (13). Other advantages of digital pulmonary angiography over cut film include rapid image acquisition and flexible display format. Images can be viewed individually or in cine format on the monitor, subtracted or unsubtracted. Masks can be selected image by image and pixels shifted to best match the anatomy. For these reasons, digital pulmonary angiography with selective intraarterial contrast injections has virtually replaced cut film studies.

One area in which digital angiography remains inferior to cut film is image resolution. For 1,024×1,024 matrix images laser printed on film, resolution is 1.6 line pairs per millimeter (lp/mm) for a 25-cm image intensifier, and 1.2 lp/mm for a 38-cm image intensifier. Cut film resolves from 4 to 7 lp/mm. Resolution on film recorded in a cine camera with a 25-cm image intensifier is 2.1 lp/mm (14).

Radiation Dose Considerations

The dose per image for digital, cut-film, and cine angiography is similar (with digital images probably slightly higher). The higher total dose for cineangiography results from the speed of serial acquisition, since the exposures occur at 30 to 60 images per second. Digital systems are now capable of running 15 images per second in a 1,024 matrix and up to 30 frames per second in a 512 matrix, at a cost of higher patient radiation dose.

The FDA has addressed x-ray-induced skin injuries due to long fluoroscopically guided procedures (15). Although it is unlikely that diagnostic pulmonary angiography would result in radiation injury, the laboratory director should ensure that the equipment operates within NCRP guidelines (16) and that its operators are well trained in its use. A medical physicist should supervise the equipment and quality improvement program. Most angiographic systems now produce a dose estimate for the patient, including both fluoroscopic times and angiographic run dose. This should be included as part of the patient's medical record. Pulsed fluoroscopy modes can reduce fluoroscopic dose. Whenever possible these should be used for the benefit of both patient and operator.

Monitoring Equipment and Personnel

Safe pulmonary arteriography requires patient monitoring equipment for continuous heart rate, cardiac rhythm, and blood pressure along with personnel skilled in its use. Virtually all patients should be placed on supplemental oxygen. A pulse oximeter or end-tidal carbon dioxide monitor should also be used. The radiologic technologists in the room should be completely familiar with all x-ray and angiographic equipment, including injectors, catheters, guidewires, and patient monitors. Certification as a vascular and interventional radiologic technologist ensures appropriate training. A qualified nurse should monitor the patient and record vital signs. The technologists should be trained in basic cardiac life support, and the physicians and nurses participating in the procedure should be trained in advanced cardiac life support. For pulmonary angiography, a crash cart should be located within the immediate area. Medical or surgical support teams, though only rarely required, must be promptly available in the event of complications.

All angiography procedures must be part of a laboratory's ongoing quality improvement monitoring process. Periodic review of indications, outcomes, and complications provides the opportunity to improve patient care.

CONTRAINDICATIONS

There are no absolute contraindications to pulmonary angiography. Individuals with left bundle branch block are at risk for developing complete heart block during right heart catheterization due to minor trauma of the right side of the ventricular septum. Nevertheless, passage of the catheter into the pulmonary artery for angiography can be performed safely as long as individuals skilled at transvenous pacing and the necessary equipment are immediately at hand.

Pulmonary hypertension has been considered a relative contraindication to pulmonary angiography. With the use of nonionic, low-osmolar contrast, and prophylactic oxygen, the risk of complications may be reduced. Pitton et al. measured hemodynamic parameters in patients with normal pulmonary pressure, moderate pulmonary hypertension, and severe pulmonary hypertension during pulmonary angiography with multiple selective injections of iopamidol (contrast total 167.9 ± 34.2 mL), a nonionic, low-osmolar iodinated contrast agent (17). All patients were on oxygen. Even in the patients with severe pulmonary hypertension (systolic pulmonary artery pressure more than 60 mm Hg), bolus injection of nonionic contrast into the pulmonary arteries caused no major hemodynamic effects in patients given supplemental oxygen (17).

In patients with a history of anaphylactoid reaction to intravenous contrast, the risk of a reaction can be reduced with use of preprocedural corticosteroids (orally if time permits or intravenously in emergent studies), and with use of nonionic low-osmolar contrast media. In patients with a history of allergy (food allergy or asthma), nonionic contrast should be used.

A number of cases of acute fatality after pulmonary angiography in patients on amiodarone have been reported. For example, Malden et al. describe a case of acute pulmonary toxicity and death after pulmonary angiography despite the use of nonionic contrast material (18). Caution must be used when considering pulmonary angiography in a patient on amiodarone.

COMPLICATIONS

Although pulmonary angiography is the definitive diagnostic test for imaging the pulmonary arteries, it is an invasive procedure that is accompanied by some risk of complication. Major complications can be defined as those that are life-threatening and do not respond promptly to therapy or that require intensive-care monitoring or prolonged hospitalization (e.g., when cardiopulmonary resuscitation, endotracheal intubation, dialysis, or blood transfusion is required). Minor complications can be defined as those that regress spontaneously without long-term morbidity, even if patients require prolonged monitoring. The complications seen during the PIOPED study (10) were tabulated according to these definitions (Table 13.2 and Table 13.3). Of note, the study involved injecting high-osmolar ionic contrast through pigtail

catheters with images recorded on conventional film.

Death	5 (0.5%)
Respiratory distress (CPR/intubated)	4 (0.4%)
Renal failure (dialysis)	3 (0.3%)
Hematoma (2-unit transfusion)	2 (0.2%)
Total	14 (1.3%)

TABLE 13.2. *Major complications of pulmonary angiography in 1,111 patients with suspected acute pulmonary embolism (10)*

Respiratory distress (prompt response to drugs)	4 (0.4%)
Renal dysfunction (responded to drug and fluid treatment)	10 (0.9%)
Angina (monitored in coronary care unit)	2 (0.2%)
Hypotension (prompt response to drugs/ fluids)	2 (0.2%)
Pulmonary congestion (prompt response to drugs)	4 (0.4%)
Urticaria, itching, or periorbital edema	16 (1.4%)
Hematoma (not transfused)	9 (0.81%)
Arrhythmia (spontaneous response to conversion/drugs)	6 (0.54%)
Subintimal contrast (dissection)	4 (0.4%)
Narcotic overdose (treated with naloxone)	1 (0.1%)
Nausea and vomiting	1 (0.1%)
Right bundle branch block	1 (0.1%)
Total	60 (5.4%)

TABLE 13.3. *Other complications of pulmonary angiography in 1111 patients with suspected acute pulmonary embolism (10)*

At least three of the deaths reported by Stein and colleagues may have been due to severe baseline cardiopulmonary compromise rather than to catheterization or angiography (10). Mills and coworkers report three deaths in patients with right ventricular end-diastolic pressure of more than 20 mm Hg and conclude elevated right ventricular filling pressures are associated with increased complications from pulmonary angiography (19). Marsh et al. reported the death of a patient with severe pulmonary hypertension after hand injection of only 10 mL of contrast material into the main pulmonary artery (20).

Unlike previous large series, no myocardial perforations occurred in the PIOPED series, attributed to the exclusive use of pigtail type rather than to straight catheters, such as the Eppendorf. Renal failure and insufficiency occurred in the PIOPED group in 0.3% and 1.0%, respectively, more often in elderly patients (10). This complication was not evaluated in the Mills study, but Stein and coworkers found the volume of contrast injected was not significantly greater in those patients having renal complications.

PROCEDURE

Venous Access

The right common femoral vein is the preferred venous access site, as it provides a relatively straight course to the inferior vena cava and right heart. This site also facilitates insertion of an inferior vena cava filter if indicated, to prevent recurrent thromboemboli in patients who are at high risk for anticoagulation (21). If iliac vein or caval thrombosis is present, the right internal jugular vein also provides excellent anatomy for accessing the pulmonary arteries or inferior vena cava. The left internal jugular vein is preferable if only angiography is required, as catheters preferentially seem to follow the circular path from access to right pulmonary artery (22). If access here is precluded, then the left femoral vein, followed by the right or left basilic vein at the antecubital fossa, can provide adequate access.

Patients who come to pulmonary angiography are frequently anticoagulated, and those in whom pulmonary embolism is found may be candidates for thrombolytic therapy. This places such patients at higher risk for hemorrhagic complications at the puncture site. A single-wall puncture technique is preferred to avoid inadvertent through-and-through puncture of the femoral artery (see also Chapter 4). Because of compression of the vein on entry, the needle may also puncture the back wall of the vein, with blood flow seen only during slow withdrawal of the needle. Once venous blood return is obtained, the position of the needle is fixed and a guidewire is introduced. Any floppy-tip, straight, or J wire can be used.

Pulmonary Catheterization

After appropriate dilation of the entry site, a 6F to 7F pulmonary catheter is placed over the wire. Catheters of this size are necessary to provide a lumen that will accommodate flow rates of 20 to 25 mL/sec. A 4F nylon pulmonary catheter has recently been reported that will allow flow rates of 20 mL/sec at 1,050 psi (23). Using a 4F catheter may reduce access site complications and, when used from a basilic vein (as it is designed for), removes the need for bedrest. A sidearm sheath can be left in place after the study if the patient is to go on to thrombolytic therapy. Recognizing that there are many techniques for selectively catheterizing the right and left pulmonary arteries, we describe three common approaches in Fig. 13.1.

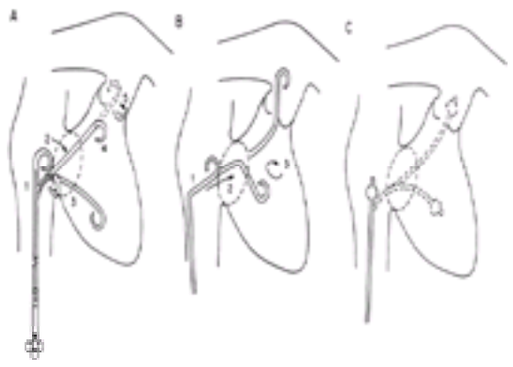

FIG. 13.1. Techniques for pulmonary artery catheterization. **(A)** Straight body pigtail catheter and tip deflecting wire. (1) The pigtail catheter is placed in the right atrium. (2) The wire is deflected to point toward the right ventricle. (3) The wire is fixed, and the catheter is advanced over it into the right ventricle. (4) The tip deflection is released. (5) Counterclockwise rotation of the catheter swings the pigtail anteriorly. Simultaneous advancement of the catheter places it into the main pulmonary artery. Advancing the catheter further usually takes it into the left main pulmonary artery. The tip-deflecting wire is utilized to direct the catheter downward and to the right for right main pulmonary artery catheterization. **(B)** Angled pigtail catheter. (1) The pigtail catheter is placed in the right atrium. (2) Advancing the catheter places the tip in the right ventricle. (3) Clockwise rotation, with simultaneous advancement places the tip in the main pulmonary artery. **(C)** Balloon catheter. The balloon is inflated under fluoroscopic guidance in the common iliac vein. It is advanced under observation through the right heart and into the main pulmonary artery. Selection of right and left pulmonary arteries is assisted with conventional or tip-deflecting wires. If a pigtail catheter is needed after use of a balloon catheter, 260-cm Rosen wire is used for the exchange.

The presence of a properly placed inferior vena caval filter does not necessarily preclude a transfemoral approach. Safe transfilter angiography has been reported with straight, 3-mm J, and 15-mm J wires through stainless steel Greenfield (Medi-tech/Boston Scientific, Watertown, MA), Vena-Tech (B. Braun Medical,), and bird's nest (Cook, Bloomington, IN) filters (24). It is important to insert and withdraw catheters only while they are straightened over a wire, to minimize the likelihood of hooking the filter. During interventional procedures that involve multiple catheter exchanges, a long sheath may be placed with its leading tip beyond the filter.

Catheter Selection

Although many catheters are available for pulmonary arteriography, virtually all are variations of two basic designs. The pigtail-type catheter confers safe passage through the right heart. There have been no reports of right ventricular perforation with a pigtail catheter (22). Various curve configurations facilitate catheterization of the pulmonary artery and the subselection of pulmonary artery branches by active catheter manipulation. The pulmonary pigtail should be tight (<1 cm), permitting use of the same catheter for subselective injections (22). In contrast, balloon-tipped catheters are passively carried by blood flow through the right heart chambers and into the pulmonary arteries. Side-holes in the catheter shaft then allow power injection in the main branches, while an end-hole makes balloon occlusion angiography possible with the same catheter (Fig. 13.2). All pigtail catheters must be removed from the pulmonary arteries straightened by a floppy-tip guidewire under fluoroscopic observation, since the catheter tip may hook a papillary muscle, chordae tendineae, or tricuspid valve leaflet during withdrawal. Balloon catheters are first deflated and can then be removed without fluoroscopy.

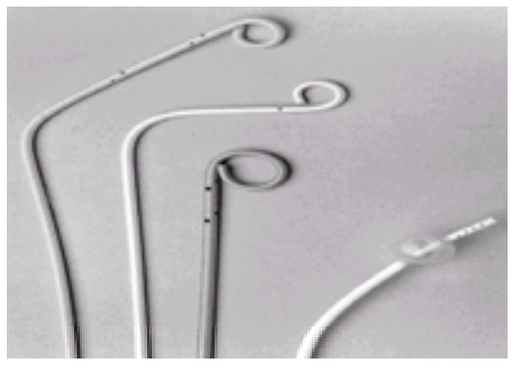

FIG. 13.2. Catheters for pulmonary angiography. Left to right: the Nyman, Grollman, and straight pigtail catheters, and the balloon occlusion catheter with side-holes distal to the balloon (Berman type).

Hemodynamic Assessment

Hemodynamic assessment should precede pulmonary angiography, allowing rational selection of appropriate supportive, therapeutic, and prophylactic measures. For example, if prompt correction of circulatory inadequacy cannot be achieved in a patient with pulmonary thromboembolism, definitive therapeutic measures to remove pulmonary emboli can be undertaken. Examination of the right heart pressures may reveal unsuspected alternative diagnoses, such as cardiac tamponade, or left ventricular failure. All right heart and pulmonary pressures need to be obtained before injection of contrast. Damping of the pressure in the main pulmonary artery may indicate massive embolism, with the catheter holes embedded in the embolus. Some clinical situations will require that a pulmonary wedge pressure be obtained. A balloon flotation catheter can be used to gain access to the pulmonary circulation for wedge pressure measurement, with subsequent exchange for a pigtail angiographic catheter.

Contrast Media

In most medical centers, low-osmolar iodinated contrast is preferentially used for pulmonary angiography, recognizing that this practice has not been shown to produce a significant reduction in mortality from contrast reaction. Moreover, changes in pulmonary hemodynamics are not significantly different when high-osmolar or low-osmolar agents are used (25). A reduction in coughing and other forms of involuntary motion with low-osmolar agents (25), however, allows the relatively motion-free images that are essential to high-quality pulmonary angiography.

Additional precautions should be taken when using low-osmolar contrast material to prevent thrombotic and embolic complications. *In vitro* activation of platelets has been demonstrated with iohexol and iopamidol in a limited number of volunteers (26). Increased plasma levels of plasminogen activator type 1 were found in patients after pulmonary angiography with iohexol, and increased thrombin–antithrombin III complexes were found after iohexol and ioxaglate (27). Prolonged contact of contrast with blood should be avoided. Some institutions utilize ionic contrast for preliminary hand injections, since ionic contrast inhibits coagulation, reserving low-osmolar agents for power injection; other institutions add heparin to low-osmolar contrast.

The amount of contrast utilized is determined by the size of and flow in the vessel selected, assessed during a test hand injection. The right and left main pulmonary arteries usually require 40 to 50 mL of contrast at 20 to 25 mL/sec. For digital recording techniques, a total of 25 mL is usually sufficient. As smaller vessels are selected, the rate and volume are decreased. For balloon occlusion angiography of segmental vessels, a hand injection of 5 to 10 mL is used.

Since the density of contrast is greater than that of blood, gravity tends to cause preferential opacification of the dependent portions of the lung in the supine patient. Pulmonary arteries of the middle lobe, lingula, and anterior segments of the upper lobe may therefore not be satisfactorily opacified (Fig. 13.3).

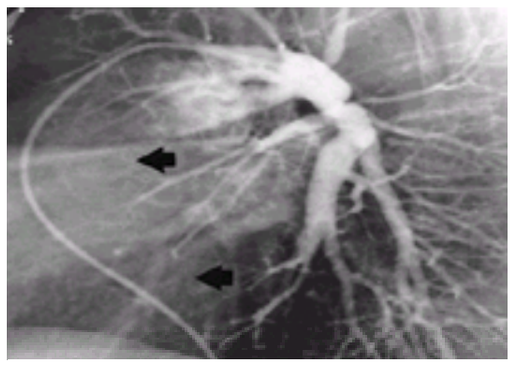

FIG. 13.3. Iodinated contrast dependency (gravitational layering). Single lateral view from a left pulmonary angiogram obtained with the patient supine demonstrates poor opacification of all the anterior pulmonary arteries *(arrows)*.

Filming

Two views of each lung are performed in the frontal and 45° ipsilateral posterior oblique (i.e., 45° right posterior oblique for the right lung) for each lung. Although the lateral is the true orthogonal view to the frontal projection, it is not desirable for most cases of pulmonary angiography, since even selective right or left injections frequently cause reflux into the opposite lung that may confuse interpretation. Use of the frontal and 45° oblique view has been validated for pulmonary embolism in a

large clinical trial (10).

Filming rates are based on the normal transit of contrast through the lung. Injected contrast reaches the capillaries in 2 to 3 seconds, and the left atrium fills in 4 to 6 seconds (28). Conventional x-ray filming rates are usually three images per second for 3 seconds and then one image per second for 6 seconds. With digital systems, a full second of masks is obtained before injection (about one cardiac cycle). For most indications, filming at six images per second is sufficient. Higher rates may be used in uncooperative patients or in situations where high flow is expected (e.g., in pulmonary arteriovenous malformations).

ANATOMY AND PHYSIOLOGY

Physiology

The pulmonary arterial system has low resistance and low pressure when compared with the systemic arterial system, with a normal main pulmonary artery pressure of 22/8 mm Hg (mean, 13 mm Hg). The main pulmonary artery is an elastic vessel (like the aorta), which serves as a reservoir for the right ventricular output. At the level of the bronchi–bronchiolar junction, muscular arteries 1.0 to 0.1 mm in diameter have a well-developed medial smooth muscle layer. Below 0.1 mm, pulmonary arteries are essentially endothelial tubes leading into the capillary networks surrounding alveoli.

The pulmonary arterial system can accommodate large changes in volume, mostly by the recruitment of previously collapsed vessels rather than by distension of open vessels. Evidence of this is seen in postpneumonectomy patients, in whom the pulmonary vascular resistance typically remains normal despite the loss of half of the pulmonary vascular bed.

Anatomy

The main pulmonary artery arises from the pulmonary conus of the right ventricle, anterior and to the left of the aorta. It ascends 4 to 5 cm in a posteromedial direction until its bifurcation into the right and left pulmonary arteries. The right pulmonary artery has a mean diameter of 23.4 mm and courses horizontally in the mediastinum anterior to the right mainstem bronchus. The right upper lobe branch arises within the mediastinum before the right hilum. The left pulmonary artery mean diameter is 26.4 mm and is a direct posterior continuation of the main pulmonary artery, passing over the left mainstem bronchus to descend posterior to the bronchus before the origin of the left upper lobe branch. Thus the proximal portion of the left pulmonary artery is foreshortened in a frontal view and is best seen in a lateral or right posterior oblique view.

Within the lung, the vessels then branch in either a bifurcational (two branches of similar size), or collateral (one small branch at a 30° to 80° angle, with the larger branch of similar size as the parent) fashion (Fig. 13.4). Lobar and segmental branching is tremendously variable but related to bronchial branching. In addition, “supernumerary” branches outnumber conventional branches and penetrate the lung directly (29). The pulmonary arteries are fairly evenly distributed throughout the lung. The segmental pulmonary veins are variable. They form two superior and two inferior veins that enter the left atrium. The left veins may join to form a common vein within the pericardium (29). The anatomy of the pulmonary arteries is displayed in Fig. 13.5.

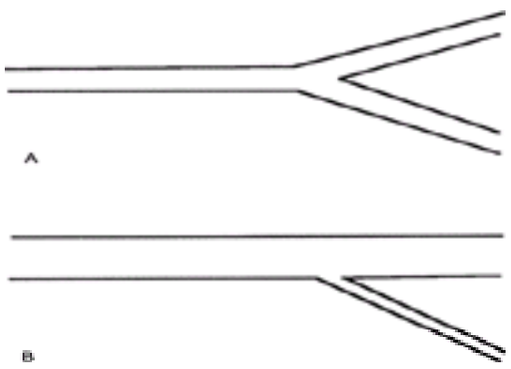

FIG. 13.4. Pulmonary artery branching. **(A)** Bifurcational branching: Diameter of the daughter branches is similar and the sum of them equals or exceeds the parent. **(B)** Collateral or disproportionate branching. The diameter of the daughter branch is much less than the parent vessel. It is important not to interpret collateral branching configurations as abnormal.

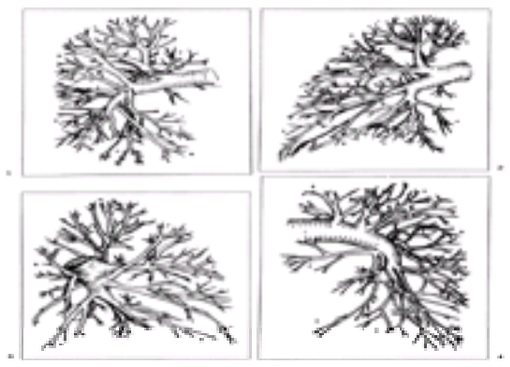

FIG. 13.5. Segmental pulmonary arterial anatomy. **(1)** Right lung, right anterior oblique view, and **(2)** right lung, left anterior oblique view. A: Right middle lobe medial segmental artery. B: Right lower lobe anterior basal segmental artery. C: Right lower lobe lateral basal segmental artery. D: Right lower lobe posterior basal segmental artery. E: Right lower lobe medial basal segmental artery. F: Right middle lobe lateral segmental artery. G: Right lower lobe superior segmental artery. H: Right upper lobe posterior segmental artery. I: Right apical segmental artery. J: Right upper lobe anterior segmental artery. **(3)** Left lung, right anterior oblique view, and **(4)** left lung, left anterior oblique view. A: Lingula, inferior segmental artery. B: Left lower lobe antero-medial basal segmental artery. C: Left lower lobe lateral basal segmental artery. D: Left lower lobe posterior basal segmental artery. E: Left upper lobe anterior segmental artery. F: Lingula, superior segmental artery. G: Left lower lobe superior segmental artery. H: Left upper lobe apical-posterior segmental artery. (From Kandarpa K, ed. *Handbook of cardiovascular and interventional radiology*.)

ANGIOGRAPHIC FINDINGS AND INTERPRETATION

Pulmonary Artery Stenosis

An increasing number of patients with repaired congenital heart disease now survive into adulthood and may present with pulmonary vascular stenoses and occlusions. Most pulmonary arterial and venous stenoses occur in association with congenital cardiac disease such as tetralogy of Fallot, truncus arteriosus, pulmonary valvular stenosis, patent ductus arteriosus, aortic stenosis, and ventricular septal defects.

Congenital single or multiple stenoses may be present without cardiac anomalies (Fig. 13.6). Stenosis may also be secondary to rubella, chronic infections (such as histoplasmosis), or infestations (such as schistosomiasis). Stenoses are associated with idiopathic hypercalcemia. Isolated stenoses may present after pulmonary artery banding after systemic to pulmonary artery shunts such as Blalock-Taussig, Waterston-Cooley, or Glenn anastamoses. Lung transplant pulmonary arterial stenoses are not common and carry a poor prognosis (30).

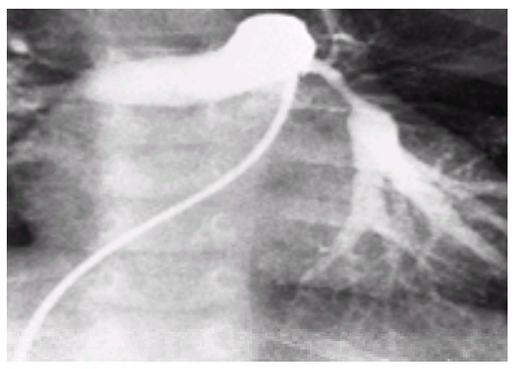

FIG. 13.6. Left interlobar pulmonary artery stenosis. Left pulmonary angiogram of isolated pulmonary arterial stenosis in an adolescent male.

It is important to measure the pressure gradient across the suspected stenosis, as the high flow in pulmonary arteries may create a significant pressure gradient despite the angiographic appearance of a mild stenosis (Fig. 13.7).

FIG. 13.7. Transplant pulmonary arterial stenosis. Left anterior oblique view of a left pulmonary arteriogram in a patient 2 months after left lung transplantation. The stenosis *(arrows)* appears mild in this view, but a pressure gradient of 20 mm Hg was measured across the stenosis.

Angioplasty and stent placement for treatment of pulmonary artery stenoses have been used primarily for treatment of congenital stenoses (31). Only sporadic case reports of angioplasty or stent placement for acquired pulmonary stenoses are in the literature (32).

Pulmonary Arteriovenous Communications

Pulmonary arteriovenous malformation (PAVM) is thought to be due to an embryologic defect in the terminal capillary loop. Polycythemia and low arterial P O_2 are manifestations of the extracardiac right-to-left shunt. Most patients with PAVMs are asymptomatic, although dyspnea, cyanosis, digital clubbing, and hemoptysis may be present. Paradoxical emboli via PAVMs can result in cerebrovascular accident or abscess. PAVMs are classified into two types (33). Simple PAVMs are usually a complex branching mass, supplied by one to three subsegmental arteries, all arising from the same segmental artery. Complex PAVMs are supplied by two or more different segmental arteries. Complex PAVMs are more frequent in the right middle lobe or lingula.

The walls of PAVMs are quite thin. Multiple PAVMs are present in one-third of cases. From 40% to 65% of PAVMs are associated with hereditary hemorrhagic telangiectasia (Rendu-Osler-Weber syndrome). PAVMs are seen rarely with Fanconi's syndrome (pancytopenia, radial ray deformities, and brown skin pigmentation).

Screening for PAVMs can be done noninvasively with bubble echocardiography or spiral CT (Fig. 13.8). When intervention is planned, selective pulmonary angiography is necessary, with frontal and both oblique views of each lung. The entire lung volume needs to be filmed, as small, subpleural PAVMs may be present (33). When PAVMs are present in the lingula or right middle lobe, lateral views should also be obtained.

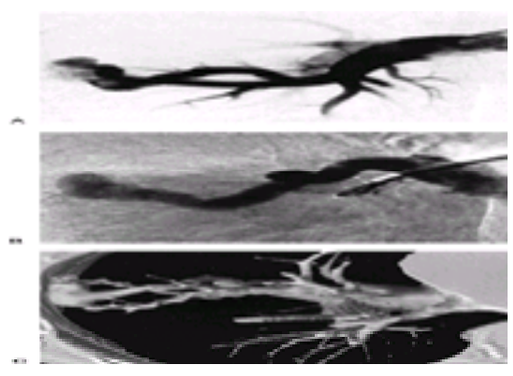

FIG. 13.8. Pulmonary arteriovenous malformation. **(A)** Digital subtraction right interlobar pulmonary angiogram demonstrates two feeding arteries, and **(B)** single draining vein in a 40-year-old dyspneic female. Shaded surface reconstructed display from her spiral CT without contrast **(C)** displays the architecture of the malformation well. (CT courtesy of G. Rubin, Stanford University Hospital, Stanford, CA.)

PAVMs can be percutaneously embolized with detachable balloons or coils (Fig. 13.9) (33). With the potential for direct systemic emboli, extreme caution must be exercised, and angiographic technique must be meticulous to avoid air embolism, catheter thrombosis and embolism, or systemic deployment of occlusion devices.

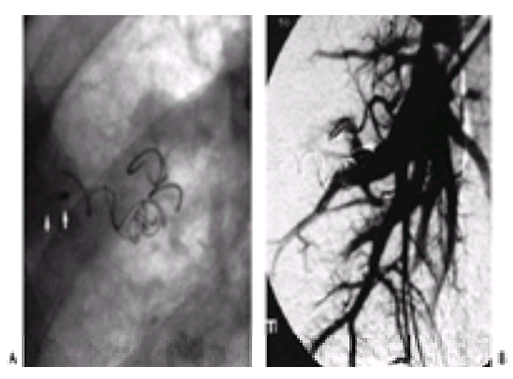

FIG. 13.9. Pulmonary arteriovenous malformation with percutaneous embolization. **A:** Digital image displaying Amplatz spider vascular occlusion device *(arrows)* trailed by multiple coils in therapeutic embolization of the arteriovenous malformation seen in Figure 13.8. **B:** Right pulmonary angiogram confirms occlusion of the

fistula.

Acquired pulmonary arteriovenous shunts can be secondary to trauma, infection, or hepatogenic angiodysplasia (34). Arteriovenous shunts seen in chronic infections of the lung may involve normal or anomalous feeding arteries and communicate with either pulmonary arteries or veins (29). Infection-related shunts are seen in bronchiectasis, invasive aspergillosis, tuberculosis, and schistosomiasis.

Diffuse or Focal Attenuation of Pulmonary Vessels

Angiography may be requested in cases of pulmonary hypertension of unknown etiology to exclude chronic pulmonary embolism. In primary pulmonary hypertension (Fig. 13.10), dilatation of the proximal pulmonary arteries is present, with smooth, rapid tapering of the vessels distally. A distal corkscrew appearance of the arteries may also be seen (29). Similar vascular findings are present in patients with secondary hypertension, but these patients will have an identifiable pulmonary, mediastinal, or cardiac cause of pulmonary hypertension.

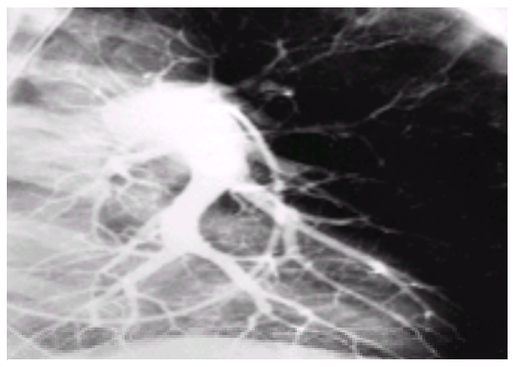

FIG. 13.10. Primary pulmonary hypertension. 45° right anterior oblique of the left pulmonary angiogram of a 30-year-old male with primary pulmonary hypertension. Note the rapid tapering of segmental vessels.

In pulmonary emphysema, peripheral vessels appear narrowed and widely spaced. Mild to moderate dilatation of central vessels may be present.

Postoperative complications involving the pulmonary circulation are rare. Torsion of a lobe or lung can occur after pulmonary resection, with diaphragmatic hernia and pneumothorax. The angiographic appearance is described in one case, after thoracotomy, as fusiform tapering of the arteries and veins at the site of torsion, with slow vascular filling (35).

Intraluminal Abnormalities

Acute Pulmonary Thromboembolism

By far the most common indication for pulmonary angiography is suspected pulmonary embolism. The clinical issues relating to diagnosis and treatment of pulmonary thromboembolism are discussed in the Profiles section of Chapter 31. Signs and symptoms, and prior imaging can guide the angiographer to particular lung segments, allowing for the most expeditious examination. A study is considered complete only when a thromboembolus is documented or when a two-view study of both lungs is negative. Primary angiographic evidence of an acute thromboembolus is a persistent central or marginal intraluminal radiolucency, or the trailing edge of an intraluminal radiolucency obstructive to contrast flow (Fig. 13.11). Secondary signs include abrupt cutoff without evidence of an intraluminal defect, oligemic or avascular regions, focal prolonged arterial phase, or abruptly tapered peripheral vessels (Fig. 13.12) (36). Examination for acute pulmonary thromboembolus ideally should be performed within 24 hours of the event. Fragmentation and partial lysis of the thromboembolus may require magnification and subselective angiography for detection of the small residual emboli.

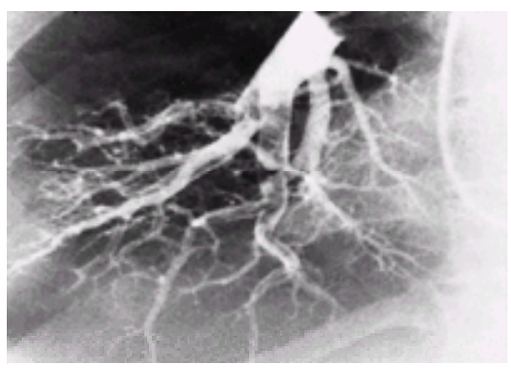

FIG. 13.11. Primary evidence of acute pulmonary thromboembolism. Single image from a balloon occlusion right lower lobe pulmonary cineangiogram demonstrates multiple intraluminal radiolucencies, almost completely outlined by contrast as primary evidence for thromboemboli.

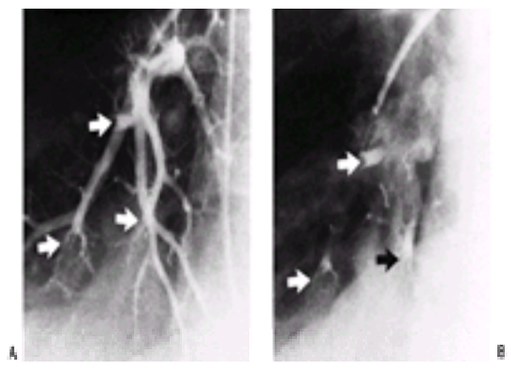

FIG. 13.12. Secondary evidence of acute pulmonary thromboembolism. **(A)** Right lower lobe balloon occlusion pulmonary cineangiogram initially demonstrates multiple vessels “cut off” *(arrows)* as an example of a secondary sign of acute pulmonary thromboembolism. When the balloon is deflated, **(B)** it becomes apparent the cutoff was the trailing edge of a thromboembolus, with a meniscus evident *(arrows)*. This sign is also considered primary evidence of acute pulmonary thromboemboli.

Methods and devices used in percutaneous mechanical thrombectomy can be utilized to treat selected cases of acute massive pulmonary thromboembolism. The

Greenfield transvenous embolectomy catheter (Medi-tech/Boston Scientific, Watertown, MA) has been available the longest, as has balloon maceration of emboli. More recently reported devices range from 14F catheters for suction embolectomy (37), to modified pigtail catheters (38), to rheolytic catheters (39). Operator or local experience probably best determines the method of choice until comparative research determines the relative efficacy of these devices for clot removal and complication.

Chronic Pulmonary Thromboembolism

In a small number of patients, pulmonary thromboemboli fail to resolve, instead organizing, recanalizing, and retracting to variable degrees (Fig. 13.13). Angiographic depiction of location and extent of disease is essential for surgical planning. Surgical thromboendarterectomy of the organized thrombus can improve or cure pulmonary hypertension and right heart dysfunction in severely affected patients. In a study of 250 patients with chronic pulmonary thromboembolism and pulmonary hypertension, Auger and coworkers report the characteristic findings of organized thrombus, confirmed surgically (Table 13.4) (40).

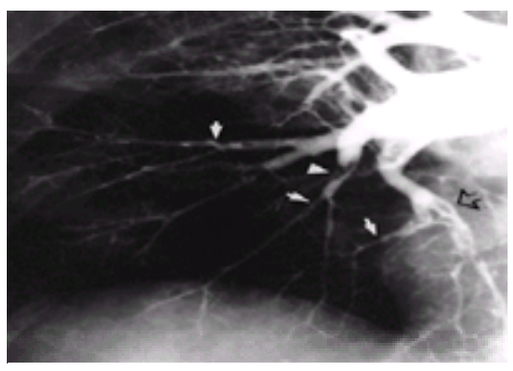

FIG. 13.13. Chronic pulmonary thromboembolism. Frontal view of right pulmonary angiogram in a 42-year-old female still dyspneic after an acute pulmonary embolus was documented 6 months earlier and treated. The proximal pulmonary arteries are dilated. The distal vessels taper rapidly and are irregular *(arrows)*. Eccentric stenoses are present *(arrowheads)*, as are intraluminal webs *(open arrow)*.

1. Pouching: contrast filling concave pouches in organized thrombus, with delayed opacification or obstruction of the distal artery
2. Webs or bands: persistent thin or thick linear radiolucencies in lobar or segmental vessels causing stenosis with or without poststenotic dilatation.
3. Luminal irregularity: scalloped arterial margins
4. Abrupt narrowing of major pulmonary arteries
5. Obstruction of lobar arteries, usually at their origin

TABLE 13.4. *Angiographic findings in chronic pulmonary thromboembolism (40)*

Pulmonary arteriography may not adequately assess the proximal extent of organized thromboemboli. In dilated proximal pulmonary arteries, concentric or smooth organized thromboembolus may mimic the appearance of a normal-sized vessel. Adjunctive imaging of the pulmonary arteries with contrast helical CT was found to be more accurate (0.79) than conventional angiography and MR in the central vessels (41). It is important to note that CT can exclude other causes of multiple stenoses and occlusions of pulmonary vessels, such as chronic infection or inflammation, Takayasu's arteritis, or neoplasm (42) (Fig. 13.14). A combination of imaging modalities may best serve the patient in the workup of chronic pulmonary embolism.

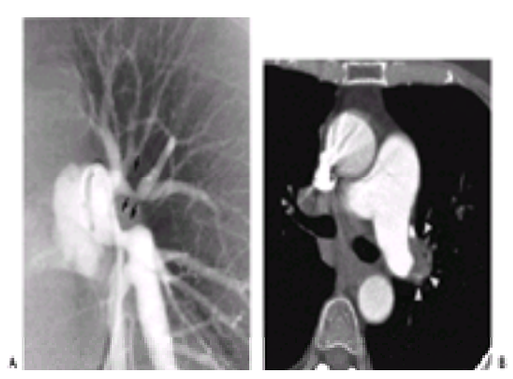

FIG. 13.14. Histoplasmosis. **A:** Left pulmonary arteriogram in a patient being evaluated for chronic pulmonary thromboembolism. Multiple eccentric stenoses are present *(arrows)*. **B:** Contrast-enhanced CT scan at the level of the left pulmonary artery demonstrates calcified, enlarged lymph nodes *(arrowheads)* in the region of angiographic abnormality. The mediastinum is diffusely abnormal, containing soft-tissue attenuation material. (Images courtesy of Ulf Nyman, Sahlgrenska University Hospital, Goteborg, Sweden.)

In situ central pulmonary arterial thrombosis can occur in severe primary pulmonary hypertension (43). Moser et al. use scintigraphy to distinguish the flow-limiting chronic thromboembolism (segmental defects present), from primary pulmonary hypertension with *in situ* thrombosis (no segmental defects).

Pulmonary Vascular Neoplasms

Leiomyosarcoma of the pulmonary artery is a rare neoplasm. It typically is seen in the main pulmonary artery in relation to the pulmonary valve. The tumor is entirely intraluminal in half of the reported cases and spreads along the lumen (29). An irregular intraluminal mass is seen at angiography. Metastases to the lung are common.

Pulmonary angiography or hemodynamic assessment may be required preoperatively when other imaging modalities have not answered all questions in mediastinal and perihilar neoplasms. Selective left or right main pulmonary angiograms are usually performed in at least two projections most likely to demonstrate the area of interest based on tumor location. It is important to evaluate the venous phase for any pulmonary venous involvement. Arterial or venous obstruction, encasement, displacement, or rarely intraluminal invasion may be identified.

Pulmonary Artery Aneurysms

Pulmonary artery aneurysms, defined as a focal increase in diameter of a vessel by 50% over its initial normal diameter, are unusual (44). They can be classified regionally as central or peripheral, in addition to morphologic/anatomic classification as fusiform, saccular, true, and false. The largest number of aneurysms occur

centrally, usually secondary to pulmonary hypertension and repairs for congenital heart disease. Congenital aneurysms result from defects in the arterial wall. Degenerative pulmonary aneurysms can be seen in Marfan's syndrome.

Almost any acute or chronic pulmonary infection can lead to the formation of pulmonary arterial aneurysms. Tuberculosis results in pulmonary artery aneurysms known as Rasmussen aneurysms. Other infectious causes of pulmonary artery aneurysms include syphilis and septic emboli. Takayasu's arteritis can rarely cause aneurysms. Multiple pulmonary artery aneurysms may be seen in Behcet's disease or the Hughes-Stovin syndrome (Fig. 13.15) (45). The presence of pulmonary aneurysms in Behcet's disease is associated with a poor prognosis (46). Rupture of pulmonary artery aneurysms usually causes fatal hemorrhage.

FIG. 13.15. Pulmonary artery aneurysms. Frontal view of right pulmonary angiogram in a young male with Hughes-Stovin syndrome demonstrates multiple saccular aneurysms. (Image courtesy of Paul Stark, V.A. Medical Center, Palo Alto, CA.)

Pseudoaneurysms of the pulmonary artery result from penetrating or catheter trauma. These and other aneurysms may be treated percutaneously by exclusion of the pseudoaneurysm sac. Ray et al. report excellent technical and clinical success in percutaneous embolization of pseudoaneurysms with coils, Gelfoam (Upjohn, Kalamazoo, MI), and suture material (47).

Inflammation

Infectious and noninfectious inflammatory diseases of the lung manifest a spectrum of findings at pulmonary arteriography. Consequently, no single finding is diagnostic of a particular disease. Noninfectious vasculitis involving the pulmonary vessels is uncommon. It can be seen in Takayasu's arteritis, where the degree of involvement has been correlated with the severity of brachiocephalic disease (48). Findings include stenosis, occlusion, and, rarely, dilatation of pulmonary arteries. CT angiography best demonstrates the wall thickening and enhancement of involved arteries (49). Systemic-to-pulmonary artery communications can exist, with bronchial arteries serving as collaterals to the occluded pulmonary arteries. Yamada and colleagues found most of the disease in the segmental and subsegmental vessels (48). Coronary-to-bronchial-to-pulmonary artery shunts can also occur (50).

Behcet's disease involves the pulmonary arteries with a nonspecific vasculitis in about 5% of patients. Angiographic finding are predominantly aneurysms, with occlusion noted less frequently (46).

In chronic thoracic infections such as histoplasmosis, granulomas can be seen in the walls or arteries, veins, or both on histologic examination. Severe mediastinitis from histoplasmosis can compress and occlude the pulmonary arteries and veins as they traverse the mediastinum. Lymph node involvement can compress adjacent arteries and veins, mimicking chronic pulmonary embolism (Fig. 13.15).

Hemorrhage

Though most life-threatening hemoptysis is of bronchial artery origin, when embolization of the bronchial arteries and other systemic collaterals fails to control hemoptysis, the pulmonary arteries should be examined in the suspected area of hemorrhage (51). Massive hemoptysis can be due to rupture of Rasmussen's aneurysms (52) or to those seen in Behcet's or Hughes-Stovin syndrome (45).

Foreign Bodies

The pulmonary arterial system is the final destination for fractured and embolized medical and nonmedical devices placed in the venous system. In most cases, a formal angiogram is not necessary as most foreign bodies encountered in this setting are radioopaque, but a hand-injected run is helpful to determine the size and orientation of the vessel containing the foreign body. Percutaneous retrieval using a nitinol snare (Microvena, White Bear Lake, MN) is highly effective and has simplified the approach to foreign-body removal. Balloons are well suited to engage lost stents and are used either to deploy the stent in a safe location or to retrieve it via a venous cutdown.

CHAPTER REFERENCES

1. Robb GP, Steinberg I. A practical method of visualization of the chambers of the heart, the pulmonary circulation, and the great blood vessels in man. *J Clin Invest* 1938;17:507.
2. Goldhaber SZ. Pulmonary embolism. *N Engl J Med* 1998;339:93.
3. ACR Standard for diagnostic arteriography in adults. American College of Radiology and Society of Cardiovascular and Interventional Radiology, Res. 8, 1993.
4. Remy-Jardin M, Remy J, Wattinne L, Giraud F. Central pulmonary thromboembolism: diagnosis with spiral volumetric CT with the single-breath-hold technique-comparison with pulmonary angiography. *Radiology* 1992;185:381.
5. Goodman LR, Curtin JJ, Mewissen MW, et al. Detection of pulmonary embolism in patients with unresolved clinical and scintigraphic diagnosis: helical CT versus angiography. *Am J Roentgenol* 1995;164:1369.
6. Drucker EA, Rivitz SM, Shepard JO, et al. Acute pulmonary embolism: assessment of helical CT for diagnosis. *Radiology* 1998;209:235.
7. Stein PD, Henry JW. Prevalence of acute pulmonary embolism in central and subsegmental pulmonary arteries and relation to probability interpretation of ventilation/perfusion lung scans. *Chest* 1997;111:1246.
8. Oser RF, Zuckerman DA, Gutierrez FR, Brink JA. Anatomic distribution of pulmonary emboli at pulmonary angiography: implications for cross-sectional imaging. *Radiology* 1996;199:31.
9. Meaney JFM, Weg JG, Chenevert TL, et al. Diagnosis of pulmonary embolism with magnetic resonance angiography. *N Engl J Med* 1997;336:1422.
10. Stein PD, Athanasoulis C, Alavi A, et al. Complications and validity of pulmonary angiography in acute pulmonary embolism. *Circulation* 1992;85:462.
11. Hagspiel KD, Polak JF, Grassi, CJ, et al. Pulmonary embolism: comparison of cut-film and digital pulmonary angiography. *Radiology* 1998;207:139.
12. Johnson MS, Stine SB, Shah H, et al. Possible pulmonary embolus: evaluation with digital subtraction versus cut-film angiography-prospective study in 80 patients. *Radiology* 1998:207:131.
13. Forauer AR, McLean GK, Wallace LP. Clinical follow-up of patients after a negative digital subtraction pulmonary arteriogram in the evaluation of pulmonary embolism. *J Vasc Interv Radiol* 1998:9:903.
14. Tomporowski S. Philips product specification database. January 1995, Philips, Shelton, CT.
15. Food and Drug Administration. Avoidance of serious x-ray induced skin injuries to patients during fluoroscopically guided procedures. Rockville, MD, 1994.
16. National Council of Radiation Protection and Measurements. Quality assurance for diagnostic imaging. Report no. 99, Bethesda, MD, 1988.
17. Pitton MB, Duber C, Mayer E, Thelen M. Hemodynamic effects of nonionic contrast bolus injection and oxygen inhalation during pulmonary angiography in patients with chronic major-vessel thromboembolic pulmonary hypertension. *Circulation* 1996;94:2485.
18. Malden ES, Tartar VM, Gutierrez FR. Acute fatality following pulmonary angiography in a patient on an amiodarone regimen--case report. *Angiology* 1993;15:152.
19. Mills SR, Jackson DC, Older RA, et al. The incidence, etiologies, and avoidance of complications of pulmonary angiography in a large series. *Radiology* 1980;136:295.
20. Marsh JD, Glynn M, Torman HA. Pulmonary angiography. Application in a new spectrum of patients. *Am J Med* 1983;75:763.
21. Becker DM, Philbrick JT, Selby JB. Inferior vena cava filters—indications, safety, and effectiveness. *Arch Int Med* 1992;152:1985.
22. Grollman JH. Pulmonary arteriography. *Cardiovasc Intervent Radiol* 1992;15:166.
23. Koizumi J, Mouri M, Watanabe M, Hiramatsu K. Transbrachial selective pulmonary angiography using a new 4Fr curved pigtail catheter and hydrophilic-coated guidewire. *Cardiovasc Intervent Radiol* 1998;21:347.
24. Hansen ME, Geller SC, Yucel EK, et al. Transfemoral venous catheterization through inferior vena caval filters: results in seven cases. *Am J Roentgenol* 1991;157:967.
25. Saeed M, Braun SD, Cohan RH, et al. Pulmonary angiography with iopamidol: patient comfort, image quality, and hemodynamics. *Radiology* 1987;165:345.
26. Hardeman MR, Konijnenberg A, Sturk A, Reekers JA. Activation of platelets by low-osmolar contrast media: differential effects of ionic and nonionic agents. *Radiology* 1994;192:563.
27. Van Beek EJR, Levi M, Reekers JA, et al. Increased plasma levels of PAI-1 after administration of nonionic contrast medium in patients undergoing pulmonary angiography. *Radiology* 1994;193:821.
28. Baum S, ed. *Abrams angiography*. Boston: Little, Brown, 1997.

29. Fraser RF, Pare JAP, Pare PD, et al. *Diagnosis of diseases of the chest,* 3rd ed. Boston: Little, Brown, 1983.
30. Clark SC, Levine AJ, Hasan A, et al. Vascular complications of lung transplantation. *Ann Thorac Surg* 1996;61:1079.
31. O'Laughlin MP, Slack MC, Grifka RG, et al. Implantation and intermediate-term follow-up of stents in congenital heart disease. *Circulation* 1993;88:605.
32. Gaubert JY, Moulin G, Thomas P, et al. Anastamotic stenosis of the left pulmonary artery after lung transplantation: treatment by percutaneous placement of an endoprosthesis. *Am J Roentgenol* 1993;161:947.
33. White RI, Pollak JS, Wirth JA. Pulmonary arteriovenous malformations: diagnosis and transcatheter embolotherapy. *J Vasc Interv Radiol* 1996;7:787.
34. Oh KS, Bender TM, Bowen A, Ledesma-Medina J. Plain radiographic, nuclear medicine and angiographic observations of hepatogenic pulmonary angiodysplasia. *Pediatr Radiol* 1983;13:111.
35. Munk PL, Vellet AD, Zwirewich C. Torsion of the upper lobe of the lung after surgery: findings on pulmonary angiography. *Am J Roentgenol* 1991;157:471.
36. Sagel SS, Greenspan RH. Nonuniform pulmonary arterial perfusion. *Radiology* 1970;99:541.
37. Lang EV, Barnhart WH, Walton DL, Raab SS. Percutaneous pulmonary thrombectomy. *J Vasc Interv Radiol* 1997;8:427.
38. Schmitz-Rode T, Janssens U, Schild HH, et al. Fragmentation of massive pulmonary embolism using a pigtail rotation catheter. *Chest* 1998;114:1427.
39. Koning R, Cribier A, Gerber L, et al. A new treatment for severe pulmonary embolism: percutaneous rheolytic thrombectomy. *Circulation* 1997;96:2498.
40. Auger WR, Fedullo PF, Moser KM, et al. Chronic major-vessel thromboembolic pulmonary artery obstruction: appearance at angiography. *Radiology* 1992;182:393.
41. Bergin CJ, Sirlin CB, Hauschildt JP, et al. Chronic thromboembolism: diagnosis with helical CT and MR imaging with angiographic and surgical correlation. *Radiology* 1997;204:695.
42. Schwickert HC, Schweden F, Schild HH, et al. Pulmonary arteries and lung parenchyma in chronic pulmonary embolism: preoperative and postoperative CT findings. *Radiology* 1994;191:351.
43. Moser KM, Fedullo PF, Finkbeiner WE, Golden J. Do patients with primary pulmonary hypertension develop extensive central thrombi? *Circulation* 1995;91:741.
44. Stark P, Jacobson F, Phillips A. Aneurysms of the pulmonary artery. *Radiology* 1994;34:323.
45. Balci NC, Semelka RC, Noone TC, Worawattanakul S. Multiple Pulmonary aneurysms secondary to Hughes-Stovin syndrome: demonstration by MR angiography. *J Magn Reson Imaging* 1998;8:1323.
46. Numan F, Islak C, Berkmen T, et al. Behcet's disease: pulmonary arterial involvement in 15 cases. *Radiology* 1994;192:465.
47. Ray CE Jr, Kaufman JA, Geller SC, et al. Embolization of pulmonary catheter-induced pulmonary artery pseudoaneurysms. *Chest* 1996;110:1370.
48. Yamada I, Shibuya H, Matsubara O. Pulmonary artery disease in Takayasu's arteritis: angiographic findings. *Am J Roentgenol* 1992;159:263.
49. Park JH, Chung JW, Im J-G, et al. Takayasu arteritis: evaluation of mural changes in the aorta and pulmonary artery with CT angiography. *Radiology* 1995;196:89.
50. Matsunaga N, Hayashi K, Sakamoto I, et al. Coronary to pulmonary artery shunts via the bronchial artery: analysis of cineangiographic studies. *Radiology* 1993;186:877.
51. Hickey NM, Peterson RA, Leech JA, et al. Percutaneous embolotherapy in life-threatening hemoptysis. *Cardiovasc Intervent Radiol* 1988;11:270.
52. Santelli ED, Katz DS, Goldschmidt AM, Thomas HA. Embolization of multiple Rasmussen aneurysms as a treatment of hemoptysis. *Radiology* 1994;193:396.

14
Angiography of the Aorta and Peripheral Arteries

Robert M. Schainfeld and Michael R. Jaff

RMS: Non-Invasive Vascular Laboratory, Tufts University School of Medicine and Division of Vascular Medicine, St. Elizabeth's Medical Center, Boston, MA 02135.
MRJ: Center for Vascular Care, Washington Hospital Center, Washington, DC 20010.

Atherosclerosis is a systemic disease that afflicts millions of patients annually in the United States. Historically, most of the clinical focus has been on its coronary artery manifestations, given their frequency and the potentially grave consequences. While vascular medicine and vascular surgical specialists, however, have long recognized that peripheral (extracardiac) arterial occlusive disease may contribute significantly to morbidity and mortality, it is only recently that invasive and interventional cardiologists have become involved in its diagnosis and management. To support that involvement, the scope of this chapter has been extended beyond the usual aortic diseases (such as dissection) to include information on atherosclerosis as it affects other major arterial territories. It reviews the natural history, clinical presentation, noninvasive diagnostic modalities, and angiographic techniques that are of value in patients with peripheral vascular disease, including aneurysmal disease of the thoracic and abdominal aorta, and atherosclerotic disease of the extracranial carotid arteries, renal arteries, and lower-extremity arteries. Additional information regarding interventional techniques is reviewed in Chapter 27, and representative case profiles are reviewed in Chapter 35.

PERIPHERAL IMAGING TECHNIQUES

Aortography and peripheral angiography have a history as long as that of cardiac catheterization. As W. Forssmann was reporting the passage of a catheter from his own arm vein into his right atrium in 1929 (1), dos Santos and colleagues described their experience in performing abdominal aortography by direct needle puncture (2). Seven years later, Nuvoli performed aortography via direct needle puncture of the ascending aorta (3). Fortunately, these direct-access techniques have now been virtually replaced by the same percutaneous (see Chapter 4) and cutdown (see Chapter 5) techniques for catheter introduction that are used for left heart catheterization, albeit with different catheters and filming techniques. Beyond these catheter-based imaging techniques, many disorders of the aorta are now diagnosed using highly refined noninvasive techniques (echocardiography, computed tomography [CT], and magnetic resonance angiography [MRA] techniques) that have the potential to provide detailed two- and even three-dimensional images.

RADIOGRAPHIC IMAGING

Radiographic invasive vascular imaging examinations have achieved a new level of complexity and sophistication over the past decade. Although many of the technical aspects are the same as those previously described for cardiac catheterization (see Chapter 2), some of the requirements for examination of the aorta and peripheral vessels are different. They are summarized in American Heart Association (AHA) task force guidelines relating to the optimal resources for the examination and endovascular treatment of peripheral and visceral vascular systems (4).

As in cardiac work, satisfactory imaging requires a radiographic gantry that is capable of angulation in both the axial and sagittal planes. It must also allow the operator to access a variety of potential catheter introduction sites, including the neck via jugular vein, arm (axillary, brachial, and radial arteries), and leg (for antegrade and retrograde femoral as well as more peripheral artery) entry sites. To capture the larger regions of interest (e.g., the entire aortic arch, the pelvic vasculature, or both legs, a larger field (14-inch or 36-cm) image intensifier is optimal. Conventionally, image recording of peripheral studies was done using film-screen radiographic techniques and mechanical rapid cut-film changers. This has now been replaced by digital angiography, which allows immediate monitor display of the acquired image, as well as electronic processing to enhance contrast, reduce noise, and subtract overlying bony and soft-tissue density. In what is known as digital subtraction angiography (DSA), a preliminary image is recorded immediately prior to contrast injection, so that any background density (bone, calcifications, soft tissue, and air densities) can be subtracted from subsequent images, which then show only the contrast-filled vessels of interest (Fig. 14.1*A*, Fig. 14.1*B*). Further postprocessing features may include reversal, magnification, pixel-shifting, picture integration, and contour enhancement of the subtracted image. Quantitative analysis (QA) may be used to assess vessel diameters and lengths, degree of luminal narrowing, and blood flow velocity. The resulting electronic images may be stored digitally and may also be transmitted to other sites for simultaneous review. Although it is not used in cardiac work (where cardiac motion precludes acquiring as suitable “mask” image), DSA is of great value in peripheral work where it can reduce the volume of contrast required for an examination (improving patient comfort, reducing the risk of local vascular and systemic contrast toxicity), shorten the time needed to perform the procedure, reduce radiation exposure, and lower film cost (because only the selected best images are captured to film).

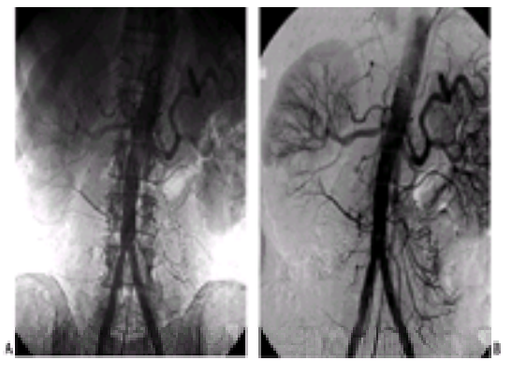

FIG. 14.1. A: Normal abdominal aortogram utilizing iodinated contrast material obtained by digital imaging technique. **B:** Same imaging data as for (A); however, enhancement of contrast-filled vessels obtained by the subtraction of all background densities (bones, soft tissue, gas) as recorded on a “mask,” immediately prior to contrast injection.

CATHETERS AND GUIDEWIRES

Just as there is a wide range of cardiac catheters and guidewires, vascular angiography and intervention have a wide range of tools to meet different anatomic challenges. In addition to standard, thin-walled 18-gauge needles that will accommodate an 0.038-inch wire, micropuncture (i.e., 21-gauge) needle sets are available that allow conversion to a standard (i.e., 0.035-inch) guidewire in situations with a high risk of bleeding, if anticipating unsuccessful needle punctures or thrombolytic therapy.

Most peripheral guidewires are made of a stainless steel coil surrounding a tapered inner core that runs the length of the wire for additional strength. A central safety wire filament is incorporated to prevent separation should the wire coil ever fracture. Standard wires vary in diameter from 0.012 to 0.052 inch, with 0.035 and 0.038 being the most commonly used sizes. The length of most standard wires is between 100 and 180 cm; longer exchange-length guidewires (measuring 260 to 300 cm) permit keeping the tip of the wire in a selected position during catheter exchange. Tip configurations include straight or angled tip and J shape. Special features may include the ability to move the wire's inner core to vary the length of the floppy tip, deflect the wire tip, or transmit torque from the shaft to the tip so that it can be steered within the vascular tree. Varying degrees of shaft stiffness (e.g., extrasupport wires) allow advancement of stiff devices through tortuous vessels, and low-friction wires with a hydrophilic coating (glidewires) have revolutionized peripheral work and made it possible to perform superselective catheterization, and traverse complex stenoses and long occlusions.

Peripheral angiographic catheters are constructed of polyurethane, polyethylene, Teflon, or nylon, with wire braid to impart torqueability. An ideal catheter has good memory, nonthrombogenicity, sufficient torque control to facilitate rotational positions, ability to accommodate high-pressure injection, and ready trackability, frequently aided by hydrophilic polymer coating. Catheters vary in French size, length, and hole pattern. They may have either a single end-hole for selective injections, both end- and side-holes, or a blocked end with side-holes only. For catheters designed to be positioned in the abdominal aorta, 60- to 80-cm lengths are sufficient; in the thoracic or carotid areas, 100- to 120-cm lengths (similar to those of left heart catheters) may be required. The most common diagnostic catheter sizes are 5F to 7F, although 3F and 4F systems have gained popularity when brachial and radial arteries are used for access.

Several catheter shapes have been designed, which ultimately determines a specific function (Fig. 14.2). They fall into these general families:

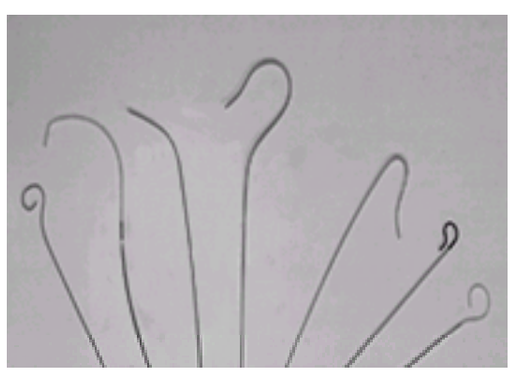

FIG. 14.2. Peripheral angiographic catheters. **Left to right:** Pigtail, cobra, multipurpose, headhunter, Simmons, SOS-OMNI, tennis-racquet.

Straight catheters with multiple side ports that are used for rapid injection into large vessels, and for exchange.

Pigtail or tennis-racquet catheters that are used for nonselective angiography in large vessels (i.e., aorta, pulmonary artery, or cardiac chambers). Multiple side-holes along the distal shaft allow rapid delivery of contrast without a single forceful jet that could cause catheter whipping or subintimal dissection, as might be seen with contrast exiting the end-hole alone.

Simple curved catheters (e.g., Berenstein, Cobra [Merit Medical, South Jordan, UT], Headhunter), that are used for vessel selection.

Complex reverse-curve catheters (e.g., Simmons [Cook Medical, Bloomington IN], Sidewinder [Cordis, a Johnson & Johnson Co., Warren, NJ], SOS-OMNI [Angio Dynamics, Queensbury, NY]), that are used for selective catheterization of certain aortic branches.

CONTRAST AGENTS

Because high-osmolar contrast materials (e.g., iothalamate, diatrizote) produce general side-effects (such as nausea, vomiting, light-headedness) as well as intense local pain, during peripheral injection, patient tolerance is improved by the use of low-osmolar agents (5). Low-osmolar agents also deliver a lesser osmotic load, thereby reducing any intravascular volume augmentation, which could be hazardous in patients with congestive heart failure or renal dysfunction. They are a necessity when there is a possibility of filling carotid, vertebral, or spinal artery branches and should be used for pulmonary arteriography to avoid pulmonary vasoconstriction.

In recent years, two new contrast agents have emerged as alternatives in patients with severe renal dysfunction or a history of life-threatening contrast allergy. *Carbon dioxide* (CO_2) as a contrast agent has been utilized extensively in many vascular beds (6,7 and 8). Its primary advantage is that it obviates any risk of allergic reaction or nephrotoxicity (8,9 and 10). Its application is limited to arteries below the diaphragm, to minimize the risk of intracerebral embolization. To be used effectively, digital subtraction equipment is required. Another agent, *gadolinium* (gadopentetate dimeglumine), has been used traditionally with magnetic resonance imaging. Recently, however, it has also been used as a contrast agent during catheter-directed radiographic peripheral vascular imaging (11,12). Like CO_2, it is relatively nontoxic, although the maximal dose is limited to 0.4 mmol/kg (approximately 60 mL). It lower K-edge absorbance energy may also require some adjustment to radiographic technique (lower kilovolts) compared with iodine-based imaging (Fig. 14.3*A*, Fig. 14.3*B*).

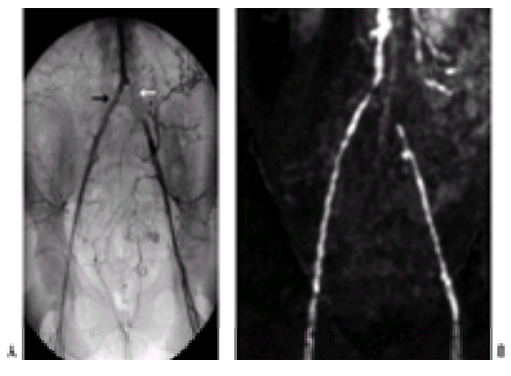

FIG. 14.3. A: Pelvic arteriogram of 75-year-old female with bilateral hip claudication demonstrating diffuse infrarenal aortic atherosclerosis, right common iliac artery

stenosis *(black arrow)* and left common iliac artery occlusion *(white arrow)* with external iliac artery reconstitution via collaterals. **B:** Corresponding MRA with two-dimensional gadolinium-enhanced technique that mirrors the DSA image.

VASCULAR ACCESS

Deciding on the optimal puncture site in the patient with peripheral vascular disease is analogous to the surgeon's planning of an incision. The goals are to facilitate the procedure, reduce the likelihood of complications, and shorten the duration of the procedure. The optimal site of access may be determined by the physical examination, complemented with data obtained by noninvasive studies (e.g., duplex ultrasonography), to avoid entry into heavily diseased or occluded vessels. The most common sites remain the common femoral and brachial arteries. If the femoral pulse is diminished or absent (e.g., due to occlusion more proximally), one of several methods may be employed to facilitate successful entry of the artery (13,14). Fluoroscopic landmarks include the facts that the common femoral artery usually overlies the medial third of the femoral head, and that arterial wall calcification is frequently present. Ultrasound guidance, and road mapping of a contrast injection performed via a catheter positioned in the distal aorta from the contralateral groin may be helpful.

One technique unique to peripheral angiography—antegrade puncture of the common femoral artery (CFA)—is required for many infrainguinal procedures. As in retrograde access, the desired site of entry is in the middle of the CFA below the inguinal ligament; therefore the skin puncture is made at or above the *top* of the femoral head (not the bottom of the femoral head as during retrograde puncture) (15) (Fig. 14.4). A less acute needle angle, generally less than 45°, should be maintained to facilitate catheter and sheath insertion by avoiding the kinking that may occur with a steeper-angled entry. Single-wall puncture of the artery (rather than the classic through-and-through Seldinger approach) may reduce bleeding complications. Great care should be exercised in advancing and manipulating catheters and guidewires in the severely diseased peripheral circulation, to reduce the chance of embolization related to the traumatic disruption of cholesterol-rich atherosclerotic plaque. This rare but devastating complication of arteriography may lead to livedo reticularis, hypertension, renal failure, gangrene, stroke, or death (see Chapter 3). Although there are no proven therapies effective in the management of this dreadful complication, prostanoids (e.g., PGE_1, PGI_2) may serve a palliative role in those cases in which it occurs (16,17).

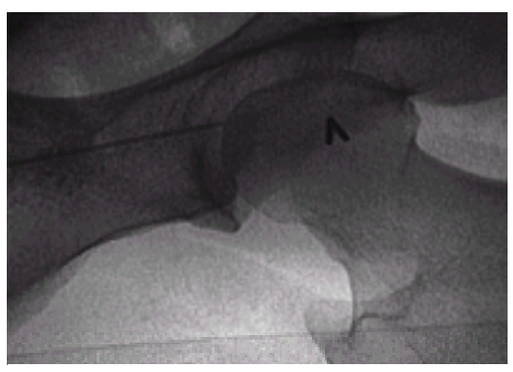

FIG. 14.4. Antegrade femoral artery puncture. The skin nick at the top of the femoral head (needle), with ideal entry at the middle of the common femoral artery with angle less than 45°.

Beyond these general peripheral imaging techniques, there are a number of important considerations relating to each portion of the arterial tree. In this and subsequent chapters relating to the peripheral circulation (Chapter 27 and Chapter 35), we will review the territories in a head-to-foot sequence.

THORACIC AORTA

Anatomy

The aortic valve is composed of three leaflets that form the three sinuses of Valsalva: right, left, and posterior (18). The ascending aorta itself begins just beyond the sinus segment and courses in a mostly anterior to posterior direction. The diameter of the ascending aorta varies between 2.2 cm and 3.8 cm in middle-aged adults, and increases slightly with advancing age (19). After it passes over the main pulmonary artery and left mainstem bronchus, the aorta gives rise to the brachiocephalic trunk and then courses posteriorly and leftward in front of the trachea. It then gives rise to the remaining arch vessels—the left common carotid, and left subclavian arteries—from its upper surface (Fig. 14.5*A*).

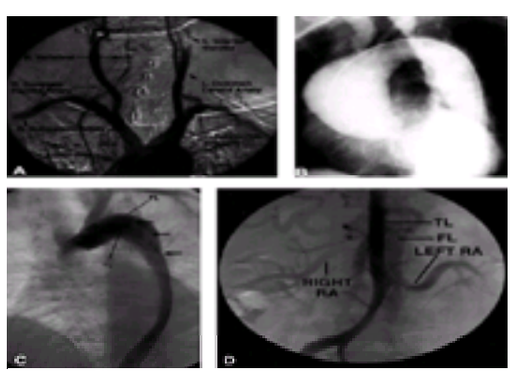

FIG. 14.5. A: Normal ascending and arch aortogram with great vessels. **B:** Ascending aortic aneurysm due to cystic medial degeneration. **C:** Stanford type A aortic dissection following aortic valve replacement. The intimal dissection flap *(arrows)* separates the contrast-filled true lumen (TL) from the false lumen (FL) that compromises the TL as it proceeds distally. **D:** The dissection extending into the abdominal aorta with origination of the left renal artery from the FL and TL supplying the right renal artery.

Distal to the origin of the left subclavian artery, the aorta narrows slightly at the site of the isthmus where the ligamentum arteriosum (the remnant of the fetal ductus arteriosus) tethers the aorta to the left pulmonary artery. Just distally to this point, a fusiform dilatation, called the aortic spindle, may occur. The descending aorta then continues anterior to the spine, with a diameter of approximately 2.5 cm. Vessels deriving from the descending portion of the aorta are nine pairs of posterior intercostal arteries (levels T-3 to T-11). The first and second posterior intercostal arteries are supplied by the superior intercostal artery, which is a branch of the subclavian artery. At the level of the fourth to sixth thoracic vertebrae, anteriorly directed bronchial arteries arise to supply each lung.

Disorders of the Thoracic Aorta

Aortic Coarctation

Coarctation of the aorta occurs in 0.02% to 0.06% of the population and may be associated with bicuspid aortic valve (33% of cases), patent ductus arteriosus, ventricular septal defect (VSD), or Turner's syndrome (20). To bypass the resulting bandlike narrowing of the aorta, collateral flow occurs retrograde into the posterior intercostal branches of the descending aorta. The resultant enlargement and tortuosity of these intercostal arteries are responsible for the “rib notching” seen on chest

roentgenograms.

Findings by aortography or MRI are a severe, discrete narrowing of the aorta at the isthmus, dilatation of the ascending aorta, and enlarged internal thoracic and intercostal arteries (21). Aortography assumes a significant role in differentiating the great variety of abnormal patterns, including complete aortic interruption, hypoplastic aorta, and the most common type—a stenosis at the site of the isthmus, distal to the origin of the left subclavian artery. Both anteroposterior (AP) and lateral (right anterior oblique [RAO] to left anterior oblique [LAO]) aortography should be initially undertaken, with contrast injection performed proximal to the presumed site of coarctation using either large-film or cineangiographic technique. When attempting to traverse the site of narrowing in retrograde fashion, care must be taken to avoid inadvertent perforation of the thin-walled poststenotic segment. Entrance to the prestenotic aorta from the brachial or axillary arteries may thus be preferred.

Patent Ductus Arteriosus

The prevalence of patent ductus arteriosus is one in 5,500 children less than 14 years of age (22). Selective aortic angiography is sensitive in demonstrating small shunts and surpasses the sensitivity of right heart catheterization with stepwise oximetry (see also Chapter 6, Chapter 28, and Chapter 34).

Aortic Aneurysms

Thoracic aortic aneurysms (TAAs) and pseudoaneurysms may have various etiologies. These include those that are related to degeneration or atherosclerosis, trauma, infection (syphilitic, bacterial), cystic medial degeneration, connective-tissue disorders, vasculitis, chronic dissection, and congenital (aneurysms of the Valsalva sinus) causes. Degenerative aneurysms involving the descending aorta account for about 75% of TAAs (23,24). Cystic medial degeneration (as seen in Marfan's syndrome, see below) may also produce aneurysms of the ascending aorta (25) (Fig. 14.5*B*). Aneurysms caused by blunt or penetrating trauma often involve the proximal descending thoracic aorta, where the mobile arch segment joins the descending segment that is fixed to the spine (26,27 and 28). They often represent pseudoaneurysms—contained ruptures that are lacking intimal and medial components and are contained only by adventitia and periaortic tissue.

The natural history of TAAs is poorly understood as compared with the extensive data available on untreated infrarenal abdominal aortic aneurysms (30). Many patients with thoracic aortic aneurysms are asymptomatic at the time of diagnosis, with the aneurysm incidentally detected during testing for an unrelated disorder. Thoracic aneurysms appear to enlarge at a more rapid rate than abdominal aneurysms (0.42 versus 0.28 cm/year), and aneurysms larger than 5 to 6 cm in diameter enlarge even faster and have a greater likelihood of rupture (29,30 and 31). The cumulative 5-year risk of rupture is increased fivefold in aneurysms 6 cm or greater in diameter. Symptoms tend to develop late in the course of the enlargement of the aorta, and are usually related to impingement on adjacent structures. In addition to presenting with catastrophic rupture, patients with TAA may report dyspnea, hoarseness, dysphagia, stridor, and plethora with edema from superior vena cava (SVC) compression. Neck or jaw pain may also be present in patients with aneurysms of the aortic arch. Dilatation of the aortic valve annulus and aortic valve may produce aortic regurgitation and congestive heart failure. Aneurysms of the descending thoracic aorta may produce pleuritic left-sided or interscapular pain, and thoracoabdominal aortic aneurysms may induce complaints of abdominal pain and left shoulder discomfort from irritation of the left hemidiaphragm.

The primary treatment for TAAs is surgical repair when the diameter exceeds 5 to 6 cm or symptoms develop (32). The standard procedure is to use a Dacron graft to replace the diseased segment. In most patients undergoing elective thoracic aorta surgical repair, aortography is required to provide information about the location of the aneurysm and its relationship to major aortic branches in the chest and abdomen. Optimal surgical approaches, as well as operative risks are best defined by imaging the coronary, brachiocephalic, visceral, and renal arteries during injections. Stent-graft devices have been successfully employed as an alternative to surgical grafting for both thoracic and aortic degenerative and posttraumatic descending TAAs (33,34 and 35). Early experience has been limited by incomplete aneurysm thrombosis, graft leak and failure. However, further refinements in the technology may make this modality a viable option in poor surgical candidates.

Aortic Dissection

Aortic dissection is a longitudinal cleavage of the aortic media by a dissecting column of blood (36). An intimal tear allows the passage of blood into the aortic wall, separating the inner and outer layers of the aortic wall and creating a “double-barrel lumen” (37). Men are affected about twice as frequently as women (38). Most patients are between 50 and 70 years of age, and have arterial hypertension (39). Other risk factors include cystic medial degeneration (40), Marfan's syndrome (41), bicuspid aortic valve (39), aortic coarctation, blunt trauma (39), pregnancy (42,43), connective-tissue disorders (41), and thoracic aorta operative procedures (44). The dissection may extend proximally from its origin to the aortic annulus, or distally to involve the entire length of the aorta and any or all of its major branches, until terminated by an aortic branch or atherosclerotic plaque. Two classification systems of aortic dissection are widely used. The *DeBakey* classification is based on the anatomic extent of the dissection (45,46). In type I, the tear originates in the ascending aorta and extends distally. Type II dissections are confined to the ascending aorta. In type III, the dissection may be confined to the descending aorta (type IIIa) or extend into the abdominal aorta and iliac arteries (type IIIb). The *Stanford* classification is based solely on the location of the origin of the dissection (47). Type A includes all cases where the ascending aorta is involved, and type B includes those where the ascending aorta is not involved (Fig. 14.5*C*, Fig. 14.5*D*).

Dissection is usually heralded by the sudden onset of excruciating pain described as “tearing, throbbing, lacerating, ripping, or burning” in the anterior chest, neck, or interscapular region (48). Similar pain may occur with rupture or sudden expansion of a chronic dissection. If the acute dissection results in compression of aortic branches, symptoms and signs of acute myocardial infarction (49), stroke or transient ischemic attack, paraparesis (50), mesenteric ischemia, renal failure (51), paraplegia, and extremity ischemia (52) may result. The majority of patients with ascending aortic extension who are treated medically die within 3 months, usually from dissection into the pericardium, mediastinum, or pleural cavity.

Once considered the “gold standard” for diagnosis of aortic dissection, aortography (which has a sensitivity of 80% and specificity of about 95%) has largely been replaced by CT, MRA, and transesophageal echocardiography (TEE) (53). Intimal flap visualization is the only direct aortographic sign that is pathognomonic of dissection. This is frequently in association with delayed or sluggish filling of a second lumen, although about 20% of patients with aortic dissection have only one visible aortic channel. The presence of a false lumen may still be suspected, however, if that single channel shows evidence of extrinsic compression by a hematoma in the false lumen. Beyond documenting the dissection, aortography provides information about aortic insufficiency and branch vessel or coronary artery involvement, particularly in cases where CT or MRI findings are equivocal and there is a strong clinical suspicion of aortic dissection (54).

When approaching a patient with suspected aortic dissection, the preferred entry point is the femoral artery with the best pulse. An atraumatic diagnostic catheter (e.g., pigtail or tennis racquet) with a soft J-tipped guidewire should be advanced under fluoroscopic guidance with frequent test injections. Since the entry to the false lumen is commonly on the greater (outer) curve of the aorta, the catheter may be used to direct the wire toward the inner curve to maximize the chance of remaining in the true lumen. If this is done successfully, structures like the aortic leaflets and coronary arteries will be observed, and it will be possible to enter the left ventricle. It is not uncommon, however, to enter the false lumen during initial catheter advancement. When this becomes apparent on test injections, care should be taken to avoid extending the false lumen, pulling the catheter back and using the techniques discussed above to reenter the true lumen.

Surgical repair of Stanford type A aortic dissections entails Dacron graft replacement of the ascending aorta (55). If the aortic valve is abnormal, it is replaced (56). In contrast, most patients with type B acute aortic dissections can be initially treated with medical therapy, reserving surgical intervention for those with signs of impending rupture (persistent pain and hypotension), ischemia of legs or mesentery, renal failure, paraparesis, or paraplegia (57). In cases of chronic dissection, operative treatment should be considered if the diameter of the descending aorta exceeds 5 to 6 cm or symptoms develop. Endovascular stents and balloon fenestration have been successfully used in treating the ischemic complications associated with aortic dissection (58,59 and 60).

Vasculitides

Vasculitis, highlighted by inflammation of the vessel wall, has two forms which commonly affect the aorta and its branches. These produce dilation of the proximal aorta, narrowing or occlusion of large aortic branches, or both. Takayasu's arteritis is characterized by irregularity of the ascending aorta, narrowing of the descending aorta, obstructions of arch vessels and aortic insufficiency or dissection (61,62 and 63). Therapeutic options include surgical bypass or balloon angioplasty demonstrating adjunctive stenting in patients with end-organ ischemia (64,65). Intervention should generally be reserved until acute inflammation has subsided.

Giant cell or temporal arteritis is a vasculitis of large and medium-sized arteries, and is likely a variant of Takayasu's arteritis. Angiographic evidence of aortic branch involvement shows long, smooth stenoses alternating with relatively normal segments. The intracranial carotid artery and its branches, or the distal subclavian arteries, are usually involved, with aortic disease relatively uncommon (66).

Connective-Tissue Disorders

Several inherited diseases—including Marfan's syndrome, Ehlers-Danlos syndrome, and hereditary annuloaortic ectasia—may be responsible for noninflammatory degeneration of the aortic wall. These may lead to aneurysm formation, rupture, or dissection.

Marfan's syndrome is a rare autosomal dominant disorder that may affect the aorta, heart, eye, and skeleton. Cardiovascular complications occur in greater than 50% of patients (67,68). Cystic medial degeneration accounts for the resultant changes in aortic root dilation with aortic ectasia, aortic insufficiency, aneurysm formation, or dissection (69). In Marfan's syndrome the aortic dilatation is primarily confined to the aortic root. Asymptomatic aortic dissection may be seen in approximately 10% of patients. Treatment for patients with Marfan's syndrome and cystic medial degenerative disease should include elective replacement of the ascending aorta and the aortic sinuses when the greatest diameter of the aorta is 5.0 to 5.5 cm (70). The most commonly performed procedure is replacement of the ascending aorta and the aortic valve with a composite graft containing Dacron and a mechanical valve prosthesis. The coronary arteries are reimplanted in the Dacron graft (71).

Ehlers-Danlos syndrome is a rare set of genetic disorders of collagen production. The literature describes more than nine types of this syndrome with features of hyperextensibility of joints and thick skin. Vascular complications include vessel thrombosis, rupture, or embolization from aneurysms (72).

Thoracic Aortography

Arch aortography has historically been used to examine the aorta for aortic valve or root disease; suspected aneurysms, dissections; congenital anomalies, such as vascular rings, coarctation, or patent ductus arteriosus; evaluation of vascular injuries associated with blunt or penetrating chest trauma; and examination of stenoses at the origins of the great vessels. TEE, CT, and MRA have made substantial inroads in the role traditionally reserved for arch aortography.

Thoracic aortography is usually performed from the femoral approach. In cases of suspected aortic dissection with diminished or absent femoral pulses or a history of catheter-related cholesterol embolization, angiography may also be performed safely via a brachial approach. A high-flow multiple-side-hole pigtail catheter is positioned in the ascending aorta, just above the sinus of Valsalva. It should be positioned there by pulling back from the sinuses, so that any unfolding that occurs during injection will not thrust the catheter across the aortic valve. Contrast (40 to 60 mL injected at 20 to 30 mL/sec) is injected using a power injector. For cine imaging, 30 (or 15) frames per second may be used; for cut-film or digital imaging three frames per second or faster should be used, with the patient instructed to breath-hold to avoid motion artifact. The LAO projection optimally delineates the aortic arch. In the RAO projection, the ascending and descending aortas are often superimposed, and the origin of the great vessels may be obscured.

ABDOMINAL AORTA

Anatomy

The abdominal aorta starts at the level of the diaphragm (T-12) and proceeds anterior to the spine and to the left of the inferior vena cava until it bifurcates into the common iliac arteries at the level of the fourth lumbar vertebra (18) (Fig. 14.6*A*). The normal diameter of the midabdominal aorta varies between 1.50 cm and 2.15 cm, with a slight increase in size with age and male gender (73). Three main branches of the aorta originate from its ventral surface. The first is the celiac artery at the level of T-12 to L-1. The second branch is the superior mesenteric artery (SMA) which takes off about 1 cm caudal to the celiac axis, at the L-1 to L-2 level. The third is the inferior mesenteric artery (IMA), which originates at the L-3 to L-4 level and takes off in an anterolateral direction, slightly to the left. The renal arteries originate posterolaterally from the aorta at the level of L-1 to L-2 (just below the SMA). Four pairs of lumbar arteries arise in a posterolateral direction, below the main renal arteries.

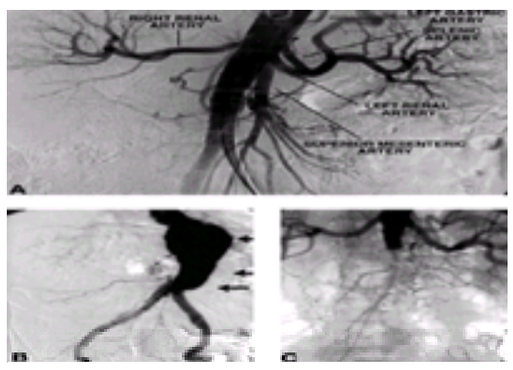

FIG. 14.6. A: Normal abdominal aortogram in anteroposterior projection. **B:** Aortogram demonstrating an infrarenal abdominal aortic aneurysm (4.7 cm) that underestimates the accurate size due to the presence of mural thrombus *(arrows)*. **C:** Distal aortic occlusion below the renal arteries.

Clinical Manifestations of Abdominal Aortic Disease

In patients with abdominal aortic aneurysms (AAA), the goals of preoperative imaging are detection, staging, surveillance, and diagnosis of rupture (74,75). Important information in planning a management strategy includes the size and length of the AAA, proximal and distal margins, number, location and patency of renal and mesenteric arteries, presence of lower-extremity occlusive disease, and any associated aneurysmal disease (e.g., iliac, hypogastric, femoral, or other intraabdominal vessels) (Fig. 14.6*B*). The role of abdominal aortography in the preoperative assessment of patients with AAA has diminished with the advent of CT, MRI, and sonography. Preoperative angiography may be useful in the cases of suspected suprarenal or juxtarenal aortic aneurysm involvement, renal or mesenteric artery stenosis, horseshoe kidney, and iliofemoral occlusive disease.

Atherosclerotic occlusive disease (ASO), or asteriosclerois obliterans, may warrant arteriographic examination of the aorta. ASO may result in complete occlusion of the aorta (76) (Fig. 14.6*C*). The etiology usually is a chronic thrombotic occlusion superimposed on severe atherosclerosis of the distal aorta and iliac arteries. Leriche syndrome is a chronic aortic occlusion that consists of buttock and thigh claudication, impotence, and the absence of femoral pulses (77). Congenital coarctation syndromes, which include Williams' syndrome (78), neurofibromatosis (79), congenital rubella (80), and tuberous sclerosis (81), may also involve the abdominal aorta and its branches. Aortography reveals a smooth, tapered proximal and midabdominal aorta with proximal renal artery involvement, and narrowing of the superior mesenteric or celiac arteries. Middle aortic syndrome (abdominal aortic coarctation) produces stenoses of the midaorta and its associated major branches (82). Treatment options include surgical bypass or percutaneous transluminal angioplasty with endovascular stenting in certain cases, although experience is limited, and the exact role of the latter is controversial (83).

Abdominal Aortography Technique

Abdominal aortography is performed from a femoral approach, utilizing a 4F or 5F multiple-side-hole pigtail or tennis-racquet diagnostic catheter. If the femoral pulse is not palpable on either side, other options include translumbar, axillary, brachial, or radial access. The tip of the catheter should be positioned at the T-12 or L-1 level, thus placing the side-holes adjacent to the first and second lumbar vertebrae. Contrast medium should be injected (30 to 60 mL at a rate of 15 to 30 mL/sec). At least three frames per second should be obtained when evaluating the mesenteric or renal arteries. Two views of the aorta—anteroposterior and lateral—generally provide sufficient information regarding the aorta and mesenteric vessels. When performing arteriography in an aorta with suspected or known aneurysmal disease or severe atherosclerotic involvement, meticulous care should be taken to avoid dislodging mural thrombus or plaque, potentially liberating distal atheroemboli.

SUBCLAVIAN AND VERTEBRAL ARTERIES

Anatomy

The brachiocephalic, left common carotid, and left subclavian arteries arise from the aortic arch after it passes over the main pulmonary artery and left main stem bronchus (18). While the right subclavian artery and right common carotid originate as branches of the brachiocephalic trunk (also known as the “innominate” artery), the left common carotid and left subclavian usually originate separately from the aortic arch. An aortic arch variant in which the brachiocephalic and left common carotid artery may have a common origin (i.e., “bovine arch”) is present in about 10% of the population (84). The major branches of the subclavian artery that deserve special attention are the internal mammary and vertebral arteries; the latter originate from the superior aspect of the vessel (opposite the internal mammary) and proceed into the skull through the cervical transverse processes.

Manifestations of Subclavian Disease

Atherosclerosis of the proximal subclavian artery may manifest clinically as arm claudication, subclavian-steal syndrome (85), or (in patients with previous internal mammary grafting) coronary ischemia (86). In classic subclavian steal, stenosis or occlusion of the proximal subclavian artery causes blood from the contralateral vertebral artery to flow antegrade across the basilar system and then retrograde down the ipsilateral vertebral to fill the subclavian artery distal to the lesion (Fig. 14.7*A*). In rare cases, this may cause cerebral ischemia during upper-extremity exercise. In patients who have undergone internal mammary artery bypass grafting to a coronary artery, a proximal subclavian obstruction may cause retrograde flow in the graft during arm exercise and lead to coronary ischemia (coronary-subclavian-steal) (Fig. 14.7*B*, Fig. 14.7*C*). Stenosis of the vertebral origin is relatively common, particularly at its origin from the subclavian artery; however, cerebral symptoms are unusual, given the dual blood supply (from both vertebrals and the carotid arteries by way of the posterior communicating artery) unless both vertebrals are diseased.

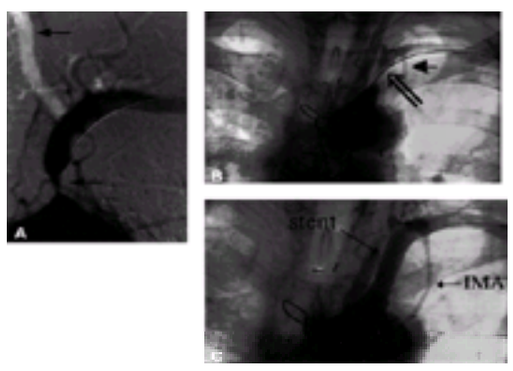

FIG. 14.7. A: Selective left subclavian arteriogram depicting severe ostial stenosis *(arrow)* and retrograde flow through left vertebral artery *(white)*. **B:** Arteriogram of subclavian artery in a patient after a coronary artery bypass graft with a left internal mammary artery (LIMA) graft and high-grade ostial stenosis *(double arrow)* resulting in poor visualization of the graft *(arrow)*. **C:** Following successful stenting of the subclavian artery stenosis and restoration of antegrade flow into the LIMA graft.

Subclavian and Vertebral Arteriography

An aortic arch arteriogram with a 5F pigtail catheter can visualize the origin of the great vessels to evaluate for atherosclerotic occlusive disease. (See the section on the thoracic arteriogram.) To catheterize the left subclavian artery selectively, a guidewire usually can be advanced directly from the descending thoracic aorta (see Chapter 11). If a proximal vertebral artery stenosis is expected, selective injection of the ipsilateral subclavian artery in the anteroposterior projection is usually diagnostic. Modest angulation may be necessary.

CAROTID ARTERIES

Anatomy

The brachiocephalic artery bifurcates into the right subclavian and right common carotid arteries as the first main branch off the aorta. The left common carotid is typically the second main branch of the aorta. Each common carotid runs within a fascial (carotid) sheath, lateral to the vertebrae, and bifurcates into an external and internal carotid artery branch at the fourth cervical vertebrae (18). While the internal carotid artery normally has no main branches prior to entering the skull, it forms a tortuous portion known as the carotid siphon within the cavernous and supraclinoid segment and thereafter divides into the anterior and posterior cerebral arteries. The external carotid artery has several major branches named for their territory of supply.

Extracranial Carotid Atherosclerosis

Approximately 700,000 strokes occur annually in the United States. It is estimated that 25% to 30% of these events are due to extracranial carotid artery disease. In the Minneapolis–St. Paul, Minnesota, metropolitan area, in 1985 there were 1,792 hospital discharges with the diagnosis of acute stroke, representing an event rate of 828/100,000 population in men and 551/100,000 in women (87). Patients with carotid disease frequently have severe coronary artery disease. In a population of 506 patients undergoing evaluation for potential carotid revascularization, 16% of patients without clinical clues suggestive of coronary heart disease were found to have severe, surgically correctable coronary artery disease (88). Even patients with *asymptomatic* carotid artery stenosis have an increased risk of coronary events. In one study of 444 male patients, the 4-year mortality rate was 37%, with 61% of the deaths due to coronary artery disease. Multivariate analysis shows diabetes mellitus, an abnormal electrocardiogram, and the presence of intermittent claudication to be associated with an increased mortality risk. (Two or three risk factors revealed annual mortality rates of 11.3% and 13%, respectively.) Just the finding of increased carotid intima-media thickness on duplex ultrasonographic examination predicts a higher risk of myocardial infarction or stroke, as much as 3.87 times that compared with patients with minimal thickness (89).

The majority of patients with extracranial carotid artery disease, often identified by the discovery of a carotid bruit on physical examination, have no referable symptoms. Estimates of the prevalence of asymptomatic carotid bruits in adults range from 1% (90) to 2.3% in patients age 45 to 54 years and 8.2% in patients more than 75 years of age (91). Among patients scheduled to undergo other vascular surgical procedures, however, the incidence of cervical bruits ranged from 6% (92) to 16% (93), with a mean prevalence of 10% (94). An asymptomatic carotid bruit carries a 1.5% annual incidence of stroke and a 3-year stroke risk of 2.1% (as demonstrated by the European Carotid Surgery Trialists). Among patients with an asymptomatic bruit and severe (70% to 99%) carotid stenosis, the 3-year risk of stroke was 5.7% (95). Absence of a bruit, however, does not imply absence of significant carotid disease. In a substudy of the North American Symptomatic Carotid Endarterectomy Trial (NASCET), 1,268 patients with recent transient cerebral ischemia or nondisabling stroke were examined for the presence of a carotid bruit. Fifty-eight percent of patients had a bruit localized to the ipsilateral carotid artery; 31% had a carotid bruit involving the contralateral vessel; and 24% had bilateral carotid bruits. The sensitivity and specificity of a focal bruit to predict high-grade ipsilateral carotid stenosis was 63% and 61%, respectively. In this patient subgroup, absence of a bruit lowered the pretest probability of a 70% to 99% carotid stenosis only from 52% to 40% (96).

Once established, extracranial carotid artery stenosis progresses in approximately 20% to 40% of cases. In one prospective natural history study of 232 patients with mild (<50%) and moderate (50% to 79%) carotid stenosis followed with annual carotid duplex ultrasonography for a mean of 7 years, 23% demonstrated disease progression. One-half of these patients developed severe stenosis (80% to 99%) or occlusion. Progression to either 80% to 99% stenosis or occlusion was more likely in patients whose initial stenosis was 50% to 79% rather than less than 50% (97). More recent data in 425 asymptomatic patients with 50% to 79% carotid stenosis followed for a mean of 38 months demonstrated progression of stenosis in 17% of 282 arteries with at least two serial carotid duplex examinations. In general, this carried a moderately low incidence of ipsilateral stroke (0.85% at 1 year; 3.6% at 3 years; 5.4% at 5 years) (98), but patients with 80% to 99% carotid stenosis had an annual neurologic event rate of 20.6% (99).

Many carotid lesions are discovered only after the patient begins to experience symptoms, which may vary from transient monocular blindness (amaurosis fugax) to expressive or receptive aphasia, hemiparesis/hemiplegia, and mental status changes. These episodic symptoms that last minutes to hours and then completely

resolve are harbingers of recurrent and potentially nonreversible events, and thus warrant urgent evaluation and therapy in an attempt to prevent a catastrophic stroke. The first study in this evaluation is carotid duplex ultrasonography, which provides two-dimensional images of the extracranial carotid arteries and may provide information about plaque morphology (Fig. 14.8*A*). Color flow can detect increased velocities of blood flow, which correlate to greater degrees of stenosis, while Doppler waveforms and velocities can also be measured to evaluate stenosis severity when performed by skilled vascular ultrasonographers (100) (Fig. 14.8*B*). Once a significant stenosis is identified, contrast or MRA can be performed to corroborate the ultrasound findings (101) (Fig. 14.8*C*). Conversely, if the ultrasound is performed by a reliable vascular laboratory, many surgeons proceed with endarterectomy based on this diagnostic test alone (102). Stent-assisted carotid angioplasty is now being offered at some centers as an alternative to surgery, particularly in patients at high risk for surgical correction (see Chapter 27 and Chapter 35) (Fig. 14.8*D*).

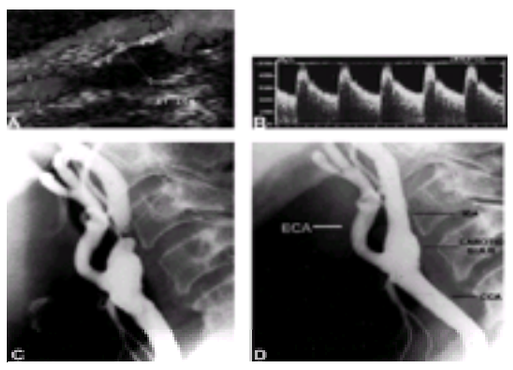

FIG. 14.8. A: Color duplex image of severely narrowed right ICA. **B:** Corresponding spectral waveform of ICA showing accelerated peak systolic and end-diastolic velocities. **C:** Carotid arteriogram confirming severe stenosis involving the right ICA. **D:** Arteriogram of carotid bifurcation following successful stenting of stenotic right ICA.

Carotid Arteriography

Carotid arteriography remains the gold standard in assessing the presence and quantitative narrowing of the carotid and intracerebral vasculature. Despite the advances made with noninvasive techniques such as duplex ultrasonography, MRA, and spiral computed tomoangiography (CTA), selective carotid catheterization may be indicated to more accurately delineate the degree of stenosis involving the distal common and internal carotid arteries and the extent of disease at the bifurcation, as well as to provide information about the intracranial circulation, including collateral flow patterns. The carotid artery may be selectively catheterized by a number of 5F (simple) catheters. Tortuous proximal great vessels, however, may require a complex-curve catheter.

Once the catheter is beyond the aortic arch, careful double-flushing is mandatory to minimize risk of embolization. Injections of low-osmolar contrast injections are typically performed at a maximum rate of 8 mL/sec for 10 cc total in the CCA, 8 mL/sec for 8 cc total in the internal carotid artery (ICA), and 7 mL/sec for a total of 7 cc in the vertebral artery. Film rates of two to four frames per second should be used during the arterial phase and slower rates should be used for the venous phase. Multiple oblique projections are necessary, including anteroposterior, lateral, and oblique views to visualize narrowing at the carotid bifurcation and proximal ICA optimally. The lateral projection is best to visualize the proximal ICA and carotid siphon. The Towne and lateral views are best for visualizing the intracerebral anatomy. The Towne view is centered like an AP skull radiograph, with slight angulation so that the petrous ridge lies over the roof of the orbit.

To calculate the percentage diameter stenosis, the projection that demonstrates the highest degree of stenosis should be used. Many different methods of calculating carotid artery stenosis have been employed in previous trials; however, the North American Symptomatic Carotid Endarterectomy Trial (NASCET) methodology is the most widely accepted. It compares the stenotic area with the most normal-appearing artery distal to the stenosis.

RENAL ARTERIES

Anatomy

The renal arteries arise from the lateral aspect of the aorta at the L-1 to L-2 level (18). Accessory renal arteries may occur in 25% to 35% of cases and usually supply the lower pole of the kidney. These may originate anywhere from the suprarenal aorta down to the iliac arteries.

Atherosclerotic Renal Artery Stenosis

Atherosclerotic renal artery stenosis (ARAS) is clearly more common than previously believed, with increasing prevalence in certain patient populations. In one series of 395 arteriograms performed in patients with abdominal aortic aneurysms, aortoiliac or infrainguinal atherosclerosis, 33% to 50% had renal artery stenosis of more than 50% (103). In 346 patients with aneurysmal or occlusive vascular disease prompting arteriography, 28% had significant ARAS. The presence of coronary artery atherosclerosis is also a marker for ARAS. In a prospective study of 1,302 patients undergoing coronary arteriography, concurrent abdominal aortography demonstrated significant ARAS in 15% of patients. The number of coronary arteries involved with atherosclerosis also appears to predict the likelihood of renal artery stenosis in this series. For example, if one coronary artery demonstrated atherosclerosis, the incidence of significant ARAS was 10.7%. If three coronary arteries and the left main trunk are involved with atherosclerosis, the incidence of ARAS was 39% (104). Conversely, 58% of patients with ARAS had clinically overt coronary artery disease.

A number of clinical clues may suggest the presence of ARAS. Patients who develop diastolic hypertension after 55 years of age who have exacerbation of previously well-controlled hypertension, who demonstrate refractory hypertension (uncontrolled hypertension despite treatment with three antihypertensive medications of synergistic classes at maximal doses), who develop azotemia after treatment with an angiotensin converting enzyme inhibitor, or who present with malignant hypertension (severe hypertension and acute myocardial infarction, acute stroke or transient ischemic attack, aortic dissection, acute renal failure) should be suspected of having renal artery stenosis. A discrepancy in renal size, the physical finding of a systolic and diastolic abdominal bruit with radiation to one or both flank regions, unexplained azotemia, or the presence of diffuse atherosclerosis with hypertension and azotemia without obvious cause must prompt the physician to search for renal artery disease. Up to 24% of patients with end-stage renal disease (ESRD) being considered for dialysis in one series had severe ARAS (105). The 15-year survival of patients committed to ESRD because of ARAS was 0, compared with 32% in patients committed to dialysis for other causes such as polycystic kidney disease.

The natural history of ARAS has been studied extensively in many retrospective series, which suggest that approximately 50% of renal arteries progress over time (106). More recent prospective data utilizing duplex ultrasonography to assess renal artery patency demonstrated that 48% of renal arteries whose baseline stenosis was less than 60% progressed to more than 60% stenosis after 36 months, compared with only 8% in vessels with no stenosis at baseline (107).

A number of noninvasive diagnostic tests have been used to determine if renal artery stenosis is present. Historically, rapid sequence intravenous pyelography was used; this has now been shown to be inaccurate. Equally inaccurate are plasma renin levels, only elevated in 50% to 80% of patients with RAS (108). Captopril stimulated nuclear renography is a prominent diagnostic test for patients with suspected renal artery stenosis, with sensitivity and specificity in the range of 90% (109). However, in a recent comparison for the diagnosis of renal artery stenosis, the isotopic renal scan was no better than the clinical prediction rule to predict renal artery stenosis, particularly in the presence of bilateral renal artery stenosis or impaired renal function.

Renal artery duplex ultrasonography can be an excellent test to diagnose renal artery stenosis if performed by a skilled operator. In one prospective series of 29 patients (58 renal arteries) who underwent contrast arteriography and duplex ultrasonography, sensitivity of the latter was 84%, specificity was 97%, and positive predictive value was 94% for detection of more than 60% stenosis (110). Utilizing criteria of peak systolic velocity within the renal artery of more than 180 cm/sec, duplex scanning was able to discern between normal and diseased renal arteries with a sensitivity of 95% and specificity of 90% (111). The ratio of peak systolic velocity (PSV) in the area of renal artery stenosis compared with the PSV within the aorta (renal to aortic ratio [RAR]) of more than 3.5 predicts the presence of more than 60% renal artery stenosis with a sensitivity of 92%. In another large prospective series of 102 consecutive patients who underwent both duplex ultrasonography

and contrast arteriography within 1 month of each other, 62 of 63 arteries with less than 60% stenosis, 31 of 32 arteries with 60% to 79% stenosis, and 67 of 69 arteries with 80% to 99% stenosis were correctly identified by duplex ultrasonography. Occluded renal arteries were correctly identified in 22 of 23 cases. The overall sensitivity of duplex ultrasonography was 98%; specificity, 99%; positive predictive value, 99%; and negative predictive value, 97% (112). Limitations of direct ultrasound visualization of the renal arteries include large body habitus and overlying bowel gas obscuring identification of the renal arteries. Some authors have suggested that renal hilar scanning is easier and as accurate as complete interrogation of the renal arteries (113). However, direct comparison of both techniques has revealed limitations of hilar scanning, including low sensitivity, inability to discriminate between stenosis and occlusion, and inadequate determination of accessory renal arteries. The sensitivity was 67% for hilar scanning, with a specificity of 89% to 99% (114). Given that many patients have both main renal artery disease and intraparenchymal disease, the addition of resistive indices within the parenchyma may help predict which patients will benefit from revascularization (115). Duplex ultrasonography is an excellent method for determining patency following revascularization (116). Given the proliferation of endovascular therapy (percutaneous angioplasty with stent deployment) (117), duplex ultrasonography is helpful in detecting restenosis.

Magnetic resonance arteriography has demonstrated great promise as a highly accurate noninvasive test for the diagnosis of renal artery stenosis (118). Limitations of this technology, predominantly overestimating degrees of stenosis, are decreasing with the addition of intravenous gadolinium, a nonnephrotoxic contrast agent (119), and perhaps, captopril (120).

Arteriography

Arteriography of the renal vasculature should begin with an aortogram to assess the degree of aortic disease, ostia of the renal arteries, and presence of accessory renal arteries. Images are obtained with a 4F or 5F pigtail or tennis-racquet catheter, with the side-holes positioned at the L-1 to L-2 level (Fig. 14.9*A*). Anteroposterior and oblique (RAO and LAO) views, often with cranial or caudal angulation, may be necessary to delineate the ostium and proximal renal arteries that are most commonly involved in atherosclerosis (Fig. 14.9*B*). Selective renal arteriography may be indicated in the case of ostial disease, accessory renal arteries not visualized by the initial arteriogram, suspected intrarenal vascular disease (e.g., fibromuscular dysplasia, Takayasu's arteritis, radiation, aneurysms, vasculitis), or need to measure pressure gradients across lesions of equivocal hemodynamic significance (Fig. 14.9*C*). The renal arteries can be engaged selectively with 4F or 5F (e.g., renal double curve, Cobra, SOS-OMNI, hockey-stick, or internal mammary) catheters. Injection rates of contrast media should be 5 to 10 mL at a rate of 5 mL/sec. Filming sequences should include the early arterial phase as well as the nephrographic phase, which demonstrates contrast in both the nephrons and capillaries. The venous phase occurs 5 to 10 seconds after the initial injection and shows filling of the renal veins. If surgical revascularization (e.g., hepatorenal or splenorenal bypass) is contemplated, a lateral view of the aorta should be obtained to delineate the origins of the celiac and superior mesenteric arteries and evaluate them for the presence of inflow disease.

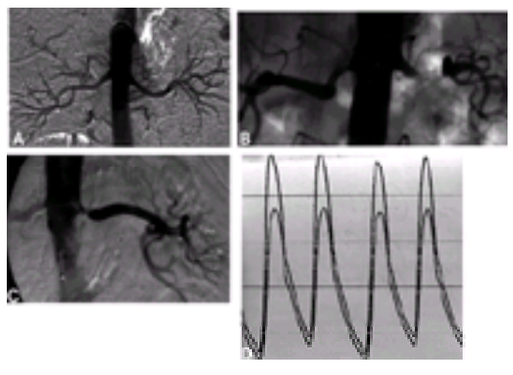

FIG. 14.9. A: Abdominal aortogram demonstrating normal renal arteries. **B:** Atherosclerosis of the aorta resulting in bilateral renal artery stenosis. **C:** Selective injection of the left renal artery depicting an apparent moderate degree of luminal narrowing. **D:** An intraarterial pressure tracing obtained across the lesion demonstrates a peak systolic and mean gradient of 23 mm Hg and 12 mm Hg, respectively, indicating a hemodynamic significant lesion.

For equivocal renal artery stenoses, measurement of a transstenotic gradient may be helpful—gradients greater than 10 mm Hg mean or 20 mm Hg systolic as measured using a 4F catheter are taken as significant (Fig. 14.9*D*). This can be done by advancing these catheters into the renal artery over flexible- or tapered-tip (e.g., Wholey, Bentson) wires to avoid trauma, spasm, embolization, or perforation of the distal renal branches. Even so, any guidewire manipulation within the renal artery should be minimized, and the operator must be prepared to move immediately to renal stenting (see Chapter 27) if measurement of the gradient causes any disruption within the renal artery stenosis).

PELVIC AND LOWER EXTREMITIES

Anatomy

The bifurcation of the abdominal aorta into the common iliac arteries (CIA) occurs at the level of L-4 to L-5 (18) (Fig. 14.10*A*). The common iliac arteries divide at the lumbosacral junction, with the internal iliac arteries (IIA) taking off medially and posteriorly, and the external iliac arteries (EIA) continuing anteriorly and laterally to the groin, where they exit the pelvis just posterior to the inguinal ligament. The inferior epigastric artery takes off medially at the junction of the EIA and common femoral artery. The deep iliac circumflex artery takes off laterally and superiorly.

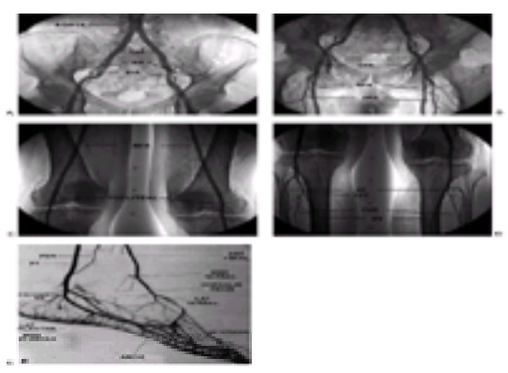

FIG. 14.10. Normal pelvic and lower-extremity arteriogram. **A:** The distal abdominal aorta bifurcating into the iliac arteries. **B:** The common femoral artery (CFA) dividing into the deep femoral (DFA) and superficial femoral arteries (SFA). **C:** The SFA traversing the thigh into the popliteal artery as it dives through the adductor (Hunter's) canal. **D:** The popliteal artery dividing laterally into the anterior tibial (AT) artery and continues directly into the tibioperoneal trunk (TPT), which bifurcates into the posterior tibial (PT) and peroneal arteries (PER). **E:** The dorsalis pedis (DP) artery originates from the AT artery beyond the ankle and PT artery, which gives off plantar branches. (CIA, common iliac arteries; IIA, internal iliac arteries; EIA, external iliac arteries.)

The common femoral artery (CFA) is an extension of the EIA, which originates at the inguinal ligament and then bifurcates (usually at the lower portion of the femoral head) into the superficial femoral artery (SFA) anteromedially and the deep femoral artery (DFA), or “profunda,” posterolaterally (Fig. 14.10*B*). The DFA has two major branches, the lateral circumflex and medial circumflex femoral arteries. The SFA proceeds down the anteromedial thigh and dives deep at adductor (Hunter's) canal, where it becomes the popliteal artery running posterior to the femur. Major popliteal branches include the sural and geniculate (superior, middle, and inferior) arteries around the knee (Fig. 14.10*C*).

Below the knee, at the border of the popliteus muscle, the popliteal artery divides, with the anterior tibial (AT) artery proceeding laterally and anterior to the tibia

toward the foot. As it passes over the ankle onto the dorsum of the foot, it continues as the dorsalis pedis (DP) artery. After the take-off of the AT, the popliteal continues as the tibio-peroneal trunk (TPT), which subsequently bifurcates into the posterior tibial (PT) and peroneal (PER) arteries. The PT courses posteromedially in the calf, while the peroneal runs near the fibula between the AT and PT arteries. The peroneal artery then rejoins the PT above the ankle via its posterior division, and the AT via its anterior division (Fig. 14.10*D*). On the dorsum of the foot, the DP artery has lateral and medial tarsal branches. After the PT artery passes behind the medial malleus, it divides into medial and lateral plantar arteries. The lateral plantar and distal DP arteries join to form the plantar arch (Fig. 14.10*E*).

Lower-Extremity Arterial Occlusive Disease

The prevalence of peripheral arterial occlusive disease (PAD) remains difficult to appreciate among the general population. Since a significant segment of the population with PAD has no symptoms of the disorder, this makes true prevalence rates even more difficult to ascertain. Patients with asymptomatic PAD are at minimal risk of developing critical limb ischemia that threatens limb survival, with the obvious exception of the patient who suffers acute limb ischemia from an embolic event or trauma. Instead, patients first develop intermittent claudication to some degree, before progressing to rest pain, a nonhealing ischemic ulcer, or gangrene.

The United States National Institutes of Health suggests that lower-extremity arterial occlusive disease causes more than 60,000 hospitalizations annually, each stay lasting an average of more than 11 days (121). Manifestations of arteriosclerosis obliterans—namely, diminished pedal pulses and femoral bruits—occur with increasing frequency as the population ages. While intermittent claudication occurs more often in men at any age, physical examination findings of peripheral arterial disease occur with identical frequency in men and women (122). Several investigators have attempted to define the prevalence of PAD using noninvasive testing modalities and symptom questionnaires. One series of 613 men and women with a mean age of 66 years, utilizing segmental limb blood pressures, Doppler flow velocities, reactive hyperemia, and pulse reappearance times found an 11.7% incidence of large-vessel PAD (123). Although 11.7% of the population thus had evidence of PAD, only 2.2% of men and 1.7% of women had intermittent claudication. In this same population, however, 20.3% of men and 22.1% of women had abnormalities in the femoral or posterior tibial artery pulse examination.

The currently accepted methods of determining the presence of PAD include an historical review of patient symptoms and atherosclerotic risk factors, physical examination, and use of noninvasive vascular tests. A common simple test is the ankle-brachial index (ABI). This test compares the blood pressure obtained with a hand-held Doppler in the dorsalis pedis or posterior tibial artery (whichever is higher) to the blood pressure in the higher of the two brachial pressures. Generally, an ABI of more than 0.9 is considered normal, one of more than 0.5 to less than 0.9 reflects mild to moderate PAD, and an ABI of less than 0.5 suggests severe arterial occlusive disease.

It is widely accepted that the presence of PAD increases the likelihood of myocardial infarction, stroke, renovascular disease (124), and cardiovascular mortality. The 5-year survival of a patient with intermittent claudication is only 70%, with 75% of these deaths attributable to cardiovascular events (125). Many studies have confirmed the association between cardiovascular morbidity and mortality and an abnormal ABI (126,127,128,129,130,131 and 132). Some have suggested that there is a significant proportion of the population with asymptomatic PAD, and their risk of cardiovascular morbidity and mortality is similar to their symptomatic counterparts. However, it is assumed that because of their lack of symptoms, this risk may not be recognized until an event has occurred.

The risk factors for the development of PAD include hypertension, hypercholesterolemia, tobacco use, and diabetes mellitus. Tobacco use remains the most important modifiable risk factor for PAD. Hughson et al. found that 56% of patients with intermittent claudication were active users of cigarettes, and 24% were former smokers. In addition, active cigarette smoking causes more severe claudication pain and diminished peripheral circulation than is found among patients who do not smoke, leading to a reduction in the exercise capacity of patients with claudication (133). Finally, the risk of progression of PAD and atherosclerosis in other vascular beds is significantly greater in patients who continue to smoke than it is in those who stop smoking. In 343 patients with intermittent claudication, only 11% stopped smoking 1 year after the diagnosis. Ischemic rest pain developed in 16% of continued smokers after 7 years, whereas none of the former smokers suffered from rest pain. The incidence of myocardial infarction 10 years after the diagnosis of claudication was 11% in former smokers and 53% in active smokers. Ten-year overall survival rates were 82% in former smokers and 46% in active smokers (134).

Diabetes mellitus and PAD is an ominous combination. Although the prevalence of PAD is higher in the diabetic than in the nondiabetic population, it is the relatively rapid progression to ischemic rest pain and ulceration that portends a poor prognosis for the patients with diabetes. There is a two- to threefold increase in risk of intermittent claudication in diabetic patients when compared with the nondiabetic population (135). This holds true for both men and women. The severity of PAD is also greater in the diabetic population. In a study of 47 patients with diabetes mellitus, all of whom had intermittent claudication at baseline, in comparison with 224 patients with intermittent claudication but no diabetes, the incidence of ischemic rest pain and/or gangrene after 6 years of follow-up was 40% and 18%, respectively (136). The duration of diabetes and the type of diabetes therapy (i.e., diet, oral hypoglycemic agent, and insulin) did not play a role in the incidence or severity of PAD.

Independent predictors of progression of PAD in diabetic patients include a decreased postexercise ankle-brachial index, increased arm systolic blood pressure, and current smoking, demonstrating the additive effects of atherosclerotic risk factors on the natural history of PAD (137). Interestingly, among the risk factors for amputation in patients with diabetes mellitus, neuropathic symptoms and lack of outpatient diabetes education are of importance and must be viewed concomitantly with the location and severity of PAD (138). Unfortunately, there remains no definitive evidence that strict glycemic control can prevent macrovascular complications from diabetes mellitus (139). There are several other potential risk factors for peripheral arterial occlusive disease, including Lp(a) (140), hyperhomocysteinemia (141), fibrinogen (142), and C-reactive protein (143). The specific role of each of these factors in the prevention and therapy of peripheral arterial disease remains unclear.

The most common symptom described by patients with peripheral arterial disease is intermittent claudication. Although the description of the symptom may vary among patients from pain, to ache, to numbness and weakness, there are several distinct characteristics of intermittent claudication. The discomfort is usually brought on by walking and alleviated by rest. The discomfort generally involves muscle groups immediately distal to the arterial segments involved (i.e., superficial femoral artery stenosis causes calf discomfort). The onset of intermittent claudication is quite predictable and occurs at similar distances, providing that the speed, incline, and terrain have remained unchanged. Patients generally stop, stand, and wait for 1 to 5 minutes for relief prior to resumption of walking.

Progression to critical limb ischemia is manifest by ischemic pain at rest, generally in the arch of the foot or toes. This occurs with the patient lying supine and is relieved by hanging the foot over the bedside. Paradoxically, patients with ischemic rest pain may note improvement in their pain with walking. Patients may resort to sleeping in a reclining chair, to provide a dependent position to the foot. Ischemic ulcerations occur as a result of trauma to toes or areas where bony prominences are exposed. Even minimal trauma, such as an ill-fitting shoe, may result in ulceration. The presence of ischemic rest pain or ulceration warrants a prompt and aggressive strategy for revascularization.

Physical examination must include palpation of all pulses, including the superficial temporal and carotid arteries, the arteries of the upper extremities, and the arteries of the lower extremities. Auscultation for bruits in the region of the cervical carotid arteries, abdomen, flank, and inguinal regions should be routinely performed, and the phase of the cardiac cycle during which the bruit occurs should be noted. Attempts to palpate the abdominal aorta for aneurysmal dilatation should me made. Close inspection of the feet and toes should include a search for ischemic ulceration or tinea infection. Kissing ulcerations between the toes in the web spaces are often subtle and easily missed on examination.

Once the ankle-brachial index has been performed, providing objective evidence of the overall severity of PAD in a limb, more specific noninvasive information can be obtained in the vascular laboratory. The addition of segmental limb pressures can aid in localizing stenoses or occlusions. Limb pressure cuffs are placed on the thigh (some centers prefer high- and low-thigh cuffs), calf, ankle, transmetatarsal region of the foot, and digit. The ABI is calculated and then the pressure is sequentially inflated in each cuff to approximately 20 to 30 mm Hg above systolic pressure. Utilizing a continuous-wave Doppler probe placed at a pedal vessel, the pressure in the cuff is gradually released, and the pressure at each segment is measured. If a decrease in pressure between two consecutive levels of more than 30 mm Hg is identified, this suggests arterial occlusive disease of the artery proximal to the cuff. In addition, comparing the two limbs, a 20 to 30 mm Hg discrepancy from one limb to the other at the same cuff level also suggests a significant arterial stenosis or occlusion proximal to the cuff (144).

Pulse volume recordings (PVR) are plethysmographic tracings that detect the changes in the volume of blood flowing through a limb. Using similar equipment as described previously, the cuffs are inflated to 65 mm Hg, and a plethysmographic tracing is recorded at various levels (145). The normal PVR is similar to the normal arterial pulse wave tracing and consists of a rapid systolic upstroke and rapid downstroke, with a prominent dicrotic notch. With increasing severity of disease, the waveform becomes more attenuated, with a wide downslope and, ultimately, virtually absent waveforms. Ankle-brachial indices, segmental pressures, and pulse volume recordings are useful objective tests in patients with suspected lower-extremity arterial occlusive disease, in those with limb discomfort without an obvious cause, as a method of evaluating the success of an intervention, and as a method of follow-up. The tests are inexpensive, painless, reproducible, and relatively easy

to perform. The equipment required to perform these examinations is significantly less expensive than modern color-flow duplex ultrasound units.

Native vessel arterial duplex ultrasonography is widely performed. This examination is generally accepted as a method of defining arterial stenoses or occlusions (Fig. 14.11*A*). The sensitivity of duplex ultrasonography to detect occlusions and stenoses has been reported to be 95% and 92%, with specificities of 99% and 97%, respectively (146). Limitations have included tandem stenoses (147), tibial vessel imaging (148), and difficulty imaging the inflow arteries (149). Using a 5.0- to 7.5-MHz transducer, imaging of the supra- and infrainguinal arteries is performed. The vessels are studied in the sagittal plane, and Doppler velocities are obtained using a 60° Doppler angle. Vessels are classified into one of five categories: normal, 1% to 19% stenosis, 20% to 49% stenosis, 50% to 99% stenosis, and occlusion. The categories are determined by alterations in the Doppler waveform and by increasing peak systolic velocities. For a stenosis to be classified as 50% to 99%, for example, the peak systolic velocity must increase by 100% in comparison with the normal segment of artery proximal to the stenosis (150) (Fig. 14.11*B*).

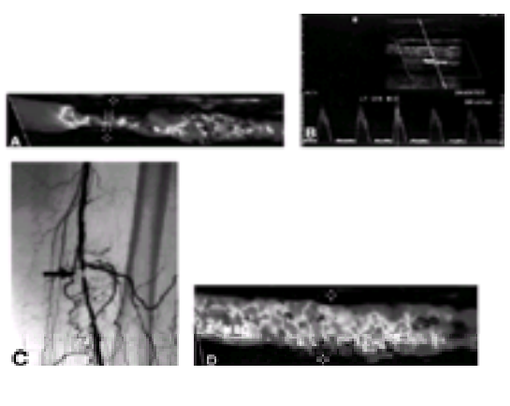

FIG. 14.11. Severe stenosis of the left superficial femoral artery (SFA) as depicted by **(A)** color duplex scanning. **B:** Spectral waveform shows an increased peak systolic velocity of 300 cm/sec. **C:** Arteriogram confirming a severe SFA stenosis at the corresponding site. **D:** Nine-month follow-up arteriogram demonstrating a widely patent SFA at the site of revascularization with adjunctive pHVEGF165 to accelerate reendothelialization.

Arterial duplex ultrasonography has been used to guide the interventionist toward appropriate access to a lesion potentially amenable to endovascular therapy (151) (Fig. 14.11*C*). This technology has also been used after endovascular therapy to determine technical success (152) and durability of the procedure (153) (Fig. 14.11*D*). Unfortunately, it appears that duplex ultrasonography soon after balloon angioplasty may overestimate residual stenosis and may limit the use of this technology after endovascular therapy (154).

In patients who have undergone surgical bypass graft revascularization, particularly with saphenous vein, stenoses will develop in 21% to 33% of cases. Once the graft becomes thrombosed, secondary patency rates are dismal. If the stenosis is detected and repaired before graft thrombosis, however, an estimated 80% of grafts can be salvaged (155). A well-organized graft surveillance program is thus crucial to preserving patency of bypass grafts. In one series of 170 saphenous vein bypass grafts, 110 stenoses were detected over a 39-month period. In those grafts that underwent surgical revision once a stenosis was detected, the 4-year patency was 88%, whereas in those grafts that did not undergo revision despite the detection of a stenosis, the 4-year patency was 57% (156). The use of an intensive surveillance program has been less beneficial in prosthetic grafts (157).

The procedure for graft surveillance is performed in a manner similar to that used in native vessel arterial duplex ultrasonography. The inflow artery to the bypass graft is initially imaged using a 5.0- to 7.5-MHz transducer and a Doppler angle of 60°. Subsequently, the proximal anastomosis; proximal, middle, and distal graft; distal anastomosis; and outflow artery are interrogated. Peak systolic and end-diastolic velocities are obtained at each segment and compared with the segment of graft proximal to the area being studied. If the ratio of the peak systolic velocity within a stenotic segment relative to the normal segment proximal to the stenosis is more than 2, this suggests 50% to 75% diameter reduction. The addition of end-diastolic velocities of more than 100 cm/sec suggests more than 75% stenosis (158).

Vein bypass grafts should be studied within 7 days of formation and then in 1 month, followed by 3-month intervals for the first year. If the graft remains normal after year 1, follow-up surveillance should be done every 6 months thereafter. Ankle pressures and waveforms should be performed at the time of each surveillance study. The development of a stenosis during a surveillance examination should prompt consideration toward arteriography, either with contrast or with magnetic resonance (159).

MRA has been promoted as an excellent method of evaluating the anatomy of the lower-extremity arteries. Initially touted as a unique and effective method of identifying angiographically occult runoff arteries that would be suitable as targets for surgical revascularization (160), investigators have studied the utility of MRA as the sole imaging modality prior to surgical revascularization (161). Recent comparative trials of MRA and standard contrast arteriography have revealed high sensitivity and specificity (97.1% and 99.2%, respectively) for MRA in patients suspected of having PAD (162).

Given the impressive advances in the field of endovascular therapy for PAD with percutaneous transluminal angioplasty, stent deployment, atherectomy, and stent grafting for aneurysmal and occlusive disease, however, diagnostic arteriography continues to play an important role in the management of patients with PAD.

Pelvic and Lower-Limb Arteriography

Arteriography is still considered the gold standard for evaluation of patients with peripheral vascular disease (PVD). With the advent of reliable noninvasive vascular laboratory testing, however, arteriography should be reserved only for patients in whom endovascular or surgical intervention is contemplated. Information obtained from the history, physical examination, and noninvasive testing should be able to provide the clinician with the ability to ascertain the level and distribution of obstructive vascular disease. Indications for arteriographic study of the upper and lower extremities include ischemia (either exertional or resting) due to atherosclerosis, embolus, thrombosis, and vasculitis. Other potential etiologies warranting arteriography are peripheral aneurysms, vascular tumors, trauma, extrinsic compression (e.g., popliteal artery entrapment syndrome, cystic adventitial disease, and vasculitis [Buerger's disease], collagen vascular disease, and radiation).

Pelvic arteriography is usually performed from a femoral approach using a pigtail or tennis-racquet side-hole catheter placed just above the aortic bifurcation (L-4 to L-5). Other options include translumbar, axillary, or brachial artery sites. Axillofemoral bypass grafts may be directly punctured as they pass over the ribs. No consensus has been reached as to which common femoral artery should be punctured, the one on the side of the more symptomatic or that on the less symptomatic leg. The advantages of accessing the less symptomatic leg are that groin complications would not interfere with surgical bypass procedures, there is less risk of iliac artery trauma (e.g., dissection or occlusion), and the possibility remains of performing an antegrade puncture of the affected leg.

When one of the iliac arteries is occluded, the catheter should be positioned just below the renal arteries to visualize the lumbar arteries that serve as important collaterals into the pelvis (Fig. 14.12). To adequately assess for iliac disease, anteroposterior (AP) and both oblique (25° to 30°) pelvic projections should be obtained, to image the iliac and femoral artery bifurcations. The RAO projection opens the left iliac and right femoral bifurcations, and the LAO projection opens the opposite bifurcations. When lower-extremity arteriography is performed, visualization of the arteries to both feet is necessary in planning definitive treatment, by either surgical or endovascular techniques. Images may be recorded on cut-film, long-leg changer or step table, digital bolus-chase method, or serial digital filming techniques. If cut-film step table technique is used, a single bolus of contrast material is injected from the catheter at the aortic bifurcation at 7 to 9 mL/sec for a volume of 70 to 120 mL and images are obtained along the course of the contrast from the aorta to the feet.

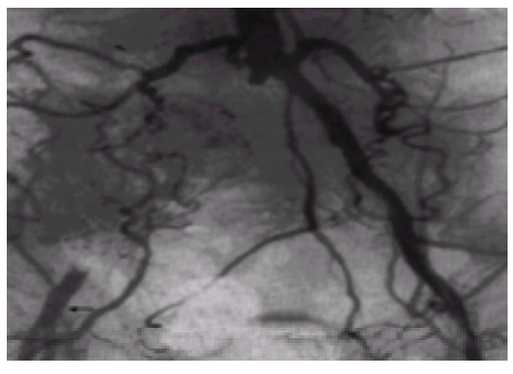

FIG. 14.12. Pelvic arteriogram showing right iliac artery occlusion with common femoral artery *(arrow)* reconstitution via collaterals.

Digital imaging affords better resolution of images with a smaller diluted contrast load than with cut film. Serial digital filming is performed by obtaining stationary images over an arterial segment while contrast material is injected at a rate of 8 to 12 mL/sec for 2 to 3 seconds. The imager is positioned over each segment with similar injections and sequence at all respective levels, until pedal arteries are visualized. The digital bolus-chase method performs angiography by acquiring digital images series without contrast material and then acquires the image as it "chases" the contrast bolus. Advantages have been previously outlined in the text.

Atherosclerotic plaque may be eccentric, particularly in the aorta, iliac, or femoral bifurcation, where it tends to be located in the posterior wall of the deep femoral artery. In these cases, multiple oblique projections are necessary to uncover significant narrowings. Even so, angiography may underestimate the degree of luminar diameter narrowing, especially in tortuous iliac arteries, in particular the ostium of the common iliac and iliac bifurcation (163). Intraarterial pressure monitoring may thus be more accurate than multiple angiographic images in assessing the hemodynamic significance of a vascular lesion (164). There exists no consensus as to the threshold that defines a significant gradient. However, a resting peak systolic gradient of 5 mm Hg or an increase of greater than 10 mm Hg after augmentation with a vasodilator (e.g., nitroglycerin) is considered of hemodynamic significance (165). Intravascular ultrasound permits direct planimetry of luminal cross-sectional narrowing, obviating the multiple, oblique views required to unwind and/or eliminate overlap, which may obscure important luminal obstructions (166).

To optimize the visualization of the tibial or pedal arteries, selective catheter positioning into the superficial femoral artery with the use of vasodilating agents, such as nitroglycerin (100 to 300 µg), papaverine (30 to 60 mg), or tolazoline (12.5 to 25 mg) may enhance digital images (167). When selection of the contralateral iliac artery is desired, a pigtail or tennis-racquet catheter, if previously placed in the distal aorta, may be used by gently unfolding it with a guidewire and engaging the aorta bifurcation. Once the guidewire is successfully advanced into the contralateral iliac artery, the catheter may be replaced with a straight catheter. Other options include Cobra, SOS-OMNI, hook, or internal mammary artery guide catheters, which are advanced over the aortic bifurcation. Reverse-curve catheters may facilitate engaging the internal iliac arteries from the ipsilateral side, although an easier access may be approached from an antegrade direction, if revascularization is a consideration.

CHAPTER REFERENCES

1. Forssmann W. Die Sondierung des rechten Herzens. *Klin Wochenschr* 1929;8:2085.
2. Dos Santos R, Lama AC, Pereira-Caldas J. Arteriografia da aorta e dos vasos abdominalis. *Med Contempo* 1929;47:93.
3. Nuvoli I. Arteriografia dell' aorta ascendente o del ventriculo. *Policlinico (Prat)* 1936;43:227.
4. Cardella JF, Casarella WJ, DeWeese JA, et al. Optimal resources for the examination and endovascular treatment of the peripheral and visceral vascular systems. *Circulation* 1994;89:1481.
5. Krouwels MM, Overbach EH, Guit GL. Iohexol vs. ioxaglate in lower extremity angiography: a comparative randomized double-blind study in 80 patients. *Eur J Radiol* 1996;22:133.
6. Hawkins IF. Carbon dioxide digital subtraction arteriography. *Am J Roentgenol* 1982;139:19
7. Weaver FA, et al. Clinical applications of carbon dioxide/digital subtraction arteriography. *J Vasc Surg* 1991;13:266.
8. Kerns SR, Hawkins IF Jr. Carbon dioxide digital subtraction angiography: expanding applications and technical evolution. *Am J Radiol* 1995;164:735.
9. Sullivan KL, Bonn J, Shapiro MJ, et al. Venography with carbon dioxide as a contrast agent. *Cardiovasc Intervent Radiol* 1995;18:141.
10. Caridi JG, Hawkins IF Jr. CO_2 digital subtraction angiography: potential complications and their prevention. *J Vasc Interv Radiol* 1997;8:383.
11. Kaufman JA, Geller SC, Waltman AC. Renal insufficiency: gadopentetate dimeglumine as a radiographic contrast agent during peripheral vascular interventional procedures. *Radiology* 1996;198:579.
12. Prince M, et al. Dynamic gadolinium-enhanced three-dimensional abdominal MR arteriography. *J Magn Reson Imaging* 1993;3:877.
13. Millward SF, Burbridge BE, Luna G. Puncturing the pulseless femoral artery: a simple technique that uses palpation of anatomic landmarks. *J Vasc Interv Radiol* 1993;4:415.
14. Khangure MS, Chow KC, Christensen MA. Accurate and safe puncture of a pulseless femoral artery. *Radiology* 1982;144:927.
15. Sacks D, Summers TA. Antegrade selective catheterization of femoral vessels with a 4- or 5-F catheter and safety wire. *J Vasc Interv Radiol* 1991;2:325.
16. Hirai M, Nakayama R. Haemodynamic effects of intra-arterial and intravenous administration of prostaglandin E1 in patients with peripheral vascular disease. *Br J Surg* 1986;73:20.
17. Gruss JD. Experience with PGE 1 in patients with postoperative trash foot. *Vasa* 1989;28[Suppl]:57.
18. Gabella G, ed. Cardiovascular system. In: Williams PL, Bannister LH, Berry MM, et al, eds. *Gray's anatomy*, 38th ed. New York: Churchill Livingstone, 1995:1505.
19. Aronberg DJ, Glazer HS, Madsen K, et al. Normal thoracic aortic diameters by computed tomography. *J Comput Assist Tomogr* 1984;8:247.
20. Hougen TJ. Congenital anomalies of the aortic arch. In: Lindsay J Jr, ed. *Diseases of the aorta*. Philadelphia: Lea & Febiger, 1994:19.
21. Ho VB, Prince MR. Thoracic MR aortography: imaging techniques and strategies. *Radiographics* 1998;18:287.
22. Perloff JK. Patent ductus arteriosus. *The clinical recognition of congenital heart disease.* Philadelphia: WB Saunders, 1994:510.
23. Rizzo RJ, McCarthy WJ, Dixit SN, et al. Collagen types and matrix protein content in human abdominal aortic aneurysms. *J Vasc Surg* 1989;10:365.
24. Milewicz DM, Michael K, Fisher N, et al. Fibrillin-1 (FBN-1) mutations in patients with thoracic aortic aneurysms. *Circulation* 1996;94:2708.
25. Kouchoukos NT, Dougenis D. Surgery of the thoracic aorta. *N Engl J Med* 1997;336:1876.
26. Creasy JD, Chiles C, Routh WD, et al. Overview of traumatic injury of the thoracic aorta. *Radiographics* 1997;17:27.
27. Parmley LF, Mattingly TW, Manison WC, et al. Non-penetrating traumatic injury of the aorta. *Circulation* 1958;17:1086.
28. Cohen AM, Crass JR, Thomas HA, Fisher RG, Jacobs DG. CT evidence for the "osseous pinch" mechanism of traumatic aortic injury. *Am J Roentgenol* 1992;159:271.
29. Hirose Y, Hamada S, Takamiya M, et al. Aortic aneurysms: growth rates measured with CT. *Radiology* 1992;185:249.
30. Dapunt OE, Galla JD, Sadeghi AM, et al. The natural history of thoracic aortic aneurysms. *J Thorac Cardiovasc Surg* 1994;107:1323.
31. Cambria RA, Glviczki P, Stanson AW, et al. Outcome and expansion rate of 57 thoracoabdominal aortic aneurysms managed nonoperatively. *Am J Surg* 1995;170:213.
32. Lawrie GM, Earle N, DeBakey ME. Evolution of surgical techniques for aneurysms of the descending thoracic aorta: twenty-nine years experience with 659 patients. *J Cardiac Surg* 1994;9:648.
33. Semba CP, Kato N, Kee ST, et al. Acute rupture of the descending thoracic aorta: repair with use of endovascular stent-grafts. *J Vasc Interv Radiol* 1997;8:337.
34. Dake MD, Miller DC, Semba CP, et al. Transluminal placement of endovascular stent-grafts for the treatment of descending thoracic aortic aneurysms. *N Engl J Med* 1994;331:1729.
35. Girardi LN, Bush HL Jr. Type B aortic dissection and thoracoabdominal aneurysm formation after endoluminal stent repair of abdominal aortic aneurysm. *J Vasc Surg* 1999;29:936.
36. Crawford ES. The diagnosis and management of aortic dissection. *JAMA* 1990;264:2537.
37. DeSanctis RW, et al. Aortic dissection. *N Engl J Med* 1987;317:1060.
38. Spittell PC, et al. Clinical features and differential diagnosis of aortic dissection: experience with 236 cases (1980 through 1990). *Mayo Clin Proc* 1993;68:642.
39. Larson EW, Edwards WD. Risk factors for aortic dissection: a necropsy study of 161 cases. *Am J Cardiol* 1984;53:849.
40. DeBakey ME, Henly WS, Cooley DA, et al. Surgical management of dissecting aneurysms of the aorta. *J Thorac Cardiovasc Surg* 1965;49:130.
41. Marsalese DL, et al. Marfan's syndrome presenting as a type 3 aortic dissection. *Chest* 1985;88:463.
42. Pumphrey CW, Fay T, Weir I. Aortic dissection during pregnancy. *Br Heart J* 1986;55:106.
43. Wahlers T, et al. Repair of acute type A aortic dissection after cesarean section in the thirty-ninth week of pregnancy. *J Thorac Caridovasc Surg* 1994;107:314.
44. Strichartz SD, Belabert HA, Moore WS. Retrograde aortic dissection with bilateral renal artery occlusion after repair of infrarenal aortic aneurysms. *J Vasc Surg* 1990;12:56.
45. DeBakey ME, et al. Dissection and dissecting aneurysms of the aorta: twenty-year follow-up of five hundred twenty-seven patients treated surgically. *Surgery* 1982;92:1118.
46. DeBakey ME, et al. Surgical management of dissecting aneurysms of the aorta. *J Thorac Cardiovasc Surg* 1965;49:130.
47. Daily PO, et al. Management of acute aortic dissections. *Ann Thorac Surg* 1970;10:237.
48. Crawford ES, et al. Aortic dissection and dissecting aortic aneurysms. *Ann Surg* 1988;208:254.
49. Glower DD, et al. Management and long-term outcome of aortic dissection. *Ann Surg* 1991;214:31.
50. Strouse PJ, et al. Aortic dissection presenting as spinal cord ischemia with a false-negative aortogram. *Cardiovasc Interv Radiol* 1990;13:77.
51. Cambria RP, et al. Vascular complications associated with spontaneous aortic dissection. *J Vasc Surg* 1988;7:199.
52. Raby N Giles J, Walters H. Aortic dissection presenting as acute leg ischaemia. *Clin Radiol* 1990;42:116.
53. Fradet G, et al. Aortic dissection: current expectations and treatment: experience with 258 patients over 20 years. *Can J Surg* 1990;33:465.
54. Soto B, et al. Angiographic diagnosis of dissecting aneurysm of the aorta. *Surgery* 1972;116:146.
55. Taniguch K, et al. Long-term survival and complications after composite graft replacement for ascending aortic aneurysm associated with aortic regurgitation. *Circulation* 1991;84[Suppl III]:III-31.
56. Wheat MW, et al. Acute dissection aneurysms of the aorta: treatment of the results in 64 patients. *J Thorac Cardiovasc Surg* 1969;57:344.
57. Glower DD, et al. Comparison of medical and surgical therapy for uncomplicated descending aortic dissections. *Circulation* 1990;82(Suppl IV):IV-39.
58. Walker PJ, et al. The use of endovascular techniques for the treatment of complications of aortic dissection. *J Vasc Surg* 1993;18:1042.
59. Dake MD, et al. Transluminal placement of endovascular stent-grafts for the treatment of descending thoracic aortic aneurysms. *N Engl J Med* 1994;331:1729.
60. Slonim SM, Nyman U, Semba CP, et al. Aortic dissection: percutaneous management of ischemic complications with endovascular stents and balloon fenestration. *J Vasc Surg* 1996;23:241.

61. Matsunaga N, Hayashi K, Sakamoto I, et al. Takayasu arteritis: protean radiologic manifestations and diagnosis. *Radiographics* 1997;17:579.
62. Yamato M, Lecky JW, Hiramatsu K, et al. Takayasu arteritis: radiographic and angiographic findings in 59 patients. *Radiology* 1986;161:329.
63. Cho YD, Lee KT. Angiographic characteristics of Takayasu arteritis. *Heart Vessels* 1992;7[Suppl]:97.
64. Sharma S, Saxena A, Talwar KK, et al. Renal artery stenosis caused by nonspecific arteritis (Takasayu disease): results of treatment with percutaneous transluminal angioplasty. *Am J Roentgenol* 1992;158:417.
65. Kumar S. Mandalam KR, Rao VRK, et al. Percutaneous transluminal angioplasty in nonspecific aortoarteritis (Takasayu's disease): experience of 16 cases. *Cardiovasc Intervent Radiol* 1990;12:321.
66. Klein RG, Hunder GG, Stanson AW, et al. Large artery involvement in giant cell (temporal arteritis). *Ann Intern Med* 1975;83:806.
67. Peyritz R. Ehlers-Danlos syndrome. In: Steinberg AG, Bearn AG, Motulsky AG, et al., eds. *Progress in medical genetics,* New series, vol. 5, *Genetics of cardiovascular disease.* Philadelphia: WB Saunders, 1983.
68. Peyritz RE, McKusick VA. The Marfan syndrome: diagnosis and management. *N Engl J Med* 1979;300:772.
69. McKusick VA, ed. *Heritable disorders of connective tissue,* 4th ed. St. Louis: CV Mosby 1972.
70. Gott VL, Peyritz RE, Cameron DE, et al. Composite graft repair of Marfan aneurysm of the ascending aorta: results in 100 patients. *Ann Thorac Surg* 1991;52:38.
71. Coselli JS, Le Maire SA, Büket S. Marfan syndrome: the variablility and outcome of operative management. *J Vasc Surg* 1995;21:342.
72. Steinberg AG, Bearn AG, Motulsky AGH, et al., eds. *Progress in medical genetics,* New series, vol. 5, *Genetics of cardiovascular disease.* Philadelphia: WB Saunders, 1983.
73. Horejs D, Gilbert PM, Burnstein S, et al. Normal aortoiliac diameters by CT. *J Comput Assist Tomogr* 1988;12:602.
74. Nuno IN, Collins GM, Bardin JA, et al. Should arteriography be used routinely in the elective management of abdominal aortic aneurysm? *Am H Surg* 1982;144:53.
75. Campbell JJ, Bell DD, Gaspar MR. Selective use of arteriography in the assessment of aortic aneurysm repair. *Ann Vasc Surg* 1990;4:419.
76. Dossa CD, Shepard AD, Reddy DJ, et al. Acute aortic occlusion: a 40-year experience. *Arch Surg* 1994;129:603.
77. Leriche R, Morel A. The syndrome of thrombotic obliteration of the aortic bifurcation. *Ann Surg* 1948;127:193.
78. Sumboonnanonda A, Robinson BL, Gedroye WMW, et al. Middle aortic syndrome: clinical and radiological findings. *Arch Dis Child* 1992;67:501.
79. Itzchak Y, Katznelson D, Boichis H, et al. Angiographic features of arterial lesions in neurofibromatosis. *Am J Roentgenol* 1974;122:643.
80. Siassi B, Klyman G, Emmanouilides GC. Hypoplasia of the abdominal aorta associated with the rubella syndrome. *Am J Dis Child* 1970;120:476.
81. Flynn PM, Robinson MB, Stapleton FB, et al. Coarctation of the aorta and renal artery stenosis in tuberous sclerosis. *Pediatric Radiol* 1984;14:337.
82. Lewis VD 3rd, Meranze SG, McLean GK, et al. The midaortic syndrome: diagnosis and treatment. *Radiology* 1988;167:111.
83. Messina LM, Reilly LM, Goldstone J, et al. Middle aortic syndrome: effectiveness and durability of complex arterial revascularization techniques. *Ann Surg* 1986;204:331.
84. Kadir S. Regional anatomy of the thoracic aorta. In: Kadir S, ed. *Atlas of normal and variant angiographic anatomy.* Philadelphia: WB Saunders, 1991:19.
85. Fisher CM. A new vascular syndrome—"The subclavian steal." *N Engl J Med* 1961;265:912.
86. Brown AH, Wellington MS. Coronary steal by internal mammary graft with subclavian stenosis. *J Thorac Cardiovasc Surg* 1976;73:690.
87. McGovern PG, Burke GL, Sprafka JM, et al. Trends in mortality, morbidity, and risk factor levels for stroke from 1960 through 1990. The Minnesota heart survey. *JAMA* 1992;268:753.
88. Hertzer NR, Young JR, Beven EG, et al. Coronary angiography in 506 patients with extracranial cerebrovascular disease. *Arch Intern Med* 1985;145:849.
89. O'Leary DH, Polak JF, Kronmal RA, et al. Carotid-artery intima and media thickness as a risk factor for myocardial infarction and stroke in older adults. *N Engl J Med* 1999;340:14.
90. Wadia NH, Monckton G. Intracranial bruits in health and disease. *Brain* 1957;80:492.
91. Heyman A, Wilkinson WE, Heyden S, et al. Risk of stroke in asymptomatic persons with cervical arterial bruits: a population study in Evans County, Georgia. *N Engl J Med* 1980;302:838.
92. Ivey TD, Strandness E, Williams DB, et al. Management of patients with carotid bruit undergoing cardiopulmonary bypass. *J Thorac Cardiovasc Surg* 1984;87:183.
93. Evans WE, Cooperman M. The significance of asymptomatic unilateral carotid bruits in preoperative patients. *Surgery* 1978;83:521.
94. Sauve J-S, Andreas Laupacis A, Ostbye T, et al. Does this patient have a clinically important carotid bruit? *JAMA* 1993;270:2843.
95. The European Carotid Surgery Trialists Collaborative Group. Risk of stroke in the distribution of an asymptomatic carotid artery. *Lancet* 1995;345:209.
96. Sauve JS, Thorpe KE, Sackett DL, et al. Can bruits distinguish high-grade from moderate symptomatic carotid stenosis? *Ann Intern Med* 1994;120:633.
97. Johnson BF, Verlato F, Bergelin RO, et al. Clinical outcome in patients with mild and moderate carotid artery stenosis. *J Vasc Surg* 1995;21:120.
98. Rockman CB, Riles TS, Lamparello PJ, et al. Natural history and management of the asymptomatic, moderately stenotic internal carotid artery. *J Vasc Surg* 1997;25:423.
99. Bock RW, Gray-Weale AC, Mock PA, et al. The natural history of asymptomatic carotid artery disease. *J Vasc Surg* 1993;17:160.
100. Carpenter JP, Lexa FJ, David JT. Determination of sixty percent or greater carotid artery stenosis by duplex Doppler ultrasonography. *J Vasc Surg* 1995;22:697.
101. Kent KC, Kuntz KM, Patel MR, et al. Perioperative imaging strategies for carotid endarterectomy: an analysis of morbidity and cost-effectiveness in symptomatic patients. *JAMA* 1995;274:888.
102. Muto PM, Welch, HJ, Mackey WC, O'Donnell TF. Evaluation of carotid artery stenosis: is duplex ultrasonography sufficient? *J Vasc Surg* 1996;24:17.
103. Olin JW, Melia M, Young JR, et al. Prevalence of atherosclerotic renal artery stenosis in patients with atherosclerosis elsewhere. *Am J Med* 1990;88:46N.
104. Harding MB, Smith LR, Himmelstein SI, et al. Renal artery stenosis: prevalence and associated risk factors in patients undergoing routine cardiac catheterization. *J Am Soc Nephrol* 1992;2:1608.
105. Scoble JE, Maher ER, Hamilton G, et al. Atherosclerotic renovascular disease causing renal impairment: a case for treatment. *Clin Nephrol* 1989;31:119.
106. Rimmer JM, Gennari FJ. Atherosclerotic renovascular disease and progressive renal failure. *Ann Intern Med* 1993;118:712.
107. Zierler RE, Bergelin RO, Davidson RC, et al. A prospective study of disease progression in patients with atherosclerotic renal artery stenosis. *Am J Hypertens* 1996;9:1055.
108. Brunner HR, Laragh JH, Baer L, et al. Essential hypertension: rennin and aldosterone, heart attacks and stroke. *N Engl J Med* 1972;286:441.
109. Mann SJ, Pickering TG, Sow TA, et al. Captopril renography in the diagnosis of renal artery stenosis: accuracy and limitations. *Am J Med* 1991;90:30.
110. Taylor DC, Kettler MD, Moneta GL, et al. Duplex ultrasound scanning in the diagnosis of renal artery stenosis: a prospective evaluation. *J Vasc Surg* 1988;7:363.
111. Strandness DE. Duplex imaging for the detection of renal artery stenosis. *Am J Kidney Dis* 1994;24:674.
112. Olin JW, Piedmonte MR, Young JR, et al. The utility of duplex ultrasound scanning of the renal arteries for diagnosing significant renal artery stenosis. *Ann Intern Med* 1995;122:833.
113. Munier MNS, Hoballah JJ, Miller EV, et al. Renal hilar Doppler analysis is of value in the management of patients with renovascular disease. *Am J Surg* 1997;174:164.
114. Isaacson JA, Zierler RE, Spittell PC, Strandness DE. Noninvasive screening for renal artery stenosis: comparison of renal artery and renal hilar duplex scanning. *J Vasc Tech* 1995;19:105.
115. Cohn EJ, Benjamin ME, Sandager GP, et al. Can intrarenal duplex waveform analysis predict successful renal artery revascularization? *J Vasc Surg* 1998;28:471.
116. Eidt JF, Fry RE, Clagett GP, et al. Postoperative follow-up of renal artery reconstruction with duplex ultrasound. *J Vasc Surg* 1988;8:667.
117. Dorros G, Jaff M, Mathiak L, et al. Four-year follow-up of Palmaz-Schatz stent revascularization as treatment for atherosclerotic renal artery stenosis. *Circulation* 1998;98:642.
118. Grist TM. Magnetic resonance angiography of the aorta and renal arteries. *Magn Reson Imaging Clin N Am* 1993;1:253.
119. De Cobelli F, Vanzulli A, Sironi S, et al. Renal artery stenosis: evaluation with breath-hold, three-dimensional, dynamic, gadolinium-enhanced versus three-dimensional, phase-contrast MR angiography. *Radiology* 1997;205:689.
120. Grenier N, Trillaud H, Combe C, et al. Diagnosis of renovascular hypertension: feasibility of captopril-sensitized dynamic MR imaging and comparison with captopril scintigraphy. *Am J Roentgenol* 1996;166:835.
121. US Department of Health and Human Services. Chartbook on cardiovascular, lung and blood diseases. *Morbidity and mortality.* Bethesda: NIH, NHLBI, 1994.
122. Abbott RD, Brand FN, Kannel WB. Epidemiology of some peripheral arterial findings in diabetic men and women: experiences from the Framingham study. *Am J Med* 1990;88:376.
123. Criqui MH, Fronek A, Barrett-Connor E, et al. The prevalence of peripheral arterial disease in a defined population. *Circulation* 1985;71:510.
124. Gross CM, Kramer J, Waigand J, et al. Relation between arteriosclerosis in the coronary and renal arteries. *Am J Cardiol* 1997;80:1478.
125. Weitz JI, Byrne J, Clagett GP, et al. Diagnosis and treatment of chronic arterial insufficiency of the lower extremities: a critical review. *Circulation* 1996;94:3026.
126. McKenna M, Wolfson S, Kuller L. The ratio of ankle and arm arterial pressure as an independent predictor of mortality. *Atherosclerosis* 1991;87:119.
127. Criqui MH, Langer RD, Fronek A, et al. Mortality over a period of 10 years in patients with peripheral arterial disease. *N Engl J Med* 1992;326:381.
128. Newman AB, Siscovick DS, Manolio TA, et al. Ankle-arm index as a marker of atherosclerosis in the cardiovascular health study. *Circulation* 1993;88:837.
129. Vogt MT, Cauley JA, Newman AB, et al. Decreased ankle/arm blood pressure index and mortality in elderly women. *JAMA* 1993;270:465.
130. Vogt MT, McKenna M, Wolfson SK, Kuller LH. The relationship between ankle brachial index, other atherosclerotic disease, diabetes, smoking and mortality in older men and women. *Atherosclerosis* 1993;101:191.
131. Kornitzer M, Dramaix M, Sobolski J, et al. Ankle/arm pressure index in asymptomatic middle-aged males: an independent predictor of ten-year coronary heart disease mortality. *Angiology* 1995;46:211.
132. Leng GC, Fowkes FGR, Lee AJ, et al. Use of ankle brachial pressure index to predict cardiovascular events and death: a cohort study. *BMJ* 1996;313:1440.
133. Gardner AW. The effect of cigarette smoking on exercise capacity in patients with intermittent claudication. *Vasc Med* 1996;1:181.
134. Jonason T, Bergstrom R. Cessation of smoking in patients with intermittent claudication: effects on the risk of peripheral vascular complications, myocardial infarction, and mortality. *Acta Med Scand* 1987;221:253.
135. Brand FN, Abbott RD, Kannel WB. Diabetes, intermittent claudication, and risk of cardiovascular events. The Framingham study. *Diabetes* 1989;38:504.
136. Jonason T, Ringqvist I. Diabetes mellitus and intermittent claudication: relation between peripheral vascular complications and location of the occlusive atherosclerosis in the legs. *Acta Med Scand* 1985;218:217.
137. Palumbo PJ, O'Fallon M, Osmundson PJ, et al. Progression of peripheral occlusive arterial disease in diabetes mellitus. What factors are predictive? *Arch Intern Med* 1991;151:717.
138. Reiber GE, Pecoraro RE, Koepsell TD. Risk factors for amputation in patients with diabetes mellitus: a case-control study. *Ann Intern Med* 1992;117:97.
139. The diabetes control and complications trial (DCCT) research group. Effect of intensive diabetes management on macrovascular events and risk factors in the diabetes control and complications trial. *Am J Cardiol* 1995;75:894.
140. Valentine JR, Grayburn PA, Vega GL, et al. Lp(a) lipoprotein is an independent, discriminating risk factor for premature peripheral atherosclerosis among white men. *Arch Intern Med* 1994;154:801.
141. Malinow MR, Kang SS, Taylor LM, et al. Prevalence of hyperhomocyst(e)inemia in patients with peripheral arterial occlusive disease. *Circulation* 1989;79:1180.
142. Lowe GDO, Fowkes FGR, Dawes J, et al. Blood viscosity, fibrinogen, and activation of coagulation and leukocytes in peripheral arterial disease and the normal population in the Edinburgh artery study. *Circulation* 1993;87:1915.
143. Ridker PM, Cushman M, Stampfer MJ, et al. Plasma concentration of C-reactive protein and risk of developing peripheral vascular disease. *Circulation* 1998;97:425.
144. Strandness DE. Noninvasive vascular laboratory and vascular imaging. In: Young JR, Olin JW, Bartholomew JR. *Peripheral vascular diseases*, 2nd ed. St. Louis: CV Mosby, 1996:33.
145. MacDonald NR. Pulse volume plethysmography. *J Vasc Tech* 1994;18:241.
146. Whelan JF, Barry MH, Moir JD. Color flow Doppler ultrasonography: comparison with peripheral arteriography for the investigation of peripheral vascular disease. *J Clin Ultrasound* 1992;20:369.
147. Allard L, Cloutier G, Durand LG, et al. Limitations of ultrasonic duplex scanning for diagnosing lower limb arterial stenoses in the presence of adjacent segment disease. *J Vasc Surg* 1994;19:650.
148. Larch E, Minar E, Ahmadi R, et al. Value of color duplex sonography for evaluation of tibioperoneal arteries in patients with femoropopliteal obstruction: a prospective comparison with anterograde intraarterial digital subtraction angiography. *J Vasc Surg* 1997;25:629.
149. Lewis WA, Bray AE, Harrison CL, et al. A comparison of common femoral waveform analysis with aorto-iliac duplex scanning in assessment of aorto-iliac disease. *J Vasc Tech* 1994;18:337.
150. Kohler TR, Nance DR, Cramer MM, et al. Duplex scanning for diagnosis of aortoiliac and femoropopliteal disease: a prospective study. *Circulation* 1987;76:1074.
151. Elsman BHP, Legemate DA, van der Heyden FWHM, et al. The use of color-coded duplex scanning in the selection of patients with lower extremity arterial disease for percutaneous transluminal angioplasty: a prospective study. *Cardiovasc Intervent Radiol* 1996;19:313.
152. Silke CM, Grouden MC, Nicholls S, et al. Noninvasive follow-up of peripheral angioplastyóa prospective study. *J Vasc Tech* 1997;21:23.
153. Mewissen MW, Kinney EV, Bandyk DF, et al. The role of duplex scanning versus angiography in predicting outcome after balloon angioplasty in the femoropopliteal artery. *J Vasc Surg*

1992;15:860.
154. Sacks D, Robinson ML, Marinelli DL, Perlmutter GS. Evaluation of the peripheral arteries with duplex US after angioplasty. *Radiology* 1990;176:39.
155. Bandyk DF. Ultrasonic duplex scanning in the evaluation of arterial grafts and dilatations. *Echocardiography* 1987;4:251.
156. Mattos MA, van Bemmelen PS, Hodgson KJ, et al. Does correction of stenoses identified with color duplex scanning improve infrainguinal graft patency? *J Vasc Surg* 1993;17:54.
157. Lalak NJ, Hanel KC, Hunt J, Morgan A. Duplex scan surveillance of infrainguinal prosthetic bypass grafts. *J Vasc Surg* 1994;20:637.
158. Bandyk DF. Postoperative surveillance of infrainguinal bypass. *Surg Clin N Am* 1990;70:71.
159. Jaff MR, Breger R, Deshur W, Pipia J. Detection of an arterial bypass graft threatening lesion by use of duplex ultrasonography and magnetic resonance angiography in an asymptomatic patient. *Vasc Surg* 1998;32:109.
160. Owen RS, Carpenter JP, Baum RA, et al. Magnetic resonance imaging of angiographically occult runoff vessels in peripheral arterial occlusive disease. *N Engl J Med* 1992;326:1577.
161. Cambria RP, Yucel EK Brewster DC, et al. The potential for lower extremity revascularization without contrast arteriography: experience with magnetic resonance angiography. *J Vasc Surg* 1993;17:1050.
162. Sueyoshi E, Sakamoto I, Matsuoka Y, et al. Aortoiliac and lower extremity arteries: comparison of three-dimensional dynamic contrast-enhanced subtraction MR angiography and conventional angiography. *Radiology* 1999;210:683.
163. Vlodaver Z, Frech R, Van Tassel RA, Edwards JE. Correlations of the antemortem arteriogram and the post-mortem specimen. *Circulation* 1973;47:162.
164. Moore W, Hall A. Unrecognized aortoiliac stenosis. *Arch Surg* 1971;103:633.
165. Legemate DA, Teeuwen C, Hoeneveld H, Eielboom BC. Value of duplex scanning compared with angiography and pressure measurement in the assessment of aortoiliac lesions. *Br J Surg* 1991;78:1003.
166. Isner JM, Rosenfield K. Enough with the fantastic voyage: will IVUS pay in Peoria? *Cathet Cardiovasc Diagn* 1992;266:192.
167. Cohen MI, Vogelzang RL. A comparison of techniques for improved visualization of the arteries of the distal lower extremity. *Am J Roentgenol* 1986;147:1021.

15
Stress Testing During Cardiac Catheterization: Exercise and Pacing Tachycardia

William Grossman

University of California, San Francisco, School of Medicine; Division of Cardiology, University of California, San Francisco Medical Center, San Francisco, California 94143

Patients with significant heart disease may have entirely normal hemodynamics when assessed in the resting state during cardiac catheterization. Because most cardiac symptoms are precipitated by exertion or some other stress, however, it also may be important to assess hemodynamic performance during some form of stress such as muscular exercise, pharmacologic intervention (e.g., dobutamine infusion), or pacing-induced tachycardia. Such an evaluation enables the physician to assess the *cardiovascular reserve* and the relationship (if any) between specific symptoms and hemodynamic impairment. Physiologic information so obtained is often valuable in prescribing specific medical therapy, selecting patients for corrective cardiac surgery, and estimating prognosis.

Muscular exercise, both dynamic and isometric, has been studied extensively in the cardiac catheterization laboratory, and the normal hemodynamic responses are reasonably well understood. There are major differences between the hemodynamic responses to dynamic exercise (done either in the supine or the erect position) and the responses to static, isometric exercise, and these two types of exercise are discussed separately.

DYNAMIC EXERCISE

During dynamic exertion, skeletal muscles are actively contracting and developing force that is translated into motion and work. This is accompanied by an increase in both carbon dioxide production and oxygen (O_2) consumption by skeletal muscle, and a corresponding increase in alveolar gas exchange needed to support the higher metabolic rate. In normal sedentary individuals, the level of O_2 consumption during maximal exercise ($\dot{V}O_2max$) can increase about 12-fold in comparison with that during the resting state (1). Age and fitness also modify $\dot{V}O_2max$. During aging, there is a decrease in $\dot{V}O_2max$ of about 5% per decade. During athletic training, $\dot{V}O_2max$ increases because of both cardiovascular and skeletal muscle adaptation. In marathon runners and Olympic-class athletes, $\dot{V}O_2max$ may represent an 18-fold increase in O_2 consumption above the resting state. The increased oxygen requirements of muscular exercise are met by both an increase in the cardiac output and an increased extraction of oxygen from arterial blood by skeletal muscle, which causes widening of the arteriovenous oxygen difference (AV O_2 difference). The need for the heart to increase cardiac output appropriately for the increase in O_2 consumption resulting from exercise is met by an increase in *heart rate* and an increase in *stroke volume*. The relative contributions of these increases to the rise in cardiac output depend on the type of exercise (supine versus upright), the intensity of exercise, the limitation of diastolic filling at high heart rates, and the response to sympathetic stimulation. Metabolic adaptations of exercising muscle include a switch from utilization of free fatty acids at rest to an accelerated breakdown of muscle glycogen stores and enhanced uptake of bloodborne glucose, which is supplied by increased hepatic gluconeogenesis. Because carbohydrate metabolism produces more carbon dioxide than fat metabolism does, the *respiratory quotient* (ratio of carbon dioxide production to O_2 consumption) rises from a resting value of 0.7 to 0.8 toward 1.0. The delivery of bloodborne oxygen and glucose to working skeletal muscle is enhanced in the presence of normal vasculature by a reduction in skeletal muscle vascular resistance mediated by metabolic byproducts and by sympathetically mediated vasoconstriction elsewhere, which causes a redistribution of blood away from the renal and splanchnic beds to exercising muscle.

Exercise depends on the adequacy of pulmonary function to increase oxygen supply. During progressive exercise, there is a linear increase in minute ventilation relative to the increase in O_2 consumption. When the intensity and duration of exercise are such that insufficient oxygen is delivered to exercising muscle, anaerobic metabolism of glucose develops, causing metabolic acidosis and an increase in respiratory quotient to values higher than 1.0; minute ventilation increases out of proportion to O_2 consumption. Beyond this *anaerobic threshold* the accumulation of hydrogen ions usually causes skeletal muscle weakness, pain, and severe breathlessness, followed by exhaustion and cessation of exercise. It is best to conduct exercise studies in the catheterization laboratory so that the patient reaches a *steady-state level of submaximal exercise* below the anaerobic threshold and exercise can be sustained for several minutes. This approach permits estimation of cardiovascular reserve and allows the physician to determine whether the increase in cardiac output is appropriate for the increase in O_2 consumption occurring at that particular level of exercise.

Oxygen Uptake and Cardiac Output

There is a linear relationship between O_2 consumption and increasing workload (Fig. 15.1). Oxygen uptake increases abruptly after initiation of dynamic exercise, reflecting additional work needed to overcome inertia of the legs, and then increases steadily over a few minutes to reach a new steady state that is directly related to the intensity or level of exercise (2,3 and 4). Simultaneously, the mixed venous blood oxygen saturation decreases to a lower steady level related to the intensity of exercise, producing an increase in the AV O_2 difference.

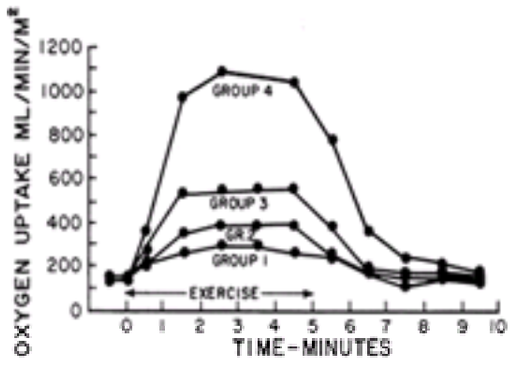

FIG. 15.1. Oxygen consumption in normal subjects during exercise. Each group represents a different level of exercise, with the most intense exercise being performed by group 4. Note the prompt increase and establishment of a new steady state in oxygen uptake that is directly related to the intensity of the exercise. (From Donald KW, et al. The effect of exercise on the cardiac output and circulatory dynamics of normal subjects. *Clin Sci* 1955;14:37, with permission.)

The cardiac output increases linearly with increasing workload during both supine and upright exercise in normal subjects (2,3,4 and 5). As can be seen from the regression equation for this relationship (Fig. 15.2, for each increment of 100 mL/min/m^2 of O_2 consumption during exercise there is an increase in cardiac output of 590 mL/min/m^2.

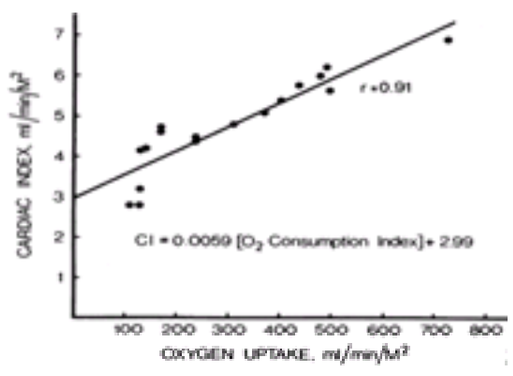

FIG. 15.2. The relationship between cardiac output and oxygen consumption (both indexed for body surface area) during supine dynamic exercise of varying intensity in normal subjects, based on the data of Dexter. As can be seen from the regression equation for this relationship, for each increment of 100 mL/min/m^2 of oxygen consumption, there is an increase in cardiac output of 0.59 L/min/m^2 or 590 mL/min/m^2. CI, cardiac index. (Data from Dexter L, et al. Effects of exercise on circulatory dynamics of normal individuals. *J Appl Physiol* 1951;3:439.)

Exercise Index

The linear relationship between oxygen uptake and cardiac output during exercise, illustrated in Fig. 15.2, may be used to assess whether the cardiac output response measured in an individual patient is appropriate to the level of exercise and increased oxygen uptake. The regression formula is CI = 0.0059X + 2.99, where CI is the cardiac index in liters per minute per square meter of body surface area (BSA) and X is the O_2 consumption in mL/min/m^2 BSA. This formula may be used to calculate the *predicted cardiac index* for a given level of O_2 consumption (X), and the predicted cardiac index may then be compared with the *measured cardiac index*. Note that this assessment can be performed at any steady-state level of exercise and does not depend on achieving any specific "target" level of exertion. This equation can be used to calculate a predicted cardiac index by measuring O_2 consumption during dynamic exercise. The patient's actual measured cardiac index during exercise is then divided by the predicted cardiac index to determine the deviation from normal:

$$\text{Exercise index} = \frac{\text{Measured cardiac index (L/min/m}^2\text{)}}{\text{Predicted cardiac index (L/min/m}^2\text{)}} \quad \textbf{(15.1)}$$

We have termed this ratio the *exercise index*, since it allows expression of exercise capacity as a percentage of the normal response. An exercise index of 0.8 or higher indicates a normal cardiac output response to exercise.

Exercise Factor

Another way of using this same relationship between cardiac output and O_2 consumption involves calculation of the *exercise factor*, which is the increase in cardiac output with exercise divided by the corresponding increase in O_2 consumption:

$$\text{Exercise factor} = \frac{\text{Increase in cardiac output (mL/min)}}{\text{Increase in O}_2\text{ consumption (mL/min)}} \quad \textbf{(15.2)}$$

A normal exercise factor would be an increase of = 600 mL/min in cardiac output per 100 mL/min increase in O_2 consumption. An exercise factor less than 6.0 indicates a subnormal response in cardiac output; like an exercise index of less than 0.8, such a factor suggests some pathologic process limiting the heart's ability to meet the exercise-induced increase in O_2 consumption with an appropriate increase in cardiac output, forcing an excessive reliance on oxygen extraction from arterial blood and widening of the AV O_2 difference.

Systemic and Pulmonary Arterial Pressure and Heart Rate

Systolic arterial pressure and mean arterial pressure also increase linearly in relation to O_2 consumption during dynamic exercise in normal subjects, although the response is somewhat variable (4,6,7 and 8). Despite this increase in arterial pressure, systemic vascular resistance decreases substantially during dynamic exercise, indicating that the elevated arterial blood pressure is secondary to increased cardiac output. Patients who are unable to generate an adequate increase in cardiac output during dynamic exercise may also increase their arterial pressure, but in this circumstance systemic vascular resistance does not decline and may actually increase.

The behavior of the pulmonary circulation in response to dynamic exercise is different from that of the systemic circulation in normal individuals. Mean pulmonary artery pressure increases almost proportionally with cardiac output (pulmonary blood flow), so that there is only a slight decrease in pulmonary vascular resistance, in contrast to the normal substantial decrease in resistance of the systemic vasculature.

Heart rate increases consistently during both supine and upright dynamic exercise and tends to increase linearly in relation to O_2 consumption. During dynamic supine exercise in the catheterization laboratory, tachycardia is the predominant factor in increasing cardiac output. Tachycardia exerts a positive inotropic effect (the

so-called treppe phenomenon), but increased sympathetic nervous system activity appears to be the most significant factor leading to enhanced myocardial contractility. In most normal subjects, supine bicycle exercise is accompanied by an increase in ejection fraction, and other ejection indices of left ventricular (LV) systolic function with a decrease in LV end-systolic volume.

Several investigators (2,3,6,7 and 8) examined the responses of cardiac output, stroke volume, and heart rate to a given intensity of supine exercise in normal subjects and showed that the increase in cardiac output is caused primarily by an increase in heart rate with a negligible contribution by increased stroke volume. During repeat exercise when heart rate is held constant, there is a comparable increase in cardiac output caused by a marked increase in stroke volume (7). When heart rate is artificially increased by electrical pacing in the absence of dynamic exercise, however, cardiac output remains unchanged and a major fall in stroke volume occurs (7), indicating that further cardiovascular adjustments are required for an adequate hemodynamic response to dynamic exercise.

Therefore, to adequately interpret the response to supine exercise in the catheterization laboratory, it is important to recognize that the increase in cardiac output in normal young subjects is caused by a proportionate increase in heart rate. As discussed later, when chronotropic reserve is depressed, an appropriate increase in cardiac output relative to O_2 consumption depends on the capacity to augment LV diastolic filling and end-diastolic fiber tension, leading to an increase in stroke volume by means of the Frank-Starling mechanism.

Upright Versus Supine Exercise

The contributions of heart rate and stroke volume to cardiac output differ in supine and upright bicycle exercise. End-diastolic volumes at rest are near maximum when normal subjects are supine, smaller when they are sitting, and smallest when they are standing (4). When subjects are in the upright position, LV end-diastolic volume, cardiac output, and stroke volume are lower than when they are in the supine position (6,8). During erect bicycle exercise, most normal subjects demonstrate an increase in ejection fraction and reduction in end-systolic volume, some enhancement of LV end-diastolic volume, and an increase in stroke volume as well as heart rate. LV end-diastolic volume and stroke volume tend to increase up to about 50% of peak O_2 consumption and then to plateau or actually decrease at high levels of exercise (4). At high levels of exercise and fast heart rates, recruitment of the Frank-Starling mechanism may be blunted by the effects of tachycardia and limitation of diastolic filling due to shortening of diastole. At high levels of upright exercise, stroke volume is preserved by a progressive decrease in end-systolic volume and increase in ejection fraction in the presence of a constant or decreased LV end-diastolic volume (4,5).

Caution must be used in interpreting the relative contributions of inotropic reserve and utilization of the Frank-Starling mechanism in patients studied during dynamic exercise in the catheterization laboratory. The effects of advancing age profoundly alter the exercise response. In healthy subjects, there appear to be no age-related changes in resting cardiac output, ejection fraction, end-systolic volume, or end-diastolic volume (9). With age, there is a reduction in both peak O_2 consumption and cardiac output during exercise. Also, with advancing age there is a reduction in heart rate and contractility response during exercise, so that the increase in cardiac output at any level of exercise is accomplished by significant increases in end-diastolic volume and in stroke volume (9,10). Therefore, as discussed earlier, studies of the effects of dynamic supine bicycle exercise in young adults have generally shown no change or a fall in LV end-diastolic pressure (LVEDP) and volume during exercise. In contrast, studies of older normal subjects or patients with atypical chest pain and normal coronary arteries have generally shown that both dynamic supine and upright bicycle exercise are associated with an increase in LVEDP (8,11), which is consistent with an age-dependent reliance on an increase in preload during exercise. For example, in a group of 10 sedentary men whose average age was 46 years, there was a rise in LVEDP from 8 ± 1 to 16 ± 2 mm Hg during supine bicycle exercise, and a rise from 4 ± 1 to 11 ± 1 mm Hg during upright bicycle exercise (8). The diminished heart rate and contractility responses during exercise and resultant increased dependence on the Frank-Starling mechanism with aging may reflect an age-related decrease in responsiveness to beta-adrenergic stimulation (12). There are also gender-related differences in the normal response to exercise. Normal men and women can achieve comparable increases in weight-adjusted peak O_2 consumption, heart rate, and blood pressure. However, normal women generally achieve increases in stroke volume during upright exercise through an increase in end-diastolic volume without an increase in ejection fraction, whereas normal men exhibit a progressive increase in ejection fraction to peak exercise (13).

The interpretation of normal versus abnormal LV systolic performance during dynamic exercise may also be complicated by the effects of chronic b-adrenergic blockade. Studies of the hemodynamic effects of chronic b-adrenergic blockade on graded exercise in hypertensive but otherwise healthy young adults have shown that no impairment of maximal exercise capacity (maximal O_2 consumption) or cardiac output response occurs during chronic b-adrenergic blockade. b-Blockade, however, causes a reduction in heart rate at any level of exercise, and this relative reduction in heart rate is compensated for by both a widening of the AV O_2 difference and an increase in stroke volume, associated with an increased LV end-diastolic volume and a reduced arterial blood pressure (decreased impedance to ejection).

In normal b-blocked subjects, increases in cardiac output during exercise depends on increasing stroke volume by means of the Frank-Starling mechanism. Therefore, the dynamic exercise response of a patient receiving chronic b-adrenergic blocking therapy may be associated with an “inappropriately” low increase in cardiac output relative to O_2 consumption, accompanied by excessive widening of the AV O_2 difference with an increased reliance on an increase in LV end-diastolic volume. During dynamic supine exercise in the catheterization laboratory, the finding that an increase in cardiac output depends on an increase in LV end-diastolic volume (and pressure) could be caused by either b-adrenergic blockade *per se* or intrinsic impairment of LV systolic function. For these reasons, strong consideration should be given to discontinuation of b-adrenergic blocking drugs at least 24 hours before catheterization if analysis of the hemodynamic response to dynamic exercise is planned to assess the adequacy of cardiovascular reserve.

Left Ventricular Diastolic Function

Interpretation of the changes in LV diastolic pressure with exercise depends greatly on an appreciation of the adaptations in diastolic function that occur. In normal subjects, multiple adjustments occur to accommodate an increased transmitral flow into the left ventricle in the face of an abbreviated diastolic filling period and to maintain low pressures throughout diastole. Exercise is associated with a progressive acceleration of isovolumetric relaxation so that enhanced diastolic filling occurs with minimal change in mitral valve opening pressure (14). The exercise-induced enhancement of diastolic relaxation and filling is probably modulated by both b-adrenergic stimulation and increased heart rate.

In normal subjects, there is either no change or a downward shift in the LV diastolic pressure-volume relation during exercise (Fig. 15.3). In the presence of ischemia or cardiac hypertrophy, however, exercise may provoke an upward shift in the LV diastolic pressure-volume relationship, so that any level of LV end-diastolic volume is associated with a much higher LVEDP. In such patients, the left ventricle may be regarded as exhibiting increased chamber stiffness (decreased distensibility) during exercise. In patients with coronary artery disease, a transient but striking upward shift in the LV diastolic pressure-volume relation is common during episodes of ischemia (15). Patients with coronary artery disease who develop angina during dynamic exercise in the catheterization laboratory commonly show a marked rise in LVEDP. A careful study of the dynamics of LV diastolic filling during exercise in patients with coronary artery disease has been reported by Carroll et al. (16). These authors studied LV diastolic pressure-volume relations in 34 patients with coronary disease who developed ischemia during exercise and compared the finding with those from 5 patients with minimal cardiovascular disease (control) and 5 patients with an akinetic area at rest from a prior infarction but no active ischemia during exercise (scar group). There was an upward shift in the LV diastolic pressure-volume relationship during exercise-induced ischemia, which was not seen in either the scar or the control group (Fig. 15.3). Therefore, interpretation of an exercise-induced rise in LVEDP in patients with coronary artery disease is complex and may be related to both a decrease in LV chamber distensibility and an increase in LV end-diastolic volume secondary to a reduction in ejection fraction (11,16).

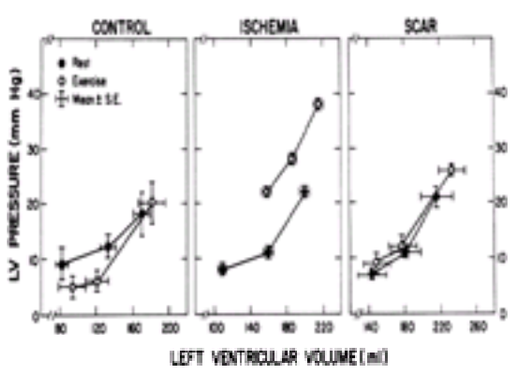

FIG. 15.3. Left ventricular (LV) diastolic pressure-volume relations at rest and during exercise in patients without heart disease (CONTROL), compared to patients with coronary disease who developed ischemia during exercise (ISCHEMIA), and patients with akinetic areas due to previous infarction but no active ischemia during exercise (SCAR). Pressure and volume are averaged at three diastolic points: early diastolic pressure nadir, mid-diastole, and end-diastole. The control group had a

downward shift of the early diastolic pressure-volume relation, but the ischemia group showed an upward and rightward shift. (From Carroll JD, Hess OM, Hirzel HO, et al. Dynamics of left ventricular filling at rest and during exercise. *Circulation* 1983;68:59, with permission.)

The presence of cardiac hypertrophy is frequently characterized by depression of the rates of LV relaxation and diastolic filling at rest, and this depression profoundly impedes LV filling during exercise-induced tachycardia. In patients with conditions such as hypertrophic cardiomyopathy or hypertensive hypertrophic cardiomyopathy, in whom baseline LV end-systolic volumes are small, there is no reserve to further enhance systolic shortening, and abnormal diastolic properties limit the capacity to recruit the Frank-Starling mechanism during exercise. Furthermore, tachycardia may provoke ischemia (owing to impaired coronary vasodilator reserve), accompanied by an upward shift in the diastolic pressure-volume relationship. These findings with exercise-induced tachycardia in patients with coronary disease and/or advanced LV hypertrophy are remarkably similar to the changes in diastolic function seen during angina induced by pacing tachycardia, as described later in this chapter.

Marked abnormalities in LV diastolic function occur with exercise in patients with clinical evidence of heart failure but normal resting systolic function (so-called diastolic heart failure). Kitzman and Sullivan (17) studied seven patients with New York Heart Association (NYHA) class III or IV heart failure with one or more documented episodes of pulmonary edema and no significant coronary artery disease. All had LV ejection fractions of ³ 50%, without echocardiographic evidence of regional wall motion abnormalities or valvular or pericardial disease. Four of these patients were elderly with a medical history remarkable only for chronic hypertension. Most patients had increased LV wall thickness and mass. Patients were studied by symptom-limited upright exercise with simultaneous hemodynamic and radionuclide measurements, and data were compared to those seen in age- and sex-matched healthy volunteers who served as controls. As can be seen in Fig. 15.4, maximum exercise capacity was reduced, and the cardiac output increased primarily as a result of tachycardia, with no change in stroke volume. Fig. 15.5 shows that LV ejection fraction was normal at rest and with exercise for both patients and control subjects, but there was a striking rise in pulmonary capillary wedge pressure in those patients with diastolic heart failure, compared with the control subjects. Accordingly, these patients clearly have “pure” diastolic heart failure: Efforts to treat their heart failure by improving systolic function (e.g., digoxin) will not be successful. As seen in Fig. 15.6, diastolic distensibility was markedly decreased with exercise in these patients.

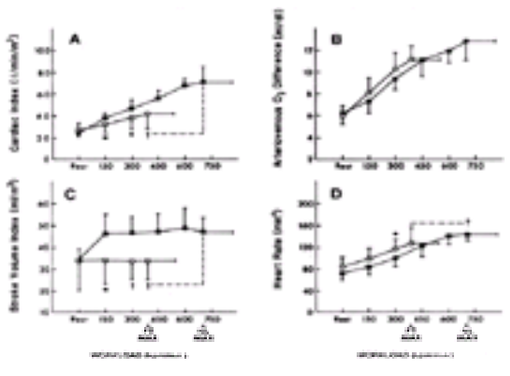

FIG. 15.4. Seven patients with heart failure and normal left ventricular systolic function *(open symbols)* compared with 10 age- and gender-matched healthy volunteers *(solid symbols)* who served as controls. All subjects underwent upright bicycle exercise with hemodynamic evaluation. Cardiac output increased for the patients with heart failure as a result of an increase in heart rate, with fixed stroke volume. PT MAX, patient maximum exercise; NL MAX, normal subject maximum exercise. (From Kitzman D, et al. Exercise tolerance in patients with heart failure and preserved left ventricular systolic function: failure of the Frank-Starling mechanism. *J Am Coll Cardiol* 1991;17:1065, with permission.)

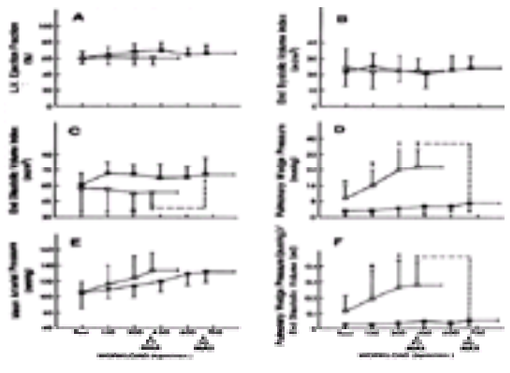

FIG. 15.5. Response of left ventricular function to upright bicycle exercise in the patients with diastolic heart failure (❑) and healthy controls (■) illustrated in Fig. 15.4. Pulmonary wedge pressure increases dramatically, but left ventricular end-diastolic volume fails to increase in the patients with heart failure, compared with healthy age- and gender-matched controls. LV ejection fraction remains normal. The intolerance to exercise is probably the result of increased pulmonary capillary wedge pressure and the resultant increased lung stiffness rather than decreased cardiac output or oxygen delivery to metabolizing tissues. PT MAX, patient maximum exercise; NL MAX, normal subject maximum exercise. (From Kitzman D, et al. Exercise tolerance in patients with heart failure and preserved left ventricular systolic function: failure of the Frank-Starling mechanism. *J Am Coll Cardiol* 1991;17:1065, with permission.)

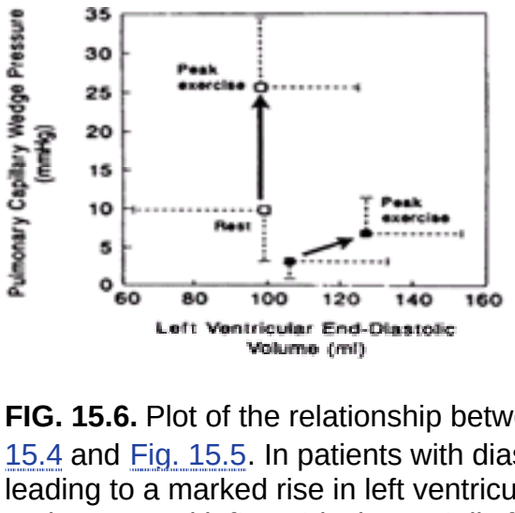

FIG. 15.6. Plot of the relationship between changes in pulmonary capillary wedge pressure and left ventricular end-diastolic volume in the patients illustrated in Fig. 15.4 and Fig. 15.5. In patients with diastolic heart failure, the stiff left ventricle cannot dilate normally (❑) in response to the increased venous return of exercise, leading to a marked rise in left ventricular filling pressure, compared to normal controls (■). (From Kitzman D, et al. Exercise tolerance in patients with heart failure and preserved left ventricular systolic function: failure of the Frank-Starling mechanism. *J Am Coll Cardiol* 1991;17:1065, with permission.)

Examples of the Use of Exercise to Evaluate Left Ventricular Failure in the Cardiac Catheterization Laboratory

Examples of the hemodynamic changes that can occur during supine bicycle exercise are shown in Table 15.1 and Table 15.2. Table 15.1 illustrates the response to 6 minutes of supine bicycle exercise of a 36-year-old woman with an idiopathic dilated cardiomyopathy (ejection fraction, 40%) whose major symptom was exertional

dyspnea. Because her ejection fraction was only moderately depressed and her hemodynamic values were almost normal at rest, resting hemodynamic data alone did not clarify whether her cardiovascular reserve was impaired and whether her exertional dyspnea was likely to be cardiac in origin. During exercise, the cardiac index increased appropriately in relation to the increase in O_2 consumption, yielding an exercise index of 1.1 and an exercise factor of 8.5:

$$\frac{\Delta \text{ cardiac index}}{\Delta \text{ } O_2 \text{ consumption}} = \frac{3{,}300}{387} = 8.5 \quad \textbf{(15.3)}$$

The increase in cardiac output, however, was accomplished at the cost of a substantial increase in mean pulmonary capillary wedge pressure, which rose from 11 to 27 mm Hg. These data suggest that the patient had some limitation of inotropic reserve and that her ability to increase cardiac output depended heavily on utilization of the Frank-Starling mechanism. Therefore, her dyspnea can be considered to be of cardiac origin.

Hemodynamic parameter	Resting	Exercise (6 min)
Oxygen consumption index (mL/min/m²)	117	504
Atrioventricular oxygen difference (mL/L)	34	75
Cardiac index (L/min/m²)	3.4	6.7
Heart rate (beats per min)	80	140
Systemic arterial pressure (mm Hg), systolic/diastolic (mean)	130/70 (95)	142/83 (110)
Right atrial mean pressure (mm Hg)	6	7
Pulmonary capillary wedge mean pressure (mm Hg)	11	27
Left ventricular pressure (mm Hg)	130/17	142/28
Exercise index	—	1.1
Exercise factor	—	8.5

TABLE 15.1. *Response to supine bicycle exercise in a 36-year-old woman with dilated cardiomyopathy*

Hemodynamic parameter	Resting	Exercise (6 min)
Oxygen consumption index (mL/min/m²)	128	469
AV O_2 difference (mL/L)	40	96
Cardiac index (L/min/m²)	3.2	4.9
Heart rate (beats per min)	90	141
Systemic arterial pressure (mm Hg), systolic/diastolic (mean)	91/62 (73)	107/67 (80)
Right atrial mean pressure (mm Hg)	5	20
Pulmonary capillary wedge mean pressure (mm Hg)	12	34
Left ventricular pressure (mm Hg)	91/16	107/34
Exercise index	—	0.85
Exercise factor	—	4.9

TABLE 15.2. *Response to supine bicycle exercise in a 60-year-old man with dilated cardiomyopathy*

A patient with more severe impairment of cardiovascular reserve is illustrated in Table 15.2, which shows the response to 6 minutes of supine bicycle exercise of a 60-year-old man with idiopathic dilated cardiomyopathy and symptoms of marked fatigue and dyspnea with minimal exertion. His chest roentgenogram showed cardiomegaly with no evidence of pulmonary edema, and his rest hemodynamics were almost normal. Supine bicycle exercise was associated with a marked rise in both left and right heart filling pressures and a marginal ability to increase cardiac output appropriately in relation to his increase in O_2 consumption. His exercise index was 0.85, with a low exercise factor at 4.9:

$$\frac{\Delta \text{ cardiac index}}{\Delta \text{ } O_2 \text{ consumption}} = \frac{1{,}700}{341} = 4.9 \quad \textbf{(15.4)}$$

The cause of exercise intolerance in some patients with LV failure is diminished cardiovascular reserve, so that inadequate oxygen is delivered to working skeletal muscle to meet the demands of aerobic metabolism. Other patients are not limited by the ability to deliver oxygen to working skeletal muscle but by the rise in pulmonary capillary wedge pressure associated with exercise (Table 15.1). As illustrated in these examples, the relative contributions of the inability of the heart to augment cardiac output versus an exercise-induced rise in pulmonary capillary wedge pressure that could impair gas exchange are controversial. Exercise tolerance in patients with congestive heart failure is highly variable and correlates poorly with ejection fraction. Studies of the hemodynamic and ventilatory response to exercise have shown that as the clinical severity of congestive heart failure worsens, there is a progressive decrease in maximal O_2 consumption, premature onset of the anaerobic threshold, and declines in both maximal cardiac output and the cardiac output achieved at levels of submaximal O_2 consumption (18,19). Studies of brief exercise performed by patients with chronic congestive heart failure have shown that arterial oxygen saturation usually increases (presumably as a result of increased ventilation) despite elevation of the pulmonary capillary wedge pressure; maximal oxygen extraction is normal, and ventilatory mechanisms do not limit maximum O_2 consumption, so that both symptomatic limitation and the inability to normally increase oxygen delivery are caused by the failure to increase cardiac output adequately. Conversely, in patients with depressed LV ejection fraction who can achieve normal levels of exercise, factors that contribute to normal exercise capacity include normal augmentation of heart rate, the ability to increase cardiac output through further increases in LV end-diastolic volume and stroke volume, and tolerance of a high pulmonary venous pressure, possibly because of enhanced lymphatic drainage.

Therefore, in patients with severe depression of LV ejection fraction, the failure to increase cardiac output normally appears to be related both to the inability to increase stroke volume and to the inability to increase heart rate, compared with age-matched subjects (20). This *impaired chronotropic response* appears to be caused by an impaired postsynaptic response to b-adrenergic stimulation that may be related to several defects, including a reduced cardiac b-receptor density, “uncoupling” of the b-receptor and adenylate cyclase activity, and deficient production of cyclic adenosine monophosphate (21).

Evaluation of Valvular Heart Disease

Valvular Stenosis

Exercise may also be used in the cardiac catheterization laboratory to evaluate valvular heart disease. Gradients across the atrioventricular and semilunar valves may become apparent during exercise and may reach levels that account for the clinical symptoms of the patient. Exercise hemodynamics are especially useful when the resting transvalvular gradient or estimated valve area has borderline significance.

An example of the hemodynamic changes during supine dynamic exercise in a patient with moderate mitral stenosis is shown in Fig. 15.7 and Table 15.3. As the result of increased mitral valve flow and a decreased diastolic filling period, the pressure gradient increased significantly, producing left atrial pressures of sufficient magnitude to cause symptoms. Cardiac output increased normally, yielding an exercise index of 1.2 and an exercise factor of 5.8:

$$\frac{\Delta \text{ cardiac output}}{\Delta \text{ } O_2 \text{ consumption}} = \frac{2{,}800}{481} = 5.8 \quad \textbf{(15.5)}$$

These data are compatible with mild mitral stenosis and illustrate the changes in a diastolic pressure gradient across the mitral valve required to produce an increase

in cardiac output appropriate to the increased oxygen requirements of strenuous exercise.

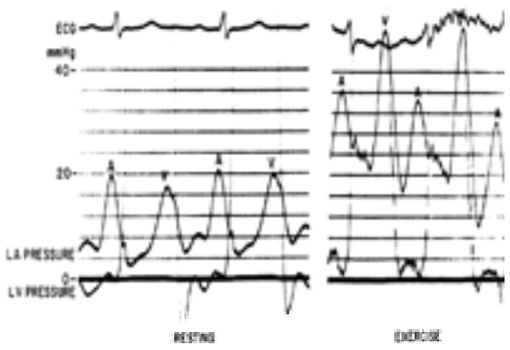

FIG. 15.7. Simultaneous pressure recordings from left atrium and left ventricle at rest and at 5 minutes of bicycle ergometer exercise in a patient with mitral stenosis. The hemodynamic data for this patient are presented in Table 15.3.

Parameter	Resting	Exercise (5 min)
Left atrial pressure (mm Hg)		
A	20	34
V	18	46
Mean diastolic	10	26
Left ventricular mean diastolic pressure (mm Hg)	1	4
Oxygen consumption (mL/min)	207	688
Atrioventricular oxygen difference (mL/L)	31	74
Cardiac output (L/min)	6.5	9.3
Heart rate (beats per min)	72	108
Mitral value area (cm^2)	1.6	1.8
Exercise index		1.2
Exercise factor		5.8

[a] Same patient as in Fig. 7.

TABLE 15.3. *Hemodynamic changes during supine dynamic exercise in a patient with mitral stenosis*[a]

In evaluating hemodynamic changes across stenotic valves during exercise, it is often found that the calculated valve area during exercise varies somewhat from that calculated on the basis of resting data (it is usually slightly larger). This variance is usually small and may be related to actual changes in the degree of valvular obstruction (i.e., a higher gradient and greater flow may force the stenotic leaflets to open farther), deficient data, or computational errors inherent in the assumptions applied to the equation for calculating valve orifice size.

Valvular Insufficiency

The hemodynamic consequences of valvular insufficiency with ventricular volume overload may be subtle at rest. Dynamic exercise, by calling on the heart to substantially augment its forward cardiac output, may elicit changes in LVEDP and volume (preload) and in systemic vascular resistance (afterload) that are useful in assessing the cardiovascular limitations imposed by the valve lesion. Of particular importance here is the inability of many patients with valvular insufficiency to increase forward cardiac output in an appropriate manner, resulting in a low exercise index and an abnormal exercise factor. Dynamic exercise testing is especially valuable in such patients because the qualitative assessment of valvular insufficiency from angiograms may be unreliable and does not correlate well with the extent of functional impairment.

Figure 15.8 shows the hemodynamic response to dynamic bicycle exercise for a 55-year-old man with rheumatic heart disease and mitral regurgitation. The patient was able to increase cardiac output normally, but mean pulmonary capillary wedge pressure increased from 18 to 30 mm Hg, with V waves to 60 mm Hg, during 6 minutes of supine bicycle exercise. This patient had successful mitral valve replacement, with relief of symptoms.

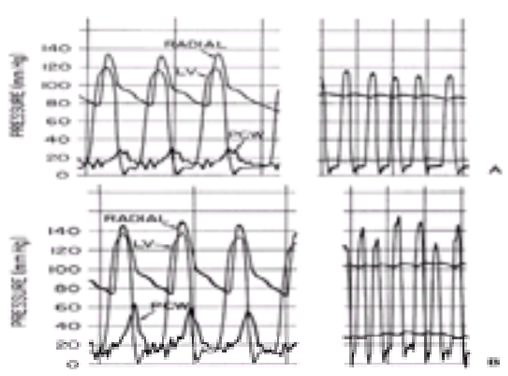

FIG. 15.8. Hemodynamic findings during exercise in a 55-year-old man ith mitral regurgitation. Left ventricular (LV), pulmonary capillary wedge (PCW), and radial artery pressure tracings are shown before **(A)** and during **(B)** the sixth minute of supine bicycle exercise. PCW mean pressure and V wave increased substantially with exercise.

Performing a Dynamic Exercise Test

Dynamic exercise during cardiac catheterization is easily performed with a bicycle ergometer while the patient is supine. A protocol detailing the exercise test should be prepared beforehand to ensure that all essential data are obtained. Pressures should be obtained so that the appropriate valve gradients can be evaluated, and LV pressure should be monitored if LV performance is in question.

Supine bicycle exercise tests are performed most easily when catheterization is done by the arm (e.g., brachial, radial) and/or neck (e.g., jugular vein) approach. However, supine bicycle exercise tests can also be done with safety when catheterization is by the femoral approach if care is taken to place the right and left heart manifolds and transducers in a stable and accessible position on the chest, away from leg motion artifact, and if the femoral venous and arterial sheaths are visualized and secured in place by the hand of one operator during exercise to ensure that catheters and sheaths are not displaced by leg movement.

We usually carry out a supine bicycle exercise test immediately after baseline hemodynamic values and cardiac output have been measured, before contrast angiography. The patient's feet are secured in the bicycle stirrups, and the right heart, left heart, and systemic arterial catheters and attached manifolds are positioned so that they are not kinked or under tension and will not be disturbed during the exercise. Next, the system for measuring O_2 consumption is put in place (see Chapter 8). Alternatively, cardiac output can be assessed with the use of an indicator-dilution technique (e.g., thermodilution), and O_2 consumption can be estimated as the quotient of cardiac output and AV O_2 difference.

Before beginning exercise, the patient is instructed that he or she will be coached to achieve a certain level of submaximal exercise over the first 1 minute that can be sustained for an additional 4 to 6 minutes. This detailed patient instruction is useful because some patients may be accustomed to the different format of progressively graded exercise aimed at achieving a transient level of maximal, exhaustion-limited exercise used in upright treadmill tests. A sufficient number of syringes for measuring systemic arterial and mixed venous (pulmonary artery) blood oxygen saturation content should be at hand.

With the patient resting quietly and feet positioned on the bicycle, all manometers are zeroed, phasic and mean pressures are recorded at 25 or 50 mm/sec paper speed (or electronic equivalent) and at the gain to be used during exercise, and cardiac output measurements are repeated to obtain an accurate preexercise baseline with legs elevated in the stirrups. Manometers are zeroed once again, all pressures are then redisplayed, and paper speed is slowed (to 5 to 10 mm/sec). Exercise is then begun with all pressures displayed continuously on the monitor and recorded at slow speed. We generally record LV phasic pressure, systemic arterial (e.g., radial or femoral artery) mean pressure, and pulmonary capillary mean pressure simultaneously. It is desirable to choose a gain setting on the recorder such that all pressures may be visualized simultaneously (as shown in Fig. 15.8). At each 1-minute interval, a brief recording of all three pressures on phasic at 25 to 50 mm/sec paper speed is accomplished, after which the pulmonary capillary and systemic arterial pressures are returned to “mean” and the paper speed is slowed to 5 to 10 mm/sec. The continuous observation and recording of pressures is important because it permits the accurate monitoring of any rise in filling pressure or fall in arterial pressure during exercise and ensures that catheters remain in correct position for measurements at peak exercise. After the patient has achieved a steady-state level of exercise for 4 minutes, simultaneous LV-systemic arterial, LV-PCW, and PCW-to-pulmonary artery pullback pressures are recorded during minutes 4 to 6, after increasing the recorder speed to 50 mm/sec without attempting to rezero the transducers. The right heart catheter is pulled back to the pulmonary artery, and exercise cardiac output is measured by the Fick or thermodilution technique, at which time systemic arterial and pulmonary artery blood samples are drawn for measurement of oxygen saturation.

Precautions should be taken during exercise to ensure patient safety. The duration and intensity of the exercise must be tailored to fit the needs of the individual patient. The electrocardiogram (ECG) should be monitored constantly to avoid serious arrhythmias, and exercise should be terminated if significant symptoms or greatly abnormal hemodynamic alterations occur. Little additional diagnostic information can be obtained by continuing the exercise to the point of producing pulmonary edema.

ISOMETRIC EXERCISE

Sustained isometric contraction of the forearm flexor muscles produces a cardiovascular reflex consisting of increases in heart rate, arterial blood pressure, and cardiac output. The precise nature of this reflex is not completely understood, but it appears to require afferent neural impulses from the exercising extremity and may be related to inhibition of vagal activity. Although the cardiac output response may be blunted, the anticipated responses in heart rate and blood pressure are not blocked by administration of propranolol, indicating that more is involved than a simple increase in b-adrenergic stimulation.

Hemodynamic Response

The hemodynamic response to isometric handgrip exercise has been studied in a series of normal subjects and patients with heart disease (22). In normal adult subjects, heart rate, systemic arterial pressure, and cardiac output increase, whereas systemic vascular resistance shows no change, indicating that the increase in systemic arterial pressure is caused by the increased cardiac output rather than by a vasoconstrictor response. No significant or consistent change in LVEDP or stroke volume occurs, whereas stroke work, a function of both arterial pressure and stroke volume, usually increases. The augmentation of LV performance during isometric exercise may be caused by both increased LV myocardial contractility (22) and the Frank-Starling mechanism.

Patients with heart disease and decreased LV function or inotropic reserve commonly show an abnormal hemodynamic and contractile response to isometric exercise (22). Although the maximum rate of rise of LV pressure, peak dP/dt, may increase in diseased hearts, the change is of less magnitude than in normal subjects. LV stroke work may increase, remain unchanged, or decrease in response to isometric exercise in pathologic states. This may itself be evidence of compromised LV function but is more apparent when the change in stroke work is compared with the change in LVEDP. Significant increases in LVEDP are seen commonly in the abnormal response to isometric exercise (22) and indicate decreased inotropic reserve, dependence on the Frank-Starling mechanism to augment LV performance, and probably some component of diastolic dysfunction.

Performing an Isometric Exercise Test

Isometric exercise is most commonly performed as sustained hand grip. The subject is first tested to evaluate maximal voluntary contraction strength. A partially inflated sphygmomanometer cuff or a specially designed handgrip dynamometer may be used. This testing may be done before cardiac catheterization and should be done well before the actual handgrip test. The patient must be coached and encouraged to grip as hard as possible at the time maximal voluntary contraction strength is determined. Baseline resting hemodynamic data should include heart rate, systemic arterial pressure (phasic and mean), LV pressure, and cardiac output. Cardiac output is most easily determined for this form of exercise by the indicator dilution method (e.g., thermodilution) or by the Fick method with the continuous O_2 consumption measurement technique.

Once baseline data are collected, the subject is asked to grip the dynamometer at a level 30% to 50% of the previously determined maximal voluntary contraction. Some coaching is usually required to ensure that the patient sustains the grip. It is important that the patient not do a Valsalva maneuver during handgrip exercise, and the respiratory pattern should be closely observed. Valsalva maneuver may be avoided simply by engaging the patient in conversation during the test. We have used 50% maximal voluntary contraction for 3 minutes, with repeat measurements of pressures and cardiac output beginning at 2.5 minutes, so that measurements are completed by 3 minutes and the test may be terminated. The ECG should be monitored continuously to exclude the appearance of arrhythmias.

PACING TACHYCARDIA

Graded tachycardia induced by atrial pacing was first introduced in 1967 by Sowton et al. (23) as a stress test that could be used in the cardiac catheterization laboratory to evaluate patients with ischemic heart disease. They noted that artificially increasing the heart rate by pacing the right atrium usually could induce angina in patients with symptomatic coronary artery disease. Moreover, they found that the degree of pacing stress needed to produce ischemia, defined in terms of pacing rate and duration, was more or less reproducible in any given patient. Since this original report, numerous investigators have described characteristic pacing-induced ECG changes (24,25,26,27,28,29 and 30), alterations in adenosine production (31,32) and myocardial lactate metabolism (25,26), hemodynamic abnormalities (33,34,35,36,37,38 and 39), regional wall motion abnormalities (40,41), and defects in thallium scintigraphy (42,43). Although agreement on the overall usefulness of atrial pacing has not been universal, it is clear that the technique can safely and reliably induce ischemia in most patients with coronary artery disease and that information obtained during the pacing-induced ischemic state is often helpful in the diagnosis and treatment of the patient's underlying disease.

Hemodynamic Effects of Pacing Tachycardia

The principal form of stress that accompanies pacing tachycardia is an increase in myocardial O_2 consumption secondary to the increased heart rate and an increase in myocardial contractility because of the treppe effect (44). Associated with this increase in myocardial O_2 consumption is a reflex coronary vasodilation with an increase in myocardial blood flow. Apart from these changes in oxygen demand and supply, pacing tachycardia appears to be associated with no major hemodynamic stress, at least in patients with normal coronary arteries. Artificially increasing the heart rate by pacing the right atrium is accompanied by a concomitant decrease in ventricular stroke volume, with little or no overall change in cardiac output. Moreover, there appears to be no significant change in ventricular afterload, venous return, or circulating catecholamines during pacing tachycardia.

Differences between Pacing Tachycardia and Exercise Stress

The physiology of pacing is distinctly different from that of dynamic or isometric exercise, in which there are not only increases in heart rate and myocardial contractility but also major changes in ventricular loading conditions and cardiac output in response to increased metabolic demands from the periphery.

Because of the differences in physiology between atrial pacing and exercise, each technique has relative advantages and disadvantages as a form of stress testing in the catheterization laboratory. Unlike pacing, exercise is associated with an increase in both heart rate and systolic blood pressure. As a result, exercise is usually capable of achieving a higher rate-pressure product (i.e., heart rate × peak systolic pressure) and represents a more severe form of stress with greater increases in

myocardial O_2 consumption. On the other hand, pacing is not associated with exercise-induced changes in cardiac output or ventricular loading conditions, and, as a result, the characterization of ventricular function is easier. In addition, atrial pacing is superior to exercise for evaluating myocardial metabolic function because the rapid rise in arterial blood lactate and adenosine levels that accompanies exercise may obscure alterations of myocardial lactate metabolism and adenosine production. Finally, unlike exercise, with the termination of pacing and the rapid diminution of myocardial oxygen requirement, myocardial ischemia almost always resolves rapidly (i.e., within 1 to 2 minutes). As a result, the physician has more control over the amount of stress that the patient experiences, with very little prolonged ischemia occurring in the poststress period.

Pacing tachycardia has been used as a form of stress testing in patients with heart disease for more than 30 years. The technique has been most useful in the assessment of patients with coronary artery disease.

Method for a Pacing Stress Test

Atrial pacing protocols usually can be conducted in the cardiac catheterization laboratory without undue prolongation of the routine catheterization procedure or significant added risks to the patient. In our experience, pacing is best conducted after the routine diagnostic aspects of catheterization and usually extends the procedure by no more than 15 to 30 minutes, depending on the details of the protocol. It is important that detailed planning of the protocol be made before the catheterization is begun, to help incorporate the atrial pacing into the routine catheterization as much as possible without unnecessary repetition of maneuvers and excessive prolongation of arterial time.

The type of catheter used for the pacing protocol can vary depending on the type of information that is to be evaluated during the pacing procedure. In general, the pacing catheter can be either unipolar or bipolar. If pacing is to be conducted with simultaneous myocardial metabolic assessment, a Gorlin or Baim-Turi pacing catheter that allows simultaneous pacing and coronary sinus lactate sampling is ideal. Sampling of both coronary sinus lactate and adenosine has been accomplished (32,45) with the use of a specially designed catheter placed in the coronary sinus. If assessment of myocardial O_2 consumption is to be made, a coronary sinus pacing catheter with the capability of measuring coronary blood flow, such as the Baim catheter (Elecath, Rahway, NJ), may be used. If pacing is to be conducted with simultaneous measurement of left heart filling pressures and cardiac output, then both a pacing catheter and a second right heart catheter (typically a thermodilution flow-directed catheter) may be inserted into the right side of the heart.

The pacing catheter may be inserted by either venous cutdown or percutaneous technique from the groin, the antecubital fossa, or the neck. Use of a coronary sinus pacing catheter usually requires a neck or arm approach for easier access into the coronary sinus.

Perhaps the most critical part of the atrial pacing technique is proper placement of the pacing lead, because accidental displacement of the pacing tip during pacing can disrupt the protocol. The pacing lead can be placed at the junction of the superior vena cava and right atrium, at the lateral right atrial wall, or in the coronary sinus. Placement of the pacing lead is most stable at either the first or last of these positions, because displacement of the lead commonly occurs from the lateral atrial wall during respiration. Stimulation of the phrenic nerve with subsequent diaphragmatic stimulation also occurs commonly with placement of the catheter against the lateral atrial wall. To avoid problems with displacement of the pacing tip, we have used a bipolar flared pacing catheter (Atri-Pace I, Mansfield Scientific, Mansfield, MA).

Once the pacing catheter is positioned in the right atrium, it is connected to the pulse generator unit. This unit should be equipped with a fixed-rate mode, pacing at least to 170 beats per minute (bpm), and a variable output from 0.5 to 10 mA. Bipolar pacing catheters may be connected directly to the pacemaker unit or attached through extension wires with alligator clamps. Unipolar catheters should have their negative pole grounded to the skin via either a needle electrode or standard ECG plates. Once the pacing catheter has been positioned properly and connected to the pulse generator, the ability of the pacemaker to stimulate the atrium and to control ventricular rate should be assessed. Initially, the output of the generator is set at 2 to 3 mA, and the pacing rate is adjusted to 10 bpm faster than the sinus rate. Pacing is then begun, and if there is atrial and ventricular capture, the pacing rate is increased by 10 bpm every 5 seconds until a rate of 150 to 160 bpm is reached. Inadequate pacing may occur secondary to an inadequate output of the pulse generator, improper lead positioning, or the development of atrioventricular block. The output of the pulse generator may be increased, but, in general, stimulating energies in excess of 7 to 8 mA frequently result in painful phrenic nerve stimulation. If excessively high energies are required for capture, the electrode lead should be repositioned. If atrioventricular block develops at high stimulatory rates, 1 mg atropine may be administered intravenously: this usually ensures adequate atrioventricular conduction up to rates of 140 bpm or more.

After the lead has been properly positioned and an adequate trial of pacing to assess capture has been performed, the actual pacing protocol may be done. A pacing stress test usually begins with pacing at approximately 20 bpm above the baseline rate, with increases of 20 bpm every 2 minutes, until angina pectoris or characteristic hemodynamic alterations occur, or until 85% of maximum age-predicted heart rate is achieved. Placement of a thermodilution balloon-tip flow-directed catheter, a left heart catheter, and a radial arterial cannula (or femoral arterial sheath sidearm) before pacing allows simultaneous assessment of right- and left-sided heart pressures, cardiac output measurement by thermodilution and/or Fick method, and determination of systemic and pulmonary vascular resistances. Assessment of LV volumes also may be accomplished with standard angiographic, echocardiographic, or radionuclide techniques.

Following the induction of chest pain during pacing tachycardia, pacing may be continued at the same heart rate safely for up to 3 to 5 minutes, during which hemodynamic, metabolic, and ECG data may be obtained. After cessation of pacing, chest pain usually resolves quickly, but it may occasionally persist for up to 1 to 2 minutes after the return to sinus rhythm.

Pacing-induced Angina

Initial reports on the use of atrial pacing tachycardia suggested that pacing-induced angina was a sensitive marker for the presence of ischemic heart disease and could serve as a suitable ischemic end point of pacing protocols (23). Specifically, the induction of angina was thought to mark a highly reproducible anginal threshold defined in terms of pacing rate and duration. Subsequent investigators have found, however, that chest pain is neither a sensitive nor a specific indicator of the presence of coronary artery disease. For example, Robson et al. (28) demonstrated that chest pain could be elicited in 80% of patients with normal coronary arteries if they were paced at extremely high rates (in excess of 180 bpm). Moreover, Chandraratna et al. (46) demonstrated the absence of angina in some patients with coronary artery disease who were stressed with pacing tachycardia at a high rate. Similarly, in terms of defining anginal threshold according to the pacing rate and duration, as many as 20% of individuals have been shown to have considerable variation in these parameters (47). In view of these results, it is clear that chest pain alone should not be used as a reliable marker for the presence of pacing-induced ischemia. However, improved sensitivity and specificity of pacing-induced chest pain are noted when additional evidence of ischemia, such as pacing-induced ECG changes or myocardial metabolic abnormalities, is present.

Electrocardiographic Changes in Response to a Pacing Stress Test

Like pacing-induced angina, the presence of ischemic ST-segment depression during pacing tachycardia has not been regarded previously as a sensitive or specific marker for the presence of coronary artery disease. For example, in terms of sensitivity, Rios and Hurwitz (27) compared pacing tachycardia and exercise in 50 patients and found diagnostic ECG changes with pacing in only 20% with pacing tachycardia, compared with 83% with exercise. Similarly, in terms of specificity, Robson et al. (28) reported ST-segment depression of 1.5 mm or more during pacing tachycardia in as many as 80% of patients with normal coronary arteries. In addition to poor overall sensitivity and specificity, pacing tachycardia is associated with certain distortions of the ECG that sometimes make interpretation of ischemic ST-segment changes difficult or impossible. Pacing is associated with prolongation of the PR interval in most patients, and extreme prolongation of this interval can cause the pacemaker spike to fall within the ST segment of the preceding paced complex, thereby obscuring potential ST-segment changes.

Despite the previously reported poor utility of pacing-induced ECG changes, work from our laboratory (29) has suggested an improved sensitivity and specificity of ischemic ST-segment depression during pacing tachycardia if certain technical guidelines of the pacing protocol are followed. Several earlier pacing trials that reported a low sensitivity of pacing ECG changes used only limited three-lead recording, and it is clear, at least with standard exercise testing, that sensitivity can be improved substantially with full 12-lead monitoring.

To maximize the utility of pacing-induced ECG changes, pacing trials should be conducted with the use of the following guidelines. First, a 12-lead ECG is used for monitoring, and the ECG is regarded as positive for myocardial ischemia if at least 1 mm or more of horizontal or downsloping ST-segment depression is produced. Second, pacing tachycardia is terminated when 85% of maximal age-predicted heart rate is achieved or when typical ischemic chest pain is accompanied by diagnostic ECG changes. Finally, if marked prolongation of the PR interval distorts the preceding ST-segment changes, the ECG is considered positive for ischemia *only if there is ST-segment depression in the first five beats after the discontinuation of the pacing stimulus.*

Using these guidelines, actual pacing protocols conducted in our experience had an overall sensitivity and specificity of 94% and 83%, respectively, with regard to pacing-induced ECG changes. In addition, distortion of the ST segment by the pacing stimulus because of marked prolongation of the PR interval appeared to occur infrequently when the peak pacing rate was no higher than 85% of the maximum age-predicted heart rate. Moreover, in at least one subgroup of patients who were tested with both atrial pacing and standard treadmill exercise (29), the concordance between pacing-induced and exercise-induced ECG changes was 90%. Examples of pacing-induced and exercise-induced ECG changes are shown for a patient with normal coronary arteries in Fig. 15.9*A* and for a patient with coronary artery disease in Fig. 15.9*B*.

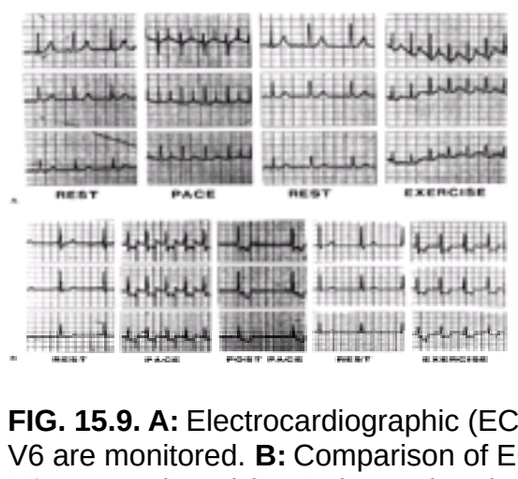

FIG. 15.9. A: Electrocardiographic (ECG) response to atrial pacing and exercise stress in a man with normal coronary arteries. From top to bottom, leads V4, V5, and V6 are monitored. **B:** Comparison of ECG response to atrial pacing and exercise stress in a man with severe three-vessel coronary artery disease. Leads V4, V5, and V6 are monitored (top to bottom) as in **A**. ST depression occurs to the same degree with both types of stress. (From Heller GV, et al. The pacing stress test: a reexamination of the relation between coronary artery disease and pacing-induced electrocardiographic changes. *Am J Cardiol* 1984;54:50, with permission.)

The sensitivity of pacing-induced ECG changes may be further improved with the use of endocardial electrograms obtained during the pacing stress test. Nabel et al. (30) reported on the use of local unipolar electrograms recorded from the tip of a 0.064-cm-diameter guidewire positioned against the endocardial surface of potentially ischemic regions. Endocardial electrograms, LVEDP, and multiple surface ECG leads were recorded before, during, and after rapid atrial pacing in 21 patients with coronary artery disease. Before pacing, endocardial electrograms in all 21 patients were free of ST-segment elevation. After rapid atrial pacing, marked ST-segment elevation was apparent in 17 of the 21 patients. This ST-segment elevation could be abolished in all patients with the use of nitroglycerin. Moreover, in several patients, endocardial ST-segment elevation after pacing was abolished by successful percutaneous coronary angioplasty of the critically stenosed artery supplying the ischemic region of myocardium. The authors concluded that endocardial electrographic changes are a reliable marker of pacing-induced myocardial ischemia and may be more sensitive than angina, pacing-induced hemodynamic changes, or ST-segment depression on the surface ECG.

Myocardial Metabolic Changes Induced by a Pacing Stress Test

Abnormal myocardial metabolism has been documented during pacing-induced ischemia by means of coronary sinus sampling and the subsequent measurement of coronary arterial and venous blood lactate. Because lactate production is a byproduct of anaerobic glycolysis, its production by the heart and appearance within the coronary sinus is a sign of myocardial ischemia. Previous investigators have noted rapid increases in coronary sinus lactate levels during pacing tachycardia in patients with coronary artery disease, often before the appearance of angina (25,26). With cessation of pacing, the elevated coronary sinus lactate concentrations fall rapidly, representing a washout of the accumulated myocardial lactate and diminished lactate production as normal oxygenation is restored. Monitoring of arterial lactate levels while coronary sinus lactate levels are rising usually shows little or no elevation, in marked contrast to arterial lactate levels during exercise. As a result, atrial pacing tachycardia is superior to exercise for evaluating abnormal myocardial metabolic function, because rapidly rising arterial lactate levels during exercise may obscure abnormal patterns of myocardial lactate metabolism.

Monitoring of coronary sinus lactate during pacing protocols is most easily accomplished with a Gorlin pacing catheter. Placement of the Gorlin catheter in the coronary sinus usually can be confirmed by injection of a small amount of contrast medium. Care must be taken not to perforate either the coronary sinus or the great cardiac vein, and not to place the pacing tip of the catheter too distally, because placement of the distal catheter into the great cardiac vein may result in ventricular rather than atrial pacing.

Arterial and coronary venous blood lactate concentrations in response to a pacing stress test are illustrated in Fig. 15.10. In the control state, the concentration of coronary sinus blood lactate is lower than lactate concentration in arterial blood, reflecting the fact that the heart normally consumes lactate as a fuel. During pacing tachycardia, coronary sinus blood lactate concentration rises progressively and exceeds arterial blood lactate concentration, reflecting a shift to anaerobic metabolism of the ischemic myocardium. The lactate falls rapidly after discontinuation of pacing because the heart rate returns to control immediately.

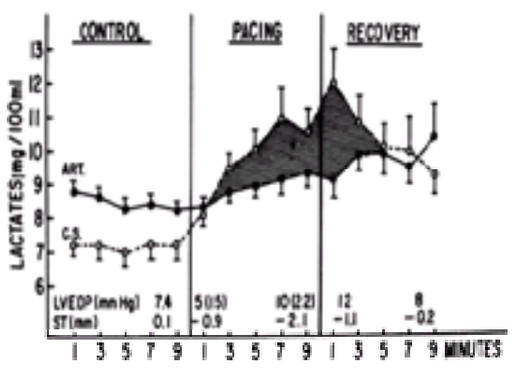

FIG. 15.10. Mean values for arterial (ART.) and coronary sinus (C.S.) blood lactate concentrate before (CONTROL), during (PACING) and after (RECOVERY) tachycardia in 17 patients with coronary artery disease. Left ventricular end-diastolic pressure (LVEDP) changed little during pacing tachycardia but was elevated during brief periods of interruption of pacing (values in parentheses). ST-segment depression developed progressively during pacing tachycardia and resolved in recovery. Lactate extraction shifted to lactate production during ischemia, and this persisted into recovery for a brief period. (From Parker JO, Chiong MA, West RO, et al. Sequential alterations in myocardial lactate metabolism, S-T segments, and left ventricular function during angina induced by atrial pacing. *Circulation* 1969;40:113, with permission.)

There has been renewed interest in using coronary sinus adenosine as a marker of myocardial ischemia. Adenosine, a metabolite released by ischemic myocardium, elicits an increase in coronary artery blood flow in response to a decrease in the ratio of myocardial oxygen supply to demand. As a result, adenosine should be a more sensitive marker of myocardial ischemia than lactate, which requires anaerobic glycolysis. An early report demonstrated that adenosine is increased in the coronary sinus blood of patients with ischemic heart disease during pacing tachycardia (31), and later Feldman et al. (32) made several methodologic improvements regarding adenosine measurements. A double-lumen “metabolic” catheter was used that allowed the addition and mixing of a solution to stop adenosine metabolism at the tip of the catheter. Adenosine has a half-life of less than 1.5 second in human blood. Furthermore, there are numerous sources of artifactual adenosine production in human blood. It is therefore essential that a solution that inhibits both the breakdown and the production of adenosine be mixed with human blood at the site of collection. Using this technique, adenosine was demonstrated to be a more sensitive marker of myocardial ischemia than lactate (32). Each patient with coronary artery disease (n = 9) atrially paced to ischemia demonstrated at least a 1.5-fold increase in coronary sinus adenosine. In contrast, only three of these nine patients had lactate production. In a subsequent study with improved methodology (48), patients with coronary artery disease (n = 17) were found to have higher coronary sinus adenosine concentrations than a control group of patients (n = 6) at rest. This finding provides evidence that release of endogenous adenosine may be

an intrinsic homeostatic mechanism to maintain resting flow distal to a stenotic coronary artery.

Hemodynamic Changes During a Pacing Stress Test

Patients without ischemic heart disease who are stressed by atrial-paced tachycardia generally demonstrate no significant change in cardiac output, mean arterial pressure, AV O_2 difference, or systemic vascular resistance. LVEDP and pulmonary capillary wedge pressure usually fall during pacing tachycardia and then return to prepacing baseline levels in the immediate postpacing period. LV end-diastolic and end-systolic volumes fall during pacing tachycardia, with a decrease in stroke volume and no significant change in ejection fraction.

Patients with coronary artery disease who are paced to ischemia likewise manifest no significant change in cardiac output, mean arterial pressure, AV O_2 difference, or systemic vascular resistance. Some investigators have documented slight decreases in cardiac output with slight increases in mean arterial pressure, AV O_2 difference, and systemic resistance. However, these differences are probably related to the intensity of pacing-induced ischemia, its duration before the measurement of hemodynamic variables, and the amount of myocardium that has become ischemic, with more extensive hemodynamic abnormalities occurring in the setting of more extensive myocardial ischemia. The most dramatic differences in pacing hemodynamics between patients with normal coronary arteries and those with coronary artery disease are seen in terms of LV pressure-volume relationships during pacing tachycardia and in the immediate postpacing period. Of note, LV filling pressures do not show the progressive decrease seen in nonischemic patients, and elevations in pulmonary capillary wedge, mean pulmonary artery, and occasionally LV end-diastolic pressures occur at maximum pacing. Most important, there is an abrupt rise in LVEDP in the immediate postpacing period. Similarly, LV end-diastolic and end-systolic volumes decrease less during pacing-induced tachycardia in patients with ischemic heart disease compared with normal subjects, and there is often a significant decrease in LV ejection fraction.

A study looking at pressure-volume relationships during pacing tachycardia conducted by us (49) illustrates well the differences between nonischemic and ischemic hemodynamic responses to pacing. In this study, 22 patients, including 11 patients with normal coronary arteries and 11 with significant coronary artery disease, underwent sequential atrial pacing with simultaneous monitoring of LV pressure and ventricular volume measured by gated radionuclide ventriculography. Using synchronized LV pressure tracings and radionuclide time-activity volume curves, three sequential pressure-volume diagrams were constructed for each patient, corresponding to baseline, intermediate, and maximum pacing levels. All 11 patients with coronary artery disease demonstrated angina and significant ST-segment depression at maximum pacing, but none of the 11 patients with normal coronary arteries showed any evidence of pacing-induced ischemia.

Figure 15.11 shows typical LV pressure-volume curves for a patient with normal coronary arteries stressed with pacing tachycardia. Notably, there is a progressive leftward shift for the loop, with an increased heart rate and a progressive downward shift in the LV diastolic pressure-volume limb of each pressure-volume curve. It is clear that changes in both systolic and diastolic function have occurred in these patients during pacing tachycardia. In terms of systolic function, the progressive leftward shift of the end-systolic portion of the loop presumably represents increased contractility secondary to a treppe effect. Other investigators (44) have likewise demonstrated a positive inotropic stimulus in response to increased heart rate, with increases in isovolumetric contraction indices (e.g., dP/dt) and ejection-phase indices (e.g., circumferential fiber shortening) during pacing tachycardia. With respect to diastolic function, the progressive downward shift of the diastolic limbs seen in Fig. 15.11 suggests that LV distensibility has increased slightly during pacing tachycardia. Whether this downward shift is related to an increase in myocardial relaxation, an alteration in viscoelastic properties, or a change in factors extrinsic to the myocardium (e.g., right ventricle, pericardium) is not known. It is notable that some investigators have documented small increases in markers of diastolic relaxation during pacing-induced tachycardia, such as peak negative dP/dt (50) and the time constant tau (51) in normal animals and the peak rate of posterior wall thinning (52) and LV internal dimension changes in humans.

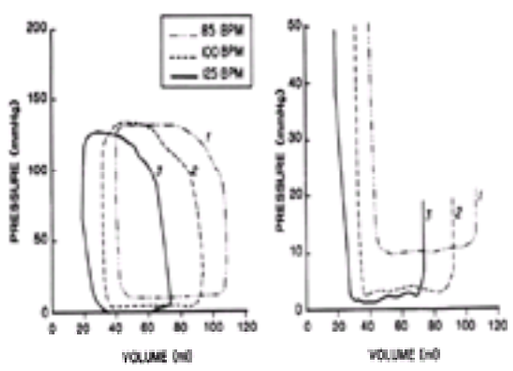

FIG. 15.11. Sequential left ventricular pressure-volume diagrams for a patient with normal coronary arteries in response to atrial pacing tachycardia at three increasing heart rates. (See text for discussion.) (From Aroesty JM, et al. Simultaneous assessment of left ventricular systolic and diastolic dysfunction during pacing-induced ischemia. *Circulation* 1985;71:889, with permission.)

Figure 15.12 shows sequential LV pressure-volume diagrams for a patient with coronary artery disease whose heart rate was increased progressively by atrial pacing. All patients in our study who developed chest pain and ischemic ECG changes demonstrated a similar pressure-volume pattern with an initial shift of the pressure-volume loop to the left at an intermediate heart rate, followed by a rightward shift at peak pacing when ischemia developed. In terms of systolic function, it is clear that pacing resulted in an initial treppe effect with a leftward shift of the end-systolic portion of the diagram at intermediate pacing, followed by systolic failure at peak pacing with an increase in ventricular volumes and a rightward shift in the end-systolic portion of the curve. Similarly, in terms of diastolic function, it is evident that the patient did not show a progressive downward shift of the diastolic limb of the LV pressure-volume curve but actually experienced an upward shift at intermediate and peak pacing. In part, the increase in LVEDP at peak pacing is related to systolic failure with an increase in ventricular volume. Because the patient did not experience evidence of systolic failure at the intermediate pacing level, however, it is also clear that this patient has experienced a primary decrease in LV diastolic distensibility so that pressure is higher at any given chamber volume throughout diastole.

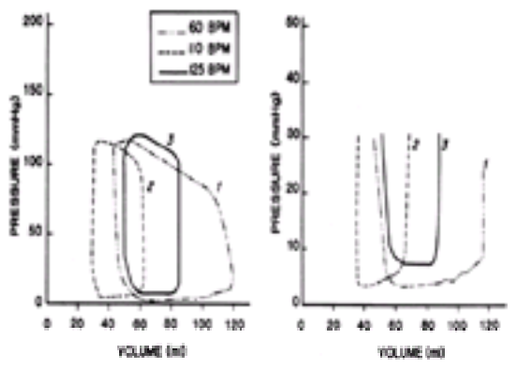

FIG. 15.12. Sequential left ventricular pressure-volume diagrams in a patient with three-vessel coronary artery disease who was paced at three increasing heart rates. The patient developed angina and ischemic ST depression at peak pacing. (See text for discussion.) (From Aroesty JM, et al. Simultaneous assessment of left ventricular systolic and diastolic dysfunction during pacing-induced ischemia. *Circulation* 1985;71:889, with permission.)

Speculation has continued over the last three decades as to whether the increase in diastolic pressures during pacing-induced ischemia is related to a primary decrease in distensibility or is secondary to systolic failure with increases in ventricular volume. At present, it seems clear that both mechanisms play some role in creating the elevated diastolic pressures. The evidence, however, suggests that changes in diastolic distensibility actually precede altered systolic function (49).

The cause of the altered diastolic distensibility during pacing-induced ischemia has been debated, and a number of different mechanisms (35,36,37 and 38,53,54)

have been proposed, including incomplete myocardial relaxation, altered diastolic tone, partial ischemic contracture of some myofibrils within the distribution of the stenotic or occluded coronary artery, altered right ventricular loading, and influence of the pericardium. At present, it seems likely that relaxation of myocardial cells within the reversibly ischemic region is slowed and does not proceed to completion by end-diastole (53,54). This may be related to impaired diastolic calcium sequestration by sarcoplasmic reticulum, but data are insufficient to permit a firm conclusion.

The postpacing rise in LVEDP is perhaps the most concrete evidence of pacing-induced ischemia during atrial pacing protocols. In our protocols, this postpacing rise has been calculated on beats 5 through 15 after discontinuation of pacing, with greater than a 5 mm Hg increase in LVEDP in comparison with the prepacing baseline being considered abnormal. Figure 15.13 and Figure 15.14 summarize hemodynamic changes in patients with normal coronary arteries and in those with ischemic heart disease in response to a pacing stress test.

FIG. 15.13. Changes in cardiac index, systemic vascular resistance (SVR), and arteriovenous oxygen (AV O_2) difference in 5 patients with normal coronary arteries and 20 patients with coronary artery disease (CAD) during pacing tachycardia. Patients with CAD showed a significant decrease in cardiac index and increases in SVR and AV O_2 difference during maximum pacing tachycardia. (From McKay RG, et al. The pacing stress test reexamined: correlation of pacing-induced hemodynamic changes with the amount of myocardium at risk. *J Am Coll Cardiol* 1984;3:1469, with permission.)

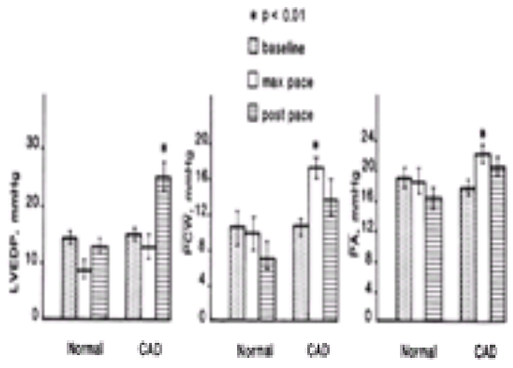

FIG. 15.14. Changes in left ventricular end diastolic pressure (LVEDP), mean pulmonary capillary wedge pressure ($\overline{\text{PCW}}$), and mean pulmonary artery pressure ($\overline{PA}$) in 5 patients with normal coronary arteries and 20 patients with coronary artery disease (CAD) during maximum pacing tachycardia and immediately after pacing. Patients with CAD showed significant elevations of PA and PCW at maximum pacing and of LVEDP immediately after pacing. (From McKay RG, et al. The pacing stress test reexamined: correlation of pacing-induced hemodynamic changes with the amount of myocardium at risk. *J Am Coll Cardiol* 1984;3:1469, with permission.)

Quantification of the hemodynamic alterations induced by pacing tachycardia may also be useful in assessing myocardial performance in patients with other forms of cardiac disease. Feldman et al. (55) used atrial pacing tachycardia to evaluate the systolic and diastolic myocardial reserve of patients with dilated cardiomyopathy. Pacing-induced changes in LV pressure and volume in seven patients with dilated cardiomyopathy (mean LV ejection fraction, 19%) were compared with findings in six patients with normal coronary arteries and normal LV function (mean LV ejection fraction, 69%). The patients with normal LV function demonstrated significant increases in LV peak positive dP/dt, LV end-systolic pressure-volume ratio, and LV peak filling rate during graded increases in heart rate with atrial pacing. They also exhibited a progressive leftward and downward shift of their pressure-volume diagrams, compatible with increased contractility and enhanced diastolic distensibility in response to pacing tachycardia. In contrast, patients with dilated cardiomyopathy demonstrated no increase in either LV peak positive dP/dt or the end-systolic pressure-volume ratio and absence of a progressive leftward shift of their pressure-volume diagrams. Moreover, patients with dilated cardiomyopathy demonstrated no increase in LV peak filling rate and a blunted downward shift of the diastolic limb of their pressure-volume diagrams. These data suggest that patients with dilated cardiomyopathy demonstrate little or no enhancement of systolic and diastolic function during atrial pacing tachycardia, indicating a depression of both inotropic and lusitropic reserve.

Regional Wall Motion Abnormalities During a Pacing Stress Test

Regional wall motion abnormalities during pacing-induced ischemia have been noted with contrast ventriculography, gated radionuclide ventriculography, and transesophageal echocardiography. Using contrast ventriculography, Dwyer (40) studied eight patients with coronary artery disease who were paced to angina and found that three developed regional hypokinesis in one area, while the remaining five developed at least two separate areas of hypokinesis or akinesis. In all cases, an associated coronary artery lesion could be identified in the vessel that supplied the area of the new regional wall motion abnormality. Similarly, Tzivoni et al. (41), using radionuclide ventriculography, found that 9 of 11 patients developed new regional wall motion abnormalities in response to pacing-induced ischemia.

The overall specificity and sensitivity of pacing-induced regional wall motion abnormalities have been defined with the development of simultaneous transesophageal two-dimensional echocardiography and atrial pacing. Lambertz et al. (56) first developed an ultrasound system in which an atrial pacing facility was incorporated. Fifty patients were evaluated prospectively by cardiac catheterization and pacing echocardiography; 44 had correlative exercise testing. Nine patients were found to have normal epicardial coronary arteries and normal pacing results (100% specificity). Thirty-eight of the 41 patients with significant coronary artery disease developed regional wall motion abnormalities with pacing (93% sensitivity). In contrast, the specificity and sensitivity for exercise testing were 50% and 53%, respectively.

Thallium Scintigraphy and the Pacing Stress Test

The incorporation of thallium scintigraphy into pacing protocols has improved the overall utility of atrial pacing as a stress test. In patients with normal coronary arteries, pacing tachycardia is associated with a homogeneous increase in myocardial O_2 consumption and a secondary increase in coronary blood flow. In patients with coronary artery disease, however, regional increases in myocardial blood flow may be limited by critical coronary stenoses. Because initial myocardial uptake of thallium 201 has been shown to reflect myocardial perfusion and viability, myocardial ischemia induced by pacing tachycardia theoretically should be detectable by thallium scintigraphy. Although early reports on the simultaneous use of atrial pacing and thallium scintigraphy suggested serious limitations (41), studies with improved methodology indicate that this approach is successful in detecting both reversible ischemia and infarcted myocardium (42,43).

To assess the utility of combined atrial pacing and thallium scintigraphy, our laboratory researchers (42) examined the correlation between pacing-induced and exercise-induced thallium defects in patients referred for evaluation of chest pain. The overall sensitivity and specificity of thallium imaging after atrial pacing were excellent. Moreover, segment-by-segment comparison of the thallium scans after either pacing or exercise stress testing revealed a correlation of 83%.

Simultaneous use of thallium scintigraphy and atrial pacing tachycardia can be accomplished by injection of 1.5 to 2.0 mCi of thallium 201 intravenously at peak pacing, followed by continued pacing for at least an additional 5 minutes. In routine thallium exercise testing, exercise is maintained for only 30 to 60 seconds after injection of the radionuclide to allow the thallium to reach the myocardium. However, because of the rapid decrease in heart rate after discontinuation of pacing and

the subsequent rapid diminution of myocardial oxygen requirements, pacing is extended to 5 minutes. After discontinuation of the pacing stimulus, while the patient is in the supine position, standard anterior, 40°, and 70° left anterior oblique views are obtained immediately in the catheterization laboratory with a mobile scintillation camera. Repeat standard views are obtained 4 hours after termination of the pacing protocol.

Clinical Uses of Atrial Pacing

The complete evaluation of a patient's cardiac function in the catheterization laboratory often requires an examination of the patient's performance under stressed conditions, when ECG, metabolic, and hemodynamic abnormalities may manifest themselves fully. The role of stress testing is particularly important in the evaluation of patients with ischemic heart disease, in whom, for example, it may be useful to determine the anginal threshold, the magnitude of hemodynamic impairment during ischemia, and the efficacy of antianginal therapy and to establish a need for coronary revascularization. Although standard dynamic and isometric exercise may serve as a form of stress for many patients, not all patients are able to exercise because of physical disabilities, old age, pulmonary disease, peripheral vascular disease, and possibly b-blockade. In each of these situations, atrial pacing may be used as a suitable form of stress.

Some material in this chapter was developed for previous editions by Drs. Beverly Lorell, Mark Feldman, and Raymond McKay.

CHAPTER REFERENCES

1. Weiner DA. Normal hemodynamic, ventilatory, and metabolic response to exercise. *Arch Intern Med* 1983;143:2173.
2. Dexter L, et al. Effects of exercise on circulatory dynamics of normal individuals. *J Appl Physiol* 1951;3:439.
3. Donald KW, Bishop JM, Cumming G, et al. The effect of exercise on the cardiac output and circulatory dynamics of normal subjects. *Clin Sci* 1955;14:37.
4. Higginbotham MB, et al. Regulation of stroke volume during submaximal and maximal upright exercise in normal man. *Circ Res* 1986;58:281.
5. Plotnick GD, et al. Use of the Frank-Starling mechanism during submaximal versus maximal upright exercise. *Am J Physiol* 1986;251:H1101.
6. Braunwald E, Sonnenblick EH, Ross J Jr, et al. An analysis of the cardiac response to exercise. *Circ Res* 1967;20[Suppl I]:44.
7. Ross J Jr, Linhart JW, Braunwald E. Effects of changing heart rate in man by electrical stimulation of the right atrium: studies at rest, during exercise, and with isoproterenol. *Circulation* 1965;32:549.
8. Thadani U, Parker JO. Hemodynamics at rest and during supine and sitting bicycle exercise in normal subjects. *Am J Cardiol* 1978;41:52.
9. Rodeheffer RJ, et al. Exercise cardiac output is maintained with advancing age in healthy human subjects: cardiac dilatation and increased stroke volume compensated for a diminished heart rate. *Circulation* 1984;69:203.
10. Port S, Cobb FR, Coleman RE, et al. Effect of age on the response of the left ventricular ejection fraction to exercise. *N Engl J Med* 1980;303:133.
11. McAllister BD, et al. Left ventricular performance during mild supine leg exercise in coronary artery disease. *Circulation* 1968;37:922.
12. Gerstenblith D, Renlund DG, Lakatta EG. Cardiovascular response to exercise in younger and older men. *Fed Proc* 1987;46:1834.
13. Higginbotham MB, et al. Sex-related differences in the normal cardiac response to upright exercise. *Circulation* 1984;70:357.
14. Murgo JP, Craig WE, Pasipoularides A. Evaluation of time course of left ventricular isovolumic relaxation in man. In: Grossman W, Lorell BH, eds. *Diastolic Relaxation of the Heart.* Boston: Martinus Nijhoff, 1986:217.
15. Aroesty JM, McKay RG, Heller GV, et al. Simultaneous assessment of left ventricular systolic and diastolic dysfunction during pacing-induced ischemia. *Circulation* 1985;71:89.
16. Carroll JD, Hess OM, Krayenbuehl HP. Diastolic function during exercise-induced ischemia in man. In: Grossman W, Lorell BH, eds. *Diastolic Relaxation of the Heart.* Boston: Martinus Nijhoff, 1986:217.
17. Kitzman D, Sullivan MJ. Exercise intolerance in patients with heart failure: role of diastolic dysfunction. In: Lorell BH, Grossman W, eds. *Diastolic Relaxation of the Heart,* 2nd ed. Boston: Kluwer, 1994:295.
18. Higginbotham MB, et al. Determinants of variable exercise performance among patients with severe left ventricular dysfunction. *Am J Cardiol* 1983;51:52.
19. Weber KT, Kinasewitz GT, Janicki JS, et al. Oxygen utilization and ventilation during exercise in patients with chronic cardiac failure. *Circulation* 1982;65:1213.
20. Colucci WS, et al. Impaired chronotropic response to exercise in patients with congestive heart failure. *Circulation* 1989;80:314.
21. Bristow MR, et al. Decreased catecholamine sensitivity and b-adrenergic receptor density in failing human hearts. *N Engl J Med* 1982;307:205.
22. Grossman W, et al. Changes in the inotropic state of the left ventricle during isometric exercise. *Br Heart J* 1973;35:697.
23. Sowton GE, Balcon R, Cross D, et al. Measurement of the angina threshold using atrial pacing. *Cardiovasc Res* 1967;1:301.
24. Lau SH, et al. Controlled heart rate by atrial pacing in angina pectoris: a determinant of electrocardiographic S-T depressions. *Circulation* 1968;38:711.
25. Parker JO, Chiong MA, West RO, et al. Sequential alterations in myocardial lactate metabolism, S-T segments, and left ventricular function during angina induced by atrial pacing. *Circulation* 1969;40:113.
26. Helfant RH, et al. Differential hemodynamic, metabolic, and electrocardiographic effects in subjects with and without angina pectoris during atrial pacing. *Circulation* 1970;42:601.
27. Rios JC, Hurwitz LE. Electrocardiographic responses to atrial pacing and multistage treadmill exercise testing: correlation with coronary anatomy. *Am J Cardiol* 1976;34:986.
28. Robson RH, Pridie R, Fluck DC. Evaluation of rapid atrial pacing in diagnosis of coronary artery disease: evaluation of atrial pacing test. *Br Heart J* 1976;38:986.
29. Heller GV, et al. The pacing stress test: a reexamination of the relation between coronary artery disease and pacing induced electrocardiographic changes. *Am J Cardiol* 1984;54:50.
30. Nabel EG, et al. Detection of pacing-induced myocardial ischemia by endocardial electrograms recorded during cardiac catheterization. *J Am Coll Cardiol* 1988;11:983.
31. Fox AC, Reed GE, Glassman E, et al. Release of adenosine from human hearts during angina induced by rapid atrial pacing. *J Clin Invest* 1974;53:1447.
32. Feldman MD, Ayers CR, Lehman MR, et al. Improved detection of ischemia-induced increases in coronary sinus adenosine in patients with coronary artery disease. *Clin Chem* 1992;38:256.
33. Parker JO, Ledwich JR, West RO, et al. Reversible cardiac failure during angina pectoris. *Circulation* 1969;34:745.
34. McCans JL, Parker JO. Left ventricular pressure-volume relationships during myocardial ischemia in man. *Circulation* 1973;48:775.
35. McLaurin LP, Rolett EL, Grossman W. Impaired left ventricular relaxation during pacing induced ischemia. *Am J Cardiol* 1973;32:751.
36. Mann T, Brodie BR, Grossman W, et al. Effect of angina on the left ventricular diastolic pressure-volume relationship. *Circulation* 1977;55:761.
37. Barry WH, Brooker JZ, Alderman EL, et al. Changes in diastolic stiffness and tone of the left ventricle during angina pectoris. *Circulation* 1974;49:225.
38. Mann T, Goldberg S, Mudge GH, et al. Factors contributing to altered left ventricular diastolic properties during angina pectoris. *Circulation* 1979;59:14.
39. Thadani U, et al. Clinical hemodynamic and metabolic responses during pacing in the supine and sitting postures in patients with angina pectoris. *Am J Cardiol* 1979;44:249.
40. Dwyer EM. Left ventricular pressure-volume alterations and regional disorders of contraction during myocardial ischemia induced by atrial pacing. *Circulation* 1970;42:1111.
41. Tzivoni D, et al. Diagnosis of coronary artery disease by multigated radionuclide angiography during right atrial pacing. *Chest* 1981;80:562.
42. Heller GV, et al. The pacing stress test: thallium 201 myocardial imaging after atrial pacing. *J Am Coll Cardiol* 1984;3:1197.
43. McKay RG, et al. The pacing stress test reexamined: correlation of pacing-induced hemodynamic changes with the amount of myocardium at risk. *J Am Coll Cardiol* 1984;3:1469.
44. Ricci D, Orlick A, Alderman E. Role of tachycardia as an inotropic stimulus in man. *J Clin Invest* 1979;63:695.
45. Shryock JC, Boykin MT, Hill JA, et al. A new method of sampling blood for measurement of plasma adenosine. *Am J Physiol* 1990;258:H1232.
46. Chandraratna PAN, et al. Spectrum of hemodynamic responses to atrial pacing in coronary artery disease. *Br Heart J* 1973;35:1033.
47. Thadani U, et al. Are the clinical and hemodynamic events during pacing in patients with angina reproducible? *Circulation* 1979;60:1036.
48. McLaughlin DP, Beller GA, Linden J, et al. Hemodynamic and metabolic correlates of dipyridamole-induced myocardial thallium 201 perfusion abnormalities in multivessel coronary artery disease. *Am J Cardiol* 1994;74:1159.
49. Aroesty JM, et al. Simultaneous assessment of left ventricular systolic and diastolic dysfunction during pacing-induced ischemia. *Circulation* 1985;71:889.
50. Karliner JS, et al. Pharmacological and hemodynamic influences on the rate of isovolumetric left ventricular relaxation in the conscious dog. *J Clin Invest* 1977;60:511.
51. Weiss JL, Fredericksen JW, Weisfeldt ML. Hemodynamic determinants of the time-course of fall in canine left ventricular pressure. *J Clin Invest* 1976;58:751.
52. Fifer MA, Borow KM, Colan S, et al. Early diastolic left ventricular function in children and adults with aortic stenosis. *J Am Coll Cardiol* 1985;5:1147.
53. Grossman W. Diastolic dysfunction in congestive heart failure. *N Engl J Med* 1991;325:1557.
54. Paulus WJ. Upward shift and outward bulge: divergent myocardial effects of pacing angina and brief coronary occlusion. *Circulation* 1990;81:1436.
55. Feldman MD, Alderman JD, Aroesty JM, et al. Depression of systolic and diastolic myocardial reserve during atrial pacing tachycardia in patients with dilated cardiomyopathy. *J Clin Invest* 1988;82:1661.
56. Lambertz H, Kreis A, Trumper H, et al. Simultaneous transesophageal atrial pacing and transesophageal two-dimensional echocardiography: a new method of stress echocardiography. *J Am Coll Cardiol* 1990;16:1143.

16
Measurement of Ventricular Volumes, Ejection Fraction, Mass, Wall Stress, and Regional Wall Motion

Michael A. Fifer and William Grossman

MAF: Harvard Medical School; Coronary Care Unit, Massachusetts General Hospital,[qcBoston, Massachusetts 02114.
WG: University of California, San Francisco, School of Medicine; Division of Cardiology, University of California, San Francisco Medical Center, San Francisco, California 94143

Cardiac angiography was introduced initially to provide qualitative information regarding anatomic abnormalities of the cardiovascular system. Subsequently, it became apparent that quantitative information derived from cineangiography could provide insight into *functional* abnormalities of the heart as well. Direct measurements of ventricular dimension, area, and wall thickness allow calculation of volume, ejection fraction, mass, and wall stress. Assessment of pressure-volume relationships provides additional information regarding systolic and diastolic function of the ventricular chambers. Finally, techniques developed to assess *regional* left ventricular wall motion have proved useful in the evaluation of patients with coronary artery disease. Therefore, the ventricular angiograms obtained by the techniques described in Chapter 12 can be used to derive quantitative descriptors of geometry and function.

VOLUMES

Technical Considerations

As discussed in detail in Chapter 12, ventriculograms are generally recorded on cine film or in digital format at 15 to 60 frames per second (fps), and radiographic contrast material is usually injected into the left ventricle at rates of 7 to 15 mL/sec for a total volume of 30 to 50 mL. Alternatively, the left ventricle may be visualized from contrast injections into the pulmonary artery, the left atrium (by the transseptal technique), or, in cases of severe aortic insufficiency, the aortic root. Attention to catheter position and injection rate minimizes the occurrence of ventricular ectopy during contrast studies; this is important because analysis of extrasystoles and postextrasystolic beats cannot be used for proper assessment of basal ventricular function.

With the widespread availability of computer systems, the technique of determining ventricular volumes has evolved from a handheld planimeter with pencil and paper (or a calculator) to semiautomated software packages. The principles important in accurate volume determination, however, apply equally to manual and computer-based techniques. For example, the need for magnification correction applies to both manual and automated techniques of volume determination.

In the first step in assessing left ventricular chamber volume, the left ventricular outline or silhouette is traced. The ventricular silhouette should be traced at the *outermost margin of visible radiographic contrast* so as to include trabeculations and papillary muscles within the perimeter (Fig. 16.1). The aortic valve border is defined as a line connecting the inferior aspects of the sinuses of Valsalva. Some computer-based systems require that the entire ventricular silhouette be traced manually; others incorporate a semiautomated edge-detection algorithm, wherein some points on the ventricular silhouette are entered manually and others are “supplied” by the computer software.

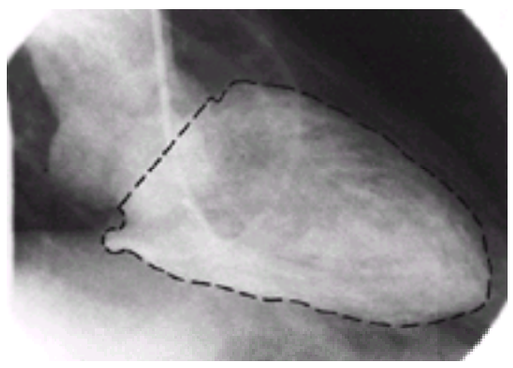

FIG. 16.1. Left ventriculogram in the 30° right anterior oblique projection. The ventricular outline has been traced, as indicated by the broken line.

To facilitate the calculation of left ventricular volume, the ventricle is usually approximated by an ellipsoid (1,2). Alternatively, techniques based on Simpson's rule, which is independent of assumptions regarding ventricular shape, may be used (3). Because the x-rays emanate from a point source, they are nonparallel; correction must therefore be made for magnification of the ventricular image onto the image intensifier. A further complicating factor is so-called pincushion distortion, which causes greater magnification at the periphery than in the center of the image, as a result of spherical aberration of the electromagnetic lens system (4). Finally, ventricular volumes calculated by most mathematical techniques overestimate true ventricular chamber volume, so that regression equations must be used to correct for the overestimation.

Biplane Formula

Biplane left ventriculography may be performed in the anteroposterior (AP) and lateral projections (2), the 30° right anterior oblique (RAO) and 60° left anterior oblique (LAO) projections (5), or angulated projections (e.g., 45° RAO and 60° LAO–25° cranial) (6). Although it is a complex geometric shape, the left ventricle can be approximated with considerable accuracy by an ellipsoid (2) (Fig. 16.2). The volume of an ellipsoid is given by the equation

$$V = \frac{4}{3}\pi\frac{L}{2}\frac{M}{2}\frac{N}{2} = \frac{\pi}{6}LMN \qquad \textbf{(16.1)}$$

where V is volume, L is the long axis, and M and N are the short axes of the ellipsoid. The long axis, L, is taken practically to be L_{max}, the longest chord that can be drawn within the ventricular silhouette in either projection. To determine M and N, each of the biplane projections of the left ventricle is approximated by an ellipse. M and N are taken to be the minor axes of these ellipses. They are calculated by the *area-length method*, as introduced by Dodge et al. (2) from the silhouette areas and long-axis lengths in each projection, using the standard geometric formula for the area of an ellipse as a function of its major and minor axes. For biplane oblique

(RAO/LAO) left ventriculography, for example, the areas of the two ventricular silhouettes are given as

$$A_{RAO} = \pi \frac{L_{RAO}}{2} \frac{M}{2} \text{ and} \tag{16.2}$$

$$A_{LAO} = \pi \frac{L_{LAO}}{2} \frac{N}{2}$$

L_{RAO} and L_{LAO} are the longest chords that can be drawn in the RAO and LAO silhouettes, respectively. The area of each traced silhouette (Fig. 16.1) is obtained by planimetry, and *M* and *N* are calculated by rearrangement as follows:

$$M = \frac{4A_{RAO}}{\pi L_{RAO}} \text{ and } N = \frac{4A_{LAO}}{\pi L_{LAO}} \tag{16.3}$$

Combining Equation (16.1), Equation (16.2), and Equation (16.3),

$$V = \frac{\pi}{6} L_{max} \left(\frac{4A_{RAO}}{\pi L_{RAO}}\right)\left(\frac{4A_{LAO}}{\pi L_{LAO}}\right) \tag{16.4}$$

$$= \frac{8}{3\pi} \frac{A_{RAO}A_{LAO}}{L_{min}}$$

where L_{min} is the shorter of L_{RAO} and L_{LAO}. Because L_{RAO} is almost always greater than L_{LAO}, L_{LAO} is usually substituted for L_{min}.

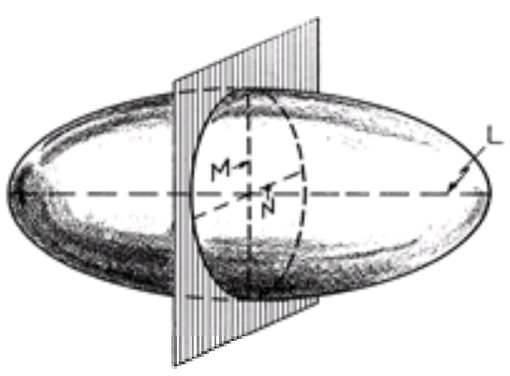

FIG. 16.2. Ellipsoid used as a reference figure for the left ventricle. The long axis, *L*, and the short axes, *M* and *N*, are shown.

Equation (16.4) is derived for projections at right angles, or *orthogonal* projections, and is applicable to biplane oblique ventriculography in the 30° RAO and 60° LAO views, as just described, or for the older AP and lateral format. Although it is not valid theoretically for nonorthogonal projections (e.g., RAO and angulated LAO), it has been demonstrated empirically to be useful in those situations as well (6).

Right ventricular volumes have been calculated from biplane AP and lateral films using a modification of the Dodge area-length technique (7,8) or Simpson's rule (8,9 and 10). Because right ventricular volumes are rarely calculated from cineangiographic studies today, the reader is referred elsewhere for methodologic details (7,8,9 and 10).

Single-plane Formula

The area-length ellipsoid method for estimating left ventricular chamber volume has been modified for use when only single-plane measurements obtained in the AP or RAO projection are available (4,11,12 and 13). Inherent in single-plane methods is the assumption that the left ventricular shape may be approximated by a prolate spheroid=mthat is, an ellipsoid in which the two minor axes are equal (12). It is assumed that the minor axis of the ventricle in the projection used is equal to the minor axis in the orthogonal plane, which was not filmed. Recalling Eq. (1) for the general case of an ellipsoid:

$$V = \frac{\pi}{6} LMN \tag{16.5}$$

If only single-plane (e.g., RAO) ventriculography is done, we assume that $M = N$ and that *L* in the plane presented is the true long axis of the ellipsoid. *M* is calculated from the single-plane silhouette area (*A*) and *L* by the area-length method as $M = 4A/pL$. Therefore, the single-plane volume calculation becomes

$$V = \frac{\pi}{6} LM^2 = \frac{\pi}{6} L \left(\frac{4A}{\pi L}\right)^2 = \frac{8A^2}{3\pi L} \tag{16.6}$$

Magnification Correction: Single-Plane

Correction accomplished by filming a calibrated grid at the estimated level of the ventricle (11) and submitting the grid to the same magnification process as the ventricle accounts for both linear magnification and pincushion distortion. Use of x-ray systems in which the center of the ventricle can be positioned at a fixed point (isocenter), around which the x-ray tubes and image intensifiers rotate, allows for magnification correction without the use of grids but does not correct for pincushion distortion.

The use of grids and other means of calculating magnification correction factors has been reassessed by Sheehan and Mitten-Lewis (14). They found that the error introduced by considering a large central square area of the grid rather than the portion encompassing a particular ventricular silhouette was negligibly small. Replacement of the grid by a circular disk did not significantly alter the calculated correction factor. Alternatively, the use of catheters with radiopaque markers separated by 1 cm also yielded accurate correction factors.

An approximation of the magnification correction may be obtained by considering the diameter of the catheter used for left ventriculography. However, there is a large potential percentage error in measurement of this small dimension, and the percentage error in volumes derived from it is roughly triple that in the linear correction factor. Furthermore, there is no correction for pincushion distortion. On the other hand, the error introduced into calculation of ejection fraction by this technique is much [bnsmaller than that in the calculation of ventricular volume; if it were not for the need for regression formulas (see later discussion), ejection fraction could be determined without regard to magnification.

In the single-plane formula, the cube of the linear correction factor adjusts the volume for magnification:

$$V = \frac{8}{3\pi}(CF)^3 \frac{A^2}{L} \quad \textbf{(16.7)}$$

H4>Magnification Correction: Biplane

In biplane studies, a correction factor (CF) must be calculated separately for each projection, yielding, in the case of biplane oblique cineangiography, CF_{RAO} and CF_{LAO}. The linear correction factor is multiplied by the measured lengths, and the square of this correction factor is multiplied by planimetered areas to convert to true lengths and areas. Accordingly, the corrected volume of the ventricle is

$$V = \frac{8}{3\pi} \frac{(CF_{RAO})^2(CF_{LAO})^2}{CF_{LAO}} \frac{A_{RAO}A_{LAO}}{L_{LAO}} \quad \textbf{(16.8)}$$

$$= \frac{8CF_{RAO}{}^2CF_{LAO}}{3\pi} \frac{A_{RAO}A_{LAO}}{L_{LAO}}$$

Regression Equations

Postmortem studies of hearts injected with contrast material have demonstrated that angiographic volumes calculated by Eq. (16.8) overestimate true left ventricular cavity volumes (2,4,5). This overestimation results in large part from the papillary muscles and trabeculae carneae, which do not contribute to blood volume but are nevertheless included within the traced left ventricular silhouette. Regression equations derived from these studies are used to adjust the calculated volumes. A list of the most commonly used regression equations is given in Table 16.1. For biplane studies in AP and lateral projections using large-film techniques, the regression equation of Dodge and Sandler (15) is used. For children (in whom this regression equation may yield a negative volume), another formula has been suggested (16). For cine studies in the 60° RAO/30° LAO projections, Wynne et al. (5) used postmortem casts, as shown in Fig. 16.3, to derive the regression equation shown in Table 16.1.

Investigator	Angiographic method	Age group	Regression equation
Wynne et al. (5)	Biplane cine RAO and LAO	Adults	$V_A = 0.969V_C - 8.1$
	Single-plane cine RAO	Adults	$V_A = 0.959V_C - 5.7$
Kennedy et al. (13)	Single-plane cine RAO	Adults	$V_A = 0.81V_C + 1.9$
Dodge et al. (2,15)	Biplane serial AP and lateral	Adults	$V_A = 0.959V_C - 3.8$
Graham et al. (16)	Biplane cine AP and lateral	Children	$V_A = 0.703V_C$
Sandler and Dodge (12)	Single-plane serial AP	Adults	$V_A = 0.951V_C - 3.0$

AP, anteroposterior; LAO, left anterior oblique; RAO, right anterior oblique; V_A, actual volume; V_C, calculated volume.

TABLE 16.1. *Regression equations to correct for overestimation in calculation of left ventricular volumes*

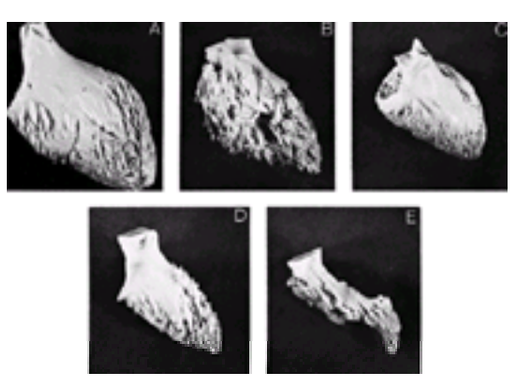

FIG. 16.3. Left ventricular casts made from fresh postmortem specimens of human hearts, using an encapsulant mixed with barium sulfate powder. The shape of the left ventricle only roughly approximates an ellipsoid of revolution; nevertheless, amazingly good correlation was obtained between true volume of these casts (measured by water displacement of the actual cast) and calculated volume. (From Wynne J, Green LH, Grossman W, et al. Estimation of left ventricular volumes in man from biplane cineangiograms filmed in oblique projections. *Am J Cardiol* 1978;41:726, with permission.)

Single-plane techniques tend to overestimate volume significantly, compared with biplane methods, and this is reflected in the single-plane regression equations (Table 16.1). Regression equations are incorporated into commercial catheterization laboratory packages.

EJECTION FRACTION AND REGURGITANT FRACTION

Visual inspection of the cine film allows selection of frames depicting maximum (end-diastolic) and minimum (end-systolic) ventricular volumes. Ejection fraction (EF) is then calculated as follows (17,18):

$$EF = (EDV - ESV)/EDV = SV/EDV \quad \textbf{(16.9)}$$

where EDV is end-diastolic ventricular volume, ESV is end-systolic ventricular volume, and SV is the angiographic stroke volume.

In patients with aortic and/or mitral regurgitation, comparison of the angiographically determined stroke volume with the forward stroke volume determined by the Fick technique or (in the absence of concomitant tricuspid regurgitation) the thermodilution technique yields the regurgitant stroke volume, that portion of the ejected volume that is regurgitated and therefore does not contribute to the net cardiac output (15). The regurgitant fraction (RF) is defined as follows (17,18 and 19):

$$RF = \frac{SV_{\text{angiographic}} - SV_{\text{forward}}}{SV_{\text{angiographic}}} \quad \textbf{(16.10)}$$

An assumption of this calculation is constancy of heart rate between the determination of forward cardiac output and the performance of left ventriculography. If the heart rate (HR) is substantially different at these two times, a mod- ified method for calculating RF must be used, wherein the angiographic minute output ($SV_{\text{angiographic}}$ × HR) is substituted for angiographic stroke volume and the forward minute output or cardiac output is substituted for the forward stroke volume. This calculation is based on the assumption that cardiac output is independent of heart rate to a first approximation.

Because the derivation of RF involves the difference between the two stroke volume measurements, both of which contain some degree of error, the error in RF itself may be significant; interpretation of this number should be influenced by qualitative assessment of the degree of regurgitation seen on the angiogram. In cases of combined aortic and mitral regurgitation, estimation of the relative contribution of the two lesions must be made from the cineangiograms.

OTHER TECHNIQUES FOR MEASURING VENTRICULAR VOLUME AND EJECTION FRACTION

Image enhancement by computerized digital subtraction techniques can be used to obtain left ventriculograms after peripheral intravenous administration of contrast material (20,21). Peripheral injection of the contrast agent eliminates the problem of ventricular extrasystoles sometimes associated with direct injection of contrast material into the ventricular chamber. Alternatively, the image enhancement provided by the digital subtraction process permits direct left ventricular injections with small volumes of contrast agents (20), possibly allowing multiple ventriculograms under varying conditions during a single catheterization procedure. Ventricular volume and ejection fraction may be calculated from digital subtraction ventriculograms using the area-length method (20), as described for standard ventriculograms. Alternatively, ejection fraction may be determined by computer analysis of the attenuation of x-rays by the contrast agent within the ventricle (21,22). This technique is independent of geometric assumptions regarding the shape of the ventricle.

A multielectrode catheter capable of measuring intracavitary electrical impedance has been introduced (23,24 and 25) and has proved useful for the measurement of ventricular volume and ejection fraction without the use of contrast agents. An early version of the catheter, consisting of 12 platinum ring electrodes mounted at 1-cm intervals along the distal end of an 8F or 9F end-hole catheter, is shown in Fig. 16.4. A 4-mA current flows through the blood of the ventricular chamber between selected ring electrodes, and the voltage needed to drive this current reflects the instantaneous electrical impedance of the blood, which has been shown to be a direct function of the blood volume. Newer catheters, only 6F in diameter, combine impedance, volume, and micromanometer pressure measurements. Validation studies (23,24) indicate that both left and right ventricular volumes can be measured by this technique. An illustration of the potential usefulness of this catheter in assessing left ventricular pressure-volume relationships is shown in Fig. 16.5.

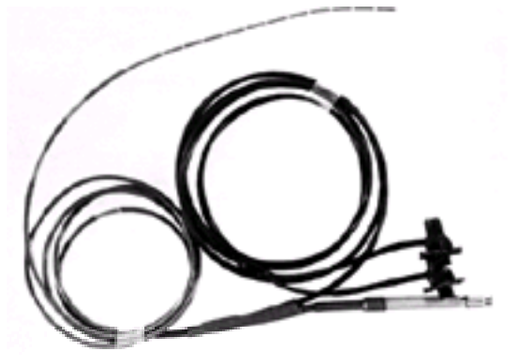

FIG. 16.4. Multielectrode impedance catheter for measurement of instantaneous chamber blood volume. (See text for description.) (From McKay RG, et al. Instantaneous measurement of left and right ventricular stroke volume and pressure-volume relationships with an impedance catheter. *Circulation* 1984;69:703.)

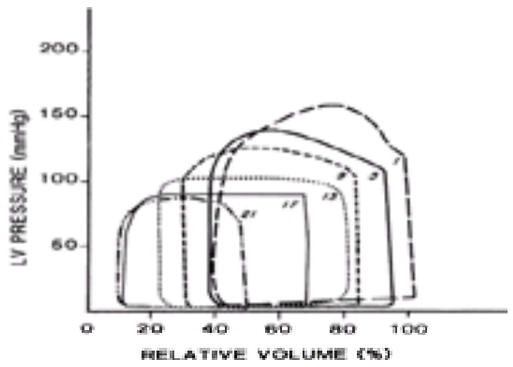

FIG. 16.5. Use of multielectrode impedance catheter, shown in Fig. 16.4, to obtain left ventricular pressure-volume loops every fourth beat during inhalation of amyl nitrate. (From McKay RG, et al. Instantaneous measurement of left and right ventricular stroke volume and pressure-volume relationships with an impedance catheter. *Circulation* 1984;69:703, with permission.)

LEFT VENTRICULAR MASS

Measurement of left ventricular wall thickness, in addition to the parameters measured for volume determination, allows calculation of left ventricular wall volume and estimation of left ventricular mass (LVM). For these calculations, it is assumed that wall thickness is uniform throughout the ventricle. Wall thickness (h) is measured at end-diastole at the left ventricular free wall roughly two thirds of the distance from the aortic valve to the apex in the AP (26) or RAO (13) projection. Appropriate magnification correction is applied. For biplane methods, the total volume of left ventricular chamber and wall, V_{C+W}, is approximated by that of the corresponding ellipsoid:

$$V_{c+w} = \frac{4}{3}\pi\left(\frac{L+2h}{2}\right)\left(\frac{M+2h}{2}\right)\left(\frac{N+2h}{2}\right) \quad \textbf{(16.11)}$$

$$= \frac{\pi}{6}(L+2h)\left(\frac{4A_{RAO}}{\pi L_{RAO}}+2h\right)\cdot\left(\frac{4A_{LAO}}{\pi L_{LAO}}+2h\right)$$

As with h, appropriate correction for magnification must be applied to A and L so that V_{C+W} represents the total volume of the left ventricular chamber and wall corrected for magnification. For single-plane methods, it is assumed that $M = N$, yielding the single-plane formula:

$$V_{c+w} = \frac{\pi}{6}(L+2h)\left(\frac{4A}{\pi L}+2h\right)^2 \quad \textbf{(16.12)}$$

The volume of the chamber is calculated by the biplane or single-plane technique. In order to exclude the volume of the papillary muscles and trabeculae from the chamber volume (and thus include their mass in LVM), the appropriate regression equation is applied, so that V_C is the regressed value for chamber volume. LVM, then, is calculated as follows:

$$LVM = 1.050\,V_w \quad \textbf{(16.13)}$$

$$= 1.050(V_{c+w} - V_c)$$

where V_W is wall volume, and 1.050 is the specific gravity of heart muscle. This method has been validated by postmortem examination of hearts (26,27); however, it may not be accurate in the presence of marked right ventricular hypertrophy or pericardial effusion or thickening, where accurate measurement of wall thickness from the RAO silhouette may be impossible. The left ventricular wall thickness may sometimes be seen well in the LAO projection in the region of the posterior wall, or it

may be measured accurately by echocardiography, computed tomography, or magnetic resonance imaging. Values obtained by any of these methods may be used for calculation of LVM.

NORMAL VALUES

A number of investigators have reported normal values in adults and children for left ventricular volume, ejection fraction, wall thickness, and mass (5,16,28,29 and 30). These are summarized in Table 16.2.

Investigator	Angiographic method	Number of patients	Age group	End-diastolic volume (mL/m²)	End-systolic volume (mL/m²)	Ejection fraction	Wall thickness (mm)	Mass (g)
Rhyne et al. (5)	Biplane (one RAO–LAO)	17	Adults	72 ± 15	20 ± 8	0.72 ± 0.08	—	—
Kennedy et al. (27)	Biplane (one AP and Lat)	15	Adults	79 ± 23	24 ± 10	0.67 ± 0.08	10.9 ± 2.9	167 ± 42
Hood (28)	Biplane (one AP and Lat)	6	Adults	79 ± 11	26 ± 6	0.67 ± 0.07	8.5 ± 1.3	164 ± 35
Hermann and Battle (29)	Biplane (one AP and Lat)	6	Adults	71 ± 20	30 ± 10	0.58 ± 0.05	—	—
Graham et al. (16)	Biplane (one AP and Lat)	19	Children less than 2 yr	42 ± 10	—	0.66 ± 0.05	—	66 ± 11*
Graham et al. (16)	Biplane (one AP and Lat)	27	Children older than 2 yr	70 ± 11	—	0.63 ± 0.05	—	66 ± 11*

AP, anteroposterior; LAO, left anterior oblique; RAO, right anterior oblique.
*g/m².

TABLE 16.2. *Normal average values for left ventricular parameters by angiocardiography (Mean ± SD)*

WALL STRESS

Whereas consideration of ventricular pressure and volume is useful for assessment of *ventricular* performance, direct evaluation of *myocardial* function requires attention to forces acting at the level of the individual myocardial fiber. In particular, correction must be made for differences in ventricular wall thickness and chamber radius (*R*), which modify the extent to which intraventricular pressure (*P*) is borne by the individual fiber; this is especially important in disease states characterized by ventricular hypertrophy or dilation or both. Such a correction may be achieved by consideration of wall stress (s) (29,31,32 and 33). Several formulas are commonly used to calculate stress, all related to the basic Laplace relation:

$$\sigma = \frac{PR}{2h} \qquad \textbf{(16.14)}$$

Assumptions of the shape of the ventricular chamber and the properties of the ventricular wall have led to a number of such formulas for wall stress components in the circumferential, meridional, and radial directions (Fig. 16.6). Consideration of circumferential and meridional stress has been particularly useful for clinical applications. A representative formula for calculation of circumferential stress, s_c is

$$\sigma_c = \frac{Pb}{h}\left(1 - \frac{h}{2b}\right)\left(1 - \frac{hb}{2a^2}\right) \qquad \textbf{(16.15)}$$

where *a* and *b* are the major and minor semiaxes, respectively, at the midwall. Meridional stress, s_m, may be calculated as follows (32):

$$\sigma_m = \frac{PR}{2h(1 + h/2R)} \qquad \textbf{(16.16)}$$

where *R* is the internal chamber radius as bounded by the endocardial surface. For more detailed consideration of wall stress formulas, the reader is referred to reviews of the subject (33).

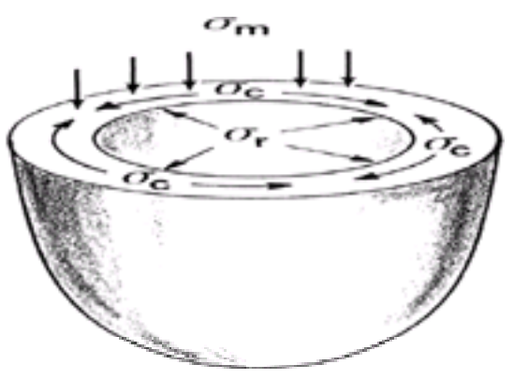

FIG. 16.6. Circumferential (s_c), meridional (s_m), and radial (s_r) components of left ventricular wall stress for an ellipsoid model. The three components of wall stress are mutually perpendicular.

Calculation of wall stress in disease states has provided information not apparent from consideration of pressure and volume data alone. For example, it has been demonstrated that peak stress does not necessarily occur at the same time in the cardiac cycle as does peak pressure and that, in “compensated” pressure overload, the increase in ventricular pressure is offset by a proportional increase in wall thickness, so that wall stress remains normal (Fig. 16.7) (32).

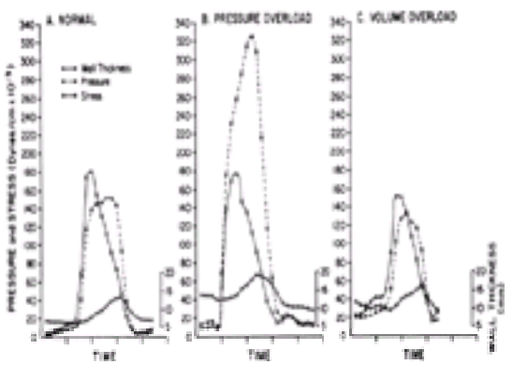

FIG. 16.7. A comparison of changes in left ventricular pressure, wall thickness, and meridional stress throughout the cardiac cycle for representative normal **(A)**, pressure-overloaded **(B)**, and volume-overloaded **(C)** ventricles. These parameters are plotted at 40-msec intervals. In all three types of ventricles, peak stress occurs earlier than peak pressure. In the pressure-overloaded ventricle, peak pressure is markedly elevated, but peak systolic stress and end-diastolic stress are normal. In

the volume-overloaded ventricle, peak systolic stress is normal, but end-diastolic stress is elevated. (From Grossman W, Jones D, McLaurin LP. Wall stress and patterns of hypertrophy in the human left ventricle. *J Clin Invest* 1975;56:56, with permission.)

PRESSURE-VOLUME CURVES

Simultaneous measurement of ventricular pressure and volume allows construction of the pressure-volume diagram (Fig. 16.8) (34,35,36 and 37). The position and slope of the diastolic portion of the pressure-volume curve provides information regarding diastolic properties of the ventricle (35,38). Construction of the systolic portion of the curve is useful for analysis of the end-systolic pressure-volume relation, a measure of ventricular contractile function (see Chapter 17).

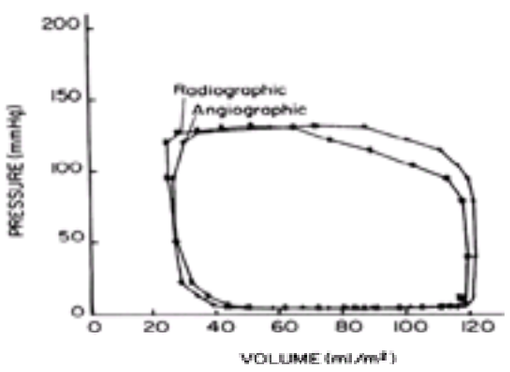

FIG. 16.8. Pressure-volume diagram for the left ventricle. In this example, the diagram derived from single-plane cineangiography is compared to that constructed from radionuclide volume data. (From McKay RG, et al. Left ventricular pressure-volume diagrams and end-systolic pressure-volume relations in human beings. *J Am Coll Cardiol* 1984;3:301, with permission.)

REGIONAL LEFT VENTRICULAR WALL MOTION

The recognition that left ventricular regional dyssynergy is a more sensitive marker of coronary artery disease than is depression of global function has led to attempts to quantify abnormalities of regional wall motion. Left ventriculography is performed in the RAO or RAO and LAO projections. The ventricle is divided into regions by one of two methods: (a) construction of lines perpendicular to the major axis that divide the major axis into equal segments (39,40) or (b) construction of lines drawn from the midpoint of the major axis to the ventricular outline at intervals of a fixed number of degrees (39). Extent of inward (or outward) movement of individual segments can then be measured, usually with the aid of computer techniques, providing quantitative measures of hypokinesis, akinesis, and dyskinesis.

An automated method of processing the left ventricular cineangiogram was reported by Sasayama et al. (41,42 and 43). End-diastolic and end-systolic ventricular silhouettes are superimposed (Fig. 16.9), and 128 radial grids are drawn from the center of gravity of the end-diastolic silhouette to the endocardial margins. Measurement of the length of each radial grid between end-diastolic and end-systolic silhouettes measures segmental systolic and diastolic function. Figure 16.9 illustrates this technique in a patient with coronary disease before and after induction of angina pectoris by rapid atrial pacing. Simultaneous measurements of left ventricular pressure permit construction of segmental left ventricular pressure-length loops for both normally perfused myocardial regions (Fig. 16.9, c and d), and regions perfused by stenotic coronary arteries (Fig. 16.9, a and b). Depressed wall motion develops during angina in the latter, and compensatory hyperkinesis develops in the former.

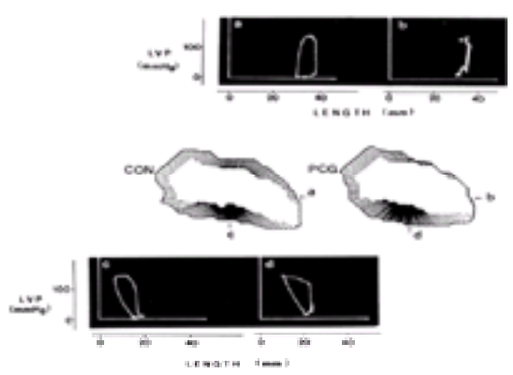

FIG. 16.9. Assessment of regional wall motion in the control state (CON) and after induction of angina pectoris by atrial pacing tachycardia (PCG). Left ventricular pressure (LVP)–length loops are plotted for a myocardial region distal to a stenotic coronary artery (a and b) and for a normally perfused region (c and d). (From Sasayama S, et al. Changes in diastolic properties of the regional myocardium during pacing-induced ischemia in man. *J Am Coll Cardiol* 1985;5:599, with permission.)

Another approach has been used by Sheehan et al. (44,45). Wall motion is measured along 100 chords constructed as perpendiculars to a line drawn midway between the end-diastolic and end-systolic left ventricular contours (Fig. 16.10). The motion of each chord is compared with a normal range established from analysis of ventriculograms from patients without heart disease. Deviations from the normal range indicate hypokinesis or hyperkinesis. In studies of wall motion after thrombolysis, availability of the LAO in addition to the RAO projection proved particularly useful in patients with left circumflex coronary artery thrombosis (45).

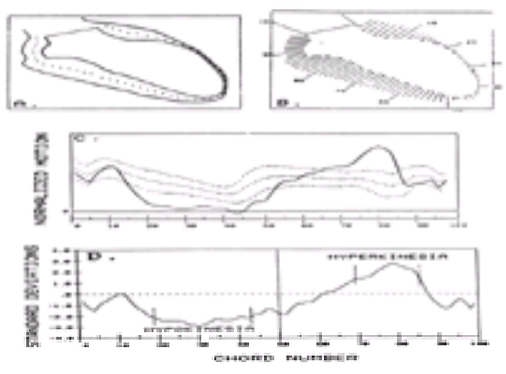

FIG. 16.10. Wall motion as assessed by the center line method. The center line (**A,** *dotted line*) is constructed midway between the end-systolic and end-diastolic silhouettes. In panel **B,** chords are drawn at right angles to the center line. The percentage of systolic shortening along each chord is plotted (**C,** *solid line*) and compared with normal mean and standard deviation values *(dashed and dotted lines)*. Deviation from normal is replotted in panel **(D)**. (From Sheehan FH, Bolson EL, Dodge HT, et al. Advantages and applications of the center line method for characterizing regional ventricular function. *Circulation* 1986;74:293, with permission.)

Software for regional wall motion analysis is now available in commercial catheterization laboratory computer systems.

CHAPTER REFERENCES

1. Arvidsson H. Angiocardiographic observations in mitral disease. *Acta Radiol* 1958;(Suppl 158).
2. Dodge HT, Sandler H, Ballew DW, et al. The use of biplane angiocardiography for the measurement of left ventricular volume in man. *Am Heart J* 1960;60:762.
3. Chapman CB, Baker O, Reynolds J, et al. Use of biplane cinefluorography for measurement of ventricular volume. *Circulation* 1958;18:1105.
4. Greene DG, Carlisle R, Grant C, et al. Estimation of left ventricular volume by one-plane cineangiography. *Circulation* 1967;35:61.
5. Wynne J, Green LH, Grossman W, et al. Estimation of left ventricular volumes in man from biplane cineangiograms filmed in oblique projections. *Am J Cardiol* 1978;41:726.
6. Rogers WJ, et al. Quantitative axial oblique contrast left ventriculography: validation of the method by demonstrating improved visualization of regional wall motion and mitral valve function with accurate volume determinations. *Am Heart J* 1982;103:185.
7. Arcilla RA, Tsai P, Thilenius O, et al. Angiographic method for volume estimation of right and left ventricles. *Chest* 1971;60:446.
8. Graham TP Jr, Jarmakani JM, Atwood GF, et al. Right ventricular volume determinations in children: normal values and observations with volume or pressure overload. *Circulation* 1973;47:144.
9. Goerke RJ, Carlsson E. Calculation of right and left cardiac ventricular volumes: method using standard computer equipment and biplane angiocardiograms. *Invest Radiol* 1967;2:360.
10. Gentzler RD, Briselli MF, Gault JH. Angiographic estimation of right ventricular volume in man. *Circulation* 1974;50:324.
11. Kasser IS, Kennedy JW. Measurement of left ventricular volumes in man by single-plane cineangiocardiography. *Invest Radiol* 1969;4:83.
12. Sandler H, Dodge HT. The use of single plane angiocardiograms for the calculation of left ventricular volume in man. *Am Heart J* 1968;75:325.
13. Kennedy JW, Trenholme SE, Kasser IS. Left ventricular volume and mass from single-plane cineangiocardiogram: a comparison of anteroposterior and right anterior oblique methods. *Am Heart J* 1970;80:343.
14. Sheehan FH, Mitten-Lewis S. Factors influencing accuracy in left ventricular volume determination. *Am J Cardiol* 1989;64:661.
15. Sandler H, Dodge HT, Hay RE, et al. Quantitation of valvular insufficiency in man by angiocardiography. *Am Heart J* 1963;65:501.
16. Graham TP Jr, Jarmakani JM, Canent RV Jr, et al. Left heart volume estimation in infancy and childhood: reevaluation of methodology and normal values. *Circulation* 1971;43:895.
17. Arvidsson H, Karnell J. Quantitative assessment of mitral and aortic insufficiency by angiocardiography. *Acta Radiol* 1964;2:105.
18. Miller GAH, Brown R, Swan HJC. Isolated congenital mitral insufficiency with particular reference to left heart volumes. *Circulation* 1964;29:356.
19. Jones JW, et al. Left ventricular volumes in valvular heart disease. *Circulation* 1964;29:887.
20. Sasayama S, et al. Automated method for left ventricular volume measurement by cineventriculography with minimal doses of contrast medium. *Am J Cardiol* 1981;48:746.
21. Nissen SE, Elion JL, Grayburn P, et al. Determination of left ventricular ejection fraction by computer densitometric analysis of digital subtraction angiography: experimental validation and correlation with area-length methods. *Am J Cardiol* 1987;59:675.
22. Tobis J, et al. Measurement of left ventricular ejection fraction by videodensitometric analysis of digital subtraction angiograms. *Am J Cardiol* 1983;52:871.
23. McKay RG, Spears JR, Aroesty JM, et al. Instantaneous measurement of left and right ventricular stroke volume and pressure-volume relationships with an impedance catheter. *Circulation* 1984;69:703.
24. Kass DA, Midei M, Graves W, et al. Use of a conductance (volume) catheter and transient inferior vena caval occlusion for rapid determination of pressure-volume relationships in man. *Cathet Cardiovasc Diagn* 1988;15:192.
25. Odake M, Takeuchi M, Takaoka H, et al. Determination of left ventricular volume using a conductance catheter in the diseased human heart. *Eur Heart J* 1992;13(Suppl E):57.
26. Rackley CE, Dodge HT, Coble YD Jr, et al. A method for determining left ventricular mass in man. *Circulation* 1964;29:666.
27. Kennedy JW, Reichenbach DD, Baxley WA, et al. Left ventricular mass: a comparison of angiocardiographic measurements with autopsy weight. *Am J Cardiol* 1967;19:221.
28. Kennedy JW, et al. Quantitative angiocardiography: I. The normal left ventricle in man. *Circulation* 1966;34:272.
29. Hood WP Jr. Wall stress in the normal and hypertrophied human left ventricle. *Am J Cardiol* 1968;22: 550.
30. Hermann HJ, Bartle SH. Left ventricular volumes by angiocardiography: comparison of methods and simplification of techniques. *Cardiovasc Res* 1968;4:404.
31. Sandler H, Dodge HT. Left ventricular tension and stress in man. *Circ Res* 1963;13:91.
32. Grossman W, Jones D, McLaurin LP. Wall stress and patterns of hypertrophy in the human left ventricle. *J Clin Invest* 1974;56:56.
33. Yin FCP. Ventricular wall stress. *Circ Res* 1981;49:829.
34. Arvidsson H. Angiocardiographic determination of left ventricular volume. *Acta Radiol* 1961;56:321.
35. Dodge HT, Hay RE, Sandler H. Pressure-volume characteristics of diastolic left ventricle of man with heart disease. *Am Heart J* 1962;64:503.
36. Bunnell IL, Grant C, Greene DG. Left ventricular function derived from the pressure-volume diagram. *Am J Med* 1965;39:881.
37. McKay RG, Aroesty JM, Heller GV, et al. Left ventricular pressure-volume diagrams and end-systolic pressure-volume relations in human beings. *J Am Coll Cardiol* 1984;3:301.
38. Grossman W. Relaxation and diastolic distensibility of the regionally ischemic left ventricle. In: Grossman W, Lorell BH, eds. *Diastolic Relaxation of the Heart.* Boston: Martinus Nijhoff, 1988:193.
39. Herman MV, Heinle RA, Klein MD, et al. Localized disorders in myocardial contraction: asynergy and its role in congestive heart failure. *N Engl J Med* 1967;277:222.
40. Sniderman AD, Marpole D, Fallen EL. Regional contraction patterns in the normal and ischemic left ventricle in man. *Am J Cardiol* 1973;31:484.
41. Sasayama, S, Nonogi H, Kawm C. Assessment of left ventricular function using an angiographic method. *Jpn Circ J* 1982;46:1177.
42. Fujita M, et al. Automatic processing of cine ventriculograms for analysis of regional myocardial function. *Circulation* 1981;63:1065.
43. Sasayama S, et al. Changes in diastolic properties of the regional myocardium during pacing-induced ischemia in human subjects. *J Am Coll Cardiol* 1985;5:599.
44. Sheehan FH, Bolson EL, Dodge HT, et al. Advantages and applications of the centerline method for characterizing regional ventricular function. *Circulation* 1986;74:293.
45. Sheehan FH, Schofer J, Mathey DG, et al. Measurement of regional wall motion from biplane contrast ventriculograms: a comparison of the 30 degree right anterior oblique and 60 degree left anterior oblique projections in patients with acute myocardial infarction. *Circulation* 1986;74:796.

17
Evaluation of Systolic and Diastolic Function of the Ventricles and Myocardium

William Grossman

University of California, San Francisco, School of Medicine; Division of Cardiology, University of California, San Francisco Medical Center, San Francisco, California 94143.

A critical aspect of most cardiac catheterization procedures is the evaluation of myocardial function. At its simplest, this consists of a visual assessment of the left ventricular (LV) contractile pattern from the left ventriculogram, together with measurements of LV end-diastolic pressure. In laboratories where most patients have right-sided heart catheterization and cardiac output measurement as part of a standard cardiac catheterization procedure, additional information about LV function may be gleaned from the cardiac output, stroke volume, and pulmonary capillary wedge pressure, whereas right ventricular (RV) function is reflected in the values for right ventricular end-diastolic pressure (RVEDP) and right atrial pressure. Measurements of pressures and cardiac output give important information about overall cardiac function but may shed little light on whether dysfunction is caused by abnormal systolic or diastolic myocardial performance. This chapter describes some of the specific methods that can be used in the cardiac catheterization laboratory to examine myocardial performance in systole and diastole.

SYSTOLIC FUNCTION

Preload, Afterload, and Contractility

Systolic function of the myocardium is a reflection of the interaction of myocardial preload, afterload, and contractility. *Preload* is the load that stretches myofibrils during diastole and determines the end-diastolic sarcomere length. For the left ventricle, this load is often quantified as the LV end-diastolic pressure (LVEDP). This pressure, taken together with LV wall thickness (*h*) and radius (*R*), determines LV end-diastolic *wall stress* (s » *PR/h*), which is an estimate of the force stretching the myocardial fibers at end-diastole. The end-diastolic stress or "stretching force" is resisted by the intrinsic stiffness or elasticity of the myocardium, and the interaction of end-diastolic stretching force and myocardial stiffness determines the extent of end-diastolic sarcomere stretch. If the myocardium is diffusely fibrotic or infiltrated with amyloid, a very high end-diastolic stretching force may be required to produce even a normal end-diastolic sarcomere length. In such a case, LVEDP may be very high (e.g., more than 25 mm Hg), and attempts to lower it by diuretic or venodilator therapy may lead to reduction in end-diastolic sarcomere stretch to subnormal values and a concomitant fall in cardiac output.

Changes in preload influence both the extent and velocity of myocardial shortening in experiments using isolated cardiac muscle preparations. Increased preload augments the extent and velocity of myocardial shortening at any given afterload. In the intact heart, the relationship is more complex because increases in preload generally produce increases in LV chamber size and LV systolic pressure. Therefore, *afterload* (the force resisting systolic shortening of the myofibrils) is also increased, and this increase tends to blunt the increases in extent and velocity of myocardial shortening caused by increased diastolic fiber stretch. This point is discussed in more detail later in this chapter, under the section on ejection phase indices of systolic function.

Afterload varies throughout systole as the ventricular systolic pressure rises and blood is ejected from the ventricular chamber. LV systolic stress approximates the force resisting myocardial fiber shortening within the wall of the ventricle. The theory and methods for calculation of wall stress are described in Chapter 16. End-systolic wall stress is considered by many to be the final afterload that determines the extent of myocardial fiber shortening, when preload and contractility are constant. An increase in end-systolic wall stress results in a decrease in myocardial fiber shortening. For the intact ventricle, an increase in afterload (end-systolic wall stress) therefore results in a fall in stroke volume and ejection fraction.

Contractility refers to the property of heart muscle that accounts for alterations in performance induced by biochemical and hormonal changes; it has classically been regarded as independent of preload and afterload. Contractility is generally used as a synonym for *inotropy*: both terms refer to the level of activation of cross-bridge cycling during systole. Contractility changes are assessed in the experimental laboratory by measuring myocardial function (extent or speed of shortening, maximum force generation) while preload and afterload are held constant. In contrast to skeletal muscle, the strength of contraction of heart muscle can be increased readily by a variety of biochemical and hormonal stimuli, some of which are listed in Table 17.1.

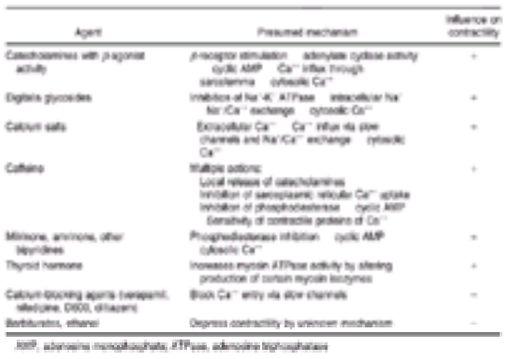

Agent	Presumed mechanism	Influence on contractility
Catecholamines with β-agonist activity	β-receptor stimulation → adenylate cyclase activity → cyclic AMP → Ca^{++} influx through sarcolemma → cytosolic Ca^{++}	+
Digitalis glycosides	Inhibition of Na⁺-K⁺ ATPase → intracellular Na^+ for $/Ca^{++}$ exchange → cytosolic Ca^{++}	+
Calcium salts	Extracellular Ca^{++} → Ca^{++} influx via slow channels and Na^+/Ca^{++} exchange → cytosolic Ca^{++}	+
Caffeine	Multiple actions: Local release of catecholamines Inhibition of sarcoplasmic reticular Ca^{++} uptake Inhibition of phosphodiesterase → cyclic AMP Sensitivity of contractile proteins of Ca^{++}	+
Milrinone, amrinone, other bipyridines	Phosphodiesterase inhibition → cyclic AMP → cytosolic Ca^{++}	+
Thyroid hormone	Increases myosin ATPase activity by altering production of certain myosin isozymes	+
Calcium-blocking agents (verapamil, nifedipine, D600, diltiazem)	Block Ca^{++} entry via slow channels	−
Barbiturates, ethanol	Depress contractility by unknown mechanism	−

AMP, adenosine monophosphate; ATPase, adenosine triphosphatase

TABLE 17.1. *Hormones and drugs that influence myocardial contractility*

Increased myocardial contractility may be present in patients with hyperadrenergic states, thyrotoxicosis, or hypertrophic cardiomyopathy or in response to a variety of drugs. It is manifested by an increase in the speed and extent of myocardial contraction at constant afterload and preload.

Experiments with isolated myocardial tissue have demonstrated that contractility is not truly independent of preload. Increased end-diastolic sarcomere stretch leads to an immediate increase in the strength of contraction due to the Frank-Starling mechanism, followed by a gradual further increase in contractile strength over 5 to 10 minutes (1,2 and 3). Evidence supports a role for both increased intracellular calcium (Ca^{++}) release and increased myofilament sensitivity to any given level of cytosolic Ca^{++} as underlying factors in the length-dependent activation seen with increased preload (2).

Assessment of systolic function requires consideration of the simultaneous influence of afterload, preload, and contractility. Systolic function should *not* be regarded as synonymous with contractility. Major depression of systolic function can occur with normal contractility, as in conditions with so-called afterload excess (see later discussion).

Isovolumic Indices

One of the oldest and most widely used measures of myocardial contractility is the maximum rate of rise of LV systolic pressure, d *P*/d*t*. Wiggers noted more than 70 years ago that in animal experiments the failing ventricle showed a reduced steepness of the upslope of the ventricular pressure pulse (4). In 1962, Gleason and Braunwald first reported measurement of d*P*/d*t* in humans (5). They studied 40 patients with micromanometer catheters. Maximum d*P*/d*t* in those patients without hemodynamic abnormalities ranged from 841 to 1,696 mm Hg/sec in the left ventricle and 223 to 296 mm Hg/sec in the right ventricle. Interventions known to increase myocardial contractility, such as exercise and infusion of norepinephrine or isoproterenol, caused major increases in d *P*/d*t*. Increased heart rate produced by intravenous atropine also caused a rise in maximum d*P*/d*t*, and the authors attributed this to the *treppe phenomenon* described by Bowditch. Acute increases in arterial pressure and afterload produced by infusion of the a-adrenergic vasoconstricting agent methoxamine produced little change in d *P*/d*t*. These points are illustrated in Fig. 17.1 and Fig. 17.2.

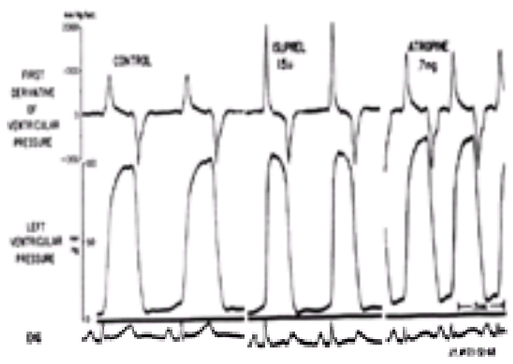

FIG. 17.1. Micromanometer recordings of left ventricular pressure and its first derivative, d *P*/d*t*, in a patient with normal left ventricular function. Isoproterenol markedly increases contractility with large increments in positive d *P*/d*t*. Atropine produces tachycardia, which results in a treppe effect and a rise in +d *P*/d*t* above control. (From Gleason WL, Braunwald E. Studies on the first derivative of the ventricular pressure pulse in man. *J Clin Invest* 1962;41:80, with permission.)

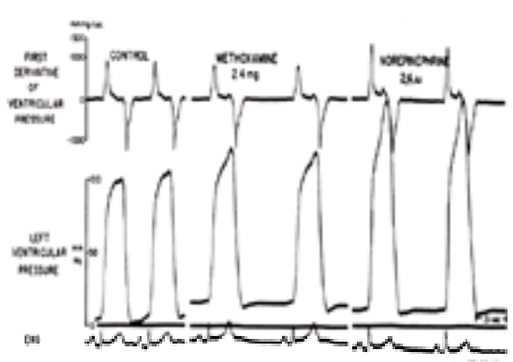

FIG. 17.2. Micromanometer recordings of left ventricular (LV) pressure and d *P*/d*t*, as in Fig. 17.1. Methoxamine raises arterial and LV systolic pressure but does not increase +d*P*/d*t*. In contrast, the combined a- and b-adrenergic effects of norepinephrine increase LV systolic pressure and +d *P*/d*t*. (From Gleason WL, Braunwald E. Studies on the first derivative of the ventricular pressure pulse in man. *J Clin Invest* 1962;41:80, with permission.)

In normal subjects and in patients with no significant cardiac abnormality, maximum d*P*/d*t* increases significantly in response to isometric exercise (6), dynamic exercise (5), tachycardia by atrial pacing (7,8) or atropine (5), b-agonists (5), and digitalis glycosides (9). Relatively few studies have been done in humans to assess the changes in d*P*/d*t* induced by alterations in afterload and preload, but some studies do indicate that maximum positive d *P*/d*t* tends to increase slightly (6% to 8%) with moderate increases in LV preload (10) and shows little change with methoxamine-induced increases (5) or nitroprusside-induced decreases (11) in mean arterial pressure of 25 to 30 mm Hg. Extensive studies in animals have examined the influence of changes in afterload, preload, and contractility on maximum d *P*/d*t* (10,12,13,14 and 15). These studies generally show that maximum d*P*/d*t* rises with increases in afterload and preload, but the changes were quite small (less than 10%) in the physiologic range.

As discussed in Chapter 7, accurate measurement of d*P*/d*t* requires a pressure measurement system with excellent frequency-response characteristics. Micromanometer catheters are usually required to achieve this frequency-response range (16). Differentiation of the ventricular pressure signal can be achieved by (a) analog techniques on-line (Fig. 17.1 and Fig. 17.2), using a resistance capacitor (RC) differentiating circuit (5,10); (b) computer digitization of the analog LV pressure tracing and subsequent differentiation of a polynomial best fit to the averaged LV isovolumic pressure (17); or (c) computer digitization of the analog LV pressure tracing with subsequent Fourier analysis and differentiation (18).

In addition to d*P*/d*t*, several other isovolumic indices have been introduced in an attempt to obtain a “pure” contractility index, completely independent of alterations in preload and afterload (10,19,20). These indices include the maximum value of (d*P*/d*t*)/*P*, where *P* is LV pressure (the maximum value of (d*P*/d*t*)/*P* is sometimes called V_{PM}); (peak d*P*/d*t*)/*IIT*, where *IIT* is the integrated isovolumic tension; (d*P*/d*t*)/*CPIP*, where *CPIP* is the common developed isovolumic pressure; V_{max}, the extrapolated value of (d*P*/d*t*)/*P* versus *P*, when *P* = 0; (d*P*/d*t*)/P_D when the developed LV pressure, P_D, equals 5, 10, or 40 mm Hg; and the fractional rate of change of power, which involves the second derivative of LV pressure.

Although changes in d*P*/d*t* reflect acute changes in inotropy in a given individual, the usefulness of d *P*/d*t* is reduced in comparisons between individuals, especially when there has been chronic LV pressure or volume overload. Peak d*P*/d*t* is generally increased in patients with chronic aortic stenosis, even though contractility is normal or decreased in most of these patients. To account for chronic changes in LV geometry and mass that occur with chronic LV overload, some investigators have examined the rate of rise of systolic wall stress (17). The peak value of ds/d*t* may be used as a contractility index, as may the spectrum plot that relates ds/d*t* to instantaneous s (Fig. 17.3).

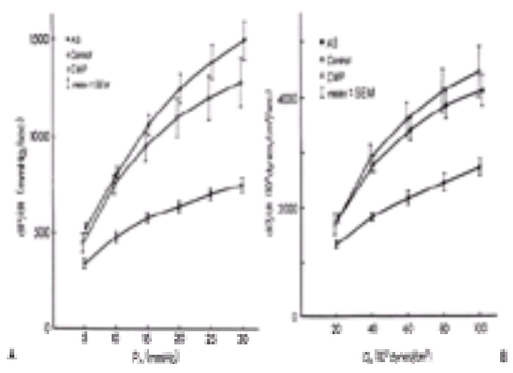

FIG. 17.3. Left ventricular (LV) isovolumic indices of contractility. **A:** Rate of pressure development (d*P*/d*t*) as a function of LV-developed pressure (P_D). Mean values in control subjects (*open circles*), patients with aortic stenosis (AS, *closed circles*), and patients with dilated cardiomyopathy (CMP, *crosses*) are shown. Brackets represent standard errors of the mean (SEM). **B:** Rate of wall stress development (ds/d*t*) as a function of LV-developed stress (s_D) for the same groups. There are no significant differences for patients with AS compared with controls, although patients with CMP clearly show depressed values for d *P*/d*t* and ds/dt at all levels of P_D and s_D. (From Fifer MA, Gunther S, Grossman W, et al. Myocardial contractile function in aortic stenosis as determined from the rate of stress development during

isovolumic systole. *Am J Cardiol* 1979;44:1318, with permission.)

Pressure-Volume Analysis

Since the time of Frank and Starling, pressure-volume (PV) diagrams have been used to analyze ventricular function. The normally contracting left ventricle ejects blood under pressure, and the relationship of its pressure generation and ejection can be expressed in a plot of LV pressure against volume. As can be seen in Fig. 17.4, end-diastole is represented by point A, isovolumic contraction by line AB, aortic valve opening by point B, ejection by line BC, end-ejection and aortic valve closure by point C, isovolumic relaxation by line CD, mitral valve opening by point D, and LV diastolic filling by line DA.

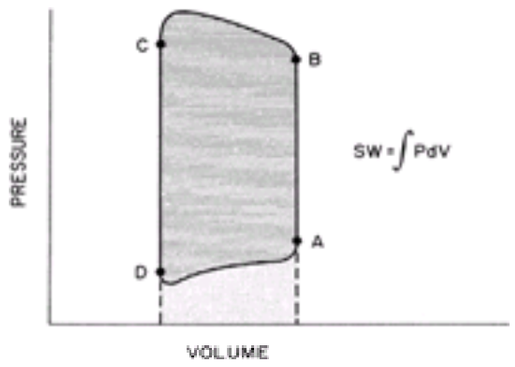

FIG. 17.4. Diagram of ventricular pressure (*P*) plotted against simultaneous ventricular volume (*V*) for a single cardiac contraction. For the left ventricle, point A represents end-diastole, segment AB is isovolumic contraction, point B is aortic valve opening, segment BC is LV ejection, point C is aortic valve closure and represents end-ejection, segment CD is isovolumic relaxation, point D is mitral valve opening, and segment DA is LV filling. LV stroke work (SW) is the cross-hatched area, and the stippled area is diastolic work done on the left ventricle by right ventricle and left atrium. (See text for details.)

Stroke Work

The area ABCD enclosed within the PV diagram in Fig. 17.4 is the external LV stroke work (SW), represented mathematically as ò*P*d*V*. Although the calculation of LVSW is most accurate when it is derived by integrating the area within complete PV diagrams, a practical approximation can be obtained as follows:

$$\mathbf{LVSW} = (\overline{\mathbf{LVSP}} - \overline{\mathbf{LVDP}})\mathbf{SV}(0.0136) \qquad \textbf{(17.1)}$$

where $\overline{\mathrm{LVSP}}$ and $\overline{\mathrm{LVDP}}$ are, respectively, the mean LV systolic and diastolic pressures (in mm Hg), SV is the LV total stroke volume (in mL), and 0.0136 is a constant for converting mm Hg-mL into g-m. $\overline{\mathrm{LVSP}}$ and $\overline{\mathrm{LVDP}}$ may be obtained from planimetry of direct pressure tracings, as shown in Fig. 17.5. When the total LV stroke volume is the same as the forward stroke volume, SV may be calculated as cardiac output divided by heart rate. In cases where LV total stroke volume differs from forward stroke volume (e.g., mitral or aortic regurgitation, ventricular septal defect), the PV diagram may differ substantially in configuration from that shown in Fig. 17.4, and LVSW cannot be calculated from Eq. (17.1). Instead, planimetric integration of the entire PV plot is required.

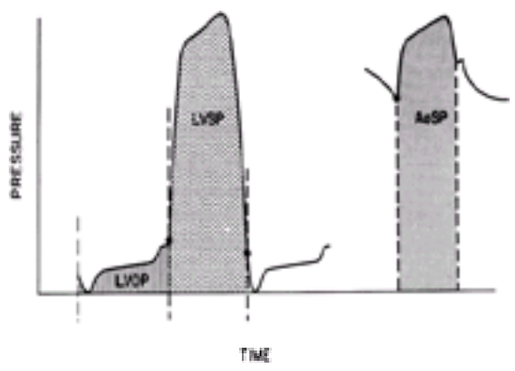

FIG. 17.5. Left ventricular (LV) and aortic pressure tracings illustrate areas planimetered to measure LV mean systolic pressure (LVSP), LV mean diastolic pressure (LVDP), and aortic mean systolic pressure (AoSP). LVSP is the area contained under the LV pressure curve, bounded by perpendicular lines defining end-diastole and mitral valve opening; LVDP is the diastolic area, similarly defined. AoSP is the area contained under the aortic pressure curve, bounded by perpendicular lines defining aortic valve opening and closure.

If LV pressure tracings are not available, in the absence of major regurgitation SW can be approximated from the aortic and pulmonary capillary wedge pressures as follows:

$$\mathbf{LVSW} = (\overline{\mathbf{AoSP}} - \overline{\mathbf{PCW}})\mathbf{SV}(0.0136) \qquad \textbf{(17.2)}$$

where $\overline{\mathrm{AoSP}}$ is the aortic systolic mean pressure (planimetered from the aortic pressure tracing, Fig. 17.5) and $\overline{\mathrm{PCW}}$ is the mean pulmonary capillary wedge pressure. A further approximation may be made by substituting mean systemic arterial pressure for AoSP, which it closely approximates.

LVSW is a reasonably good measure of LV systolic function in the absence of volume or pressure overload conditions, both of which may substantially increase calculated LVSW. The normal LVSW in adults is approximately 90 ± 30 g-m (mean ± SD); in adult patients with dilated cardiomyopathy or heart failure from extensive prior myocardial infarction, LVSW is often less than 40 g-m. Values less than 25 g-m indicate severe LV systolic failure, and when LVSW is less than 20 g-m the prognosis is grave.

LVSW is a measure of total LV chamber function and can be considered to reflect myocardial contractility only when the ventricle is reasonably homogeneous in its composition, as in most patients with dilated cardiomyopathy. For patients with coronary artery disease and extensive myocardial infarction, LVSW may be depressed even though well-perfused areas of the myocardium with normal contractility remain.

Because power is the rate at which work is done, LV power in the normal heart is the integral of the product of LV pressure during ejection and aortic flow. LV power may be regarded as a measure of overall LV contractile function; with refinement (such as the measurement of preload-adjusted maximal power), it can be used as a measure of inotropic state (21).

Ejection Phase Indices

LV systolic function can be assessed using only the volume data from the PV diagram. One of the most widely used indices of LV systolic performance is the ejection

fraction (EF), which is defined as follows:

$$\mathrm{EF} = (\mathrm{LVEDV} - \mathrm{LVESV})/\mathrm{LVEDV} \quad \textbf{(17.3)}$$

where LVEDV and LVESV are the LV end-diastolic and end-systolic volumes, respectively. In the cardiac catheterization laboratory, left ventricular EF (LVEF) is most often derived from the LV angiogram, as discussed in Chapter 16. If the EF is divided by the ejection time (ET), measured from the aortic pressure tracing, the quotient is called *mean normalized systolic ejection rate* (MNSER).

$$\mathrm{MNSER} = \frac{(\mathrm{LVEDV} - \mathrm{LVESV})}{(\mathrm{LVEDV})(\mathrm{ET})} \quad \textbf{(17.4)}$$

Finally, another ejection phase index of LV systolic function is the velocity of circumferential fiber shortening, V_{CF} (22). This is calculated as the rate of shortening of a theoretic LV myocardial fiber in a circumferential plane at the midpoint of the long axis of the ventricle. For convenience, mean V_{CF} is used most often, rather than instantaneous or peak V_{CF}. Mean V_{CF} is obtained by subtracting the end-systolic endocardial circumferential fiber length (p D_{ES}) from the end-diastolic endocardial circumferential fiber length (pD_{ED}), then dividing by ET and normalizing for end-diastolic circumferential fiber length:

$$V_{CF} = (\pi D_{ED} - \pi D_{ES})/\pi D_{ED}(\mathrm{ET}) \quad \textbf{(17.5)}$$
$$= (D_{ED} - D_{ES})/D_{ED}(\mathrm{ET})$$

D_{ED} and D_{ES} are end-diastolic and end-systolic minor axis dimensions. Although V_{CF} can be calculated from angiographic data using the area-length method ($D = 4A/pL$), it is most commonly calculated from values for D measured by M-mode echocardiography. Normal values for isovolumic and ejection phase indices are given in Table 17.2.

Contractility indices	Normal values (mean ± SD)	References
Isovolumic indices		
Maximum dP/dt	1610 ± 200 mm Hg/sec	7
	1073 ± 320 mm Hg/sec	23
	1061 ± 325 mm Hg/sec	19
Maximum dP/dt/P	44 ± 8.4 sec^{-1}	19
		23
V_{cf} or peak $\left[\frac{dP/dt}{DP}\right]$	1.47 ± 0.19 ML/sec	
$dP/dt/P_d$ at P_d = 40 mm Hg	37.6 ± 12.2 sec^{-1}	19
Ejection phase indices		
LVSWI	61 ± 23 g-m	6
LVSWI	53 ± 22 g-m/m^2	23 & 24, combined
	41 ± 12 g-m/m^2	26
EF (Angiographic)	0.70 ± 0.08	27
MNSER		
Angiographic	3.32 ± 0.84 EDV/sec	19
Echographic	2.29 ± 0.39 EDV/sec	28
Mean V_{CF}		
Angiographic	1.83 ± 0.56 ED circ/sec	19
	1.90 ± 0.27 ED circ/sec	22
Echographic	1.88 ± 0.12 ED circ/sec	28

dP/dt, rate of rise of left ventricular (LV) pressure; P_d, developed LV pressure; ML, muscle length; MNSER, mean normalized systolic ejection rate; ED, end-diastolic; V, volume; circ, circumference; EF, ejection fraction.

TABLE 17.2. *Evaluation of left ventricular systolic performance: normal values for some isovolumic and ejection phase indices*

Ejection phase indices are obtained easily from LV angiography and can also be derived reliably from a variety of noninvasive techniques such as radionuclide ventriculography and echocardiography. The most widely used ejection phase index, the EF, is generally depressed when myocardial contractility is diminished. However, the ejection indices depend heavily on preload and afterload and cannot be regarded as reliable indices of contractility in conditions associated with altered loading conditions. For example, increases in preload cause the EF (and other ejection indices) to rise; consequently, LVEF may be increased in patients with mitral or aortic regurgitation, severe anemia, or other causes of increased diastolic LV inflow and may mask underlying deterioration of myocardial contractility. Conversely, increases in afterload cause the EF to fall; consequently, LVEF may be low in patients with severe aortic stenosis or other causes of increased resistance to systolic ejection and may falsely suggest underlying depression of myocardial contractility.

In practice, acute elevation of LV preload causes some increase in LV chamber size and aortic pressure, and these increases in afterload (systolic s resisting shortening) tend to decrease the EF and other ejection indices, offsetting the rise in EF that a pure rise in preload would produce. Rankin and coworkers (28) produced changes in venous return by total body tilt in normal subjects; despite substantial changes in LV end-diastolic dimension and volume, there were no significant changes in EF, MNSER, or V_{CF}. Similarly, acute elevation of afterload caused by raising aortic pressure causes an increase in LVEDP, and the resultant rise in preload (end-diastolic fiber stretch) tends to increase the EF and other ejection indices, offsetting the fall in EF produced by a pure rise in afterload. These physiologic adjustments explain why the ejection indices are much more useful clinically than might be expected on the basis of studies in the isolated heart or muscle preparation.

An LVEF of less than 0.40 indicates depressed LV systolic pump function, and if there is no abnormal loading to account for it, an LVEF of 0.40 or less can be taken to signify depressed myocardial contractility. An LVEF of less than 0.20 corresponds to severe depression of LV systolic performance and is usually associated with a poor prognosis. Interpretation of EF and other ejection indices is improved by consideration of the ventricular preload and afterload, and the latter values are defined most precisely by end-diastolic and end-systolic wall stresses, respectively.

End-Systolic Pressure-Volume and s-Length Relations

Over the past 20 years, several groups have shown that the LV end-systolic PV, pressure-diameter, and s-length relationships accurately reflect myocardial contractility, independent of changes in ventricular loading. This has been established in a series of studies in animals (29,30,31,32,33,34 and 35) and humans (36,37,38,39,40,41 and 42). The fundamental principle of end-systolic PV analysis is that at end-systole there is a single line relating LV chamber pressure to volume, unique for the level of contractility and independent of loading conditions. The LV end-systolic PV line can be generated by producing a series of PV loops (such as the one in Fig. 17.4) over a range of loading conditions (Fig. 17.6 and Fig. 17.7). The line connecting the upper left corners of the individual PV diagrams is the end-systolic PV line, characterized by a slope and by an x-axis intercept, called V_0 (the extrapolated end-systolic volume when end-systolic pressure is zero). Current evidence indicates that an increase in contractility shifts the end-systolic PV line to the left with a steeper slope, and a depression in contractility is associated with a displacement of the line downward and to the right, with a reduced slope. Although there is some uncertainty as to the meaning of V_0, it is generally agreed that an increase in slope of the end-systolic PV line is a sensitive indicator of an increase in contractility. However, the technique of end-systolic analysis may not be as useful in comparisons among subjects as it is in comparisons of values in a single subject measured before and after an intervention. The end-systolic PV lines for groups of patients with normal, intermediate, and depressed LV contractility are shown in Fig. 17.8.

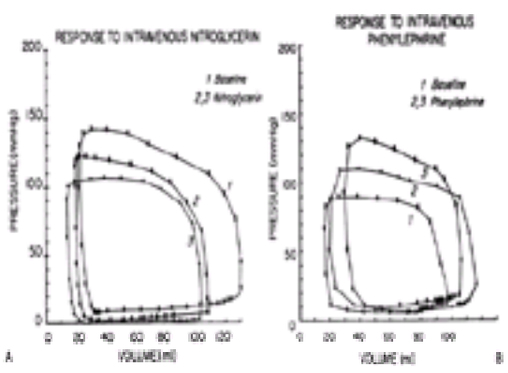

FIG. 17.6. Left ventricular (LV) pressure-volume (PV) plots constructed using radionuclide ventriculography to measure LV volume simultaneously with measurement of LV pressure during cardiac catheterization. **A:** Three sequential plots measured during baseline and at two sequential doses of intravenous nitroglycerin to lower

LV pressure. **B:** Similar plots in a patient whose baseline LV systolic pressure was low: In this case, phenylephrine was used in increasing doses to produce three levels of systolic loading. The upper left (end-systolic) corners of the three PV plots in each panel define a straight line, the LV end-systolic PV line. (See text for discussion.) (From McKay RG, Aroesty JM, Heller GV, et al. Left ventricular pressure-volume diagrams and end-systolic pressure relations in human beings. *J Am Coll Cardiol* 1984;3:301, with permission.)

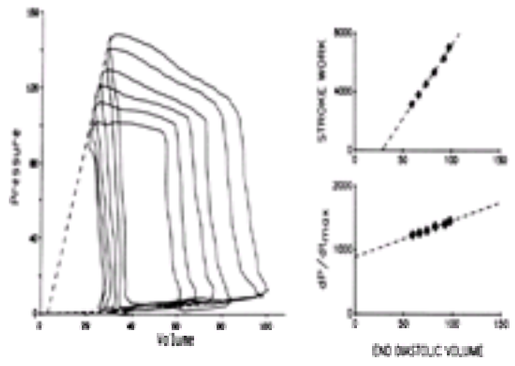

FIG. 17.7. The left panel shows left ventricular (LV) pressure-volume loops obtained during rapid LV unloading achieved by inferior vena cava (IVC) balloon occlusion in a patient undergoing cardiac catheterization. Volume was obtained by a conductance catheter technique. The right panels show relationships between stroke work *(upper right)*, maximum rate of rise of LV systolic pressure, d*P*/d*t (lower right)*, and LV end-diastolic volume. (From Kass DA, Maughan WL. From E_{Max} to pressure-volume relations: a broader view. *Circulation* 1988;77:1203, with permission.)

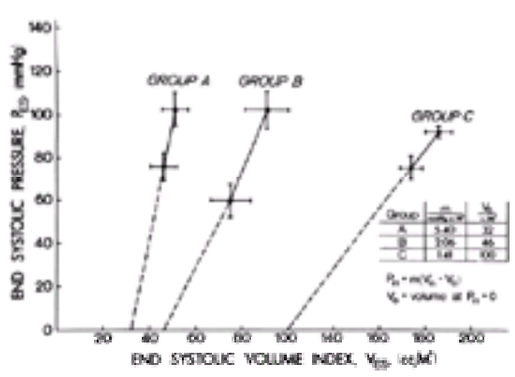

FIG. 17.8. Left ventricular (LV) end-systolic pressure (P_{ES}) plotted against end-systolic volume index (V_{ES}) at two levels of loading for each of three patient groups: Group A, patients with normal LV contractile function; Group B, patients with moderate depression of LV contractile performance; Group C, patients with marked depression of LV contractility. Depressed contractility shifts the P_{ES}-V_{ES} relation to the right, with a reduced slope (m) and increased intercept (V_0). (From Grossman W, Braunwald E, Mann JT, et al. Contractile state of the left ventricle in man as evaluated from end-systolic pressure relations. *Circulation* 1977;45:845, with permission.)

To measure the end-systolic PV line, one can use aortic dicrotic notch pressure as end-systolic LV pressure and minimum LV chamber volume as end-systolic volume. LV volume can be measured by angiography, using either direct LV injection or right-sided injection with image enhancement by digital subtraction angiography. Alternatively, LV volume can be measured by radionuclide techniques, ultrasonic techniques, or a specially designed impedance (conductance) catheter (42,43).

Relationship Between Peak dP/dt and End-diastolic Volume

Little and coworkers (44) have examined the relationship between LV d*P*/dt_{max} and end-diastolic volume and have proposed the slope of this relationship as an index of contractile state. They have shown that, on theoretic grounds, this relationship can be derived from the LV end-systolic PV relationship; both provide estimates of maximal myocardial elastance. This relationship is simpler to derive because both LV end-diastolic volume and d *P*/dt_{max} are more readily defined than either end-systolic pressure or volume. One does not need to be concerned about a lack of coincidence between end-systole and maximal elastance, as with the end-systolic PV relationship. The d*P*/dt_{max}–end-diastolic volume relationship, however, has yet to be evaluated extensively in the clinical setting. Also, the end-systolic PV relationship can be estimated clinically by entirely noninvasive methods (45). Nevertheless, the d*P*/dt_{max}–end-diastolic volume relationship represents an intriguing concept and may prove a valuable index of contractile state.

Stress-shortening Relationships

Another approach to the assessment of LV systolic performance and myocardial contractility involves measuring the extent of cardiac muscle shortening and relating this shortening to the systolic wall stress (s) resisting shortening.

If a ventricle is presented with progressively increasing resistance to ejection, s rises while the extent of myocardial shortening declines. Therefore, a plot of systolic s on the horizontal axis against myocardial shortening expressed as EF, V_{CF}, or percent fractional shortening (DD) on the vertical axis yields a tight inverse relationship (Fig. 17.9). Data from studies of individual patients may then be compared with these normal values. In Fig. 17.9, if the point relating end-systolic s (s_{ES}) and DD for a given patient lies within the confidence lines of the normal population, myocardial contractility is likely to be normal; however, if the s_{ES}-DD point lies below the normal range, contractility is depressed even if DD is normal. Fig. 17.10 shows that the s_{ES}-DD relationship is shifted upward by an increase in contractility resulting from a dobutamine infusion. One caution concerning the s_{ES}-DD relationship is that it is preload sensitive. That is, increases in preload will increase DD for any level of s_{ES}. There is some evidence that when V_{CF} is substituted for DD the preload dependence of the stress-shortening relationship is attenuated or abolished.

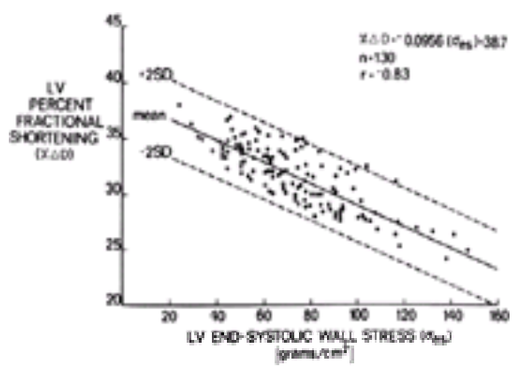

FIG. 17.9. Relationship between left ventricular (LV) end-systolic wall stress (s_{ES}) and % fractional shortening (%D*D*) measured by echocardiography for 130 control points, at rest (o) or during methoxamine infusion (·). The inverse relationship defines normal LV myocardial contractility. (From Borow KM, Green LH, Grossman W,

et al. Left ventricular end-systolic stress-shortening and stress-length relations in humans. *Am J Cardiol* 1982;50:1301, with permission.)

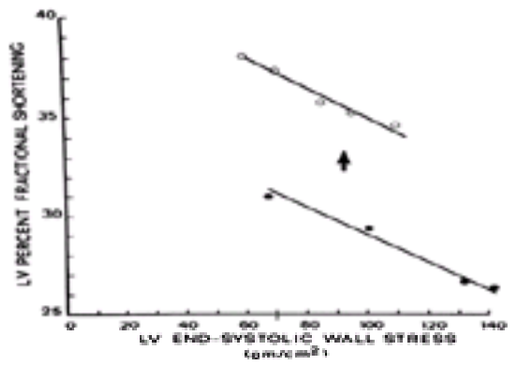

FIG. 17.10. Upward shift in the left ventricular (LV) end-systolic stress-shortening relation resulting from dobutamine infusion. (See text.) (From Borow KM, et al. Left ventricular end-systolic stress-shortening and stress-length relations in humans. *Am J Cardiol* 1982;50:1301, with permission.)

Plots of systolic wall stress against LVEF have been analyzed for patients with a variety of conditions, including LV pressure overload (Fig. 17.11). In these plots, comprised of multiple individual data points (each point relating LV wall s and EF for an individual patient) an inverse systolic s-EF relationship is apparent for patients with chronic LV pressure overload. This suggests that the depressed LVEF in some of these individuals is caused by excessive systolic s; that is, the load resisting systolic shortening is abnormally high and is responsible for a reduced extent of shortening. This combination of high s and low EF is sometimes referred to as *afterload mismatch* (46,47 and 48), and it implies that hypertrophy has been inadequate to return systolic wall stress to its relatively low normal level. Patients in whom LVEF is diminished out of proportion to any increase in systolic wall stress can be assumed to have depressed myocardial contractility (Fig. 17.12).

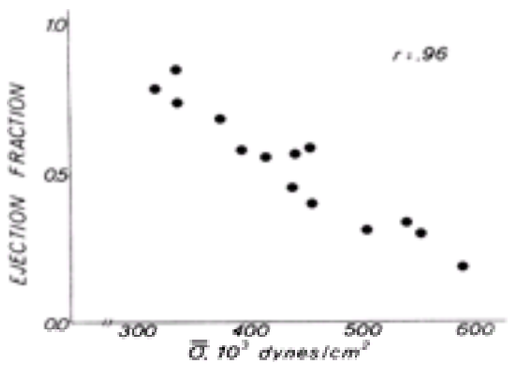

FIG. 17.11. Left ventricular (LV) ejection fraction plotted against mean systolic circumferential wall stress, s, for 14 patients with pure aortic stenosis (normal coronary arteries, no other valve disease) and varying degrees of LV decompensation. The inverse relationship is consistent with afterload excess as a principal cause of the decreased ejection fraction. (From Gunther S, Grossman W. Determinants of ventricular function in pressure-overload hypertrophy in man. *Circulation* 1979;59:679, with permission.)

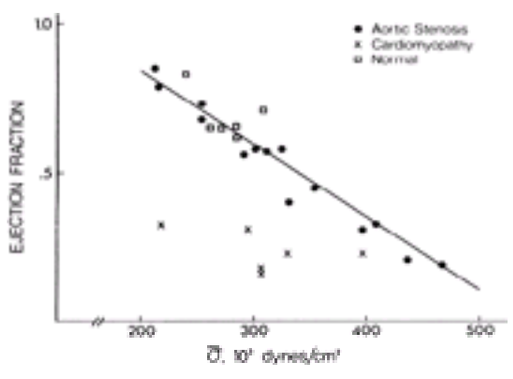

FIG. 17.12. Plot of left ventricular (LV) ejection fraction against systolic s, similar to Fig. 17.11 but including patients with aortic stenosis *(solid dots)*, dilated cardiomyopathy *(crosses)*, and normal ventricular function *(open squares)*. The regression line was constructed from the patients with normal LV function and those with aortic stenosis. (See text for discussion.) (From Gunther S, Grossman W. Determination of ventricular function in pressure overload hypertrophy in man. *Circulation* 1979;5:679, with permission.)

A refinement of this approach involves measuring the relation between end-systolic LV wall stress and the heart rate–corrected velocity of fiber shortening. This approach was found to be sensitive and preload independent in an assessment of LV response to nitroprusside and dopamine infusions in patients with dilated cardiomyopathy (49). In that study, this approach was more sensitive to detecting increased contractility than was LV d *P*/d*t*.

The advantage of s-shortening analysis over PV diagram analysis is that wall s takes into consideration changes in LV geometry and muscle mass that occur in response to chronic alterations in loading. For example, a systolic pressure of 250 to 300 mm Hg imposed acutely on a normal left ventricle would result in considerable reduction in LVEF, perhaps down to the 20% to 30% range. This change occurs because, in the absence of any increase in LV wall thickness or decrease in chamber radius, systolic s would more than double in response to such an acute pressure overload, and this would lead to a major reduction in LVEF. However, if the increase in systolic pressure to 250 to 300 mm Hg occurs gradually and is matched by the development of sufficient hypertrophy in the appropriate pattern, systolic wall s remains normal and fiber shortening and LVEF do not decrease. Therefore, in the presence of significant hypertrophy and/or altered LV geometry, s-shortening analysis may have considerable value.

DIASTOLIC FUNCTION

Left Ventricular Diastolic Distensibility: Pressure-Volume Relationship

As pointed out by Henderson in 1923, “In the heart, diastolic relaxation is a vital factor and not merely the passive stretching of a rubber bag. Being vital, it is variable” (50). Analysis of diastolic function today requires appreciation that diastolic compliance is variable and may change substantially in a given patient from one minute to the next. Diastolic function is summated physiologically in the relation between LV pressure and volume during diastole (Fig. 17.4, segment DA). Traditionally, an upward shift in this diastolic PV relation is regarded as indicating increased LV diastolic chamber stiffness, and a downward shift indicates decreased stiffness or increased LV diastolic chamber compliance. In the terminology of physics and engineering, stiffness, and its opposite, compliance, relate a change in pressure (DP) to a change in volume (DV); therefore, some investigators have restricted these terms to refer to the slope of the diastolic PV relation. In this regard, as seen in segment

DA of Fig. 17.4, LV diastolic stiffness (DP/DV) is low early in diastole and rises steadily throughout diastolic filling.

Figure 17.13 shows theoretic LV diastolic PV plots for patients with normal, stiff, and compliant ventricular chambers. Several problems arise when stiffness and compliance are defined strictly in terms of the slope of the diastolic PV diagram, and these problems are illustrated in Fig. 17.14. First, in some clinical conditions (e.g., angina pectoris), the LV diastolic PV plot shifts upward in a parallel fashion, without a noticeable change in slope. These patients have increased LV filling pressure, often with normal chamber volumes, and from a hydrodynamic point of view the LV chamber must be regarded as presenting increased resistance to diastolic filling. To say that LV diastolic stiffness and compliance are normal in such patients because the upward shift has been a parallel one (without slope change) seems inappropriate. In other cases (e.g., after nitroprusside infusion in patients with heart failure), there is a downward shift in the LV diastolic PV plot, with an increase in the steepness of the plot; again, to say that such patients exhibit increased LV diastolic stiffness seems inappropriate, because they require a lower filling pressure to achieve the same diastolic chamber dimension and fiber stretch. Therefore, the LV diastolic PV plot can show changes of two types: displacement (movement of the entire relationship upward, downward, or laterally) and configuration change (including change in curvature). In our studies, we have referred to upward or downward displacement changes as being associated with a change in ventricular distensibility (51). Therefore, if the LV diastolic PV plot shifts upward, we would say that the LV chamber has become less distensible; a higher diastolic pressure is required to fill or distend the chamber to its earlier volume (Fig. 17.14). Similarly, a downward shift in the diastolic PV plot would be said to indicate an increase in LV diastolic distensibility. The changes in curvature and/or configuration that may accompany these displacement changes are difficult to quantify and to interpret.

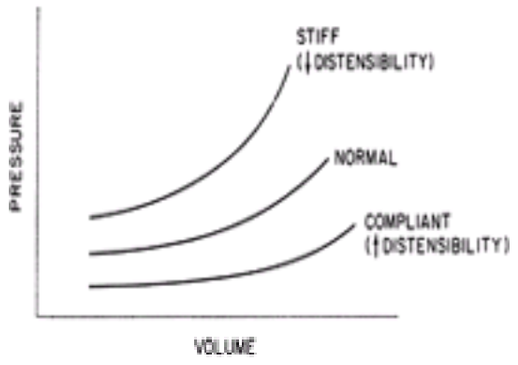

FIG. 17.13. Diagrammatic representation of ventricular diastolic pressure-volume relations for normal, stiff, and compliant ventricles. (See text for discussion.)

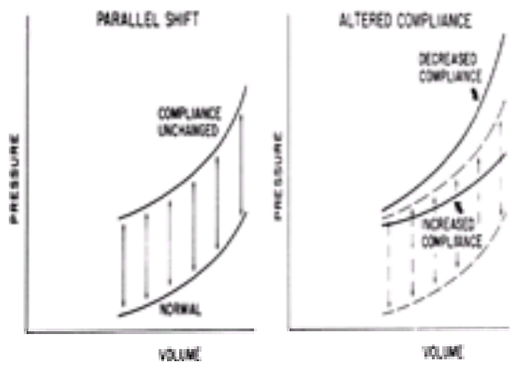

FIG. 17.14. Schematic illustration of the difference between diastolic distensibility and compliance. On the left, the left ventricular diastolic pressure-volume (PV) relation has undergone a parallel upward shift. Distensibility is decreased (higher diastolic pressure required to fill the ventricle to the same chamber volume), but compliance, defined as the slope of the PV relation, is unchanged. On the right, superimposed on the parallel upward shift, are curves whose slopes are steeper (decreased compliance) or less steep (increased compliance) than either of the two parallel PV curves. This illustrates the importance of distinguishing distensibility from compliance, because the curve labeled “increased compliance” nevertheless exhibits decreased diastolic distensibility, compared with the normal PV relation. (From Grossman W. Relaxation and diastolic distensibility of the regionally ischemic left ventricle. In: Grossman W, Lorell BH, eds. *Diastolic Relaxation of the Heart.* Boston: Martinus Nijhoff, 1988:193.)

Various formulas have been developed for analyzing the curvature of the LV diastolic PV plot (52,53,54 and 55). These generally assume that the curvature is exponential, an assumption that is often but not always reasonable. Diastolic PV and P–segment length (SL) plots constructed from a series of end-diastolic points have been used in animal experiments to assess LV diastolic compliance (56), and this technique has been applied to clinical studies. When a series of end-diastolic PV or P-SL points are plotted, the relation is more strictly exponential, and application of mathematical models and analysis is more easily justified by the good agreement of measured data and mathematical predictions.

Clinical Conditions Influencing Diastolic Distensibility

Factors that influence the position of the LV diastolic PV plot (that is, factors that influence LV diastolic *distensibility*) are listed in Table 17.3. *Constrictive pericarditis* and *pericardial tamponade* are associated with a striking upward shift in the diastolic PV relation. This upward shift is a parallel shift, without substantial change in curvature. Pericardial restraint is also important in the mechanism whereby altered RV loading can alter the LV diastolic PV relation. When distended, the right ventricle can decrease LV diastolic distensibility by exerting an extrinsic pressure on the LV chamber in diastole through the shared interventricular septum, which may actually bulge into the LV chamber. *Acute RV infarction* causes dilatation of the RV chamber that, in the presence of an intact, previously unstressed pericardium, may lead to extrinsic compression of the LV in diastole with a hemodynamic pattern resembling cardiac tamponade (57). The effect of increased RV loading on LV diastolic distensibility is an example of ventricular interaction, which is more prominent in the presence of an intact and relatively snug pericardium. In animal experiments, it is difficult to demonstrate diastolic ventricular interaction once the pericardium has been opened wide (55).

I. Factors extrinsic to the LV chamber
A. Pericardial restraint
B. Right ventricular loading
C. Coronary vascular turgor (erectile effect)
D. Extrinsic compression (e.g., tumor, pleural pressure)
II. Factors intrinsic to LV chamber
A. Passive elasticity of LV wall (stiffness or compliance when myocytes are completely relaxed)
1. Thickness of LV wall
2. Composition of LV wall (muscle, fibrosis, edema, amyloid, hemosiderin) including both endocardium and myocardium
3. Temperature, osmolality
B. Active elasticity of LV wall due to residual cross-bridge activation (cycling and/or latch state) through part or all of diastole
1. Slow relaxation affecting early diastole only
2. Incomplete relaxation affecting early-, mid-die-, and end-diastolic distensibility
3. Diastolic tone, contracture, or rigor
C. Elastic recoil (diastolic suction)
D. Viscoelasticity (stress relaxation, creep)

TABLE 17.3. *Factors that influence left ventricular (LV) diastolic chamber distensibility*

Coronary vascular turgor can influence LV diastolic chamber stiffness (58). The LV wall has a rich blood supply, and engorgement of the capillaries and venules with blood makes the wall relatively stiff: for obvious reasons, this has been referred to as the erectile effect. Although the erectile effect is probably not of much

importance when coronary blood flow and pressure (the two components determining the degree of turgor) are in the physiologic range, a marked fall in coronary flow and pressure (as occurs distal to a coronary occlusion when collateral flow is poor or absent) is associated with a decrease in stiffness of the affected myocardium and an increase in LV diastolic distensibility.

Experimental evidence (59) supports an important role for *increased coronary venous pressure* as a major determinant of coronary vascular turgor. Increases in right atrial pressure from 0 to 15 and 30 mm Hg led to substantial upward shifts in the LV end-diastolic PV relation that could not be attributed to right ventricular distention and a shift in the interventricular septum.

Extrinsic *compression of the heart by tumor* may cause decreased LV diastolic distensibility and may mimic cardiac tamponade.

When an upward shift in the diastolic PV relation is present and the extrinsic factors listed in Table 17.3 cannot clearly explain the altered distensibility, a change in one of the intrinsic determinants of LV distensibility is likely to be present. Altered passive elasticity caused by *amyloidosis*, edema, or diffuse fibrosis may cause a restrictive cardiomyopathic pattern, with high LV diastolic pressure relative to volume in the presence of reasonably well-preserved systolic function. Clinically, heart failure may be present. Endomyocardial biopsy of the right or left ventricle may be needed to establish the diagnosis (see Chapter 20).

Myocardial Ischemia

Abnormal diastolic relaxation can cause the diastolic PV relation to shift upward strikingly. During *angina pectoris*, a 10 to 15 mm Hg rise in average LV diastolic pressure may occur with little or no change in diastolic volume; if this persists for a sufficient duration (more than 10 to 20 minutes), pulmonary edema may occur. Such episodes of *flash pulmonary edema* in patients with essentially normal LV systolic function and normal LV chamber size generally indicate a large mass of ischemic myocardium (60) and suggest three-vessel or left main coronary artery obstruction. The decreased LV distensibility during ischemia may be prevented in many patients by a Ca^{++} channel blocking agent (61). The mechanism of impaired myocardial relaxation during the ischemia of angina pectoris is not understood completely but may be associated with diastolic Ca^{++} overload of the ischemic myocytes, in part related to ischemic dysfunction of the sarcoplasmic reticulum (62). During the ischemia of acute coronary occlusion, an upward shift of the diastolic PV relation may occur if sufficient collateral blood flow is present to permit continued systolic contraction of the ischemic segment. If ischemia is sufficiently severe to cause complete akinesis of the affected myocardium, however, altered distensibility does not occur: *incomplete relaxation* can occur only in myocytes when there has been systolic cross-bridge activation. Also, the marked decrease in coronary vascular turgor distal to a coronary occlusion with poor or absent collaterals, together with local accumulation of hydrogen ion (H^{+}), contributes to an increase in regional distensibility, so that the net effect on the ventricular diastolic PV relation may be one of no change.

Cardiac Hypertrophy

Impaired relaxation with decreased LV diastolic distensibility is also seen in patients with *hypertrophic cardiomyopathy* and during angina pectoris in patients with *aortic stenosis* and normal coronary arteries.

Indices of Left Ventricular Diastolic Relaxation Rate

Much attention has been given to measures of LV diastolic relaxation during the isovolumic relaxation period and during early, middle, and late diastolic filling. These indices may be considered as either pressure-derived or volume flow-derived and may assess either global or regional diastolic relaxation (63,64,65,66,67,68,69,70,71,72,73,74,75,76,77,78,79,80,81,82 and 83). A listing of some of these indices and their normal values is given in Table 17.4.

Parameter	Normal values	References
Peak − *dP/dt*	2500 ± 700 mm Hg/sec	7
	2522 ± 756 mm Hg/sec	80
	1894 ± 398 mm Hg/sec	81
	1825 ± 251 mm Hg/sec	82
T [logarithmic method, Eq. (17.7)]	36 ± 7 msec	80
	33 ± 8 msec	81
	31 ± 3 msec	82
	55 ± 12 msec	82
	47 ± 10	83
P_b [derivative method, Eqs. (17.8) and (17.9)]	−25 ± 9 mm Hg	82
PFR	3.3 ± 0.6 EDV/sec	73
Time to PFR	130 ± 23 msec	73
Peak − *dh/dt* (posterior wall)	8.4 ± 3.0 cm/sec	77
	8.2 ± 3.7 cm/sec	78

LV, left ventricular; Peak − *dp/dt* = maximum rate of LV isovolumic pressure decline; *T* = time constant of LV isovolumic relaxation, calculated assuming both zero pressure intercept [Eq. (17.7)] and variable pressure (P_b) intercept [Eqs. (17.8) and (17.9)]; PFR = LV peak filling rate, from radionuclide ventriculography, normalized to end-diastolic volumes (EDV) (sec); Peak − *dh/dt* = maximum rate of posterior wall thinning, measured by echocardiography

TABLE 17.4. *Evaluation of left ventricular diastolic performance: normal values for some indices of relaxation and filling*

Isovolumic Pressure Decay

The time course of LV pressure decline after aortic valve closure is altered in conditions known to be associated with abnormalities of myocardial relaxation. One of the simplest ways of quantifying the time course of LV pressure decline is to measure the maximum rate of pressure fall, peak –d *P*/d*t*. Although peak negative d*P*/d*t* is altered by conditions that change myocardial relaxation, it is also altered by changes in loading conditions. For example, LV peak –d *P*/d*t* increases (i.e., rises in absolute value) when aortic pressure rises. For example, an increase in LV peak –d *P*/d*t* from –1,500 to –1,800 mm Hg/sec could be caused by an increase in the rate of myocardial relaxation, a rise in aortic pressure, or both. An increase in peak negative d *P*/d*t* when aortic pressure is unchanged or declining, however, signifies an improvement of LV relaxation. LV peak –d*P*/d*t* is decreased during the myocardial ischemia of either angina pectoris or infarction and is increased in response to b-adrenergic stimulation and the phosphodiesterase inhibitor milrinone (63). It is not increased by digitalis glycosides.

Time Constant of Relaxation

Because of the load dependency of peak negative d*P*/d*t* and the fact that it uses information from only one point on the LV pressure-time plot, other indices have been introduced that analyze the time course of LV isovolumic pressure fall more completely. In 1976, Weiss and coworkers introduced the time constant *T* (or tau) of LV isovolumic pressure decline (64). They pointed out that LV isovolumic pressure decline could be fit by the equation

$$P = e^{At+B} \tag{17.6}$$

where *P* is LV isovolumic pressure, *t* is time after peak negative d*P*/d*t*, and A and B are constants. This can also be expressed as

$$\ln P = At + B \tag{17.7}$$

A plot of the natural logarithm of LV pressure versus time allows calculation of the slope A, a negative number whose units are sec^{-1}. The time constant *T* of isovolumic pressure fall is then defined as –1/A, expressed in milliseconds, and is the time that it takes *P* to decline 1/*e* of its value. Studies by the Johns Hopkins group have suggested that myocardial relaxation is normally complete by approximately 3.5 *T* after the onset of isovolumic relaxation. The normal value for *T* as calculated using a plot of ln *P* versus *t* is 25 to 40 msec in humans. Therefore, by 140 msec after the dicrotic notch, LV diastolic PV relations should be determined primarily by passive elastic properties of the myocardium. Because the normal LV diastolic filling period is more than 400 msec, it is unlikely, according to this concept, that late- and end-diastolic PV relations are still influenced by the relaxation process. However, there is now considerable evidence that even in the normal myocardium cross-bridge cycling persists to some extent throughout diastole. This resting myocardial activity or tone makes it difficult to know what significance to apply to the concept that relaxation is complete at 3.5 *T*. Nevertheless, it is important to emphasize that the relaxation process does progress with time through diastole, so that slowing of the process (prolongation of *T*) or shortening of the diastolic filling period (e.g., tachycardia) results in a greater resistance to early and even late diastolic filling.

Another approach to the measurement of *T* uses a more general equation to describe LV isovolumic pressure decline (65):

$$P = P_o e^{-t/T} + P_B \quad \textbf{(17.8)}$$

In this formulation, if diastole were infinite in duration (*t* = ¥), *P* would decay to a residual pressure, P_B. In the initial formulation by Weiss and coworkers (64), *P* always declines toward zero in long diastoles. The more general formula allows for two variables: *T* (which equals –1/A) and P_B. Work by Carroll and coworkers (66), as well other groups (63), has shown that both P_B and *T* can vary with physiologic maneuvers (e.g., exercise, ischemia). The biologic meaning of P_B is uncertain, although there has been speculation that it may reflect the level of diastolic myocardial tone. A problem with both P_B and *T* is that there is experimental evidence that the speed of the relaxation process itself is altered by myofiber stretch that occurs after mitral valve opening.

When *T* is to be derived from the formulas that assume a variable pressure intercept (P_B), the calculation is often accomplished by taking the first derivative (65):

$$P = P_o e^{-t/T} + P_B \quad \textbf{(17.9)}$$

$$dP/dt = -\frac{1}{T}(P - P_B)$$

Here, a plot of d*P*/d*t* versus ($P - P_B$) has the slope –1/*T*.

Normal values in humans for *T* calculated by either the logarithmic method (asymptote = 0) or the derivative method (variable asymptote) are listed in Table 17.4.

Interesting experimental data comparing the two methods of calculating *T* with a “gold standard” were published by Paulus and coworkers (67). They measured LV pressure decay with a micromanometer catheter during isovolumic beats generated using an Inoue balloon to occlude the mitral valve orifice in patients with mitral stenosis who were undergoing balloon valvuloplasty. LV pressure declined to an asymptote of 2 ± 3 mm Hg, and *T* was calculated from a monoexponental curve fit using the measured asymptote pressure. This *T* was considerably shorter than the *T* calculated by the derivative (variable asymptote) method and was much closer to the value obtained by the original Weiss logarithmic method (64), which assumes a zero asymptote.

Not only slow myocardial relaxation but also asynchrony of the relaxation process within the ventricular chamber results in a prolongation of *T*. In addition, *T* is probably not completely independent of loading conditions, although the influence of altered loading is relatively small. Measurement of *T* should be attempted only from LV pressure tracings obtained with high-fidelity, micromanometer-tipped catheters, or from fluid-filled systems with demonstrated optimal damping and high (more than 25 Hz) natural frequencies (see Chapter 7). Of interest, investigators have reported the *noninvasive assessment* of LV relaxation by continuous wave Doppler echocardiography in patients with some degree of mitral regurgitation (68,69). The Doppler mitral regurgitant velocity profile is recorded, digitized, and converted to ventriculoatrial pressure gradient curves with the use of the simplified Bernoulli equation and differentiated into instantaneous d*P*/d*t*. The relaxation time constant is then calculated assuming a zero-pressure asymptote (Fig. 17.15). In general, close correlations are seen between measurements of *T* made by this technique and those made from simultaneous LV micromanometer pressure measurements (68,69). However, accurate prediction of actual *T* was improved substantially when a measure of left atrial pressure was incorporated in the analysis.

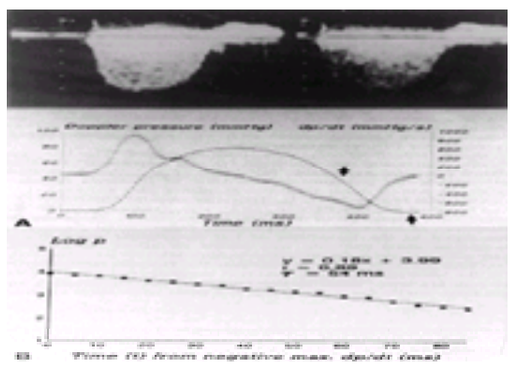

FIG. 17.15. Doppler technique for measuring left ventricular (LV) rate of pressure fall, d*P*/d*t*, and the time constant of LV relaxation (*T*, using Doppler mitral regurgitant velocity spectrum (**A,** *top*), LV–left atrial pressure gradient and its first derivative (**A,** *bottom*), and linear plot of log LV-estimated pressure (*p*) versus time (**B**), with *T* = 1/slope. (From C Chen et al. Doppler derived d*P*/d*t* and *T* in mitral regurgitation. *J Am Coll Cardiol* 1994;23:970, with permission.)

Volume-Derived Indices of Relaxation

Peak Filling Rate

After mitral valve opening, ventricular filling usually proceeds briskly with an initial rapid filling phase, a middle slow filling phase, and a terminal increase in filling rate associated with atrial systole. The rapid filling phase may be characterized by a maximum or peak filling rate (PFR) and time-to-PFR. PFR is usually determined by plotting LV volume against time, fitting the initial portion of this plot after mitral valve opening to a third- (or higher-) order polynomial, and solving for the first derivative of this polynomial. LV volume for this calculation may be obtained from the LV cineangiogram or from radionuclide techniques. As one might expect, PFR is preload dependent: interventions that raise left atrial pressure increase PFR, and interventions that reduce pulmonary venous return and left atrial pressure cause PFR to decrease (70). However, an increase in PFR that occurs when LV filling pressure (pulmonary capillary wedge pressure, left atrial pressure, or LV diastolic pressure) is unchanged or falling can reasonably be taken as an indication that LV relaxation has improved. For example, PFR has been shown to decrease during angina pectoris (71) when LV filling pressure is increasing. Because the rise in LV filling pressure by itself would cause an increase in PFR, the fall in PFR that is actually observed most likely indicates slowed relaxation of the myocardium, consistent with the other findings in this condition (fall in peak negative d*P*/d*t*, prolongation of *T*) that suggest impaired relaxation of the ischemic myocardium. PFR is reduced in patients with coronary stenoses, even in the absence of overt ischemia, and improves after coronary angioplasty (72). PFR is also reduced in patients with hypertrophic cardiomyopathy and improves after administration of a calcium-blocking agent (73). PFR is usually normalized for end-diastolic volume (EDV) and expressed as EDV/sec. Cardiac dilatation by itself tends to depress PFR, exaggerating its preload dependence.

Regional Diastolic Dysfunction

Diastolic dysfunction of specific regions of the left ventricle may be difficult to assess solely by examination of a global parameter of LV diastolic function such as the time constant of relaxation or the PFR. As pointed out by Pouleur and Rousseau (74), the time course of LV isovolumic pressure decline underestimates the severity of regional impairment in the rate of relaxation. Marked slowing of regional relaxation in an area of myocardial ischemia is partially masked by normal or enhanced rates of relaxation in adjacent normal regions of myocardium. Regional wall stress measurements have been proposed as an ideal way to assess regional rates of relaxation, but these can be made only by having knowledge of simultaneous LV pressure wall thickness and geometry (74).

A more practical way of assessing regional LV myocardial relaxation involves measurement of changes in regional LV chamber volume during isovolumic relaxation (Fig. 17.16) as well as regional PFR (75,76 and 77). Regional LV area may not be constant for each segmental area during “isovolumic” relaxation in the dysfunctional ventricle. Instead, some regions may increase while others decrease in area, due to either asynchrony or regional slowing of the relaxation process, with resultant differences in active wall tension in different parts of the left ventricle. An example of the application of this approach to measurement of regional myocardial relaxation is seen in a hemodynamic study by Friedrich and coworkers (75) of 20 adult patients with LV hypertrophy resulting from aortic stenosis (mean aortic valve area, 0.7 ± 0.2 cm^2). LV global diastolic function was abnormal, with a *T* of 58 ± 4 msec, and a time-to-PFR of 378 ± 63 msec. Enalaprilat, an angiotensin-converting

enzyme inhibitor, was infused into the left coronary artery, and regional LV diastolic function was assessed in both the anterior wall (perfused by enalaprilat) and the inferior wall. LV area change during isovolumic relaxation increased in anterior segments and decreased in inferior segments (Fig. 17.17), suggesting improved diastolic relaxation of the hypertrophied myocardium in response to angiotensin-converting enzyme inhibition (75), something seen previously only in animal experiments (76).

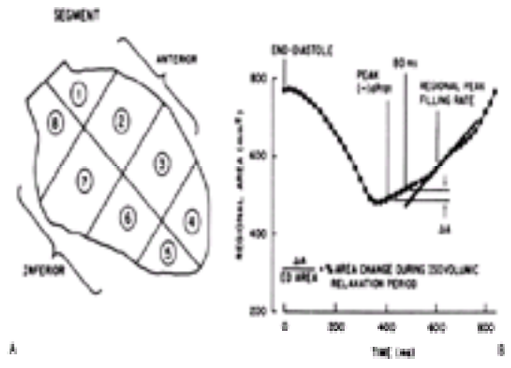

FIG. 17.16. Analysis of diastolic left ventricular (LV) regional wall motion. **A:** The LV silhouette is divided into eight segments. **B:** Regional area is plotted throughout the cardiac cycle, and the change in area (DA) during isovolumic relaxation (defined as the first 80 msec after peak rate of LV pressure fall) and regional peak filling rate are calculated. –d*P*/d*t*, maximum rate of LV pressure fall; ED, end-diastolic. (From Friedrich S, Lorell BH, Rousseau M, et al. Intracardiac angiotensin-converting enzyme inhibition improves diastolic function in patients with LV hypertrophy due to aortic stenosis. *Circulation* 1994;90:2761, with permission.)

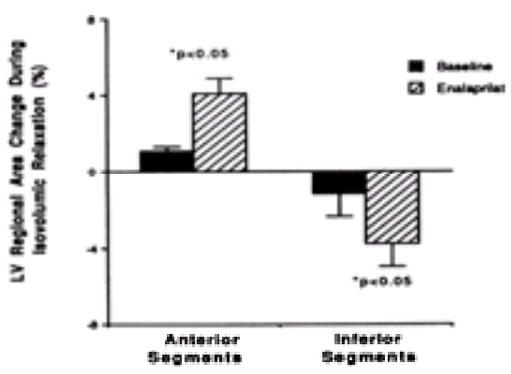

FIG. 17.17. Left ventricular (LV) regional area change during isovolumic relaxation before and after selective left intracoronary angiotensin-converting-enzyme (ACE) inhibition with enalaprilat in patients with marked LV hypertrophy and normal coronary arteries. Because total LV volume is constant during isovolumic relaxation, the increase in anterior segment area (presumably caused by improved myocardial relaxation due to regional ACE inhibition) is exactly counterbalanced by a decrease in inferior segment area. (From Friedrich S, et al. Intracardiac angiotensin-converting-enzyme inhibition improves diastolic function in patients with LV hypertrophy due to aortic stenosis. *Circulation* 1994;90:2761, with permission.)

Rate of Wall Thinning

Another index of diastolic function, similar in some ways to PFR, is the peak rate of diastolic LV wall thinning. This can be measured echocardiographically by plotting posterior or septal wall thickness against time, fitting the data to a polynomial, and taking the first derivative (77,78 and 79). The posterior wall thickness, *h*, and its first derivative, d*h*/d*t*, reflect regional diastolic function of the posterior wall myocardium. An advantage of peak negative d *h*/d*t* over PFR is that it assesses regional myocardial function, whereas PFR describes behavior for the whole ventricle and is insensitive when equal and opposite changes in diastolic function are occurring in different parts of the LV chamber. Peak negative d*h*/d*t* decreases during angina, even though LV filling pressure rises (79).

Various other indices of diastolic myocardial relaxation have been proposed. Most are imperfect, as are the ones discussed here. However, important information about diastolic relaxation and distensibility usually can be gleaned from examination of the parameters discussed in this chapter, taken in the context of the clinical setting and other hemodynamic findings in an individual patient.

CHAPTER REFERENCES

1. Parmley WW, Chuck L. Length-dependent changes in myocardial contractile state. *Am J Physiol* 1973;224:1194, 1973.
2. Lakatta EG. Starling's Law of the Heart is explained by an intimate interaction of muscle length and myofilament calcium activation. *J Am Coll Cardiol* 1987;10:1157, 1987.
3. Lew WYW. Time-dependent increase in left ventricular contractility following acute volume loading in the dog. *Circ Res* 1988;63:635, 1988.
4. Wiggers CJ. Studies on the cardiodynamic actions of drugs: I. The application of the optical methods of pressure registration in the study of cardiac stimulants and depressants. *J Pharmacol Exp Ther* 1927;30:217, 1927.
5. Gleason WL, Braunwald E. Studies on the first derivative of the ventricular pressure pulse in man. *J Clin Invest* 1962;41:80, 1962.
6. Grossman W, McLaurin LP, Saltz S, et al. Changes in inotropic state of the left ventricle during isometric exercise. *Br Heart J* 1973;35:697, 1973.
7. McLaurin LP, Rolett EL, Grossman W. Impaired left ventricular relaxation during pacing induced ischemia. *Am J Cardiol* 1973;32:751, 1973.
8. Feldman MD, Alderman J, Aroesty JM, et al. Depression of systolic and diastolic myocardial reserve during atrial pacing tachycardia in patients with dilated cardiomyopathy. *J Clin Invest* 1988;82:1661, 1988.
9. Mason DT, Braunwald E. Studies on digitalis: IX. Effects of ouabain on the nonfailing human heart. *J Clin Invest* 1963;42:1105, 1963.
10. Grossman W, Haynes F, Paraskos J, et al. Alterations in preload and myocardial mechanics. *Circ Res* 1972;31:83, 1972.
11. Brodie BR, Grossman W, Mann T, et al. Effects of sodium nitroprusside on left ventricular diastolic pressure-volume relations. *J Clin Invest* 1977;59:59, 1977.
12. Wallace AG, Skinner NS, Mitchell JH. Hemodynamic determinants of the maximal rate of rise of left ventricular pressure. *Am J Physiol* 1963;205:30, 1963.
13. Zimpfer M, Vatner SF. Effects of acute increases in left ventricular preload on indices of myocardial function in conscious, unrestrained and intact, tranquilized baboons. *J Clin Invest* 1981;67:430, 1981.
14. Broughton A, Korner PI. Steady-state effects of preload and afterload on isovolumic indices of contractility in autonomically blocked dogs. *Cardiovasc Res* 1980;14:245, 1980.
15. Barnes GE, Horwitz LD, Bishop VS. Reliability of the maximum derivatives of left ventricular pressure and internal diameter as indices of the inotropic state of the depressed myocardium. *Cardiovasc Res* 1979;13:652, 1979.
16. Gersh BJ, Hahn CEW, Prys-Roberts C. Physical criteria for measurement of left ventricular pressure and its first derivative. *Cardiovasc Res* 1971;5:32, 1971.
17. Fifer MA, Gunther S, Grossman W, et al. Myocardial contractile function in aortic stenosis as determined from the rate of stress development during isovolumic systole. *Am J Cardiol* 1979;44:1318, 1979.
18. Arentzen CE, et al. Force-frequency characteristics of the left ventricle in the conscious dog. *Circ Res* 1978;42:64, 1978.
19. Peterson KL, et al. Comparison of isovolumic and ejection phase indices of myocardial performance in man. *Circulation* 1974;49:1088, 1974.
20. Grossman W, Brooks HL, Meister SG, et al. New technique for determining instantaneous myocardial force-velocity relations in the intact heart. *Circ Res* 1971;28:290, 1971.
21. Sharir T, Feldman MD, Haber H, et al. Ventricular systolic assessment in patients with dilated cardiomyopathy by preload-adjusted maximal power. *Circulation* 1994;89:2045, 1994.
22. Paraskos JA, et al. A non-invasive technique for the determination of velocity of circumferential fiber shortening in man. *Circ Res* 1971;29:610, 1971.
23. Krayenbuehl HP, et al. High-fidelity left ventricular pressure measurements for the assessment of cardiac contractility in man. *Am J Cardiol* 1973;31:415, 1973.
24. Ross J Jr, et al. Left ventricular performance during muscular exercise in patients with and without cardiac dysfunction. *Circulation* 1966;34:597, 1966.
25. Ross J Jr, Braunwald E. The study of left ventricular function in man by increasing resistance to ventricular ejection with angiotensin. *Circulation* 1964;29:739, 1964.
26. McLaurin LP, Grossman W, Stefadouros M, et al. A new technique for the study of left ventricular pressure-volume relations in man. *Circulation* 1973;48:56, 1973.
27. Wynne J, Green LH, Grossman W, et al. Estimation of left ventricular volumes in man from biplane cineangiograms filmed in oblique projections. *Am J Cardiol* 1978;41:726, 1978.
28. Rankin LS, Moos S, Grossman W. Alterations in preload and ejection phase indices of left ventricular performance. *Circulation* 1975;51:910, 1975.
29. Suga H, Sagawa K, Shoukas AA. Load independence of the instantaneous pressure-volume ratio of the canine left ventricle and effects of epinephrine and heart rate on the ratio. *Circ Res* 1973;32:314, 1973.
30. Weber KT, Janicki JS, Reeves RC, et al. Factors influencing left ventricular shortening in isolated canine heart. *Am J Physiol* 1976;230:419, 1976.
31. Maughan WL, Sunagawa K, Burkhoff D, et al. Effect of heart rate on the canine end-systolic pressure-volume relationship. *Circulation* 1985;72:654, 1985.
32. Kass DA, Yamazaki T, Burkhoff D, et al. Determination of left ventricular end-systolic pressure-volume relationships by the conductance (volume) catheter technique. *Circulation* 1986;73:586, 1986.

33. Burkhoff D, Sugiura S, Yue DT, Sagawa K. Contractility-dependent curvilinearity of end-systolic pressure-volume relations. *Am J Physiol* 1987;252:H1218, 1987.
34. McKay RG, Miller MJ, Ferguson JJ, et al. Assessment of left ventricular end-systolic pressure-volume relations with an impedance catheter and transient inferior vena cava occlusion: use of this system in the evaluation of the cardiotonic effects of dobutamine, milrinone, Posicor and epinephrine. *J Am Coll Cardiol* 1986;8:1152, 1986.
35. Sagawa K, Suga H, Shoukas AA, et al. Endsystolic pressure/volume ratio: a new index of ventricular contractility. *Circulation* 1981;63:1223, 1981.
36. Grossman W, Braunwald E, Mann JT, et al. Contractile state of the left ventricle in man as evaluated from end-systolic pressure-volume relations. *Circulation* 1977;45:845, 1977.
37. McKay RG, Aroesty JM, Heller GV, et al. Assessment of the end-systolic pressure-volume relationship in human beings with the use of a time-varying elastance model. *Circulation* 1986;74:97, 1986.
38. Aroney CN, Herrmann HC, Semigran M, et al. Linearity of the left ventricular end-systolic pressure-volume relation in patients with severe heart failure. *J Am Coll Cardiol* 1989;14:127, 1989.
39. Starling MR, Walsh RA, Dell'Italia LJ, et al. The relationship of various measures of end-systole to left ventricular maximum time-varying elastance in man. *Circulation* 1987;76:32, 1987.
40. Borow KM, Neumann A, Wynne J. Sensitivity of end-systolic pressure-dimension and pressure-volume relations to the inotropic state in humans. *Circulation* 1982;65:988, 1982.
41. Konstam MA, Cohen SR, Salem DN, et al. Comparison of left and right ventricular end-systolic pressure-volume relations in congestive heart failure. *J Am Coll Cardiol* 1985;5:1326, 1985.
42. Kass DA, Midei M, Graves W, et al. Use of a conductance (volume) catheter and transient inferior vena caval occlusion for rapid determination of pressure-volume relationships in man. *Cathet Cardiovasc Diagn* 1988;15:192, 1988.
43. McKay RG, Spears JT, Aroesty JM, et al. Instantaneous measurement of left and right ventricular stroke volume and pressure-volume relationships with an impedance catheter. *Circulation* 1984;69:703, 1984.
44. Little WC. The left ventricular d P/dt_{max}–end-diastolic volume relation in closed-chest dogs. *Circ Res* 1985;56:808, 1985.
45. Marsh JD, Green LH, Wynne J, et al. Left ventricular end-systolic pressure-dimension and stress-length relations in normal human subjects. *Am J Cardiol* 1979;44:1311, 1979.
46. Ross J Jr. Afterload mismatch and preload reserve: a conceptual framework for the analysis of ventricular function. *Prog Cardiovasc Dis* 1976;18:255, 1976.
47. Gunther S, Grossman W. Determinants of ventricular function in pressure-overload hypertrophy in man. *Circulation* 1979;59:679, 1979.
48. Grossman W. Cardiac hypertrophy: useful adaptation or pathologic process? *Am J Med* 1980;69:576, 1980.
49. Borow KM, Neumann A, Marcus RH, et al. Effect of simultaneous alterations in preload and afterload on measurements of left ventricular contractility in patients with dilated cardiomyopathy: comparisons of ejection phase, isovolumetric and end-systolic force-velocity indexes. *J Am Coll Cardiol* 1992;20:787, 1992.
50. Henderson Y. Volume changes of the heart. *Physiol Rev* 1923;3:165, 1923.
51. Grossman W. Relaxation and diastolic distensibility of the regionally ischemic left ventricle. In: Grossman W, Lorell BH, eds. *Diastolic Relaxation of the Heart: Basic Research and Current Applications for Clinical Cardiology.* Boston: Martinus Nijhoff, 1988:193.
52. Glantz SA. Computing indices of diastolic stiffness has been counterproductive. *Fed Proc* 1980;39:162, 1980.
53. Zile MR. Diastolic dysfunction: detection, consequences, and treatment. Part 1: Definition and determinants of diastolic function. *Mod Concepts Cardiovasc Dis* 1989;58:67, 1989.
54. Gaasch WH, et al. Left ventricular stress and compliance in man: with special reference to normalized ventricular function curves. *Circulation* 1972;45:746, 1972.
55. Glantz SA, et al. The pericardium substantially affects the left ventricular diastolic pressure-volume relationship in the dog. *Circ Res* 1978;42:433, 1978.
56. Momomura SI, Bradley AB, Grossman W. Left ventricular diastolic pressure-segment length relations and end-diastolic distensibility in dogs with coronary stenoses: an angina physiology model. *Circ Res* 1984;55:203, 1984.
57. Lorell BH, et al. Right ventricular infarction: clinical diagnosis and differentiation from cardiac tamponade and constriction. *Am J Cardiol* 1979;43:465, 1979.
58. Vogel WM, et al. Acute alterations in left ventricular diastolic chamber stiffness: role of the “erectile” effect of coronary arterial pressure and flow in normal and damaged hearts. *Circ Res* 1982;51:465, 1982.
59. Watanabe J, Levine MJ, Bellotto F, et al. Effects of coronary venous pressure on left ventricular diastolic chamber distensibility. *Circ Res* 1990;67:923, 1990.
60. McKay RG, Aroesty JM, Heller GV, et al. The pacing thallium test reexamined: correlation of pacing-induced hemodynamic changes with the amount of myocardium at risk. *J Am Coll Cardiol* 1984;3:1469, 1984.
61. Lorell BH, Turi Z, Grossman W. Modification of left ventricular response to pacing tachycardia by nifedipine in patients with coronary artery disease. *Am J Med* 71:667, 1981.
62. Paulus WJ, Serizawa T, Grossman W. Altered left ventricular diastolic properties during pacing-induced ischemia in dogs with coronary stenosis: potentiation by caffeine. *Circ Res* 1982;50:218, 1982.
63. Monrad ES, McKay RG, Baim DS, et al. Improvements in indices of diastolic performance in patients with congestive heart failure treated with milrinone. *Circulation* 1984;70:1030, 1984.
64. Weiss JL, Frederiksen JW, Weisfeldt ML. Hemodynamic determinants of the time-course of fall in canine left ventricular pressure. *J Clin Invest* 1976;58:751, 1976.
65. Raff GL, Glantz SA. Volume loading slows left ventricular isovolumic relaxation rate. *Circ Res* 1981;48:813, 1981.
66. Carroll JD, Hess OM, Hirzel HO, et al. Exercise-induced ischemia: the influence of altered relaxation on early diastolic pressure. *Circulation* 1983;67:521, 1983.
67. Paulus WJ, Vantrimpont PJ, Rousseau MF. Diastolic function of the nonfilling human left ventricle. *J Am Coll Cardiol* 1992;20:1524, 1992.
68. Chen C, et al. Continuous wave Doppler echocardiography for noninvasive assessment of left ventricular d P/dt and relaxation time constant from mitral regurgitant spectra in patients. *J Am Coll Cardiol* 1994;23:970, 1994.
69. Nishimura RA, Schwartz RS, Tajik AJ, et al. Noninvasive measurement of rate of left ventricular relaxation by Doppler echocardiography: validation with simultaneous cardiac catheterization. *Circulation* 1993;88:146, 1993.
70. Chong CY, Herrmann HC, Weyman AE, et al. Preload dependence of Doppler-derived indexes of left ventricular diastolic function in humans. *J Am Coll Cardiol* 1987;10:800, 1987.
71. Aroesty JM, McKay RG, Heller GV, et al. Simultaneous assessment of left ventricular systolic and diastolic dysfunction during pacing-induced ischemia. *Circulation* 1985;71:889, 1985.
72. Bonow RO, et al. Improved left ventricular diastolic filling in patients with coronary artery disease after percutaneous transluminal coronary angioplasty. *Circulation* 1982;66:1159, 1982.
73. Bonow RO, et al. Effects of verapamil on left ventricular systolic function and diastolic filling in patients with hypertrophic cardiomyopathy. *Circulation* 1981;64:787, 1981.
74. Pouleur H, Rousseau M. Regional diastolic dysfunction in coronary artery disease: clinical and therapeutic implications. In: Grossman W, Lorell BH, eds. *Diastolic Relaxation of the Heart: Basic Research and Current Applications for Clinical Cardiology.* Boston: Martinus Nijhoff, 1988:245.
75. Friedrich SP, Lorell, BH, Rousseau MF, et al. Intracardiac angiotensin-converting enzyme inhibition improves diastolic function in patients with left ventricular hypertrophy due to aortic stenosis. *Circulation* 1994;90:2761, 1994.
76. Hayashida W, Kumada T, Kohno F, et al. Left ventricular regional relaxation and its nonuniformity in hypertrophic nonobstructive cardiomyopathy. *Circulation* 1991;84:1496, 1991.
77. Mason SJ, et al. Exercise echocardiography: detection of wall motion abnormalities during ischemia. *Circulation* 1979;59:50, 1979.
78. St. John Sutton MG, Tajik AJ, Smith HC, et al. Angina in idiopathic hypertrophic subaortic stenosis. *Circulation* 1980;61:561, 1980.
79. Bourdillon PD, Lorell BH, Mirsky I, et al. Increased regional myocardial stiffness of the left ventricle during pacing-induced angina in man. *Circulation* 1983;76:316, 1983.
80. Pouleur H, et al. Force-velocity-length relations in hypertrophic cardiomyopathy: evidence of normal or depressed myocardial contractility. *Am J Cardiol* 1983;52:813, 1983.
81. Hirota Y. A clinical study of left ventricular relaxation. *Circulation* 1980;62:756, 1980.
82. Thompson DS, et al. Analysis of left ventricular pressure during isovolumic relaxation in coronary artery disease. *Circulation* 1982;65:690, 1982.
83. Nonogi H, Hess OM, Bortone AS, et al. Left ventricular pressure-length relation during exercise-induced ischemia. *J Am Coll Cardiol* 1989;13:1062, 1989.

18
Evaluation of Myocardial Blood Flow and Metabolism

Tony M. Chou, Christian Zellner, and Morton J. Kern

TMC: University of California, San Francisco, School of Medicine, San Francisco, California 94143
CZ: Division of Cardiology, Cardiovascular Research Institute, University of California, San Francisco, School of Medicine, San Francisco, California 94143
MJK: Division of Cardiology, Saint Louis University School of Medicine, J.G. Mudd Cardiac Catheterization Laboratory, St. Louis, Missouri 63110

Measurement of myocardial blood flow for research studies and in clinical practice has enhanced our understanding of the coronary circulation in health and disease. Despite the refinements in measurement techniques of epicardial coronary anatomy provided by quantitative angiographic techniques and, more recently, by intravascular ultrasound, direct measurement of coronary blood flow provides important additional insights into functional aspects of coronary artery disease. In this chapter, we will review the wide variety of techniques that have been used to evaluate myocardial metabolism and blood flow with a focus on catheter-based methods. Particular emphasis will be placed on intracoronary translesional Doppler flow velocity and pressure measurements as simple and safe techniques for determination of coronary artery blood flow that can be clinically applied in the cardiac catheterization laboratory.

MYOCARDIAL METABOLISM

The myocardium relies almost exclusively on oxidative (aerobic) metabolism for its energy needs. Even at rest, transmyocardial oxygen extraction is already near maximal, with coronary venous oxygen saturation (25% to 35%) being the lowest in the body (1). Any increase in myocardial oxygen demand can thus be met primarily by a proportional increase in myocardial blood flow, chiefly mediated by a reduction in coronary arteriolar resistance. Such adjustments in coronary arteriolar resistance in response to alterations in demand (so-called autoregulation) permit the coronary circulation to maintain appropriate myocardial perfusion in the face of varying coronary perfusion pressure and oxygen demand (2,3).

Regional myocardial blood flow tracks mechanical activity by linkage through metabolic substrates: oxygen, glucose, free fatty acids, lactate, amino acids, and ketones. These substrates are critical for the generation of high-energy phosphates [adenosine triphosphate (ATP) and creatine phosphate] (4,5 and 6) that supply the energy requirements of the myocardium. At rest, the rate of force development and the frequency of force generation per unit time account for approximately 60% of myocardial energy utilization; myocardial relaxation accounts for approximately 15% of energy utilization; electrical activity accounts for 3% to 5%; and basal cellular metabolism accounts for the remaining 20% of energy utilization (5) (Fig. 18.1, Table 18.1). As workload increases, myocardial contractile function consumes an even greater fraction of high-energy phosphate availability. Any compromise in substrate availability causes the myocardium to minimize energy expenditure on mechanical work and divert the remaining high-energy substrates for the continued maintenance of cellular integrity.

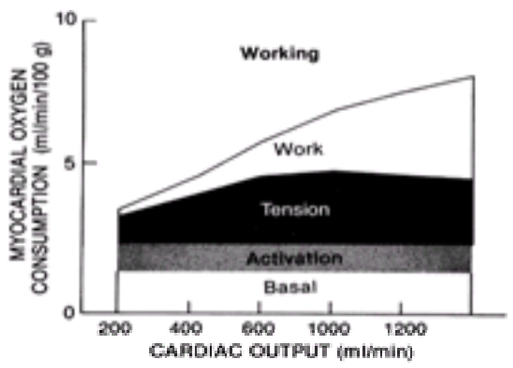

FIG. 18.1. Basal metabolism, activation energy, tension-related energy, and energy for external work as components of myocardial oxygen consumption in dogs at various levels of cardiac output. (With permission from Ando H, Nakano E, Ueno Y, Tokunaga K. New techniques for analysis of cardiac energetics using a modified Fenn equation. *J Thorac Cardiovasc Surg* 1989;97:565.)

Distribution			
Basal	20%	Volume work	15%
Electrical	1%	Pressure work	64%
Effects on MVO_2 of 50% increases in			
Wall stress	25%	Heart rate	50%
Contractility	45%	Volume work	4%
Pressure work	50%		

Note: The table demonstrates the dominant contribution to myocardial oxygen consumption (MVO_2) made by pressure work and prominent effects of increasing pressure work and heart rate on MVO_2. (Reproduced with permission from Gould KL. *Coronary artery stenosis*. New York: Elsevier, 1991:8.)

TABLE 18.1. *Myocardial oxygen consumption components total: 6–8 ml/min/100 g*

Under normal aerobic conditions, several substrates contribute simultaneously to meeting myocardial energy needs: free fatty acid (65%), glucose (15%), lactate and pyruvate (12%), and amino acids (5%) (4, 5 and 6). Under aerobic conditions, glycolysis plays only a minor role. Lactate is extracted by the myocardium, converted into pyruvate, and oxidized by way of the Krebs cycle (6).

In the fasting state, when serum fatty acids are high, myocardial glucose uptake tends to be suppressed by fatty acid utilization. After an oral glucose load, or when a fall in myocardial blood flow or oxygen supply leads to a reduction or loss in mechanical function, glucose uptake is enhanced and fatty acid oxidation declines (6). While glucose metabolism is initially aerobic, as oxygen availability decreases, high-energy phosphate stores are depleted and ATP breakdown products (adenosine diphoshpate, adenosine monophosphate, and other nucleosides) accumulate. The myocardium then turns toward enhancing glycogenolysis and glycolysis to augment ATP production. In doing so, the pyruvate-lactate equilibrium is shifted toward lactate formation, causing net transmyocardial lactate production rather than extraction. Under extreme conditions, increasing cytosolic lactate and hydrogen ion concentrations lead to inhibition of residual glycolysis and deprives the cell of even anaerobic ATP production, a sequence of biochemical events that may lead to complete cessation of energy production with irreversible cellular injury.

REGULATION OF CORONARY BLOOD FLOW IN HUMANS

Coronary blood flow is regulated primarily by the need to keep myocardial oxygen supply in balance with variations in oxygen demand resulting from changes in myocardial work. In the setting of constant aortic pressure, changes in coronary blood flow are modulated by coronary vascular resistance (CVR = coronary pressure/flow). Coronary vascular resistance, in turn, may be considered as the sum of three distinct resistance components (3): R_1 resides in the large epicardial coronary conduit vessels that function primarily as vascular capacitors and contribute minimally to total coronary vascular resistance in the absence of fixed or dynamic epicardial obstructions; R_2 resides in the precapillary arterioles and is the major component of coronary vascular resistance; and R_3 resides in the intramural coronary capillary vessels, where resistance increases markedly during systole due to mechanical compression during ventricular contraction. This phasic variation in R_3 explains the diastolic predominance of coronary blood flow.

Changes in epicardial (R_1) and arteriolar (R_2) coronary resistances during physiologic or pharmacologic stimuli can be considered either primary or secondary vasomotor events (Fig. 18.2). Primary vasodilation signifies an alteration in myocardial vessel tone and perfusion with no preceding change in myocardial oxygen demand. Secondary vasodilation refers to changes in vessel tone and blood flow that occurs in response to alterations in myocardial oxygen consumption (7).

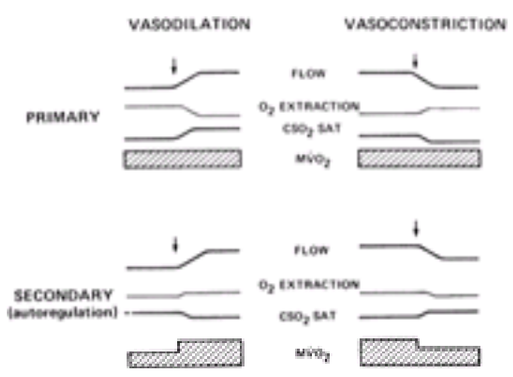

FIG. 18.2. Primary and secondary coronary vasomotion as determined by the simultaneous measurement of coronary blood flow (FLOW) and coronary venous oxygen saturation (CSO_2 SAT). Primary vasodilation causes a rise in flow at constant myocardial oxygen consumption ($M\dot{V}O_2$), resulting in lower transmyocardial oxygen extraction. In contrast, in secondary coronary vasodilation, an increase in myocardial oxygen consumption obliges a secondary rise in coronary blood flow with either constant or reduced coronary sinus oxygen saturation. (With permission from Baim DS, Rothman MT, Harrison DC. Simultaneous measurement of coronary venous blood flow and oxygen saturation during transient alterations in myocardial oxygen supply and demand. *Am J Cardiol* 1982;49:743.)

Coronary vasodilator reserve (also known as flow reserve) is the ability of a coronary vascular bed to increase coronary blood flow in response to stimuli that produce a maximal or near maximal hyperemic response. Such stimuli include the reactive hyperemia that follows transient coronary occlusion or the administration of various pharmacologic agents (8) (Fig. 18.3). Coronary flow reserve is expressed as the ratio of maximal hyperemic flow to resting coronary flow–a ratio that averages 4 to 7 in experimental animals and 2 to 5 in man (8,9). In experimental animal studies, increasing conduit stenosis (R_1) produces a predictable decline in coronary flow reserve, beginning at about a 60% artery diameter narrowing. At diameter stenoses of more than 80% to 90%, all available coronary reserve has been exhausted and resting flow begins to decline (10,11 and 12). This relationship between increasing stenosis severity and reduced available flow reserve has been used to assess the effective physiologic severity of any given coronary lesion and forms the basis of many noninvasive test modalities for ischemia. For individual patients, however, this relationship has been less predictable, given complex three-dimensional anatomy, imprecise correlation between angiographic estimate of diameter stenosis reduction and true lumen cross-sectional area, and thus the uncertain hemodynamic significance of a given lesion. In addition, flow measured in regions proximal to a stenosis in branching systems may not reflect poststenotic flow responses.

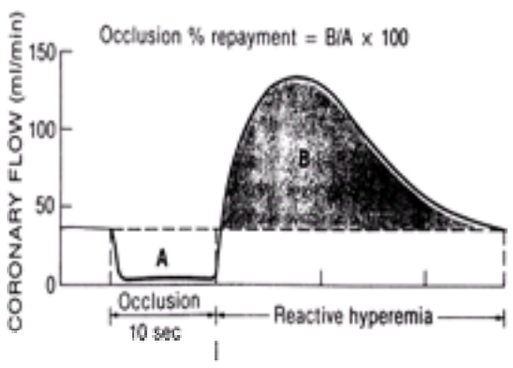

FIG. 18.3. Mean coronary flow before, during, and after coronary occlusion. *Arrow* indicates the release of occlusion. Area A represents the flow debt and area B its repayment. (With permission from Gould KL. *Coronary artery stenosis.* New York: Elsevier, 1991:13.)

Because coronary reserve flow represents a ratio of maximal over basal flow, the level of basal coronary flow also has an important effect on the reserve value (Fig. 18.4) (13). Increases in resting flow will lower the apparent reserve ratio in the absence of any other alterations. When using Doppler flow techniques, poststenotic flow reserve may differ from proximally measured flow reserve, depending on the contribution of prestenotic branch vessel distribution relative to the stenosis.

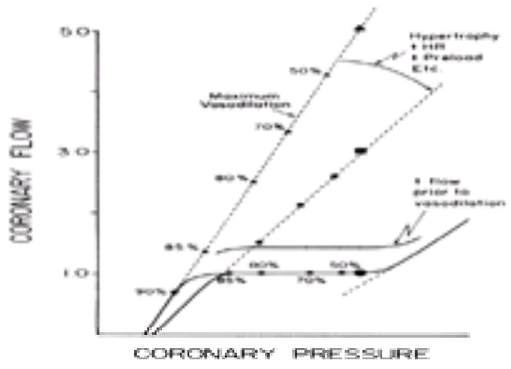

FIG. 18.4. Resting and maximally vasodilated coronary pressure—flow relationships. Coronary flow reserve, the ratio of maximally vasodilated over resting flow, can be seen to be a complex function of the actual position of the maximally vasodilated and resting flow curves. (With permission from Klocke FJ. Measurements of coronary flow reserve: defining pathophysiology versus making decisions about patient care. *Circulation* 1987;76:1183.)

MEASUREMENT OF MYOCARDIAL METABOLISM

Measurement of myocardial metabolism may be performed noninvasively (i.e., positron emission tomography scanning) or invasively by transmyocardial sampling techniques that involve acquisition of simultaneous arterial and coronary venous (i.e., coronary sinus) blood. Specialized blood products commonly used in the determination of changes in myocardial metabolism include serum pyruvate, lactate, oxygen content, and other metabolic or hematologic blood components. The transmyocardial extraction of pharmaceutical agents after systemic or intracoronary delivery can also be determined by the transmyocardial sampling technique. In studies involving ischemic myocardial metabolism, the most commonly measured products are lactate and oxygen. Specialized chilled collection tubes containing an agent (perchloric acid) to stop red cell metabolism and prevent clotting are prepared. Samples should be obtained in pairs and serial containers labeled in advance of the procedure. Measurement assays need to be geared to measuring small differences in “normal” lactate levels across the myocardium. Clinical laboratory tests geared to measuring high lactate levels in lactate acidosis are unsuitable for transmyocardial measurements. Myocardial catecholamines (norepinephrine, epinephrine) and other mediator products, such as prostaglandins, can be measured if sample tubes are placed immediately in ice to prevent platelet activation on withdrawal through a long, narrow catheter lumen. Large-bore (6F) heparin-coated catheters may be required to assess platelet products. In the setup of any measurement system for myocardial metabolism, advanced preparation of the sampling tubes should be made so that the operators can quickly draw and pass the blood to the technicians for insertion into the collection tubes. Additional equipment beyond the specific sample tubes may be needed, such as an iced bath, a centrifuge (in the laboratory), or a series of dilutional tubes. Although the techniques are not complicated, advanced preparation with correct labeling and anticipation of the tubes required during the various maneuvers in the laboratory will facilitate studies of myocardial metabolism without error or unnecessary prolongation of the study.

METHODS OF MEASURING BLOOD FLOW: INDIRECT AND NONINVASIVE TECHNIQUES

Several historically important techniques, including radionuclide clearance techniques and myocardial and coronary videodensitometry, have been described in detail in previous editions of this textbook. Other noninvasive diagnostic techniques such as positron emission tomography and magnetic resonance imaging play an increasingly important role in the determination of myocardial blood flow and function in clinical practice. The focus of this textbook lies in catheter-based methodologies that are reviewed in the following paragraphs.

ANGIOGRAPHIC ASSESSMENT OF CORONARY FLOW

Since its introduction by the Thrombolysis in Myocardial Infarction (TIMI) investigators in 1985 (14), a simple, qualitative grading of coronary flow (grade 0 through 3) to assess the efficiency of reperfusion therapy has become a standard in assessing coronary obstruction and restoration of flow in clinical trials. The reproducible angiographic quantification of coronary artery flow by TIMI grade is now widely accepted as a standard in the angiographic grading of coronary blood flow (15,16) and TIMI grade 3 flow has been associated with improved outcome (17,18 and 19).

According to the TIMI description (14,20), when assessing TIMI flow, cardiac catheterization should be performed using 6F or 7F diagnostic catheters. Cineangiograms should be filmed at 30 frames per second following administration of sublingual or intravenous nitroglycerin and thus can be incorporated very easily in the routine catheterization. Care should be taken to film vessel filling and emptying completely with careful panning.

The TIMI group defined the observed flow grades as follows: TIMI flow grade 0 represents no perfusion: There is no antegrade flow beyond the obstruction in an occluded artery. TIMI flow grade 1 represents penetration without perfusion: Contrast material passes beyond the area of obstruction but fails to opacify the entire coronary bed distal to the obstruction for the duration of the angiographic panning. TIMI flow grade 2 represents partial perfusion: Contrast material passes across the obstruction and opacifies the coronary artery distal to the obstruction. However, the rate of entry of contrast material into the vessel distal to the obstruction or its rate of clearance from the distal bed, or both, is perceptibly slower than the flow into or rate of clearance from comparable areas not perfused by the previously occluded or infarct-related vessel (e.g., opposite coronary artery or the coronary bed proximal to the obstruction). TIMI flow grade 3 represents complete perfusion: Antegrade flow into the bed distal to the obstruction, and clearance of contrast material from the involved bed is as rapid as clearance from an uninvolved bed in the same vessel or the opposite artery.

By nature, TIMI flow grading is qualitative rather than quantitative, and differences in TIMI flow grading by investigators and angiographic core laboratories have been reported (20). Anatomic differences between coronary arteries and global (multivessel) reduction in coronary flow after myocardial infarction contribute further to heterogeneity of coronary flow grading (20,21). Even a patent vessel with TIMI grade 3 flow may not be able to identify “normal” flow after myocardial infarction (20). The range of velocities that constitute TIMI flow grade 3 is wide (22) and velocities are frequently abnormal in both culprit and nonculprit arteries following myocardial infarction.

TIMI Frame Count

To overcome limitations of the initial TIMI classification, Gibson et al. introduced a quantitative and continuous measure, the TIMI frame count (20). The TIMI frame count is a standardized assessment of coronary flow using a simple continuous index: the number of cineframes required for contrast material to first reach standard distal coronary landmarks in the infarct-related artery. The first frame used for TIMI frame counting is the first frame in which dye fully spans the artery's takeoff. This occurs when three criteria are met: (a) a column of nearly full or fully concentrated dye must extend across the entire width of the origin of the artery; (b) dye must touch both borders of the origin of the artery; and (c) there must be antegrade motion of the dye (Fig. 18.5) . If the left anterior descending coronary artery is subselectively engaged and the left circumflex coronary artery is the culprit vessel, the TIMI frame count begins when dye first touches both borders at the origin of the left circumflex coronary artery. The same rule holds for subselective engagement of the left circumflex artery. The last frame is counted or included as one of the frames and is defined as the frame when dye first enters the distal landmark branch. Full opacification of the distal branch is not required. Often the last frame is best determined by running the cinefilm past the initial opacification of the end point branch and then moving frame by frame in reverse until the end point branch disappears. Care must be taken to advance one frame forward once the dye disappears to identify the frame in which dye first appears. The following distal landmark branches are used for analysis: the distal bifurcation of the left anterior descending coronary artery (i.e. the “mustache,” “pitchfork,” or “whale's tail”; Fig. 18.6, top); in the circumflex system, the distal bifurcation of the segment with the longest total distance that includes the culprit lesion (Fig. 18.6, middle); and in the right coronary artery, the first branch of the posterolateral artery (Fig. 18.6, bottom). Proper panning is essential for counting the number of cineframes required to first opacify the

distal artery, particularly with the left anterior descending. The TIMI frame count of the left anterior descending and circumflex arteries often is assessed best in either the right or left anterior oblique views with caudal angulation, and the right coronary artery often is assessed best in the left anterior oblique projection with steep cranial angulation. Because of the frame rate variations in catheterization laboratories, frame counts need to be adjusted to 30 frames per second.

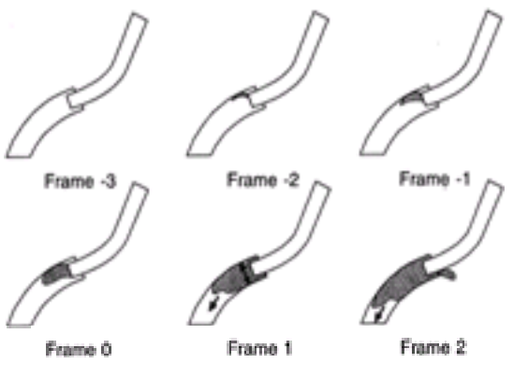

FIG. 18.5. Definitions of the first and last frames used for TIMI frame counting. The first frame used for TIMI frame counting is the first frame in which dye fully enters the artery. This occurs when three criteria are met: (a) A column of nearly full or fully concentrated dye must extend across the entire width of the origin of the artery; (b) dye must touch both borders of the origin of the artery; and (c) there must be antegrade motion of the dye. Dye may initially track down a single wall of the artery as it leaks from catheter before the injection, and these frames are not included in the TIMI frame count. (With permission from Gibson CM, Cannon CP, Daley WL, et al. TIMI frame count: a quantitative method of assessing coronary artery flow. *Circulation* 1996;93:879.)

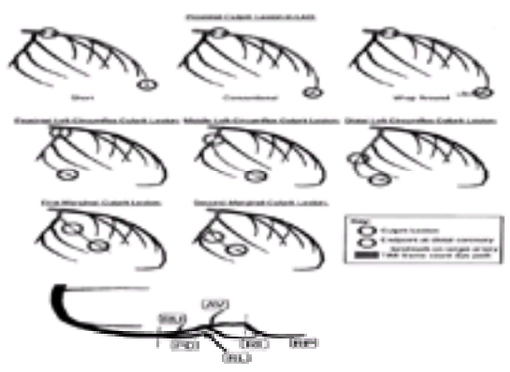

FIG. 18.6. Top: Anatomic landmarks used for TIMI frame counting in the left anterior descending coronary artery. The distal-most branch in the left anterior descending coronary artery (referred to as the “pitchfork,” “mustache,” or “whale's tail”) usually occurs at the apex of the heart. In a wraparound left anterior descending coronary artery, the branch closest to the apex of the heart is used. Middle: Anatomic landmarks used for TIMI frame counting in the left circumflex coronary artery. The branch of the left circumflex coronary artery used for TIMI frame counting is determined as follows: The artery used for TIMI frame counting is the artery with the longest total distance along which dye travels in the left circumflex coronary artery system and yet passes through the culprit lesion. When the culprit lesion is proximal to two arteries with equal total dye path distances, the artery that arises more distally from the left circumflex coronary artery is used. For example, when the culprit lesion is located in the proximal left circumflex coronary artery, the marginal branch with the longest total dye path distance is used, regardless of whether it is the first, second, or third marginal branch. If these second and third marginals have equal total dye path distances, the third marginal branch is the target artery. The target artery is always the first marginal branch when the culprit lesion is in the first marginal and, likewise, always the second marginal branch when the culprit lesion is in the second marginal. In left and balanced dominant systems, the target artery is no further distal than the marginal branch that lies at the border of the inferior and lateral walls, usually the third or fourth marginal. The anatomic end point is the distal-most branch in the target artery. Usually, this end point branch can be found at approximately the midpoint of the distal third of the artery (five-sixths of the distance down the vessel from its origin), but occasionally it is located just before the termination of the artery. **Bottom:** Anatomic landmarks used for TIMI frame counting in the RCA. The distal landmark is the first branch arising from the posterior lateral extension of the RCA after the origin of the posterior descending (PD) artery, regardless of the size of this branch. As shown, this branch will often be located just distal to the bifurcation and may be oriented either superiorly (RU) or inferiorly (RL). In some cases, this branch will lie further along the extension of the distal RCA and either will course superiorly as the AV nodal artery (AV) or will be oriented inferiorly as the right inferior branch (RI). In the event that a very proximal posterior descending stenosis is the culprit lesion, the first branch off the posterior descending artery after the stenosis is the end point. Infrequently, the distal portion of the posterior descending artery is supplied by a proximally arising acute marginal branch, and the proximal portion of the posterior descending artery arises at the base of the heart. In these cases, it is the extension of the distal RCA past the posterior descending artery at the base of the heart and not the proximal acute marginal branch that is used for determining the TIMI frame count. In patients with left dominant anatomy, the TIMI frame count end point is the distal-most branch of the RCA once it is no longer in the atrioventricular groove. (Modified with permission from Gibson CM, Cannon CP, Daley WL, et al. TIMI frame count: a quantitative method of assessing coronary artery flow. *Circulation* 1996;93:879.)

The Corrected TIMI Frame Count (CTFC) for the Left Anterior Descending Coronary Artery

The initial experience with the TIMI frame count demonstrated that the length of the left anterior descending coronary artery influences the observed frame count. The TIMI frame count in the left anterior descending coronary artery requires recalculation before comparing flow in the three major coronary conduits and is called the corrected TIMI frame count. Anatomically, the left anterior descending is the longest of the three coronary conduits. The approximate distance to the TIMI landmark in the average human left anterior descending coronary artery is 14.7 cm; in the right coronary artery, 9.8 cm; and in the left circumflex coronary artery, 9.3 cm (20). The corrected TIMI frame count (CTFC) accounts for the longer distance dye has to travel to opacify the left anterior descending coronary artery. The frame rate required for full opacification of the distal end point of the left anterior descending is 1.7 times longer when compared with the right coronary artery and the left circumflex coronary artery. The CTFC divides the absolute frame count in the left anterior descending coronary artery by 1.7 to standardize the distance dye and has to travel in all three coronary conduits. TIMI frame count and CTFC reference values are shown in Table 18.2.

	Average	RCA	LCx	CTFC (LAD)	LAD
Normal	21.0 ± 3.1 (16–31)	20.4 ± 3.0 (16–26)	22.2 ± 4.1 (16–31)	21.1 ± 1.5 (18.8–24.1)	36.2 ± 2.6 (32–41)
Nonculprit at 90 min	35.5 ± 9.8 (16–57)	24.6 ± 7.1 (13–36)	22.5 ± 8.3 (10–52)	30.6 ± 11.5 (16.5–57.1)	52.3 ± 19.6 (28–97)
Culprit at 90 min	59.2 ± 20.0 (13–164.7)	37.2 ± 19.3 (13–112)	33.7 ± 9.8 (19–61)	43.8 ± 22.6 (17.1–164.7)	74.5 ± 38.4 (29–280)

Note: TIMI Frame Counts and Corrected TIMI Frame Counts (CTFC) in coronary arteries without epicardial stenoses (normal) and in nonculprit and culprit arteries 90 minutes after myocardial infarction. Where RCA is right coronary artery, LCx is left circumflex coronary artery, and LAD is left anterior descending coronary artery. Values are expressed as frames ± standard deviation and 95% confidence intervals. (Adapted with permission from Gibson CM, Cannon CP, Daley WL, et al. TIMI frame count: a quantitative method of assessing coronary artery flow. *Circulation* 1996;93:879.)

TABLE 18.2. *Reference values for TIMI frame counts*

Angioplasty Guidewire Velocity

A new method recently proposed to measure absolute coronary velocity and absolute flow uses TIMI frame counting and a guidewire-derived measure of intravascular distance between ostium and TIMI landmark (23) (Fig. 18.7). Velocity is then calculated using the following formula:

$$\text{Velocity (cm/sec)} = \text{Distance separating Kelly clamps (cm)} / (\text{frame count/frames per second})(\text{sec})$$

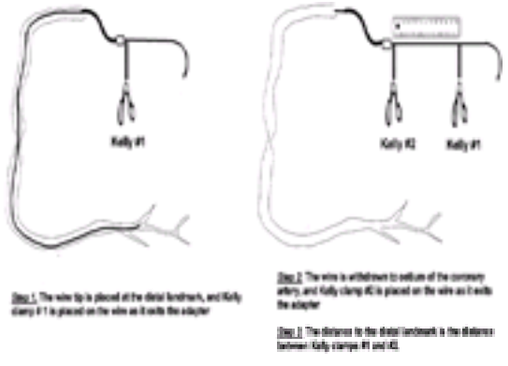

FIG. 18.7. Method of measuring the distance from coronary ostium to the distal TIMI frame count landmark using the guidewire pullback technique. A standard guidewire is positioned with its tip at the TIMI landmark. A Kelly clamp (no. 1) is placed on the guidewire where it exits the Y-adapter. The wire is then withdrawn to the guiding catheter tip. A second Kelly clamp (no. 2) is then placed on the wire. The distance between the two clamps represents the distance from the guiding catheter tip to the coronary landmark. (With permission from Gibson CM, Dodge JT Jr, Goel M, et al. Angioplasty guidewire velocity: a new simple method to calculate absolute coronary blood velocity and flow. *Am J Cardiol* 1997;80:1536.)

The angioplasty guidewire velocity may prove useful as a measure of coronary flow. When compared with the CTFC, it may be superior because it takes into account variability in artery length from patient to patient. Usefulness and applicability in clinical practice remain to be evaluated.

Limitations and Practical Use of the TIMI Flow and TIMI Frame Count

Gibson et al. (20) and Kern et al. (22) suggested that visual estimates of TIMI flow in the usual clinical setting bear little relationship to the more precise TIMI frame count or Doppler flow measurements, and that even noninfarct-related coronary arteries show prolonged flow when compared with normal values. Most likely, prolonged TIMI frame counts are associated with microvascular dysfunction (21), even in the presence of an open artery. Gibson et al. (24) further investigated the predictive value of CTFC on clinical outcome in patients undergoing thrombolytic therapy in the TIMI 4, 10A, and 10B trials. They found that a CTFC of less than 20 frames per second (or brisk flow) was associated with a low risk for adverse outcomes, both for in- and out-of-hospital events (24). This was particularly true for a subgroup of patients with hyperemic flows of less than 14 frames per second. CTFCs of greater than 20 but less than 40 frames per second (the cutoff value for TIMI grade 3 flow) showed a higher risk for adverse outcome (24). Prolonged CTFCs 4 weeks after myocardial infarction appear to be associated with impaired infarct-artery-related flow at 1 year (25) and may give insight into why complete reperfusion by invasive strategies does not uniformly translate into better outcome.

Technique can also impact on the rate of angiographic opacification. For example, the rate of contrast injections can cause variations in CTFCs. Dodge et al. (26) investigated the impact of injection rate on the CTFC. Using standard 7F diagnostic catheters, they found that a mean increase of 1.0 mL/sec of standard hand injections (10th to 90th percentile of left coronary injections: 1.5 to 2.5 mL/sec; right coronary injections: 1.1 to 2.1 mL/sec) induced a decrease of two frames in the CTFC.

In summary, TIMI frame counting is a simple, reproducible method for the assessment of coronary flow that is applicable in virtually every patient and catheterization laboratory. TIMI frame counting provides additional valuable information related to treatment success and clinical outcome.

CATHETER TECHNIQUES FOR MEASUREMENT OF CORONARY BLOOD FLOW

Coronary Sinus Thermodilution and Oximetry

The measurement of coronary venous flow is inexpensive and can be performed with only right heart cardiac catheterization. Unlike coronary arterial flow, however, coronary venous flow occurs predominantly during *systole*. Approximately two-thirds of left anterior descending coronary artery flow drains into the great cardiac vein, the continuation of the anterior intraventricular vein as it reaches the atrioventricular groove. The great cardiac vein then becomes the coronary sinus, at the point marked by the valve of Vieussens and the oblique vein of Marshall (a left atrial venous remnant of the embryonic left-sided superior vena cava). The remaining portion of left anterior descending venous drainage enters the coronary sinus along with blood from the circumflex territory, by way of the left marginal vein and circumflex venous branches. Great cardiac vein flow thus represents primarily left anterior descending venous outflow, whereas coronary sinus flow represents a mixture of both left anterior descending and left circumflex coronary artery outflow, accounting for 80% to 85% of total left coronary outflow drained by this route (27,28).

Measurement of coronary venous flow is based on the principle of thermodilution, with the principle that the heat loss by blood equals the heat gained by a cold indicator solution (Fig. 18.8). Room temperature fluid (5% dextrose or normal saline) is injected upstream in the coronary sinus for 20 to 30 seconds at a rate of 35 to 55 mL/min (using a 200-mL Harvard pump or angiographic power injector to ensure turbulent mixing with venous blood). Coronary venous flow is then computed according to the following formula (28,29):

$$Q = F \times C \times (T_m - T_I)/(T_b - T_m)$$

where Q is coronary venous flow, F is the rate of injection of the thermodilution indicator, C is the ratio of the specific heats of blood and the injectate (equaling 1.08 for 5% dextrose and 1.19 for normal saline), and T_m, T_I, and T_b are the temperatures of the mixture, the injectate, and blood, respectively.

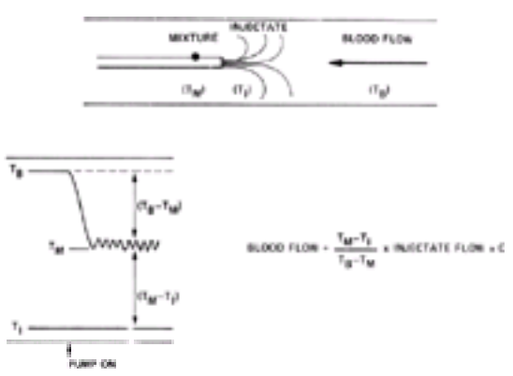

FIG. 18.8. Schematic diagram of the thermodilution technique. The thermal indicator (injectate) at temperature T_I is infused at fixed rate, typically 50 mL/min. The ensuing turbulence causes mixing of the injectate with coronary venous blood at temperature T_B, resulting in a mixture at temperature T_M. The temperatures monitored by the catheter tip (T_B and T_M) and injectate (T_I) thermistors are recorded continuously on a uniform temperature scale. Because the heat lost by blood is gained by the injectate, coronary venous flow can be calculated using the respective measured temperatures, the rate of indicator injection, and a constant derived from the specific heats of blood and injectate. (With permission from Bradley BA, Baim DS. Measurement of coronary blood flow in man: methods and implication for clinical

practice. *Cardiovasc Clin* 1985;15:67.)

Coronary sinus catheters are currently only available upon request for investigational studies (Cordis Webster, Baldwin Park, CA; Baim Electro-catheter, Rahway, NJ). Their clinical utility is enhanced by incorporation of various key features. The presence of two sampling thermistors allows simultaneous selective measurement of left anterior descending and more proximal coronary sinus flow by a catheter whose tip is positioned at the great cardiac vein (Fig. 18.9). Pacing electrodes facilitate the measurement of blood flow changes at a constant heart rate maintained by coronary sinus pacing. Reflectance oximetry allows the continuous measurement of great cardiac vein oxygen saturation and permits on-line determination of regional myocardial oxygen consumption ($M\dot{V}O_2$) (7):

$$M\dot{V}O_2 = Q \times (A_{O_2} - CS_{O_2})$$

where Q equals coronary venous flow, A_{O_2} is arterial, and CS_{O_2} is coronary sinus oxygen contents, respectively.

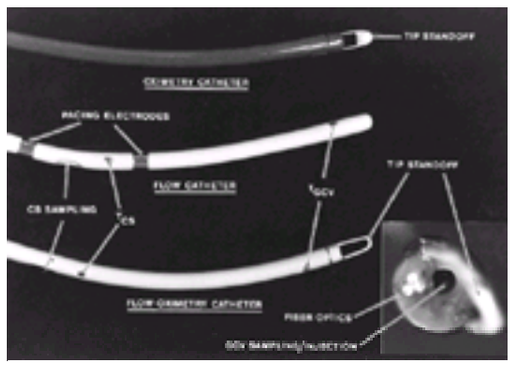

FIG. 18.9. Coronary venous oximetry, thermodilution flow, and combined flow oximetry catheters (top to bottom). The flow and flow oximetry catheters have the following features in common: two lumina for indicator injection or sampling at the great cardiac vein (see inset) and coronary sinus sites and two great cardiac vein (T_{GCV}) and coronary sinus (T_{CS}) thermistors for regional flow determinations. The flow catheter additionally has two pacing electrodes. The oximetry and flow oximetry catheters have fiberoptic bundles for the continuous measurement of great cardiac vein oxygen saturation. (With permission from Baim DS, Rothman MT, Harrison DC. Simultaneous measurement of coronary venous flow and oxygen saturation during transient alterations in myocardial oxygen supply and demand. *Am J Cardiol* 1982;49:743.)

The coronary sinus is located posteriorly and slightly caudal to the tricuspid annulus. Coronary sinus cannulation has traditionally been performed from a left brachial approach because a catheter with a single curve easily enters the ostium of the coronary sinus from the left arm in the majority of patients. Although a right brachial or femoral venous approach is feasible using a reverse loop technique in which the catheter is rotated so that its tip lies posterior to its shaft in the right anterior oblique projection, the easiest approach to the coronary sinus is via the right internal jugular vein. With this approach, the catheter tip is initially pointed laterally toward the right atrial border. The catheter is then rotated counterclockwise and advanced slightly until it just enters the right ventricle (detected by pressure waves or premature ventricular contractions). After slight additional counterclockwise rotation, the catheter is withdrawn slowly until an atrial pressure tracing is restored. Gentle readvancement of the catheter from this position leads to cannulation of the coronary sinus. Should the right ventricle be reentered, the same maneuver is repeated with accentuation of counterclockwise rotation.

Successful coronary sinus entry is confirmed by the maintenance of a right atrial pressure waveform as the catheter is smoothly advanced across the plane of the tricuspid valve. During catheter advancement, catheter resistance suggests impingement on venous branches or the valve of Vieussens. If slight catheter repositioning fails to correct the situation, the anatomic obstacle can usually be crossed with a 0.018-inch soft-tipped angioplasty guidewire, allowing advancement of the catheter over this wire to reach the desired sampling site in the great cardiac vein. The coronary sinus is a thin-walled venous structure that can be easily perforated with the application of force. Care should be taken to ascertain correct intravascular position before catheter manipulation.

Reproducible coronary sinus or venous flow measurements require a stable catheter position to avoid variable inclusion of blood entering from venous tributaries adjacent to the temperature thermistor. The proximal (coronary sinus) thermistor needs to be positioned at least 2 to 3 cm from the sinus ostium to avoid reflux of right atrial blood contaminating the coronary sinus temperature profile. Typically, the most stable position for the catheter tip is near the point where the anterior interventricular vein meets the great cardiac vein. This position also provides a selective measurement of left anterior descending coronary artery territory outflow (Fig. 18.10).

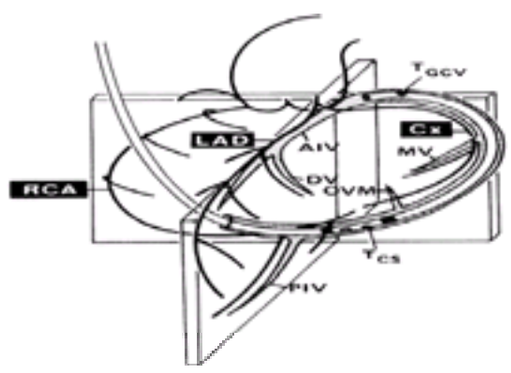

FIG. 18.10. Schematic diagram of the cannulated coronary venous system in relation to the coronary artery anatomy: diagonal vein (DV), anterior interventricular vein (AIV), marginal vein (MV), oblique vein of Marshall (OVM), posterior interventricular vein (PIV), and the right, left anterior descending, and circumflex coronary arteries (RCA, LAD, CX, respectively). (With permission from Baim DS, Rothman MT, Harrison DC. Simultaneous measurement of coronary venous flow and oxygen saturation during transient alterations in myocardial oxygen supply and demand. *Am J Cardiol* 1982;49:743.)

Coronary venous flow measurements are easy to perform, are inexpensive, and can be done at low risk to the patient. The approach allows insights into regional (left anterior descending) myocardial flow and metabolic changes. Serial measurements can be performed to detect transient changes in flow and oxygen extraction (30). The technique, however, has several limitations. It does not allow assessment of phasic or very rapid changes in coronary flow. Transmural myocardial perfusion also cannot be assessed. Regionality of flow measurements is confined to the left anterior descending territory. The technique is extremely sensitive to alterations in catheter position and is insufficiently validated for flow measurements in severe coronary artery disease. Coronary venous flow data tend to significantly underestimate coronary flow reserve. Rarely, coronary sinus thrombosis has been reported to occur as a result of right atrial and coronary sinus instrumentation, particularly in the setting of heart failure.

Coronary Arterial Flow: Doppler Guidewire Techniques

The change in sound frequency as a transmitter moves to or away from a receiver is called the Doppler effect (Christian Johann Doppler, 1803 to 1853). The change in frequency is related to the transmitter's velocity. In practice, a piezoelectric crystal that both emits and receives high-frequency sounds can be mounted on the tip of

an intravascular catheter to measure the velocity of red blood cells flowing through an artery (Fig. 18.11). Coronary flow velocity is calculated from the difference between the transmitted and returning frequency (call the Doppler frequency shift), using the following equation:

$$\text{Velocity} = \frac{(f_o - f_d)(C)}{(2F_0)(\cos\ \phi)}$$

where *V* is the velocity of blood flow, f_o is the transmitting (transducer) frequency, f_d is the returning frequency, *C* is a constant (speed of sound in blood), and f is the angle of incidence, respectively.

FIG. 18.11. Diagram of the Doppler concept. High-frequency ultrasound (f_o) is emitted from the Doppler crystal and is reflected off the moving red cell at frequency f_d. The difference between these two frequencies is termed the *Doppler shift* and is directly related to the velocity of red cells moving. (With permission from Kern MJ, Aguirre FV, Bach RG, Caracciolo EA, Donohue TJ, Labovitz AJ. Fundamentals of translesional pressure-flow velocity measurements. *Cathet Cardiovasc Diagn* 1994;31:137.)

When the transducer beam is nearly parallel to blood flow and f is zero (cos f = 1), velocity can be measured optimally with changes in blood flow velocity reflected by changes in the Doppler frequency shift. Intracoronary Doppler has several advantages for the assessment of coronary blood flow. It measures red blood cell velocity directly so that indicator-dilution markers are not required. Volumetric blood flow can be calculated as the product of angiographically measured vessel cross-sectional area and mean flow velocity with a correction factor for parabolic flow profile across the vessel. When the vessel cross-sectional area remains constant, however, changes in Doppler coronary flow velocities can be used to represent changes in absolute coronary flow. Technical advances using spectral signal analysis and guidewire-mounted Doppler crystals have improved the reliability and safety of intracoronary blood flow velocity measurements.

Intracoronary Doppler Guidewire

The advent of a Doppler-tipped guidewire (FloWire, Endosonics, Rancho Cordova, CA) has overcome the limitations of catheter-based determination of intracoronary Doppler velocity measurements. The flowire is an 0.014- to 0.018-inch diameter, 175-cm-long, flexible and steerable guidewire with a 12- to 15-MHz piezoelectric ultrasound transducer integrated onto the tip (Fig. 18.12). The forward-directed ultrasound beam diverges at 27° from the Doppler transducer so that the Doppler sample volume is approximately 0.65 mm thick by 2.25 mm in diameter when range-gated to 5.2 mm beyond the transducer (31). The signal transmitted from the piezoelectric transducer is processed from the quadrature Doppler audio signal by real-time spectral analyzer using on-line fast Fourier transformation providing a scrolling gray scale spectral display (Fig. 18.13).

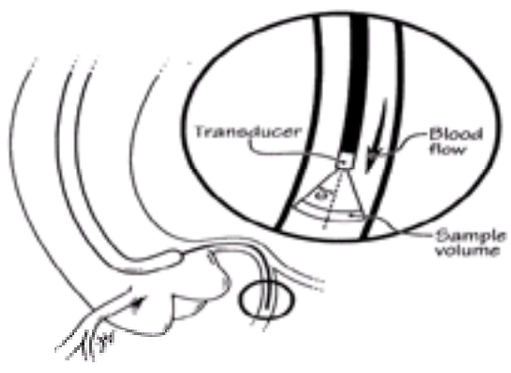

FIG. 18.12. Diagram of coronary Doppler flowire placed in the proximal segment of a coronary artery through a diagnostic catheter. The 12-MHz transducer has a sample volume located approximately 5.2 mm from the tip with a beam spread of 27°. The angle of incidence (theta) is less than 17°. Magnitude and direction of flow are easily determined by the spectral flow velocity. (With permission from Ofili EO, Kern MJ, Labovitz AJ, et al. Analysis of coronary blood flow velocity dynamics in angiographically normal and stenosed arteries before and after endolumen enlargement by angioplasty. *J Am Coll Cardiol* 1993;21:308.)

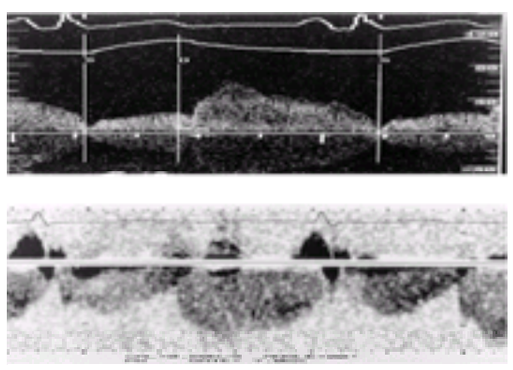

FIG. 18.13. Comparison of coronary spectral flow velocity by two Doppler techniques. **Top:** Flow velocity spectra in a normal coronary artery using the intracoronary Doppler guidewire. **Bottom:** Flow velocity in the left anterior descending artery obtained with transesophageal echocardiography. Note the similarities of phasic pattern, although the direction of flow is inverted for the transesophageal Doppler signal. Scale for top panel: 0 to 160 cm/sec. Scale for bottom panel: 20 cm/division. Peak flow velocity for both signals is approximately 50 cm/sec.

Poststenotic regional flow velocity can be accurately recorded. Since the Doppler guidewire has a minimal cross-sectional area of 0.164 mm^2, it tends to be nonobstructive within any but the tightest coronary lesion and to create less disturbance of the flow profile distal to its tip, even when placed within small coronary arteries. The physical properties of the Doppler guidewire are designed for crossing intracoronary arterial obstructions and maintaining a stable position in the distal coronary artery during coronary angioplasty and other interventional procedures. Easily recognized phasic coronary flow velocity measurements are readily incorporated into a typical angioplasty procedure without adding new or unnecessary complex technical maneuvers.

The Doppler guidewire has been validated during intravascular measurements of coronary arterial flow velocity by Doucette et al. (31), who found an excellent correlation (r^2= 0.936) between Doppler spectral flow velocity using the guidewire and electromagnetic flow probes in proximal coronary arteries in dogs. The Doppler guidewire accurately measures phasic flow velocity patterns and linearly tracks changes in flow rates in small, predominantly straight coronary arteries.

Setting up of the guidewire system usually takes less than 10 minutes. It is easily incorporated into routine angioplasty procedures and provides additional physiologic information on lesion severity and responses to balloon occlusions; it also monitors flow in the postprocedural period without the need for frequent contrast injections.

Measurement of Translesional Velocity

Complete assessment of an epicardial stenosis utilizing arterial flow velocity requires access to both proximal and poststenotic flow velocity data. After diagnostic angiography and before angioplasty, the Doppler guidewire is passed through a standard angioplasty Y-connector attached to either an angiographic or guiding catheter. The flowire is then advanced into the target artery. Baseline flow velocity data are obtained at least 1 cm proximal to the target lesion. The flowire is then advanced distally by a distance equivalent to approximately five to ten times the arterial diameter (2 cm) beyond the stenosis. Placement in any side branch is avoided. Distal flow velocity data are then obtained in a similar manner. If the ratio of proximal-to-distal flow velocity integral is more than 1.7:1, the stenosis is significant (see later discussion).

Pharmacologic Agents Used to Induce Maximal Hyperemia

Stenosis severity can be assessed more accurately using flow measurements during maximal hyperemia. Widely used vasodilator agents are dipyridamole, papaverine, and adenosine. The hyperosmolar ionic and low-osmolar nonionic contrast media have also been used, but they do not produce maximal vasodilatation. On the other hand, maximal hyperemia can be obtained by intracoronary injections of adenosine (8 to 18 µg in the right coronary artery and 12 to 18 µg in the left coronary artery), or papaverine (10 to 12 mg). Papaverine (8 to 12 mg) produced a response equal to that of an intravenous infusion of dipyridamole in a dose of 0.56 to 0.84 mg/kg of body weight (32) but can occasionally cause ventricular arrhythmias. Nitrates also cause similar increases in volumetric flow, but since these agents also dilate epicardial conductance vessels, the increase in coronary flow velocity is less pronounced.

Intracoronary papaverine, which produces maximal coronary vasodilation, has been reported to increase coronary blood flow velocity four to six times over the resting value in patients with normal coronary arteries (33). In these series, however, a highly selected patient population was studied, with the exclusion of patients with myocardial hypertrophy, previous myocardial infarction, or any other condition known to increase baseline flow (such as anemia, hyperthyroidism). Pharmacologically induced coronary flow reserve measured in normal arteries in the cardiac catheterization laboratory more realistically ranges from 2.5 to 3.5 (34).

The hyperemic response after intravenous or intracoronary adenosine is comparable to that of intracoronary papaverine. The time to peak hyperemia, as well as the total duration of the hyperemic response with adenosine, however, is four times shorter than that of papaverine (35). *Intracoronary adenosine has an extremely high safety profile in low doses and has become the pharmacologic stimulus of choice in the cardiac catheterization laboratory.*

Impairment of Coronary Blood Flow Reserve

Coronary flow reserve is computed as hyperemic flow velocity divided by basal mean flow velocity (Fig. 18.14). Work by Gould and colleagues (10,11 and 12) has established coronary flow reserve as an excellent parameter by which to assess the severity of a stenosis located in a major epicardial vessel, with reduction in flow reserve serving as an objective indicator of stenosis severity.

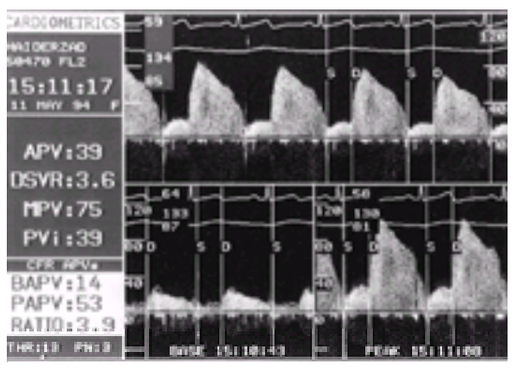

FIG. 18.14. Method of measuring coronary vasodilatory reserve using flow velocity. Spectral flow velocity signals are displayed in a continuous strip along the top panel with heart rate and systolic and diastolic blood pressure displayed in the upper left corner of the top panel. The phasic signal demonstrates a normal hyperemic velocity with a small systolic component and large diastolic component. Systolic and diastolic periods are demarcated by the S and D, respectively. The lower panel is split into two sections: baseline and hyperemic response. Baseline average peak velocity (BAPV) is 14 cm/sec. The peak hyperemic flow velocity obtained 25 seconds later after 18 µg of intracoronary adenosine is peak average peak velocity (PAPV) of 53 cm/sec, producing a coronary vasodilatory reserve ratio of 3.9. The diastolic to systolic velocity ratio (DSVR) for the peak hyperemic response was 3.6; that is, diastolic to systolic velocity ratio with a maximal peak velocity (MPV) was 75 cm/sec and the peak velocity integral, which is the average velocity integral over two cycles during maximal hyperemia, was 39 units.

Although physiologically attractive, the coronary flow reserve concept has certain limitations. Coronary flow reserve is influenced by microcirculatory responses independent from the hydrodynamic characteristics of the stenotic lesion. Thus changes in basal resting flow without changes in hyperemic flow or vice versa will affect coronary flow reserve calculations. Basal systemic hemodynamic variables (e.g., heart rate, preload) and myocardial composition (e.g., hypertrophy, microvascular disease) will affect the hyperemic pressure—flow relationship and modify the flow reserve, thus possibly altering the assessment of lesion severity independent of lesion-specific factors (36). To minimize the influence of coexistent microvascular disease and elevated baseline resting flow on coronary flow reserve, the additional determination of coronary flow reserve in a reference vessel may contribute to a more lesion-specific index. The ratio of coronary vasodilator reserve in the target to coronary vasodilator reserve in a normal reference zone (37,38) provides both, a lesion-specific index and information on the cardiac microvascular function.

Normal Coronary Flow Velocity

Because the microvascular circulation is subject to biologic variations between individuals, the range of normal coronary flow velocities at baseline and during hyperemia is variable. In one study, simultaneous flow velocity measurements were performed in 55 angiographically normal proximal and distal coronary arteries (right coronary artery = 12, left circumflex artery = 19, left anterior descending coronary artery = 24) (39). Coronary hyperemic flow was produced with intracoronary administration of 8 to 18 µg of adenosine. The normal proximal left anterior descending and circumflex time-averaged peak velocity was approximately 25 to 30 cm/sec with peak diastolic velocity ranging from 40 to 50 cm/sec and peak systolic velocity ranging from 10 to 20 cm/sec. In the right coronary artery and in some distal left coronary locations, flow velocity values may be reduced by 15% to 20%. There was no difference in proximal and distal velocities in normal arteries at baseline or during hyperemia, with a diastolic predominant pattern (diastolic/systolic flow velocity ratio of more than 1.5) in all arterial segments.

Limitations of Intracoronary Doppler Measurements

Intracoronary Doppler velocity measurements have important limitations that should be recognized by the operator. The method may be affected by the stenosis geometry, intracoronary velocity profile, and angle between the piezoelectric crystal and the flow vector of the blood (40). In addition, the sample volume is small and may fail to capture the maximal velocity of the bloodstream (40). Doppler methods measure coronary blood flow velocity, not absolute volumetric blood flow. The use of flow velocity as a surrogate for coronary blood flow assumes that the cross-sectional area of the vessel under investigation remains constant while measurements are made. It also assumes that the velocity profile across the vessel is not grossly distorted by luminal disease and is, in general, a parabolic configuration so that a correction factor of 0.5 can be used to calculate mean velocity from peak velocity. Furthermore, the Doppler catheter or guidewire, to reflect the true flow velocity,

must lie within an angle of less than 30° to the flow stream for the cosine of the angle to be within 15% of the assumed value (41).

Problems in Coronary Flow Velocity Signal Acquisition

Occasionally, it may be difficult to find the maximal distal flow velocity signals and conclude falsely that a significant flow reduction is bbeing caused by a particular stenosis. Therefore, the Doppler velocity signal should be examined during several different tip orientations to identify the maximal and most intense velocity spectra. In tortuous segments, stable distal signals can usually be obtained, but more guidewire manipulation may be needed to record a satisfactory Doppler envelope. In some patients, guidewire manipulation may not be successful due to tortuosity or lesion complexity. In these instances, the Doppler wire may be placed distally through a small-diameter catheter (Tracker, Target Therapeutics, Boston Scientific Co., Quincy MA), positioned over a standard angioplasty guidewire. Both translesional pressure and flow velocity can then be measured.

An elevated distal flow velocity may falsely normalize the proximal-to-distal flow velocity ratio. In a region with diffuse distal disease, flow velocity acceleration may occur secondary to distal luminal narrowing. In patients with serial lesions or diffuse distal disease, the proximal-to-distal flow ratio should not be used. In these cases, confirmation of lesion significance with coronary vasodilatory reserve and translesional pressure gradients may be needed.

Guide catheter obstruction to inflow at the ostium of the coronary artery may interfere with interpretation of both pressure and distal velocity signals. For this reason, intermediate lesions can be assessed at the time of diagnostic catheterization with small (6F) diagnostic or guiding catheters, or with the catheter disengaged from the coronary ostium.

Intracoronary Pressure-Derived Blood Flow Measurements

Historically, Andreas Grüntzig used coronary-pressure gradients to judge lesion severity and angioplasty success as the technique began in 1977 (42). Grüntzig showed that reductions in mean pressure gradient correlated well with reduction in lesion stenoses (Fig. 18.15). Impeded flow by the balloon catheter, however, frequently led to overestimation of translesional gradients, and angiography subsequently evolved as the gold standard of procedural success. Miniature fiber-optic and electronic pressure guidewires have overcome these limitations and renewed interest in the initial concept. Theoretical models of flow—pressure relationships in the coronary circulation were initially described by Gould and Kirkeeide (43) and later refined by Pijls et al. (44). In the basal state, pressure gradients are determined primarily by coronary autoregulation of vascular resistance. Myocardial resistance responds to changes in hemodynamics, myocardial oxygen demand, and coronary vasomotion, followed by alterations in pressure and flow. In the absence of coronary stenoses, pressure is constant throughout a vascular bed and the ratio of distal to proximal pressure equals 1. Theoretically, coronary flow can be predicted by coronary pressure if coronary resistance remains constant. This condition occurs during maximum vasodilation when all coronary resistances are close to minimal. Under these circumstances, coronary pressure measurements are also able to quantify collateral flow and their contribution to maximal coronary blood flow.

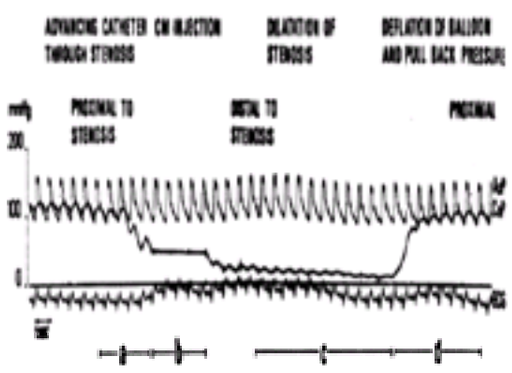

FIG. 18.15. Original tracing with recording of mean pressure and electrocardiogram during dilation, September 16, 1977, in a 39-year-old man with severe angina and 85% stenosis of the left anterior descending coronary artery. (With permisssion from Gruntzig AR, Senning A, Siegenthaler WE. Nonoperative dilatation of coronary-artery stenosis: percutaneous transluminal coronary angioplasty. *N Engl J Med* 1979;301(2):61.

Pressure Guidewire System

Pressure measurements can be easily incorporated in routine cardiac catheterization using pressure guidewire systems. The most commonly used pressure-monitoring guidewire is a 0.014-inch guidewire equipped with a high-fidelity, electronic, miniaturized pressure sensor (PressureWire, Radi Medical Systems, Uppsala, Sweden), located 3 cm proximal to the flexible tip. The sensor is a piezoresistive pressure sensor coupled in a Wheatstone bridge. The linear working range of the sensor is -30 to 300 mm Hg and the bandwidth is 0 to 1,000 Hz. The wire is connected to a small interface that allows display of the pressure signal on standard monitors and calibration outside the patient's body. Baseline pressure drift is less than 5 mm Hg/hour according to the manufacturer. The wire is advanced to the tip of the guiding catheter where it is verified that the pressure recorded by the guidewire sensor and the guiding catheter are equal. The wire is then advanced into the coronary artery and positioned distal to the stenosis with continuous monitoring and simultaneous display of phasic pressure tracings. In very tortuous anatomy, the pressure wire may not cross a specific lesion. A regular guidewire with optimal steerability and torquability may be used to pass the lesion, and the pressure guidewire then can be advanced using an infusion catheter or multifunctional probing catheter. The fractional flow reserve of the coronary artery and its dependent myocardium is then calculated as the mean distal pressure (from the pressure guidewire), divided by the mean proximal pressure (from the catheter tip) at hyperemia (peak effect of intravenous adenosine at a rate of 140 µg/kg/min (45), or subselective intracoronary injections as outlined earlier). During balloon inflation, coronary wedge pressure can be recorded and the following calculations of myocardial and coronary fractional flow reserve (FFR_{myc} and FFR_{cor}) are performed:

$$FFR_{myo} = (P_d - P_v)/(P_a - P_v)$$

$$FFR_{cor} = (P_d - P_w)/(P_a - P_w)$$

where P_d represents mean pressure distal to a stenosis, P_a represents mean aortic pressure, P_v represents mean central venous pressure at maximal hyperemia, and P_w represents distal coronary wedge pressure. Frequently, P_v is estimated as 5 mm Hg, which simplifies the determination of FFR_{myc}. At the end of the case the guidewire is withdrawn to the ostium and pressure tracings are superimposed again to exclude drift.

Myocardial, Coronary, and Collateral Fractional Flow Reserves

Myocardial fractional flow reserve reflects antegrade and collateral contribution to maximal myocardial flow. In contrast, coronary fractional flow reserve measures only antegrade flow. The difference between myocardial and coronary fractional flow reserve represents the collateral contribution to hyperemic myocardial perfusion and allows the assessment of collateral flow. In the absence of antegrade flow ($FFR_{cor} = 0$), the collateral contribution averaged 30% of the expected value for hyperemic myocardial perfusion in patients with coronary disease (46).

Practical Uses of Flow Velocity and Pressure Gradients in the Assessment of Stenosis Severity

Coronary angiography cannot delineate the functional severity of many epicardial stenoses. Intracoronary velocity and pressure, measured with sensor-tipped angioplasty guidewires during cardiac catheterization, provide immediate data discriminating the physiologic significance of coronary stenoses. Functional analysis provides objective criteria for refining the selection of cases for revascularization, and prospective clinical data have confirmed the safety of deferring intervention on lesions with normal physiologic assessment (47, 48). The following physiologic indexes complement both diagnostic and therapeutic aspects of coronary catheterization: (a) Coronary vasodilatory reserve (CVR), the ratio of hyperemic to basal mean velocity, represents the summed result of flow through the coronary artery and myocardial microvasculature (49). A CVR within the normal range identifies both a normal coronary conduit and microvascular response, excluding a coronary lesion from being flow-limiting. To identify coexistent microvascular disease, relative coronary vasodilator reserve (rCVR, computed as the ratio of coronary

vasodilator reserve in the target to coronary vasodilator reserve in a normal reference zone, $CVR_{target}/CVR_{reference}$) has been proposed (37,38). rCVR has a normal range of 0.8 to 1.0 (37,38) and appears to be a more lesion-specific index than absolute coronary flow reserve (aCVR). (b) Another approach to assessing coronary blood flow uses the hyperemic poststenotic pressure in the computation of the fractional flow reserve of the myocardium (FFR_{myo}) (50). FFR_{myo} represents the maximal blood flow to the myocardium across the stenosis compared with the theoretical normal maximal flow in the same vessel without the stenosis. A FFR_{myo} between 1.0 and 0.75 is considered normal (51).

Flow Velocity and Coronary Vasodilator Reserve

Translesional flow velocity can be used for assessment of coronary lesion significance, subject to two assumptions: first, that changes in flow velocity accurately reflect changes in volumetric blood flow, requiring that the cross-sectional area of a vessel remain constant; second, that epicardial artery cross-sectional area diminishes in proportion to volumetric flow as the parent gives off daughter branches (Fig. 18.16), so that flow velocity is maintained nearly constant from proximal to distal locations in segments 2.5 mm in diameter. A ratio of proximal-to-distal flow velocity approaching 1 is present in normal arteries (39). Significant epicardial lesions produce increased resistance and divert blood flow to branches proximal to the lesion, reducing flow velocity in the poststenotic region (Fig. 18.17*A*). Initial studies (39,52) demonstrated that a decrease in poststenotic flow velocity, such that the ratio of proximal-to-distal velocity integral was more than 1.7, was related to translesional pressure loss resulting in gradients of more than 30 mm Hg in branching arterial systems (52) (Fig. 18.17*B*). However, flow velocity measured in normal and abnormal vessels proximal to a stenosis demonstrated significant overlap in flow velocity parameters, thus limiting the predictive accuracy of proximal values.

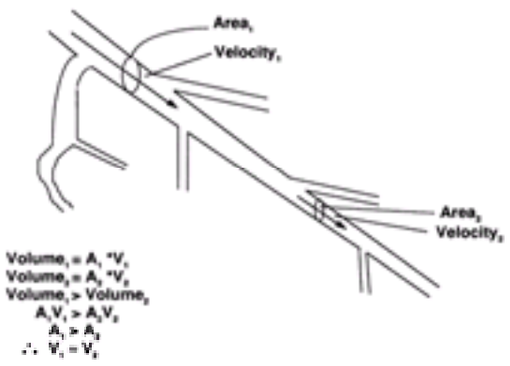

FIG. 18.16. Diagram of branching coronary artery illustrating three major principles: (a) that volumetric flow is proportional to velocity and cross-sectional area; (b) that coronary arteries normally taper; and (c) that blood flow is distributed through the branches across the myocardium as the vessel traverses the myocardium. Because coronary vessels normally taper, cross-sectional area is reduced and volumetric flow is reduced. Thus the relative relationship between proximal and distal velocities approaches 1. (With permission from Kern MJ, Aguirre FV, Bach RG, Caracciolo EA, Donohue TJ. Translesional pressure-flow velocity assessment in patients: part I. *Cathet Cardiovasc Diagn* 1994;31:49.)

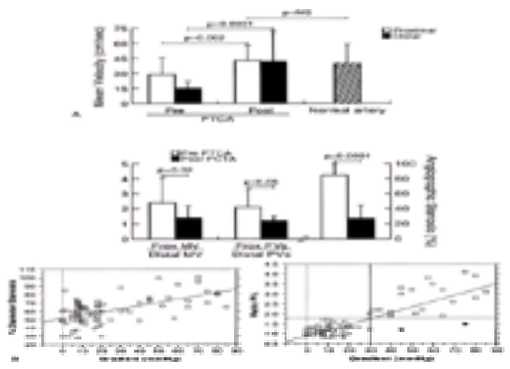

FIG. 18.17. A: Top: Changes in mean velocity before and after coronary angioplasty in relation to a normal reference artery. **Bottom:** Ratio of proximal-to-distal mean velocity (MV), proximal-to-distal peak systolic velocity (PVs) before and after angioplasty. These changes correspond to angiographic success of the intervention. (With permission from Ofili EO, Kern MJ, Labovitz AJ, et al. Analysis of coronary blood flow velocity dynamics in angiographically normal and stenosed arteries before and after endolumen enlargement by angioplasty. *J Am Coll Cardiol* 1993;21:308.)

B: Left: Percent diameter stenosis by quantitative coronary angiography versus translesional pressure gradient; **right:** ratio of proximal-to-distal peak velocity integral versus gradient. Patients in this study with proximal-to-distal velocity ratios of less than 1.7 had translesional pressure gradients of less than 30 mm Hg, with two exceptions (*dark boxes*) in which flow velocity was measured in the proximal right coronary artery. This ratio is sensitive but not specific for translesional pressure gradients and may not be applicable in ostial lesions, diffuse distal disease, or serial lesions for assessment of pressure gradients. However, it is one of three indices used to assess intermediate lesion severity. (With permission from Donohue TJ, Kern MJ, Aguirre FV, et al. Assessing the hemodynamic significance of coronary artery stenoses: analysis of translesional pressure-flow velocity relations in patients. *J Am Coll Cardiol* 1993;22:449.)

Coronary Blood Flow Velocity During Angioplasty

Characterization of severe coronary stenosis during angioplasty is associated with three major alterations of the intracoronary flow velocity in the poststenotic region. These alterations are as follows: (a) A decrease in mean velocity [usually less than 20 cm/sec—for lesions in branching artery systems, a mean proximal-to-distal flow velocity integral ratio of more than 1.7 (52) is generally associated with translesional gradients greater than 30 mm Hg]; (b) An impaired phasic pattern of coronary flow (53,54) with diastolic to systolic velocity ratio of less than 1.5; and (c) Impaired poststenotic coronary hyperemia flow reserve (less than 2.0 × basal values) (52).

Phasic Coronary Flow and the Diastolic/Systolic Velocity Ratio

Early experimental animal studies demonstrated a reduction in the normal diastolic predominant phasic flow pattern distal to experimentally induced critical stenoses (55). Intraoperative studies in patients confirmed a reduction of diastolic flow velocity and unchanged systolic flow velocity during graft occlusion (54). Using Doppler guidewire techniques during angioplasty, stenotic arteries were demonstrated to have a reduced diastolic flow velocity with relatively preserved systolic flow velocity (53) (Fig. 18.18, Fig. 18.19, Fig. 18.20). The systolic predominant pattern was seen in more than 50% of abnormal arteries and none of the normal arteries (39,53). Normalization of the diastolic to systolic velocity ratio after successful angioplasty was confirmed by Segal et al. and other investigators (53,56).

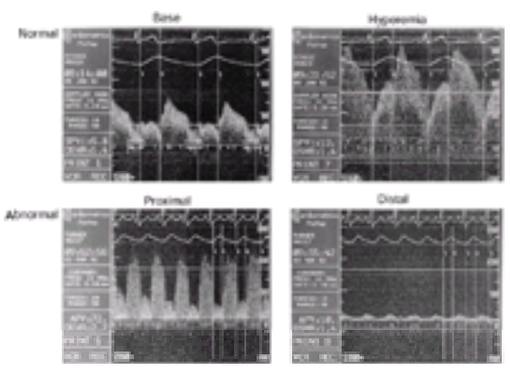

FIG. 18.18. Comparison of normal hyperemic flow velocity response to flow velocity response distal to a severe stenosis. **Top:** Normal flow velocity at rest and during intracoronary adenosine hyperemia demonstrates a 2.5-fold increase in flow velocity. Note increase in systolic and diastolic flow velocity components. SPVi = systolic peak velocity index; DSVR = diastolic/systolic velocity ratio. Mean velocity in the normal artery increases from 28 to 60, for a coronary vasodilatory reserve of 2.3. **Bottom:** In the abnormal velocity response, proximal velocity is elevated, indicating that a jet velocity has been acquired at the site of the lesion. Peak velocity is 120 cm/sec, mean velocity is 60 cm/sec. In the poststenotic region (distal) flow velocity demonstrates loss of phasic pattern with a low diastolic/systolic velocity ratio of 1.4, mean velocity of 15 cm/sec, and no hyperemic response.

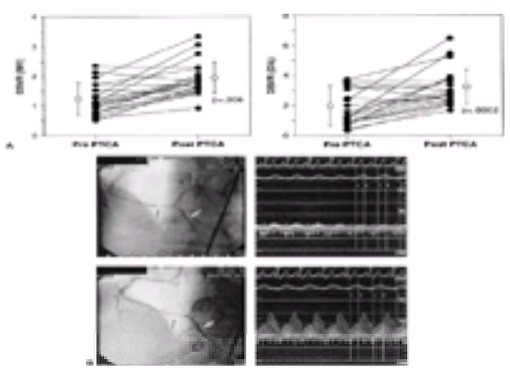

FIG. 18.19. A: Changes in diastolic to systolic velocity ratio (DSVR) before and after angioplasty using mean velocity (MV) (**left**) and diastolic/systolic velocity integral (**right**). Improvement in phasic pattern in general accompanies a successful coronary angioplasty. (With permission from Segal J, Kern MJ, Scott NA, et al. Alterations of phasic coronary artery flow velocity in man during percutaneous coronary angioplasty. *J Am Coll Cardiol* 1992;20:276.)

B: Left: Angiograms before and after angioplasty. **Right:** Poststenotic flow velocity in the posterior descending artery in the location of the *white arrow,* demonstrating poor phasic flow and reduced mean velocity before angioplasty and increased mean velocity and normalized distal coronary flow after coronary angioplasty. Flow velocity measurements reflect the region in which velocity data are acquired.

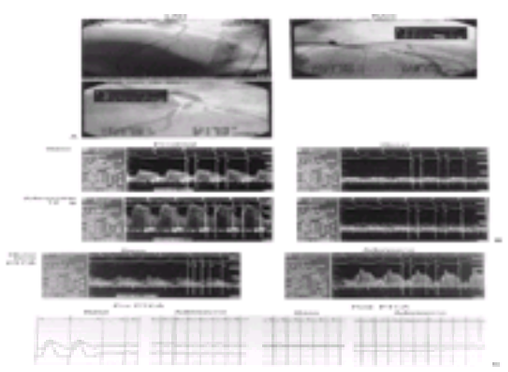

FIG. 18.20. Angiogram of a left anterior descending (LAD) stenosis. (LAO, left anterior oblique projection; RAO, right anterior oblique projection.) Coronary angiography revealed a 60% diameter narrowing in the proximal left anterior descending coronary artery in this young man 6 days after an anterior myocardial infarction. In-laboratory assessment of the stenosis was performed before and after angioplasty. Basal and hyperemic flow velocity data were obtained 1 cm proximal to the stenosis. The Doppler guidewire was advanced across the stenosis. Distal (more than ten artery diameters or 2 cm) basal and hyperemic flow responses were obtained. Intracoronary adenosine (12 to 18 µg) was administered through the guide catheter to evaluate poststenotic coronary reserve.

B: Analysis of the flow velocity data revealed normal mean proximal velocity (32 cm/sec), with a normal phasic pattern and coronary flow reserve (2.5 × basal) (Fig. 18.20*B*, **top and bottom left**). Poststenotic flow velocity, however, was abnormal (reduced mean velocity 17 cm/sec), with a proximal tp distal velocity ratio of 32:17 = 1.9 (Fig. 18.20*B*, **top right**). In addition, the ratio of phasic diastolic to systolic velocity was abnormally low (1.3 in the distal vessel; a normal left coronary ratio is more than 1.5). Distal coronary flow reserve was also impaired (1.42 × basal flow) (Fig. 18.20*B*, **bottom right**). These findings were associated with a basal translesional pressure gradient of 40 mm Hg (increasing to 48 mm Hg during maximal hyperemia) (Fig. 18.20*C*, **bottom left**).

C: Coronary angioplasty was successfully performed. The stenosis was reduced (less than 30% diameter narrowing) with normalization of the distal phasic flow velocity pattern (diastolic to systolic ratio of 1.6), augmentation of basal mean velocity (33 cm/sec), and increase in distal flow reserve (1.96) (Fig. 18.20*C*, **top panels**). The velocity data corresponded to a postangioplasty translesional pressure gradient of 8 mm Hg (20 mm Hg during maximal hyperemia) (Fig. 18.20*C*, **bottom right**). (With permission from Kern MJ, Flynn MS, Caracciolo EA, Bach RG, Donohue TJ, Aguirre FV. Use of translesional coronary flow velocity for interventional decisions in a patient with multiple intermediately severe coronary stenoses. *Cathet Cardiovasc Diagn* 1993;29:148.)

Poststenotic Coronary Hyperemia

As previously discussed, coronary flow reserve has been shown to correlate with the physiologic severity of a coronary stenosis in experimental animal studies. Subselective coronary flow reserve measurements have been employed in patients with variable results in a number of studies to aid in determining the functional significance of a given coronary stenosis. Unlike animal studies that are performed in nonbranching segments of coronary arteries, in patients, proximally measured coronary flow reserves are contaminated by branch vessels between the Doppler crystal and the lesion in question. The usefulness of distally measured (poststenotic) coronary flow reserve measurements in predicting Tc-99m sestamibi perfusion imaging during pharmacologic stress has been demonstrated (57). Coronary flow reserves equal to or less than 2.0 had a strong correlation with the presence of a reversible perfusion defect (57).

The Doppler Endpoints Balloon Angioplasty Trial Europe (DEBATE) study (58) found that a combined procedural end point (angiographic residual diameter stenosis of 35% or less and coronary flow reserve of less than 2.5) was associated with a favorable clinical outcome at 6 months. In a subgroup of patients with both poor anatomic and functional results, further therapy (i.e., with stenting) could be contemplated in view of the highly predictable outcome of these patients. Two ongoing trials, DEBATE II and Doppler Endpoint Stenting International Investigation (DESTINI) (59), will give further insight if coronary vasodilator reserve aids in the development of lesion-specific interventional strategies.

Pressure Guidewire and Fractional Flow Reserve

Myocardial fractional flow reserve (FFR_{myc}) is an index of the functional severity of coronary stenoses derived from coronary pressure measurements. The index represents the maximal blood flow to the myocardium in the presence of a stenosis of a supplying artery, divided by the theoretical normal maximal flow in the same distribution (Fig. 18.21, Fig. 18.22). Unique features of FFR_{myc} are that the index is independent of changes in systemic blood pressure or heart rate and that it takes into account the contribution of collateral blood supply to maximal myocardial perfusion (60). The concept of FFR_{myc} has been carefully validated (61) and shows a high reproducibility and a well-defined cutoff value for inducible ischemia. A FFR_{myc} of more than 0.75 appears to be uniformly associated with the absence of exercise-inducible myocardial ischemia (51) and correlated better with dobutamine stress echocardiography than with angiographic indexes of stenosis severity (62,63 and 64). In symptomatic patients, deferral of intervention of an intermediate stenosis on the basis of an FFR_{myc} of more than 0.75 is safe and is associated with a low clinical event rate (65). The value of FFR_{myc} in the evaluation of coronary interventions such as angioplasty and stenting is currently under investigation. Similar to

coronary vasodilator reserve, preliminary results suggest that FFR_{myc} may aid in the decision process during interventional procedures and is associated with low restenosis rates (66).

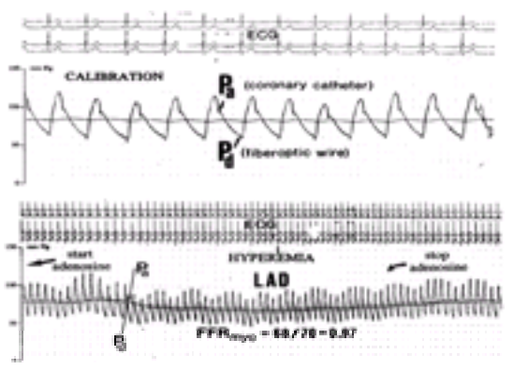

FIG. 18.21. Example of phasic and mean pressure recording in a patient with normal angiogram. LAD indicates left anterior descending coronary artery. (With permission from Pijls NH, Van Gelder B, Van der Voort P, et al. Fractional flow reserve: a useful index to evaluate the influence of an epicardial coronary stenosis on myocardial blood flow. *Circulation* 1995;92:3183.)

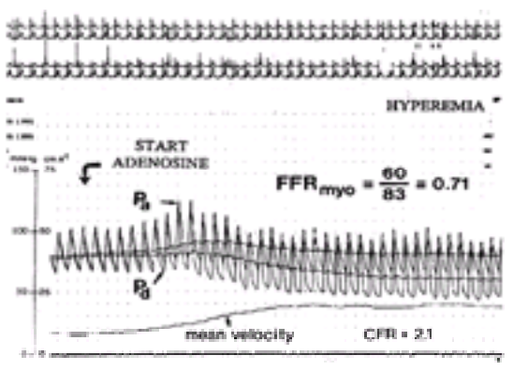

FIG. 18.22. Procedure for calculating myocardial flow reserve (FFR_{myc}) from coronary pressure measurements. After calibration (**top**), a translesional gradient is clearly seen when the pressure sensor crosses the stenosis (**middle**). At steady-state maximum hyperemia (**bottom**) FFR_{myc} is calculated as indicated. (Adapted with permission from Pijls NH, Bech GJ, De Bruyne B, van Straten A. Clinical assessment of functional stenosis severity: use of coronary pressure measurements for the decision to bypass a lesion. *Ann Thorac Surg* 1997;63[Suppl]:S6.)

Limitations of Coronary Vasodilator Reserve and Fractional Flow Reserve

Although coronary vasodilator reserve was initially devised to quantify limitation of flow caused by an epicardial coronary stenosis, microvascular dysfunction can influence both maximal or baseline flow. Increased extravascular forces such as elevated left ventricular diastolic pressure compress the intramyocardial microvasculature and limit peak flow rates. Structural alterations of the resistance vessel wall occur in hypertension, diabetes, and hypertrophic cardiomyopathy and limit vasodilation, thereby impairing maximal flow rates. Hyperlipidemia and other metabolic disorders may also impair coronary resistance vessel dilation. While adenosine induces vasodilation in arterioles with a diameter of less than 100 µm, a substantial amount of coronary resistance lies within small arteries with a size 100 to 400 µm. A flow increase though arterioles will induce shear-stress-mediated release of nitric oxide and vasodilation in these small arteries. Impaired vasodilator reserve thus may be mediated by endothelial dysfunction in resistance vessels with a diameter between 100 and 400 µm.

All functional studies are limited by submaximal hyperemic vasodilation. Lesion assessments relying on velocity and pressure measurements are invalid if inadequate hyperemic vasodilation occurs and may underestimate lesion severity. The presence of diffuse epicardial disease in the reference vessel may also lead to a reduction in reference CVR and thus to an underestimation of target-lesion severity in using rCVR (67). Additionally, similar to the TIMI frame count observations, CVR is frequently reduced in the perfusion territory of the culprit artery after myocardial infarction (68,69 and 70).

Conclusions

Measurements of coronary blood flow and myocardial metabolism have given important insights into cardiac function in health and disease. While there continues to be a role for noninvasive techniques in patient screening, catheter-derived estimates of coronary flow provide similar and potentially greater precision in measurement. With the availability of guidewire-based Doppler flow velocity and pressure measurements, clinically relevant measurements of coronary flow can be estimated during interventional procedures to evaluate patient-by-patient results, as well as enhance our understanding of coronary physiology and its response to intervention. Acceptance of traditional CVR to assess stenosis severity has been hampered by variable threshold values. Pressure-derived FFR, a well-validated and accepted concept to assess lesion-specific significance, and rCVR circumvent these problems and may serve as valid and more accurate measures of stenosis severity in the clinical setting.

ACKNOWLEDGMENT

Some of the material in this chapter was developed from previous editions by Drs. Arlene Levine, Donald S. Baim, and Thomas J. Donohue.

CHAPTER REFERENCES

1. Weber KT, Janicki JS. The metabolic demand and oxygen supply of the heart: physiologic and clinical considerations. *Am J Cardiol* 1979;44:722.
2. Bache RJ, Dymek DJ. Local and regional regulation of coronary vascular tone. *Prog Cardiovasc Dis* 1981;24:191.
3. Klocke FJ. Coronary blood flow in man. *Prog Cardiovasc Dis* 1976;19:117.
4. Opie LH. Metabolism of the heart in health and disease. Part I. *Am Heart J* 1968;76:685. Part II 1969;77:100. Part III 1969;77:383.
5. Scheuer J, Penpargkul S. Myocardial metabolism. In: Willerson S, Sanders C, eds. *Clinical cardiology.* New York: Stratton, 1977.
6. Krasnow N, et al. Myocardial lactate and metabolism. *J Clin Invest* 1962;41:2075.
7. Baim DS, Rothman MT, Harrison DC. Simultaneous measurement of coronary venous blood flow and oxygen saturation during transient alterations in myocardial oxygen supply and demand. *Am J Cardiol* 1982;49:743.
8. Wilson RF, Marcus ML, White CW. Prediction of the physiologic significance of coronary arterial lesions by quantitative lesion geometry in patients with limited coronary artery disease. *Circulation* 1987;75:723.
9. McGinn AL, Wilson RF, Olivari MT, Homans DC, White CW. Coronary vasodilator reserve after human orthotopic cardiac transplantation. *Circulation* 1988;78:1200.
10. Gould KL, Lipscomb K, Hamilton GW. Physiologic basis for assessing critical coronary stenosis: instantaneous flow response and regional distribution during coronary hyperemia as measures of coronary flow reserve. *Am J Cardiol* 1974;33:87.
11. Gould KL, Kelley KO. Physiological significance of coronary flow velocity and changing stenosis geometry during coronary vasodilation in awake dogs. *Circ Res* 1982;50:695.
12. Gould KL, Kirkeeide RL, Buchi M. Coronary flow reserve as a physiologic measure of stenosis severity. *J Am Coll Cardiol* 1990;15:459.
13. Klocke FJ. Measurements of coronary flow reserve: defining pathophysiology versus making decisions about patient care. *Circulation* 1987;76:1183.
14. The Thrombolysis in Myocardial Infarction (TIMI) trial. Phase I findings. TIMI Study Group. *N Engl J Med* 1985;312:932.
15. Cannon CP, Sharis PJ, Schweiger MJ, et al. Prospective validation of a composite end point in thrombolytic trials of acute myocardial infarction (TIMI 4 and 5). Thrombosis In Myocardial Infarction. *Am J Cardiol* 1997;80:696.
16. Barbagelata NA, Granger CB, Oqueli E, et al. TIMI grade 3 flow and reocclusion after intravenous thrombolytic therapy: a pooled analysis. *Am Heart J* 1997;133:273.
17. The effects of tissue plasminogen activator, streptokinase, or both on coronary artery patency, ventricular function, and survival after acute myocardial infarction. The GUSTO Angiographic Investigators. *N Engl J Med* 1993;329:1615.

18. Simes RJ, Topol EJ, Holmes DR, Jr, et al. Link between the angiographic substudy and mortality outcomes in a large randomized trial of myocardial reperfusion. Importance of early and complete infarct artery reperfusion. GUSTO-I Investigators. *Circulation* 1995;91:1923.
19. Fath-Ordoubadi F, Huehns TY, Al-Mohammad A, Beatt KJ. Significance of the Thrombolysis in Myocardial Infarction scoring system in assessing infarct-related artery reperfusion and mortality rates after acute myocardial infarction. *Am Heart J* 1997;134:62.
20. Gibson CM, Cannon CP, Daley WL, et al. TIMI frame count: a quantitative method of assessing coronary artery flow. *Circulation* 1996;93:879.
21. Uren NG, Crake T, Lefroy DC, de Silva R, Davies GJ, Maseri A. Reduced coronary vasodilator function in infarcted and normal myocardium after myocardial infarction. *N Engl J Med* 1994;331:222.
22. Kern MJ, Moore JA, Aguirre FV, et al. Determination of angiographic (TIMI grade) blood flow by intracoronary Doppler flow velocity during acute myocardial infarction. *Circulation* 1996;94:1545.
23. Gibson CM, Dodge JT Jr, Goel M, et al. Angioplasty guidewire velocity: a new simple method to calculate absolute coronary blood velocity and flow. *Am J Cardiol* 1997;80:1536.
24. Gibson CM, Murphy SA, Rizzo MJ, et al. The relationship between the TIMI frame count and clinical outcomes after thrombolytic administration. *Circulation* 1999;99:1945.
25. French JK, Ellis CJ, Webber BJ, et al. Abnormal coronary flow in infarct arteries 1 year after myocardial infarction is predicted at 4 weeks by corrected Thrombolysis in Myocardial Infarction (TIMI) frame count and stenosis severity. *Am J Cardiol* 1998;81:665.
26. Dodge JT, Jr, Rizzo M, Nykiel M, et al. Impact of injection rate on the Thrombolysis in Myocardial Infarction (TIMI) trial frame count. *Am J Cardiol* 1998;81:1268.
27. Nakazawa HK, Roberts DL, Klocke FJ. Quantitation of anterior descending vs. circumflex venous drainage in the canine great cardiac vein and coronary sinus. *Am J Physiol* 1978;234:H163.
28. Ganz W, Tamura K, Marcus HS, Donoso R, Yoshida S, Swan HJ. Measurement of coronary sinus blood flow by continuous thermodilution in man. *Circulation* 1971;44:181.
29. Baim DS, Rothman MT, Harrison DC. Improved catheter for regional coronary sinus flow and metabolic studies. *Am J Cardiol* 1980;46:997.
30. Pepine CJ, Mehta J, Webster WW, Jr, Nichols WW. *In vivo* validation of a thermodilution method to determine regional left ventricular blood flow in patients with coronary disease. *Circulation* 1978;58:795.
31. Doucette JW, Corl PD, Payne HM, et al. Validation of a Doppler guide wire for intravascular measurement of coronary artery flow velocity. *Circulation* 1992;85:1899.
32. Rossen JD, Simonetti I, Marcus ML, Winniford MD. Coronary dilation with standard dose dipyridamole and dipyridamole combined with handgrip. *Circulation* 1989;79:566.
33. Wilson RF, White CW. Intracoronary papaverine: an ideal coronary vasodilator for studies of the coronary circulation in conscious humans. *Circulation* 1986;73:444.
34. Kern MJ, Bach RG, Mechem CJ, et al. Variations in normal coronary vasodilatory reserve stratified by artery, gender, heart transplantation and coronary artery disease. *J Am Coll Cardiol* 1996;28:1154.
35. Wilson RF, Wyche K, Christensen BV, Zimmer S, Laxson DD. Effects of adenosine on human coronary arterial circulation. *Circulation* 1990;82:1595.
36. Strauer BE. The significance of coronary reserve in clinical heart disease. *J Am Coll Cardiol* 1990;15:775.
37. Kern MJ, Donohue TJ, Bach RG, Aguirre FV, Caracciolo EA, Wolford TL. Assessment of intermediate coronary stenosis by relative coronary flow velocity reserve. *J Am Coll Cardiol* 1997;29:21A.
38. Baumgart D, Haude M, Goerge G, et al. Improved assessment of coronary stenosis severity using the relative flow velocity reserve. *Circulation* 1998;98:40.
39. Ofili EO, Kern MJ, Labovitz AJ, et al. Analysis of coronary blood flow velocity dynamics in angiographically normal and stenosed arteries before and after endolumen enlargement by angioplasty. *J Am Coll Cardiol* 1993;21:308.
40. Hatle L, Angelsen B. Physics of blood flow. *Doppler ultrasound in cardiology.* Philadelphia: Lea & Febiger, 1985:8.
41. Doucette JW, Corl PD, Payne HM, et al. Validation of a Doppler guide wire for intravascular measurement of coronary artery flow velocity. *Circulation* 1992;85:1899.
42. Grüntzig AR, Senning A, Siegenthaler WE. Nonoperative dilatation of coronary-artery stenosis: percutaneous transluminal coronary angioplasty. *N Engl J Med* 1979;301:61.
43. Kirkeeide RL, Gould KL, Parsel L. Assessment of coronary stenoses by myocardial perfusion imaging during pharmacologic coronary vasodilation. VII. Validation of coronary flow reserve as a single integrated functional measure of stenosis severity reflecting all its geometric dimensions. *J Am Coll Cardiol* 1986;7:103.
44. Pijls NH, van Son JA, Kirkeeide RL, De Bruyne B, Gould KL. Experimental basis of determining maximum coronary, myocardial, and collateral blood flow by pressure measurements for assessing functional stenosis severity before and after percutaneous transluminal coronary angioplasty. *Circulation* 1993;87:1354.
45. Van der Voort PH, van Hagen E, Hendrix G, van Gelder B, Bech JW, Pijls NH. Comparison of intravenous adenosine to intracoronary papaverine for calculation of pressure-derived fractional flow reserve. *Cathet Cardiovasc Diagn* 1996;39:120.
46. Bartúnek J, Sys SU, Heyndrickx GR, Pijls NH, De Bruyne B. Quantitative coronary angiography in predicting functional significance of stenoses in an unselected patient cohort. *J Am Coll Cardiol* 1995;26:328.
47. Kern MJ, Puri S, Randall C, Bach R, Donohue TJ. Hemodynamic rounds series II: coronary hemodynamics for angioplasty and stenting after myocardial infarction: use of absolute, relative coronary velocity and fractional flow reserve. *Cathet Cardiovasc Diagn* 1998;45:174.
48. Baumgart D, Haude M, Liu F, Ge J, Goerge G, Erbel R. Current concepts of coronary flow reserve for clinical decision making during cardiac catheterization. *Am Heart J* 1998;136:136.
49. Gould KL, Kirkeeide RL, Buchi M. Coronary flow reserve as a physiologic measure of stenosis severity. *J Am Coll Cardiol* 1990;15:459.
50. Pijls NH, De Bruyne B, Peels K, et al. Measurement of fractional flow reserve to assess the functional severity of coronary artery stenoses. *N Engl J Med* 1996;334:1703.
51. De Bruyne B, Bartunek J, Sys SU, Heyndrickx GR. Relation between myocardial fractional flow reserve calculated from coronary pressure measurements and exercise-induced myocardial ischemia. *Circulation* 1995;92:39.
52. Donohue TJ, Kern MJ, Aguirre FV, et al. Assessing the hemodynamic significance of coronary artery stenoses: analysis of translesional pressure-flow velocity relations in patients. *J Am Coll Cardiol* 1993;22:449.
53. Segal J, Kern MJ, Scott NA, et al. Alterations of phasic coronary artery flow velocity in humans during percutaneous coronary angioplasty. *J Am Coll Cardiol* 1992;20:276.
54. Kajiya F, Tsujioka K, Ogasawara Y, et al. Analysis of flow characteristics in poststenotic regions of the human coronary artery during bypass graft surgery. *Circulation* 1987;76:1092.
55. Wiesner TF, Levesque MJ, Rooz E, Nerem RM. Epicardial coronary blood flow including the presence of stenoses and aorto-coronary bypasses. II: Experimental comparison and parametric investigations. *J Biomech Eng* 1988;110:144.
56. Serruys PW, Di Mario C, Kern MJ. Intracoronary Doppler. In: Topol EE, ed. *Textbook of interventional cardiology*, vol. 2. Philadelphia: WB Saunders, 1993:1069.
57. Miller DD, Donohue TJ, Younis LT, et al. Correlation of pharmacological 99mTc-sestamibi myocardial perfusion imaging with poststenotic coronary flow reserve in patients with angiographically intermediate coronary artery stenoses. *Circulation* 1994;89:2150.
58. Serruys PW, di Mario C, Piek J, et al. Prognostic value of intracoronary flow velocity and diameter stenosis in assessing the short- and long-term outcomes of coronary balloon angioplasty: the DEBATE Study (Doppler Endpoints Balloon Angioplasty Trial Europe). *Circulation* 1997;96:3369.
59. Di Mario C, Muramatsu T, Moses J, et al. Aggressive dilatation strategy to optimize the angiographic and functional PTCA results: preliminary results of the DESTINI study. *Eur Heart J* 1997;18:238.
60. De Bruyne B, Bartunek J, Sys SU, Pijls NH, Heyndrickx GR, Wijns W. Simultaneous coronary pressure and flow velocity measurements in humans. Feasibility, reproducibility, and hemodynamic dependence of coronary flow velocity reserve, hyperemic flow versus pressure slope index, and fractional flow reserve. *Circulation* 1996;94:1842.
61. De Bruyne B, Baudhuin T, Melin JA, et al. Coronary flow reserve calculated from pressure measurements in humans: validation with positron emission tomography. *Circulation* 1994;89:1013.
62. Bartunek J, Marwick TH, Rodrigues AC, et al. Dobutamine-induced wall motion abnormalities: correlations with myocardial fractional flow reserve and quantitative coronary angiography. *J Am Coll Cardiol* 1996;27:1429.
63. Pijls NH, Van Gelder B, Van der Voort P, et al. Fractional flow reserve: a useful index to evaluate the influence of an epicardial coronary stenosis on myocardial blood flow. *Circulation* 1995;92:3183.
64. Pijls NH, Bech GJ, De Bruyne B, van Straten A. Clinical assessment of functional stenosis severity: use of coronary pressure measurements for the decision to bypass a lesion. *Ann Thorac Surg* 1997;63:S6.
65. Bech GJ, De Bruyne B, Bonnier HJ, et al. Long-term follow-up after deferral of percutaneous transluminal coronary angioplasty of intermediate stenosis on the basis of coronary pressure measurement. *J Am Coll Cardiol* 1998;31:841.
66. Pijls NHJ, Bruyne Bd. Fractional flow reserve for evaluation of coronary interventions. *Coronary pressure.* Boston: Kluwer Academic Publishers, 1997:261.
67. Baumgart D, Haude M, Goerge G, et al. Improved assessment of coronary stenosis severity using the relative flow velocity reserve. *Circulation* 1998;98:40.
68. Moore JA, Kern MJ. Coronary flow velocity during coronary angioplasty in regions of myocardial infarction. *Cathet Cardiovasc Diagn* 1994;32:187.
69. Miller DD, Esparza-Negrete J, Donohue TJ, et al. Periprocedural Doppler coronary blood flow predictors of myocardial perfusion abnormalities and cardiac events after successful coronary interventions. *Am Heart J* 1996;131:1058.
70. Mazur W, Bitar JN, Lechin M, et al. Coronary flow reserve may predict myocardial recovery after myocardial infarction in patients with TIMI grade 3 flow. *Am Heart J* 1998;136:335.

19
Intravascular Ultrasound

Tony M. Chou, Peter J. Fitzgerald, and Paul G. Yock

TMC: University of California, San Francisco, School of Medicine, San Francisco, California 94143
PJF: Division of Cardiology, Center for Research in Cardiovascular Interventions, Stanford University, Stanford, California 94305
PGY: Center for Research in Cardiovascular Interventions, Stanford University, Stanford, California 94305

Angiography has been useful for clinical assessment of stenoses caused by atherosclerosis and as a guide for surgical and catheter-based revascularization. However, the two-dimensional luminal imaging of an angiogram provides incomplete information about the coronary artery disease process. This chapter will discuss intravascular ultrasound (IVUS), a technique that visualizes the arterial wall in a tomographic format that is analogous to a histologic cross-section. The initial experience with IVUS began in the late 1980s and since then has gained rapid acceptance. The qualitative and quantitative information generated by IVUS is significantly more detailed and potentially more accurate than angiography. As IVUS has developed, it has become an important diagnostic aid in the clinical interventional lab as well as a powerful research tool to improve our understanding of atherosclerosis and response to intervention.

IMAGING SYSTEMS AND PROCEDURES

There are two approaches to IVUS imaging—solid state and mechanical scanning. Both types of catheters generate a 360°, cross-sectional image plane that is perpendicular to the catheter and guidewire. In the solid-state approach, individual transducers are radially mounted on the catheter. An imaging beam is swept around the catheter by electronically varying the activation of individual elements in the transducer array. The elements receive the ultrasound signal and the resulting echo information is processed and routed to a computer where the images are reconstructed and presented in a near-real-time format. Complex miniaturized integrated circuits mounted in the catheter tip are responsible for the timing and integration of the transducer activation. The mechanical coronary catheters create images by rotating a single transducer element inside the tip of a catheter using a flexible cable as a driveshaft. The transducer is rotated at 1,600 to 1,800 rpm by the cable, which runs the length of the catheter. The rotational speed of the transducer is controlled by an external motor drive. The transducer operates within a protective sheath that is transparent to the ultrasound beam and has a separate degree of freedom to allow movement within the catheter without requiring motion of the catheter within the artery.

As of early 1999 three domestic manufacturers produced IVUS scanners. At present there is only one FDA-approved solid-state catheter (Endosonics, Inc., Rancho Cordova, CA), which has 64 transducer elements arranged radially near the catheter tip with a center frequency of 20 to 25 MHz (1). The catheters are produced in both over-the-wire and rapid-exchange formats. The current solid-state coronary catheters are 3F at the tip (1.0 mm diameter). A central guidewire lumen is utilized and thus there is no guidewire artifact. Since there are no moving parts, no rotational distortion is seen. The catheter acts as a fixed transducer and imaging in a longitudinal axis requires movement of the catheter within the artery. The catheter has excellent guidewire tracking and is in general more hardy than the mechanical systems. A combination balloon angioplasty/IVUS device based on this technology has been approved and has imaging elements mounted immediately proximal to a compliant angioplasty balloon (Oracle Micro, Oracle Combination Systems, Endosonics, Rancho Cordova, CA). Development of a second solid-state catheter is under way in England with clinical trials in progress (Intravascular Resources Limited [IRL]2, Middlesex, England).

There are two currently available mechanical systems in use for coronary imaging (Boston Scientific Corp., Sunnyvale, CA; and Hewlett Packard Corp., Andover, MA) (2). Hewlett Packard has recently announced that it is ending its commitment to IVUS and plans to phase out its system. Mechanical catheters are sold in a variety of sizes, frequencies, and configurations for coronary, peripheral, and intracardiac use. The current coronary catheters have a transducer frequency of 30 to 45 MHz. Two styles of catheter delivery are used; both are based on a monorail and rapid-exchange design. In one design, a 15-mm monorail is positioned at the distal tip and acts as the guidewire lumen. The imaging portion of the catheter is a 15-cm clear plastic segment proximal to the monorail. The guidewire runs parallel to the shaft of the catheter and thus is imaged creating a point artifact within the vessel lumen. This short monorail design currently has sizes from 2.6F to 3.2F (0.83 to 1.1 mm diameters). Care must be taken in using this system as the short monorail does not track like over-the-wire or standard monorail systems, and looping or folding of the guidewire can occur if the distal catheter tip approaches the end of the guidewire. There is a radioopaque marker fixed at 0.5 cm from the catheter tip that should be kept well clear of the guidewire tip. A second 2.9F configuration has a long rapid-exchange sleeve that is shared with the imaging transducer. It too is manipulated in a monorail fashion but tracks the guidewire better due to the longer lumen length. The distal 30 cm of the catheter is a shared or common lumen and is utilized by both guidewire and imaging transducer alternately. The transducer is pulled proximally when the catheter is positioned under fluoroscopy with guidewire in the vessel. Once in place, the guidewire is pulled back to a radioopaque marker and the imaging element can be advanced into the vessel and scanning begun. Care must be taken to keep the imaging element sufficiently back from the guidewire during catheter placement; similarly, the guidewire needs to be fully retracted before advancing the transducer. This configuration, although more cumbersome in preparation and operation, offers the benefit of a lower profile and imaging without guidewire artifact. The current profile is 2.9F or 0.92 mm, compatible with most 6F guiding catheters. With both designs of the mechanical catheters, the rotating transducer can be advanced or retracted inside the catheter for a 15-cm imaging segment, allowing the vessel to be scanned without moving the catheter itself. This allows the transducer to be moved through a segment of interest in a precise and controlled manner and is especially advantageous during automated pullback. At the most forward position, the transducer is approximately 1 cm from the catheter tip. This is important to keep in mind to ensure that the transducer is beyond the area of interest when pullback is begun and when imaging specific areas guided by the angiography. In Europe, a third manufacturer (Dumed, Rotterdam, The Netherlands) has developed a mechanical imaging catheter system that has a micromotor on the catheter tip. This is not available in the United States. Aloka and Terumo have demonstrated prototype mechanical systems.

In head-to-head comparisons, mechanical transducers have offered an overall advantage compared with the solid-state systems, but the gap has narrowed. Both systems have had image quality improvements and can image standard coronary anatomy and devices well. The far-field resolution of the mechanical transducers is poorer. With mechanical systems, nonuniform rotational distortion (NURD) can occur when the driveshaft has sufficient bend or hindrance to cause imperfect one-to-one rotation of driveshaft to transducer. Even small disturbances such as a twist in the catheter or placement of the catheter in tortuous anatomy can cause this artifact. This results in a wedge-shaped smeared-image appearance in one or more segments of the image that can affect image interpretation. Efforts should be made to straighten the catheter and motor drive assembly and lessen guiding catheter tension when NURD is seen.

With both solid-state and mechanical approaches, the catheter is attached to an interface unit that in turn is connected to the imaging console. The console has a monitor for image display and controls that allow image manipulation and on-line measurements to be made and recorded. The IVUS image is often relayed or “slaved” to a larger catheterization laboratory monitor. The fluoroscopic or angiographic image can also be incorporated into the IVUS console screen if desired. The controls mimic many of the controls found on standard echocardiography machines and thus allow adjustment of “zoom,” gain, gray scale (contrast), and noise elimination threshold (reject). Most systems have digital storage memory to allow freeze frame capability and allow playback from VHS video tape or CD off-line storage.

BASIC PROCEDURES

IVUS studies, especially in the coronary arterial tree, should only be performed by experienced interventional cardiologists. Catheter systems presently allow access to the coronary tree via 6F and larger guiding catheters, and 8F guiding catheters are preferred for positioning to allow intermittent injection of contrast medium and free rotation to reduce the risk of NURD with mechanical systems. The manipulation of IVUS probes is similar to standard angioplasty balloon catheters. Additional care to avoid torsion of the imaging catheters should be taken. A stable guide catheter position is desirable since imaging catheters have larger profiles and are less trackable than most balloon catheters. Angulation of angiography to lay out the target vessel is important to assess adequate guidewire positioning. The short monorail catheters are prone to prolapse and kink the wire, so the guidewire should be placed well distal to the imaging catheter tip. For tortuous anatomies, a long-rail (rapid-exchange) or over-the-wire catheter should be selected if possible. Prior to IVUS imaging, an intravenous injection of 5,000 to 10,000 units of heparin should be given if not done previously, and intracoronary injection of 100 to 300 mg nitroglycerin or 1 to 3 mg isosorbide dinitrate given prior to catheter insertion.

A standard operating procedure is recommended for IVUS examination with careful catheter preparation. Imaging outside the body should be performed for verification and optimization of image gray scale. Use of the mechanical and solid-state catheters is similar except that the mechanical catheters require flushing with saline prior to insertion to eliminate any air in the path of the beam. Incomplete flushing can leave bubbles adjacent to the transducer, resulting in poor image quality once the catheter is inserted. Holding the catheter upright and flicking the tip with the transducer forward during flushing often helps release air that is trapped alongside the transducer. An acceptable image should be obtained before advancing the imaging catheter into the body. With both systems this should appear as a central catheter image with concentric bright echo arcs or rings radiating outward from the center. In the solid-state systems, ring-down artifact (a “halo” surrounding the catheter) is typically subtracted electronically.

The imaging catheter is positioned within the coronary artery using standard interventional techniques. As the catheter is advanced, kinks and bends in the mechanical catheter should be avoided so that drive shaft and other assemblies remain intact. Images tend to be optimal when the catheter is coaxial within the vessel and slight manipulation may be necessary by the interventionist to improve the image. It is the norm for the catheter to be slightly off center; however, every effort should be taken to keep the catheter coaxial, as the off-center ultrasound signal will produce artifactual intensity findings because of backscatter and elliptical distortion of structures.

All current systems allow the operator to rotate the image electronically to achieve a standard image presentation. Although there is no standard orientation, it is intuitive to rotate the image so that when viewing the left anterior descending (LAD) artery, the left circumflex (LCX) departs at 9 o'clock. With this orientation, the septal perforators will come off between 2 and 8 o'clock (bottom of arc) and the diagonal branches to the left, between 8 and 12 o'clock. Similarly, when imaging the LCX, orient the image so that the LAD comes off at 3 o'clock. In the LCX, the obtuse marginal branches should depart at 12 and 6 o'clock. Using a guiding catheter with side-holes can help facilitate orientation (3). The use of this type of positioning allows for consistency with serial imaging and helps the inexperienced viewer orient quickly.

After the IVUS catheter is positioned distal to the area of interest, imaging can commence and a continuous automated pullback should be started. Automated pullback devices are available from all manufacturers. The use of motorized devices for pullback (most commonly at 0.5 mm/sec to 1.0 mm/sec) is strongly recommended to allow reproducibility and longitudinal image interpretation (4). This is important for two reasons: It gives the ability to measure or register the position of a given cross-section for repeat studies, and it provides the potential for a reasonably accurate longitudinal or three-dimensional representation of a segment.

IMAGE INTERPRETATION

An understanding of the normal coronary artery morphology is important as a background for image interpretation. From the vantage point of the blood-filled vessel lumen, the first tissue layer that is encountered is the superficial endothelial cell layer that covers a small layer of connective tissue and smooth muscle cells, the subintima. Collectively, this layer is called the intima. The intima begins as a single cell layer at birth, increases to a thickness of about 60 mm during childhood, to about 200 mm at age 30, and to 250 mm by age 40. Diffuse intimal thickening can be seen in older patients and may not represent atherosclerotic disease. Additionally, the intima can be physiologically thickened at points where there is increased wall tension such as within tortuous segments and at bifurcations. A sheet of elastic tissue known as the internal elastic lamina separates the intima from the media. The media is a muscular layer composed of primarily smooth muscle cells with smaller amounts of connective tissue. The thickness of the media ranges from 125 to 350 mm and averages about 200 mm. Medial thinning occurs with age and with atherosclerotic disease. A second sheet of elastic tissue known as the external elastic lamina (EEL) separates the media from the adventitia. The adventitia is composed of collagen and elastic tissue and merges with the surrounding periadventitial tissue and is 300 to 500 mm in thickness.

In vitro studies with IVUS have suggested high degrees of correlation between cross-sectional morphology from histology and the ultrasound-determined vessel appearance. IVUS images from all current systems present in a two-dimensional cross-section format. Interpretation of the images begins with the identification of two key landmarks: the luminal border with the vessel wall (at the intima) and the media/adventitia interface (Fig. 19.1). The luminal border is the first bright interface beyond the catheter and is generally easy to locate on IVUS images by its bright contrast with the intraluminal blood. Blood exhibits a “speckled” low-intensity pattern that increases with increased ultrasound frequencies. Blood appears as a faint echo and is essentially not visible at 20-Mhz frequencies. At 30 MHz, blood speckle is typically seen as a chaotic continuous pattern but is so low in intensity that tissue structures can easily be visualized. At higher frequencies, blood speckling may become so prominent that it will obscure the tissue boundary, and specific subtraction algorithms are necessary. At times, the appearance of blood speckle is useful for delineating dissection planes where flow is present in the false lumen or when false channels are present within the plaque matrix. Injecting saline through the guiding catheter can be useful to delineate the true vessel border if unclear. Saline will cause the lumen to appear darker (by temporarily displacing blood targets), resulting in a sharper differentiation between blood and intima. Radiographic contrast does not give as much clarity or uniformity as saline.

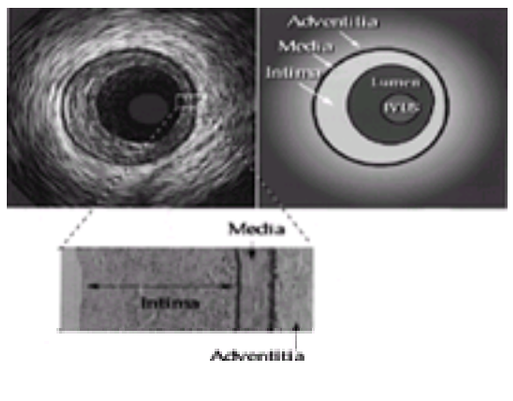

FIG. 19.1. Cross-sectional format of a typical intravascular ultrasound image. The bright-dark-bright three-layered appearance is seen in the image with corresponding anatomy as defined. IVUS represents the IVUS catheter in the blood vessel lumen. Histologic correlation with intima, media, and adventitia is shown. The media has lower ultrasound reflectance due to a lack of collagen and elastin compared with neighboring layers. Because the intimal layer reflects ultrasound more strongly than the media, there is a spillover in the image that results in a slight overestimation of the thickness of the intima and a corresponding underestimation of the medial thickness.

The media/adventitia border is a second key landmark that must be identified. In particularly clear images, the media of coronary arteries stands out as a discrete, thin band that is darker than the intima or adventitia. The media has a low echodensity because it contains much less echoreflective material than the intima or adventitia, particularly collagen and elastin. The intima, media, and adventitia form a bright-dark-bright appearance that has been referred to as the “three-layered appearance” (5). Though considered the norm, there can be significant variations, and a large fraction of patients do not have this pattern. The media does not always appear as a completely distinct layer and can drop out or cover only part of the circumference of the vessel. Loss of the media can be seen in atherosclerotic disease where the media is thinned and may not be visualized (5). In truly normal arteries, it may also be difficult to appreciate a three-layered appearance despite the presence of an intact media. In young patients, the intima may not be thick enough to register as a separate layer (the resolution at 30 MHz is about 150 μm, so higher-resolution systems will have fewer problems). By age 40, intimal thickness is typically 250 μm and can usually be well visualized by IVUS. Additionally, there may be instances where the media has more collagen and elastin, such as in the proximal vessel segments and at branch points. At these sites, the media may blend with the

surrounding layers (5).

Because the intimal layer reflects ultrasound more strongly than the media, there is a spillover effect known as “blooming” in the image that results in a slight overestimation of the thickness of the intima and a corresponding underestimation of the medial thickness by encroachment (Fig. 19.1). On the other hand, the media/adventitia border is accurately rendered because there is a step-up in echoreflectivity at this boundary and no blooming occurs. The adventitia and periadventitial tissues are similar enough in echoreflectivity that a clear outer adventitial border cannot be defined.

The IVUS beam penetrates beyond the artery, providing images of perivascular structures, including the cardiac veins, the myocardium, and the pericardium. These structures have a characteristic appearance when viewed from different positions within the arterial tree, so they provide useful landmarks regarding the position of the imaging plane.

The left main coronary artery arises from the left sinus of Valsalva. It ranges in length between 1 and 25 mm and its diameter ranges from 2.0 to 5.5 mm (mean 4 mm) (6,7 and 8). It passes between the pulmonary artery and left atrium before typically bifurcating into left LAD and LCX branches, in one-third of cases giving rise to a ramus intermedius. IVUS visualization of the left main coronary artery, observed when exiting the guiding catheter, often produces a dark crescent-shaped shadow. This large echo-free defect, the transverse sinus, represents a potential space as the pericardium drapes from the aorta to the surface of the heart. This space becomes more prominent in the image when there is pericardial fluid accumulation (7).

As the imaging catheter is advanced into the left main, the bifurcation into the LAD and LCX can be easily seen as a large interruption in the circular arc of the vessel. The LAD is 10 to 13 cm in length with a mean diameter of 3.6 mm (typically ranging from 2.0 to 5.0 mm) (8) and turns downward toward the apex in the anterior interventricular groove, giving off diagonal branches, which supply the lateral margin of the heart, and septal branches, which supply the anterior septum. A large, triangular, echo-free space can be seen from the very proximal LAD that is bounded by the LAD, LCX, and great cardiac vein (GCV). This space is known by anatomists as the Triangle of Brock and Mouchet. It too is filled with pericardial fluid and can vary in size with fluid as seen by IVUS (7). The first perforating septal branch is usually within 1 cm of the LAD origin and is often the largest branch that arises from the LAD. In the mid-LAD, pericardium is often visualized as an echo-dense, thick structure that moves back and forth with the cardiac cycle. This can be used as a guide for LAD branching as the diagonal branches tend to take off orthogonally to the pericardial signals while the septal branches head away or opposite the pericardium. The distal LAD can be identified by the presence of one or two anterior interventricular veins (AIV) paralleling the vessel. More proximally, the AIV gives rise to the GCV, which also runs parallel to the LAD (Fig. 19.2). The middle and distal LAD may be surrounded by myocardium. The branching pattern in the LAD also is distinctive by IVUS. The septal perforators generally branch at a wider angle (more perpendicular) than the diagonals so that on the IVUS scan the septals appear to bud away from the LAD much more abruptly than the diagonals. Diagonal branches can often be seen in the far field and gradually move toward the LAD on pullback. They ultimately appear to exit the LAD in a similar direction as the LCX (7).

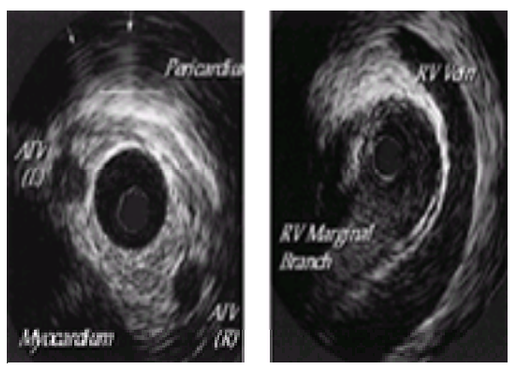

FIG. 19.2. Perivascular landmarks. The left panel represents a distal cross-section from the LAD. The right and left branches of the anterior interventricular vein (AIV) are seen to frame the coronary artery. The pericardium appears as a bright arc with reverberations emitting from it *(arrows)*. The right panel represents typical imaging at the level of the middle right coronary artery. Bridging veins arch over the artery, typically at a position just adjacent to the RV marginal branches.

The LCX is typically 6 to 8 cm long, with a mean diameter of 3.0 mm (range of 1.5 to 5.5 mm) (8). It runs along the anterior interatrial furrow and then down the left atrioventricular sulcus. It typically gives rise to large marginal branches, depending on the dominance of the right coronary system. With ultrasound imaging, the LCX is noticeably more mobile than the LAD as it lies in the atrioventricular groove. The GCV (proximally) and coronary sinus (distally) can be seen adjacent to the LCX running superiorly (on the atrial side) and occasionally across the artery. The venous structures typically have significantly larger diameters than the artery and often assume a crescent shape. Obtuse marginal branches typically take off from the LCX opposite these venous structures and away from the atrium in the same general direction as the LAD.

A dominant right coronary artery (RCA) usually runs 12 to 14 cm before giving rise to the posterior descending artery (PDA) and/or atrioventricular nodal artery (6,7 and 8). While the LAD and LCX typically taper throughout their course, the RCA remains generally constant (mean diameter of 3.2 mm; range 1.5 to 5.5 mm) (8) until just before the takeoff of the PDA. The PDA extends along the posterior longitudinal (interventricular) sulcus toward the terminal or apical portion of the LAD. On IVUS examination, the RCA is similar to the LCX in that its position in the atrioventricular groove leads to large motion relative to the catheter transducer. The RCA can be easily identified by the presence of crossing anterior cardiac veins that arch in a “rainbow-like” fashion over the artery, often adjacent to RV marginal branches (Fig. 19.2). Recurrent atrial branches originate opposite the RV marginal ostia and are usually much smaller (7).

The combination of perivascular landmarks and branching patterns allows the experienced operator to identify the vessel and segment from the IVUS image alone. It is important to keep in mind that unless the image is specifically adjusted, the rotational orientation of the structures presented on the screen is arbitrary and can vary between imaging runs. The branching pattern and perivascular landmarks, once understood, provide a reference for the rotational orientation.

QUANTITATIVE ASSESSMENT

The use of quantitative measures is of great utility during IVUS examination. Unlike quantitative coronary angiography, IVUS systems do not require routine calibration. All systems have software that provides superimposed calibrated measurement (diameters and areas). Measurements are typically performed at the stenosis site where the minimum lumen area is present and in reference segments both proximal and distal to the lesion. While the stenosis site is usually unequivocal, the selection of the reference is operator dependent and should be in an angiographically normal segment. Criteria for reference selection have been suggested for stent implantation (5 mm from both ends of the stented territory), but precisely reproducible references are more difficult in other interventions. It must be remembered that it is common for the reference site to have significant plaque present.

All current systems have software that allows rapid quantitation of useful distance and area measurements. Commonly used area measurements include the lumen area, total vessel area, and plaque area. The lumen area is determined by tracing the leading edge of the blood/intima border (Fig. 19.1). Often, real-time playback can help clarify this border for accurate tracing. The IVUS standard for total vessel area is taken as the mean area enclosed by the outermost interface between media and adventitia, which coincides with the EEL. Measurement of the IEL would theoretically allow the calculation of true intimal or plaque area, but the IEL is not well delineated in most cases. Vessel area is often obscured by calcium shadowing, and extrapolation must be made based on the closest identifiable media/adventitia or EEL border. Plaque area (or more accurately, the “plaque + media” area) is calculated as the difference between total vessel and lumen areas. From this it is straightforward to calculate the percentage plaque area or “percentage plaque burden,” which has also been called the “percent cross-sectional narrowing” by some investigators.

Lumen diameters are critically important in everyday clinical practice where interventional sizing is needed. Direct measurement of the maximum and minimum diameter within a stenosis is the most widely used technique. While the maximum lumen diameter is usually easy to define, the selection of the minimum lumen diameter can be problematic when borders of the lumen are irregular. The minimum lumen diameter is measured as the smallest diameter in any direction passing through the midpoint of the maximum diameter. The ratio of maximum to minimum diameter defines a symmetry measure with ratios lower than 1.0, suggesting

increasing lumen asymmetry (8).

Care should be taken to avoid or account for artifactual errors in measurement. Alignment of the catheter in a noncoaxial plane can result in an elliptical image rather than an accurate, usually more circular cross-sectional imaging plane. Image distortion, such as NURD, can result in rotational angle artifacts. Additionally, there are variations with the cardiac cycle which must be accounted for. The maximum areas are present in midsystole and the minimum areas, in late diastole (except in the presence of arteries that are tunneled into the muscle layer, so-called myocardial bridges, where there is systolic compression). The cyclic variation in lumen area is on the average of 8% in native coronary arteries (8). Quantitative angiography typically uses end-diastolic frames for measurement by convention. An argument can be made that a more physiologically correct approach with IVUS is to measure dimensions in systole, when there is maximum distending pressure to minimize effects of a false lumen when present.

ARTERIAL DISEASE

Atherosclerotic tissue consists of fat and lipid with cholesterol, fibrin, and calcium deposits. Plaque is often infiltrated by macrophages and lymphocytes. The early changes of atherosclerotic disease, so-called fatty streaks, are represented histologically by disruption of the internal elastic lamina and are not capable of being visualized with the current resolution of IVUS. With progression of atherosclerosis, intimal thickening occurs and can be imaged. With advanced disease, different disease patterns appear. The atherosclerotic plaque presents as intimal thickening with duplication, fragmentation, and eventually disintegration of the internal elastic lamina so that the intimal/medial border becomes blurred. As plaque develops, the acoustic properties allow identification of several basic tissue types. A highly cellular fibromuscular plaque with extensive lipid/fat infiltration has low echoreflectivity and appears as “soft plaque.” Denser fibrous lesions then form with lower lipid concentration, more heterogeneous cell types, and connective tissue. Occasionally, within this fibrous plaque, localized areas of lipid deposition and necrotic tissue can be seen as a lipid pool. Tissue within this substrate often forms a fibrous cap over the lipid pool. The furthest end of the spectrum is calcified plaque, which can have a very heterogeneous distribution. It can form in layers superficially on the rim of the luminal border, or form more punctate granules or lie deep within the intima/media.

The easiest tissue type to identify by IVUS is calcified plaque. Calcium deposits are recognized by bright reflections that produce shadowing, which obscures the true depth of the calcified plaque and all deeper tissue structures due to failure of the ultrasound signal to penetrate the dense tissue (Fig. 19.3). Shadowing can be accompanied by “reverberations” or ghost images of the calcium that appear as spaced arcs radiating from the real calcified lesion. Calcium is visualized in 60% to 80% of target lesions undergoing intervention when IVUS is performed, compared with 40% visualization by fluoroscopy/angiography (9,10). A rough rule of thumb is that an arc of calcium that occupies less than two quadrants (180°) on IVUS will not be visible on fluoroscopy. Interestingly, the presence of calcium on IVUS imaging appears to correlate with total coronary plaque burden but does not correlate well with severity of luminal obstruction by angiography (10). Calcium on IVUS is seen more frequently with increasing age and in patients with stable (as opposed to unstable) angina (10).

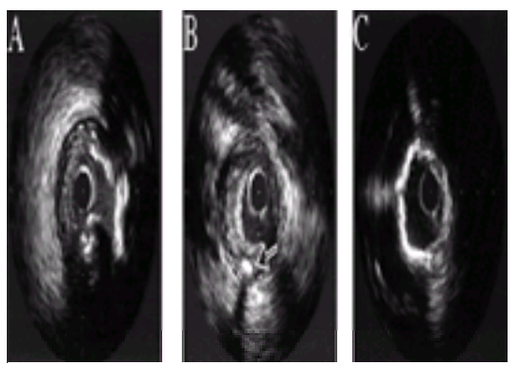

FIG. 19.3. Examples of coronary calcification. **A:** A complex calcified plaque is seen between 12 and 6 o'clock. There is superficial and deep calcium and a disrupted appearance. **B:** Heterogeneous tissue density is shown with a rim of fibrofatty plaque and a deep deposit of calcium at 7 o'clock (*arrow*). **C:** Superficial circumferential calcification gives a “napkin ring” appearance. Two zones of reverberation are seen at 5 o'clock and 9 o'clock. The external elastic lamina and adventitia are obscured by the shadowing of the superficial calcium layer.

Dense fibrous tissue has a bright, heterogeneous appearance on IVUS and can have a spotty appearance. The echoreflectivity is usually at the same intensity or higher than the adventitia. Occasionally, fibrous tissue will also shadow the ultrasound beam, and this can be difficult to distinguish from calcium. Usually, however, dense fibrous plaque has a less intense IVUS image than calcium and is less echogenic or less “bright.” Compared with calcium, the beam penetrates a short distance into the fibrous tissue beyond the luminal interface. The extent of shadowing is dependent on both the thickness and density of the fibrotic region, as well as the transducer strength.

Soft or fatty plaque is less bright than fibrous plaque. The brightness of the adventitia can be used as a gauge to discriminate predominantly fatty from fibrous plaque. Using the adventitia as a standard, when an area of plaque appears darker, it is generally fatty. In an image of extremely good quality, the presence of a lipid pool can be inferred from the appearance of a dark region within the plaque. Suspected lipid pools may be false channels, however, which can give a similar appearance. Occasionally, shadowing from an adjacent region of calcification or fibrosis may look much like a lipid pool.

One of the major limitations of IVUS in terms of identifying tissue is the difficulty in discriminating thrombus from soft plaque. These two tissue types often have a similar signal or “texture” and a comparable intensity or brightness. With IVUS, there are clues to the presence of thrombus that can be useful in some cases. Thrombus is much more likely than soft plaque (a) if there is a nodular appearance or there are clefts; (b) if small channels can be identified within the tissue; (c) if there is a scintillating appearance (reminiscent of amyloidosis on transthoracic echocardiography); or (d) if there is tissue motion during the cardiac cycle that suggests more flexibility than motion seen with plaque. There is promise that computer-enhanced processing of the raw ultrasound signal may help the discrimination between thrombus and plaque.

The application of IVUS in clinical practice has given us many insights into the nature of coronary disease that angiography did not afford. For example, in patients with coronary artery disease, IVUS generally reveals a much larger plaque burden than would be estimated by angiography (11,12 and 13). IVUS reminds us that coronary disease is a systemic process. When a vessel appears to have one discrete stenosis by angiography, IVUS almost invariably shows that considerable atherosclerotic disease is present throughout the entire length of the vessel. Studies have shown that the reference segment for an intervention—which by definition is normal or near normal angiographically—has on average of 35% to 51% of its cross-sectional area occupied by plaque (Fig. 19.4) (13,14). It is unusual in patients with clinical coronary disease to find any portion of an artery that is completely clear of plaque accumulation in at least some part of its circumference.

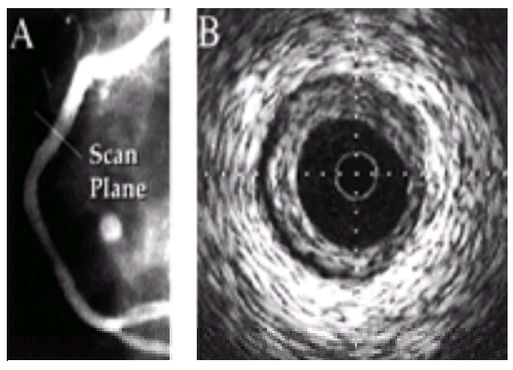

FIG. 19.4. Angiographically silent disease. The angiogram of the right coronary artery suggests minimal disease **(A)**. IVUS images **(B)**, however, show significant circumferential plaque ranging from 0.5 to 1.5 mm thickness throughout its length. The lumen is large, round, and regular, accounting for the benign angiographic

appearance.

IVUS also gives a very precise representation of the distribution of plaque within the vessel wall and the variation of intimal thickness—specifically the eccentricity and concentricity of atherosclerotic plaque—and the relationship of plaque volume to vessel wall area. Contrasted with IVUS, angiography has demonstrated significant limitations in its ability to characterize the degree of plaque eccentricity. Phase I of the GUIDE trial (Guidance by Ultrasound Imaging for Decision Endpoints) compared the assessment of eccentricity by angiography to an IVUS-determined eccentricity ratio of the thinnest-to-thickest segment of plaque (9). In plaques that were judged to be concentric by angiography, there was a broad distribution of actual eccentricity ratios from plaques with a ratio near 1 (truly concentric) to plaques with a ratio as low as 1:5 (highly eccentric). Conversely, many diseased segments judged to be eccentric by angiography were relatively concentric when viewed directly by IVUS (9).

The phenomenon of remodeling, as originally described by the pathologist Glagov (15), is often seen by IVUS (14). Remodeling is a localized expansion of the vessel wall in areas of high plaque burden—as if the vessel has stretched to accommodate the accumulation of plaque. This would lessen the degree of luminal narrowing to less than what would be expected if the vessel had remained a consistent caliber. IVUS studies have demonstrated that the remodeling response is in fact heterogeneous, with some segments showing the positive remodeling of the typical Glagov paradigm and others showing negative remodeling, “shrinkage” or constriction, in the area of lumen stenosis (15,16,17,18,19 and 20). At present we have no clear understanding of the variables that influence the type and extent of remodeling. The same heterogeneity appears to occur as part of the restenosis process following coronary intervention (21).

Many studies have suggested that atherosclerosis occurs in particular areas of the arterial circulation such as branch sites and curved segments where there are disturbed blood flow patterns. Clinically, this is illustrated with the predilection for plaque formation in the proximal LAD (22,23). Consistent with postmortem studies, IVUS has demonstrated that proximal LAD lesions are localized on the opposite wall of the branch divider, the crux of the left main, consistent with the theory that abnormally low shear forces may contribute to this clinically important site (22). Similarly, studies have shown that atherosclerotic plaque tends to form on the inner curvature of the vessel arc, which can be determined as the wall opposite the pericardium when seen on IVUS.

DIAGNOSTIC APPLICATIONS

IVUS has been used to clarify situations when angiography shows lesion severity to be equivocal or “intermediate.” Angiographically, difficult lesions typically occur at an ostial location or in tortuous segments where angiography may not lay out the vessel well for interpretation (23,24 and 25). Ultrasound can be useful but should be used judiciously. Plaque burden can be high in areas of stenosis that are not hemodynamically restrictive and may not warrant treatment. Assessment of physiologic obstruction is beyond the anatomic information that IVUS provides and no criteria are established for hemodynamic significance by IVUS. A percent luminal stenosis can be determined by comparing cross-sectional areas at the target and reference sites, similar to angiography. Area stenosis by IVUS of 70% is equivalent to a 50%-diameter stenosis. The finding of a meaningful angiographic equivalent, however, does not mean that the lesion will impede flow. Alternatively, some have suggested minimum-lumen diameter can be used as an assessment. In a large vessel, 1.5 mm has been suggested as a cutoff point and is usually visualized when plaque is completely encircling, or “cuffing,” the IVUS catheter. In uncertain situations, it may be more appropriate to assess lesion severity with functional testing, either in he catheterization laboratory with Doppler or pressure measurement or via noninvasive stress testing.

When coronary angiography is normal in patients with suspected coronary artery disease, IVUS has been used to assess for the presence of plaque. In these patients, plaque has been observed in 48% of cases (26). If Doppler-derived coronary flow reserve is also assessed, only 36% of patients are found to be entirely normal (26). While this does suggest a new classification for patients with syndrome X or chest pain without significant epicardial coronary obstruction, the clinical relevance for treatment and lack of evidence for an alteration in prognosis makes IVUS imaging in this setting of unclear utility.

Similarly, IVUS has been utilized to assess the accelerated coronary artery disease seen after heart transplantation (27,28). The vasculopathy seen typically consists of concentric intimal proliferation that progresses to diffuse arterial obliteration. Especially early in disease, angiography has been found to be limited in diagnostic yield. IVUS has shown that proliferation occurs in the first 2 years after transplantation with the development of more complex plaque with calcium and focal stenoses later on in areas where there is failure of vessel wall compensation (8,28). Unfortunately, while IVUS can describe the process very precisely, effective treatments remain to be discovered.

GUIDANCE FOR INTERVENTIONS

Preintervention Imaging

IVUS imaging has been useful in selecting appropriate catheter-based intervention as well as in optimizing the results of coronary procedures (29,30). With current technology, more than 90% of lesions can be imaged before intervention, providing valuable information about the extent, length, and circumferential location of plaque and the nature of the tissue involved (12). This can lead to a change in interventional strategy in 20% to 40% of cases (29,30). The presence, location, and extent of calcium can significantly affect the performance of balloon angioplasty, atherectomy, and stent deployment (see later discussion). The distribution of plaque can also be determined and may favor certain ablative procedures such as rotational and directional atherectomy. Precise delineation of lesion length can guide debulking procedures as well as stent selection. Cross-sectional vessel sizing is also a useful measurement that allows for the appropriate sizing of devices to be employed.

Balloon Angioplasty

Insights into Mechanism of Action

IVUS has provided many insights into the mechanism of action involved with balloon angioplasty. Tearing or dissection of plaque is a frequent and important feature of PTCA and occurs in 45% to 70% of cases as seen by IVUS imaging compared with 20% to 45% by angiography (Fig. 19.5) (9,31,32 and 33). Angioplasty success may depend on dissection as a mechanism as presence of dissections is associated with a greater acute gain (increase in lumen diameter) than the absence of any tearing after PTCA (12). Ultrasound has shown that dissections are often localized to calcified areas where shearing forces from dilation are high at the junction with surrounding plaque (33). When plaque is eccentric in morphology, tears typically occur at the junction between plaque and normal vessel wall where the elastic, nondiseased wall stretches away from the more rigid plaque. Elastic recoil is an important countermechanism to balloon angioplasty and can be dramatic with reduction in lumen size observed when IVUS imaging is done soon after balloon dilatation. Data from the GUIDE trial suggest that lesions with dissections have less recoil than lesions that have not had intimal disruption, suggesting that once the dissection threshold is reached, the constrictive process that causes mechanical recoil may be lessened (9).

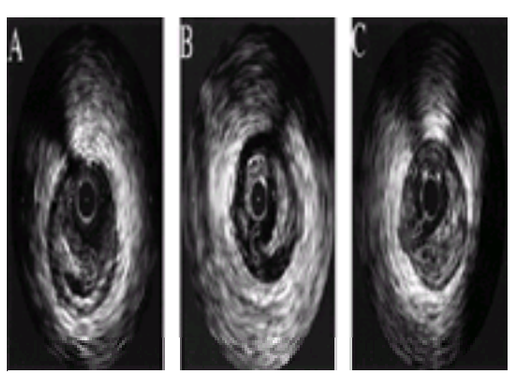

FIG. 19.5. Examples of dissections. **A:** A superficial dissection starting at 6 o'clock and extending clockwise. The dissection flap does not extend far into the vessel lumen. **B:** A deeper dissection with dissection flap that extends into the lumen and may compromise flow or precede abrupt closure. Injection of contrast in this setting can demonstrate free fluid flow behind the flap to better define the dissection plan. **C:** Eccentric plaque with a deep dissection at 8 o'clock that penetrates the external

elastic lamina and extends into the adventitia.

High-quality IVUS imaging can demonstrate the depth of dissections, especially with regard to the involvement of media or adventitia (Fig. 19.5) (9,31). This may have implications with respect to increased response to injury and worsened long-term outcome. Prospective study has shown that severe dissections that predispose to abrupt closure are difficult to predict by IVUS before intervention (32). Firm IVUS criteria to predict the likelihood of vessel closure are not established and would likely require an integration of longitudinal and circumferential information with dissection depth.

Guidance of Procedures

IVUS has been used effectively to guide balloon sizing in PTCA. The CLOUT (ClinicalOutcomes with Ultrasound Trial) examined whether aggressive balloon sizing guided by IVUS measures was safe and effective (34). Investigators chose balloon sizes that were determined by the measured average of reference vessel and lumen diameters leading to an average oversizing of the balloon by angiography of 0.5 mm. This strategy led to an average postprocedure residual stenosis of 18%, without an increase in complications. The approach was expanded and confirmed by two single-center studies where balloon sizing based on vessel diameter alone with high-pressure inflation saw a large acute lumen gain with safe procedural outcomes (35,36). Six-month follow-up also showed stent-like angiographic restenosis rates of about 20% (35,36).

Arguments have been made that with IVUS sizing of balloons and subsequent treatment site examination, a strategy of IVUS-guided “provisional PTCA” as a method to decrease stent usage can be supported. This two-step approach would include preinterventional imaging to assess the vessel diameter and select balloon size followed by postinterventional imaging to assess whether the angiographic appearance is acceptable to assess the need for stenting. Proceeding to stenting is then based on the specific criteria of a small minimum luminal diameter (<2.0 mm) or large residual plaque area (>65%). Using this strategy, stenting was avoided in 38% of lesions treated with large lumen gain and low target lesion revascularization rate of 17% in an unpublished single-center experience.

Insights into Outcome

Quantitative angiographic measures are poor predictors of long-term results from balloon angioplasty. Several efforts have examined the use of IVUS to predict restenosis. The PICTURE (Post Intra-Coronary Treatment Ultrasound Restenosis Evaluation) studied 200 patients with IVUS after final balloon inflation and found no correlation between IVUS-defined lesion composition, quantitative measures, dissection presence and long-term clinical and angiographic results (37). In contrast, Mintz and coworkers studied lesions after transcatheter intervention and found that residual plaque burden as measured by IVUS was an independent predictor of restenosis (38). A plot of residual plaque burden with 6-month restenosis saw a curvilinear relationship with restenosis occurring in more than 50% of lesions where more than 70% residual plaque burden was observed immediately after intervention. In phase II of the GUIDE trial, operators were blinded to the IVUS information on scans done immediately after 500 PTCA and directional coronary atherectomy procedures. Analysis of data without discriminating between PTCA and atherectomy revealed that residual plaque burden and minimal lumen diameter by IVUS were predictive of recurrence of symptoms at 6 months. No angiographic parameters were predictive. Morphologic IVUS variables such as calcification or presence or type of dissection were also not predictive of long-term outcome. An additional single-center experience found similar results. The cumulative data suggest that residual plaque area is an important predictor of restenosis with PTCA (30).

Anatomic information provided by IVUS imaging gives insight into the mechanism of restenosis. The restenotic process can be divided into two major components: tissue proliferation and arterial remodeling. In nonstented patients with restenosis, most late lumen loss is due to arterial remodeling or vessel shrinkage (a decrease in vessel cross-sectional area). Only about a quarter of the restenosis effect is due to tissue proliferation (39). In some patients, there is enlargement of vessel area after intervention and restenosis is infrequent when this adaptive response occurs even in the presence of increased plaque (39). This is contrary to the mechanism of restenosis after stent implantation where tissue proliferation is the only contribution to late lumen loss as vessel constriction is largely abolished.

Directional Atherectomy

Insights into Mechanism of Action

Directional coronary atherectomy (DCA) was designed to treat lesions by selective plaque removal. IVUS studies have demonstrated that plaque removal only accounts for 50% to 70% of lumen gain with this technique, the remaining portion being due to mechanical expansion by the device passage—the “Dottering” effect and balloon dilatation (40). Using standard DCA techniques where angiographic success is seen with residual stenoses of less than 20%, IVUS imaging revealed that an average of 60% residual plaque burden is present, which may contribute to the significant restenosis rates seen with DCA (40).

Guidance of Procedures

IVUS imaging has been used successfully as an adjuvant to DCA. The presence of calcium, especially when it is superficial and forms a “rim,” is problematic and reduces tissue retrieval (41,42). When calcium is deep and near the medial border or when it is deposited in a granular pattern, DCA can cut effectively and can be used aggressively, sometimes with less concern for medial invasion. Using IVUS as a directional aid to improve plaque removal has the theoretical advantage of providing greater lumen sizes with more complete plaque removal. This must be done with a methodical approach and a good understanding of the three-dimensional coronary anatomy as defined by IVUS and angiography. Typically, the area of greatest plaque accumulation is identified by IVUS. Then, utilizing a branch point near the stenosis for orientation, the DCA cutter can be aligned similar to the IVUS catheter at the branch point by angiography. The DCA device can then be positioned at the treatment site and, with IVUS-determined rotation, the cutting device can be “aimed” at the target plaque area. Serial ultrasound examination with repeated reorientation is required for aggressive debulking.

Insights into Outcome

Trials have demonstrated that approaches using IVUS-guided DCA can be effective. The Optimal Atherectomy Restenosis (OARS) trial confirmed that IVUS guidance achieved an improved immediate result with residual stenoses that were “stent-like” (7% residual stenosis) (43) with high procedural success. However, the angiographic restenosis rate was 29% with subsequent target vessel revascularization or major ischemic event rate of 20%. The Adjunctive Balloon Angioplasty following Coronary Atherectomy Study (ABACAS) trial saw even more complete plaque removal than OARS (45% vs. 57% residual plaque burden), which resulted in a reduction in 6-month angiographic restenosis to 21%.

As with PTCA, studies verify that the mechanism of restenosis with DCA is largely due to arterial remodeling leading to late lumen loss. In a study where serial IVUS imaging was performed after DCA, more than 60% of lumen loss seen at 6 months was due to vessel shrinkage (43,44). Whether more complete excision of plaque will ultimately impact on vessel shrinkage remains to be seen.

Rotational Atherectomy

Insights into Mechanism of Action

In contrast to directional atherectomy, rotational atherectomy effectively ablates calcific and densely fibrotic plaque, particularly when calcium is located at or near the luminal surface (45,46 and 47). The lumen created by rotational atherectomy, when examined by IVUS, has a smooth, round appearance in calcified plaque with a lumen size that is 90% to 100% of the burr size. Rotational atherectomy results in a decrease in plaque area with no significant impact on total vessel area (45), suggesting that there is very little vessel stretch. In noncalcified plaque, however, the lumen tends to be more irregular and smaller in diameter, perhaps due to a combination of recoil and/or arterial spasm. Effective ablation still occurs, however, even with lesions that do not demonstrate calcium on preintervention IVUS (45).

Guidance of Procedures

As an aid to rotational atherectomy technique, IVUS can guide burr sizing. It is common for a satisfactory rotational atherectomy angiographic result to have extensive plaque on IVUS scanning. Using IVUS can help the operator avoid use of burrs that are undersized for the vessel. Usually, a reference segment remote from the

lesion must be employed since shadowing from calcium can obscure measurement of vessel dimensions at the stenosis. Similarly, burr sizes have been shown to be accurately gauged using IVUS before treatment of in-stent restenosis, especially when stents are small in diameter (48). IVUS allows the safe aggressive sizing of rotational atherectomy burrs in most clinical situations. Additionally, IVUS can be used to assess the severity of guidewire bias where the burr guidewire may be aligned with vessel structures, particularly bifurcations, that may lead to unwanted trauma.

Stents

Insights into Mechanism of Action

The most common clinical application of IVUS technology to date has been in the imaging of coronary stents (8,48,49 and 50). Stents are easily visualized on IVUS examination as a collection of very bright distinct echoes, allowing definition of the stent structure within the lumen of the vessel. Each stent and stent type has a distinctive IVUS appearance (Fig. 19.6). Stents essentially fix the vessel wall in place, leaving a rigid scaffold and a vessel area on IVUS that generally does not change with serial examination over time (particularly with rigid stents such as the slotted tubes). The plaque at the intervention site, however, does not remain fixed. IVUS has demonstrated that similar to balloon angioplasty (51), noncalcified plaque that is present at the stent site extrudes in an axial direction from under the stented area during stent deployment. Careful analysis has demonstrated that the plaque volume lost at the stented region is gained at distal and proximal reference sites and may explain the angiographic appearance of a “step up/step down.”

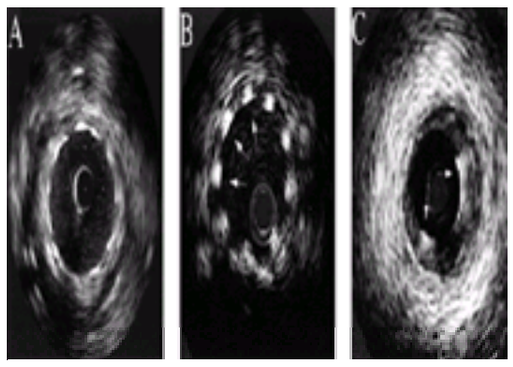

FIG. 19.6. Stent signatures. **A:** Typical cellular design stents (Scimed NIR, Boston Scientific Scimed, Maple Grove, MN) with good apposition has an IVUS appearance where stent struts create bright echos in a radial pattern. **B:** The IVUS image from a self-expanding nickel-titanium design stent (Scimed Radius stent) shows the struts as discrete points *(arrows)*. **C:** The IVUS image from a coil design stent (Gianturco-Roubin stent, Cook Cardiology, Bloomington, IN) displays the stent architecture as two arcs *(arrows)* where the ultrasound beam plane has intersected a short length of the coil.

Artifacts specific to stents on IVUS can be seen because of the high reflectance of the stent metal, typically stainless steel. For example, when strut echoreflectance is strong, stent “ghosts” can be seen within the lumen of the vessel. With mechanical transducers, signals can be detected by the back of the rotating transducer as weak images creating an image within the lumen that can mimic the presence of intraluminal struts. The presence of a ghost can be detected by observing that the motion of the ghost artifact is opposite to the motion of the adjacent wall and concordant with the opposite wall. Lateral distortion or “whitecaps” are seen more frequently with solid-state transducer systems. Poor lateral resolution can lead to a smearing of the strut image and give the false impression that the strut is protruding into the vessel lumen. These artifacts should be less problematic as improved imaging systems are developed.

Guidance of Procedures

In the deployment of stents, issues of greatest concern as seen by IVUS are incomplete apposition and incomplete expansion (Fig. 19.7). Incomplete apposition occurs when part of the stent structure is not fully imprinted into the vessel wall. This may cause local flow disturbances and increase the risk for subacute thrombosis. Incomplete apposition is seen in 3% to 10% of stent cases and most commonly involves the stent edges, particularly the proximal edge. Incomplete expansion occurs when a portion of the stent is fully pressed into the vessel wall but inadequately expanded compared with the distal and proximal reference dimensions. Incomplete expansion occurs most frequently in areas of the vessel where dense fibrocalcific or fully calcified plaque is present. At bend points, where plaque buildup tends to be larger, incomplete expansion also tends to be common.

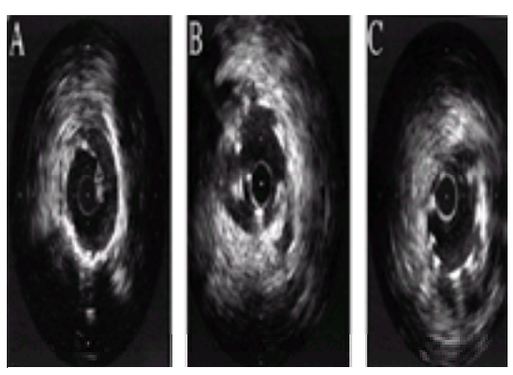

FIG. 19.7. IVUS-detected problems with stent deployment. The left image **(A)** shows an edge tear or “pocket flap” with a disruption of plaque at the stent margin with little compromise of the lumen. When there is incomplete apposition **(B)**, there is a gap between a portion of the stent and the vessel wall (between 4 and 12 o'clock on the IVUS image). The apparent thickness of the stent struts in this area is due to reverberations. Injection of contrast or saline or blood speckling on a dynamic image can help define this lumen boundary. The right image **(C)** shows incomplete apposition and expansion. Expansion of the lumen is assessed relative to the ends of the stent and the reference segments. Apposition of the stent is dependent on definition of the lumen boundary, which can be seen beyond the stent struts at 3 o'clock and 9 and 10 o'clock.

Early in the stent experience abnormalities in stent deployment had been seen on IVUS in up to 88% of cases even when patients had angiographically optimal results (50). These IVUS findings were described in patients where stents were deployed at 6 to 8 atmospheres inflation pressure and led to the application of high-pressure inflation strategies to achieve better IVUS measures of stent deployment. Generally, criteria for stent deployment have focused on achieving adequate apposition and expansion. The Multicenter Ultrasound-guided Stent Implantation in Coronaries (MUSIC) trial required that IVUS-guided stenting result in (a) complete apposition over the entire stent length, (b) in-stent minimal lumen area greater than or equal to 90% of the average of the reference areas or 100% of the smallest reference area, and (c) symmetric stent expansion with minimal/maximal lumen diameter greater than or equal to 0.7 (8). Similar criteria have been established for other stent trials.

Insights into Outcome

Procedural criteria such as MUSIC have been utilized and were confirmed to be effective in several IVUS studies with reduced rates of subacute thrombosis to less than 2% (52,53). Subsequent studies demonstrated that stenting at high pressures could be performed without IVUS to achieve similar low rates of subacute thrombosis (54,55). Because of improvements in stent techniques and the difficulty in performing a trial large enough to demonstrate what would be a small benefit from routine IVUS imaging, the use of IVUS with intracoronary stent placement does not appear to be a cost-effective measure to reduce the now low risk of subacute thrombosis.

Are there subsets of patients who are at higher thrombotic risk and may benefit from poststent IVUS imaging? The Predictors and Outcomes of Stent Thrombosis (POST) registry examined IVUS recordings and angiography in 55 patients who suffered stent thrombosis and found that 90% of patients had suboptimal IVUS results such as incomplete apposition (47%), incomplete expansion (52%), and evidence of thrombus (24%). Reexamination of imaging studies revealed that only 25% of patients had abnormalities on angiography. This suggests that when it is done, IVUS may be able to prospectively predict subacute closure. Thus it has been suggested that an intermediate strategy to evaluate for subacute thrombosis risk after stent deployment would be to utilize IVUS selectively when thrombosis is more likely (bifurcation lesions, small vessels, long lesions, slow angiographic flow) or when consequences would be particularly catastrophic (unprotected left main or left main equivalent).

Longer-term studies after stent implantation have shown that IVUS imaging at the time of implantation can predict outcomes at 6 months and beyond. In MUSIC, use of IVUS optimization criteria resulted in a low target vessel revascularization rate of 9% at 6 months (8). Other studies have shown that the IVUS-determined minimal in-stent cross-sectional area is a predictor of restenosis and target vessel revascularization, especially when less than 7 mm^2. In the CRUISE (Can Routine Ultrasound Improve Stent Expansion) trial, IVUS guidance by operator preferences significantly decreased the percentage of stents with minimum lumen areas below 7 mm^2 and led to a 44% reduction in target vessel revascularization to 6.7% at 9 months compared with when IVUS guidance was not used. The Angiography Versus IVUS-Directed (AVID) stent placement trial randomized 800 patients to IVUS guidance versus standard angiography. Preliminary data saw that the use of IVUS resulted in an average increase of almost 2 mm^2 gained in minimum stent area (increase of more than 25% in area) compared with angiography alone. Data on target vessel revascularization at 6 months and 12 months are pending. The RESIST (Restenosis after IVUS-guided Stenting) trial randomized 164 patients to IVUS-guided stent placement versus angiography alone and saw a similar increase in minimum stent area (56). Interestingly, the IVUS group saw a 60% rate of inadequate stent deployment in patients with acceptable angiographic results of whom 80% were treated until criteria were met. There was a 50% reduction in 6-month restenosis rate to a rate of 15% in the IVUS-guided group that did not reach statistical significance. Though a significant reduction in restenosis was not seen, the authors felt the trend toward lower restenosis, a larger stent lumen diameter, and improved minimum lumen diameter by angiography could not exclude the benefit of IVUS imaging with stent deployment. The OPTICUS (Optimal IntraCoronary UltraSound to reduce restenosis) trial randomized 550 patients to examine if IVUS-guided stent implantation to meet MUSIC criteria would see a reduction in restenosis rates at 6 months. Preliminary data with off-line analysis saw 68% of the IVUS group meet all the MUSIC criteria with similar procedure times and balloon and stent usage. Final analysis of this trial, however, found that there was no difference between angiographic and IVUS-guided strategies in angiographic restenosis as would have been predicted by the similar immediate postprocedural lumen diameters seen between the two groups. In a recent large real-world experience with IVUS-guided stent implantation, Kasaoka et al. reported on 2,343 lesions treated with stent implantation at high pressures over a 4-year period. Patients were examined with immediate postprocedural IVUS in more than 75% of cases, leading to further balloon inflations in 34% of cases and further stent implantation in 19% (57). This approach saw restenosis significantly reduced from 29% to 24% with IVUS guidance. Multivariate analysis suggested that IVUS guidance, larger lumen diameter, larger IVUS cross-sectional area, decreased stent length, and use of a single stent were important procedural variables that predicted a decrease in in-stent restenosis. Taken in aggregate, studies have shown that IVUS-guided stent implantation consistently increased lumen areas with similar patient safety and reduced long-term events and particularly restenosis rate. Whether the advantage gained by IVUS will be cost-effective in the stent setting will await the cumulative analysis of these data.

In-stent restenosis is clearly a different process from restenosis in the nonstented patient (Fig. 19.8) (38,58,59). IVUS studies have demonstrated that the primary process involved is neointimal proliferation rather than vessel shrinkage in slotted-tube stent designs. When an articulation is present in the stent, the contribution of vessel shrinkage can lead to a focal stenosis; however, the in-stent restenosis process tends to be uniformly distributed along the stent segment and neighboring vessel (58,59). The restenotic process shows similar measures of lumen size, plaque area, and remodeling with IVUS imaging in native arteries and in vein grafts as well as in multistent settings (58). As in nonstented interventions, the intimal growth process seems to be more aggressive in diabetic patients (60). In a single-center experience, multivariate analysis of angiographic and IVUS predictors of in-stent restenosis revealed that an ostial location, preinterventional lesion plaque burden, and postinterventional lumen dimension were all predictive of restenosis (61).

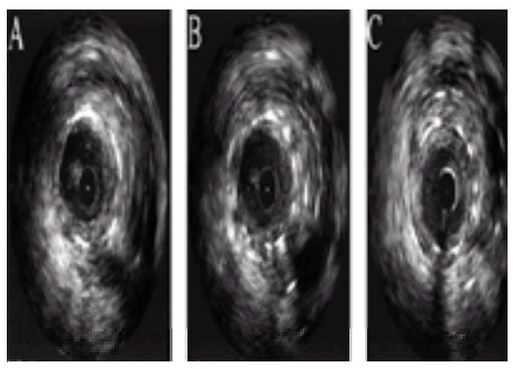

FIG. 19.8. In-stent restenosis. Intimal hyperplasia can be seen within the stent architecture of a coil stent **(A)** or slotted tube stent **(B,C)**. The pattern is typically concentric **(C)** or mildly eccentric **(A** and **B)**.

Unfortunately, treatment of in-stent restenosis has been complicated by a high recurrence rate. IVUS can be helpful in guiding therapy, especially if ablative therapies are being considered and concentricity and lumen size are important. When imaging, the in-stent tissue can be difficult to visualize because of low echoreflectance and may require careful gray scale adjustment. Observational studies suggest that the in-stent restenosis intervention is followed by reintrusion of tissue that is not angiographically evident. About 40 minutes after intervention, repeat IVUS imaging shows the reintrusion process with minimal lumen area decrease of about 20% (62). The degree of reintrusion correlates with the amount of intimal plaque seen as well as stent length (62). This finding may help explain why it appears that ablative therapies appear to have better outcomes than balloon angioplasty for in-stent restenosis.

SAFETY

As with other interventional procedures, the possibility of spasm, dissection, and thrombosis exists when intravascular imaging catheters are used. Hausmann and colleagues (63) examined the issue of safety of intracoronary ultrasound in a multicenter retrospective survey of 2,207 patients. The most common complication seen was spasm, which occurred in 2.9% of patients during IVUS imaging. In 0.4% of patients, complications other than spasm were judged to have a “certain relation” to IVUS, including acute procedural events in six and major events in three patients. The complication rate was higher in patients with unstable angina or acute myocardial infarction (2.1% events) as compared with patients with stable angina pectoris and asymptomatic patients, 0.8% and 0.4%, respectively (63). These complications were also more frequent in patients undergoing interventions (1.9%) than in those with transplant and nontransplant patients undergoing diagnostic IVUS imaging (0 and 0.6%), as has been noted in other studies (27). No association was detected between these events and the size or type of IVUS catheter used.

COSTS

In the United States, current retail sales prices for the stand-alone single-use imaging catheters range between $600 and $850. In 1997 to 1998, IVUS was used in approximately 6% of catheter-based coronary interventional cases in the United States, 3% of cases in Europe, and 20% of cases in Japan. There were an estimated 128,000 coronary IVUS cases in the world in 1998. IVUS systems were available in 39% of catheterization laboratories in the United States as of 1998.

The 1998 usage statistics suggest a 30% increase in usage compared with 1997, driven in part by improved reimbursement. The Health Care Financing Administration approved reimbursement for the IVUS procedure and interpretation for Medicare patients in 1997. For intracoronary ultrasound, reimbursement is based on the number of vessels imaged and varies for the different geographic regions in the country. A number of other carriers have also approved reimbursement for IVUS, although payment is on a region-by-region basis.

FUTURE DIRECTIONS

The technology of IVUS continues to evolve on many fronts. Device improvements have moved toward lower-profile probes with improved handling with higher frequencies. Image quality has seen significant gains due to higher-frequency imaging at 40 to 45 MHz. Prototype work with 50-MHz imaging catheters has shown

improved image quality, though issues remain with blood artifact (64). Imaging guidewires remain a difficulty and present an attractive technical challenge. The continued miniaturization of ultrasound transducers is of obvious benefit in integration of imaging into interventional procedures more seamlessly. A mechanical transducer 0.035-inch imaging core guidewire has been developed for peripheral application that requires replacement of a standard guidewire within a catheter and images through the catheter material to assess vessel anatomy (65). Prototypes for standard coronary dimensions, 0.018 inch and 0.014 inch, are being explored (65,66). Forward-viewing IVUS catheter systems offer the advantage of imaging features without actually passing wire and catheter into the site of interest. Prototype mechanical systems have been developed and are larger than current cross-sectional imaging catheters (67,68). These would offer the hope of being able to guide chronic total occlusion intervention.

The addition of flow information to IVUS imaging has been achieved to provide a color flow signal, displayed as a real-time pulsatile color pattern in response to blood speckle. This color coding can aid in defining the luminal border. One step beyond this is combination devices under development where side-imaging IVUS catheters have simultaneous forward Doppler velocimetry, providing real-time measurement of volumetric blood flow (the product of cross-sectional area and average forward-velocity vector).

Integration of serial two-dimensional IVUS into three-dimensional reconstructions of coronary anatomy has been successfully developed (Fig. 19.9) (69). In three-dimensional format, IVUS can render entire coronary segments and allow examination in several orientations, allowing detailed insights into the geometry of atherosclerotic plaques and effects of intervention. The main limitation of the three-dimensional reconstruction is the difficulty in representing the curvature of the vessel in an accurate manner. Instrumentation has been developed to provide ECG-gated automated quantitative three-dimensional IVUS reconstruction, reducing the analysis time and the subjectivity of boundary tracing (70).

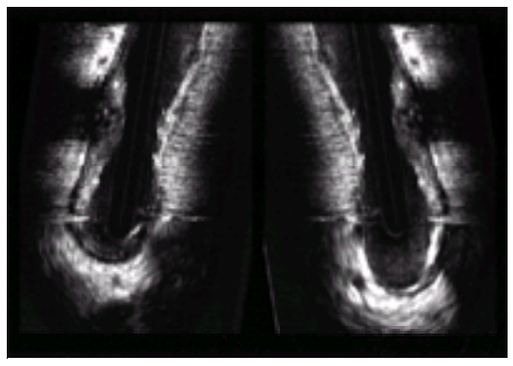

FIG. 19.9. Three-dimensional reconstruction of IVUS cross-sectional images acquired at constant pullback speed (0.5 mm/sec) in the left anterior descending artery. The IVUS study was performed over an eccentric plaque in the proximal portion of the LAD. Spatial relationship between vascular structures are clearly depicted. The catheter itself is represented by the solid tube in the center of the vessel.

Beta and gamma radiation are being actively explored as therapies to counteract restenosis associated with balloon angioplasty and stent placement. Initial results have shown great promise, but dosing and positioning of source within the coronary artery are critical. IVUS is being utilized in conjunction with this new technology, as it allows real-time information on centering and vessel size (71). The role IVUS will play if and when this therapy becomes commonly accepted remains to be seen.

There has been great interest in finding diagnostic methodologies to identify the vulnerable plaque and discriminate features of the plaque tissue (72). Although catheter-based techniques have been focused on treatment of fixed lesions within the coronary tree that are hemodynamically obstructive, acute plaque disruption often occurs at nonobstructive sites, leading to the acute coronary syndromes. With high-quality images, IVUS can identify features that suggest a potential site of a future event—lipid pools and fibrous cap—vascular architecture thought to be a precursor to thrombotic events. Greater promise lies in the analysis of raw ultrasound and radiofrequency signals to add information regarding tissue structure and "vulnerability." Studies have already demonstrated an ability to differentiate thrombus and soft atherosclerotic plaque (73,74). Other imaging technologies that may enhance tissue characterization and are being developed for catheter-based intravascular application include optical coherence tomography (OCT) and magnetic resonance imaging (MRI).

IVUS examination remains a very helpful aid in the cardiac catheterization laboratory. It offers additional information in many clinical settings. Vessel findings beyond angiography can be seen with IVUS that can aid in all forms of coronary intervention. It continues to add to our understanding of atherosclerotic disease. IVUS has been and remains a critical tool for interventionalists in understanding mechanisms of disease progression and response to therapy.

ACKNOWLEDGMENTS

We would like to acknowledge Ali Hassan for his work with the figures for this chapter and Jennifer Witcher for administrative assistance.

CHAPTER REFERENCES

1. Nissen SE, Grines CL, Gurley JC, et al. Application of a new phased-array ultrasound imaging catheter in the assessment of vascular dimensions. *In vivo* comparison to cineangiography. *Circulation* 1990;81:660.
2. Yock PG, Linker DT, Angelsen BA. Two-dimensional intravascular ultrasound: technical development and initial clinical experience. *J Am Soc Echocardiogr* 1989;2:296.
3. Schwarzacher SP, Fitzgerald PJ, Metz JA, et al. Enhancement of spatial orientation of intravascular ultrasound images with side holes in guiding catheters. *Am Heart J* 1998;135:1063.
4. Fuessl RT, Mintz GS, Pichard AD, et al. *In vivo* validation of intravascular ultrasound length measurements using a motorized transducer pullback system. *Am J Cardiol* 1996;77:1115.
5. Fitzgerald PJ, St GF, Connolly AJ, et al. Intravascular ultrasound imaging of coronary arteries. Is three layers the norm? *Circulation* 1992;86:154.
6. Waller BF, Orr CM, Slack JD, Pinkerton CA, Van TJ, Peters T. Anatomy, histology, and pathology of coronary arteries: a review relevant to new interventional and imaging techniques—Part I. *Circulation* 1992;85:2305.
7. Fitzgerald PJ, Yock C, Yock PG. Orientation of intracoronary ultrasonography: looking beyond the artery. *J Am Soc Echocardiogr* 1998;11:13.
8. DiMario C, Gorge G, Peters R, et al. Clinical application and image interpretation in intracoronary ultrasound. *Eur Heart J* 1998;19:207.
9. Fitzgerald PJ, Yock PG. Mechanisms and outcomes of angioplasty and atherectomy assessed by intravascular ultrasound imaging. *J Clin Ultrasound* 1993;21:579.
10. Mintz GS, Pichard AD, Popma JJ, et al. Determinants and correlates of target lesion calcium in coronary artery disease: a clinical, angiographic and intravascular ultrasound study. *J Am Coll Cardiol* 1997;29:268.
11. Hausmann D, Johnson JA, Sudhir K, et al. Angiographically silent atherosclerosis detected by intravascular ultrasound in patients with familial hypercholesterolemia and familial combined hyperlipidemia: correlation with high density lipoproteins. *J Am Coll Cardiol* 1996;27:1562.
12. Mintz GS, Popma JJ, Pichard AD, et al. Limitations of angiography in the assessment of plaque distribution in coronary artery disease: a systematic study of target lesion eccentricity in 1446 lesions. *Circulation* 1996;93:924.
13. St Goar F, Pinto FJ, Alderman EL, Fitzgerald PJ, Stadius ML, Popp RL. Intravascular ultrasound imaging of angiographically normal coronary arteries: an *in vivo* comparison with quantitative angiography. *J Am Coll Cardiol* 1991;18:952.
14. Mintz GS, Painter JA, Pichard AD, et al. Atherosclerosis in angiographically "normal" coronary artery reference segments: an intravascular ultrasound study with clinical correlations. *J Am Coll Cardiol* 1995;25:1479.
15. Glagov S, Weisenberg E, Zarins CK, Stankunavicius R, Kolettis GJ. Compensatory enlargement of human atherosclerotic coronary arteries. *N Engl J Med* 1987;316:1371.
16. Hermiller JB, Tenaglia AN, Kisslo KB, et al. *In vivo* validation of compensatory enlargement of atherosclerotic coronary arteries. *Am J Cardiol* 1993;71:665.
17. Nishioka T, Luo H, Eigler NL, Berglund H, Kim CJ, Siegel RJ. Contribution of inadequate compensatory enlargement to development of human coronary artery stenosis: an *in vivo* intravascular ultrasound study. *J Am Coll Cardiol* 1996;27:1571.
18. Mintz GS, Kent KM, Pichard AD, Salter LF, Popma JJ, Leon MB. Contribution of inadequate arterial remodeling to the development of focal coronary artery stenoses: an intravascular ultrasound study. *Circulation* 1997;95:1791.
19. Pasterkamp G, Wensing PJ, Post MJ, Hillen B, Mali WP, Borst C. Paradoxical arterial wall shrinkage may contribute to luminal narrowing of human atherosclerotic femoral arteries. *Circulation* 1995;91:1444.
20. Berglund H, Luo H, Nishioka T, et al. Highly localized arterial remodeling in patients with coronary atherosclerosis: an intravascular ultrasound study. *Circulation* 1997;96:1470.
21. Post MJ, Borst C, Kuntz RE. The relative importance of arterial remodeling compared with intimal hyperplasia in lumen renarrowing after balloon angioplasty. *Circulation* 1994;89:2816.
22. Montenegro MR, Eggen DA. Topography of atherosclerosis in the coronary arteries. *Lab Invest* 1968;18:586.
23. Kimura BJ, Russo RJ, Bhargava V, McDaniel MB, Peterson KL, DeMaria AN. Atheroma morphology and distribution in proximal left anterior descending coronary artery: *in vivo* observations. *J Am Coll Cardiol* 1996;27:825.
24. Iwami T, Fujii T, Miura T, et al. Importance of left anterior descending coronary artery curvature in determining cross-sectional plaque distribution assessed by intravascular ultrasound. *Am J Cardiol* 1998;82:381.
25. Hermiller JB, Buller CE, Tenaglia AN, et al. Unrecognized left main coronary artery disease in patients undergoing interventional procedures. *Am J Cardiol* 1993;71:173.

26. Erbel R, Ge J, Bockisch A, et al. Value of intracoronary ultrasound and Doppler in the differentiation of angiographically normal arteries: a prospective study in patients with angina pectoris. *Eur Heart J* 1996;17:880.
27. St Goar FG, Pinto FJ, Alderman EL, et al. Intracoronary ultrasound in cardiac transplant recipients. *In vivo* evidence of "angiographically silent" intimal thickening. *Circulation* 1992;85:979.
28. Pethig K, Heublein B, Wahlers T, Haverich A. Mechanism of luminal narrowing in cardiac allograft vasculopathy: inadequate vascular remodeling rather than intimal hyperplasia is the major predictor of coronary artery stenosis. Working Group on Cardiac Allograft Vasculopathy. *Am Heart J* 1998;135:628.
29. Mintz GS, Pichard AD, Kovach JA, et al. Impact of preintervention intravascular ultrasound imaging on transcatheter treatment strategies in coronary artery disease. *Am J Cardiol* 1994;73:423.
30. Gorge G, Ge J, Erbel R. Role of intravascular ultrasound in the evaluation of mechanisms of coronary intervention and restenosis. *Am J Cardiol* 1998;81:91G.
31. Honye J, Mahon DJ, Jain A, et al. Morphological effects of coronary balloon angioplasty *in vivo* assessed by intravascular ultrasound imaging. *Circulation* 1992;85:1012.
32. Athanasiadis A, Haase KK, Wullen B, et al. Lesion morphology assessed by pre-interventional intravascular ultrasound does not predict the incidence of severe coronary artery dissections. *Eur Heart J* 1998;19:870.
33. Fitzgerald PJ, Ports TA, Yock PG. Contribution of localized calcium deposits to dissection after angioplasty: an observational study using intravascular ultrasound. *Circulation* 1992;86:64.
34. Stone GW, Hodgson JM, St Goar FG, et al. Improved procedural results of coronary angioplasty with intravascular ultrasound-guided balloon sizing: the CLOUT pilot trial. *Circulation* 1997;95:2044.
35. Haase KK, Athanasiadis A, Mahrholdt H, et al. Acute and one year follow-up results after vessel size adapted PTCA using intracoronary ultrasound [see comments]. *Eur Heart J* 1998;19:263.
36. Colombo A, Kobayashi Y. Intravascular ultrasound-guided PTCA [Editorial]. *Eur Heart J* 1998;19:196.
37. Peters RJG, Kok WEM, DiMario C, et al. Prediction of restenosis after coronary balloon angioplasty: results of the PICTURE (Post-IntraCoronary Treatment Ultrasound Result Evaluation). A prospective multicenter intracoronary ultrasound imaging study. *Circulation* 1997;95:2254.
38. Mintz GS, Popma JJ, Pichard AD, et al. Intravascular ultrasound predictors of restenosis following percutaneous transcatheter coronary revascularization. *J Am Coll Cardiol* 1996;27:1678.
39. Mintz GS, Popma JJ, Pichard AD, et al. Arterial remodeling after coronary angioplasty: a serial intravascular ultrasound study. *Circulation* 1996;94:35.
40. Safian RD, Gelbfish JS, Erny RE, Schnitt SJ, Schmidt DA, Baim DS. Coronary atherectomy. Clinical, angiographic, and histological findings and observations regarding potential mechanisms. *Circulation* 1990;82:69.
41. Popma JJ, Mintz GS, Satler LF, et al. Clinical and angiographic outcome after directional coronary atherectomy: a qualitative and quantitative analysis using coronary arteriography and intravascular ultrasound. *Am J Cardiol* 1993;72:55E.
42. Matar FA, Mintz GS, Pinnow E, et al. Multivariate predictors of intravascular ultrasound end points after directional coronary atherectomy. *J Am Coll Cardiol* 1995;25:318.
43. Simonton CA, Leon MB, Baim DS, et al. "Optimal" directional coronary atherectomy: final results of the Optimal Atherectomy Restenosis Study (OARS). *Circulation* 1998;97:332.
44. Kimura T, Kaburagi S, Tamura T, et al. Remodeling of human coronary arteries undergoing coronary angioplasty or atherectomy. *Circulation* 1997;96:475.
45. Dussaillant GR, Mintz GS, Pichard AD, et al. Effect of rotational atherectomy in noncalcified atherosclerotic plaque: a volumetric intravascular ultrasound study. *J Am Coll Cardiol* 1996;28:856.
46. Kovach JA, Mintz GS, Pichard AD, et al. Sequential intravascular ultrasound characterization of the mechanisms of rotational atherectomy and adjunct balloon angioplasty. *J Am Coll Cardiol* 1993;22:1024.
47. Mintz GS, Potkin BN, Keren G, et al. Intravascular ultrasound evaluation of the effect of rotational atherectomy in obstructive atherosclerotic coronary artery disease. *Circulation* 1992;86:1383.
48. Schiele F, Meneveau N, Vuillemenot A, Gupta S, Bassand JP. Treatment of in-stent restenosis with high speed rotational atherectomy and IVUS guidance in small <3.0 mm vessels. *Cathet Cardiovasc Diagn* 1998;44:77.
49. Goldberg SL, Colombo A, Nakamura S, Almagor Y, Maiello L, Tobis JM. Benefit of intracoronary ultrasound in the deployment of Palmaz-Schatz stents. *J Am Coll Cardiol* 1994;24:996.
50. Nakamura S, Colombo A, Gaglione A, et al. Intracoronary ultrasound observations during stent implantation. *Circulation* 1994;89:2026.
51. Mintz GS, Pichard AD, Kent KM, Satler LF, Popma JJ, Leon MB. Axial plaque redistribution as a mechanism of percutaneous transluminal coronary angioplasty. *Am J Cardiol* 1996;77:427.
52. Colombo A, Hall P, Nakamura S, et al. Intracoronary stenting without anticoagulation accomplished with intravascular ultrasound guidance. *Circulation* 1995;91:1676.
53. Gorge G, Haude M, Ge J, et al. Intravascular ultrasound after low and high inflation pressure coronary artery stent implantation. *J Am Coll Cardiol* 1995;26:725.
54. Goods CM, Al SK, Yadav SS, et al. Utilization of the coronary balloon-expandable coil stent without anticoagulation or intravascular ultrasound. *Circulation* 1996;93:1803.
55. Nakamura S, Hall P, Gaglione A, et al. High pressure assisted coronary stent implantation accomplished without intravascular ultrasound guidance and subsequent anticoagulation. *J Am Coll Cardiol* 1997;29:21.
56. Schiele F, Meneveau N, Vuillemenot A, et al. Impact of intravascular ultrasound guidance in stent deployment on 6-month restenosis rate: a multicenter, randomized study comparing two strategies—with and without intravascular ultrasound guidance. RESIST Study Group. REStenosis after Ivus guided STenting. *J Am Coll Cardiol* 1998;32:320.
57. Kasaoka S, Tobis JM, Akiyama T, et al. Angiograhic and intravascular ultrasound predictors of in-stent restenosis. *J Am Coll Cardiol* 1998;32:1630.
58. Hoffmann R, Mintz GS, Dussaillant GR, et al. Patterns and mechanisms of in-stent restenosis: a serial intravascular ultrasound study. *Circulation* 1996;94:1247.
59. Mintz GS, Hoffmann R, Mehran R, et al. In-stent restenosis: the Washington Hospital Center experience. *Am J Cardiol* 1998;81:7E.
60. Kornowski R, Mintz GS, Kent KM, et al. Increased restenosis in diabetes mellitus after coronary interventions is due to exaggerated intimal hyperplasia. *Circulation* 1997;95:1366.
61. Hoffmann R, Mintz GS, Mehran R, et al. Intravascular ultrasound predictors of angiographic restenosis in lesions treated with Palmaz-Schatz stents. *J Am Coll Cardiol* 1998;31:43.
62. Shiran A, Mintz GS, Waksman R, et al. Early lumen loss after treatment of in-stent restenosis: an intravascular ultrasound study. *Circulation* 1998;98:200.
63. Hausmann D, Erbel R, Alibelli CM, et al. The safety of intracoronary ultrasound: a multicenter survey of 2207 examinations. *Circulation.* 1995;91:623.
64. Foster FS, Knapik DA, Machado JC, Ryan LK, Nissen SE. High-frequency intracoronary ultrasound imaging. *Semin Interv Cardiol* 1997;2:33.
65. Hamm MA, Lowe GE, Koger JD. Technical aspects of ultrasound imaging guidewires. *Semin Interv Cardiol* 1997;2:63.
66. Hiro T, Hall P, Maiello L, et al. Clinical feasibility of 0.018-inch intravascular ultrasound imaging device. *Am Heart J* 1998;136:1017.
67. Evans JL, Ng KH, Vonesh MJ, et al. Arterial imaging with a new forward-viewing intravascular ultrasound catheter, I. Initial studies. *Circulation* 1994;89:712.
68. Ng KH, Evans JL, Vonesh MJ, et al. Arterial imaging with a new forward-viewing intravascular ultrasound catheter, II. Three-dimensional reconstruction and display of data. *Circulation* 1994;89:718.
69. Von Birgelen C, Li W, Bom N, Serruys PW. Quantitative three-dimensional intravascular ultrasound. *Semin Interv Cardiol* 1997;2:25.
70. Von Birgelen C, de Vrey EA, Mintz GS, et al. ECG-gated three-dimensional intravascular ultrasound: feasibility and reproducibility of the automated analysis of coronary lumen and atherosclerotic plaque dimensions in humans. *Circulation* 1997;96:2944.
71. Carlier SG, Marijnissen JPA, Coen VLMA, et al. Guidance of intracoronary radiation therapy based on dose-volume histograms derived from quantitative intravascular ultrasound. *IEEE Trans Med Imag* 1998;17:772.
72. Kleber FX, Dopfmer S, Thieme T. Invasive strategies to discriminate stable and unstable coronary plaques. *Eur Heart J* 1998;19:C44.
73. Moore MP, Spencer T, Salter DM, et al. Characterisation of coronary atherosclerotic morphology by spectral analysis of radiofrequency signal: *in vitro* intravascular ultrasound study with histological and radiological validation. *Heart* 1998;79:459.
74. Picano E, Landini L, Urbani MP, Mazzarisi A, Paterni M, Mazzone AM. Ultrasound tissue characterization techniques in evaluating plaque structure. *Am J Card Imaging* 1994;8:123.

20
Endomyocardial Biopsy

Donald S. Baim

Harvard Medical School; Center for Innovative Minimally Invasive Therapy, Brigham and Women's Hospital, Boston Massachusetts 02115

Examination of fragments of right or left ventricular endomyocardium recovered during cardiac catheterization (endomyocardial biopsy) remains an important tool in the detection of transplant rejection and identification of specific disease process that cause primary myocardial dysfunction (1). This chapter focuses on the currently available techniques for endomyocardial biopsy and reviews the disease states in which evaluation of myocardial histology appears most valuable. As the indications for endomyocardial biopsy are reviewed, the reader should keep in mind that the definition, frequency, natural history, and optimal treatment of many of these myocardial disorders are still in dispute. As a result, centers may differ significantly in their use of endomyocardial biopsy in the routine evaluation of patients with myocardial disease.

BIOPSY DEVICES

Cardiac biopsy was initially performed in the 1950s by means of limited thoracotomy. Subsequent attempts at transthoracic needle biopsy were frustrated by an almost 10% incidence of major complications, including pneumothorax, tamponade, and coronary laceration (2,3). Over the past several decades, these techniques have been replaced by a series of catheter-based biopsy systems (or bioptomes) that permit rapid and safe transvascular biopsy of either the left or right ventricular endomyocardium. There are two basic types of bioptomes: (a) stiff devices that are maneuvered independently through the vasculature and (b) more flexible devices that can be positioned only with the aid of a long sheath or introducing catheter.

Independent Bioptomes

The Konno Bioptome

In 1962, Sakakibara and Konno developed a biopsy catheter capable of transvascular introduction and retrieval of endomyocardial biopsy samples from either the left or right ventricular chamber (4). The original device consisted of a 100-cm catheter shaft with two sharpened cups (diameter either 2.5 or 3.5 mm) at its tip. These cups could be opened or closed under the control of a single wire, activated by a sliding assembly attached to the proximal end of the catheter. Because of the large size of the catheter head, it was usually introduced by cutdown entry of the saphenous or basilic vein (or the femoral or brachial artery), maneuvered into the desired ventricle under fluoroscopic guidance, and applied to the endocardial surface with its jaws closed. The catheter was then withdrawn slightly, opened, readvanced into contact with the endocardium, reclosed, and withdrawn. Although the Konno bioptome is still in limited use, the stiffness of its shaft complicates intravascular and intracardiac manipulation, which has led to the development of a variety of improved devices based on the same theme.

The Kawai Bioptome

Developed by Kawai and Kitaura in 1977, this device has a highly flexible tip that can be deflected up to 40° in one direction and up to 10° in the opposite direction by rotation of a knob on the operating handle (5,6) (Fig. 20.1). This allows easy maneuvering through the vasculature and across the aortic or tricuspid valve for right or left ventricular biopsy. Because of its extremely flexible tip, a stylet must be advanced into the catheter shaft before excision of an endomyocardial sample.

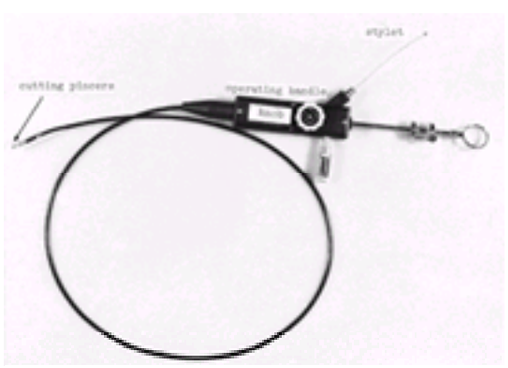

FIG. 20.1. The Kawai flexible endomyocardial biopsy catheter. (From Kawai C, Matsumori A, Kawamura K. Myocardial biopsy. *Annu Rev Med* 1980;31:139, with permission.)

The Stanford (Caves-Schulz) Bioptome

This device was developed as a modification of the Konno bioptome and was designed specifically for right ventricular biopsy by way of the right internal jugular vein (7,8) (Fig. 20.2). It has had wide application in the United States. The device consists of a somewhat flexible coil shaft fabricated from stainless steel and coated by clear plastic tubing (Sholten Surgical Supply, Palo Alto, CA). The tip of the catheter has two hemispheric cutting jaws with a combined diameter of 3.0 mm (9F); one jaw is opened and closed by a stainless steel wire running through the center of the bioptome shaft, while the other jaw remains stationary. The control wire is attached to a ratcheting surgical mosquito clamp by means of a pair of spring-loaded adjustable nuts that allow the operator to set the amount of force that is applied during opening and closing of the surgical clamp. These nuts should be adjusted so that the two biopsy jaws touch just as the two halves of the ratchet mechanism make contact. The distal end of the catheter is equipped with a curve that can be varied between 45° and 90° (depending on whether the clamp is closed to its first or second click). To facilitate orientation within the heart, the distal curve lies in the same orientation as the handle of the clamp. With adequate care and cleaning, each instrument can be used for more than 50 procedures without the need for sharpening or service.

FIG. 20.2. Stanford (Caves-Schulz) bioptome. The surgical clamp drives the control wire by way of its connection through the two adjustable nuts, thereby controlling the position of the single mobile jaw.

Other Independent Bioptome Designs

Disposable urethane-coated independent bioptomes are now available for use by the internal jugular approach. The use of disposable biopsy equipment may be wise in view of widespread concern over acquired immunodeficiency syndrome (AIDS) and other bloodborne infectious diseases. A special 7F pediatric Stanford bioptome is also available and may be used from the subclavian vein in adults with difficult jugular venous access. Use of any rigid bioptome from the subclavian vein is more difficult than from the right internal jugular vein, however, and the possibility of using one of the long-sheath techniques from an alternate site should be considered (see next section).

Long-sheath Devices

Whereas the independent bioptomes are designed to be maneuvered as a stand-alone catheters once they are introduced into the vascular system, the next group of bioptomes lack this ability and must be conveyed from the introduction site to the chamber targeted for biopsy through a long introducing sheath. This sheath also helps to orient the biopsy catheter toward the desired wall of the chamber (e.g., the septum of the right ventricle), although limited directionality of the bioptome itself is possible. The only remaining function of the long-sheath devices, then, is to be advanced into contact with the ventricular wall, obtain a sample of myocardial tissue, and retain it while the catheter is withdrawn through the sheath.

The King Bioptome

The King bioptome is a modification of the stainless steel Olympus bronchoscopic biopsy forceps (Olympus Corporation of America, Lake Success, NY), which is widely used in Europe (9,10) (Fig. 20.3). Its double-opening scissor-action jaws are controlled by an inner drive wire attached to a proximal control handle. A compression spring on the control handle keeps the jaws in their closed position unless the handle's thumb ring is pushed in. The flexible forceps shaft and closed jaws have an outer diameter of 1.8 mm, allowing the catheter to be introduced into the desired ventricle through a radiopaque 6F or 7F sheath that has been previously placed within the desired chamber. The sample is retrieved as described for the Stanford bioptome in the next paragraph.

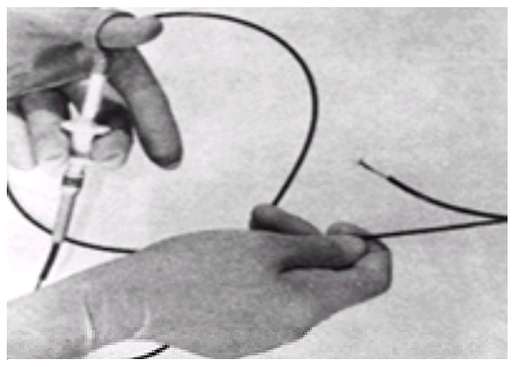

FIG. 20.3. The Olympus bioptome positioned through a modified Stanford biopsy sheath. (From Anderson JL, Marshall HW. The femoral venous approach to endomyocardial biopsy: comparison with internal jugular and transarterial approaches. *Am J Cardiol* 1984;53:833, with permission.)

The Stanford Left Ventricular Bioptome

The original Stanford bioptome was modified for left ventricular biopsy by doubling its length to 100 cm and reducing its outer diameter to 6F (8). With this reduction in shaft diameter, the catheter is no longer capable of independent movement through the vasculature and must be positioned with the aid of an 8F 90-cm curved Teflon sheath, which is itself introduced into the left ventricle over a conventional 100-cm 6.7F pigtail catheter (Stanford Biopsy Set, Cook Inc., Bloomington, IN). The tip of the sheath is positioned distal to the mitral apparatus and away from the posterobasal wall and apex, which are thinner and more easily perforated than other areas of the left ventricle. The pigtail catheter is then removed, the sheath is flushed, and the bioptome is introduced.

The Stanford left ventricular sheath was modified by Anderson to permit biopsy of the right ventricular septum by way of the percutaneous femoral venous approach (11). In his original description, the Teflon sheath of the Stanford Biopsy Set was heated over a forming wire to create an 8-cm distal semicircular curve with 70° posterior angulation of the final 3 cm (Fig. 20.3). When this sheath was placed in the right ventricle over the 6.7F pigtail catheter (itself heated to form a distal Cournand-like curve), the posterior angulation caused the sheath to rest against the septum (Fig. 20.4), allowing safe biopsy of that structure without risk of free wall perforation. This field modification is no longer required, because commercial guiding sheaths (Cordis Corporation, Miami, FL) that have been preformed into the desired distal curves (12) are now available for use with either the Stanford left ventricular bioptome or a variety of disposable transfemoral bioptomes (see next paragraph). A similar long-sheath system has been used to permit transseptal catheterization and endomyocardial biopsy of the left ventricle in children (13).

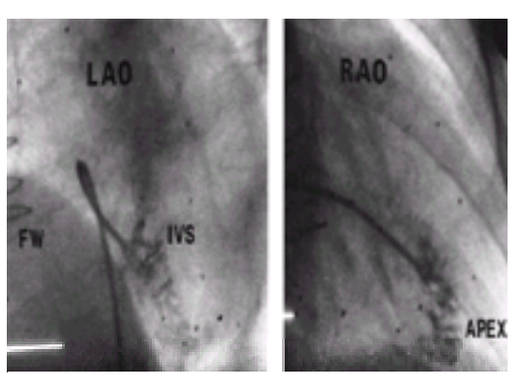

FIG. 20.4. Contrast injection in the left anterior oblique (LAO, *left*) and right anterior oblique (RAO, *right*) projections demonstrates correct position of the long sheath against apical-septal wall. FW, free wall of right ventricle; IVS, interventricular septum.

Disposable Long-sheath Bioptomes

Disposable 50- and 104-cm versions of a King-type bioptome are now available (Cordis Corporation; Mansfield Scientific, Inc., Mansfield, MA), with jaw sizes of 5.4F or 7F. These devices can be used from a variety of entry sites, in conjunction with various sheaths and guiding catheters. The *7F format,* however, requires a larger sheath internal diameter (at least 0.095 inch), such as the preshaped 8F, 98-cm curved Teflon introducing sheath marketed by Cordis. It is equipped with a back-bleed valve and side-arm flush mechanism and can be positioned within the right ventricular chamber over a conventional (pigtail or balloon flotation) catheter to allow subsequent biopsy using the 104-cm disposable bioptome. The *5.4F format* provides smaller tissue samples but allows the use of conventional 8F right coronary guiding catheter or one of the “Tampa Bay” shape (internal diameter at least 0.078 inches) as an alternative to the stiffer 8F Teflon sheath required by the 7F bioptome (14). The Tampa Bay guiding catheter has a 7-cm radius followed by a 1.1-cm distal angulated tip segment, allowing it to be stable within the right ventricle. It therefore resembles the preshaped Cordis sheath. In addition to using the preshaped sheath or guiding catheter, my colleagues and I usually manually bend the distal 1 cm of the bioptome by 45°, so that we can rotate the proximal shaft to orient the jaws more directly toward the septum.

The shorter (50-cm) disposable bioptome can be employed for right ventricular biopsy using a 35-cm sheath inserted by way of the internal jugular or subclavian vein on either side of the patient (15). This versatility of access site may be of value when serial biopsies must be performed in patients with thrombosis of the right internal jugular vein and restricted access from below (e.g., a vena caval filter).

BIOPSY TECHNIQUE

There are many different techniques that have been described for using the biopsy instruments previously described. This chapter concentrates on the two most common approaches.

The Stanford Bioptome Used from the Internal Jugular Vein

Internal Jugular Vein Puncture

The right ventricular endomyocardial biopsy procedure is usually performed via the right internal jugular vein. Although the internal jugular vein is widely used for hemodynamic monitoring or temporary pacing in the coronary care unit, it is used relatively infrequently in the cardiac catheterization laboratory, where access to the patient's neck from the head of the bed is limited by the presence of the x-ray gantry. The technique described here is designed to be used with the operator standing beside the patient.

Percutaneous puncture of the right internal jugular vein is performed with the patient lying supine without a pillow, with the head turned to the far left. With the patient in this position, the operator should be able to identify the relevant landmarks: the sternal notch, the sternal and clavicular heads of the right sternocleidomastoid muscle, and the top of the clavicle (Fig. 20.5). These anatomic features can be defined more easily by having the patient lift the head just off the table. With a 25-gauge needle, a small intradermal bleb of 1% lidocaine (Xylocaine) is injected near the center of the triangle formed by the two muscle heads and the clavicle, at a point approximately two fingerbreadths above the top of the clavicle. A skin nick is created with the tip of a no. 11 blade and enlarged with a small mosquito clamp. A 6-mL non-Luer syringe is filled with 2 mL of Xylocaine and attached to a 22-gauge, 1.5-inch needle. This needle is advanced through the skin nick at an angle 30° to 40° from the vertical and 20° to 30° right of the sagittal plane. Continuous suction is applied until the vein is entered, usually at a depth of 1 to 2.5 cm below the skin, using the steep angle of entry described. If desired, small boluses of Xylocaine can be injected into the soft tissues along the way, but the total volume injected should be kept to less than 1 mL to avoid compression of the vein within the carotid sheath. If the vein is not found, the needle should be withdrawn to the skin under continued suction, and puncture should be attempted with a slightly more lateral angulation. Only if this fails should a more medial angulation be tried, because medial angulation increases the risk of puncturing the carotid artery, which lies just deep and medial to the internal jugular vein. This uncertainty can be reduced by performing internal jugular puncture under ultrasound guidance, using a 7.5-MHz dedicated sector scanner (SiteRite, Dynamax Corporation, Pittsburgh PA) (16). Regardless of the approach, jugular venous puncture may be facilitated in patients with normal or low right atrial pressure by elevating the legs on a linen pack, using the Trendelenburg (head-down) position, or a having the patient perform a Valsalva maneuver. This increases central venous pressure and greatly distends the internal jugular vein, making it an easier target for needle puncture (Fig. 20.6).

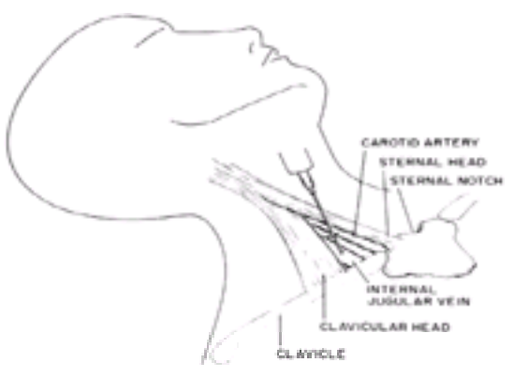

FIG. 20.5. Regional anatomy for right internal jugular vein puncture. With the patient's head rotated to the left, the sternal notch, clavicle, and the sternal and clavicular heads of the sternocleidomastoid muscle are identified. A skin nick is made between the two heads of the muscle, two fingerbreadths above the top of the clavicle, and the needle is inserted at an angle of 30° to 40° from vertical and 20° to 30° right of sagittal. This approach leads to reliable puncture of the internal jugular vein and aims the needle away from the more medially located carotid artery.

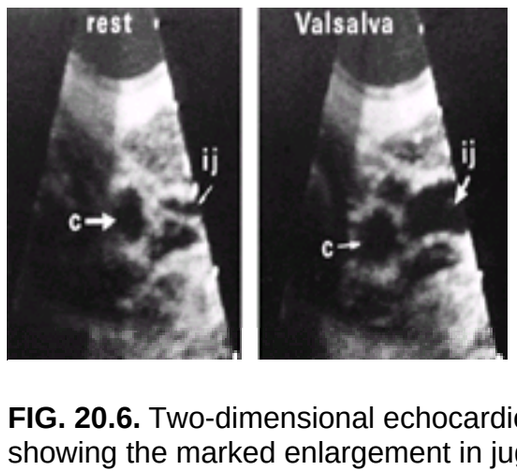

FIG. 20.6. Two-dimensional echocardiographic image of the carotid artery (c) and the internal jugular vein (ij) at rest *(left)* and during a Valsalva maneuver *(right)*, showing the marked enlargement in jugular venous caliber with increased distending pressure.

Once the vein has been entered, we usually leave the “test” needle in place and perform a parallel puncture using a 2.75-inch, 18-gauge, thin-wall needle (UMI, Universal Medical Instruments, Ballston Spa, NY), through which a 40-cm J guidewire is then advanced into the right atrium. The “test” needle is removed, and a 9F sheath with a side-arm and back-bleed valve (Cordis Corporation) is advanced over the guidewire and attached to a continuous intravenous drip adjusted to a moderate flow rate.

Biopsy Performance

The bioptome is inserted into the sheath, with its clamp closed on its first click, and advanced under fluoroscopy until its tip lies against the lower third of the lateral right atrial wall (Fig. 20.7). The catheter is then rotated counterclockwise (into an anteromedial orientation) and simultaneously advanced across the tricuspid valve. As the valve is being crossed, this counterclockwise rotation is continued so that the handle clamp points almost straight posteriorly as the tip of the bioptome approaches the apical half of the right ventricular cavity. To correctly position the bioptome, this maneuver must be performed with both finesse and assurance, because the stiff bioptome can perforate the thin free wall of the right atrium or ventricle if it is advanced too vigorously in the wrong orientation (Fig. 20.8). Two-dimensional echocardiography has been reported to be a useful alternative or adjunct to fluoroscopy for guiding endocardial biopsy, particularly in situations where fluoroscopy should be avoided (i.e., pregnancy) or where cardiac anatomy is distorted (e.g., heterotopic transplantation) (17), but fluoroscopy alone is usually adequate.

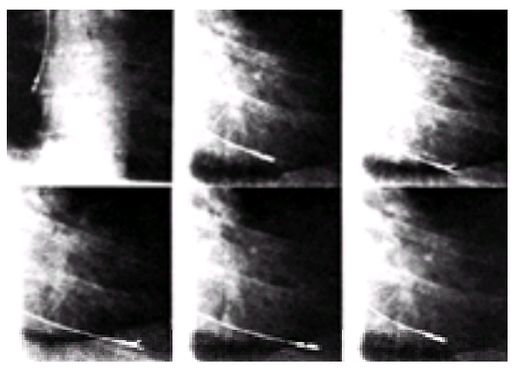

FIG. 20.7. Cineangiographic frames obtained during right ventricular endomyocardial biopsy using the Stanford bioptome. From left to right, the top row shows the bioptome against the lateral right atrial wall, against the ventricular septum, and withdrawn slightly with jaws opened. In the bottom row, the bioptome is reapplied to the septum, with subsequent closure of the jaws, and withdrawal of the sample.

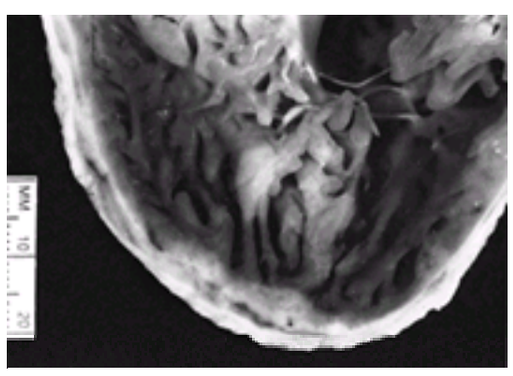

FIG. 20.8. Postmortem specimen shows the heavy trabeculation of the interior surface of the right ventricle and the thinness of the right ventricular free wall.

When this sequence has been followed, the tip of the bioptome will be directed toward the interventricular septum. On fluoroscopy, it should appear to lie across the spine and below the upper margin of the left hemidiaphragm. If there is any doubt about the final position of the bioptome in the right ventricle and against the septum, correct orientation can be confirmed further by fluoroscopy in both the 30° right anterior oblique (RAO) and 60° left anterior oblique (LAO) views. On occasion these views have disclosed unintentional positioning of the bioptome in the coronary sinus (i.e., in the atrioventricular groove in the RAO projection) or in an infradiaphragmatic vein (i.e., under the heart and beyond the left heart border in the LAO projection). If the bioptome is not in the correct position, it must be withdrawn into the atrium and repositioned appropriately before sampling is attempted. In some patients, successful positioning requires closing the handle clamp to its second click, to further increase the curve of the bioptome (i.e., to 90°).

Contact with the ventricular myocardium is recognized by the lack of further advancement, the occurrence of premature ventricular contractions, and the transmission of ventricular impulses to the operator's hand.

Once the biopsy catheter is in the desired position against the septal endocardium, it is withdrawn about 1 cm, the jaws are opened, and the catheter is gently readvanced into contact with the endocardium (Fig. 20.7). The jaws are closed and allowed a brief delay to sever the tissue. The catheter is then gently withdrawn with its enclosed sample. Although there is frequently a slight “tug” on the catheter as the sample is removed from the wall, forceful tugging with multiple premature ventricular contractions and inward retraction of the ventricular wall suggests that the jaws may have trapped a sample that includes the pericardium, in which case the jaws should be opened and the bioptome withdrawn without the sample. Otherwise, the presumption should be that a piece of tissue *has* been collected whenever the jaws have been closed, and the bioptome must be withdrawn in its closed position and inspected before another pass is attempted. *Three to five separate biopsies should usually be obtained to reduce sampling error,* although larger samples may be divided to allow a portion of a sample to be sent for frozen section or electron microscopic examination while most of the material is placed in formalin for light microscopy.

The Long-Sheath Cordis Bioptome Used from the Femoral Vein

Access to the right femoral vein is obtained as described for right-sided heart catheterization from the femoral percutaneous approach (see Chapter 4). The long 0.035-inch guidewire used for left-sided heart catheter introduction is passed through the diaphragm of the venous sheath, to the level of the right atrium. This wire is kept in place as the venous sheath is withdrawn. The angled pigtail from the Cordis biopsy set is introduced into the preshaped 8F long sheath, and the pigtail-sheath combination is threaded onto the free end of the guidewire and inserted to the level of the right atrium. The wire is then withdrawn, and the hub of the pigtail catheter is attached to the coronary manifold and flushed. When the pigtail and sheath have both been rotated clockwise so that they face anteromedially, they usually can be advanced across the tricuspid valve and into the right ventricle. If the right atrium is enlarged, the bend of the pigtail may need to be accentuated to reach the tricuspid valve. One quick way is to curl the stiff end of the long guidewire and introduce it to (but never out of) the end of the pigtail catheter. Another is to replace the pigtail catheter with a balloon flotation right heart catheter (see Chapter 4), which is passed to the right ventricle and used to support advancement of the sheath.

Once the tip of the pigtail or balloon flotation catheter is in the right ventricle, the long sheath is advanced over the pigtail until the tip of the sheath lies in the midventricle region. The broad curve set into the sheath should conform to the arc from the inferior vena cava to the midventricle and should keep the tip pointing down rather than allowing it to rise toward the right ventricular outflow track. The out-of-plane bend of the terminal portion of the catheter serves to further orient the tip of the sheath toward the septum. The pigtail catheter is withdrawn from the sheath, while care is taken to keep the sheath in position. The sharp leading edge of the sheath must never be pushed forward so that it points directly toward the inferior wall of the ventricle, where it may produce perforation. At this point, I like to hook the side-arm of the sheath to the coronary manifold, flush, and gently clear the sheath with contrast material. Fluoroscopy in the RAO and LAO views (Fig. 20.4) confirms correct orientation of the sheath toward the septum of the right ventricle midway along its long axis.

At this point, the disposable bioptome is prepared for introduction. I like to bend the distal 2 cm of the catheter at an angle of 30° to 45° and check the jaw mechanism for free operation. The bioptome is then advanced into the sheath. The passage of the bioptome into the right ventricle should be monitored under fluoroscopy in the RAO projection, because the stiff bioptome may cause the sheath to rise unacceptably toward the right ventricular outflow track or advance unacceptably toward the apex or inferior wall. If these movements are observed, the bioptome should be withdrawn into the right atrium and the sheath position adjusted slightly so that its position is better maintained as the bioptome is readvanced. After the bioptome has been brought to the tip of the sheath, the sheath should be withdrawn slightly as

the bioptome is kept in place. This type of “unsheathing” of the bioptome is preferable to advancing the bioptome out of the end of the sheath, which may already be in direct contact with the right ventricular wall. Switching to the LAO view, the bioptome itself can be rotated so that the bend placed on its distal 2 cm points directly toward the wall. It is then pulled back slightly, jaws opened, readvanced into contact, and jaws closed to obtain a biopsy sample. With the jaws maintained closed, the bioptome is withdrawn, and the sheath is reflushed and reoriented if necessary to prepare for obtaining the next sample. After the last sample has been obtained, the sheath is withdrawn.

COMPLICATIONS

Transvascular endomyocardial biopsy of either the left or right ventricle can be performed safely by any of the techniques described. A worldwide survey of more than 6,000 cases showed a procedure-related mortality rate of approximately 0.1% (18).

A variety of *local complications* related to the venous entry site (hematoma, pneumothorax, injury to the recurrent laryngeal nerve, Horner's syndrome), or creation of *transient right bundle branch block* if the bioptome bumps against the upper septum (instead of the desired midseptum). A number of less serious complications of endomyocardial biopsy have been described, including transient arrhythmias and tricuspid valve dysfunction due to trauma during repeated biopsy procedures. Coronary artery–to–right ventricular fistula is now a recognized complication (of doubtful clinical significance) that may occur when endomyocardial biopsy resects small- to medium-sized coronary arterioles that then communicate with the ventricular chamber (19,20 and 21).

The most serious specific hazard of endomyocardial biopsy (using any of the biopsy techniques) is *cardiac perforation*. This occurs in 0.3% to 0.5% of cases and can rapidly lead to tamponade and circulatory collapse (1,18). This risk is minimal in patients with cardiac transplantation or prior cardiac surgery, because of adhesive pericardium overlying the right ventricular free wall. To minimize the risk of clinical perforation in other (nontransplantation) patients, careful attention must be paid to catheter position, catheter advancement, and continuous patient monitoring. Right ventricular biopsy should also be avoided in a patient whose prothrombin time exceeds 18 seconds or who has received intravenous heparin for the preceding diagnostic catheterization (unless it has been reversed with protamine). This caveat does not apply to left ventricular biopsy, however, where the risk of perforation is far lower (as long as one avoids the thin inferolateral walls, apex, and areas of thinning from any recent myocardial infarction) and heparinization is desired to reduce the risk of thromboembolism.

Any biopsy passes that are associated with chest pain or that produce samples that float in 10% formalin (suggesting the presence of epicardial fat) are of particular concern. When these events occur, monitoring of the blood pressure, the right atrial pressure, and the fluoroscopic appearance of the heart border should be done for at least 10 minutes after the final biopsy sample has been obtained. Frank cardiac perforation is usually heralded by sudden bradycardia and hypotension, resulting from vagal stimulation by blood in the pericardium. Atropine may help transiently (see Chapter 3), but hypotension progresses, associated with loss of the normal fluoroscopic motion of the right atrial and left ventricular heart borders (22). If the diagnosis of perforation with hemopericardium is in question in a hemodynamically stable patient, it may be desirable to confirm the presence of pericardial effusion by means of a portable echocardiogram in the cardiac catheterization laboratory, but the operator must be prepared to perform pericardiocentesis without hesitation if hemodynamic compromise develops. In most cases, simple aspiration or temporary catheter drainage of the pericardial space allows nonoperative management of biopsy-induced cardiac perforation in a patient with normal coagulation parameters. Because these complications are invariably evident before the patient leaves the catheterization laboratory, most centers are currently performing serial right ventricular biopsies (in cardiac transplantation or myocarditis patients) on an outpatient basis.

An additional hazard of cardiac biopsy is *embolization*. Right-sided thromboembolism can occur during cardiac biopsy but is rare with continuous flushing of the entry sheath (23). Air embolization has been described, however, as the result of the smaller size of the bioptome shaft in relation to its head. This allows aspiration of air through any sheath lacking a suitable back-bleed valve when the bioptome is used in a patient with a low central venous pressure. The possibility of paradoxic air or thromboembolism constitutes a relative contraindication for right ventricular biopsy in patients with significant right-to-left intracardiac shunting. Of course, embolization poses a greater potential problem during left ventricular biopsy, where cerebral embolization has been reported despite careful technique, systemic angiocoagulation, and avoidance of patients with mural thrombi.

TISSUE PROCESSING

The operator has the responsibility not only for obtaining an adequate tissue sample but also for performing the initial preparations that permit subsequent pathologic evaluation. It is usually recommended that *five* separate specimens be obtained from either the right or the left ventricle, to minimize sampling errors. Most myocardial diseases affect both ventricles, so that either chamber may be sampled, depending on operator experience and preference. Selective left ventricular involvement may be present in certain diseases (endomyocardial fibrosis, scleroderma, left-sided heart radiation, and cardiac fibroelastosis of infants and newborns). Left ventricular biopsy may be performed in these conditions and in patients in whom right ventricular biopsy has been unsuccessful or nondiagnostic. In the remaining patients, we usually prefer right (rather than left) ventricular biopsy because of greater ease, speed, and less likelihood of morbidity.

The safest and most elegant techniques of endomyocardial biopsy and sample preparation are useless without expert pathologic interpretation. The availability of a cardiac pathologist who is fully trained in the evaluation of biopsy-obtained tissue and conversant with the latest classification schemes (see later discussion) is mandatory in any biopsy program. Artifacts such as crushing or contraction bands are frequently present in endomyocardial biopsy specimens and may be overinterpreted by an inexperienced pathologist or one used to evaluating only postmortem specimens. The operator may assist the pathologist by appropriately handling the tissue in the catheterization laboratory. Biopsy specimens should be removed gently from the jaws of the bioptome with a fine needle and placed on moistened filter paper to be transferred immediately to the appropriate fixative: 10% formalin for light microscopy or 2.5% buffered glutaraldehyde for electron microscopy. Frozen specimens may be prepared in the catheterization laboratory by placing samples in a suitable fluid embedding medium and immersing them in liquid nitrogen or a dry ice–isopentane mixture to allow immediate interpretation (as in the case of transplant rejection) or subsequent immunologic staining. Immunoperoxidase staining using monoclonal antibodies to CD45 (common leukocyte antigen) or CD3 may be helpful in highlighting lymphocytic infiltrates, even when the classic histologic findings of myocarditis are absent. Additional special sample preparation or staining (e.g., iron staining, amyloid staining) may be indicated for the evaluation of specific disease states (see next section).

FINDINGS IN SPECIFIC DISEASE STATES

The value of endomyocardial biopsy in the management of myocardial disease depends on the perceived balance between the risk of performance (which is very low in experienced hands) and the yield of positive findings (1). The great majority of endomyocardial biopsies performed in patients with suspected myocardial disease, in fact, are abnormal in that they show myocyte hypertrophy, abnormal myocyte nuclei, and interstitial fibrosis that are not seen in normal hearts. These findings, however, are not specific for any particular cause.

In contrast, about 20% of patients have findings that are “specific” for a particular cause (e.g., myocarditis, amyloid, sarcoid) (1,24). About 5% of patients undergoing biopsy have findings that lead to a specific change in therapy (e.g., chelation, immunosuppressive agents). The threshold for performing an endomyocardial biopsy therefore depends on the operator's experience, the availability of pathology expertise, and the institutional view of how important the findings are for diagnosis and management in the individual patient (25). Given that the presence of severe heart muscle disease reduces life expectancy by as much as many malignancies do, I believe that an attempt to get a tissue diagnosis in any patient who comes to the cardiac catheterization laboratory (and is found not to have coronary or valvular pathology to explain myocardial dysfunction) is entirely appropriate. Some of the clinical situations in which biopsy results may be helpful are described in the following paragraphs.

Transplant Rejection

Endomyocardial biopsy has been the cornerstone of monitoring of antirejection therapy in patients with heart or heart-lung transplants (26,27). Biopsy allows the detection of early rejection before clinical findings of advanced cardiac damage (arrhythmias, third heart sound, congestive heart failure) become manifest, and it confirms the adequacy of pulsed immunosuppressive therapy to control each acute rejection episode. Surveillance biopsies are performed frequently during the first 6 months after transplantation, because of the high (more than 50%) incidence of rejection during this early period. No methodology thus far investigated has demonstrated a sensitivity or predictive accuracy high enough to replace endomyocardial biopsy in the detection of rejection in adults, although scintigraphy after the administration of indium 111 (^{111}In)–labeled antimyosin Fab fragments may correlate best with biopsy findings (28). Because immunologic transplant rejection is a diffuse process, sampling errors are rare. The light-microscopic histologic features of rejection include interstitial edema, inflammatory infiltration, and immunoglobulin deposition. More severe rejection is marked by myocytolysis and even interstitial hemorrhage. The original Stanford grading system (1981) defined absent, mild, moderate, and severe grades of rejection, the later two showing both lymphocytic infiltrates and myocyte damage. The newer (1989) grading scale of the International Society of Heart and Lung Transplantation (27) distinguishes four grades of rejection. *Milder rejection*—grade 1 (focal perivascular [1A] or diffuse [1B] sparse infiltrate

without necrosis) and grade 2 (single focus of aggressive infiltration and/or myocyte damage)—does not warrant active treatment. In contrast, *more severe rejection*—grade 3 (multifocal aggressive infiltrates and/or myocyte damage [3A] or diffuse inflammation with necrosis [3B]) and grade 4 (diffuse polymorphous infiltrate with necrosis and variable degree of edema, hemorrhage, or vasculitis)—warrants aggressive immunosuppression even if the patient is asymptomatic.

Adriamycin Cardiotoxicity

Doxorubricin hydrochloride (Adriamycin) is a potent anthracycline antibiotic that is active against many tumors but whose usefulness is limited by its tendency to cause progressive and irreversible dose-related cardiotoxicity (29). The incidence is 4% at doses lower than 500 mg/m^2, 18% between 500 and 600 mg/m^2, and 36% at doses higher than 600 mg/m^2. One approach to safe clinical use has been to limit the total cumulative dose to 500 mg/m^2, but this constitutes an unnecessary limitation in patients who can tolerate substantially higher doses without cardiotoxicity and who depend on the drug for tumor control. At the same time this approach fails to protect patients who have preexisting heart disease, who have undergone prior radiotherapy or cyclophosphamide administration, or who are older that 70 years of age and may develop cardiac toxicity at substantially lower doses. Because overt impairment of cardiac function is a relatively late finding in Adriamycin toxicity, noninvasive testing may fail to disclose whether additional doses of Adriamycin can be given safely.

Nevertheless, Bristow and coworkers (30) demonstrated that a progressive series of histologic changes (including electron microscopic evidence of myofibrillar loss and cytoplasmic vacuolization) takes place during the development of Adriamycin cardiotoxicity. The extent of these changes can predict whether a patient is likely to develop clinical cardiotoxicity during the subsequent chemotherapy cycle. The five-step grading system relates grade to the percentage of cells that show these histologic changes: 1 = less than 5%; 1.5 = 5% to 15%; 2 = 16% to 25%; 2.5 = 26% to 35%; and 3 = more than 35%. A biopsy score of 2.5 or higher indicates that doxorubricin therapy should be terminated; lower scores allow administration of the next cycle of therapy followed by rebiopsy, thus permitting maximal yet safe dosing with Adriamycin while substantially decreasing the incidence of morbidity and mortality from Adriamycin cardiotoxicity.

Dilated Cardiomyopathy

Dilated cardiomyopathy—primary myocardial failure in the absence of underlying coronary, valvular, or pericardial disease—has an age-adjusted prevalence of 36 per 100,000 population in the United States and causes approximately 10,000 deaths each year (31). The prevalence is 2.5 times higher in blacks and males. The clinical syndrome, which includes advanced congestive heart failure with dilation of both ventricles, chest pain, and arrhythmias, can be caused to a variety of toxins, metabolic abnormalities, inflammatory or infectious causes, neuromuscular diseases, or familial syndromes (Table 20.1). The classification scheme was updated by the World Health Organization in 1995 (32).

Toxins
Ethanol
Chemotherapy agents
Heavy metals (cobalt, lead, mercury)
Cocaine
Antiretroviral agents
Metabolic abnormalities
Nutritional deficiencies (thiamine, selenium, carnitine)
Endocrine (thyroid, acromegaly, Cushing's disease, pheochromocytoma, diabetes mellitus)
Electrolyte disorders (hypocalcemia/phosphatemia)
Infectious
Viral (coxsackie, cytomegalovirus, human immunodeficiency virus)
Rickettsia
Diphtheria
Mycobacteria
Fungal
Parasitic (toxoplasmosis, trichinosis, Chagas' disease)
Inflammatory
Collagen vascular (scleroderma, lupus, dermatomyositis)
Hypersensitivity
Sarcoidosis
Peripartum
Neuromuscular syndromes
Duchenne's muscular dystrophy
Facioscapulohumeral muscular dystrophy
Erb's limb-girdle dystrophy
Myotonic dystrophy
Friedreich's ataxia
Familial cardiomyopathies

Modified from Olsen EGJ, Fowler W. Idiopathic dilated cardiomyopathy. *N Engl J Med* 1984;301:1084.

TABLE 20.1. *Some known causes of dilated cardiomyopathy*

By the time of clinical presentation, most patients with dilated cardiomyopathy already have well-established cardiac damage. Although the course is highly variable and may include transient periods of improvement, the 1-year mortality rate may be as high as 25% to 30% (31). Because dilated cardiomyopathy carries a substantial mortality, our approach to any young or middle-aged patient who presents with dilated cardiomyopathy includes an invasive evaluation that incorporates coronary angiography and endomyocardial biopsy. The former may be helpful, because clinical signs and symptoms (chest pain or a history of myocardial infarction) are neither sensitive nor specific for distinguishing idiopathic dilated from ischemic cardiomyopathy: both factors may be present in patients with classic dilated cardiomyopathy (with angiographically normal coronaries) and both may be absent in up to half of patients with ischemic cardiomyopathy (despite a high incidence of triple-vessel disease). Because some patients with a “myopathic” presentation of extensive coronary artery disease do well with revascularization, coronary angiography is an important part of the evaluation.

Unfortunately, endomyocardial biopsy in patients with dilated cardiomyopathy generally displays only the monotonous histologic findings of myocyte hypertrophy, interstitial and replacement fibrosis, and endocardial thickening (1,31). Occasional small clusters of lymphocytes—fewer than five per high-power (300 ´ to 400 ´) field—may be present without meeting the criteria for diagnosis of myocarditis. The amount of collagen, particularly rigid type I collagen, is increased, potentially accounting for an increase in diastolic stiffness (33). As such, the histologic findings in dilated cardiomyopathy generally do not aid in establishing cause, long-term prognosis, or appropriate specific therapy. However, there clearly are patients with otherwise “garden-variety” dilated cardiomyopathy in whom *specific processes* can be diagnosed by endomyocardial biopsy (Table 20.2). The yield of endomyocardial biopsy findings that significantly alter either therapy or long-term prognosis in dilated cardiomyopathy, however, is admittedly low (1,24,25).

Diagnosis	Frequency	%
Idiopathic dilated cardiomyopathy	654	51.2
Myocarditis (2/3 active, 1/3 borderline)	117	9.2
Coronary artery disease	98	7.7
Peripartum cardiomyopathy	58	4.5
Hypertension	54	4.2
Human immunodeficiency virus infection	46	3.6
Amyloidosis	41	3.2
Connective tissue disease (mostly scleroderma/lupus)	40	3.1
Drug-induced (mostly adriamycin)	30	2.3
Chronic alcohol abuse	30	2.3
Familial cardiomyopathy	25	2.0
Valvular heart disease	19	1.5
Sarcoid	16	0.9
Endocrine (mostly thyroid)	11	0.9
Hemochromatosis	9	0.7
Neoplastic	6	0.5

Modified from Felker GM, Hu W, Hare JM, et al. The spectrum of dilated cardiomyopathy: The Johns Hopkins experience with 1,278 patients. *Medicine* 1999;78:270.

P>**TABLE 20.2.** *Final clinical plus biopsy diagnoses from 1,278 patients with dilated cardiomyopathy*

Myocarditis

In contrast to the “burned-out” condition of the myocardium in dilated cardiomyopathy, myocarditis is an acute or subacute inflammatory illness in which there is variable lymphocytic infiltration in conjunction with myocardial cell damage (1,34,35). Epidemiologic studies suggest that approximately 5% of a coxsackie B virus–infected population show some evidence of cardiac involvement (31), and replicating enteroviral RNA may be recovered in myocardial samples (36). Infection and inflammation may resolve spontaneously or may become chronic with perpetuation of an autoimmune process that causes ongoing myocardial damage (37). Similar processes can result from various viral, protozoal, metazoal, and bacterial infections (Table 20.1). Patients with myocarditis typically present with symptoms of chest pain, arrhythmias, or heart failure, with a clinical course that may vary from days to months. Newer noninvasive tests, such as scintigraphy after administration of ^{111}In-labeled antimyosin Fab (in which a ratio of counts over the heart to counts over the lung in the anterior view higher than 1.6 is considered “positive”) may help identify cases of myocarditis, but it has a low sensitivity (66%) compared with endomyocardial biopsy (35). In patients in whom myocarditis is strongly suspected but not confirmed by scintigraphy, biopsy should still be performed.

Much of the confusion in this field has stemmed from the use of various definitions for “myocarditis,” some of which (e.g., more than five lymphocytes per high-power field) were fairly liberal. In contrast, the Dallas criteria (38) adopted in 1986 require that infiltrating lymphocytes be adjacent to myocyte necrosis or degeneration to

diagnose “active” myocarditis. If lymphocyte infiltration is present without adjacent myocyte damage, the diagnosis is “borderline” myocarditis. Roughly 9% of biopsies done for the evaluation of dilated cardiomyopathy show myocarditis (about two thirds active and one third borderline) (1). Biopsy samples that were previously read as showing myocarditis may now be read as borderline or even frankly negative by the Dallas criteria. If the biopsy shows nondiagnostic abnormalities (particularly if “borderline” changes are present), the patient may still turn out to have active myocarditis on repeat biopsy (39). If confirmation of active myocarditis is clinically relevant, repeat right ventricular biopsy is usually sufficient, because the incidence of right versus left ventricular discordance in myocarditis is apparently low (39,40).

Using both clinical and histopathologic criteria (1,41,42), the Johns Hopkins group classified myocarditis as *fulminant* (intense infiltration, acute onset with progression to death or recovery within 1 month, poor response to immunosuppressives); *acute* (less distinct onset, active inflammation, potentially good response to immunosuppressives); *chronic active* (progressive decline in cardiac function, a biopsy that shows mixed inflammation and fibrosis, and only a brief response to immunosuppressives); or *chronic persistent* myocarditis (histologic evidence of myocarditis, near-normal ventricular function, unaffected by immunosuppressives). Positive biopsies for myocarditis may be found in patients presenting with new- or recent-onset congestive heart failure, including patients with peripartum cardiomyopathy during the last month of pregnancy or within the first 5 months after delivery (43) and in survivors of cardiac arrest who have no other evident organic heart disease (44). Several series of patients with AIDS have shown serious clinical cardiac abnormalities associated with myocarditis (45,46 and 47).

Given this high apparent prevalence of myocarditis among patients with both acute and chronic illness, uncontrolled use of immunosuppressive treatment (analogous to that used in the treatment of transplant rejection) was reported in the 1980s (48). Patients with active inflammation appeared to show histologic and some clinical improvement. However, immunosuppressive therapy also caused significant complications, and it was not clear that the frequency of improvement exceeded that seen spontaneously in many patients with myocarditis. This general confusion about the prevalence and optimal treatment of myocarditis led to the conduct of the Myocarditis Treatment Trial (49). Between October 1986 and October 1990, 2,233 patients who underwent nontransplantation-related endomyocardial biopsy within 2 years after symptom onset at one of 30 participating centers were screened. Histopathologic evidence of myocarditis was found in 214 (10%), of whom 111, who had a left ventricular ejection fraction less than 45% and no medical contraindication, were randomly assigned to receive either placebo or 24 weeks of cyclosporine/prednisone (after an initial azothiprine/prednisone arm was dropped). There was no significant benefit in the primary end point (improvement in left ventricular ejection fraction from baseline to 28 weeks) between the patients receiving immunosuppression and those receiving conventional stepped drug therapy for congestive heart failure. Despite initial screening by expert pathologists, only 6% of baseline biopsies met rigorous Dallas criteria for active myocarditis when overread by the core laboratory, and the trial was seriously underpowered to detect even substantial clinical benefit. Therefore, some physicians still consider use of immunosuppressives for patients with biopsy-proven myocarditis and a deteriorating clinical picture, particularly with a clinical picture of active myocarditis. Of course, such patients should also be screened for cardiac transplantation, should their condition continue to deteriorate.

Restrictive Versus Constrictive Disease

Heart failure caused by impaired diastolic functioning of a normal-sized or mildly dilated left ventricle is an uncommon but important clinical entity. In some cases, this condition may be caused by pericardial constriction, in which instance endomyocardial biopsy would offer no further information. A restrictive pattern (32,50) may be seen in some patients with hypertrophic myopathy, associated with a pattern of myocyte fiber disarray. More important, diastolic dysfunction may also be caused by one of a series of diseases that can be readily diagnosed with endomyocardial biopsy, thus sparing the patient inappropriate medical or surgical therapy (i.e., pericardial stripping) (51). These disorders include primary amyloidosis, Loeffler's endomyocardial fibrosis, carcinoidosis, Fabry's disease, and the glycogen storage diseases.

Of these, amyloid (AL) disease is one of the most common (1,000 to 3,000 new U.S. cases per year) (52,53). It also has one of the worst prognoses (the typical survival time of patients with amyloid, 12 months, reduced to 5 months in those with cardiac involvement). Trials suggest that treatment with melphalan and prednisone significantly prolongs survival time (54), so definitive diagnosis is important. Although most patients with cardiac amyloidosis have evidence of the disease on biopsy of more accessible organs or urinary light chain excretion, about 10% do not. Cardiac biopsy should be performed in patients with thick walls and a small, hypokinetic ventricle, particularly if the myocardium has the characteristic speckled appearance on echocardiography.

Sarcoid is also relatively common (more than 10,000 new U.S. cases per year) (55,56). Although serious cardiac dysfunction is detected in only 5% to 10% of patients, more than three fourths have cardiac involvement on autopsy. About half of the patients have electrocardiographic abnormalities of conduction or repolarization, and some have papillary muscle dysfunction, infiltrative cardiomyopathy, or pericarditis. Hemochromatosis may manifest with either a dilated or restrictive pattern and is found in roughly 1% of endomyocardial biopsies (1,57). It is important to identify this condition given the benefits of iron chelation therapy.

FUTURE DIRECTIONS

Endomyocardial biopsy remains the “gold standard” for the diagnosis of transplant rejection and anthracycline cardiotoxicity, and it is a highly valuable tool for the diagnosis of myocarditis. The use of highly specific molecular probes to look for viral genetic material or autoimmune activity in endomyocardial biopsy specimens promises to further sharpen the diagnostic potential of this technique. Although the lack of positive findings in the Myocarditis Treatment Trial has somewhat dampened enthusiasm for widespread performance of this procedure in patients who present with congestive heart failure, we still believe it is appropriate to perform this safe and potentially helpful procedure as part of an overall invasive evaluation given the poor prognosis of such patients. Despite ongoing uncertainty of its correct place in the clinical workup (58), endomyocardial biopsy plays an important role in the evaluation of patients with recent-onset or rapidly deteriorating cardiomyopathy or potential cardiac involvement of certain systemic diseases, as well as the furtherance of our understanding of the pathophysiology and treatment of diseases of the heart muscle.

CHAPTER REFERENCES

1. Felker GM, Hu W, Hare JM, et al. The spectrum of dilated cardiomyopathy: the Johns Hopkins experience with 1278 patients. *Medicine* 1999;78:270.
2. Shugoll GI. Percutaneous myocardial and pericardial biopsy with the Menghini needle. *Am Heart J* 1973;85:35.
3. Shirey EK, Hawk WA, Mukerji D, Effler DB. Percutaneous myocardial biopsy of the left ventricle: experience in 198 patients. *Circulation* 1972;46:112.
4. Sakakibara S, Konno S. Endomyocardial biopsy. *Jpn Heart J* 1962;3:537.
5. Kawai C, Kitaura Y. New endomyocardial biopsy catheter for the left ventricle. *Am J Cardiol* 1977;40:63.
6. Kawai C, Matsumori A, Kawamura K. Myocardial biopsy. *Annu Rev Med* 1980;31:139.
7. Caves PK, Stinson EB, Dong E Jr. New instrument for transvenous cardiac biopsy. *Am J Cardiol* 1974;33:264.
8. Mason JW. Techniques for right and left ventricular endomyocardial biopsy. *Am J Cardiol* 1978;41:887.
9. Richardson PJ. King's endomyocardial bioptome. *Lancet* 1974;1:660.
10. Brooksby IAB, et al. Left ventricular endomyocardial biopsy. *Lancet* 1974;2:1222.
11. Anderson JL, Marshall HW. The femoral venous approach to endomyocardial biopsy: comparison with internal jugular and transarterial approaches. *Am J Cardiol* 1984;53:833.
12. Anastasiou-Nana MI, et al. Validation of a new femoral venous method of endomyocardial biopsy: comparison with internal jugular approach. *J Interven Cardiol* 1988;1:263.
13. Rios B, Nihill MR, Mullins CE. Left ventricular endomyocardial biopsy in children with the transseptal long sheath technique. *Cathet Cardiovasc Diagn* 1984;10:417.
14. Canedo MI. Tampa Bay catheter: a new guiding catheter for endomyocardial biopsy via femoral approach. *Cathet Cardiovasc Diagn* 1992;25:71.
15. Corley DD, Strickman N. Alternative approaches to right ventricular endomyocardial biopsy. *Cathet Cardiovasc Diagn* 1994;31:236.
16. Denys BG, Uretsky BF, Reddy PS. Ultrasound-assisted cannulation of the internal jugular vein: a prospective comparison to the external landmark-guided technique. *Circulation* 1993;87:1557.
17. Miller LW, Labovitz AJ, McBride LA, et al. Echocardiography-guided endomyocardial biopsy. a 5-year experience. *Circulation* 1988;78[Suppl III]:III-99.
18. Sekiguchi M, Take M. World survey of catheter biopsy of the heart. In: Sekiguchi M, Olsen EGJ, eds. *Cardiomyopathy: clinical, pathological, and theoretical aspects.* Baltimore: University Park Press, 1980:217.
19. Henzlova MJ, Nath H, Bucy RP, et al. Coronary artery to right ventricle fistula in heart transplant recipients: a complication of endomyocardial biopsy. *J Am Coll Cardiol* 1989;14:258.
20. Fitchett DH, Forbes C, Guerraty AJ. Repeated endomyocardial biopsy causing coronary arterial-right ventricular fistula after cardiac transplantation. *Am J Cardiol* 1988;62:829.
21. Sandhu JS, Uretsky BF, Zerbe TR, et al. Coronary artery fistula in the heart transplant patient: a potential complication of endomyocardial biopsy. *Circulation* 1989;79:350.
22. Friedrich SP, Berman AD, Baim DS, et al. Myocardial perforation in the cardiac catheterization laboratory: incidence, presentation, diagnosis, and management. *Cathet Cardiovasc Diagn* 1994;32:99.
23. Kreher SK, Ulstad VK, Dirk CD, et al. Frequent occurrence of occult pulmonary embolism from venous sheaths during endomyocardial biopsy. *J Am Coll Cardiol* 1992;19:581.
24. Kasper EK, Agema WRP, Hutchins GM, et al. The causes of dilated cardiomyopathy: a clinicopathologic review of 673 consecutive patients. *J Am Coll Cardiol* 1994;23:586.
25. Mason JW. Endomyocardial biopsy and the causes of dilated cardiomyopathy [Editorial comment]. *J Am Coll Cardiol* 1994;23:591.
26. Miller LW, et al. Task force 5: complications. *J Am Coll Cardiol* 1993;22:41.
27. Billingham ME, Cary NR, Hammond ME, et al. A working formulation for the standardization of nomenclature in the diagnosis of heart and lung rejection. *J Heart Lung Transplant* 1990;9:587.
28. Ballester M, Bordes R, Tazelaar HD, et al. Evaluation of biopsy classification for rejection: relation to detection of myocardial damage by monoclonal antimyosin antibody imaging. *J Am Coll Cardiol* 1998;31:1357.
29. Singal PK, Iliskovic N. Doxorubicin-induced cardiomyopathy. *N Engl J Med* 1998;339:900.
30. Bristow MR, Mason JW, Billingham ME, et al. Doxorubricin cardiotoxicity: evaluation of phonocardiography, endomyocardial biopsy, and cardiac catheterization. *Ann Intern Med* 1978;88:168.
31. Dec GW, Fuster V. Idiopathic dilated cardiomyopathy. *N Engl J Med* 1994;331:1564.
32. Richardson P, MCKenna W, Bristow M, et al. Report of the 1995 World Health Organization/International Society and Federation of Cardiology task force on the definition and classification of cardiomyopathies. *Circulation* 1996;93:841.

33. Marijianowski MMH, Teeling P, Mann J, et al. Dilated cardiomyopathy is associated with an increase in the type I/type III collagen ratio: a quantitative assessment. *J Am Coll Cardiol* 1995;25:1263.
34. Herskowitz A, Campbell S, Deckers J, et al. Demographic features and prevalence of idiopathic myocarditis in patients undergoing endomyocardial biopsy. *Am J Cardiol* 1993;71:982.
35. Kuhl U, Lauer B, Souvatzoglu M, et al. Antimyosin scintigraphy and immunohistologic analysis of endomyocardial biopsy in patients with clinically suspected myocarditis: evidence of myocardial cell damage and inflammation in the absence of histologic signs of myocarditis. *J Am Coll Cardiol* 1998;32:1371.
36. Pauschinger M, Doerner A, Kuehl U, et al. Enteroviral RNA replication in the myocardium of patients with left ventricular dysfunction and clinically suspected myocarditis. *Circulation* 1999;99:889.
37. Kawai C. From myocarditis to cardiomyopathy: mechanisms of inflammation and cell death. *Circulation* 1999;99:1091.
38. Aretz HT, Billingham ME, Edwards WB, et al. Myocarditis: a histopathologic definition and classification. *Am J Cardiovasc Pathol* 1986;1:3.
39. Dec GW, Fallon JT, Southern JF, et al. "Borderline" myocarditis: an indication for repeat endomyocardial biopsy. *J Am Coll Cardiol* 1990;15:283.
40. Hauck AJ, Kearney OL, Edwards WD. Evaluation of postmortem endomyocardial biopsy specimens from 38 patients with lymphocytic myocarditis: implications for role of sampling error. *Mayo Clin Proc* 1989;64:1235.
41. Lieberman EB, Hutchins GM, Rose NR, et al. Clinicopathologic description of myocarditis. *J Am Coll Cardiol* 1991;18:1617.
42. McCarthy RE, Boehmer JP, Hruban RH, et al. Long term outcome of fulminant myocarditis as compared with acute (nonfulminant) myocarditis. *N Engl J Med* 2000;342:690.
43. Midei MG, DeMent SH, Feldman AM, et al. Peripatrum myocarditis and cardiomyopathy. *Circulation* 1990;81:922.
44. Frustaci A, Belloci F, Olsen EGJ. Results of biventricular endomyocardial biopsy in survivors of cardiac arrest with apparently normal hearts. *Am J Cardiol* 1994;74:890.
45. Reilly JM, et al. Frequency of myocarditis, left ventricular dysfunction and ventricular tachycardia in the acquired immune deficiency syndrome. *Am J Cardiol* 1988;62:789.
46. Herskowitz A, Vlahov D, Willoughby S, et al. Prevalence and incidence of left ventricular dysfunction in patients with human immunodeficiency syndrome. *Am J Cardiol* 1993;71:955.
47. Barbaro G, Di Lorenzo G, Grisorio B, et al. Incidence of dilated cardiomyopathy and detection of HIV in myocardial cells of HIV-positive patients. *N Engl J Med* 1998;339:1093.
48. Mason JW, Billingham ME, Ricci DR. Treatment of acute inflammatory myocarditis assisted by endomyocardial biopsy. *Am J Cardiol* 1980;45:1037.
49. Mason JW, O'Connell JB, Herskowitz A, et al. A clinical study of the efficacy of immunosuppressive therapy for myocarditis. *N Engl J Med* 1995;333:269.
50. Keren A, Popp RL. Assignment of patients into the classification of cardiomyopathies. *Circulation* 1992;86:1622.
51. Schoenfeld MH, Supple EW, Dec GW, et al. Restrictive cardiomyopathy versus constrictive pericarditis: role of endomyocardial biopsy in avoiding unnecessary thoracotomy. *Circulation* 1987;75:1012.
52. Kyle RA. Amyloidosis. *Circulation* 1995;91:1269.
53. Falk RH, Comenzo RL, Skinner M. The systemic amyloidoses. *N Engl J Med* 1997;337:898.
54. Kyle RA, Gertz MA, Greipp PR, et al. A trial of three regimens for primary amyloidosis: colchicine alone, melphalan and prednisone, and melphalan, prednisone and colchicine. *N Engl J Med* 1997;336:1202.
55. Newman LS, Rose CS, Maier LA. Sarcoidosis. *N Engl J Med* 1997;336:1224.
56. Yazaki Y, Isobe M, Hiramitsu S, et al. Comparison of clinical features and prognosis of cardiac sarcoidosis and idiopathic dilated cardiomyopathy. *Am J Cardiol* 1998;82:537.
57. Olson LJ, Edwards WD, Holmes DR, et al. Endomyocardial biopsy in hemochromatosis: clinicopathologic correlates in six cases. *J Am Coll Cardiol* 1989;13:116.
58. Williams JF, Bristow MR, Fowler MC, et al. Guidelines for the evaluation an management of heart failure (ACC/AHA Task Force). *Circulation* 1995;92:2764.

21
Intraaortic Balloon Counterpulsation and Other Circulatory Assist Devices

Julian M. Aroesty

Harvard Medical School; Department of Clinical Cardiology, Beth Israel Deaconess Medical Center, Boston, Massachusetts 02115

As cardiac catheterization and intervention have been applied to patients with unstable hemodynamic and ischemic conditions, the availability of effective devices for circulatory support has assumed increasing importance. The first such device was the *counterpulsation intraaortic balloon pump* (IABP), which improved the myocardial oxygen supply/demand ratio and provided limited circulatory support. It remains the most widely used and practical system today, although more complicated devices, such as the left ventricular support device (LVAD) and the cardiopulmonary support (CPS) system, have been introduced to provide more *complete* circulatory support in special circumstances. This chapter reviews the design, function, indications, and technique for use of these important adjunctive devices for circulatory support in the cardiac catheterization laboratory.

THE INTRAAORTIC BALLOON PUMP

The well-deserved popularity of the intraaortic balloon is related to its simplicity, ease and rapidity of insertion, ease of operation, long clinical record, and relatively low cost. The concept of using timed inflation of a balloon to generate a positive pressure pulse during diastole (to improve coronary flow), and then withdrawing that volume during systole by balloon deflation (to reduce resistance to systolic ejection, thereby reducing myocardial oxygen requirements), was first conceived by Claus et al., in 1961 (1,2) and applied clinically by Kantrowitz in 1968 (3). At first it was used only in patients with cardiogenic shock (1,2), but soon it was successfully applied to patients with medically refractory unstable angina (4). Insertion of the balloon catheter was initially performed surgically, but this has been almost completely supplanted by percutaneous insertion techniques that offer rapid and simple balloon insertion during an emergency (5).

Intraaortic Balloon Pump Equipment

The intraaortic balloon catheter consists of a long (roughly 10 cm) polyurethane bladder that is mounted on a flexible shaft so that it can be positioned in the descending aorta just distal to the origin of the left sublcavian artery. This bladder is inflated abruptly with helium immediately after aortic valve closure, causing an increase in aortic diastolic pressure. Inflation is maintained until just before the beginning of systolic ejection (the opening of the aortic valve), when the gas control system rapidly deflates the balloon to produce a sharp fall in systolic aortic pressure and a decrease in the impedance to left ventricular (LV) ejection. The inflation-deflation cycle is triggered by the surface electrocardiogram (ECG), although a fixed cycle can be generated internally for patients in ventricular fibrillation or on cardiopulmonary bypass. The console allows fine adjustment of the timing of balloon inflation and deflation to optimize the hemodynamic effect, as monitored in the arterial pressure waveform.

Although early balloons were single-lumen devices (with just the gas lumen for inflation and deflation), most IABP balloons are now double-lumen catheters. A central lumen allows delivery over a guidewire and then monitoring of the central aortic pressure. In order to minimize damage to the adjacent aortic intima, the inflated balloon diameter should be no more than 90% of the aortic diameter. The 40-cc balloon is generally satisfactory for most adults, and a 30- to 34-cc balloon is reserved for small patients. Pediatric balloons are available in 2.5-, 5.0-, 12.0-, and 20-cc sizes (Table 21.1). Early balloon consoles used carbon dioxide because of its excellent solubility in blood were the balloon ever to leak or rupture. Because the shaft size of balloon catheters has decreased, a gas with a lower molecular weight (i.e., helium) is now used to maintain fast gas shuttle times for crisp inflation and deflation. Because of the low solubility of helium in blood, however, the consoles must have a reliable mechanism to detect and react to balloon leak or rupture, by rapidly withdrawing all helium from the balloon and shutting down the counterpulsation cycle to minimize the risk of serious helium embolization.

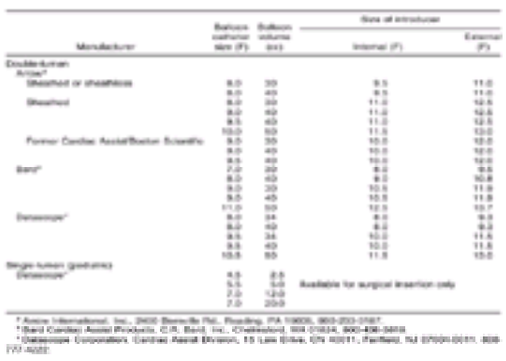

TABLE 21.1. *Percutaneous intraaortic balloons*

Percutaneous Insertion

Unless the IABP is being used because of instability during induction of anesthesia for surgery or difficulty in weaning from cardiopulmonary bypass, the IABP catheter is inserted percutaneously. The large diameter can cause serious vascular complications, and careful preprocedure evaluation is in order.

If feasible, clotting parameters (prothrombin time, partial thromboplastin time, and platelet count) should be checked before balloon insertion. A careful history should be obtained to determine the possible presence of claudication or prior peripheral vascular surgery. Both catheterization and IABP insertion can be performed via femoral artery grafts if special attention is paid to puncture technique (6). Noninvasive evaluation of the peripheral arterial circulation before balloon insertion forms a valuable point of reference for later monitoring of circulatory compromise by the IABP catheter.

Although early single-lumen balloons were inserted directly through a cutdown or large (11F) sheath, currently balloons are inserted percutaneously over a guidewire using either a small (8F to 9F) sheath or sheathless insertion. The technique for correct preparation and puncture of the common femoral artery is described in Chapter 4. If balloon placement is being performed as a stand-alone procedure, the artery is predilated with a 7F or 8F dilator after the wire has been advanced to the

level of the diaphragm. Firm pressure is maintained over the puncture site to prevent hematoma as the dilator is removed and the wire is wiped clean. Either the appropriate-size sheath or the balloon catheter itself, if sheathless technique is chosen, is introduced over the wire. When balloon placement is being performed at the conclusion of a catheterization (particularly an intervention performed via an 8F sheath), one of the new, low-profile IABP catheters can be placed via the existing 8F sheath. In this case, it is helpful to place the special balloon guidewire at the level of the diaphragm before the final diagnostic or interventional guiding catheter is removed, thereby obviating the need to renegotiate tortuous iliac vessels.

Before the IABP is handled, powder residue should be washed from the operator's sterile gloves to prevent alteration of the nonthrombogenic properties of the balloon surface. All air is evacuated from the balloon via a large (40- to 50-cc) syringe attached to the one-way valve supplied, so as to maintain the lowest possible profile during introduction. The guidewire lumen is flushed with heparin saline solution, and the balloon is loaded onto the special, stiff 0.021-inch guidewire supplied with the insertion kit. With the guidewire maintained above the carina (bifurcation of the trachea into left and right mainstem bronchi), the balloon should advance to that level with minimal resistance. When the radiopaque tip-marker reaches the carina (generally just distal to the left subclavian artery), the guidewire is removed, the central lumen of the balloon catheter is aspirated and flushed vigorously, and the central lumen is attached to either the coronary manifold or a pressurized flushing device equipped with a pressure transducer (Intraflow, Naimic, Glens Falls, NY) that delivers 3 mL/hr to maintain lumen patency. Special care must be taken to prevent inadvertent injection of air bubbles or thrombi, because the tip of the catheter is only a short distance below the aortic arch. The balloon shaft may be equipped with an outer sleeve, which can be advanced to the hub of the introducer sheath to maintain sterility if subsequent adjustment is required. If a long (23-cm) sheath has been used to negotiate a tortuous iliac artery, it must be partially withdrawn before initiation of counterpulsation, so that the distal end of the sheath does not overlie the distal end of the balloon.

Sheathless Insertion

Although insertion through a sheath is quite easy, most current balloons have a tapered nose to allow them to be inserted directly over a guidewire (i.e., without use of a sheath). Because the balloon shaft is roughly 1.5F (0.5 mm) smaller than the corresponding sheath outer diameter, sheathless insertion results in less femoral arterial trauma and less obstruction to the limb circulation in patients with small or atherosclerotic arteries. Care must be taken to adequately predilate the soft-tissue track and to avoid kinking either the guidewire or the balloon catheter during insertion, and the balloon catheter should not be rotated as it is passed through the soft tissues. If undue resistance is encountered, consideration should be given to reverting to a sheathed insertion.

Care of Central Lumen

Once the balloon is positioned, the central lumen is attached to a transducer with a 3 mL/hr continuous infusion system pressurized to 300 mm Hg. Air must be purged from the system to prevent inadvertent air embolism, and heparin should be added to the flush solution at a concentration of 10 IU/mL. Power flushing with the continuous infusion system (which runs at 1.5 mL/sec when the valve is pulled open) should be avoided, in favor of syringe aspiration with one syringe and flushing with a second, unless counterpulsation is suspended temporarily. The central lumen should not be used for drawing blood samples. If the central lumen pressure waveform becomes damped and the cause is not related to a loose connection in the system, aspiration of the central lumen should be attempted. If there is marked resistance to aspiration of blood, *do not flush*. A thrombus may have formed within the lumen, which should then be considered occluded and capped off.

Initiation of Counterpulsation

Following connection to the console with the appropriate connector, the system is purged with helium inflation gas. The balloon is filled to half volume and counterpulsation is begun at the 1:2 setting (every other beat) so that preliminary timing adjustments can be made (see later discussion). Fluoroscopy confirms appropriate placement of the balloon proximally, full exit from the sheath distally, and uniform expansion without twists or kinks. If it is necessary to adjust the position of the balloon, it may be moved within the sheath but must never be adjusted by advancing the sheath itself, because the latter maneuver may produce arterial damage at the distal end of the introduction sheath as it advances within the artery without the protection of a snug-fitting internal dilator.

Once the half-filled balloon is operating satisfactorily, the balloon should be increased to its full rated volume, and fluoroscopy should again verify that the balloon position is appropriate and that the balloon has assumed a uniform symmetric, cylindrical shape at full inflation. The balloon shaft and sheath (if used) are sewn to the skin, povidone-iodine (Betadine) ointment is applied to the entrance site, a mark is placed across the balloon shaft and the skin to detect any subsequent balloon migration, and a sterile dressing is applied. Five thousand units of aqueous heparin is given intravenously as soon as the balloon is inserted, followed by continuous intravenous heparin.

Adjusting Counterpulsation Timing

Maximal benefit depends on proper timing of inflation and deflation (Table 21.2). Timing should be done by inspection of the central aortic pressure tracing through the balloon guidewire lumen, because the change in contour and the timing of the pulse wave as it moves from the central aorta to the periphery can make accurate timing of counterpulsation difficult. Timing is best done with the console set at 1:2 pumping (i.e., counterpulsation of every other beat), so that arterial pressure tracings with and without counterpulsation can be compared (Fig. 21.1).

Timing error	Waveform	Correction
Inflation too early	Dicrotic notch obliterated by early rise of augmented pressure as IABP inflates	Set inflation so it occurs at dicrotic notch
Inflation too late	Dicrotic notch visible but diastolic augmentation is not at peak value	Set inflation so it occurs at dicrotic notch
Deflation too early	Assisted and unassisted systolic pressures are equal	Move deflation later until a "U" shape appears in aortic pressure trace; assisted systolic and end-diastolic aortic pressures should be lower than corresponding unassisted pressures
Deflation too late	Balloon aortic end-diastolic pressure is higher than native end-diastolic pressure	Move inflation earlier until the assisted aortic end-diastolic pressure and systolic pressure are less than the corresponding unassisted pressures

TABLE 21.2. *Timing of inflation and deflation of the intraaortic balloon pump (IABP)*

FIG. 21.1. Appropriately timed counterpulsation of every other beat producing a decrease in both the end-diastolic pressure and the peak systolic pressure.

Inflation

While observing a high-fidelity central aortic pressure tracing, slowly move the inflation timing toward later inflation until the dicrotic notch becomes visible. Inflation should then be moved back to a slightly earlier time until the inflation upstroke fuses with the central aortic dicrotic notch to form a “U” (Fig 21.1). Earlier inflation should be avoided, because it would require a portion of LV ejection to be made against the resulting increased central aortic pressure, which can have disastrous consequences in a critically ill patient.

Deflation

Deflation should be timed to take place just before the opening of the aortic valve. Starting with deflation that is clearly too early (before the R wave), delay the timing of deflation progressively until the maximum reduction in aortic systolic pressure is observed in the following beat. This is usually accompanied by a parallel 10 to 15 mm Hg decrease in the nadir of central aortic diastolic pressure.

In the presence of *atrial fibrillation* or marked *irregularity of the cardiac rhythm*, balloon timing is best adjusted so that deflation occurs on the peak of the R wave to avoid LV ejection against an inflated balloon during occasional short R-R intervals. *Atrial pacing* may also produce timing difficulties if the console misinterprets the atrial pacing spike as the peak of the R wave. This can be overcome by timing the balloon off of the arterial pressure contour, by choosing a monitor lead that magnifies the difference between the ECG R wave and the atrial pacing spike, or by setting the console to the mode that discriminates between the pacing spike and R wave by sensing both the height and duration of the signal.

Balloon Pressure Wave Form

Although most timing decisions are made by reference to the central *aortic* pressure waveform, the console also has the capacity to display the pressure waveform in the helium drive system (the *balloon* waveform) (Fig. 21.2). The balloon waveform ordinarily has a rectangular appearance, onto which a sharp positive overshoot artifact is superimposed just before the peak inflation pressure and a negative deflation artifact at the end of deflation. Loss of these inflation and deflation artifacts produces a waveform with a blunted or somewhat rounded top, which may be seen when the balloon is too large for the aorta, there is a kink in the balloon catheter or connecting tubing, or the balloon is not fully unwrapped.

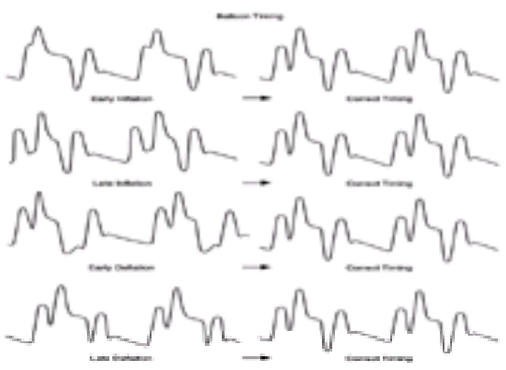

FIG. 21.2. Early inflation—This is characterized by absence of the dicrotic notch on the arterial pressure tracing with encroachment of the diastolic augmentation pulse on the prior systole. Late inflation—There is a prominent dicrotic notch, indicating that balloon inflation has occurred well after aortic valve closure. The timing is adjusted until the dicrotic notch just disappears. Early deflation—Timing is adjusted until the aortic end-diastolic pressure is at its lowest value. Late inflation—The balloon remains inflated beyond the end of diastole and into the start of systole, resulting in an *increase* in resistance to ejection and cardiac work. The timing is adjusted earlier in diastole until the end-diastolic pressure is at its nadir.

Angiography During Counterpulsation

Whenever possible, we like to perform angiography or intervention first, before balloon placement through the same access site. Very unstable patients, however, require counterpulsation *during* the catheterization procedure. In this case, the balloon catheter is placed first, and cardiac angiography is then be performed via either the brachial artery or the opposite femoral artery. If the contralateral femoral approach is used for angiography, a few precautions should be taken to avoid damaging the balloon membrane. The guidewire and catheters should be advanced beyond the level of the balloon with inflation suspended briefly and with the point of the tip of the catheter pointed away from the balloon toward the wall of the aorta (7). Once the catheter is in the ascending aorta, counterpulsation can be resumed. Counterpulsation does not interfere with catheter manipulation past the operating balloon, but the operator should remember to suspend balloon operation temporarily when the next catheter exchange is performed.

Patient Management During Counterpulsation

During counterpulsation, there should be daily evaluation for evidence of sepsis, thrombocytopenia, blood loss, hemolysis, vascular obstruction, thrombus, embolus, or dissection. Mild to moderate thrombocytopenia is expected as a result of platelet destruction, but the platelet count rarely falls below 50,000 to 100,000 per milliliter unless there is some other problem such as heparin-induced thrombocytopenia or disseminated intravascular coagulation. After balloon removal, the platelet count rapidly returns to normal (8).

The level of heparin anticoagulation must be monitored closely, maintaining the partial thromboplastin time at 50 to 70 seconds to prevent serious thrombotic or embolic complications. Evaluation of the circulation to the involved limb should take place once during each 8-hour nursing shift. Dorsalis pedis and posterior tibial pulses should be palpated and graded on a scale of 1+ to 4+ during each shift. The ratio of the Doppler systolic pressure of the calf to that of the upper arm, known as the ankle-brachial index, is a useful technique for evaluating the development of limb ischemia. An index that is trending downward or is less than 0.5 indicates the presence of serious limb ischemia that may require early balloon removal.

Local sepsis can be minimized by good aseptic insertion technique, daily changes of dressings with application of providone-iodine (Betadine) at the insertion site, careful technique in changing bottles of flush solution, and avoidance of prolonged pumping (beyond 5 days). During insertion prophylactic antibiotics are not given routinely, but they should be administered if there is any compromise in sterile technique. Disseminated sepsis, an uncommon complication, mandates urgent balloon removal.

During counterpulsation, patients must be kept at bed rest. Hip flexion is restricted, and the head of the bed should not be elevated beyond 30°. A limb restraint is attached to the involved leg to maintain appropriate leg position during periods of sleep, confusion, or discomfort. Sedation may be required to achieve this goal.

Weaning from Counterpulsation and Balloon Removal

Balloon counterpulsation is a temporary support measure. The balloon is usually removed once the patient's condition has stabilized after the acute insult (usually 24 to 48 hours of support). Before removal of an intraaortic balloon, the patient is weaned progressively from support, by decreasing the counterpulsation mode from 1:1, to 1:2, and then to 1:3 counterpulsation. Sufficient time should elapse between each stage to ensure that the patient is tolerating the progressive decrease in the level of hemodynamic support without exhibiting clinical deterioration. In order to reduce the chance of clot formation, pumping should not be reduced below 1:8 until immediately before balloon removal. Heparin should be stopped, and clotting parameters should have an activated clotting time of less than 160 seconds or a partial thromboplastin time of less than 50 seconds.

At this point, the balloon is turned off and a 50-mL syringe and stopcock is attached to the balloon inflation port to create a vacuum. The balloon is withdrawn to but not into the insertion sheath, because the latter maneuver may tear or even embolize a portion of the balloon membrane. After the skin sutures are cut, the sheath and balloon are withdrawn as a single unit. A small spurt of blood should be allowed to escape while the artery is compressed distally to help flush out any adherent thrombus above the site. The proximal vessel is then compressed while distal back-bleeding is allowed. The site is then firmly compressed by hand or with a

mechanical compression device for 30 to 60 minutes. Distal limb circulation is checked during and after compression. The patient is kept at bed rest, avoiding hip flexion on the involved side, for the next 24 hours.

Complications

The success rate for percutaneous insertion is greater than 90%, but balloon counterpulsation can have serious complications. These have decreased progressively with improvement in balloon profile (usable through 8F and even 7F sheaths) and increased use of the sheathless technique. Still, operators must be aware of and try to prevent complications of the use of this valuable device.

Limb Ischemia

The most common IABP complication is local vascular insufficiency that resolves without permanent sequelae once the balloon pump is removed (9). Usually it is apparent within a few hours after insertion and is related to mechanical obstruction at or above the insertion site. The development of local thrombus may produce late ischemia. If the patient's status is too precarious to permit discontinuation of counterpulsation, a new balloon may be placed in the contralateral femoral artery, or cross-femoral grafting can be performed to relieve the ischemia without interrupting IABP support (10).

When balloon French size was much larger (10F and 11F), the rate of significant vascular complications was approximately 10%, with permanent morbidity about 5% and balloon-related mortality about 1% (9,11,12,13,14,15,16,17,18,19,20,21,22,23,24 and 25). Currently, limb ischemia requiring IABP removal and that requiring surgical intervention should each be less than 5% (23). An evaluation of the rate of complications in a single institution documented the adverse effects of larger balloons and more prolonged counterpulsation (25) (see later discussion).

To minimize ischemic vascular complications, the balloon pump catheter must be placed in the common femoral artery (see Chapter 4). The profunda and superficial femoral branches of the common femoral artery are too small to allow intraaortic balloon insertion without severe compromise of flow. If the puncture is made too low and the balloon is inserted distal to the common femoral artery, it is likely that evidence of severe obstruction will develop immediately, requiring balloon removal and contralateral insertion or ipsilateral reinsertion at the time of surgical balloon removal and vascular repair.

Arterial Dissection

Retrograde dissection (26,27) may occur as an iatrogenic event at the time of wire advancement. The IABP may then be inserted and may even appear to function normally in the false lumen of the aorta, although severe back pain is often present. There is great danger of aortic rupture. Dissection was much more common when intraaortic balloons were inserted surgically, without the benefit of a guidewire. Echocardiography has been useful both in making the diagnosis and in avoiding the complication (28,29).

The best defense against this complication is to avoid using stiff guidewires, avoid forcing the guidewire through the vascular system when there is resistance to advancement or pain with advancement, and avoid introducing the guidewire unless there is excellent pulsatile flow through the puncture needle. If there is any doubt concerning intraluminal position of the guidewire or the anatomy, a 5F dilator should be inserted over the guidewire; if there is good backflow of blood, gentle hand injections of contrast should be made to help define the anatomy before balloon insertion.

Loss of Limb

This is a rare complication that is usually related to prolonged shock, extensive thrombus formation, or cholesterol embolization (30). The latter is an especially ominous complication because surgical intervention is often ineffective in restoring adequate circulation. It is heralded by bilateral painful, cold, mottled limbs (livedo reticularis) shortly after the intervention. Many patients exhibit increased eosinophils in blood and urine sediment and throbocytopenia. Rapidly progressive renal failure is common; it is most often permanent (31) and therefore unlike contrast-related nephropathy. Some authorities believe that chronic anticoagulation is contraindicated because further embolization may be promoted by the failure to form an organized thrombus over the eroded plaque (32).

Cerebrovascular Accident

Embolic cerebrovascular accident may occur if the balloon has been placed too proximally or if the central lumen of the balloon has been flushed vigorously to correct thrombus-induced damping of the central arterial pressure. As expected, this complication is more common with thoracic balloon placement. Except in extreme emergencies, the central lumen of the intraaortic balloon should not be used as a site for obtaining arterial blood or samples for chemistries. If venous access is difficult, a venous cannula or a side-arm cannula for right-sided heart catheterization can be placed in the internal jugular vein. An arterial cannula in the radial artery is a convenient site for frequent arterial blood samples.

Sepsis

If counterpulsation is carried out for less than 3 to 7 days, there is little correlation between the duration of counterpulsation and the development of local or disseminated sepsis. Although there are few studies of longer-term counterpulsation, most show increased local and disseminated sepsis when counterpulsation is carried out for longer than 1 week, suggesting that sepsis is a secondary event that may respond to the same kind of meticulous cleansing techniques applied to total parenteral nutrition catheters (33).

Balloon Rupture

This uncommon complication has been reported largely as a result of iatrogenic factors or equipment malfunction. Because helium is so insoluble in blood, helium embolization is a serious event, producing prolonged ischemia or stroke (34). Balloon rupture may produce massive helium embolization if there is failure of the console to recognize the problem. Hyperbaric oxygen treatment has been applied to maintain tissue viability until helium excretion has taken place (35).

Balloon rupture may occur as a result of heavy calcification of the aorta (36). In addition to helium leakage, it may result in thrombus formation within the balloon that makes percutaneous removal impossible. Usually the balloon has been removed surgically in these instances (37,38 and 39), but percutaneous removal of a ruptured entrapped IABP has been accomplished by flushing out the thrombus within the balloon (40).

Risk Factors for Complications

Percutaneous Versus Surgical Insertion

Because of the simplicity and rapidity of insertion, percutaneous insertion has almost completely replaced the direct surgical insertion technique. The newer, low-profile balloons and the increased use of the sheathless percutaneous insertion (41,42) have contributed to the low complication rate of the percutaneous technique, relegating surgical insertion to those balloons inserted as an emergency in the course of cardiac surgery. If severe peripheral vascular disease precludes the use of a femoral approach during thoracic surgery, thoracic insertion has been applied (43,44 and 45), with IABP-related complication rates as low as 4% (46). Although early studies suggested a lower complication rate associated with direct surgical insertion (41,42), this is no longer the case with current devices and insertion techniques (23).

Sheathed Versus Sheathless Insertion

Sheathless insertion has decreased the IABP complication rate (47,48). The technique is somewhat more demanding than the standard sheathed insertion technique, requiring a special guidewire with a stiff body and firm pressure over the puncture site during insertion to prevent artery laceration or balloon damage. Sheathless insertion may not be feasible in the presence of marked obesity or dense scar tissue at the puncture site related to prior femoral artery surgery.

Catheter Size

As the catheter size has decreased, there has been a progressive decline in vascular complications. A review of 381 patients between 1977 and 1995 found a vascular complication rate of 30% for surgical insertion, 21% for 12F catheters, 10% for 10.5F catheters, and 8.4% for 9.5F catheters. Additional independent risk factors were duration of counterpulsation beyond 48 hours, peripheral vascular disease, and shock (25). The recent development of 7F and 8F IABP catheters is likely to improve these figures even further.

Thoracic Aorta Insertion

This technique is largely limited to patients with severe peripheral vascular disease who require counterpulsation at the end of their cardiac surgery (43,44 and 45). Despite the high risks associated with the technique and with the patient population to which it is applied, the IABP-related complication rate for ascending aorta insertion could be as low as 4% (46). The SupraCor balloon (ABIOMED Cardiovascular, Inc., Danvers, MA) is similar to the existing intraaortic balloon but is designed for placement in the ascending rather than the descending aorta. In an animal study, conventional IABP had no effect on graft flow, whereas the ascending aorta device increased internal mammary bypass flow by 70% and increased venous conduit flow by 50% (49).

Miscellaneous Clinical Factors

The risks of a vascular complication from intraaortic counterpulsation are increased in the presence of vascular disease, female gender, and diabetes. A 1984 report noted that patients with peripheral vascular disease had a vascular complication rate of up to 31% after percutaneous insertion, compared with 16% after surgical insertion. Female gender was an additional risk factor (15% vs. 3.5%), but age, duration of counterpulsation, and indications for insertion were not (18). A single institution retrospective review of 436 IABP patients over a 14-year period in which the indications for counterpulsation were intraoperative pump failure (42%), unstable angina (24%), preoperative prophylaxis (22%) and preoperative shock (9%) found that only the absence of pedal pulses on admission correlated with an increased incidence of vascular complications (50). Kantrowitz reviewed 733 patients, a large proportion of whom had received a surgically implanted IABP for cardiogenic shock. The vascular complication rate was increased in the presence of diabetes, hypertension, or female gender but was not related to duration of counterpulsation. Bacteremia was positively correlated with the duration of counterpulsation, and local or systemic infection was more common in coronary care unit insertion compared with operating room insertion (26% vs. 12%) (19).

An early analysis of the Beth Israel Hospital experience with 10.5F and 12F percutaneous sheath insertion balloons revealed some degree of limb ischemia in more than 40% of patients, almost one third of whom required balloon removal. Limb ischemia was related to the presence of diabetes, peripheral vascular disease, female gender, and an ankle-brachial pressure index of less than 0.8. There was no association between limb ischemia and age, body surface area, or 10.5F versus 12F balloon size (9). Of the 7,333 patients undergoing percutaneous left-sided heart catheterization procedures at the Beth Israel Hospital between 1980 and 1987, only 1% required operative repair of catheterization-related vascular complications, but the incidence of operative repair after transfemoral intraaortic balloon placement was 11.5%. Most of the patients developing limb ischemia after balloon placement did not require surgical repair, because limb ischemia often resolved with removal of the intraaortic balloon (20,24).

The increased use of sheathless technique and the development of smaller-profile balloons have been accompanied by a dramatic decrease in the complication rate. A review of 200 consecutive patients undergoing sheathless insertion revealed a major complication rate of only 4.8% and acute limb ischemia requiring surgery in only 4%. At a mean follow-up of 17 months, there was only one false aneurysm and one new case of intermittent claudication (51). Other high-volume catheterization laboratories have duplicated these outstanding results (47).

Indications and Contraindications

Although it was designed initially as a support device for patients with cardiogenic shock, current indications for intraaortic balloon pumping have expanded from purely hemodynamic support to the management of refractory ischemia, even when it occurs in the absence of hemodynamic compromise (see Table 21.3 and Table 21.4). Balloon pumping may even be instituted prophylactically before high-risk intervention in the setting of severe baseline hemodynamic dysfunction or intervention on a vessel that supplies a large part of the remaining viable myocardium.

Hemodynamic compromise
Cardiogenic shock secondary to acute myocardial infarction with continuing ischemia, ventricular septal defect, or mitral valve reflux (52–54)
Cardiogenic shock due to reversible causes (e.g., transient ischemia, myocarditis, sepsis, drug toxicity) (55,56)
Inability to wean from bypass after cardiac surgery (57)
Hemodynamic support while awaiting transplantation (58)
Serious arrhythmia due to refractory ischemia (59–60)
Medically refractory ischemia
Medically refractory unstable angina (4)
Failed PTCA with refractory ischemia (61)
Prophylactic high-risk intervention
High-risk PTCA due to left ventricular dysfunction and/or large territory at risk (62–64)
PTCA during acute myocardial infarction (65,66)
Stabilization in patients with severe aortic stenosis (67)
Severe multivessel or left main coronary artery disease requiring urgent cardiac or noncardiac surgery (68–70)
Large myocardial infarction (71–72)

PTCA, percutaneous transluminal coronary angioplasty.

TABLE 21.3. *Indications for intraaortic balloon pump therapy*

Significant aortic regurgitation
Abdominal aortic aneurysm
Aortic dissection
Uncontrolled septicemia
Uncontrolled bleeding diathesis
Severe bilateral peripheral vascular disease uncorrectable by peripheral angioplasty or cross-femoral surgery
Bilateral femoral-popliteal bypass grafts for severe peripheral vascular disease

TABLE 21.4. *Contraindications for intraaortic balloon pump therapy*

Clinical Results

A large number of studies have been conducted to examine the hemodynamic effects of counterpulsation and its benefit in various clinical situations. Although the number of such studies is too large to review here, the most important ones are summarized.

Hemodynamic Effects of Counterpulsation

The rapid expansion of the balloon in early diastole produces an increase in diastolic pressure and thus coronary perfusion pressure. The abrupt deflation of the balloon at end-diastole removes effective aortic volume, decreasing aortic systolic pressure and thus the resistance to LV ejection (Fig. 21.1). These two effects—a decrease in myocardial oxygen requirements with a concomitant increase in coronary diastolic perfusion pressure—improve the myocardial supply/demand balance. The enhancement in LV emptying improves forward output and decreases left heart filling pressure, although to a lesser extent than the circulatory assist devices

discussed later in this chapter.

Cardiogenic Shock

The effect of counterpulsation on systemic and coronary circulation is very much dependent on the extent of hemodynamic decompensation before initiation of intraaortic balloon pumping. When instituted relatively early in the course of cardiogenic shock in dogs, counterpulsation produces a 19% to 25% reduction in peak LV wall stress, with an increase in coronary blood flow (73,74 and 75) and a reduction in extent and severity of ischemia (76). Improvement in hemodynamics is especially prominent when cardiogenic shock is accompanied by a mechanical defect such as a ventricular septal defect or acute mitral regurgitation (77). Generally, the institution of counterpulsation in cardiogenic shock produces a marked rise in systemic diastolic pressure and a 5 to 10 mm Hg fall in LV filling pressure, accompanied by a variable effect on systemic pressure and cardiac output (78).

The effect of counterpulsation on coronary hemodynamics in patients with shock is more difficult to characterize. Animal studies have not shown uniform increases in regional or global coronary flow, probably because of failure to control for other variables such as the degree of hypotension, degree of coronary stenosis, or presence of collateral vessels (79). Coronary flow is increased in IABP only when the pressure beyond a coronary stenosis has fallen below the level at which autoregulation can compensate fully (about 40 to 60 mm Hg). When the distal pressure is higher than this level, IABP may not change or may even decrease coronary flow if myocardial oxygen requirements have also been attenuated by an IABP-mediated decrease in LV wall stress. In the clinical setting with the added variable of multivessel disease, different degrees of collateralization, and variation in the severity of coronary stenosis, it is not surprising that the effect of counterpulsation on total coronary flow in patients with shock can be highly variable. In the presence of profound shock, however, both systemic and coronary flows increase significantly after initiation of intraaortic balloon pumping (80). At least in the short term, there is no effect of counterpulsation on renal blood flow or oxygen consumption of patients in shock (81).

Seventy percent of patients in cardiogenic shock studied 14 hours after IABP insertion showed no change or a fall in coronary blood flow with counterpulsation and no significant change in myocardial lactate extraction (74). A comparable group of patients studied 4 to 6 hours after initiation of counterpulsation showed an 18% decrease in LV systolic pressure and a 38% increase in cardiac index. Coronary sinus studies in these patients documented a 34% increase in coronary blood flow and a change from 6% lactate production to 15% extraction—that is, a change toward normal nonischemic myocardial metabolism (82). With multiple ECG leads in a dog model and in humans, counterpulsation produced a marked decrease in the extent and severity of myocardial ischemia (as determined by the sum of ST-segment elevations in multiple ECG chest leads) if it was applied within 3 hours after coronary occlusion (73).

In addition to the suggested benefits on coronary blood flow and ischemia just described, the initiation of counterpulsation in patients with shock has produced a uniform improvement in LV performance. Cardiac index and mean arterial pressure increase significantly, while LV filling pressure decreases substantially (75,78,79,80,81,82,83,84 and 85).

Initial improvement in hemodynamics is usually followed by recurrent deterioration after 3 to 4 days, if definitive revascularization or corrective surgery is performed (86). Although the usual treatment for cardiogenic shock is rapid stabilization followed by percutaneous transluminal coronary angioplasty (PTCA) or surgery, several days of counterpulsation may improve the high mortality rate of cardiogenic shock even if immediate revascularization is not feasible (87).

A retrospective community hospital study of patients with acute infarction accompanied by cardiogenic shock found that the addition of IABP to thrombolysis led to a much-improved hospital survival rate (93% vs. 37%). Although this was a retrospective study, age, systolic pressure, pulmonary capillary wedge pressure, incidence of anterior infarction, and presence of diabetes mellitus did not differ between the two groups (88). A subgroup analysis of 310 patients presenting with shock in the international multicenter Global Utilization of Streptokinase and Tissue Plasminogen Activator for Occluded Coronary Arteries (GUSTO) study revealed a wide disparity in the use of the IABP. There was a trend toward lower 30-day and 1-year mortality rates in patients undergoing counterpulsation, more than 80% of whom were from the centers in the United States, yet only one third of cardiogenic shock patients presenting to U.S. centers underwent IABP insertion (89). Differences in aggressive diagnostic and therapeutic interventions in the United States compared with the other centers included IABP use (35% vs. 7%), PTCA (26% vs. 8%), and cardiac catheterization (58% vs. 23%), but also lower 30-day (50% vs. 66%) and 1-year (56% vs. 70%) mortality rates (90).

In the absence of early revascularization, the mortality rate of cardiogenic shock is more than 85%. Patients with multiple infarctions or serious comorbidity, those requiring mitral valve replacement or repair for concomitant mitral regurgitation, and those with coronary anatomy that is unfavorable for bypass have the worst prognosis with surgery (84). Nonrandomized studies in which the survival rate for patients with successful revascularization was compared with that for patients in whom no attempt was made or the attempt failed have all shown a much worse survival rate in the latter group (older studies, reference 85; current studies, reference 91). A report of 200 consecutive patients presenting with acute infarction and cardiogenic shock found that the hospital survival rate was 67% with a patent infarct-related artery and 25% if the artery was occluded. In-hospital mortality was related to age, lowest recorded cardiac index, and the presence of left main coronary artery disease as well as infarction (54).

Delay in revascularization has a profound deleterious effect on survival. In a nonrandomized study, the in-hospital survival rate was 77% in patients revascularized within 24 hours but only 10% in those undergoing successful revascularization more than 24 hours after the onset of shock (53). The SHOCK Registry was a randomized trial of direct invasive strategy for patients with cardiogenic shock complicating an acute infarction. The mortality rate varied from 84% in patients with acute mitral regurgitation or ventricular rupture to 53% in patients with nonanterior infarction (92).

Counterpulsation has also produced favorable responses in patients with shock due to a nonischemic cause. In a reported series of noncoronary shock patients, most with acute myocarditis, IABP therapy was instituted in ventilated patients for whom pharmacologic support had failed. Three to 4 days of counterpulsation was sufficient to allow adequate recovery of ventricular function in 25% of the patients. The remainder required an LVAD or a biventricular support device for 3 to 79 days. At follow-up (7 to 54 months), all patients had recovered normal ventricular function and were asymptomatic, suggesting that patients with severe noncoronary shock may be supported for up to several weeks before transplantation is considered (93).

The IABP may be especially useful in mitigating the ischemic and hemodynamic abnormalities that accompany a failed angioplasty with abrupt closure. Even when catheter technique rescue is unsuccessful, rapid stabilization with mechanical support followed by prompt surgery can yield a favorable result (61). Of course these events have become unusual in the era of stenting to reverse abrupt closure (see Chapter 23), but counterpulsation should not be forgotten in the rare patient who still requires emergency bypass in the setting of profound ischemia.

Duplex scanning of the common carotid artery in patients during counterpulsation revealed an increase in diastolic flow but a *reversal* in systolic flow, resulting in no net change in total carotid flow (94).

Unstable Angina, Acute Myocardial Infarction

Patients with medically refractory unstable angina make up the large proportion of those treated by IABP. During counterpulsation, they may exhibit only modest decreases in peak systolic pressure and in LV filling pressure, with unchanged cardiac output, LV volumes, LV ejection fraction (LVEF), and regional contraction, as determined by angiographic chordal shortening (95). In patients with anterior wall ischemia, measurements of coronary sinus flow from the ischemic area may improve with counterpulsation, but this is not a uniform response (96).

In patients who were hemodynamically stable, coronary flow velocity was studied using an *intracoronary Doppler wire* (see Chapter 18). There was no increase in mean coronary flow velocity beyond a critical coronary stenosis (97), despite an increase in peak coronary flow velocity (98). This counterpulsation-induced effect on peak coronary flow beyond a critical stenosis was not observed in a carefully controlled study on normotensive dogs (99). In contrast, counterpulsation produced a dramatic increase in the integral of coronary flow velocity, a measure of coronary flow, in hypotensive patients with acute infarction or cardiogenic shock (100). It has been postulated that counterpulsation might improve unstable angina by increasing collateral flow to the ischemic area. In a small series of patients with acute infarction or unstable angina, there was a significant increase in collateral flow in the presence of angiographically documented collaterals but no change in collateral flow when collateral vessels were absent or too small to be seen by angiography (80).

In a dog study of thrombolysis with recombinant tissue plasminogen activator (r-TPA), IABP did not change the mean systemic pressure or coronary blood flow but did decrease the time to reperfusion, suggesting that the time to thrombolysis may be a pressure-dependent variable (101). A Doppler wire study of coronary flow velocity in patients with acute infarction and successful angioplasty revealed no change in mean coronary flow by counterpulsation, but peak velocity of flow increased from 35 to 47 cm/sec (98). A report of patients with anterior infarction and PTCA randomly assigned to either 24 hours of counterpulsation or conventional therapy found

reocclusion rates of 2.4% in the IABP group and 17.7% in the conventional therapy group (102). Retrospective review of the Thrombolysis and Angioplasty in Myocardial Infarction (TAMI) study noted a similar effect on reinfarction or reocclusion (103), and a study that randomly assigned patients with failed angioplasty to either conventional therapy or 48 hours of counterpulsation found a marked improvement in TIMI-3 flow in the counterpulsation group at the 3-week angiography (74% vs. 32% of patients), suggesting that counterpulsation may be a reasonable alternative in rescuing angioplasty to achieve late patency of the infarct-related artery (104).

There have been two large, multicenter, randomized trials of counterpulsation to maintain patency of the infarct-related artery. The first, reported in 1994, confirmed the benefit of this strategy (65). Patients in whom patency was restored within 24 hours after acute infarction were randomly assigned to standard therapy or to 48 hours of counterpulsation. Repeat angiography was performed on day 5. Reocclusion was present in 8% of the IABP patients but in 21% of those receiving standard care, who also were almost twice as likely to suffer death, stroke, or a recurrent ischemic event (65). This benefit was accomplished without any substantial increase in hospital costs (105).

The enthusiasm for counterpulsation to prevent reocclusion after angioplasty has been tempered, however, by the results of a large multicenter study, the Second Primary Angioplasty in Myocardial Infarction (PAMI-II). This prospective, randomized trial studied 1,100 patients within 12 hours after acute infarction. Clinical and angiographic variables were used to stratify patients undergoing primary PTCA into high-risk and low-risk groups. The high-risk patients were randomly assigned to 36 to 48 hours of IABP or standard care. Although IABP produced a decrease in recurrent ischemia (13.3% vs. 19.6%) and unscheduled recatheterization (7.6% vs. 13.3%), it did not reduce the rate of infarct-related artery occlusion (6.7% vs. 5.5%), reinfarction (6.2% vs. 8.0%), or death (4.3 % vs. 3.1%). The authors concluded that prophylactic IABP after primary PTCA in hemodynamically stable high-risk patients with acute myocardial infarction did not decrease the rate of infarct-related artery reocclusion or reinfarction, promote myocardial recovery, or improve overall clinical outcome (106). The reocclusion rate in the control group was extraordinarily low, and the disparity between these two studies may be related to both the clinical characteristics of the patients and the rapidly evolving changes in the techniques of intervention and anticoagulation. The control group reocclusion rate in the more recent study was less than that of the IABP group in the 1994 investigation (5.5% vs. 8%). Counterpulsation may offer little extra benefit for decreasing reocclusion in current intervention practice.

Prophylactic Intraarticular Balloon Pump Therapy in High-Risk Angioplasty

The application of new devices, most especially stents and atherectomy, has resulted in a dramatic decrease in the need for prophylactic IABP support. It is prudent to have the IABP console and catheters immediately available and, especially in high-risk interventions, to have placed a 5F dilator in the contralateral femoral artery so that counterpulsation can be instituted with minimal delay. Although prophylactic counterpulsation has been applied successfully and with a surprisingly low complication rate in this very sick group of patients (62,63,64,65 and 66,107), in one series high-risk patients did equally well but had fewer vascular complications when *prophylactic* IABP was not used (108). The National Registry of Supported Angioplasty reported the results in 801 patients with supported or standby-supported angioplasty. Patients older than 70 years of age and those with left main coronary artery stenosis were at higher risk, and those with LVEF less than 20% did better with prophylactic support. However, those with greater than 50% of myocardium in jeopardy and low LVEF can undergo intervention with a 7.2% in-hospital mortality rate with either prophylactic or standby IABP support (109). With standby CPS, the in-hospital mortality rate for a similar group of patients was 6.0% (110). A nonrandomized comparison of prophylactic IABP with prophylactic CPS did not reveal any differences in myocardial infarction, stroke, emergency bypass surgery, or death, but there was a higher rate of peripheral vascular complications in the CPS group (111). This suggests that the mortality rate is more a function of the baseline characteristics of the patient than of the support device used.

A retrospective analysis of 159 consecutive high-risk patients undergoing rotational atherectomy revealed that the 28 patients with elective preprocedure IABP placement had the same occurrence of slow flow (18% vs. 17%), equal hospital stay, and similar vascular complication rate, compared with controls. However, among the patients developing slow flow, there were no non–Q wave myocardial infarctions in the IABP group, compared with 27% in the control group (112).

Emergency Coronary Artery Bypass Grafting for Failed Percutaneous Transluminal Coronary Angioplasty

A retrospective review of emergency coronary artery bypass grafting (CABG) operations for failed PTCA documented a marked change over a single decade. Of 9,145 patients undergoing PTCA from 1980 through 1990, the group treated from 1980 to 1985 was compared with the subset treated from 1986 through 1990. Although the incidence of emergency CABG within 24 hours after PTCA fell from 3.8% to 2.3%, the mortality rate rose from 4.6% to 7.6%. The patients in the more recent period had a higher incidence of prior PTCA and class III or IV symptoms, but the major determinant of in-hospital mortality after emergency surgery for failed PTCA remained the hemodynamic status at the time of surgery. Patients who required cardiopulmonary resuscitation or were in shock had a mortality rate of 28% (13/46), whereas those with stable hemodynamics at time of emergency CABG had a mortality rate of only 1.4% (3/207). Preoperative IABP use increased from 13% in the first period to 33% in the second. Late survival was excellent, 92% at 2 years and 87% at 5 years (113).

Bridge to Cardiac Transplantation

IABP has been successful at maintaining severely decompensated patients awaiting suitable donor hearts. Although the support is less impressive than that delivered by CPS or the ventricular assist device, the IABP is much more easily maintained over the intermediate term and often is enough to supply the required degree of hemodynamic support (114).

Enhanced External Counterpulsation.

Enhanced external counterpulsation (EECP) has been used to achieve some of the benefits of the IABP with a noninvasive device that produces serial inflation of three sets of cuffs wrapped around the calves, the thighs, and the buttocks, timed to inflate in diastole according to the surface ECG. (Commercial systems are available from Vasomedical Inc., Westbury, NY, and from Cardiomedics Inc., 18872 Bardeen Ave, Irvine, CA 90612.) In a randomized trial comprising 258 patients with acute infarction, application of EECP for 3 hours within 24 hours after presentation resulted in a reduction in mortality in the subgroup of elderly patients (115). When EECP was applied 1 hour each day for 7 weeks to a group of 18 patients with chronic stable angina, exercise treadmill studies revealed improvement in exercise duration, resolution of thallium defects in 12 patients, decreased ischemic area in 4 patients, but no change in systolic blood pressure × pulse double product (116). At 3-year follow-up, 13 of the 18 patients remained free of angina (117). In some patients the EECP has produced dramatic improvement in symptoms and radionuclide stress tests after failure of all other usual modalities of treatment (118). It is presumed that the mechanism for improvement is collateral development, which is dependent on patency of neighboring vessels, there being less improvement in patients with residual three-vessel disease. Although the improvement in the thallium study suggests that there is a decrease in ischemia, the unchanged double product indicates that the improvement is partly related to decreased peripheral vascular resistance and the heart rate response to exercise (119). By means of Doppler techniques to study flow velocity, mean carotid flow velocity was shown to increase by 22% and mean renal artery flow velocity by 19% during sequential external counterpulsation (120).

In the Multicenter Study of Enhanced External Counterpulsation (MUST-EECP), 139 patients were randomly assigned to either hemodynamically inactive counterpulsation or active counterpulsation. In the latter group, total exercise time was increased by almost 1 minute. Angina episodes decreased in the active counterpulsation group only, but hospitalization rates were the same in both groups (121).

Pulmonary Artery Counterpulsation

Rare case reports of pulmonary artery counterpulsation have shown favorable hemodynamic effects on the failing right ventricle, but these patients had profoundly abnormal hemodynamics and most did not survive (122,123 and 124). Placement in these cases was in the operating room under direct vision, but percutaneous deployment has been possible in animals (125).

PERCUTANEOUS CARDIOPULMONARY SUPPORT

Although the IABP provides effective circulatory assistance or ischemia relief for the majority of patients, it usually does not increase the cardiac output by more than 1 L/min. This is not adequate to completely support patients with severely compromised pump function. Newer and more potent forms of CPS have been developed for this purpose, some of which can even support the circulation in the presence of full cardiac arrest. Because these devices markedly decrease cardiac work and myocardial oxygen consumption, they may also be much less effective in reversing myocardial ischemia in the presence of a complete coronary occlusion. The increase in hemodynamic support is accomplished at the cost of much increased complexity and expense for the ventricular assist device and for the CPS device.

Bard Cardiopulmonary Support System

Design

The Bard percutaneous cardiopulmonary support system (PCPS, C.R. Bard, Billerica, MA) is analogous to the heart-lung machine used during open heart surgery. The basic design is shown in Fig. 21.3. Venous blood is withdrawn from the right atrium and vena cavae, through the Bio-medicus pump, heat exchanger, and membrane oxygenator, after which it is pumped back into the aorta via the percutaneously inserted arterial cannula. The system is battery powered and mounted in a portable cart. Initially the cannulae were inserted surgically, but this has been supplanted by percutaneous femoral artery and vein insertion.

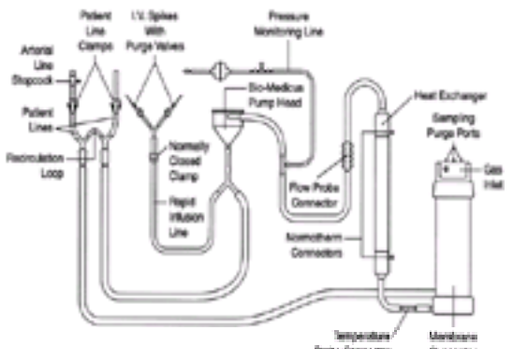

FIG. 21.3. The Bard cardiopulmonary support system (C.R. Bard, Billerica, MA) uses a Bio-medicus pump to pass venous blood through a heat exchanger and membrane oxygenator and into the arterial system. The extra lines are available to provide pressure monitoring, a recirculation loop, and a purging circuit.

Prophylactic Versus Standby Cardiopulmonary Support

In contrast to prophylactic use of PCPS, which is defined as the implementation of bypass support before coronary angioplasty, *standby-supported* angioplasty refers to a planned situation in which both PCPS equipment and personnel are available in the cardiac catheterization laboratory should hemodynamic collapse develop. Most high-risk PTCAs can be performed safely without advance placement of cannulae or initiation of bypass so long as cardiopulmonary bypass support is immediately available. Iliac angiography is performed, followed by placement of 5F sheaths in the artery and vein contralateral to that being used for intervention. Unplanned cardiopulmonary bypass support has been much less effective, in large part because even a short hiatus between cardiac arrest and the institution of hemodynamic support has a major impact on survival. In a high-volume catheterization laboratory that is very experienced in the CPS system, elective coronary interventions have been performed without formal surgical backup but with immediately available standby CPS, which was required in 0.4% of the cases—none of which fell into the high-risk category for PTCA. The importance of rapid initiation of CPS is supported by the lower mortality rate for patients sustaining hemodynamic collapse in the catheterization laboratory (126).

Contraindications

The contraindications for PCPS are similar to those for IABP counterpulsation—aortic regurgitation, uncontrolled sepsis, uncontrolled bleeding diathesis, contraindication to anticoagulation, severe peripheral vascular disease, aortic dissection, or severe aortic aneurysm.

Elective Cardiopulmonary Support Technique

Because of the large diameter of the cannulae, insertion is preceded by iliofemoral angiography to ascertain feasibility of cannulae placement. Care is taken to ensure that puncture is below the inguinal ligament but in the common femoral artery. Access is achieved in both the femoral artery and the ipsilateral femoral vein using a 0.038 inch J guidewire and 8F long dilator. Anticoagulation is instituted with heparin and followed with regular determinations of activated clotting time. The wire is then replaced with a 0.038-inch heavy-duty guidewire with a stiff body and a flexible tip. The femoral artery and vein are progressively dilated, first with an 8F, then a 12F and a 14F dilator, followed by the 18F cannulae, which are positioned in the middle right atrium and in the aorta at the bifurcation. The pump uses a disposable system that must be primed, but this can be accomplished simultaneously with catheter insertion. Venous return is via active suction, not gravity, making it essential that patients be well hydrated and that all venous lines remain closed to prevent air embolism. For this reason *central venous access should not be attempted while the pump is operating*. Cardiopulmonary bypass is initiated at 2.0 L/min and progressively advanced as needed in increments of 0.5 L/min. Pumping can be performed for up to 6 hours before changes in pulmonary and hematologic function require discontinuation. Beyond 6 hours, platelet aggregation, hemolysis, a bleeding diathesis, and increased capillary permeability with plasma loss become major problems. If the cannulae were inserted to perform a high-risk angioplasty, the patient can be weaned over a 15-minute period, with a further 30-minute period of observation prior to removal of the cannulae. Hemostasis is achieved with the use of a mechanical clamp.

Cardiopulmonary Support Physiology

In a study of the hemodynamic effects in 14 patients undergoing high risk PTCA, pulmonary artery pressure decreased from 45/23 to 27/14 mm Hg, and the mean pulmonary arterial pressure went from 30 to 18 mm Hg. Aortic systolic pressure decreased from 129 to 106 mm Hg, and mean aortic pressure from 89 to 84 mm Hg, but diastolic pressure and heart rate remained unchanged. Calculated end-systolic wall stress decreased from 122 to 96 dynes-cm ^{2} (127). A similar study in 20 patients receiving CPS support found a comparable reduction in afterload and in LV wall stress but no change in LV size or global LV function. Regions supplied by vessels with greater than 50% stenosis deteriorated during CPS, whereas those supplied by normal vessels did not. During balloon inflation under CPS support, two-dimensional echocardiography revealed evidence of regional myocardial dysfunction in the area supplied by the vessel being dilated (128).

Results

When PCPS has been placed outside of the catheterization laboratory for cardiac arrest, the long-term survival has been disappointing, despite short-term improvement, because of the delay between the acute event and the institution of PCPS. Patients with severe hemodynamic compromise experience marked hemodynamic improvement in almost all cases, but the long-term survival rate is disappointing (110,129,130,131,132,133 and 134). The application of PCPS is most effective when performed in a catheterization laboratory that is already prepared for insertion and technical support (135).

Supported High-Risk Percutaneous Transluminal Coronary Angioplasty

The group at Washington Adventist Hospital (Takoma Park, MD) reported on 107 patients with unstable presentation and severely depressed LVEF managed by PCPS-supported intervention. Mean LVEF was 19%, 47% of patients were deemed unsuitable for bypass surgery, and 54% had only one remaining patent artery. Ninety eight percent were successfully dilated with an in-hospital mortality rate of 4.7% and a 21% further mortality rate within 2 years after the procedure. LVEF increased from 21% to 29% in the patients in whom it was measured. Survival free of cardiac symptoms at 1 and 2 years was 83% and 77%, respectively (136). The multicenter registry reported the results in 105 patients with similar anatomic and hemodynamic profiles. The angioplasty success rate was 95%, and the in-hospital mortality rate was 7.6%. Half of the hospital mortality occurred in patients older than 75 years of age who had left main coronary artery disease. If those patients were omitted, the mortality rate fell to 2.6%. Over the next 12 months of follow-up, there were only three additional cardiac-related deaths (137).

Prophylactic Versus Standby Percutaneous Cardiopulmonary Support

As interventional catheter techniques have advanced, the necessity for prophylactic support has diminished markedly. A retrospective comparison was made of 389 patients undergoing prophylactic PCPS for a high-risk angioplasty and 180 standby patients for whom preparations were made but PCPS was not initiated before

intervention. Only 13 (7.2%) of the standby group sustained a *hemodynamic* collapse, 12 of whom underwent successful PCPS within 5 minutes. Procedural success was equivalent: 88.7% in the prophylactic group and 84.4% in the standby group. Femoral access complications and the requirement for transfusion were more frequent in the prophylactic group (42%) than in the standby group (12%) (110). Standby PCPS requires immediate access to the technical support required to operate the system but provides a comparable success rate with a much lower morbidity.

Emergency Percutaneous Cardiopulmonary Support for Cardiac Arrest

The national registry experience confirms the importance of early initiation of PCPS. The long-term survival rate was 38% for patients in whom PCPS was operating within 20 minutes after the acute event and only 18% for those requiring more than 20 minutes (133). From a practical standpoint, this means that the device is not likely to be useful for cardiac arrest out of the catheterization laboratory, or even for catheterization laboratory emergencies unless the pump technician and equipment are available immediately (134,135,136 and 137). A subset of patients with hemodynamic collapse due to massive pulmonary embolization may respond well to PCPS, permitting stabilization for emergency embolectomy (138). In at least one case of critical aortic stenosis with cardiac arrest during diagnostic catheterization and unsuccessful cardiopulmonary resuscitation for 45 minutes, institution of peripheral CPS restored cardiac rhythm and blood pressure, with a subsequent successful aortic valve replacement (139).

Complications

Most of the complications are caused by local vascular problems, but there has been a dramatic reduction in the vascular complication rate reported with PCPS, which is now less than 1.5% in elective patients. This improvement has been largely related to changes in anticoagulation protocol and in the duration of support.

Conclusion

In the current interventional era, the full hemodynamic support provided by PCPS is rarely necessary, and the continuous technical back-up required for operation of the CPS device is a major impediment to its widespread use. Furthermore, the failure of the PCPS system to provide increased myocardial perfusion distal to a total occlusion is a serious limitation of the technique: despite the presence of excellent systemic flows and extreme reduction in myocardial oxygen demand, an occluded coronary artery may continue to produce significant myocardial ischemia unless an autoperfusion catheter can be advanced across the occlusion. Therefore, even in the presence of affective PCPS support, acute coronary occlusion after PTCA that cannot be stabilized by catheter technique should be treated with CABG to prevent a large myocardial infarction. The availability of PCPS does not change the requirement for rapid CABG surgery in the event of abrupt and uncorrectable coronary occlusion after PTCA.

Temporary Left Ventricular Assist Devices

Design

The Hemopump (Medtronic Hemodynamics, Minneapolis, Minnesota, 800-678-2500) is a temporary LVAD that uses a single coaxial catheter inserted into the LV cavity by surgical exposure of the femoral artery (21F catheter) or by percutaneous insertion via the femoral artery (14F catheter). A flexible silicone cannula is placed across the aortic valve into the LV cavity. The surgically implanted 21F device can achieve flows of 6 L/min, but the percutaneous 14F catheter can reach only 2 L/min. A rotating turbine fits snugly within the cannula and imparts both a rotational and a longitudinal velocity to the blood. To eliminate the rotational motion of the blood as it exits the catheter, static vanes are mounted downstream from the rapidly rotating turbine pump. Power to the pump is provided by means of a magnetically coupled sheath drive cable, providing a system that is entirely enclosed, with no contact between blood and the drive motor. The pump can be driven at speeds up to 25,000 rpm to provide a pumping rate of up to 3.5 L/min in a continuous, nonpulsatile manner. Forty percent dextrose in water is used to lubricate the 9F sheath that contains the drive cable as well as the pump itself. The control console is compact and easily portable.

Originally designed as an LVAD, the unit has been modified to be used as a right ventricular assist device (RVAD) or biventricular support device (BiVAD).

Percutaneous Insertion Technique

This is similar to the technique required for the PCPS system described, except that only arterial access is necessary for the support system. Single-wall puncture is used, the iliofemoral anatomy is defined, the guidewire is exchanged for a heavy-duty, stiff guidewire, and the femoral artery is progressively dilated to accommodate the 16F sheath. The pump is advanced to the abdominal aorta, turned on at minimum flow, and then advanced slowly over the guidewire until it enters the left ventricle. Proper placement of the pump is critical. The pump should be 4 cm above the aortic valve sinus to prevent damage to the aortic valve leaflets.

Management During Pumping

Before insertion, arterial blood gas analysis, complete blood count with platelet and differential counts, liver function tests, fibrinogen, fibrin split products, partial thromboplastin time, prothrombin time, and activated clotting time measurements are obtained. A pulmonary arterial catheter and intravenous line should be in place, and a baseline echocardiogram is obtained. Prophylactic antibiotics are administered. Care must be taken to avoid damage to the surface of the cannula to maintain its resistance to thrombus formation. After insertion of the pump, anticoagulation is achieved with the use of intravenous heparin. The pump rotation speed is increased progressively until a satisfactory pumping level has been achieved. A chest x-ray is obtained to monitor cannula position. During the use of the Hemopump, the patient should be monitored closely for signs of complications including coagulation abnormalities, sepsis, arrhythmias, embolization of LV thrombus either systemically or within the 21F pump cannula, decreased peripheral circulation, and cannula migration. A daily chest x-ray should be obtained to check on cannula placement.

Discontinuation of Pumping

A trial of reduced speed pumping is performed every 24 hours with close monitoring of arterial blood gases, cardiac output, heart rate, right-sided heart pressures, and systemic pressures. If this is tolerated well, pumping is reduced gradually every 4 hours. When the patient has been weaned to the lowest pump speed without evidence of hemodynamic deterioration, the pump may be removed.

Indications and Contraindications

This device has been used for cardiac support during high-risk intervention, as a bridge to transplantation, and to treat patients with severe hemodynamic compromise due to acute myocardial infarction, myocarditis, valve disease, or other condition. It is contraindicated in patients with sepsis, bleeding diathesis, aortic dissection or large aortic aneurysm, prosthetic aortic valve, aortic stenosis, aortic insufficiency, or LV or left atrial thrombi. As is true for the PCPS system, severe peripheral vascular disease is a relative contraindication that can sometimes be overcome by antecedent femoral or iliac artery intervention.

Clinical Applications

High-Risk Catheter Intervention

The Hemopump was first used in 1994 for this purpose, and the favorable outcome in two patients encouraged further use (140). The percutaneous Hemopump was used in 32 high-risk patients undergoing catheter intervention. There was good unloading of the left ventricle and maintenance of cardiac output during periods of severe ischemia. In three patients with cardiac arrest, the mean aortic pressure was maintained at 50 mm Hg. However, mortality was high (12.5%), as was procedure-related morbidity. Femoral artery occlusion occurred in two patients, and severe bleeding requiring transfusion was present in four patients (141,142).

Acute Myocardial Infarction Complicated by Shock

In comparison to the intraaortic balloon, LVAD has shown improvement in regional myocardial blood flow, LV unloading, and infarct salvage in a dog model (143). In patients, initial studies using the 21F surgically inserted device showed an associated mortality rate of 64% while receiving support or immediately after its removal. Although hemodynamics improved substantially within 24 hours (pulmonary capillary wedge pressure decreased from 26 to 16 mm Hg, and cardiac index from 1.6 to

2.4 L/min/m^2), the overall survival rate remained only 36% (144). Despite these disappointing long-term results, there have been reports of remarkable recovery from profound shock with near-fatal stunning after acute infarction with LVAD insertion (145). In an animal study, the addition of IABP to Hemopump LVAD support resulted in an increase in myocardial blood flow to ischemic regions, restoring the flows to normal while the perfusion of peripheral organs remained unaltered (146).

Bridge to Transplantation

Although emergency temporary support can be accomplished with the units described earlier, these patients usually require a longer period of hemodynamic support, which is best supplied by surgically implanted LVAD or BiVAD units.

CHAPTER REFERENCES

1. Clauss RH, Birtwell WC, Albertal G, et al. Assisted circulation: I. The arterial counterpulsator. *J Thorac Cardiovasc Surg* 1961;41:447.
2. Moulopoulos SD, Topaz S, Kolff WJ. Diastolic balloon pumping (with carbon dioxide) in the aorta: a mechanical assistance to the failing circulation. *Am Heart J* 1962;63:669.
3. Kantrowitz A, Tjonneland S, Freed PS, et al. Initial clinical experience with intraaortic balloon pumping in cardiogenic shock. *JAMA* 1968;203:113.
4. Weintraub RM, Aroesty JM, Paulin S, et al. Medically refractory unstable angina pectoris: I. Long-term follow-up of patients undergoing intraaortic balloon counterpulsation and operation. *Am J Cardiol* 1979;43:877.
5. Bregman D, Casarella WJ. Percutaneous intraaortic balloon pumping: initial clinical experience. *Ann Thorac Surg* 1980;29:153.
6. LaMuraglia GM, Vlahakes GJ, Moncure AC, et al. The safety of intraaortic balloon pump catheter insertion through suprainguinal prosthetic vascular bypass grafts. *J Vasc Surg* 1991;13:830.
7. Aroesty JM, Schlossman D, Weintraub RM, et al. Transfemoral selective coronary artery catheterization during intra-aortic balloon by-pass pumping. *Radiology* 1974;111:307.
8. McCabe JC, Abel RM, Subramamianian VA, et al. Complications of intra-aortic balloon insertion and counterpulsation. *Circulation* 1978;57:769.
9. Alderman J, Gabliani GI, McCabe CH, et al. Incidence and management of limb ischemia with percutaneous wire guided intraaortic balloon catheters. *J Am Coll Cardiol* 1987;9:524.
10. Alpert J, Parsonnet V, Goldenkranz RJ, et al. Limb ischemia during intra-aortic balloon pumping: indication for femorofemoral crossover graft. *J Thorac Cardiovasc Surg* 1980;79:729.
11. Shahian DM, Neptune WB, Ellis FH Jr, et al. Intraaortic balloon pump morbidity: a comparative analysis of risk factors between percutaneous and surgical techniques. *Ann Thorac Surg* 1983;36:644.
12. Naunheim KS, Swartz MT, Pennington DG, et al. Intraaortic balloon pumping in patients requiring cardiac operations: risk analysis and long-term followup. *J Thorac Cardiovasc Surg* 1992;104:1654.
13. Isner JM, Cohen SR, Virmani R, et al. Complications of the intraaortic counterpulsation device: clinical and morphological observations in 45 necropsy patients. *Am J Cardiol* 1980;45:260.
14. Vignola PA, Swaye PS, Gosselin AJ. Guidelines for effective and safe percutaneous intraaortic balloon pump insertion and removal. *Am J Cardiol* 1981;48:660.
15. Harvey JC, Goldstein JE, McCabe JC, et al. Complications of intraaortic balloon pumping. *Circulation* 1981;64[Suppl II]:II-114.
16. Weintraub RM, Thurer RL. The intraaortic balloon pump: a ten year experience. *Heart Transplant* 1983;3:8.
17. Vignola PA, Swaye PS, Gosselin AJ. Percutaneous intraaortic balloon pumping: new problems and dilemmas. *Cathet Cardiovasc Diagn* 1983;9:317.
18. Gottlieb SO, Brinker JA, Borkon AM, et al. Identification of patients at high risk for complication of intraaortic balloon counterpulsation: a multivariate risk factor analysis. *Am J Cardiol* 1984;53:1135.
19. Kantrowitz A, Wasfie T, Freed PS, et al. Intraaortic balloon pumping 1967–1982: analysis of complications in 733 patients. *Am J Cardiol* 1986;57:976.
20. Skillman J, Kim DS, Baim DS. Vascular complications of percutaneous femoral interventions. *Arch Surg* 1988;123:1207.
21. Akins CW, Buckley MJ, Daggett WM, et al. Reoperative coronary grafting: changing patient profiles, operative indications, techniques and results. *Ann Thorac Surg* 1994;58:359.
22. Alvarez JM, Gates R, Rowe D, et al. Complications from intra-aortic balloon counterpulsation: a review of 303 cardiac surgical patients. *Eur J Cardiothorac Surg* 1992;6:530.
23. Eltchaninoff H, Dimas AP, Whitlow PL. Complications associated with percutaneous placement and use of intraaortic balloon counterpulsation. *Am J Cardiol* 1993;71:328.
24. Busch T, Sirbu H, Zenker D, et al. Vascular complications related to intraaortic balloon counterpulsation: an analysis of ten years experience. *Thorac Cardiovasc Surg* 1997;45:55.
25. Scholz KH, Ragab S, von zur Muhlen F, et al. Complications of intra-aortic counterpulsation: the role of catheter size and duration of support in a multivariate analysis of risk. *Eur Heart J* 1998;19:458.
26. Biddle TL, Stewart S, Stuard ID. Dissection of the aorta complicating intra-aortic balloon counterpulsation. *Am Heart J* 1976;92:781.
27. Yuen JC, Riggs OE. Aortoiliac dissection after percutaneous insertion of an intra-aortic balloon pump. *South Med J* 1991;84:1135.
28. Jacobs LE, Fraifeld M, Kotler MN, et al. Aortic dissection following intraaortic balloon insertion: recognition by transesophageal echocardiography. *Am Heart J* 1992;124:536.
29. Nakatani S, Beppu S, Tanaka N, et al. Application of abdominal and transesophageal echocardiography as a guide for the insertion of intraaortic balloon in aortic dissections. *Am J Cardiol* 1989;64:1082.
30. Allen RC, Schneider J, Longenecker L, et al. Acute lower extremity ischemia after cardiac surgery. *Am J Surg* 1993;166:124.
31. Kassirer JP. Atheroembolic renal disease. *N Engl J Med* 1969;280:812.
32. Hyman BT, Landas SK, Ashman RF, et al. Warfarin-related purple toes syndrome and cholesterol microembolization. *Am J Med* 1987;82:1233.
33. Aksnes J, Abdelnoor M, Berge V, et al. Risk factors of septicemia and perioperative myocardial infarction in a cohort of patients supported with intra-aortic balloon pump (IABP) in the course of open heart surgery. *Eur J Cardiothorac Surg* 1993;7:153.
34. Myers GJ, Landymore RW, Leadon RB, et al. Fracture of the internal lumen of a Datascope Percor Stat-DL balloon, resulting in stroke. *Ann Thorac Surg* 1994;57:1335.
35. Frederiksen JW, Smith J, Brown P, et al. Arterial helium embolism from a ruptured intraaortic balloon. *Ann Thorac Surg* 1988;46:690.
36. Rajani R, Keon WJ, Bedard P. Rupture of an intra-aortic balloon. *J Thorac Cardiovasc Surg* 1980;79:301.
37. Aru GM, King JT Jr, Hovaguimanian H, et al. The entrapped balloon: report of a possibly serious complication. *J Thorac Cardiovasc Surg* 1986;91:146.
38. Millham FH, Hudson HM, Woodson J, et al. Intraaortic balloon pump entrapment. *Ann Vasc Surg* 1991;5:381.
39. Shafei H, Webb G, Lennox SC. Entrapping of the clotted intra-aortic balloon in the descending aorta. *Eur J Cardiothorac Surg* 1991;5:165.
40. Takazawa A, Tsuchida K, Kijima M, et al. A case report of successful removal of entrapped IABP by Lambert's method. *Kyobu Geka* 1993;46:435.
41. Goldberg MJ, Rubenfire M, Kantrowitz A, et al. Intraaortic balloon pump insertion: a randomized study comparing percutaneous and surgical techniques. *J Am Coll Cardiol* 1987;9:515.
42. Lundell DC, Hammond GL, Geha AS, et al. Randomized comparison of the modified wire-guided and standard intraaortic balloon catheters. *J Thorac Cardiovasc Surg* 1981;81:297.
43. Hazelrigg SR, Auer JE, Seifert PE. Experience in 100 transthoracic balloon pumps. *Ann Thorac Surg* 1992;54:528.
44. Baciewicz FA Jr, Kaplan BM, Murphy TE, et al. Bilateral renal artery thrombotic occlusion: a unique complication following removal of a transthoracic intraaortic balloon. *Ann Thorac Surg* 1982;33:631.
45. McGeehin W, Sheikh F, Donahoo JS, et al. Transthoracic intraaortic balloon pump support: experience in 39 patients. *Ann Thorac Surg* 1987;44:26.
46. Macoviak J, Stephenson LW, Edmunds LH Jr, et al. The intraaortic balloon pump: an analysis of five years experience. *Ann Thorac Surg* 1980;29:451.
47. Nash IS, Lorell BH, Fishman RF, et al. A new technique for sheathless percutaneous intraaortic balloon catheter insertion. *Cathet Cardiovasc Diagn* 1991;23:57.
48. Tartar H, Cicek S, Demirkilic U, et al. Vascular complications of intraaortic balloon pumping: unsheathed versus sheathed insertion. *Ann Thorac Surg* 1993;55:1518.
49. Gitter R, Cate CM, Smart CK, et al. Influence of ascending versus descending balloon counterpulsation on bypass graft blood flow. *Ann Thorac Surg* 1998;65:365.
50. Makhoul RG, Cole CW, McCann RL. Vascular complications of the intra-aortic balloon pump: an analysis of 436 patients. *Am Surg* 1993;59:564.
51. Eltchaninoff H, Whitlow PL. Immediate and long-term complications of counterpulsation balloon: recent data apropos of a series of 200 consecutive patients. *Arch Mal Coeur Vaiss* 1993;86:1465.
52. Bolooki H. Emergency cardiac procedures in patients in cardiogenic shock due to complications of coronary artery disease. *Circulation* 1989;79:1137.
53. Moosvi AR, Khaja F, Villanueva L, et al. Early revascularization improves survival in cardiogenic shock complicating acute myocardial infarction. *J Am Coll Cardiol* 1992;19:907.
54. Bengtson JR, Kaplan AJ, Pieper KS, et al. Prognosis in cardiogenic shock in the interventional era. *J Am Coll Cardiol* 1992;20:1482.
55. Shub C, Gau GT, Sidell PM, et al. The management of acute quinidine intoxication. *Chest* 1978;73:173.
56. Frierson J, Bailly D, Shultz T, et al. Refractory cardiogenic shock and complete heart block after unsuspected verapamil-SR and atenolol overdose. *Clin Cardiol* 1991;14:933.
57. Creswell LL, Rosenbloom M, Cox JL, et al. Intraaortic balloon counterpulsation: patterns of usage and outcomes in cardiac surgery patients. *Ann Thorac Surg* 1992;54:11.
58. Lazar JM, Ziady GM, Dummer SJ, et al. Outcome and complications of prolonged intraaortic balloon counterpulsation in cardiac patients. *Am J Cardiol* 1992;69:955.
59. Franciosa JA, Heckel R. Significance of hypotension preceding fatal ventricular tachyarrhythmias in post-coronary obstruction sudden death. *Am Heart J* 1981;101:421.
60. Fitzpatrick AP, Dawkins K, Conway N. Emergency percutaneous transluminal angioplasty for intractable ventricular arrhythmias associated with acute anterior myocardial infarction. *Br Heart J* 1993;69:453.
61. Hochberg MS, Gregory JJ Jr, McCullough J, et al. Early emergent coronary bypass after failed angioplasty. *N J Med* 1993;90:385.
62. Kahn JK, Rutherford BD, McConahay DR, et al. Supported “high risk” coronary angioplasty using intraaortic balloon pump conterpulsation. *J Am Coll Cardiol* 1990;15:1151.
63. Aguirre FV, Kern MJ, Bach R, et al. Intraaortic balloon pump support during high risk coronary angioplasty. *Cardiology* 1994;84:175.
64. Stevens T, Kahn JK, McCallister BD, et al. Safety and efficacy of percutaneous transluminal coronary angioplasty in patients with left ventricular dysfunction. *Am J Cardiol* 1991;68:313.
65. Ohman EM, George BS, White CJ, et al. Use of aortic counterpulsation to improve sustained coronary artery potency during acute myocardial infarction: results of a randomized trial. The Randomized IABP Study Group. *Circulation* 1994;90:792.
66. Gacioch GM, Ellis SG, Lee L, et al. Cardiogenic shock complicating acute myocardial infarction: the use of coronary angioplasty and the integration of the new support devices into patient management. *J Am Coll Cardiol* 1992;19:647.
67. Folland ED, Kemper AJ, Khuri SF, et al. Intraaortic balloon counterpulsation as a temporary support measure in decompensated critical aortic stenosis. *J Am Coll Cardiol* 1985;5:711.
68. Vijayanagar R, Bognolo DA, Eckstein PE, et al. The role of intra-aortic balloon pump in the management of patients with main left coronary artery disease. *Cathet Cardiovasc Diagn* 1981;7:397.
69. Siu SC, Kowalchuk GJ, Welty FK, et al. Intra-aortic balloon counterpulsation support in the high-risk cardiac patients undergoing urgent noncardiac surgery. *Chest* 1991;99:1342.
70. Christenson JT, Badel P, Simonet F, et al. Preoperative intraaortic balloon pump enhances cardiac performance and improves the outcome of redo CABG. *Ann Thorac Surg* 1997;64:1237.
71. O'Rourke MF, Norris RM, Campbell TJ, et al. Randomized controlled trial of intraaortic balloon counterpulsation in early myocardial infarction with acute heart failure. *Am J Cardiol* 1981;47:815.
72. Flaherty JT, Becker LC, Weiss JL, et al. Results of a randomized prospective trial of intraaortic balloon counterpulsation and intravenous nitroglycerin in patients with acute myocardial infarction. *J Am Coll Cardiol* 1985;6:434.
73. Spotnitz HM, Covell JW, Ross J Jr, et al. Left ventricular mechanics and oxygen consumption during arterial counterpulsation. *Am J Physiol* 1969;217:1352.
74. Leinbach RC, Buckley MJ, Austen WG, et al. Effects of intraaortic balloon pumping on coronary flow and metabolism in man *Circulation* 1971;43–44[Suppl I]:77.
75. Mueller H, Ayres SM, Gianelli S, et al. Effect of isoproteronol, L-norepinephrine and intraaortic counterpulsation on hemodynamics and myocardial metabolism in shock following myocardial infarction. *Circulation* 1972;43:335.
76. Maroko PR, Bernstein EF, Libby P, et al. Effects of intraaortic balloon counterpulsation on the severity of myocardial ischemic injury following acute coronary occlusion. *Circulation* 1972;45:1150.
77. Mundth ED. Surgical treatment of cardiogenic shock and of acute mechanical complications following myocardial infarction. *Cardiovasc Clin* 1977;8:241.
78. Aroesty JM: Cardiogenic shock. In: Donoso E, Cohen S, eds. *Current Cardiovascular Topics* 1979;5:51.
79. Sasayama S, Osakada G, Takahashi M, et al. Effects of intraaortic balloon counterpulsation on regional myocardial function during acute coronary occlusion in the dog. *Am J Cardiol* 1979;43:59.
80. Flynn MS, Kern MJ, Donohue TJ, et al. Alterations of coronary collateral blood flow velocity during intraaortic balloon pumping. *Am J Cardiol* 1993;71:1451.
81. Haywood GA, Keeling PJ, Parker DJ, et al. Short-term effects of intra-aortic balloon pumping on renal blood flow and renal oxygen consumption in cardiogenic shock. *J Card Fail* 1995;1:217.

82. Mueller H, Ayres SM, Gregory JJ, et al. The effects of intraaortic counterpulsation on cardiac performance and metabolism in shock associated with acute myocardial infarction. *J Clin Invest* 1971;50:1885.
83. Dunkman WB, Leinbach RC, Buckley MJ, et al. Clinical and hemodynamic results of intraaortic balloon pumping and surgery for cardiogenic shock. *Circulation* 1972;46:465.
84. Dilley RB, Ross J Jr, Bernstein EF. Serial hemodynamics during intraaortic balloon counterpulsation for cardiogenic shock. *Circulation* 1973;47–48[Suppl III]:99.
85. Bardet J, Masquet C, Kahn JC, et al. Clinical and hemodynamic results of intraaortic balloon counterpulsation for cardiogenic shock. *Am Heart J* 1977;93:280.
86. O'Rourke MF, Sammel N, Chang VP. Arterial counterpulsation in severe heart failure complicating acute myocardial infarction. *Br Heart J* 1979;41:308.
87. Waksman R, Weiss AT, Gottsman MS, et al. Intra-aortic balloon counterpulsation improves survival in cardiogenic shock complicating acute myocardial infarction. *Eur Heart J* 1993;14:71.
88. Kovack PJ, Rasak MA, Bates ER, et al. Thrombolysis plus aortic counterpulsation: improved survival in patients who present to community hospitals with cardiogenic shock. *J Am Coll Cardiol* 1997;29:1454.
89. Anderson RD, Ohman EM, Holmes DR Jr, et al. Use of intraaortic balloon counterpulsation in patients presenting with cardiogenic shock: observations from the GUSTO-I Study. Global Utilization of Streptokinase and TPA for Occluded Coronary Arteries. *J Am Coll Cardiol* 1997;30:708.
90. Holmes DR Jr, Califf RM, van de Werf F, et al. Difference in countries' use of resources and clinical outcome for patients with cardiogenic shock after myocardial infarction: results from the GUSTO trial. *Lancet* 1997;349:75.
91. Lee L, Erbel R, Brown TM, et al: Multicenter registry of angioplasty therapy of cardiogenic shock: Initial and long-term survival. *J Am Coll Cardiol* 1991;17:599.
92. Hochman JS, Boland J, Sleeper LA, et al., and the SHOCK Registry Investigators. Current spectrum of cardiogenic shock and effect of early revascularization on mortality: results of an international registry. *Circulation* 1995;91:873.
93. Dembitsky WP, Moore CH, Holman WL, et al. Successful mechanical circulatory support for noncoronary shock. *J Heart Lung Transplant* 1992;11:129.
94. Applebaum RM, Wun HH, Katz ES, et al. Effects of intraaortic balloon counterpulsation on carotid artery blood flow. *Am Heart J* 1998;135:850.
95. Aroesty JM, Weintraub RM Paulin S, O'Grady GP. Medically refractory unstable angina pectoris: II. Hemodynamic and angiographic effects of intraaortic balloon counterpulsation. *Am J Cardiol* 1979;43:883.
96. Williams DO, Korr KS, Dewirtz H, et al. The effect of intraaortic balloon counterpulsation on regional myocardial blood flow and oxygen consumption in the presence of coronary artery stenosis in patients with unstable angina. *Circulation* 1982;66:593.
97. Kern M, Aguirre F, Bach R, et al. Augmentation of coronary blood flow by intra-aortic balloon pumping in patients after coronary angioplasty. *Circulation* 1993;87:500.
98. Ishihara M, Sato H, Tateishi H, et al. Effects of intraaortic balloon pumping on coronary hemodynamics after coronary angioplasty in patients with acute myocardial infarction. *Am Heart J* 1992;1224:1133.
99. Anderson RD, Gurbel PA. The effect of intra-aortic balloon counterpulsation on coronary blood flow velocity distal to coronary artery stenoses. *Cardiology* 1996;87:306.
100. Kern MJ, Aguirre FV, Tatineni S, et al. Enhanced coronary blood flow velocity during intraaortic balloon counterpulsation in critically ill patients. *J Am Coll Cardiol* 1993;21:359.
101. Gurbel PA, Anderson RD, MacCord CS, et al. Arterial diastolic pressure augmentation in intra-aortic balloon counterpulsation enhances the onset of coronary artery reperfusion by thrombolytic therapy. *Circulation* 1994;89:361.
102. Ishihara M, Sato H, Tateishi H, et al. Intraaortic balloon pumping as the postangioplasty strategy in acute myocardial infarction. *Am Heart J* 1991;122:385.
103. Ohman EM, Califf RM, George BS, et al. The use of intraaortic balloon pumping as an adjunct to reperfusion therapy in acute myocardial infarction: The Thrombolysis and Angioplasty in Myocardial Infarction (TAMI) Study Group. *Am Heart J* 1991;121:895.
104. Kono T, Morita H, Nishina T, et al. Aortic counterpulsation may improve late patency of he occluded coronary artery in patients with early failure of thrombolytic therapy. *J Am Coll Cardiol* 1996;28:876.
105. Talley JD, Ohman EM, Mark DB, et al. Economic implications of the prophylactic use of intraaortic balloon counterpulsation in the setting of acute myocardial infarction: The Randomized IABP Study Group. *Am J Cardiol* 1997;79:590.
106. Stone GW, Marsalese D, Brodie BR, et al. A prospective, randomized evaluation of prophylactic intraaortic balloon counterpulsation in high risk patients with acute myocardial infarction treated with primary angioplasty: Second Primary Angioplasty in Myocardial Infarction (PAMI-II) Trial Investigators. *J Am Coll Cardiol* 1997;29:1459.
107. Mueller HS. Role of intra-aortic counterpulsation in cardiogenic shock and acute myocardial infarction. *Cardiology* 1994;84:168.
108. Feld H, Herz I, Fried G, et al. Cardiopulmonary support increases morbidity and mortality in high-risk coronary angioplasty. *Am J Cardiol* 1991;68:790.
109. Tommaso CL, Vogel RA. National Registry for Supported Angioplasty: results and follow-up of three years of supported and standby supported angioplasty in high-risk patients. *Cardiology* 1994;84:238.
110. Teirstein PS, Vogel RA, Dorros G, et al. Prophylactic versus standby cardiopulmonary support for high risk percutaneous transluminal coronary angioplasty. *J Am Coll Cardiol* 1993;21:590.
111. Shreiber TL, Kodali UR, O'Neill WW, et al. Comparison of acute results of prophylactic intraaortic balloon pumping with cardiopulmonary support for percutaneous transluminal coronary angioplasty (PTCA). *Cathet Cardiovasc Diagn* 1998;45:115.
112. O'Murchu B, Foreman RD, Shaw RE, et al. Role of intraaortic balloon pump counterpulsation in high risk coronary rotational atherectomy. *J Am Coll Cardiol* 1995;26:1270.
113. Boylan MJ, Lytle BW, Taylor PC, et al. Have PTCA failures requiring emergent bypass operations changed? *Ann Thorac Surg* 1995;59:283.
114. Birovljev S, Radovancevic B, Burnett CM, et al. Heart transplantation after mechanical circulatory support: four years experience. *J Heart Lung Transplant* 1992;11:240.
115. Amsterdam EA, Banas J, Criley JM, et al. Clinical assessment of external pressure circulatory assistance in acute myocardial infarction: report of a cooperative clinical trial. *Am J Cardiol* 1980;45:349.
116. Lawson WE, Hui JC, Soroff HS, et al. Efficacy of enhanced external counterpulsation in the treatment of angina pectoris. *Am J Cardiol* 1992;70:859.
117. Lawson WE, Hui JC, Zheng ZS, et al. Three-year sustained benefit from enhanced external counterpulsation in chronic angina pectoris. *Am J Cardiol* 1995;75:840.
118. Lawson WE, Hui JC, Oster ZH, et al. Enhanced external counterpulsation as an adjunct to revascularization in unstable angina. *Clin Cardiol* 1997;20:178.
119. Lawson WE, Hui JC, Zheng ZS, et al. Improved exercise tolerance following enhanced external counterpulsation: cardiac or peripheral effect? *Cardiology* 1996;87:271.
120. Applebaum RM, Kasliwal R, Tunick PA, et al. Sequential external counterpulsation increases cerebral and renal blood flow. *Am Heart J* 1997;133:611.
121. Arora RR, Chou TM, Jain D, et al. The Multicenter Study of Enhanced External Counterpulsation (MUST-EECP): Effect of EECP on exercise-induced myocardial ischemia and anginal episodes. *J Am Coll Cardiol* 1999;33:1833.
122. Skillington PD, Couper GS, Peigh PS, et al. Pulmonary artery balloon counterpulsation for intraoperative right ventricular failure. *Ann Thorac Surg* 1991;51:658.
123. Moran JM, Opravil M, Gorman AJ, et al. Pulmonary artery balloon counterpulsation for right ventricular failure: II. Clinical experience. *Ann Thorac Surg* 1984;38:254.
124. Symbas PN, McKeown PP, Santora AH, et al. Pulmonary artery balloon counterpulsation for treatment of intraoperative right ventricular failure. *Ann Thorac Surg* 1985;39:437.
125. Letsou GV, Franco KL, Detmer W, et al. Pulmonary artery balloon counterpulsation: safe after peripheral placement. *Ann Thorac Surg* 1993;55:741.
126. Overlie PA, Walter PD, Hurd HP II, et al. Emergency cardiopulmonary support with circulatory support devices. *Cardiology* 1994;84:231.
127. Stack RK, Pavlides GS, Miller R, et al. Hemodynamic and metabolic effect of venoarterial cardiopulmonary support in coronary artery disease. *Am J Cardiol* 1991;67:1344.
128. Pavlides GS, Hauser AM, Stack RK, et al. Effect of peripheral cardiopulmonary bypass on left ventricular size, afterload and myocardial function during elective supported coronary angioplasty. *J Am Coll Cardiol* 1991;18:499.
129. Shawl FA, Domanski MJ, Hernandez TJ, et al. Emergency percutaneous cardiopulmonary bypass with cardiogenic shock from acute myocardial infarction. *Am J Cardiol* 1989;64:967.
130. Shawl FA, Domanski MJ, Wish MH, et al. Emergency cardiopulmonary bypass support in patients with cardiac arrest in the catheterization laboratory. *Cathet Cardiovasc Diagn* 1990;19:8.
131. Hill JG, Bruhn PS, Cohen SE, et al. Emergent applications of cardiopulmonary support: a multiinstitutional experience. *Ann Thorac Surg* 1992;54:699.
132. Dembitsky WP, Moreno-Cabral J, Adamson RM, et al. Emergency resuscitation using portable extracorporeal membrane oxygenation. *Ann Thorac Surg* 1993;55:304.
133. Overlie PA. Emergency use of cardiopulmonary bypass. *J Interv Cardiol* 1995;8:239.
134. Grambow DW, Deeb GM, Pavlides GS, et al. Emergent cardiopulmonary bypass in patients having cardiovascular collapse in the cardiac catheterization laboratory. *Am J Cardiol* 1994;73:872.
135. Overlie PA, Walter PD, Hurd HP, et al. Emergency cardiopulmonary support with circulatory support devices. *Cardiology* 1994;84:231.
136. Shawl FA, Quyyumi AA, Bajaj S, et al. Percutaneous cardiopulmonary bypass-supported coronary angioplasty in patients with unstable angina pectoris or myocardial infarction and a left ventricular ejection fraction less than or equal to 25%. *Am J Cardiol* 1996;77:14.
137. Vogel RA, Shawl FA, Tommaso CL, et al. Initial report of the National Registry of Elective Cardiopulmonary Bypass Supported Coronary Angioplasty. *J Am Coll Cardiol* 1990;15:22.
138. Ohteki H, Norita H, Sakai M, et al. Emergency pulmonary embolectomy with percutaneous cardiopulmonary bypass. *Ann Throac Surg* 1997;63:1584.
139. Pavlides GS, Sieszkowski J, Timmis GC, et al. Successful resuscitation of a patient with critical aortic stenosis and cardiac arrest by peripherial cardiopulmonary support system. *Cathet Cardiovasc Diagn* 1990;20:120.
140. Scholz KH, Figulla HR, Schweda F, et al. Mechanical left ventricular unloading during high risk coronary angioplasty: first use of a new percutaneous transvalvular left ventricular assist device. *Cathet Cardiovasc Diagn* 1994;31:61.
141. Scholz KH, Dubois-Rande JL, Urban P, et al. Clinical experience with percutaneous hemopump during high-risk coronary angioplasty. *Am J Cardiol* 1998;82:1107.
142. Wampler RK, Baker BA, Wright WM. Circulatory support of cardiac interventional procedures with the Hemopump cardiac assist system. *Cardiology* 1994;84:194.
143. Smalling RW, Cassidy DB, Barrett R, et al. Improved regional myocardial blood flow, left ventricular unloading, and infarct salvage using an axial flow, transvalvular left ventricular assist device: a comparison with intra-aortic balloon counterpulsation and reperfusion alone in a canine infarction model. *Circulation* 1992;85:1152.
144. Wampler RK, Frazier OH, Lansing AM, et al. Treatment of cardiogenic shock with the Hemopump left ventricular assist device. *Ann Thorac Surg* 1991;52:506.
145. Smalling RW, Sweeney M, Lachterman B, et al. Transvalvular left ventricular assistance in cardiogenic shock secondary to acute myocardial infarction: evidence for recovery from near fatal myocardial stunning. *J Am Coll Cardiol* 1994;23:637.
146. Meyns B, Nishimura Y, Racz R, et al. Organ perfusion with Hemopump device assistance with and without intraaortic balloon pumping. *J Thorac Cardiovasc Surg* 1997;114:243.

22
Implantable Devices for the Treatment of Cardiac Arrhythmia

Timothy W. Smith, Jane Chen, and Laurence M. Epstein

TWS: Boston Medical Center, Boston University School of Medicine, Boston, Massachusetts 02118
JC: Beth Israel Deaconess Medical Center, Boston, Massachusetts 02215
LME: Brigham and Women's Hospital, Harvard University School of Medicine, Boston, Massachusetts 02115

The availability of catheter techniques for recording intracardiac electrograms and ablating portions of the myocardium and specialized conducting tissue to modify or terminate cardiac arrhythmia has led to the development of a specialized field of catheterization known as electrophysiology. Although this field was reviewed in previous editions of *Cardiac Catheterization, Angiography, and Intervention,* it has become too complex and specialized for review here. The reader seeking more information about electrophysiology is referred to one of the specialized textbooks in this area (1,2 and 3). One area that has been retained, however, concerns the implantation of "devices" for control of the cardiac rhythm. Pacemakers may be implanted in the cardiac catheterization laboratory by cardiologists who perform other invasive procedures and who may have undergone some additional electrophysiologic training. Because of the complexity of programming and testing, implantable cardioverter defibrillators (ICDs) should be implanted only by full-time electrophysiologists.

With increasing sophistication and miniaturization, implanted devices that can monitor and diagnose the cardiac rhythm, pace the atrium or ventricle, and/or deliver a countershock have become first-line (and potentially life-saving) therapy for many arrhythmic disorders. Both pacemakers and ICDs are now small enough to be implanted in the pectoral region through a small incision. In addition to their clear therapeutic potential, the ability of these devices to record, store, and transmit data has made them powerful diagnostic tools.

DEVICES FOR THE TREATMENT OF BRADYCARDIA: PACEMAKERS

The first electronic pacemaker was a transcutaneous device developed by Zoll in 1952 for the treatment of life-threatening bradycardia (4). With miniaturization of the pulse generator and direct myocardial leads, implantation of the first *internal* pacemaker was performed in 1958 (5). Compared with these early fixed-rate devices, modern pacemakers have highly sophisticated microprocessors to apply diagnostic and therapeutic algorithms that have dramatically increased their versatility. The relative ease and low risk of implantation make them an attractive choice of therapy in a variety of bradyarrhythmic conditions.

The American College of Cardiology/American Heart Association Task Force on Practice Guidelines, Committee on Pacemaker Implantation periodically publishes guidelines for the implantation of pacemakers (6). The guidelines also address implantable cardioverter-defibrillators (ICDs) and the use of pacing to terminate tachyarrhythmias (discussed in another section).

Temporary Pacing

Indications

Temporary pacing is indicated in any patient with profound bradycardia and hemodynamic compromise and occasionally for prophylaxis when the risk of such an occurrence is high.

The ACC/AHA Task Force on Practice Guidelines (Committee on Management of Acute Myocardial Infarction) has published guidelines for temporary pacing in the setting of acute myocardial infarction (MI) (7). They are summarized in Table 22.1. In inferior infarction, atrioventricular (AV) block usually occurs in the AV node and is second degree, type I. It usually is transient, though it may last for several days. If third-degree AV block occurs, it usually develops after progressing from prolonged AV conduction (first-degree AV block) and then second-degree AV block. Because of hemodynamically effective escape rhythms originating below the AV node, this type of heart block is often asymptomatic and resolves within a week or less (8). In anterior infarctions, on the other hand, AV block usually occurs below the AV node, may be quite sudden in onset, and often lacks an effective escape rhythm resulting in cardiovascular collapse. Moreover, heart block in anterior infarction is usually a sign of extensive infarction and carries a poor prognosis (9).

Class I	Class IIa	Class IIb	Class III
Asystole	RBBB and LAFB or LPFB (new or of indeterminate age)	Bifascicular block of indeterminate age	Prolonged AV conduction
Symptomatic bradycardia (including sinus bradycardia and type I second-degree AV block with hypotension not responsive to atropine)	RBBB with prolongation of AV conduction	New or age-indeterminate isolated RBBB	Mobitz type I second-degree AV block with normal hemodynamics
Bilateral BBB (alternating BBB or RBBB with abnormality LAFB and LPFB) new or of indeterminate age	LBBB, new or of indeterminate age		Accelerated idioventricular rhythm
New or indeterminate-age bifascicular block (RBBB with LAFB or LPFB, or LBBB) with PR interval prolongation	Incessant VT, for atrial or ventricular overdrive pacing		BBB or fascicular block known to exist before acute MI
Mobitz type II second-degree AV block	Recurrent sinus pauses, greater than 3 seconds, not responsive to atropine		

AV, atrioventricular; BBB, bundle branch block; LAFB, left anterior fascicular block; LBBB, left bundle branch block; LPFB, left posterior fascicular block; MI, myocardial infarction; RBBB, right bundle branch block; VT, ventricular tachycardia.

TABLE 22.1. *Indications for temporary pacemaker placement in acute myocardial infarction*

A temporary pacemaker may be placed prophylactically during right heart catheterization in the patient with preexisting left bundle branch block, where catheter contact with the right bundle branch may produce complete heart block. Although less common, the same outcome may develop when left heart catheterization is

performed in a patient with preexisting right bundle branch block (see Chapter 3).

Other indications for temporary pacemaker placement include the prevention of pause- or bradycardia-dependent tachycardias, or the pace termination of tachyarrhythmias.

Venous Access

Temporary pacemakers can be inserted using any of the right heart catheterization sites discussed in Chapter 4. Careful selection of the access site is indicated, based on the advantages and disadvantages shown in Table 22.2. The femoral site is frequently used in the electrophysiology laboratory or catheterization laboratory, since the need for the temporary pacemaker is usually short-term, sterile technique is easily observed, the patient remains essentially immobile, and fluoroscopy is readily available. In the intensive care unit, however, the internal jugular and subclavian veins are used more commonly, for ease of placement, stability, and longer dwell time without thrombosis or infection. On the other hand, use of a vein that will be needed for a subsequent *permanent* pacemaker should be avoided (most often the left subclavian vein). Another option is one of the antecubital veins, particularly the basilic vein (the more medial of the antecubital veins), which takes a more direct course to the central vasculature than the cephalic (the more lateral antecubital vein) (see Chapter 5). Antecubital access reduces the risk of bleeding in patients who are anticoagulated or have received thrombolytic therapy, but the patient must keep the arm nearly immobile to minimize the risk of perforation or dislodgment.

Site	Advantages	Disadvantages
Femoral vein	Easy access	Leg must remain immobilized High infection risk Fluoroscopy required for pacer placement Patient must lie flat
Internal jugular vein	Good site for pacer placement (right better than left)	Risk of pneumothorax, inadvertent carotid artery puncture Patient must lie flat for access; Trendelenberg position preferred to avoid air embolism
Subclavian vein	Good site for pacer placement (left better than right)	Risk of pneumothorax, hemothorax with inadvertent subclavian artery puncture Patient must lie flat for access; Trendelenberg position preferred to avoid air embolism
Antecubital vein (Basilic, median basilic, or cephalic)	Access is low risk	Risk of dislodgment; arm must remain immobilized
	Good site for pacer placement (left better than right)	Basilic or median basilic preferred (cephalic has tortuous course to central veins)
		Fluoroscopy required for pacer placement

TABLE 22.2. *Advantages and disadvantages of venous access sites for temporary pacing catheter insertion*

Lead Placement

Fluoroscopy is invaluable to guide a standard bipolar pacing catheter into the right ventricular apex, and its use is recommended for temporary lead placement whenever possible. Care must be taken to avoid excess forward pressure on the catheter, which may lead to perforation, especially in the setting of inferior MI with right ventricular involvement. The best location for the catheter tip is along the inferior or septal surface of the right ventricle, about two-thirds of the way toward the apex. Free wall or outflow tract placements carry more risk of dislodgment, perforation, or ectopy, and should be avoided. Once placed in a suitable anatomic location, the capture threshold of the lead should be determined. Good placement should have a threshold of less than 1 mA; if the threshold is higher, consideration should be given to repositioning the lead. The integrity of all the components and connections of the system should be ensured to avoid repeated manipulation of the lead in an attempt to improve capture when the fault is in a connector wire. After adequate pacing has been ensured, the lead and sheath should be secured as well as possible with suture to prevent dislodgment.

If fluoroscopy is not available, placement of a pacing catheter from the femoral or antecubital veins should be avoided. Instead a balloon-tipped catheter pacing lead can be placed via internal jugular or subclavian vein access. The distal tip electrode is connected to the precordial (V) lead of an ECG to allow monitoring of the (unipolar) electrogram as the catheter is advanced (Fig. 22.1). When the distal tip of the catheter is in the atrium, there will be a large atrial electrogram (P wave) with a smaller ventricular electrogram (QRS). When the catheter tip enters the ventricle, however, the ventricular electrogram will grow larger than the atrial electrogram. When the catheter tip touches the endocardium, a current of injury can be recorded, and the catheter should be advanced no further. Alternatively, the electrodes can be connected to the temporary pacemaker pulse generator, which is then activated. As the catheter is advanced into the ventricle, paced QRS complexes appear when contact is made with the endocardium. This may be particularly helpful in the setting of severe bradycardia or asystole, where observing spontaneous electrical activity may be difficult.

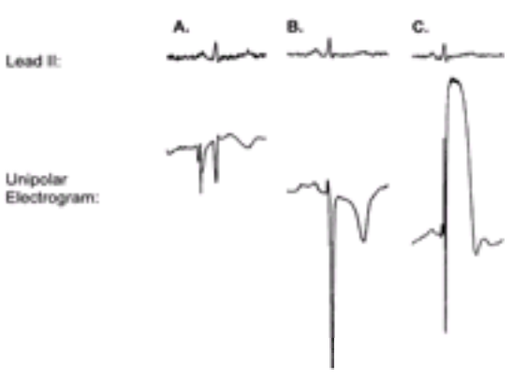

FIG. 22.1. Unipolar electrograms recorded during placement of temporary pacing catheter by clipping lead V_1 to the distal electrode of the catheter. The catheter is being placed via a right internal jugular vein introducer. Lead II is also shown. **A:** The catheter tip is in the right atrium. The P wave is as large as the QRS complex. **B:** The catheter tip is in the right ventricle. The amplitude of the QRS complex is markedly increased, and the P-wave amplitude has decreased. **C:** The catheter tip is in contact with the right ventricular endocardium. The massive ST segment elevation represents a current of injury.

A 12-lead ECG of the paced complexes should always be examined to ensure correlation with presumed position of the catheter. Pacing from the typical right ventricular apical position should produce a wide left bundle branch block/superior axis pattern. Pacing from the left ventricle (via a septal defect, for example), in the cardiac veins, or in the pericardial space will yield a different QRS morphology.

Temporary AV Sequential Pacing

Occasionally, patients who need temporary pacing may benefit from preserving AV synchrony, particularly in the setting of right ventricular infarction with heart block (10,11). If the only conduction system abnormality is sinus node dysfunction, this may be achieved by atrial pacing alone. If there is concurrent AV node dysfunction, however, maintaining an optimal AV temporal relationship requires placement of both atrial and ventricular pacing catheters. Unfortunately, stable atrial lead positioning is difficult with a passive fixation electrode. Options include the use of a temporary active fixation lead or placement of the catheter in the coronary sinus to allow left atrial pacing. Capture thresholds in coronary sinus pacing are typically higher than those seen pacing a catheter in direct contact with the endocardium.

After placement of the temporary pacemaker is completed, a chest x-ray is indicated to document placement of the lead. Pneumothorax must also be excluded after internal jugular or subclavian vein puncture. The duration of temporary pacing should be minimized (usually < 72 hours) to reduce risks of infection, dislodgment, and perforation. Although in place, the capture threshold of temporary pacemakers should be checked at least twice a day to avoid sudden, unexpected loss of capture. When checking thresholds, the rate of pacing should be gradually reduced to allow for the emergence of an escape rhythm.

Permanent Pacemaker Implantation

The guidelines for placement of permanent pacemakers are summarized in Table 22.3, Table 22.4, Table 22.5, Table 22.6, Table 22.7, Table 22.8, Table 22.9, Table 22.10 and Table 22.11. The guidelines are best understood by considering what benefit may be afforded the patient by implantation of a permanent pacemaker.

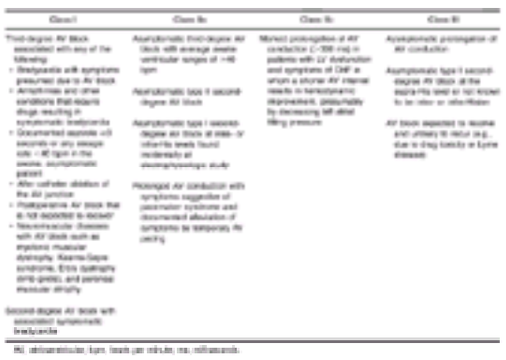

TABLE 22.3. *Indications for permanent pacing in acquired atrioventricular block in adults*

Class I	Class IIa	Class IIb	Class III
Intermittent third-degree AV block	Syncope not proved to be due to AV block when other likely causes have been excluded, specifically ventricular tachycardia	None	Fascicular block without AV block or symptoms
Type II second-degree AV block	Incidental finding of electrophysiologic study of HV interval ≥100 ms in the asymptomatic patient Incidental finding of electrophysiologic study of pacing-induced infra-His block that is not physiologic		

AV, atrioventricular; ms, milliseconds.

TABLE 22.4. *Indications for permament pacing in chronic bifascicular and trifascicular block*

Class I	Class IIa	Class IIb	Class III
Persistent second-degree AV block in the His-Purkinje system with bilateral BBB or third-degree AV block within or below the His-Purkinje system Transient advanced (second- or third-degree) infranodal AV block and associated BBB. If site of block is uncertain, electrophysiologic study may be necessary Persistent and symptomatic second- or third-degree AV block	None	Persistent second- or third-degree AV block at the AV node level	Transient AV block in the absence of intraventricular conduction defects Transient AV block in the presence of isolated left anterior fascicular block Acquired left anterior fascicular block in the absence of AV block Persistent AV conduction prolongation in the presence of BBB that is old or age indeterminate

Abbreviations: AV, atrioventricular; BBB, bundle branch block.

TABLE 22.5. *Indications for permanent pacing in atrioventricular block after the acute phase of myocardial infarction*

Class I	Class IIa	Class IIb	Class III
Sinus node dysfunction with documented symptomatic bradycardia, including frequent sinus pauses that produce symptoms. In some patients, bradycardia is iatrogenic and will occur as a consequence of essential long-term drug therapy of a type and dose for which there are no acceptable alternatives Symptomatic chronotropic incompetence	Sinus node dysfunction occurring spontaneously or as a result of necessary drug therapy, with heart rate <40 bpm when a clear association between significant symptoms consistent with bradycardia and the actual presence of bradycardia has not been documented	In the minimally symptomatic patient with chronic heart rate <30 bpm while awake	Sinus node dysfunction in the asymptomatic patient, including those in whom sinus bradycardia (<40 bpm) is a consequence of drug therapy Sinus node dysfunction in patients with symptoms suggestive of bradycardia that are clearly documented as not associated with a slow heart rate Sinus node dysfunction with symptomatic bradycardia due to nonessential drug therapy

Abbreviations: bpm, beats per minute.

TABLE 22.6. *Indications for permanent pacing in sinus node dysfunction*

Class I	Class IIa	Class IIb	Class III
Sustained, pause-dependent VT, with or without prolonged QT interval, in which the efficacy of pacing is thoroughly documented	Congenital long QT syndrome in the patient at high risk for tachyarrhythmia	AF-resistant or AV nodal-resistant tachycardia not responsive to medical or ablative therapy Prevention of symptomatic, drug-refractory, recurrent atrial fibrillation	Frequent or complex ventricular ectopic activity without sustained VT in the absence of the long QT syndrome Long QT syndrome due to reversible causes

Abbreviations: AF, atrioventricular; VT, ventricular tachycardia.

TABLE 22.7. *Indications for permanent pacing to prevent tachyarrhythmias*

Class I	Class IIa	Class IIb	Class III
Recurrent syncope caused by carotid sinus stimulation; minimal carotid sinus pressure induces ventricular asystole of >3 seconds duration in the absence of medication that depresses the sinus node or AV conduction	Recurrent syncope without clear, provocative events and with a hypersensitive cardioinhibitory response	Neurally mediated syncope with significant bradycardia reproduced by head-up tilt with or without isoproterenol or other provocative maneuvers	Hyperactive cardioinhibitory response to carotid sinus stimulation in the absence of symptoms
	Syncope of unexplained origin when major abnormalities of the sinus node or AV conduction are discovered or provoked at electrophysiologic study		Hyperactive cardioinhibitory response to carotid sinus stimulation in the presence of vague symptoms, such as dizziness and/or lightheadedness Recurrent syncope, lightheadedness, or dizziness in the absence of a hyperactive cardioinhibitory response Situational vasovagal syncope in which avoidance behavior is effective

Abbreviations: AV, atrioventricular.

TABLE 22.8. *Indications for permanent pacing in hypersensitive carotid sinus syndrome and neurally mediated sycope*

Class I	Class IIa	Class IIb	Class III
[illegible]	[illegible]	[illegible]	[illegible]
[illegible]	[illegible]	[illegible]	[illegible]
[illegible]	[illegible]	[illegible]	[illegible]
[illegible]	[illegible]		
[illegible]			

Abbreviations: AV, atrioventricular; bpm, beats per minute.

TABLE 22.9. *Indications for pacing in children and adolescents*

Class I	Class IIa	Class IIb	Class III
Class I indications for sinus node dysfunction or AV block as described in previous tables	None	Medically refractory symptomatic hypertrophic cardiomyopathy with significant resting or provoked LV outflow tract obstruction Symptomatic, drug-refractory dilated cardiomyopathy with prolonged PR interval when acute hemodynamic studies have demonstrated hemodynamic benefit of pacing	Hypertrophic cardiomyopathy in the patient who is asymptomatic or medically controlled Hypertrophic cardiomyopathy in the symptomatic patient without evidence of LV outflow obstruction Asymptomatic dilated cardiomyopathy Symptomatic dilated cardiomyopathy when patients are rendered asymptomatic by drug therapy Symptomatic ischemic cardiomyopathy

Abbreviations: AV, atrioventricular; LV, left ventricular.

TABLE 22.10. *Indications for permanent pacing in hypertrophic cardiomyopathy and dilated cardiomyopathy*

Class I	Class IIa	Class IIb	Class III
Symptomatic bradyarrhythmias/ chronotropic incompetence not expected to resolve and other class I indications	None	Symptomatic bradyarrhythmias/ chronotropic incompetence that, although transient, may persist for months and require intervention	Asymptomatic bradyarrhythmias after cardiac transplantation

TABLE 22.11. *Indications for permanent pacing after cardiac transplantation*

When the underlying bradyarrhythmia is chronic or recurring, the most appropriate therapy will often be a permanent pacemaker. However, indication for pacemaker implantation is not simply the presence of bradycardia. Like any medical or surgical therapy, implantation of a permanent pacemaker should offer either or both of the following:

1. Alleviation of symptoms
2. Prevention of future morbidity or mortality

Some of the indications are discussed later.

Alleviation of Symptoms

Symptomatic bradycardia is a general term that encompasses several disorders of the sinus node and the atrioventricular (AV) node. The symptoms of bradycardia are caused by poor organ perfusion in the setting of inadequate cardiac output. They include fatigue, lightheadedness or dizziness, and frank syncope. Bradycardia may also exacerbate myocardial ischemia, causing angina or precipitating congestive heart failure.

Sinus node dysfunction is addressed in Table 22.6 and is one of the most common causes of profound symptomatic bradycardia. The sick sinus syndrome, in which the sinus node fails to generate an adequate heart rate, is an example. In the tachy-brady variant of sick sinus syndrome, profound bradycardia or long pauses usually occur after the termination of a paroxysm of tachycardia (such as atrial fibrillation or atrial tachycardia), due to a prolonged recovery time of adequate sinus node function. This may result in severe lightheadedness or syncope at the time of conversion from the rapid rhythm. Other syndromes include “chronotropic incompetence,” in which an adequate heart rate at rest fails to elevate with exertion or physiologic stress, often leading to decreased exercise tolerance and dyspnea on exertion. This may be due either to dysfunction of the sinus node or to dysfunction of the autonomic nervous system. Inadequacy of the chronotropic response should be confirmed after discontinuation of any unnecessary bradycardic drugs (beta- or calcium channel blockers, for example) prior to implantation of a pacemaker.

Sinus bradycardia itself is rarely an indication for pacing in the absence of symptoms. Highly trained athletes often have baseline heart rates in the 40s or even 30s. Less highly trained individuals may have similarly low heart rates during times of high vagal activity, particularly while sleeping. Before deciding on pacemaker implantation, the bradycardia should be shown to be associated with symptoms. Ambulatory monitoring, especially patient-triggered “cardiac event” monitoring is a

useful tool in this regard. The patient whose episodic bradycardia does not correlate with symptoms does not have a clear indication for a pacemaker.

Disorders of AV conduction frequently cause symptoms and are shown in Table 22.3. Prolongation of the AV conduction time is rarely symptomatic but may be so if the PR interval becomes so long that atrial activation occurs during ventricular systole, with the atria contracting against closed AV valves. Patients often feel this as an uncomfortable throbbing in the neck or head. This situation is closely related to “pacemaker syndrome,” which occurs when ventricular pacing is not synchronized to atrial contraction or there is retrograde (ventricular–atrial) conduction that causes the atria to contract against closed AV valves (12,13). Occasionally, patients develop symptoms when proper timing of atrial and ventricular contraction is disturbed, and loss of the atrial contribution to ventricular filling reduces cardiac output. Second- or third-degree AV block may also cause symptoms, depending on the rate of the infranodal escape mechanism. Higher degrees of heart block, even when asymptomatic, may be indications for pacing to reduce morbidity and mortality (see later discussion).

Prevention of Morbidity and Mortality

Some conditions may produce no immediate symptoms but herald the possibility of severe events.

Type II second-degree AV block and third-degree AV block are usually caused by disease in the His-Purkinje system, and type II second-degree AV block may progress unpredictably to third-degree block (14). Since third-degree AV block is likely to have an unreliable ventricular escape mechanism, there is a risk of profound bradycardia as well as pause-dependent tachyarrhythmias. Therefore type II second- and third-degree heart block, even in the absence of symptomatic bradycardia, is considered an indication for pacing (Table 22.3). On the other hand, type I second-degree (Wenckebach) AV block usually occurs in the AV node, does not progress to higher-degree AV block, and is therefore not considered an indication for pacing in the absence of symptoms.

Table 22.4 shows indications for pacing as related to the manifestations of a diseased His-Purkinje system on ECG. Block of a single fascicle without symptoms should not be considered an indication for pacemaker implantation. Bifascicular and trifascicular block refers to evidence of impairment of two or three of the three fascicles below the His bundle. There may not be complete conduction block in all three fascicles at all times (equivalent to third-degree AV block), but there may be conduction delay or intermittent block. Chronic bifascicular block progresses only slowly to third-degree AV block and is not usually an indication for permanent pacing unless it is accompanied by additional evidence of compromise (a markedly prolonged His-to-Ventricle (HV) interval, abnormal infra-His block during electrophysiology study, or syncope likely to be due to intermittent third-degree AV block; that is, it cannot be attributed to any ther cause).

The need for permanent pacing after acute MI is related to the site of the MI, its extent, and the type of block. The need for temporary pacing during the acute phase of a MI is not in itself an indication for permanent pacing (Table 22.5) (6,7). This is particularly true in inferior MI, where AV block is more likely to be related to intranodal block and is usually transient, lasting a few days (15,16,17 and 18). In anterior MI, AV block is usually related to damage to the conduction system in the setting of a large infarct. The AV block is a marker for the extent of infarct and is rarely a cause of death in itself (19).

Permanent pacing may also be indicated to prevent the morbidity caused by pause-dependent tachyarrhythmias (Table 22.7) (20,21). Pacing at rates faster than the intrinsic sinus rate shortens the action potential duration and reduces after-depolarizations, possibly decreasing the risk of arrhythmia induction (22,23).

Neurally Mediated Syncope

Neurally mediated syncope is a particularly difficult problem, since the symptoms may be the result of bradycardia or vasodilation. Such patients frequently have a cardioinhibitory component, and bradycardia is common (24). Since vasodilation is also a part of the syndrome, however, pacing may not prevent syncope. Pacemaker manufacturers have devised algorithms that attempt to avoid sudden decreases in the heart rate and overcome any vasodepressor activity by pacing at fast rates (see the following section entitled “ Hysteresis”). Carotid sinus hypersensitivity in patients with syncope is generally considered an indication for pacing (Table 22.8). Head-up tilt-table testing may also be helpful, but its use is severely limited by poor reproducibility and lack of sensitivity and specificity (25,26).

Other Indications and Potential Indications

Some novel indications, not always associated directly with bradycardia, have received recent attention.

One group of patients who may find symptomatic benefit from pacing in the absence of bradycardia is those with hypertrophic obstructive cardiomyopathy (HOCM). It is thought that the abnormal ventricular activation associated with right ventricular pacing may relieve outflow tract obstruction and increase cardiac output (27). Some trials have shown benefit of pacing in terms of both symptoms and reduction of outflow tract gradients. It is not clear whether these benefits related directly to altered ventricular contraction pattern with pacing or to the ability to use higher doses of negatively inotropic and/or chronotropic agents, or perhaps to placebo effect alone (28,29,30,31 and 32).

It has been suggested that AV synchronous pacing can benefit patients with dilated cardiomyopathy. Some of the benefit may result from minimizing mitral and tricuspid regurgitation, which may be seen in late diastole in the dilated heart, particularly if there is intraventricular conduction delay. Preliminary data have not been conclusive (33,34,35 and 36).

Some have suggested that atrial pacing may help prevent recurrence of atrial fibrillation; dual-site atrial pacing may be even more beneficial (37,38). At present, atrial pacing cannot be considered first-line therapy for prevention of recurrence of atrial fibrillation.

Pacemaker Systems and Function

Transvenous permanent pacemakers typically are made up of a pulse generator implanted in a subcutaneous or submuscular pocket connected to one or two leads whose distal tips are placed against the right atrial and/or ventricular wall. The pulse generator is set to sense and pace one or both of the chambers in any one of a variety of programmable modes.

Pacemaker function is described by a code established by the North American Society for Pacing and Electrophysiology (NASPE) and the British Pacing and Electrophysiology Group (BPEG). The pacer mode is identified by at least three letters signifying (in order): (a) the chamber paced, (b) the chamber sensed, and (c) the response to sensed events. Additional letters may be appended to signify: (d) programmability or rate modulation, and (e) antitachycardia functions. The entire code is shown in Table 22.12. The code is very useful in the discussion of the many potential pacing modalities that follow. Most pacing modes can be adequately identified using the first three positions of the code. Each of the typical single- and dual-chamber modes can exist with or without rate responsiveness (an “R” in the fourth position of the code), which is discussed later.

I Chamber(s) paced	II Chamber(s) sensed	III Response to sensing	IV Programmability, rate modulation	V Antitachyarrhythmia functions
O, none	O, none	O, none	O, none	O, none
A, atrium	A, atrium	T, triggered	P, simple programmable	P, pacing (antitachycardia)
V, ventricle	V, ventricle	I, inhibited	M, multiprogrammable	S, shock
D, dual (A & V)	D, dual (A & V)	D, dual (T & I)	C, communicating	D, dual (P & S)
*S, single	*S, single		R, rate modulation	

*S is used to designate pacemaker pulse generators for use as a single-chamber pacemaker (atrial or ventricular).

TABLE 22.12. *The NASPE/BPEG generic pacemaker code*

The Basics of Pacing

Reduced to the most essential level, pacemakers perform three basic functions: pacing, sensing, and timing, which are discussed in the following sections.

Pacing

If an electrical impulse is introduced by an electrode pair and depolarizes enough myocardium to initiate propagation of an activation wave front throughout the myocardium, the chamber can be said to have been *paced.* Sometimes the term *capture* is used to denote successful pacing. The minimum total energy required to pace successfully is the stimulation threshold.

The amplitude of the depolarization stimulus (in volts for constant voltage stimulation or in milliamps for constant current stimulation) that is required for capture varies with the duration of the stimulus (referred to as *pulse width,* in milliseconds). Minimizing the energy of the pacing impulse is important to minimize battery depletion, but a safety margin is always included to allow for inevitable variations in the stimulation threshold. In the stable situation, there should be either a threefold safety margin in pulse width or a twofold margin in amplitude. Some newer pacemakers can detect changes in capture threshold and modulate their output accordingly. This allows energy drainage to be minimized to prolong battery life.

Sensing

For a pacemaker to coordinate pacing with any intrinsic activity of the heart, there must be a means of sensing electrograms and differentiating the true electrogram of depolarization from extrinsic signals and the repolarization electrogram.

As the wave of depolarization approaches a recording electrode in contact with the endocardium, a deflection is recorded due to the potential difference between the recording electrode and the indifferent electrode. As the wave front passes under the recording electrode and proceeds away from it, a deflection in the opposite direction is recorded. The transition from the approaching to receding deflection is called the *intrinsic deflection.* The slope of the intrinsic deflection (the rate of change of potential, *dV/dt*) is called the *slew rate.* Lower-frequency deflections before and after the intrinsic deflection represent depolarization of surrounding myocardium. Finally, there is also a deflection as the wave of repolarization approaches and then passes by the recording electrode.

The pacemaker system has an amplifier to increase the signal from the recording electrode and a bandpass filter to remove signals with frequencies too high or low to be the intrinsic deflection. Whenever the amplitude of the filtered signal exceeds the sensing threshold (which may be programmed), the electrogram is “sensed” and the appropriate timing circuits of the pulse generator are reset.

Timing Cycles The pacemaker's timing circuits allow complicated interactions between sensed and paced events and, in dual-chamber pacemakers, between atrial and ventricular events. The nature of these interactions is determined by the programmed mode of the pacemaker, discussed later. The pacemaker's program makes use of a series of timers that are reset by specific sensed or paced events. The programmed mode of the pacemaker is the combination of timers and their reaction to sensed and paced events.

Cycle Lengths and Rates Intervals and cycle lengths are expressed in units of time, usually milliseconds (ms), with rates expressed in the inverse of time, such as beats per minute (bpm) or pulses per minute (ppm). For practical purposes, it is a simple matter arithmetically to convert between cycle length and rate. Rate in bpm or ppm can be found by dividing 60,000 by the cycle length in milliseconds; conversely, cycle length in milliseconds can be found by dividing 60,000 by the rate in beats per minute or pulses per minute.

Single-Chamber Pacing The timing cycles of single-chamber pacemakers are simpler and will be considered first. The simplest case is a single-chamber asynchronous mode (AOO or VOO). No intrinsic electrograms are sensed, and pacing stimuli are delivered regardless of any intrinsic activity. The only timer is that of the basic cycle length or *lower rate limit.* The timer is reset when the pacing stimulus is delivered. When the timer reaches its programmed time, another pacing stimulus is delivered, resetting the timer again. Asynchronous pacing like this is now only used in temporary situations in which the pacemaker may be inappropriately inhibited (e.g., by surgical electrocautery) or when sensing is unreliable (as in the case of lead dislodgment or lead fracture). VOO pacing is shown schematically in Fig. 22.2A.

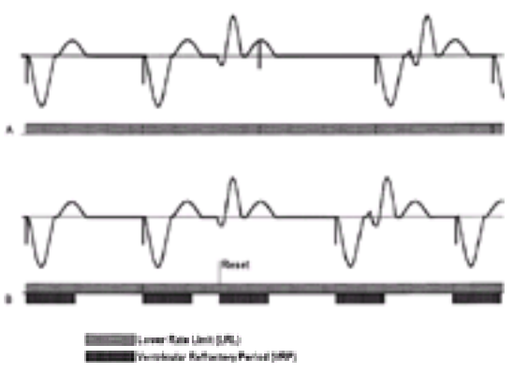

FIG. 22.2. Schematic representation of asynchronous (A) and inhibited (B) ventricular pacing. The bars indicate the duration of the indicated timing circuit. (For simplicity, no atrial activity is shown.) **A:** V00 pacing. Pacing stimuli occur when the lower rate limit timer completes its cycle and the timer is reset. There is no sensing of intrinsic electrical events; therefore the timer completes its cycle regardless of the native QRS complexes. **B:** VVI pacing. The lower rate limit and the ventricular refractory period timers are shown. The lower rate limit timer is reset by a pacing stimulus or by a sensed intrinsic event that does not fall within the refractory period. An intrinsic QRS that is detected within the refractory period does not reset the lower rate limit timer.

The so-called demand or inhibited modes (in which the pacing only occurs in the absence of intrinsic activity) require sensing of intrinsic events. The basic cycle length timer can now be reset by either a paced or a sensed event. However, it would be undesirable for the timer to be reset by an early premature beat, which may not generate an effective stroke volume. Therefore an additional timer is introduced, the ventricular (or atrial) *refractory period* (VRP or ARP). The refractory period also prevents inappropriate sensing of the repolarization wave as an electrogram (e.g., the T wave). During the refractory period, intrinsic events are not sensed and the lower rate limit timer is not reset. The refractory period occurs during the first part of the basic cycle, starting when an electrogram is sensed or when a pacing stimulus is delivered. VVI pacing is shown schematically in Fig. 22.2B.

Practically speaking, the only modes commonly used with single-chamber pacemakers are *AAI* and *VVI.* Rate responsiveness can be added in either case (AAIR or VVIR). In these inhibited modes, the pacer output is inhibited when it senses an impulse within the appropriate time period after the last paced or sensed event.

In *triggered* modes, a sensed event causes the delivery of a pacing stimulus. Triggered pacing is intended to prevent inappropriate (and possibly dangerous) inhibition by incorrectly sensed events, such as skeletal myopotentials. Though triggered pacing is now uncommonly used clinically, it may be used temporarily to assist in pacemaker interrogation to test sensing. In triggered mode, a pacing stimulus indicates that an electrogram has been sensed. As the sensitivity is decremented, disappearance of pacing artifacts indicates loss of sensing.

Dual-Chamber Pacing Dual-chamber pacing dramatically increases the complexity of the programming that is possible. Interaction of paced and sensed events in two chambers allows for multiple pacing modes and multiple possible responses to intrinsic cardiac activity. It follows therefore that the number and complexity of the timings circuits also increase.

DOO Mode In the *DOO mode* (asynchronous dual-chamber pacing), the atrium and ventricle are paced sequentially; no intrinsic electrical activity is sensed. Therefore pacing stimuli are delivered regardless of any intrinsic activity. The atrial and ventricular pacing stimuli are separated by the *AV interval* (AVI), which is

reset each time an atrial pacing stimulus is delivered.

Modes in which sensing of electrograms is necessary (for inhibition or triggering) require additional timing circuits to coordinate the paced and sensed events in the two chambers. First among these is the *blanking period,* which is a short period (usually less than 100 ms) starting at the delivery of a pacing stimulus in the opposite channel. That is, when an atrial stimulus occurs, the ventricular channel is “blanked” for several milliseconds, so that the leading edge of the pacing stimulus itself is not sensed inappropriately. Though the leading edge of the atrial pacing stimulus is not sensed due to the blanking period, the remainder of the pacing spike may be sensed. If this is the case, ventricular pacing is inhibited and inappropriate inhibition in this setting can be very dangerous in the pacemaker-dependent patient. This problem prompts the addition of another timer, the *cross-talk detection* window. The cross-talk detection window timer begins at the end of the blanking period and, like the blanking period, is a part of the AVI (see later).

Another important timer is the *postventricular atrial refractory* period, or PVARP. The PVARP begins when a ventricular event is sensed or a ventricular pacing stimulus is delivered. The atrial channel is refractory to sensed events during the PVARP. Its primary purpose is to prevent sensing of retrograde P waves and subsequent triggered pacing of the ventricle, which may initiate pacemaker-mediated tachycardia (see later discussion).

The *atrial escape interval* (AEI) is the time between a sensed or paced ventricular event and time at which the next atrial stimulus is delivered (if no atrial event is sensed). The AEI corresponds to the VA interval on a sinus rhythm ECG.

The *upper rate limit* (URL) or *maximum tracking rate* (MTR) is the maximum rate at which ventricular pacing will occur in response to sensed atrial events. The URL is programmable and may be set at a high rate in the vigorous patient who requires a relatively high heart rate during activity. The rate may be set lower in other patients who may not tolerate high rates, particularly if they are prone to atrial arrhythmias.

Atrial Versus Ventricular-Based Timing The timing of a dual-chamber pacemaker must be based on either the ventricular timing or atrial timing.

In ventricular-based timing, the VV interval is considered paramount and is not allowed to drop below the LRL interval. The VV interval is composed of AEI + AVI. This AEI is kept constant and equals the LRL – AVI. The consequence of this is that if the patient's AV node function is intact and the PR interval is less than the programmed AVI, the actual ventricular rate will be slightly faster than the programmed rate. That is: AEI + PR < AEI + AVI. Since the ventricular rate is most important, a sensed R wave always resets the entire basic cycle and therefore resets the AEI timer.

If the timing is atrial based, the AA interval is considered paramount and is held constant. In this case, rapid AV conduction does not change the AA interval. However, if the AV conduction is not rapid in the next cycle, the ventricular cycle length (which equals the VA interval [AA minus the previous PR] plus the AVI) may slightly exceed the lower rate limit cycle length. Since the AA interval remains fixed, the following VV cannot be longer than the basic cycle length. So though a single VV cycle can exceed the lower rate limit cycle length, the overall rate cannot drop significantly below the lower rate limit.

In most atrial-based timing systems, a ventricular premature complex resets the AA interval. The AA interval and the following AVI pass before the next ventricular pacing stimulus occurs, another situation in which the VV cycle length exceeds the lower rate limit cycle length. Some manufacturers have added further complexity by modifying these basic atrial-based and ventricular-based systems.

Complex Dual-Chamber Pacing Modes

Having discussed some of the details of timing cycles of dual-chamber pacing, we can proceed to discuss how these concepts are applied in several of the more commonly used dual-chamber modes.

In the *DDD mode* (fully physiologic dual-chamber pacing), the pacer senses both chambers and is inhibited by sensed events. If atrial activity faster than the programmed lower rate limit is sensed, the atrial stimulus in inhibited; if the atrial activity is not sensed within time period allowed by the lower rate limit, an atrial stimulus is produced. A ventricular stimulus is triggered (after an appropriate programmed AV delay) by sensed or paced atrial activity, but inhibited if the intrinsic ventricular activity is sensed before the end of the AV delay. In this sense, the DDD mode is a triggered mode as well and an inhibited mode, as the D (for *dual*) in the third position of the NASPE/BPEG code suggests.

DDD (with or without rate responsiveness) is the most commonly used mode in current dual-chamber pacemakers. It allows for physiologic AV synchrony whether the atrium is sensed or paced, and it allows for normal ventricular activation through the intrinsic conduction system if AV nodal conduction occurs. Ventricular pacing will “track” the sensed atrial rate (up to the upper rate limit), allowing the patient's intrinsic atrial rate to dictate the ventricular rate. It should be noted that in patients with AV node dysfunction but with normal sinus node function and chronotropic competence, DDD mode is more physiologic than DDDR, since the ventricular pacing rate is determined by the patient's intrinsic sinus rate alone. DDD pacing is shown schematically in Fig. 22.3.

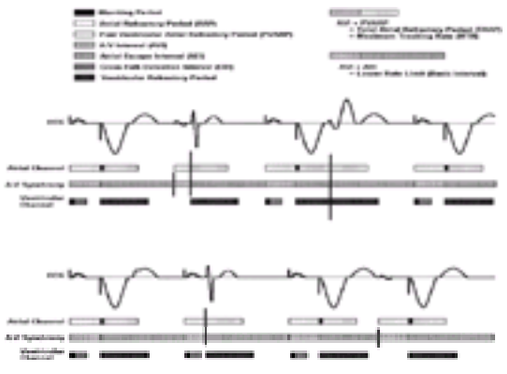

FIG. 22.3. Schematic representation of DDD pacing. Three sets of timers are shown: atrial timers, ventricular timers, and timers that coordinated AV synchrony. Resetting of a timer by sensed intrinsic events is shown by a heavy vertical line. In DDD mode, both the atrial and ventricular channels are inhibited by sensed intrinsic events. In addition, an atrial paced or sensed event triggers ventricular pacing after an appropriate AV delay, if no intrinsic R wave is sensed. An atrial pacing stimulus is delivered if the atrial escape interval timer expires before an intrinsic P wave is sensed. See text for discussion of refractory periods and blanking periods.

DDI mode (AV sequential, non-P-wave synchronous pacing) allows for physiologic AV synchrony on fully paced cycles. Pacing output is inhibited by intrinsic activity from either chamber. However, ventricular pacing is not triggered by sensed atrial activity. Therefore ventricular pacing does not track the atrial rate. Atrial rates faster than the lower rate limit inhibit atrial stimuli, but in the absence of sensed ventricular activity, ventricular pacing occurs at the lower rate limit, making for nonphysiologic AV dissociation. DDI may be used to prevent inappropriately fast ventricular pacing during paroxysms of atrial fibrillation or atrial tachycardia while allowing AV sequential pacing when the intrinsic rate is low. Pacemakers with *mode-switching* capability can automatically switch to DDI (or another mode that prevents atrial tracking, such as VVI) when the sensed atrial rate exceeds a programmed limit. The development of mode switching has decreased the need for the DDI mode.

DVI mode (AV sequential pacing) allows for pacing both the atrium and ventricle but cannot sense intrinsic atrial activity. A sensed R wave therefore inhibits atrial as well as ventricular pacing. However, atrial pacing is not inhibited by intrinsic atrial activity. The presence of both intrinsic and paced atrial activity (entirely unsynchronized) may induce atrial fibrillation or other atrial arrhythmias. DVI is now uncommonly used in permanent pacemakers. However, some dual-chamber temporary pulse generators do not sense atrial activity, so their mode is DVI.

VDD mode (P-wave synchronous pacing) can be used in the patient with good sinus node function and an intact chronotropic response. The ventricle is the only chamber paced. Ventricular pacing, after an appropriate AV delay, is triggered by sensed atrial activity but inhibited by sensed ventricular activity. If no atrial or ventricular activity is sensed within the time period appropriate for the lower rate limit, a ventricular stimulus occurs. VDD operates like DDD when the atrial rate is faster than the lower rate limit and like VVI when the atrial rate is lower than the lower rate limit. Like DDD, ventricular pacing will track the atrial rate (up to the

programmed upper rate limit). In dual-chamber/dual-lead systems, VDD pacing confers no significant advantage over DDD mode. However, single-lead VDD systems are available, avoiding the technical difficulty and risks of implanting a second lead. In addition to the ventricular bipolar electrodes, the lead has a more proximal electrode pair mounted more proximally on the lead for sensing the atrial activity.

Rate Responsiveness

The most commonly used parameter in the fourth and fifth positions of the NASPE/BPEG code is an “R” in the fourth position to indicate rate responsiveness. Many advanced pacemakers have this feature, in which the lower-paced rate increases in response to the patient's activity. Other parameters, such as the AVI, may also be adjusted to sensed activity.

Rate-responsive pacemakers must have a sensor of patient activity. Ideally, such a sensor would match the lower rate limit to the metabolic demands associated with increased patient activity, in the same way the normal sinus node does.

The most commonly used sensor is the motion sensor. This consists of a piezoelectric crystal mounted on the case of the pulse generator. Vibration of the crystal results in an electrical signal that can be used to estimate the intensity of the patient's activity (39). A similar activity sensor is the accelerometer. The accelerometer's piezoelectric crystal is isolated from the case of the pulse generator and is intended to detect patient motion in a single axis (e.g., in the anteroposterior direction) (40).

Another strategy to estimate metabolic demand is to sense minute ventilation. Minute ventilation can be estimated by measuring impedance across the thoracic cavity. The impedance is measured frequently (many times per second) by delivering a low-amplitude pulse between the tip of the lead and the pulse generator. Since the impedance increases as the chest expands, it is dependent on the respiratory rate and depth of respiration. These results can be used to estimate minute ventilation and thereby modulate that pacing rate (41,42).

Other sensor strategies are used less commonly and are still in development. These include central venous temperature (43,44), changes in the QT interval with autonomic activity (45,46), and mixed venous oxygen saturation (47,48).

It should be obvious that all these sensors are vulnerable to various artifacts and inaccuracies. Some newer pacemakers utilize a combination of sensor strategies (e.g., motion and minute ventilation) in an attempt to mimic physiologic rate response more accurately. However, rate responsiveness still cannot replace intact sinus node function with intact response to the autonomic nervous system.

Hysteresis

Some syncope syndromes, such as vasovagal syncope and carotid sinus hypersensitivity, are often characterized by precipitous decreases in heart rate. The patient may need rapid pacing at the times of the would-be syncopal episodes but may not need pacing at all at any other time. The hysteresis function was designed to address this problem. In typical programming, the pacemaker will pace when the intrinsic heart rate falls below the lower rate limit, at a rate equal to the lower rate limit. When hysteresis is programmed, pacing is initiated whenever the intrinsic heart rate falls below a programmed lower rate limit, but the pacing rate is faster than the lower rate limit. If the intrinsic rate has recovered (to a programmed rate), pacing ceases until the patient's rate again declines below the programmed minimum.

Some Common Problems and Solutions

Interactions between the patient's intrinsic activity and pacemaker output may make for results that are surprising to the uninitiated. Safety features have been built in to prevent many of these problems.

Pacemaker Syndrome

Most of the problems in this section are related to the complicated relationships between sensed and paced events. Pacemaker syndrome, in contrast, is most often a problem of single chamber ventricular pacemakers. The symptoms vary from patient to patient but may include fatigue, malaise, headache, a sensation of throbbing in the neck, and lightheadedness or syncope. The symptoms are thought to result from lack of physiologic AV synchrony (49,50). P waves occurring during ventricular systole result in atrial contraction against closed mitral and tricuspid valves and retrograde transmission of the pressure of atrial contraction (a cannon A wave). The symptoms are attributed to depressed cardiac output due to loss of “atrial kick” or to the elevated venous pressure associated with cannon A waves. In patients with intact retrograde AV nodal conduction, there may a retrograde P wave and a cannon A wave with every paced beat, and the symptoms can be debilitating.

The only solutions for pacemaker syndrome are reduction of the ventricular pacing lower rate limit so that pacing rarely occurs (if feasible), or upgrade to a dual-chamber pacemaker.

2:1 AV Block

When a dual-chamber pacemaker senses atrial activity and paces the ventricle (e.g., in the case of complete heart block with normal sinus node function), 2:1 AV block occurs at a predictable rate for a given set of programmed parameters. The 2:1 cycle length is equal to the total atrial refractory period (TARP); the TARP is equal to the AV interval plus the postventricular atrial refractory period (PVARP); that is,

$$\begin{aligned} \text{2:1 block cycle length} &= \text{TARP} \\ &= \text{AVI} + \text{PVARP} \end{aligned}$$

The implication of this formula is that an atrial event that is sensed before the expiration of total atrial refractory period will not be followed by a ventricular stimulus from the pacemaker. Therefore sinus tachycardia or an atrial tachycardia that occurs faster than this cycle length will result in lack of ventricular pacing after every second atrial event (Fig. 22.4). This 2:1 block may occur precipitously at the time that atrial rate exceeds the 2:1 block rate and is often quite symptomatic. For example, 2:1 block may occur suddenly with sinus tachycardia during exercise, causing the patient to experience a sudden halving of the ventricular rate. Many modern pacemakers have rate-smoothing algorithms that anticipate 2:1 block and change the pacing rate gradually to prevent sudden ventricular rate decreases.

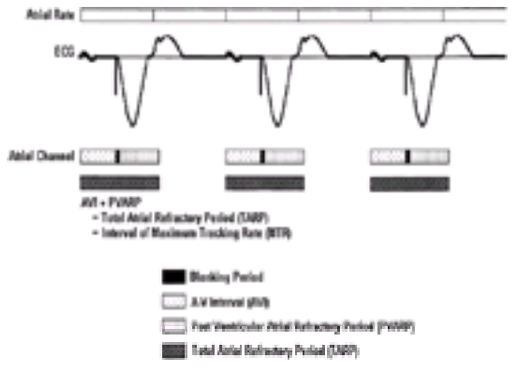

FIG. 22.4. Schematic representation of pacemaker 2:1 AV block in a patient with complete heart block. The pacemaker is in DDD mode. The atrial rate exceeds the maximum tracking rate (MTR). The MTR interval is equal to the total atrial refractory period (TARP), which in turn is equal to the sum of the AV interval (AVI) and the PVARP. When an intrinsic atrial event falls within the TARP, it does not trigger a ventricular pacing stimulus. The next P wave does trigger a ventricular stimulus and the cycle continues as long as the atrial rate exceeds the MTR.

Pacemaker Wenckebach

The 2:1 AV block rate is defined by the TARP. When the upper rate limit of the pacer is set below the 2:1 AV block rate, pacemaker Wenckebach may occur. When the patient's sinus rate exceeds the programmed upper rate limit, the pacemaker will pace the ventricle only as fast as the upper rate limit. The result is progressive prolongation of the AV delay until one of the sensed P waves occurs within the refractory period after the paced ventricular event. There is no ventricular pacing after this P wave, and the cycle repeats itself with the next sensed P wave. On the surface ECG, this strongly resembles typical AV Wenckebach block, except the QRS complexes are paced. The remedy for pacemaker Wenckebach, which may be symptomatic in the active patient, is an increase in the upper rate limit of ventricular pacing. If the 2:1 AV block rate is slower than the programmed upper rate limit, it serves as the effective upper rate limit because 2:1 AV block will occur before the programmed upper rate limit is reached.

Pacemaker-Mediated Tachycardia

Any tachycardia in which the pacemaker participates falls into the category of pacemaker-meditated tachycardia. The term usually refers to an *endless-loop tachycardia* in which the pacemaker AV sequential pacing serves as the antegrade limb of a reentrant tachycardia (51,52). The endless-loop tachycardia occurs when retrograde AV nodal conduction results in atrial activity that is sensed by the pacemaker and triggers ventricular output. If the patient's intrinsic retrograde conduction is consistent, this cycle will occur repeatedly until an intervention is performed (Fig. 22.5).

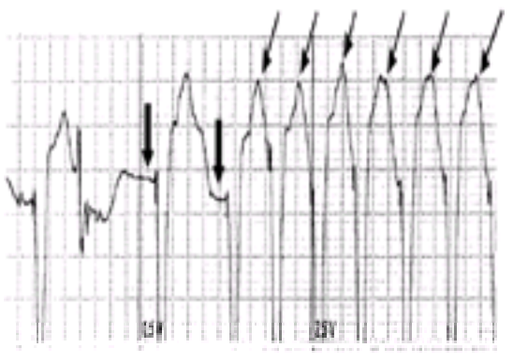

FIG. 22.5. Pacemaker-mediated tachycardia (PMT) or endless-loop tachycardia. During atrial threshold testing in DDD mode, atrial capture is lost when the atrial output is decreased *(heavy arrows)*. The occurrence of a retrograde P wave *(light arrow)* triggers ventricular pacing. PMT, repeated retrograde P waves with ventricular tracking, was thus initiated. Telemetry from the pacemaker confirmed that P waves were being sensed though they are obscured by the T wave in the ECG tracing. The PMT was terminated by temporarily extending the postventricular atrial refractory period (PVARP). Ventricular pacing is then not triggered by the P wave falling within the PVARP, and the cycle is broken. (Courtesy M. Daoust, RN, BIDMC Pacemaker Clinic.)

Treatment for endless-loop tachycardia is aimed at creating a block in one of the limbs of the reentrant circuit. The simplest approach is to place a magnet over the pulse generator. Magnet application trips a magnetic reed switch in the generator that changes the pacing mode to asynchronous (DOO) pacing. When the pacer stops sensing and tracking retrograde P waves, there is a block in the antegrade limb of the tachycardia circuit.

Prevention of endless-loop tachycardia requires reprogramming. Changing modes permanently prevents tracking of retrograde P waves, but sacrifices the advantages of DDD mode. Extension of the Post-Ventricular Atrial Refractory Period (PVARP) is usually effective, and DDD mode can still be used. However, the PVARP cannot be extended too far. As discussed earlier, increase of the PVARP reduces the rate at which 2:1 block occurs, which may be especially troublesome in patients with prolonged VA conduction. Most new pacemakers have “PMT intervention” designed to interrupt an endless-loop tachycardia. For example, a temporary prolongation of the PVARP may be programmed to occur after pacing at the upper rate limit occurs for a given period of time. The retrograde atrial activation that occurs within the prolonged PVARP is not sensed, and the tachycardia is terminated. Endless-loop tachycardia can be prevented by a temporary prolongation of the PVARP after sensation of intrinsic ventricular activity without preceding atrial activity (most likely a ventricular premature complex).

Cross-talk

Cross-talk refers to inappropriate sensing of the stimulus of one lead by the other lead. For example, in DDD mode, cross-talk can result in inhibition of ventricular pacing due to inappropriate sensing of the atrial stimulus artifact by the ventricular channel. In the patient dependent on ventricular pacing, cross-talk can be catastrophic. This may be a matter of incorrect sensitivity programming. However, another cause may be dislodgment of the atrial lead into the ventricle. *Safety pacing* is designed to prevent inappropriate inhibition of ventricular pacing by the sensed atrial stimulus artifact. If an electrogram is sensed by the ventricular lead within the cross-talk detection window, a ventricular stimulus is delivered. Safety pacing prevents inappropriate inhibition, but the source of inappropriate sensing must also be sought. Examination of a chest x-ray is important to ensure good lead positioning. If a lead has been dislodged, revision is necessary. If the leads are in good position, reprogramming of the ventricular sensitivity is required. Examples of safety pacing are shown schematically in Fig. 22.6.

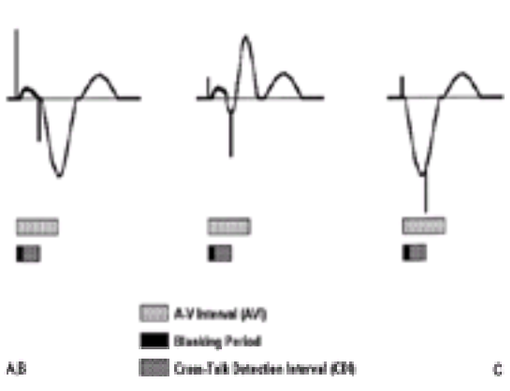

FIG. 22.6. Schematic representation of safety pacing. In each case the ventricular channel senses an event during the cross-talk detection interval (CDI), prompting delivery of a ventricular pacing stimulus at the end of the CDI. **A:** The decay of the atrial pacing stimulus is sensed by the ventricular channel after the expiration of the ventricular blanking period. Note the size of the atrial stimulus artifact. Safety pacing occurs and the resulting AV delay is shorter than the programmed AV delay. **B:** A ventricular premature complex occurs during the CDI, prompting safety pacing. **C:** The atrial lead has dislodged into the ventricle. The atrial pacing stimulus captures the ventricle. Ventricular activation is detected in the ventricular channel during the CDI, prompting safety pacing.

Tracking Atrial Tachyarrhythmias

In DDD mode, ventricular pacing is triggered by sensed atrial activity, and the ventricular rate “tracks” the atrial rate. If the atrial rhythm is abnormal, tracking the atrial rate may be inappropriate. The most prominent examples are atrial tachycardia and atrial fibrillation. If these were tracked without limit by ventricular pacing, ventricular rates could easily achieve dangerously high levels, particularly in atrial fibrillation. This eventuality is prevented by the existence of the maximum tracking rate. However, atrial tachycardias in which the atrial rate exceeds the maximum tracking rate will cause ventricular pacing at the maximum tracking rate.

The possibility of inappropriate tracking must be considered in patients prone to develop atrial fibrillation and atrial tachycardia. One option is not to use DDD mode. DDI allows dual-chamber pacing and prevents bradycardia but sacrifices the advantages of atrial tracking when the patient is in sinus rhythm. *Mode switching* was

developed to solve this problem. When a pacemaker with mode-switching programmed on senses an atrial rate exceeding a programmed mode-switch rate, the mode changes to a nontracking one, such as DDI or VVI. The pacer's mode-switching circuit continues to monitor the atrial rate. When the atrial arrhythmia is terminated, the mode is switched back to DDD.

Pacemaker Leads

Pacing, sensing, and timing are functions of the pacemaker pulse generator. Pacemaker leads provide the direct electrical connection between the pulse generator and the heart. Each lead consists of one or two exposed metal electrodes, which are placed in contact with the heart, connectors specifically designed to fit into the head of the pulse generator, and insulated wires connecting the connectors to the electrodes.

Pacemaker leads are either *unipolar* (meaning that a single electrode is incorporated into the lead [typically the cathode] and the other electrode [typically the anode] is incorporated into the casing of the pacemaker generator) or *bipolar* (meaning that the anode and cathode are both incorporated into the distal end of the lead). Uni- or bipolarity applies both to pacing and sensing. The potential difference created or sensed using bipolar lead occurs over a few millimeters, while the difference using a unipolar lead is over the chest, from the tip of the lead to the generator. For this reason, unipolar pacing spikes are much more prominent on surface ECG; the pacing artifact of bipolar leads is sometimes difficult to discern, occasionally providing a challenge for even the experienced ECG reader.

Some operators still prefer unipolar leads, which have a long track record and are usually of smaller caliber than bipolar leads. However, bipolar leads have now proven quite successful and have several advantages over unipolar leads:

- No sensing of skeletal muscle myopotentials, which may result in inappropriate inhibition of pacing.
- Less chance of “cross-talk” between the two leads of dual-chamber pacemakers.
- Less chance of interference with an ICD. ICDs should not be used in conjunction with unipolar pacing.
- Less chance of stimulating skeletal muscle.
- If necessary (e.g., in the event of lead damage), unipolar pacing is still possible if the pulse generator has unipolar pacing capability.

For these reasons we advocate the use of bipolar leads.

Leads are currently insulated with either silicone or polyurethane. Silicone has been used for many years with good results. The original polyurethane formulations (e.g., P80A) were subject to unacceptable levels of deterioration and fracture (53,54). Later formulations have resulted in improvements, making polyurethane a useful material. The P55D formulation currently in use has been quite successful over more than a decade of use. Choice of insulation is a matter of personal preference. Silicone leads tend to be more flexible, and many find the firmer polyurethane leads more manipulable. Silicone leads slide poorly against each other, though lubricant coatings have been applied to minimize this problem.

Placement of leads initiates an inflammatory reaction at the site of electrode contact with the myocardium. The inflammation in turn results in insulation of the myocardium from the electrode and an increase in pacing threshold (55,56 and 57). The threshold usually peaks 3 to 6 weeks after implantation. Over time, the inflammatory reaction diminishes and the capture threshold gradually decreases, reaching a stable “chronic” level after about 3 months (Fig. 22.7). Anticipation of the acute threshold rise should prompt programming high output at the time of implant to maintain a good safety margin as the threshold rises. In rare instances, the acute threshold rise can exceed the output of the pacemaker, a potentially dangerous situation in the pacemaker-dependent patient, possibly requiring placement of a temporary pacemaker. Systemic steroid therapy had been used to reduce the inflammatory response (58). Currently, the problem of acute threshold rise has largely been circumvented by the development of steroid eluting leads. The leads have a reservoir of steroid near the electrode that flows slowly through the porous electrode into the myocardium. Steroid-eluting leads reduce the magnitude of the inflammatory response and the acute rise in capture threshold (Fig. 22.7) (59,60 and 61).

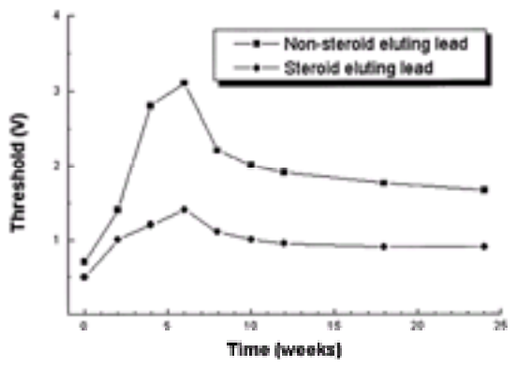

FIG. 22.7. Typical time course of capture threshold changes for two hypothetical ventricular leads. The threshold amplitude at a fixed pulse width of 0.5 ms rises sharply in the first few weeks after implantation, then declines to a level that is greater than the threshold at original implantation. The effect is markedly attenuated in steroid-eluting leads.

All currently used leads have some form of fixation mechanism, passive or active. Passive fixation mechanisms include tines, talons, and fins, designed to become entrapped in trebeculations in the heart to provide stability of positioning. Active fixation devices are designed to penetrate the myocardium and remain embedded in it. Most of these are helical screws, which are twisted into the myocardium. Passive fixation leads work well in the right ventricular apex and right atrial appendage, which are trebeculated. Active fixation leads allow greater versatility in choice of implantation sites and reduce the risk of dislodgment of the atrial lead. Active fixation leads generate a more exuberant inflammatory response; both acute and chronic pacing thresholds are higher than those of passive fixation electrodes.

DEVICES FOR THE TREATMENT OF TACHYCARDIAS: IMPLANTABLE CARDIOVERTER-DEFIBRILLATORS (ICDS)

Sudden cardiac death (SCD) affects approximately 450,000 people per year in the United States, and at least 1 million people per year develop conditions that place them at risk for SCD in the future. Survivors of one SCD episode have a recurrence rate of approximately 30% to 50% within 2 years, with malignant ventricular arrhythmias most often responsible. Options for treatment of these arrhythmias now include antiarrhythmic agents, catheter-based or surgical ablation, and implantation of implantable cardioverter defibrillators (ICD). This section of the chapter will focus on the indications for ICDs, description of the defibrillator system and device function, and follow-up of patients with ICDs.

The development of the ICD is primarily the result of pioneering work by Michel Mirowski. The first human implant was performed on February 4, 1980, and the first device was approved by the Food and Drug Administration (FDA) in 1985. Early, retrospective studies had established that ICDs can effectively detect and terminate ventricular arrhythmias and suggested that they improved survival (62,63 and 64). Subsequently, several randomized trials have attempted to define which patients benefit from ICD therapy.

Indications for ICD Therapy

Secondary Prevention

The most common indication for implantation of ICDs remains the secondary prevention of sudden cardiac death. There are currently three prospective, randomized trials comparing ICD with the best medical regimen as first-line therapy for patients who have survived one SCD episode, using total mortality as primary endpoint (65,66 and 67). These studies are reviewed in Table 22.13. Preliminary metaanalysis data from the Antiarrhythmics Versus Implantable Defibrillators (AVID), Canadian Implantable Defibrillator Study (CIDS), and Cardiac Arrest Study Hamburg (CASH) trials were presented at the 1999 North American Society of Pacing and Electrophysiology (NASPE) Scientific Sessions. In patients with cardiac arrest or hemodynamically unstable ventricular tachycardia, subgroup analysis based on ejection fractions showed a clear benefit of ICD implantation over amiodarone therapy in patients with ejection fractions (EF) of less than 35% but no benefit in those

with EF of 35% or more (unpublished data).

	AVID 1995–1997 (66)	CIDS 1990–1998 (65)	CASH 1987–1998 (67)
Protocol	ICD vs. empiric amiodarone or sotalol (mainly amiodarone)	ICD vs. empiric amiodarone	ICD vs. empiric amiodarone, metoprolol, or propafenone†
Sample size	N: 1,016 AAD: 509 ICD: 507	N: 659 Amiodarone: 331 ICD: 328	N: 346 Amiodarone: 90 Metoprolol: 97 Propafenone†: 96 ICD: 86
Patient inclusion criteria	VF VT with syncope VT with EF 40%	VF VT with syncope VT with CHD, length 400 ms and EF 40%	VF (no EF requirements)
Mortality in medical therapy arm	1 year: 17.9% 2 years: 25.3% 3 years: 35.9%	3 years: 39%	2 years: 19.6%
Mortality in ICD arm	1 year: 10.7% 2 years: 16.4% 3 years: 24.6%	3 years: 24%	2 years: 12.1%
P value	<0.02	0.017	0.0478

ms, milliseconds; VF, ventricular fibrillation; VT, ventricular tachycardia.
† Enrollment discontinued due to significantly increased mortality compared with the other arms.
‡ ICD arm vs. amiodarone arm (risk nonsignificant).

TABLE 22.13. *ICD Therapy vs. antiarrhythmic drugs (aad): secondary prevention trials*

Primary Prevention

Recently, one prospective study has attempted to establish the role of ICD in primary prevention of SCD. The Multicenter Automatic Defibrillator Implantation Trial (MADIT) randomized 196 patients with a history of MI, EF of 35% or less, asymptomatic nonsustained ventricular tachycardia (NSVT), and inducible ventricular arrhythmias during electrophysiology study (EPS) that were not suppressible with IV procainamide, to either ICD implantation or conventional medical therapy (68). The trial was terminated prematurely due to the significant improvement in survival in the ICD group by almost 50% compared with the control group. Another study evaluated the effect on survival of prophylactically implanted ICDs in patients with LV dysfunction and abnormal signal-averaged ECGs at the time of their coronary artery bypass surgery (69). Although this study found no evidence of improved survival among patients with prophylactic ICDs, it did confirm the importance of adequate revascularization in patients with CAD who are at high risk for ventricular arrhythmias. A follow-up to MADIT, the MADIT II, is currently in progress (70). The only prerequisites for enrollment in MADIT II are a history of MI and EF of 30% or less. Another primary prevention study currently in progress is the Sudden Cardiac Death in Heart Failure Trial (SCD-HeFT) (71). This trial tests the hypothesis that amiodarone or ICD, or a combination of both, can improve overall survival when compared with placebo in patients with clinical heart failure (New York Heart Association [NYHA] II or III) and low ejection fraction (<36%). A summary of the available data for some of the secondary and primary prevention ICD trials is shown in Table 22.13 and Table 22.14.

	MADIT 1990–1996 (68)	CABG-Patch 1990–1997 (69)
Protocol	ICD vs. conventional medical therapy*	ICD vs. conventional medical therapy
Sample size	N: 196 ICD: 95 Medical therapy: 101	N: 900 ICD: 446 Medical therapy: 454
Patient inclusion criteria	• Prior MI • EF < 36% • Asymptomatic NSVT • Inducible VT on EPS, not suppressed by procainamide	• Undergoing CABG • EF 36% • Abnormal signal-averaged ECG
Mortality in medical therapy arm	5 years: 35.6%	4 years: 24%
Mortality in ICD arm	5 years: 15.8%	4 years: 27%
P value	0.009	0.084

CABG, coronary artery bypass grafting; EF, left ventricular ejection fraction; ICD, implantable cardioverter defibrillator; MI, myocardial infarction.
* Significant numbers on amiodarone.

TABLE 22.14. *ICD therapy vs. conventional therapy: primary prevention trials*

Specific Cardiac Diseases

Recent information is now available, suggesting that certain underlying cardiac conditions, such as idiopathic dilated cardiomyopathy, hypertrophic obstructive cardiomyopathy, or congenital long QT syndrome, may predispose patients to malignant ventricular arrhythmias. Although no definitive data are available regarding the efficacy of ICDs in these patients, the severity of the disease states may influence the decision and the timing of ICD implantation.

Dilated Cardiomyopathy

In patients with idiopathic dilated cardiomyopathy, the combination of poor LV ejection fraction and nonsustained ventricular tachycardia (VT) is associated with increased risk of sudden death. In addition, electrophysiology studies in these patients is of limited value due to the low rate of inducibility. Results are available from two trials comparing amiodarone with standard therapy for primary prevention of sudden death in patients with heart failure and left ventricular dysfunction. In the GESICA trial, there was a 27% reduction in sudden death and a 28% reduction in total mortality in the amiodarone group (72). It is important to recognize that this study included approximately 20% of patients in each arm with idiopathic dilated cardiomyopathy. A second study, the Survival Trial of Antiarrhythmic Therapy in Congestive Heart Failure (STAT-CHF), failed to show any significant difference in overall mortality or sudden death rate between the amiodarone and placebo groups (73). However, the study did find a trend toward a reduction in overall mortality among the patients with nonischemic cardiomyopathy who received amiodarone. Although ICD may be the preferred treatment for patients with symptomatic VT or ventricular fibrillation (VF), and in patients with nonischemic cardiomyopathy and asymptomatic non-sustained VT—or who are not optimal candidates for ICD implantation—the results of GESICA and STAT-CHF trials suggest that amiodarone may be beneficial.

Long QT Syndrome

The congenital long QT syndrome has variable clinical manifestations, from asymptomatic to recurrent syncope to sudden death due to *torsades de pointes.* Because it is primarily an electrical disorder and not associated with structural heart disease, long-term prognosis is excellent if arrhythmias can be controlled or prevented. Conventionally, beta blockers are used in patients with syncope or in asymptomatic patients with a strong family history of sudden death. Sympathectomies, as well as permanent pacing to avoid bradycardia-dependent arrhythmias, are also effective in selected patients. ICD implantation is recommended in these patients with recurrent syncope and sustained ventricular arrhythmias, sudden death despite drug therapy, and sudden death as initial presentation. ICD as primary therapy may be considered in patients with a strong family history of sudden death, or in whom drug compliance may be an issue (74).

Idiopathic Ventricular Fibrillation/Tachycardia

Approximately 10% of young patients resuscitated from cardiac arrest have no clear etiology of VF despite extensive evaluation. EP studies can usually induce polymorphic VT or VF, which is often suppressible with class IA agents, but the long-term efficacy of antiarrhythmic agents in these patients is unknown. Despite limited data, it is generally accepted practice to implant ICDs in patients with idiopathic VF, given the guarded prognosis and often the young age of the affected patients.

Hypertrophic Cardiomyopathy

Hypertrophic cardiomyopathy can be a cause of ventricular arrhythmias and should be suspected as a cause of sudden death in young athletes. Sudden death may be the first manifestation of the disease in previously asymptomatic people. Because patients with hypertrophic cardiomyopathy may have ventricular arrhythmias, it has been suggested that they should be routinely screened by Holter monitoring for the presence of nonsustained VT, which may in turn be a marker for sustained

VT. No definitive data are available to support this routine screening, and risk stratification in this population remains ill defined.

The degree of outflow obstruction does not correlate with increased risk of sudden death, but inducibility of sustained ventricular arrhythmias on EP testing may be of prognostic value and appears to be associated with increased risk of cardiac arrest and syncope in some patients. Beta blockers and calcium channel blockers are often used for their negative inotropic properties to decrease outflow obstruction. Their efficacy in preventing sudden death, however, is not established. Empiric use of amiodarone has been used with some efficacy, but this remains controversial (75). Sudden death survivors should be considered for ICD therapy (76). The role of ICD in patients with hypertrophic cardiomyopathy with nonsustained VT and presyncope or syncope is not yet proven and remains controversial.

Right Ventricular Dysplasia

An important cause of congestive heart failure and ventricular arrhythmias is right ventricular dysplasia. Patients with RV dysplasia are considered to be at particularly high risk for sudden death if they have a strong family history of sudden death or if they have a history of syncope. Drug therapy is often ineffective. Ablations are sometimes useful and should be attempted first if VT is tolerated. In patients with cardiac arrest, recurrent arrhythmias, or syncope despite drugs or ablations, ICD implantation should be considered to prevent hemodynamically unstable VT or sudden death (77).

Syncope

Syncope is a common presenting symptom for which, in most cases, there is often no known etiology despite extensive evaluation. Although syncope of unknown etiology usually has a benign prognosis, syncope attributable to cardiovascular causes is associated with increased sudden death and mortality. Therefore high-risk patients with a history of infarctions and low LVEF who have syncope without apparent etiologies and in whom clinically relevant VT/VF is induced at EP study, may be considered candidates for ICD therapy.

Heart Failure

ICD therapy has also recently been considered for patients with heart failure and in those awaiting cardiac transplantation. The stages of heart failure (NYHA classes I to III) appear to correlate with overall mortality and occurrence of ventricular arrhythmias. Preliminary data suggest that ICDs may prolong life in patients with NYHA functional classes I to III, with the initial benefit greatest in patients with classes II and III (78). In patients with end-stage heart failure awaiting heart transplantation, about 20% die suddenly while waiting for the donor organ. ICD therapy in this group of patients appears to decrease the incidence of sudden death. However, the rate of nonsudden deaths, mostly from pump failure, are slightly increased in this group. This raises the question as to whether ICDs can truly prolong survival in patients with end-stage heart failure or are merely changing the mode of their death (79).

Contraindications to ICD Therapy

ICD therapy or implantation is not recommended in patients in whom VT/VF is due to a reversible cause, such as acute myocardial infarction or severe electrolyte abnormalities. Patients with LV dysfunction undergoing routine bypass graft surgery without inducible sustained VT should also not have ICDs implanted (69). Patients with Wolff-Parkinson-White syndrome with VF due to atrial fibrillation should not receive ICD therapy but should instead undergo catheter ablation of their accessory bypass tracts. Patients with terminal illnesses and life expectancy of less than 6 months are unlikely to benefit from ICD therapy. Patients with ongoing infections should not have ICD implanted until the infection has been clearly resolved. Severe psychiatric disorders that may be worsened with ICDs or may preclude follow-up are relative contraindications for ICD implants. Patients with incessant VTs that are refractory to drugs may not benefit from ICDs because the arrhythmias would constantly trigger shocks. Rather, surgical or catheter ablation should be attempted before ICD implantation.

Guidelines

The American College of Cardiology and the American Heart Association have published guidelines for ICD implantation in the same document in which pacemaker guidelines are discussed (7). Table 22.15 is a summary of those guidelines.

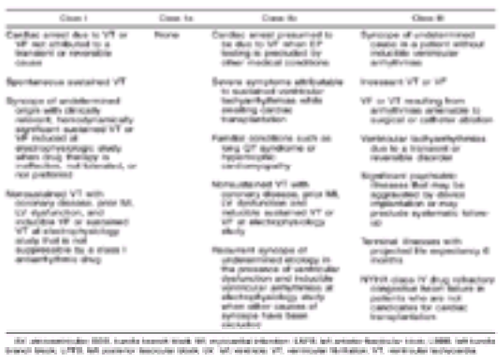

TABLE 22.15. *Indications for ICD therapy*

Cardioverter-Defibrillator Systems

First-generation ICDs consisted of a large generator placed in an abdominal pocket, capable only of high-energy shocks. In the nearly 20 years since the first implantation in humans, advances in technology have resulted in significantly smaller devices, with sophisticated detection algorithms and tiered therapies. Ongoing developments in defibrillation systems are to continue to decrease the size of generators without sacrificing maximal available energy, to improve sensing and detection of arrhythmias, and to find ways to deliver the lowest energy possible that can defibrillate successfully—the defibrillation threshold (DFT). Despite these advances, the primary goal of the ICD continues to be the rapid and effective treatment of ventricular arrhythmias. The defibrillation system consists of the pulse generator and the leads. The generator supplies low-energy current to power the basic functions of the device as well as high current density for depolarizing the myocardium. The leads set up optimally uniform current density for defibrillation and may provide sensing and backup pacing.

Pulse Generators

The first-generation devices were large (180 cm^3 device volume) and were implanted in the abdomen. Evolving ICD technologies have focused on decreasing the size of the generators, which would allow pectoral implantation, decrease local pocket complications, and improve patient comfort. The bulk of the generator consists of the lithium silver vanadium oxide battery and the capacitor. ICD generators must meet the following requirements: They must monitor electrical status through sense amplifiers, analyze waveforms for abnormal arrhythmias, deliver appropriate therapy, be reliable, and have significant lifetime before battery depletion.

The power for the ICD system is supplied by the battery, which serves as the energy storage reservoir. Capacitors store the energy drawn from the battery, because the battery itself cannot deliver a current fast enough for defibrillation, and it cannot deliver a voltage high enough for defibrillation.

Before an arrhythmia can be treated, it must be sensed by the electrodes. Local bipolar electrograms and amplifying systems are used to permit accurate sensing of small electrograms such as seen in VF (80).

ICDs, like pacemakers, can be subject to oversensing or undersensing. Oversensing occurs when the device detects an event that is not due to ventricular depolarization and may result in inappropriate shocks. Examples of oversensing are T-wave sensing, cross-talk (sensing electrical signals from another chamber, e.g., atrium), myopotential or diaphragmatic sensing, or lead fracture leading to electrical noise (Fig. 22.8). Undersensing occurs when the device does not register an event. This occurs most often when the electrogram is smaller than the sensitivity setting of the device. Changes in electrograms can occur with lead dislodgment,

infarction at the site of the lead, inflammation or fibrosis at the electrode site, new bundle branch block, and lead fracture. Undersensing is particularly a concern with ICDs, which must deal with having to sense not only normal R waves, which may be up to 20 mV in amplitude, but also VF with R waves that can be less than 1 mV. Because of the variations in the amplitudes of the electrograms, fixed gain and sensitivity settings, such as those used in pacemakers, may result in undersensing of VF. Some devices attempt to enhance VF sensing with auto-amplifiers. The two most common types of amplifiers currently used in ICDs are the automatic gain control and autoadjustable threshold (Fig. 22.9).

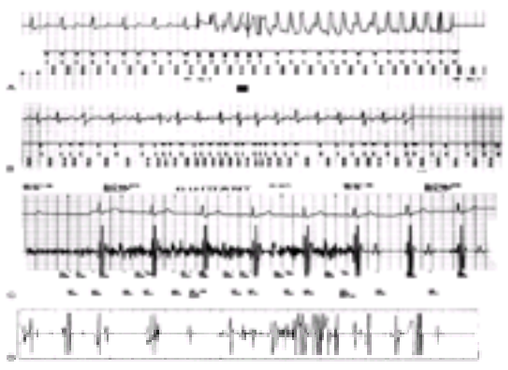

FIG. 22.8. Examples of ICD oversensing. **A:** T-wave oversensing. During sinus rhythm, double counting of R and T waves led to VT detection (TD), triggering therapy with antitachycardiac pacing (ATP). ATP resulted in true VF, which was detected and treated with a single shock. (Courtesy of N. Hallette, RN, BIDMC Device Clinic.) **B:** Cross-talk. In this example, the ventricular lead is sensing not only R waves from the ventricle, but also activity in the right atrium. The patient is in atrial fibrillation, which is sensed by the device as VF. The patient subsequently received a shock. (Courtesy of N. Hallette, RN, BIDMC Device Clinic.) **C:** Oversensing of diaphragmatic myopotentials. The patient in this example received multiple shocks while having a bowel movement. Interrogation showed sensing of diaphragmatic myopotentials with valsalva maneuvers, sensed by the ICD as VF. (Courtesy of Donald Love, M.D.) **D:** Lead fracture. Electrical noise (large, sharp spikes) was detected as VF. In this particular case, the shock was aborted when decreased noise at a later strip allowed for detection of sinus rhythm. (Courtesy of N. Hallette, RN, BIDMC Device Clinic.)

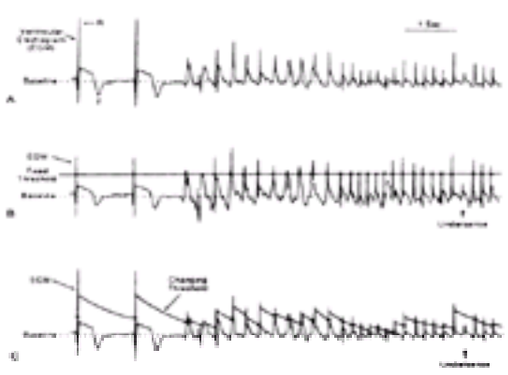

FIG. 22.9. Sinus rhythm and ventricular fibrillation (VF) sensing. **A:** Raw electrograms. **B:** Sensing with automatic gain control. **C:** Sensing with automatic adjusting threshold. (See text for details. From Olsen WH. Tachyarrhythmia sensing and detection. In: Singer I, ed. *Implantable cardioverter defibrillator.* New York: Futura Publishing, 1994:77.)

Leads

Although the pulse generator provides the power for defibrillation and contains circuitry for sensing and detection, the leads set up the current flow for defibrillation and provide the actual sensing of local electrograms. Initial electrodes used for defibrillation were patches which were sewn onto the epicardium or pericardium. With the advent of transvenous systems epicardial patches are now rarely used. Initially, sensing was achieved from the high-voltage patch electrodes. Oversensing, however, prompted the use of a separate sensing lead, either epicardial or endocardial (81).

Endocardial leads are made of high-voltage conductors. At least one conductor is used for the defibrillation coil, which is usually located near the tip of the lead and meant to be placed along the posterior wall of the right ventricle. Defibrillation leads can have either a single coil (one conductor) or two shocking coils (two conductors). The second coil is located more proximally to the distal coil. When a dual coil lead is implanted, the lead would be positioned with the distal coil in the right ventricle (RV) and the proximal coil anywhere from the subclavian vein (SVC) to the right atrium, depending on the anatomy of the patient. Alternatively, separate leads with a single shocking coil each may be implanted in the RV, SVC, coronary sinus (CS), or a combination thereof. Leads placed in the RV must also have sensing and pacing capabilities, whereas leads in the SVC or CS would not be required to have these features.

With the implant of devices in the pectoral region the housing of the pulse generator itself can serve as a second electrode. Because the pulse generator has a large surface area and can provide more even current distribution, defibrillation using the active pulse generator as one of the electrodes can be achieved with lower energies than defibrillation with a combination of leads. The defibrillation threshold (DFT) is the lowest clinically obtained energy that can achieve defibrillation. DFT achieved with a single RV coil and an active pulse generator are comparable to that of epicardial lead systems (82).

Three electrodes may also be used to attempt to lower DFT. The most common electrodes used in practice are the RV, the SVC, and the active pulse generator. Two electrodes may be connected together, with the current flowing between the two joined electrodes (anodes) and a third common electrode (cathode) (Fig. 22.10).

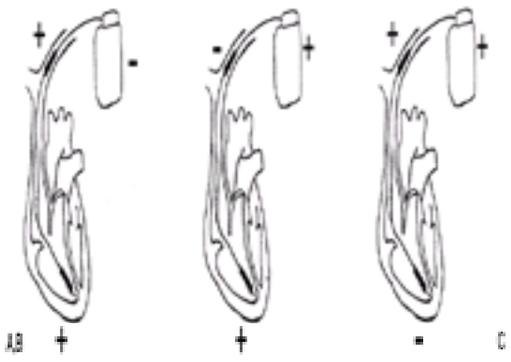

FIG. 22.10. Possible configurations with three electrodes. **A:** Pulse generator as cathode: area of low current density is across the RV. **B:** SVC coil as cathode: area of low current density is across the LV apex and LV free wall. **C:** Optimal configuration, with RV coil as cathode: area of low current density is extracardiac.

Sensing in an endocardial system is achieved through a distal electrode at the tip of the lead. The same conductor can be used for backup pacing. Unipolar leads have only one high-voltage conductor, for defibrillation, and thus do not have pace/sense capabilities. These leads are usually placed in the SVC or CS positions. Bipolar leads consist of two conductors, one for shocking and the other for sensing. Sensing, in this case, occurs between the tip of the lead and anywhere along the

length of the shocking coil, and is termed *integrated bipolar sensing.* Because of the distance between the tip and the coil and the size of the coil, sensing in these leads is more susceptible to noise, farfield artifacts, and postshock undersensing than true bipolar sensing (83). True bipolar sensing occurs between the distal tip of the lead and a ring located approximately 1 cm proximally from the tip. Sensing is thus local and much more reliable. New lead technologies are testing quadrapolar leads, consisting of two shocking coils, a distal tip, and a proximal ring, which would allow for true bipolar sensing at the same time, giving the option for using dual defibrillation coils (Fig. 22.11).

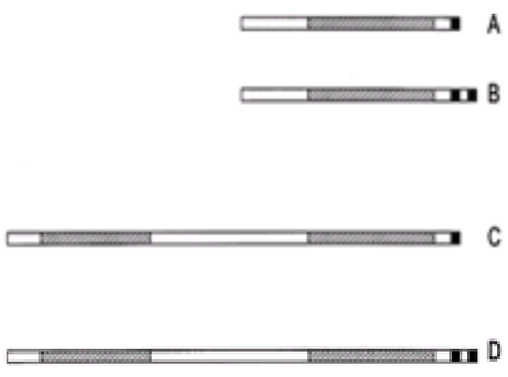

FIG. 22.11. Diagram of four possible RV leads. **A:** Bipolar, single coil with integrated sensing. **B:** Tripolar, single coil with true bipolar sensing. **C:** Tripolar, dual coil with integrated sensing. **D:** Quadripolar, dual coil with true bipolar sensing (investigational). Striped areas, coils; dark areas, electrodes (proximal, ring; distal, tip).

Tachyarrhythmia Detection

As described earlier, an event is sensed when the detected R wave is above a set threshold. The time interval between two sensed events is the cycle length (CL). Detection is the process of analyzing recent cycle lengths and R-wave morphologies to classify rhythms and determine appropriate programmed therapy. It should be a rapid process so that therapy can be delivered before a patient develops symptoms or before an electrogram deteriorates, but not too rapid because some arrhythmias are nonsustained. Because ventricular arrhythmias can be sustained or self-limiting, hemodynamically stable or unstable, ICDs should be able to respond to each episode. The rate cutoff is defined as the heart rate above which the device will be triggered to deliver therapy. The original devices were not programmable, and the cutoff rate and sensitivity level were preset at the factory. Devices today have not only multiple zones of detection, but also specific therapies that can be individually programmed into each zone, termed *tiered therapy.* Detection zones are ranges of CLs that are programmable. An average of the most recent cycle lengths of the sensed events is compared against various detection zones, and the CL is counted if it falls within a specific zone. For example, if the VF zone is programmed to 320 ms (188 bpm), and the VT zone is programmed at 400 ms (150 bpm), a detected CL will be classified into the VF zone if it is less than 320 ms and will be counted in the VT zone if it is between 300 and 400 ms. If the CL is greater than 400 ms, it would fall outside tachyarrhythmia detection zones and would therefore not be classified (Fig. 22.12).

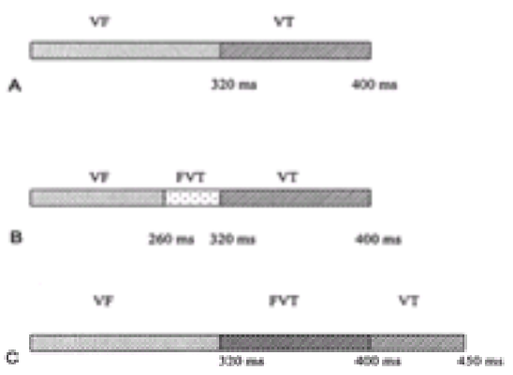

FIG. 22.12. Examples of the multiple detection zones available with current devices. **A:** Ventricular tachycardia (VT) will be detected between 440 and 320 ms. Above 320 ms, ventricular fibrillation (VF) will be detected. **B:** Addition of a "fast" VT zone (FVT) as part of the VF detection window. **C:** Addition of a "fast" VT zone (FVT) as part of the VT detection window. Different therapies can be programmed for each zone.

Although detection based on cycle lengths of sensed ventricular electrograms is highly reliable, this method can sometimes lead to inappropriate shocks. This most commonly occurs with atrial fibrillation (83) and sinus tachycardia, when the rates of these and other nonventricular arrhythmias fall into the detection zones. To decrease the risk of inappropriate shocks, newer devices offer additional detection parameters to increase the specificity of VT detection. These include sudden onset criterion, rate stability criterion, and criterion based on electrogram morphology, and are only available, for safety reasons, in the lowest VT rate cutoff zones.

Sudden onset is intended to distinguish sinus tachycardia with a gradual increase in rate from VT with a sudden onset. Rate stability criterion allows the ICD to withhold VT detection for rapid, supraventricular rhythms with irregular intervals, and can be used to differentiate VT with minor rate variability from atrial fibrillation with large variations in cycle lengths. The electrogram width and/or morphology criterion is based on the premise that rhythms of ventricular origin generally have different intracardiac electrograms than those of supraventricular origin. Although the use of these detection enhancement parameters may increase specificity of VT detection, the concern exists that these parameters may mistakenly inhibit therapy for true VT or delay time to detection.

The first ICDs were "committed" devices in that once detection occurred and therapy was initiated, it could not be aborted. Current devices can confirm a rhythm before discharge of energy, and therapy can be aborted if the tachycardia is nonsustained, thereby minimizing unnecessary and painful shocks. Confirmation does not occur before delivery of antitachycardia pacing (ATP), however, because ATP is meant to be delivered rapidly and painlessly. Examples of an older, committed device and a newer device capable of aborting therapy are shown in Fig. 22.13.

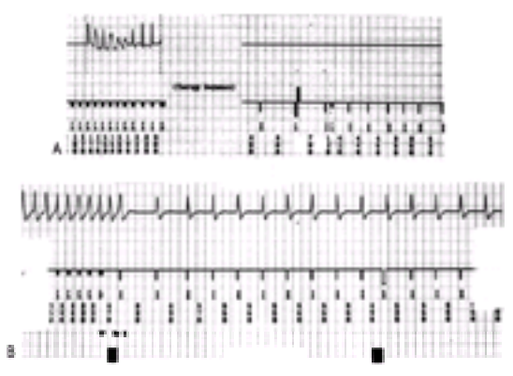

FIG. 22.13. Confirmation. **A (top strip):** Older device with committed therapy only. VF is sensed (FS) and detected (FD). During charging (no EGMs available on this device during charging), VF spontaneously terminated as shown by a sensed ventricular beat (VS) outside the VF detection zone. Because therapy is committed, charge is delivered (CD) despite termination of VF. **B (bottom strip):** Newer, noncommitted device. VF is detected at the left of the strip (FD) and charging begins, followed by spontaneous termination. At the end of the charging period (CE), sinus rhythm was detected during confirmation, and no shock was delivered.

If therapy either is diverted or is unsuccessful in restoring sinus rhythm, redetection of tachyarrhythmia will begin. Most algorithms use a smaller number of intervals for meeting redetection criteria, and most devices will not allow for confirmation in the redetection period after a diverted or unsuccessful therapy. In essence, therapy after redetection of VT/VF following a diverted or unsuccessful shock is committed, so that the overall duration of an episode is kept to a minimum. It is important to recognize that an episode does not terminate just because a therapy has been aborted. Termination of an episode requires that a specific number of CLs fall outside the detection zones and results in the resetting of all detection algorithms and therapies to zero.

Dual-Chamber ICDs

The newest generation of ICDs is made up of the dual-chamber pacemaker-defibrillators. The major advantages of a dual-chamber ICD/pacemaker are improvement in the detection and identification of arrhythmias to prevent inappropriate therapy, and availability of dual-chamber pacing capabilities. About 10% to 25% of patients receiving ICDs may require dual-chamber pacing at some point. Although older ICDs can provide backup bradycardia pacing, they are not meant to be used as permanent pacemakers, since the battery drain would be too great with the current systems and they are only capable of fixed-rate pacing. Dual-chamber ICDs add an atrial lead to improve detection specificity and to provide DDD pacing. Implantation of a dual-chamber system has the additional benefit of eliminating pacemaker/ICD interactions in patients who require both. The new dual-chamber ICDs must ensure that pacing function is not affected by shocks that may transiently lower sensing capabilities or increase pacing thresholds; that the defibrillation function is able to operate in all pacing modes; and that the mode-switch function of the pacemaker does not interfere with tachyarrhythmia detection.

Therapy

Early devices were limited to a single form of therapy with a single high-energy shock. Today's devices offer a range of therapies, from programmable high-energy defibrillation shocks to low-energy synchronized cardioversion to antitachycardia pacing.

High-Energy Defibrillation

The process of defibrillation involves halting ventricular fibrillation wave fronts within a critical mass of myocardium and is a statistical process. Changes in the autonomic or metabolic state of a person can mean that a shock strength is able to defibrillate at a given time but not at others. In addition, each episode of fibrillation has different activation wavefronts and may require different shock strengths. There appears to be a range of energy over which defibrillation can occur, with the probability of successful defibrillation increasing with increasing energy. Clinically, the lowest energy that successfully converts VF to sinus rhythm during ICD testing is taken as the DFT. This value is usually lower than the minimum energy required for consistently successful defibrillation, which is not an obtainable value clinically. A safety margin of usually at least 10 joules (J) must be demonstrated between the maximum output of a device and the DFT.

Many patients undergoing ICD implantation are also on antiarrhythmic drug (AAD) therapy, and the effects of AADs on the DFT should be taken into consideration. Such class IC and IB agents as encainide, flecainide, lidocaine, and mexiletine cause a reversible, dose-dependent increase in energy requirements for successful defibrillation (84,85,86 and 87). Amiodarone appears to have a bimodal effect on DFT. Acute administration may lower DFT in the animal model, but chronic use may elevate DFT (88). Type IA drugs, such as procainamide and quinidine, do not appear to affect DFT significantly (89), whereas sotalol and N-acetyl-procainamide have been shown to lower DFT (90).

One method of lowering DFT is by improving defibrillation waveforms, which describe the manner with which the energy is delivered across the myocardium. Defibrillation waveforms can be delivered as a single monophasic pulse, sequential or simultaneous monophasic pulses, biphasic pulses with the two phases in opposite polarity, or triphasic pulses with the first and third pulses in the same polarity. Current data show that biphasic waveforms achieve the lowest DFT and are commonly used in devices today.

Low-Energy Synchronized Cardioversions

Although VF often requires a relatively higher energy for termination, some ventricular tachycardias can be terminated with very low energies. Low-energy synchronized cardioversions have the advantage of faster delivery of therapy, may cause less discomfort, and can conserve battery when compared with high-energy shocks. Although each patient's pain threshold may vary, most tolerate a shock of 1 J or less (91). Although the advantages of being able to terminate ventricular tachycardias rapidly and with little discomfort are evident, the risks of utilizing this therapy are acceleration of stable VT to VF and delay of time to successful treatment if initial cardioversion was unsuccessful.

Antitachycardia Pacing

The ability to terminate tachycardias with pacing had been available before the advent of the ICD. However, due to the potential risk of acceleration of VT to VF, the use of ATP devices was limited to the treatment of SVTs until the ability to defibrillate the heart was also available. Similar to low-energy cardioversion, the advantages of ATP include rapid delivery of therapy, less discomfort to the patient, and conservation of battery life. The concept of ATP in termination of VT is based on the observation that ventricular arrhythmias, such as those in patients with prior coronary artery disease, are due to reentrant circuits involving the border zones of prior infarctions. In a reentrant circuit, the leading wavefront of activation must encounter excitable tissue for continuing propagation. Progressively more premature stimuli encroach on the refractory tail end of the wavefront. Termination of VT occurs when a stimulus interacts with the circuit both orthodromically (forward) and antidromically (backward), causing bidirectional block (92). Multiple extrastimuli increase the probability of a stimulus to interact with the tachycardia circuit, at the slightly increased risk of accelerating VT. An example of VT accelerating to VF after ATP, and successful treatment of VF with a synchronized shock, is shown in Fig. 22.14.

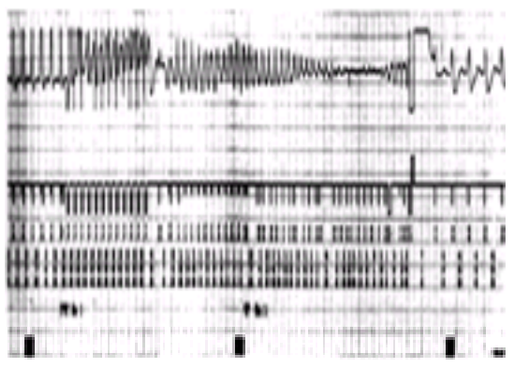

FIG. 22.14. Acceleration of VT to VF by ATP. A continuous strip is shown. VT is detected in the first part of the rhythm strip (TF), followed by a 12-beat burst of ATP (TP), which accelerated the tachycardia to VF (FS). VF is detected (FD) and charging begins. A synchronized shock is then delivered (CD), resulting in sinus rhythm. (Courtesy of N. Hallette, RN, BIDMC Device Clinic.)

The two most commonly used methods of ATP are rate-adaptive burst pacing and autodecremental or ramp pacing. With rate-adaptive burst pacing (Fig. 22.15A), the device is programmed to deliver a set number of pulses at a constant coupling interval based on a percentage of the VT CL. The sequence may be repeated in successive trains if VT is redetected. Each sequence is titrated by decrementing the coupling interval between pulses by a set amount per sequence, usually 10 ms. In the autodecremental or ramp pacing mode (Fig. 22.15B), the initial coupling interval within a sequence is also based on a percentage of the tachycardia cycle length. Within a sequence, each coupling interval is decremented by a set amount, usually 10 ms. The sequence is titrated by the addition of an extrastimulus at the end of each sequence until the coupling interval reaches the programmed minimum value. Comparisons of the two methods with regard to success of VT termination and acceleration of VT to VF have shown no significant differences between the two methods when 10-ms decrements are used (Table 22.16) (111,112 and 113).

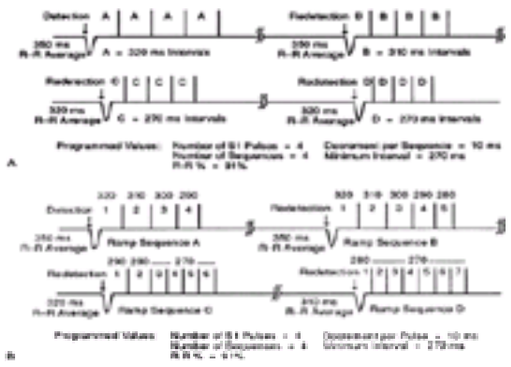

FIG. 22.15. A: Rate-adaptive burst. The ICD is programmed to deliver on detection of VT an adaptive burst at 91% of the tachycardia cycle length. The number of pulses within the burst is programmed to four and the sequence will repeat itself on redetection of the tachycardia four times. The programmed decrement per sequence is 10 ms but not to shorten to less than a programmed minimum interval of 270 ms. In the example, a tachycardia at 350 ms is detected. The first burst sequence (A) should be 320 ms (350 ms × 91% = 320 ms). The first pulse is delivered accordingly at 320 ms from the R wave that fulfilled the programmed detection criteria. All subsequent pulses of this sequence are separated by 320 ms. Assuming that the VT is redetected and the RR interval remains at 350 ms, a second burst sequence (B) is decremented by 10 ms (320 ms – 10 ms = 310 ms). In the example, sequence (B) results in the acceleration of the tachycardia to 320 ms, which is again redetected. The alculated pulse interval (C) is now 270 ms (320 ms × 91% = 290 ms – 20 ms decrement = 270 ms). Assuming that the tachycardia is unaffected and redetected at 320 ms, the fourth and final burst sequence (D) will be 270 ms (the programmed minimum interval) despite the fact that the calculated pulse interval would have been 260 ms (320 ms × 91% = 290 ms – 30 ms decrement = 260 ms). **B:** Autodecremental ramp. The ICD is programmed in this case to deliver an autodecremental ramp of four pulses, starting at 91% of the average sensed RR, continuing on redetection for four sequences with a decrement per pulse of 10 ms, not to exceed a minimum interval of 270 ms. The first ramp sequence (A) should start at 320 ms (350 ms × 91% = 320 ms) with each interval thereafter shortened by 10 ms so that the fourth interval equals 290 ms. Assuming that the tachycardia is redetected (B), the initial ramp pulse will be 320 ms, with decrements of 10 ms with the ramp as above but with the addition of a fifth beat at 280 ms. Before the third ramp sequence (C), the average RR shortens to 320 ms. Accordingly, the initial pulse is 290 ms (320 ms × 91% = 290 ms). After a decrement of 10 ms for interval 2; intervals 3, 4, and 5; and the additional sixth are all delivered at the programmed minimum of 270 ms. Acceleration of the tachycardia to 310 ms determines that the first pulse will be delivered at 280 ms, with intervals 2 to 6 and the additional seventh at the minimum programmed value of 270 ms.

Reference	Average VT CL(ms)	Termination (%)			Acceleration (%)		
		Ramp	Burst	*p* value	Ramp	Burst	*p* value
Calkins 111	324 ± 64	72	70	>.1	18	21	>.1
Gillis 112	324 ± 56	69	76	n/a	11	3	.16
Newman 113	364 ± 74	84	75	.31	6	15	.43

Calkins: Calkins H, El-Atassi R, Kaltbfleisch S, Langberg J, Moradyj F. Comparison of fixed burst versus decremental burst pacing for termination of ventricular tachycardia. *Pacing Clin Electrophysiol* 1993;16:36.

Gillis: Gillis AM, Leitch JW, Sheldon RS, et al. A prospective randomized comparison of autodecremental pacing to burst pacing for termination of ventricular tachycardia. *Am J Cardiol* 1993;72:146.

Newman: Newman D, Dorian P, Hardy J. Randomized controlled comparison of antitachycardia pacing algorithms for termination of ventricular tachycardia. *J Am Coll Cardiol* 1992;19:1413.

TABLE 22.16. *Comparison of ramp vs. burst antitachycardia pacing*

Programming of ATP can be performed using a number of methods. If an EP study is performed before ICD implant and ATP was able to terminate the induced VT, ATP can be programmed accordingly. Alternatively, noninvasive programmed stimulation (NIPS) can be performed after implantation through the device, and ATP can then be tailored to determine the setting that would best terminate VT without accelerating it to VF. ATP can also be programmed empirically, which is a reasonable approach since the success of termination may be different between induced and spontaneous VT.

The Technique of Pacemaker and ICD Implantation

Permanent Pacemaker Implantation

Currently, pacemaker and ICD leads are usually implanted transvenously and the pulse generator is implanted in a subcutaneous or submuscular pocket in the pectoral region. Venous access can be afforded by the subclavian, cephalic, or axillary vein. The technique of dual-chamber device implantation is described. Single-chamber device implantation follows the same technique without the placement of the second lead. Transvenous, pectoral implantation of ICDs utilizes the same techniques as pacemaker implantation, with the addition of defibrillation testing.

Preparation

We prefer the left pectoral location for ease of lead introduction and positioning. For right-handed patients the left side is also preferable. The right side can also be used if the left is inaccessible or if preferable (examples include very active left handed golfers or tennis players). The left side is preferred for ICD implantation in which one shocking electrode is housed in the pulse generator (even in the left-handed patient), because the field orientation for defibrillation (can to electrode) is superior to that of the right-sided device position.

Informed consent should be obtained from the patient (or a designated guardian if the patient cannot understand or give consent) before the procedure. The procedure and its risks (see Complications section later) should be explained, and the patient's questions should be answered.

Before the procedure, the history and physical and laboratory examinations should be reviewed with an emphasis on issues important to pacemaker implantation.

The history and physical examination should consider the possibility of injury or pathology in the potential region of device implantation. Injury or previous surgery suggests that abnormal venous anatomy may be present, making venous access more difficult. Allergies or intolerances to antibiotics, radiographic contrast agents, local anesthesia, and sedatives should be noted. Ongoing infection or signs or symptoms of infection (e.g., fever, leukocytosis, chills, productive cough, dysuria) should prompt investigation and resolution before implantation. Congestive heart failure therapy should be optimized to allow the patient to lie flat throughout the procedure. Similarly, the respiratory status should be evaluated and optimized before the procedure.

Some basic laboratory data should be scrutinized before the procedure. The chest x-ray and ECG are part of the original evaluation in most patients. The hematocrit and coagulation parameters should be known to avoid bleeding complications. Coumadin should be discontinued at least 4 days before implantation, and the INR should be 1.5 or less, though a recent study suggests the feasibility of pacemaker implantation in patients receiving oral warfarin (93). Aspirin should be discontinued 1 week before the procedure if possible.

The patient should be in the fasting, postabsorptive state. Meticulous sterile technique should be exercised throughout, with thorough scrubbing and draping of the region to be incised. General anesthesia is not necessary, but local anesthesia should be used liberally. Judicious use of an intravenous benzodiazepine (e.g., midazolam) and a narcotic (e.g., fentanyl) reduces both anxiety and discomfort. The drugs should be short-acting to minimize the risk of severe respiratory depression. A peripheral intravenous line in the arm ipsilateral to the implant is useful, should the need for an injection of intravenous radiographic contrast arise.

Prophylactic antibiotic therapy is still somewhat controversial, but we favor its use. A recent metaanalysis of seven randomized trials of antibiotic use at the time of

pacemaker implant suggested that antibiotics do reduce the risk of wound infection, pacemaker erosion, and septicemia (94). At our institution, patients receive a dose of intravenous cefazolin or vancomycin during the procedure followed by 48 hours of therapy.

Venous Access

A variety of techniques are available for gaining venous access. The cephalic, axillary, and subclavian veins can all be utilized. We prefer the cephalic vein cutdown approach when possible. Using this approach, venous access is achieved under direct visualization and there is no risk of pneumothorax. In addition, some believe that there is a lower incidence of lead fracture due to crushing at the junction between the first rib and the clavicle.

After the preparation and draping, the deltopectoral groove should be identified by palpation. An incision is made after infiltration of local anesthesia. We use a mixture of lidocaine and bupivicaine (which has a longer duration of action and helps prevent postoperative discomfort). The incision may be oblique, overlying the deltopectoral groove, or it may be transverse, about 2 cm inferior to the clavicle with its lateral margin crossing the deltopectoral groove (Fig. 22.16). Some prefer the oblique incision because it allows greater exposure of the cephalic vein. Others prefer the transverse incision since it increases the chance of finding the deltopectoral groove. The incision is made with a no. 10 blade, perpendicular to the skin. Enough pressure should be applied to cut through the epidermis and dermis with a single incision. The incision is extended down to the prepectoral fascia. Blunt dissection should be used primarily; sharp dissection and electrocautery should be minimized to prevent inadvertent division of unrecognized structures (especially arteries and arterioles). Moreover, large areas of charred tissue from electrocautery heal poorly and increase the risk of infection or wound dehiscence.

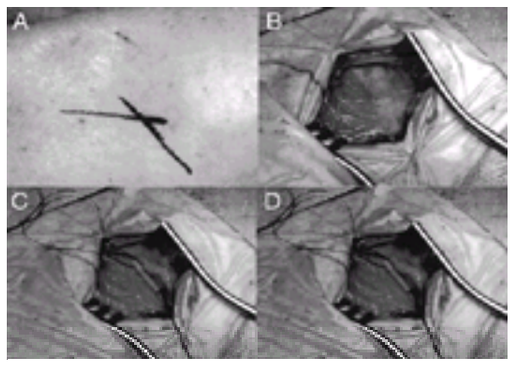

FIG. 22.16. Cephalic vein cutdown. **A:** Surface anatomy of the deltopectoral region. The incision can be made in the groove or across the groove as noted by the marks. **B:** A fat streak is often seen in the groove between the pectoral and deltoid muscles. The cephalic vein lies just under this streak. **C:** The vein isolated with distal and proximal ties in place. **D:** After incising the vein a 5F sheath is introduced followed by a guidewire.

The deltopectoral groove can be identified by the fatty streak between the deltoid and pectoralis muscles. The orientation of the fibers of the two muscles is also different, which can help identify the deltopectoral groove in the very lean patient. The cephalic vein runs in the deltopectoral groove. Once it is identified, it is dissected free of fat and connective tissue and isolated. We typically ligate the vein distally to minimize bleeding. A suture is also passed under the vessel proximally and not tied; traction on this suture is used to control bleeding after the vessel is incised. The vein may be small in caliber and may collapse further with ligation but is usually sufficiently distensible for insertion of introducer sheaths and leads. The vein is incised with iris scissors. Although the lead can be inserted directly into the vein, we prefer to cannulate with a 5F introducer. Through the introducer, a guidewire is advanced (under fluoroscopic guidance) to the superior vena cava through the right atrium and into the inferior vena cava. If the guidewire is not advanced easily, radiographic contrast can be injected either through introducer or through the peripheral intravenous line, to confirm that the introducer is intraluminal and to help guide advancement of the wire. Venography will also reveal venous occlusion if present.

If the cephalic vein cannot be used, we then consider use of the *axillary* vein (95). The vein can be visualized by injection of radiographic contrast into a peripheral arm vein. Although contrast remains in the vein, it is cannulated under fluoroscopic guidance with an 18-gauge needle (Fig. 22.17) and a guidewire is then advanced to the inferior vena cava as described earlier.

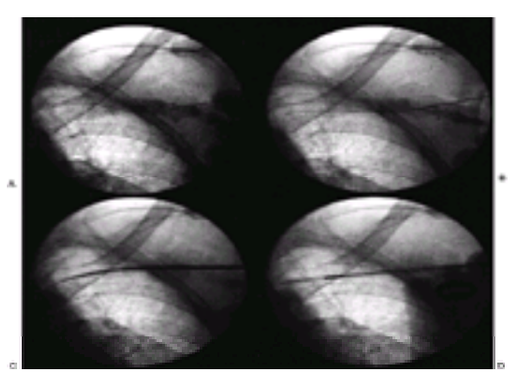

FIG. 22.17. Fluoroscopic image of venographically guided axillary vein cannulation. Contrast was injected through a left arm peripheral intravenous line. **A:** The 18-gauge needle is entering the contrast-filled vein. **B:** A guidewire is passed through the needle and into the subclavian vein. **C:** The sheath and dilator are advanced over the wire. **D:** The lead is advanced through the sheath.

Alternatively, the *subclavian* vein can be used. From within the incision, the subclavian vein is cannulated with an 18-gauge needle and a guidewire is advanced into the vein. Since the subclavian puncture is performed without direct visualization of the vein, there is a risk of pneumothorax and subclavian artery puncture. Before placing the sheath, the position of the wire within the vein should be confirmed with fluoroscopy. A chest x-ray to exclude pneumothorax is therefore mandatory after completion of the procedure.

The subclavian approach is less desirable because of the risk of pneumothorax and the potential for crush injury to the lead(s) that may occur as they pass between the clavicle and first rib. Subclavian puncture often penetrates the ligaments connecting the first rib and the clavicle, making the lead at risk for being entrapped there and increasing the incidence of crush. Cannulation of the subclavian vein as lateral as possible helps minimize the risk of crush.

Lead Placement

Once venous access has been achieved and a guidewire is in place, the wire is used to guide the insertion of venous sheaths to introduce the leads into the vein. The sheath is of the “peel-away” type, to allow its removal after the lead is introduced. The sheath should be large enough to contain the guidewire with the ventricular lead. When the sheath's dilator is removed, the sheath itself should be pinched to prevent both excessive bleeding and air embolism. The lead should be inserted immediately to minimize the time that the sheath is open to air, and the patient may be instructed to stop breathing during this process (without taking a deep breath first).

The ventricular lead is first advanced to the right atrium. Pacemaker leads are intentionally designed to be flexible; this lack of axial stiffness helps prevent cardiac perforation by the leads. However, such flexible leads are not easily manipulated, and the use of a stiffening wire stylet is required. The sheath is then withdrawn from the vein and removed (retaining the guidewire if another lead is to be placed). We then shape a stylet with a curve at its distal 10 to 12 cm. Using the curved stylet, the lead is advanced across the tricuspid valve and into the right ventricular outflow tract/pulmonary artery. Then, using a straight stylet (tapered at its tip to reduce

stiffness that might lead to perforation), the lead is withdrawn from the outflow tract and then advanced to the apex of the right ventricle. As the lead is withdrawn from the outflow tract, the stylet is simultaneously advanced to the tip of the lead. The lead frequently becomes caught in the trebeculations of the right ventricle; some manipulation is often necessary to advance the lead toward the apex of the right ventricle. Ventricular ectopy is common during lead manipulation and almost always stops when the lead position is stable. If ventricular tachycardia persists, the lead should be repositioned. If ventricular tachycardia continues still, appropriate steps must be taken to terminate the rhythm.

Good ventricular lead positioning is shown in the anteroposterior and lateral orientations in the chest x-rays in Fig. 22.18A and Fig. 22.18B. Right anterior oblique imaging can assist in ventricular lead positioning, since the length of the right ventricle can be viewed *en face,* without the foreshortening seen in the anteroposterior view. In any case, the lead should be viewed in the right anterior oblique and left anterior oblique projections to ensure location of the tip of the lead along the floor of the RV septum and in the apex. Sensing of the R waves and pacing threshold are then checked for acceptable function. An ECG should be examined (especially lead V_1) during pacing to ensure the presence of a left bundle branch block pattern. Right bundle branch block suggests pacing from the left ventricle, which may occur if the lead crossed the atrial or ventricular septum, if the lead is inadvertently placed in one of the cardiac veins via the coronary sinus, or if the lead has perforated the heart and pacing is occurring from the left ventricular epicardium. Inadequate sensing or pacing despite a good anatomic site suggests an injured area of myocardium, though the integrity of the lead, the testing equipment, and all connections must be confirmed before repositioning. After good ventricular lead placement is achieved, it must be maintained during placement of a second lead (if applicable). Some operators place an anchoring suture at this stage. However, if the lead is nonetheless dislodged, removal of this anchoring suture is usually required for repositioning. Lead stability is improved by retaining the stylet in place while inserting the second lead; withdrawing it approximately halfway helps maintain proximal stability while reducing axial stiffness at the tip and thereby reducing the risk of perforation.

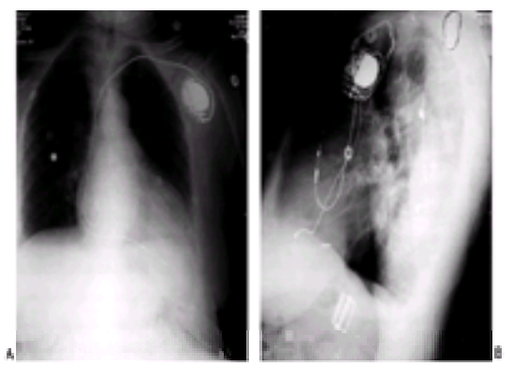

FIG. 22.18. Posteroanterior **(A)** and lateral **(B)** chest x-rays showing typical dual-chamber pacemaker placement. This patient has biventricular enlargement. The ventricular lead is in the right ventricular apex, and the atrial lead is in the right atrial appendage.

Using the retained wire as a guide, a second peel-away sheath is advanced into the vein. The atrial lead is then advanced and placed in the atrium. In the patient who has not had previous cardiopulmonary bypass (and therefore whose right atrial appendage is intact), the right atrial appendage is the ideal site for lead placement. If the lead is of the preformed “J” shape, the straight stylet may be withdrawn partially after the lead has been advanced to the right atrium. Partial withdrawal causes the lead to resume a 90° angle. Torque applied to the stylet rotates the tip of the lead to the desired anteromedial position of the right atrial appendage. Further manipulation may be necessary to ensure good contact with the endocardium. If a straight atrial lead is used, a “J”-shaped stylet is used for lead placement. The stylet is placed to produce a 90° angle in the lead, and torque applied to the stylet is used to position the lead in the desired location. The straight atrial lead is easier to manipulate using the curved stylet, making it more desirable when sites other than the right atrial appendage are likely to be explored.

A lead in the right atrial appendage has a characteristic movement with each cardiac cycle, as shown in Fig. 22.19. During atrial systole, the tip of the lead moves laterally while the loop moves medially. In the patient with no right atrial appendage, a stable site in the anterolateral right atrium is sought. In either case, we prefer active fixation for the atrial lead to minimize the risk of lead dislodgment. With stylet in place to provide some pressure against the endocardium, the helical screw electrode is rotated to engage the myocardium. Some leads have a retracted screw, which is extruded and retracted by a rotating mechanism at the proximal end of the lead. Others have a fixed helical screw, requiring rotation of the entire lead. After the electrode is screwed into the myocardium, careful withdrawal of the stylet usually confirms fixation of the electrode. In addition, when using active fixation leads we examine the electrogram from the lead to ensure atrial sensing and the presence of current indicating that the electrode has indeed penetrated the myocardium (Fig. 22.20). Sensing and pacing parameters are then checked for the ventricular lead. Care must be taken to avoid displacement of the ventricular lead during atrial lead manipulation. Acceptable implant valves are shown in Table 22.17.

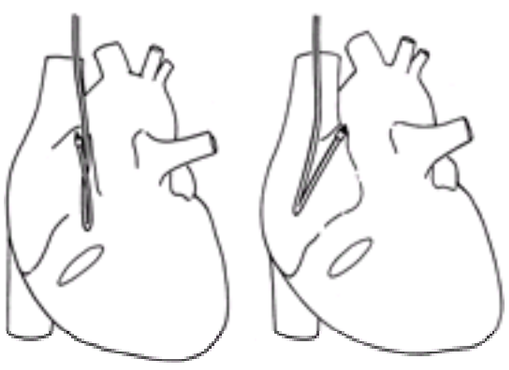

FIG. 22.19. Motion of pacing lead in the right atrial appendage. **A:** During atrial systole, the tip appears to move in a lateral direction, and the loop moves in a medial direction. **B:** During atrial diastole, the tip moves medially, and the loop moves laterally.

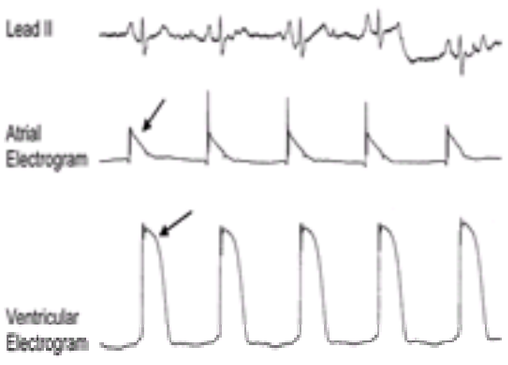

FIG. 22.20. Unfiltered bipolar electrograms obtained from leads during implantation of a dual-chamber pacemaker. Both leads were of the retractable screw type of active fixation. Lead II of the surface ECG is also shown. The tracings are simultaneous. A current of injury can be seen in both electrograms *(arrows)*.

	Atrial lead		Ventricular lead	
	desirable	Acceptable	desirable	Acceptable
Sensed P/R wave	>2.5 mV	>1.5 mV	>10 mV	>5 mV
Stimulation threshold	<1.0 V	<2.0 V	<0.7 V	<1.0 V
Impedance		400–1,000 Ω		400–1,000 Ω

Abbreviations: mV, millivolts; V, Volts; Ω ohms

TABLE 22.17. *Lead parameters at implantation*

After satisfactory positions for both leads are found, the leads should be examined under fluoroscopy while the patient inspires deeply and while he/she coughs vigorously to ensure that the lead tips are not dislodged with these actions. The leads should be examined in the left and right anterior oblique orientations to confirm the positions of the lead tips. Pacing at high output should be performed to ensure that there is no pacing of the diaphragm, particularly by the atrial lead, since the right phrenic nerve courses along the lateral right atrium. Once good positioning of both leads has been confirmed they are anchored to the deltoid and pectoralis fascia using a strong nonabsorbable suture, such as no. 0 silk. Three sutures for each lead are recommended. The sutures are tied around an anchoring sleeve that should be advanced over the lead to a position in the deltopectoral groove. Lead parameters are again checked to ensure that no detrimental change has occurred while the anchoring sutures are placed. Some improvement in capture threshold is often seen after the lead has been in place for several minutes, particularly for active fixation leads.

Pulse Generator Implantation and Pocket Closure

After further local anesthesia, a subcutaneous or submuscular pocket is made with blunt and sharp dissection, then irrigated liberally with antibiotic solution. We use a liter of saline with 1 g of vancomycin (or 1 g of cefazolin) and 80 mg of gentamicin added. The pacemaker pulse generator is connected to the lead(s), ensuring that the correct lead is placed in the correct position in the header of the generator and that the leads are secured in place. The system is then implanted into the pocket with the lead(s) coiled behind the generator to minimize the risk of damage to the leads in the event of reincision. The ECG monitor is then examined to ensure appropriate pacing and sensing. If the patient is in sinus rhythm at a rate exceeding the lower rate of the pacemaker, we place a sterile magnet over the generator to ensure that it will pace in asynchronous mode. The pocket is then closed with two layers of an absorbable suture. We typically use a continuous subcuticular stitch of absorbable suture to close the skin. We place adhesive tapes over the incision and then a gauze dressing over the area.

Pulse Generator Change

Pulse generator changes are necessary due to the finite lifetime of the pacemaker battery. The procedure is simpler than the original implantation because the leads need not be placed or moved (though great care must be taken not to damage the leads while dissecting the pacemaker generator free). A temporary transvenous pacemaker is indicated for pacemaker-dependent patients and for those at risk for profound bradycardia. In this setting, femoral vein access is the recommended route, since fluoroscopy is available, the need for transvenous pacing is brief, and the patient will be lying still for the duration of the procedure (Table 22.2).

The pacemaker lead(s) and pulse generator should be examined fluoroscopically. After administration of local anesthesia, an incision should be made that will provide access to the pacemaker pocket and that will minimize the risk of damage to the leads. This will often be the site of the previous incision. In the patient with significant amounts of scarring, the scar from the old incision can be excised with an elliptic incision.

Blunt dissection to the pacemaker pocket and careful incision of its fibrous capsule allow delivery of the generator from the pocket. After disconnection of the generator from the lead(s) using the appropriate tool, the lead parameters should *without fail* be checked to ensure lead integrity. Before implantation of the new generator, the capsule should be disrupted to prevent creation of an isolated pocket that is more likely to harbor infection. The pocket should then be irrigated with antibiotic solution. The new pulse generator is connected to the lead(s) and implanted into the pocket, which is then closed as described earlier. Before the procedure, the type of existing lead(s) and its connector type should be determined. Every effort should be made to use a new generator compatible with the lead connector type, since the use of adapters increases the risk of malfunction. The new generator must be compatible with the uni- or bipolar nature of the existing lead(s). Postprocedure wound care, including prophylactic antibiotic therapy, is similar to postprocedure care for a patient undergoing an original implant. An overnight hospital stay is unnecessary in the uncomplicated case, since the leads are chronic and the risk for dislodgment is low.

Before any procedure in which the pacemaker generator is manipulated, the pacemaker should be interrogated. Rate responsiveness should be programmed *off* to prevent an inappropriate increase in pacing rate with manipulation of the generator. Electrocautery should be minimized to prevent damage to leads and to prevent inappropriate inhibition of pacing, which may be dangerous in the pacemaker-dependent patient. Vigilance is required, and it is often necessary to program the temporary pacemaker to pace asynchronously during use of cautery.

In the case of procedures involving previously implanted ICDs, electrocautery or manipulation of the generator may be sensed by the ICD as tachycardia or fibrillation, prompting inappropriate therapy. Therefore the ICD detection and/or therapy should be programmed *off* to avoid inappropriate shocks by the ICD.

Techniques Specific to ICD Implantation

Surgical approaches for implantation of epicardial patches include the anterolateral thoracotomy, subcostal thoracotomy, subxiphoid, and median sternotomy (96). As stated earlier, this approach has been essentially abandoned since the development of the transvenous system.

The first transvenous systems required abdominal implant due to the size of the pulse generator. Transvenous leads were tunneled subcutaneously to the abdomen. Additionally, since early devices used monophasic waveforms for defibrillation, subcutaneous patches or arrays were often required to achieve adequate DFT. Abdominal implants are now placed rarely, and usually only in patients in whom a pectoral implant would carry significant risks of pocket erosion, in patients with previous multiple pectoral pocket infections, or in patients whose anatomy preludes pectoral implants. By the early 1990s, the size of the pulse generator had decreased sufficiently to allow for pectoral implantation. With the device in this location, the large surface area of the pulse generator could be used as an active electrode, which resulted in further lowering of DFT to the range seen with epicardial implantation (97,98 and 99). Currently, left pectoral implants using techniques similar to those used with pacemaker implants are the first choice for most institution. Right pectoral locations can be used but are often associated with slightly higher DFT, due to the greater distance from the heart. Occasionally, submuscular implants are desired by some patients for cosmetic purposes. However, this location may be associated with increased complications of bleeding, damage of the thoracoacromial nerves, and pectoralis major atrophy (100), as well as discomfort due to muscle sliding over the pulse generator.

Initially, ICDs were implanted by cardiothoracic surgeons in the operating room, and this practice continues in some hospitals. However, in most institutions today with an active electrophysiology program, implantation of ICDs has become the responsibility of electrophysiologists. Implantation under ocal anesthesia combined with intravenous sedation, performed by electrophysiologists in a laboratory with air-filtering facilities similar to those used in the operating room, has been shown to have high success and low complication rates, short implantation and fluoroscopy time, and is associated with earlier discharge from the hospital (101,102).

Connecting ICD leads to the device is slightly different from connecting pacemaker leads to pacemaker generators. All ICD pulse generators have at least three ports. One is for the sense/pace conductor, and one for the defibrillation coil. The third port can be connected to a second defibrillation lead, such as SVC coil or subcutaneous patch, or may be capped if only one defibrillation coil is used. The newest-generation dual-chamber ICDs have a fourth port, for the atrial sense/pace lead.

Defibrillation Testing at the Time of ICD Implantation

Fundamental to successful ICD implantation is the ability to reliably sense and reproducibly defibrillate VF. Therefore meticulous testing of leads and device function must be carried out at the time of implant. The lead must be tested for adequate sensing in sinus rhythm, as assessed by R-wave amplitudes, which should be no less than 5 to 6 mV and preferably greater than 10 mV. Care must be taken to obtain a stable lead position and to rule out oversensing of myopotentials and diaphragmatic pacing. Pacing threshold must also be acceptably low to ensure reliable backup pacing after defibrillation. Repositioning of the lead must be carried out if any of the parameters are unsatisfactory.

An important part of ICD implantation procedure that is not part of pacemaker implantation is the testing of the device to determine DFT. This is generally performed before closing the wound, after satisfactory lead positions and parameters are obtained, the leads are connected to the ICD, and the system is implanted into the subcutaneous pocket. In our laboratory, anesthesia is often administered by the Anesthesiology Service, usually using short-acting agents such as Propofol. However, conscious sedation with a combination of narcotics and benzodiazepines can be used effectively. The testing is usually performed through a programmer, with a sterile programming wand placed over the implanted pulse generator. Occasionally, testing may be performed through an emulator, which substitutes for the actual pulse generator and connects the defibrillation lead to the programmer. This allows for the decision regarding the ICD model used to be made after the DFT is determined. An initial low-energy (1 to 2 J) synchronized shock may be utilized to ensure that all connections are intact and to determine the high-voltage lead impedance before VF induction. VF is commonly induced by critically timed T-wave shocks or high-frequency pacing. Alternatively, rapid-burst pacing at 50 Hz can be delivered, with the length of time of delivery at the discretion of the operator.

The DFT may be determined in several ways. The DFT testing protocol uses a series of inductions to determine the lowest energy that produces successful defibrillation. For example, with a device capable of a maximum energy output of 34 J, one may begin the test with a shock at 24 J. If successful, then a shock at 12 J can be tested, decreasing to 6 J or even 3 J. The lowest energy that successfully defibrillates VF is the DFT. This method more accurately determines DFT, but multiple VF inductions are needed. Alternatively, the margin-verification protocol requires testing of one selected energy that would allow for an adequate safety margin without having to determine the lowest energy that would successfully defibrillate. Fewer numbers of VF inductions are needed with the latter method and may be used in patients who may not tolerate repeated episodes of VF. In most patients, however, we favor the “step-down” approach because having at least one shock that fails to defibrillate allows for redetection also to be tested. Redetection problems are encountered more frequently with integrated bipolar sensing leads than with true bipolar sensing leads. During testing, we choose to set the second shock at device maximum output. If the first shock fails, the device is allowed to redetect VF and deliver a second shock, and if this fails, we deliver a 360-J shock externally. Usually, 5-minute intervals are allowed between each VF induction.

In addition to sensing, pacing, and determination of DFT, other parameters, such as the impedance and charge time, must also be assessed during intraoperative testing to ensure that the device is performing adequately. If an unacceptable value is repeatedly obtained during testing, replacement of the lead, or the device, may be necessary. Charge time is the time needed to charge the capacitor for energy delivery and may vary with generators, but should be short (less than 10 seconds) for new and well-functioning devices.

When adequate DFT is not achievable with a single-coil endocardial lead, reversing shocking polarity by designating the RV lead as the anode and the active can as the cathode may occasionally lower DFT. Also, repositioning the lead to be as close to the RV apex as possible may help to lower shocking energy. Alternatively, using another electrode in the SVC by changing to a dual-coil lead or by inserting a separate SVC or CS lead, or adding a subcutaneous patch or array, may be helpful. With today's devices, a subcutaneous patch or array is rarely required. The entire system should be implanted and the wound closed only after satisfactory sensing in both sinus rhythm and VF is verified, pacing thresholds are low, and lead impedances are acceptable. Because of the possibility of increases in the required defibrillation energy over time due to fibrosis around the tip of the lead, migration of the lead, changes in underlying cardiac status, or addition of antiarrhythmic drugs, a safety margin must be added to the DFT to compensate for future changes. This can usually be accomplished by adding 7 to 10 J to the DFT when programming therapies (103).

An important note should be mentioned regarding patients who have separate permanent pacemakers and ICDs. If pacing spikes are large, ICDs may sense pacer stimulus artifacts and count them as R waves, which would lead to “double-counting” and may trigger inappropriate shocks. A more significant concern is that electrograms from VF are often small and may not be sensed by the pacemaker, thus triggering pacing. The pacing spikes may reset the amplifier (decrease the gain) of the ICD, which may result in failure to sense VF. Unipolar leads are particularly problematic, since they produce large pacing spikes. For this reason, implantation of a unipolar pacing lead is absolutely contraindicated in patients with preexisting ICD. During intraoperative testing of a new ICD system in the setting of an existing pacemaker, the pacemaker should be programmed to full output (maximum amplitude and pulse width), pacing at either DOO or VOO mode to maximize pacer stimulus artifact size. If the pacemaker lead is not a committed bipolar lead, then it should be reprogrammed to unipolar during testing. The ICD is programmed at the least sensitive setting, to set up a worst-case scenario. Testing of the ICD must then include determination that these spikes do not interfere with VF sensing. Alternatively, the preexisting pacemaker may be extracted and a dual-chamber ICD implanted to avoid pacemaker/ICD interactions.

Postprocedure Care After successful pacemaker or ICD implantation, the primary risk in the early postprocedure period is lead dislodgment. Therefore we place the arm ipsilateral to the implant in a sling and keep the patient at bedrest overnight. After 24 hours the patient is encouraged to move the arm but is admonished not to lift any object weighing more than 10 pounds and not to raise the arm above shoulder level for 6 weeks. Anticoagulation is withheld for several hours to minimize the risk of bleeding and hematoma in the pocket.

As noted earlier, we prescribe prophylactic antibiotic therapy for 48 hours after implantation. Intravenous antibiotics may be switched to an oral equivalent if the patient is to be discharged before the end of 48 hours.

Before discharge, the pacemaker (or ICD) is interrogated to ensure that no marked changes in lead impedance, pacing threshold, or sensing have occurred. Such changes raise the possibility of lead dislodgment. A posteroanterior and lateral chest x-ray is also examined for stability of lead placement. As noted earlier, a portable chest x-ray is taken immediately after the procedure in the case of subclavian vein cannulation to exclude pneumothorax as well as to verify lead position. An immediate postprocedure chest x-ray does not change the need for the posteroanterior and lateral chest x-ray the following day. The patient is then asked to follow up in the Pacemaker Clinic 7 to 10 days after implant to evaluate wound healing and to interrogate the device.

There is controversy about whether routine noninvasive programmed stimulation (NIPS) is necessary before discharge of the ICD patient, to test for acute changes in DFT or lead problems. One study noted that in 97 patients undergoing routine predischarge testing, three had ineffective shocks at maximum device energy, despite an adequate safety margin during implant. No change in lead positions was detected on chest x-rays or under fluoroscopy in those patients (104). However, the devices implanted in that study were abdominal units, and these problems may be less likely with implantations of active can generators. At our institution, we do not routinely perform NIPS before discharge if lead positions are verified by chest x-ray and interrogation of the device is satisfactory.

Complications As stated earlier, the risk associated with transvenous implantation of a permanent pacemaker or ICD is low (101,105,106). Nonetheless, complications do occur, and the patient should be apprised of the risks in the informed consent process before the procedure.

The patient should be told of the risk of bleeding and vascular injury inherent in any vascular procedure. Placement of leads is often accompanied by ectopy. Sustained tachycardia requiring therapy is rare, and it is uncommon that urgent cardioversion or defibrillation is necessary. However, personnel should be prepared to treat atrial and ventricular arrhythmias induced by lead manipulation.

There is a small risk of perforation of the thin-walled right ventricle or atrium with the leads. Vigilance is necessary and the index of suspicion for pericardial tamponade should be high during and after the procedure. Tamponade may present as an apparent “vagal” episode, though the heart rate will be supported by the pacemaker. Since bradycardia and chronotropic incompetence are common indications for pacemaker implantation, the tachycardia that typically accompanies pericardial tamponade may be absent in the pacemaker patient.

As noted earlier, there is a risk of pneumothorax associated with subclavian vein puncture, and a portable chest x-ray is recommended after implantation using the subclavian vein for access.

Lead dislodgment is most likely to occur early after implantation (within a day). Therefore pacemaker interrogation and chest x-ray are recommended the day following the procedure. In the event of lead dislodgment, lead revision should be carried out as soon as feasible to minimize the scarring and fibrosis around the lead. When the inflammatory response has progressed far, lead revision and/or extraction becomes more difficult and risky.

The most feared complication of pacemaker implantation is infection. If there is evidence of systemic infection (fever, positive blood cultures), removal of the entire

system (pacemaker and lead[s]) is indicated to allow antibiotic therapy to clear the infection completely. This situation is even more unfortunate in the pacemaker-dependent patient, in whom a temporary pacemaker is often required between the time of removal of the infected system and implantation of a new one. The gravity of the risk of infection should serve to emphasize the need for attention to sterile technique, both at primary implantation and during generator change. Some procedure-related complications are listed in Table 22.18.

Early complications	Infection Bleeding Pneumothorax/hemothorax Air embolism Arterial cannulation Perforation of heart/tamponade Atrial fibrillation Heart block induced by contact with conduction system Deep vein thrombosis Lead damage/fracture Lead dislodgment Ventricular tachycardia Pocket hematoma Incorrect connection of leads to pulse generator
Late complications	Lead dislodgment Erosion of skin over pocket Pain Infection Lead fracture Lead insulation failure Infection Migration of pulse generator Twisting and fracture of leads due to manipulation of generator—Twiddler's syndrome

TABLE 22.18. *Complications of transvenous pacemaker or ICD implantation*

Limitations of the Pacemaker or ICD Patient

Pacemaker implantation is intended to free the patient from health-related limitations, not impose additional ones. Patients, however, are frequently anxious that their "condition" of having an implanted device will result in more illness, not less. The patient should be reassured that after recovery from the implantation procedure, with the limitations discussed earlier (see " Postprocedure Care"), he or she should be able to proceed with the normal activities of life.

The single most important limitation is that magnetic resonance imaging is contraindicated, since exposure to the strong magnetic field may affect device function unpredictably. Similarly, exposure to other high electromagnetic fields, such as those produced by arc welding, is contraindicated. Activities that cause direct trauma to the pulse generator are contraindicated.

Recent policies on driving advise patients with ICDs to avoid operating a vehicle for a minimum of 3 months, preferably 6 months, after the last symptomatic arrhythmic event, or until a stable pattern of VT/VF can be established (107).

High-dose radiation therapy directly to the pulse generator can damage the device. In the case of the patient whose neoplasm is located such that the pacemaker cannot be kept out of the field, it may be necessary to relocate the pulse generator. An entirely new device can be implanted from the opposite side, or the pulse generator may be placed in the abdomen and the lead(s) tunneled to the new site.

Medical equipment such as x-ray equipment and computed tomography scanning equipment do not interfere with ICDs or pacemakers. Similarly, common household appliances should have no effect on the devices. Many patients are concerned about exposure to microwave ovens. Modern microwave ovens are well shielded, however, and pose no threat to the pacemaker or ICD patient. There has been recent concern about airport metal detectors and antishoplifting devices. One publication reported multiple shocks delivered to a patient with an ICD who had inadvertently stood within an antitheft device for a prolonged period of time (108). Usually, however, antitheft devices or airport security systems do not cause interference problems if the patient does not linger within the device itself. Similarly, it is possible that such a device might inhibit a pacemaker, though only temporarily. Like ICD patients, pacemaker patients should avoid long periods in close proximity to such devices.

Recent concern has been raised about the effect of cellular phones on pacemakers and ICDs. A study to address this problem concluded that ordinary use of a cellular phones poses very low risk for malfunction (109). Holding a cellular phone directly over the device is not recommended. All hand-held electronic devices should be kept more than 6 inches away from the device.

Transthoracic defibrillation may damage the circuits of an implanted device if very high output is used or if the electrodes are in close proximity to the pulse generator. When transthoracic shocks take place, the electrodes should be placed at least a few inches away from the pulse generator, and it is recommended that the device be interrogated after transthoracic defibrillation has taken place.

Care and Follow-up of the Patient with a Permanent Pacemaker or ICD

Routine Pacemaker Follow-up

After the first follow-up visit to ensure adequate wound healing and consistency of sensing and thresholds, further follow-up should occur periodically. Interrogation of the pacemaker is discussed later. The Pacemaker Clinic visits following the first visit for a wound check can be timed to follow the postimplantation threshold rise. For example, a 1-month visit would be near the peak of the threshold rise. Another visit at 3 months would coincide with the threshold reaching the chronic state. The output of the pacing stimulus can then be reduced (maintaining an adequate safety margin) to maximize battery life.

Routine follow-up should always include a history of any new symptoms as well as an examination of the pocket site for erythema, edema, tenderness, or threatened erosion.

Transtelephonic follow-up can be used to follow battery status. A single-lead rhythm strip can be transmitted over the phone with and without a magnet applied to the pulse generator. The Pacemaker Clinic personnel can monitor for malfunction detectable by ECG. The ECG recorded while the magnet is applied gives an indication of the battery status for most pacemakers (see later discussion).

As the battery life declines, the *elective replacement indicator* (ERI) is signaled. Plans should be made at this time to undergo pulse generator change. At *end of life* (EOL), the mode of most pacemakers changes to signify need for generator change, which should proceed as soon as possible.

Routine ICD Follow-up

After discharge, all patients with ICDs must have regular, meticulous follow-up to ensure proper functioning of the system. Generally, the first follow-up visit is scheduled within 1 or 2 weeks after time of implant, to check that the wound is healing properly and that leads have not dislodged. Follow-up visits afterward should take place approximately every 3 to 6 months. During these visits, the patients are interviewed as to whether the device has delivered any shocks and whether the patients had any symptoms before the shocks. A review of all current medications is necessary because of the potential effects of all antiarrhythmic agents on the defibrillation threshold. Interrogation of the device should include checking the battery status, assessing sensing and pacing parameters, evaluating event logs to record the number of sustained and nonsustained ventricular arrhythmias, as well as the number of delivered and aborted shocks. Current devices are capable of automatically reforming capacitors. In older devices, however, manual reformation of capacitors is performed during interrogations.

Noninvasive testing during follow-up is performed in patients who have begun a new antiarrhythmic agent, to ensure adequate safety margin of DFT on the medication. Data on routine noninvasive testing in patients who have never received any shocks from the device are controversial, but many support annual testing to assess the integrity of the system (110).

Magnet Application

Pacemakers

Placement of a magnet over a pacemaker pulse generator can be a therapeutic, diagnostic, or prophylactic maneuver. Therapeutic use, as in pacemaker-mediated tachycardia, has already been discussed. The diagnostic and prophylactic uses of magnet application lie in its inhibition of all sensing.

Application of a magnet over the pacemaker pulse generator temporarily changes its mode to asynchronous (DOO, VOO, or AOO). The rate will vary from model to model and will change as the battery status changes. These changes are specific to each manufacturer and in many cases are related to the programmed rate. Armed with appropriate information from the manufacturer, the magnet rate can therefore be used as a simple method to evaluate the battery status, and this method is commonly used for transtelephonic pacemaker follow-up.

Magnet application is prophylactic whenever there is a risk of inhibition due to inappropriate sensing. A common example is the use of electrocautery for surgical procedures. The pacemaker in the inhibited mode may sense the electrocautery, and pacing will be inhibited. The likelihood of inappropriate sensing is reduced by the use of bipolar leads. In magnet mode, the pacemaker will not sense any activity and will pace asynchronously. Extracorporeal shock-wave lithotripsy (ESWL), electroconvulsive therapy (ECT), and electrical cardioversion are other instances in which electric fields are brought into close contact with the patient. As with electrocautery, the risk of serious interaction, such as reprogramming or permanent damage, with the pacemaker is small, particularly if the stimulus is far from the pulse generator and electrodes. Inhibition of pacing due to inappropriate sensing of the stimulus remains a risk. Short durations of stimulus can limit the inhibition to a few cardiac cycles at a time. As with cautery, however, magnet application is a simple way to eliminate inappropriate inhibition. *Noise reversion* circuits provide a further safety feature. If electrograms are sensed at a rate faster than the noise reversion rate, the pacing mode is changed to an asynchronous one. The noise reversion mode will persist until the pacemaker is reprogrammed. Interrogation of the pacemaker to ensure appropriate programming and function after any procedure using electrical equipment is reasonable. In the absence of any sign of malfunction, interrogation can be done on an elective basis.

Complications of asynchronous pacing are rare, though some may worry about the risk of induction of ventricular arrhythmia. It is true that ventricular fibrillation is reliably induced by a shock timed to fall on the T wave for ICD testing. The amplitude of such a shock is usually 1 J or more orders of magnitude greater than that of a pacemaker stimulus.

ICDs

External stimuli can often result in oversensing and can trigger delivery of inappropriate shocks to the patient. For this reason when patients with ICDs undergo any surgery in which electrocautery will be used, they should have their device inactivated or have the detection suspended. The safest method is to turn off detection via a programmer. When the programmer is not available, a magnet may be used to suspend detection and therapy temporarily. When a magnet is applied over an ICD, detection and therapy will be suspended without affecting antibradycardia pacing. For most of the commonly used ICDs, such as Medtronic, Intermedics, Ventritex, and Telectronics models, all detection and therapy are resumed when the magnet is removed. The new CPI devices, such as the Ventak Mini and AV series, behave slightly differently in response to magnet application. As with ICDs from other manufacturers, a magnet applied over CPI devices will temporarily inhibit detection and therapy. However, CPI devices have an optional “change tachy mode with magnet” feature that can be programmed on or off. When this feature is off, the ICD behaves similar to models from other manufacturers and will resume detection and therapy once the magnet is removed. If the “change tachy mode with magnet” feature is on, a magnet placed over the ICD for more than 30 seconds will permanently inactivate the device. A magnet placed over these devices will also produce an audible tone, which is synchronized to R waves when the device is active and continuous if the device is inactive. Listening to the tone is one method of determining whether the device has been permanently inactivated by the magnet. Interrogation of the device after removal of a magnet to ensure that there has been no change in the programming is always prudent.

Interrogation of the Pacemaker or ICD

The cardiology consultant is often asked to “interrogate” a pacemaker or ICD to rule out any malfunction because of symptoms in a patient who has an implanted device. In the case of a pacemaker, the consulting physician may be searching for a cause of symptoms apparently related to bradycardia, such as syncope, lightheadedness, and dyspnea. If there is no evidence of malfunction on ECG or telemetry, the search for malfunction can only be general. If there is electrocardiographic evidence of a specific failure (e.g., failure to capture or failure to sense), the search for the cause and solution may be more focused. In the case of an ICD, interrogation may be prompted by inappropriate antitachycardia therapy or by concern for malfunction in antibradycardia pacing.

Sometimes there is a desire to make a specific change in the programming of the device, rather than seek a malfunction. Examples include changing the mode or the rate. The detection criteria for tachyarrhythmia or the nature of antitachycardia therapy can be changed in an ICD. In pacemakers with rate responsiveness, its “aggressiveness” can be adjusted. That is, the rate and degree of acceleration and deceleration of the lower pacing rate can be adjusted. Exercise testing can be of assistance in optimizing these settings. In the patient who has experienced endless-loop tachycardia, the PVARP should be adjusted or the PMT intervention should be turned on. In the absence of any suspected failure, the desired changes can be made without seeking malfunction.

The technical details of interrogation vary with the programmer, and some experience is necessary (preferably with a knowledgeable tutor) to gain facility with each one. However, the principles of interrogation are the same regardless of manufacturer. If the goal is simply to screen for malfunction, the basic functions and parameters must be checked. Unfortunately, a detailed discussion of this procedure is beyond the scope of this chapter.

Troubleshooting

A complete list of possible problems is beyond the scope of this chapter. Some common ones are listed here. Some are remediable by programming; others need more extensive intervention.

Undersensing

Undersensing is usually manifested by the appearance of stimulus artifacts despite the presence of ECG signs of intrinsic activity in the chamber in question (i.e. P waves or QRS complexes). The amplitude of the sensed electrograms can be determined by interrogation (see earlier discussion). Notice that *reducing* the value (in millivolts) of the sensitivity setting *increases* sensitivity (and vice versa).

Some possible causes of undersensing are the following:

- Lead dislodgment with loss of contact between the electrode and the endocardium, usually accompanied by loss of capture or increase in capture threshold.
- Lead insulation deterioration. If the body of the lead is exposed, the exposed portion acts an electrode, and the “electrogram” (or lack thereof) attenuates the electrogram signal from the true electrode.
- Inflammatory reaction. The inflammation initiated by lead implantation can affect sensing as well as pacing by insulating the electrode from the myocardium.
- Decrease in amplitude of the electrogram. This may be reversible, as in the case of added medication (especially antiarrhythmic agents) or metabolic abnormalities, such as hyperkalemia or acidosis. Alternatively, the cause may be irreversible, as in the case of progressive cardiomyopathy or new myocardial infarction.
- Programming error. This error can be avoided by carefully reviewing the programmed parameters when finishing a programming session.

In some cases, these problems may only be remedied by invasive correction, such as revising or replacing the lead. In other cases, reprogramming the sensitivity can correct the problem. Nominal sensitivity of the atrial channel is usually 0.5 to 1.0 mV; for the ventricular channel, 1.5 to 2.5 mV is typical. For most pacemakers the sensitivity can be increased if undersensing occurs.

Oversensing

Oversensing is manifest on the surface ECG by the absence of an expected pacing stimulus artifact. A pacing spike is expected when a pause exceeds the length allowed by the pacemaker's lower rate limit. It should be kept in mind that bipolar pacing spikes may be very low amplitude and may not be visible in all leads. Both

physiologic phenomena and extrinsic signals may be inappropriately sensed as electrograms.

- Myopotential sensing. Skeletal muscle myopotentials are rarely sensed in bipolar lead systems, but this problem may occur in unipolar systems with high sensitivity settings.
- T-wave sensing. Usually, the T-wave amplitude is low relative to the R wave, and adjustment of the sensitivity is effective.
- Lead fracture. Intermittent contact of the lead fragments can create noise; the amplitude may be high enough to be sensed as electrograms.
- Inner insulation failure. This may allow contact between the conductor of the two electrodes in a bipolar lead, and the resulting noise may be inappropriately sensed.
- External electromagnetic interference. External signals may be inappropriately sensed as electrograms. These include surgical electrocautery, magnetic resonance imaging, extracorporeal shock wave lithotripsy, transcutaneous nerve stimulation, radiofrequency ablation, and arc welding. These sources of inappropriately sensed impulses are rarely difficult to diagnose. As discussed earlier, temporary programming to asynchronous pacing (as with magnet application) may be appropriate in some cases (e.g., magnetic resonance imaging).
- Inappropriate programming.

Oversensing can be disastrous in the case of a pacemaker-dependent patient. If oversensing results in complete inhibition of pacing, magnet application is the appropriate immediate action. Pacing will be asynchronous, and the oversensed signals will be irrelevant. The sensitivity should be checked with the programmer and reprogrammed if indicated. Further evaluation, including interrogation of lead impedance and examination of the chest x-ray for fracture, is required.

Abnormal Lead Impedance

Abnormally high lead impedance suggests a discontinuity in the circuit of the lead in question. The most likely cause is fracture of the lead. The two parts of the divided lead may be in contact intermittently, which may make the abnormal lead impedance (and failure) intermittent. If the lead fragments are separated by air, the impedance will approach infinity and will not function.

Abnormally low lead impedance suggests a short circuit in the system. This may be due to loss of integrity of the lead insulation, lead dislodgment, or lead perforation.

Lead failure can rarely be solved merely by programming. Dislodged leads can be revised, but fractured leads must be replaced. Insulation failure is often in the part of the lead in the pacemaker pocket and results from friction against the pulse generator. These failures can be sought and often repaired. If the damage cannot be found or malfunction persists after repair, the lead must be replaced to regain full function. If a bipolar lead has damaged outer insulation, the distal electrode (and inner conductor) can be used as a unipolar lead (if the pulse generator is capable of unipolar pacing).

High Capture Threshold

The pacing stimulus output should exceed the capture threshold with a comfortable safety margin. For a chronic lead (older than 8 weeks) the safety margin should be twice the amplitude threshold or three times the pulse width threshold. An acute change in the threshold of a chronic lead raises the possibility of disruption of the system. Lead impedance should be checked and a chest x-ray should be obtained to exclude lead dislodgment.

The possibility of perforation of the myocardium by the lead should be borne in mind. Good sensing with poor pacing may be a sign of perforation, since the ring electrode of a bipolar lead is likely to remain in contact with the myocardium when the tip of the lead has advanced through to the ventricular wall. Pacing of the diaphragm at relatively low outputs is also a strong indicator that the lead has perforated.

As noted earlier, an acute (4 to 6 weeks) threshold rise is common after lead implantation. Therefore higher output should be programmed at the time of implantation. Some medications and electrolyte imbalances may change pacing thresholds, making a greater margin of safety desirable in patients likely to undergo changes in these factors.

Battery Depletion

Pulse generator change should occur soon after the ERI (elective replacement indicator) appears, since battery depletion to this extent does not change pacemaker function. In some pacemakers, when the battery reaches EOL (end of life), there is a change in the rate and/or mode, which may be symptomatic. The modes and rates are specific to individual pacemakers. These need not be memorized, since an unexpected change of mode should prompt interrogation. Battery depletion should not come as a surprise under normal circumstances with good follow-up. However, if some change occurs that dramatically increases current used to pace (such as a large decrease in lead impedance), the rate of battery depletion may increase rapidly. Only rarely will battery depletion cause frank failure. In this case, the programmer may no longer be able to communicate with the pacemaker. Such a failure can be catastrophic in the pacemaker-dependent patient; therefore the follow-up should be particularly frequent as the life of the battery nears its end.

CHAPTER REFERENCES

1. Fogoros RN. *Electrophysiologic testing,* 2nd ed. Oxford: Blackwell Science, 1995.
2. Josephson ME. *Clinical cardiac electrophysiology: techniques and interpretations,* 2nd ed. Philadelphia: Lea & Febiger, 1993.
3. Zipes DP, Jalife J, eds. *Cardiac electrophysiology: from cell to bedside,* 2nd ed. Philadelphia: WB Saunders, 1995.
4. Zoll PM. Resuscitation of the heart in ventricular standstill by external electrical stimulation. *N Engl J Med* 1952;247:768.
5. Furman S, Schweidel JB. An intracardiac pacemaker for Stokes-Adams seizures. *N Engl J Med* 1959;261:943.
6. Gregoratos G, Cheitlin MD, Conill A, et al. ACC/AHA Guidelines for Implantation of Cardiac Pacemakers and Antiarrhythmia Devices: A Report of the American College of Cardiology/American Heart Association Task Force on Practice Guidelines (Committee on Pacemaker Implantation). *J Am Coll Cardiol* 1998;31:1175.
7. Ryan TJ, Anderson JL, Antman EM, et al. ACC/AHA Guidelines for the management of patients with acute myocardial infarction: a report of the American College of Cardiology/American Heart Association Task Force on Practice Guidelines. *J Am Coll Cardiol* 1996;28:1328.
8. Fiegl D, Ashkenazy J, Kishon Y. Early and late atrioventricular block in acute inferior myocardial infarction. *J Am Coll Cardiol* 1984;4:35.
9. Hindman MC, Wagner GS, Ja Ro M, et al. The clinical significance of bundle branch block complicating acute myocardial infarction. 1. Clinical characteristics, hospital mortality, and one year follow-up. *Circulation* 1978;58:679.
10. Maveric Z, Zaputovic L, Matana A, et al. Prognostic significance of complete atrioventricular block in patients with acute inferior myocardial infarction with and without right ventricular involvement. *Am Heart J* 1990;119:823.
11. Topol EJ, Goldschlager N, Ports TA, et al. Hemodynamic benefit of atrial pacing in right ventricular myocardial infarction. *Ann Intern Med* 1982;96:594.
12. Kim YH, O'Nunain S, Trouton T, et al. Pseudopacemaker syndrome following inadvertent fast pathway ablation for atrioventricular nodal reentrant tachycardia. *J Cardiovasc Electrophysiol* 1993;4:178.
13. Barold SS. Indications for permanent cardiac pacing in first degree AV block: class I, II, or III? *Pacing Clin Electrophysiol* 1996;19:747.
14. Dhingra RC, Denes P, Wu D, Chuquimia R, Rosen KM. The significance of second degree atrioventricular block and bundle branch block: observations regarding site and type of block. *Circulation* 1976;49:638.
15. Dubois C, Pierard LA, Smeets JP, Carlier J, Kulbertus HE. Long-term prognostic significance of atrioventricular block in inferior acute myocardial infarction. *Eur Heart J* 1989;10:816.
16. Nicod P, Gilpin E, Dittrich H, Polikar R, Henning H, Ross J Jr. Long-term outcome in patients with inferior myocardial infarction and complete atrioventricular block. *J Am Coll Cardiol* 1988;12:589.
17. Goldberg RJ, Zevallos JC, Yarzebski J, et al. Prognosis of acute myocardial infarction complicated by complete heart block. *Am J Cardiol* 1992;69:1135.
18. Clemmensen P, Bates ER, Califf RM, et al. Complete atrioventricular block complicating inferior wall acute myocardial infarction treated with reperfusion therapy. *Am J Cardiol* 1991;67:225.
19. Col JJ. The incidence and mortality of intraventricular conduction defects in acute myocardial infarction. *Am J Cardiol* 1972;29:344.
20. Eldar M, Griffin JC, Abbott JA, et al. Permanent cardiac pacing in patients with the long QT syndrome. *J Am Coll Cardiol* 1987;10:600.
21. Eldar M, Griffin JC, Van Hare GF, et al. Combined use of beta-adrenergic blocking agents and long-term cardiac pacing for patients with the long QT syndrome. *J Am Coll Cardiol* 1992;20:830.
22. Jackman WM, Friday KJ, Anderson JL, et al. The long QT syndromes: a critical review, new clinical observations, and a unifying hypothesis. *Progr Cardiovasc Dis* 1988;31:115.
23. El-Sherif N, Bekheit SS, Henkin R. Quinidine-induced long QTU interval and torsade de pointes: role of bradycardia-dependent early afterdepolarizations. *J Am Coll Cardiol* 1989;14:252.
24. Sutton R, Petersen M, Brignole M, Raviele A, Menozzi C, Giani P. Proposed classification for tilt-induced vasovagal syncope. *Eur J Card Pacing Electrophysiol* 1992;2:180.
25. Ruiz GA, Scaglione J, Gonzalez-Zuelgaray J. Reproducibility of head-up tilt test in patients with syncope. *Clin Card* 1996;19:215.
26. Brooks R, Ruskin JN, Powell AC, Newell J, Garan H, McGovern BA. Prospective evaluation of day-to-day reproducibility of upright tilt table testing in unexplained syncope. *Am J Cardiol* 1993;71:1289.
27. Wigle ED, Rakowski H, Kimball BP, Williams WG. Hypertrophic cardiomyopathy—clinical spectrum and treatment. *Circulation* 1995;92:1680.
28. Fananapazir L, Cannon RO, Tripodi D, Panza JA. Impact of dual-chamber permanent pacing in patients with obstructive hypertrophic cardiomyopathy with symptoms refractory to verapamil and beta-adrenergic blocker therapy. *Circulation* 1992;85:2149.
29. Fananapazir L, Epstein ND, Curiel RV, Panza JA, Tripodi D, McAreavey D. Long-term results of dual-chamber (DDD) pacing in obstructive hypertrophic cardiomyopathy; evidence for progressive symptomatic and hemodynamic improvement and reduction of left ventricular hypertrophy. *Circulation* 1994;90:2731.
30. McDonald K, McWilliams E, O'Keefe B, Maurer B. Functional assessment of patients treated with permanent dual chamber pacing as a primary treatment for hypertrophic cardiomyopathy. *Eur Heart J* 1988;9:893.

31. Jeanrenaud X, Goy JJ, Kappenberger L. Effects of dual-chamber pacing in hypertrophic obstructive cardiomyopathy. *Lancet* 1992;339:1318.
32. Nishimura RA, Trusty JM, Hayes DL, et al. Dual-chamber pacing for hypertrophic cardiomyopathy: a randomized, double-blind, crossover trial. *J Am Coll Cardiol* 1997;29:435.
33. Gold MR, Feliciano Z, Gottlieb SS, Fisher ML. Dual-chamber pacing with a short atrioventricular delay in congestive heart failure: a randomized study. *J Am Coll Cardiol* 1995;26:967.
34. Innes D, Leitch JW, Fletcher PJ. VDD pacing at short atrioventricular intervals does not improve cardiac output in patients with dilated heart failure. *Pacing Clin Electrophysiol* 1994;17:959.
35. Cazaeu S, Ritter P, Lazarus A, Gras D, Mujica J. Multisite pacing for congestive heart failure. *Pacing Clin Electrophysiol* 1996;19:568.
36. Saxon LA, Cahalan MK, Merrick SH, et al. Effects of multi-site ventricular pacing in dilated cardiomyopathy. *Pacing Clin Electrophysiol* 1996;19:641.
37. Attuel P, Pellerin D, Mugica J, Coumel P. DDD pacing: an effective treatment modality for atrial arrhythmias. *Pacing Clin Electrophysiol* 1979;11:1647.
38. Saksena S, Prakash A, Hill M, et al. Prevention of recurrent atrial fibrillation with chronic dual site right atrial pacing. *J Am Coll Cardiol* 1996;28:687.
39. Anderson KM, Moore AA. Sensors in pacing. *Pacing Clin Electrophysiol* 1986;9:954.
40. Matula M, Alt E, Fotuhi P, et al. Influence of varied types of exercise on the rate adaptation of activity pacemakers. *Pacing Clin Electrophysiol* 1992;15:578.
41. Mond H, Strathmore N, Kertes P, et al. Rate responsive pacing using a minute ventilation sensor. *Pacing Clin Electrophysiol* 1988;11:1886.
42. Alt E, Heinz M, Hirgsletter C, et al. Control of pacemaker rate by impedance-based respiratory minute ventilation. *Chest* 1987;92:247.
43. Griffin JC, Jutzy KR, Claude JP, et al. Central body temperature as a guide to optimal heart rate. *Pacing Clin Electrophysiol* 1983;6:498.
44. Sugiura T, Kimura M, Shizui M, et al. Cardiac pacemakers regulated by respiratory rate and blood temperature. *Pacing Clin Electrophysiol* 1989;11:1077.
45. Richards AF, Donaldson RM, Thalen HJT. The use of QT interval to determine pacing rate: early clinical experience. *Pacing Clin Electrophysiol* 1983;6:346.
46. Oda E. Changes in QT interval during exercise testing in patients with VVI pacemakers. *Pacing Clin Electrophysiol* 1986;9:36.
47. Wirtzfeld W, Heinze R, Stangl K, et al. Regulation of pacing rate by variations of mixed venous saturation. *Pacing Clin Electrophysiol* 1984;7:1257.
48. Snell J, Cohen D, Hedberg SE. *In vivo* performance of a hemo-reflective type oxygen sensor for rate responsive pacing. *Pacing Clin Electrophysiol* 1988;11:504.
49. Ellenbogen KA, Thames MD, Mohanty PK. New insights into pacemaker syndrome gained from hemodynamic, humoral and vascular responses during ventriculoatrial pacing. *Am J Cardiol* 1990;65:53.
50. Ausubel K, Furman S. The pacemaker syndrome. *Ann Intern Med* 1985;103:420.
51. Den Dulk K, Lindemans FW, Bar FW, Wellens HJJ. Pacemaker-related tachycardias. *Pacing Clin Electrophysiol* 1982;5:476.
52. Furman S, Fisher JD. Endless loop tachycardia in an AV universal (DDD) pacemaker. *Pacing Clin Electrophysiol* 1982;5:486.
53. Raymond RD, Nanian KB. Insulation failure with bipolar polyurethane pacing leads. *Pacing Clin Electrophysiol* 1984;7:378.
54. Hanson JS. Sixteen failures in a single model of bipolar polyurethane-insulated ventricular pacing lead: a 44 month experience. *Pacing Clin Electrophysiol* 1984;7:389.
55. Platia EV, Brinker JA. Time course of transvenous pacemaker stimulation impedance, capture threshold, and electrogram amplitude. *Pacing Clin Electrophysiol* 1986;9:620.
56. Luceri RM, Furman S, Hurzeler P, et al. Threshold behavior of electrodes in long-term ventricular pacing. *Am J Cardiol* 1977;40:184.
57. Furman S, Hurzeler P, Mehra R: Cardiac pacing and pacemaker IV. Threshold of cardiac stimulation. *Am J Cardiol* 1977;94:115.
58. Nagatomo Y, Ogawa T, Kumagae H, et al. Pacing failure due to markedly increased stimulation threshold two years after implantation: successful management with oral prednisolone: a case report. *Pacing Clin Electrophysiol* 1989;12:1034.
59. Pirzada FA, Moschitto LJ, Diorio D. Clinical experience with steroid-eluting unipolar electrodes. *Pacing Clin Electrophysiol* 1988;11:1739.
60. Mond H, Stokes K, Helland J, et al. The porous titanium steroid eluting electrode: a double blind study assessing the stimulation threshold effects of steroid. *Pacing Clin Electrophysiol* 1988;11:214.
61. Kruse IM, Terpstra B. Acute and long-term atrial and ventricular stimulation thresholds with a steroid eluting electrode. *Pacing Clin Electrophysiol* 1985;8:45.
62. Thomas AC. Implantable defibrillation: eight years clinical experience. *Pacing Clin Electrophysiol* 1988;11:2053.
63. Fogoros RN, et al. Efficacy of the automatic implantable cardioverter-defibrillator in prolonging survival in paitients with severe underlying cardiac disease. *J Am Coll Cardiol* 1990;16:381.
64. Gottlieb SS. Dead is dead—artificial definitions are no substitute. *Lancet* 1997;349:662.
65. The Antiarrhythmics Versus Implantable Defibrillators (AVID) Investigators. A comparison of antiarrhythmic-drug therapy with implantable defibrillators in patients resuscitated from near-fatal ventricular arrhythmias. *N Engl J Med* 1997;337:1576.
66. Connolly SJ, Gent M, Roberts RS, et al. Canadian Implantable Defibrillator Study (CIDS): study design and organization. *Am J Cardiol* 1993;72:103F.
67. Siebels J, Cappato R, Ruppel R, et al. Preliminary results of the Cardiac Arrest Study Hamburg (CASH). *Am J Cardiol* 1993;72:109F.
68. Moss AJ, Hall WJ, Cannom DS, et al. Improved survival with an implanted defibrillator in patients with coronary disease at high risk for ventricular arrhythmia. *N Engl J Med* 1996;335:1933.
69. Bigger JT, for the Coronary Artery Bypass Graft (CABG) Patch Trial Investigators. Prophylactic use of implanted cardiac defibrillators in patients at high risk for ventricular arrhythmias after coronary-artery bypass graft surgery. *N Engl J Med* 1997;337:1569.
70. Moss AJ, Cannom DS, Daubert JP, for the Madit II Investigators. Multicenter Automatic Defibrillator Implantation Trial II (MADIT II): design and clinical protocol. *Ann Noninvas Electrocardiol* 1999;4:83.
71. Bardy GH, Lee KL, Mark DB, and the SCD-HeFT Pilot Investigators. The Sudden Death in Heart Failure Trial: pilot study. *Pacing Clin Electrophysiol* 1997;20:1148.
72. Doval HC, Nul DR, Grancelli HO, et al. Randomised trial of low dose amiodarone in severe congestive heart failure. *Lancet* 1994;344:493.
73. Singh SN, Fletcher RD, Fisher SG, et al. Amiodarone in patients with congestive heart failure and asymptomatic ventricular arrhythmia. Survival trial antiarrhythmic therapy in congestive heart failure. *N Engl J Med* 1995;333:77.
74. Groh WG, Silka MG, Oliver RP, Halperin BD, McAnulty JH, Kron J. Use of implantable cardioverter-defibrillators in the congenital long QT syndrome. *Am J Cardiol* 1996;78:703.
75. McKenna WJ, Franklin RC, Nihoyannopoulos P, Robinson KC, Deanfield JE. Arrhythmia and prognosis in infants, children, and adolescents with hypertrophic cardiomyopathy. *J Am Coll Cardiol* 1988;11:147.
76. Hamilton RM, Dorian P, Gow RM, Williams WG. Five-year experience with implantable defibrillators in children. *Am J Cardiol* 1996;77:524.
77. Breithardt G, Wichter T, Haverkamp W, et al. Implantable cardioverter defibrillator therapy in patients with arrhythmogenic right ventricular cardiomyopathy, long QT syndrome, or no structural heart disease. *Am Heart J* 1994;127:1151.
78. Bocker D, Bansch D, Heinecke A, et al. Potential benefit from implantable cardioverter-defibrillator therapy in patients with and without heart failure. *Circulation* 1998;98:1636.
79. Sweeney MO, Ruskin JN R, Garan H, et al. Influence of the Implantable cardioverter/defibrillator on sudden death and total mortality in patients evaluated for cardiac transplantation. *Circulation* 1995;92:3273.
80. Cook JR, Kirchhoffer JB, Fitzgerald TH, Lajzer DA. Comparison of decremental and burst overdrive pacing as treatment for ventricular tachycardia associated with coronary artery disease. *Am J Cardiol* 1993;70:311.
81. Reid WH, Mirowski M, Mower MM, et al. Clinical evaluation of the internal automatic cardioverter-defibrillator in survivors of sudden cardiac death. *Am J Cardiol* 1983;51:1608.
82. Poole JE, Bardy GH, Kudenchuk PJ, et al. Prospective randomized comparison biphasic waveform tilt using a unipolar defibrillation system. *Pacing Clin Electrophysiol* 1995;18:1369.
83. Grimm W, Flores BF, Marchlinski FE. Electrocardiographically documented unnecessary, spontaneous shocks in 241 patients with implantable cardioverter defibrillators. *Pacing Clin Electrophysiol* 1992;15:1667.
84. Fain FS, Dorian P, Davy JM, Kates RE, Winkle RA. Effects of encainide and its metabolites on energy requirements for defibrillation. *Circulation* 1986;73:1334.
85. Reiffel JA, Coromilas J, Zimmerman JM, Spotnitz HM. Drug device interactions: clinical considerations. *Pacing Clin Electrophysiol* 1985;8:369.
86. Dorian P, Fain FS, Davy JM, Winkle RA. Lidocaine causes a reversible, concentration-dependent increase in defibrillation energy requirements. *J Am Coll Cardiol* 1986;8:347.
87. Marinchak RA, Friehling TD, Kline RA, Stohler J, Kowey PR. Effect of antiarrhythmic drugs on defibrillation threshold: case report of an adverse effect of mexiletine and review of the literature. *Pacing Clin Electrophysiol* 1988;11:7.
88. Guarnieri T, Levine JH, Veltri EP, et al. Success of chronic defibrillation and the role of antiarrhythmic drugs with the automatic implantable cardioverter/defibrillator. *Am J Cardiol* 1987;60:1061.
89. Deeb GM, Hardesty RL, Griffith BP, Thompson ME, Heiman MS, Myerowitz RL. The effects of cardiovascular drugs on the defibrillation threshold and the pathological effects on the heart using an automatic implantable defibrillator. *Ann Thorac Surg* 1983;4:361.
90. Movsowitz C, Marchlinski FE. Interactions between implantable cardioverter-defibrillator and class III agents. *Am J Cardiol* 1998;82:411.
91. Lok NS, Lau CP, Tse HF, Ayers GM. Clinical shock tolerability and effect of different right atrial electrode locations on efficacy of low energy human transvenous atrial defibrillators using an implantable lead system. *J Am Coll Cardiol* 1997;30:1324.
92. Josephson ME. Recurrent ventricular tachycardia. In: Josephson ME, ed. *Clinical cardiac electrophysiology: techniques and interpretations,* 2nd ed. Philadelphia: Lea & Febiger, 1993:417.
93. Goldstein DJ, Losquadro W, Spotnitz HM. Outpatient pacemaker procedures in orally anticoagulated patients. *Pacing Clin Electrophysiol* 1998;21:1730.
94. Da Costa A, Kirkorian G, Cucherat M, et al. Antibiotic prophylaxis for permanent pacemaker implantation: a meta-analysis. *Circulation* 1998;97:1976.
95. Ramza BM, Rosenthal L, Hui R, et al. Safety and effectiveness of placement of pacemaker and defibrillator leads in the axillary vein guided by contrast. *Am J Cardiol* 1997;80:892.
96. Block M, Breithardt G. Long-term follow-up and clinical results of implantable cardioverter-defibrillators. In: Zipes DP, Jalife J, eds. *Cardiac electrophysiology: from cell to bedside,* 2nd ed. Philadelphia: WB Saunders, 1995:1412.
97. Schmitt C, Alt E, Plewan S, Schomig A. Initial Experience with implantation of internal cardioverter-defibrillator under local anesthesia by electrophysiologists. *Eur Heart J* 1996;17:1710.
98. Pinosky ML, Reeves ST, Fishman RL, Alpert CC, Dorman BH, Kratz JM. Intravenous sedation for placement of automatic implantable cardioverter-defibrillator. *J Cardiothorac Vasc Anesth* 1996;10:764.
99. Pacifico A, Wheelan KR, Nasir N, et al. Long-term follow-up of cardioverter-defribrillator implanted under conscious sedation in prepectoral subfascial position. *Circulation* 1997;95.
100. Gold MR, Peters RW, Johnson JW, Shorofsky SR. Complications associated with pectoral cardioverter-defibrillator implantation: comparison of subcutaneous and submuscular approaches. *J Am Coll Cardiol* 1996;28:1278.
101. Rugge FP, Savalle LH, Schalij MJ. Subcutaneous single-incision implantation of cardioverter defibrillators under local anesthesia by electrophysiologists in the electrophysiology laboratory. *Am J Cardiol* 1998;81:302.
102. Fitzpatrick AP, Lesh MD, Epstein LM, et al. Electrophysiology laboratory, electrophysiologist-implanted, nonthoracotomy-implantable cardioverter/defibrillators. *Circulation* 1994;89:2503.
103. Fotuhi PC, Epstein AE, Ideker RE. Energy levels for defibrillation: what is of real clinical importance. *Am J Cardiol* 1999;83:24D.
104. Goldberger JJ, Horvath G, Inbar S, Kadish AH. Utility of predischarge and one-month transvenous implantable defibrillator tests. *Am J Cardiol* 1997;79:822.
105. Phibbs B, Marriott HJL. Complications of permanent transvenous pacing. *N Engl J Med* 1985;312:1428.
106. Mueller X, Sadeghi H, Kappenberger L. Complications after single versus dual chamber pacemaker implantation. *Pacing Clin Electrophysiol* 1990;13:711.
107. Epstein AE, Miles WM, Benditt DG, et al. Personal and public safety issues related to arrhythmias that may affect consciousness: implications for regulation and physician recommendations: a medical/scientific statement from the American Heart Association and North American Society of Pacing and Electrophysiology. *Circulation* 1996;94:1147.
108. Santucci PA, Haw J, Trohman RG, Pinski SL. Interference with an implantable defibrillator by an electronic antitheft-surveillance device. *N Engl J Med* 1998;339:1371.
109. Fetter JG, Ivans V, Benditt DG, Collins J. Digital cellular telephone interaction with implantable cardioverter-defibrillators. *J Am Coll Cardiol* 1998;31:623.
110. Zito P, Weiss DN, Luceri RM. Late retesting of system performance in ICD patients without spontaneous shocks. *Pacing Clin Electrophysiol* 1999;22:197.
111. Calkins H, El-Atassi R, Kalbfleisch S, Langberg J, Morady F. Comparison of fixed burst versus decremental burst pacing for termination ventricular tachycardia. *Pacing Clin Electrophysiol* 1993;16:26.
112. Gillis AM, Leitch JW, Sheldon RS, et al. A prospective randomized comparison of autodecremental pacing to burst pacing in device therapy for chronic ventricular tachycardia secondary to coronary artery disease. *Am J Cardiol* 1993;72.
113. Newman D, Dorian P, Hardy J. Randomized controlled trial of antitachycardia pacing algorithms for termination of ventricular tachycardia. *J Am Coll Cardiol* 1993;21:1413.

23
Coronary Angioplasty

Donald S. Baim

Harvard Medical School; Center for Innovative Minimally Invasive Therapy, Brigham and Women's Hospital, Boston, Massachusetts 02115

The concept of transluminal angioplasty—enlargement of the lumen of a stenotic vessel by a catheter technique—was first proposed by Dotter and Judkins in 1964 (1). Their idea was to advance a spring-coil guidewire across an atherosclerotic arterial stenosis. As this guidewire remained in place, it would serve as a rail over which a series of progressively larger rigid dilators could be advanced to enlarge the vessel lumen. Although this technique proved to be effective in peripheral arteries, the need to insert large-caliber rigid dilators through the arterial puncture (and the high shear forces applied by the dilators as they crossed the atherosclerotic lesion) ultimately limited the clinical application of this “Dotter” technique. In 1974, Gruentzig (2) modified the technique, by replacing the series of rigid dilators with an inflatable nonelastomeric balloon mounted on a comparatively smaller catheter shaft. The balloon catheter could be introduced percutaneously with minimal trauma, advanced easily across a vascular stenosis in its smaller (collapsed) state, and then inflated with sufficient force to enlarge the stenotic lumen. Although others had speculated about the possibility of balloon dilatation, Gruentzig was the first to develop it into a practical device, and perfect it as a usable clinical tool. Within 4 years he and his colleagues (3) had performed a series of experiments in animals, cadavers, peripheral arteries, and the coronary arteries of patients undergoing bypass surgery, culminating in their performance of the first percutaneous balloon angioplasty of a stenotic coronary artery in a conscious human (September 16, 1977).

Although the new technique of balloon angioplasty was viewed with skepticism by most, a small number of cardiologists around the world recognized the great potential it might hold (4). In 1979 they met to form a registry of all coronary angioplasty cases worldwide under the sponsorship of the National Heart, Lung, and Blood Institute (NHLBI). That registry grew to 3,000 cases by 1981, although no more than 1,000 angioplasties were performed in any given year during that period. From these humble beginnings, progressive improvements in equipment and technique have produced dramatic growth in percutaneous transluminal coronary angioplasty (PTCA), transforming it into a major therapeutic modality that is used to benefit large numbers of patients with ischemic syndromes caused by anatomically suitable coronary artery lesions (5) (Fig. 23.1). Roughly 35% of the 1.4 million people who undergo diagnostic cardiac catheterization each year are referred for revascularization by catheter-based techniques exceeding the number referred for revascularization by bypass surgery. Despite a progressive broadening in its clinical and anatomic indications, the success rate for coronary angioplasty has risen to 98%, with a procedural mortality rate and an emergency bypass rate each less than 1%.

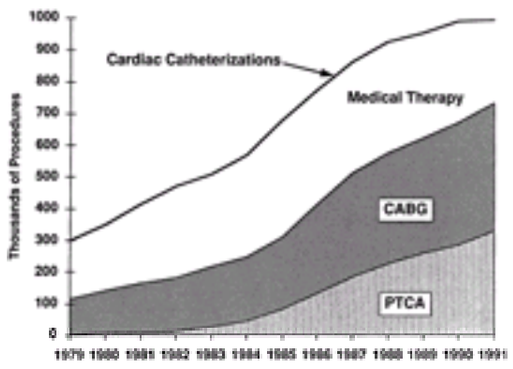

FIG. 23.1. Growth in the number of coronary angioplasty procedures between 1979 and 1991 is shown by the bottom *(stippled)* band, increasing from less than 1,000 per year in 1979–1981 to more than 300,000 per year in 1991. This was similar to the annual number of bypass operations *(cross-hatched band)*. The number of annual catheterizations has now grown to approximately 1.4 million, with one of three patients who undergo diagnostic cardiac catheterization being referred for coronary angioplasty, compared with one of four being referred for bypass surgery. CABG, coronary artery bypass grafting; PTCA, percutaneous transluminal coronary angioplasty. (From American College of Cardiology; see also Bittl JA. Advances in coronary angioplasty. *N Engl J Med* 1996;335:1290.)

Much of the improvement over the past 6 to 8 years, however, has come from the introduction of new adjunctive technologies such as atherectomy and stent implantation (see Chapter 24 and Chapter 25), as well as refinements in anticoagulant and antiplatelet pharmacology. Newer devices are now used in more than 80% of coronary interventions, so that stand-alone plain old balloon angioplasty (POBA) has become a minority interventional procedure. But balloon predilation or postdilation still plays an important *adjunctive* role in almost all such procedures (5), and the roots for our understanding of the strengths and weaknesses of any percutaneous coronary intervention lie in the history of balloon angioplasty. The intent of this chapter is to examine the basic equipment, strategy, results, and current indications of balloon angioplasty, indicating the situations in which newer stent and atherectomy devices have become dominant through their ability to address the previous limitations of stand-alone balloon angioplasty (6). Even more importantly, this chapter makes it clear that the evolution of catheter-based intervention is continuing, at an ever-increasing pace. The coronary interventionalist must have strong grounding in these fundamental principles, as well as the flexibility to master rapidly changing techniques and indications as they develop, if his or her patients are to receive the greatest benefits of safety, predictability, and durability from percutaneous coronary intervention.

EQUIPMENT

A coronary angioplasty system consists of three basic components (Fig. 23.2): (a) a guiding catheter, which provides stable access to the coronary ostium, a route for contrast administration, and a conduit for the advancement of the dilatation equipment; (b) a leading guidewire that can be passed through the guiding catheter, across the target lesion, and well into the distal coronary vasculature to provide a rail over which a series of therapeutic devices can be advanced; and (c) a

nonelastomeric balloon dilatation catheter filled with liquid contrast medium. Technologic advances lead to refinements in specific equipment each year, so any detailed description of current products would be outdated too soon to be of value here, but some general principles hold true.

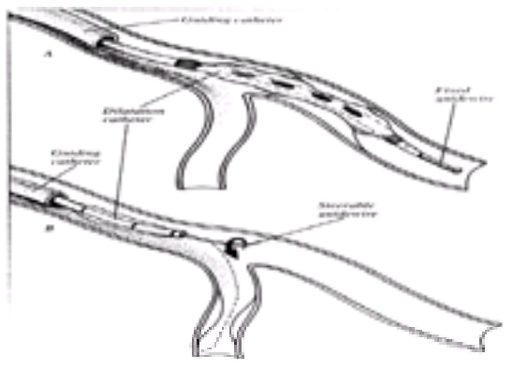

FIG. 23.2. Components of the coronary angioplasty system. The original Gruentzig fixed guidewire balloon **(A)** is compared with the steerable guidewire system **(B)**. Although both are advanced through a guiding catheter positioned in the coronary ostium, neither the wire shape nor its orientation could be changed once the original Gruentzig catheter was introduced, whereas the steerable design allows the guidewire to be advanced, withdrawn and reshaped, and steered independently of the balloon catheter to select the desired vessel. Once in place in the distal vessel beyond the target lesion, the guidewire serves as a rail over which the angioplasty balloon or other device can be advanced. (From Willerson JT, ed. *Treatment of heart diseases.* New York: Gower Medical, 1992.)

Guiding Catheters

Guiding catheters remain a crucial component in PTCA. Compared with the small lumens, minimal torque control, and sharp edges of the crude initial Teflon guiding catheters, current designs more closely emulate the performance of catheters used for diagnostic coronary angiography. To allow passage of therapeutic instruments, however, guiding catheters must have a lumen diameter at least twice that of a typical diagnostic catheter (e.g., 0.080-inch [2 mm] vs. 0.040-inch [1 mm]). To achieve this lumen in a catheter whose outer diameter is 8F (2.7 mm, or 0.107-inch), the wall thickness must be less than 0.010-inch (0.5 mm). Yet the catheter must still incorporate a Teflon liner to reduce friction, metal or plastic braid to transmit torque and provide sufficient stiffness to offer “backup” support during device advancement, and a smooth outer coating to resist thrombus formation. The complexity of this design goal requires use of special materials whose properties are typically varied along the length of the catheter to optimize the balance between support and flexibility at each point. Most guiding catheters now also include a very soft material in the most distal 2 mm of the catheter to reduce the chance of vessel trauma during engagement of the nontapered tip. Current guiding catheters are available in shapes similar to conventional Judkins and Amplatz curves, as well as a wide range of custom shapes, such as hockey-stick, multipurpose, and Voda (7), that are designed to ease engagement or provide better support for balloon advancement.

Although 9F guiding catheters predominated in the early 1980s, 8F (2.7 mm) catheters are in common use today. Improvements in catheter design have enabled routine lumen diameters of 0.088 inches in 8F guiding catheters to facilitate passage of bulkier devices such as stents and Rotablator burrs. Smaller (7F and even 6F) guiding catheters are also available, with a more restricted inner diameter (0.076 inches or 1.9 mm), well suited to the current generations of balloon catheters and bare-mounted stents and ideal for use from alternative access sites such as the radial artery (see Chapter 4). Larger (9F and 10F) guiding catheters with lumen diameters up to 3 mm (0.120 inch) are still used occasionally for certain procedures such as directional or extraction atherectomy. The standard guiding catheter length is 100 cm, but shorter (90 cm) guides are available to allow more distal passage of devices with limited working lengths during procedures on distal lesions in saphenous vein or internal mammary grafts (see later discussion). Much of the technology developed for interventional guiding catheters (e.g., thin walls, soft tips) has now been fed back into the design of diagnostic catheters to allow safer coronary engagement and brisk contrast injections through 6F (and even 5 or 4F) catheters.

To function adequately, the guiding catheter must be able to selectively engage the ostium. This requires the selection of an appropriate catheter shape and the ability to manipulate the catheter under fluoroscopic guidance (see Chapter 11). Engagement of the desired vessel, however, must not interfere with arterial inflow. Although this is routinely possible in the left coronary artery, damping of the guiding catheter in the right coronary artery ostium was once a common and vexing problem before the introduction of guiding catheters equipped with side-holes that allow ongoing perfusion despite wedged engagement. However, because the guiding catheter must deliver small boluses of contrast medium into the involved vessel (as needed to visualize vascular side branches and the target lesion for angioplasty), contrast flow out of such side-holes may increase the total contrast load used during a procedure. A second important function of the guiding catheter is to provide adequate support for advancement of the dilatation catheter across the target stenosis. This support derives from the intrinsic stiffness of the guiding catheter material, a catheter shape that buttresses it against the opposite aortic wall, and/or deep engagement of the guiding catheter into the coronary ostium (Fig. 23.3). Deep engagement was routinely required in the mid-1980s, when poor balloon catheter performance demanded a large measure of support if the balloon was to be forced across a severe stenosis. Unfortunately, deep engagement of the guiding catheter was also a well recognized cause of complication (i.e., ostial dissection). Although deep-guiding catheter engagement is still required on occasion (particularly with smaller, 6F guiding catheters), guiding catheter–induced dissection has become far less frequent with the incorporation of an atraumatic bumper on the tip of most guiding catheters and deep engagement of the guiding catheter only by its coaxial advancement over the balloon catheter. When a deeply engaged guiding catheter is used to push a dilatation balloon or other device across the lesion, the operator cannot forget to then withdraw the guiding catheter back to a more neutral position (just within the vessel ostium) to avoid its migration into an even deeper position as the device is withdrawn. In this sense, the ability to actively use the guiding catheter constitutes one of the important skills required for effective management of the overall angioplasty equipment system.

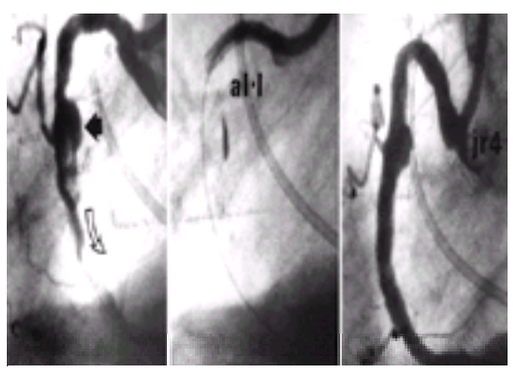

FIG. 23.3. Use of deep-guiding catheter engagement to facilitate coronary intervention. **Left:** Complex lesion in the right coronary artery including aneurysm *(dark arrow)* and diffuse distal disease *(open curved arrow)*. **Center:** Left Amplatz guiding catheter (AL-1) is deeply engaged to provide optimal support for stent placement. **Right:** After stent placement, the vessel is widely patent, but replacement of the Amplatz catheter with a conventional right Judkins catheter (JR4) shows how effective the Amplatz has been in straightening out a severe upward bend (shepherd's hook) in the proximal right coronary artery. Although progressive improvements in device profile and trackability have made such deep engagement less necessary, the technique is still of great value in selected cases. Deep seating of the guiding catheter needs to be done with great care and with coaxial advancement of the guiding catheter over a balloon catheter, to avoid injuring the proximal coronary artery.

Guidewires

The original dilatation catheter designed by Gruentzig had a short segment of guidewire (spring coil) attached to its tip to help it follow the vessel lumen and avoid subintimal passage as the catheter was passed to and across the stenosis (Fig. 23.2). Because the shape and orientation of this leading wire could not be modified once the catheter had been introduced, it provided the operator relatively little control over whether the catheter followed the desired path or was diverted into a side branch proximal to the lesion. In contrast, the movable guidewire system designed by Simpson in the early 1980s contained a standard 0.018-inch Teflon-coated wire

that extended and moved freely through the central lumen of the dilatation catheter (8). If this guidewire selected the desired vessel, it could continue to be advanced until it crossed the target lesion. If the guidewire instead selected a more proximal side branch, the balloon catheter could be advanced into the main vessel to a point just before the side branch to hold that place as the wire was withdrawn and reshaped in an effort to choose the desired path beyond. By a series of such iterative advancements of wire and dilatation catheter, many lesions could be crossed with the guidewire and then with the dilatation catheter. The first “steerable” guidewires were introduced in 1983, and guidewire technology has continued to improve with the evolution of a wide range of wire sizes (down to 0.009-inch), tip stiffness, shaft support, and lubricious coating.

In contrast to crude early guidewires, modern guidewires are designed to combine tip softness, trackability around curves, radiographic visibility, and precise torque control, which allow the guidewire to be steered past vascular side branches and through tortuous or stenotic segments. With these refinements, crossing a subtotal lesion with the guidewire has become a task that takes seconds rather than minutes to hours, helping to open up the more distal portions of the coronary circulation to a variety of interventional devices. The basic guidewire consists of a solid core (stainless steel or the superelastic alloy known as nitinol) that is ground to a progressive taper in its distal portion. This taper helps retain torque control when the wire is steered around the series of bends located in the guiding catheter and proximal coronary anatomy and allows the stiffer proximal portions of the wire to follow the soft tip into side branches. This core is covered by a spring coil, which is usually Teflon-coated stainless steel on the body of the wire and platinum on the distal 3 to 25 cm (for greater radiographic visibility). A family of plastic-covered guidewires with a hydrophilic coating is available to aid in crossing vessels with extreme tortuosity or total occlusion, but the spring-coil design is still dominant. At the tip of the guidewire, the coil is welded to the tapered core, either directly or through an intermediary shaping ribbon that allows the operator to kink or bend the tip of the wire to a shape that is appropriate for navigating the vessel features it must pass—such as larger-diameter bends for selecting left anterior descending (LAD) versus circumflex artery, smaller kinks or bends for selecting diagonal versus LAD. If greater probing force is required (e.g., for crossing a chronic total occlusion), stiffer tip designs (intermediate or “standard” rather than floppy) are available. When more shaft support is needed to help advance a stiff device (e.g., a stent) around a bend, extra support wires are available with a thicker and stiffer inner core. To allow exchange of one device for another, double-length (300-cm) exchange wires are widely available. I use these exchange-length wires as my initial wire in most cases, because they help retain access to the distal vessel as a series of devices (balloons, rotational atherectomy burrs, stents) is employed, without the risk of subintimal passage of the second guidewire as it crosses the partially dilated segment (9). A similar strategy can be followed with shorter (175 cm) guidewires if “rapid-exchange” balloon catheters and stent delivery systems are used (see later discussion). These advanced features are now obtainable in guidewires whose diameters range from 0.010 to 0.018 inch (0.25 to 0.5 mm) in 0.002-inch increments. The largest-diameter guidewire that is compatible with the lumen of the particular device (usually 0.014 inch in current practice) is employed, to minimize any potential mismatch between the wire and the tapered tip of the balloon catheter that might impede smooth passage. Although the movable guidewire concept (implemented in the current spectrum of highly sophisticated steerable guidewires) has simplified, shortened, and improved the success rate of coronary angioplasty, it is still important to heed the advice of Dotter and Judkins (1) that “the guidewire is passed across the atheromatous block more by the application of judgment than of force.”

Dilatation Catheters

The dilatation catheters for coronary angioplasty have undergone radical evolution since 1977. As described previously, the original Gruentzig catheters were designed with a short segment of guidewire permanently affixed to the catheter tip to decrease the risk of subintimal passage during advancement down the coronary tree. The shaft of this catheter had two lumens—one for inflation and deflation of the balloon and one for distal pressure measurement and/or contrast injection. This reflected the reliance on monitoring of transstenotic (i.e., aortic root to distal coronary) pressure gradients as a way of assessing lesion severity, given the difficulty in performing adequate contrast injections through small-lumen guiding catheters around the large (4.3F, or 1.3 mm) shafts of early balloon catheters. In contrast, virtually all dilatation catheters since 1982 have used an independently movable and/or steerable guidewire extending the entire length of the dilatation catheter, as described by Simpson and coworkers (Fig. 23.2). The central lumen of such dilatation catheters must have a sufficient caliber to allow free movement of the guidewire, but it is generally no longer used for either pressure measurement or contrast injection. The concept of using transstenotic pressure gradients to evaluate the significance and completeness of correction of coronary stenoses, however, has undergone renewed interest with the advent of solid-state pressure measurement guidewires (see Fractional Flow Reserve in Chapter 18).

An important feature of the dilatation catheter is the diameter of the smallest opening through which the deflated balloon can be passed (its “profile”). Compared with the 0.060-inch (1.5-mm) profile of the original Gruentzig design, current over-the-wire dilatation catheters have profiles of 0.032 in (0.8 mm) or less. Specially designed “fixed-wire” devices, which consist of a balloon mounted directly on a steerable wire core, were developed and used widely in the late 1980s to provide deflated profiles as small as 0.020 in (0.5 mm). Ongoing refinements in balloon technology, however, have allowed competitive performance from over-the-wire systems, thereby restricting the use of such fixed-wire devices to special situations (e.g., dilating side branches through the struts of a stent placed in the parent vessel). To preserve the best balloon profile, a “negative” or “aspiration” preparation (rather than a “positive” preparation, in which the balloon is first aspirated and then inflated with contrast material) is generally preferred, maximizing the probability that the balloon will cross a severe lesion. Although the primary and secondary (i.e., after an initial inflation) balloon profiles are important aspects of performance, the ability of the balloon to bend so as to advance easily through tortuous vascular segments (trackability) and the presence of sufficient shaft stiffness (pushability) to force it through the stenosis are also important. Delivery of the balloon is also aided by the incorporation of a friction-resistant coating (silicone or a hydrophilic coating such as polyethylene oxide) to improve surface lubricity. Other specialized properties of balloon catheters include whether the catheter travels over the wire along its full length or just in its tip (rapid-exchange or monorail style) to allow quick removal and reinsertion of a catheter over a short (i.e., 175-cm) guidewire. So-called “perfusion balloon” catheters also have been designed with either a series of side-holes in the shaft proximal and distal to the balloon segment or a spiral channel within the balloon to allow ongoing antegrade blood flow and thereby mitigate myocardial ischemia during prolonged balloon inflations (Fig. 23.4). Although prolonged inflations do help control elastic recoil and stabilize some dissections (10), they do not improve long-term results (freedom from restenosis). In the era when stents are used for recoil and dissection, the use of perfusion balloons has become rare.

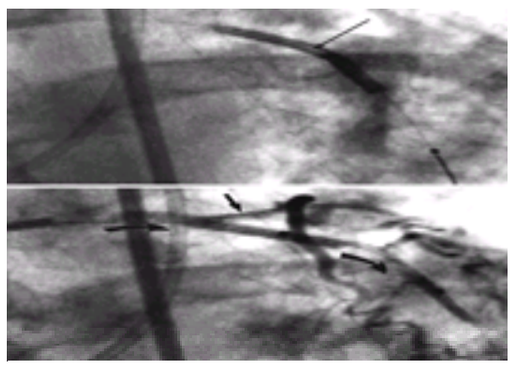

FIG. 23.4. Use of a perfusion balloon catheter. **Top:** The inflated perfusion balloon *(arrow)* is shown in the left anterior descending artery (LAD) and can be recognized by the presence of the non-contrast-filled *(white)* perfusion lumen running through the center of the balloon. **Bottom:** Injection through the guiding catheter *(left curved arrow)* shows direct opacification of the circumflex *(straight arrow)* as well as contrast flow into the distal LAD: this flow enters through proximal side-holes, passes through the perfusion lumen within the balloon, and flows out into the distal vessel *(right curved arrow)*. The 40- to 60-mL/min flow to the distal vessel through the perfusion lumen helps mitigate myocardial ischemia during prolonged balloon inflations, but use of such high-profile devices has become less common since the advent of more effective ways (i.e., stents) to stabilize coronary dissections.

Other than these factors that influence the ability to deliver the balloon catheter across the target lesion, the most important characteristic of the dilatation catheter is its ability to inflate to a precisely defined diameter despite application of pressures that average 10 atm (150 psi). This was not possible with early balloons manufactured from polyvinyl chloride, whose compliance led to balloon oversizing and rupture at pressures as low as 6 atm. More suitable performance can be readily achieved today with balloons manufactured from polyethylene, polyethylene teraphalate (PET), polyolyfin (POC, SciMed), or nylon, with a wall thickness as low as 0.0003 to 0.0005 inch. More compliant balloon materials such as polyolofin tend to reach their rated (nominal) diameter at 6 atm (90 psi) and then grow by up to 20% above their nominal size (e.g., a 3.0-mm balloon growing to 3.5 mm) at 10 atm. Semicompliant balloon materials such as polyethylene or nylon grow by less than 10% over this pressure range, whereas truly noncompliant balloon materials such as PET can retain their defined diameter up to 20 atm (300 psi) to allow dilatation of calcific stenoses or full expansion of coronary stents (Fig. 23.5).

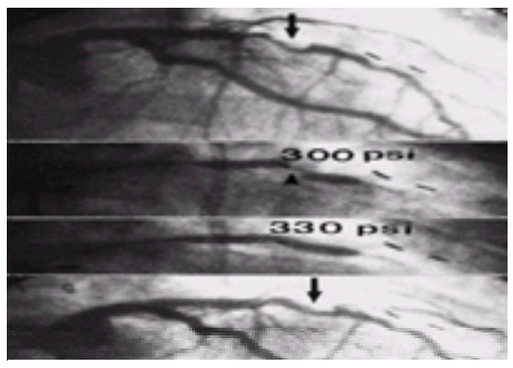

FIG. 23.5. Successful dilatation of a rigid calcific lesion. This rigid lesion (**top,** *arrow*) in the middle left anterior descending coronary artery of a patient who had undergone coronary artery bypass surgery (note surgical clips) resisted dilatation at 300 psi (20 atm) but yielded to an inflation pressure of 330 psi (22 atm) **(middle two photographs)**, with an excellent angiographic result (**bottom**). Such pressures are obtainable only with special high-pressure balloon construction, because most standard angioplasty balloons have rated rupture pressures of only 180 psi (12 atm). In current practice, such lesions would more likely be treated by rotational atherectomy (see Chapter 24).

Balloon compliance characteristics must be kept in mind especially whenever a compliant or semicompliant balloon is inflated to pressures above 6 to 8 atm (90 to 120 psi), to avoid overdistending the adjacent normal vessel. Because the noncompliant balloon materials preclude growth in normal segments upstream and downstream of a rigid lesion, they may be desirable whenever high pressures are needed, and they may also help to treat resistant lesions by concentrating dilating force on the stenosis itself (rather than in balloon growth and dilatation of the adjacent vessel). Regardless of which balloon type is used, staying within the prescribed range of inflation pressures is also important to prevent balloon rupture. This pressure range is specified in terms of the *rated burst pressure* (i.e., an inflation pressure at which the probability of balloon rupture is less than 0.1%). Taking any balloon catheter above its rated burst pressure increases the risk of balloon rupture, with the potential for air embolization (if the balloon was incompletely purged), local dissection, or difficulty in removing the balloon from an incompletely dilated lesion (11). This risk grows the further above rated burst pressure that the balloon is inflated, until it reaches 50% risk of rupture when the average burst pressure is reached. With the availability of effective therapies for calcified or fibrotic lesions (e.g., rotational atherectomy [see Chapter 24]), it is usually unnecessary to take any balloon catheter to pressures more than 1 to 2 atm above the rated burst pressure except in rare circumstances such as stent postdilatation in a calcified or fibrotic lesion that has not been adequately predilated or pretreated with rotational atherectomy.

Dilatation catheters that meet these design specifications are currently available from a variety of manufacturers with inflated diameters of 1.5 to 4.0 mm, in 0.5-mm increments, to match the size of the coronary artery in which the stenosis is located. Larger balloons (i.e., 4.5, 5.0, and 6.0 mm) are occasionally needed for treatment of large right coronary arteries or saphenous vein grafts. These once had to be obtained as special orders of the bulkier balloons used for peripheral vascular intervention, but large-size coronary balloons are now available in most coronary balloon lines. Quarter-sized balloons (e.g., 2.25, 2.75, and 3.25 mm) are also available, but that degree of precision probably exceeds the operator's ability to gauge vessel size, and stocking “quarter-sizes” tends unfavorably to increase the size of a laboratory's balloon inventory. The usual length of the inflatable balloon segment is 20 mm, but most balloons can be obtained with inflated segment lengths that are shorter, such as a 10- or 15-mm length for a high-pressure dilation completely within a 15-mm stent, or longer, such as 30 or 40 mm for dilation of a diffusely diseased segment (12,13). Most lesions can be dilated effectively with balloon catheters from any of the several manufacturers, but the fact that there are still subtle differences in performance characteristics that can make the difference between success and failure makes it necessary for each interventional laboratory to stock a variety of balloon types. Although competition has brought the average balloon price down substantially (from its high of almost $700 to less than $300), continued pressure on catheterization laboratory budgets has raised the possibility of resterilization and reuse. At least one recent trial of this concept, however, showed an increase in procedure time and device failures for resterilized product (14).

PROCEDURE

In that catheters are introduced under local anesthesia, a coronary angioplasty procedure bears a superficial resemblance to diagnostic cardiac catheterization. However, because angioplasty involves superselective cannulation of diseased coronary arteries with guidewires and balloon catheters, temporary occlusion of antegrade coronary arterial flow, and an attempt to manipulate the offending atherosclerotic lesion by balloon inflation, the procedure is a great deal more complicated and entails roughly 10 times the risk (i.e., 1% vs. 0.1%) associated with diagnostic catheterization (15). These risks should be discussed in detail with the patient and family before the procedure. The potential use of new devices and any alteration in management related thereto (e.g., need for additional antiplatelet therapy including oral agents or intravenous platelet IIb/IIIa integrin receptor blockers) should also be discussed, along with the probability that a repeat intervention may be necessary if restenosis of the dilated segment occurs. Special problems, such as the risk of “no reflow” during vein graft intervention or loss of involved side branches, should be described, if relevant. These small but very real risks of major complications highlight why angioplasty should be attempted only by experienced personnel in a setting where full cardiac surgical and anesthetic support is available (16).

Although patients were once admitted the night before elective angioplasty, current cost-driven protocols delay admission until the morning of the procedure. Details of the patient evaluation, informed consent, and preprocedure laboratory work usually have been completed in a separate outpatient visit or are compressed into a very brief encounter immediately before the procedure. This is particularly true for patients who come to catheter-based intervention at the conclusion of what began as a diagnostic catheterization (“ad hoc angioplasty” or “catheterization with angioplasty standby”). The patient should have been prepared by proscription of oral intake after midnight on the evening before the procedure, and pretreatment with a calcium channel blocker (to prevent vessel spasm at the treatment site) and aspirin 325 mg/day to diminish platelet deposition on the disrupted endothelium (17). Other antiplatelet agents, including low-molecular-weight dextran and dipyridamole 200 mg/day, were once administered in conjunction with angioplasty but have now been abandoned due to lack of demonstrated efficacy, potential allergic or volume-overload side effects with dextran, and the availability of more potent antiplatelet agents. The increasing use of stents and the importance of oral platelet adenosine diphosphate–receptor antagonists (ticlopidine and clopidogrel) (18), as well as the important benefit of intravenous platelet IIb/IIIa integrin receptor blockers in preventing periprocedural infarction and emergency revascularization for vessel closure (19) (Table 23.1), has made either or both classes of agents commonplace additions to aspirin therapy. Controlled trials have yet to show that any type of antiplatelet therapy consistently decreases the incidence of subsequent restenosis. Because aspirin reduces late cardiac mortality in patients with coronary disease, it is generally continued indefinitely after the procedure. In the aspirin-allergic patient, use of these alternative antiplatelet agents (sometimes with the addition of oral sulfinpyrazone) is mandatory.

Factors associated with abrupt vessel closure	Factors associated with increased mortality
Preprocedure	**Clinical factors**
Clinical factors	Female gender
Female gender	Unstable angina
Unstable angina	Age >65 yr
Insulin-dependent diabetes mellitus	Congestive heart failure
Inadequate antiplatelet therapy	Chronic renal failure
Angiographic factors	**Angiographic factors**
Intracoronary thrombus	Left main coronary artery disease
Stenosis >90%	Three-vessel disease
Stenosis length >2 luminal diameters	Left ventricular ejection fraction <0.30
Stenosis at branch point	Myocardial jeopardy score
Stenosis on bend (>45°)	Proximal right coronary artery stenosis
Right coronary artery stenosis	Collaterals originate from dilated vessel
Postprocedure	
Intimal dissection >10 mm	
Residual stenosis >50%	
Transient in-lab closure	
Residual transtenotic gradient 20 mm Hg	

[a] Except for female gender and unstable angina, the risk factors associated with abrupt closure and increased mortality differ. Factors associated with abrupt closure are mostly lesion-based and are heavily influenced by a poor postprocedure result (i.e., residual stenosis or dissection). In contrast, factors associated with procedural mortality are mostly patient-based, reflecting poor left ventricular function and the extent of disease (see Ryan TJ, et al. Guidelines for percutaneous transluminal angioplasty: a report of the ACC/AHA task force. J Am Coll Cardiol 1993;22:2033).

TABLE 23.1. *Factors associated with abrupt closure or increased mortality with coronary angioplasty*[a]

Angioplasty may be done by the brachial approach, although more than 90% of current procedures are done from the femoral approach. Although most catheter-based interventions can be performed safely without right-sided heart catheterization, I still prefer to place a right heart catheter to allow potentially valuable measurement of baseline and intraprocedure filling pressures in patients with abnormal baseline left ventricular function or who are undergoing treatment of major vascular territories. The venous sheath also allows rapid initiation of ventricular pacing, although experience shows that placement of a prophylactic pacemaker is

seldom needed in patients undergoing coronary angioplasty (20). After placement of the arterial sheath, intravenous heparin (70 units/kg, or 7,000 to 10,000 units) is administered. Because there is wide patient-to-patient variability in heparin binding and activity, the activated clotting time (ACT) should be measured, and additional heparin should be administered as needed to prolong the ACT to 275 to 300 seconds before any angioplasty devices are introduced and to maintain it at this level throughout the case. Lower levels of ACT (less than 250 seconds) are associated with a marked increase in the incidence of occlusive complications (21), although ACTs in the 275-second range are acceptable when adjunctive IIb/IIIa receptor blockade is used. Higher ACTs (greater than 300 to 350 seconds) tend to increase the risk of bleeding. In setting the target ACT, it is important to understand which machine is being used, because measurement with the Hemochron system (International Technidyne, Edison, NJ) tends to give values 30 to 50 seconds higher than those measured by the rival HemoTech machine (Medtronic Hemodynamics, Minneapolis, MN). Preliminary testing suggests that other direct thrombin inhibitors (e.g., low-molecular-weight heparin, hirudin, bivalirudin [Hirulog], argatroban) may find increasing use during angioplasty, based on more predictable dose-response characteristics than heparin and potentially greater efficacy against clot-bound thrombin (22,23,24 and 25). They may also be useful in patients with the heparin-induced thrombocytopenia or thrombosis syndrome (see Chapter 3).

Baseline angiograms are then obtained of one or both coronary arteries, using either standard diagnostic catheters or the angioplasty guiding catheter. When the guiding catheter is used for baseline angiography, it must be manipulated carefully, because its large diameter and nontapered tip increase the risk of ostial injury. Coronary injections should be repeated after the administration of 200 mg of intracoronary nitroglycerin to demonstrate that spasm is not a significant component of the target stenosis and to minimize the occurrence of coronary spasm during the subsequent angioplasty. My colleagues and I have seen cases where the intended target of a catheter-based intervention resolved with intracoronary nitroglycerin, and an unnecessary intervention was avoided! Baseline angiography also serves to evaluate any changes in angiographic appearance (interval development of total occlusion, thrombus formation) that have occurred since the diagnostic catheterization and to permit the selection of those angiographic views that allow optimal visualization of the stenoses and their surrounding branch vessels.

The appropriate guiding catheter is connected to the pressure manifold (see Chapter 11) by way of an extension tube and a rotating hemostatic valve (Tuohy-Borst valve) and positioned in the coronary ostium. The hemostatic valve contains an adjustable O ring that allows introduction and free movement of the angioplasty balloon while maintaining a sufficient seal around the balloon shaft to permit pressure measurement and contrast injection. The angioplasty guidewire is then steered across the target lesion, guided by puffs of contrast material through the guiding catheter, in a projection that shows the desired path free of foreshortening or overlapping side branches. Some operators advance the guidewire through a dilatation catheter that has been placed into the guiding catheter through the hemostatic valve so that it lies just inside the distal tip of the guiding catheter. Others (myself included) prefer a *bare-wire* technique, in which an exchange-length guidewire is placed into the hemostatic valve through a needle-like guidewire introducer. This permits free movement of the wire during advancement through the guiding catheter and down the involved coronary vessel, while preserving excellent contrast injections absent an obstructing balloon catheter. Once the position of the wire tip in the distal vasculature has been confirmed by contrast angiography, the introducer is removed from the hemostatic valve, and the desired angioplasty balloon or other device is selected.

Experience has shown that the best and safest angioplasty results are obtained with a balloon whose diameter closely approximates that of the presumably nondiseased “reference segment” adjacent to the site being treated (balloon/artery ratio, 0.9:1.1) (26,27). A slightly larger balloon (1.1 to 1.2 the reference lumen) may be used if an intravascular ultrasound study (see Chapter 19) shows that the outer vessel diameter in the reference segment (external elastic membrane diameter) is significantly larger than the reference lumen. On the other hand, a slightly smaller initial balloon may be chosen if it is difficult to estimate the correct reference size in a diffusely diseased or rapidly tapering vessel, or if great difficulty is anticipated in crossing the lesion. The selected balloon is prepared by flushing the central (guidewire) lumen with heparinized saline and filling the balloon inflation lumen with a dilute radiographic contrast material (Renografin-60, or Renografin-76 diluted to half strength). When balloon rupture was more frequent, contrast filling was accomplished by a “positive” preparation, in which the balloon was inflated with contrast material and then aspirated to remove any air. With more robust balloon materials, however, it is now more common to perform only a “negative” preparation, in which a contrast-filled syringe is used to pull air from the balloon lumen and then to let the balloon aspirate a small amount of contrast material when vacuum on the syringe is released. This method of preparing the balloon catheter avoids inflation of the balloon before it is across the target lesion and therefore helps to maintain the lowest possible deflated profile for crossing a severe stenosis. The prepared and flushed balloon catheter is then loaded onto the free end of the guidewire. The tip of this balloon is brought down to the O-ring, which is loosened to permit passage of the balloon into the guiding catheter, down the proximal vessel, and across the lesion.

Once the dilatation catheter has been positioned within the target stenosis, the balloon is inflated progressively using a screw-powered, handheld inflation device equipped with a pressure dial. At low pressure (i.e., 2 to 4 atm, or 30 to 60 psi), the balloon typically has an “hourglass” appearance due to its central restriction by the coronary stenosis being treated. In soft lesions, this restriction, or waist, may expand as pressure is gradually increased, allowing the balloon to assume its full cylindrical shape. In more rigid lesions, the restriction may remain prominent until the balloon expands abruptly at a “stenosis yield pressure” that may be anywhere between 4 and 10 atm (60 to 150 psi) (28). Some operators increase pressure rapidly until all balloon deformity resolves, in the hope that pushing rigid lesions to higher pressure will produce further balloon expansion, but this increases the risk of dissection when a fibrotic or calcified plaque yields suddenly. With the availability of effective tools for dealing with such fibrotic or calcific plaques (i.e., the Rotablator; see Chapter 24), one must then consider whether it is preferable to treat a plaque that resists expansion at 10 atm by rotablation, rather than pushing to the pressures (15 to 20 atm, or 225 to 300 psi; Fig. 23.5) that may be required for full dilation. Calcified or fibrotic rigid stenoses resist expansion at conventional pressures, but elastic (usually eccentric) stenoses are also problematic. These lesions allow full balloon expansion at low pressures but then tend to recoil promptly once the balloon is deflated. This type of lesion was once treated by repeated inflations or cautious use of oversized balloons, but they are now treated routinely by stenting (with or without prior debulking by directional atherectomy). The “cutting balloon,” its surface modified by the application of three to four microscopic blades that protrude slightly above the balloon surface when inflated, has also been used for fibrotic or elastic lesions (29).

Despite the more than 20-year history of balloon angioplasty, there is still little objective science behind the speed and maximal pressure used to inflate a dilatation balloon. The classic approach is to go deliberately (over 10 to 15 seconds) to a pressure that resolves the balloon waist, and then maintain that pressure for 1 minute. On the other hand, some operators prefer a slower speed of inflation and are prepared to tolerate mild persistent balloon deformities that have failed to resolve at moderate (6 to 8 atm) pressure (30) (Fig. 23.6), although the evidence for improved outcome is still inconclusive (31). In addition to this operator-to-operator variability in inflation speed, there is wide variation in the duration of inflation. Early data from Kaltenbach et al. (32) suggested that inflations of 1 minute might offer more benefit than the 30-second inflations used in the early 1980s. Even longer (15-minute) inflations with a perfusion balloon may produce slightly better acute results, with no difference in long-term patency (10).

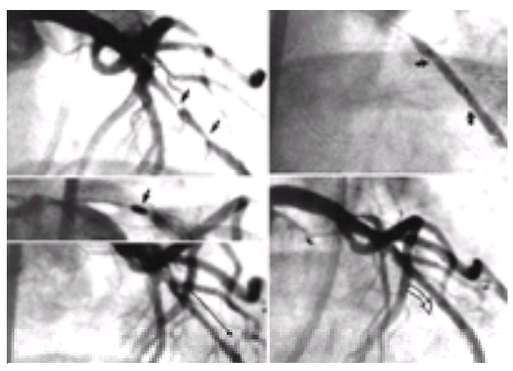

FIG. 23.6. Demonstration of low-pressure balloon inflation (2 atm, or 30 psi) **Left, top:** Long calcified lesion in the middle left anterior descending coronary artery *(small arrows)*. **Left, center:** Rotablator burr (1.75 mm, *arrow*) being advanced across the lesion. **Left, bottom:** Result after application of Rotablator shows residual stenosis despite improvement in lumen *(long arrow)*. **Right, top:** Low-pressure inflation of a 2.5 × 30 mm balloon shows full expansion of the balloon at either end of the lesion but tubular mild constriction throughout the lesion *(arrows)*. **Right, bottom:** Despite absence of full balloon inflation, a postdilation angiogram shows excellent luminal patency without dissection *(open arrow)*. Although higher inflation pressure might have produced further lumen enlargement, it would probably have caused prominent local dissection, resulting in the need for stent implantation despite the unfavorable small caliber and long length of the target lesion.

Whatever inflation strategy is selected, the response of each lesion to balloon dilatation must then be assessed individually so that the dilatation protocol can be tailored to achieve the best possible result. The most common way to assess lesion response to balloon dilatation is repeat angiography performed through the guiding catheter. By leaving the exchange-length guidewire in place during such angiography, access to the distal vessel and the ability to perform additional intervention (e.g., repeat balloon inflation, stent placement) are maintained. Complete normalization of the vessel lumen would be the ideal end result of coronary angioplasty. Given the mechanism of angioplasty (see later discussion), the more typical result of a successful angioplasty is a 30% residual diameter stenosis (i.e., a

1.9-mm lumen in a 3-mm vessel) with some degree of intimal disruption (reflected as localized haziness, filling defect, or dissection). The operator must decide whether this result is adequate or whether further treatment is needed. Some additional benefit frequently can be obtained by repeated or more prolonged balloon inflation, (i.e., 3 to 5 minutes rather than the usual 1 minute), which may require use of a perfusion balloon to attenuate associated myocardial ischemia. A larger balloon may provide greater lumen enlargement. This possibility can be explored by exploiting any compliance in the initial balloon (e.g., inflating it to higher pressure, such as 10 rather than 6 atm) or by using the next-larger balloon size. In doing so, however, one must weigh any potential benefits against the clear risk of using an oversized balloon: Although dilatation with a larger balloon may improve luminal caliber, it also may increase the risk of producing a large dissection leading to abrupt vessel closure (26). This creates a clear dilemma, however, because “better is frequently the enemy of good”: Striving for “perfect” luminal enlargement with balloon angioplasty not uncommonly led to conversion of a patient with a fair result to one who had to go to immediately to the operating room for treatment of a dissection caused by “one more balloon inflation.”

In the stent era, of course, much less emphasis is placed on pushing the results of balloon angioplasty to the maximum. Most lesions that *can* be stented *are* stented. Even if stenting is not planned, the mere *availability* of stenting to treat balloon-induced dissection has helped improve the results of balloon angioplasty by allowing the operator to push for the best result, knowing that stenting is always available to fine-tune the angioplasty results if there is persistent stenosis of more than 20% or to repair a balloon-induced dissection. It remains uncertain what percentage of patients must be stented for such a “provisional” stent strategy to have its results approach those of preemptive stenting (see also Chapter 25). In trials evaluating provisional stenting, upwards of 40% of balloon angioplasty patients received stents before short and long-term results were as good as those in patients who underwent preemptive stenting (see Chapter 25). But even stenting in the approximately 15% of patients with the worst angioplasty outcomes has substantially improved the results of balloon angioplasty (both acute success and complications, as well as long-term freedom from clinical and angiographic restenosis) in the “control” arm of trials comparing new devices to balloon angioplasty performed after the 1994 introduction of widespread stenting in the United States. In the current view, the best position for stand-alone balloon angioplasty is in lesions that are poorly suited to stenting—vessels smaller than 2.5 mm, with lesions longer than 30 mm, particularly in patients with diabetes mellitus.

Given the importance of achieving the best acute angiographic result and the uncertainty about the adequacy of the acute result as assessed angiographically, a number of other techniques have been employed to grade the quality of an angioplasty result. In the initial years of PTCA, operators relied heavily on the transstenotic gradient as an index of dilatation adequacy, seeking a postdilation pressure difference of less than 15 mm Hg between the aortic pressure (measured through the guiding catheter) and the distal coronary artery pressure (measured through the tip of the dilatation catheter). In practice, measurement of the gradient is complicated by the presence of the dilatation catheter within the stenosis and the small size of the dilatation catheter lumen; these factors, together with the switch to low-profile over-the-wire dilatation catheters, led to abandonment of the gradient measurement by 1988 (33). There has been some recent reawakened interest based on the availability of newer, solid-state *pressure-measuring* guidewires that can be used to assess the transstenotic gradient at baseline flow and during maximal hyperemia (34).

The fractional flow reserve (FFR) is defined as the ratio of distal coronary pressure to aortic pressure during adenosine-induced hyperemia (see Chapter 18), with a goal FFR greater than 0.95 after a successful angioplasty. The same type of physiologic assessment can be done using Doppler *flow-measuring* guidewires to assess diastolic/systolic flow ratios or coronary flow reserve (CFR) as an index of baseline lesion significance and a confirmation of adequate dilation. Alternatively, *intravascular ultrasound* (IVUS; see Chapter 19) can more accurately measure lumen diameter and cross-sectional area after dilation. IVUS has been helpful in procedures (such as directional atherectomy or stenting) where additional dilation is likely to provide further improvement in luminal caliber. It has provided important mechanistic insights into balloon angioplasty but is not used in more than 10% to 15% of routine clinical cases because of the added procedural time and expense. In most laboratories, the postdilation angiogram remains the “gold standard” for determining whether an adequate result has been obtained. If the intent is to perform stand-alone balloon angioplasty and the angiogram shows that a technically appropriate attempt at conventional dilatation has produced a poor result (residual stenosis greater than 50%, prominent dissection, frank abrupt closure), secondary use of a new device such as a stent is indicated.

Once adequate dilatation is deemed to have been achieved, it is common to withdraw the balloon catheter completely from the guiding catheter. The exchange-length guidewire is then left across the dilated segment for several minutes, while the treated vessel is observed over several minutes for angiographic deterioration. Injections through the guiding catheter with the balloon removed provide excellent angiographic visualization, while the indwelling guidewire provides easy access to the dilated segment to permit readvancement of the balloon if needed. With more predictable interventions such as stenting, however, a single set of postprocedure angiograms in orthogonal views is usually sufficient to document a suitable result in the treated lesion and the absence of dissections or branch occlusions in the adjacent portions of the vessel. Once stability of the dilated segment has been established, the guidewire is withdrawn, and other significant lesions are dilated similarly or the patient is transferred to a recovery area.

POSTPROCEDURE MANAGEMENT

Although the heparin administered during PTCA was once reversed to allow immediate removal of the femoral sheaths, it later became routine to leave the sheaths in place overnight with continued heparin infusion, perfusion of the sheath lumen (Intra-flow II, 30 mL/hr), and monitoring for distal limb ischemia. This practice allowed prompt vascular reaccess should delayed abrupt closure occur (35). In current interventional practice, however, such delayed abrupt closure occurs so infrequently (well less than 1%) that most laboratories now remove the sheaths later the same day, as soon as the heparin effect wears off. There is no evidence that prolonged postprocedure heparin infusion improves outcome (36), and there are compelling data that same-day ACT-guided sheath removal has lowered the incidence of femoral complications and facilitated next-morning discharge. The current standard is thus to give no further heparin after an uncomplicated procedure that has had a good angiographic result, and then to perform same-day sheath removal once the ACT has fallen below 160 seconds. When angioplasty is performed with 7F or 8F sheaths, control of the arterial puncture site during sheath removal can be achieved with the same manual compression techniques used for diagnostic catheterizations. With larger sheaths (or more intense anticoagulation protocols), however, prolonged compression (more than 30 minutes) may be required; this is better performed with the use of a mechanical aid, such as Femo-stop (USCI) or Compressar (Instromedix, San Diego, CA). The other alternative is to perform immediate sheath removal in the setting of full heparinization by using one of the several arterial puncture sealing devices now available (see Chapter 4).

After sheath removal, the patient typically remains at bedrest for 18 to 24 hours and then ambulates before discharge. On discharge, patients are usually given a calcium channel blocker for 6 weeks (longer if required for another indication such as hypertension) and aspirin (325 mg/day) indefinitely. Patients who received a stent are also given additional antiplatelet therapy (ticlopidine or clopidogrel) for 2 to 4 weeks. With a good angiographic result in the treated lesions, marked relief of ischemic symptoms should be expected unless other significant disease has been left behind. In the patient with multivessel disease (see later discussion), it may be particularly helpful to evaluate the postangioplasty physiologic state by a maximal exercise test in the first few weeks after discharge. Earlier (i.e., predischarge) exercise testing was once performed on a routine basis but has now been largely abandoned due to the potential for groin rebleeding, delay of discharge, or the small risk of precipitating thrombotic closure of the dilatation site. Patients may return to full activity within 72 hours, by which time the groin puncture site should have healed sufficiently to allow even brisk physical activity.

Patients should expect to have no anginal symptoms early after discharge. Ongoing anginal symptoms suggest persistent untreated disease or a poor result at the treatment site. On the other hand, initial symptomatic relief followed by recurrence of symptoms after 2 to 6 months suggests restenosis of the dilated segment. Recurrence of symptoms 1 or more years after successful angioplasty suggests progression of disease at another site. Along with education regarding these possibilities and their proposed management (repeat exercise testing and catheterization, with the possibility of more catheter intervention or bypass surgery), the acute angioplasty admission should be viewed as an opportunity to educate the patient and family about changes in lifestyle or drug therapy (to control hypertension or lipid abnormalities), and to reduce the risk for the progression of atherosclerotic disease (37).

MECHANISM OF PERCUTANEOUS TRANSLUMINAL CORONARY ANGIOPLASTY

According to the original explanation proposed by Dotter and Judkins (1) and by Gruentzig et al. (3), the enlargement of the vessel lumen after angioplasty was ascribed to compression of the atheromatous plaque—akin to footprints in the snow. In fact, true plaque compression accounts for the minority of the observed improvement (38). Extrusion of liquid components from the plaque does permit some compression of soft plaques but contributes minimally to improvement in more fibrotic lesions, even when balloon inflation is prolonged to 1 minute. Absent significant reduction in plaque volume, most luminal improvement after PTCA seems to result from plaque redistribution—more like footprints in wet sand. Some of this takes place by longitudinal displacement of plaque upstream and downstream from the lesion. Most improvement in the lumen, however, results from controlled overstretching of the entire vessel segment by the PTCA balloon. This stretching leads to fracture of the intimal plaque, partial disruption of the media and adventitia, with consequent enlargement of both the lumen and the overall outer diameter of the vessel (38) (Fig. 23.7). Although use of a full-sized balloon (balloon/artery ratio of 1:1) should theoretically eliminate all narrowing at the treatment site, the overstretched vessel wall invariably exhibits elastic recoil (39,40) after balloon deflation, as well as some degree of local vasospasm (41). These processes typically leave the stretched vessel with a 30% residual stenosis (i.e., a 2-mm lumen in a 3-mm vessel that has been dilated with a 3-mm balloon). Newer devices such as stenting or directional atherectomy are able to provide lower (0% to 10% rather than 30%) postprocedural residual stenosis, by reducing or even eliminating this

elastic recoil and vascular tone.

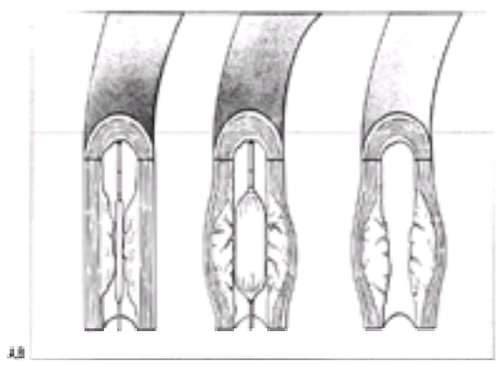

FIG. 23.7. Proposed mechanism of angioplasty. **A:** Deflated balloon positioned across stenosis. **B:** Inflation of the balloon catheter within the stenotic segment causes cracking of the intimal plaque, stretching of the media and adventitia, and expansion of the outer diameter of the vessel. **C:** After balloon deflation, there is partial elastic recoil of the vessel wall, leaving a residual stenosis of 30% and local plaque disruption that would be evident as “haziness” of the lumen contours on angiography. (From Willerson JT, ed. *Treatment of heart diseases.* New York: Gower Medical, 1992.)

In addition to wrestling with tendencies of the deeper vessel wall to exhibit elastic recoil, the operator also must contend with the problems produced by localized trauma to more superficial plaque components. This trauma is apparent as an almost universal haziness of the lumen margin in the post-PTCA angiogram, reflecting superficial plaque injury (42). Greater degrees of disruption are reflected by intimal filling defects (Fig. 23.8), contrast caps outside the vessel lumen, or spiral dissections that may interfere with antegrade blood flow (Fig. 23.9). This local disruption has been seen on IVUS, on angioscopy, and on histologic examination of postmortem angioplasty specimens, and its extent correlates with the risk of an occlusive complication (43) (see Abrupt Closure). Given the amount of “angioblasty” that takes place, it is remarkable that dislodgment and distal embolization of plaque fragments seemed to be infrequent in both experimental studies (44) and most early angioplasty procedures. Disruption of the plaque, however, may clearly lead to embolization of atherosclerotic debris in patients undergoing dilatation of a saphenous vein bypass graft and in those with large thrombi adherent to the lesion (45). In these patient, distal embolization of large (more than 1 mm) plaque elements is usually manifested as an abrupt “cutoff” of flow in the embolized distal vessel. In contrast, *micro*embolization of plaque debris or adherent thrombus may be more common than suspected (46) and may contribute to postprocedure chest pain and enzyme elevation. In 2% to 5% of angioplasties (particularly of vein grafts or platelet-rich thrombi in patients with recent myocardial infarction [MI]) there may be a dramatic reduction in antegrade flow with manifestations of severe ischemia (chest pain, ST-segment elevation). This may be caused by release of vasoactive agents (including serotonin, which may cause intense arteriolar vasospasm of the distal microvasculature) or by liberation of a very large number of microemboli that physically plug the distal microcirculation. It is important to distinguish this “no-reflow” phenomenon from more proximal causes of flow restriction (dissection, spasm, proximal thrombosis), because the no-reflow phenomenon can usually be quickly reversed by administration of low doses of intracoronary calcium channel blockers (e.g., 100 µmg of verapamil or 500 µ *m*g of diltiazem) into the distal vessel (47,48). Others have reported reversal with distal injections of other vasodilators such as adenosine or nitroprusside, but the syndrome is usually *not* responsive to nitrates. When drug therapy is not effective at restoring normal flow, the patient with no reflow will almost certainly go on to sustain a substantial MI, and consideration should be given to intraaortic balloon counterpulsation support. In patients with vein graft disease, alternative approaches (distal occlusion aspiration devices or debris filters) are being investigated to prevent this problem before it occurs (see Chapter 24).

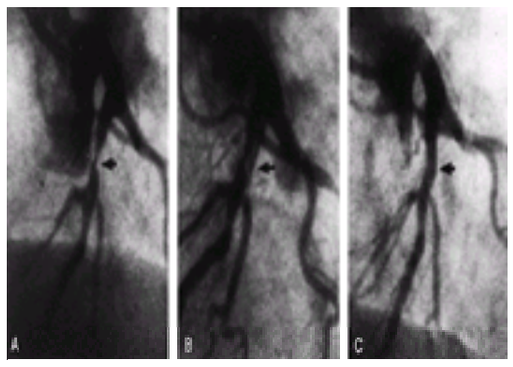

FIG. 23.8. Normal healing of percutaneous transluminal coronary angioplasty (PTCA)–related coronary dissection. Compared with the baseline angiogram **(A)**, the immediate post-PTCA angiogram **(B)** shows enlargement of the left anterior descending coronary artery lumen with two small filling defects typical of an uncomplicated coronary dissection. **C:** Follow-up angiogram 3 months later shows preservation of luminal caliber with complete healing of the localized dissection. (From Baim DS. Percutaneous transluminal coronary angioplasty. In: Braunwald E, ed. *Harrison's principles of internal medicine: update VI.* New York: McGraw-Hill, 1985.)

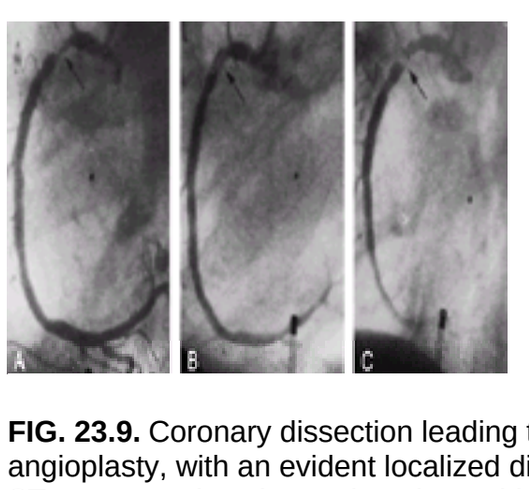

FIG. 23.9. Coronary dissection leading to abrupt reclosure. The appearance of a right coronary artery stenosis before **(A)** and immediately after **(B)** coronary angioplasty, with an evident localized dissection. Within 15 minutes after removal of the dilatation catheter, the patient experienced chest pain associated with inferior ST-segment elevation and angiographic evidence of progressive dissection with impeded antegrade flow **(C)**. Standard management in 1980 (when this case was done) consisted of emergency bypass surgery, which was accomplished without complication. Current practice would be to attempt to recross the lesion and “tack down” the dissection by repeat balloon inflation or, more likely, to place a stent. (From Baim DS. Percutaneous transluminal angioplasty: analysis of unsuccessful procedures as a guide toward improved results. *Cardiovasc Intervent Radiol* 1982;5:186.)

Although it is a theoretical possibility with sufficient local stretching trauma, frank vessel rupture has turned out to be a rare consequence during conventional balloon angioplasty, barring the use of significantly oversized balloons (49). Such vessel perforation is more common (approximately 1% incidence) when new atherectomy devices such as directional atherectomy, rotational atherectomy, or laser angioplasty are used (50) (see Chapter 24).

ACUTE RESULTS OF ANGIOPLASTY

Early published data on coronary angioplasty success derive mostly from the 3,000-patient NHLBI Angioplasty Registry, which collected all procedures performed

between 1977 and September of 1981 (51). Although case selection in the registry focused on “ideal” PTCA candidates—those with proximal, discrete, concentric, subtotal, noncalcified stenoses of a single vessel—the primary success rate of 63% would be considered disappointing by current standards. The main explanations for this low rate were failure to cross the lesion with the dilatation system (29% of cases) and failure to dilate the lesion adequately once having crossed it (12% of cases). These failures resulted from two factors: the relative lack of experience of operators contributing cases to the registry (the “learning curve”) and the use of original Gruentzig fixed-wire dilatation catheters, which had limited maneuverability, a comparatively high deflated balloon profile, and a low peak inflation pressure.

Despite the inclusion of patients with more difficult coronary anatomy, progressive improvement in equipment (with widespread availability of steerable guidewires since 1983) has allowed progressive improvement in the primary success rate of coronary angioplasty (5). The second PTCA registry enrolled patients at 14 centers between 1985 and 1986 (52), with a success rate of 90%. Moreover, analysis of complications in the 1985–1986 registry (53) shows a concomitant reduction in the incidence of emergency bypass surgery (from 5.8% to 3.5%) and a reduction in the mortality rate for patients with single-vessel disease (SVD) (from 0.85% to 0.2%), although overall procedural mortality remained close to 1% because of the inclusion of greater numbers of patients with multivessel disease. In the late 1980s and early 1990s, success was obtained in roughly 85% of patients undergoing balloon angioplasty, with major complications occurring in roughly 6% of patients and including death in 1.5%, Q-wave MI in 1.5%, and emergency surgery in 3%. These outcomes have improved further with the introduction of new devices (late 1990s), with acute procedural success rising to more than 95% and major adverse cardiac events falling to roughly 3% (death, 1%; emergency surgery, 0.7%; and Q-wave or large non–Q wave MI, 1.3%).

Anatomic improvement after an angiographically successful PTCA correlates with elimination of anginal symptoms and improved function on atrial pacing or conventional exercise testing (54,55). Studies using thermodilution, videodensitometry, and Doppler flow measurement have shown restoration of coronary flow reserve after successful coronary angioplasty, although full normalization may take a matter of weeks to return (see Chapter 18).

COMPLICATIONS

As a specialized form of cardiac catheterization, coronary angioplasty is attended by the usual risks related to invasive cardiac procedures (see Chapter 3). In contrast to diagnostic procedures, the larger-caliber guiding catheter used for angioplasty is more likely to result in damage to the proximal coronary artery and to cause local bleeding complications at the catheter introduction site. Selective advancement of guidewires and dilatation catheters into diseased coronary arteries may lead to vessel injury if they are manipulated too aggressively. The most common complications of coronary angioplasty, however, relate directly to local injury at the dilatation site caused as part of the angioplasty process (56), as described in the section concerning mechanisms (see earlier discussion).

Coronary Artery Dissection

Although plaque dissection may be caused by overly vigorous attempts to pass the guidewire through a tortuous stenotic lumen, most dissections are the result of the “controlled injury” induced intentionally by inflation of the dilatation catheter (37,38). In fact, localized dissections can be found routinely in animal or cadaveric models of angioplasty and are evident angiographically in approximately one half of patients immediately after angioplasty (42). When these dissections are small and nonprogressive and do not interfere with antegrade flow in the distal vessel, they have no clinical consequence other than transient mild pleuritic chest discomfort. Follow-up angiography as soon as 6 weeks after the angioplasty procedure usually demonstrates complete healing of the dissected segment (Fig. 23.8), although localized formation of aneurysm at the site of dissection has occasionally been described (57,58).

Abrupt Closure

Although small dissections may be well tolerated, large progressive dissections may interfere with antegrade flow and lead to total occlusion of the dilated segment (a phenomenon known as abrupt closure; Fig. 23.9). With the use of balloon angioplasty alone (before the advent of new devices), abrupt closure occurred in approximately 5% of patients as the result of compression of the true lumen by the dissection flap (43), with superimposed thrombus formation, platelet adhesion, or vessel spasm. In one study (59), postangioplasty dissections were evident angiographically in 40% of dilated lesions, with spiral (type D) dissections (51) in 3.5% of patients. The presence of a type D dissection increased the risk of frank or “threatened” abrupt closure (residual stenosis greater than 50%, with reduced antegrade flow) from a baseline of 6.1% to 28%. This finding supports the earlier findings of Ellis et al. (60), showing a five-fold increase in abrupt closure with postprocedure dissection and stressing the relative importance of the postprocedure result (as opposed to preprocedure clinical or angiographic variables; Table 23.1) on the risk of abrupt closure.

Most abrupt closures after stand-alone balloon angioplasty developed within minutes after the final balloon inflation, so that it was desirable to observe the patient for 10 minutes before leaving the catheterization laboratory. Abrupt closure could also occur up to several hours later (in 0.5% to 1% of cases), particularly as the heparin anticoagulation wore off. Under those circumstances, it was heralded by severe chest pain and clear electrocardiographic changes (usually ST-segment elevation) similar to those observed during prolonged balloon inflation. Before 1985, most patients who experienced abrupt closure of a major epicardial coronary artery went directly to emergency surgery, in an effort to minimize the amount of consequent myocardial damage. The rate of emergency surgery was 5% to 6%, but even with emergency surgery within 90 minutes after the onset of vessel occlusion, up to 50% of patients sustained a Q-wave MI (61). The development of “perfusion” catheters—infusion catheters or angioplasty balloons with multiple sideholes along their distal shaft to allow 40 to 60 mL/min of blood to enter proximal to the site of occlusion, flow through the central lumen, and reexit into the lumen distal to the point of occlusion—allowed patients to go to the operating room in a nonischemic state (Fig. 23.4), reducing the incidence of transmural infarction during emergency surgery to approximately 10% (62). Once it was realized that many abrupt closures can be reversed by simply readvancing the balloon dilatation catheter across the lesion to “tack up” the dissection via repeated balloon inflation (35) (Fig. 23.10), the emergency surgery rate fell in half, to roughly 3%. Prolonged balloon inflations—up to 20 minutes, using an autoperfusion balloon (63) to limit ongoing ischemia—further improved the ability to reverse abrupt closure.

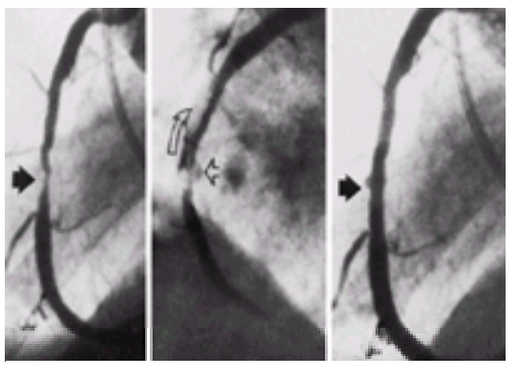

FIG. 23.10. Reversal of abrupt closure by repeat balloon inflation. Eccentric stenosis in the mid-right coronary artery (**left,** *arrow*) dilates **(center)** with production of a large dissection *(curved arrow)*, focal dye stain *(open arrow)*, and retarded distal flow. Repeat inflations with a 0.5-mm-larger balloon catheter, using inflation durations of up to 5 minutes, “tacked up” the dissection to provide a stable luminal appearance (**right,** *arrow*). Approximately 50% of abrupt closure events can be reversed in this manner, with up to 90% reversal by use of a coronary stent.

Since 1993, the availability of coronary stents has increased the certainty of reversing abrupt closure to almost 90% (64). This success has made it routine to stent any patient with a large postprocedure dissection, as a preemptive treatment for “threatened” abrupt closure even when flow compromise is not apparent. With elective stenting of more than 80% of interventional procedures, this problem has been largely eliminated, and emergency surgery rates having fallen below 0.5%. Because emergency surgery is still required in some cases, the recommendation is still in place to perform elective coronary angioplasty only in settings where the resources for prompt emergency bypass surgery are available (16).

Beyond the mechanical issues of residual stenosis and local dissection, it is now clear that platelet-rich clots contribute significantly to the abrupt closure process. The presence of thrombus, reflected as a globular filling defect, increases the risk of abrupt closure from 7.2% to 27.8% (59). The role of thrombus in abrupt closure is further supported by an increased risk of abrupt closure in patients with a subtherapeutic ACT value (20) and by the reduction of ischemic end points seen in patients treated with a bolus plus infusion of various platelet IIb/IIIa integrin blockers (Table 23.2) (17). Although platelets may adhere to damaged vessel walls through other

receptors, it is the activation of the 50,000 to 80,000 glycoprotein IIb/IIIa receptors on each platelet's surface that allows them to bind avidly to fibrinogen to cause platelet aggregation and thrombosis. Vessels with moderate local dissection but preserved antegrade flow are more likely to stay patent in the presence of agents that reduce the affinity of the activated IIb/IIIa receptor for fibrinogen, thereby reducing the incidence of emergency surgery or unplanned (bailout) stent placement. These agents also appear to reduce the incidence of periprocedural MI, particularly the incidence of creatine kinase (CK) elevations (non–Q wave MIs) that are seen in 10% to 30% of patients undergoing coronary intervention (65). Until it is clear that prophylactic use of such agents improves hard end points such as mortality or emergency surgery, however, the expense and increased bleeding risks associated with the use of these agents has constrained their use in most laboratories to the 30% to 40% of patients who have high-risk lesion morphologies or a suboptimal mechanical result after mechanical intervention.

Tradename	Agent	Manufacturer	Loading dose[a]	Infusion (for 24 hr)
ReoPro	Abciximab	Lilly/Centocor	250 μg/kg (0.25 mg/kg)	0.125 μg/kg/min (max 10 μg/min)
Aggrastat	Tirofiban	Merck	12 μg/kg (over 3 minutes)	0.1 μg/kg/min (one-half dose for C_{Cr} < 30)
Integrilin	Eptifibatide	Key/Cor	180 μg/kg (may be repeated 10 min later)	2.0 μg/kg/min

[a] Various dose regimens of these agents are in use in different laboratories, and the ability to monitor platelet receptor occupancy is still limited. Care should be taken to avoid excess heparin administration (activated clotting time, >350 sec) when IIb/IIIa blockers are given and to check for early profound thrombocytopenia (incidence approximately 1%) as well as potentially serious excessive bleeding that may require discontinuation of the infusion or administration of fresh platelets. Although tirofiban and eptifibatide have short (half-lives (approximately 90 min) after discontinuation, abciximab has persistent effects for 24–48 hours after discontinuation of the infusion. (See Dobesh PP, Latham KA. Advancing the battle against acute ischemic syndromes—a focus on the GP IIb/IIa inhibitors. *Pharmacotherapy* 1998;18:563, for additional information on these agents.)

TABLE 23.2. *Intravenous blockers of the platelet glycoprotein IIb/IIIa receptors used during coronary intervention at Beth Israel Deaconess Medical Center*

In certain subgroups—those with extensive prior or ongoing myocardial damage, multivessel disease, a large myocardial territory perfused by the target stenosis, or prior coronary bypass surgery—the consequences of abrupt closure may be more severe. Before the widespread availability of stenting, these patients had a procedure-related mortality rate several times higher than the 0.3% to 0.6% rate seen with elective coronary angioplasty (66). This required the most vigilant surgical standby and immediate availability of hemodynamic support devices, including intraaortic balloon counterpulsation and, potentially, percutaneous cardiopulmonary support (CPS) via 18F femoral arterial and venous cannulas (67,68) (see Chapter 21). More recently, however, the high degree of reliability of stent intervention has meant that such patients do well with nothing more than prophylactic intraaortic balloon counterpulsation.

Other Complications

A number of other complications have been described as the result of coronary angioplasty. Q-wave MI occurs in approximately 1% of patients (53), often as a result of abrupt closure or “snowplow” loss of a major side branch originating within or in close proximity to the lesion being treated. If creatine kinase MB (CK-MB) isoenzyme levels are measured routinely, however, 10% to 30% of patients show some elevation after apparently uncomplicated procedures (65), usually as the result of distal microembolization or loss of smaller side branches. The importance of these “infarctlets” is still the subject of some debate. Certainly larger non–Q wave infarctions—those with absolute CK-MB levels greater than 5 times the upper limit of normal or those associated with new ST-T wave abnormalities—probably have the same import as a periprocedural Q-wave infarction. Overnight electrocardiographic monitoring is prudent, and discharge should be delayed for 24 to 48 hours to ensure clinical stability. The debate, however, centers on smaller elevations of CK-MB, between 1 and 5 times normal. These events do not significantly impair ventricular function or increase the 1-year mortality rate, and in our laboratory we do *not* generally classify such enzymatic abnormalities as significant infarctions or delay the timing of planned discharge (69). On the other hand, a number of large studies have demonstrated that patients with CK-MB elevations 1 to 5 times greater than normal have an increased incidence of adverse events (variously identified as death, repeat MI, repeat revascularization) at 3 to 5 years. Were this a *cause-and-effect* relationship, one would expect those randomized device trials in which one study arm had greater CK elevation (e.g., directional atherectomy) to show higher mortality, which has not been the case (70). One would also expect that drug interventions that decrease the frequency of CK-MB elevation (e.g., IIb/IIIa platelet receptor blockers) would significantly lower mortality, but this has been seen only for *post hoc* selected subgroups. In a pooled analysis of more than 12,000 interventional patients enrolled in randomized trials of IIb/IIIa receptor blockers versus placebo, the odds ratio for mortality at 6 months was 0.90 (95% confidence interval, 0.70 to 1.16; $p = .41$) (17). If the relationship is not cause-and-effect, the other possibility is that *both the CK elevations and the variety of late events are related to a common factor* (a confounder), such as the diffuseness of atherosclerotic disease. By analogy to the example of the association of carrying matches and lung cancer (through the confounder of cigarette smoking), devices or drugs that decrease the incidence of CK elevation would not change the underlying disease process or its late manifestations (any more than banning matches would eliminate smoking-related lung cancer). Until and unless a cause-and-effect relationship is demonstrated (i.e., through an across-the-board reduction in late mortality by periprocedural IIb/IIIa blocker administration), the practice in my laboratory is to use these agents only for the approximately 30–40% of patients who have certain high-risk lesions or lesions in which the best attempt at mechanical revascularization still fails to provide an angiographically perfect result.

Other than embolization of plaque constituents, embolization of large thrombi that are adherent to the stenosis may occur and should be taken into account during angioplasty of patients with unstable angina or acute MI (see earlier discussion). This may include overnight intracoronary infusion of a thrombolytic agent or use of one of the new mechanical thrombectomy devices (see Chapter 24). Embolization of smaller thrombus or plaque particulates, which can cause slowed antegrade perfusion and transmural ischemia in the absence of proximal vessel compromise or distal cutoffs, known as the “no reflow” phenomenon (45). It is most common (2% to 8%) in patients who undergo treatment of a lesion responsible for recent MI or treatment of a saphenous vein graft. The mechanism may include embolization of platelet-rich thrombi that release vasoconstrictive substances (e.g., serotonin) which can cause intense vasospasm of the distal microcirculation, or release of atherosclerotic plaque debris (particularly during vein graft intervention) that can “sludge” the distal vessels (46).

Occlusion of branch vessels originating from within the stenotic segment occurs in 14% of vessels at risk during angioplasty of the main vessel, according to what has been called the “snowplow effect” (71) (Fig. 23.11). If the branch vessel is small, this event usually has no significant clinical sequelae and should not discourage attempted angioplasty. On the other hand, if a large branch vessel originates from within the stenosed segment, simultaneous dilatation of the main vessel and the involved branch with two separate dilatation systems (the “kissing balloon” technique) may be required for preservation of both vessels (72). This originally required two separate guiding catheter and balloon dilatation catheter systems (Fig. 23.12). Alternatively, two guidewires were inserted through a single guiding catheter (one guidewire being placed into the main vessel and one into the involved side branch), to allow advancement of a balloon catheter into one and then the other vessel (73). Current large-lumen guiding catheters and low-profile dilatation systems now allow actual kissing balloon inflations through a single guiding catheter. The results can be improved, however, by performing atherectomy of both the parent and branch vessel (74) (see Chapter 24). When the involved side branch is noncalcified and larger than 2.5 mm, directional atherectomy of the main vessel and then the side-branch ostium has proved to be an effective way of maintaining patency of both vessels (Fig. 23.13). For smaller branches or calcified bifurcations, rotational atherectomy provides similar benefit. Various stent strategies have been used in bifurcation lesions, but at this time none offers significant benefit in long-term patency over the atherectomy approaches followed by kissing balloon dilatation.

FIG. 23.11. The “snowplow” effect. Dilatation of mid-right coronary artery stenosis **(left)** resulted in occlusion of a diseased right ventricular branch that originated from within the stenotic segment **(right)**. There were no clinical sequelae. Approximately 14% of involved branches suffer a similar fate. (From Baim DS. Percutaneous transluminal angioplasty. In: Braunwald E, ed. *Harrison's principles of internal medicine: update VI.* New York: McGraw-Hill, 1985.)

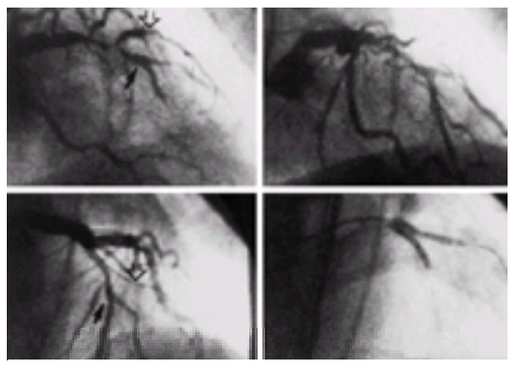

FIG. 23.12. “Kissing balloon” treatment of a bifurcation lesion. **Left, top:** A severe stenosis involves the bifurcation of the left anterior descending (LAD) coronary artery *(dark arrow)* and a large diagonal branch *(open arrow)*. With conventional dilatation of the LAD, the diagonal branch would be at risk for “snowplow” occlusion, which did occur **(left, bottom)**. Note, however, a second guidewire *(open arrow)*, which was placed in the diagonal branch before LAD dilatation to allow alternating dilatation of the LAD and the diagonal branch. When this failed to provide adequate improvement in both vessels, a true “kissing balloon” procedure (simultaneous inflation of two balloon catheters) was performed **(right, bottom)**. Although some luminal thrombus was present **(right, top)**, it had resolved at follow-up angiography the next day.

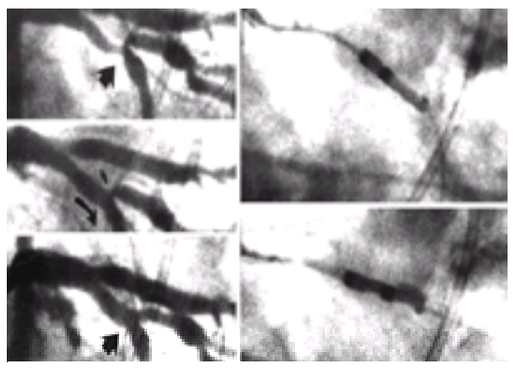

FIG. 23.13. Bifurcation atherectomy. **Left, top:** Bifurcation stenosis involving the circumflex *(arrow)* and the large obtuse marginal branch. **Left, center:** Directional atherectomy of circumflex has provided a large smooth lumen *(curved arrow)*, with ongoing stenosis of the origin of the marginal branch *(small arrow)*. **Left, bottom:** After atherectomy of the marginal branch, excellent patency of both the main vessel and the involved side branch have been secured. **Right, top:** Position of the directional atherectomy catheter during cuts in the circumflex. **Right, bottom:** Position of atherectomy catheter during cuts in the marginal branch. Atherectomy of the main branch and involved side branch, followed by kissing balloon dilatation, remains an effective way to approach such lesions (see reference 74), although several stent-based approaches are being developed (see Chapter 25).

Perforation of the coronary artery with a stiff guidewire occurs rarely and does not necessarily have dire consequences, unless a device is passed over the wire or the wire perforation takes place in a patient receiving a platelet IIb/IIIa receptor blocker. Frank rupture of the coronary artery resulting from use of too large a dilatation balloon or use of an atherectomy device (see Chapter 24) can cause vessel perforation that leads to rapid tamponade and hemodynamic collapse (49,50). Tamponade also may result from perforation of the right atrium or right ventricle during placement of temporary pacemaker electrode catheters, particularly in angioplasty patients who are receiving antiplatelet therapy in addition to full heparinization. This potential complication and the infrequency (less than 1%) of severe bradycardiac complications support our recommendation against prophylactic pacing during coronary angioplasty (19). Ventricular fibrillation occurs in approximately 1% of angioplasty procedures (53), usually as the result of prolonged ischemia during balloon advancement or inflation. In addition to causing electrical instability, ischemia during balloon inflation may cause marked electrocardiographic changes, (75) abnormalities in regional left ventricular systolic and diastolic function (76,77), and regional myocardial lactate production.

Although angioplasty guidewires and catheters are extremely reliable devices, failures can occur when any device is subjected to severe operating stresses, as when a guidewire is rotated repeatedly in a single direction while its tip is held fixed in a total occlusion or when a balloon catheter is inflated past its operating pressure range in an attempt to dilate a resistant stenosis. In a small percentage of cases, this may lead to detachment of a part of the wire or dilatation catheter, with a fragment remaining in the coronary artery (78). In the stent era, this also includes dislodgment of a bare-mounted stent from its delivery balloon. To avoid the need for surgical removal, the angioplasty operator should be familiar with the techniques of catheter retrieval (79). Finally, the operator must be careful to limit the amount of contrast material administered (usually to 3 or at most 4 mL/kg) to avoid renal toxicity, particularly during complex or multivessel procedures.

THE HEALING RESPONSE TO CORONARY ANGIOPLASTY: RESTENOSIS

After successful balloon angioplasty, the body attempts to repair the damage caused by the procedure-related mechanical injury. Within minutes, a carpet of platelets and fibrin is deposited. Within hours to days, inflammatory cells begin to infiltrate the site, cytokines are released, and vascular smooth muscle cells begin to migrate from the media toward the lumen. These smooth muscle cells and fibroblasts convert from their normal phenotype to a synthetic phenotype and remain in this form as they undergo hypertrophy, proliferate, and begin to secrete extensive extracellular matrix. The luminal surface is simultaneously colonized by endothelial cells that slowly regain their normal barrier function and secretory functions in making tissue plasminogen activator (tPA) and endothelial-derived relaxation factor. Along with this proliferative neointimal response, there may be further elastic recoil and fibrotic contraction of the vessel wall during this period. Different arteries and interventions appear to result in different degrees of proliferation and vessel contraction—for example, stents renarrow exclusively by neointimal hyperplasia, whereas most other devices also undergo a significant amount of late narrowing due to contraction (unfavorable remodeling) of the entire vessel wall (80). There are also significant patient-to-patient variations in the late healing response after coronary intervention, reflected in variables amounts of “late loss” in lumen diameter between the completion of the intervention and the time when the repair process stabilizes (roughly 6 months) (Fig. 23.14). Follow-up angiography shows continued maintenance of lumen diameter at the treated site beyond 6 to 9 months (81).

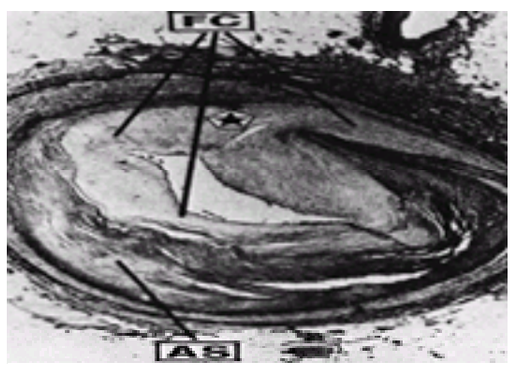

FIG. 23.14. Mechanisms of restenosis: cross-section of a restenotic lesion in the left anterior descending coronary artery 5 months after initial coronary angioplasty shows the original atherosclerotic plaque (AS), the crack in the medial layer induced by the original procedure (star), and the proliferation of fibrocellular tissues (FC) that constitutes the restenotic lesion. (From Serruys PW, et al. Assessment of percutaneous transluminal coronary angioplasty by quantitative coronary angiography:

diameter versus videodensitometric area measurements. *Am J Cardiol* 1984;54:482.)

If the healing response is excessive, however, most or all of the gain in lumen diameter produced by the initial intervention may be lost to the healing process. This causes the return of a severe stenosis and ischemic symptoms—a phenomenon known as *restenosis* of the dilated segment (82) (Fig. 23.15). Throughout the 1980s, restenosis was considered to be a dichotomous outcome (i.e., it either did or did not develop). A large number of competing dichotomous restenosis definitions (e.g., loss of half the gain, late loss more than 0.72 mm) were developed, adding to the general confusion about restenosis rates. Although a great deal was learned about restenosis from the study of conventional angioplasty patients (e.g., its time course, histology, various clinical factors correlating with an increased incidence of restenosis) (83), data derived from stent and atherectomy procedures have led to new paradigms for evaluating restenosis (84). It is now considered more useful to consider restenosis as a continuous variable. A cumulative distribution curve may be used to show the ranked population distribution of the late result, expressed either in terms of late lumen diameter or late percent diameter stenosis, for the whole treated population (Fig. 23.16). On the diameter stenosis curve, the percentage of the population with a late diameter stenosis of more than 50% (analogous to the original dichotomous Emory definition) serves as a useful benchmark for comparing the angiographic “restenosis rates” between different populations or treatment groups.

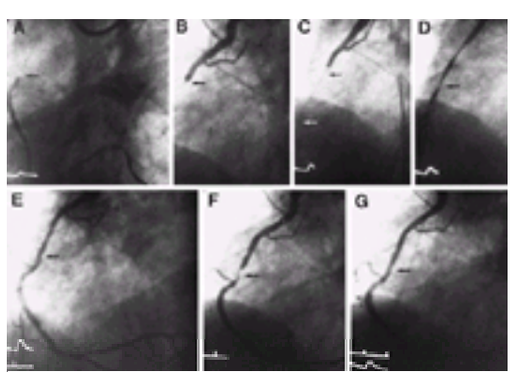

FIG. 23.15. Clinical restenosis. **A** through **D:** A totally occluded right coronary artery with filling of the distal vessel by way of left to right collaterals. **E:** The essentially normal appearance of the right coronary artery after successful angioplasty. **F:** The appearance 6 weeks later, when angina had recurred. **G:** The appearance after successful repeat percutaneous transluminal coronary angioplasty (PTCA). Restenosis developed again after 6 weeks, but the patient has now been asymptomatic after a third PTCA procedure. (From Dervan JP, Baim DS, Cherniles J, et al. Transluminal angioplasty of occluded coronary arteries: use of a movable guidewire system. *Circulation* 1983;68:776.)

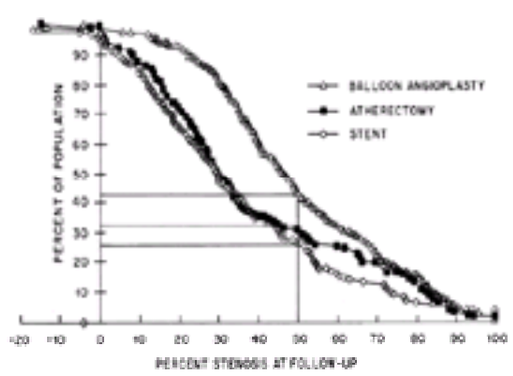

FIG. 23.16. The view of restenosis as a continuous process that takes place to some degree in every treated segment favors displaying the late result (here, percent stenosis at follow-up) for the whole treated population. For patients treated by balloon angioplasty, directional atherectomy, or stenting, the y-axis shows the percentage of patients who have a stenosis greater than the value on the x-axis. The ability of stenting and atherectomy to lower restenosis is shown by a shift of their “cumulative distribution function” curves to the left. If a dichotomous definition of restenosis is applied, the intersection of each curve with a late diameter stenosis of 50% *(vertical line)* corresponds to a dichotomous restenosis rate of 43% for angioplasty, 31% for atherectomy, and 26% for stenting. (From Kuntz RE, et al. Novel approach to the analysis of restenosis. *J Am Coll Cardiol* 1992;19:1493.)

Further understanding is gained by comparing the acute gain in lumen produced by the intervention to the late loss in lumen diameter that results from the healing process. Every treated lesion undergoes some degree of late loss, but this process usually negates only part (roughly half) of the acute gain, so that a long-term net gain in lumen diameter (and alleviation of ischemia) results. Another important finding is the tendency toward a linear relationship between late loss in lumen diameter (caused by the proliferative and fibrotic reaction of the artery during the healing phase) and the acute gain in lumen diameter caused by the intervention. The slope of this relationship (the *loss index*) is roughly 0.5 for most interventions, corresponding to the payment of a late loss “tax” equal to about half of the acute gain. Larger lumen diameters immediately after intervention translate into larger lumen diameters at 6-month angiographic restudy (the “bigger is better” dictum). To date, all new mechanical devices (e.g., stents, directional atherectomy) that have lowered the restenosis rate compared with balloon angioplasty have done so by providing a larger acute lumen diameter (more acute gain). Once minimal lumen diameter is included in the statistical model, the particular device used (stent or atherectomy versus PTCA) is no longer an important determinant of restenosis (Fig. 23.17).

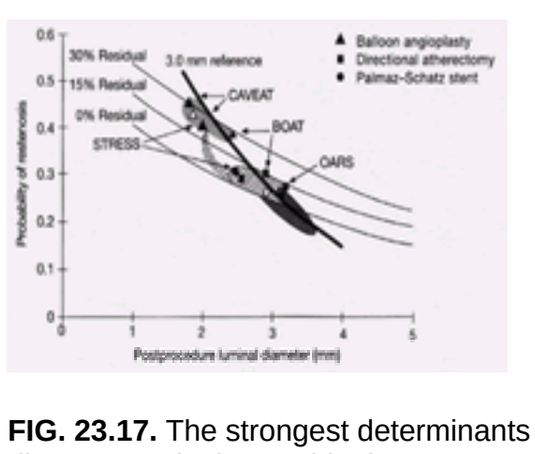

FIG. 23.17. The strongest determinants of the probability of restenosis (using a definition of late diameter stenosis greater than 50%) are a large postprocedure lumen diameter and a low residual percent stenosis. Once these variables are taken into account, it no longer matters which device was used—it is the result and not the device that matters. Balloon angioplasty *(triangles)* resulted in a 2- to 2.3-mm lumen with a 40% restenosis rate, whereas stenting produces a 2.9- to 3.2-mm lumen with a 20% restenosis rate (slightly worse results with stenting in the STRESS study are shown, as well). Directional atherectomy *(squares)* had an angioplasty-like result in CAVEAT but a more stent-like result in BOAT and OARS (see Chapter 24 and Chapter 25). (Modified from Kuntz RE, et al. A generalized model of restenosis following conventional balloon angioplasty, stenting, and directional atherectomy. *J Am Coll Cardiol* 1993;21:15.)

The importance of postprocedure geometry to the late result does not, however, mean that other biologic variables are unimportant. A number of biologic factors (e.g., diabetes, LAD lesion location, prior restenosis, the presence of previously activated smooth muscle cells) have been shown to increase the loss index to as high as

0.70 (84), a level at which even perfect (0% residual stenosis) acute results are associated with a large late loss, a small net gain, and a high restenosis rate in vessels smaller than 4 mm. From this perspective, a drug or other treatment that could decrease the loss index "tax" rate would be dramatically effective in reducing restenosis. Efforts to reduce the restenosis rate by manipulating procedure-related variables such as duration of conventional balloon inflation (10) have been largely unrewarding unless, like stenting, they produce markedly more favorable acute results (i.e., a larger posttreatment minimal luminal diameter). Similarly, trials of numerous drug regimens (e.g., aspirin, nifedipine, ticlopidine, steroids, prolonged heparin administration, fish oil, mevinolin, ketanserin) have shown no beneficial effect against restenosis. The search for such treatments is vital, however, since finding an agent that would decrease the loss index even slightly (e.g., from 50% to 35%), would have a major impact on angiographic restenosis rate. Because the complex healing response involves so many mechanisms (smooth muscle cell proliferation, matrix synthesis, recoil, and fibrotic vessel contraction), and because it appears to be driven by a variety of agonists (e.g., platelet-derived growth factor, thrombin), agents (such as antisense DNA to the protooncogene c-*myc*) that selectively inhibit a final common pathway (smooth muscle cell division) may be of benefit (85). In conventional angioplasty, where late vessel contraction (in addition to the neointimal proliferation response) plays an important role, drugs such as probucol, which seem to favorably affect late remodeling, may be of value (86). On the possibility that antirestenosis drugs might have to be delivered locally or in high concentration or prolonged duration to the treatment site, a number of local drug delivery systems and sustained-delivery vehicles are being investigated (87). The other promising approach is local radiation therapy (brachytherapy). Studies with both µ *g*- and µ*b*-radiation (88,89,89a) suggest that a dose of roughly 1,400 to 1,800 rad (cGy) delivered to the treatment site by a catheter system retards the local proliferative response and may be a promising primary or secondary treatment for restenosis, particularly the purely proliferative restenosis that takes place within stents.

LONG-TERM RESULTS OF ANGIOPLASTY

Although the preceding discussion of restenosis emphasizes mechanistic and quantitative angiographic analyses of late outcome (with an emphasis on the status of the treated site), the long-term *clinica*ı benefit of coronary angioplasty as a strategy for treating patients with coronary artery disease derives from its ability to prevent subsequent ischemic events. The traditional measure of this ability has been the freedom of angioplasty patients from any subsequent events, including death, MI, or a repeat revascularization procedure (either repeat PTCA or late bypass surgery). As trials of new devices have unfolded, however, it has become increasingly important to distinguish whether the cause of a late cardiac event or repeat revascularization is *restenosis of the dilated segment* or the *unchecked natural history of coronary artery disease* (i.e., the persistence or progression of disease elsewhere in the coronary tree). In general, the events that develop during the restenosis window—the first 8 months after successful angioplasty—reflect predominantly restenosis of the treated segment (84). Given the quiescence of the dilated lesion beyond 6 months (81,90), most of the events that develop after 8 months reflect the progression of disease at other sites (Fig. 23.18). Because most late events trigger a repeat cardiac catheterization, it is possible to decide whether the originally treated lesion was responsible, thus "filtering" late clinical end points into those that are and are not related to failure at the original treatment site (target lesion revascularization, or TLR). Such distinctions have become commonplace when reporting or comparing the incidence of clinical events after a particular coronary intervention. On the other hand, when strategies for treating the patient with coronary artery disease are compared (i.e., medicine versus angioplasty or angioplasty versus bypass surgery), the more meaningful comparison remains the occurrence of any late clinical event.

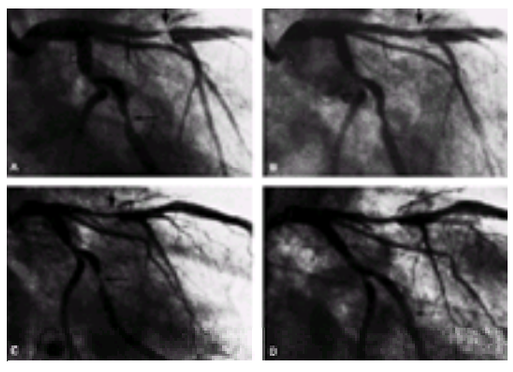

FIG. 23.18. Recurrent angina caused by progressive disease in a nondilated segment. Left coronary artery in right anterior oblique projection before **(A)** and after **(B)** successful dilatation of the middle left anterior descending (LAD) coronary artery. Despite the presence of a moderate lesion in the circumflex marginal branch, this patient had an entirely normal exercise tolerance test until the recurrence of symptoms 1 year later. **C** and **D:** Preserved patency of the LAD but interval progression of the circumflex stenosis, which was then dilated successfully to restore an asymptomatic status. (From Baim DS. Percutaneous transluminal coronary angioplasty: analysis of unsuccessful procedures as a guide toward improved results. *Cardiovasc Intervent Radiol* 1982;5:186.)

The concept of collecting and analyzing late clinical and angiographic follow-up data began with Gruentzig's original series of 169 patients, of whom 133 underwent a successful procedure, in Zurich between 1977 and 1980. A 10-year follow-up study on that group (91) showed an overall survival rate of 89.5%, higher in the 81 patients with SVD than in the 52 patients with multivessel disease (95% vs. 81%, respectively). This was comparable to the 92% survival rate in the 36 patients who underwent unsuccessful PTCA, of whom 32 had coronary artery bypass graft (CABG) surgery (emergency in 13 and elective CABG in 19). Angiography at 6 months showed recurrence in 38 patients (a 31% restenosis rate), 36 of whom had associated symptoms. Only 4 additional patients who had a patent angioplasty site at 6 months developed restenosis later during follow-up (a 3% later restenosis rate), although 25 patients (18%) went on to develop significant narrowing at other nondilated sites during follow-up. At 10 years, patients with single-vessel versus multivessel disease at the time of initial PTCA had substantially better clinical outcomes, with a lower actuarial incidence of MI (9% vs. 29%); MI or bypass surgery (26% vs. 48%); and MI, bypass surgery, or repeat PTCA (37% vs. 44%). They also had better symptomatic status, with freedom from angina in 79% versus 67%, respectively.

These long-term data from this "index" angioplasty series are mirrored in more recent studies (except for a much higher initial procedural success rate). Because most of the late events relating to the treatment site occur in the first 6 to 8 months, it is appropriate to concentrate on a shorter follow-up period (i.e., 1 year). A follow-up report on 838 patients with SVD in the 1985–1986 Registry (92) showed mortality in 1.6%, MI in 1.9%, repeat angioplasty in 18.1%, and bypass surgery in 6.2% within the first year after hospital discharge. In more recent studies, in which balloon angioplasty has included stenting of the worst acute results (see earlier discussion of provisional stenting), the incidence of repeat revascularization within the first year in patients with single-vessel intervention has fallen further, with a TLR rate (by either catheter intervention or bypass surgery) of only 17%, and similarly-defined 1-year TLR rates in some stent trials as low as 12%.

The repeat revascularization rates for patients with multivessel disease are clearly higher (see later discussion). In the 1985–1986 Registry, patients with multivessel disease had a higher in-hospital mortality rate than those with single-vessel disease (1.7% vs. 0.2%); adverse events within the first year after hospital discharge were only slightly more common (mortality in 2.8%, MI in 3.4%), but patients with multivessel disease had an increased need for repeat revascularization. This has been borne out in the randomized trials (e.g., Bypass Angioplasty Revascularization Investigation [BARI]) comparing angioplasty with bypass surgery for patients with multivessel coronary artery disease, where up to 35% of angioplasty patients (but only 5% of surgery patients) required a repeat revascularization within the first year after treatment (92). Newer studies, in which patients with multivessel disease are treated with stenting (rather than with conventional balloon angioplasty alone, as in the studies performed in the late 1980s), have a reduced (approximately 20%) late need for repeat revascularization.

Until a practical and completely effective means of preventing restenosis is established, patients who develop recurrent symptoms in the months after a successful angioplasty should be presumed to have a problem with restenosis. They should be scheduled for repeat coronary angiography, with the anticipation that, should the presence of restenosis of the dilated segment be confirmed, a repeat intervention (Fig. 23.15) will be performed during the same procedure. When repeat balloon angioplasty was the only such procedure available, it was noted that the acute success and safety rates of a repeat angioplasty for restenosis were somewhat higher than those of first angioplasties, but that at least 30% of such patients would go on to develop a second restenosis (93). At particularly high risk (94) were men with long lesions or associated disease progression at other sites who presented with recurrent stenosis within 5 months after the first dilatation. Subsequent restenoses were treated by third, fourth, or even fifth dilatations, although the restenosis rate approached 50% as the number of repeat dilatations increased (95). Many patients with recurrent restenosis ultimately chose the alternative of surgical revascularization. In the new device era, most such patients will have undergone stent placement for these lesions at some point in their treatment history. Although this may decrease the incidence of subsequent restenosis, when it does occur the special considerations relating to the treatment of in-stent restenosis apply (see Chapter 24 and Chapter 25). With recent studies suggesting that local radiation (brachytherapy) is the key to controlling in-stent restenosis, however, this long-standing limitation of angioplasty may be largely controlled.

Several other causes of recurrent symptoms after apparently successful coronary angioplasty should be considered. The first is coronary artery spasm, which may be exacerbated within the first 6 weeks after the procedure (96). Many groups use calcium channel blockers during this period, particularly given the suggestion that

uncontrolled spasm may increase the chance of organic restenosis (97). A second cause of recurrent symptoms after successful angioplasty is persistence of disease in undilated segments. Whereas cardiac surgeons routinely bypass all significant stenoses at the time of surgery, most angioplasty operators confine their efforts to the severe (greater than 70%) stenoses (98), leaving behind more moderate lesions that are unlikely to cause persistent symptoms. The rationale for this approach is that dilatation of these milder lesions requires additional time and administration of contrast medium, exposes the patient to additional hazards of abrupt vessel closure, and may initiate progressive restenosis leading to a more severe lesion than was present initially (99). On the other hand, failure to dilate significant and clinically relevant lesions in patients with multivessel disease may cause persistent symptoms leading to subsequent need for revascularization (Fig. 23.18). When symptoms recur more than 6 months after successful dilatation, disease progression is the most likely explanation (100). Whether symptom recurrence is triggered by restenosis or lesion progression, repeat catheter-based intervention is usually effective in long-term nonoperative management (101). Late stenosis at the left or right coronary ostium (presumably the result of guiding catheter–induced injury) also has been reported as a rare cause of late symptom recurrence (102) and is readily apparent on angiographic restudy.

CURRENT INDICATIONS

With the improvements in equipment and technique that have been described, coronary angioplasty has grown progressively through the 1980s and 1990s (Fig. 23.1). By 1990, more than 400,000 angioplasty procedures were performed annually, represent almost half all revascularizations (angioplasty plus bypass) performed in the United States each year (5). By the end of the 1990s, the number of percutaneous catheter-based revascularizations (including both conventional balloon angioplasty and the ever-growing family of newer devices) had grown to more than 500,000. The fact that there has been no demonstrable fall in the use of bypass surgery during this period suggests that the use of angioplasty has moved beyond the narrow group of patients who would have undergone bypass surgery (as had been suggested in the original NHLBI registry guidelines) to the point where it is now also seen as an alternative to medical therapy in selected patients.

These trends toward greater reliance on catheter-based intervention are also evident in the record of individual programs. Since the mid-1980s, about one third of all patients coming through our diagnostic laboratory have been treated by coronary angioplasty. Data from Emory between 1981 and 1988 (103) show a similar pattern. The percentage of diagnostic catheterization patients going on to coronary angioplasty increased from 4.3% to 30.3%, while the percentage undergoing bypass surgery decreased only from 44.0% to 28.5%. Therefore, almost as much of the growth in angioplasty procedures over that period was explained by contraction of the fraction of patients treated medically (from 51.7% to 41.2%) as by the shift from surgery to angioplasty. In a survey of practice extending from 1989 to 1997 at the 17 U.S. sites that participated in the BARI trials (see Multivessel Coronary Artery Disease), the percentage of all revascularizations that were catheter based (versus surgical) increased from 52.2% to 62% by 1997, with a corresponding growth of new devices from 11.6% to 67% of all catheter-based procedures (104).

Because the person who is responsible for case selection is often the person who will perform the angioplasty, it is critically important that operators have a full understanding of the indications and outcomes so that only suitable patients are treated. The issues that need to be addressed include (a) how compelling is the clinical justification for revascularization, (b) do the “culprit” lesions have anatomic features that suggest reasonable level of safety and probability of successful dilatation, (c) what combination of conventional balloon angioplasty and newer interventional devices would offer the best short- and long-term outcomes, and (d) does angioplasty compare favorably (or at least equally) with the other therapeutic options such as bypass surgery or continued medical therapy. This evaluation process involves integration of complex clinical, angiographic, pathophysiologic, and technical knowledge to decide whether a particular patient is a “candidate” for angioplasty and therefore constitutes an important component of angioplasty operator training (see earlier discussion).

With the rapid growth of coronary angioplasty, several cardiology organizations have prepared position statements that attempt to outline its “correct” utilization (16,105) (Table 23.3). These statements are useful compilations that outline some well accepted indications and contraindications for coronary angioplasty, but they each consign situations in which decisions are difficult and individualized to a “possibly indicated” category. In an effort to review some aspects of these evolving or controversial indications, the following discussion of various anatomic clinical applications of coronary angioplasty is offered.

Potential indications	Potential absolute or relative contraindications
Significant stenosis of one or more major epicardial arteries, which subtend at least a moderate-sized area of viable myocardium, in a patient with any of the following:	High-risk anatomy, including significant left main coronary artery disease in which vessel closure would probably result in hemodynamic collapse
Recurrent ischemic episodes after myocardial infarction or major ventricular arrhythmia	Severe, diffuse, and/or extensive coronary artery disease better treated surgically
Angina that has not responded adequately to medical therapy	Target lesion morphology (type C) with anticipated success less than 60%, unless PTCA is the only reasonable treatment option
Clear evidence of myocardial ischemia on resting, ambulatory or exercise electrocardiography	No coronary stenosis greater than 50% diameter reduction
Objective evidence of myocardial ischemia that increases the overall risk of required noncardiac surgery	No objective or compelling clinical evidence of myocardial ischemia
Acute myocardial infarction with obstruction or severe stenosis of the infarct-related vessel	Absence of on-site surgical backup, qualified PTCA operators, or adequate radiographic imaging equipment

[a] General concepts behind patient selection for PTCA favor anatomically suitable lesions in a patient with a convincing clinical presentation suggesting benefit from revascularization. The application of these concepts to individual patients requires considerable clinical judgment.

Modified from Ryan TJ, et al. Guidelines for percutaneous transluminal coronary angioplasty: a report of the ACC/AHA task force. J Am Coll Cardiol 1990;22:2033.

TABLE 23.3. *Clinical indications for percutaneous transluminal coronary angioplasty (PTCA)*[a]

Single-Vessel Coronary Disease

When the NHLBI registry was formed in 1979, patients were selected in the context of the abilities of then-current angioplasty equipment and the considerable risk of the new therapeutic modality. To be candidates for coronary angioplasty, a patient was required to have medically refractory angina, objective evidence of myocardial ischemia, and single-vessel coronary disease (51), with a lesion that was proximal, discrete, subtotal, concentric, and noncalcified. Although these criteria (in the form of the American College of Cardiology/American Heart Association [AHA/ACC] lesion classification scheme) continue to identify patients with the highest likelihood of success (Table 23.4), major improvements in equipment and technique have permitted the safe and effective application of coronary angioplasty in patients with far less than this ideal anatomy. Steerable guidewires, dilatation catheters with smaller deflated profiles, and adjunctive devices such as stenting, directional atherectomy, rotational atherectomy, and excimer laser have allowed operators to attempt dilatation of progressively more complex anatomic lesions, in progressively sicker patients, with ever-improving results. Recent data suggest that a lesion's high AHA/ACC class does not itself correlate with unfavorable success or complication probability—rather, that specific morphologies such as bifurcation lesions or degenerated saphenous vein grafts are more predictive (106, 106a)—and that experienced operators are able to select lesions at low, medium, or high risk of complication in a way that transcends their AHA/ACC class (107).

Type A lesions (minimally complex)	Type B lesions (moderately complex)	Type C lesions (severely complex)
Discrete (length < 10 mm)	Tubular (length 10–20 mm)	Diffuse (length >2 cm)
Concentric	Eccentric	Excessive tortuosity of proximal segment
Readily accessible	Moderate tortuosity of proximal segment	Extremely angulated segments (>90°)
Nonangulated segment (<45°)	Moderately angulated segment (45°–90°)	Total occlusions >3 mo old and/or bridging collaterals
Smooth contour	Irregular contour	Inability to protect major side branches
Little or no calcification	Moderate or heavy calcification	Degenerated vein grafts with friable lesions
Less than totally occlusive	Total occlusions <3 mo old	
Not ostial in location	Ostial in location	
No major side branch involvement	Bifurcation lesions requiring double guidewires	
Absence of thrombus	Some thrombus present	

[a] Although the A,B,C lesion classification was generated by consensus rather than prospective analysis, it still correlates well with the expected outcome of the procedure. Minimally complex (type A) lesions have the highest probability of success and the lowest probability of complication. Moderately complex (type B) lesions have somewhat lower probability of success and a somewhat higher probability of complication, particularly if multiple type B factors are present. Severely complex (type C) lesions have the lowest probability of success and the highest probability of complication and are generally avoided. The availability of new devices has "upgraded" some traditional B and C morphologies. For example, calcified lesions respond well to rotational atherectomy, bifurcation lesions respond well to directional atherectomy, and vein grafts respond well to stenting.

TABLE 23.4. *Characterization of lesion suitability (AHA/ACC A,B,C Classification)*[a]

However the clinical and anatomic circumstances have changed, patients with a single lesion needing treatment still account for the majority of angioplasty procedures. In the Emory data from 1988, 318 (46%) of 692 patients with SVD were treated by angioplasty, compared with 159 (30.1%) of 528 patients with double-vessel disease and 43 (10.6%) of 405 patients with triple-vessel disease (103). In those patients with SVD, the intent of angioplasty is not to improve life

expectancy (which is already excellent with medical therapy), although Duke databank analysis does suggest a slightly higher 5-year survival rate with angioplasty (95%, vs. 93% with CABG and 94% with medical therapy) (108). Rather, the primary intent in the patient with angina due to SVD is to improve quality of life by alleviating angina. The Veterans Administration (VA) Angioplasty Compared to Medical Therapy (ACME) trial (109) suggested that even conventional balloon angioplasty is better able to achieve this goal than is ongoing medical therapy. Despite a PTCA success rate of only 80%, 64% of PTCA patients (compared with 46% of medically treated patients) were free of angina at 6 months, with the PTCA patients showing a greater increase (2.1 minutes) in exercise time off antianginal medication (compared with a 0.5-minute increase in the medical patients receiving antianginal drugs). The price paid for this symptomatic improvement was a small risk of acute complications (2% emergency bypass, 1% Q-wave MI) and a 23% need for a repeat procedure (PTCA in 16%, bypass surgery in 7%) in the cohort assigned to PTCA. In contrast, 9% of the group assigned to medical therapy had late angioplasty for refractory symptoms. At 6 months, there was one death in the medical group and none in the angioplasty group. Follow-up to 3 years showed ongoing symptomatic benefit in the angioplasty group. Based on these data, not all patients with stable angina resulting from SVD need to undergo angioplasty, particularly if they are reasonably content with their quality of life on medical therapy. Most patients, however, seek better exercise tolerance or relief from medication side effects, if angioplasty for an anatomically suitable single-vessel lesion can be offered at a low risk. This would appear to be an even more compelling option since the possibility of stent placement has further reduced the short-term risk of failure or complication, as well as the long-term risk of restenosis. In the setting of unstable angina or acute MI, the use of angioplasty to treat SVD becomes even more reasonable (see later discussion).

Total Coronary Occlusion

Although total occlusion was initially a contraindication to attempting angioplasty, it has been clear since the early to mid-1980s that many chronic total occlusions can be dilated successfully. The main reason to attempt such a procedure is if the distal myocardium receives collaterals that are adequate to maintain viability but inadequate to meet the increased demand of exercise (Fig. 23.19). The main challenge in angioplasty of a total occlusion is the need to pass a guidewire through the area of occlusion and into the vessel lumen beyond. This is best done by crossing through the path of least resistance (i.e., the “latent” true lumen), without causing vascular dissection or perforation in the attempt. The traditional approach is to use a series of guidewires (progressing from soft- to stiff-tipped) to gently probe the stump of the occlusion until the latent vascular channel is entered. The wire is then rotated and advanced millimeter by millimeter through the total occlusion until it emerges into the distal coronary artery beyond. Even in experienced hands, this approach has a primary success rate in cases of chronic total occlusion of only 60% to 70% (110), mostly because of inability to advance the guidewire across the occlusion. The presence of one or more chronic total occlusions is one of the most common reasons for sending a patient to bypass surgery rather than attempting angioplasty. Until alternative approaches (such as drug- or laser-induced angiogenesis to enhance collateral inflow or more effective mechanical devices) are developed, the biggest factors in approaching total occlusions successfully will be careful case selection and operator expertise.

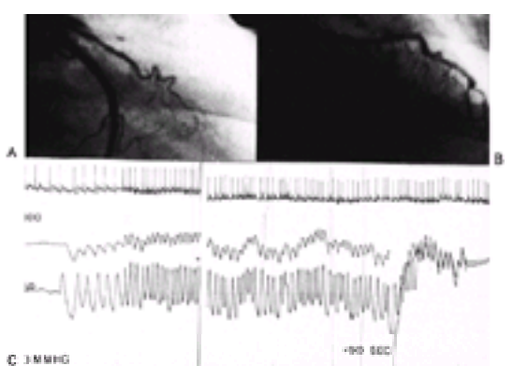

FIG. 23.19. Angioplasty of a totally occluded left anterior descending (LAD) coronary artery, shown before **(A)** and after **(B)** angioplasty. **C:** The proximal (PROX) and distal (DIST) LAD presence. This patient had normal anterior wall motion because of the presence of right-to-left collaterals capable of maintaining a distal occluded LAD pressure of almost 50 mm Hg, but not capable of meeting flow requirements during exertion. (From Dervan JP, Baim DS, Cherniles J, et al. Transluminal angioplasty of occluded coronary arteries: use of a movable guidewire system. *Circulation* 1983;68:776.)

The success rate may be higher for chronic occlusions that have a tapered or funnel-like entry suggesting the presence of a small (0.010-inch) residual lumen (111). The presence of bridging (vasa vasora) collaterals across the area of total occlusion has been thought to be a negative predictor of success, but with careful technique (staying within the lumen rather than exiting into the vasa) success and safety comparable to that seen without such collaterals can be achieved (112). This is facilitated by aiming deliberately toward the continuation of the vessel, which can be aided by performing separate contrast injections into the contralateral (collateral-supplying) coronary artery to opacify the target vessel beyond the area of total occlusion, and by visualizing the anatomy with biplane fluoroscopy or frequent alternation of the single-plane projection. The success of crossing such lesions has improved with the introduction of stiffer and lubricious coated guidewires (Choice-PT, SciMed; Shinobi, Cordis Corporation, Miami, FL) (113) and ball-tip wires (Magnum, Sci Med) (114). A variety of other approaches have been evaluated, including low-speed rotational angioplasty (115), ultrasound vibrational angioplasty (116), and the excimer laser guidewire (117). None of these more aggressive techniques has significantly increased the ability to cross the chronic total occlusion, and they tend to increase the incidence of vessel perforation or extensive local dissection. Still newer techniques (including forward-looking imaging) are under development. If a device can be found that safely improves crossing success for these difficult lesions, it will greatly increase the number of patients who can be served by coronary angioplasty.

Once the guidewire has been passed into the distal vessel, treatment of the total occlusion proceeds as does any other catheter-based intervention. If crossing the lesion has been difficult or has required the use of aggressive guidewire manipulation, it is appropriate to confirm that the distal wire position is in fact intraluminal before advancing or inflating larger devices by performance of a distal injection through an infusion catheter (e.g., Ultrafuse-X, Boston Scientific, Natick, MA). This injection also evaluates the distal anatomy for additional areas of disease. Once these issues are clear, the lesion can be crossed with a balloon catheter and dilated in the usual manner. Perhaps because of competitive flow by way of distal collaterals, plaque bulk, or other lesional characteristics, successfully dilated total occlusions appear to have a higher (40% to 50%) restenosis rate than do subtotal stenoses (110). Several randomized trials have shown that long-term patency can be improved by the use of coronary stents, which further improve the acute lumen caliber, with a restenosis rate of 32% after stenting compared with 74% with balloon angioplasty alone (118).

Multivessel Coronary Artery Disease

With the improved success rate in single-vessel coronary angioplasty, extension of the technique to patients with multivessel disease seemed natural. Selected patients with severe stenosis of two or even all three coronary arteries began to be considered for true multivessel angioplasty in the late 1980s. But most patients with multivessel disease who received angioplasty actually underwent single-vessel dilatation, with the hope that correction of the most severe “culprit” lesions would control ischemic symptoms even though milder lesions in other vessels remained untreated (98). Although it is possible to attempt angioplasty on these milder residual lesions, experience showed that these dilatations carried a significant risk of acute vessel occlusion and their treatment could initiate the restenosis process, resulting in the formation of a severe stenosis within a matter of months (99). On the other hand, leaving significant lesions untreated increased the chance of a late repeat procedure (angioplasty or bypass surgery). In one analysis (119), performing incomplete revascularization (leaving behind stenoses greater than 50% in vessels greater than 1.5 mm in diameter) more than doubled the chance of a late event and increased the risk of 5-year events by 50% even after adjustment for other variables such as left ventricular function, angina class, and territory at risk. This is an important consideration, because fewer than half of the patients undergoing angioplasty in the setting of multivessel disease meet these strict criteria for complete revascularization (92,120). Furthermore, angioplasty in multivessel disease is more demanding technically than single-vessel angioplasty and carries a higher risk of complications should vessel occlusion occur (52,53).

Reanalysis of the medicine versus surgery trials from the 1970s only strengthened the conclusion that bypass surgery offers a clear benefit over medical therapy in patients with multivessel disease (121). It was therefore important to determine how well angioplasty as an initial strategy would compare with bypass surgery. Registries such as the Duke database suggested that surgery would have a survival benefit over angioplasty in patients with triple-vessel disease or double-vessel disease involving severe stenosis of the proximal LAD (108). To gain a clearer picture, several randomized trials of angioplasty versus surgery in multivessel disease were performed in the late 1980s. Several of the trials have been summarized in a metaanalysis by Pocock (122), and two are discussed here in some detail.

Both the Emory EAST trial (123) and BARI (92) showed that fewer than 15% of screened patients with multivessel disease could even be considered suitable for angioplasty—chief exclusions being one or more chronic occlusions, left main coronary artery disease, or a left ventricular ejection fraction of less than 25%. About

60% of the randomized group had double-vessel disease and 40% had triple-vessel disease. In EAST, angioplasty (compared with surgery) provided somewhat less complete initial revascularization (73% vs. 99%), a slightly lower incidence of major in-hospital complications (death, 1%; MI, 3% vs. 10%; stroke, 0.5% vs. 1.5%), and a lower initial hospital cost. Over the next 3 years, although patients treated by initial angioplasty had a similar total mortality rate (7.1% vs. 6.2%), they were much more likely to undergo an additional revascularization procedure (repeat angioplasty, 41% vs. 13%; bypass surgery, 22% vs. 1%) to treat angina due to restenosis of the dilated segment or a territory not revascularized during the initial procedure. Although this eroded much of the initial hospital savings, it did not increase the incidence of late irreversible events (i.e., death, MI). In the randomized portion of the BARI trial of 1,829 patients (92), all lesions were successfully dilated in only 57% of patients (an average 1.9 of 3.5 significant lesions per patient); in comparison, there was complete surgical revascularization in 91% of patients (3.1 coronaries bypassed). Despite a slightly lower incidence of in-hospital death or Q-wave MI (3.0% vs. 5.8%) and a similar 5-year survival rate (86.3% vs. 89.3%), patients treated with initial angioplasty were more likely to undergo a repeat revascularization (54%, including 31% with subsequent CABG) than patients undergoing initial bypass (8%). Of concern in BARI, patients with diabetes fared significantly worse with angioplasty than with surgery, with 5-year all-cause mortality rates of 34.5% and 19.4%, respectively (95% confidence interval for difference, 1.4% to 28.9%). This may reflect the more diffuse nature of coronary disease and the higher incidence of restenosis in diabetics (see Restenosis). The difference between surgery and angioplasty was much less pronounced in the BARI Registry (5-year mortality rate, 14.4% vs. 14.9% for surgery) (124). With the freedom of the registry, operators generally performed angioplasty on diabetic patients who had more localized angiographic disease. For example, the incidence of triple-vessel disease in registry was 35% for angioplasty and 60% for bypass; in the randomized BARI cohort, these figures were 43% and 45%, respectively. This complex issue needs to be addressed further in the 7 and 10-year follow-up of BARI (124a) and the planned BARI-II trial, but it is reasonable to continue to offer catheter-based revascularization to those diabetics who have reasonably discrete lesions while referring patients with more diffuse disease to bypass surgery (125).

Based on these data, fewer than 20% of patients with multivessel disease are likely to be judged as good candidates for coronary angioplasty, compared with more than half of those with SVD (103,123,124). These selected patients can be offered initial angioplasty without increasing their risk of subsequent death or MI, but they must be prepared to accept a four-fold (e.g., 54% vs. 13%) increased need for a subsequent revascularization procedure, including a 22% chance that they will ultimately need bypass surgery anyway. Otherwise, bypass surgery should remain the standard approach to patients with diffuse multivessel coronary artery disease, in whom it provides a more durable benefit than angioplasty, particularly in patients with underlying diabetes. The durability of the result may be improved, however, through the use of other non-balloon technologies such as coronary stenting. Preliminary data suggest that patients treated by multivessel stent placement have a lower and acceptable incidence of late revascularization, with repeat angioplasty rates of 25% to 30% and a low incidence of late bypass surgery (less than 5%) in anatomically suitable patients (126,127).

Trials comparing surgery versus stenting are in progress to reexamine the question in the context on the modern new device era, but even these trials do not include newer modalities such as minimally invasive bypass of the LAD combined with catheter-based treatments of the circumflex and right coronary artery (128), or the inclusion of catheter-based treatments of significant left main coronary artery stenosis. Balloon angioplasty of left main lesions not “protected” by a patent graft to the LAD or circumflex was previously demonstrated to have a poor long-term outlook. Experience in the stent era indicates good acute results in elective left main procedures, but sill a high (10% or more) mortality rate in the first year, probably reflecting restenosis (129). As the predictability and durability of catheter-based intervention continue to improve, it is likely that its indications will encompass more patients with left main or multivessel disease.

Bypass Grafts

Bypass surgery provides excellent early symptomatic benefit, but 40% of saphenous vein conduits become occluded and many more develop severe narrowing within 10 years after surgery (130). Although only 2% of such patients require angioplasty or repeat bypass surgery within the first 5 years, 31% require a repeat revascularization by year 12 (including 20% reoperation and 15% PTCA) (131). Internal mammary conduits have a better long-term track record (132), but some of these grafts develop early significant stenosis at the distal anastomosis. Finally, patients with previous bypass surgery frequently develop new or progressive disease beyond a graft insertion site or in a nongrafted vessel over time. By these various mechanisms, it is common for the patient who has undergone a previous bypass operation to develop recurrent angina. Although this can be managed by repeat bypass surgery, repeat surgery is a higher-risk procedure in a patient population that is older and sicker than those undergoing initial bypass. With the progressive growth of coronary angioplasty, many such patients can be managed by catheter-based intervention on the diseased graft or a stenotic native vessel, and angioplasty of postoperative patients accounts for approximately 20% of current volume. Although angioplasty has a lower in-hospital mortality rate than reoperation (1.2% vs. 6.8%), late mortality is similar and angioplasty carries a higher incidence of repeat interventions, including a 24% 5-year risk of requiring reoperation (133).

When attempting angioplasty in a patient with previous bypass surgery, the operator should keep in mind that the extensive mediastinal fibrosis and risk of injuring functional anterior grafts would prolong the time required for emergency surgery should a complication of angioplasty occur. Although vein-graft stenoses that occur within the first year after surgery are caused most commonly by intimal hyperplasia and respond quite well to balloon dilatation, late vein-graft stenoses (average, 8 years after surgery) are caused more commonly by diffuse atherosclerosis that has a distinct tendency to fragment and/or embolize into the distal coronary bed during dilatation (134,135) (Fig. 23.20). In a 1993 report of their experience with angioplasty for bypass grafts, de Feyter et al. (135) found a primary success rate of 88%, with complications including death (1%), MI (4%), emergency bypass (2%), and distal embolization (3%). Although these acute results may be acceptable, they also found that dilated graft lesions had a high restenosis rate (42% overall), and the rate was even higher in the midportion and body of the graft (58% and 52%, respectively). Other factors associated with increased risks of a poor acute result included grafts older than 3 to 4 years, multiple lesions or diffuse disease, small graft diameter, and the presence of intragraft thrombus, each of which increased the restenosis rate to almost 80%. In addition to plaque friability, older grafts frequently contain thrombus, which may embolize during attempted angioplasty. Grafts with large thrombotic filling defects were often pretreated by intracoronary infusion of a thrombolytic agent (136), such as urokinase 50,000 to 100,000 IU/hour or recombinant tissue plasminogen activator (r-tPA) 20 mg over 20 minutes, to dissolve clot and allow the underlying stenosis to be dilated (Fig. 23.21). More recently, such grafts have been approached with extraction atherectomy (TEC) or rheolytic thrombectomy (Possis AngioJet, Minneapolis, MN) to remove thrombi before definitive mechanical intervention (see Chapter 24). A similar approach can be used on grafts that are more chronically occluded, but poor long-term patency gives such procedures only marginal utility (137).

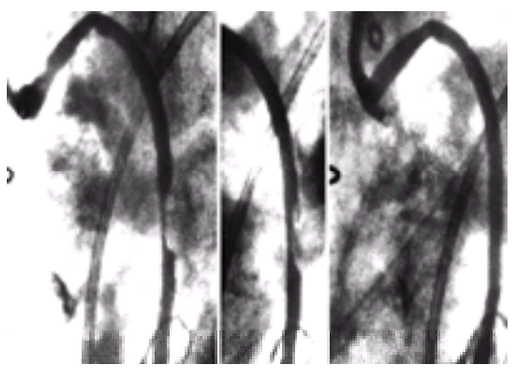

FIG. 23.20. Saphenous vein graft intervention. **Left:** Eccentric stenosis in the midportion of an 8-year-old saphenous vein graft to the left anterior descending coronary artery. **Center:** After conventional balloon angioplasty, there is marked disruption of the plaque and elastic recoil, leaving a 70% residual stenosis. **Right:** After placement of a single Palmaz-Schatz stent, there is a smooth lumen with no residual stenosis. These excellent acute results, plus the favorable late restenosis rate, make stenting the treatment of choice for the focally diseased saphenous vein graft.

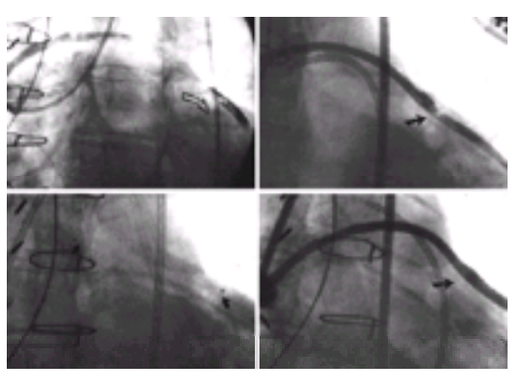

FIG. 23.21. Thrombus-laden graft. **Top left:** Recently occluded saphenous vein graft in a patient with unstable angina shows long, lobulated filling defect consistent with thrombus. **Bottom left:** A drug infusion catheter (Tracker, Target Therapeutics) with 6 cm of side-holes between the gold markers *(small arrows)* has been placed across the thrombotic segment. **Top right:** After overnight infusion of urokinase (50,000 IU/hour), there has been marked cleanup of the thrombus, revealing the underlying focal stenosis in the distal third of the graft. **Bottom right:** Placement of a single Palmaz-Schatz coronary stent normalizes this area of focal disease. Recent trials with the rheolytic thrombectomy catheter have shown mechanical thrombectomy to be superior to prolonged infusion of a thrombolytic agent (see Chapter 24).

As with other lesion types, the availability of new devices has improved the results of vein graft treatment. Directional atherectomy has been used successfully, but the randomized CAVEAT-II trial failed to show significant benefit in long-term outcome (see Chapter 24). On the other hand, stenting has consistently shown superior short- and long-term results (Fig. 23.20). Early registries from both my institution (138) and the Washington Hospital Center (139) in the early 1990s used Palmaz-Schat coronary and biliary stents in a population whose mean graft age exceeded 8 years and achieved a 98% acute success, almost 0% residual stenosis, acute complications in less than 2%, and an angiographic restenosis rate in the 17% to 25% range. Although quite small (approximately 200 patients total) the randomized SAphenous VEin graft Disease (SAVED) trial confirmed these benefits over conventional balloon angioplasty (140) and made stenting the preferred therapy for treatment of the diseased vein graft. With the introduction of second-generation stent designs starting in 1997, more flexible stent deigns are now available, including the self-expanding Wallstent (see Chapter 25). But even effective local treatments like stents are unable to prevent late failures at other (nonstented) portions of the same or other vein grafts, contributing substantially to the need for repeat procedures in follow-up after successful vein graft intervention (141).

Despite the successes of stenting, the problem of distal embolism has continued to plague treatment of these older vein grafts (45,46 and 47). Even without angiographically evident filling defects, these diffusely diseased older grafts may contain sufficient debris to increase their risk of developing frank “no reflow” syndrome. This syndrome involves marked diminution in antegrade flow with profound myocardial ischemia, even though the proximal vessel is free of stenosis or dissection and there are no “cutoffs” in the distal vessel. When this condition represents distal microvascular spasm caused by the release of serotonin from platelet-rich thrombi, it can be reversed quickly by distal injection of a calcium channel blocker (see Chapter 3). In vein grafts, however, many such episodes are refractory to vasodilators and go on to cause large MIs and a substantial (20%) in-hospital mortality. Recent work with a distal occlusion/aspiration device (GuardWire, PercuSurge, Sunnyvale, CA) (142) has demonstrated that the cause of “no reflow” in vein grafts is embolization of atherosclerotic debris (e.g., cholesterol clefts, foam cells), for which the best therapy is likely to be use of distal protective devices (including occlusion devices and filters). The advent of stents with impermeable coverings may also help control this distal embolization problem.

Unlike saphenous veins, *internal mammary artery grafts* are generally resistant to disease, with a 10-year patency rate of better than 90% (132). Still, some patients develop recurrent angina early (within 6 months) after bypass surgery due to stenosis of the internal mammary–native artery anastomosis. These lesions can be dilated effectively with the use of low-profile, trackable dilatation catheters (143), with a moderate (approximately 20%) restenosis rate (Fig. 23.22). Second-generation stents may easily track through internal mammary grafts to treat these distal anastomotic lesions. When evaluating patients with recurrent ischemia in the distribution of an internal mammary graft, it is also important to investigate the possibility of subclavian or brachiocephalic stenosis proximal to the internal mammary origin, which can now be treated by angioplasty or stent placement (144). Limited data regarding angioplasty of gastroepiploic artery grafts suggest similar results of angioplasty in these arterial conduits (145). Although they are technically also a “graft,” the response of the diffuse lesions characteristic of cardiac homografts (accelerated allograft vasculopathy) to coronary angioplasty have not been well characterized (146).

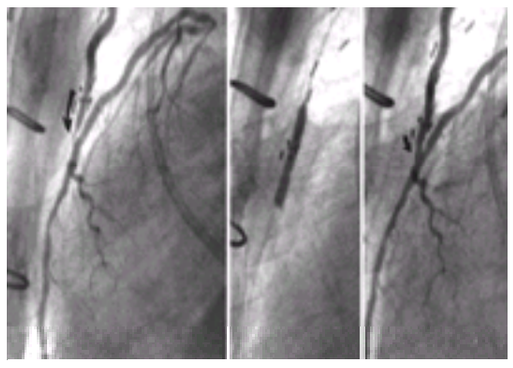

FIG. 23.22. LIMA angioplasty. This 58-year-old man developed recurrent angina 5 months after bypass surgery that had involved grafting of the left internal mammary artery (IMA) to the left anterior descending (LAD) coronary artery (whose proximal segments had exhibited early restenosis after two rotational atherectomy procedures). **Left:** In the left lateral projection, severe stenosis *(curved arrow)* is seen at the distal anastomosis, where the IMA meets the LAD. **Center:** Inflation of a 3.0 mm over-the-wire angioplasty balloon at 70 psi. **Right:** Posttreatment angiography shows 20% residual stenosis. This site and timing (as well as the favorable response to conventional balloon angioplasty) are typical for postoperative problems with the IMA graft.

Stable Angina

The initial group of patients who were candidates for coronary angioplasty were patients with stable but medically refractory angina pectoris and suitable coronary anatomy. Occasionally patients with milder symptoms and ideal anatomy are candidates if they have favorable coronary anatomy and objective evidence of ischemia, and are willing to accept the small risk that angioplasty will lead to emergency bypass surgery and the 20% risk that they will need repeat intervention for the treatment of restenosis (105). This approach was borne out for patients with SVD in the VA ACME trial (109), which showed better freedom from angina and better exercise tolerance in patients randomly assigned to angioplasty treatment, at the expense of more repeat procedures for restenosis. However, patients with mild symptoms should be aware that the ACME trial failed to demonstrate any improvement in the already excellent rates of survival or freedom from infarction seen with medical therapy in a stable angina population with SVD. Of course, the ACME trial was performed before the widespread use of stenting, which has substantially improved the success, safety, and durability of catheter-based intervention, so that similar studies would have to be redone to provide relevant data for today's practice. The findings of the recent Asymptomatic Cardiac Ischemia Pilot study (ACIP) involving 558 patients with ambulatory electrocardiographic evidence of ischemia in the absence of significant symptoms (147) suggest that even these patients may benefit from catheter-based revascularization.

One group worthy of separate mention is elderly patients with severe stable or unstable angina. Unlike bypass surgery (which carries a higher risk and a longer recovery period in the elderly), angioplasty has almost as favorable an outlook in this group as it does in younger patients (148). Although such patients tend to have more challenging anatomy (multiple, diffuse, or calcified lesions), they frequently can be offered palliation by angioplasty as an alternative to bypass surgery. Patients older than 65 years of age now constitute more than 35% of the 1988 Emory angioplasty population (103); 39% of the current patients at Beth Israel are 65 to 79 years of age, and 8% are age 80 or older.

Unstable Angina

Patients with unstable angina (including angina at rest, post-MI angina, accelerating angina, and new-onset angina) have accounted for the majority of interventions in most institutions. Early reports are available from the ThoraxCenter (149), and the 1985–1986 NHLBI PTCA registry (150). In the Registry, 857 patients had unstable angina, 79% of whom had rest angina. The majority of patients with new-onset angina had SVD, largely severe focal stenosis of the LAD coronary artery. Angioplasty was attempted on a mean of 1.6 lesions per patient, with success in 85% and major complications including death (1.4%), nonfatal MI (2.7%), and emergency surgery (4.3%). Complications were greatest in the subgroup of 219 patients with acute coronary insufficiency (rest pain for more than 30 minutes without diagnostic enzyme elevation).

This approach to the patient with unstable angina was evaluated further in the Thrombolysis in Myocardial Infarction (TIMI) IIIB trial, which examined the role of r-tPA

as well as management strategy in 1,473 patients with unstable angina or non–Q-wave MI (151). In the early invasive strategy, patients underwent diagnostic catheterization at a mean of 1.5 days, which led to revascularization in 61% (38% by PTCA and 25% by bypass surgery). PTCA in this group of patients had a favorable outcome (success, 93%; death, 0.4%; nonfatal MI, 2.9%; emergency bypass, 0.7%). Of the patients assigned to a conservative (noncatheterization) strategy, 60% required catheterization primarily for failure of initial therapy, with revascularization in 49% of the patients assigned to this strategy (26% by PTCA and 24% by CABG) within 6 weeks after enrollment. Although there was no difference in the composite end point (death, MI, or positive exercise test) at 6 weeks, patients in the conservative arm required more repeat hospitalizations, more hospital days, and more medications to achieve this end. At 1-year follow-up, the patients receiving early invasive treatment showed a nonsignificant trend toward less death or MI (10.8% vs. 12.2%; p = NS), with fewer repeat hospitalizations (26 vs. 35%; p = .038), and only slightly higher cumulative revascularization rates (64% vs. 58%) with equal bypass rates (30%) at 1 year. The authors concluded that early catheterization after 18 to 48 hours of antiischemic therapy can be carried out safely, clarifies the therapeutic options, and allows prompt delivery of revascularization when appropriate.

The benefits of early catheterization and revascularization for patients with unstable angina were less clear in the 920 patient, VA-based VANQWISH trial (152), but this trial has been criticized for the relatively low use of revascularization in both arms (44% invasive, 33% conservative), the 11% surgical mortality in the invasive arm, and differentially high mortality in nonrevascularized patients (9% in the invasive arm, 5% in the conservative arm). In contrast, the recent Scandinavian trial, Fast Revascularization during Instability in Coronary artery disease (FRISC-II) showed clear benefits, in terms of mortality, readmission, and cost, for the strategy of brief initial medical stabilization (with anticoagulants as well as newer antiplatelet agents including IIb/IIIa blockers), followed by cardiac catheterization and (if anatomically suitable) catheter-based revascularization including the use of coronary stents (153). Of the 2,457 patients, 91% of those treated invasively had an intervention within 10 days after hospital admission, and the invasive arm showed a 21% relative reduction in the 6-month composite of death or MI (9.5% vs. 12.0%), with an even greater reduction among males (9.1% vs. 13.9%), who also had a significantly reduced mortality rate (1.5% vs. 3.2%). Most U.S. centers now follow a similar strategy, with initial medical stabilization followed by a diagnostic catheterization performed with “angioplasty standby” so that suitable lesions can be treated by balloon dilatation or other catheter-based therapies during the same procedure.

Acute Myocardial Infarction

The treatment of acute MI has undergone a major revolution over the past 15 years, with the recognition that intracoronary thrombosis is the final mechanism of vessel occlusion and the understanding that prompt reestablishment of vessel patency offers significant clinical benefit (154). Current “front-loaded” or “double-bolus” regimens using potent thrombolytic agents (e.g., r-tPA) can open almost 75% of infarct vessels within 90 minutes after intravenous administration. A purely pharmacologic approach to the management of MI has not proved completely satisfactory, however, because approximately 15% of vessels fail to open in response to thrombolytic therapy, only half of the open vessels have normal (TIMI grade 3) flow, and at least 10% of vessels opened by thrombolysis either reocclude or cause recurrent angina during hospitalization due to the persistence of an underlying high-grade atherosclerotic stenosis (155). Although newer combinations of thrombolytics with platelet IIb/IIIa receptor blockers may achieve higher rates of initial patency (156), they do so with an increase in bleeding complications.

These shortcomings of thrombolysis prompted several large clinical trials in the late 1980s to explore the optimal strategy of combining thrombolysis with mechanical revascularization using balloon angioplasty (if possible) or bypass surgery. These trials demonstrated that immediate catheterization and angioplasty carry an increased risk and offer no additional benefit in terms of survival or recovery of left ventricular function (157). In fact, the TIMI IIB trial reported that even routine delayed catheterization (18 to 48 hours after thrombolysis) offered no additional benefit over a conservative strategy in which catheterization and angioplasty were reserved for patients with recurrent spontaneous or exercise-provoked ischemia (158).

On the other hand, some operators reported excellent results using primary angioplasty instead of thrombolysis to open occluded vessels in the early hours of infarction (159) (Fig. 23.23). In the early 1990s, the Primary Angioplasty in Myocardial Infarction (PAMI) (160), the Zwolle (161) trials, and a metaanalysis of the four principal trials (total of 2,606 patients) (162) established that prompt primary angioplasty offered better acute patency, fewer reinfarctions, better mortality (3% to 4% vs. 6% to 7%), and fewer strokes than a strategy based on primary administration of a thrombolytic agent. Of course, these studies enrolled only thrombolytic-eligible patients, excluding elderly patients, patients with central nervous system disease, those with cardiogenic shock, and those who had ongoing ST-segment elevation after thrombolytic administration, who have an even higher mortality rate (15% to 20%) with medical therapy and would only be treatable only by acute angioplasty. While excluded patients have a higher mortality rate with primary angioplasty than do thrombolytic-eligible patients, there is strong evidence that acute revascularization does reduce the mortality in such patients with cardiogenic shock. In an analysis from the GUSTO I trial, patients with acute cardiogenic shock who underwent revascularization within the first 30 days (predominantly by angioplasty) had a significantly better 1-year mortality rate than those who did not (37% vs. 70%) (163). Similarly, there is evidence that patients with failed thrombolysis have an acute angioplasty success rate of 88% and a mortality rate of 8.6% after successful rescue PTCA that is similar to the 5.2% mortality rate for successful thrombolysis in GUSTO I (164).

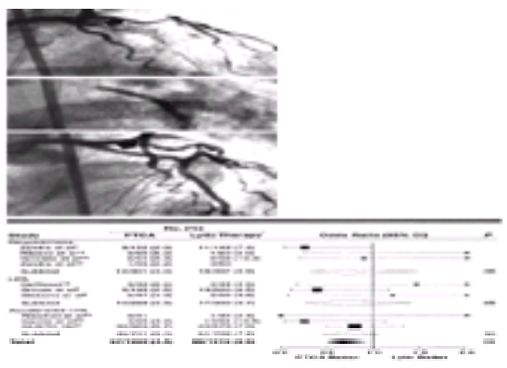

FIG. 23.23. Primary angioplasty for acute myocardial infarction (MI). A primary angioplasty procedure **(left, top)** shows baseline total occlusion of the proximal left anterior descending coronary artery *(arrow)* 2 hours into acute anterior MI with cardiogenic shock. Primary angioplasty **(left, center)** is shown with placement of a perfusion balloon across the area of occlusion. After angioplasty **(left, bottom)**, there is no residual stenosis *(arrow)* and brisk antegrade flow. Despite a peak creatine kinase values approaching 2,000, this patient's hemodynamic status recovered promptly, with normal wall motion on gated nuclear ventriculography 6 weeks later. **Below:** Metaanalysis of more than 2,600 patients from studies comparing primary angioplasty with thrombolytic therapy shows significant reduction in mortality (from roughly 6% to 4%) with primary angioplasty. CABG, coronary artery bypass graft surgery; PTCA, percutaneous transluminal coronary angioplasty. (From Weaver WD, Simes J, Betriu A, et al. Comparison of primary coronary angioplasty and intravenous thrombolytic therapy for acute myocardial infarction: a quantitative review. *JAMA* 1997;278:2093, with permission.)

Based on those studies, our institution began in 1994 to offer primary angioplasty as our around-the-clock frontline therapy for acute MI. This requires a team of experienced angioplasty operators and catheterization personnel who can be in the cardiac catheterization laboratory within 30 minutes, so that a patient can be brought to the laboratory within 60 minutes and have the infarct-related artery open within 90 minutes after emergency room presentation (165). Results of primary angioplasty have improved further with the use of stenting and IIb/IIIa blockers during the procedure. Some studies have even suggested that community hospitals that do not themselves have cardiac surgery or elective angioplasty programs but are staffed by active interventional cardiologists can also deliver primary angioplasty effectively, although this activity is not included in the most recent (1999) revision of the ACC/AHA guidelines for management of acute MI (166). As thrombolytic regimens (and associated antithrombin and antiplatelet drugs) improve, it is likely that the role of mechanical versus pharmacologic thrombolysis will need to be reexamined, but at present we believe that primary angioplasty (where it is available) constitutes the best revascularization strategy for the patient with acute MI.

FINANCIAL AND REGULATORY CONSIDERATIONS

Because coronary angioplasty is performed in a cardiac catheterization laboratory under local anesthesia, it is attended by substantially lower in-hospital costs than coronary bypass surgery (167). On the other hand, this cost benefit is partially eroded by the greater need for repeat procedures to treat restenosis within the first year. The net cost savings therefore depend on the extent to which an intervention improves acute outcome and late freedom from restenosis, as well as its cost. In patients with SVD, stenting has proved to be a cost-effective or even cost-saving technology, whereas in patients with extensive multivessel disease catheter-based revascularization may be a more costly approach than bypass surgery. In general, however, catheter-based revascularization strategies offer less patient morbidity, faster return to work, and equivalent mortality benefit and symptom relief (barring the restenosis) and are therefore preferred when anatomically possible. Because the

decision frequently is being made by the same operator (i.e., the cardiologist who performs the diagnostic catheterization, makes the decision about treatment, and then performs the coronary angioplasty), the large expense associated with catheter revascularization has increasingly made angioplasty a target for scrutiny in the managed-care environment (168).

In addition to issues about the appropriateness of angioplasty procedures and markedly different utilization rates across the country (169), there is also a major question about whether every hospital should offer bypass surgery or angioplasty. In fact, only about 1,500 of the nation's 7,000 hospitals do so, but there is continued pressure on those that do not to open such programs (170). Data from California (171) and a nationwide study of 217,836 Medicare beneficiaries who underwent coronary angioplasty (172) clearly show excess mortality and emergency surgery rates in hospitals that perform fewer than 200 angioplasty procedures per year.

These same issues concern the training and continued caseload for angioplasty operators (173). Early in the development of coronary angioplasty, physicians active in diagnostic catheterization learned to perform angioplasty by attending live demonstration courses and watching or assisting on a small number of procedures (i.e., 10 to 20) under the guidance of a knowledgeable operator. Given the ever-increasing complexity of the procedure, however, virtually all new angioplasty operators since the mid-1980s have received formal training consisting of a third (or third and fourth) year of interventional fellowship beyond completion of their training in diagnostic coronary angiography. During the interventional fellowship, a trainee should perform a minimum of 250 procedures (173a). There is evidence that operators who maintain an annual interventional caseload of fewer than 75 procedures have a higher rate of risk-adjusted complications than higher-volume operators, not just for all patients, but also for low-complexity (AHA/ACC A or B1) lesions (174), and even for stenting (175). To further standardize interventional training in 1999, the Accreditation Council for Graduate Medical Education (ACGME) began certifying interventional fellowship programs, and the Board of Internal Medicine began offering an examination- and caseload-based Certificate of Additional Qualification in Interventional Cardiology (176). These changes will almost certainly put pressure on the more than 7,000 “angioplasty operators” in the United States, most of whom perform less than half of the recommended annual caseload of 75 interventions. As catheter-based interventions continue to evolve toward progressively more challenging clinical and anatomic situations, and as the development of new technologies for coronary intervention continues, increasing functional specialization will be required of “interventional” cardiologists. This action is in keeping with the recommendations of the 1993 ACP/ACC/AHA task force, which advised that “the proliferation of small-volume operators should be curtailed by appropriate institutional review” (16).

ROLE OF CONVENTIONAL ANGIOPLASTY IN THE NEW DEVICE ERA

Between its introduction in 1977 and 1990, conventional balloon angioplasty (POBA) was the only mechanical intervention available for percutaneous coronary revascularization. The choice of devices was very much like the situation described by Mark Twain: “To the man with a hammer, everything looks like a nail.” In contrast, the period from 1988 through 1994 saw unparalleled investigation of a wave of new stent and atherectomy devices (177). The first of the new devices (directional coronary atherectomy) was approved by the U.S. Food and Drug Administration (FDA) in 1990, followed by approval of two other atherectomy devices (rotational and extraction atherectomy), excimer lasers, and two balloon-expandable stents by 1994. Second generations of these devices have been developed, and even newer classes of devices (e.g., thrombectomy, distal protection, radiation) have continued to be introduced. Over only a few years, these new devices have progressively replaced POBA as the dominant stand-alone tool for coronary intervention.

To be chosen over balloon angioplasty, a new device must be expected to provide an advantage in terms of (a) the predictability of the acute result, (b) the quality of the acute result (less residual stenosis), (c) the ability to treat a lesion that would have been refractory to conventional angioplasty, or (d) the ability to reduce the incidence of subsequent restenosis. Moreover, such treatment must be provided in a cost-effective way (if it costs more, it also must provide a clinical benefit worth that extra cost [178]), and it must not unduly increase the complication rate. Although balloon angioplasty remains unmatched in its simplicity, anatomic versatility, and broad clinical applicability, the availability of new devices has made balloon angioplasty more of an adjunctive treatment (for predilation to aid in device passage or postdilation to improve the new device–created result) than a stand-alone treatment. Coronary stents have become heir apparent to balloon angioplasty and are currently being used in more than 80% of catheter-based interventions (see Chapter 25). The atherectomy technologies (directional and rotational atherectomy) are still beneficial for debulking certain lesion types (ostial, calcified, bifurcation lesions), as definitive treatment or to improve the results of subsequent stent placement. These same debulking treatments are also effective in treating in-stent restenosis, particularly when combined with local radiation therapy to inhibit regrowth of the proliferative neointima (see Chapter 24).

Although there is still some uncertainty about which new device is best for which lesion, I believe that “lesion-specific new device therapy” is here to stay. In our practice, as shown in Fig. 23.24, the percentage of interventional procedures in which a new device was used has risen from roughly 50% in 1994 to more than 80% in 1998. During this time, there has been a progressive fall (from 5% to 1.5%) in the incidence of major adverse clinical events, including virtual elimination of emergency bypass surgery (less than 0.2%) and a stable mortality rate of 0.6% in non–acute-infarction patients, despite the treatment of an older, sicker patient population with more complex lesion anatomy. Although much of the research focus in interventional cardiology has shifted to understanding the mechanism, technique, and optimal indications for these new devices, I believe that balloon angioplasty will continue to play a crucial role as an adjunct to new device therapies. Whatever new modalities are introduced—be they forms of angiogenesis (179,180), laser direct myocardial revascularization (181), or nonsurgical septal reduction for hypertrophic obstructive cardiomyopathy (182)—the skills, knowledge, and judgment derived from balloon angioplasty will continue to form the foundation on which broader interventional skills are built in coming years.

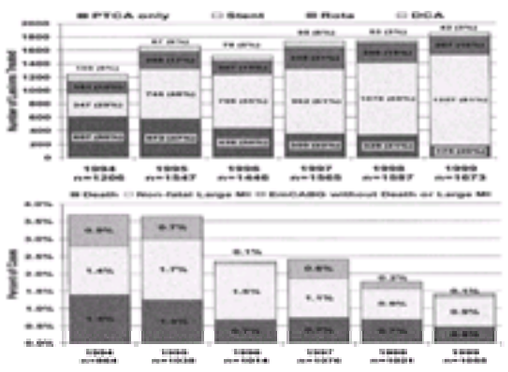

FIG. 23.24. Changing new device use and results at Beth Israel Deaconess Medical Center during the “new device era.” **Upper panel:** During the 6-year period from 1994 through 1999, inclusive, there was a dramatic increase in the use of stenting (from 29% to 81% of interventions) as well ongoing use of atherectomy (directional plus rotational atherectomy from approximately 20% of interventions), but a corresponding decrease in the use of stand-alone balloon angioplasty (from 50% to 20% of interventions). **Lower panel:** The clinical benefits of this trend are reflected in the ability to treat a broader range of lesion types, an increasing primary success rate (from 92% to 98%), and a halving in the incidence of major complications—death, large myocardial infarction (MI) (i.e., Q-wave MI or creatine kinase more than 5 times normal), or emergency surgery—from 3.7% to 1.5%. By 1999, intravenous blockers of platelet glycoprotein IIb/IIIa receptor were used in approximately 30–40% of patients in whom a perfect mechanical result could not be achieved by catheter-based techniques.

CHAPTER REFERENCES

1. Dotter CT, Judkins MP. Transluminal treatment of arteriosclerotic obstruction: description of a new technique and a preliminary report of its application. *Circulation* 1964;30:654.
2. Gruentzig A, Kumpe DA. Technique of percutaneous transluminal angioplasty with the Gruentzig balloon catheter. *AJR Am J Roentgenol* 1979;132:547.
3. Gruentzig AR, Senning A, Siegenthaler WE. Non-operative dilatation of coronary artery stenosis–percutaneous transluminal coronary angioplasty. *N Engl J Med* 1979;301:61.
4. King SB. Angioplasty from bench to bedside. *Circulation* 1996;93:1621.
5. Bittl JA. Advances in coronary angioplasty. *N Engl J Med* 1996;335:1290.
6. Baim D, Kent KM, King SB 3rd, et al. Evaluating new devices: acute (in-hospital) results from the New Approaches to Coronary Intervention Registry. *Circulation* 1994;89:471.
7. Mehta S, et al. Voda guiding catheter is superior to Amplatz guiding catheter for performing left circumflex PTCA. *J Invasive Cardiol* 1994;6:229.
8. Simpson JB, Baim DS, Robert EW, et al. A new catheter system for coronary angioplasty. *Am J Cardiol* 1982;49:1216.
9. Dervan JP, McKay RG, Baim DS. The use of an exchange wire in coronary angioplasty. *Cathet Cardiovasc Diagn* 1985;11:207.
10. Ohman EM, Marquis JF, Ricci DR, et al. A randomized comparison of the effects of gradual prolonged versus standard primary balloon inflation on early and late outcome: results of a multicenter clinical trial. *Circulation* 1994;89:1118.
11. Carell ES, Schroth G, Ali A. Circumferential balloon rupture and catheter fracture due to entrapment in a calcified coronary stenosis. *Cathet Cardiovasc Diagn* 1994;32:34.
12. Tenaglia AN, Zidar JP, Jackman JD Jr, et al. Treatment of long coronary artery narrowings with long angioplasty balloon catheters. *Am J Cardiol* 1993;71:1274.

13. Cannon AD, Roubin GS, Hearn JA, et al. Acute angiographic and clinical results of long percutaneous transluminal coronary angioplasty and adjuvant stenting for long narrowings. *Am J Cardiol* 1994;73:635.
14. Plante S, Strauss BH, Goulet G, et al. Reuse of balloon catheters for coronary angioplasty: a potential cost-saving strategy? *J Am Coll Cardiol* 1994;24:1475.
15. O'Meara JJ, Dehmer GJ. Care of the patient and management of complications after percutaneous coronary artery interventions. *Ann Intern Med* 1997;127:458.
16. Ryan TJ, et al. Guidelines for percutaneous transluminal coronary angioplasty: a report of the ACC/AHA task force. *J Am Coll Cardiol* 1993;22:2033.
17. Fuster V, Dyken ML, Vokonas PS, et al. Aspirin as a therapeutic agent in cardiovascular disease: AHA medical scientific statement. *Circulation* 1993;87:659.
18. Leon MB, Baim DS, Popma JJ, et al. A randomized trial comparing three anti-thrombotic drug regimens following coronary-artery stenting. *N Engl J Med* 1998;339:1665.
19. Kong DF, Califf RA, Miller DP, et al. Outcomes of therapeutic agents that block the platelet glycoprotein IIb/IIIa integrin in ischemic heart disease. *Circulation* 1998;98:2829.
20. Harvey JR, Wyman RM, McKay RG, et al. Use of balloon flotation pacing catheters for prophylactic temporary pacing during diagnostic and therapeutic cardiac catheterization. *Am J Cardiol* 1988;62:941.
21. Ferguson JJ, Dougherty KG, Gaos CM, et al. Relation between procedural activated coagulation time and the outcome after percutaneous transluminal coronary angioplasty. *J Am Coll Cardiol* 1994;23:1061.
22. Popma JJ, Weitz J, Bittl JA, et al. Antithrombotic therapy in patients undergoing coronary angioplasty. *Chest* 1998;114:728S.
23. Lefkovits J, Topol EJ. Direct thrombin inhibitors in cardiovascular medicine. *Circulation* 1994;90:1522.
24. Karsch KR, Preisack MB, Baildon R, et al. Low molecular heparin (Reviparin) in percutaneous transluminal coronary angioplasty: results of a randomized, double-blind, unfractionated heparin and placebo-controlled multicenter trial (REDUCE trial). *J Am Coll Cardiol* 1996;28:437.
25. Burchenal JEB, Marks, DS, Mann JT, et al. Effect of direct thrombin inhibition with bivalrudin (Hirulog) on restenosis after coronary angioplasty. *Am J Cardiol* 1998;82:511.
26. Roubin GS, Douglas JS Jr, King SB 3rd, et al. Influence of balloon size on initial success, acute complications, and restenosis after percutaneous transluminal coronary angioplasty. *Circulation* 1988;78:557.
27. Nichols AB, Smith R, Berke AD, et al. Importance of balloon size in coronary angioplasty. *J Am Coll Cardiol* 1989;13:1094.
28. Chenu P, Zakhia R, Marchandise B, et al. Resistance of the atherosclerotic plaque during coronary angioplasty: a multivariable analysis of clinical and angiographic variables. *Cathet Cardiovasc Diagn* 1993;29:203.
29. Muramatsu T, Tsukahara R, Ho M, et al. Efficacy of cutting balloon angioplasty for lesions at the ostium of the coronary arteries. *J Invasive Cardiol* 1999;11:201.
30. Shawl FA. Minimally invasive angioplasty: acute and long-term results of low-pressure dilation with a non-compliant balloon during percutaneous transluminal coronary angioplasty. *J Invasive Cardiol* 1993;5:122.
31. Blankenship JC, Kruckoff MJ, Werns SW, et al. Comparison of slow oscillating versus fast balloon inflation strategies for coronary angioplasty. *Am J Cardiol* 1999;83:675.
32. Kaltenbach M, Beyer J, Walter S, et al. Prolonged application of pressure in transluminal angioplasty. *Cathet Cardiovasc Diagn* 1984;10:213.
33. Anderson HV, Roubin GS, Leimgruber PP, et al. Measurement of transstenotic pressure gradient during percutaneous transluminal coronary angioplasty. *Circulation* 1986;73:1223.
34. Bech GJW, Pijls NHJ, DeBruyne B, et al. Usefulness of fractional flow reserve to predict clinical outcome after balloon angioplasty. *Circulation* 1999;99:883.
35. Simpendorfer C, Belardi J, Bellamy G, et al. Frequency, management and follow-up of patients with acute coronary occlusions after percutaneous transluminal coronary angioplasty. *Am J Cardiol* 1987;59:267.
36. Friedman HZ, Cragg DR, Glazier SM, et al. Randomized prospective evaluation of prolonged versus abbreviated intravenous heparin therapy after coronary angioplasty. *J Am Coll Cardiol* 1994;24:1214.
37. Pearson T, Raaport E, Criqui M, et al. Optimal risk factor management in the patient after coronary revascularization: a statement for healthcare professionals from an American Heart Association Writing Group. *Circulation* 1994;90:3125.
38. Sanborn TA, Faxon DP, Haudenschild C, et al. The mechanism of transluminal angioplasty: evidence for formation of aneurysms in experimental atherosclerosis. *Circulation* 1983;68:1136.
39. Rensig BJ, Hermans WR, Beatt KJ, et al. Quantitative angiographic assessment of elastic recoil after percutaneous transluminal coronary angioplasty. *Am J Cardiol* 1990;66:1039.
40. Rozenman Y, Gilon D, Welber S, et al. Clinical and angiographic predictors of immediate recoil after successful coronary angioplasty and relation to late restenosis. *Am J Cardiol* 1993;72:1020.
41. Fischell TA, Derby G, Tse TM, et al. Coronary artery vasoconstriction after percutaneous transluminal coronary angioplasty: a quantitative arteriographic analysis. *Circulation* 1988;78:1323.
42. Holmes DR Jr, Vlietstra RE, Mock MB, et al. Angiographic changes produced by percutaneous transluminal coronary angioplasty. *Am J Cardiol* 1983;51:676.
43. Black AJR, Namay DL, Niederman AL, et al. Tear or dissection after coronary angioplasty: morphologic correlates of an ischemic complication. *Circulation* 1989;79:1035.
44. Sanborn TA, Faxon DP, Waugh D, et al. Transluminal angioplasty in experimental atherosclerosis: analysis for embolization using an in vitro perfusion system. *Circulation* 1982;66:917.
45. Baim DS, Carozza JP, Kuntz RE, et al. Managing the “embolization” problem during saphenous vein graft intervention. *Cathet Cardiovasc Interventions* 1999;47:155.
46. Topol EJ, Yadov JS. Recognition of the importance of embolization in atherosclerotic vascular disease. *Circulation* 2000;101:570.
47. Piana R, Paik GY, Moscucci M, et al. Incidence and treatment of “no reflow” after percutaneous coronary intervention. *Circulation* 1994;89:2514.
48. Weyrens FJ, Mooney J, Lesser J, et al. Intracoronary diltiazem for microvascular spasm after interventional therapy. *Am J Cardiol* 1995;75:849.
49. Saffitz JE, Rose TE, Oaks JB, et al. Coronary artery rupture during coronary angioplasty. *Am J Cardiol* 1983;51:902.
50. Ellis SG, Ajluni S, Arnold AZ, et al. Increased coronary perforation in the new device era: incidence, classification, management, and outcome. *Circulation* 1994;90:2725.
51. Kent KM, Mullin SM, Passamani ER, eds. Proceedings of the National Heart, Lung, and Blood Institute Workshop on the Outcome of Percutaneous Transluminal Angioplasty, June 7–8, 1983. *Am J Cardiol* 1984;53:1C.
52. Detre K, Holubkov R, Kelsey S, et al. Percutaneous transluminal coronary angioplasty in 1985–1986 and 1977–1981: the NHLBI registry. *N Engl J Med* 1988;318:265.
53. Holmes DR Jr, Holubkov R, Vlietstra RE, et al. Comparison of complications during percutaneous transluminal coronary angioplasty from 1977 to 1981 and from 1985 to 1986: the NHLBI PTCA registry. *J Am Coll Cardiol* 1988;12:1149.
54. Kent KM, Bonow RO, Rosing DR, et al. Improved myocardial function during exercise after successful percutaneous transluminal coronary angioplasty. *N Engl J Med* 1982;306:441.
55. Hirzel HO, Neusch K, Gruentzig AR, et al. Short- and long-term changes in myocardial perfusion after percutaneous transluminal coronary angioplasty assessed by thallium-201 exercise scintigraphy. *Circulation* 1981;63:1001.
56. Bredlau CE, Roubin GS, Leimgruber PP, et al. In-hospital morbidity and mortality in patients undergoing elective coronary angioplasty. *Circulation* 1985;72:1044.
57. Hill JA, Margolis JR, Feldman RL, et al. Coronary arterial aneurysm formation after balloon angioplasty. *Am J Cardiol* 1983;52:261.
58. Vassarelli C, Turri M, Morando G, et al. Coronary artery aneurysm formation after PTCA: a not uncommon finding at follow-up angiography. *Int J Cardiol* 1989;22:151.
59. Ferguson JJ, et al. The relation of clinical outcome to dissection and thrombus formation during coronary angioplasty. *J Invasive Cardiol* 1995;7:2.
60. Ellis SG, Roubin GS, King SB 3rd, et al. Angiographic and clinical predictors of acute closure after native vessel coronary angioplasty. *Circulation* 1988;77:372.
61. Talley JD, Jones EL, Weintraub WS, et al. Coronary artery bypass surgery after failed elective percutaneous transluminal coronary angioplasty: a status report. *Circulation* 1989;79:I126.
62. Paik GY, Kuntz RE, Baim DS: Perfusion therapy to resolve myocardial ischemia en route to emergency bypass grafting for failed percutaneous transluminal angioplasty. *J Intervent Cardiol* 1995;8:319.
63. de Muinck ED, den Heijer P, van Dijk RB, et al. Autoperfusion balloon versus stent for acute or threatened closure during percutaneous transluminal coronary angioplasty. *Am J Cardiol* 1994;74:1002.
64. George BS, Voorhees WD 3rd, Roubin GS, et al. Multicenter investigation of coronary stenting to treat acute or threatened closure after percutaneous transluminal coronary angioplasty: clinical and angiographic outcomes. *J Am Coll Cardiol* 1993;22:135.
65. Kelly D, Arora D. Prognostic significance of myocardial enzyme release after coronary interventions. *Cathet Cardiovasc Interventions* 1999;46:292.
66. Hartzler GO, Rutherford BD, McConahay DR, et al. “High-risk” percutaneous transluminal coronary angioplasty. *Am J Cardiol* 1988;61:33G.
67. Vogel RA, Shawl F, Tommaso C, et al. Initial report of the National Registry of Elective Cardiopulmonary Bypass-Supported Coronary Angioplasty. *J Am Coll Cardiol* 1990;15:23.
68. Teirstein PS, Vogel RA, Dorros G, et al. Prophylactic versus standby circulatory support for high risk percutaneous transluminal coronary angioplasty. *J Am Coll Cardiol* 1993;21:590.
69. Kugelmass AD, Cohen DJ, Moscucci M, et al. Elevation of the creatine kinase myocardial isoform following otherwise successful directional coronary atherectomy and stenting. *Am J Cardiol* 1994;74:748.
70. Baim DS, Cutlip DE, Sharma SK, et al. Final results of the Balloon vs. Optimal Atherectomy Trial (BOAT). *Circulation* 1998;97:322.
71. Meier B, Gruentzig AR, King SB 3rd, et al. Risk of side branch occlusion during coronary angioplasty. *Am J Cardiol* 1984;53:10.
72. Meier B: Kissing balloon coronary angioplasty. *Am J Cardiol* 1984;54:918.
73. Osterle SN, McAuley BJ, Buchbinder M, et al. Angioplasty at coronary bifurcations: single-guide, two-wire technique. *Cathet Cardiovasc Diagn* 1986;12:57.
74. Dauerman HL, Higgins PJ, Sparano AM, et al. Mechanical debulking versus balloon angioplasty for the treatment of true bifurcation lesions. *J Am Coll Cardiol* 1998;32:1845.
75. Wohlgelernter D, Cleman M, Highman HA, et al. Regional myocardial dysfunction during coronary angioplasty: evaluation by two-dimensional echocardiography and 12 lead electrocardiography. *J Am Coll Cardiol* 1986;7:1245.
76. Bertrand ME, Leblanche JM, Fourrier JL, et al. Left ventricular systolic and diastolic dysfunction during acute coronary artery balloon occlusion in humans. *J Am Coll Cardiol* 1988;12:341.
77. Serruys PW, Wijns W, van den Brand M, et al. Left ventricular performance, regional blood flow, wall motion, and lactate metabolism during transluminal angioplasty. *Circulation* 1984;70:25.
78. Hartzler GO, Rutherford BD, McConahay DR. Retained percutaneous transluminal coronary angioplasty equipment components and their management. *Am J Cardiol* 1987;60:1260.
79. Serota H, Deligonul U, Lew B, et al. Improved method for transcatheter retrieval of intracoronary detached angioplasty guidewire segments. *Cathet Cardiovasc Diagn* 1989;17:248.
80. Mintz GS, Popma JJ, Pichard AD, et al. Arterial remodeling after coronary angioplasty: a serial intravascular unltrasound study. *Circulation* 1996;94:35.
81. Serruys PW, Luijten HE, Beatt KJ, et al. Incidence of restenosis after successful coronary angioplasty: a time related phenomenon. A quantitative angiographic follow-up study of 342 patients. *Circulation* 1988;77:361.
82. McBride W, Lange RA, Hillis LD. Restenosis after successful coronary angioplasty. *N Engl J Med* 1988;318:1734.
83. Hirshfeld JW Jr, Schwartz JS, Jugo R, et al. Restenosis after coronary angioplasty: a multivariable statistical model to relate lesion and procedure variables to restenosis. *J Am Coll Cardiol* 1991;18:647.
84. Kuntz RE, Baim DS. Defining coronary restenosis: newer clinical and angiographic paradigms. *Circulation* 1993;88:1310.
85. Braun-Dullaeus RC, Mann MJ, Dzau VJ. Cell cycle progression: new therapeutic target for vascular proliferative disease. *Circulation* 1998;98:82.
86. Cote G, Tardif J, Lesperance J, et al. Effects of probucol on vascular remodeling after coronary angioplasty. *Circulation* 1999;99:30.
87. Lincoff AM, Ellis SG. Local drug delivery for the prevention of restenosis: fact, fancy, and future. *Circulation* 1994;90:2070.
88. Teirstein PS, Massullo V, Jani S, et al. Catheter-based radiotherapy to inhibit restenosis after coronary stenting. *N Engl J Med* 1997;336:1697.
89. King SB, Williams DO, Chougule P, et al. Endovascular beta-radiation to reduce restenosis after coronary balloon angioplasty: results from the Beta Energy Restenosis Trial (BERT). *Circulation* 1998;97:2025.

89a. Kuntz RE, Baim DS. Prevention of coronary restenosis—the evolving evidence base for radiation therapy. *Circulation* 2000;101:2130.

90. Saito T, Date H, Taniguchi I, et al. Outcome of target sites escaping high-grade (> 70%) restenosis after percutaneous transluminal coronary angioplasty. *Am J Cardiol* 1999;83:857.
91. King SB, Schlumpf M. Ten-year completed follow-up of percutaneous transluminal coronary angioplasty: the early Zurich experience. *J Am Coll Cardiol* 1993;22:353.
92. Detre K, Holubkov R, Kelsey S, et al. One-year follow-up results of the 1985–1986 National Heart, Lung, and Blood Institute's percutaneous transluminal coronary angioplasty registry. *Circulation* 1989;80:421.
93. Black AJR, Anderson HV, Roubin GS, et al. Repeat coronary angioplasty: correlates of a second restenosis. *J Am Coll Cardiol* 1988;11:714.
94. Leimgruber PP, Roubin GS, Hollman J, et al. Restenosis after successful coronary angioplasty in patients with single vessel disease. *Circulation* 1986;73:710.
95. Tierstein PS, Hoover CA, Ligon RW, et al. Repeat coronary angioplasty: efficacy of a third angioplasty for a second restenosis. *J Am Coll Cardiol* 1989;13:291.
96. Hollman J, Austin GE, Gruentzig AR, et al. Coronary artery spasm at the site of angioplasty in the first two months after successful percutaneous transluminal coronary angioplasty. *J Am Coll Cardiol* 1983;2:1039.

97. Bertrand ME, Leblanche JM, Fourrier JL, et al: Relation of restenosis after percutaneous transluminal coronary angioplasty to vasomotion of the dilated arterial segment. *Am J Cardiol* 1989;63:277.
98. Wohlgelernter D, Cleman M, Highman HA, et al. Percutaneous transluminal coronary angioplasty of the "culprit lesion" for management of unstable angina in patients with multivessel coronary artery disease. *Am J Cardiol* 1986;58:460.
99. Ischinger LT, Gruentzig AR, Hollman J, et al. Should coronary arteries with less than 60% diameter stenosis be treated by angioplasty? *Circulation* 1983;68:148.
100. Joelson JM, Most AS, Williams DO. Angiographic findings when chest pain recurs after successful percutaneous transluminal coronary angioplasty. *Am J Cardiol* 1987;60:792.
101. Lehmann KG, Maas AC, van Domburg R, et al. Repeat interventions in the management of progressive coronary artery disease. *J Am Coll Cardiol* 1996;27:1398.
102. Lowe HC, Chesternab CN, Khachigian LM. Left main coronary artery stenosis after percutaneous transluminal coronary angioplasty: importance of remaining "minimally invasive." *Cathet Cardiovasc Diagn* 1999;46:254.
103. Weintraub WS, Jones EL, King SB, et al. Changing use of coronary angioplasty and coronary bypass surgery in the treatment of chronic coronary artery disease. *Am J Cardiol* 1990;65:183.
104. Holubkov R, Detre KM, Sopko G, et al. Trends in coronary revascularization 1989–1997: the Bypass Angioplasty Revascularization Investigation (BARI) survey of procedures. *Circulation* 1999;84:157.
105. Gibbons RJ, Chatterjee K, Daley J, et al. ACC/AHA/ACP-ASIM Guidelines for the management of patients with chronic stable angina: executive summary and recommendations. *Circulation* 1999;99:2829.

106a. Ellis SG, Gutta V, Miller D, et al. Relation between lesion characteristics at risk with percutaneous intervention in the stent and glycoprotein IIb/IIc era. *Circulation* 1999;100:1971.

106. Zaacks SM, Allen JE, Calvin JE, et al. The value of the American College of Cardiology/American Heart Association stenosis morphology classification for coronary interventions in the late 1990s. *Am J Cardiol* 1998;82:43.
107. Brueren BRG, Suttorp MJ, Ernst JMPG, et al. How good are experienced interventional cardiologists in predicting the risk and difficulty of a coronary angioplasty procedure: a prospective study to optimize surgical standby. *Cathet Cardiovasc Interventions* 1999;46:257.
108. Mark DB, Nelson CL, Califf RM, et al. Continuing evolution of therapy for coronary artery disease: initial results from the era of coronary angioplasty. *Circulation* 1994;89:2015.
109. Parisi AF, Folland ED, Hartman P. A comparison of medical therapy in the treatment of single-vessel coronary artery disease. *N Engl J Med* 1992;326:10.
110. Puma JA, Sketch MH, Tcheng JF, et al. Percutaneous revascularization of chronic coronary occlusions: an overview. *J Am Coll Cardiol* 1995;26:1.
111. Katsuragawa M, Fijiwara H, Miyamae M, et al. Histologic studies in percutaneous transluminal coronary angioplasty for chronic total occlusion: comparison of tapering and abrupt type of occlusion and short and long occluded segments. *J Am Coll Cardiol* 1993;21:604.
112. Kinoshita I, Katoh O, Nariyama J, et al. Coronary angioplasty of chromic total occlusions with bridging collateral vessels: immediate and follow-up outcome from a large single-center experience. *J Am Coll Cardiol* 1995;26:409.
113. Freed M, Boatman JE, Siegel N, et al. Glidewire treatment of resistant coronary occlusion. *Cathet Cardiovasc Diagn* 1993;30:201.
114. Meier B, Carlier M, Finci L, et al. Magnum wire for balloon recanalization of chronic total occlusion. *Am J Cardiol* 1989;64:148.
115. Kaltenbach M, Vallbracht C, Hartman A. Recanalization of chronic coronary occlusion by low speed rotational angioplasty (ROTACS). *J Intervent Cardiol* 1991;4:155.
116. Siegel RJ, Gunn J, Ahsan A, et al. Use of therapeutic ultrasound in percutaneous coronary angioplasty: experimental in vitro studies and initial clinical experience. *Circulation* 1994;89:1587.
117. Hamburger JN, Serruys PW, Scabra-Gomes R, et al. Recanalization of total coronary occlusions using the laser guidewire. *Am J Cardiol* 1997;80:1419.
118. Sirnes PA, Golf S, Myreng Y, et al. Stenting in chronic coronary occlusion (SICCO): a randomized, controlled trial of adding stent implantation after successful angioplasty. *J Am Coll Cardiol* 1996;28:1444.
119. Cowley MJ, Vandermael M, Topol EJ, et al. Is traditionally defined complete revascularization needed for patients with multivessel disease treated by elective coronary angioplasty? *J Am Coll Cardiol* 1993;22:1289.
120. Bourassa MG, Holubkov R, Yeh W, et al. Strategy of complete revascularization in patients with multivessel coronary artery disease (a report from the 1985–1986 NHLBI PTCA registry). *Am J Cardiol* 1992;70:174.
121. Yusuf S, Zucker D, Peduzzi P, et al. Effect of coronary artery bypass surgery on survival: overview of 10-year results from randomized trials by the Coronary Artery Bypass Surgery Trialists. *Lancet* 1994;344:563.
122. Pocock SJ, Henderson RA, Rickards AF, et al. Meta-analysis of randomised trials comparing coronary angioplasty with bypass surgery. *Lancet* 1995;346:1184.
123. King SB, Lembo NJ, Weintraub WS, et al. A randomized trial comparing coronary angioplasty with coronary bypass surgery. *N Engl J Med* 1994;331:1044.
124. Detre KM, Guo P, Holubkov R, et al. Coronary revascularization in diabetic patients: a comparison of the randomized and observational components of the Bypass Angioplasty Revascularization Investigation (BARI). *Circulation* 1999;99:633.

124a. The BARI Investigators. Seven-year outcome in the Bypass Angioplasty Revascularization Investigation (BARI) by treatment and diabetic status. *J Am Coll Cardiol* 2000;35:1122.

125. Kuntz RE. Importance of considering atherosclerosis progression when choosing a coronary revascularization strategy: the diabetes-percutaneous transluminal coronary angioplasty dilemma. *Circulation* 1999;99:847.
126. Laham RJ, Ho KKL, Baim DS, et al. Multivessel Palmaz-Schatz stenting: early results and one-year outcome. *J Am Coll Cardiol* 1997;30:180.
127. Moussa I, Reimers B, Moses J, et al. Long-term angiographic and clinical outcome of patients undergoing multivessel coronary stenting, *Circulation* 1997;96:3873.
128. Cohen HA, Zenati M, Smith AJC, et al. Feasibility of combined percutaneous transluminal angioplasty and minimally invasive direct coronary artery bypass in patients with multivessel coronary artery disease. *Circulation* 1998;98:1048.
129. Baim DS. Is it time to offer elective percutaneous transluminal treatment of the unprotected left main coronary artery? *J Am Coll Cardiol* 2000;35:1551.
130. Fizgibbon GM, Kafka HP, Leach AJ, et al. Coronary bypass graft fate and patient outcome: angiographic follow-up of 5,065 grafts related to survival and reoperation in 1,388 patients during 25 years. *J Am Coll Cardiol* 1996;28:616.
131. Weintraub WS, Jones EL, Craver JM, et al. Frequency of repeat coronary bypass or coronary angioplasty after coronary artery bypass surgery using saphenous venous grafts. *Am J Cardiol* 1994;73:103.
132. Loop FD, Lytle BW, Cosgrove DM, et al. Influence of internal-mammary-artery graft on 10-year survival and other cardiac events. *N Engl J Med* 1986;314:1.
133. Weintraub WS, Jones EL, Morris DC, et al. Outcome of reoperative coronary bypass surgery versus coronary angioplasty after previous bypass surgery. *Circulation* 1997;95:868.
134. Waller BF, Rothbaum DA, Gorfinkel HJ, et al. Morphologic observations after percutaneous transluminal angioplasty of early and late aortocoronary saphenous vein bypass grafts. *J Am Coll Cardiol* 1984;4:784.
135. deFeyter P, van Suylen RJ, de Jaegere PP, et al. Balloon angioplasty for the treatment of lesions in saphenous vein bypass grafts. *J Am Coll Cardiol* 1993;21:1539.
136. Hartmann JR, McKeever SLS, O'Neill WW, et al. Recanalization of chronically occluded aortocoronary saphenous vein bypass grafts with long-term, low-dose direct infusion of urokinase (ROBUST): a serial trial. *J Am Coll Cardiol* 1996;27:60.
137. de Feyter PJ, Serruys P, van den Brand M, et al. Percutaneous transluminal angioplasty of a totally occluded venous bypass graft: a challenge that should be resisted. *Am J Cardiol* 1989;64:88.
138. Piana RN, Moscucci M, Cohen DJ, et al. Palmaz-Schatz stenting for treatment of focal vein graft stenosis: immediate results and long-term outcome. *J Am Coll Cardiol* 1994;23:1296.
139. Wong SC, Popma JJ, Pichard AD, et al. Comparison of clinical and angiographic outcomes after saphenous vein graft angioplasty using coronary versus "biliary" tubular slotted stents. *Circulation* 1995;91:339.
140. Savage MP, Douglas JS, Fishman DL, et al. Stent placement compared with balloon angioplasty for obstructed coronary bypass grafts. *N Engl J Med* 1997;337:740.
141. Ellis SG, Brener SJ, DeLuca S, et al. Late myocardial ischemic events after saphenous vein graft intervention: importance of initially "non-significant" vein graft lesions. *Am J Cardiol* 1997;79:1460.
142. Webb JG, Carere RG, Virmani R, et al. Retrieval and analysis of particulate debris following saphenous vein graft intervention. *J Am Coll Cardiol (in press)*.
143. Hearne SE, Davidson CJ, Zidar JP, et al. Internal mammary artery graft angioplasty: acute and long-term outcome. *Cathet Cardiovasc Diagn* 1998;44:153.
144. Kugelmass AD, Kim D, Kuntz RE, et al. Endoluminal stenting of a subclavian artery stenosis to treat ischemia in the distribution of a patent left internal mammary artery graft. *Cathet Cardiovasc Diagn* 1994;33:175.
145. Isshiki T, Yamaguchi T, Tamura T, et al. Percutaneous angioplasty of stenosed gastroepiploic artery grafts. *J Am Coll Cardiol* 1993;22:727.
146. Topaz O, Cowley MJ, Mohanty PK, et al. Percutaneous revascularization modalities in heart transplant recipients. *Cathet Cardiovasc Interventions* 1999;46:227.
147. Davies RF, Goldberg AD, Forman S, et al. Asymptomatic cardiac ischemia pilot (ACIP) study two-year follow-up: outcomes of patients randomized to initial strategies of medical therapy versus revascularization. *Circulation* 1997;95:2037.
148. Forman DE, Berman A, McCabe CH, et al. PTCA in the elderly: "young old" versus the "old old." *J Am Geriatr Soc* 1992;40:19.
149. deFeyter PJ, Serruys PW, van den Brand M, et al. Emergency angioplasty in refractory unstable angina. *N Engl J Med* 1985;313:342.
150. Bentivoglio LG, Detre K, Yeh W, et al. Outcome of percutaneous transluminal coronary angioplasty in unstable angina pectoris: a report from the 1985–1986 National, Heart, Lung, and Blood Institute Percutaneous Transluminal Coronary Angioplasty Registry. *J Am Coll Cardiol* 1994;24:1195.
151. Anderson HV, Cannon CP, Stone PH, et al. One-year results of the Thrombolysis in Myocardial Infarction (TIMI) IIIB clinical trial: a randomized comparison of tissue-type plasminogen activator versus placebo and early invasive versus early conservative strategies in unstable angina and non–Q wave myocardial infarction. *J Am Coll Cardiol* 1995;26:1643.
152. Boden WE, O'Rourke RA, Crawford MH, et al. Outcomes in patients with acute non-Q-wave myocardial infarction randomly assigned to an invasive as compared with a conservative management strategy (VANQWISH). *N Engl J Med* 1998;328:1785.
153. No authors listed. Invasive compared with non-invasive treatment in unstable coronary-artery disease: FRISC prospective randomised multicentre study. FRagmin and Fast Revascularisation during InStability in Coronary artery disease Investigators. 1999;354:708.
154. Ryan TJ, Anderson JL, Antman EM, et al. ACC/AHA guidelines for the management of patients with acute myocardial infarction: executive summary. *Circulation* 1996;94:2341.
155. White HD, Van de Werf FJJ. Thrombolysis for acute myocardial infarction. *Circulation* 1998;97:1632.
156. Antman EM, Giugliano RP, Gibson CM, et al. Abciximab facilitates the rate and extent of thrombolysis: results of the Thrombolysis In Myocardial Infarction (TIMI) 14 trial. *Circulation* 1999;99:2720.
157. Rogers WJ, Baim DS, Gore JM, et al. Comparison of immediate invasive, delayed invasive and conservative strategies after tissue-type plasminogen activator: results of the TIMI IIA trial. *Circulation* 1990;81:1457.
158. The TIMI Study Group. Comparison of invasive and conservative strategies after treatment with intravenous tissue plasminogen activator in acute myocardial infarction. *N Engl J Med* 1989;320:618.
159. O'Keefe JH, Rutherford BD, McConahay DR, et al. Early results and long-term outcome of direct coronary angioplasty for acute myocardial infarction in 500 consecutive patients. *Am J Cardiol* 1989;64:1221.
160. Grines CL, Browne KF, Marco J, et al. A comparison of immediate angioplasty with thrombolytic therapy for acute myocardial infarction. *N Engl J Med* 1993;328:673.
161. deBoer MJ, Hoorntje JC, Ottervanger JP, et al. Immediate coronary angioplasty versus intravenous streptokinase in acute myocardial infarction: left ventricular ejection fraction, hospital mortality, and reinfarction. *J Am Coll Cardiol* 1994;23:1004.
162. Weaver WD, Simes J, Betriu A, et al. Comparison of primary coronary angioplasty and intravenous thrombolytic therapy for acute myocardial infarction: a quantitative review. *JAMA* 1997;278:2093.
163. Berger PB, Tuttle RH, Holmes DR, et al. One-year survival among patients with acute myocardial infarction complicated by cardiogenic shock, and its relation to early revascularization: results from the GUSTO-I trial. *Circulation* 1999;99:873.
164. Ross AM, Lundergan CF, Rohrbeck SC, et al. Rescue angioplasty after failed thrombolysis: technical and clinical outcomes in a large thrombolysis trial. *J Am Coll Cardiol* 1998;31:1511.
165. Caputo RP, Ho KKL, Stoler RC, et al. Effect of continuous quality improvement analysis on the delivery of primary percutaneous transluminal coronary angioplasty for acute myocardial

infarction. *Am J Cardiol* 1997;79:1159.
166. Ryan TJ, Antman EM, Brooks NH, et al. 1999 Update: ACC/AHA guidelines for the management of patients with acute myocardial infarction. *J Am Coll Cardiol* 1999;34:890.
167. Ellis SG, Brown KJ, Ellert R, et al. Cost of cardiac care in three years after coronary catheterization in a contained care system: clinical determinants and implications. *J Am Coll Cardiol* 1998;31:1306.
168. Langa KM, Sussman EJ. The effect of cost-containment policies on rates of coronary revascularization in California. *N Engl J Med* 1993;329:1784.
169. Topol EJ, Ellis SG, Cosgrove DM, et al. Analysis of coronary angioplasty practice in the United States with an insurance-claims data base. *Circulation* 1993;87:1489.
170. Robinson JC, Garnick DW, McPhee SJ. Market and regulatory influences on the availability of coronary angioplasty and bypass surgery in US hospitals. *N Engl J Med* 1987;317:85.
171. Ritchie JL, Philips KA, Luft HS. Coronary angioplasty: statewide experience in California. *Circulation* 1993;88:2735.
172. Jolis JG, Peterson ED, DeLong ER, et al. The relation between the volume of coronary angioplasty procedures at hospitals treating Medicare beneficiaries and short-term mortality. *N Engl J Med* 1994;331:1625.
173. Hirshfeld JW, Ellis SG, Faxon DP, et al. Recommendations for the assessment and maintenance of proficiency in coronary interventional procedures. *J Am Coll Cardiol* 1998;31:722.
174. Ellis SG, Weintraub W, Holmes D, et al. Relation of operator volume and experience to procedural outcome of percutaneous coronary revascularization at hospitals with high interventional volumes. *Circulation* 1997;96:2479.
175. Ryan TJ. Stents: expanding the case for volume minimums in interventional cardiology. *J Am Coll Cardiol* 1998;32:977.
176. Parmley WW. Interventional cardiology: an aded qualification to the cardiovascular boards. *J Am Coll Cardiol* 1998;30:716.
177. Baim DS, Leon MB, Popma JJ, et al. Problems in the evaluation of new devices for coronary intervention: what have we learned since 1989? *Am J Cardiol* 1997;80[Suppl]:3K.
178. Cohen DJ, Breall JA, Ho KK, et al. Evaluating the potential cost-effectiveness of stenting as a treatment for symptomatic single-vessel coronary disease: use of a decision-analytic model. *Circulation* 1994;89:1859.
179. Losordo DW, Vale PR, Symes JF, et al. Gene therapy for myocardial angiogenesis: initial results with direct myocardial injection of phVEGF-165 as sole therapy for myocardial ischemia. *Circulation* 1998;98:2800.
180. Kornowski R, Leon MB, Fuchs S, et al. Electromagnetic guidance for catheter-based trans-endocardial injection: a platform for intramyocardial angiogenesis therapy. *J Am Coll Cardiol* 2000;35:1031.
181. Shawl FA. Percutaneous transluminal myocardial revascularization: an emerging technology. *J Invasive Cardiol* 1999:11:169.
182. Knight C, Kurbaan AS, Seggewiss H, et al. Nonsurgical septal reduction for hypertrophic obstructive cardiomyopathy: outcome in the first series of patients. *Circulation* 1997;95:2075.

24
Coronary Atherectomy, Atheroablation, and Thrombectomy*

Richard E. Kuntz and Donald S. Baim

REK: Harvard Medical School, Division of Clinical Biometry, Brigham and Women's Hospital, Boston, Massachusetts 02115
DSB: Harvard Medical School; Center for Innovative Minimally Invasive Therapy, Brigham and Women's Hospital, Boston, Massachusetts 02115

Unlike balloon angioplasty (Chapter 23) or stent placement (Chapter 25), which widen the coronary lumen by merely displacing atherosclerotic plaque, the family of atherectomy techniques seeks to widen the lumen by actually removing tissue (plaque or thrombus) from the vessel wall. A variety of specific devices and mechanisms of action are available, ranging from cutting and retrieval (directional [1,2] and transluminal excisional atherectomy [3]) to atheroablation without recovery of the resulting debris (rotational [4,5] and laser atherectomy [6]). Also included are the recently approved Possis AngioJet thrombectomy suction catheter (which has no cutting elements but uses a highly efficient vacuum generation system to provide efficient removal of intracoronary thrombus) and the new class of embolus containment devices (which do not act on the lesion itself, but rather trap and recover atheroembolic debris liberated from the lesion by other devices).

The proportion of interventions involving atherectomy has diminished (to roughly 20% in our laboratory) since reaching its zenith (at about 30%) from 1992 to 1994, largely because stenting generally provides a simpler, easier, and often less costly option. But atherectomy continues to be used for indications that are unfavorable for stenting, or where atherectomy before stenting improves results. It is therefore important to understand the techniques available and how to match available devices to patient and lesion characteristics, so as to optimize the final posttreatment lumen diameter and procedural safety. Given the wide variety of devices and associated mechanisms, the design, technique, results, and applications of each will be reviewed separately.

DIRECTIONAL CORONARY ATHERECTOMY

Device Description

The directional coronary atherectomy (DCA) catheter, also called the Simpson AtheroCath (Guidant, Santa Clara, CA), was first used in human peripheral vessels in 1985 (1) and in coronary arteries in 1986 (7). The coronary device was approved in 1990, following a large multicenter experience (8). Despite several minor improvements, the basic concept remains intact—a windowed steel housing is pressed up against the lesion by a low-pressure positioning balloon. Any plaque that protrudes into the window is then shaved from the lesion and trapped in the device nose cone by a spinning cup-shaped cutter that is advanced across the window opening. The coronary device tracks over a 0.014-inch guidewire (Fig. 24.1), and wire braid allows the shaft to be rotated to reduce friction as the device is advanced across the lesion and to allow precise rotational orientation of the cutting window. During cuts, a separate battery-powered motor drive unit spins the cup-shaped cutter at approximately 2,500 rpm, as it is advanced manually by a small lever on the motor drive unit.

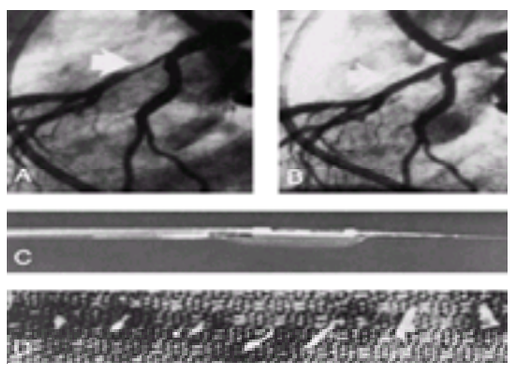

FIG. 24.1. Directional coronary atherectomy. Left coronary angiography (lateral view) reveals a long eccentric stenosis in the mid–left anterior descending (LAD) artery (**A**). After atherectomy, the lumen is smooth, and there is no significant residual stenosis or dissection (**B**). A 7F AtheroCath was employed (**C**), and several pieces of atheroma were retrieved (**D**).

Three different sizes of housing are available for coronary use, with diameters of 5F, 6F, and 7F (1.7, 2.0, and 2.3 mm, respectively). A 7F-graft device with a larger-diameter positioning balloon is also available. A newer design (Flexi-Cut) now in clinical trials uses a single 6F housing with a wider (160° versus 120° window

opening), and different size positioning balloons to achieve different effective working diameters.

Directional Atherectomy Procedure

The large size of the device requires special 9.5F and 10F guiding catheters, which are constructed with gentle curves rather than sharp angles to facilitate passage of the rigid housing (Fig. 24.2). Some large-lumen 9F catheters are capable of delivering the 6F and 7F devices, and a new flexi-cut design promises 8F guiding catheter compatibility. The size of the atherectomy device is determined by the size of the normal vessel adjacent to the stenosis (the reference segment). The 6F device is generally used when the reference diameter is less than 3 mm, and the 7F device, when the reference diameter is between 3 and 4 mm or when a residual stenosis remains despite use of the 6F device with balloon inflation pressures up to 40 psi. The 7F graft device uses a larger-diameter positioning balloon on the 7F housing to treat vessels of more than 4 mm. A smaller, 5F device may be used rarely (e.g., subtotal lesions in calcified or moderately tortuous vessels) to partially debulk the plaque and thereby facilitate passage of a larger (definitive) device. Predilation with a small (e.g., 2-mm) conventional balloon also may be used to facilitate passage of the AtheroCath, but larger predilating balloons should not be used to avoid causing dissections or making recovery of tissue more difficult during subsequent atherectomy cuts.

FIG. 24.2. Guiding catheters for directional coronary atherectomy (devices for vascular intervention) are constructed with gentle curves rather than sharp angles. **Left:** The 11F JCL 3.5 guiding catheter for coronary atherectomy. **Right:** The 9F JCL 4 guiding catheter for conventional PTCA.

After flushing the central lumen and filling the balloon lumen with dilute contrast material, the device is passed into the guiding catheter over an exchange-length guidewire that has been positioned well across the target lesion through a large-bore rotating hemostatic valve. To advance the device across the target lesion, the device is gently advanced until its nose cone passes into the proximal portion of the vessel. Gentle withdrawal or rotation of the guiding catheter helps align the device with the long axis of the vessel, and gentle forward pressure is applied during continuous rotation of the atherectomy catheter. If the device does not pass easily, attempts to force it into the lesion or around curves in the vessel should be avoided, since forceful advancement of the rigid housing through a stiff, calcified, tortuous vessel could traumatize the vessel wall. Likewise, deep seating the guiding catheter (a common maneuver in PTCA) should be avoided during atherectomy, since the stiff guiding catheter itself may cause injury to the coronary ostium or proximal vessel.

Once the device is in position at the target lesion, a fluoroscopic projection is utilized that maximizes visualization of the target lesion and its eccentricity. In that projection, the device is rotated until the cutting window is seen to point toward the greatest plaque burden. The cutter is withdrawn to the proximal end of the window, and the positioning balloon is inflated to 10 to 20 psi. The motor is activated, and the cutter is advanced slowly (>5 seconds) across the window. After each cut, the balloon is deflated as the device is rotated by 45° to 90° to reorient it toward additional plaque burden. To prevent embolization of plaque, the balloon is inflated to 10 psi during cutter withdrawal prior to making the next cut. Higher balloon inflation pressures (30 to 40 psi) may be used on subsequent cuts to retrieve remaining plaque, but cuts oriented toward nondiseased walls should be avoided to minimize the risk of vessel perforation. After four to six cuts, or if incomplete cutter advancement indicates that the nose cone collecting chamber is full, the device should be removed and emptied before additional cuts are made.

The number of passes and the final size of the device are determined based on the size of the reference segment and the presence of any angiographic residual stenosis. Intravascular ultrasound (Chapter 19) may be helpful in assessing the lumen diameter as well as the amount and location of residual plaque burden. Atherectomy is considered successful if there is tissue removal, a residual stenosis is less than 50% after atherectomy, and there are no major complications (death, Q-wave myocardial infarction [MI], or emergency coronary bypass surgery).

Mechanisms of Lumen Enlargement

Directional atherectomy was designed to excise atherosclerotic plaque (2). While lumen enlargement is predicated on plaque removal, the acute result is actually due to a combination of plaque removal and dilation. Early data showed that the amount of plaque removed (averaging 18.5 mg) accounts for less than half the observed gain in volume seen at the lesion site (9,10), with the rest resulting from “facilitated angioplasty” (Fig. 24.3). Even after a successful atherectomy that has normalized the angiographic vessel lumen relative to that of the adjacent reference segments, a substantial amount of plaque (40% to 50% of the outer vessel [external elastic lamina, or EEL] cross-sectional area) remains, reflecting the substantial Glagov remodeling that typically has taken place at the lesion site (11).

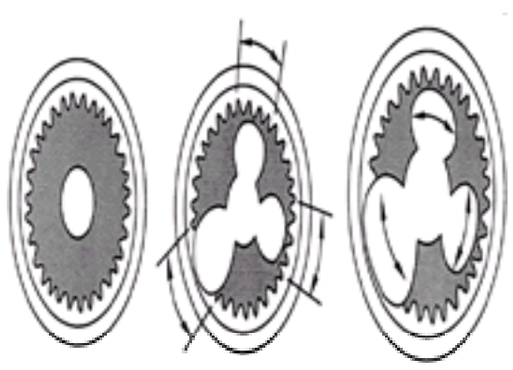

FIG. 24.3. Schematic representation of mechanism of directional coronary atherectomy and the concept of “facilitated angioplasty.” **Left:** Concentric stenosis in a coronary artery. The shaded area represents intimal plaque contained within the internal elastic lamina (*wavy line*). **Center:** Excision of plaque and media at 8 o'clock results in thinning of the vessel wall; subsequent cuts at 1 and 4 o'clock do not penetrate the media. **Right:** With disruption of the internal elastic lamina, radial compliance increases so that subsequent balloon inflations cause focal stretching of the vessel wall within the channels produced by previous atherectomy cuts (“facilitated angioplasty”). The resulting lumen appears smooth and free of residual stenosis in any angiographic projection, despite only partial atherectomy with the continued presence of residual intimal plaque.

Since atherectomy improves the radial compliance of the diseased and stiff coronary segment and since the mechanism of lumen enlargement is due in part to dilation, it stands to reason that postatherectomy balloon angioplasty should impart additional volume expansion. Although early studies considered such an application of balloon angioplasty after successful atherectomy to be tantamount to a “crossover,” current “optimal” atherectomy practice makes routine use of low-pressure postdilation to further enlarge the treated lumen (12,13 and 14).

Procedural Results

There has been considerable experience with directional coronary atherectomy (with the Simpson AtheroCath), with more than 200,000 procedures performed

worldwide. Published experience includes single-center reports (15,16) and results from two multicenter registries (8,17), five multicenter randomized trials (Table 24.1, Table 24.2, Table 24.3 and Table 24.4) (13,14,18,19 and 20). Device success rate (defined as achievement of more than 20% gain and less than 50% residual stenosis with tissue removal) is greater than 95%, with overall procedural success (defined as less than 50% residual stenosis, with adjunctive postatherectomy balloon angioplasty or other device) greater than 98%. Major complications are generally quite similar to balloon angioplasty except for the higher incidence of perforation (approximately 1%) and CK elevation greater than three times normal (approximately 15%). The importance of the high incidence of clinically silent elevations in creatine kinase myocardial band (CK-MB) enzymes following directional atherectomy remains unsettled and controversial, but in the Balloon versus Optimal Atherectomy Trial (BOAT) (14) there was no association with deaths at 1 or 3 years and there tended to be more late deaths by 1 year in the balloon angioplasty arm compared with the DCA arm (eight deaths vs. three deaths, p = .14).

	Lesion (n)	Device success (%)	Residual stenosis (%)
Beth Israel Hospital (15)	225	98	7
Sequoia Hospital (16)	447	94	12
NACI (17)	1084	94	13
WHC (18)	306	95	14
Multicenter preapproval (8)	1032	92	N/A
CAVEAT I (19)	512	N/A	29
CCAT (19)	136	94	26
OARS (13)	216	98	7
BOAT (14)	989	99	15
ABACAS (20)	210	99	13

TABLE 24.1. *Clinical studies and trials with directional atherectomy (see text)*

	Major			Other	
	Death (%)	CABG (%)	Q MI (%)	Non-Q MI (%)	Perforation (%)
Beth Israel Hospital	0	0.5	0	7.4	6.5
Sequoia Hospital	0.2	3.0	0.8	N/A	1.3
NACI	0.6	1.6	1.0	4.8	N/A
WHC	0.7	2.0	0.3	9.8	N/A
DCA investigators	0.5	4.0	0.9	5	6.6
CAVEAT I	0	3	2	19	6.4
CCAT	0	1.4	0.7	3.6	N/A
OARS	0	1.0	1.5	14	1.0
BOAT	0	1.0	2.0	16	1.4
ABACAS	0	0	0.5	0.8	0.5

TABLE 24.2. *Complications of directional atherectomy*

	Angiographic restenosis	Clinical restenosis
Beth Israel Hospital	32%	26%
Sequoia Hospital	30%*	N/A
WHC	N/A	28%
CAVEAT I	50%	37%
CCAT	46%	28%
OARS	29%	21%
BOAT	31%	25%
ABACAS	21%	17%

* De novo native coronary lesions or one previous treatment.

TABLE 24.3. *Angiographic and clinical restenosis after directional atherectomy*

Variable	Before intervention	After intervention	Follow-up
QCA			
Reference diameter (mm)	3.39 ± 0.47	3.51 ± 0.46	3.22 ± 0.44
MLD (mm)	1.21 ± 0.39	3.22 ± 0.47	2.00 ± 0.72
DS (%)	64 ± 10	8 ± 10	38 ± 20
IVUS			
Reference EEM CSA (mm^2)	18.3 ± 7.5	19.1 ± 7.7	17.6 ± 8.0
Reference lumen CSA (mm^2)	10.2 ± 3.9	10.8 ± 3.9	9.5 ± 4.6
Reference P + M CSA (mm^2)	8.1 ± 4.4	8.4 ± 4.6	8.1 ± 4.3
Lesion EEM CSA (mm^2)	17.7 ± 5.7	19.7 ± 5.6	16.9 ± 6.2
Lesion lumen CSA (mm^2)	2.0 ± 1.3	8.8 ± 2.5	5.5 ± 4.0
Lesion P + M CSA (mm^2)	15.6 ± 5.3	10.9 ± 4.2	11.3 ± 3.6

IVUS, Intravascular ultrasound; QCA, quantitative coronary angioplasty.

TABLE 24.4. *IVUS analysis of acute and late results of directional atherectomy (OARS)*

The main differences among trials concern the residual stenosis and the subsequent rate of angiographic restenosis. For the two early (1990 to 1991) randomized trials, high (>25%) residual stenoses (29% for CAVEAT I and 26% for CCAT) (18,19) reflected cautious tissue removal and the discouragement of adjunctive balloon postdilatation. In contrast, more recent experiences utilizing the optimal atherectomy technique have used more aggressive tissue removal and routine (> 75% of cases) adjunctive postdilation angioplasty to obtain much lower residual stenoses (<15%). The benefit of this approach in lowering restenosis compared with stand-alone balloon angioplasty has been confirmed in the OARS (13), BOAT (14), and ABACAS (20) studies with angiographic restenosis rates of 21% to 31%, compared with the 46% to 50% restenosis rates in the earlier trials. In BOAT, the lower residual stenosis for DCA versus PTCA (14% vs. 28%) led to significantly lower angiographic restenosis rates (31% vs. 40%).

The mechanism of late lumen narrowing has been carefully evaluated for directional atherectomy using intravascuar ultrasound (IVUS). Analysis of the OARS multicenter registry IVUS substudy (11) and the Serial Ultrasound Restenosis (SURE) trial (21) demonstrated that lumen renarrowing following directional atherectomy occurs between 1 and 6 months after the procedure and is due primarily to shrinkage (negative remodeling) of the external elastic membrane as well as some neointimal hyperplasia. The results of the OARS intravascular substudy are summarized in Table 24.4.

Tissue Analysis and Consequences of Deep-Wall Resection

Atherectomy provides a unique opportunity for studying the pathophysiology of atherosclerosis and coronary restenosis in human coronary arteries (22). Standard light microscopy demonstrates that atherosclerotic plaque (97%), media (66%), adventitia (30%), and thrombus (43%) are commonly recovered. Remarkably, retrieval

of deep-wall components seems to be well tolerated acutely, and at 6 months, angiographic follow-up (23,24) shows no relationship between deep-wall resection and restenosis, although the risk of late aneurysm formation may be increased (25,26).

Histologic analysis of DCA specimens shows intimal hyperplasia in 93% of restenotic lesions, with proliferating-phenotype smooth muscle cells interspersed with ground substance. Surprisingly, however, 44% of primary (*de novo*) lesions have intimal hyperplasia that is histologically indistinguishable from intimal hyperplasia seen in lesions with prior restenosis (27).

Use in Specific Lesion Types

Bifurcation Lesions

Plaque obstruction in large epicardial coronary arteries that involves the origin of a large branch, such as the left anterior descending/diagonal branch bifurcation, presents a special problem to the interventionist. The treatment of such true bifurcation lesions using conventional balloon angioplasty techniques is limited due to plaque shifting that occurs between the parent vessel and the ostium of the branch vessel (Chapter 23). In contrast, directional atherectomy provides superior treatment of bifurcation lesions, since the mechanism of lumen enlargement includes excision of the tissue that might otherwise be displaced into the branch ostium (28,29 and 30). The preferred technique involves sequential atherectomy of the main vessel and its branch, if the branch is large enough to accommodate the device (Fig. 24.4).

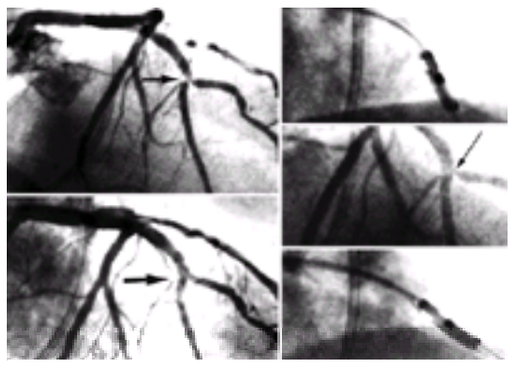

FIG. 24.4. Bifurcation atherectomy. **Upper left:** “Mercedes Benz” lesion involving the bifurcation of the left anterior descending (LAD) and diagonal branch (*arrow*). **Upper right:** Directional atherectomy of LAD, leaving tight stenosis of the diagonal origin (*right center, arrow*). **Lower right:** Atherectomy of the diagonal origin leaves excellent result (*lower left*). (From Friedman HZ, et al. Mechanical rotary atherectomy: the effects of microparticle embolization on myocardial blood flow and function. *J Interv Card* 1989;2:77, with permission.)

The acute and long-term results of directional atherectomy for the treatment of true bifurcation lesions were compared with balloon angioplasty by Dauerman (31). The atherectomy group had lower acute residual diameter stenosis and lower target vessel revascularization rate (28% for atherectomy vs. 53% for balloon angioplasty. $P = .01$). DCA should only be performed in noncalcified bifurcation lesions where the main vessel and involved side branch are larger than 2.5 mm (otherwise, rotational atherectomy should be used). We first position the 0.014-inch guidewire into the distal parent vessel and perform initial cuts directed toward the ostium of the branch vessel in an effort to minimize “snowplow” branch compromise. Next, the guidewire is withdrawn and redirected into the branch vessel, where additional cuts are performed. Finally, kissing balloon inflation in the parent and branch vessel is performed, with stent placement reserved for situations in which there is excessive recoil or dissection.

Aortoostial Stenoses

The ostium of the right coronary artery or saphenous vein graft is located within the thick-walled aorta, where substantial elastic recoil makes the use of stand-alone balloon angioplasty problematic (see Chapter 23). Such recoil has been overcome by tissue excision using directional atherectomy (Fig. 24.5) (32,33). This requires delivery of the device coaxially with the proximal portion of the target vessel. The guiding catheter must be disengaged before performing atherectomy cuts (to avoid cutting the tip of the guiding catheter itself). This requires use of bony landmarks for positioning the device at the ostium, since the disengaged guide can no longer provide adequate contrast angiography. Generally, postatherectomy balloon angioplasty or stent placement may be used to further “upsize” the lumen result beyond the working diameter of the AtheroCath. The presence of intracoronary calcium, especially at the lumen surface, is a relative contraindication for directional atherectomy of ostial stenoses, and such lesions are more suited for rotational atherectomy (see later discussion).

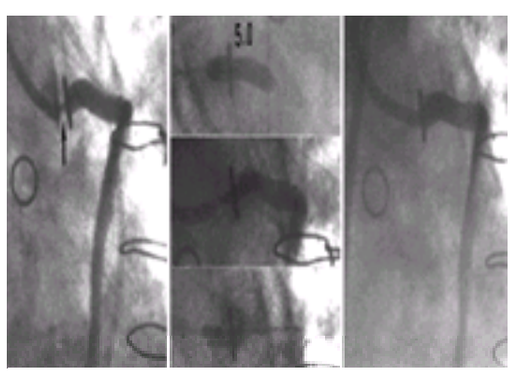

FIG. 24.5. Aortoostial saphenous vein graft atherectomy. **Left panel:** Ostial stenosis of saphenous vein graft (*arrow*) represents stenosis within the wall of the aorta, based on its location between the aortic lumen and the ring marker. This was refractory to dilatation with a 5-mm balloon (*center, top*) but responded to directional atherectomy (*center, bottom*) with favorable results (**right panel**). Such lesions are currently treated with stent placement (see Chapter 25).

Salvage Atherectomy

Directional coronary atherectomy can be used successfully to rescue failed or suboptimal balloon angioplasty (34,35), particularly when plaque recoil results in plaque avulsion into the intraluminal space. This application has become quite rare with the widespread use of stent placement to stabilize abrupt or threatened closure after balloon angioplasty and should not be attempted when there are deep spiral dissections in which attempted resection may result in perforation.

In-Stent Restenosis

Although coronary stenting has been proven to reduce the incidence of restenosis compared with balloon angioplasty, the high recurrence rate (50% to 80%) of treating diffuse restenosis within stent in-stent restenosis has become evident. Debulking techniques using laser, rotational atherectomy, or DCA have been shown in case-matched series to cut this recurrence rate roughly in half (36,37 and 38), although further substantial reductions in recurrence have now been seen with beta or gamma radiation of the in-stent restenosis (39). Directional atherectomy, which offers potentially the highest debulking capacity of the atherectomy and atheroablative devices, has been shown to be safe and effective in achieving less than 20% residual in-stent diameter stenoses and subsequent clinical restenosis rates of less than 30% (Fig. 24.6). In some atherectomy procedures for in-stent restenosis, the tissue sample may include a small section of stent strut, although without apparent clinical consequence.

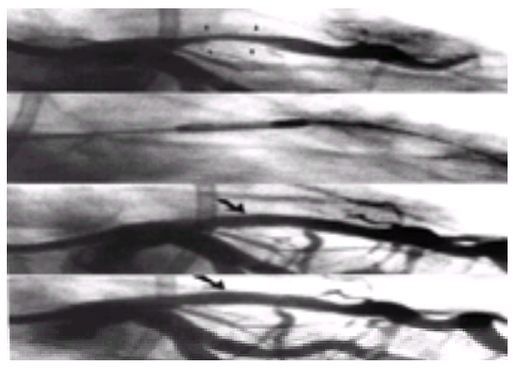

FIG. 24.6. Directional atherectomy of in-stent restenosis. **Top:** Restenosis within stent in the mid-left anterior descending artery (*arrows* denote stent struts). **Upper center:** Directional atherectomy catheter positioned within stent. **Lower center:** Enlarged lumen following atherectomy (*arrow*). **Bottom:** Final result after balloon dilatation.

Debulking Before Coronary Stenting

The concept of stand-alone “optimal” atherectomy was validated in the OARS, BOAT, and ABACAS studies (13,14,20). Recent studies have suggested that performing directional atherectomy before stenting may improve long-term stent results. In the Stenting after Optimal Lesion Debulking (SOLD) study (40), 71 patients underwent directional atherectomy of coronary lesions before stenting, achieving an angiographic restenosis rate of 11%. Interestingly, this was due both to a slightly larger acute result reduction and to a reduced late loss index (33% vs. the more typical 50%) compared with stenting alone. A similar experience has been reported by Kiesz and coworkers (the ADAPTS study), in which 89 lesions in 60 patients were treated with a combination of DCA debulking followed by stenting (41). Two more definitive randomized trials, AMIGO and DESIRE, are currently under way to test the hypothesis that directional coronary atherectomy before stenting may result in a lower restenosis rate than stenting alone.

TRANSLUMINAL EXTRACTION CORONARY ATHERECTOMY

Device Description

The transluminal extraction catheter (TEC) (Interventional Technologies, Inc., San Diego, CA) uses a tip-mounted cutting blade and an external vacuum source to macerate and aspirate thrombus and soft plaque material (Fig. 24.7 and Fig. 24.8). A trigger on the handle of the motor drive unit activates shaft and blade rotation at 750 rpm, and a sliding lever on top of the motor drive unit permits advancement or retraction of the cutter over the 300-cm-long 0.014-inch guidewire. Warm, heparinized lactated Ringer's solution is infused during atherectomy passes to produce a thin slurry of blood and tissue that is then continuously aspirated into the external suction bottle during cutter activation.

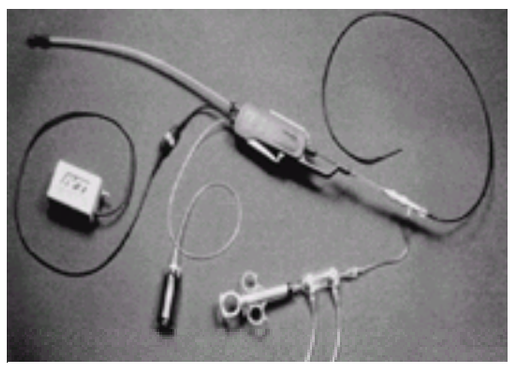

FIG. 24.7. Components of the transluminal extraction catheter (TEC), including the cutter, motor drive unit, battery pack, and vacuum bottle. (Reproduced with permission from Interventional Technologies, Inc., and Physician's Press.)

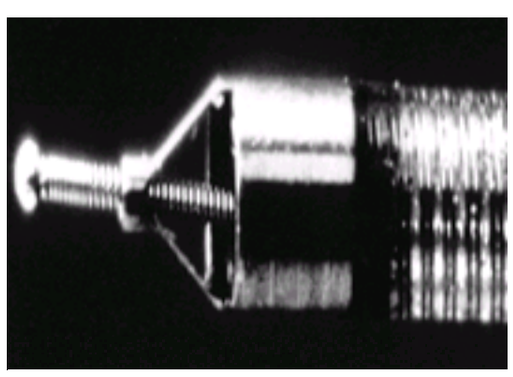

FIG. 24.8. Close-up view of the conical cutting head and stainless steel blades of the transluminal extraction catheter (TEC) and special 0.014-inch TEC guidewire. (Reproduced with permission from Interventional Technologies, Inc., and Physician's Press.)

TEC Atherectomy Procedure

Device selection remains empirical, with the largest cutter being 1 to 1.5 mm smaller than the normal vessel diameter. For coronary use, TEC cutters range from 5.5F (1.8 mm), 6F (2 mm), 6.5F (2.15 mm), and 7F (2.3 mm) to 7.5F (2.5 mm). The larger cutters (7F or 7.5F) should be reserved for vessels greater than 3.5 mm in diameter or for lesions associated with large amounts of thrombus. Special 10F tungsten-braided soft-tip guiding catheters are recommended for all TEC atherectomy procedures, but a 9F guiding catheter can be used for TEC cutters of 6.5F or less. Guiding catheters with an inner diameter of more than 0.105 inch are required for 7F or 7.5F cutters.

After engaging the vessel ostium with the guiding catheter, the target lesion should be crossed with the special TEC guidewire using a bare-wire technique. The floppy tip of the guidewire should be positioned in the distal vessel so the stiff shaft of the wire is across the lesion. If difficulty is anticipated crossing the lesion, a conventional wire may be used first and then exchanged for the TEC wire using a transport catheter that will accommodate the 0.021-inch ball at the tip of the special TEC guidewire. Once the guidewire is in proper position, the TEC cutter should be advanced up to the lesion, and the infusion of warmed lactated Ringer's is begun through the guiding catheter. The operator then depresses the trigger to activate cutter rotation and slowly advances the lever to traverse the entire lesion. Two to five passes should be made slowly through the lesion (15 to 30 seconds per 10-mm segment) until there is no further resistance to cutter advancement. After retracting the cutter into the guiding catheter, repeat angiography should be performed to determine the need for a larger device or adjunctive angioplasty.

Mechanism of Action

TEC atherectomy theoretically enlarges the lumen by cutting, aspirating, and removing thrombus, plaque, and other debris. In contrast to the discrete tissue fragments commonly retrieved by directional atherectomy, TEC results in a slurry of blood and debris that does not lend itself easily to tissue analysis. In angioscopic studies of saphenous vein grafts, TEC resulted in partial or complete removal of fresh thrombus in more than 75% of lesions in which thrombus was identified (42,43) but was less effective in removing laminated thrombus. Other angioscopic findings included the frequent development of intimal flaps and dissection. By intravascular ultrasound, plaque fissures and residual plaque were identified in 100% of lesions after TEC, and intimal dissections were identified in 36% of lesions (44). Others have suggested that most of the improvement results from mechanical dilatation rather than removal of plaque or thrombus (45).

Results

The treatment of saphenous vein grafts with luminal irregularities or the presence of frank thrombus is unfavorable for any coronary device, because of high rates of distal embolization, no reflow, and recurrent ischemia and restenosis, but may be suited for the TEC device with its potential to cut and aspirate thrombus and "grummous" material (Fig. 24.9) (Table 24.5). The overall procedure success rate ranges from 80% to 90% (3,46,47; Table 28.4), but modest quantitative angiographic improvement in lumen diameter immediately after TEC required adjunctive balloon angioplasty in approximately 90% of cases (48). Although lesions containing thrombus have been shown to be associated with lower procedure success for the TEC device than that achieved in lesions without thrombus (49), TEC atherectomy before stenting may be better than conventional balloon or stent treatment alone for thrombotic lesions (50).

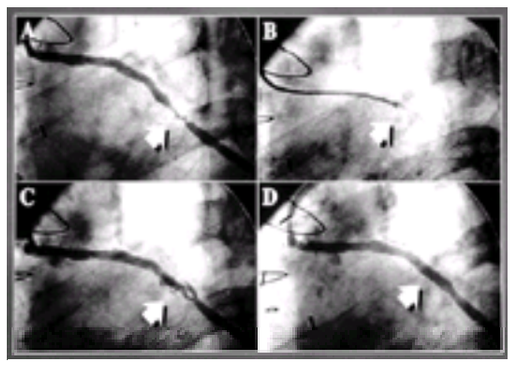

FIG. 24.9. Bypass graft angiography (left anterior oblique [LAO] projection) and angioscopy before and after TEC atherectomy. **A:** Angiography of a vein graft to the obtuse marginal branch reveals a tubular stenosis in the midbody of the graft. There is no definite thrombus by angiography. **B:** TEC atherectomy is performed with a 6.5F cutter. **C:** Angiography immediately after TEC reveals a complex residual stenosis with dissection and/or thrombus. **D:** A single Palmaz-Schatz P204 biliary stent is inserted and further dilated to 14 atm. After adjunctive angioplasty, there is no residual stenosis, dissection, or filling defect.

Author (Ref.)	Vessel	n	PTCA (%)	Success (%)	Death (%)	CABG (%)	QMI (%)
Popma (44)	SVG, N	51	86	82	5.9	3.9	7.8
Safian[a]	SVG	158	91	84	2.6	0.7	2.3
Trezzak (46)	SVG	88	95	86	0	1.5	4.4
NACI (57)	SVG, N	240	89	80	5.7	0.9	1.4
Safian (51)	N	181	84	84	2.3	3.4	2.8

Abbreviations: n = number of lesions; PTCA = adjunctive balloon angioplasty; success = final diameter stenosis <50% in the absence of death, emergency bypass surgery (CABG), or Q-wave myocardial infarction (QMI); SVG = saphenous vein bypass graft; N = native coronary artery.

[a] Safian RD, et al. Clinical and angiographic results of transluminal extraction coronary atherectomy in saphenous vein bypass grafts. Circulation 1994;89:932.

TABLE 24.5. *Angiographic results and major clinical complications after TEC atherectomy*

The incidence of death (0 to 5.9%), emergency bypass surgery (0.7% to 3.9%), and MI (2% to 7.8%), however, is generally similar to the incidence of death (0 to 5%), emergency bypass surgery (0 to 3%), and MI (0 to 9%) for patients with vein graft lesions treated by conventional angioplasty (3,17,44,46). Angiographic follow-up confirmed the high incidence of restenosis, with 52% to 69% of lesions having a follow-up diameter stenosis of more than 50% (44,46), and late vessel total occlusion in 29% of lesions.

In native coronaries, the TEC device has a procedure success rate that ranges from 85% to 95%, with adjunctive angioplasty required in approximately 80% (Table 24.5) (51). The final incidence of major in-hospital complications was death in 2.3%, emergency bypass surgery in 2.8%, and Q-wave MI in 3.4%, which was somewhat higher than the incidence of major complications for comparable lesions treated with balloon angioplasty. Other TEC-induced angiographic complications included side-branch occlusion in 2.7%, distal embolization in 0.5%, guiding catheter dissection in 2.2%, coronary artery perforation in 2.2% of lesions (Fig. 24.10 and Fig. 24.11).

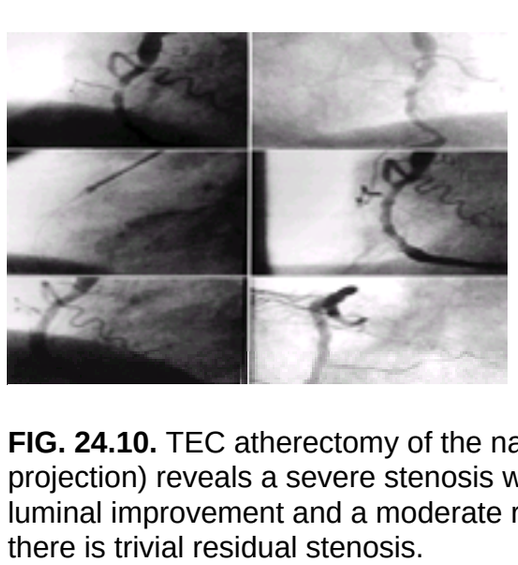

FIG. 24.10. TEC atherectomy of the native right coronary artery (RCA). Baseline angiography (**top left,** LAO projection; **top right,** right anterior oblique [RAO] projection) reveals a severe stenosis with intraluminal haziness in the mid-RCA. TEC atherectomy is performed with a 7F cutter (**middle left**), resulting in significant luminal improvement and a moderate residual stenosis (**middle right**). After adjunctive angioplasty (**bottom left,** LAO projection; **bottom right,** RAO projection), there is trivial residual stenosis.

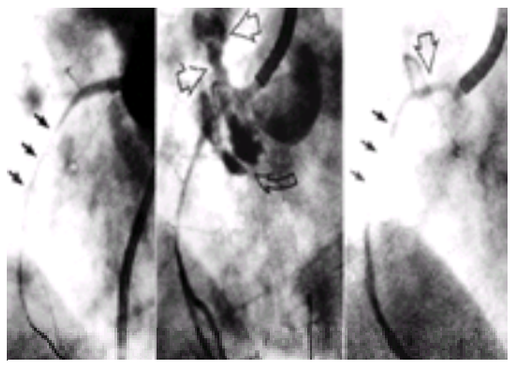

FIG. 24.11. Perforation of the right coronary artery (RCA, LAO projection) after TEC atherectomy. Baseline angiography reveals a long stenosis in the proximal RCA (**left panel, black arrows**). After TEC atherectomy with a 7F cutter, there is a jet of free contrast extravasation into the pericardium (**middle panel, open arrowheads**) and deep periadventitial contrast staining (**middle panel, open arrow**). After prolonged inflation with a perfusion balloon and pericardiocentesis, there is no residual contrast extravasation (**right panel, open arrowhead**), although there is a mild residual stenosis at the site of the original lesion (**right panel, black arrows**).

Since TEC atherectomy has not been shown to consistently remove plaque, the immediate angiographic results of TEC atherectomy in native coronary arteries do not appear to be superior to balloon angioplasty, and most lesions were treated with adjunctive angioplasty after TEC, the value of TEC in native coronary arteries remains uncertain. Procedural costs for TEC are also significantly higher than those for conventional angioplasty of similar lesions (52). One exception may be the use of TEC to remove thrombus in the setting of acute MI, especially where large thrombus burdens are present (53,54).

Randomized Trials

Thrombus-Containing Lesions Trial

The TEC or PTCA in Thrombus-Containing Lesions (TOPIT) Trial was a 245-patient multicenter randomized trial comparing TEC plus optional balloon angioplasty with balloon angioplasty for patients with either a clinical likelihood for coronary thrombus (unstable angina or postinfarction angina) or angiographically apparent thrombus (55). The procedure success rate was 97% for both groups, owing to the frequent (35%) rate of stent use to repair dissections. The primary end point—a composite rate of in-hospital major adverse cardiac events (death, MI, bailout intervention, or emergent surgery)—was noted in 11.2% of patients randomized to balloon angioplasty versus 4.5% for those randomized to TEC (p = .06). A secondary end point of CK-MB isoenzyme peak elevation greater than three times normal was observed more frequently in the balloon angioplasty group (15.4% vs. 4.5%, p = .03).

Transluminal Extraction Coronary. . . (TECBEST)

The Transluminal Extraction Coronary (TECBEST) trial examined the potential role of TEC compared with balloon predilation before stenting in saphenous vein grafts (56). There was no improvement in acute angiographic results by TEC pretreatment, and the incidence of distal embolization and periprocedural MI was not reduced.

Contraindications and Limitations of TEC

TEC is contraindicated for the treatment of dissection caused by other devices and should not be used in cases of extreme angulation or calcification and where vessels are less than 2.5 mm in diameter. The theoretical benefits of TEC atherectomy suggest that its benefit is generally limited to thrombus-containing vein grafts. Published data disclose inadequate lumen enlargement as a “stand-alone” device, a high incidence of serious angiographic complications, frequent need for adjunctive angioplasty, high procedural cost, and high incidence of clinical and angiographic restenosis (57). Even in the cases of large thrombi, the use of newer thrombectomy devices (see later discussion) may offer safer and more efficient thrombus removal.

HIGH-SPEED MECHANICAL ROTATIONAL ATHERECTOMY (ROTABLATOR)

Device Description

The high-speed mechanical rotational atherectomy device, or Rotablator (Boston Scientific, Boston, MA) (4,5,58), consists of an olive-shaped stainless steel or brass burr whose surface is embedded with diamond chips measuring 30 to 120 mm in diameter (Fig. 24.12). The burr is attached to a hollow, flexible drive shaft that permits passage of a steerable, movable 0.009-inch guidewire with a 0.014-inch platinum coil at its tip. The drive shaft is encased within a Teflon sheath through which warm, heparinized Ringer's lactate solution is pumped into the sheath to lubricate and cool the drive shaft and burr. A compressed-air turbine rotates the drive shaft at 150,000 to 200,000 rpm (Fig. 24.13). Burrs for coronary use are available in diameters of 1.25, 1.5, 1.75, 2.0, 2.15, 2.25, and 2.5 mm (Table 24.6).

FIG. 24.12. Close-up view of the Rotablator burr embedded with diamond chips and special 0.009-inch guidewire. (Reproduced with permission from Heart Technology, Inc., and Physician's Press.)

FIG. 24.13. Schematic overview of the original Rotablator assembly. (Reproduced with permission from Boston Scientific, and Physician's Press.) In the current Rota-link design, the drive unit is separate and can be used with a series of different burr cables.

Rotablator Burr Size (mm)	Guiding Catheter ID
1.25	0.059
1.50	0.069
1.75	0.078
2.0	0.088
2.15	0.092
2.25	0.097
2.5	0.107

Abbreviation: ID = inner diameter (in).

TABLE 24.6. *Inner diameter of guiding catheters to accommodate rotablator burrs*

Rotablator Atherectomy Procedure

As with conventional balloon angioplasty, all patients should be pretreated with aspirin at least 24 hours before the procedure, and intravenous heparin adequate to maintain the activated clotting time at approximately 300 seconds. Intracoronary nitroglycerin (100- to 200-µg bolus), and intravenous nitroglycerin (20- to 100-µg/min infusion) should be administered as tolerated. For patients with target lesions in the distribution of the right coronary artery, prophylactic temporary pacemaker insertion is recommended, frequently in the form of a right heart catheter that combines capabilities for pacing and monitoring pulmonary artery pressure. Conventional angioplasty guiding catheters may be used for Rotablator atherectomy as long as their lumen is at least 0.020 inch larger than the largest burr to be used (Table 24.6). Two guidewires are available, a floppy guidewire and an extra-support guidewire. The floppy wire has the advantage of minimizing guidewire bias—a phenomenon in which a stiff guidewire tends to straighten out curved vessel segments and cause deep cuts or dissection as the burr is forced against the tautly stretched lesser curvature of the vessel. On the other hand, the floppy guidewire may fail to adequately control the travel of the burr around tight bends, leading to uncontrolled cutting on the greater curvature of the vessel. If difficulty is anticipated crossing the target lesion with the Rotablator guidewire using a bare-wire technique, the lesion may be crossed with a conventional angioplasty wire and exchanged for the Rotablator guidewire using a suitable transport catheter.

Once the guidewire is across the lesion, the burr should be advanced to within a few centimeters of the rotating hemostatic valve, with the lines for compressed air supply and tachometer readout attached to the drive console. The system should be tested by depressing the foot pedal adjusting the turbine to maintain burr speeds of 140,000 to 160,000 rpm. During the test, the operator should also confirm adequate flow of heparinized flush through the Teflon sheath, free motion of the advance lever, and a firm grip of the wire brake. Once this test has been completed, the burr can be advanced into and through the guiding catheter. Any resistance encountered as the burr is passed around the primary curve of the guiding catheter can be overcome by firm traction on the guidewire, but this is less common with the use of gentle (“Q”) curves analogous to those used for DCA. The guiding catheter must be well seated in the vessel ostium while advancing the burr to prevent kinking of the guidewire in the aortic root. Once the burr has been advanced to 1 to 2 cm proximal to the target lesion, the advancer lever should be unlocked and pulled all the way back to its proximal limit so as to take up any slack in the drive shaft that might otherwise cause the burr to lurch forward into the lesion upon activation.

Under fluoroscopy, the burr is then activated by stepping on the pedal, and adjusted to the desired “platform” speed (160,000 rpm for smaller burrs and 140,000 rpm for burrs bigger than 2 mm) before engaging the lesion. Advancement of the lever then brings the spinning burr slowly into contact with the lesion. It is important to be aware of the sound of the turbine, the rotational speed display, and tactile feedback during “rotablation,” to avoid speed drops of more than 5,000 rpm during advancement. Greater speed drops caused by excessive pressure on the burr may result in the liberation of larger particles, frictional heating of the plaque, or torsional dissection. Brief (1- to 3-second) periods of plaque contact should be alternated with longer (3- to 5-second) periods of reperfusion provided by pulling the burr back from the plaque face, to aid in clearance of particulate debris through the distal circulation. After 15 to 30 seconds of operation, the device should be withdrawn into the proximal vessel and rotation should be suspended for a similar time before reactivating and advancing the burr again. This sequence should be repeated until the device can be advanced through the full length of the lesion without any fluoroscopic or tactile resistance to burr advancement and with no audible change in the pitch of the turbine or reduction in burr speed. If a second, larger burr is to be used, the initial burr is then removed during continuous rotation (decreased to 90,000 rpm, in the “dynaglide” mode).

The selection of burr sizes is largely empirical but should progress to a final burr/artery ratio of roughly 0.7 (e.g., 2.15-mm burr in a 3-mm vessel). In treating long segments of disease, heavily calcified lesions, and subtotal de novo lesions, it is generally a good idea to start with a smaller (1.5 or 1.75 mm) burr and step up to the final burr size in 0.5-mm increments. With the Rota-Link system, this involves changing only the burr with reuse of a single-drive turbine throughout the procedure. With a maximum burr-to-artery ratios of 0.7, optimal improvement in vessel lumen requires liberal use of adjunctive angioplasty (or other devices). When adjunctive postdilation is desired, most operators use low inflation pressures (<2 atm) to minimize barotrauma, but there are no published data to suggest that this technique results in lower residual stenoses or fewer complications than other approaches.

Mechanisms of Rotablator

Unlike other atherectomy devices, which rely on tissue cutting and retrieval (directional atherectomy) or cutting and aspiration (TEC atherectomy), high-speed mechanical rotational atherectomy relies on plaque abrasion and pulverization. By the principle of differential cutting, the Rotablator tends to selectively abrade inelastic tissue (i.e., plaque) while elastic tissue (i.e., normal vessel wall) is deflected away from the burr (59). The abraded plaque is pulverized into particles 20 to 50 µm in diameter that pass through the coronary microcirculation and undergo phagoctyosis in the liver, spleen, and lung (4,60,61). Although these particles have long been felt to not interfere with the coronary microcirculation (62), the reported benefit of glycoprotein IIb/IIIa receptor blockers against transient hypoperfusion suggests a role for platelet-mediated microvascular flow reduction during rotational atherectomy (63). Reisman has confirmed ex vivo platelet activation, with greater activation at higher burr speeds (64), as well as greater vessel heating. These findings have encouraged the use of lower (<160,000 rpm) speed during rotational atherectomy, although this necessitates longer cumulative burr time.

Although two independent studies demonstrated no immediate or long-term impact on left ventricular ejection fraction (65,66), other studies show a significant incidence of non–Q-wave MI and no reflow (67), particularly in longer lesions (>2 mm). These problems could be secondary to particle embolization, spasm, microcavitation caused when the burr surface velocity exceeds the speed of sound in water (Bernoulli phenomenon) (68). Microcavitations or hemolysis of red blood cells may also contribute to transient bradycardia and atrioventricular (A-V) block, whereas mechanical stimulation and the loss of endothelium in the lesion and adjacent normal wall may explain the propensity for severe vasospasm during rotational atherectomy. Accordingly, liberal use of nitroglycerin and calcium channel blockers is routine, and temporary pacing should be considered, as discussed earlier.

Results

Immediate Results

Following Rotablator, the average residual diameter stenosis was 37% to 54% (65,67,69,70,71,72 and 73), but this high residual diameter stenosis may reflect an increase in vessel tone after rotational atherectomy. Reisman thus demonstrated that the lesion site diameter was significantly larger 24 hours after rotational atherectomy than it was immediately after the procedure (74). IVUS may be useful for identifying which lesions are best suited to Rotablator and for guiding the use of larger burrs, balloon angioplasty, directional atherectomy, or stenting (75). In general, superficial calcium deposits are most amenable to Rotablator, since deep calcium deposits do not come in contact with the burr surface. Hoffman and coworkers demonstrated that treatment of calcified lesions with rotational atherectomy before stenting resulted in larger posttreatment lumen diameters and higher 9-month event-free survival than with stenting alone (76). The use of adjunctive low-pressure balloon angioplasty is frequent after Rotablator (70) (Table 24.7), and Rotablator pretreatment improves vessel compliance and therefore stent expansion (77). This “rota-stent” approach is our standard technique for calcified ostial and left main lesions (78,79) although it showed no significant advantage in the

randomized SPORT trial of non- or minimally-calcified lesions. Rotablator is also an effective technique for debulking in-stent restenosis (Fig. 24.14) (36).

Author	n	Adjunctive PTCA (%)	Success (%)	Death (%)	MI (%) Q/non-Q	CABG (%)	Restenosis (%)
Topol (67)	42	0	76	2.0	0/10.0	2.0	69
Bertrand (65)	129	29	88	0	2.3/5.4	1.6	38
Zacca (38)	36	0	97	0	0/3.2	3.2	NR
Henson[a]	462	82	95	1.0	0.7/NR	2.2	NR
Safian (70)	116	77	75	0.9	4.4/2.7	1.8	51
Stertzer (71)	346	77	94	0	3.3/11.0	1.2	37
Gimore[b]	140	69	92	0.5	0.9/2.5	2.8	NR
Bertrand (66)	1688	70	95	0.9	1.0/5.4	2.3	48
Ellis (72)	400	82	90	0.3	2.2/5.7	0.9	NR
Warth (73)	674	NR	95	0.8	0.9/3.5	1.7	38
NAC[c]	340	82	97	0.8	1.5/4.3	0.4	NR
Ytiig[d]	574	39	94	1.0	0.8/4.8	2.4	38

Abbreviations: n = number of lesions; PTCA = adjunctive balloon angioplasty; success = final diameter stenosis <50% in the absence of a major complication (death, emergency bypass surgery, or Q-wave myocardial infarction); MI = Q-wave myocardial infarction/non-Q-wave myocardial infarction; CABG = emergency bypass surgery).

[a] Henson KD. *Am J Cardiol* 1993;71:962.
[b] Gilmore. *Clin Cardiol* 1993;16:311.
[c] Brown DL. *Am J Cardiol* 1997;80:801.
[d] Ytiig. *Intervent Cardiol* 1993;8:126.

TABLE 24.7. *Angiographic results and major clinical complications after rotablator atherectomy*

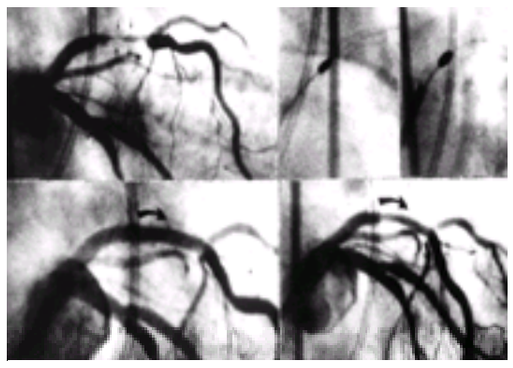

FIG. 24.14. Rotablator for in-stent restenosis (**upper left**). Severe restenosis is present in the proximal left anterior descending (note stent struts, *small arrows*). **Upper center and upper right:** Rotational atherectomy with 1.75- and 2.15-mm burrs. **Lower right:** Appearance post-Rotablator. **Lower left:** Appearance after final balloon dilatation.

Rotablator atherectomy may be particularly indicated for specific lesion subsets where balloon angioplasty is known to be associated with suboptimal angiographic results. For calcified lesions, ostial lesions (Fig. 24.15), nondilatable lesions, and chronic total occlusions, Rotablator success has been reported to be 92% to 97%, with an acceptably low incidence of major clinical complications (80) (Table 24.7). Quantitative angiographic studies using matching lesion subsets suggest that pretreating many types of lesions with Rotablator can facilitate the results of adjunctive angioplasty (81) (Fig. 24.16).

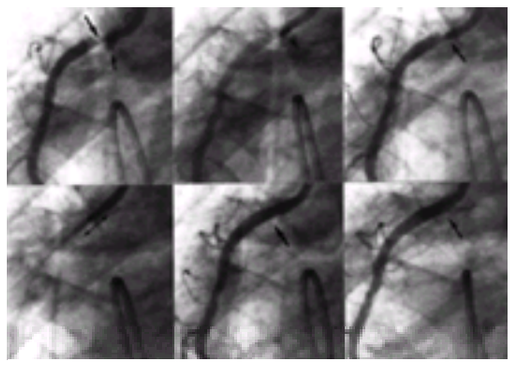

FIG. 24.15. Ostial RCA rota-stent. **Upper left:** Severe ostial right coronary stenosis (*long arrow*) with heavy calcification (*short arrow*). **Upper center:** 1.75-mm Rotablator burr positioned just outside the lesion. **Upper right:** Modest lumen enlargement after rotational atherectomy. **Bottom left:** The resulting lumen, however, allowed advancement of a PS 104 biliary stent. **Bottom center:** Stent deployment. **Bottom right:** Final result postdilatation.

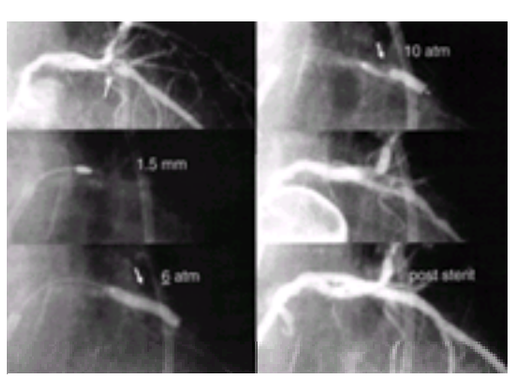

FIG. 24.16. Resistant calcified lesion becomes responsive after Rotablator. **Upper left:** Severe stenosis in the proximal left anterior descending artery (*arrow*). **Upper right:** Persistent waist despite inflation of angioplasty balloon to 10 atm. **Center left:** Advancement of a 1.5-mm Rotablator burr (note the heavy calcium shadows). **Center right:** Modest lumen enlargement following Rotablator. **Bottom left:** Following Rotablator, however, the same balloon now expands completely at 6 atm. **Bottom right:** Final result after stent placement.

While early studies indicated significant angiographic complications in nearly 40% of lesions after Rotablator—including angiographic dissection in 29%, side-branch occlusion in 1.8%, distal embolization in 0.9%, no reflow in 6.1%, abrupt closure in 11.2%, and severe spasm in 13.8%, and perforation in 1% to 2% of lesions—current technique has made the complication rate comparable to other catheter-based techniques (81a). Like DCA, there is a higher incidence of non–Q-wave MI after Rotablator, which was 19% in one study of long lesions (67).

Late Results

In the Excimer, Rotablator, Balloon Angioplasty for Complex Lesions (ERBAC) study, a randomized trial of rotational atherectomy, excimer laser angioplasty, or balloon angioplasty (see later, in the laser section), the final diameter stenosis after Rotablator and adjunctive angioplasty was significantly lower than that for adjunctive angioplasty after excimer laser or balloon angioplasty alone, but angiographic restenosis at 6 months was not significantly different at 45% to 50% (82). Other observational studies suggest a clinical restenosis rate of 38% and an angiographic restenosis rate between 31% and 59% (Table 24.6). The 500-patient

randomized STRATAS trial compared aggressive rotational atherectomy, defined as high (>0.75) burr-to-artery ratio, with standard burr sizing (<0.7) to evaluate the impact of greater debulking (83). There was no difference in acute outcomes (except for a higher trend of non–Q-wave MI in the aggressive arm), with 6-month restenosis rates of 58% for the aggressive arm versus 52% for the conventional arm; *p* = NS.

Recommendations for Use of Rotablator Atherectomy

Although detailed randomized trial data are limited, we recommend the use of Rotablator for those lesions that are least likely to benefit from conventional angioplasty, such as long, ostial, and heavily calcified lesions, including protected left main arteries calcified bifurcation lesions (84), as well as the rare (1% to 2%) lesion that cannot be dilated successfully at inflation pressures of 12 atm (Table 24.8). Lesions that cannot be crossed with a balloon catheter due to lesion rigidity or excessive tortuosity of the proximal vessel may also be amenable to Rotablator (80). Rotablator has also proven to be an excellent tool for the debulking of in-stent restenosis, with some studies suggesting a substantial reduction in recurrence rates after Rotablator plus balloon dilatation of such lesions (36,85,86 and 87).

Author	Lesion	n	Success (%)	Death (%)	CABG (%)	QMI (%)
Whitlow	Calcified	NR	96	1.5	1.3	1.3
Leon	Calcified	229	95	0.5	1.1	1.6
Kent	Ostial	147	93	2.1	3.5	0
Motwani [78]	Ostial	119	97	0	0	0.8
Reisman	Nondilatable	34	97	0	2.9	0
Rosenblum [82]	Nondilatable	41	98	0	0	0
Worth [73]	Chronic TO	68	93	1.5	0	0

Abbreviations: n = number of lesions; success = final diameter stenosis <50% in the absence of death, emergency bypass surgery (CABG), or Q-wave myocardial infarction (QMI); TO = total occlusion.

TABLE 24.8. *In-hospital results of rotablator atherectomy for specific lesion subsets*

Rotablator should be avoided soon after attempted angioplasty, particularly if there is any evidence for local dissection. Other contraindications to Rotablator include the presence of visible thrombus or extremely eccentric lesions in a severe bend in which the normal vessel wall lies on the outer curve of the bend. Although Rotablator is technically feasible in long lesions, it may be associated with a significant incidence of no reflow or non–Q-wave MI, and there are as yet no data to suggest superiority to conventional angioplasty using long balloons.

Despite its ability to facilitate the immediate results of balloon angioplasty for a variety of lesions, Rotablator has a clear learning curve for safe use. It is further limited by the maximum 2.5-mm burr diameter, the frequent need for adjunctive balloon angioplasty or stenting, the high cost of procedures, and the lack of a confirmed impact on restenosis. While the complications of distal embolization, no reflow, severe coronary vasospasm, bradycardia, and perforation are uncommon with refinement in Rotablator technique as described earlier, they can clearly occur and stand as a reason that Rotablator use is uncommon for low-volume operators.

ABLATIVE LASER TECHNIQUES

It was hoped that laser angioplasty would permit precise plaque removal with fewer acute complications and lower incidence of clinical restenosis (88). Despite the evolution of catheter system designs over the years, restenosis rates following laser angioplasty have not been lower than those with balloon angioplasty alone (6,82). Given the lack of clinical benefit over other mechanical therapies and the significant capital cost ($100,000 to $250,000) for acquiring a laser system, hopes for laser angioplasty have shifted from a mainstream stand-alone therapy to an infrequently used adjunctive treatment to debulk plaque before balloon angioplasty or stenting in coronary lesions with large atherosclerotic and restenosis plaque burdens, or to debulk in-stent restenosis. Because laser systems are still in use in some laboratories, newer applications may still be found. The body of theoretical and clinical data will be reviewed.

Laser Generation

Light amplification by stimulated emission of radiation (LASER) is the process of creating an in-phase (coherent) beam of monochromatic light with high energy. The lasing medium is “pumped” by an external energy source to force most of the atoms or molecules from their lower-energy ground state to a higher-energy excited state. After a brief time—measured in nanoseconds—the atoms begin to relax to their ground state by giving off a photon whose wavelength is determined by the energy difference between the excited and ground states, by the equation $E = hn$, where h = Planck's constant and $n = c/l$ (c, speed of light; l, wavelength). One spontaneously released photon of precisely matched energy (hn) can induce other excited atoms in the lasing medium to relax to the ground state and emit photons that are identical in direction, wavelength, and phase to the stimulating photon (stimulated emission). As this wave passes through the laser cavity, light coalesces into a single wave front whose intensity increases exponentially as it travels along the optical axis of the laser cavity and is reflected back and forth between the mirrors positioned at either end of the chamber. This standing wave of intense, monochromatic, coherent light then permeates the optical coupler, from which it travels down the optical fibers within the multifiber laser catheter whose other end is positioned within the coronary artery lumen so as to illuminate the obstructing plaque with a burst of laser light.

Laser/Tissue Interactions

The interaction between laser light and biologic tissue depends on the wavelength, the mode of laser operation (continuous-wave or pulsed), the energy density of the laser light (fluence), any interposed fluid medium (saline or blood) and the tissue's intrinsic absorption characteristics. For coronary laser angioplasty, lasers can be divided into ultraviolet lasers (e.g., XeCl excimer lasers, 300 nm) in which ablative energy is absorbed directly by atherosclerotic plaque absorption, and near-infrared/infrared lasers (e.g., holmium or neodynium YAG [yttrium-aluminum-garnet], 2,000 nm) in which thermal energy produced by water absorption leads to secondary photocoagulation. It is also important to distinguish continuous-wave laser systems, in which laser light is emitted in an uninterrupted manner, from newer pulsed systems that deliver peak laser over a very short pulse followed by a long interpulse interval to reduce heating of surrounding tissue. Despite these theoretical advantages, all pulsed laser systems still produce some thermal effects that are detectable with histologic examination after holmium and excimer laser radiation (89,90).

While water is almost completely transparent to ultraviolet light at wavelengths greater than 193 nm, it absorbs infrared light strongly due to excitement of the translational, vibrational, and rotational frequencies of the H—O bond. On the other hand, blood, x-ray contrast agents (such as ioxaglate), and tissue DNA absorb ultraviolet (UV) light avidly. When laser light encounters biologic tissue, tissue vaporization occurs if the light contains wavelengths that are absorbed by the tissue, and if the absorbed energy exceeds the threshold for triggering a phase transformations. Tissue ablation then takes place through one of three mechanisms: vaporization of tissue (photothermal effects), ejection of debris (photoacoustic effect), or direct breakdown of molecules (photochemical dissociation) (91).

Because early experimental studies involving free-laser beams in air (88) showed tidy ablation of biologic tissue with clean margins and no histologic evidence of thermal injury (Fig. 24.17), it was initially thought that photodissociation was the predominant mechanism of excimer laser ablation of atherosclerotic plaque *in vivo.* Studies under saline or blood, however, disclosed less efficient plaque ablation and significant dissection of adjacent tissue due to formation and implosion of vapor bubbles at the impact site. This observation has immediate implications for excimer laser angioplasty. The use of intracoronary saline infusion to displace blood and radiographic contrast in the excimer laser field may thus reduce the risk of vessel dissection during excimer laser angioplasty (Fig. 24.18).

FIG. 24.17. Ablation of postmortem human aortic tissue with pulsed excimer laser radiation at 193 nm in air.

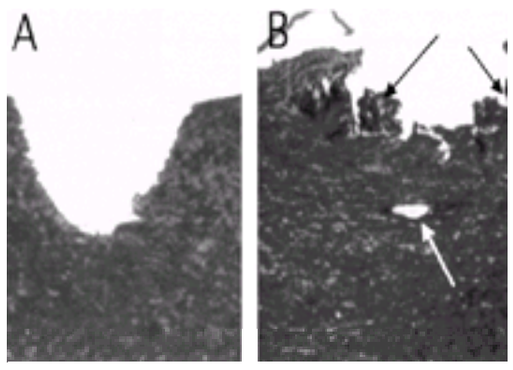

FIG. 24.18. Ablation of porcine aortic tissue after pulsed excimer laser angioplasty at 308 nm with multifiber laser catheters under saline (**A**) or blood (**B**). (Photomicrographs courtesy of L. Wells, Spectranetics, Colorado Spring, CO.)

Catheter Delivery Systems

The history of laser angioplasty includes experimentation with bare laser fibers, coaxial fiber-centering balloons, laser-heated metal tips, the laser balloon for local vessel heating, and “smart” laser systems that used a diagnostic laser to interrogate the vessel and confirm the presence of plaque rather than normal vessel wall before firing the therapeutic laser. None of these techniques have survived clinical investigation. All current clinical laser systems share common elements: a laser generator, an energy coupler, and a catheter delivery system—a trackable, flexible, over-the-wire or monorail catheter that contain several hundred optical fibers. Each optical fiber is composed of a transmitting material (such as a purified silica for excimer laser angioplasty) surrounded by a cladding. Since the cladding and silica fibers have different refractive indices, this creates an interface that promotes internal reflection and transmission of light down the length of fiber with negligible energy loss. The brittle fiber and cladding materials are surrounded by a flexible protective coating to allow bending without fissuring. Efficient coupling of energy between the laser generator and the optical fibers requires critical tolerances for alignment and precise polishing of the fiber ends.

The Technique of Laser Angioplasty

Conventional, commercially available guiding catheters can be used for excimer laser angioplasty. Because laser catheters are stiffer than balloon catheters and have difficulty negotiating acute angles into the target vessel, coaxial alignment is imperative. A stiff guiding catheter helps delivery, but firm guide support theoretically is not needed to advance the activated laser catheter through the target lesion, and excessive pushing of the catheter across the lesion may increase the risk of vessel dissection.

To maximize the likelihood of a safe outcome and reduce the risk of vessel perforation with excimer laser angioplasty, it is important to select a laser catheter with a diameter at least 1 mm smaller than the reference diameter of the target vessel (e.g., a 2-mm catheter for a 3-mm vessel). For diffuse disease or total and subtotal occlusions, an even smaller laser catheter (1.3 or 1.4 mm) should be used initially to cross the lesion. The current recommendation is thus to limit ablation to one pass of a laser catheter per lesion.

After the target lesion is crossed with the guidewire, the laser catheter is advanced to lie at the proximal end of the lesion. This catheter position should be documented on cine. Before activating the laser and beginning ablation of the lesion, every effort must be made first to remove all contrast medium from the target vessel by flushing the guide catheter with at least 30 mL of saline. This is important because the interaction between excimer laser radiation and any retained contrast medium may increase the generation of shock waves with disruption of adjacent tissue planes (92).

During pulsed excimer laser angioplasty, laser energy is delivered at a fluence of 40 to 70 mJ/mm ^{2} at a frequency of 20 to 25 Hz for a duration of 1 to 5 seconds as the tip of the catheter is advanced through the lesion. For soft lesions such as saphenous vein graft lesions and restenosis lesions, laser ablation may commence at a fluence of 40 mJ/mm^2, but for calcified lesions and *de novo* lesions in the native coronary arteries, the initial fluence should be 50 mJ/mm ^{2}. As the laser is activated, the catheter is advanced slowly under fluoroscopic guidance through the lesion at an average rate of 0.5 to 1 mm/sec. After each 1- to 5-second train of laser pulses, the laser catheter should “rest” for 10 seconds, to avoid potential attenuation of energy transmission through the optical fibers. If the laser catheter meets resistance and cannot pass through the lesion at the initial fluence, the energy output should be increased by increments of 10 mJ/mm ^{2} to a maximum of 60 or 70 mJ/mm^2. If the laser catheter still cannot be advanced at higher fluence levels, the repetition rate also can be increased by increments of 5 Hz to a maximum of 40 Hz. If the laser catheter still fails to make progress through a stenotic segment after 15 seconds of laser time, the temptation for forceful advancement of the catheter should be avoided, since this will only increase the risk of vessel perforation. Once the laser catheter has been advanced completely through the stenotic segment, adjunctive balloon postdilatation will be required in about 90% of laser angioplasty procedures to reduce the residual stenosis to below 30% (93,94 and 95). Further improvement can be achieved by following excimer laser angioplasty by stent placement or directional atherectomy in selected cases.

Clinical Results of Laser Angioplasty

Clinical success with the excimer laser, defined as less than 50% residual stenosis (after all treatments) and absence of major in-hospital complications, has been reported in 84% to 94% of patients with saphenous vein graft lesions, aortoostial stenoses, total occlusions, long lesions, and undilatable lesions (82,93,94 and 95). Early clinical experience with holmium laser coronary angioplasty in 331 patients demonstrated a procedural success rate of 94% and a perforation rate of 1.9% (96). Because of the similarities for both excimer laser and holmium laser interaction with tissue, the clinical results for the two systems are probably quite similar.

Despite increased clinical success with catheter improvements, the rates of vessel dissection and perforation have remained constant. Indeed, the incidence of propagating dissection as high as 22% (Fig. 24.19) has continued to limit the usefulness of excimer laser angioplasty (93,95). Although coronary artery dissection is not unique to laser angioplasty, extension of the dissection beyond the treated site is probably more common following laser angioplasty than after use of balloon angioplasty or other devices. Vessel perforation occurs during laser angioplasty in 1% to 2% of patients treated (97) and commonly leads to a major complication (death, MI, cardiac tamponade, or bypass surgery). Risk factors for perforation include the use of oversized laser catheters, bifurcation lesions, and diabetes mellitus (98). The use of a saline flush during lasing has been shown to reduce the incidence of dissection and perforation both experimentally (99) and clinically.

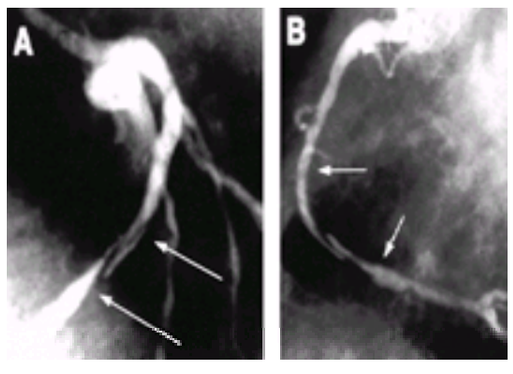

FIG. 24.19. Coronary artery dissections after excimer laser angioplasty. Treatment of a long lesion in the left anterior descending artery (**A**, *proximal arrow*) was associated with propagating dissection (*distal arrow*). Treatment of a total occlusion in the midportion of the right coronary artery (**B**, *proximal arrow*) was associated with propagating dissection to the distal right coronary artery (distal arrow).

Although laser angioplasty was developed initially to reduce restenosis by ablating atheromatous plaque without injuring the normal components of the arterial wall, restenosis has been reported in approximately 50% of patients (100).

Undilatable Lesions

Some fibrotic and calcified lesions cannot be dilated with balloon angioplasty at high pressures. Excimer laser angioplasty is associated with successful treatment in 89% of 36 patients with lesions that could be crossed with a guidewire but could not be dilated with balloon angioplasty (101). Although the excimer laser angioplasty is of value, rotational atherectomy is more commonly used for this indication. Neither should be attempted, however, in cases where dilation attempts resulted in local vessel dissection. Under such circumstances, excimer laser angioplasty is invariably associated with worsened dissection or perforation.

Total Occlusions

Total occlusions crossable with a guidewire are associated with procedural success rates of 84% to 90% with excimer laser angioplasty (102,103). Many dissections that occur with excimer laser angioplasty, especially in the treatment of total occlusions, arise because the guidewire has traveled along an extraluminal course. It is therefore important to ensure that the guidewire is in the true lumen of the vessel by frequent contrast injections and confirming that the distal tip remains mobile, before advancing the laser catheter. The long-term success after excimer laser treatment of total occlusions is limited by the development of restenosis in approximately 50% of patients. In the randomized Amsterdam-Rotterdam (AMRO) trial (94), no restenosis benefit was seen for excimer laser compared with balloon angioplasty in a subset of 103 patients who presented with total occlusions.

For total occlusions not crossable with a conventional guidewire, a new approach with an excimer laser-based guidewire recently has entered clinical investigation. The Prima laser guidewire system (Spectranetics Corp., Colorado Springs, CO) consists of an 0.018-inch fiberoptic bundle coupled to a pulsed excimer laser operating at a tip fluence of 60 mJ/mm^2 at 25 to 40 Hz. The system uses a centering balloon for blinded tissue ablation through the obstruction.

The Prima system was also evaluated more formally in two prospective trials in which the laser guidewire was used only after conventional guidewire techniques were performed and documented to fail. The U.S. TOTAL trial evaluated the learning phase of the lasing strategy in a 179-patient registry (104). Using the Prima catheter alone or in combination with a conventional guidewire, 61% of the refractory total occlusions were successfully crossed. Major complications were low, with a 1.1% death rate and a 1.7% rate of perforation leading to tamponade. A similar European feasibility trial demonstrated a 59% successful recanalization rate in 39 patients who could not be treated with conventional guidewire techniques (105). The European TOTAL surveillance study was a multicenter trial done to evaluate the safety and performance of the excimer laser system among 345 patients with a median occlusion age of 29 weeks (106). The recanalization rate was 59%, with no deaths, emergency surgery, or Q-wave MIs. While coronary perforations (laser “exits”) were seen in 21% of cases, only 1% had tamponade. The independent covariates associated with success were occlusion age less than 40 weeks and lesion length less than 30 mm.

Calcified Lesions

Calcified lesions initially were thought to be an indication for excimer laser angioplasty (107), but results of more recent studies have tempered the enthusiasm for this indication. In the Excimer Laser Rotational Atherectomy Balloon Angioplasty Comparison (ERBAC) trial involving 620 patients (82), excimer laser angioplasty was compared with conventional balloon angioplasty and percutaneous transluminal rotational atherectomy for type B and C lesions and a high proportion of calcified lesions. The procedural success rate was 84% for balloon angioplasty, 88% for excimer laser angioplasty, and 93% for rotational atherectomy. The incidence of major complications (death, MI, or bypass surgery) was greater after excimer laser angioplasty than after rotational atherectomy or balloon angioplasty (6.2% vs. 2.3% and 4.8%, respectively). At 6-month follow-up, the incidence of clinical events (death, MI, bypass surgery, or repeat intervention) was greater after treatment with rotational atherectomy than after balloon angioplasty (53% vs. 45%; $p < .05$), whereas treatment with excimer laser angioplasty was associated with an intermediate rate of clinical events (49%). This does not support the use of laser in calcified lesions.

Long Lesions

Although long lesions were identified initially as the most promising indication for excimer laser angioplasty (93,94 and 95), recent analyses have suggested that long lesions are associated with trends toward reduced success, and strategies using long balloons and selective use of coronary stent placement (108) may result in superior success rates.

In a randomized comparison of excimer laser angioplasty with balloon angioplasty for lesions greater than 10 mm in length in 308 patients, the AMRO trial reported equivalent results for both types of treatment (109). In 151 patients randomly assigned to excimer laser angioplasty, 126 patients (80%) had procedural success and 50 (33%) experienced at least one cardiac event (death, MI, bypass surgery, or repeat angioplasty) within 6 months of the procedure. In 157 patients assigned to balloon angioplasty alone, 132 patients (79%) had procedural success and 47 (30%) experienced at least one cardiac event (death, MI, bypass surgery, or repeat angioplasty) within 6 months. Laser did not appear to confer a better acute or long-term benefit than balloon angioplasty for patients with lesions greater than 10 mm in length.

In-Stent Restenosis

Laser angioplasty may be used successfully as a debulking treatment for in-stent restenosis. Excimer laser angioplasty with adjunctive balloon dilatation was evaluated in 527 in-stent lesions in 440 patients previously treated with a variety of coronary stents (110). There was a 92% laser angioplasty success, with serious adverse events, including death (1.6%), Q-wave MI (0.5%), perforation (0.9%), and dissections after laser (4.8%) or postdilatation (9.3%). Mehran and coworkers compared the results of balloon angioplasty alone with excimer laser followed by balloon angioplasty in 98 cases of in-stent restenosis (111). By quantitative angiography and intravascular ultrasound, excimer laser was found to safely provide greater acute gain, plaque reduction, larger cross-sectional lumen area, and a trend for lower clinical restenosis than seen with balloon angioplasty.

MECHANICAL THROMBECTOMY

The pathogenesis of acute myocardial ischemic syndromes in native coronary arteries and saphenous aortocoronary vein grafts clearly involves thrombus formation (112,113 and 114). Often the small amount of thrombus formation at the surface of a ruptured plaque is sufficient to interrupt coronary flow, may not be evident by coronary angiography, but may permit larger thrombi to propagate beyond the culprit plaque or into a proximal area of stagnant flow. Such large thrombi may be evident on angiography, and attempted intervention in such lesions tends to produce significant clinical problems (distal embolization, no reflow, abrupt closure). They were previously treated by infusions of thrombolytic drugs, but these large thrombi—recognized by certain angiographic and clinical clues (recent onset of symptoms,

a mobile, rat-tail filling defect)—are now considered to be suitable targets for mechanical thrombectomy devices.

Earlier Pharmacologic Strategies to Remove Thrombus

Before the development of mechanical thrombectomy, standard therapy involved direct intracoronary or intragraft infusion of urokinase (115,116 and 117). The safety and efficacy of this approach was evaluated in the ROBUST trial (118), in which 107 patients were treated with direct urokinase infusion through a 0.035-inch infusion wire. After 25.4 hours of urokinase infusion to a mean dosage of 3.7 million units, 69% recanalization success rate was observed with major complications, including a 3% stroke rate and a 6.5% death rate. Broader use of adjunctive urokinase infusion during intervention has, however, been associated with a worsening of clinical outcomes (119).

In an attempt to avoid systemic lytic complications, urokinase has also been delivered directly to the thrombus surface using specialized delivery catheters. The Dispatch (Boston Scientific, Natrick, MA) catheter is an over-the-wire, nondilatation catheter with a 20-mm spiral inflation coil whose inflation creates an external space apposed to the vessel surface into which urokinase may be infused. The initial experience showed complete dissolution of thrombus in patients with angiographically evident thrombus in native coronary and vein graft obstructions (120,121). Urokinase may also be absorbed into a hydrogel balloon coating to transfer urokinase locally to the site of thrombotic obstruction (122).

Mechanical Thrombectomy

The limitations in speed, efficacy, and bleeding complications have fostered the development of catheter-based techniques for direct thrombus removal. Catheter-based systems can be categorized broadly into systems designed to disintegrate thrombus (e.g., the therapeutic ultrasound Acolysis device and the vortex-creating rotational Amplatz device), and systems designed to aspirate and remove thrombus from the body (e.g., the Possis AngioJet, the Hydrolyzer, TEC [see earlier discussion]).

The mechanical cutting and aspirating TEC device (see earlier discussion) has been advocated as a potential strategy for the treatment of thrombus-containing native coronaries and vein grafts (46,47,48,49 and 50), but has problems with distal embolization and vessel injury. The Cordis Hydrolyzer has had limited European exposure in humans in peripheral vessels (123), hemodialysis shunts (124), and coronary arteries and vein grafts (125,126).

The Amplatz thrombectomy device is another mechanical thrombectomy device that macerates thrombus. There is limited experience in peripheral artery thrombosis and occluded hemodialysis shunts (127,128,129 and 130). The Acolysis system employs therapeutic coronary ultrasound (at 41.9 kHz) to produce thrombolysis by fragmentation (131,132). Of 20 patients treated with the coronary ultrasound thrombolysis for vein graft disease (75% had total occlusions), there was a 70% device success (defined as final Thrombolysis in Myocardial Infarction [TIMI] 2 or 3 flow in occluded vessels or reduction in thrombus in patent vessels) with only one patient (5%) having evident distal embolization.

Possis AngioJet Catheter Design and Technique

The AngioJet is a 5F catheter with a stainless steel tip connected to a high-pressure hypotube (Fig. 24.20). Saline is injected into the tip via the hypotube, where it exits as three high-speed jets directed back into the main catheter lumen. By the Venturi-Bernoulli principle, this creates a low-pressure region at the tip (Fig. 24.21) that approaches a perfect vacuum (–760 mm Hg). With a normal pressure in the arterial lumen of +100 mm Hg, this produces a driving pressure of 860 mm Hg that pulls surrounding fluid (blood, thrombus, and saline) into the tip opening. There the jets break the thrombus into subcellular-sized particles and propel them proximally through the catheter lumen and out of the body. A hemostasis valve allows for the evacuation lumen to be sealed around a 0.014- to 0.018-inch diameter guidewire, over which the catheter is advanced down the coronary vessel. Previous *in vivo* histologic studies have shown that the catheter produces minimal or no vessel wall damage (133).

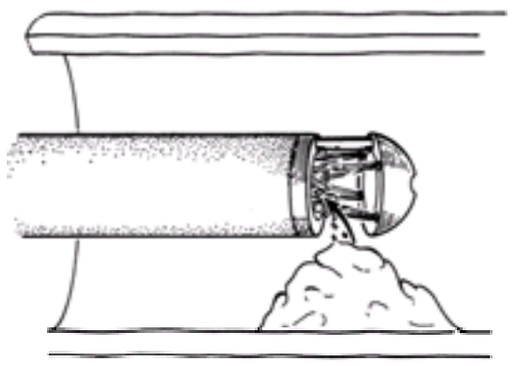

FIG. 24.20. Principle of rheolytic thrombectomy with the Possis AngioJet. High-speed saline jets exit orifices near the catheter tip and spray back into the mouth of the catheter. This creates intense local suction by the Venturi effect, which pulls thrombus into the jets, where the thrombus is macerated and propelled down the catheter lumen for external collection.

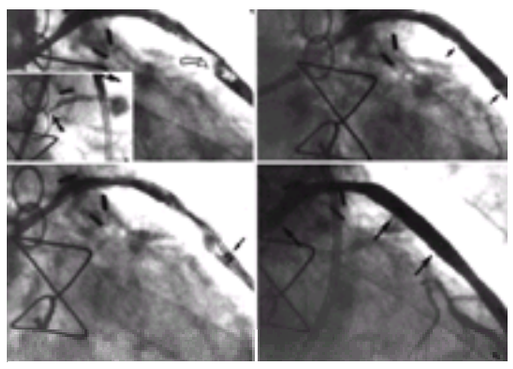

FIG. 24.21. Rheolytic thrombectomy with the Possis AngioJet in a patient with an occluded saphenous vein graft (*upper left, insert*). **Upper left:** Following balloon angioplasty of the graft ostium, a large filling defect (*open arrow*) is apparent in the body of the graft. **Lower left:** The AngioJet (*arrow*) is advanced beyond the presumptive thrombus, activated, and pulled back slowly. **Upper right:** Following AngioJet treatment, only small defects remain. **Bottom right:** Placement of Palmaz-Schatz biliary stents in the ostium and body of the graft provides near-normal appearance and antegrade flow.

Once the culprit lesion is identified, it is crossed using a 0.014- to 0.018-inch guidewire. The 5F AngioJet is then advanced over the wire and distal to the thrombotic lesion. The saline jets are then activated and the catheter is withdrawn slowly across the lesion at 0.5 to 1 mm/sec. Angiography is then performed after the first such withdrawal, and repeated passes of the Angiojet may be performed until angiography shows no further evidence of improvement in the lumen diameter or thrombus burden. The AngioJet has been used successfully to remove thrombus in elective situations such as thrombotic vein grafts (Fig. 24.21) and acute coronary ischemic scenarios, including acute MI (Fig. 24.22) (134,135 and 136).

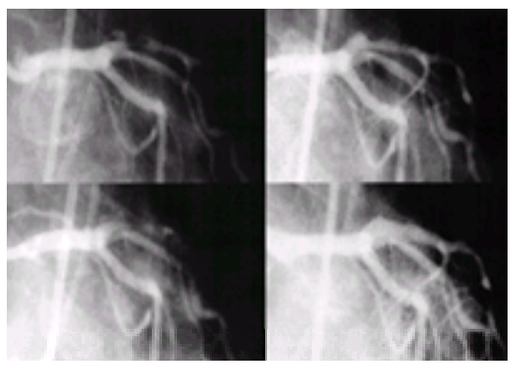

FIG. 24.22. AngioJet for AMI. **Upper left:** Primary angioplasty for acute anterior wall myocardial infarction shows thrombotic occlusion of the proximal left anterior descending. **Bottom left:** Passage of the AngioJet distal to thrombus. **Top right:** Following aspiration with the AngioJet, the thrombotic filling defect is gone. **Bottom right:** Following stent placement, a large, smooth lumen and brisk antegrade flow are present.

Studies

VEGAS I

The Vein Graft AngioJet Study (VEGAS I) consisted of multicenter registry of 90 patients with acute ischemic syndromes demonstrated. It showed that the AngioJet rheolytic thrombectomy catheter system reduced the angiographically measured thrombus burden within native coronary arteries or saphenous vein bypass grafts by an average of 86% (137).

VEGAS II

The Vein Graft AngioJet Study randomized trial (VEGAS II) was designed as a 500-patient multicenter randomized trial comparing the AngioJet rheolytic thrombectomy system with direct urokinase infusion for safety and effectiveness of thrombus removal before stenting for the treatment of saphenous vein grafts or native coronaries with angiographically apparent intraluminal thrombus (138). Because the 30-day event-free survival for major adverse cardiac events (defined as freedom from death, MI, emergent bypass surgery, target lesion revascularization, or stroke) was significantly lower for the AngioJet group after enrollment of 300 patients, the data safety committee recommended early termination at a final enrollment of 349 patients (180 in the AngioJet arm and 169 in the urokinase arm). The results of VEGAS I and VEGAS II were used by the Food and Drug Administration to approve the device in June of 1998.

DISTAL EMBOLIZATION PROTECTION DEVICES

Each of the devices discussed earlier actively seeks to remove plaque or thrombus from the target lesion, but it is now clear that even such interventions as balloon angioplasty or stent placement may break free fragments of friable plaque. This appears to be one of the main causes of no reflow during saphenous vein graft intervention, and may cause distal embolic events during carotid artery intervention (see Chapter 27). Various devices have been introduced recently for clinical trial evaluation that seek to trap such embolic material and remove it from the circulation (Fig. 24.23). As such, they are technically members of the “atherectomy” family. As their development progresses, it is likely that distal embolus protection will be used in combination with a broad variety of interventional devices (such as thrombectomy and stent placement, Fig. 24.24) to protect the distal circulation from embolization and consequent no-reflow.

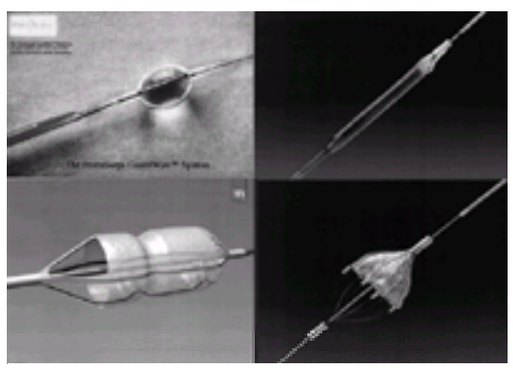

FIG. 24.23. Distal embolus retrieval devices. **Upper left:** The PercuSurge Guardwire shown during inflation of the low-pressure distal occlusion balloon and passage of the Export aspiration catheter to aspirate liberated debris. **Lower left:** The MedNova filter device shown open with collected debris in the filter, and the AngioGuard filter shown collapsed during delivery (*upper right*) and expanded (*lower right*) for collection of embolic material.

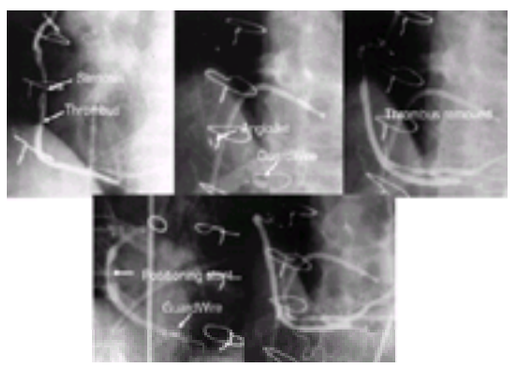

FIG. 24.24. Combination of distal protection and rheolytic thrombectomy. **Upper left:** Severe stenosis and adherent distal thrombus are present in this vein graft to the right coronary artery. **Upper center:** The PercuSurge Guardwire has been passed into the distal vessel and inflated, with advancement of the AngioJet over the Guardwire. **Upper right:** After removal of the thrombus, the Guardwire is deflated, and injection shows the residual stenosis. **Lower left:** Reinflation of the Guardwire allows placement of a stent. **Lower right:** Following aspiration of any liberated atheroembolic debris, the Guardwire is again deflated to restore flow.

The Guardwire (PercuSurge, Sunnyvale, CA) is a compliant balloon mounted on a hypotube that can function as a 0.014-inch steerable guidewire (139). Once it is positioned across the target lesion, the balloon can be inflated to block the flow of blood in the vessel, as the mechanical intervention is performed. With any liberated debris still trapped by the inflated Guardwire, an aspiration catheter is brought into the vessel and removes the blood and suspended debris. The Guardwire is then deflated to restore flow into the distal vessel. Preliminary analysis of the aspirate shows extensive plaque debris, and a randomized trial (SAFER) is now under way to evaluate whether performing vein graft angioplasty with such protection is associated with a lowering in the incidence of periprocedural slow flow and CK release. Preliminary results in the carotid artery is also encouraging.

There are also a series of semiporous filter devices that can be advanced into the distal vessel and deployed during intervention, to catch and remove liberated emboli. The first devices that will undergo clinical trial evaluation are the Emboshield (MedNova), the AngioGuard, and the Filter Wire (Embolic Protection Inc., San

Carlos, CA). All (Johnson & Johnson Medical) devices are nitinol expandable polymer filters located on the distal end of a modified 0.014-inch guidewire, which is deployed using specialized delivery and retrieval catheters. The shaft of the device can then function as a rail for advancement of over-the-wire platform for percutaneous coronary devices. After intervention, the filter is collapsed and withdrawn with any trapped debris.

SUMMARY

Although they have proven no more effective than stenting for the treatment of routine lesions, mechanical and laser-based atherectomy techniques continue to play an important adjunctive role in coronary intervention. These techniques are of particular value in treating ostial, bifurcation, or in-stent restenotic lesions, in debulking before stenting, and in treating long, fibrotic, or calcified lesions. In general, they are more challenging to use than balloon and stent techniques, and frequently carry a higher cost and an increased risk of some complications (such as per-procedure CK elevation, perforation, or dissection). But they have survived as important parts of interventional cardiology simply because they extend the range of lesions treatable by catheter-based therapy. The newer devices for thrombus removal and distal embolic protection also extend the range of treatable lesions and improve procedural results. Still newer atherectomy concepts are under development, including some with on-board ultrasound guidance to facilitate safe and more complete plaque removal, making it likely that atherectomy will remain as a strong minority player in an interventional world dominated by stenting.

---

* Drs. Robert D. Safian and John Bittl were contributors to this chapter in the previous editions.

CHAPTER REFERENCES

1. Simpson JB, Selmon MR, Robertson GC, et al. Transluminal atherectomy for occlusive peripheral vascular disease. *Am J Cardiol* 1988;61:96G.
2. Simpson JB. How atherectomy began: a personal history. *Am J Cardiol* 1993;72:3E.
3. Safian RD, et al. Clinical and angiographic results of transluminal extraction coronary atherectomy in saphenous vein bypass grafts. *Circulation* 1994;89:302.
4. Ahn SS, Auth D, Marcus DR, Moore WS. Removal of focal atheromatous lesions by angioscopically guided high-speed rotary atherectomy. *J Vasc Surg* 1988;7:292.
5. Fourrier JL, et al. Percutaneous coronary rotational atherectomy in humans: preliminary report. *J Am Coll Cardiol* 1989;14:1278.
6. Bittl JA. Clinical results with excimer laser coronary angioplasty. *Semin Interv Cardiol* 1996;1:129.
7. Hinohara T, Selmon MR, Robertson GC, Braden L, Simpson JB. Directional atherectomy: new approaches for treatment of obstructive coronary and peripheral vascular disease. *Circulation* 1990;81[Suppl IV]:IV-79.
8. Baim DS, et al. Results of directional coronary atherectomy during multicenter preapproval testing. *Am J Cardiol* 1993;72:6E.
9. Penny WF, Schmidt DA, Safian RD, Erny RE, Baim DS. Insights into the mechanism of luminal improvement after directional coronary atherectomy. *Am J Cardiol* 1991;67:435.
10. Matar FA, Mintz GA, Farb A, et al. The contribution of tissue removal to the lumen improvement after directional coronary atherectomy. *Am J Cardiol* 1994;74:647.
11. Lansky AJ, Mintz GS, Popma JJ, et al. Remodeling after directional coronary atherectomy (with and without adjunct percutaneous transluminal coronary angioplasty): a serial angiographic and intravascular ultrasound analysis from the Optimal Atherectomy Restenosis Study. *J Am Coll Cardiol* 1998;32:329.
12. Gordon PC, Kugelmass AD, Cohen DJ, et al. Balloon postdilation can safely improve the results of successful (but suboptimal) directional coronary atherectomy. *Am J Cardiol* 1993;72:71E.
13. Simonton CA, Leon MB, Baim DS, et al. "Optimal" directional coronary atherectomy: final results of the Optimal Atherectomy Restenosis Study (OARS). *Circulation* 1998;97:332.
14. Baim DS, Cutlip DE, Sharma SK, et al. Final results of the Balloon vs Optimal Atherectomy Trial (BOAT). *Circulation* 1998;97:322.
15. Fishman RF, Kuntz RE, Carrozza JP, et al. Long-term results of directional coronary atherectomy: predictors of restenosis. *J Am Coll Cardiol* 1992;20:1101.
16. Hinohara T, Rowe MH, Robertson GC, et al. Effect of lesion characteristics on outcome of directional coronary atherectomy. *J Am Coll Cardiol* 1991;17:1112.
17. Waksman R, Popma JJ, Kennard ED, et al. Directional coronary atherectomy—a report from the NACI Registry. *Am J Cardiol* 1997;80[Suppl]:50K.
18. Topol EJ, Leya F, Pinkerton CA, et al. A comparison of directional atherectomy with coronary angioplasty in patients with coronary artery disease. *N Engl J Med* 1993;329:221.
19. Adelman AG, et al. A comparison of directional atherectomy with balloon angioplasty for lesions of the left anterior descending coronary artery. *N Engl J Med* 1993;329:228.
20. Suzuki T, Hosokawa H, Katoh O, et al. Effects of adjunctive balloon angioplasty after intravascular ultrasound-guided optimal directional atherectomy—results of the ABACAS study. *J Am Coll Cardiol* 1999;34:1028.
21. Lansky AJ, Mintz GS, Popma JJ. Remodeling after directional coronary atherectomy (with or without percutaneous adjunct transluminal coronary angioplasty)—a serial angiographic and intravascular ultrasound analysis from the Optimal Atherectomy Restenosis Study. *J Am Coll Cardiol* 1998;32:329.
22. Schnitt SJ, Safian RD, Kuntz RE, Schmidt DA, Baim DS. Histologic findings in specimens obtained by percutaneous directional coronary atherectomy. *Hum Pathol* 1992;23:415.
23. Kuntz RE, Hinohara T, Safian RD, Selmon MR, Simpson JB, Baim D. Restenosis following directional coronary atherectomy: the effects of luminal diameter and deep wall excision. *Circulation* 1992;86:1394.
24. Holmes DR Jr, Garratt KN, Isner JM, et al. Effect of subintimal resection on initial outcome and restenosis for native coronary lesions and saphenous vein graft disease treated by directional coronary atherectomy. A report from the CAVEAT I and II investigators. Coronary Angioplasty Versus Excisional Atherectomy Trial. *J Am Coll Cardiol* 1996;28:645.
25. Bell MR, Garratt KN, Bresnahan JF, Edwards WD, Holmes DR Jr. Relation of deep arterial resection and coronary artery aneurysms after directional coronary atherectomy. *J Am Coll Cardiol* 1992;20:1474.
26. Imai Y, Hara K, Yamasaki M, et al. Mid-term follow-up of coronary artery aneurysm after directional coronary atherectomy. *J Cardiol* 1999;33:201.
27. Miller MJ, Kuntz RE, Friedrich SP, et al. Frequency and consequences of intimal hyperplasia in specimens retrieved by directional atherectomy of native primary coronary artery stenoses and subsequent restenoses. *Am J Cardiol* 1993;71:652.
28. Mansour M, Fishman RF, Kuntz RE, et al. Feasibility of directional atherectomy for the treatment of bifurcation lesions. *Coron Artery Dis* 1992;3:761.
29. Safian RD, Screiber TL, Baim DS. Specific indications for directional atherectomy: origin left anterior descending coronary artery and bifurcation lesions. *Am J Cardiol* 1993;72:35E.
30. Eisenhauer AC, Clugston RA, Ruiz CE. Sequential directional atherectomy of coronary bifurcation lesions. *Cathet Cardiovasc Diagn* 1993;[Suppl 1]:54.
31. Dauerman HL, Higgins PJ, Sparano AM, et al. Mechanical debulking versus balloon angioplasty for the treatment of true bifurcation lesions. *J Am Coll Cardiol* 1998;32:1845.
32. Popma JJ, Dick RJ, Haudenschild CC, Topol EJ, Ellis SG. Atherectomy of right coronary ostial stenoses: initial and long-term results, technical features and histologic findings. *Am J Cardiol* 1991;67:431.
33. Jain SP, Liu MW, Dean LS, et al Comparison of balloon angioplasty versus debulking devices versus stenting in right coronary ostial lesions. *Am J Cardiol* 1997;79:1334.
34. McKeever LS, Marek JC, Kerwin PM, et al. Bail-out directional atherectomy for abrupt coronary artery occlusion following conventional angioplasty. *Cathet Cardiovasc Diagn* 1993;[Suppl 1]:31.
35. Harris WO, Berger PB, Holmes DR Jr, et al. "Rescue" directional coronary atherectomy after unsuccessful percutaneous transluminal coronary angioplasty. *Mayo Clin Proc* 1994;69:717.
36. Dauerman HL, Baim DS, Cutlip DE, et al. Mechanical debulking versus balloon angioplasty for the treatment of diffuse in-stent restenosis. *Am J Cardiol* 1998;82:277.
37. Strauss BH, Umans VA, van Suylen RJ, et al. Directional atherectomy for treatment of restenosis within coronary stents: clinical, angiographic and histologic results. *J Am Coll Cardiol* 1992;20:1465.
38. Mahdi NA, Pathan AZ, Harrell L, et al. Directional coronary atherectomy for the treatment of Palmaz-Schatz in-stent restenosis. *Am J Cardiol* 1998;82:1345.
39. Teirstein PS, Massullo V, Jani S, et al. Catheter-based radiotherapy to inhibit restenosis after coronary stenting. *N Engl J Med* 1997;336:1697.
40. Moussa I, Moses J, Di Mario C, et al. Stenting after optimal lesion debulking (SOLD) registry: angiographic and clinical outcome. *Circulation* 1998;98:1604.
41. Kiesz RS, Rozek MM, Mego DM, et al. Acute directional coronary atherectomy prior to stenting in complex coronary lesions: ADAPTS Study. *Cathet Cardiovasc Diagn* 1998;45:105.
42. Annex BH, Larkin TJ, O'Neill WW, Safian RD. Thrombus removal by transluminal extraction coronary atherectomy (TEC): evaluation by percutaneous coronary angioscopy. *Am J Cardiol* 1994;74:606.
43. Kaplan BM, Safian RS, Grines CL, et al. Usefulness of adjunctive angioscopy and extraction atherectomy before stent implantation in high risk narrowings in aorto-coronary artery saphenous vein grafts. *Am J Cardiol* 1995;76:822.
44. Popma JJ, et al. Results of coronary angioplasty using the transluminal extraction catheter. *Am J Cardiol* 1992;70:1526.
45. Pizzulli L, Kohler U, Manz M, luderitz B. Mechanical dilatation rather than plaque removal as major mechanism of transluminal extraction atherectomy. *J Intervent Cardiol* 1993;6:31.
46. Twidale N, Barth CW, Kipperman RM, et al. Acute results and long-term outcome of transluminal extraction catheter atherectomy for saphenous vein graft stenoses. *Cathet Cardiovasc Diagn* 1994;31:187.
47. Meany TB, Leon MB, Kramer BL, et al. Transluminal extraction catheter for the treatment of diseased saphenous vein grafts: a multicenter experience. *Cathet Cardiovasc Diagn* 1995;34:112.
48. Sullebarger JT, Dalton RD, Tauth JG, Matar FA. One-year follow-up of recanalization of totally occluded aortocoronary saphenous vein grafts using transluminal extraction atherectomy. *Am J Cardiol* 1998;81:636.
49. Dooris M, et al. Comparative results of transluminal extraction atherectomy in saphenous vein graft lesions with and without thrombus. *J Am Coll Cardiol* 1995;25:1700.
50. Braden GA, Xenopoulos NP, Young T, et al. Transluminal extraction catheter atherectomy followed by immediate stenting in treatment of saphenous vein grafts. *J Am Coll Cardiol* 1997;30:657.
51. Safian RD, et al. Detailed clinical and angiographic analysis of transluminal extraction coronary atherectomy for complex lesions in native coronary arteries. *J Am Coll Cardiol* 1995;25:848.
52. Nino CL, et al. Procedural cost of new interventional devices. *Am J Cardiol* 1994;74:1165.
53. Kaplan BM, Larkin T, Safian RD, et al. Prospective study of extraction atherectomy in patients with acute myocardial infarction. *Am J Cardiol* 1996;78:383.
54. Topaz O, Miller G, Vetrovec GW. Transluminal extraction catheter for acute myocardial infarction. *Cathet Cardiovasc Diagn* 1997;40:291.
55. Kaplan BM, Gregory M, Schreiber TL, et al. Transluminal extraction atherectomy versus balloon angioplasty in acute ischemic syndrome. *Circulation* 1996;94:I317.
56. Kaplan BM. Results of the TECBEST trial. Presented at Trancatheter Therapeutics, September 22–25, 1999, Washington DC.
57. Sketch MH, Davidson CJ, Yeh W, et al. Predictors of acute and long-term outcome with transluminal extraction atherectomy: the new approaches to coronary intervention registry. *Am J Cardiol* 1997;80[Suppl]:68K.
58. Zacca NM, et al. Treatment of symptomatic peripheral atherosclerotic disease with a rotational atherectomy device. *Am J Cardiol* 1989;63:77.
59. Auth DC. Angioplasty with high speed rotary ablation. In: Serruys PW, et al, eds. *Restenosis after intervention with new mechanical devices.* Boston: Kluwer Academic Publishers, 1992:275.
60. Hansen DD, et al. Rotational atherectomy in atherosclerotic rabbit iliac arteries. *Am Heart J* 1988;115:160.
61. Hansen DD, et al. Rotational endarterectomy in normal canine coronary arteries: preliminary report. *J Am Coll Cardiol* 1988;11:1073.
62. Friedman HZ, et al. Mechanical rotary atherectomy: the effects of microparticle embolization on myocardial blood flow and function. *J Intervent Card* 1989;2:77.
63. Koch KC, Vom Dahl J, Kleinhans E, et al. Influence of platelet Gp IIb/IIIa receptor antagonist on myocardial hypoperfusion during rotational atherectomy as assessed by myocardial Tc-99m sestamibi scintigraphy. *J Am Coll Cardiol* 1999;33:998.
64. Reisman M, Shuman BJ, Dillard D, et al. Analysis of low-speed rotational atherectomy for the reduction of platelet aggregation. *Cathet Cardiovasc Diagn* 1998;45:208.
65. Bertrand ME, et al. Percutaneous transluminal coronary rotary ablation with Rotablator (European experience). *Am J Cardiol* 1992;69:470.
66. O'Neill WW. Mechanical rotational atherectomy. *Am J Cardiol* 1992;69:12F.
67. Teirstein PS, et al. High-speed rotational coronary atherectomy for patients with diffuse coronary artery disease. *J Am Coll Cardiol* 1991;18:1694.
68. Zotz R, et al. Analysis of high-frequency rotational angioplasty-induced echo contrast. *Cathet Cardiovasc Diagn* 1991;22:137.
69. Zacca NM, et al. Rotational ablation of coronary artery lesions using single, large burrs. *Cathet Cardiovasc Diagn* 1992;26:92.
70. Safian RD, et al. Detailed angiographic analysis of high-speed mechanical rotational atherectomy in human coronary arteries. *Circulation* 1993;88:961.
71. Stertzer SH, et al. Coronary rotational ablation: initial experience in 302 procedures. *J Am Coll Cardiol* 1993;21:287.

72. Ellis SG, et al. Relation of clinical presentation, stenosis morphology, and operator technique to the procedural results of rotational atherectomy and rotational atherectomy-facilitated angioplasty. *Circulation* 1994;89:882.
73. Warth DC, et al. Rotational atherectomy multicenter registry: acute results, complications and 6-month angiographic follow-up in 709 patients. *J Am Coll Cardiol* 1994;24:641.
74. Reisman M, Buchbinder M, Harms V, et al. Quantitative angiography of coronary artery dimensions 24 hours after rotational atherectomy. *Am J Cardiol* 1998;81:1427.
75. Mintz GS, et al. Intravascular ultrasound evaluation of the effect of rotational atherectomy in obstructive atherosclerotic coronary artery disease. *Circulation* 1992;86:1383.
76. Hoffman R, Mintz GS, Kent KM, et al. Comparative early and nine-month results of rotational atherectomy, stents, and the combination of both for calcified lesions in large coronary arteries. *Am J Cardiol* 1998;81:552.
77. Henneke KH, Regar E, Konig A, et al. Impact of target lesion calcification on coronary stent expansion after rotational atherectomy. *Am Heart J* 1999;137:93.
78. Motwani JG, Raymond RE, Franco I, et al. Effectiveness of rotational atherectomy of right coronary artery ostial stenosis. *Am J Cardiol* 2000;85:563.
79. Lopez JJ, Ho KKL, Stoler RC, et al. Percutaneous treatment of protected and protected left main coronary stenosis with new devices—immediate angiographic results and intermediate-term follow-up. *J Am Coll Cardiol* 1997;29:345.
80. Rosenblum J, et al. Rotational ablation of balloon angioplasty failures. *J Invas Cardiol* 1992;4:312.
81. Safian RD, Freed M, Reddy V, et al. Do excimer laser angioplasty and rotational atherectomy facilitate balloon angioplasty? Implications for lesion-specific coronary intervention. *J Am Coll Cardiol* 1996;27:552.

81a. King A, Marmur JD, Duvvuri S, et al. Rotational atherectomy-improved procedural outcome with evolution of techniques and equipment. Single0center results of the first 1,000 patients. *Cathet Cardiovasc Interv* 1999;46:1522.

82. Reifart N, Vandormael M, Krajcar M, et al. Randomized comparison of angioplasty of complex coronary lesions at a single center. Excimer Laser, Rotational Atherectomy, and Balloon Angioplasty Comparison (ERBAC) Study. *Circulation* 1997;96:91.
83. Ferguson J., Meeting highlights—46th annual session of the American College of Cardiology. *Circulation* 1997;96:367.
84. Rihal CS, Garratt KN, Holmes DR Jr. Rotational atherectomy for bifurcation lesions of the coronary circulation: technique and initial experience. *Int J Cardiol* 1998;65:I-9.
85. Sharma SK, Duvvuri S, Dangas G. Rotational atherectomy for in-stent restenosis: acute and long-term results of the first 100 cases. *J Am Coll Cardiol* 1998;32:1358.
86. Lee SG, Lee CW, Cheong SS, et al. Immediate and long-term outcomes of rotational atherectomy versus balloon angioplasty alone for the treatment of diffuse in-stent restenosis. *Am J Cardiol* 1998;82:140.
87. vom Dahl J, Radke PW, Haager PK, et al. Clinical and angiographic predictors of recurrent restenosis after percutaneous transluminal rotational atherectomy for treatment of diffuse in-stent restenosis. *Am J Cardiol* 1999;83:862
88. Linsker R, Srinivasan R, Wynne JJ, Alonso DR. Far-ultraviolet laser ablation of atherosclerotic lesions. *Laser Surg Med* 1984;4:201.
89. Clarke R, Isner JM, Donaldson RF, Jones GI. Gas chromatography light microscopic correlation of excimer laser photoablation of cardiovascular tissues: evidence for a thermal mechanism. *Circ Res* 1987;60:429.
90. Isner JM, Rosenfield K, White CJ, et al. *In vivo* assessment of vascular pathology resulting from laser irradiation: analysis of 23 patients studied by directional atherectomy immediately after laser angioplasty. *Circulation* 1992;85:2185.
91. Bonner R, Smith PD, Prevosti LD, Leon MB. New sources for laser angioplasty: Er:YAG, excimer lasers, and nonlaser hot-tip catheters. In: Vogel JHK, King SB III, eds. *Interventional cardiology: future directions.* St Louis: Mosby, 1989:101.
92. Appelman YE, Piek JJ, Verhoofstad GG, Gijsbers GH, Van Gemert MJ. Tissue ablation and gas formation of two excimer laser systems: an *in vitro* evaluation on porcine aorta. *Lasers Surg Med* 1996;18:197.
93. Stone GW, de Marchena E, Dageforde D, et al. Prospective, randomized, multicenter comparison of laser-facilitated balloon angioplasty versus stand-alone balloon angioplasty in patients with obstructive coronary artery disease. The Laser Angioplasty Versus Angioplasty (LAVA) Trial Investigators. *J Am Coll Cardiol* 1997;30:1714,
94. Appelman YE, Koolen JJ, Piek JJ, et al. Excimer laser angioplasty versus balloon angioplasty in functional and total coronary occlusions. *Am J Cardiol* 1996;78:757.
95. Litvack F, Eigler N, Margolis J, et al. Percutaneous excimer laser coronary angioplasty: results in the first consecutive 3,000 patients. *J Am Coll Cardiol* 1994;23:323.
96. de Marchena EJ, Mallon SM, Knopf WD, et al. Effectiveness of holmium laser-assisted coronary angioplasty. *Am J Cardiol* 1994;73:117.
97. Holmes DR Jr, Reeder GS, Ghazzal ZMB, et al. Coronary perforation after excimer laser coronary angioplasty: the Excimer Laser Coronary Angioplasty Registry experience. *J Am Coll Cardiol* 1994;23:330.
98. Baumbach A, Bittl JA, Fleck E, et al. Acute complications of coronary excimer laser angioplasty: analysis of two multicenter registries. *J Am Coll Cardiol* 1994;23:1305.
99. Tcheng JE, Wells LD, Phillips HR, Deckelbaum LI, Golobic RA. Development of a new technique for reducing pressure pulse generation during 308 nm excimer laser coronary angioplasty. *Cathet Cardiovasc Diagn* 1995;34:15.
100. Bittl JA, Kuntz RE, Estella P, Sanborn TA, Baim DS. Analysis of late lumen narrowing after excimer laser-facilitated coronary angioplasty. *J Am Coll Cardiol* 1994;23:1314.
101. Bittl JA, Sanborn TA, Tcheng JE, Watson LE. Excimer laser-facilitated angioplasty for undilatable coronary lesions: results of a prospective, controlled study. *Circulation* 1993;88:I-23 (abst).
102. Holmes DR Jr, Forrester JS, Litvack F, et al. Chronic total obstruction and short-term outcome: the excimer laser angioplasty registry experience. *Mayo Clin Proc* 1993;68:5.
103. Schofer J, Kresser J, Rau T, et al. Recanalization of chronic coronary artery occlusions using laser followed by balloon angioplasty. *Am J Cardiol* 1996;78:836.
104. Oesterle SN, Bittl JA, Leon MB, et al. Laser wire for crossing chronic total occlusions: “learning phase” results from the U.S. TOTAL trial. Total Occlusion Trial with Angioplasty by using a laser wire. *Cathet Cardiovasc Diagn* 1998;44:235.
105. Hamburger JN, Gijsbers GH, Ozaki Y, et al. Recanalization of chronic total coronary occlusions using a laser guide wire: a pilot study. *J Am Coll Cardiol* 1997;30:649.
106. Hamburger JN, Serruys PW, Scabra-Gomes R, et al. Recanalization of total coronary occlusions using a laser guidewire (the European TOTAL Surveillance Study). *Am J Cardiol* 1997;80:1419.
107. Cook SL, Eigler NL, Shefer A, Goldenberg T, Forrester JS, Litvack F. Percutaneous excimer laser coronary angioplasty of lesions not ideal for balloon angioplasty. *Circulation* 1991;84:632.
108. Cannon AD, Roubin GS, Hearn JA, et al. Acute angiographic and clinical results of long balloon percutaneous transluminal coronary angioplasty and adjuvant stenting for long narrowings. *Am J Cardiol* 1994;73:635.
109. Appelman YEA, Piek JJ, Strikwerda S, et al. Randomized trial of excimer laser versus balloon angioplasty for the treatment of obstructive coronary disease. *Lancet* 1996;347:79.
110. Koster R, Hamm CW, Seabra-Gomes R, et al. Laser angioplasty of restenosed coronary stents—results of a multicenter surveillance trial. *J Am Coll Cardiol* 1999;34:25.
111. Mehran R, Mintz GS, Satler LF, et al. Treatment of in-stent restenosis with excimer laser coronary angioplasty: mechanisms and results compared with PTCA alone. *Circulation* 1997;96:2183.
112. Mizuno K, Satomura K, Miyamoto A, et al. Angioscopic evaluation of coronary-artery thrombi in acute coronary syndromes. *N Engl J Med* 1992;326:287.
113. Sherman CT, Litvack F, Grundfest WS, et al. Coronary angioscopy in patients with unstable angina pectoris. *N Engl J Med* 1986;315:913.
114. Ambrose JA, Weinrauch M. Thrombosis in ischemic heart disease. *Arch Intern Med* 1996;156:1382.
115. Hartmann JR, McKeever LS, Stamato NJ, et al. Recanalization of chronically occluded aortocoronary saphenous vein bypass grafts by extended infusion of urokinase: initial results and short-term clinical follow-up. *J Am Coll Cardiol* 1991;18:1517.
116. Bell C, Kern MJ, Kaiser G. Sequential proximal and distal infusion of urokinase resulting in recanalization of acutely occluded aortocoronary bypass graft after coronary angioplasty. *Cathet Cardiovasc Diagn* 1992;26:224.
117. Chapekis AT, George BS, Candela RJ. Rapid thrombus dissolution by continuous infusion of urokinase through an intracoronary perfusion wire prior to and following PTCA: results in native coronaries and patent saphenous vein grafts. *Cathet Cardiovasc Diagn* 1991;23:89.
118. Hartmann JR, McKeever LS, et al. Recanalization of Chronically Occluded Aortocoronary Saphenous Vein Bypass Grafts With Long-Term, Low Dose Direct Infusion of Urokinase (ROBUST): a serial trial. *J Am Coll Cardiol* 1997;27:60.
119. Ambrose JA, Almeida OD, Sharma SK, et al. Adjunctive thrombolytic therapy during angioplasty for ischemic rest angina. Results of the TAUSA trial. TAUSA Investigators. Thrombolysis and Angioplasty in Unstable Angina trial. *Circulation* 1994;90:69.
120. McKay RG, Fram DB, et al. Treatment of intracoronary thrombus with local urokinase infusion using a new, site-specific drug delivery system: the Dispatch catheter. *Cathet Cardiovasc Diagn* 1994;33:181.
121. Glazier JJ, Kiernan FJ, et al. Treatment of thrombotic saphenous vein bypass grafts using local urokinase infusion therapy with the Dispatch catheter. *Cathet Cardiovasc Diagn* 1997;41:261.
122. Mitchel JF, Azrin MA, et al. Inhibition of platelet deposition and lysis of intracoronary thrombus during balloon angioplasty using urokinase-coated hydrogel balloons. *Circulation* 1994;90:1979.
123. Rousseau H, Sapoval M, et al. Percutaneous recanalization of acutely thrombosed vessels by hydrodynamic thrombectomy (Hydrolyser). *Eur Radiol* 1997;7:935.
124. Overbosch EH, Pattynama PM, et al. Occluded hemodialysis shunts: Dutch multicenter experience with the Hydrolyser catheter. *Radiology* 1996;201:485.
125. van Ommen VG, van den Bos AA, et al. Removal of thrombus from aortocoronary bypass grafts and coronary arteries using the 6Fr Hydrolyser. *Am J Cardiol* 1997;79:1012.
126. van den Bos AA, van Ommen V, Corbeij HM. A new thrombosuction catheter for coronary use: initial results with clinical and angiographic follow-up in seven patients. *Cathet Cardiovasc Diagn* 1997;40:192.
127. Rilinger N, Gorich J, et al. Short-term results with use of the Amplatz thrombectomy device in the treatment of acute lower limb occlusions. *J Vasc Interv Radiol* 1997;8:343.
128. Uflacker R, Rajagopalan PR, Vujic I, Stutley JE. Treatment of thrombosed dialysis access grafts: randomized trial of surgical thrombectomy versus mechanical thrombectomy with the Amplatz device. *J Vasc Interv Radiol* 1996;7:185.
129. Uflacker R, Strange C, Vujic I. Massive pulmonary embolism: preliminary results of treatment with the Amplatz thrombectomy device. *J Vasc Interv Radiol* 1996;7:519.
130. Uflacker R. Mechanical thrombectomy in acute and subacute thrombosis with use of the Amplatz device: arterial and venous applications. *J Vasc Interv Radiol* 1997;8:923.
131. Rosenschein U, Roth A, Rassin T, et al. Analysis of coronary ultrasound thrombolysis endpoints in acute myocardial infarction (ACUTE trial). Results of the feasibility phase. *Circulation* 1997;95:1411.
132. Rosenschein U, Gaul G, Erbel R, et al. Percutaneous transluminal therapy of occluded saphenous vein grafts. *Circulation* 1999;99:26.
133. Drasler WJ, Jenson ML, Wilson GJ, et al. Rheolytic catheter for percutaneous removal of thrombus. *Radiology* 1992;182:263.
134. Weisenaunt BK, Baim DS, Kuntz RE, Garcia LA, Ramee SR, Carrozza JP. Rheolytic thrombectomy with the Possis AngioJet—technical considerations and initial clinical experience. *J Invas Cardiol* 1999;11:421.
135. Nakagawa Y, Matsuo S, Kiura T, et al. Thrombectomy with AngioJet catheter in native coronary arteries for patients with acute or recent myocardial infarction. *Am J Cardiol* 1999;83:994.
136. Hamburger JN, Serruys PW. Treatment of thrombus containing lesions in diseased vein bypass grafts using the AngioJet Rapid Thrombectomy System. *Herz* 1997;22:318.
137. Ramee SR, Schatz RA, Carozza JP, et al. Results of the VEGAS-I pilot study of the Possis coronary AngioJet thrombectomy catheter. *Circulation* 1996;94:3622.
138. Ramee SR, Baim DS, Popma JJ, et al. A randomized, prospective, multi-center study comparing intracoronary urokinase to rheolytic thrombectomy with the Possis AngioJet catheter for intracoronary thrombus—final results of the VEGAS-2 trial. *Circulation* 1998;98:437.
139. Webb JG, Carere RG, et al. Retrieval and analysis of particulate debris follow saphenous vein graft intervention. *J Am Coll Cardiol* 1999;34:461.

25
Coronary Stenting

Joseph P. Carrozza, Jr. and Donald S. Baim

Harvard Medical School; Section of Invasive Cardiology, Beth Israel Deaconess Medical Center, Boston, Massachusetts 02215

Stents are metallic scaffolds that are deployed within a diseased segment of coronary artery to establish and then maintain a widely patent lumen. Just 6 years after the 1994 approval of the balloon-expandable Palmaz-Schatz slotted tube stent in the United States, stents are utilized in upwards of 80% of interventions and have revolutionized catheter-based treatment. Given the rapid evolution in stent design, techniques, and indications, the goal of this chapter is to highlight some of the underlying principles and concepts and to summarize the key trials on which current stent use is based, expecting that many of the nuances of stent design will continue to evolve.

HISTORICAL PERSPECTIVE

As described in Chapter 23, despite progressive improvement in the results of conventional balloon angioplasty, it remains limited by abrupt vessel closure (which leads to emergency bypass surgery in 1% of patients) and restenosis (which prompts a repeat revascularization procedure in 30% of patients). The attraction of stenting is that it addresses both of these shortcomings.

Although the concept of an endovascular prosthesis to seal dissections and overcome recoil was first proposed by the late Charles Dotter in 1964 (1), the first implantation of stents in human arteries did not occur until 1985, when Sigwart et al. (2) reported the successful placement of self-expanding Wallstents in the peripheral and coronary arteries of eight patients. One year later, however, Serruys (3) reported a much less favorable multicenter experience using this device, with 18% thrombotic occlusion and 8% mortality at 1 year. However, those patients who did not experience subacute thrombotic occlusion had a 6-month angiographic restenosis rate of only 14%, suggesting for the first time that stenting could reduce angiographic restenosis. This encouraged Gianturco and Roubin (4) to begin work on a balloon-expandable coil stent, which consisted of stainless steel wire wrapped around a deflated balloon in a serpiginous manner. A phase II study began in 1988 using this stent to reverse postangioplasty acute or threatened vessel closure (5), which led to U.S. Food and Drug Administration (FDA) approval in June 1993. Concurrently, Palmaz introduced a balloon-expandable stent in 1984 (6,7), in which rectangular slots were cut into thin-walled stainless steel tubing, so that balloon inflation within the stent deformed these rectangular slots into diamond-shaped windows or cells. The rigidity of this design made it difficult to pass through guiding catheters and tortuous vessels, until 1989 when Schatz (8,9) added a 1-mm central articulation to join two rigid 7-mm segments, creating the Palmaz-Schatz stent. In 1989, enrollment commenced in two randomized multicenter studies—the U.S. Stent Restenosis Study (STRESS) and the European Belgium Netherlands Stent (Benestent) trial (10,11)—comparing balloon angioplasty with *elective* Palmaz-Schatz stenting, which showed a 30% reduction in angiographic restenosis compared with conventional balloon angioplasty. This led to the 1994 FDA approval of the Palmaz-Schatz stent for elective treatment of focal *de novo* lesions in native vessels, 3 to 4 mm in diameter.

Despite the impressive acute and long-term results observed in the STRESS and Benestent trials, widespread application remained limited by the 3% incidence of thrombosis and a significantly higher incidence of hemorrhagic complications and length of hospital stay associated with the draconian anticoagulation regimens employed as prophylaxis against thrombosis (11). In the early 1990s, Colombo and colleagues, using intravascular ultrasound (IVUS), demonstrated that the majority of stents were inadequately expanded despite excellent angiographic appearance (12). By employing routine high-pressure adjunctive dilatation, he and other European investigators showed that such “optimal stenting” reduced the incidence of stent thrombosis to less than 1% to 2% using only aspirin and a second antiplatelet agent, ticlopidine, rather than prolonged warfarin therapy (13). Subsequently, two randomized trials—the German Intracoronary Stenting and Antithrombotic Regimen (ISAR) study (14) and the U.S. multicenter STent Anticoagulation Restenosis Study (STARS) (15)—definitively established the superiority of dual antiplatelet therapy (with aspirin and ticlopidine) over anticoagulation (with warfarin) for prevention of stent thrombosis. Additional trials showed the efficacy of stenting in broader anatomic and clinical situations (beyond focal *de novo* native vessel lesions). With the more effective antiplatelet regimens and expanding indications (16,17,18 and 19), which included saphenous vein bypass grafts, chronic total occlusions, prior restenosis, and acute myocardial infarction (MI), as well as the introduction since 1997 of a wide range of newer stent designs with improved flexibility, visibility, and profile, stent placement is now used in approximately 80% of percutaneous revascularizations.

STENT DESIGNS

As of 2000, more than 30 stent types have been implanted in the human coronary circulation (Fig. 25.1). Stent types differ in their *composition* (e.g., stainless steel, tantalum, nitinol), *architecture* (e.g., slotted tube, coiled wire), and *mode of implantation* (e.g., self-expanding, balloon-expandable) (Table 25.1). In theory, the perfect coronary stent would be made of a relatively nonthrombogenic material and have sufficient flexibility in its unexpanded state to allow passage through guiding catheters and tortuous vessels. Despite its flexibility and low profile in the collapsed state, it should have an expanded configuration that provides uniform scaffolding of the vessel wall with low recoil and maximal radial strength. In addition, the stent should be sufficiently radioopaque to allow fluoroscopic visualization but not so opaque as to obscure important vascular details. All clinically tested coronary stents have been constructed from metallic alloys, including stainless steel, tantalum, nitinol, and cobalt/platinum. The largest experience has been with stainless steel. Although each stent design is unique, they can be divided into broad categories

based on whether they are balloon-expandable or self-expanding, and subcategorized based on architecture (e.g., coil, tube, hybrid tube-coil).

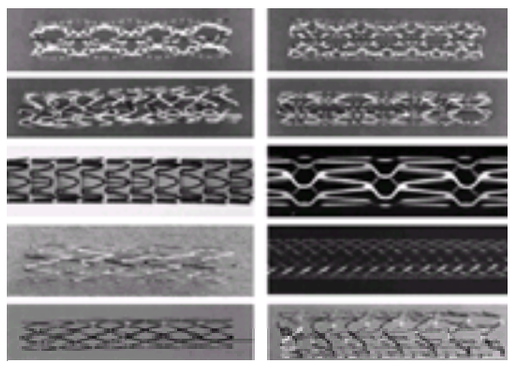

FIG. 25.1. Ten contemporary stent designs evaluated in humans as of January 2000. **Left to right, top row:** Crown Stent, Minicrown Stent. **Second row:** CrossFlex LC Stent, BX Stent. **Third row:** Duet Stent, NIR Stent. **Fourth row:** Radius Stent, Wallstent. **Bottom row:** GFX stent, BeStent.

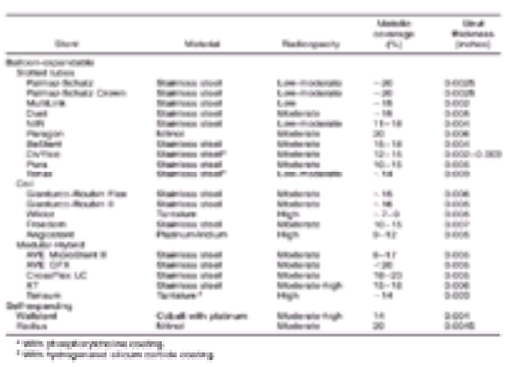

Stent	Material	Radiopacity	Coverage (%)	Thickness (inches)
Balloon-expandable				
Slotted tubes				
Palmaz-Schatz	Stainless steel	Low–moderate	~20	0.0035
Palmaz-Schatz Crown	Stainless steel	Low–moderate	~20	0.0035
MultiLink	Stainless steel	Low	~16	0.002
Duet	Stainless steel	Moderate	~16	0.006
NIR	Stainless steel	Low–moderate	15–18	0.004
Paragon	Nitinol	Moderate	20	0.006
BeStent	Stainless steel	Moderate	16–18	0.004
DaVinci	Stainless steel[a]	Moderate	12–15	0.003–0.003
Pura	Stainless steel	Moderate	16–18	0.004
Ismar	Stainless steel[a]	Low–moderate	~14	0.003
Coil				
Gianturco-Roubin Flex	Stainless steel	Moderate	~16	0.006
Gianturco-Roubin II	Stainless steel	Moderate	~16	0.005
Wiktor	Tantalum	High	~2–9	0.005
Freedom	Stainless steel	Moderate	10–15	0.007
Angiostent	Platinum/iridium	High	9–12	0.005
Modular/ Hybrid				
RVE MicroStent II	Stainless steel	Moderate	9–11	0.005
RVE GFX	Stainless steel	Moderate	~20	0.005
CrossFlex LC	Stainless steel	Moderate	18–23	0.005
BX	Stainless steel	Moderate-high	15–18	0.006
Tensum	Tantalum[a]	High	~14	0.003
Self-expanding				
Wallstent	Cobalt with platinum	Moderate-high	14	0.004
Radius	Nitinol	Moderate	20	0.0045

[a] Within phosphorylcholine coating.
[b] Within hydrogenated silicone carbide coating.

TABLE 25.1. *Stent designs*

Balloon-Expandable Stents

Balloon-expandable stents are delivered into the coronary artery in their collapsed state, mounted on a delivery balloon. Once in the desired location, inflation of the delivery balloon expands the stent and imbeds it into the arterial wall. Within the balloon-expandable stent category, all stents can be assigned to one of three subgroups, based on construction: wire coils, slotted tubes, and modular designs.

Wire Coils

The Gianturco-Roubin FlexStent (Cook Cardiology, Indianapolis, IN) was the initial coil stent prototype. It was constructed by winding stainless steel wire into a serpiginous pattern of reversing loops and then folding that pattern onto a compliant balloon to create an interdigitating coil. Although this device was the first stent to receive FDA approval (in 1993), its mechanical deficiencies (e.g., low axial and radial strength and a tendency for plaque to prolapse through large gaps between adjacent loops) largely limited its use to acute or threatened vessel closure. To address these deficiencies, a second-generation Gianturco-Roubin II (GR-II) stent incorporated a longitudinal spine to enhance radial and axial strength. For ease of manufacture, the desired geometry was actually cut from a flat sheet, and small dots of gold solder were placed at each end of the stent to enhance radiographic visualization. Although this design retained the excellent flexibility and deliverability of the original, the GR-II was still troubled by plaque prolapse and excessive recoil after deployment (up to 30% of cross-sectional area); this must be compensated by intentional oversizing of the delivery balloon (ratio of balloon to artery diameter, about 1.2) (24,25), which may lead to edge dissections or even vessel perforation.

Slotted Tubes

In the mid 1980s, Palmaz introduced the concept of an endovascular prosthesis whose wall was made of offset rows of rectangular slots, each of which was plastically deformed into a “diamond” during expansion. In their expanded state, these diamonds (like the trusses of a bridge) made the stent relatively resistant to recoil and compression. The initial Palmaz prototypes, however, were relatively rigid and difficult to deliver through angulated guiding catheters or tortuous vasculature. Schatz therefore modified the original Palmaz design by breaking the 15-mm rigid length into two 7-mm segments joined by a 1-mm central articulation. When bare-mounted on an angioplasty balloon by the operator, the Palmaz-Schatz stent proved susceptible to being stripped off the balloon, leading to systemic embolization if the target lesion could not be crossed. To overcome this problem, a protective 5F delivery sheath was introduced in 1990 (Palmaz-Schatz Coronary Stent Delivery System, Cordis Corporation, Miami, FL); this helped to prevent snagging of the stent on coronary irregularities during advancement and precluded embolization during withdrawal if advancement across the lesion proves unsuccessful. Although this was the design released in 1994 and used for the pivotal randomized trials of stenting, this relatively inflexible stent and its bulky (5F) delivery sheath required large-lumen (more than 0.084-inch) guiding catheters, was difficult to deliver in tortuous anatomy or to distal lesions, and provided suboptimal scaffolding at the articulation site.

In an effort to preserve the radial strength and wall coverage of the tubular design but improve flexibility in the collapsed state, a number of newer (second- and third-generation) slotted-tube stents were developed. These included the modified Palmaz-Schatz geometry of the Crown (Cordis), the MultiLink and Duet (Guidant Corporation, Santa Clara, CA), and the NIR (Medinol, Israel) stent. Each involves laser cutting of a unique multicellular pattern into a metallic tube, which increases the overall flexibility of the stent by distributing bending throughout the stent length without compromising radial strength or elastic recoil (see later discussion). The newer stents have also been marketed in a broader range of stent lengths (8 to 32 mm) and diameters (2.25 to 6.0 mm) to facilitate stenting of long lesions, small vessels, saphenous vein grafts, and distal lesions. With better balloon materials and techniques for crimping and retaining the stent on the delivery balloon, the concept of a protective sheath has proved unnecessary. All current slotted tube designs are “bare mounted” on a delivery balloon, with deflated profiles smaller than 0.040-in. (1 mm), comparable with the best angioplasty balloons of only a few years ago.

Modular Stents

Despite enhanced flexibility, even second-generation slotted-tube stents are sometimes difficult to deliver through tortuous and noncompliant vessels. In an effort to enhance flexibility and deliverability without sacrificing the excellent scaffolding of the slotted-tube stents, the modular or hybrid stents are constructed by flexibly joining multiple, short repeating modules to each other. The initial modular stent was the MicroStent (Arterial Vascular Engineering, Santa Rosa, CA), in which 4-mm-long stainless steel corrugated ring subunits were welded to each other. Although this first-generation MicroStent was extremely deliverable, it was limited by low surface coverage and radial strength. Subsequent designs incorporated an elliptorectangular strut profile and reduced the length of the individual modules to 3 mm (Micro II), 2 mm (GFX), and 1.5 mm (S670), with further reductions in crossing profile and increased surface area coverage.

Self-Expanding Stents

The prototype self-expanding stent—the Wallstent (Boston Scientific, Minneapolis, MN)—is a direct descendent of the first coronary stent used in 1985. It is manufactured from 16 stainless steel wire strands that are woven together to form a mesh tube (Table 25.1; Fig. 25.1). The stent is positioned on the delivery system in its collapsed state, constrained by an outer membrane. Retraction of the membrane allows the stent to reassume its unconstrained (expanded) geometry, which can be reinforced by balloon dilatation within the stent, if necessary. In the original Wallstent design, a double-layer outer membrane rolled over itself during retraction but gave the delivery system a large diameter (5F); this has been replaced by a single-layer sliding membrane in current designs. In an effort to reduce thrombogenicity

and the amount by which the stent shortens during delivery, the braiding angle of the mesh wires has also been reduced by approximately 40° (the Less Shortening Wallstent). The present-generation Wallstent (the Magic Wallstent) incorporates a platinum core within the wires (to increase radioopacity), further modification of the braiding angles, and the ability to readvance the delivery sheath to recapture a partially deployed stent.

The Radius stent (Boston Scientific) is a self-expanding nitinol stent that makes use of the shape memory of the nickel—titanium alloy, nitinol. Once baked at high temperature in its expanded diameter, the superelasticity of this material allows it to be compressed to small diameter and constrained by a membrane on the delivery catheter. The stent is placed within the target lesion and the membrane is withdrawn; the stent then springs back to its memory diameter. The advantage of this design over the Wallstent is the fact that minimal shortening takes place during expansion.

Self-expanding stents typically are selected to have an unconstrained diameter that is oversized by 0.50 to 1.0 mm relative to the diameter of the adjacent reference segment. This ensures contact with the vessel wall and increases the expansile force, but final optimization of stent expansion usually requires inflation of an angioplasty balloon within the stent. (The diameter of that balloon must never exceed the unconstrained stent diameter in air.) Although self-expanding stents are extremely flexible and can be delivered through tortuous vessels without risk of dislodgement, the difficulties relating to accurate sizing and precise placement necessitate a longer operator “learning curve” and render these stents unsuitable for the treatment of ostial lesions or involved side branches.

INDICATIONS FOR STENTING

Acute or Threatened Closure

Balloon expansion within an arterial stenosis causes luminal enlargement by overall vessel expansion and fracture of atheromatous plaque, but the combination of medial dissection and elastic recoil causes sufficient luminal compromise to culminate in abrupt vessel closure in roughly 5% of lesions treated by balloon angioplasty (see Chapter 23). One of the major benefits of stenting is the ability to definitively reverse abrupt closure due to dissection and recoil, and thus eliminate the need for high-risk emergency bypass surgery. A 518-patient multicenter registry of the Gianturco-Roubin FlexStent as a definitive treatment for acute or “threatened” vessel closure (local dissection, reduced antegrade flow, or clinical evidence of ongoing ischemia) was conducted from 1988 through 1991 (5) (Fig. 25.2). Although 95% of patients were successfully stented, 7.7% of patients with frank closure (and 2.7% of those with threatened closure) still required surgery, and there was an 8.7% incidence of stent thrombosis, particularly in smaller stents (2.5 mm or less).

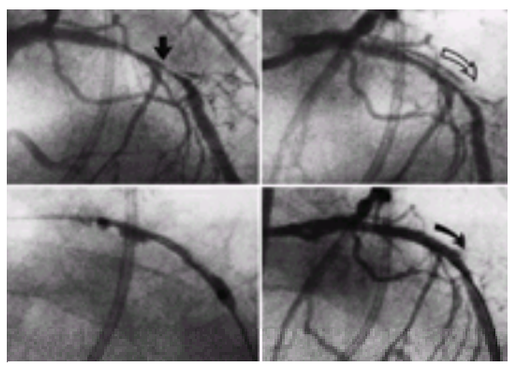

FIG. 25.2. Early example of placement of a Gianturco-Roubin coil stent for threatened abrupt closure. A long lesion is present in the left anterior descending coronary artery **(upper left)**, with a long dissection after angioplasty (**upper right,** *open arrow*). Placement of a coil stent **(lower left)** results in effacement of the dissection and elimination of the need for emergency bypass **(lower right)**.

Two small, randomized trials compared bailout stenting with prolonged inflations with perfusion balloons. In the Trial of Angioplasty and Stents in Canada (TASC II), patients with abrupt or threatened closure were randomly assigned to treatment with a perfusion balloon or stent placement (20). Even though about 25% of the patients assigned to balloon angioplasty crossed over to bailout stenting, the 6-month restenosis rate was significantly lower for stented lesions (22% vs. 50%). In the STENT-BY study, 100 patients were randomly assigned to prolonged balloon inflations or Palmaz-Schatz placement; they showed similar reductions in rate of target vessel revascularization at 6 months (24% vs. 65%) (21). Although bailout stenting is therefore a very effective technique (Fig. 25.3), the exponential growth in *elective* stenting during the past 5 years has left very few vessels that require bailout stenting, as the need for emergency bypass surgery to less than 0.5% between.

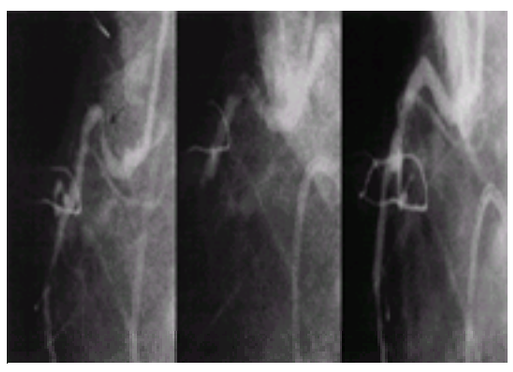

FIG. 25.3. Stenting as definitive treatment for acute vessel closure. A high-grade stenosis is present in an angulated segment of the proximal right coronary artery *(arrow)*. After balloon dilatation, a grade F dissection is seen **(middle)**. After stent placement, normal flow is restored **(right)**.

Elective Stenting of Focal, De Novo Native Coronary Lesions

This indication was used in two landmark studies—STRESS (11) and Benestent I (10)—to establish the ability of the Palmaz-Schatz coronary stent to significantly lower incidence of angiographic and clinical restenosis, compared with balloon angioplasty, in focal *de novo* lesions in 3- to 4-mm native coronary arteries (Table 25.2). These trials also confirmed that this benefit was a result of the ability of the stent to provide a larger acute lumen compared with balloon angioplasty. The strongest predictor of freedom from restenosis was a large posttreatment lumen diameter, and once posttreatment lumen diameter was incorporated into the statistical model of restenosis, there was not any independent effect attributable to the stent itself (22). Other randomized trials comparing stenting with balloon angioplasty (Table 25.2) have consistently demonstrated the superiority of stenting for focal, *de novo* lesions in 3- to 4-mm native coronary arteries.

Study Author (ref)	Major findings	Stent (%)	PTCA (%)
STRESS, Fischman et al. (11)	Procedure success	92	85
	Restenosis	31	42
	TVR	14	22
Benestent I, Serruys et al. (10)	Procedure success	87	86
	Restenosis	22	32
	TVR	18	27
	Vascular surg	10	2
Benestent II, Serruys et al. (55)	Procedure success	96	95
	Restenosis	16	31
	EFS	84	78
LAD, Versaci et al.[a]	Procedure success	95	93
	Restenosis	19	40
	EFS (12 mo)	87	76
TASC II, Penn et al. (30)	Major events	16	14
START, Serra et al. (56)	Restenosis	22	37
	TVR	11	22

EFS, event-free survival; PTCA, percutaneous transluminal coronary angioplasty; TVR, target vessel revascularization.
[a] De novo lesions in the left anterior descending coronary artery (Versaci).

TABLE 25.2. *Trials of stenting versus PTCA for de novo lesions in native coronary arteries*

The superior acute and long-term clinical outcomes reported in the STRESS and Benestent trials heightened the interest in evaluating stenting in other lesion subsets—chronic total occlusions, aortoostial location, and saphenous vein graft lesions—that respond poorly to conventional angioplasty due to marked elastic recoil, a predisposition to dissection, and high restenosis rates. Each of these "non-STRESS/Benestent" lesion categories is reviewed separately below.

Saphenous Vein Graft Lesions

The most common cause of recurrent ischemia after coronary artery bypass surgery is atheromatous degeneration within the body of the saphenous vein graft. Balloon angioplasty and atherectomy techniques have high rates of angiographic restenosis (40% to 50%) and long-term clinical failure (23,24 and 25), but early single-center registries suggested that stenting of saphenous vein graft lesions had lower rates of angiographic restenosis (17% to 25%) and repeat revascularization of the target site (26,27). This finding was evaluated further in the randomized SAphenous VEin graft Disease (SAVED) trial (28), which compared Palmaz-Schatz stenting with balloon angioplasty for treatment of relatively focal, *de novo* lesions in 3.0- to 5.0-mm saphenous vein grafts. Stenting had greater technical success (residual stenosis less than 50% by QCA, 95% vs. 75%); greater procedural success (technical success in the absence of a major adverse event, 92% vs. 69%); and a lower incidence of adverse clinical events (death, MI, or subsequent revascularization, 26% vs. 38%). Although the angiographic restenosis rates were not statistically different (due to inadequate sample size), the incidence of major adverse events was significantly reduced in stented patients (26% vs. 38%).

The lack of stents that could be expanded beyond 4 mm, however, limited the ability to treat many vein grafts. One option for treatment of large grafts was to use hand-crimped larger Palmaz-Schatz *biliary* stents (Cordis) which could be expanded up to 6 mm (50). With the development of longer stents and those that can be expanded beyond 4 mm (e.g., the Wallstent and the nine-cell NIR stent [Boston Scientific]), vein graft stenting has become easier, although there are still issues relating to "no reflow" and distal embolization (see Chapter 23). Finally, even though the incidence of repeat revascularization triggered by failure of the stented *site* is low (less than 20%), the incidence of clinical events approaches 50% by 5 years owing to progression of disease at nontarget sites within the treated graft, as well as attrition of other grafts and progression of native coronary disease (26).

Restenosis After Previous Angioplasty

Retreatment of lesions that have restenosed after previous angioplasty generally has a higher incidence of recurrent restenosis, even after correction for confounding factors such as diabetes mellitus or small reference vessel diameter that might have predisposed to the original restenosis (29). The subset of such patients undergoing treatment of restenotic lesions in the TASC I trial had a significantly lower incidence of repeat revascularization (4.5% vs. 25%) than those in the percutaneous transluminal coronary angioplasty (PTCA) cohort (30). Similarly, the Restenosis Stent Study (REST) randomly assigned 383 patients with prior restenosis to either balloon angioplasty or the Palmaz-Schatz stent and found reductions in angiographic restenosis (18% vs. 32%) and subsequent need for revascularization of the target vessel (10% vs. 27%) with stenting (19). Using aspirin and ticlopidine, Colombo reported an angiographic restenosis rate of 25% with a low (0.8%) incidence of subacute thrombosis in patients with prior restenosis (31).

Chronic Total Occlusions

Balloon angioplasty of chronically occluded coronary arteries is associated with a high incidence (approximately 50%) of restenosis, reocclusion, and recurrent symptoms, compared with treatment of subtotal stenoses (see Chapter 23). Three randomized trials have compared stenting with conventional balloon angioplasty alone for treatment of chronic total occlusions. In the Stenting in Chronic Coronary Occlusion (SICCO) trial, which compared balloon angioplasty with Palmaz-Schatz stenting for treatment of chronic total occlusion in native coronary arteries, a lower incidence of both angiographic restenosis (32% vs. 74%) and target vessel revascularization (22% vs. 42%) was found with stenting (21,32). The Gruppo Italiano di Studio Stent Nelle Occlusioni Coronariche (GISSOC) trial also showed a lower incidence of restenosis (32% vs. 68%), reocclusion (8% vs. 34%), and target lesion revascularization (5% vs. 22%) in patients assigned to stenting (33). Likewise, in the Total Occlusion Study of Canada (TOSCA), angiographic restenosis and target vessel revascularization were reduced in patients treated with stents compared with conventional angioplasty (34).

Acute Myocardial Infarction

With the completion of several large registries and randomized trials of acute MI demonstrating better outcomes in patients treated with primary angioplasty rather than thrombolytic therapy, "mechanical reperfusion" has become the preferred treatment for acute MI in many institutions (see Chapter 23). Despite successful initial reperfusion, however, there is a 10% to 15% incidence of reocclusion and a 30% to 50% incidence of restenosis after primary angioplasty (35,36). Although the presence of acute MI was initially considered to be a contraindication to stent placement (because of concerns that this prothrombotic milieu would be associated with an unacceptably high incidence of acute thrombosis), the use of stents to treat suboptimal results and as "upfront" therapy in the treatment of MI has now become widespread. Bauters and colleagues showed that stenting of the infarct-related artery is associated with reduction in the incidence reocclusion (1% vs. 14%) and restenosis (27% vs. 52%) compared with balloon angioplasty (37). Data from several small randomized trials have also suggested that stenting may offer acute and long-term benefits (primarily a reduction in repeat revascularizations) compared with balloon angioplasty alone (38,39,40 and 41) (Table 25.3).

Study (reference)	Early MACE		Restenosis		TVR		EFS	
	PTCA (%)	Stent (%)	PTCA (%)	Stent (%)	PTCA (%)	Stent (%)	PTCA (%)	Stent (%)
GFWM (38)	12	3.8	–	–	13	9.6	65	83
Sunyaprantata (39)	–	–	–	–	17	4.0	80	95
FRESCO (41)	8.3	1.0	52	12	25	7.0	–	–

EFS, event-free survival; MACE, major adverse cardiac event; PTCA, percutaneous transluminal coronary angioplasty; TVR, target vessel revascularization.

TABLE 25.3. *Stenting versus balloon angioplasty in acute myocardial infarction*

It is less clear that routine stenting of infarct vessels improves already good acute outcomes. The large Stent Primary Angioplasty in Myocardial Infarction (Stent-PAMI) study (balloon angioplasty vs. heparin-coated Palmaz-Schatz stent) randomly assigned 900 patients with acute MI to either PTCA alone or stenting with the heparin-coated Palmaz-Schatz coronary stent. Although patients assigned to stenting had a lower incidence of recurrent ischemia with ST-segment elevation during hospitalization (1.2% vs. 3.5%), angiographic restenosis (12.8% vs. 21.9%), and target vessel revascularization by 6 months (16.3% vs. 20%) (42), they more commonly exhibited reduced posttreatment TIMI flow compared with balloon angioplasty. This question is being evaluated further in the Controlled Abciximab and Device Investigation to Lower Late Angioplasty Complications (CADILLAC), in which patients with acute MI are randomly assigned to stenting (vs. PTCA) and then to abciximab (vs. heparin alone).

Long Lesions

Lesion length is associated with an increased incidence of acute complications and restenosis after conventional balloon angioplasty, as well as directional and rotational atherectomy (43,44 and 45). Early randomized trials (e.g., STRESS, Benestent) excluded lesions longer than 15 mm because of the lack of availability of longer stents and the concern that placement of multiple overlapping stents would be associated with a high incidence of subacute thrombosis and restenosis. With the availability of longer stents, improvements in stenting technique, and use of antiplatelet therapy, stenting of longer lesions and diffusely diseased arteries has

become a viable option. In the early multicenter registry, lesions treated with multiple Palmaz-Schatz coronary stents had a 65% rate of restenosis (46) and an 8.9% incidence of subacute thrombosis (47). Despite high-pressure dilatation and use of antiplatelet therapy in more than 7,000 patients enrolled in five recently completed stent trials, Cutlip and colleagues found that total stent length was independently associated with stent thrombosis, with an odds ratio of 1.2 for each additional 10 mm of stent placed (48).

The pivotal question remains whether stenting will have any impact on the high rates (more than 50%) of restenosis observed with balloon angioplasty or atheroablative techniques in such lesions. Single-center and registry data suggest an almost linear relation between stent length and restenosis even with contemporary stenting techniques (49). Although total stent length is associated with increased risk for clinical and angiographic restenosis, it is uncertain whether total stent number or the ratios of stent to lesion length also independently affect restenosis. In the multicenter randomized trial comparing the GR-II stent (Cook) to the Palmaz-Schatz stent, the stent-to-lesion ratio was significantly greater (2.5 vs. 1.9) for patients randomly assigned to the GR-II cohort despite similar baseline lesion lengths, which may have contributed to the higher incidence of restenosis (47% vs. 21%) with that device (50). Similarly, data from Albiero and colleagues suggest that high stent-to-lesion ratios are associated with high rates of restenosis (37% to 40%) in both discreet and long lesions (51). This has led some to advocate the use of “spot stenting,” whereby aggressive balloon angioplasty or rotational atherectomy is performed in diffusely diseased segments and short stents are placed only in areas of high residual plaque burden or residual stenosis exceeding 20% (52). With current devices, it seems that both lesion length and stent length exert an independent effect on subsequent restenosis (53).

Small Vessels

Small (less than 3.0 mm) vessels were formally excluded from the early randomized stent trials (8), although a significant number of vessels in both the STRESS and Benestent trials were actually smaller than 3.0 mm by quantitative coronary angiography (most between 2.75 and 3.0 mm). Most trials have suggested a higher incidence of subacute thrombosis and restenosis for stenting in vessels smaller than 3 mm compared with larger vessels. Despite this higher risk, there are emerging data from subgroup analyses of the randomized “stent versus PTCA” trials to suggest that stenting of vessels smaller than 3.0 mm may be associated with better clinical and angiographic outcome compared with balloon angioplasty (Table 25.4) (10,11,54,55 and 56). It must be cautioned, however, that good trials comparing stenting with balloon angioplasty in small vessels (2.0 to 2.7 mm) are lacking, and that the current stent systems for vessels 2.5 mm and smaller are based on the abrupt closure indication rather than elective stenting in these vessels. Finally, there is the unproven hope that stents specifically designed for smaller vessels, such as the MiniCrown (Cordis), may result in benefit from lower metal coverage with correspondingly lower restenosis rates.

Study (reference)	Binary restenosis (%)		TLR (%)	
	PTCA	Stent	PTCA	Stent
STRESS (11)	55	34	27	16
Benestent I (10)	–	–	41	31
START (56)	43	24	–	–
Benestent II (53)	28	19	–	–

PTCA, percutaneous transluminal coronary angioplasty; START, Stent Versus Angioplasty Restenosis Trial; STRESS, Stent Restenosis Study; TLR, target lesion revascularization.
$p < .05$ for all comparisons of PTCA vs. stent.

TABLE 25.4. *Angiographic and clinical outcome of stenting versus balloon angioplasty for small vessels (<3.0 mm)*

Aortoostial Lesions

True aortoostial lesions extend proximal to the coronary ostia into the walls of the aorta, where abundant elastic fibers contribute to elastic recoil and poor outcome (57). By resisting recoil, stents may provide significantly larger lumens and lower the risk of restenosis in this lesion subset. Although randomized trials comparing stenting with balloon angioplasty or atherectomy techniques as a treatment for aortoostial lesions have not been performed, Rocha-Singh (58) reported a restenosis rate of 27.8%, and Rechavia (59) a repeat revascularization rate of only 9% after stent placement. Accurate stent placement and expansion in the ostium is often technically challenging, however, because the lesion must be covered completely without excessive protrusion of the stent into the aortic lumen. This is aided by the use of an angiographic projection that shows the coronary ostium and wall of the aorta in profile, by the use of a radioopaque stent, and by first debulking the lesion with rotational atherectomy (see Chapter 24). These techniques have allowed successful treatment of left main as well as ostial right coronary lesions (60,61,62 and 63), although the risk of restenosis of an “unprotected” left main lesion manifesting as sudden cardiac death is a concern (see Chapter 23).

Bifurcation Lesions

Lesions involving the bifurcation of a coronary artery and a major side branch are associated with increased procedural complications and poor long-term outcome owing to recoil and plaque shifting at the origin of the side branch (64). Dauerman and colleagues (65) demonstrated that atherectomy debulking of such lesions (see Chapter 24) reduces the need for subsequent revascularization, but optimal performance may be technically demanding. Other investigators have explored a number of approaches to stenting of bifurcation lesions (Fig. 25.4). If the parent vessel is large and the side branch is relatively small, a stent can simply be deployed across the side branch, and the compromised side branch can be “rescued” by balloon dilatation out through the wall of the stent, using a low-profile balloon positioned half in the parent vessel and half in the jailed side branch.

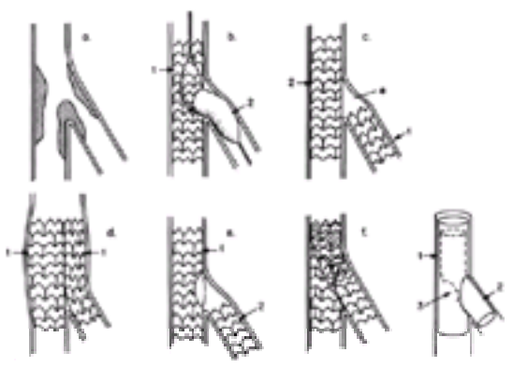

FIG. 25.4. Various techniques for stenting bifurcation stenoses. **A:** A typical bifurcation lesion with involvement of both the main vessel and the side branch. **B:** Stenting of the main vessel (1) with side branch rescue by dilatation through the stent struts (2). **C:** T-stent technique with initial placement of a stent in the side branch (1) followed by a second stent (2) in the parent vessel. Note the nonstented gap (*) caused by a side branch angle less than 90°. **D:** Kissing stents with simultaneous placement of two stents that then run side-by-side in the main vessel proximal to the bifurcation. **E:** Reverse T-stenting with placement of the main vessel stent and rescue as per **B**, but with placement of a second stent (2) into the side branch through the dilated cell of the parent vessel stent. **F:** Culotte stenting, in which the stent is placed in one vessel first (1), the side branch is dilated (as per **B**), and a second stent is placed into the side branch (as per **E**) but extending well into the proximal vessel (2). The procedure is completed (3) by dilating back into the main vessel through the side of the second stent (or with a kissing balloon inflation). None of these techniques is completely reliable, and their complexity and high restenosis rates lead us to favor debulking approaches for most such lesions (see Chapter 24).

When both the parent vessel and the side branch are large (more than 2.5 mm) and involved in the bifurcation lesion, optimal treatment may require stenting of both. With the “T stent” technique, a stent is deployed at the ostium of the side branch, followed by a second stent in the parent vessel. Unless the angle of origin of the

side branch is 90°, however, the operator is faced with the dilemma of whether it is better to leave a portion of the ostial side branch lesion unstented, or risk having part of the stent protrude into the parent vessel (making subsequent advancement of the parent vessel stent difficult or impossible). The “culotte” technique involves placement of a stent into the side branch with extension into the proximal aspect of the parent vessel. A wire is then passed through the side of this stent and into the distal parent vessel. After balloon dilatation, a second stent is passed into the distal vessel through the side of the first stent, so that the proximal ends of the first and second stents overlap in the proximal vessel. Ideally, this and other bifurcation stent approaches should be finished by “kissing balloon” inflations—simultaneous inflation of balloons in the main and branch vessel—to optimize both lumens (66). Other approaches to stenting of bifurcation lesions include placement of “kissing” stents, whereby stents are simultaneously deployed in the parent vessel and side branch, allowing the operator to shift the “carina” or bifurcation more proximally in the vessel. *All of these techniques are technically difficult and may result in significant difficulty in accessing the parent vessel or side branch because of overlapping metallic elements.* Future purpose-specific bifurcation stents such as the Bifurcate Stent (AVE, Santa Rosa, CA) or the Jostent Bifurcation stent (Jomed International, Helsingborg) may facilitate treatment of this problematic subset and provide more durable long-term results (66a).

Intramyocardial Bridging and Refractory Coronary Vasospasm

Systolic compression of a coronary artery that courses within the myocardium is a common observation during coronary angiography and occasionally causes myocardial ischemia (see Chapter 13). Using the Doppler flow wire, Klues and colleagues (67) demonstrated that severe myocardial bridging is characterized by abrupt acceleration of diastolic flow velocity, followed by a mid-diastolic plateau, and retrograde systolic flow. In 12 patients, these alterations in coronary flow were completely normalized and all patients symptomatically improved after stent placement (Fig. 25.5*A*). Stent placement has also been used successfully to treat coronary vasospasm refractory to vasodilators (68) (Fig. 25.5*B*).

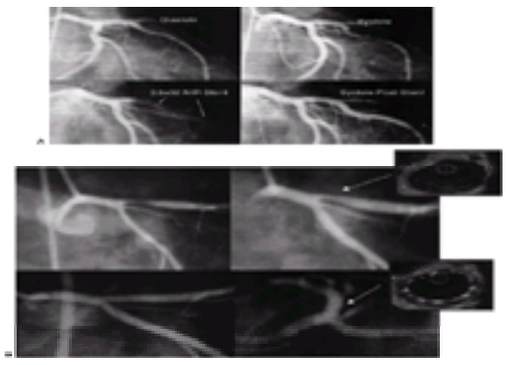

FIG. 25.5. Unusual applications of stenting. **A:** Stenting of a severe muscle bridge. Upper panels show the left anterior descending (LAD) coronary artery in diastole and compressed in systole. Hemodynamic significance was established by thallium scintigraphy and Doppler flow wire. In the lower panels, systolic compression has been eliminated by placement of a 3.5 × 32 mm NIR stent within the bridged segment. **B:** Stenting as treatment for refractory coronary vasospasm. A young woman developed intermittent chest pain associated with reversible T-wave inversions in the precordial leads despite calcium blockers and nitroglycerin. **Top:** Angiography demonstrated a high-grade stenosis in the proximal LAD *(left)*, which improved after intracoronary nitroglycerin administration *(right)*. **Top, inset:** Intravascular ultrasound revealed moderate, eccentric soft plaque. Angiography and intravascular ultrasound after placement of a Crown stent.

Multivessel Stenting

In the past decade, six multicenter, randomized trials compared outcomes after multivessel balloon angioplasty and coronary artery bypass grafting (See Chapter 23) and failed to demonstrate a significant difference in mortality among patients randomly assigned to either mode of revascularization. All of these trials, however, showed a significantly higher incidence of recurrent angina and need for repeat revascularization within the first year after multivessel angioplasty. After multivessel stenting, approximately a 1-year event-free survival rate of 80% has been reported (69,70 and 71), and the randomized ARTS trial has confirmed a reduction of roughly 50% in the incidence of excess repeat revascularization procedures, compared with initial surgical treatment, when multivessel stenting is used instead of conventional balloon angioplasty.

COMPARISONS AMONG STENTS

Approval of the first-generation (Gianturco-Roubin and Palmaz-Schatz) stents was based on the knowledge that they reduced the incidence of emergency surgery for abrupt closure and the rate of restenosis after elective stenting of favorable lesions (see earlier discussion). Once the improved second-generation stent designs were ready for testing (1995–1998), the success of the early stents meant that operators were no longer willing to compare a new stent against balloon angioplasty in a randomized trial. To meet the FDA's requirement for a randomized pivotal trial, a new “stent versus stent” design was developed to show that a new stent was “equivalent” to the gold-standard Palmaz-Schatz design. A number of such randomized studies—ASCENT (MultiLink), NIRVANA (NIR), SMART (MicroStent II), EXTRA (XT), WINS (Wallstent), PAS (Paragon), SCORES (Radius), and BEST (BeStent)—were performed to compare newer investigational stents with the Palmaz-Schatz coronary stent, using an “equivalency” design (Table 25.5) (71,72,73,74 and 75). Only the GR-II stent (whose stent recoil, undersizing, and excessive stent length appear to have contributed to higher restenosis rates) failed to show equivalency, but none of the new stents showed significantly better performance than the Palmaz-Schatz stent. In part, this was a result of the inclusion of only lesion types that were stentable with the original Palmaz-Schatz stent. The most technically challenging patient and lesion subsets (e.g., severe calcification and tortuosity), which form such a large part of stent placement in today's practice, were excluded. This explains why the second-generation stents have completely replaced the Palmaz-Schatz stent in clinical practice since the mid-1997 approval of the MultiLink. Although study-to-study differences in patient and lesion complexity factors preclude direct comparison of one new stent with another, the stent-versus-stent studies have provided a broad database about acceptable stent performance that can be used to develop objective performance characteristics for stent approval, akin to those now used to approve new heart valves.

Study (reference)	Investigational stent	Restenosis rate (%)		Target lesion revascularization (%)	
		PS	New stent	PS	New stent
ASCENT (71)	MultiLink	21	16	11.0	10.8
NIRVANA (72)	NIR	21	17	9.0	7.1
GR-II (53)	GR-II	21	47	26.6	14.6
SCORES (73)	Radius	16	17	9.0	7.1
EXTRA (74)	XT	26	35	9.0	8.2
SMART (75)	Microstent II	23	25	10.9	11.2

PS, Palmaz-Schatz coronary stent; GR-II, Gianturco-Roubin II stent.

TABLE 25.5. *Randomized trials comparing newer coronary stents with the Palmaz-Schatz coronary stent*

COMPLICATIONS OF STENTING

Thrombotic and Hemorrhagic Complications

Surface charge, surface texture, and surface energy all contribute to the thrombogenic potential of metallic endovascular prostheses. Although all stents attract platelets, they then undergo passivation as proteinaceous material is deposited on metallic surfaces, thereby altering the resting potential of the alloy (76).

At 9 to 12 days after stent placement, a neointima composed of macrophages and a-actin–negative spindle cells (77) forms over this initial coating and reduces the risk of stent thrombosis.

Early Experience

Based on animal work, the original stent regimen was a combination of antiplatelet agents (aspirin, dipyridamole, and low-molecular-weight dextran). However, the incidence of stent thrombosis was still 16% to 20% for the early Palmaz-Schatz and Wallstent data (3,9). This prompted the addition of uninterrupted anticoagulation (a transition from intravenous heparin to warfarin therapy sufficient to prolong the prothrombin time to 16 to 18 seconds, for 4 to 8 weeks) in the multicenter Palmaz-Schatz registry and subsequent early randomized trials. Although this regimen reduced the incidence of stent thrombosis to 3%, results were less satisfactory in bailout indication, stenting of small vessels, residual thrombus or dissection after stent placement, presence of inflow or outflow obstruction, incomplete stent expansion, and subtherapeutic anticoagulation (4,5,78,79 and 80). And the combination of aggressive antiplatelet and anticoagulation therapies increased the duration of hospitalization (8 vs. 3 days) and increased the incidence of hemorrhagic complications (14% vs. 3%) compared with balloon angioplasty (10,11).

Contemporary Experience

A major breakthrough in understanding the pathogenesis of stent thrombosis by Colombo was the demonstration that most stents (approximately 80%) with an excellent angiographic appearance after low-pressure deployment were seen to be incompletely expanded by IVUS (13) (see Chapter 19). Only after high-pressure (18 to 20 atm) dilatation within the stent were full stent expansion and full apposition of struts to the vessel wall observed. Using this strategy of ultrasound-guided high-pressure dilatation, it appeared that antiplatelet therapy alone (with aspirin and ticlopidine) was sufficient to reduce stent thrombosis to less than 1%. This was confirmed in a large, multicenter French registry (81) and in a series of randomized trials (Table 25.6) (14,15,82,83 and 84) that demonstrated reduction in subacute thrombosis to 0.6% after optimal stent expansion followed by aspirin and ticlopidine for 4 weeks. In addition, the timing of subacute thrombosis was shortened, from a median of 6 days with coumadin-containing regimens, to 1 to 2 days (84a). The incidence of groin complications, which had fallen with better sheath removal strategies even before the switch away from coumadin (see Chapter 4) was not reduced further, but the length of stay fell to approximately 2 days with aspirin and ticlopidine therapy.

Study (reference)	Aspirin	Aspirin + ticlopidine	Aspirin + warfarin
Stent thrombosis (%)			
STARS (optimal stents)	2.3	0.5	2.7
ISAR (all)	—	0.8	5.4
ISAR (MI)	—	0.0	9.7
FANTASTIC (all)	—	2.8	3.4
MACE (%)			
STARS	3.8	0.5	2.7
MATTIS (high-risk)		5.6	11.0
ISAR (all)		1.6	6.2
ISAR (MI)		3.3	21.0
FANTASTIC		13.5	21.0

FANTASTIC, Full Anticoagulation versus Aspirin and Ticlopidine Study; ISAR, Intracoronary Stenting and Antithrombotic Regimen; MACE, major adverse cardiac events; MATTIS, Multicenter Aspirin and Ticlopidine Trial after Intracoronary Stenting; MI, myocardial infarction; STARS, Stent Anticoagulation Restenosis Study.

TABLE 25.6. *Randomized trials comparing adjunctive pharmacologic regimens after stenting*

Ticlopidine, however, has a delayed onset of action (up to 3 days), causes rash and gastric upset in many patients, and is associated with neutropenia in about 1.5% of patients and life-threatening thrombotic thrombocytopenia purpura in a small minority of patients (85). These shortcomings have led many investigators to substitute a related platelet adenosine diphosphate–receptor antagonist (clopidogrel) for ticlopidine. The theoretic advantages of clopidogrel include the ability to achieve a high level of platelet inhibition after an oral loading dose, the absence of a significantly higher incidence of bone marrow suppression compared with aspirin alone, a low incidence of gastrointestinal and dermatologic side effects, and the convenience of once-a-day dosing (86). Moussa and colleagues found no significant difference in the incidence of stent thrombosis or major adverse cardiac events in patients treated with ticlopidine or clopidogrel after stenting (87). However, the incidence of side effects was significantly lower in patients treated with clopidogrel (5.3% vs. 10.6%). Randomized trials comparing outcome in patients treated with ticlopidine versus clopidogrel have failed to show a significant difference between these two agents, and most centers have switched to the better tolerated clopridogrel (88).

One circumstance has remained constant is that stent thrombosis, when it occurs, causes dire clinical consequences. In the STRESS trial, subacute thrombosis was associated with a 20% mortality rate; all patients had a major complication (either death, Q-wave MI, or emergency bypass surgery) (89). In the contemporary era, the 7,170-patient Cardiovascular Data Analysis Center database shows that 78% of patients with stent thrombosis experienced an acute MI, with a 30-day mortality rate of 15% and a 6-month rate of 19% (48). When thrombosis does occur, recanalization of the occluded stent was possible in 90% of patients by emergency balloon angioplasty or rheolytic thrombectomy (see Chapter 24), often in conjunction with administration of a platelet glycoprotein IIb/IIIa receptor antagonist (90). In patients who are at high risk because of either patient-related factors (e.g., hypercoagulable state, thrombocytosis) or lesion-related factors (e.g., long stents, bifurcation lesions [Fig. 25.6], residual dissection, small vessels, reduced final lumen diameter, slow flow), the addition of an intravenous platelet glycoprotein IIb/IIIa receptor antagonist is strongly recommended. In the future, the use of coatings with antithrombotic or antiplatelet activity may further reduce the incidence of stent thrombosis. In four studies, the use of the heparin-coated Palmaz-Schatz coronary stent (Cordis) was associated with a low incidence (0% to 0.8%) of stent thrombosis (18,55,91,92). Further studies must be performed to determine whether these benefits will also be seen when this device is placed for more challenging lesion subsets, such as small vessels or long lesions.

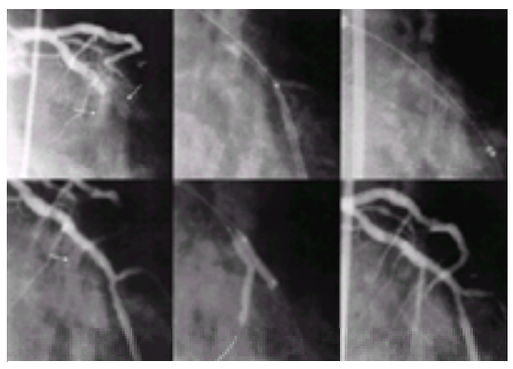

FIG. 25.6. Stent thrombosis 10 days after “T-stenting” the bifurcation of the left circumflex and its obtuse marginal branch **(top, left)**. The lesion is crossed with a hydrophilic guidewire and an infusion catheter to establish extent of thrombus and exclude passage under stent struts **(top, center)**. The Possis Angiojet is positioned distal to the bifurcation **(top, right)**. After aspiration with the Angiojet, antegrade flow is restored and filling defects are no longer apparent **(bottom, left)**. However, flow is decreased in the atrioventricular groove portion of the bifurcation *(arrow)*. Kissing balloon angioplasty is performed **(bottom, middle)**, restoring normal flow in both branches **(bottom, right)**.

In-stent Restenosis

Despite overwhelming evidence that stenting reduces restenosis compared with conventional angioplasty alone, the exponential growth in stent usage has led to new challenges in the treatment of in-stent restenosis. Restenosis after stent placement is caused almost exclusively by smooth muscle hyperplasia (93), superimposed on a small amount of initial recoil. Although this proliferative response peaks at 8 weeks in dogs (94), serial angiographic and angioscopic studies in humans

demonstrate that the greatest proliferation occurs between 1 and 6 months after placement, with only a small fraction of stents exhibiting further narrowing between 6 and 12 months (95,96 and 97). Thereafter, the proliferating smooth muscle cells are replaced by relatively inactive ground matrix and fibrosis. This transformation of the neointima from active proliferation to a quiescent, fibrotic matrix also explains the extremely low incidence (less than 2%) of late (more than 1 year) target site revascularization observed clinically (98).

Effect of "Optimal" Stenting Techniques

Although the risk of restenosis after stenting is clearly influenced by biologic factors such as diabetes mellitus and unalterable geometric factors such as small vessel size, there is a clear relationship between the immediate poststent lumen diameter and the freedom from subsequent restenosis. It is therefore up to the operator to achieve an optimal lumen at the time of stent deployment despite any lesion resistance and elastic recoil. The difficulty in achieving this goal is reflected in the findings of poststent IVUS, which can show poor expansion and apposition of stents that are apparently well deployed angiographically. Achieving an in-stent minimal cross-sectional area equal to at least 55% of the average (proximal/distal) reference cross-sectional area reduces the chance of subsequent restenosis by almost one half, compared with failure to do so (99). Other IVUS criteria have been proposed (see Chapter 19) based on large studies including the Angiography Versus Intravascular Ultrasound Directed Coronary Stent Placement (AVID) trial, the Strategy of ICUS Guided PTCA and Stenting (SIPS) trial, the Optimization with ICUS to Reduce Stent Restenosis (OPTICUS) trial, the Restenosis after IVUS-guided Stenting Trial (RESIST), and the Can Routine Ultrasound Influence Stent Expansion (CRUISE) substudy of the STARS trial. These studies have addressed whether routine use of IVUS guidance is associated with improvements in angiographic and clinical outcome after stenting (Table 25.7). In the RESIST, AVID, and CRUISE studies, IVUS-guided stenting was associated with slightly larger stent minimum lumen diameters or cross-sectional areas, but the clinical benefit has been less consistent. Given the added expense and time, formal recommendations regarding routine use of IVUS guidance for stenting cannot be made until the final long-term results from these studies are available and the criteria for optimal stenting are standardized.

Study (reference)	Design	Major findings
MUSIC (100)	Registry	81% of lesions met criteria for optimal stenting; larger MLD achieved with IVUS guidance (compared with ticlopidine II); very low angiographic (9.7%) and clinical restenosis (4.5%)
RESIST (101)	Randomized trial	Stent CSA larger with IVUS (7.85 mm^2) vs. angiographic (7.16 mm^2) guidance; no difference in postprocedure stenosis (19% by angiography vs. 16% by IVUS); no difference in angiographic restenosis (29% by angiography vs. 22% by IVUS)
OPTICUS	Randomized trial	No difference in major adverse cardiac events with IVUS vs. angiographic guidance; no difference in angiographic restenosis
AVID	Randomized trial	Stent MLD larger with IVUS (3.28 mm) vs. angiographic (3.05 mm) guidance; follow-up pending
CRUISE*	Randomized trial	Stent CSA larger with interactive IVUS (7.76 mm^2) vs. documentary IVUS (7.11 mm^2); target vessel revascularization lower with interactive IVUS (8.3%) vs. documentary IVUS (14.8%)

AVID, Angiography Versus Intravascular Ultrasound Directed Stent Placement trial; CRUISE, Can Routine Intravascular Influence Stent Expansion; CSA, cross-sectional area; MLD, minimum lumen diameter; MUSIC, Multicenter Ultrasound Stenting in Coronaries study; OPTICUS, Optimization with ICUS to Reduce Restenosis trial; RESIST, Restenosis after IVUS-guided Stenting Trial.
*CRUISE was a substudy of the Stent Anticoagulation Restenosis Study (STARS); sites were assigned to no-IVUS, documentary (blinded) IVUS, or interactive IVUS.

TABLE 25.7. *Studies of intravascular ultrasound (IVUS)-guided stent placement*

One alternative is to perform physiologic assessments of stent deployment, measuring coronary flow reserve or the transstent pressure gradient at peak flow (see Chapter 18). Hanekamp and colleagues showed that a fractional flow reserve of 0.94 or more (measured with a pressure wire) was highly correlated with IVUS-derived parameters of optimal stenting (100). Preliminary observations with coronary flow reserve have also suggested that reduced coronary flow reserve (less than 2.5) after stenting may be associated with major adverse events at 6 months (101).

Despite these measures, 20% to 40% of stents fail to meet criteria for optimal expansion (102,103). Factors contributing to this problem of inadequate stent expansion include balloon underexpansion and acute stent recoil. Although it was originally thought that stents eliminated elastic recoil, more recent data show 7% to 15% diameter recoil after deflation of the deployment or postdilating balloon (104,105) (Fig. 25.7). To achieve the desired luminal diameter or area, the deployment or postdilating balloon must stretch the stent approximately 10% beyond the desired diameter (e.g., 3.3 mm for a final 3.0 mm result), which is one of the effects produced by inflating a semicompliant balloon to 14 to 16 atm. Contrary to early uncontrolled data, there is no evidence that such high-pressure stent expansion increases the incidence of subsequent restenosis (106), so current practice favors deployment at this pressure level.

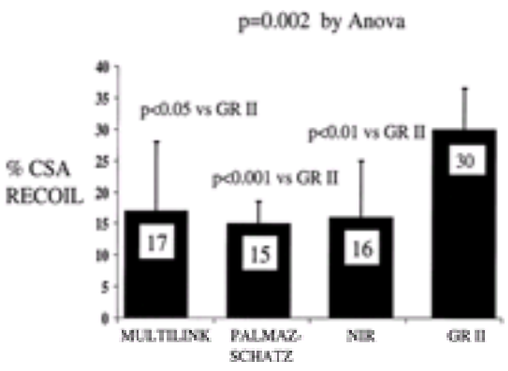

FIG. 25.7. Acute cross-section area (CSA) recoil for four different stents, as measured in normal porcine arteries using a 0.018-inch ultrasound imaging probe within the deployment balloon. (From Carrozza JP Jr, Hosley, SE, Cohen DJ, Baim DS. In-vivo assessment of stent expansion and recoil in normal porcine coronary arteries: Differential outcome by stent design. *Circulation* 1999;100:756, with permission).

In vessels with bulky eccentric or fibrocalcific plaques, balloon underexpansion may account for more than 20% of the discordance between expected and measured balloon cross-sectional area. In such lesions, vascular compliance may be improved by removing plaque from the lesion through pretreatment with high-speed rotational atherectomy (107) (see Chapter 24), thereby lowering the incidence of target vessel revascularization compared with stenting alone (Fig. 25.8 and Fig. 25.9). There is also preliminary evidence that debulking of large eccentric plaques with *directional atherectomy* before stenting reduces the amount of in-stent proliferation and lowers the incidence of angiographic restenosis (108,109). These techniques are being evaluated in the randomized SPORT (using rotational atherectomy) and AMIGO (using directional atherectomy) trials.

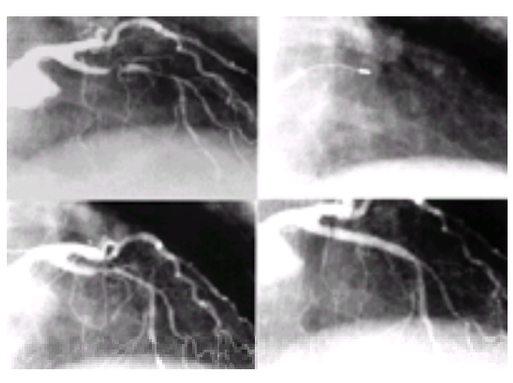

FIG. 25.8. Rota-stenting. A long, calcified stenosis is present in the left anterior descending coronary artery **(top, left)**. After application of the rotational atherectomy burr **(top, right)**, a smooth lumen with significant residual stenosis is present **(bottom, left)**. After stent deployment, excellent expansion is observed **(bottom, right)**.

Without Rotablator pretreatment, stent passage and full stent expansion would each have been unlikely.

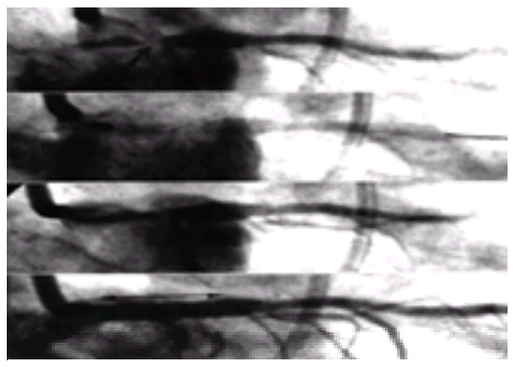

FIG. 25.9. Rota-stenting for “protected” left main coronary artery lesion. **Top:** Severe stenosis in the distal left main, which supplies only the left anterior descending coronary artery, given a patent graft to the circumflex (not shown). **Upper center:** 1.75 mm Rotablator burr. **Lower center:** After rotational atherectomy, there is modest lumen improvement but enhanced lesion compliance. **Bottom:** After stent placement, excellent lumen dimension is established.

Pharmacotherapy to Reduce In-stent Restenosis

A number of agents—including heparin, angiopeptin, angiotensin-converting enzyme inhibitors, and antioxidants—have shown promise in reducing the exuberant proliferative response evoked by stenting in experimental models. However, there are few data available that support their efficacy in reducing the incidence of human in-stent restenosis. Although data from the EPIC trial suggested that the platelet glycoprotein IIb/IIIa receptor antagonist abciximab might be associated with a reduction in restenosis after balloon angioplasty, preliminary observations from the randomized ERASER trial showed no reduction in neointimal volume or restenosis after stenting with abciximab (110). In the larger EPISTENT trial, only diabetic patients who underwent stenting had a lower incidence of 6-month clinical restenosis events with abciximab (90). Given the difficulty in achieving high tissue concentrations of an agent administered systemically, local delivery may be required to place therapeutic levels of effective agents directly into the arterial wall. However, in neither the HIPS trial (using intraarterial heparin) nor the ITALICS (intraarterial antisense oligonucleotides against c-*myc*) study was active therapy associated with reductions in restenosis after stenting, compared with placebo (111,112).

Treatment of In-stent Restenosis

Luminal narrowing within stents follows a Gaussian distribution (30). In patients *without* recurrent symptoms or provocable ischemia, mild to moderate degrees of in-stent restenosis (40% to 70% diameter stenosis) are associated with a favorable long-term prognosis and therefore can be treated with medical therapy alone (113). When in-stent restenosis results in recurrent coronary ischemia, however, treatment is indicated. The initial experience in treatment of in-stent restenosis involved balloon dilatation within the stent. The procedural success rate was almost 100%, and because the metallic struts were not reexposed to blood elements anticoagulation was not necessary (114), but the rate of recurrent restenosis exceeded 50% for dilatation of diffuse in-stent restenotic lesions (115,116). One reason is that much of the hyperplastic material that has been compressed and extruded through the stent struts returns to the stent lumen within 30 minutes after the final balloon inflation (117). In an effort to improve on the suboptimal long-term results of diffuse in-stent restenosis, several groups have investigated the strategy of plaque removal from within the stent before balloon dilatation, using atheroablative techniques (see Chapter 24). Dauerman (118) and Sharma (119) reported a larger initial lumen and reduction in subsequent target vessel revascularization (from 46% to 26–28%) in lesions treated with rotational atherectomy compared with balloon angioplasty alone. Similar results have also been reported after directional atherectomy (see Chapter 24) or excimer laser angioplasty (120,121 and 122). Although controlled, randomized clinical trials using less aggressive debulking and postplacement dilatation have not uniformly confirmed this benefit, the preponderance of evidence favors the concept that strategies incorporating tissue removal (rather than plaque compression alone) result in larger posttreatment lumen diameters and lower rates of target vessel revascularization.

Despite these reductions in repeat revascularizations observed with debulking of in-stent restenosis, almost 30% of these patients require additional interventions to treat this aggressive proliferative response. Because recurrent luminal narrowing after stenting is almost entirely the result of a smooth muscle cellular proliferative process, therapies such as radiation that are effective in the treatment of other benign proliferative disorders (e.g., Graves' exophthalmos, keloid formation) are particularly attractive. Teirstein demonstrated a marked reduction in angiographic restenosis (17% vs. 54%), target lesion revascularization (12% vs. 45%), and major adverse cardiac events (19% vs. 62%) in patients treated by g-irradiation with iodine 192 after stent placement (123). These dramatic benefits of g-irradiation were confirmed in the larger, multicenter Gamma 1 study (124) and the Washington Radiation for In-Stent Restenosis Trial (WRIST) study. The long-term outcome of patients with in-stent restenosis was also favorably influenced by b-radiation with a 47% reduction in angiographic restenosis (46% to 24%), and a 34% reduction in target vessel revascularization (24% to 16%) in the active arm (124a). Although randomized trials of primary irradiation have not been completed, data from the Beta Energy Restenosis (BERT) trial using an encapsulated strontium 90/yttrium b source (Beta-Cath, Novoste Corporation, Norcross, GA) also suggested a reduction in late loss and restenosis (15%) after balloon angioplasty (125). The effect of primary irradiation on restenosis after initial angioplasty or stenting is currently being studied.

Side Branch Occlusion

In the early experience with the Palmaz-Schatz stent, Fischman et al. (126) and Iniguez et al. (127) reported a 5% incidence of acute branch occlusion when the stent was placed across a major (more than 1 mm) side branch. In all such cases, ostial stenoses greater than 50% had been present in the involved side branch. Although such side branch occlusion had a low morbidity in these series, it should be noted that stenting across large, diseased side branches was specifically avoided and that stent-induced occlusion of a large side branch clearly may result in significant myocardial ischemia. Because stenting may induce vasospasm in the involved side branch, administration of intracoronary nitroglycerin alone is sometimes adequate to restore normal flow. More commonly, side branch compromise results from the “snowplow” mechanism—shifting of plaque during stent deployment or high-pressure dilatation. If significant ischemia persists, a guidewire can be advanced out through a stent cell and into the effected side branch, to allow advancement of a low-profile angioplasty balloon catheter. The proximal end of the balloon catheter should always be kept in the parent vessel, to avoid the risk of entrapment in the side branch (128). The size of side branch dilatation may be limited by stent cell size (e.g., NIR, Palmaz-Schatz stents), and elastic recoil commonly observed at the origin of side branches may contribute to a high likelihood of repeat restenosis. If restenosis of a “jailed” side branch occurs, rotational atherectomy can safely be performed through the side of previously dilated stent cells to improve acute angiographic appearance (Fig. 25.10).

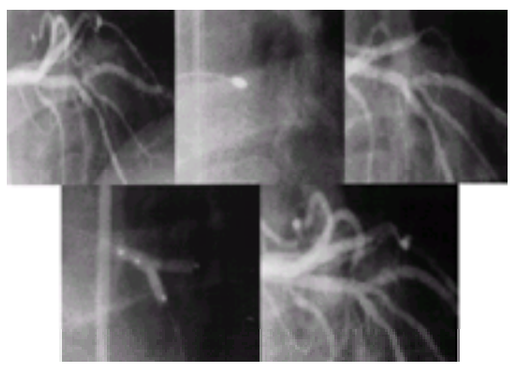

FIG. 25.10. Rotational atherectomy of a restenotic branch “jailed” by an NIR stent in the left anterior descending coronary artery **(top, left)**. A 2.15-mm Rotablator burr is seen positioned just proximal to the stent **(top, middle)**. After rotational atherectomy through the side of the stent, significant luminal enlargement is seen **(top,**

right). Kissing balloon angioplasty **(bottom, left)** is performed, resulting in a large lumen in both the left anterior descending and diagonal arteries **(bottom, right)**.

Stent Embolization

In the initial multicenter registry, in which the Palmaz-Schatz coronary stent was hand-mounted on a conventional angioplasty balloon and no sheath was used, stent embolization occurred in 2.5% of patients. There were no reported clinical sequelae (9), but clearly every effort should be made to avoid this complication. Sheathed delivery systems, such as the Palmaz-Schatz Stent Delivery System (Cordis) or the Sheathed MultiLink System (Guidant), reduce the chance of embolization but may impede delivery owing to their large profiles. Present-generation *bare* stents have significantly higher crimp strength and unique attachment features (e.g., NIR on Sox system, Boston Scientific), retentive balloon coatings (e.g., Power Grip balloon, Cordis) or nesting of the stent into the balloon material, which improve stent retention. Nevertheless, virtually any stent may be dislodged from the balloon if it catches on the edge of the guiding catheter during forceful retraction after unsuccessful placement. If guidewire position has been maintained in the distal coronary artery, the delivery balloon or another low-profile balloon may be placed back through the stent, allowing it to be repositioned across the target lesion. If the stent cannot be repositioned, the balloon can be placed distal to the stent and inflated to trap the stent between the balloon and guiding catheter as they are withdrawn into the descending aorta and recovered into the sheath. If guidewire position has been lost and the unexpanded stent is located in a proximal portion of the coronary artery or has embolized into a peripheral artery, it may be removed by use of a variety of snare devices. Alternatively, a second stent may be expanded adjacent to the dislodged stent to trap it against the vessel wall and effectively exclude it from the lumen. If the stent cannot be removed or effectively "excluded" from the coronary lumen, strong consideration should be given to referring the patient for coronary artery bypass surgery.

Incomplete Expansion

Incomplete stent expansion may result from rupture of the delivery balloon or failure of the balloon to be expanded adequately in calcified or fibrotic vessels The risk of incomplete expansion is significantly higher during "primary stenting," when the operator deploys a stent without predilation or debulking. This practice is therefore best avoided in heavily calcified vessels or when deploying long stents. In such vessels, full stent expansion may be achieved at lower balloon pressures when the vessel is pretreated with rotational atherectomy.

When the delivery balloon ruptures before the stent is embedded adequately in the vessel wall, further expansion can be achieved by rapidly increasing pressure within the balloon using a power injector or a conventional manual inflation device. A new noncompliant balloon can then be placed within the stent to achieve full expansion. If the stent is markedly underexpanded at the end of the procedure, the administration of a platelet glycoprotein IIb/IIIa receptor antagonist may reduce the risk of stent thrombosis.

Perforation

Although the routine use of high-pressure postplacement dilatation improves stent expansion, the significant barotrauma imparted to the vessel may result in frank perforation (129). In a retrospective analysis, Ellis and colleagues documented a 0.1% incidence of perforation (130). Colombo showed that high-pressure dilatation of appropriately sized balloons (balloon-artery ratio, 1.1) is safe but that the use of markedly oversized balloons (ratio, 1.2) carries a risk of perforation and vessel rupture of 1.2% to 0% (13). Most small perforations can be sealed with prolonged balloon inflations and reversal of anticoagulation with protamine, unless a platelet glycoprotein IIb/IIIa receptor antagonist has been given. In the event of a large perforation, or when balloon dilatation is unsuccessful in sealing the leak, pericardial tamponade may ensue. The operator must be prepared to block the involved vessel with an angioplasty balloon, to perform emergency pericardiocentesis, and to obtain cardiac surgical consultation. In the future, deployment of a covered stent may provide reliable sealing and obviate the need for emergency surgery.

Infectious Endarteritis

Placement of a foreign body endovascular prosthesis carries a theoretic risk of bacterial endarteritis. In an experimental porcine model, after transient bacteremia, a significant number of recently placed coronary stents cultured positive for bacteria (131). In the early stenting experience, all patients received 48 hours of antibiotic prophylaxis during and after stent placement. Because the risk of suppurative endarteritis in stented coronary arteries is extremely rare, with only three documented cases in the literature (132,133 and 134), periprocedural antibiotic therapy is no longer recommended. However, if sterile technique has been breached, or if the patient requires an invasive procedure associated with transient bacteremia during the first 4 weeks after stenting, antibiotic prophylaxis should still be strongly considered.

Cost

In the present era of cost-consciousness, new technologies that affect not only clinical outcome but also resource utilization have come under intense scrutiny. There is no better example than coronary stenting, where the cost of a single stent (approximately $1,200) may exceed that of an angioplasty balloon by a factor of 4. In two early, single-center observational studies, stenting was associated with significantly higher initial hospital costs than other modalities of catheter-based revascularization. Cohen and colleagues (135) compared the costs of stenting and balloon angioplasty for patients treated in the STRESS trial and found that the initial hospital costs of Palmaz-Schatz stenting exceeded those of balloon angioplasty by $2,200 (based on a stent price of $1,400). Despite significant cost savings from the reduction in subsequent hospitalizations and repeat revascularizations, the overall cost of stenting still exceeded that of PTCA by $800 at 1 year. This excess cost may have fallen somewhat with the adoption of optimal stenting techniques, the replacement of warfarin-based regimens with antiplatelet therapy, and the concomitant reductions in length of stay and vascular complications. In the randomized Benestent II trial (in which optimal stenting techniques and dual antiplatelet therapy were used), stenting was still associated with a greater overall cost ($1,020 higher) than balloon angioplasty at 1 year (55), but it was still *cost-effective* (with an acceptable cost-effectiveness ratio of $23,600 per quality-adjusted life-year gained) due to the reduction in the need for subsequent procedures (136).

FUTURE TECHNOLOGY

Coated Stents

Metallic stents are inherently thrombogenic and also provoke an exuberant hyperplastic response within the first year after deployment. Given these limitations, modifications to the metallic surface to reduce its thrombogenicity and alter the long-term arterial response to injury would be desirable. Most stent coatings are polymers, which can be divided into biodegradable and nonbiodegradable groups (137). Biodegradable polymers such as polyurethane, polyethylene terephtalate, and polyorganophosphazene (138,139,140 and 141) were investigated but were found to provoke intense inflammatory reactions. An example of a nonbiodegradable coating that has been used clinically is Biogold, a 30-nm-thick hydrocarbon layer applied by gas exchange to the Wallstent (138). Other nonbiodegradable coatings that are presently under investigation include phosphorylcholine (DivYsio stent, Biocompatibles, Ltd., Surrey, U.K.), amorphous hydrogenated silicon carbide (Tensum and Tenax stents, Biotronik, Berlin, Germany) (137), diamond-like carbon, and pyrolitic carbon (Carbostent, Sorin BioMedica, Italy) (137a).

Drug-eluting Stents

In the future, stent coatings may also serve as reservoirs for the local delivery of active antiplatelet, antithrombotic, and antiproliferative agents. The largest experience to date with a coated stent has been with the heparin-coated Palmaz-Schatz coronary stent, in which heparin molecules are covalently bound by end-point attachment to a polymerized surface. The stent does not elute heparin, but it allows heparin to function as an " *in situ*" catalyst for activation of antithrombin III. Low rates of thrombosis have been observed in the four large studies using this device (18,55,91,92), without any demonstrable antiproliferative effect.

The other approach is to use biodegradable polymers to slowly release pharmacologically active agents. Animal studies have demonstrated that drugs such as forskolin (142) and dexamethasone (143), when embedded into a polymer matrix, can be incorporated into the arterial wall at concentrations several orders of magnitude higher than serum levels. Although the notion of a "therapeutic stent" is attractive, significant hurdles remain, such as identifying appropriate therapeutic agents and noninflammatory polymers, as well as defining optimal delivery kinetics and dosage. Finally, stents may be seeded with cells that secrete biologically active proteins (144).

Radioactive Stents

Fischell and colleagues (145) showed that stent wires impregnated with a b emitter (phosphorus 32) inhibited subsequent growth and migration of cultured smooth muscle cells. The concept of a radioactive stent offers several theoretic advantages over other methods of endovascular brachytherapy, but clinical trials with the ^{32}P b-emitting Isostent, in which a Palmaz-Schatz coronary stent is impregnated with ^{90}Sr (half-life, 14 days) (Cordis), have shown mixed results. At low doses (1 µCi of total radiation), there was no significant reduction in restenosis (146). At higher doses (0.75 to 6.0 µCi), hyperplasia within the stent seemed to be reduced but significant luminal narrowing at the edges of the stents—termed “candy wrapper restenosis”—still occurred (147). Whether this problem can be overcome by increasing the dosage at the edge of the stent or by avoiding balloon injury to this vulnerable area remains to be seen.

Covered Stents

The difficulty in coating stents with noninflammatory polymers has led to the investigation of stents covered completely by artificial or natural material. Stefanidis described a technique for sewing thin segments of autologous veins or arteries to a metallic stent (148). The initial clinical experience with these autologous stents in thrombus-containing lesions and degenerated saphenous vein grafts has been encouraging, but the long-term outcome compared with uncovered stents has not been studied prospectively (149,150). A more practical approach has been the use of stents covered by synthetic material. The Jostent (Jomed) Coronary Stent Graft is layer of polytetrafluoroethylene (PTFE) “sandwiched” between two layers of slotted-tube stent (Fig. 25.11). This covered stent has a relatively low crimped profile and may be an ideal choice for sealing perforations, excluding coronary aneurysms, and decreasing distal embolization when stents are placed in friable lesions. Although initial clinical results suggest that the PTFE-covered portions of the stent are largely free of hyperplasia, pharmacologic regimens to prevent thrombosis and avoidance of restenosis at the uncovered edges are ongoing issues (151).

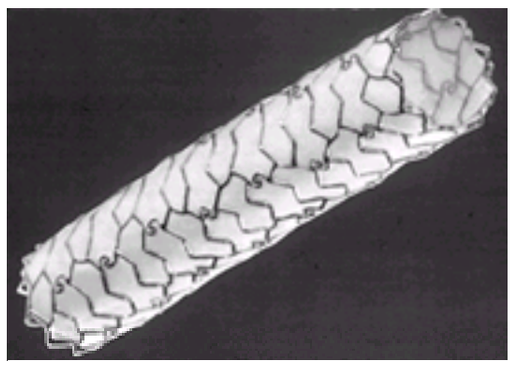

FIG. 25.11. Covered stent. The Jomed Jostent consists of a polytetrafluoroethylene membrane trapped between an inner and an outer Jostent. Such devices are potentially useful in treating vessel perforations, aneurysms, or occluding coronary sinus fistulas.

CONCLUSIONS

More than 30 years after Charles Dotter first proposed the concept of an endovascular prosthesis, coronary stenting has emerged as the dominant technology for catheter-based coronary revascularization. The availability of stents with excellent deliverability and scaffolding, the demonstration that stenting improves acute and long-term outcome in a wide variety of lesion types, and the development of effective and better-tolerated regimens to prevent stent thrombosis have facilitated the application of stenting to almost every lesion subset. In the future, stents also have the potential to provide regional arterial delivery of bioactive drugs or radiation to help prevent both thrombosis and subsequent restenosis.

CHAPTER REFERENCES

1. Dotter CT. Transluminally placed coil spring arterial tube grafts: Long-term patency in canine popliteal artery. *Invest Radiol* 1969;4:329.
2. Sigwart U, Puel J, Mirkovitch V, et al. Intravascular stents to prevent occlusion and restenosis after transluminal angioplasty. *N Engl J Med* 1987;316:701.
3. Serruys PW, Strauss BH, Beatt KJ, et al. Angiographic follow-up after placement of a self-expanding coronary artery stent. *N Engl J Med* 1991;324:13.
4. Roubin GS, Robinson KA, King SB III, et al. Early and late results of intracoronary arterial stenting after coronary angioplasty in dogs. *Circulation* 1987;76:891.
5. George BS, Voohees III WD, Roubin GS, et al. Multicenter investigation of coronary stenting to treat acute or threatened closure after percutaneous transluminal coronary angioplasty: Clinical and angiographic outcomes. *J Am Coll Cardiol* 1993;22:135.
6. Palmaz JC, Windeler SA, Garcia F, et al. Balloon expandable intraluminal grafting of atherosclerotic rabbit aortas. *Radiology* 1986;160:723.
7. Palmaz JC, Sibbitt RR, Reuter SR, et al. Expandable intraluminal graft: Preliminary study. *Radiology* 1985;156:73.
8. Schatz RA. A view of vascular stents. *Circulation* 1989;79:445.
9. Schatz RA, Baim DS, Leon MB, et al. Clinical experience with the Palmaz-Schatz coronary stent: Initial results of a multicenter study. *Circulation* 1991;83:148.
10. Serruys PW, de Jaegere P, Kiemeneij F, et al. A comparison of balloon-expandable stent implantation with balloon angioplasty in patients with coronary artery disease. *N Engl J Med* 1994;331:489.
11. Fischman DL, Leon MB, Baim DS, et al. A randomized comparison of coronary stent placement and balloon angioplasty in the treatment of coronary artery disease. *N Engl J Med* 1994;331:489.
12. Nakamura S, Colombo A, Gaglione A, et al. Intracoronary ultrasound observations during stent implantation. *Circulation* 1994;89:2026.
13. Colombo A, Hall P, Nakamura S, et al. Intracoronary stenting without anticoagulation accomplished with intravascular ultrasound guidance. *Circulation* 1995;91:676.
14. Schomig A, Neumann FJ, Kastrati A, et al. A randomized comparison of antiplatelet therapy and anticoagulation therapy after placement of coronary artery stents. *N Engl J Med* 1996;334:1084.
15. Leon MB, Baim DS, Popma JJ, et al. A clinical trial comparing three antithrombotic-drug regimens after coronary-artery stenting. *N Engl J Med* 1998;339:1665.
16. Holmes DR Jr, Hirshfeld J Jr, Faxon D, et al. ACC Expert Consensus Document on Coronary Artery Stents. *J Am Coll Cardiol* 1998;32:1471.
17. Sirnes PA, Golf S, Myreng Y, et al. Stenting in Chronic Coronary Occlusion (SICCO): A randomized, controlled trial of adding stent implantation after successful angioplasty. *J Am Coll Cardiol* 1996;28:1444.
18. Stone GW, Brodie BR, Griffin JJ, et al. Prospective multicenter study of the safety and feasibility of primary stenting in acute myocardial infarction—in-hospital and 30-day results of the PAMI-Stent pilot trial. *J Am Coll Cardiol* 1998;31:23.
19. Erbel R, Haude M, Hopp HW, et al. Coronary-artery stenting compared with balloon angioplasty for restenosis after initial balloon angioplasty. *N Engl J Med* 1998;339:1672.
20. Ricci DR, Ray S, Buller CE, et al. Six month follow-up of patients randomized to prolonged inflation or stent for abrupt occlusion during PTCA: Clinical and angiographic data—TASC II. *Circulation* 1995;92[Suppl 1]475a(abst).
21. Haude M, Erbel R, Hoepp HW, and the STENT-BY Study group. STENT-BY Study: A prospective randomized trial comparing immediate stenting versus conservative treatment strategies in abrupt vessel closure or symptomatic dissections during coronary balloon angioplasty. *Eur Heart J* 1996;17[Suppl]:172a(abst).
22. Serruys PW, Kay P, Disco C, et al. Procedural quantitative coronary angiography after Palmaz-Schatz stent implantation predicts restenosis rate at six months. *J Am Coll Cardiol* 1999;34:1067.
23. Platko WP, Hollman J, Whitlow PL. Percutaneous transluminal angioplasty of saphenous vein graft stenosis: Longterm follow-up. *J Am Coll Cardiol* 1989;14:1645.
24. Holmes DR, Topol EJ, Califf RM, et al. A multicenter, randomized trial of coronary angioplasty versus directional atherectomy for patients with saphenous vein bypass graft lesions. *Circulation* 1995;91:1966.
25. Bittl JA, Sanborn TA, Yardley DE, et al. Clinical success, complications and restenosis rates with excimer laser coronary angioplasty. *Am J Cardiol* 1992;70:1533.
26. Piana RN, Moscucci M, Cohen DJ, et al. Palmaz-Schatz stenting for treatment of focal vein graft stenosis: Immediate results and longterm outcome. *J Am Coll Cardiol* 1994;23:1296.
27. Wong SC, Popma JJ, Pichard AD, et al. Comparison of clinical and angiographic outcomes after saphenous vein graft angioplasty using coronary versus biliary tubular slotted stents. *Circulation* 1995;91:339.
28. Savage MP, Douglas JS, Fischman DL, et al. Stent placement compared with balloon angioplasty for obstructed coronary bypass grafts. *N Engl J Med* 1997;337:740.
29. Moscucci M, Piana RN, Kuntz RE, et al. Effect of prior coronary restenosis on the risk of subsequent restenosis after stent placement or directional atherectomy. *Am J Cardiol* 1994;73:1147.
30. Penn IM, Ricci DR, Almond DG, et al. Coronary artery stenting reduces restenosis: Final results from the Trial of Angioplasty and Stents in Canada (TASC) I. *Circulation* 1995;92[Suppl 1]:279a(abst).
31. Colombo A, Ferraro M, Itoh A, et al. Results of coronary stenting for restenosis. *J Am Coll Cardiol* 1996;28:830.
32. Sirnes PA, Golf S, Myreng Y, et al. Sustained benefit of stenting chronic coronary occlusion: Long-term clinical follow-up of the Stenting in Chronic Coronary Occlusion (SICCO) Study. *J Am Coll Cardiol* 1998;32:305.
33. Rubartelli P, Niccoli L, Verna E, et al. Stent implantation versus balloon angioplasty in chronic coronary occlusions: Results from the GISSOC trial. *J Am Coll Cardiol* 1998;32:90.
34. Title LM, Buller CE, Knudtson ML, et al. Efficacy of stenting vs. balloon angioplasty in small diameter (less than 3 mm) total coronary occlusions: A Total Occlusion Study of Canada substudy. *Circulation* 1998;98[Suppl 1]:639a(abst).
35. Brodie BR, Grines CL, Ivanhoe R, et al. Six-month clinical and angiographic follow-up after direct angioplasty for acute myocardial infarction. *Circulation* 1994;89:156.
36. Nakagawa Y, Iwasaki Y, Kimura T, et al. Serial angiographic follow-up after successful direct angioplasty for acute myocardial infarction. *Am J Cardiol* 1996;78:980.
37. Bauters C, Lablanche JM, van Belle E, et al. Effects of coronary stenting on restenosis and occlusion after angioplasty of the culprit vessel in patients with recent myocardial infarction. *Circulation* 1997;96:2854.
38. Rodriguez A, Bernardi V, Fernandez M, et al. In-hospital and late results of coronary stents versus conventional balloon angioplasty in acute myocardial infarction. *Am J Cardiol* 1998;81:1286.

39. Suryapranata H, van't Hof AW, Hoorntje JC, et al. Randomized comparison of coronary stenting with balloon angioplasty in selected patients with acute myocardial infarction. *Circulation* 1998;97:2502.
40. Garcia-Canter E, Spaulding C, Corlos T, et al. Stent implantation in acute myocardial infarction. *Am J Cardiol* 1996;77:451.
41. Antoniucci D, Santoro GM, Bolognese L, et al. A clinical trial comparing primary stenting of the infarct-related artery with optimal primary angioplasty for acute myocardial infarction: Results from the Florence Randomized Elective Stenting in Acute Coronary Occlusions (FRESCO) trial. *J Am Coll Cardiol* 1998;31:1234.
42. Grines Cl, et al. STENT PAMI: Primary endpoint results of a multicenter, randomized trial of heparin-coated stenting vs. primary PTCA for AMI. *Circulation* 1998;98[Suppl 1]:22a(abst).
43. Tenaglia AN, Zidar JP, Jackman JD Jr, et al. Treatment of long coronary artery narrowings with long angioplasty balloon catheters. *Am J Cardiol* 1993;71:1274.
44. Popma JJ, De Cesare NB Ellis SG, et al. Clinical, angiographic and procedural correlates of quantitative coronary dimensions after directional coronary atherectomy. *J Am Coll Cardiol* 1991;18:1183.
45. Ellis SG, Popma JJ, Buchbinder M, et al. Relation of clinical presentation, stenosis morphology, and operator technique to the procedural results of rotational atherectomy and rotational-atherectomy facilitated angioplasty. *Circulation* 1994;89:882.
46. Ellis SG, Savage M, Fischman D, et al. Restenosis after placement of Palmaz-Schatz stents in native coronary arteries: Initial results of a multicenter experience. *Circulation* 1992;86:1836.
47. Mathew V, Hasdai D, Holmes DR Jr, et al. Clinical outcome of patients undergoing endoluminal coronary artery reconstruction with three or more stents. *J Am Coll Cardiol* 1997;30:676.
48. Cutlip DE, Baim DS, Ho KKL, et al. Stent thrombosis in the modern era: A pooled analysis of 7,171 patients from multi-center clinical trials conducted by the Cardiovascular Data Analysis Center (CDAC) *(in press)*.
49. Kereiakes D. Duet registry. *Circulation (in press)*.
50. Leon MB, Popma JJ, O'Shaughnessy C, et al. Quantitative angiographic outcomes after Gianturco-Roubin II stent implantation in complex lesion subsets. *Circulation* 1997;96[Suppl 1]:653a(abst).
51. Albiero R, Marsico F, Vaghetti M, et al. The role of lesion length and stent length in restenosis after stenting. *Circulation* 1998;98[Suppl 1]:284a(abst).
52. DeGregorio J, et al. Intravascular ultrasound guided PTCA with spot stenting. *J Am Coll Cardiol* 1998[Suppl].
53. Kobayashi Y, DeGregorio J, Kobayashi N, et al. Stented segment length as an independent predictor of restenosis. *J Am Coll Cardiol* 1999;34:651.
54. Savage MP, Fischman DL, Rake R, et al. Efficacy of coronary stenting versus balloon angioplasty in small coronary arteries: Stent Restenosis Study (STRESS) investigators. *J Am Coll Cardiol* 1998;31:307.
55. Serruys PW, van Hout B, Bonnier H, et al. Randomised comparison of implantation of heparin-coated stents with balloon angioplasty in selected patients with coronary artery disease (Benestent II). *Lancet* 1998;352:673.
56. Serra A, Masotti M, Fernandez-Aviles, et al. Stent vs. Angioplasty Restenosis Trial (START): Influence of vessel size on angiographic restenosis. *Circulation* 1996;94[Suppl]:92a(abst).
57. Kereiakes DJ. Percutaneous transcatheter therapy of aorto-ostial stenoses. *Cathet Cardiovasc Diagn* 1996;38:292.
58. Rocha-Singh K, Morris N, Wong SC, et al. Coronary stenting for treatment of ostial stenoses of native coronary arteries or aortocoronary saphenous venous grafts. *Am J Cardiol* 1995;75:26.
59. Rechavia E, Litvack F, Macko G, et al. Stent implantation of saphenous vein graft aorto-ostial lesions in patients with unstable ischemic syndromes: Immediate angiographic results and long-term clinical outcome. *J Am Coll Cardiol* 1995;25:866.
60. Lopez JJ, Ho KK, Stoler RC, et al. Percutaneous treatment of protected and unprotected left main coronary stenoses with new devices: Immediate angiographic results and intermediate-term follow-up. *J Am Coll Cardiol* 1997;29:345.
61. Karam C, Fajadet J, Cassagneau B, et al. Results of stenting of unprotected left main coronary artery stenosis in patients at high surgical risk. *Am J Cardiol* 1998;82:975.
62. Park SJ, Park SW, Hong MK, et al. Stenting of unprotected left main coronary artery stenoses: Immediate and late outcome. *J Am Coll Cardiol* 1998;31:37.
63. Ellis SG, Tamai H, Nobuyoshi M, et al. Contemporary percutaneous treatment of unprotected left main coronary stenoses: Initial results from a multicenter registry analysis 1994–1996. *Circulation* 1997;96:3867.
64. Meier B, Gruentzig AR, King SB 3d, et al. Risk of sidebranch occlusion during coronary angioplasty. *Am J Cardiol* 1984;53:10.
65. Dauerman HL, Higgins PJ, Sparano AM, et al. Mechanical debulking versus balloon angioplasty for the treatment of true bifurcation lesions. *J Am Coll Cardiol* 1998;22:1845.
66. Chevalier B, Glatt B, Royer T, et al. Placement of coronary stents in bifurcation lesions by the “culotte” technique. *Am J Cardiol* 1998;82:943.

66a. Cervinka P, Foley DP, Sabate M, et al. Coronary bifurcation stenting using dedicated bifurcation stents. *Cathet Cardiovasc Intervent* 2000;49:105.

67. Klues HG, Schwarz ER, vom Dahl J, et al. Disturbed intracoronary hemodynamics in myocardial bridging: Early normalization by intracoronary stent placement. *Circulation* 1997;96:2913.
68. Kultursay H, H Can L, Payzin S, et al. A rare indication for stenting: Persistent coronary artery spasm. *Heart Vessels* 1996;11:165.
69. Laham RJ, Ho KK, Baim DS, et al. Multivessel Palmaz-Schatz stenting: Early results and one-year outcome. *J Am Coll Cardiol* 1997;30:180.
70. Kornowski R, Mehran R, Satler LF, et al. Procedural results and late clinical outcomes following multivessel coronary stenting. *J Am Coll Cardiol* 1999;33:420.
71. Moussa I, Reiners B, Moses J, et al. A long-term clinical and angiographic outcome of patients undergoing multivessel coronary stenting. *Circulation* 1997;96:3873.
72. Baim DS, Cutlip DE, Midei M, et al. Acute, 30-day and late clinical events in the randomized parallel-group comparison of the ACS Multi-link coronary stent system and the Palmaz-Schatz stent. *Circulation* 1997;96(suppl 1):1.
73. Baim DS, Cutlip DE, Lansky AJ, et al. Results of the NIRVANA equivalency trial comparing the NIR Primo stent to the Palmaz-Schatz stent. *Circulation* 1998;98(suppl 1):1.
74. Heuser R, Kuntz R, Lansky A, et al. Six-month clinical and angiographic results of the START trial. *J Am Coll Cardiol* 1998;31(suppl A):64A.
75. Han RO, Schwartz RA, Lansky A, et al. Influence of mandated coronary angiography on the target vessel revascularization rate in the SCORES trial. *Circulation* 1998;98[Suppl 1]:499a(abst).
76. DePalma VA, Baier RE, Ford JW, et al. Investigation of three surface properties of several metals and their relation to blood compatibility. In: Homsy C, Armeniades CD, eds. *Biomaterials for skeletal and cardiovascular applications.* New York: Wiley, 1972:37.
77. Komatsu R, Ueda M, Naruko T, et al. Neointimal tissue response at sites of coronary stenting in humans: Macroscopic, histologic, and immunohistochemical analyses. *Circulation* 1998;98:224.
78. Nath FC, Muller DWM, Ellis SG, et al. Thrombosis of a flexible coil stent: Frequency, predictors and clinical outcome. *J Am Coll Cardiol* 1993;21:622.
79. Haude M, Erbel R, Issa H, et al. Subacute thrombotic complications after intracoronary implantation of Palmaz-Schatz stents. *Am Heart J* 1993;126:15.
80. Sutton JM, Ellis SG, Roubin GS, et al. Major clinical events after coronary stenting: The multicenter registry of acute and elective Gianturco-Roubin stent placement. *Circulation* 1994;89:1126.
81. Karrillon GJ, Morice MC, Benveniste E, et al. Intracoronary stent implantation without ultrasound guidance and with replacement of conventional anticoagulation by antiplatelet therapy. *Circulation* 1996;94:1519.
82. Bertrand ME, Legrand V, Boland J, et al. Randomized multicenter comparison of conventional anticoagulation versus antiplatelet therapy in unplanned and elective coronary stenting. The Full Anticoagulation Versus Aspirin and Ticlopidine (FANTASTIC) study. *Circulation* 1998;98:1597.
83. Schomig A, Neumann FJ, Kastrati A, et al. A randomized comparison of antiplatelet and anticoagulant therapy after the placement of coronary-artery stents. *N Engl J Med* 1996;334:1084.
84. Urban P, Macaya C, Rupprecht HJ, et al. Randomized evaluation of anticoagulation versus antiplatelet therapy after coronary stent implantation in high-risk patients: The Multicenter Aspirin and Ticlopidine Trial after Intracoronary Stenting (MATTIS). *Circulation* 1998;98:2126.

84a. Wilson SH, Rihal CS, Bell MR, et al. Timing of coronary stent thrombosis in patients treated with aspirin and ticlopidine. *Am J Cardiol* 1999;83:1006.

85. Bennett CL, Weinberg PD, Rosenberg BK, et al. Thrombotic thrombocytopenia purpura associated with ticlopidine. *Ann Intern Med* 1998;128:541.
86. Quinn MJ, Fitzgerald DJ. Ticlopidine and clopidogrel. *Circulation* 1999;100:1667.
87. Moussa I, Oetgen M, Roubin G, et al. Effectiveness of clopidogrel and aspirin versus ticlopidine and aspirin in preventing stent thrombosis aster coronary stent implantation. *Circulation* 1999;99:2364.
88. CLASSICS, presented in late-breaking clinical trials. 48 th Annual Scientific Session of the American College of Cardiology, March 1999.
89. Shaknovich A, Moses JW, Bailey S, et al. Subacute stent thrombosis in the Stent Restenosis Study (STRESS): Clinical impact and predictive factors. *Circulation* 1994;90:650A.
90. The EPISTENT Investigators. Randomised controlled trial to assess safety of coronary stenting with use of abciximab. *Lancet* 1998;352:85.
91. Serruys PW, Emanuelsson H, van der Giessen W, et al. Heparin-coated Palmaz-Schatz stents in human coronary arteries: Early outcome of the Benestent-II Pilot Study. *Circulation* 1996;93:412.
92. Stone GW, Brodie BR, Griffin JJ, et al. Prospective, multicenter study of the safety and feasibility of primary stenting in acute myocardial infarction: In-hospital and 30-day results of the PAMI stent pilot trial. Primary Angioplasty in Myocardial Infarction Stent Pilot Trial Investigators. *J Am Coll Cardiol* 1998;31:23.
93. Gordon PC, Gibson CM, Cohen DJ, et al. Mechanisms of restenosis and redilation within coronary stents: Quantitative angiographic assessment. *J Am Coll Cardiol* 1993;21:1166.
94. Mintz GS, Popma JJ, Hong MK, et al. Intravascular ultrasound to discern device-specific effects and mechanisms of restenosis. *Am J Cardiol* 1996;78[Suppl 3A]:18.
95. Asakura M, Ueda Y, Nanto S, et al. Remodeling of in-stent neointima, which became thinner and transparent over 3 years: Serial angiographic and angioscopic follow-up. *Circulation* 1998;97:2003.
96. Kimura T, Nosaka H, Yokoi H, et al. Serial angiography follow-up after Palmaz-Schatz stent implantation: Comparison with conventional balloon angioplasty. *J Am Coll Cardiol* 1993;21:1557.
97. Farb A, Sangiorgi G, Carter AJ, et al. Pathology of acute and chronic coronary stenting in humans. *Circulation* 1999;99:44.
98. Laham RJ, Carrozza JP, Berger C, et al. Long-term (4–6 year) outcome of Palmaz-Schatz stenting: Paucity of late clinical stent-related problems. *J Am Coll Cardiol* 1996;28:820.
99. Moussa I, Moses J, DiMario C, et al. Does the specific intravascular ultrasound criterion used to optimize stent expansion have an impact on the probability of stent restenosis? *Am J Cardiol* 1999;83:1012.
100. Hanekamp CE, Koolen JL, Pijls NH, et al. Comparison of quantitative coronary angiography, intravascular ultrasound, and coronary pressure measurement to assess optimum stent deployment. *Circulation* 1999;99:1015.
101. Di Francesco LD, Di Mario C, De Gregorio J, et al. Clinical, angiographic and physiologic predictors of major adverse cardiac events (MACE) after stent implantation. *J Am Coll Cardiol* 1999;33[Suppl A]:12a.
102. de Jaegere P, Mudra H, Figulla H, et al. Intravascular ultrasound-guided optimized stent deployment: Immediate and 6 months clinical and angiographic results from the Multicenter Ultrasound Stenting in Coronaries Study (MUSIC) Study. *Eur Heart J* 1998;19:1214.
103. Schiele F, Meneveau N, Vuillemenot A, et al. Impact of intravascular ultrasound guidance in stent deployment on 6-month restenosis rate: A multicenter, randomized study comparing two strategies-with and without intravascular ultrasound guidance. *J Am Coll Cardiol* 1998;32:320.
104. Bermejo J, Botas J, García E, et al. Mechanisms of residual lumen stenosis after high-pressure stent implantation: A quantitative coronary angiography and intravascular ultrasound study. *Circulation* 1998;98:112.
105. Carrozza JP Jr, Hosley, SE, Cohen DJ, Baim DS. In-vivo assessment of stent expansion and recoil in normal porcine coronary arteries: Differential outcome by stent design. *Circulation* 1999;100:756.
106. Dirschinger J, Kastrati A, Neumann F, et al. Influence of balloon pressure during stent placement in native coronary arteries on early and late angiographic and clinical outcome. A randomized evaluation of high-pressure inflation. *Circulation* 1999;100:918.
107. Hoffmann R, Mintz GS, Kent KM, et al. Comparative early and nine-month results of rotational atherectomy, stents, and the combination of both for calcified lesions in large coronary arteries. *Am J Cardiol* 1998;81:552.
108. Moussa I, Moses J, Di Mario C, et al. Stenting after Optimal Lesion Debulking (SOLD) Registry: Angiographic and clinical outcome. *Circulation* 1998;98:1604.
109. Prati F, Di Mario C, Moussa I, et al. In-stent neointimal proliferation correlates with the amount of residual plaque burden outside the stent: An intravascular ultrasound study. *Circulation* 1999;99:1011.
110. Ellis SG, Serruys PW, Popma JJ, et al. Can abciximab prevent neointimal proliferation in Palmaz-Schatz stents? The final ERASER results. *Circulation* 1997;96[Suppl 1]:87a(abst).
111. Kutryk MJ, Serruys PW, Bruining N, et al. Randomized trial of antisense oligonucleotide against c- *myc* for the prevention of restenosis after stenting: Results of the Thoraxcenter “ITALICS” trial. *Eur Heart J* 1998;19[Suppl]:659a(abst).

112. Wilensky RL, Tanguay JF, Ito S, et al. The Heparin Infusion Prior to Stenting (HIPS) Trial: Angiographic and IVUS results. *J Am Coll Cardiol* 1998;31[Suppl]:100a.
113. Gordon PC, Friedrich SP, Piana RN, et al. Is 40–70% diameter at the site of previous stenting or directional coronary atherectomy clinically significant? *Am J Cardiol* 1994;74:26.
114. Baim DS, Levine MJ, Leon MB, et al, for the U.S. Palmaz-Schatz Stent Investigators: Management of restenosis within the Palmaz-Schatz coronary stent (the U.S. multicenter experience). *Am J Cardiol* 1993;71:364.
115. Bauters C, Banos JL, Van Belle E, et al. Six-month angiographic outcome after successful repeat percutaneous intervention for in-stent restenosis. *Circulation* 1998;97:318.
116. Kimura T, Tamura T, Yokoi H, et al. Long-term clinical and angiographic follow-up after placement of Palmaz-Schatz coronary stent. *J Interv Cardiol* 1994;7:129.
117. Shiran A, Mintz GS, Waksman R, et al. Early lumen loss after treatment of in-stent restenosis: An intravascular ultrasound study. *Circulation* 1998;98:200.
118. Dauerman HL, Baim DS, Cutlip DE, et al. Mechanical debulking versus balloon angioplasty for the treatment of diffuse in-stent restenosis. *Am J Cardiol* 1998;82:277.
119. Sharma SK, Duvvuri S, Dangas G, et al. Rotational atherectomy for in-stent restenosis: Acute and long-term results of the first 100 cases. *J Am Coll Cardiol* 1998;32:1358.
120. Strauss BH, Umans VA, van Suylen RJ, et al. Directional atherectomy for treatment of restenosis within coronary stents: Clinical, angiographic and histologic results. *J Am Coll Cardiol* 1992;20:1465.
121. Mahdi NA, Pathan AZ, Harrell L, et al. Directional coronary atherectomy for the treatment of Palmaz-Schatz in-stent restenosis. *Am J Cardiol* 1998;82:1345.
122. Mehran R, Mintz GS, Satler LF, et al. Treatment of in-stent restenosis with excimer laser coronary angioplasty: Mechanisms and results compared with PTCA alone. *Circulation* 1997;96:2183.
123. Teirstein PS, Massullo V, Jani S, et al. Catheter-based radiotherapy to inhibit restenosis after coronary stenting. *N Engl J Med* 1997;336:1697.
124. Leon MB, Teirstein PS, Lansky AJ, et al. Intracoronary gamma radiation to reduce in-stent restenosis: The multicenter Gamma 1 randomized clinical trial. *J Am Coll Cardiol* 1999;33[Suppl A]:19a.

124a. Popma JJ, Heuser R, Suntharalingam M, et al. Late clinical and angiographic outcomes after use of $^{90}Sr/^{90}y$ beta-radiation for the treatment of in-stent restenosis. Results from the Stents and Radiation Therapy (START) trial. Presented at the 49th Scientific Session of the American College of Cardiology, March 12, 2000.

125. King SB III, Williams DO, Chougule P, et al. Endovascular b-radiation after coronary balloon angioplasty: Results of the Beta Energy Restenosis Trial (BERT). *Circulation* 1998;97:2025.
126. Fischman DL, Savage MP, Leon MB, et al. Fate of lesion related side branches after coronary artery stenting. *J Am Coll Cardiol* 1993;22:1641.
127. Iniguez A, Macaya C, Alfonso F, et al. Early angiographic changes of side branches arising from a Palmaz-Schatz stented coronary segment: Results and clinical implications. *J Am Coll Cardiol* 1994;23: 911.
128. Caputo RP, Chafizadeh ER, Stoler RC, et al. Stent jail: A minimum-security prison. *Am J Cardiol* 1996;77:1226.
129. Alfonso F, Goicolea J, Hernandez R, et al. Arterial perforation during optimization of coronary stents using high-pressure balloon inflations. *Am J Cardiol* 1996;78:1172.
130. Ellis SG, Ajluni S, Arnold AZ, et al. Increased coronary perforation in the new device era: Incidence, classification, management, and outcome. *Circulation* 1994;90:2725.
131. Thibodeaux LC, James KV, Lohr JM, et al. Infection of endovascular stents in a swine model. *Am J Surg* 1996;172:151.
132. Leroy O, Martin E, Prat A, et al. Fatal infection of coronary stent implantation. *Cathet Cardiovasc Diagn* 1996;39:168.
133. Bouchart F, Dubar A, Bessou JP, et al. *Pseudomonas aeruginosa* coronary stent infection. *Ann Thorac Surg* 1997;64:1810.
134. Gunter HU, Strupp G, Volmar J, et al. Koronare Stentimplantation: Infektion and Abszedierung mit Lentalem Ausgang. *Z Kardiol* 1993;82:521.
135. Cohen DJ, Krumholz HM, Sukin CA, et al. In-hospital and 1-year economic outcomes after coronary stenting or balloon angioplasty: Results from a randomized clinical trial. *Circulation* 1995;92:2490.
136. Cohen DJ, Breall JA, Ho KL, et al. Evaluating the potential cost-effectiveness of stenting as a treatment for single-vessel coronary disease: Use of a decision analytic model. *Circulation* 1994;89:1859.
137. Bertrand OF, Sipehia R, Mongrain R, et al. Biocompatibility aspects of new stent technology. *J Am Coll Cardiol* 1998;32:562.

137a. Antoniucci D, Bartorelli A, Valenti R, et al. Clinical and angiographic outcome after coronary arterial stenting with the Carbostent. *Am J Cardiol* 2000;85:821.

138. Van der Giessen WJ, van Beusekom HM, van Houten CD, et al. Coronary stenting with polymer-coated and uncoated self-expanding endoprostheses in pigs. *Coron Artery Dis* 1992;3:631.
139. Murphy JG, Schwartz RS, Edwards WD, et al. Percutaneous polymeric stents in porcine coronary arteries: Initial experience with polyethylene terephthalate stents. *Circulation* 1992;86:1596.
140. van der Giessen W, Lincoff AM, Schwartz R, et al. Marked inflammatory response sequelae to implantation of biodegradable and non-biodegradable polymers in porcine coronary arteries. *Circulation* 1996;94:1690.
141. De Scheerder I, Wilczek K, Verbeken E, et al. Biocompatibility of polymer-coated oversized metallic stents implanted in normal porcine coronary arteries. *Atherosclerosis* 1995;114:105.
142. Lambert TL, Dev V, Rechavia E, et al. Localized arterial wall drug delivery from a polymer-coated removable metallic stent: Kinetics, distribution, and bioactivity of forskolin. *Circulation* 1994;90:1003.
143. Lincoff A, Furst J, Ellis S, et al. Sustained local delivery of dexamethasone by a novel intravascular eluting stent to prevent restenosis in the porcine coronary injury model. *J Am Coll Cardiol* 1997;29:808.
144. Dichek DA, Neville RF, Zweibel JA, et al. Seeding of intravascular stents with genetically engineered cells. *Circulation* 1989;80:1347.
145. Fischell TA, Kharma BK, Fischell DR, et al. Low-dose beta particle emission from stent wires results in complete, localized inhibition of smooth muscle cell proliferation. *Circulation* 1994;90:2956.
146. Baim DS, Fischell T, Weissman NJ, et al. Short-term (1 month) results of the IRIS feasibility study of a beta-particle emitting radioisotope stent. *Circulation* 1997;96[Suppl 1]:218a(abst).
147. Albiero R, De Gregorio J, Kobayashi N, et al. Acute and 6-month follow-up results of ^{32}P radioactive b-emitting stent implantation in patients with CAD: The Milan BX Dose-response study. *J Am Coll Cardiol* 1999;33[Suppl A]:20a.
148. Stefanidis C, Toutouzas K, Tsiamis E, et al. Stents wrapped in autologous vein: An experimental study. *Circulation* 1996;28:1039.
149. Stefanadis C, Tsiamis E, Vlachopoulos C, et al. Autologous vein graft-coated stents for the treatment of thrombus-containing coronary artery lesions. *Cathet Cardiovasc Diagn* 1997;40:217.
150. Stefanadis C, Toutouzas K, Tsiamis E, et al. Total reconstruction of a diseased saphenous vein graft by means of conventional and autologous tissue-coated stents. *Cathet Cardiovasc Diagn* 1998;43:318.
151. Elsner M, Britten M, Auch-Schwelk W, et al. Distribution of neointimal proliferation in human coronary arteries treated with polytetrafluorethylene stent-grafts. *J Am Coll Cardiol* 1999;33[Suppl A]:17a.

26
Balloon Valvuloplasty

Thomas A. Ports and William Grossman

University of California, San Francisco, School of Medicine, San Francisco, California 94143

Balloon valvuloplasty techniques and equipment have continued to evolve over the last two decades. With this expanded experience, there has been refinement in patient selection and a clearer understanding of the benefits, limitations, and long-term results of balloon valvuloplasty. In this chapter the mechanisms, indications, techniques and clinical results of balloon valvuloplasty of the mitral, pulmonic, and aortic valves are described.

PERCUTANEOUS BALLOON MITRAL VALVULOPLASTY

Percutaneous mitral valvuloplasty is an important therapeutic tool in the treatment of rheumatic mitral stenosis. Although the prevalence of rheumatic heart disease has declined significantly in the United States, this procedure remains an important therapeutic option for the symptomatic patient with mitral stenosis. In developing countries where rheumatic heart disease is very prevalent, percutaneous mitral valvuloplasty has emerged as the treatment of choice for mitral stenosis (1,2 and 3).

Mechanisms

Percutaneous mitral valvuloplasty should perhaps more appropriately be called percutaneous mitral commissurotomy, because the balloon dilatation improves the valve orifice by opening the fused mitral commissures. As shown by echocardiographic, fluoroscopic, and anatomic studies, the expanding balloon splits fused commissures in much the same way as a surgical commissurotomy (4,5).

Patient Selection

Patients should be selected for percutaneous mitral valvuloplasty based on both clinical and anatomic factors. In almost all cases, they should be symptomatic. Mitral valve area, as measured by echocardiography and hemodynamics, should be less than 1.5 cm^2. If they have anatomically suitable valves, patients with pulmonary hypertension, severe mitral stenosis, and variable left ventricular function can undergo this procedure. Similarly, patients with anatomically suitable valves who have developed restenosis (commissural refusion) after prior surgical commissurotomy can undergo percutaneous mitral valvuloplasty, with results almost as good as those of previously untreated patients (6,7). Although the procedure can be performed for patients of almost any age, the best clinical results are observed in younger patients; less predictable good long-term results occur in patients older than 70 years of age, who most likely have long-standing fibrotic valves. Percutaneous mitral valvuloplasty is a particularly valuable tool for the treatment of critical symptomatic mitral stenosis in pregnant women. It can also be a life-saving emergency procedure in the patient with mitral stenosis and refractory pulmonary edema or cardiogenic shock (8).

Contraindications

Although the procedure can be performed with thrombus localized to the left atrial appendage, thrombus within the left atrium itself is a contraindication to this procedure. Moderate or greater mitral regurgitation (2+ on a scale of 0 to 4, determined angiographically) is also a contraindication to percutaneous mitral valvuloplasty. Patients with mitral stenosis and severe coronary artery disease or aortic or tricuspid valve lesions that require cardiac surgery should not undergo a percutaneous mitral commissurotomy.

Anatomic Factors in Patient Selection for Balloon Mitral Valvuloplasty

High-quality transthoracic and transesophageal echocardiography (TEE) is an essential part of proper patient selection. TEE before the planned valvuloplasty procedure excludes the presence of left atrial thrombus and moderate or greater mitral regurgitation. In addition to ensuring that there are no anatomic contraindications, TEE provides valuable information that helps the interventional cardiologist select patients and predict results (9). The ideal patient has pliable, noncalcified mitral leaflets and mild subvalvular disease. As the degree of subvalvular disease increases, the quality of the result with percutaneous mitral commissurotomy decreases. Similarly, increasing degrees of calcification of the mitral valve diminish the effectiveness of mitral valve dilatation and increase the complication rate. Although flecks of leaflet calcium can be tolerated, the presence of calcium within the commissures is particularly to be avoided. Dilatation of mitral valves with commissural calcification may lead to leaflet tearing along noncommissural lines and severe mitral regurgitation (10). Massive calcification of the valve and bicommissural calcification are contraindications to successful percutaneous mitral valvuloplasty.

Many find the echocardiographic scoring system of Wilkins et al. (11) to be useful in assessing patients for percutaneous mitral valvuloplasty. This echocardiographic classification system is shown in Table 26.1. Points are given for leaflet mobility, valve thickening, subvalvular thickening, and valvular calcification. The final score is determined by adding up the points from each category. Higher scores indicate more severe anatomic disease and a lower likelihood of a successful procedure. The maximum score is 16. Percutaneous mitral commissurotomy results are generally excellent in patients with an echocardiographic score of less than 8, indicating favorable anatomy (i.e., pliable leaflets, mild or moderate subvalvular disease, and mild or absent valve calcification). A review of more than 1,500 patients undergoing balloon mitral valvuloplasty was used to develop a logistic model to improve patient selection (12). As expected, younger patients with echocardiographic evidence of less severe disease had a better outcome.

Leaflet mobility	
1. Highly mobile valve with restriction of only the leaflet tips	
2. Midportion and base of leaflets have reduced mobility	
3. Valve leaflets move forward in diastole mainly at the tips	
4. Little or minimal forward movement of the leaflets in diastole	
Valvular thickening	
1. Leaflets near normal (4—5 mm)	
2. Mid-leaflet thickening, marked thickening of the margins	
3. Thickening extends through the entire leaflets (5—8 mm)	
4. Marked thickening of all leaflet tissue (—8—10 mm)	
Subvalvular thickening	
1. Minimal thickening of chordal structures just below the valve	
2. Thickening of chordae extending up to one third of chordal length	
3. Thickening extending to the distal third of the chordae	
4. Extensive thickening and shortening of all chordae extending down to the papillary muscle	
Valvular calcification	
1. A single area of increased echo brightness	
2. Scattered areas of brightness confined to leaflet margins	
3. Brightness extending into the midportion of leaflets	
4. Extensive brightness through most of the leaflet tissue	

[a] Adding each of the components, determine the final score (minimum, 16 points).

Wilkins GT, Weyman AE, Abascal VM, et al. Percutaneous balloon dilatation of the mitral valve: An analysis of echocardiographic variables related to outcome and the mechanism of dilatation. Br Heart J 1988;60:299–308.

TABLE 26.1. *Echocardiographic scoring system*[a]

Technique

There are several basic techniques of percutaneous mitral valvuloplasty in use. The most common are transvenous antegrade techniques, using either a double balloon or the Inoue balloon system (2,3). These are the two techniques with which we have experience at the University of California, San Francisco. For the last 10 years we have been using the Inoue balloon introduced via an antegrade technique exclusively.

Retrograde transarterial techniques, used alone or in combination with antegrade (transseptal puncture) techniques, have been used in some centers (13). They offer the advantage of not requiring transseptal puncture or using only minimal dilatation of the intraatrial septum. Disadvantages of these techniques include the opportunity for arterial injury because of the larger balloons used. In addition, the procedures can be technically difficult and time-consuming. More common techniques are the transvenous antegrade approaches. The double-balloon technique uses a double-balloon guidewire system from the femoral vein to the left atrium, across the mitral valve, and to the left ventricle (14). The two balloons are then inflated simultaneously across the mitral valve. Figure 26.1 illustrates the two-balloon technique. In this patient the mitral valve was first dilated with a single balloon, then two balloons were used to achieve the desired hemodynamic result. The double-balloon technique, when properly performed, results in excellent improvement in mitral valve area (15,16). Multiple studies have shown no significant difference in hemodynamic results (mitral valve gradient or mitral valve area) after the procedure between the double-balloon technique and the Inoue balloon system (17). In our experience, the Inoue balloon technique is faster and less cumbersome and usually requires less fluoroscopy time (18). The Inoue balloon allows simple upsizing of the balloon without its withdrawal from the left atrium, and this is an important advantage if larger balloon sizes are needed. The Inoue balloon system may result in a slightly higher incidence of mitral regurgitation (19).

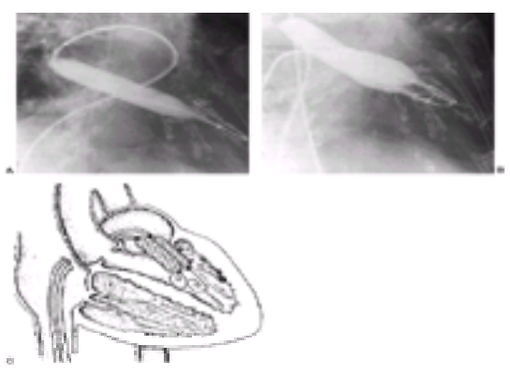

FIG. 26.1. Mitral balloon valvuloplasty in a 72-year-old woman who presented with progressive dyspnea on exertion. Her hemodynamic evaluation showed a mean mitral valve gradient of 22 mm Hg. This was reduced to 10 mm Hg after single-balloon valvuloplasty **(A)** and to 4 mm Hg after double-balloon dilatation **(B)**.

Inoue Balloon Technique

All antegrade approaches begin with the crucial step of successful transseptal catheterization. This technique, which is described in Chapter 4, not only allows access to the left atrium but also must be carried out through the proper part of the atrial septum to allow easy access to the mitral valve. After successful placement of a Mullins-type dilator and sheath into the left atrium and confirmation of its position by a hand injection of contrast material, the patient is anticoagulated with heparin. Baseline hemodynamics are then recorded, confirming the appropriate degree of mitral stenosis. Subsequently, a special heavy-duty, solid-core coiled guidewire is introduced into the left atrium, and the Mullins sheath dilator system is removed. The femoral vein and interatrial septum are then dilated with a long dilator over the coiled guidewire within the left atrium. The previously prepared, tested, and now slenderized Inoue balloon is introduced over the guidewire into the left atrium. The Inoue balloon (Fig. 26.2) is made of a nylon and rubber micromesh. The balloon has three distinct parts, each with a specific elasticity, and each part can be inflated sequentially. This allows for stable positioning of the balloon catheter across the mitral valve. After the slenderized balloon has been positioned within the left atrium, the stretching tube is removed. The preshaped “J” configuration stylet is then introduced into the Inoue balloon. We usually fill the distal portion of the balloon slightly, to aid in crossing the valve and to prevent intrachordal passage. With a combination of maneuvering the balloon catheter and rotating and withdrawing the stylet, the balloon tip moves anteriorly and inferiorly toward the mitral orifice. After the balloon catheter is across the mitral orifice, the distal portion of the balloon is inflated and the catheter is pulled back gently to confirm that the inflated portion is secure across the mitral valve.

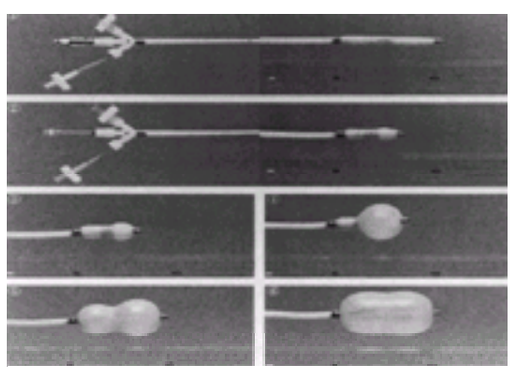

FIG. 26.2. The Inoue balloon in varying stages during deployment. **1:** The balloon is stretched or “slenderized.” **2:** The inner stretching tube is withdrawn, allowing the balloon to relax to its normal confirguration. **3:** The tip of the balloon is inflated with 2 to 3 mL of dilute contrast-saline mixture to facilitate flotation across the mitral valve without tangling in the chordae tendinae. **4:** The proximal portion of the balloon is inflated. As inflation continues, the distal portion of the balloon inflates **(5)**, and finally, the midportion of the balloon completely inflates **(6)**. (Photography courtesy of Toray, Inc., Tokyo, Japan)

Figure 26.3 illustrates the sequential filling and positioning of the Inoue balloon. The balloon is filled to its preselected diameter, then emptied and withdrawn into the left atrium. The Inoue balloon system allows for a stepwise dilatation technique to be used. We routinely measure the pressure gradient across the mitral valve after the first balloon dilatation, and also use echocardiography in the catheterization laboratory to assess the mitral valve area and the degree of mitral regurgitation. If the first inflation has not resulted in a satisfactory increase in mitral valve area and the degree of mitral regurgitation has not increased, the balloon is readvanced across

the mitral valve and inflation is repeated with the balloon diameter increased by 1 or 2 mm. This stepwise dilatation process is repeated until the desired result is achieved. The Inoue balloon comes in four sizes (24, 26, 28, and 30 mm, the size indicating the fully inflated balloon diameter), and these balloon sizes are pressure dependent, allowing the diameter to be varied up to 3 to 4 mm as required. We generally choose the initial balloon catheter size based on the height of the patient: one-tenth the height in centimeters + 10 mm. It is important to start with a small balloon size, especially for valves that are very thickened or rigid or have moderate amounts of subvalvular disease, to minimize the development of mitral regurgitation. Mitral regurgitation can still develop suddenly with as little as a 1- to 2-mm increase in diameter of inflation size. We believe that it is important to test for mitral regurgitation with Doppler echocardiography, in addition to looking for the presence and size of V-waves in the left atrial pressure tracing, before proceeding to the next inflation size. After successful mitral valve dilatation, the Inoue balloon is reslenderized by first reintroducing the guidewire and then the stretching tube. The slenderized balloon is subsequently withdrawn from the body over a guidewire. We then insert a 10F sheath into the femoral vein over the guidewire, remove the guidewire, and take the patient from the catheterization laboratory for later sheath removal.

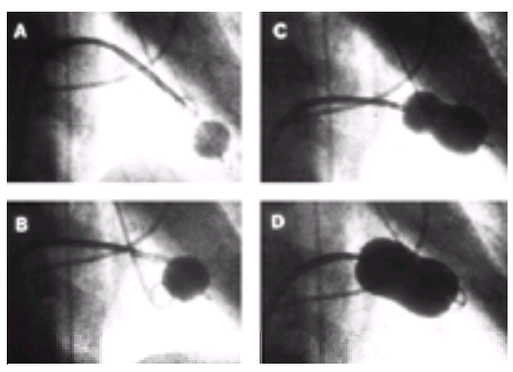

FIG. 26.3. Ballon mitral valvuloplasty in a 42-year-old man who presented with dyspnea on exertion. **A:** Distal tip of the Inoue balloon has crossed the mitral valve. **B:** With the distal tip of the balloon filled, the catheter was withdrawn to straddle the mitral valve. **C:** Partial filling of the balloon. **D:** Complete filling of the Inoue balloon across the mitral valve. This dilation reduced the mitral valve gradient from 18 to 2 mm Hg.

Immediate Results

Immediate results of mitral valvuloplasty are assessed by a combination of Doppler echocardiographic measurements and hemodynamics. Repeat evaluation of mitral valve area during the procedure by hemodynamic measurements can be performed with a reasonable degree of accuracy in catheterization laboratories equipped with computer analysis systems. There is some inaccuracy to the Gorlin formula in the presence of an atrial shunt or mitral regurgitation. Nevertheless, in successful procedures the mitral valve gradient will be observed to be substantially reduced.

Figure 26.4 illustrates a typical reduction in left atrial pressure and transmitral gradient immediately after balloon mitral valvuloplasty. The mitral valve orifice area is usually increased by more than 1 cm^2/m^2 body surface area. By echocardiographic assessment in the laboratory, particularly planimetry of the mitral valve orifice image in the two-dimensional echocardiogram short-axis view, another confirmation of improvement of mitral valve orifice area can be measured. The accuracy of Doppler measurements during valvuloplasty can be variable, but color Doppler assessment is the method of choice for sequential evaluation of the degree of mitral regurgitation (20,21). The new appearance of mitral regurgitation or an increase greater than 1 grade on the 0 to 4 classification of preexisting mitral regurgitation in general signals an end point of the procedure. Additionally, if the mitral valve area has increased to more than 2 cm^2, or if there has been a complete opening of at least one commissure on echocardiography, the procedure has been completed successfully. The clinical circumstances and anatomic factors of each individual patient must be considered carefully in determining the end point of the procedure.

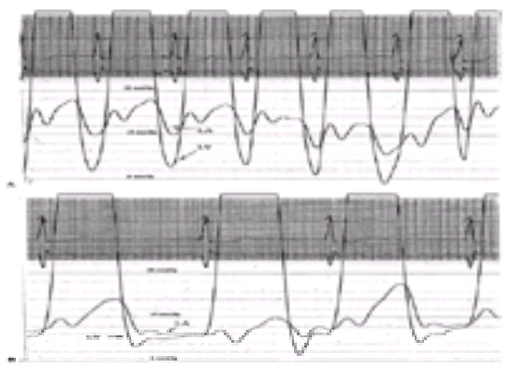

FIG. 26.4. Pressure tracings in a patient with severe mitral stenosis, showing simultaneous left atrial (LA) and left ventricular (LV) pressures before **(A)** and after **(B)** balloon mitral valvuloplasty.

Long-term Hemodynamic Results

Numerous studies have demonstrated the effectiveness of balloon valvuloplasty in increasing mitral valve area (1,12). There is almost always a near-doubling of effective mitral valve area, a decrease in left atrial pressure, and usually a slight increase in cardiac output. Over time, there is a gradual decrease in pulmonary artery pressure and pulmonary vascular resistance (22). Longer-term follow-up analyses of up to 5 years are now available. These studies show quite satisfactory results for this technique. Table 26.2 looks at the 4- and 5-year follow-up results in patients from four series (23,24,25 and 26). In a fifth series, the National Heart, Lung, and Blood Institute (NHLBI) Balloon Valvuloplasty Registry reported multicenter results in 736 patients older than 18 years of age who were monitored for 4 years (27). The actuarial survival rates at 1, 2, 3, and 4 years were 93%, 90%, 87%, and 84%, respectively. The rates of event-free survival (freedom from death, mitral valve surgery, or repeat balloon valvuloplasty) at 1, 2, 3, and 4 years were 80%, 71%, 66%, and 62%, respectively. Multivariate predictions of mortality were New York Heart Association (NYHA) functional class IV, echocardiographic mitral valve score greater than 12, postprocedure systolic pulmonary artery pressure greater than 40 mm Hg, and left ventricular end-diastolic pressure greater than 15 mm Hg.

Author (reference)	No. of patients	Mean age (yr)	Follow-up (mo)	Survival (%)	Freedom from operation (%)	NYHA class I–II and freedom from operation
Palacios et al. (23)	307	54	48	90	79	86
Cohen et al. (24)	146	59	60	76	51	–
Pan et al. (25)	359	45	60	94	91	85
Long et al. (26)	606	45	60	94	74	86

NYHA, New York Heart Association.

TABLE 26.2. *Long-term results of balloon mitral valvuloplasty for mitral stenosis*

Complications

In skilled hands, the failure rate of the procedure should be less than 5%. Failure usually results from the inability to puncture the interatrial septum safely because of anatomic difficulties or, in some cases, to position the balloon catheter successfully across the mitral valve. The procedural mortality rate varies from 0% to 3% in most series (12,28). Hemopericardium related to transseptal catheterization, atrial puncture, or, rarely, apex perforation by balloon or wires varies in incidence from 0.5% to 10%. Systemic embolization has been encountered in 0.5% to 5% of cases. These complications diminish with increasing operator experience.

Severe mitral regurgitation is uncommon, ranging in incidence from 2% to 9%, and is usually related to noncommissural leaflet tearing. It may also be associated with chordal rupture. Usually, in these circumstances, one or both of the mitral commissures were too tightly fused to be split successfully by the balloon, and the leaflets tore along noncommissural lines. Most cases of severe mitral regurgitation occur in patients with unfavorable mitral valve anatomy. Usually, even severe mitral regurgitation is well tolerated for a time by the patient, but in general elective surgical replacement of the valve is necessary because of the severity of the underlying valvular and subvalvular disease (29).

Comparison of Percutaneous Balloon Mitral Valvuloplasty and Surgery

Two prospective, randomized studies of young patients in India and South Africa compared the clinical and hemodynamic results of percutaneous balloon valvuloplasty with those of closed surgical valvotomy (30,31). The valvuloplasty results compared favorably with those obtained surgically. In one study, better functional and hemodynamic results occurred in the patients treated with percutaneous balloon valvuloplasty (31). An additional trial looked at 60 patients who were randomly assigned prospectively to percutaneous balloon valvuloplasty or open surgical commissurotomy (32). Initial mitral valve area increased from a mean of 0.9 to 2.1 cm^2 in the balloon valvuloplasty group and from 0.9 to 2.0 cm^2 in the surgical patients. However, after 3 years the patients treated with balloon valvuloplasty had a higher average mitral valve area (2.4 vs. 1.8 cm^2) and a greater likelihood of NYHA class I status (72% vs. 57%).

Open surgical commissurotomy, closed surgical commissurotomy, and percutaneous balloon valvuloplasty were compared in a trial of 90 patients (33). Short- and long-term (7-year) outcomes were not as good with closed surgical commissurotomy. The increase in mitral valve area was greater after percutaneous balloon valvuloplasty (from 0.9 to 2.2 cm^2) and open commissurotomy (from 0.9 to 2.0 cm^2) than after closed commissurotomy (from 0.6 to 1.6 cm^2). Early and late mortality and thromboembolism were similar among the three groups. At 7 years follow-up, NYHA class I was present in 87%, 90%, and 33% of patients for balloon valvuloplasty, open commissurotomy, and closed commissurotomy, respectively, and freedom from repeat intervention was 90%, 93%, and 53% respectively.

PULMONIC VALVULOPLASTY

Pulmonary valve stenosis is a relatively common congenital defect. Mild to moderate pulmonary stenosis in children has generally a benign clinical course, with a high rate of survival into adulthood. Therefore, the adult interventional cardiologist will encounter previously undetected and untreated patients who are candidates for balloon valvuloplasty.

Pathophysiology

The typical patient with valvular pulmonic stenosis has a trileaflet valve, with varying degrees of fibrous thickening and fusion of the commissures. These restricted valve leaflets have a characteristic dome-shaped, or conical, appearance during systole on angiography or echocardiography. Bicuspid pulmonic valves are uncommon (less than 20%), and heavy calcification of the stenotic valve is rare. These features make the stenotic pulmonary valve well suited for balloon valvuloplasty. Other forms of congenital pulmonic stenosis not well suited for valvuloplasty include dysplastic valves (Noonan's syndrome) and primary fibromuscular subvalvular narrowing.

Balloon valvuloplasty evolved from a long surgical experience with mechanical valve dilatation, valvulotomies (Brock procedure), bougies, and finally, under cardiopulmonary bypass, direct incision of fused pulmonic valve commissures. Since the initial balloon valvuloplasty of the pulmonary valve in 1979 with an angiographic balloon catheter, larger-diameter, longer-length polyethylene balloon catheters have been developed to allow this procedure to be performed successfully and safely in children and adults (34,35). The proposed mechanism for successful balloon valvuloplasty is predominantly mechanical separation of congenitally fused commissures. Also, there appears to be in some patients minor tearing of valve leaflets, and occasionally avulsion of the cusps.

Patients with moderate pulmonic stenosis and a gradient of 50 to 100 mm Hg who have symptoms of exercise intolerance will probably benefit from balloon valvuloplasty. Patients with severe pulmonic stenosis, defined as a gradient greater than 100 mm Hg, may benefit from balloon valvuloplasty even in the absence of symptoms, because of the significant afterload that the obstructive pulmonary valve places on the right ventricle (36).

Technique

After careful selection of a symptomatic patient with a moderate or severe gradient across the pulmonary valve by echocardiographic and Doppler evaluation, successful pulmonary valvuloplasty begins with a careful right-sided heart catheterization to document the pulmonary valve gradient and to exclude a significant supravalvular or subvalvular component. We usually place a 5F sheath in the left femoral artery for pressure monitoring and perform the procedure from the right femoral vein after the introduction of an 8F sheath. A right ventricular angiogram is done in the anteroposterior and lateral projections to determine the exact location of the pulmonary valve and to allow sizing of the pulmonary annulus. For sizing, we usually use external markers on the chest at the level of the pulmonary valve, such as a nickel taped to the chest, and we use either a pigtail catheter with tantalum markers spaced 1 cm apart or a balloon angiographic catheter whose inflated balloon is approximately 1 cm in diameter. We usually employ the dual-balloon technique in adult patients, initially selecting balloon sizes approximating the diameter of the annulus and then increasing the size, if necessary, to abolish the gradient. It is often necessary to oversize the calculated annulus diameter by as much as 25%.

After angiographic localization of the pulmonary valve, the valve is crossed with a dual-lumen balloon flotation catheter. This catheter is useful for measuring the gradient from its end-hole lumen, as well as its side-hole lumen, 5 cm from the tip. Pressure gradients can be measured by this catheter before and after balloon dilatation. Both lumens are passed distally into the pulmonary artery, and two 0.038-inch, heavy-duty exchange-length guidewires are passed into the distal pulmonary artery, one through the end-hole lumen and one through the side-hole lumen. The catheter is then removed, leaving the wires in place in the pulmonary artery exiting the body through the femoral vein. The pulmonary valvuloplasty balloons, having been previously purged of air and filled with diluted radiographic contrast, are then inserted one after the other in tandem into the femoral vein. They are positioned one at a time with the aid of both the external markers and the balloon markers so that the midportion of the valvuloplasty balloon is straddling the pulmonary valve. When both balloon catheters are in place, they are rapidly and simultaneously filled with the dilute radiographic contrast solution. The balloons are filled until the “waist” is seen to disappear on fluoroscopy . The balloon catheters are emptied and then withdrawn from the body sequentially over the two heavy-duty “J” wires. A 12F sheath is introduced into the femoral vein over the guidewires, and the dual-lumen catheter is reintroduced through the sheath and positioned across the pulmonary valve over one of the wires. That guidewire is then removed, and a careful determination is made of the residual valvular gradient, if any. In a successful balloon pulmonic valvuloplasty, the valvular gradient is almost always abolished, or nearly so. However, on occasion the operator encounters a previously undetected *subvalvular* gradient after the valvular gradient has been eliminated. This subvalvular gradient usually diminishes and disappears over the ensuing weeks, with regression of the right ventricular hypertrophy. Repeat dilatation of the pulmonary valve should be performed with larger balloons only when there is a persistent and significant *valvular* gradient. Repeat dilatation of the pulmonary valve for a subvalvular gradient is contraindicated.

Clinical Results and Complications

The impressive acute and long-term results of this procedure in adolescents and adults make balloon valvuloplasty the treatment of choice for valvular pulmonic stenosis. A pooled analysis involving 784 patients of all ages showed that clinical success was achieved with balloon valvuloplasty in 98% of patients (37). Procedural mortality was less than 0.5%, and the average peak valve gradient fell from 85 to 33 mm Hg. Several series have looked at the long-term efficacy of balloon valvuloplasty. Chen and colleagues reported on a series of 53 adolescent and adult patients, ages 13 to 55 years, treated between 1985 and 1995 (38). The systolic pressure gradient across the pulmonary valve fell from 91 ± 46 to 38 ± 32 mm Hg after the procedure. On late follow-up (average, 7 years), the gradient had fallen further. Seven of 53 patients developed pulmonary insufficiency immediately after the valvuloplasty, but none had this complication at late follow-up evaluation.

Procedural complications are rare during the procedure, and at our institution pulmonic valvuloplasty is usually planned as an outpatient procedure. Patients may have arrhythmias and occasional hypotension during balloon inflation. Transient right bundle branch block has been observed. Despite the use of large balloon catheters, bleeding and vascular complications are very infrequent because this procedure is done through the femoral vein.

BALLOON AORTIC VALVULOPLASTY

Dilatation of the stenotic aortic valve, whether by surgical technique or percutaneous balloon valvuloplasty, has not enjoyed the same level of success as therapy for the pulmonic and mitral valves. Surgical mechanical dilatation of the stenotic adult aortic valve has been attempted since the 1950s, but the use of various valvulotomies has failed to provide a significant solution for the problem of calcific aortic stenosis and has been abandoned in favor of aortic valve replacement. Open surgical valvotomy remains an option for infants and children with critical aortic stenosis, in whom it is desirable to postpone a definitive aortic valve replacement.

Noncalcific Aortic Stenosis

Percutaneous balloon aortic valvuloplasty was first performed in children and young adults by Lababidi in 1984 (39). Balloon dilatation resulted in a significant decrease in peak aortic valve gradient. Considerable experience exists with balloon valvuloplasty in children and adolescents with noncalcified congenital stenotic aortic valves, with excellent short-term and satisfactory long-term results (40,41 and 42). The predominantly fibrotic nature of these congenitally stenotic valves makes them well suited for balloon valvuloplasty. The procedure is effective 80% to 90% of the time, with a mortality rate of approximately 0.7%. Survival at 8 years has been reported to be 95%, with the need for repeat intervention 25% at 4 years and 50% at 8 years (43). There may be a role for balloon valvuloplasty in the young adult without significant valve calcification. A study of young adults ages 17 to 40 years (mean, 23 years) with congenital aortic stenosis showed that balloon aortic valvuloplasty produced a significant reduction in the gradient across the aortic valve and an increase in the aortic valve area (44). In this series there were no deaths or embolic cerebrovascular events. Intermediate follow-up at 38 months showed that 50% of patients required no further intervention. The absence of significant valve calcification is an important predictor of a good short- and long-term result.

Calcific Aortic Stenosis

The more typical patient encountered by the adult cardiologist is the elderly patient with acquired calcific aortic stenosis. Although experience with successful balloon valvuloplasty for this condition dates back to 1986 (45,46), the procedure has *a very limited role at present because of the unpredictability of the initial benefit and the very high rate of recurrence or "restenosis."* Virtually all symptomatic patients with calcific aortic stenosis should undergo aortic valve replacement as the treatment of choice. There are, however, certain settings where balloon valvuloplasty may play an important palliative role in patients who are not candidates for immediate valve replacement. These are listed in Table 26.3. Balloon aortic valvuloplasty is useful in the patient presenting with cardiogenic shock due to aortic stenosis and can serve as a successful bridge to definitive surgery in these hemodynamically unstable patients (47). It may also be used for palliation in patients with serious comorbid conditions. The technique is also used in patients with critical aortic stenosis who require urgent noncardiac surgery if it is thought that more conservative medical therapy presents excessive risk.

Cardiogenic shock
Bridge to aortic valve surgery
Symptomatic critical aortic stenosis requiring emergency noncardiac surgery
Poor surgical risk, age >90 yr
Diagnostic test in low-gradient/low-output setting
Congenital aortic stenosis
Rheumatic aortic stenosis

TABLE 26.3. *Indications for balloon aortic valvuloplasty in adults with aortic stenosis*

Mechanism of Improved Aortic Orifice Area

Postmortem and intraoperative dilatations have shown how balloon aortic valvuloplasty improves calcific degenerative aortic stenosis in the adult (48). Balloon dilatation increases the mobility of leaflets, thus enlarging the aortic valve orifice. The mechanism of dilatation appears to be predominantly fracturing of the calcific aortic valve nodules (48). In addition, in some elderly patients there may be separation of postinflammatory fused commissures.

Technique

The retrograde aortic technique for balloon aortic valvuloplasty is the one most commonly used. In the typical patient we use both femoral arteries. A 5F pigtail catheter is inserted from the left femoral artery and positioned in the ascending aorta for pressure monitoring and gradient determination. Right-sided heart catheterization is done from the left femoral vein. A balloon flotation thermodilution catheter is placed in the pulmonary artery and remains there throughout the procedure. Cardiac output is determined by both Fick and thermodilution techniques. Using the right femoral artery, an 8F sheath is introduced, through which left-sided heart catheterization is performed. A 0.038-inch straight-tip guidewire is used to cross the aortic valve. A pigtail catheter is placed in the left ventricle, the aortic valve gradient is measured, and the aortic valve area is determined by the Gorlin formula. All patients are heparinized before any attempt is made to cross the aortic valve. After these prevalvuloplasty measurements, a heavy-duty 0.038-inch exchange-length (300-cm) guidewire (Schneider-Boston Scientific, Maple Grove, MN) with a double curve placed at its tip is inserted into the left ventricle. The previously placed pigtail catheter is removed, and a 12F sheath is placed over this wire into the femoral artery. It is important that the groin be anesthetized adequately to avoid discomfort and possible vagal reaction during sheath exchange. Through the sheath the previously prepared dilatation balloon is advanced over the guidewire. To keep its profile minimal, the balloon (purged of air) is kept completely deflated by constant negative pressure from a syringe and is introduced with a counterclockwise rotation.

Under fluoroscopy, using two operators, the heavy-duty guidewire is kept in the left ventricle as the balloon valvuloplasty catheter is advanced and positioned to straddle the aortic valve. Using the proximal and distal markers of the balloon, the operator attempts to place the middle of the balloon at the level of the calcific aortic valve. Figure 26.5 illustrates the unfilled balloon straddling the aortic valve.

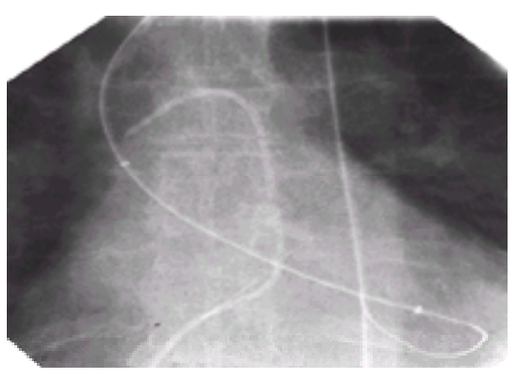

FIG. 26.5. Anteroposterior projection shows passage of the deflated aortic valvuloplasty balloon across a stenotic aortic valve. Balloon markers are positioned so that the balloon straddles the calcified aortic valve.

In most normal-sized adults with an adequate aortic valve annulus, we begin with a 20-mm diameter, 5.5-cm long balloon. In very small or frail patients, the operator can start with an 18-mm balloon or (very rarely) a 15-mm balloon. The balloon is filled with diluted contrast medium using either a very large syringe or an angioplasty end-deflator–type device. Care must be taken to maintain balloon position within the valve orifice to achieve an effective dilatation. The balloon catheter may tend to jump either forward or backward with the force of ventricular systole. To achieve a stable balloon position, we initially fill the balloon slowly, while one operator fixes the balloon in a stable position. Once a good position is achieved, the balloon is filled rapidly to its maximum diameter. We constantly monitor the electrocardiogram for arrhythmia and ischemia. The aortic pressure is also monitored continuously. If tolerated, the balloon is left filled for 15 to 20 seconds. The balloon is then emptied and withdrawn into the aorta, keeping the guidewire in the left ventricle. If significant hypotension, ischemia, or sustained ventricular tachycardia occurs, the balloon is emptied immediately. A period of stabilization to allow blood pressure and electrocardiographic changes to return to baseline should be allowed before further dilatations. It is often necessary to exert considerable force on these balloons to expand them fully and relieve the “waist” caused by the stenotic aortic valve.

After several dilatations with a single balloon or after balloon rupture (a frequent occurrence), the balloon is withdrawn through the sheath, leaving the exchange-length, heavy-duty wire in place. It is frequently necessary to remove the 12F sheath along with the deflated valvuloplasty balloon, because the valvuloplasty balloons do not always rewrap adequately to allow removal through the sheath. The pigtail catheter is then reintroduced over the guidewire back into the left ventricle, and measurements of the pressure gradient and cardiac output are repeated. The aortic valve area is calculated. Our usual goal is to increase the aortic valve area by more than 100% and to achieve a valve area of at least 1 cm^2. If a desirable result has not been achieved, we change to a 23-mm diameter balloon and repeat the procedure. If an adequate result is not achieved with the single 23-mm balloon, we then employ a dual-balloon technique, using a pair of 15- or 18-mm balloons if aortic annulus size permits. For this technique the other femoral artery is used to access the aorta and left ventricle. Pressure is monitored through the side-arm of the 12F sheath during the procedure. Figure 26.6 illustrates the dual balloon technique, and Fig. 26.7 shows the progressive reduction in gradient with single, followed by dual, balloon valvuloplasty. After a successful procedure, patients are placed in a recovery area or in the coronary care unit for continued observation. The femoral artery sheaths are removed after the coagulation parameters are in the normal range, and hemostasis is maintained either by manual pressure or a fem-stop device.

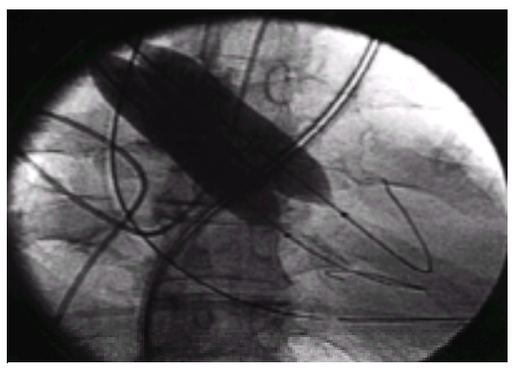

FIG. 26.6. Balloon aortic valvuloplasty using the double-balloon technique in a 94-year-old woman who presented with syncope and failure. Full inflation of two 18-mm diameter, 5.5-cm SciMed balloons across the stenotic aortic valve is shown.

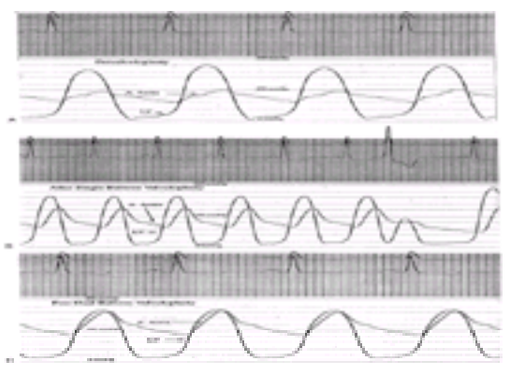

FIG. 26.7. Balloon aortic valvuloplasty in an elderly patient with severe calcific aortic stenosis. **A:** Baseline pressure gradient across the stenotic aortic valve measured with one catheter in the left ventricle (LV) and a separate pigtail catheter in the ascending aorta (A-AORTA). There is a 58 mm Hg mean gradient and an 80 mm Hg peak-to-peak gradient across the valve. **B:** Reduction in the aortic valve gradient after a series of progressive single-balloon dilatations of the aortic valve. **C:** Marked reduction in aortic valve gradient after dual-balloon valvuloplasty.

Clinical Results and Complications

In the large Mansfield balloon aortic valve registry, data were collected from 27 clinical centers across the United States and Europe from 6,742 patients with calcific aortic stenosis undergoing balloon aortic valvuloplasty between 1986 and 1987 (49). Balloon aortic valvuloplasty resulted in an increase in aortic valve area from 0.5 ± 0.18 to 0.81 ± 0.18 cm^2, and a decrease in mean aortic valve pressure gradient from 60 ± 24 to 30 ± 14 mm Hg. There was also an accompanying increase in cardiac output, from 3.86 ± 0.55 to 4.01 ± 0.51 L/min. Complications were experienced in 22.6% of patients, including a procedural death rate of 4.9%, death within 7 days 2.6%, emboli 2.2%, ventricular perforation 1.4%, and emergency aortic valve replacement 1.2%. The most common complication was local vascular injury, which required surgical repair in 5.7% of patients (50). The NHLBI balloon valvuloplasty registry enrolled patients from 1987 to 1989 at 24 clinical centers (51). Similar results were obtained, with balloon aortic valvuloplasty increasing aortic valve area from 0.5 ± 0.2 to 0.8 ± 0.5 cm^2, decreasing aortic valve pressure gradient from 57 ± 30 to 29 ± 13 mm Hg, and increasing cardiac output from 3.9 ± 1.2 to 4.1 ± 1.2 L/min. Complications included procedural death (2%), cardiac arrest (5%), emergency aortic valve replacement (1%), left ventricular perforation (2%), and embolic stroke and systemic emboli (1%).

The use of newer balloons with smaller deflated profiles and the use of large vascular sheaths may be reducing the incidence of vascular trauma. Ventricular arrhythmias and left bundle branch block are very commonly induced during the procedure; however, both are usually transient.

Long-Term Results

Restenosis with recurrent symptoms is very common in the first year after balloon valvuloplasty in the adult with calcific aortic stenosis (52,53 and 54). In the NHLBI-sponsored balloon valvuloplasty registry, the survival rates at 1, 2, and 3 years were 55%, 35%, and 23%, respectively, in the 674 patients undergoing balloon aortic valvuloplasty (51). The 1-year survival rate in the Mansfield registry of 492 patients was 64%, with an event-free survival rate of 43% (49,55). Therefore, it must be emphasized that, when at all feasible, definitive aortic valve replacement is the technique of choice for managing the adult patient with severe calcific aortic stenosis.

Short-term clinical improvements associated with balloon aortic valvuloplasty may be accompanied by improvement in systolic and diastolic left ventricular function in some patients (56). Patients with significantly depressed left ventricular function undergoing this procedure have a very poor long-term prognosis (57). In the patient with cardiogenic shock who has been stabilized with successful balloon aortic valvuloplasty, cardiac surgery with definitive aortic valve replacement should be undertaken soon after the patient's condition stabilizes (47,58).

CHAPTER REFERENCES

1. Carroll JD, Feldman T. Percutaneous mitral balloon valvotomy and the new demographics of mitral stenosis. *JAMA* 1993;207:1731.
2. Inoue K, Owaki T, Nakamura T, et al. Clinical application of transvenous mitral commissurotomy by a new balloon catheter. *J Thorac Cardiovasc Surg* 1984;87:394.
3. Lock JE, Kalilullah M, Shrivastava S, et al. Percutaneous catheter commissurotomy in rheumatic mitral stenosis. *N Engl J Med* 1985;313:1515.
4. Inoue K, Feldman T. Percutaneous transvenous mitral commissurotomy using Inoue balloon catheter. *Cathet Cardiovasc Diagn* 1993;28:119.
5. McKay RG, Lock JE, Safian RD, et al. Balloon dilatation of mitral stenosis in adult patients: Postmortem and percutaneous mitral valvuloplasty studies. *J Am Coll Cardiol* 1987;9:723.
6. Al KW, Ding ZP, Gao W, et al. Percutaneous balloon mitral valvuloplasty in patients with mitral restenosis after previous surgical commissurotomy. *Eur Heart J* 1996;17:1367.
7. Gupta S, Vora A, Lokhandwalla Y, et al. Percutaneous balloon mitral valvotomy in mitral restenosis. *Eur Heart J* 1996;17:1560.
8. Lokhandwala YY, Banker D, Vora AM, et al. Emergent balloon mitral valvotomy in patients presenting with cardiac arrest, cardiogenic shock or refractory pulmonary edema. *J Am Coll Cardiol* 1998;32:154.
9. Padial LR, Freitas N, Sagie A, et al. Echocardiography can predict which patients will develop severe mitral regurgitation after percutaneous mitral valvulotomy. *J Am Coll Cardiol* 1996;27:1225.
10. Cannan CR, Nishimura RA, Reeder GS, et al. Echocardiographic assessment of commissural calcium: A simple predictor of outcome after percutaneous mitral balloon valvotomy. *J Am Coll Cardiol* 1997;29:175.
11. Wilkins GT, Weyman AE, Abascal VM, et al. Percutaneous balloon dilatation of the mitral valve: An analysis of echocardiographic variables related to outcome and the mechanism of dilatation. *Br Heart J* 1988;60:299.
12. Iung B, Cormier B, Ducimetiere P, et al. Immediate results of percutaneous mitral commissurotomy: A predictive model on a series of 1,514 patients. *Circulation* 1996;94:2124.
13. Babic UU, Dorros G, Pejcic P, et al. Percutaneous mitral valvuloplasty: Retrograde, transarterial double-balloon technique utilizing the transseptal approach. *Cathet Cardiovasc Diagn* 1988;14:229.
14. Zaibag M, Alkasab S, Ribiero PA, et al. Percutaneous double balloon mitral valvotomy for rheumatic mitral valve stenosis. *Lancet* 1986;I:757.
15. Vahanian A, Michel PL, Cormier B, et al. Results of percutaneous mitral commissurotomy in 200 patients. *Am J Cardiol* 1989;63:847.
16. Tuzcu EM, Block PC, Palacios IF, et al. Comparison of early versus late experience with percutaneous mitral balloon valvuloplasty. *J Am Coll Cardiol* 1991;17:1121.
17. Rihal CS, Holmes DR. Percutaneous balloon mitral valvuloplasty: Issues involved in comparing techniques. *Cathet Cardiovasc Diagn* 1994;2:8.
18. Feldman T, Herrmann HC, Inoue K. Technique of percutaneous transvenous mitral commissurotomy using the Inoue balloon catheter. *Cathet Cardiovasc Diagn* 1994;2:26.
19. Roth BR, Block PC, Palacios IF. Predictors of increased mitral regurgitation after percutaneous mitral balloon valvotomy. *Cathet Cardiovasc Diagn* 1990;20:17.
20. Otto CM, Davies KB, Holmes DR, et al. Methodologic issues in clinical evaluation of stenosis severity in adults undergoing aortic or mitral balloon valvuloplasty. *Am J Cardiol* 1992;69:1607.
21. Pitsavos CE, Stafanadis CG, Stratos CG, et al. Assessment of accuracy of the Doppler pressure half-time method in the estimation of the mitral valve area immediately after balloon mitral valvuloplasty. *Eur Heart J* 1998;18:455.
22. Levine MJ, Weinstein JS, Diver DJ, et al. Progressive improvement in pulmonary vascular resistance following percutaneous mitral valvuloplasty. *Circulation* 1989;79:1061.
23. Palacios IF, Tuzcu ME, Weyman AE, et al. Clinical follow-up of patients undergoing percutaneous mitral balloon valvotomy. *Circulation* 1995;91:671.
24. Cohen DJ, Kuntz RE, Gordon SPF, et al. Predictors of long-term outcome after percutaneous balloon mitral valvuloplasty. *N Engl J Med* 1992;327:1329.
25. Pan M, Medina A, Lezo JJ, et al. Factors determining late success after mitral balloon valvulotomy. *Am J Cardiol* 1993;71:1181.
26. Iung B, Cormier B, Ducimetiere P, et al. Functional results 5 years after successful percutaneous mitral commissurotomy in a series of 528 patients and analysis of predictive factors. *J Am Coll Cardiol* 1996;27:407.
27. Dean LS, Mickel M, Bonan R, et al. Four-year follow-up of patients undergoing percutaneous balloon mitral commissurotomy: A report from the National Heart, Lung, and Blood Institute Balloon Valvuloplasty Registry. *J Am Coll Cardiol* 1996;28:1452.
28. The National Heart, Lung, and Blood Institute Balloon Valvuloplasty Registry. Complications and mortality of percutaneous balloon mitral commissurotomy. *Circulation* 1992;85:2015.
29. Acar C, Jebara VA, Grare PH, et al. Traumatic mitral insufficiency following percutaneous mitral dilation of anatomic lesions and surgical implications. *Eur J Cardiothorac Surg* 1992;6:660.
30. Turi ZG, Reyes VP, Raju BS, et al. Percutaneous balloon versus closed commissurotomy for mitral restenosis: A prospective, randomized trial. *Circulation* 1991;83:1179.
31. Patel JJ, Sharma D, Mitha AS, et al. Balloon valvuloplasty versus closed commissurotomy for pliable mitral stenosis: A prospective hemodynamic study. *J Am Coll Cardiol* 1991;18:1318.
32. Reyes VP, Raju BS, Wynne J, et al. Percutaneous balloon valvuloplasty compared with open surgical commissurotomy for mitral stenosis. *N Engl J Med* 1994;331:961.
33. Farhat MB, Ayari M, Maatoul F, et al. Percutaneous balloon versus surgical closed and open mitral commissurotomy: Seven-year follow-up results of a randomized trial. *Circulation* 1998;97:245.
34. Semb BKH, Tjonneland S, Stake G, et al. Balloon valvulotomy of congenital pulmonary valve stenosis with tricuspid insufficiency. *Cardiovasc Radiol* 1979;2:239.
35. Kan J, White RI, Mitchell SE, et al. Percutaneous balloon valvuloplasty: A new method for treating congenital pulmonary valve stenosis. *N Engl J Med* 1982;307:540.
36. Johnson LW, Grossman W, Dalen JE, et al. Pulmonic stenosis in the adult: Long-term follow-up results. *N Engl J Med* 1972;287:1159.
37. Stanger P, Cassidy SC, Girod DA, et al. Balloon pulmonary valvuloplasty: Results of the Valvuloplasty and Angioplasty of Congenital Anomalies Registry. *Am J Cardiol* 1990;65:775.
38. Chen C-R, Cheng TO, Huant T, et al. Percutaneous balloon valvuloplasty for pulmonic stenosis in adolescents and adults. *N Engl J Med* 1996;335:21.
39. Lababidi Z, Wu JR, Walls JT. Percutaneous balloon aortic valvuloplasty: Results in 23 patients. *An J Cardiol* 1984;53:194.
40. Rocchini AP, Beekman RH, Shachar GB, et al. Balloon aortic valvuloplasty: Results of the valvuloplasty and angioplasty of congenital anomalies registry. *Am J Cardiol* 1990;65:784.
41. Rao PS, Thapar MK, Wilson AD, et al. Intermediate-term follow-up results of balloon aortic valvuloplasty in infants and children with special reference to causes of restenosis. *Am J Cardiol* 1989;64:1356.
42. O'Connor BK, Beekman RB, Rocchini AP, et al. Intermediate-term effectiveness of balloon valvuloplasty for congenital aortic stenosis. *Circulation* 1991;84:732.
43. Moore P, Egito E, Mowrey H, et al. Midterm results of balloon dilation of congenital aortic stenosis: Predictors of success. *J Am Coll Cardiol* 1996;27:1257.
44. Rosenfeld HM, Landzberg MJ, Perry SB, et al. Balloon aortic valvuloplasty in the young adult with congenital aortic stenosis. *Am J Cardiol* 1994;73:1112.
45. McKay RG, Safian RD, Lock JE, et al. Balloon dilatation of calcific aortic stenosis in elderly patients: Post-mortem, intra-operative and percutaneous valvuloplasty studies. *Circulation* 1986;74:119.
46. Cribier A, Savin T, Berland J, et al. Percutaneous transluminal balloon valvuloplasty of adult aortic stenosis: Report of 92 cases. *J Am Coll Cardiol* 1987;9:381.
47. Smedira NG, Ports TA, Merrick SH, et al. Balloon aortic valvuloplasty as a bridge to aortic valve replacement in critically ill patients. *Ann Thorac & Cardiovasc Surg* 1993;55:914.
48. Safian RD, Mandell VS, Thurer RE, et al. Post-mortem and intraoperative balloon valvuloplasty of calcific aortic stenosis in elderly patients: Mechanisms of successful dilatation. *J Am Coll Cardiol* 1987;9:665.
49. O'Neill WW. Mansfield Scientific Registry Experience. Predictors of long-term survival after percutaneous aortic valvuloplasty: Report of the Mansfield Valvuloplasty Registry. *J Am Coll Cardiol* 1991;17:193.
50. Holmes DR Jr, Nishimura RA, Reeder GS, Mansfield Scientific Registry Experience. In-hospital mortality after balloon aortic valvuloplasty: Frequency and associated factors. *J Am Coll Cardiol* 1991;17:189.
51. National Heart, Lung, and Blood Institute Balloon Valvuloplasty Registry Participants. Percutaneous balloon aortic valvuloplasty: Acute and 30-day follow-up results in 674 patients from the NHLBI Balloon Valvuloplasty Registry. *Circulation* 1991;84:2383.
52. Safian RD, Berman AD, Diver DJ, et al. Balloon aortic valvuloplasty in 170 consecutive patients. *N Engl J Med* 1988;319:125.
53. Lieberman EB, Bashore TM, Hermiller JB, et al. Balloon aortic valvuloplasty in adults: Failure of procedure to improve long-term survival. *J Am Coll Cardiol* 1995;26:1522.
54. Otto CM, Mickel MC. Kennedy W, et al. Three-year-outcome after balloon aortic valvuloplasty: Insights into prognosis of valvular aortic stenosis. *Circulation* 1994;89:642.
55. Bashore TM, Davidson CJ. Mansfield Scientific Registry Experience. Follow-up recatheterization after balloon aortic valvuloplasty. *J Am Coll Cardiol* 1991;17:1188.
56. McKay RG, Safian RD, Lock JE, et al. Assessment of left ventricular and aortic valve function after balloon valvuloplasty in adult patients with aortic stenosis. *Circulation* 1987;75:192.
57. Davidson CJ, Harrisson JK, Leithe ME, et al. Failure of aortic balloon valvuloplasty to result in sustained clinical improvement in patients with depressed left ventricular function. *Am J Cardiol* 1990;65:72.
58. Moreno PR, Ik-Kyung J, Newell JB, et al. The role of percutaneous aortic balloon valvuloplasty in patients with cardiogenic shock and critical aortic stenosis. *J Am Coll Cardiol* 1990;65:72.

27
Peripheral Intervention

Kenneth Rosenfield

Tufts University School of Medicine, Division of Vascular Medicine, St. Elizabeth's Medical Center, Boston, Massachusetts 02135

Although their primary focus remains in the diagnosis and treatment of cardiac disorders, cardiovascular specialists increasingly are moving toward a strategy of "global vascular management" that also involves the noncoronary manifestations of atherosclerosis. This is appropriate since peripheral arterial disease (PAD) and coronary artery disease (CAD) may coexist in the same patient, may each cause disabling or life-threatening symptoms (stroke, renal ischemia, claudication, or limb loss), and since treatment of one may influence treatment of the other. For example, patients requiring vascular surgery generally have an increased cardiac risk because of the increased prevalence of CAD in this group; patients with severe carotid artery disease have an increased incidence of stroke during coronary bypass surgery; and patients with severe renal artery disease and associated hypertension are liable to worsening underlying cardiac conditions and have an increased risk for contrast-induced renal dysfunction during coronary intervention.

In reality, however, few invasive or interventional cardiologists have undergone the additional training required to develop the knowledge base regarding the natural history, noninvasive workup, angiography, and therapeutic alternatives (medical, surgical, and particularly catheter-based) that are relevant to the management of these conditions. This chapter is thus one of three newly included in the sixth edition of this book to provide some of the necessary resources. (The reader is also referred to Chapter 14 for additional information on angiography of the aorta and peripheral arteries, and to Chapter 35 for integration of clinical, diagnostic, and therapeutic aspects in "real-life" case profiles.) The main focus of this chapter is on catheter-based interventional techniques, organized in the same "head-to-foot" sequence as that of regional techniques.

GENERAL CONSIDERATIONS

The pathophysiologic basis of atherosclerosis of the peripheral arteries is identical to that in coronary arteries and is associated with the same risk factors—positive family history, tobacco smoking, diabetes mellitus, hypertension, hyperlipidemia, advanced age, and inactivity. The estimated prevalence of PAD in people 65 years of age and over is approximately 20%, likely underestimated by the large number of patients whose PAD symptoms are overlooked or falsely attributed to other etiologies (deconditioning, arthritis, sciatica). As is the case in CAD, symptoms related to PAD generally do not occur until the atherosclerotic process has narrowed the vessel diameter by at least 50%; similarly, the mere presence of a lesion of 50% or more does not imply that the patient will be symptomatic (i.e., if an ample collateral supply is present).

The range of symptoms depends on the vascular territory involved. In the limbs, the most common symptom is intermittent claudication, described variably as pain, tightness, aching, soreness, hardness, or heaviness that occurs in the calf, hip, buttocks, or arch of the foot during ambulation and resolves with rest, similar to the pattern of exertional angina in CAD. This may range from mild lower extremity discomfort during intense exercise to severe symptoms on minimal exertion or even at rest. More advanced ischemia leads to tissue necrosis, manifested as painful ulceration or frank gangrene. In the cerebral circulation, the dominant symptom is transient neurologic dysfunction due to embolic events or poststenotic ischemia, or permanent cerebral damage due to occlusion (stroke). In mesenteric vessels, the extensive collateral circulation generally prevents symptoms from developing until several major vessels are occluded, at which point abdominal angina or bowel infarction may ensue. Renal artery stenosis, in contrast, may cause progressive loss in renal mass and function, or severe arterial hypertension via activation of the renin-angiotensin system, since collateral supply is limited. The cardiovascular disease specialist must be familiar with the range of symptoms and findings related to vascular disease in each arterial territory, the natural history, the indications for intervention, and the therapeutic alternatives.

As indicated in Chapter 14, approximately 70% of PAD patients will remain unchanged or become even less symptomatic after 5 to 10 years, fewer than 30% will progress to require intervention, and fewer than 10% will need amputation. The slow progression of symptoms (1,2) should thus generally temper aggressive recommendations for invasive therapy in PAD, except in two unique subgroups: patients with diabetes mellitus (who have a higher likelihood of developing critical limb ischemia and seven times greater chance of progressing to amputation), and patients who develop *acute* limb ischemia (ALI). ALI most commonly occurs as a result of embolic arterial occlusion (usually from a cardiac source such as atrial fibrillation), *in situ* thrombosis of a diseased native extremity vessel or bypass graft, or spontaneous thrombosis as the result of a hypercoagulable state. The clinical presentation of acute limb ischemia is typically a dramatic one; there is the acute onset of severe pain, followed shortly by paresthesia and, ultimately, motor dysfunction (e.g., paralysis). On examination, the extremity is cool, pale, and pulseless. Rutherford and colleagues (3) have described a series of clinical categories of limb ischemia (Table 27.1), with well-defined diagnostic criteria that help determine whether the affected limb is viable, in imminent jeopardy (e.g., "threatened"), or already irreversibly damaged. These are analogous to the Rutherford criteria for *chronic* limb ischemia (Table 27.2). Paradoxically, it is the patient with less underlying atherosclerotic PVD and poorly developed collateral circulation (e.g., the patient with atrial fibrillation who embolically occludes a normal common femoral or popliteal artery) who develops the most acute ischemia.

Category	Description	Capillary return	Muscle weakness	Sensory loss	Doppler signals	
					Arterial	Venous
Viable	Not immediately threatened	Intact	None	None	Audible (ankle pressure >30 mm Hg)	Audible
Threatened	Salvageable if promptly treated	Intact, slow	Mild, partial	Mild, incomplete	Inaudible	Audible
Irreversible	Major tissue loss, amputation regardless of treatment	Absent (mottling)	Profound, paralysis	Profound, anesthetic	Inaudible	Inaudible

Adapted from Rutherford RB, Flanigan DP, Gupta SK. Suggested standards for reports dealing with lower extremity ischemia. J Vasc Surg 1986;4:80.

TABLE 27.1. *Clinical categories of acute limb ischemia*

Grade	Category	Clinical description	Objective criteria
0	0	Asymptomatic	Normal treadmill/stress test
I	1	Mild claudication	Completes treadmill exercise*, ankle pressure after exercise <50 mm Hg but >25 mm Hg less than brachial
	2	Moderate claudication	Between categories 1 and 3
	3	Severe claudication	Cannot complete treadmill exercise and ankle pressure after exercise <50 mm Hg
II	4	Ischemic rest pain	Resting ankle pressure <40 mm Hg, flat or barely pulsatile ankle or metatarsal pulse volume recording; toe pressure <30 mm Hg
	5	Minor tissue loss—nonhealing ulcer, focal gangrene with diffuse pedal ischemia	Resting ankle pressure <50 mm Hg, ankle or metatarsal pulse volume recording flat or barely pulsatile; toe pressure <40 mm Hg
III	6	Major tissue loss—extending above transmetatarsal level, functional foot no longer salvageable	Same as category 5

Adapted from Rutherford RB, Flanigan DP, Gupta SK. Suggested standards for reports dealing with lower extremity ischemia. J Vasc Surg 1986;4:80.
*Five minutes at 2 mph on a 12% incline.

TABLE 27.2. *Clinical categories of chronic limb ischemia*

Once the indications for invasive therapy are clear (Table 27.3) and the anatomic substrate has been defined, the choice will be between conventional surgery and catheter-based techniques. The details of surgical therapy are beyond the scope of this chapter but typically involve placement of natural (saphenous vein) or prosthetic (Dacron or PTFE materials) to bypass or substitute for the diseased native artery. In some situations, such as the carotid artery, the native vessel is treated by surgical removal of the obstructing atheroma (i.e., carotid endarterectomy). In general, these operations are undertaken using general anesthesia, with significant blood loss and fluid shifts, in patients who may have profound involvement of other critical organ supply (e.g., extensive coronary artery disease). When it is possible to provide a similar level of correction and durability of benefit with catheter-based (e.g., endovascular) treatments, risk and disability may be minimized.

1. Natural history of the disease (likelihood of progression/regression)
2. Degree of ischemia (Rutherford category)
3. Current effect of the disease on mortality, morbidity, and lifestyle
4. Anticipated benefit of interventional therapy
5. Anticipated cost
6. Potential for complications

TABLE 27.3. *Factors influencing decisions regarding invasive therapy for peripheral vascular disease*

Endovascular therapy—the subject of this chapter—shares the same heritage as coronary intervention (see Chapter 23), through the pioneering work of Dotter, Judkins, Gruentzig, and others (4,5). In fact, most of the techniques now used in the coronaries (balloon dilatation, stenting, atherectomy) were first employed in the peripheral circulation. Recent innovations that have made such therapies safer and more effective include lower profile catheters, lubricious guidewire coating, debulking techniques, and endovascular stents (Fig. 27.1) (6,7 and 8). Outcome has also been improved by innovations and improvements in imaging techniques, such as digital enhancement of conventional contrast images (see Chapter 14) and intravascular ultrasound (IVUS) (see Chapter 19). The latter provides a cross-sectional view of the vessel similar to a histologic section and better comprehension of the mechanisms responsible for successful angioplasty (9,10,11,12,13,14 and 15). When catheter-based therapy is possible, it is attractive to patients, providers, and insurers, since it can usually be performed as a cost-saving "same-day" procedure with low morbidity and rapid convalescence. Even in instances where the degree of revascularization is not as complete or where symptomatic improvement may not be as durable, the reduced morbidity of a catheter-based therapy may make it attractive in high-risk patients (such as those with both severe CAD and limb-threatening ischemic ulceration due to infrapopliteal disease, where restoration of antegrade flow is required for ulcer healing and long-term limb salvage) (16). Lower-risk, *partial* revascularization by percutaneous means may thus be preferable to higher-risk attempts at *complete* surgical revascularization, particularly in high-risk patients with advanced age or other cardiovascular disease. The availability of effective, "less-invasive" percutaneous options for revascularization has also led to a reevaluation and reduction of the threshold for intervention. For example, a patient whose claudication is not severe enough to warrant major surgical bypass may nonetheless be appropriate for percutaneous transluminal angioplasty (PTA) (Fig. 27.1).

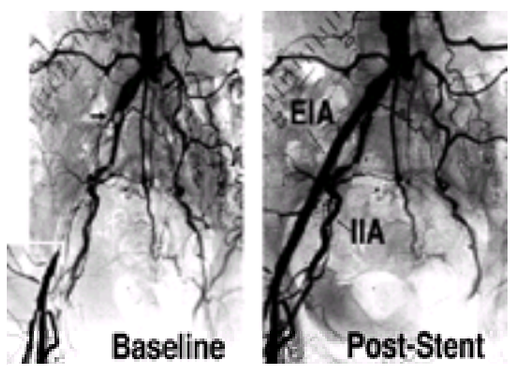

FIG. 27.1. Percutaneous revascularization in an 84-year-old female whose ability to live independently is compromised due to bilateral iliac artery occlusion and resulting severe (Rutherford class III) claudication. Lubricious, hydrophilic guidewire (Glidewire) facilitates traversal of lengthy, chronic iliac occlusion, low-profile high-pressure balloon provides effective dilation, and stenting enables a result superior to balloon angioplasty alone. Availability of these technologies enhances outcome and lowers threshold for intervention in such high-risk patients, who would not meet the higher threshold required for major surgical bypass. In this patient, anticipated fem-fem grafting was canceled, since symptoms improved enough to resume independent living after PTA/stent.

The current recommendations for revascularization at various peripheral sites are summarized in Table 27.4. Since therapy for many sites is evolving rapidly, vascular specialists must have a comprehensive understanding of all aspects of a given revascularization procedure, including (a) the indications for intervention, (b) the therapeutic alternatives available and their expected outcomes, (c) the techniques employed during an intervention, and (d) the potential complications. In the remainder of this chapter, we will review the various percutaneous treatments available for disorders in each region of the body, progressing from the thorax to the lower extremities.

TABLE 27.4. *Current revascularization strategy for various locations*

THORACIC AORTA

Disorders of the thoracic aorta requiring correction include coarctation, dissection, aneurysm, and patent ductus arteriosis (see Chapter 14). Until recently, surgery (often high-risk surgery) was the only option available for intervention at this level. The introduction of very large, low-profile balloons and oversized stents married to prosthetic graft material (stent grafts) has enabled the endovascular repair of many thoracic aortic disorders, particularly in patients with other comorbid conditions that may have previously excluded them from complex surgical correction.

Coarctation of Thoracic Aorta

Coarctation in Infancy

Coarctation of the thoracic aorta is a rare congenital disorder that typically presents early in life (less than 5 years). Although it may be isolated or idiopathic, it is more commonly associated with a variety of congenital cardiac disorders, including bicuspid aortic valve, hypoplastic left heart syndrome, or ventricular septal defect (VSD). For severe cases, correction is typically required during the first year of life to prevent complications such as congestive heart failure (CHF), severe hypertension, and cardiomyopathy (see also Chapter 28 and Chapter 34).

Adult Coarctation

De novo coarctation can also present in adulthood. Although there is not universal agreement about the treatment of these patients, a consensus is developing that balloon angioplasty should be utilized as the initial treatment modality (17,18,19 and 20), although others have recommended its restriction to patients with recurrent coarctation after surgery. In a series of 970 patients (17), the acute and long-term results of PTA for native and recurrent coarctation were found to be equivalent or slightly better in the native group. The treatment may be further improved by stenting (18,21), including the use of covered stent grafts for treatment for the pseudoaneurysm or aneurysm that may occur as a delayed complication of balloon angioplasty or surgical therapy of thoracic coarctation. To minimize dissection and recoil and to reduce the relatively high incidence of restenosis (up to 44%) (22), some interventionalists believe that primary stenting is appropriate. Long-term follow-up, however, will be necessary on a larger number of patients before establishing these catheter-based approaches as the primary therapy for coarctation.

Technique

Access to the coarctation is largely dependent on its location. Most lesions are at the isthmus, adjacent to the ligamentum arteriosum and just distal to the subclavian artery. Prograde access via the left subclavian or innominate artery (brachial approach) is possible, though the large profile of the balloons/stents required for treatment may present an increased risk for brachial artery injury. The retrograde femoral approach may therefore be preferable. A “pull-through” technique, using combined femoral and brachial (or transseptal) access, enables control of both ends of a single (0.035-inch) guidewire (“rail”) and may be helpful in counteracting the forceful jet of aortic blood flow, to facilitate accurate placement of a stent or stent graft. Balloon diameter should not exceed 1.1 times the size of the adjacent isthmus or descending aorta. Sizing to the diameter of the poststenotic dilation may lead to aortic rupture or dissection, particularly in the thin-walled poststenotic segment. Intravascular ultrasound may be of great utility for assessing vessel size and the result of intervention.

Thoracic Aortic Aneurysm

Considerable controversy exists regarding the indications and threshold for repair of thoracic aortic aneurysms (TAAs) (23,24 and 25). The relative infrequency (compared with abdominal aortic aneurysm), lack of associated symptoms, and perception that conventional surgical repair is associated with significant risk of spinal cord ischemia and paralysis limit enthusiasm for aggressive diagnosis and referrals for repair. Despite the tendency to ignore or treat medically, available data suggest that the natural history of TAA may be similar to that of AAA: both can be expected to progress and potentially rupture, particularly if the diameter is 6 cm or more, or there is associated dissection (see Chapter 14). For patients selected for surgery, significant morbidity or mortality in the hands of even the most experienced surgeons remains in the range of 10% or greater. The advent of stent grafts has provided a catheter-based alternative treatment, especially for high-risk patients. In a landmark report, Dake and colleagues (26) described the first series of patients undergoing endovascular TAA repair using stent grafts (see Chapter 35). While this study was not controlled or randomized, updated preliminary results from the same group (27) show a 6.8% 30-day mortality, which is superior to surgical series of TAA repairs.

TAA stent grafting remains highly experimental and is being performed by only a very select group of investigators. Anatomically favorable TAAs do not involve the great vessels of the aortic arch, have a 1- to 2-cm “neck” of aorta (beyond the subclavian origin) to anchor the stent, and suitable distal aortoiliac vessels to enable access with the large (22F to 28F) sheath. The etiology and extent of the aneurysm and coexisting distal disease thus must be clearly defined (by chest x-ray, spiral CT scan with three-dimensional reconstruction, and formal angiography) before undertaking stent grafting. A strategic approach must be developed in advance to ensure optimal stent deployment and avoid potential adverse events like graft migration by systolic flow. A number of purpose-specific newer stent-graft designs are being developed for treatment of TAA, to replace the homemade devices used in early clinical experience. As is the case with stent grafts placed at other sites, collaboration among specialists (surgeons and endovascular specialists) is essential for the successful completion of these procedures.

Aortic Dissection

Acute dissection of the aorta is catastrophic illness. Although the incidence is relatively low (approximately two cases per 100,000 of population), the consequences are potentially devastating. Left untreated, dissections of the ascending aorta (DeBakey type I or II/Stanford type A) have a nearly 90% 3-month mortality, because of extension with cardiac tamponade, aortic regurgitation, myocardial infarction, and/or CVA. Although dissections of the descending aorta (DeBakey type III/Stanford type B) are associated with a lower mortality (approximately 20%), their consequences include the possibility of ischemia in visceral organs or the lower extremity ischemia due to compromise of branches that arise from the abdominal aorta. Mortality for surgical repair in the setting of end-organ ischemia approaches 50% (28,29 and 30), particularly in patients with ongoing infarction of visceral organs (bowel, kidney, and others) or hemodynamic instability. Two novel strategies for treating acute aortic dissection have developed during this decade—balloon fenestration of the dissection flap and aortic stent grafting of the entry site.

Balloon fenestration (Fig. 27.2) seeks to relieve end-organ ischemia and prevent further extension of the dissection by creating a channel between the true and the false lumens that equalizes their internal pressure, improves blood flow to vessels arising from the false channel, and retards the forces responsible for distal propagation of the dissection (31,32). Although fenestration can be very effective in restoring flow to compromised branches, the aorta is still subject to delayed consequences such as rupture (as much as 20% of patients with chronic type B dissections) (33). Alternatively, Dake (34) and Kato (35) have used endovascular stent grafts to close the primary entry tear in the descending thoracic aorta. Type I and II (Stanford type A) dissections are more challenging for percutaneous techniques. Standard therapy for these dissections is surgical reconstruction of the aortic arch, which should be performed early to prevent the sudden and devastating consequences of retrograde dissection into the pericardium, right coronary artery, and cerebral vessels. The surgeon typically completes the repair of the aortic arch but does not address the remaining portion of the dissection flap, which extends into the descending and sometimes abdominal aortic segments. Early

results using stent grafts, either in conjunction with surgery or at a later time to complete the repair of the dissected aorta, have been encouraging (35).

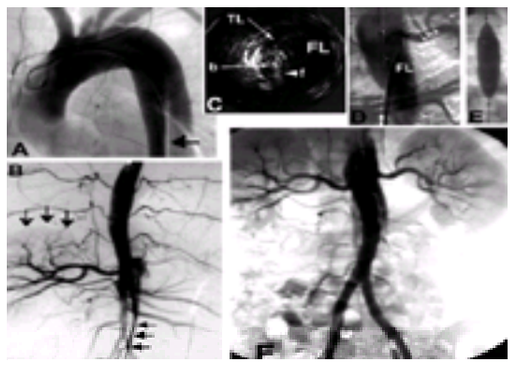

FIG. 27.2. Aortic fenestration for acute aortic dissection in a 42-year-old male with refractory severe hypertension, persistent pain due to extending dissection, and ongoing lower extremity ischemia and acidosis. Considering hemodynamic instability and anticipated difficult recovery from surgery, resulting from partial spinal cord paralysis, fenestration was erformed after diagnostic angiography. Bilateral femoral access required. **A:** Angiography shows classic flap (*arrow*) in thoracic aorta. **B:** Compression by false lumen obliterates descending aortic true lumen below renal arteries. Nephrogram seen on right (*arrows*), but not on left; underperfusion of left kidney is responsible for refractory hypertension (HTN). **C:** Intravascular ultrasound shows false lumen (FL) compressing true lumen (TL) and directs Brockenbrough needle (b) toward aortic flap (f). **D:** After fenestration, injection through Mullins dilator shows contrast in false lumen and left renal artery. **E:** Large balloon enlarges fenestration. **F:** Final angiogram after fenestration and stenting of distal abdominal aorta and common iliac arteries shows simultaneous filling of both renal arteries, restoration of outflow, and scaffolding of dissection flap. Patient's hemodynamic status corrected instantaneously and recovery/rehabilitation were greatly accelerated by absence of surgical incision and general anesthetics. Patient walking and stable 2 years postfenestration. Aortic size unchanged.

Treatment Considerations and Technique

Experience with percutaneous aortic fenestration is limited to only a few centers. Time is of the essence in making decisions about best treatment (conventional surgical fenestration vs. percutaneous fenestration). Noninvasive imaging (with TEE, CT, or MRI) must be performed to identify the primary entry site and Stanford type. If the dissection is type A, surgical repair of the thoracic aorta takes precedence. If the dissection is type B, fenestration may proceed. This requires bilateral femoral access, carefully advancing guidewires to retain their position within the true lumen. Complete aortography (starting with the LAO projection) from the aortic arch down to the abdominal aorta and iliac arteries should be performed before endovascular manipulation. On occasion, natural fenestrations may have occurred at sites where the native vessels are shorn off from the true lumen; these may be traversed and used as a starting point for balloon dilation. In most instances, however, the intimal flap will need to be punctured with a Brockenbrough (or similar) needle under intravascular ultrasound guidance, followed by balloon dilatation and stenting of the intimal flap below the fenestration site. The fenestration creates a new egress for blood flow from the false channel and may improve organ and limb perfusion by resolving compression of the true lumen (Fig. 27.2).

VESSELS OF THE AORTIC ARCH

Subclavian and Innominate Arteries

The vast majority of disease in these vessels is due to atherosclerosis, although giant cell arteritis (Takayasu) and fibromuscular dysplasia (FMD) can also cause clinically relevant disease (see Chapter 14) (36). Clinical indications for subclavian revascularization are listed in Table 27.5 (see also Fig. 27.3). Routine examination (measurement of cuff pressure and palpation of pulses in both upper extremities, plus auscultation over the supra- and subclavicular areas) will uncover a substantial number of vascular patients with asymptomatic subclavian disease. Such patients do not require treatment initially but should be followed closely for the development of related symptoms, especially if coronary bypass surgery has or will likely be performed and preservation of the internal mammary conduit is important.

Symptomatic ischemia of the posterior fossa (e.g., vertebral-basilar insufficiency)
Symptomatic subclavian steal syndrome
Disabling upper extremity claudication
Preservation of flow to LIMA/RIMA preop coronary bypass surgery, where LIMA/RIMA will be utilized
Postop CABG with ischemia in LIMA/RIMA territory (± coronary-subclavian steal syndrome)
Preservation of inflow to axillary graft or dialysis conduit
"Blue-digit" syndrome (embolization to fingers) (See. Fig. 27-3.)
Inability to measure blood pressure
Extensive cerebral territory completely subtended by the affected vessel

LIMA, left internal mammary artery; RIMA, right internal mammary artery.

TABLE 27.5. *Indications for subclavian or innominate artery revascularization*

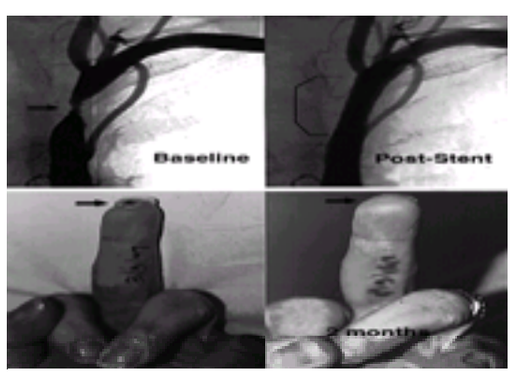

FIG. 27.3. Subclavian artery stenting for "blue digit" syndrome. **Upper left:** Severe irregular stenosis in left subclavian, associated with 60 mm Hg reduction in left brachial cuff pressure and (**lower left**) painful embolic ulcer at fingertip. **Upper right:** PTA/stenting (Palmaz P-204) performed via femoral approach using 85-cm-long, 7F sheath. Care used to avoid stenting over vertebral origin. **Lower right:** Healed ulcer 2 months after stent.

Until recently, surgical treatment (carotid-subclavian, aorto-subclavian, or axilloaxillary bypass or endarterectomy) has been considered to be the treatment of choice for subclavian disease. Subclavian and brachiocephalic (innominate) PTA was first performed in 1980 (37) and has potential advantages over surgery: It eliminates the need for general anesthesia, shortens hospital stay, is less invasive, and reduces overall morbidity. It also avoids concern about potential stenosis in the carotid artery, which serves as the donor for carotid-subclavian bypass. Most published series of subclavian PTA consistently report technical success and complication rates of more than 90% and less than 10%, respectively (38,39 and 40). Stenting may further improve the results, as recent series using primary stenting indicate (41,42 and 43). Complications are generally minor and infrequent but may include problems at the femoral or brachial access site, as well as inadvertent "jailing," dissection, or embolization of the vertebral or left internal mammary artery (LIMA), the latter of which may resolve after lytic therapy (44). Recurrence rates are generally low (5%

to 10%).

Direct comparison between surgery and PTA for subclavian disease is hampered by the absence of randomized controlled studies. Hadjipetrou et al., in their recent multicenter analysis, compared the results of primary subclavian stenting (in 108 patients) with those of 2,496 surgical patients reported in 52 papers from the literature (1966 and 1998) (45). The surgical series had complications of stroke in 3%, mortality in 2%, and overall complications in 13% of patients; the stent series had no strokes, no deaths, and 6% overall complications. Recurrence rate was 12% for surgical series and 3% for stent series, although follow-up was shorter in the latter. These data, however, mostly relate to *stenotic* disease rather than *occlusive* disease, which has a lower chance of success (5% to 75%) and an increased risk of embolization of thrombus or atheroma into the cerebral, upper extremity, or coronary circulation.

Treatment Considerations and Technique

Preprocedure

Thorough evaluation of the patient before undertaking subclavian or brachiocephalic angioplasty is essential. Noninvasive testing should include duplex evaluation, with determination of the direction of flow in the vertebral arteries (antegrade or retrograde, the latter indicating the presence of a steal syndrome) and documentation of associated carotid disease. If there is a clinical suggestion of vasculitis, then the erythrocyte sedimentation rate (ESR) should be measured. Premedication with aspirin is standard, with optional addition of clopidogrel bisulfate (Plavix, Bristol-Myers Squibb, Hillside, NJ) or ticlopidine hydrochloride (Ticlid, Roche Laboratories, Nutley, NJ). In cases of subclavian occlusion, because nascent thrombus may occur in the segment immediately beyond the occlusion, patients may benefit from anticoagulation (in conjunction with antiplatelet therapy) for a period of several weeks before revascularization.

Access

The femoral approach is used most commonly but requires careful catheter manipulation in the diseased aortic arch to avoid atheroembolic complications. The brachial approach, described by Dorros (3,9), may be useful for total occlusions, especially for those that are “flush” with the aorta. Embolization to the brachial artery can be controlled with this approach, particularly if it is done via a cutdown. However, a higher access-related complication rate has been reported when using brachial entry, whether percutaneous or cutdown.

Catheters and Guidewires

A nonselective aortic arch angiogram, using a multiple side-hole catheter, such as a pigtail, should be obtained to provide a “road map” before gaining selective access into the subclavian or innominate artery. It may be possible to steer a guidewire directly across a stenosis from the aortic sheath, but crossing a total occlusion generally requires prior selective cannulation of the subclavian with a diagnostic catheter (JR4, cobra, Simmons, etc.) and advancement of the guidewire through the catheter. The diagnostic catheter is then advanced across the stenosis (or occlusion) over the wire, where it is used to measure a baseline pressure gradient and place a longer or heavier guidewire, if necessary, to allow exchange of the diagnostic catheter for either a long-sheath (6F or 7F, 80 to 90 cm) or an 8F to 9F coronary multipurpose or right Judkins guiding catheter.

Balloons and Stents

With the guiding catheter placed into the proximal vessel, predilation is performed with an undersized (usually 4 to 5 mm in diameter) balloon. The guiding catheter or sheath is then advanced over the balloon into the distal vessel, to facilitate passage of the stent. A stent of appropriate size and length to cover the lesion should be selected. Both balloon-expandable and self-expanding steel or nitinol stents have been used, but no stent has yet received specific approval by the Food and Drug Administration (FDA) for use in the subclavian artery.

If the lesion is adjacent to or spans across the origins of the vertebral and/or IMA, attempts should be made to avoid placing these vessels into “stent jail.” Most left subclavian lesions are located proximal to the vertebral artery, where use of either balloon-expandable or self-expanding stents is reasonable. For lesions located beyond the internal mammary artery, self-expanding stents should be used to avoid the potential for late stent compression by extravascular structures at the thoracic outlet. When stenting the brachiocephalic (innominate artery), care should be taken to avoid impinging upon the origin of the right common carotid artery with a stent. Stents should be postdilated at 8 to 18 atmospheres, to match the size of the subclavian artery (generally between 5 and 8 mm). Overdilation should be avoided to minimize the risk of dissection that might extend into the vertebral artery or internal mammary artery. If such dissections do occur, they can often be salvaged by placement of a stent within the origin of affected branch vessel, although distal extension of the dissection within the branch vessel may render attempts at salvage futile. Following postdilatation, completion angiography and pressure gradients should be obtained, demonstrating complete elimination of the gradient.

Follow-up

No data exist regarding the use of Plavix or Ticlid, though many maintain this regimen for 4 weeks following the procedure. During clinical follow-up, the resolution of symptoms should be documented, equalization of blood pressures in both upper extremities should be confirmed, and the duplex study should show triphasic brachial wave forms with restoration of normal antegrade flow in the vertebral arteries. Restenosis within subclavian arteries occurs in 10% to 20% of patients and may be treated by stenting (if not stented initially) or balloon angioplasty (for in-stent restenosis). Stent “compression” should be treated by balloon reexpansion and placement of a self-expanding stent within the old device.

Vertebral and Basilar Arteries

Vertebral artery stenosis is a common finding in patients undergoing arch or subclavian angiography. Although the vertebral artery is usually easy to access, revascularization is indicated *only* in patients with indisputable symptoms of vertebral basilar insufficiency (VBI) (Table 27.6). In rare instances, a patient with an obstructed carotid may present with classic carotid, as opposed to vertebral, ischemia. In such cases, if the vertebral gives rise to collaterals (via posterior communicating artery), then PTA of the stenotic vertebral lesion is justified (Fig. 27.4). The significant “down side” of failed or complicated vertebral PTA (including potentially fatal brainstem CVA) makes case selection critical. Before undertaking vertebral intervention, therefore, it is important to define the pattern of intracerebral blood flow and collateral circulation (with MRA or four-vessel angiography).

Visual disturbance	Diplopia
Language/speech disturbance	Global aphasia, dysarthria
Altered state of consciousness	Confusion, syncope
Vestibular dysfunction	Dizziness, vertigo

TABLE 27.6. *Symptoms of vertebral-basilar insufficiency (VBI)*

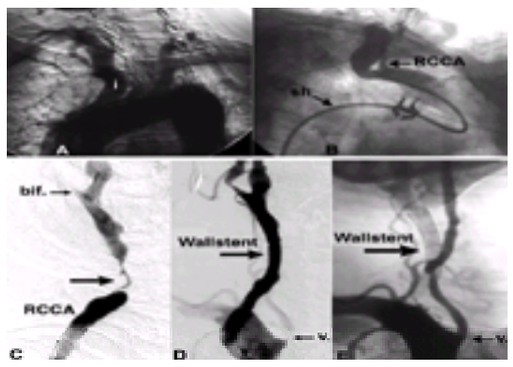

FIG. 27.4. Right carotid and vertebral stenting in 65-year-old male with prior radical neck dissection and irradiation for laryngeal CA [residual tracheostomy, prior left hemispheric CVA due to left internal carotid artery (ICA) occlusion, left vertebral occlusion, and recurrent syncopal episodes from global cerebral ischemia]. **A:** Initial attempt to obtain guiding catheter or sheath access in extremely tortuous right innominate (i) failed. **B:** Second attempt succeeded using 8F Arrow Flex sheath (sh), which provided adequate support for carotid/vertebral angiography and stenting. Flow pattern to CNS is via collaterals (thyrocervical to external carotid, then retrograde in ECA to bifurcation [bif.] and antegrade up ICA). Right ICA then cross-fills to left ICA. **C:** Critical RCCA stenosis (*arrow*) at baseline. **D:** Status post PTA/Wallstent RCCA. Antegrade flow restored to ECA; however, vertebral artery origin (v.) is severely narrowed. **E:** Vertebral patent after coronary stent (Multilink). Symptoms completely resolved. Stents patent at 6-month follow-up angiography.

Intervention in the basilar artery is considered to be even more dangerous than in the vertebral, because it is a “terminal vessel” that is responsible alone for perfusion to a number of critical central nervous system (CNS) areas, especially the brainstem. Accordingly, basilar artery PTA is reserved for the rare instances in which patients present with symptoms unequivocally related to a critical stenosis or acute occlusion. Revascularization in the latter case often requires use of thrombolytic therapy (46,47,48,49 and 50) and can produce dramatic recovery of patients who were previously near death. Given the high stakes involved in vertebral/basilar instrumentation, the Neurology Department should be involved in any decisions regarding therapy for the posterior cerebral circulation.

Treatment Considerations and Technique

The technique of vertebral angioplasty is similar to that for subclavian (or ostial coronary) PTA. The femoral approach is generally used, and a coronary guiding catheter or long sheath (Fig. 27.4) is advanced into the proximal subclavian artery over an “introducing” catheter or dilation to avoid scraping any proximal disease. The vertebral artery stenosis is crossed with a 0.014-inch or 0.018-inch wire, over which a coronary or small vessel balloon (2.5 to 4.5 mm) is advanced to dilate the vessel. Careful neurologic evaluation should be performed during and after the balloon inflation. Intraarterial nitroglycerin should be administered in cases of distal spasm, to be distinguished from pleating or “pseudostenosis” caused by guidewires straightening a tortuous vessel. Patients should be well heparinized and extreme caution should be applied to prevent air embolism. Unlike many other vascular sites, routinely crossing the dilated site with the guiding catheter is not recommended, because of the potential for additional disruption of the lesion and plaque embolization. For stenting ostial lesions, stents should be placed either flush with the origin or protruding 0.5 to 1.0 mm into the subclavian artery. Completion angiography with intracerebral views and postprocedure neurologic reevaluation are both useful.

Carotid Arteries

Atherosclerotic disease occurs predominantly at the common carotid bifurcation, a site that is conveniently accessible for surgical carotid endarterectomy (CEA). Stenosis at the origin or proximal aspect of the common carotid artery is less common, and surgical treatment may require thoracotomy or subclavian-carotid bypass. Since the first CEA more than 30 years ago, the morbidity, mortality, cost, and patient inconvenience associated with this procedure have been reduced considerably. The landmark North American Symptomatic Carotid Endarterectomy Trial (NASCET) and Asymptomatic Carotid Artery Study (ACAS) trial demonstrated that surgical endarterectomy, when performed for carotid bifurcation disease by experienced vascular surgeons on appropriately selected patients, is more effective in reducing the likelihood of stroke than is medical therapy (51,52). Therefore CEA is currently recognized as the gold standard of therapy for conventional patients deemed to require carotid revascularization.

Carotid balloon angioplasty (CPTA) was performed as early as 1983, but due to the excellent results associated with CEA and concerns about the potential for distal embolization (53) and vessel recoil/thrombosis, the use of PTA for carotid disease (especially at the bifurcation) was limited to single-center, anecdotal reports (54,55,56 and 57). In the 1990s, work by Roubin, Iyer, Yadav, Vitek (58,59), and others (60,61 and 62) has demonstrated superior results for primary (as opposed to provisional) stenting in carotid arteries, apparently due to more complete effacement of the plaque and associated ulcerations (Fig. 27.5), reduction in elastic recoil, and restoration of laminar flow.

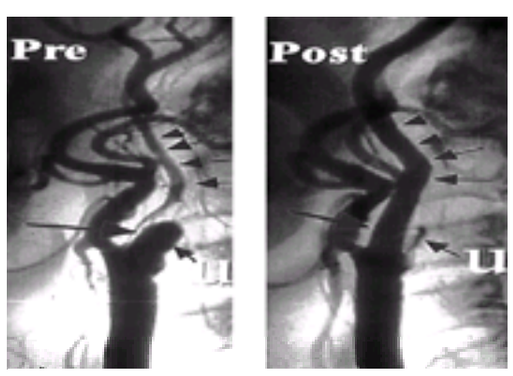

FIG. 27.5. Carotid PTA/stent deployment in 77-year-old male with unstable angina on IV nitroglycerin, awaiting CABG. Contralateral internal carotid artery (ICA) is occluded, and ipsilateral (left) is critically narrowed (*large arrow*). Distal ICA (*small arrow*) is atretic due to underperfusion. Large ulcer (u) is located at ICA origin. Surgeon reluctant to do CABG until carotid revascularized. CPTA/stent performed via 7F Cook “shuttle” catheter placed in CCA. Atraumatic 0.014-inch coronary guidewire used to cross lesion, predilation performed with 3.5-mm coronary balloon, then Wallstent placed, extending back into CCA. Post stent, distal ICA restored to normal caliber, ulcer (U) is compressed and was absent on 6-month follow-up angiogram. Patient had uneventful CABG and remains asymptomatic at 4 years.

Not since the advent of balloon angioplasty itself has a single issue within cardiovascular medicine raised as much controversy as the topic of carotid angioplasty and stent placement (63,64,65,66 and 67). In most institutions, percutaneous treatment of carotid arteries has been reserved for those circumstances wherein the surgical risk is increased (59,61,68,69,70,71,72 and 73) (Table 27.7). But favorable intermediate-term results are now available (74,75 and 76), suggesting safety and efficacy comparable to CEA. This is particularly true when the selection of patients at higher risk for surgery is taken into account (Fig. 27.4 and Fig. 27.5). In Roubin's update as of May 1999 (personal communication), a total of 482 patients (569 vessels) underwent elective stent placement over a 5-year period. Mean age was 69 years, with a range of up to 89 years, and other high-risk features included severe CAD in 80%; hypertension in more than 60%; ongoing tobacco abuse in 40%; and diabetes mellitus in 20%. Approximately 40% had symptomatic cerebral ischemia, and higher-risk anatomic features included contralateral occlusion (10%), prior ipsilateral CEA (17%), and many causes of unfavorable surgical anatomy (high or low lesion location, prior irradiation and/or radical neck dissection, subtotal occlusion with underperfusion of distal vessels). Despite these challenges, the technical success (ability to dilate and stent the lesion, and reduce narrowing to less than 30%) was 98%. There was one early case of stent thrombosis, and acute (30-day) results were comparable to CEA for this cohort: Eight patients (1.6%) died (half not related to the procedure); 4 (0.8%) had major CVA; and 29 (5.1%) had minor, nondisabling stroke (lasting more than 24 hours but resolved by 30 days). Despite the use of stents and delivery systems never intended for application in carotid arteries, the successful outcomes in this and other smaller series has led to speculation that this less invasive approach might be applied more widely for the treatment of carotid artery disease, even for traditional average-risk surgical candidates. Prospective randomized trials have been initiated to compare the percutaneous versus surgical modalities (66).

TABLE 27.7. *Proposed classification and strategy for patients currently undergoing carotid revascularization*

Treatment Considerations and Technique

For a list of treatment considerations and technique considerations for extracranial carotid PTA/stenting see Table 27.8.

TABLE 27.8. *Treatment considerations and technique for extracranial carotid PTA/stenting*

Preprocedure Evaluation

Before undertaking carotid stenting in an individual patient, a complete neurologic examination should be performed by a board-certified neurologist, with documentation of the National Institutes of Health (NIH) stroke scale. A baseline computed tomography (CT) or magnetic resonance imaging (MRI) evaluation of the head and carotid duplex should be obtained. Complete informed consent should be obtained from the patient, with participation of the family. Premedication should include aspirin (325 mg) once or twice daily, and Plavix (at least 375 mg before intervention), and prehydration to minimize hypotension. Baseline angiographic information should include nonselective angiography of the aortic arch (left anterior oblique [LAO] projection) with selective four-vessel (or at least two-vessel) cerebral study. Formal NASCET measurements must be made on the offending lesion.

Carotid Angioplasty Procedure

Some equipment required for CPTA/stenting is listed in Table 27.9. Femoral access is the standard approach. Using either a 9F coronary guiding catheter or a special 7F, 85-cm-long nonkinkable sheath (Cook [Bloomington, IN] “Shuttle” catheter or “Arrowflex” sheath). The long sheath minimizes the size of the puncture and tends to lie more coaxially within the common carotid artery, but it may be more difficult to manipulate. Selective cannulation of carotid arteries may be difficult in some instances because of the angle at which they arise from the aorta. This problem can usually be overcome by using a Vitek or Simmons catheter for selective common carotid cannulation, followed by placement of stiffer guidewires into distal *external* carotid artery, ultimately allowing the guiding catheter to be advanced into the common carotid over a smaller catheter or inner dilator. If the distal common carotid artery has a severe stenosis, then this site should be avoided by maintaining guidewire position proximal to the stenosis. It is also advisable to have available equipment suitable for opening intracerebral branches that may be occluded by distal embolization from the carotid lesion (so-called neurovascular rescue, Table 27.10, with an operator trained in intracerebral intervention.

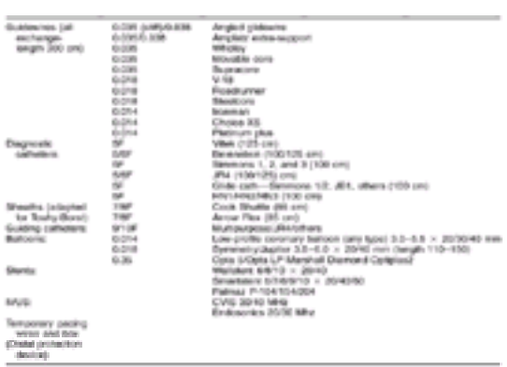

TABLE 27.9. *Equipment for carotid PTA/stenting (1999)*

Wires
Transcend (0.014-inch, 185 cm) (BSC) soft coronary wire (any brand) (hydrophilic and nonhydrophilic)
Micro catheters for infusion/exchange
Rapid Transit (3F, 150 cm) (Cordis)
or
Renegade (3F, 150 cm) (BSC)
Guiding catheters
Envoy—multipurpose or angled (6F, 120 cm) (Cordis) balloons
Ninja 2 mm × 10/15/20 mm (150 cm) (Cordis)
or
Stealth 2 mm × 10/15/20 mm (150 cm) (Target)
Alternatives: Predator (Cordis) or Ranger (BSC)
Pharmacolytics—urokinase, tPA, Retavase
IIb/IIIa inhibitors
Air filters
Pressurized bags of heparinized saline

TABLE 27.10. *Typical neurovascular “rescue” kit*

There are certain principles to which one must always adhere when treating carotid or cerebral vessels: First, catheters should always be bled back, so as to avoid any air or cholesterol/plaque embolization. Second, anticoagulation should commence before advancing any catheters into the carotid system. Third, less time in the carotid system is better. Although one should be cautious and deliberate in the performance of these procedures, the number of complications increases with additional intraarterial time. Fourth, catheter advancement should always be over a wire, and larger catheters should be transitioned in a stepwise, coaxial fashion over smaller catheters. Fifth, only atraumatic guidewires should be advanced into the internal carotid artery, to minimize the risk of spasm or dissection. Sixth, predilation is strongly advised, so as to confirm the ability to dilate the stenosis. Seventh, the use of self-expanding stents is preferred for the carotid bifurcation and other "compressible" sites (77,78 and 79). Balloon-expandable stents should be used only for aortoostial carotid lesions and distal (e.g., intracranial) internal carotid artery lesions. Eighth, when encountering resistance during advancement of balloons or stent delivery systems, removal and redilation with lower profile devices is appropriate. If a self-expanding stent will not easily cross a predilated lesion, it should not be forced. If redilation and readvancement are unsuccessful, placement of a short balloon-expandable stent to "scaffold" the plaque may facilitate subsequent placement of a self-expanding stent. Ninth, careful periprocedural hemodynamic monitoring is essential. Manipulation within the area of the carotid sinus can cause both acute and prolonged hypotension and/or bradycardia (80), requiring fluid resuscitation, atropine, or alphaadrenergic agents. Pacing is rarely needed but should be readily available (81,82). Postprocedure hypertension must also be avoided, so as to minimize the chances of "hyperperfusion syndrome," a potentially devastating entity that is occasionally seen following revascularization, particularly in elderly patients with previous near occlusion and underperfused CNS. Tenth, postdilation should be performed to relatively low or nominal pressure. Complete elimination of the stenosis is not necessary to achieve an excellent result (83). Indeed, attempts to reduce the stenosis to zero relative to the reference segment may lead to distal embolization or dissection.

Stent Selection

It remains to be determined what will be the best stent design for use in the carotid arteries. Balloon-expandable Palmaz biliary stents were used initially by many groups, with excellent results reported by Wholey (68), Diethrich (60), and Satler (74). However, the infrequent but troublesome occurrence of stent compression (78,79) has led most investigators to favor the use of self-expanding stents (such as the Wallstent) at the carotid bifurcation. There is more limited experience with the newer nitinol stents (BSC Integra, Cordis Smart, Bard Memotherm, and Guidant Acculink), all of which have undergone feasibility trials in the United States. Most investigators agree that the future of carotid stenting will employ nitinol, self-expanding stents that are lower profile, 0.014- to 0.018-inch based, and able to be placed accurately.

Distal Protection

There is tremendous enthusiasm surrounding the development of distal protection devices to avoid embolization during carotid angioplasty. Clinical trials have already begun in Europe, using both balloon occlusion devices and filter devices. It is anticipated that these may significantly reduce the embolic complications associated with CPTA/stenting.

ABDOMINAL AORTA

Abdominal Aortic Aneurysm

The endovascular repair of abdominal aortic aneurysms using stent grafts represents one of the most dramatic advances in the "less invasive" treatment of vascular disease. Although this field is still in its infancy, great strides have been made with the devices and technology so that most patients with abdominal aortic aneurysmal disease requiring repair would likely qualify anatomically for one of the available devices. Nonetheless the current gold standard for treatment of this disorder remains open surgical repair, against which any proposed alternative must be compared.

The indications for repair of abdominal aortic aneurysms (AAA) have been discussed previously (see Chapter 14). A substantial number of patients who have aneurysms greater than or equal to 5 cm in diameter are not deemed to be candidates for surgery because of unsuitable anatomy or the presence of comorbid conditions. The prognosis is grim for these patients, as described by Perko et al. (84). Of the 170 patients deemed inoperable, 132 patients (78%) died during the period of the study; 78 patients (59%) died specifically from rupture. For those who *are* surgical candidates, the operative mortality of aneurysm resection is between 1.4% and 7.6% (85) but increases substantially for those whose aneurysms are symptomatic. The potential for endovascular stent grafts to lower the morbidity and mortality in these high-risk or inoperable patients has provided a compelling reason to actively pursue the development of these devices. The first stent graft in a human was performed by Parodi in Argentina (86), who implanted a straight Dacron tube graft affixed at its proximal end to a large balloon-expandable Palmaz stent. A distal stent was subsequently added to the device to control retrograde flow into the aneurysm sac (endoleak). Several stent grafts have since been developed and subjected to clinical trials: Guidant EVT, Boston Scientific Vanguard, Medtronic AVE AneuRx, Medtronic AVE Talent, Cook Zenith, Corvita Endograft, and Gore Prograft. Two (the AneuRx and EVT devices) received FDA approval in 1999 and are commercially available. To address the fact that abdominal aortic pathology in these patients frequently extends into the iliac vessels, most abdominal endografts are now bifurcated or aortomonoiliac devices that extend into the distal vasculature to achieve a more complete seal. In the case of the latter, the other iliac artery may be perfused via a fem-fem bypass graft.

More than 5,000 stent-graft procedures for abdominal aortic aneurysm exclusion have been performed worldwide. D'Ayala, Hollier, and Marin summarized the results in 767 patients: success rate, 74% to 100%; persistent endoleaks in 14% (one-third of which closed spontaneously); 81% conversion to open AAA repair; and 4% mortality (87). More recently, a published series describe the multicenter prospective experience with the AneuRx stent graft (88) and the Boston Scientific Vanguard (85) devices. Both demonstrate success rates approaching 90%, endoleaks in approximately 10%, and less morbidity than with conventional repair, but both have a steep learning curve that entails mastering device and patient selection issues. Aneurysms with a short or absent proximal neck (distance between the lower border of the renal artery and the beginning of the aneurysm) are more difficult to treat, although some device iterations now incorporate additional bare stent material designed to be deployed proximally overlying the renal vessels, with the graft material beginning just below the renal arteries. Other issues remain, such as the obligatory sacrifice of one or both of the internal iliac arteries (which sometimes have deleterious consequences) and the large device caliber (12F to 28F). As with endovascular treatment of other vascular sites, the success of most endovascular stent-graft programs is due in large part to the spirited collaboration between vascular surgeons and endovascular specialists in cardiology and/or radiology.

Renal Arteries

Renal artery stenosis is a relatively common manifestation of generalized atherosclerosis that tends to be underdiagnosed and undertreated. The goals of renal artery revascularization are to improve control of hypertension, preserve or restore renal function, and/or treat other potential adverse physiologic effects of severe renal artery stenosis (congestive heart failure, recurrent flash pulmonary edema, and angina) (89,90). The options available for renal artery revascularization include surgery (endarterectomy, aortorenal bypass, or "extraanatomic" bypass using hepatorenal, splenorenal, iliorenal, or SMA-renal anastamoses) and PTA, with or without stent deployment. Balloon angioplasty of the renal arteries was first performed and by Gruntzig (91) in 1978 and, with the advent of stenting, has gradually superseded surgery as the treatment of choice for most patients with renal vascular disease. When analyzing indications and results, it is important to distinguish between the two major etiologies of renal artery stenosis: fibromuscular dysplasia (FMD) and the more common atherosclerotic disease.

Fibromuscular Dysplasia

When FMD is localized within the main renal artery or its primary branches, it can be treated quite effectively with balloon angioplasty alone (92) (see Fig. 35.10). Initial technical success exceeds 90%, and initial clinical success (elimination or significant reduction in hypertension at 6-month follow-up) is roughly 87%, with a 5-year recurrence rate under 10%. FMD that involves multiple branch vessels and/or aneurysmal disease, however, is better treated surgically, potentially utilizing the technique of "bench" (e.g., extracorporeal) reconstruction of the branch vessels.

Atherosclerotic Renal Artery Stenosis

Percutaneous treatment of atherosclerotic renal artery stenosis (ARAS), which causes the vast majority of renal artery narrowing, has been less gratifying than that of FMD. During the 1980s, balloon angioplasty proved to be safe and effective but had a restenosis rate that approached 70% at 6 to 12 months. The high restenosis rate following balloon angioplasty previously served as a compelling reason to recommend primary surgical revascularization in appropriately selected patients who were good surgical candidates, despite surgical mortality of 2% to 17% (93).

In the 1990s, however, numerous investigators have demonstrated more complete amelioration of the stenosis and transstenotic pressure gradient following stent

deployment in aortoostial lesions, compared with balloon angioplasty alone, with a lower restenosis rate. In a recent position paper, Palmaz (90) summarized the results of stenting in 349 patients from eight series, followed for a mean duration of 10.9 months. Hypertension was improved in 56% and cured in 10%; renal function improved in 27% and stabilized (e.g., no further deterioration) in 38%. Restenosis occurred in approximately 16% of patients, with major complications in 4.9%, but these were reduced in the more recent series. Palmaz speculated on the “clear” and “not-so-clear” indications for revascularization of RAS (Table 27.11). In general, the current indications for renal artery PTA and stenting are threefold: (a) control of hypertension (Fig. 27.6); (b) elimination of congestive heart failure/flash pulmonary edema (Fig. 27.6); (c) preservation or salvage of renal function (Fig 27.7).

“Clear” or primary indications:
Renal failure
1. RAS in patient with dialysis-dependent renal failure
2. RAS in patient with recurrent flash pulmonary edema
3. RAS in patient with nondialysis-dependent renal failure
“Not-so-clear” or secondary indications:
Normal renal function.
(In decreasing order of relevance)
1. Bilateral RAS in patients with hypertension that is difficult to control
2. RAS in patients with single functional kidney
3. Unilateral RAS in patients with hypertension that is difficult to control
4. Unilateral RAS in the asymptomatic, elderly patient
5. Unilateral RAS in the asymptomatic, young patient

RAS, renal artery stenosis.
After Palmaz. *J Vasc Interv Radiol* 1998;9:530.

TABLE 27.11. *Indications for revascularization of RAS*

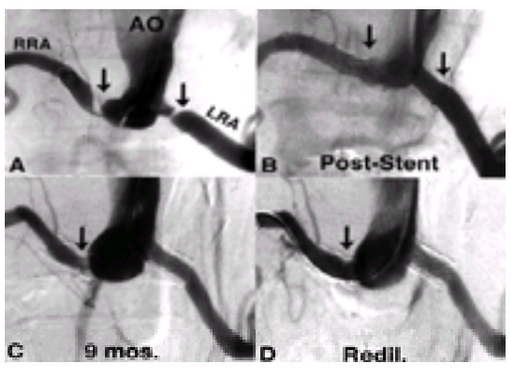

FIG. 27.6. Most renal artery stenting is performed via femoral access (Fig. 27.7 and Fig. 35.9, Fig. 35.10, Fig. 35.11, Fig. 35.12, Fig. 35.13, Fig. 35.14, Fig. 35.15, Fig. 35.16, Fig. 35.17, Fig. 35.18 and Fig. 35.19). However, in this 68-year-old female with progressive hypertension (BP = 230) despite five medications, brachial access is required due to chronic occlusion of infrarenal aorta. **A:** A long, nonkinkable 6.5F or 7F sheath was placed for baseline angiography. **B:** After predilation, bilateral critical stenoses are stented in a clinical trial using Palmaz P-154s. Clinical response was immediate. **C:** At 9 months follow-up, clinically silent moderate restenosis seen in RRA. **D:** This generally responds well to repeat dilation alone.

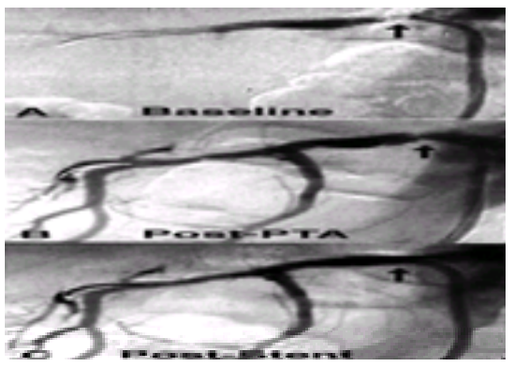

FIG. 27.7. Reversal of renal failure with stenting. Seventy-four-year-old male with baseline renal insufficiency (creatinine 2.8) who developed acute anuric renal failure following CABG. **A:** After doing poorly on dialysis for 3 weeks, angiogram was performed, showing critical stenosis to solitary kidney. **B:** Suboptimal result after PTA, due to recoil/plaque fracture. **C:** After stent, patient no longer required dialysis and remains off dialysis at 3-year follow-up.

Many patients who undergo renal artery revascularization, however, fail to demonstrate any significant clinical response. For patients with hypertension, the following clinical factors are predictive of a successful outcome: (a) rapid acceleration of hypertension over a number of weeks or months, where blood pressure was previously well controlled on a stable medical regimen; (b) presence of “malignant” hypertension (e.g., “end organ” effect); (c) hypertension in association with flash pulmonary edema; (d) contemporaneous rise in creatinine; and (e) development of azotemia in response to ACE inhibitors, administered for control of hypertension. For patients with congestive heart failure, those with episodic flash pulmonary edema (as opposed to gradual fluid retention), especially in the absence of ischemic coronary disease or LV dysfunction, have the best response. For salvage or preservation of renal function, those with (a) recent rapid rise in creatinine, unexplained by other factors; (b) azotemia resulting from ACE inhibitors; and (c) absence of diabetes or other causes of intrinsic kidney disease have the best response. One strongly predictive anatomic factor is the presence of “global renal ischemia,” wherein the entire functioning renal mass is subtended by critical bilateral stenosis or unilateral stenosis in a solitary kidney. On the other hand, patients with unilateral RAS, normal renal function, and mild or moderate hypertension that is well controlled medically, may derive little immediate benefit and should probably be followed longitudinally, with careful reevaluation of renal function, kidney size, and control of blood pressure. At the other extreme, patients with severe baseline renal insufficiency secondary to nephrosclerosis (e.g., diabetic nephropathy) with superimposed RAS but minimal associated pressure gradient, or a kidney shrunken to less than 8 cm in length, are unlikely to benefit from renal artery intervention.

Treatment Considerations and Technique

Access. Renal artery angioplasty and stenting are usually performed via the retrograde femoral approach. Because the proximal renal artery segment initially courses inferiorly and posteriorly, some interventionalists prefer the brachial approach to allow more coaxial alignment, despite the greater incidence of vascular entry site complications. Except for when the aorta is occluded distally (Fig. 27.6) or the renal artery takeoff is so severely angulated as to preclude stent delivery from below, the femoral approach is preferred by most interventionalists.

Diagnostic Angiography. Diagnostic angiographic techniques are described in Chapter 14. Nonselective arteriography is recommended before selective cannulation to identify the location of the renal ostia and the configuration of the aorta, and minimize the need for catheter manipulation in a diseased, atherogenic aorta. Once the ostia are identified, selective cannulation may be performed with several shaped catheters (IMA, Simmons, Sos-Omni), and the guidewire is passed across the lesion so that the diagnostic catheter can be advanced over it to measure a baseline pressure gradient. A significant pressure gradient is anything in excess of 10 mm Hg mean and/or 20 mm Hg peak (as measured through a 4F or 5F catheter). Below this level of gradient, a patient is unlikely to benefit dramatically with respect to blood pressure control or renal function, although an argument could be made to treat in order to prevent progression.

Balloon Inflation and Stent Deployment. Following diagnostic measurements, the diagnostic catheter is exchanged over the guidewire for a guiding catheter (renal double curve or hockey stick) that is advanced with the nose of the predilatation balloon protruding. Predilatation with a slightly undersized balloon is recommended, and the guiding catheter is then advanced into the mid-renal artery over the deflating balloon. This then allows stent advancement across the lesion within the guiding

catheter, which is in turn withdrawn slightly to expose the stent for expansion. After confirmation of appropriate stent position, taking into account any expected foreshortening of the stent and the need for the stent to extend slightly (0.5 to 2 mm) into the aorta to cover true ostial lesions, the stent is deployed. Postdilation to high pressure (10 to 14 atm) is performed with care to avoid overdilation (heralded by severe discomfort) or dissection of the distal, nonstented vessel. Final angiography, pressures measurement, and intravascular ultrasound (IVUS) can be used to assess the outcome, especially if there remains a question regarding stent apposition or lumen size (Fig. 27.8). The guiding catheter is then removed over the wire.

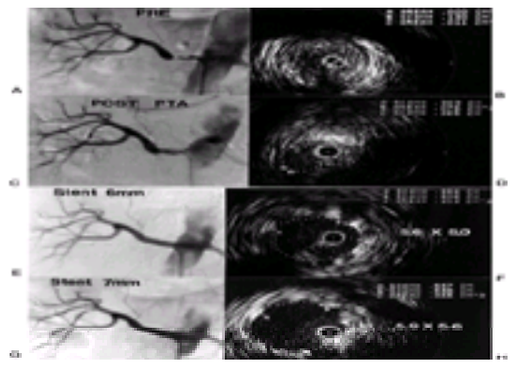

FIG. 27.8. PTA of proximal renal artery lesion, guided by intravascular ultrasound (IVUS). **A:** Baseline angiogram depicts severe proximal renal artery stenosis. **B:** Corresponding IVUS image shows plaque abutting catheter circumferentially. **C:** Post-PTA, irregular lumen with plaque fracture and residual stenosis. **D:** IVUS post-PTA shows only modest enlargement of lumen. **E:** Deployment and dilation of Palmaz stent with 6-mm balloon; angiographic result much improved over PTA alone. **F:** IVUS shows doubling in lumen diameter over PTA alone. However, in spite of excellent angiographic appearance, IVUS shows that diameter of treated segment is still less than "reference segment." **G:** After inflation with 7-mm balloon, the angiographic result is slightly better. **H:** IVUS now shows that the size of the stented vessel is equal to that of the reference segment. This case highlights the utility of IVUS in renal angioplasty.

Periprocedure Care. Fluids should be administered liberally before, during, and following the procedure. Diuretics can be used to prevent volume overload. Postprocedure monitoring of the hemodynamic state is mandatory. Some patients with "global renal ischemia" may experience a significant fall in blood pressure as the high-renin state abates, particularly if they have been allowed to become volume depleted. Blood pressure medications may be reduced in anticipation of this response, but complete withdrawal of all antihypertensive medications is ill advised in patients with coexisting coronary artery disease. Since the full clinical response to renal artery revascularization may not occur until 1 to 2 weeks after the intervention, blood pressure, creatinine, and medications should be reevaluated at 2 to 4 weeks follow-up.

Complications. Complications related to balloon angioplasty and/or stenting of renal arteries occur in less than 10% of patients and most commonly involve access. The most feared complication, however, is that of atheroembolism into either the renal or peripheral vascular bed. This is more likely to occur with aggressive manipulation of the diagnostic and/or guiding catheters; vigorous catheter manipulation can be avoided through identification of the renal ostia on a nonselective angiogram before selective cannulation with a soft, atraumatic diagnostic catheter. The signs of cholesterol embolization include persistent hypertension despite successful renal artery revascularization, gradual rise in creatinine over the succeeding weeks or months, presence of livido reticularis on the abdominal wall or in the lower extremities, and presence of eosinophilia on a peripheral blood smear. There is no known effective treatment for the renal manifestations of cholesterol embolization once it occurs, although some have reported the effective resolution of ischemic rest pain and ulceration using intravenous prostaglandin (94).

Other complications of percutaneous renal revascularization include dissection of the renal artery or the wall of the aorta, acute or delayed thrombosis, infection, and rupture of the renal artery.

Mesenteric Arteries

Indications for Treatment and Results

Stenosis of mesenteric vessels is a frequent finding during routine angiographic studies of the abdominal aorta, but ischemic consequences of those stenoses are rare due to redundant blood supply. The classic syndrome of mesenteric angina includes postprandial abdominal pain, gas, diarrhea, food avoidance, and weight loss; it is uncommon absent severe global compromise of blood supply to the mesentery (such as occlusion of two out of three mesenteric vessels, and a critical stenosis in the third). Patients with lesser degrees of ischemia will present with variable symptoms, including mild postprandial discomfort, diarrhea, nausea, or gaseousness. The angiographic diagnosis can be as ambiguous and difficult as the clinical manifestations. Because the mesenteric vessels originate and project anteriorly from the aorta, the origins of these vessels are rarely seen during a conventional "AP" angiogram. Therefore extremely angulated and/or lateral views are required to define aortoostial lesions in these vessels.

As is the case with many other vascular sites, the standard of therapy for mesenteric disease has until recently been surgical (endarterectomy or bypass) with a mortality rate that approaches 6% (95). Balloon angioplasty can be effective in restoring acute patency, although restenosis rates are 50% or more due to the ostial location of these lesions. Treatment with stents reduces acute recoil and may lead to better long-term patency (see Chapter 35, Case 8), although formal prospective studies have yet to be done. The biggest dilemma in patients with mesenteric disease is deciding who is and is not likely to benefit. Decisions to intervene should clearly be symptom driven. Certainly, the incidental findings of a stenotic mesenteric vessel during routine angiography does not necessarily indicate the need for treatment. At the other extreme, percutaneous treatment is also ill advised in patients with acute mesenteric ischemia in whom bowel infarction has already taken place, where surgical repair and intestinal resection is preferred.

Treatment Considerations and Technique

Aortoostial mesenteric disease is similar in most respects to aortoostial renal artery disease. Therefore the approach to balloon angioplasty and stenting is identical. Thus far, there are no controlled trials, nor any large series reported using stents in mesenteric arteries. Despite similar results and techniques, three factors distinguish the mesenteric vessels from the renals: First, the celiac and superior mesenteric arteries both tend to arise off of the aorta at a more downward angle than do the renal arteries, making access from below somewhat more difficult. Second, visualization of the target lesion may be more difficult in these vessels than for the renal arteries; use of the lateral projection is often required. Third, the complications related to failure and/or embolization may include bowel infarction, sepsis, and death. Therefore extreme caution and careful technique must be employed.

Aortoiliac Obstructive Disease

Most infrarenal abdominal aorta and iliac arteries disease is atherosclerotic in origin. Treatment of atherosclerotic lesions within the distal aorta and iliac arteries is similar, and therefore will be considered together. Leriche first recognized the effects of impaired inflow at the level of the terminal aorta and iliac arteries in his classic 1923 publication (96). Surgical revascularization commenced with endarterectomy in the 1940s and bypass surgery in the 1950s. In 1979, Gruentzig and Kumpe described their experience with balloon angioplasty of iliac lesions, which yielded a 2-year patency rate of 87% (97). Although balloon dilatation has been applied to atherosclerotic disease at every site in the body, nowhere have the results been superior to those achieved in the aortoiliac vessels.

Indications for Intervention and Results

Aortoiliac revascularization is currently recommended for three indications:

1. Relief of symptomatic lower extremity ischemia, including claudication, rest pain, ulceration or gangrene, or embolization causing blue-toe syndrome (Fig. 27.1; Chap. 35, Case 13).
2. Restoration and/or preservation of inflow to the lower extremity in the setting of preexisting or anticipated distal bypass (Fig. 27.9).

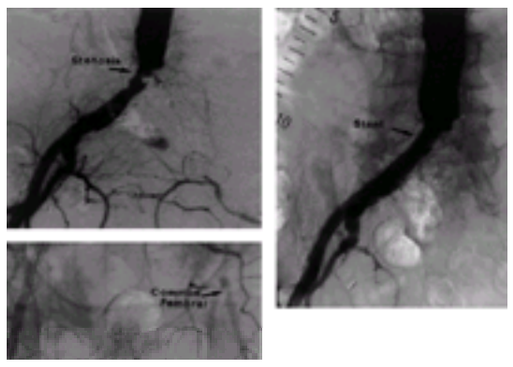

FIG. 27.9. Preparatory role of iliac PTA in patient undergoing surgical revascularization for distal disease. Patient had chronic lymphoma with extensive retroperitoneal and inguinal adenopathy and was a poor candidate for major (aortofemoral) reconstructive surgery. Surgical risk was therefore reduced by strategy of sequential PTA/stent and surgical bypass. **Upper left:** Stenosis in right common iliac artery. **Lower left:** Reconstitution of left common femoral artery. **Right:** After stent deployment, normal flow and pressure restored to right iliac artery, which subsequently served as the "donor" vessel for cross-femoral grafting.

3. Procurement of access to more proximal vascular beds for anticipated invasive procedures (e.g., cardiac catheterization/PTCA, intraaortic balloon insertion—see Chapter 35, Case 14). Occasionally, revascularization is indicated to rescue flow-limiting dissection complicating access for other invasive procedures (Fig. 27.10).

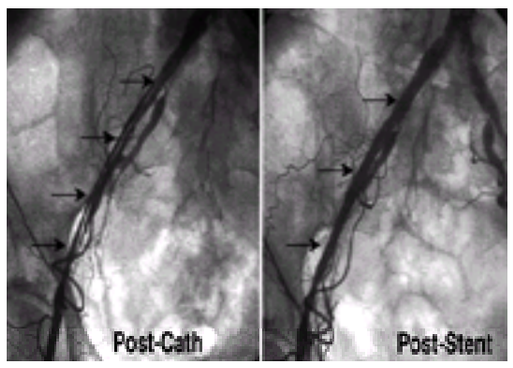

FIG. 27.10. An 84-year-old female complaining of increasing right leg pain and coolness during cardiac catheterization. Following catheterization, iliac angiogram demonstrates flow-limiting, lengthy spiral dissection (*arrows*). Flow restored after treatment with Wallstent and PTA. Severe left iliac disease is also noted. When encountering new symptoms of lower extremity ischemia during catheterization, angiographic delineation of the cause is preferable to removing the sheath and hoping for restoration of flow.

Aortobifemoral bypass has a long-term patency of 90% at 1 year, 75% to 80% at 5 years, and 60% to 70% at 10 years but carries a mortality of 2% to 3%. Accordingly, surgical intervention has been reserved for patients with critical limb ischemia or advanced degrees of disability (Rutherford category 3 or above). Because percutaneous angioplasty is less invasive, has fewer complications, and is less expensive, the threshold at which intervention is offered to patients with aortoiliac disease may be lower (Fig 27.1) (98).

Relatively few studies examine the outcome of PTA in isolated aortic segments (Fig. 27.11), because of the relatively uncommon occurrence of this entity (compared with combined aortoiliac disease). Most atherosclerotic aortic disease thus extends into the iliac arteries and requires dilation of both territories. In fact, revascularization at the aortic bifurcation commonly utilizes either "kissing balloons" or "kissing stents" (99) (see Chapter 35, Case 13). As the merits of PTA and stenting have become evident over the past 15 years, revascularization strategy for this disease has changed significantly. Considerable controversy remains in some circles concerning the "optimal" treatment (100), however, with interventionalists generally supporting angioplasty and stenting and many vascular surgeons supporting "definitive" revascularization by aortobifemoral bypass, especially in young patients or those with advanced or diffuse disease (101).

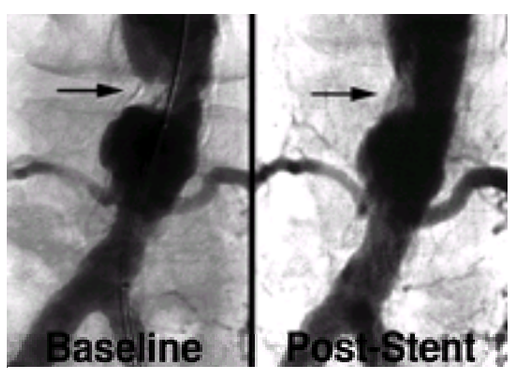

FIG. 27.11. PTA/stent of isolated infrarenal aortic stenosis, causing Rutherford category II claudication in a 63-year-old female. Long (35 cm) 8F sheath is used to "protect" Palmaz P-308 stent until it is delivered to the site. To minimize profile and optimize positioning, initial deployment is with a 9-mm balloon. After postdilation to 12 mm, lumen size is improved; in the aorta, there is no indication (and there may be a contraindication) to enlarge the stent to the size of the adjacent (ectatic) vessel. However, subsequent guidewire passage must be performed cautiously, as stent struts may be nonapposed.

The results of balloon angioplasty alone for iliac *stenoses*, particularly focal lesions, are excellent, with acute technical and clinical success in excess of 90%, based on a large number of reports (102,103). One-, 3- and 5-year patencies range from approximately 75% to 95%, 60% to 90%, and 55% to 85%, respectively. The wide disparity of these results is a reflection of multiple factors, including variations in selection criteria, discrepancies in measurements of outcome, and evolution of technique over time. Factors associated with good results include short, focal lesion; large vessel size; common iliac (as opposed to external iliac); single lesion (as opposed to multiple serial lesions); male gender; lesser Rutherford category (claudication as opposed to critical limb ischemia); and presence of good runoff. The results in patients with diffuse disease, smaller vessels, diabetes mellitus, female gender, critical limb ischemia, and poor runoff are less favorable. The results for aortoiliac *occlusions* are also less favorable.

Stents for Aortoiliac Disease

In 1993, the FDA approved the use of Palmaz balloon-expandable stents (P-308 series) for iliac arteries. Specific indications were for failed PTA (defined as a residual mean gradient of greater than or equal to 5 mm, residual stenosis of more than 30%, or presence of a flow-limiting dissection) (104). The self-expanding Wallstent prosthesis was approved for similar indications in 1996 (105). The favorable acute results, relative ease of use, and paucity of complications encountered during aortoiliac stenting, however, have led to expanded use of these devices to reduce recoil and improve on the immediate hemodynamic and angiographic result of PTA. Using stents, acute technical success is in the range of 90% to 100%, with average 1-year patency of 90% and average 3-year patency of 75% (TASC document "in press"). Because of these superior cosmetic and hemodynamic results, a strategy of primary stent deployment for aortoiliac vessels has been adopted by many, though others reserve stenting only for suboptimal angioplasty results. Tetteroo and colleagues (102) published a randomized trial between balloon angioplasty and primary stenting that showed no difference in the primary end point when balloon angioplasty patients were allowed to "cross over" to stenting for a residual stenosis of 50% or a residual gradient of 10 mm Hg mean or more (43% of provisional patients did so). If analyzed on a "per protocol" basis, stenting was far

superior. Clinical and hemodynamic success rates were approximately 77% and 85%, respectively, at 24 months, comparable to many surgical series of aortobifemoral bypass. Even more compelling is the metaanalysis performed by Bosch et al. (103) on 14 recent studies (all published after 1990) involving more than 2,100 patients undergoing aortoiliac PTA. This metaanalysis showed superior immediate success rate for stents than for PTA alone (96% vs. 91%), with a subsequent 4-year primary patency rate for *stenotic* lesions of 77% for stenting versus 65% for PTA alone. For *occlusions*, 4-year patency rates were 61% for stents and 54% for PTA.

Treatment Consideration and Technique

Before undertaking aortoiliac PTA, careful consideration should be given to the issue of arterial access. Baseline angiographic and/or noninvasive studies form the basis of decisions regarding access. When treating unilateral disease that ends above the common femoral artery, we prefer ispilateral retrograde access, which provides the most direct approach to the stenotic (or occlusive) lesion and facilitates stent deployment. The contralateral approach using “cross-over” sheaths and guiding catheters is selected when the target lesion is located near the common femoral artery or the femoral head, when the groin below the target is either scarred or the common femoral artery is heavily calcified, or when there is particular concern about impeding the “outflow” during sheath removal following revascularization of an iliac lesion. The contralateral approach is also used when more distal revascularization is to be pursued in the same sitting, but should be avoided in cases of acutely angulated aortic bifurcations or stenosis at the origin of the common iliac artery. For iliac occlusions, either retrograde or contralateral access is appropriate, and frequently both are required to successfully recanalize occluded segments. For lesions involving the aortic bifurcation, a bilateral retrograde femoral approach is recommended to enable placement of “kissing stents.” Occasionally, brachial access can be useful for patients with aortic occlusion or, for example, a target lesion that involves the distal iliac artery in one leg (near the femoral head), with the coexistent occlusion of the contralateral iliac (precluding a contralateral approach).

Role of Pressure Gradients and IVUS

Pressure gradients are routinely measured across iliac and aortic lesions (Fig. 27.12), but there are few objective data regarding what constitutes a significant hemodynamic stenosis. By convention, a 5 mm Hg mean resting pressure gradient is taken as indicative of a significant residual stenosis. If the resting gradient is borderline, a persistent (e.g., more than 60-second) mean pressure gradient of more than 15 mm Hg after administration of a vasodilator (200 to 300 µg of nitroglycerin) is considered significant. IVUS is superior to contrast angiography in demonstrating detailed vessel anatomy and can be of great utility during aortoiliac angioplasty by measuring the dimensions of the reference site, the degree of narrowing, and the characteristics of the vessel wall (e.g., calcium) (12,15,106).

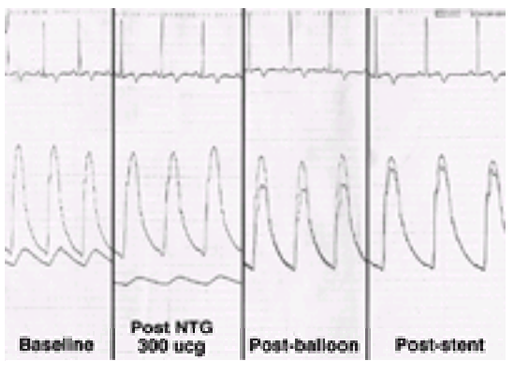

FIG. 27.12. Pressure gradients obtained during revascularization of iliac occlusion from patient in FIG. 27.1. **A:** Baseline gradient. **B:** Gradient after distal administration of NTG. **C:** Postballoon, significant resting gradient remains, even without provocation. **D:** Gradient eliminated after stenting, demonstrating superior hemodynamic result.

Thrombolytic Therapy

The utility of thrombolytic therapy in iliac occlusions is controversial. For occlusions in peripheral vessels, catheter-directed thrombolysis is much more effective than systemic fibrinolysis. The technical aspects of use vary among investigators. There is agreement that the catheter must penetrate into the occlusion for the lytic agent to have any effect. Some prefer going one step further and crossing the occlusion primarily, to “lace” the lytic agent throughout the occlusion and enhance the efficiency of thrombolysis. Others prefer crossing the occlusion and administering the lytic in “pulsed spray” fashion. This technique may accelerate clot dissolution but is associated with a slightly higher incidence of distal embolization. Urokinase has previously been the agent of choice, with alternatives of tPA (107) and Retavase.

Use of Aortoiliac PTA in Conjunction with Surgery

Many patients with aortoiliac disease also have infrainguinal disease. In such cases, the aortoiliac disease is treated first to improve inflow, which often obviates the need for reconstruction more distally (Fig. 27.13). In some instances, PTA of the “donor” iliac may be performed to preserve inflow to a planned cross-femoral graft (Fig. 27.9). The same strategy underlies the preparatory role of iliac angioplasty in patients undergoing surgical revascularization for treatment of distal disease. For example, common femoral artery cutdown, intraoperative balloon angioplasty, and iliac stent deployment may be followed by fem-pop or fem-fem bypass in the same sitting. Likewise, revascularization may be staged with proximal PTA first, followed by surgery some 3 to 4 weeks later. These approaches constitute a natural extension of the use of endovascular techniques to minimize morbidity and mortality, and maximize the benefit for the patient.

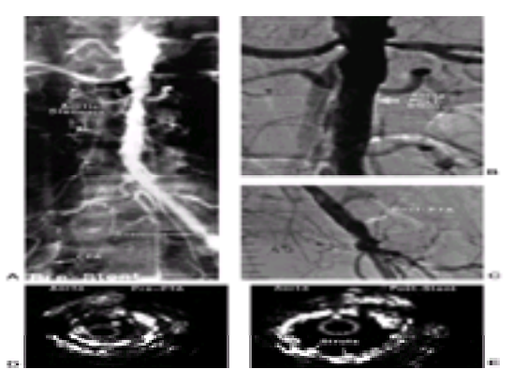

FIG. 27.13. PTA of aorta and common iliac artery in nonischemic (left) side in preparation for cross-femoral graft leads to unexpected resolution of ischemic pain. The patient is a 62-year-old woman, a poor surgical candidate, with rest pain and severe claudication in the right leg. **A:** Occlusion of right common iliac artery and stenoses in infrarenal aorta and left common iliac artery pre-PTA. Initial strategy was to dilate the stenotic sites, then graft from left to right common femoral artery (CFA). After **(B)** PTA/stent of aorta and **(C)** PTA alone of iliac artery, patient's right (contralateral) leg symptoms disappeared, presumably due to increased left-to-right collateral flow via internal iliac artery tributaries. Planned cross-femoral bypass surgery was therefore canceled. PTA was guided by intravascular ultrasound (IVUS), which demonstrates marked improvement in lumen cross-sectional area of aortic lesion from pre-PTA **(D)** to poststent **(E)**.

In summary, percutaneous therapy represents the first line of therapy for aortoiliac obstructive disease. With the exception of patients with very extensive disease, PTA with or without stent deployment is associated with a highly successful acute and long-term outcome. Furthermore, if this strategy fails, subsequent surgical intervention remains feasible. In the guidelines for peripheral PTA published by the AHA in 1994 (98), four categories of iliac disease were described: Category 1 includes stenoses of less than 3 cm in length, concentric and noncalcified, for which PTA is recommended. Category 2 includes stenoses 3 to 5 cm in length or calcified or eccentric stenoses less than 3 cm in length. For these, PTA was also felt to be well suited. Category 3 lesions include stenoses 5 to 10 cm in length or

occlusions less than 5 cm in length. In this category, it was recommended that PTA could be performed but that the initial chance of technical success or long-term benefit might not be as good as with bypass surgery. However, PTA as a first approach might be indicated in these patients, depending on the patient risk-factor profile. Category 4 lesions included stenoses more than 10 cm long, occlusions more than 5 cm in length, extensive bilateral aortoiliac atherosclerosis, or lesions in association with abdominal aortic aneurysm or other lesions requiring surgical repair. For category 4 lesions, the percutaneous approach was not recommended. These guidelines are evolving, as the benefits of stenting become manifest and the limits of percutaneous therapy are extending. For the present, they are helpful for stratifying patients by potential risks versus benefits.

Complications

Complications are relatively infrequent with aortoiliac angioplasty (less than 6% based on multiple series). Most common are access site complications, including local or retroperitoneal bleeding, pseudoaneurysm, and arteriovenous (AV) fistula. At the site of angioplasty, thrombotic occlusion is extremely rare, as is rupture. The latter, however, can have devastating consequences. This, as well as retroperitoneal bleeding, can be fatal if not controlled. Arterial rupture must be recognized promptly and controlled by inflation of a balloon within the lesion (balloon tamponade), reversal of anticoagulation, and volume resuscitation. Surgery may be required infrequently. In the future, stent grafts may be made readily available to treat this complication. Other complications include distal embolization, which was said to occur with alarming frequency in early studies of recanalized total iliac occlusion. More recent studies indicate an incidence of less than 5% (98). Systemic complications, such as contrast or atheroembolic induced renal failure, myocardial infarction, CVA, and death, all occur with very low frequency (less than 0.5%). Complications requiring surgical repair are also relatively infrequent, in the range of 2%.

LOWER EXTREMITY

Common Femoral Artery

Revascularization of the common femoral artery has long been considered the exclusive purview of the vascular surgeon, whose approach through a local incision (often under local anesthesia) allows endarterectomy and/or patch angioplasty with outstanding results. Concerns about elastic recoil, mechanical crush of stents, and possibility of dissecting or thrombosing the only site of inflow to the entire leg have raised concerns about catheter-based intervention in this region. Lesion characteristics play a significant role in determining the success of femoral PTA, with the best results in lesions that are focal, concentric, or bandlike, without extensive plaque burden. More complex lesions, including those with “cauliflower,” calcified plaque, and a large plaque burden that extends into the origins of the superficial femoral and profunda tend not to respond as well.

Treatment Considerations and Technique

The common femoral artery can be approached either via the contralateral approach using a cross-over guiding catheter or sheath, or from the brachial approach. In occasional instances, the lesion will be far enough from the sheath insertion site that ipsilateral antegrade access is possible, though more challenging technically. We occasionally use the ipsilateral approach utilizing directional atherectomy (Fig. 27.14) but usually perform balloon angioplasty via the contralateral approach (Fig. 27.15). When the lesion involves the bifurcation of the common femoral into profunda and superficial femoral artery (SFA) branches, kissing balloons must occasionally be used. The biggest albatross within the common femoral artery, however, is restenosis, which is generally accepted to be greater than 50%. Nonetheless, patients often experience persistent relief of critical symptoms, even in the face of moderate or moderately severe restenosis. Stenting the common femoral artery renders subsequent surgical repair much more complicated and should be avoided.

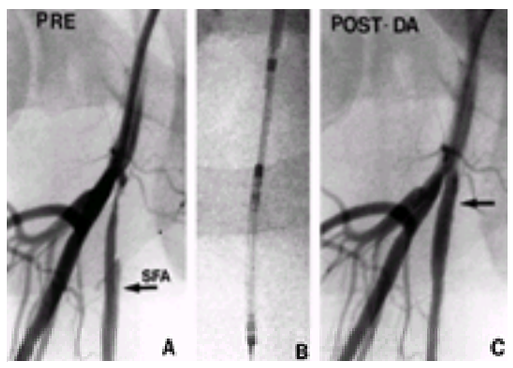

FIG. 27.14. Directional atherectomy (DA of right superficial femoral artery [SFA] via antegrade puncture). **A:** Angiography via antegrade puncture into right common femoral artery demonstrates high-grade stenosis in proximal SFA, not favorable for balloon angioplasty because of ostial location/eccentricity. **B:** 8F directional atherectomy catheter introduced via sheath, which is then pulled back to common femoral artery. **C:** Angiography following DA demonstrates excellent result.

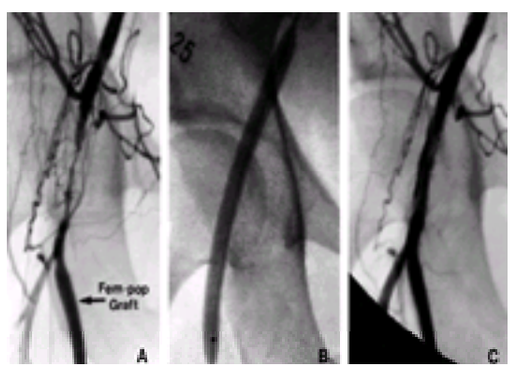

FIG. 27.15. Balloon angioplasty (PTA) of common femoral artery in patient with multiple previous right leg surgical interventions, resulting in severe scarring of right groin. **A:** High-grade, diffuse stenosis in right common femoral artery, with extensive collateral flow, supplying profunda and femoropopliteal (fem-pop) graft. **B:** PTA via contralateral approach. Balloon inflated to 15 atm. **C:** Post-PTA angiogram demonstrates mild plaque fracture, with excellent patency. Patient's claudication symptoms resolved, and he continues to be minimally symptomatic 4 years later.

Profunda Femoris Artery

Indications for Intervention and Results

The deep femoral artery is the main source of collaterals to the lower extremity. In the face of occlusion of the SFA or of a fem-pop bypass graft, the profunda alone becomes responsible for maintaining viability of the lower extremity. Surgery for disease involving the ostia of the SFA and profunda involves endarterectomy and patch angioplasty. Balloon angioplasty has been reserved for situations in which severe ischemia is present (Rutherford category 4, 5, or 6) and surgery is absolutely contraindicated, or when critical lesions involve the middle or distal portions of the descending branch of the profunda that are less accessible to the surgeon. Technically satisfactory results of profunda PTA have been described and suggest that this is a relatively safe procedure (see Chapter 35, Case 17). However, because of the potential for producing limb-threatening ischemia or limb loss if the vessel occludes, treatment of this site should generally be reserved for patients with rest pain or critical limb ischemia, in whom no good surgical options are available.

Treatment Considerations and Technique

Angioplasty of the profunda, similar to that for the common femoral artery, is best performed from the contralateral side. Antegrade access is sometimes appropriate, depending on the location of the stenosis and the condition of the common femoral artery. If the lesion is immediately adjacent to the common femoral, then it may be problematic to treat. Directional atherectomy may be performed in an antegrade fashion at this site. Since the profunda is the “vessel of last resort” for maintaining blood flow to the lower extremity, a conservative posture should be maintained with respect to balloon size and inflation pressure. The outcome of stenting in the profunda is unknown, so that stenting should be reserved for cases of true flow-limiting dissection after balloon angioplasty, wherein patency of the vessel and viability of the limb might be threatened without maintaining an open vessel.

Superficial Femoral and Popliteal Arteries

The frequency of symptomatic femoral-popliteal disease is two or more times greater than that of iliac disease; it tends to occur in older patients who have a greater incidence of coronary artery disease. Any enthusiasm for revascularization must thus be tempered by the lower likelihood of long-term success, with either surgical or percutaneous approaches. Despite a mean vessel diameter between 5 and 6 mm, restenosis is nearly twice (40% to 60%) that for coronary interventions. Since experience has failed to document any significant difference in either acute or long-term results for PTA of the SFA versus the popliteal artery, these vessels will be considered together with respect to indications, results, and techniques of PTA.

Indications for Revascularization and Results

Patients with superficial femoral/popliteal disease usually present with claudication. Less frequently, the presenting sign is critical limb ischemia. The presence of the profunda femoris as a major source of collaterals to the lower limb protects patients with SFA occlusion from the dire consequences of critical limb ischemia, so that even patients with proximal SFA occlusion may have only mild claudication, or no claudication at all. Decisions regarding intervention, whether surgery or PTA, for infrainguinal disease must take into account the degree to which the patient is disabled, the presence of comorbid factors, and the anticipated short- and long-term outcome. In general, patients with mild, nondisabling claudication should *not* undergo interventional therapy for SFA disease, but rather should be placed on conservative treatment with an exercise program to augment collateral flow. Less than a quarter of these patients will progress to the point of developing more disabling symptoms or a threatened limb, which mandate therapy.

There remains considerable controversy as to the relative role of percutaneous therapy versus surgery. The results of balloon angioplasty in the SFA have improved over time. In a recent review, Murray and colleagues (108) noted that the technical success improved from 70% to 91% between 1980 and 1989 with excellent acute and long-term efficacy even for lesions greater than 10 cm in length. Similarly, the success rate in crossing *occluded* segments of the SFA and popliteal have improved dramatically, likely as a consequence of technical advances. Foremost among these is the use of hydrophilic guidewires. Among eight large series of patients undergoing PTA of femoral-popliteal stenoses and occlusions, most of whom were claudicants, the acute technical success was between 82% and 96% (108,109,110,111,112,113,114 and 115). Primary patency rates at 1, 3, and 5 years averaged approximately 60%, 50%, and 45%. Several factors influence long-term outcome following SFA-pop angioplasty. Patients with intermittent claudication (versus tissue loss), a more severe lesion at baseline, and lower posttreatment residual stenosis tend to have a *better* outcome at 1 year; those with diabetes, threatened limb loss, or diffuse atherosclerotic vascular disease with no or one vessel runoff have a worse outcome. The recent analysis of Hunink and colleagues (116) examined the relative benefit and cost-effectiveness of PTA versus bypass surgery for 5-year outcomes in approximately 4,800 PTA and 4,500 bypass procedures performed since 1995. Their conclusion was that, for patients with *disabling claudication* due to femoral-popliteal stenosis *or* occlusion, PTA is the preferred initial treatment, whereas for patients with *chronic critical ischemia* due to femoral-popliteal *occlusion*, bypass surgery is the preferred treatment (if feasible).

Adjunct Therapies

For stenoses of the SFA and popliteal, the standard approach is that of balloon angioplasty. Various technologies, including stents, directional atherectomy, rotational atherectomy, and laser angioplasty, have been investigated as a means of improving long-term patency and reducing restenosis in the SFA. In contrast to the documented benefits achieved by the use of endovascular stents for iliac PTA, experience thus far in the SFA has been less favorable. SFA/popliteal stenting therefore presently should be limited to cases of flow-limiting dissection or clearly failed PTA. Neither directional (Fig. 27.16) nor rotational atherectomy has thus far been demonstrated to have an advantage for SFA/pop revascularization, save for those rare patients in whom the extent of calcific deposits renders the lesion refractory to alternative techniques. Laser angioplasty has been used in SFA/pop revascularization, though no study thus far has demonstrated definitive benefit of this device. A trial (PELA) that employs the strategy of debulking with excimer laser, followed by balloon angioplasty for revascularization of lengthy SFA occlusions, has recently begun (see Chapter 35, Case 15).

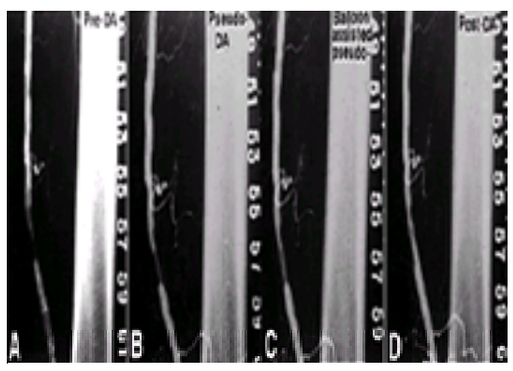

FIG. 27.16. Incremental luminal patency resulting from individual components of directional atherectomy (DA). **A:** Angiogram shows high-grade stenosis in superficial femoral artery (SFA), pre-DA. **B:** Angiogram shows improved luminal patency resulting from Dotter effect of advancing DA catheter through lesion (no balloon inflation, no atherectomy). **C:** Angiogram shows further improvement in luminal patency resulting from balloon inflation (2 atm) without activating cutter. **D:** Angiogram shows final result accomplished by activating cutter.

For occluded femoral-popliteal arteries, whether or not to use thrombolytic therapy in advance of PTA is controversial. Lytic therapy can be successful in some patients even with *chronic* total occlusion, because the occlusion in lower extremity arteries is often characterized by a lengthy, gelatin-like thrombus superimposed on a high-grade atherosclerotic lesion. Thus lytic therapy can convert a long occlusion to one that is either shorter or nonocclusive, which may then respond better to PTA.

Some promising strategies lie on the horizon for treating the vexing problem of SFA restenosis: First, endovascular brachytherapy, which is currently being tested in coronary arteries (see Chapter 23), is also undergoing study (PARIS trial) in conjunction with SFA/pop PTA. Similarly, it is hoped that covered stents or local drug delivery might reduce the incidence of restenosis. Alternatively, Isner and colleagues (117,118 and 119) have effectively transferred genetic material to induce “therapeutic angiogenesis,” in limb salvage situations where direct arterial recanalization was impossible.

Treatment Considerations and Technique

Access

There are four potential routes of access to the SFA and popliteal: antegrade common femoral artery puncture, contralateral retrograde access over the aortic bifurcation, retrograde popliteal artery access, and brachial access. The most common route of access has been the antegrade approach, which is more challenging than retrograde common femoral puncture. Familiarity with the local anatomy at the level of the common femoral artery is essential (see Chapter 14). As new catheters have been developed to facilitate contralateral access, that approach has become increasingly popular, especially among cardiovascular specialists who are more familiar with the retrograde approach. The use of a kink-resistant sheath is critical to maintaining access around the bifurcation of the aorta, especially in the case of the acutely angulated bifurcation. Any number of curved (Cobra, LIMA) or retroflexed (Sos Omni, Simmons) catheters can be used to obtain access to the contralateral common iliac artery. The advantages to this approach include the ability to image the common femoral and its bifurcation, and the ability to treat iliac and

infrainguinal disease in the same sitting. The disadvantage is that of “working from a distance,” with exchange-length wires and balloons. In addition, traversal of critically narrowed or occluded sites can be problematic because of lack of support. The third approach, retrograde popliteal, is reserved for rare cases where the antegrade or contralateral approach fails to enable traversal of an occluded segment, or in the event that a subintimal channel has been created. Complications associated with this approach are more frequent, because of the vital structures in the popliteal fossa, the small size of the vessel, and the lack of familiarity with this access. The brachial approach has the advantage of providing better radiation protection, since one is working far from the actual target site but requires the use of lengthy wires and devices.

When considering choice of access, it is important to use all the information at one's disposal, including prior angiographic examination, duplex study, and physical findings of disease along the planned access route. For example, if the contralateral iliac artery is severely diseased or occluded, then contralateral access may be excluded. In the case of an aortic aneurysm, one might wish to avoid brachial access. If duplex shows severe calcification and diffuse disease in the popliteal artery, then that access site should be avoided. Likewise, if the common femoral artery has severe and diffuse disease or if the origin of the SFA is the target lesion site, then access other than ipsilateral antegrade should be considered.

Infrapopliteal Arteries

Dotter and Judkins (4), in their original description of peripheral angioplasty in 1964, included two cases of angioplasty of infrapopliteal vessels. Since their original report, the development of techniques and delineation of indications for intervention below the knee have evolved more slowly than for larger, more proximal vessels. Published clinical experience involving PTA of the anterior tibial, tibioperoneal trunk, posterior tibial, and peroneal arteries has been far more limited than that described for aortoiliac and SFA/pop sites, and reflects multiple limitations: The relatively small size of these vessels (1.5 to 3.5 mm) and their distal location limits both access and success, and it is rare for claudication to be due to isolated disease in one or two infrapopliteal arteries; knee-to-foot patency of only one of the three major branches is regarded as sufficient to prevent lower limb ischemia or claudication. Restenosis rates in infrapopliteal vessels appear to be considerably higher than those for more proximal sites, and disease in the infrapopliteal vessels is often occlusive, diffuse, and/or complicated by the presence of heavy calcific deposits. Furthermore, many patients with infrapopliteal disease have diabetes, which is associated with atretic and diffusely calcified vessels, which respond poorly to balloon dilation.

As technological advances have been made, including the development of low-profile balloons and atraumatic coronary guidewires, the ability to treat infrapopliteal disease has improved. Over the past decade, since Schwarten and colleagues (120) reported the first sizable series of patients undergoing infrapopliteal revascularization, the application of these techniques has become more widespread. Infrapopliteal stenoses and occlusions can be revascularized percutaneously with remarkably low risk and technical success rates in the range of 80% to 95%. In one recent large series reported by Dorros et al. (121), success was achieved in 406 out of 417 patients (96%); success rate in stenoses (98%) was superior to that in occlusions (76%). In-hospital complications were extremely low. Follow-up is incomplete; however, the vast majority of patients with critical limb ischemia (95%) improved following revascularization. Such improvement does not necessarily imply ongoing patency. Restoration of flow through only one of the three major vessels to the foot may be sufficient to heal a distal ischemic lesion. And once healed, most patients will do well even in the face of documented reocclusion or restenosis.

For patients with claudication, infrapopliteal disease usually coexists with more proximal disease; revascularization alone is often sufficient to achieve symptomatic relief. This differs from patients with ischemic ulceration, in whom restoration of uninterrupted patency to the foot is generally required to heal the lesion. There is a subset of patients who claudicate due solely to infrapopliteal disease, in whom there is an increasing body of experience of treatment with percutaneous therapy. Such a strategy should be reserved, at least for the present, for patients who have severe symptoms (Rutherford category 3). Infrapopliteal PTA may also be justified in claudicants who undergo proximal revascularization (either with surgery or PTA), in whom the runoff is severely impaired. Indeed, data presented previously show that outflow is the principal determinant of long-term patency for fem-pop PTA. By recanalizing the outflow vessels, it is conceivable that the proximal PTA site or the bypass graft may be more likely to remain patent. This theory has not been formally tested in peripheral vessels, though it certainly seems to be the case in coronary arteries.

Many of the patients treated with infrapopliteal angioplasty to date were too high risk or otherwise unqualified for bypass surgery (16). The latter is still considered to be the standard of care for patients with critical limb ischemia due to infrapopliteal disease. Regardless of the conduit (reversed vein, *in situ* vein, or prosthetic material) patency rates are inferior to those of more proximal reconstruction. It is conceivable that the long-term clinical outcome of percutaneous therapy may ultimately equal that of distal bypass grafting. A randomized controlled trial will be required to address this issue. It is also conceivable that both of these revascularization strategies will be replaced in many instances by the strategy of therapeutic angiogenesis (122). If the body can be stimulated to create its own new microcirculation, then the issues of restenosis, reocclusion, and graft closure become moot.

Techniques

The technical aspects of infrapopliteal angioplasty are similar to those for coronary vessels. Antegrade common femoral access is preferred, so as to optimize the ability to manipulate catheters in the vessels below the knee. Selective injection via catheter placed at the level of the knee is advised to optimally visualize the distal vascular pattern. Digital subtraction is preferred. Not infrequently, anatomic variants will be present, such as the anterior tibial arising above the knee joint. Also, it is not unusual to mistake one of the small side branches or collaterals for the main arterial trunk. Adequate anticoagulation is critical, and administration of vasodilator therapy (nitroglycerin or papaverine) may be useful. Initial attempts to cross stenoses or occlusions should employ small, coronary-type guidewires (0.014 or 0.018 inch), though 0.035-inch hydrophilic-type wires can also be used if necessary to cross difficult occlusions. Confirmation of presence within the distal vessel should be obtained before dilating, by removing the wire from the catheter and injecting a small amount of dilute contrast through the guidewire lumen into the distal vessel.

When performing infrapopliteal PTA, particular care should be taken to be sure that subsequent surgical options are not compromised. For example, overdilation and disruption of a previously uncompromised distal vessel may prohibit subsequent bypass to that site.

Rotational atherectomy or excimer laser angioplasty (Fig. 27.17) can be useful as adjunctive therapy. Specifically, lesions that have unfavorable morphology, such as total occlusions, heavy calcification, and ostial disease, may benefit from these “niche” devices (123,124). A prospective registry employing the excimer laser for infrapopliteal lesions in the setting of limb salvage is about to be initiated (laser angioplasty for critical ischemia—LACI trial). Previous studies with rotational atherectomy have shown it to be useful acutely, though data on long-term follow-up do not suggest a benefit over balloon angioplasty alone. To summarize, the percutaneous therapy of infrapopliteal vessels is in a stage of evolution, and indications are expanding. It is not unreasonable, especially for patients with threatened limbs who are high-risk surgical candidates, for experienced operators to attempt percutaneous revascularization of offending infrapopliteal lesions before committing the patient to surgery. Although the brestenosis/reocclusion rates are high, long-term limb salvage can be successfully achieved. For the rare patients who have severe intermittent claudication on the basis infrapopliteal disease alone, PTA may be a reasonable option. Finally, when SFA/popliteal disease occurs in conjunction with infrapopliteal lesions, revascularization below the knee may be reasonable to increase the outflow following recanalization of the proximal vessel.

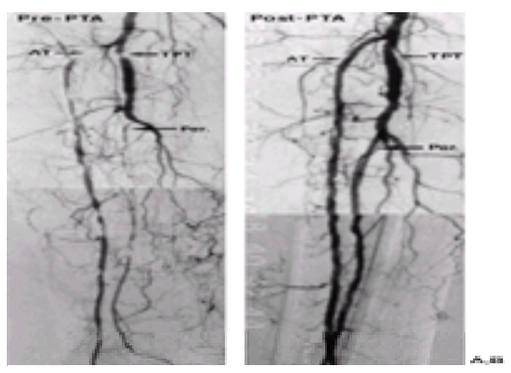

FIG. 27.17. PTA of occluded anterior tibial artery, tibioperoneal trunk, and peroneal artery in elderly patient with foot ulceration and threatened limb loss. **A:** Baseline angiogram demonstrates 2-cm occlusion of anterior tibial artery (AT), high-grade stenosis of tibioperoneal trunk (TPT), and lengthy occlusion of peroneal artery (per.). All three segments were recanalized with Glidewire, followed by excimer-laser angioplasty and PTA. **B:** Final angiogram after PTA demonstrates widely patent anterior tibial, tibioperoneal trunk, peroneal artery.

Lower Extremity Bypass Grafts

Stenosis in a lower extremity bypass graft can threaten the patency of the graft and shorten its life. The etiology of bypass graft stenoses is variable. Stenoses that occur within the first few weeks or months of graft placement usually indicate a technical problem, which is best treated by repeat surgery and graft revision. Graft failure within a later time frame (several months to years) can be due to myointimal hyperplasia, atherosclerosis, or progressive fibrosis of a poor venous conduit. Several other factors may contribute to graft failure, including the presence of poor inflow or outflow, low cardiac output, a hypercoagulable state, compromise of the graft due to patients crossing their legs, or external compression of the graft by sclerosis and fibrosis (e.g., from a scarred groin). Prosthetic conduits are more likely to present with abrupt occlusion, whereas native venous conduits tend to present with a progressive downhill course. Of course, even in the case of the latter, abrupt thrombosis and acute limb ischemia can occur.

Indications for Intervention

Graft failure, or impending graft failure, is often not heralded by increasing clinical symptoms. Accordingly, a strategy of regular graft surveillance using duplex ultrasonography is recommended to preserve and extend the life of the graft. For impending graft failure, either detected by duplex ultrasonography or by increasing symptoms, immediate arteriography is recommended, followed by either surgical or percutaneous revascularization. As stated in the AHA task force in 1993 (98), focal lesions of the distal anastomosis of a fem-pop or fem-tib graft are amenable to PTA (Fig. 27.18). Other lesions that may be amenable include focal stenoses of proximal graft anastomoses or short-segment lesions (3 cm or less) occurring within the bypass graft. Lengthy lesions (especially more than 10 cm) and stenoses associated with anastamotic aneurysms are recommended to undergo surgical revision.

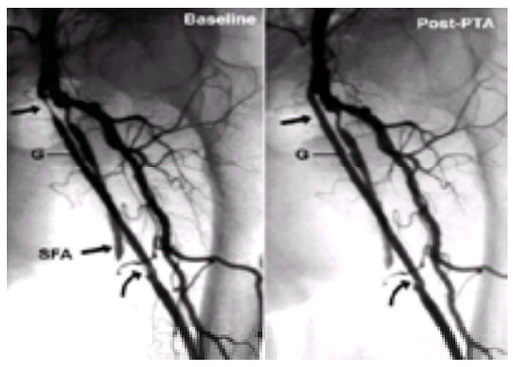

FIG. 27.18. Right anterior oblique view of critical stenosis (*straight arrow*) at origin of fem-pop graft (G) and moderate irregular lesion (*curved arrow*) at distal end of jump-graft placed during previous graft revision. SFA is occluded proximally. Lesions were detected during routine surveillance (patient asymptomatic). Because of proximity of lesions to ipsilateral common femoral artery, contralateral access may be preferred. After PTA, stenoses are eliminated but regular surveillance will be essential to prevent graft failure.

Patients presenting with acute or subacute graft thromboses (less than 14 days) are best treated with catheter-directed thrombolysis (Fig. 27.19) (125,126). An alternative is balloon embolectomy, though the latter strategy may be associated with a higher morbidity and mortality over the ensuing year (126). The one exception to this is the recently placed graft that fails almost immediately, which should return immediately to the operating room for surgical thrombectomy and revision. For patients with long-standing grafts that fail, determination of the factors responsible may require reestablishing enough flow to visualize the graft angiographically. In cases of early graft failure, examination of angiographic studies may provide clues previously overlooked, such as stenosis of an inflow vessel, poor or inadequate distal runoff, or presence of a venous side branch that was not sutured.

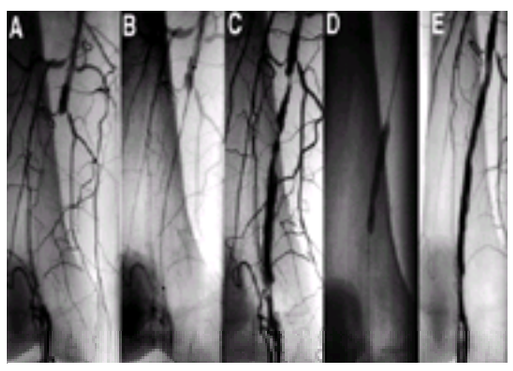

FIG. 27.19. Thrombolysis, rheolytic thrombectomy, and PTA for subacute thrombosis of SFA-to-popliteal Dacron graft. **A:** Distal SFA occluded at proximal graft anastamosis; popliteal reconstitutes by collaterals, so the limb is not imminently in jeopardy. **B:** Infusion catheter placed across thrombosed graft, after traversing with hydrophilic wire; tPA administered for 6 hours at 3 mg/hr. Residual hazy filling defect treated with Possis AngioJet. **C:** Postlysis and Possis, underlying inflow and outflow stenoses (caused by “pseudointima”) and responsible for flow compromise and graft thrombosis were identified and (**D**) dilated. **E:** Final result shows restoration of normal flow/caliber.

Technique

For patients presenting with impending graft failure based on a duplex study, access should be obtained so as to optimize the therapeutic alternatives. For example, after angiography documents the presence of a proximal or distal anastamotic lesion, it is conceivable that the lesion may be resistant to balloon dilation alone. In these cases, we and others have found that directional atherectomy is a useful tool for salvaging the graft and improving the outcome of the percutaneous intervention. The results using directional atherectomy appear to be comparable to those of surgical revision, although direct head-to-head comparison has not been carried out. Likewise, although stents have been advocated by some for use in failing vein grafts, their utility has not been studied in any formal trials to date.

CHAPTER REFERENCES

1. Pentecost MJ, Criqui MH, Dorros G, et al. Guidelines for peripheral percutaneous transluminal angioplasty of the abdominal aorta and lower extremity vessels. *Circulation* 1994;89:511.
2. Weitz JI, Byrne J, Clagett P, et al. Diagnosis and treatment of chronic arterial insufficiency of the lower extremities: a critical review. *Circulation* 1996;94:3026.
3. Rutherford RB, Becker GJ. Standards for evaluating and reporting the results of surgical and percutaneous therapy for peripheral arterial disease. *Radiology* 1991;181:277.
4. Dotter CT, Judkins MP. Transluminal treatment of arteriosclerotic obstruction: description of a new technic and a preliminary report of its application. *Circulation* 1964;30:654.
5. Gruentzig AR. Transluminal dilatation of coronary artery stenosis (letter to editor). *Lancet* 1978;1:263.
6. Isner JM, Rosenfield K. Redefining the treatment of peripheral artery disease: role of percutaneous revascularization. *Circulation* 1993;88:1534.
7. Blum U, Krumme B, Flugel P, et al. Treatment of ostial renal artery stenoses with vascular endoprostheses after unsuccessful balloon angioplasty. *New Engl J Med* 1997;336:459.
8. Dorros G, Jaff M, Mathiak L, et al. Four-year follow-up of Palmaz-Schatz stent revascularization as treatment for atherosclerotic renal artery stenosis. *Circulation* 1998;98:642.
9. Isner JM, Rosenfield K, Kelly K, et al. Percutaneous intravascular ultrasound examination as an adjunct to catheter-based interventions: preliminary experience in patients with peripheral vascular disease. *Radiology* 1990;175:61.
10. Rosenfield K, Kaufman J, Pieczek A, Langevin RE Jr, Razvi S, Isner JM. Human coronary and peripheral arteries: on-line three-dimensional reconstruction from two-dimensional intravascular US scans. *Radiology* 1992;184:823.
11. Mecley M, Rosenfield K, Kaufman J, Langevin RE, Razvi S, Isner JM. Atherosclerotic plaque hemorrhage and rupture associated with crescendo claudication. *Ann Intern Med* 1992;117:663.
12. Rosenfield K, Losordo DW, Ramaswamy K, et al. Three-dimensional reconstruction of human coronary and peripheral arteries from images recorded during two-dimensional intravascular ultrasound examination. *Circulation* 1991;84:1938.
13. Rajachandran M, Rosenfield K, Schainfeld R, Haley L, Wuensch D, Isner JM. Is there a role for intravascular ultrasound in carotid artery stenting? *J Am Coll Cardiol* 1997;29:363A(abst).

14. Isner JM, Rosenfield K, Losordo DW, et al. Combination balloon-ultrasound imaging catheter for percutaneous transluminal angioplasty. *Circulation* 1991;84:739.
15. Losordo DW, Rosenfield K, Pieczek A, Baker K, Harding M, Isner JM. How does angioplasty work? Serial analysis of human iliac arteries using intravascular ultrasound. *Circulation* 1992;86:1845.
16. Isner JM, Pieczek A, Rosenfield K. Untreated gangrene in patients with peripheral artery disease. *Circulation* 1994;89:482.
17. McCrindle BW, Jones TK, Morrow WR. Acute results of balloon angioplasty of native coarctation versus recurrent aortic obstruction are equivalent. *J Am Coll Cardiol* 1996;28:1810.
18. Giovanni JV, Lip GY, Osman K. Percutaneous balloon dilation of aortic coarctation in adults. *Am J Cardiol* 1996;77:435.
19. Storey GS, Marks MP, Dake M. Vertebral artery stenting following percutaneous transluminal angioplasty. *J Neurosurg* 1996;84:883.
20. Lababidi Z. Percutaneous balloon coarctation angioplasty: long-term results. *J Intervent Cardiol* 1992;5:57.
21. Rao PS. Stents in treatment of aortic coarctation. *J Am Coll Cardiol* 1997;30:1853.
22. Zellers TM. Balloon angioplasty for recurrent coarctation of the aorta in patients following staged palliation for hypoplastic left heart syndrome. *Am J Cardiol* 1999;84:231.
23. Crawford ES, Hess KR, Cotten ES. Ruptured aneurysm of the descending thoracic and thoracoabdominal aorta: analysis according to size and treatment. *Ann Surg* 1991;213:417.
24. Cambria RA, Gloviczki P, Stanson AW, et al. Outcome and expansion rate of 57 thoracoabdominal aortic aneurysms managed nonoperatively. *Am J Surg* 1995;170:213.
25. Juvonen T, Ergin A, Galla JD. Prospective study of the natural history of thoracic aortic aneurysms. *Ann Thorac Surg* 1997;63:1533.
26. Dake MD, Miller DG, Semba CP, Mitchell RS, Walker PJ, Liddell BA. Transluminal placement of endovascular stent-grafts for the treatment of descending thoracic aortic aneurysms. *N Engl J Med* 1994;331:1729.
27. Mitchell RS, Dake MD, Sembra CP. Endovascular stent graft repair of thoracic aneurysm. *J Thorac Cardiovasc Surg* 1996;11:1054.
28. Miller DC, Mitchell RS, Oyer PE, Stinson EB, Jamieson SW, Shumway NE. Independent determinants of operative mortality for patients with aortic dissection. *Circulation* 1984;70:I-153.
29. Ergin MA, Phillips RA, Galla JD. Significance of distal false lumen after type A dissection repair. *Ann Thorac Surg* 1994;57:820.
30. Crawford ES, Svensson LG, Coselli JS, Safi HJ, Hoss KR. Aortic dissection and dissecting aortic aneurysms. *Ann Surg* 1988;208:254.
31. Slonim SM, Nyman URO, Semba CP, Miller DC, Mitchell RS, Dake MD. Aortic dissection: percutaneous management of ischemic complications with endovascular stents and balloon fenestration. *J Vasc Surg* 1996;23:241.
32. Williams DM, Lee DY, Hamilton BH. The dissected aorta: percutaneous treatment of ischemic complications—principles and results. *J Vasc Interv Radiol* 1997;8:605.
33. Kouchoukos NT, Dougenis D. Surgery of the thoracic aorta. *N Engl J Med* 1997;1876.
34. Dake MD, Noriyuki K, Mitchell RS, et al. Endovascular stent-graft placement for the treatment of acute aortic dissection. *N Engl J Med* 1999;1546.
35. Kato M, Matsuda T, Mitsunori K, et al. Outcomes of stent-grafts treatment of false lumen in aortic dissection. *Circulation* 1998;98:II-305.
36. Arend WP, Michel BA, Bloch DA, Hunder GG, Calabrese LH, Edworthy SM. The American College of Rheumatology 1990 criteria for the classification of Takayasu arteritis. *Arthritis Rheum* 1990;33:1129.
37. Bachman DM, Kim RM. Transluminal dilatation for subclavian steal syndrome. *Am J Roentgenol* 1980;135:995.
38. Millaire A, Trinca ZM, Marache P, de Groote P, Jabinet JL, Ducloux G. Subclavian angioplasty: immediate and late results in 50 patients. *Cathet Cardiovasc Diagn* 1993;29:8.
39. Dorros G, Lewin RF, Jamnadas P, Mathiak LM. Peripheral transluminal angioplasty of the subclavian and innominate arteries utilizing the brachial approach: acute outcome and follow-up. *Cathet Cardiovasc Diagn* 1990;19:71.
40. Dueber C, Klose KJ, Marache PH, Schmiedt W. Percutaneous transluminal angioplasty for occlusion of the subclavian arteries: short- and long-term results. *Cardiovasc Intervent Radiol* 1992;15:205.
41. Kumar K, Dorros G, Bates CM, Palmer L, Mathiak L, Dufek C. Primary stent deployment in occlusive subclavian artery disease. *Cathet Cardiovasc Diagn* 1995;34:281.
42. Ansel GM, Barry SG, Yakubov JS. Primary stenting of symptomatic subclavian artery stenosis. *Circulation* 1996;94[Suppl I]:58.
43. Al-Mubarak N, Liu MW, Dean LS, et al. Immediate and late outcomes of subclavian artery stenting. *Cathet Cardiovasc Interv* 1999;46:169.
44. Sullivan TM, Gray BH, Bacharach M, et al. Angioplasty and primary stenting of the subclavian, innominate, and common carotid arteries in 83 patients. *J Vasc Surg* 1998;28:1059.
45. Hadjipetrou P, Cox S, Piemonte T, Eisenhauer A. Percutaneous revascularization of atherosclerotic obstruction of aortic arch vessels. *J Am Coll Cardiol* 1999;33:1238.
46. Becker KJ, Purcell LL, Hacke W, Hanley DF. Vertebrobasilar thrombosis: diagnosis, management, and the use of intraarterial thrombolytics. *Crit Care Med* 1996;24:1729.
47. Cross DT, Moran CJ, Akins PT, Angtuaco EE, Diringer MN. Relationship between clot location and outcome after basilar artery thrombolysis. *Am J Neuroradiol* 1997;18:1221.
48. Hacke W, Zeumer H, Ferbert A, Bruckmann H, del Zoppo GJ. Intra-arterial thrombotic therapy improves outcome in patients with acute vertebrobasilar occlusive disease. *Stroke* 1998;19:1216.
49. Brandt T, von Kummer R, Muller-Kuppers M, Hacke W. Thrombolytic therapy of acute basilar artery occlusion: variables affecting recanalization and outcome. *Stroke* 1996;27:875.
50. Connors JJ. Emergency treatment of ischemic stroke. *J Invas Cardiol* 1999;11:93.
51. North American Symptomatic Carotid Endarterectomy Trial Collaborators. Beneficial effect of carotid endarterectomy in symptomatic patients with high-grade stenosis. *New Engl J Med* 1991;325:445.
52. Hobson RW, Weiss DG, Fields WS, et al. Efficacy of carotid endarterectomy for asymptomatic carotid stenosis. *N Engl J Med* 1993;328:221.
53. Ohki T, Marin ML, Lyon RT, et al. *Ex vivo* human carotid artery bifurcation stenting: correlation of lesion characteristics with embolic potential. *J Vasc Surg* 1998;27:463.
54. Kachel R, Endert G, Basche S, Grossmann K, Glaser FH. Percutaneous transluminal angioplasty (dilatation) of carotid, vertebral, and innominate artery stenoses. *Cardiovasc Intervent Radiol* 1987;10:142.
55. Dublin AB, Baltaxe HA, Cobb CA. Percutaneous transluminal carotid angioplasty in fibromuscular dysplasia. Case report. *J Neurosurg* 1983;59:162.
56. Theron J, Raymond J, Casasco A. Percutaneous angioplasty of atherosclerotic and postsurgical stenosis of carotid arteries. *Am J Neuroradiol* 1987;8:495.
57. Mathias K. Catheter treatment of arterial occlusive disease of supraaortic vessels. *Radiologe* 1987;27:547.
58. Roubin GS, Yadav S, Iyer SS, Vitek J. Carotid stent-supported angioplasty: a neurovascular intervention to prevent stroke. *Am J Cardiol* 1996;78:8.
59. Yadav JS, Roubin GS, King P, Iyer SS, Vitek J. Angioplasty and stenting for restenosis after carotid endarterectomy. *Stroke* 1996;27:2075.
60. Diethrich EB, Ndiaye M, Reid DB. Stenting in the carotid artery: initial experience in 110 patients. *J Endovasc Surg* 1996;3:42.
61. Guterman LR, Budny JL, Gibbons KJ, Hopkins LN. Thrombolysis of the cervical internal carotid artery before balloon angioplasty and stent placement: report of two cases. *Neurosurgery* 1996;38:620.
62. Mathur A, Roubin GS, Iyer SS. Predictors of stroke complicating carotid artery stenting. *Circulation* 1998;97:1239.
63. Beebe HG, Archie JP, Baker WH, et al. Concern about safety of carotid angioplasty. *Stroke* 1996;27:197.
64. Bettmann MA, Katzen BT, Whisnant J, et al. Carotid stenting and angioplasty: a statement for healthcare professionals from the Councils on Cardiovascular, Radiology, Stroke, Cardio-Thoracic and Vascular Surgery, Epidemiology, and Prevention, and Clinical Cardiology, American Heart Association. *Circulation* 1998;97:121.
65. Diethrich EB. Carotid angioplasty and stenting. Will they match the gold standard? *Tex Heart Inst J* 1998;25:1.
66. Hobson RW. Status of carotid angioplasty and stenting trials. *J Vasc Surg* 1998;27:791.
67. Hobson RW, Brott T, Ferguson R, et al. Regarding “Statement regarding carotid angioplasty and stenting” [letter]. *J Vasc Surg* 1998;25:1117.
68. Vozzi CR, Rodriguez AO, Paolantonio D, Smith JA, Wholey MH. Extracranial carotid angioplasty and stenting: initial results and short-term follow-up. *Tex Heart Inst J* 1997;24:167.
69. Waigand J, Gross CM, Uhlich F, et al. Elective stenting of carotid artery stenosis in patients with severe coronary artery disease. *Eur Heart J* 1998;19:1365.
70. Mathur A, Roubin GS, Yadav JS, Iyer SS, Vitek JJ. Combined coronary and bilateral carotid stenting: a case report. *Cathet Cardiovasc Diagn* 1997;40:202.
71. Mathur A, Roubin GS, Gomez CR. Elective carotid artery stenting in the presence of contralateral occlusion. *Am J Cardiol* 1998;81:1315.
72. Russell EJ. Carotid artery balloon angioplasty and stenting (CABAS): a neuroradiologic perspective. *Am J Neuroradiol* 1998;19:1535.
73. Hobson RW, Goldstein JE, Jamil Z. Carotid restenosis: operative and endovascular management. *J Vasc Surg* 1999;29:228.
74. Satler LF, Hoffmann R, Lansky A, et al. Carotid stent-assisted angioplasty: preliminary technique, angiography, and intravascular ultrasound observations. *J Invas Cardiol* 1996;8:23.
75. Yadav JS, Roubin GS, Iyer S, et al. Elective stenting of the extracranial carotid arteries. *Circulation* 1997;95:376.
76. Wholey MH, Wholey M, Bergeron P. Current global status of carotid artery stent placement. *Cathet Cardiovasc Diagn* 1998;44:1.
77. Rosenfield K, Schainfeld R, Pieczek A, Haley L, Isner JM. Restenosis of endovascular stents due to stent compression. *J Am Coll Cardiol* 1997;29:328.
78. Mathur A, Dorros G, Iyer SS, Vitek JJ, Yadav SS, Roubin GS. Palmaz stent compression in patients following carotid artery stenting. *Cathet Cardiovasc Diagn* 1997;41:137.
79. Mathur A, Dorros G, Iyer SS, Vitek JJ, Yadav SS, Roubin GS. Palmaz stent compression in patients following carotid artery stenting. *Cathet Cardiovasc Diagn* 1997;41:137.
80. Dorros G. Complications associated with extracranial carotid artery interventions. *J Endovasc Surg* 1996;3:166.
81. Mendelsohn FO, Weissman NJ, Lederman RJ, et al. Acute hemodynamic changes during carotid artery stenting. *Am J Cardiol* 1998;82:1077.
82. Al-Mubarak N, Liu MW, Dean LS. Incidence and outcomes of prolonged hypotension following carotid artery stenting. *J Am Coll Cardiol* 1999;33:65A(abst).
83. Piamsomboon C, Roubin GS, Liu MW. Relationship between oversizing of self-expanding stents and late loss index in carotid stenting. *Cathet Cardiovasc Diagn* 1998;45:139.
84. Perko MJ, Norgaard M, Herzog TM. Unoperated aortic aneurysms: a survey of 170 patients. *Ann Thorac Surg* 1995;59:1204.
85. Blum U, Voshage G, Beyersdorf F, et al. Endoluminal stent-grafts for infrarenal abdominal aneurysms. *N Engl J Med* 1997;336:13.
86. Parodi JC, Criado FJ, Barone HD, Schonholz C, Queral LA. Endoluminal aortic aneurysm repair using a balloon-expandable stent-graft device: a progress report. *Ann Vasc Surg* 1994;8:523.
87. D'Ayala M, Hollier LH, Marin ML. Endovascular grafting for abdominal aortic aneurysms. *Cardiothorac Vasc Surg* 1998;78:491.
88. Zarins CK, White RA, Schwarten D, et al. AneuRx stent graft versus open surgical repair of abdominal aortic aneurysms: multicenter prospective clinical trial. *J Vasc Surg* 1999;29:292.
89. Begelman SM, Olin JW. Renal artery stenosis. *Curr Treat Opt Cardiovasc Med* 1999;1:55.
90. Palmaz JC. The current status of vascular intervention in ischemic nephropathy. *J Vasc Interv Radiol* 1998;9:539.
91. Gruntzig A, Kuhlmann U, Lutolf U, Vetter W, Meier B, Siegenthaler W. Treatment of renovascular hypertension with percutaneous transluminal dilation of a renal-artery stenosis. *Lancet* 1978;1:801.
92. Klinge J, Mali WP, Puijlaert CB, Geyskes GG, Becking WB, Feldbert MA. Percutaneous transluminal renal angioplasty: initial and long-term results. *Radiology* 1989;171:501.
93. Rimmer JM, Gennari FJ. Atherosclerotic renovascular disease and progressive renal failure. *Ann Intern Med* 1993;118:712.
94. Dormandy JA. Prostanoid drug therapy for peripheral arterial occlusive disease—the European experience. *Vasc Med* 1996;1:155.
95. Johnson KW, Lindsay TF, Walker PM. Early and late results and suggested surgical approach for chronic and acute mesenteric ischemia. *Surgery* 1995;118:1.
96. Leriche R. Des oblitérations artérielles hautes (oblitération de la terminaison de l'aorte) comme causes des insuffisances circulatoires des membres inférieurs. *Bull Mem Soc Chir* 1923;1404.
97. Gruntzig A, Kumpe DA. Technique of percutaneous transluminal angioplasty with the Gruntzig balloon catheter. *Am J Roentgenol* 1979;132:547.
98. Pentecost MJ, Criqui MH, Dorros G. Guidelines for peripheral percutaneous transluminal angioplasty of the abdominal aorta and lower extremity vessels. A statement for health professionals from a special writing group of the councils on cardiovascular radiology, arteriosclerosis, cardio-thoracic and vascular surgery, clinical cardiology, and epidemiology and prevention, the American Heart Association. *Circulation* 1994;89:511.
99. Mendelsohn FO, Santos RM, Crowley JJ, et al. Kissing stents in the aortic bifurcation. *Am Heart J* 1998;136:600.
100. Brewster MD. Current controversies in the management of aortoiliac occlusive disease. *J Vasc Surg* 1997;25:365.
101. Sullivan TM, Childs MB, Bacharach JM, Gray BH, Piedmonte MR. Percutaneous transluminal angioplasty and primary stenting of the iliac arteries in 288 patients. *J Vasc Surg* 1997;25:829.
102. Tetteroo E, van der Graaf Y, Bosch JL, et al. Randomised comparison of primary stent placement versus primary angioplasty followed by selective stent placement in patients with iliac-artery occlusive disease. Dutch Iliac Stent Trial Study Group. *Lancet* 1998;351:1153.
103. Bosch JL, Hunink MG. Meta-analysis of the results of percutaneous transluminal angioplasty and stent placement for aortoiliac occlusive disease. *Radiology* 1997;204:87.
104. Palmaz JC, Garcia OlJ, Schatz RA, et al. Placement of balloon-expandable intraluminal stents in iliac arteries: first 171 procedures. *Radiology* 1990;174:969.
105. Martin EC, Katzen BT, Benenati JF, et al. Multicenter trial of the wallstent in the iliac and femoral arteries. *J Vasc Interv Radiol* 1995;6:843.
106. Rosenfield K, Isner JM. Intravascular ultrasound in patients undergoing coronary and peripheral arterial revascularization. In: Topol EJ, ed. *Textbook of interventional cardiology,* 2nd ed. Philadelphia: WB Saunders, 1994:1153.
107. Weaver FA, Comerota AJ, Youngblood M, Froehlich J, Hosking JD, Papanicolaou G. Surgical revascularization versus thrombolysis for nonembolic lower extremity native artery occlusions: results of a prospective randomized trial. *J Vasc Surg* 1996;24:513.

108. Murray JG, Apthorp LA, Wilkins RA. Long-segment (>10 cm) femoropopliteal angioplasty: improved technical success and long-term patency. *Radiology* 1995;195:158.
109. Gallino A, Mahler F, Probst P, Nachbur B. Percutaneous transluminal angioplasty of the arteries of the lower limbs: a 5-year follow-up. *Circulation* 1984;70:619.
110. Krepel VM, van Andel HJ, van Erp WFM, Breslau BJ. Percutaneous transluminal angioplasty of the femoropopliteal artery: initial and long-term results. *Radiology* 1985;165:325.
111. Capek P, McLean GK, Berkowitz HD. Femoropopliteal angioplasty: factors influencing long-term success. *Circulation* 1991;83:I-70.
112. Jeans WD, Armstrong S, Cole SEA. Fate of patients undergoing transluminal angioplasty for lower-limb ischemia. *Radiology* 1990;177:559.
113. Johnston KW. Femoral and popliteal arteries: reanalysis of results of balloon angioplasty. *Radiology* 1992;183:767.
114. Hunink MG, Donaldson MC, Meyerovitz MF, et al. Risks and benefits of femoropopliteal percutaneous balloon angioplasty. *J Vasc Surgery* 1993;17:183.
115. Matsi PJ, Manninen JI, Vanninen RL, et al. Femoropopliteal angioplasty in patients with claudication: primary and secondary patency in 140 limbs with 1–2-year follow-up. *Radiology* 1994;191:727.
116. Huink MGM, Wong JB, Donaldson MC, Meyerovitz MF, de Vries J, Harrington DP. Revascularization for femoropopliteal disease: a decision and cost-effectiveness analysis. *JAMA* 1995;274:165.
117. Isner JM, Pieczek A, Schainfeld R. Clinical evidence of angiogenesis following arterial gene transfer of phVEGF $_{165}$. *Lancet* 1996;348:370.
118. Isner JM, Asahara T. Angiogenesis and vasculogenesis as therapeutic strategies for postnatal neovascularization (Persective). *J Clin Invest* 1999;103:1231.
119. Isner JM, Walsh K, Rosenfield K, et al. Arterial gene therapy for restenosis. *Hum Gene Ther* 1996;7:989.
120. Schwarten DE, Cutclif WB. Arterial occlusive disease below the knee: treatment with percutaneous transluminal angioplasty performed with low-profile catheters and steerable guide wires. *Radiology* 1988;169:71.
121. Dorros G, Jaff MR, Murphy KJ, Mathiak L. The acute outcome of tibioperoneal vessel angioplasty in 417 cases with claudication and critical limb ischemia. *Cathet Cardiovasc Diagn* 1998;45:251.
122. Baumgartner I, Pieczek A, Manor O. Constitutive expression of phVEGF $_{165}$ following intramuscular gene transfer promotes collateral vessel development in patients with critical limb ischemia. *Circulation* 1998;97:1114.
123. Isner JM, Rosenfield K. Redefining the treatment of peripheral artery disease. *Circulation* 1993;88:1534.
124. Henry M, Amor M, Ethevenot G, Henry I, Allaoui M. Percutaneous peripheral atherectomy using the rotablator: a single-center experience. *J Endovasc Surg* 1995;2:51.
125. The STILE Investigators. Results of a prospective randomized trial evaluating surgery versus thrombolysis for ischemia of the lower extremity. *Ann Surg* 1994;220:251.
126. Ouriel K, Shortell CK, DeWeese JA, et al. A comparison of thrombolytic therapy with operative revascularization in the initial treatment of acute peripheral arterial ischemia. *J Vasc Surg* 1994;19:1021.

28
Pediatric Interventions

Stanton B. Perry, John F. Keane, and James E. Lock

Harvard Medical School; Department of Cardiology, Children's Hospital, Boston, Massachusetts 02115

A growing list of transcatheter interventions is now available for treating patients with congenital and acquired heart disease. Among these procedures are creation of interatrial defects by balloon and blade septostomy (1,2), balloon dilation of stenotic vessels and valves, and closure of unwanted intracardiac and extracardiac defects and vessels. This chapter focuses on several interventions: balloon pulmonary and aortic valvuloplasty, angioplasty of aortic coarctation and of branch pulmonary artery stenosis, coil embolization of unwanted vessels including patent ductus arteriosus (PDA), device closure of atrial septal defects (ASDs) and ventricular septal defects (VSDs), and implantation of intravascular stents in patients with congenital heart disease.

BALLOON DILATATION VALVULOPLASTY

Balloon valvuloplasty (alternatively called balloon valvulotomy) is discussed in Chapter 26, but this section deals with application of this technique in the (predominantly pediatric) population with congenital heart disease. As with adult valvuloplasty, choosing the most appropriate balloon catheter is important not only to maximize the likelihood of successful dilation but also to avoid or minimize complications. The most common type consists of a single, cylindrical balloon mounted on a shaft that is delivered to the stenotic lesion over a guidewire. Although this type of catheter distributes wall stress equally around the circumference and folds to a relatively small collapsed profile, it tends to completely obstruct blood flow during inflation. Catheters with two or three balloons mounted on the same shaft help overcome such obstruction to flow, but their failure to distribute wall stress evenly may engender a variety of other clinical consequences. Other specialized balloons include Inoue's unique balloon for dilating mitral stenosis and a variety of balloons designed for coronary angioplasty, such as those mounted directly on a guidewire (see Chapter 23).

It is important to know the maximal pressure to which a balloon can be inflated before rupture. This pressure varies with the balloon material and inversely with the balloon diameter. High pressures are rarely needed when dilating valves but are essential in some applications, such as dilation of most pulmonary artery stenoses. Balloons are designed to rupture and tear longitudinally. If the tear is transverse, as occurs most commonly when the balloon ruptures on calcium, the distal half of the balloon will fold back on itself, making removal difficult. For this reason and to minimize the risk of vessel rupture, which is more likely to occur when the balloon ruptures (3), intentional balloon rupture should generally be avoided by limiting the inflation pressure to the rated burst pressure. A pressure gauge should be used to monitor inflation pressure when dilating lesions that require high pressure.

Balloons are manufactured to achieve certain maximal diameters. The actual inflated diameter varies depending on inflation pressure and balloon compliance. Balloon length, by convention, refers to the cylindrical portion of the balloon, excluding the taper at either end. Long balloons are more stable during inflation and easier to keep positioned as the heart contracts and ejects. As the balloon straightens during inflation, however, the ends of a long balloon may damage adjacent structures. Examples include damage to the right ventricular outflow tract when dilating valvar pulmonary stenosis (4). Therefore, 2- or 3-cm balloons are used for most lesions. An exception would be aortic valvuloplasty in older patients, where use of a long balloon is necessary to avoid its ejection from the valve orifice during inflation. The balloon profile, defined as the diameter of the deflated balloon, can be several French sizes larger than the shaft, depending on balloon size and material. High-profile balloons are more likely to damage vessels at the entry site and may be difficult to pass across tight stenoses. Balloons also vary in terms of the length of the shoulders at each end of the balloon. Although a longer taper may make entry at the groin easier, the taper when combined with a long distal tip may make centering of the balloon in the lesion more difficult. For example, when the stenotic orifice in mitral stenosis is nearer the left ventricular apex, a long taper and tip may prevent the balloon's being advanced far enough to allow dilation of the stenosis.

Most valvuloplasty balloons are mounted on shafts between 4F and 9F. A large shaft offers the potential advantages of increased stiffness, use of a larger guidewire, and a larger inflation/deflation lumen. However, a large shaft is more likely to damage the femoral vessels, which is the most common complication in pediatric patients undergoing balloon dilation. We therefore generally choose the smallest shaft size available with the desired balloon diameter. Stiffer shafts make groin entry easier and help to stabilize the balloon position during inflation, but may make following the guidewire around sharp turns more difficult. The tip of the catheter, the part of the shaft that extends beyond the balloon, varies in length and degree of tapering. Although longer tips with a more gradual taper are easier to pass through the groin puncture site, the long tip may prevent proper positioning of the balloon. It is also important to have the catheter lumen closely match the diameter of the guidewire to prevent entrapping of tissue at the tip of the catheter.

Two or more balloons may be positioned and inflated simultaneously to achieve a larger effective diameter than is possible with a single balloon. We use Yeager's formula (5) for calculating the effective combined diameter of two balloons.

Percutaneous Balloon Pulmonary Valvuloplasty

Reports of the use of blade or balloon catheters to perform pulmonary valvuloplasty appeared as early as 1953 (6,7). However, the static balloon technique, reported by Kan et al., (8) in 1982, was the first to be applied widely. Subsequent results (9,10,11 and 12) have demonstrated the safety and effectiveness of this technique and have established it as the treatment of choice for children and adults with isolated pulmonary valve stenosis (see Chapter 26).

Technique

A complete precatheterization Doppler echocardiogram defines valve morphology, measures the pulmonary annulus, and rules out associated defects. With the patient under routine sedation, a sheath is placed percutaneously in the femoral vein and a balloon-tip end-hole catheter is used to measure right-sided heart oxygen saturations and pressures. After placement of a small pigtail catheter in the femoral artery for monitoring of the arterial pressure, the patient is heparinized. The gradient across the pulmonary outflow is measured, and the location of the valve is defined with the use of fluoroscopy and a right ventriculogram in the anteroposterior and lateral projections. The pulmonary annulus is measured at the hinge points of the valve, and the balloon diameter is chosen to be 1.2 to 1.4 times that of the annulus (Fig. 28.1). Animal studies (4) and results in patients (9) have demonstrated that the use of such oversized balloons is safe and yields improved results. When the annulus is larger than 20 mm, such overdilation usually requires simultaneous inflation of two balloons.

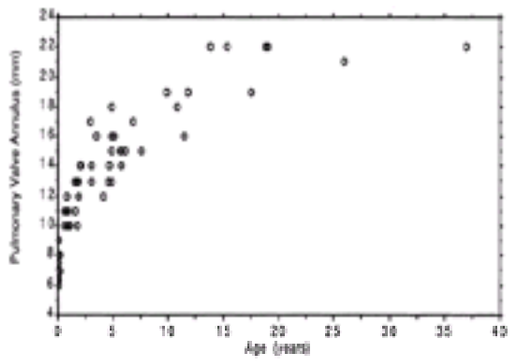

FIG. 28.1. The pulmonary valve annulus diameter measured from angiograms versus patient age.

An end-hole catheter is advanced to the distal right or left pulmonary artery, and the venous catheter and sheath are removed over an exchange wire and replaced with a sheath large enough to accommodate the balloon dilatation catheter. Once the balloon has been centered across the pulmonary valve, it is inflated rapidly until the “waist” disappears and then deflated and withdrawn to the inferior vena cava. Video playback is reviewed to ensure proper balloon position and size.

A pressure pullback is performed to measure the transvalvar gradient and to look for a subvalvar gradient that sometimes develops after dilation. A residual transvalvar gradient of more than 20 to 30 mm Hg is unusual and suggests improper position of the balloon during dilation, improper balloon size, or a dysplastic valve. If the subvalvar gradient is more than 30 mm Hg, a right ventriculogram is performed to evaluate the location and extent of subvalvar obstruction. The cardiac output is also remeasured to calculate valve area.

Patients with critical pulmonary stenosis may not tolerate the prolonged presence of a catheter across the valve because of further restriction of functional valve area. In patients with systemic right ventricular pressure, we perform the initial right ventriculogram before crossing the valve. If the patient deteriorates after the valve has been crossed, the catheter is removed without measuring a gradient, and only the exchange wire is left in place. In these patients, a relatively small balloon is frequently used for the initial dilation, followed by an oversized balloon for definitive dilations.

Neonates presenting with critical pulmonary stenosis are commonly cyanotic due to right-to-left shunts at the atrial level and are dependent on a patent ductus for pulmonary blood flow. Because of the atrial and ductal shunts, both systemic and pulmonary blood flows tend to be maintained during balloon inflation. Crossing the valve can be difficult, however, because of both the small, hypertrophied right ventricle and the pinhole opening in the valve. We attempt to cross the valve with a balloon-tip end-hole catheter, but if this is unsuccessful, we use a 3F or 4F preformed catheter (60° to 90° short bend at the distal end). This catheter is manipulated to the right ventricular outflow tract. If it does not cross the valve directly, a 0.018-inch torque-control guidewire is used to probe the outflow tract until the valve is crossed. Once the instrument is across the valve, we dilate initially with a small balloon and then with a balloon 20% to 40% larger than the annulus.

Results

Excluding neonates, the first 66 patients to undergo balloon pulmonary valvotomy at our institution included 9 patients who had undergone a previous surgical valvotomy—usually for critical pulmonary stenosis as neonates. In these nine patients, the transvalvar gradient was decreased from a average of 60 to 19 mm Hg using a balloon-to-annulus ratio of 1.24, with no significant complications. Of the remaining 57 patients, 54 valves were dilated successfully with a balloon-to-annulus ratio of 1.27. The transvalvar gradient decreased from 74 to 15 mm Hg and the right ventricular pressure from 101 to 50 mm Hg with no significant change in cardiac output. The postdilation transvalvar gradient in the 54 successful cases was less than 30 mm Hg regardless of the predilation gradient or age. Small subvalvar gradients were common, but 4 of 54 patients had subvalvar gradients of more than 30 mm Hg (45, 60, 75, and 80 mm Hg). The subvalvar gradient resolved in each case within 1 year. There were four failures in three patients with severely dysplastic valves. No cases of significant restenosis have been identified. The only significant complication occurred early in the series in a patient who developed transient complete heart block.

In 35 consecutive neonates at our institution with critical pulmonary stenosis, the valve was crossed and dilated in 34. The transvalvar gradient decreased from an average of 63 to 24 mm Hg, and the right ventricular-to-systemic pressure ratio (systolic) decreased from 1.5 to 0.8. The balloon-to-annulus ratio for the largest balloon used was 1.25. Complications included perforation and tamponade in two patients and one death due to overwhelming sepsis. During follow-up, six patients were redilated, five successfully. An additional two patients had surgery for a dysplastic valve. Only three patients had gradients greater than 30 mm Hg, and all gradients were less than 50 mm Hg.

Our results, combined with those from other centers, demonstrate that balloon pulmonary valvotomy, using oversized balloons, is safe and effective in relieving pulmonary valve stenosis in all age groups and in patients who have undergone surgical valvotomies. We currently attempt balloon pulmonary valvotomy in any patient with a transvalvar gradient greater than 40 mm Hg and in neonates with critical pulmonary stenosis.

Percutaneous Balloon Aortic Valvuloplasty

Balloon aortic valvuloplasty was first reported in 1983 in a child with congenital aortic stenosis (13). It has been performed since then in large numbers of patients with both congenital and acquired stenoses (14,15,16,17 and 18). Although initial results in adults with calcific stenosis were encouraging, the modest relief of stenosis achieved, combined with a high rate of early restenosis, has limited its use in this group of patients. Most adult centers now prefer valve replacement, reserving balloon valvuloplasty for patients who are high-risk candidates for surgery. In most patients with congenital aortic stenosis, the alternative to balloon dilation is a surgical valvotomy. Because the results of balloon valvuloplasty appear comparable to those obtained by such surgery (in terms of relief of obstruction and restenosis rate), we continue to use balloon dilation in patients with congenital aortic stenosis.

Technique

With the patient under routine sedation, a femoral vein and artery are entered percutaneously and the patient is heparinized. The venous catheter measures right-sided heart pressures and cardiac output before and after dilation. In older patients, aortic valves can be dilated from the femoral vein using a transseptal approach, but the retrograde approach via the femoral artery remains the most common technique. We start with an appropriately sized sheath in the artery and a pigtail catheter 1F size smaller than the sheath. This allows simultaneous pressure measurements through the sheath and pigtail. Any intrinsic gradient is determined by comparing the pressure measured through the pigtail catheter in the iliac artery and then in the ascending aorta with the pressure recorded through the side-arm of the sheath.

The easiest technique for retrograde crossing of the stenotic aortic valve is to advance the soft end of a straight wire out of a pigtail catheter and use it to probe for the valve orifice (see Chapter 4). This probing need not be entirely random if precatheterization echocardiograms have defined the valve morphology and position of the orifice. In congenitally stenotic valves, even unicommissural valves, the commissure that lies between the left and noncoronary cusp is the one that is almost always open. Therefore, during probing with the wire, the pigtail catheter is manipulated to direct the wire posteriorly and to the left. The probing must be done gently to avoid perforating a cusp or damaging the coronary arteries. When the left ventricle is entered, a transvalvar gradient is measured by simultaneously recording pressure from the pigtail and the femoral sheath. If the valve was easy to cross, a pressure pullback is performed, followed by an aortogram for aortic regurgitation. A left ventriculogram is performed, and the aortic annulus is measured at the hinge points of the valve.

The balloon diameter is chosen to be 75% to 90% of the annulus diameter (Fig. 28.2). Animal and clinical studies (19,20) demonstrate that aortic valvuloplasty with a balloon-to-annulus ratio greater than 1.0 is more likely to be associated with damage to the outflow tract and increased aortic regurgitation. Double balloons are used when the annulus is larger than 22 mm. The pigtail catheter is exchanged for the dilatation catheter over an exchange wire, and the balloon is flushed with carbon dioxide and dilute contrast material in the thoracic aorta. The balloon is centered across the valve, inflated and deflated rapidly, and pulled back to the descending aorta. Videotapes are reviewed to check balloon size and position.

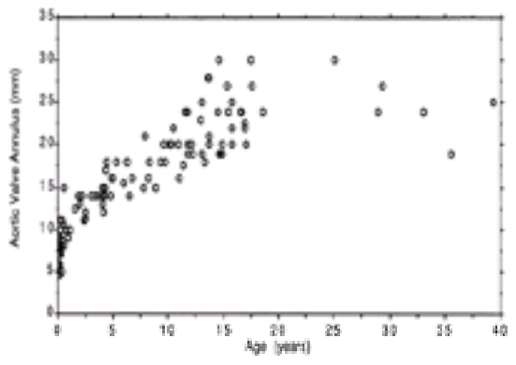

FIG. 28.2. The aortic valve annulus diameter measured from angiograms versus patient age.

The gradient and cardiac output are remeasured after dilation, and an aortogram is performed to look for aortic regurgitation. If the residual gradient is greater than 55 mm Hg and an aortogram shows no more than mild regurgitation, a larger balloon is used. A final pressure pullback and aortogram are then performed.

It can be difficult to keep the inflated balloon positioned in the valve against the force of left ventricular ejection. A stiff catheter shaft, a long balloon, and a stiff or extra-stiff exchange wire help stabilize the position. In addition, balloon ejection is counteracted by advancing the catheter so that it lies along the top of the aortic arch rather than around the underside of the arch. Finally, the double-balloon technique, which does not totally obstruct flow, may make it easier to maintain balloon position.

Although the overall approach is similar to that used in older patients (see Chapter 26), several special techniques are useful in neonates. The umbilical artery usually can be used in the first week of life. Catheter manipulation is more difficult from the umbilical artery, but its use avoids damage to the femoral artery. In addition, many centers use the carotid artery, an approach that makes crossing the valve very easy. As with older patients, a transseptal approach can be used, from either the femoral or the umbilical vein. To cross the aortic valve retrograde, a 3F or 4F pigtail catheter with the tail partially cut off is used to direct the guidewire posteriorly and leftward toward the open commissure. Because neonatal valves are very easy to perforate, we use a 0.018-inch torque-control guidewire with a very soft tip. Any difficulty in getting the pigtail or balloon catheter to follow the wire across the valve suggests cusp perforation.

Results

The results and complications in the first 149 patients are considered in two groups: neonates (younger than 1 month) and older patients. In the 122 older patients, the transvalvar gradient was reduced by 56%, from 76 to 33 mm Hg. The valve area index increased 51%, from 0.53 to 0.80 cm^2/m^2 of body surface area. The percent gradient reduction was unrelated to age (1 month to 39 years), history of prior surgical valvotomy (n = 18), predilation gradient, or final balloon-to-annulus ratio (mean, 0.98; range, 0.71 to 1.33). Aortic regurgitation (on a scale of 0 to 5) increased from grade 0.57 to grade 1.18. We have previously shown an inverse relation between gradient reduction and increased regurgitation (14). The risk of a greater than 1 grade increase in regurgitation rose from 11% (6/55) when the balloon-to-annulus ratio was less than 1.0 to 30% (6/20) when the ratio was greater than 1.0. Approximately 10% to 15% of patients have at least grade 3/5 aortic regurgitation after dilation. During follow-up, the degree of regurgitation tends to increase. No deaths occurred in these older patients. Complications included pulse loss in 30% of patients (60% in patients younger than 2 years of age, including neonates, and 15% in patients older than 2 years); this loss was permanent in 10%. The femoral artery was torn in one patient, and a pseudoaneurysm developed in a second. Complications involving the femoral artery have decreased with the availability of lower-profile balloons. Transient left bundle branch block occurred in 15% and ventricular arrhythmias requiring cardioversion in 3% (14). Follow-up analyses have shown that 50% of patients are free from reintervention at 8 years and survival is 95% (18).

Neonates are a different group in terms of results and complications (21). In the first 27 consecutive neonates with critical aortic stenosis at our institution, the valves were dilated regardless of clinical condition, valve morphology, left ventricular size or function, or degree of mitral regurgitation. They ranged from 1 to 30 days of age and from 2.2 to 5 kg. Unicommissural valves were present in 17 and bicommissural valves in 10. The left ventricular volume was greater than 80% of predicted normal in 16, 60% to 80% of normal in 7, and less than 60% of normal in 4. Using a balloon-to-annulus ratio of 0.90, the peak systolic ejection gradient was reduced from 58 to 27 mm Hg and the left ventricular end-diastolic pressure also was reduced significantly. New aortic regurgitation developed in 11 patients; it was mild in 8 and severe in 3 who died. However, because of poor ventricular function and the common presence of a PDA with right-to-left flow, gradients are an unreliable indicator of the degree of obstruction and outcome. If failure is defined as death (n = 9) or need for stage I palliation for hypoplastic left heart syndrome (n = 2), there were 11 failures, with 9 occurring in the 11 patients with left ventricular volumes less than 80% of normal. It is clear that not all patients are suited to valvotomy alone, whether by a surgical or balloon technique. Further analysis of a group of patients with critical aortic stenosis undergoing surgical valvotomy or balloon dilation has led to a scoring system based on echocardiographic measurement of left-sided structures that can be used to choose those patients who are most likely to survive with two ventricles (22). Other patients are converted to single ventricles using the stage I palliation for hypoplastic left heart syndrome.

We currently dilate congenitally stenotic aortic valves in patients who have transvalvar gradients greater than 55 mm Hg and no more than mild aortic regurgitation and in neonates with critical aortic stenosis who have adequate left heart size.

PERCUTANEOUS BALLOON ANGIOPLASTY

Coarctation and Postoperative Aortic Obstructions

Percutaneous balloon angioplasty of coarctation was first described in 1982 (23) and has since been used in large numbers of patients with native coarctation (unoperated) and postoperative recoarctation (24,25,26,27,28,29,30,31,32 and 33). A study of experimental coarctation in lambs (34) demonstrated that relief of obstruction occurs by tearing of the intima and media. Short- and long-term complications seen in that study, including perforation resulting in death and late aneurysm formation, have now been described in patients.

Technique

With the patient under routine sedation, the femoral vein and artery are entered percutaneously and the patient is heparinized. Coarctations can be dilated via an antegrade, transseptal approach, but the retrograde femoral arterial approach is preferred for most patients. Right- and left-sided heart hemodynamics are measured (including cardiac output), and a careful pullback is performed to localize gradients. Biplane aortography is performed in either anteroposterior and lateral or right anterior oblique and long axial oblique projections. More than one aortogram may be required to profile the lesion. The diameters of the narrowest area of coarctation and of the normal proximal and distal aorta are measured.

For postoperative recoarctations, the balloon is chosen to be approximately 2.5 to 3 times the narrowest area but not greater than 1.5 times the normal proximal or distal aorta. For native coarctations, the balloon is commonly chosen to be equal to the diameter of the aorta at the isthmus. Relatively long balloons can be used in distal coarctations, but short balloons should be used in the transverse arch. High inflation pressures often are required in recoarctations. The balloon dilatation catheter is advanced through a sheath over an exchange wire and purged with carbon dioxide and dilute contrast material in the descending aorta. It is centered across the coarctation, inflated until the “waist” disappears or to maximal inflation pressure, and deflated. Video playback is reviewed to ensure proper position and balloon size. The balloon catheter is exchanged for a pigtail catheter, which can be used to measure a pullback gradient by using the single pigtail over the wire with a side-arm adaptor, or by placing a second arterial line. The dilated area should be crossed only over a guidewire because of the danger of perforation. An aortogram is performed after dilation to determine the diameter of the narrowing and to detect tears, ruptures, or dissections. If significant obstruction remains despite disappearance of the balloon “waist” during inflation, a larger balloon can be used. Chest pain is common during balloon inflation, but persistent pain suggests aortic rupture or dissection.

Results

Of the first 64 angioplasties at our institution, in 62 patients ranging in age from 3 days to 67 years, 5 were native and 59 were postoperative coarctations. The

gradient was reduced from 39 to 13 mm Hg, and the diameter of the lesion was increased from 4.9 to 8.2 mm. Procedures are considered successful if the gradient is reduced by more than 50% and the diameter is increased by more than 30%. Based on these criteria, 54 (83%) of these procedures were successful. The balloon-to-lesion ratio was 3.0 for the successful group and 1.6 for the failures. The failures had significantly lower predilation gradients, had significantly larger predilation lesion diameters, and were significantly older. Because of the relatively large predilation diameters in the failed group, use of larger balloons in an effort to improve gradient reduction, would risk injuring the normal aorta (35). Results in recoarctations are unrelated to the type of previous surgery. The success rate for patients with restenosis after repair of interrupted aortic arch or hypoplastic left heart syndrome is similar. In patients with hypoplastic left heart syndrome, dilation is commonly performed via the femoral vein.

The most common complication is loss of the arterial pulse, and one baby died after iliac artery rupture and a retroperitoneal hemorrhage. The incidence of femoral artery injury has decreased with the availability of lower-profile balloons. The only other significant short-term complication in our series was an aortic dissection that occurred immediately after dilation in a 67-year-old woman with a native coarctation. During follow-up, three patients were found to have small, asymptomatic aneurysms (two of these procedures were performed after surgery for interrupted aortic arches, and one was a dilation of a native coarctation).

Aneurysm formation after dilation of recoarctation and native coarctation has been reported by several groups. At present, we routinely dilate recoarctations but tend to send younger patients with native coarctations to surgery unless their surgical risks are increased. In older patients we are increasingly using stents (see later discussion). Other investigators routinely dilate selected native coarctations that are discrete or membranous, reporting minimal residual gradients and a low incidence of complications and aneurysms. Defining the indications in terms of gradient and coarctation diameter is difficult, but our results suggest that conventional balloon dilation is unlikely to be successful in patients with low gradients and a relatively large coarctation luminal diameter.

Branch Pulmonary Artery Stenosis

Branch pulmonary artery stenosis or hypoplasia may be acquired (e.g., at sites of shunts, bands, conduits, or pulmonary emboli) or congenital. Anatomy ranges from single stenotic areas, to multiple stenoses, to diffuse hypoplasia. Successful dilation generally results in tearing of the intima and media (3). Indications for angioplasty include greater than half systemic right ventricular pressure, hypertension in unaffected portions of the vascular bed, marked decrease in flow to an affected portion, and/or symptoms.

Technique

Pulmonary arteries are most commonly dilated from the femoral veins but can be dilated from the subclavian or internal jugular vein or from the femoral arteries in patients with systemic-to-pulmonary artery shunts. Though it is less commonly used, the subclavian or internal jugular approach is easier in many patients. A small pigtail catheter is placed in the femoral artery to monitor pressure, and the patient is heparinized. Right-sided heart hemodynamics are measured, and the magnitude and location of gradients in the pulmonary arteries are determined. In patients with suprasystemic right ventricular pressure or right ventricular failure, creation of an atrial septal defect before dilation may decrease morbidity and mortality. Pulmonary angiograms should include selective injections (anteroposterior and lateral) in each lung and in affected lobes or segments. This is most efficiently accomplished with the use of a side-arm adaptor with a cutoff pigtail over a guidewire. This arrangement allows pressure measurements, angiograms, and dilations to be performed without losing wire position. Angiograms that opacify both lungs are generally not very useful. Lower lobe stenoses in particular are often better seen on the lateral projection, and with the lungs superimposed it may not be possible to visualize stenoses or to differentiate the right from the left lung.

An exchange wire should be positioned in the largest vessel distal to the stenosis to minimize the risk of aneurysm formation, which may occur after overdilation of small distal vessels. The ideal balloon has a low profile, a short distal tip, and a high maximal inflation pressure. The balloon diameter is chosen to be 2 to 4 times the diameter of the lesion, but not more than 2 times the diameter of the normal vessel on either side (29,30). The balloon is inflated until the “waist” disappears or until the maximum inflation pressure is reached. If the “waist” does not disappear at low inflation pressures, a pressure gauge is used and balloon rupture should be avoided. Inflation time ranges from 10 to 60 seconds, depending on the response of the “waist” and how well the cardiac output is maintained. After dilation, the balloon catheter is exchanged over the guidewire for a cutoff pigtail catheter and pressure measurements are repeated. Successful dilation may result in a decrease in proximal pressures, a decrease in the gradient, or an increase in the pressure distal to the stenosis. Angiograms are repeated to measure the diameter of the stenosis and to look for tears and aneurysms.

Multiple lesions can be dilated at the same procedure, but care must be taken to avoid previously dilated areas because of the risk of dissection or perforation at the site of a tear. In general, when multiple lesions are present, distal lesions are dilated before proximal lesions and severe stenoses before milder ones.

Results

The criteria for successful dilation have been arbitrarily defined as an increase in diameter of more than 50%, an increase in flow in the affected segment of more than 20%, and/or a decrease of more than 20% in the systolic right ventricular-to-aortic pressure ratio. Using these criteria, the success rate with low-pressure balloons was approximately 60% (36,37). The use of high-pressure balloons with inflation pressures as high as 21 atm increased the rate to 75% (38). The success rate for postoperative stenoses is higher than for congenital stenoses. The incidence of restenosis is approximately 15%. Complications have included death in approximately 1% of patients secondary to pulmonary artery rupture or pulmonary edema. Dilatation within 4 to 6 weeks after surgery should be avoided because of the risk of vessel rupture. Aneurysms occur in 3% of dilations and are most common in small vessels distal to the stenosis. By positioning the wire in the largest vessel distal to the stenosis and avoiding distal migration of the balloon, the incidence of aneurysms has been decreased. Although the success rate using low-pressure balloons has changed little over the years, the complication rate has decreased due primarily to improved technique. The use of high-pressure balloons does not seem to have significantly altered the complication rate. The success rate has been further increased by the use of intravascular stents (Fig. 28.3) (see later discussion).

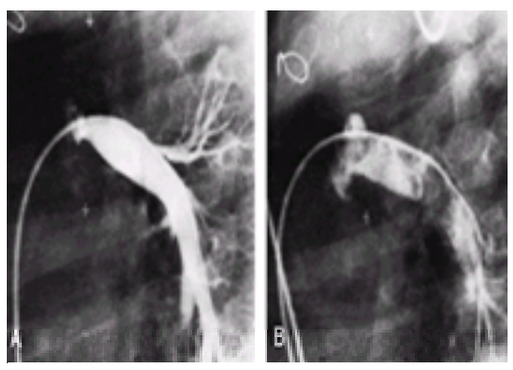

FIG. 28.3. A selective left pulmonary artery injection before **(A)** and after **(B)** balloon dilation of the stenotic origin.

COIL EMBOLIZATION OF CONGENITAL AND ACQUIRED THORACIC VESSELS

Therapeutic embolization of unwanted thoracic vessels was first reported in 1974 (39). A number of materials and devices have been used to successfully occlude aortopulmonary collaterals, arteriovenous malformations, Blalock-Taussig shunts, venous collaterals and venae cavae, coronary artery fistulas, and PDAs (40,41,42,43,44,45 and 46). This section discusses the use of Gianturco coils in these lesions.

Coils (Occluding Spring Emboli, Cook, Inc., Bloomington, IN) are stainless steel wires, either 0.018, 0.025, 0.035, 0.038, or 0.052 inches in diameter, embedded with Dacron strands to promote thrombosis. The coil is delivered by positioning a catheter in the vessel to be embolized and then extruding the coil from the catheter by insertion of a guidewire. As the wire coil is extruded from the catheter, it coils to a predetermined diameter (commonly 2 to 12 mm) and shortens significantly compared with the uncoiled length, which varies between 1.2 and 10 cm.

Technique

Routine sedation is used, and intravenous heparin (100 units/kg of body weight) is given when vascular access has been obtained. Patients are given an antibiotic (usually cefazolin) before coil embolization and for 24 hours after embolization.

Vascular access for coil embolization depends on which vessels are to be embolized. Most aortopulmonary collaterals, PDAs, and shunts are closed via the femoral or, rarely, the axillary artery. A number of catheters are used to perform angiograms, test occlude vessels, and deliver the coils, and therefore a sheath in the artery is helpful. A major advantage of coils in pediatric patients is that they can be delivered through catheters as small as 3F. Venous collaterals, venae cavae, and pulmonary arteriovenous malformations are closed from the venous side using the femoral, subclavian, or internal jugular vein.

To decide whether to close a particular vessel, one needs to know the hemodynamic consequences of closure and the technical feasibility of embolization. The hemodynamic consequences of closure depend on the vessel to be closed, the presence of other defects, and what surgery the patient has undergone.

Closure of aortopulmonary collaterals, a source of pulmonary blood flow, in patients with cyanotic congenital heart disease results in increased cyanosis if any intracardiac defects remain unrepaired. However, if there are multiple collaterals (or other sources of pulmonary blood flow, such as shunts), closure of some collaterals before complete repair may be possible. This is tested by occluding each collateral with a balloon and measuring the systemic oxygen saturation. If a collateral is the only source of pulmonary blood flow to a segment of lung (i.e., no supply by the native pulmonary arteries), embolization may lead to pulmonary infarction. As with collaterals, test balloon occlusion of surgically created systemic-to-pulmonary artery shunts is required before embolization unless intracardiac defects have been corrected.

Most veins considered for embolization are in patients with Glenn- or Fontan-like procedures. These veins are associated with right-to-left shunts, diminished pulmonary blood flow, and systemic desaturation. Closure eliminates the systemic desaturation but can raise pulmonary artery or right-sided heart pressures. This possibility can be tested by transient balloon occlusion. Similarly, occlusion of a left superior vena cava (SVC) in the absence of an innominate or adequate connecting veins can critically raise pressure above the occlusion, and this should be assessed by test occlusion. Finally, we have seen several patients with atresia of the ostium of the coronary sinus in whom the coronary sinus drains via a persistent left SVC. The presence and anatomy of branches need to be defined. For example, when embolizing a left SVC, one must be careful to position the coils so that the azygos vein does not drain to the left side of the heart.

The most difficult part of most procedures is entering the vessel to be embolized. The availability of a variety of preformed catheters and specialty wires, including tip deflectors and torque-control wires, has made this task easier. Once the vessel has been entered, selective angiograms are used to define the length, the proximal and distal anatomy, the presence of stenoses, and the diameter of the vessel. It is important to realize that the diameter may increase once the vessel is occluded. This is rarely a problem in arteries, but veins are more distensible, and it is therefore best to perform angiograms with the vessels balloon-occluded. Failure to do so can lead to migration of the coils as the vessel enlarges after embolization. Criteria for proceeding with embolization include availability of an appropriately sized coil and a vessel long enough to accept the coil. The presence of distal stenoses decreases the risk of distal migration. The length and shape of the coil when embolized depend on a number of factors, including the coil-to-vessel diameter ratio, the distensibility of the vessel, and the diameter of the wire in the coil. If the coil diameter is too large for a vessel, it will tend to remain straight rather than coil and push the catheter out of the vessel. We choose the first coil to be about 10% to 40% larger than the vessel diameter.

The type of catheter used to deliver the coil depends on the anatomy of the vessel to be embolized. Attempts are made to avoid acute angles in the catheter course (which make passage of the coil through the catheter difficult) and to fix the position of the catheter tip during delivery of the coil with the use of preformed catheter curves. Coils are extruded from the catheter using the soft end of appropriately sized guidewires. Occasionally, particularly with tortuous catheter courses, the coil cannot be extruded. If it is still entirely within the catheter, the catheter and coil are removed. If the coil is partially out the end of the catheter and appropriately positioned, the coil is delivered by rapid flushing of the catheter lumen with saline using a 1-cc tuberculin syringe.

If the vessel remains patent 5 to 10 minutes after coil placement, additional coils, often smaller than the first, are placed or blood flow in the vessel is interrupted by balloon occlusion to promote thrombosis. The procedure is terminated when the vessel is completely occluded or when no space remains for additional coils.

Modified Blalock-Taussig shunts (Gore-Tex tubes), as a group, are technically difficult to coil embolize for several reasons. Although most native vessels tend to expand or bulge in response to the coil (a property that tends to fix the coil), rigid Gore-Tex tubes do not. Combined with the high flow and common lack of distal stenoses, this increases the risk of distal coil migration. Also, coils that are even slightly too large tend to straighten and may push the catheter out of the shunt. If this happens, the coil may be pulled out of the shunt and embolize to a systemic artery. For these reasons, we choose coils slightly larger than the shunt and, in some cases, occlude the distal end of the shunt with a balloon dilatation catheter in the pulmonary artery during coil delivery.

Coronary artery fistulas can be closed either retrograde from the aorta or from the venous side by entering the distal opening that is commonly into the right atrium. Although standard coronary catheters can be used, the fistulas can be entered easily with balloon-tip flow-directed catheters owing to their size and high flow. Angiograms should demonstrate whether there are multiple distal openings, the presence of stenoses, and the location of normal coronary branches so that one can decide where to position the coils. Test balloon occlusion at that site before coil embolization is prudent.

Coils have been used to routinely close small PDAs. In contrast to other vessels, coil occlusion of a PDA does not involve positioning the coil inside the PDA. Rather, the coil is positioned to straddle the PDA, with one or two loops on the pulmonary artery side and two or three loops on the aortic side. The coil is chosen to be twice the diameter of the narrowest area of the PDA and long enough to have 4 loops when coiled. The coils can be delivered via venous or arterial access. Using a retrograde approach from the femoral artery, the catheter is advanced through the PDA into the pulmonary artery. Approximately one third (1 to 1.5 loops) of the coil is advanced out the catheter, and the catheter is pulled back until the loops are at the pulmonary end of the duct. The catheter is then withdrawn over the coil and guidewire, and the rest of the coil is delivered on the aortic side of the PDA. Multiple coils can be delivered simultaneously or sequentially with minimal risk of migration.

Results

Coil embolization is a very common intervention in our catheterization laboratory, and hundreds of vessels have been embolized (Fig. 28.4). Many embolizations eliminate the need for surgery, but more commonly, as with aortopulmonary collaterals or left SVC, they simplify surgery and allow the surgeon to concentrate on the intracardiac anatomy. The success rate for coil embolization is very high. With torque-control wires and a variety of preformed catheters and tracker systems, almost any vessel can be cannulated and coil-embolized. Of those embolized, more than 90% are completely occluded, and the recanalization rate is less than 5%. The most common complication, occurring in fewer than 1% of cases, remains migration of the coil out of the vessel being embolized. The coil can almost always be retrieved with the use of a snare or basket.

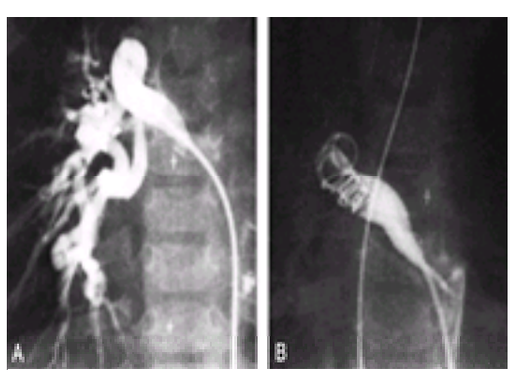

FIG. 28.4. An aortopulmonary collateral from the descending aorta to the right lung before **(A)** and after **(B)** coil embolization.

The results of coil embolizations of PDAs are excellent. Approximately 95% of PDAs smaller than 2.5 to 3 mm can be completely occluded with a single coil. Larger PDAs can also be coil-occluded, but they commonly require multiple coils. The technique has several advantages over other devices, including technical ease, smaller delivery catheters, and decreased cost. Most PDA devices are now designed for large PDAs.

DEVICE CLOSURE OF ATRIAL OR VENTRICULAR SEPTAL DEFECTS, AND PATENT DUCTUS ARTERIOSUS

Transcatheter closure of a PDA was first reported by Porstmann et al., in 1971 (47) using a plug that is still used successfully in some centers (48). King and Mills (49) reported the first transcatheter closure of ASDs by a double-disk device in 1976. In the 1980s, Rashkind developed a single umbrella (50) to close ASDs, but its use was associated with multiple problems and few successes. He later developed a double umbrella (51) to close PDAs and it was used successfully in large numbers of patients. Lock et al., first used this double umbrella to close selected ASDs and VSDs and later developed the Bard Clamshell Device (52,53,54,55,56,57 and 58), which was the first device to be used in large numbers of patients to close ASD secundum, patent foramen ovale (PFO), and VSDs. It was also used in a variety of other defects, including coronary artery fistulas, left ventricular apex-to-descending aorta conduits, SVC-to-right atrial communications occurring after Glenn shunts, SVC and azygos veins, Potts anastomoses, large aortopulmonary collaterals, large arteriovenous malformations, and paravalvar leaks. The last several years have witnessed an explosion in the device field. The double umbrella has continued to undergo modifications, and new devices have been appearing with increasing frequency. Most of the new devices were developed initially for ASD closure, but some have been modified to allow closure of PDAs and VSDs. The current list of ASD devices includes the CardioSEAL (a modified clamshell) (Nitinol Medical, Boston, MA) and its modification, the STARFlex; the button device (Custom Medical Devices, Amarillo, TX); the ASDOS device (Osypka Corporation, Germany); the Das-Angel Wings device (Microvena, Vadnais, MN); and the Amplatzer Septal Occluder (AGA Medical Corporation, Golden Valley, MN) (59,60,61,62,63,64,65,66,67 and 68). Many of these devices are used routinely outside the United States, but currently none has been approved by the U.S. Food and Drug Administration. Of the current devices, the double umbrella (CardioSEAL and STARFlex) and the Amplatzer appear to be the most promising; they are discussed in the following sections.

Closure of Atrial Septal Defects

Technique

Although the techniques for loading, positioning, and releasing the various devices differ, the overall approach for transcatheter closure of ASDs is similar for most devices (Fig. 28.5). The devices are designed to close a secundum ASD or PFO, but primum and sinus venosus ASDs are not closed because of their proximity to the atrioventricular valves and pulmonary veins, respectively. Devices are positioned by a combination of fluoroscopy and transesophageal echocardiography. The latter technique is especially useful for secundum ASD (69), but it is generally not needed for small PFOs. In most cases, general anesthesia is used and the patient is heparinized and receives prophylactic antibiotics. Access for closure is almost always via the femoral vein, although a few devices have been implanted via the internal jugular or the hepatic vein. After routine hemodynamic measurements, the defect is sized in two ways. First, it is measured echocardiograpically, and then the stretched diameter is measured by pulling a sizing balloon across the defect or using a static balloon. In general, the stretched diameter is 20% to 30% larger than the unstretched diameter. The choice of device size is usually based on the stretched diameter.

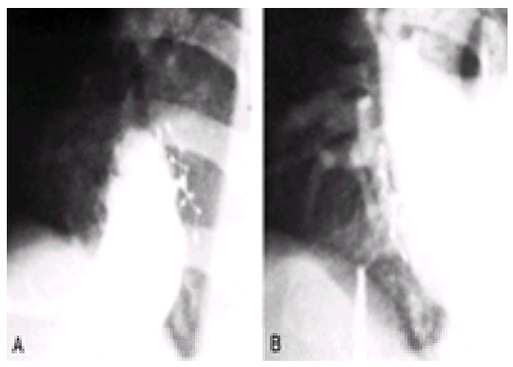

FIG. 28.5. A right atrial injection **(A)** with levophase **(B)** demonstrating complete closure of a secundum atrial septal defect with a 27-mm clamshell umbrella.

The CardioSEAL consists of two square Dacron umbrellas, each supported by four spring-loaded arms constructed of MP35N. It is available in 17-, 23-, 28-, 33-, and 40-mm sizes, the size corresponding to the diagonal of the square. The delivery system normally requires an 11F sheath. The STARFlex is a modification in which flexible nitinol springs run back and forth between the arm tips of the two umbrellas, a system that promotes self-centering. In addition, the delivery system has been modified to allow use of a 10F long sheath for delivery and more flexibility of the device before release. In general, the CardioSEAL is chosen to be twice the diameter of the stretched diameter of the ASD. With the self-centering mechanism, a smaller STARFlex device, 1.6 to 1.8 times the diameter of the defect, can be used. After balloon-sizing, a long sheath is advanced over a guidewire from the femoral vein to the left atrium, and the dilator and guidewire are removed. One must be very careful to avoid emboli through the long sheath. The double umbrella is loaded into the delivery system by collapsing the left atrial umbrella distally and the right atrial umbrella proximally. The delivery system is then advanced to the end of the long sheath. Retraction of the long sheath allows the left atrial umbrella to open. The entire system is then withdrawn under echocardiographic guidance until the left atrial umbrella is near the septum. The sheath is then withdrawn to allow the right atrial umbrella to open. If all of the arms are correctly positioned by echocardiography, the device is released. The device can be pulled back into the sheath if only the left atrial umbrella has been opened. Retrieval is more difficult if both umbrellas have been opened, but it can almost always be retrieved with the use of transcatheter techniques.

The Amplatzer Septal Occluder is constructed of 0.004- to 0.005-inch nitinol wires that are tightly woven into a right and left atrial button connected by a 4-mm waist. The device size is determined by the waist and, currently, multiple sizes between 4 and 34 mm are available. The device is filled with polyester threads to enhance thrombogenicity. The device is loaded by stretching, which eliminates the discs and waist. The smaller sizes can be delivered through a 7F long sheath. The device is designed to stent the defect open and the device size is chosen so that the waist is equal to the stretched diameter. Delivery is similar to the double umbrella in that the left atrial disc is opened first, followed by the right atrial disc. One advantage of the Amplatzer is that the device can be pulled back into the sheath even if both discs have been opened.

Results

There is a rapidly growing literature regarding the results of device closure of ASDs (70,71,72,73,74,75,76,77,78 and 79). Because it has been available in one modification or another, the double umbrella device has the largest and longest follow-up. With the original clamshell device, successful implantation was accomplished in 94% of cases, with an incidence of severe complications of 6% (death, cerebral vascular accident, need for emergent operation, tamponade, cardiac arrest, or severe dysrhythmia). The complication rate decreased in later studies with the use of the CardioSEAL. In follow-up reviews of more than 500 patients, the incidence of late transient ischemic attacks and arrhythmias was less than 1% and endocarditis was not seen. Residual leaks occurred in 39% but were significant in only 6%. Preliminary results with the STARFlex modification suggest that it has significantly higher closure rates than the CardioSEAL.

The Amplatzer device was successfully implanted in 100% of patients and achieved complete closure in 95% at 3 months. The incidence of severe complications at the time of implantation was 1.7%. Complications early in follow-up were uncommon but included both transient ischemic attacks and endocarditis. Long-term follow-up results are not yet available.

Although the procedure is not yet approved in the United States, many centers elsewhere routinely close secundum ASDs. With ongoing modifications to existing instruments and the advent of new ones, it should not be long before such devices are approved in this country. In addition to clinical trials for secundum ASDs, trials are also underway to determine the efficacy of devices for closing fenestrated Fontans and for closing PFOs in stroke patients.

Closure of Ventricular Septal Defects

Transcatheter closure of VSDs was first reported by Lock et al., in 1988 (53). They used the Rashkind PDA double umbrella to close small defects. The development of the clamshell device allowed closure of larger defects (80), and the CardioSEAL and STARFlex modifications of the clamshell are now used for VSD closure (Fig. 28.6). The Amplatzer device has been modified to allow closure of VSDs (81). Currently available devices do not lend themselves to closure of the most common type of VSD, the perimembranous defect, owing to the proximity to the aortic valve. Rather, device closure is used for muscular defects, congenital or postinfarction, and for patch margin defects. These are the defects with which surgeons have the most difficulty.

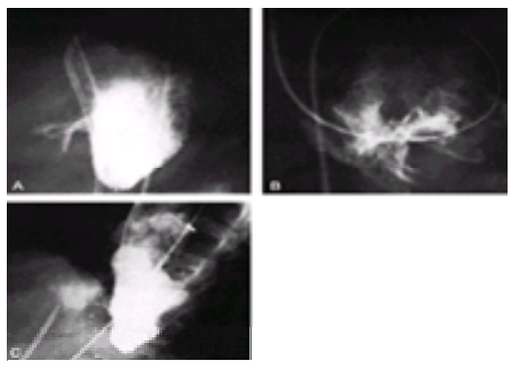

FIG. 28.6. A: Left ventriculogram demonstrating a midmuscular ventricular septal defect (VSD). **B:** Selective injection in the VSD with a pigtail over a wire from the femoral vein through the atrial septum and VSD and out the superior vena cava and internal jugular vein. **C:** Left ventriculogram taken after umbrella placement demonstrates complete closure. The contrast material in the right ventricle is from a malalignment VSD, which was closed surgically.

Technique

Precatheterization Doppler echocardiograms should define the number, location, and size of the VSDs and the relationship of these defects to the atrioventricular and semilunar valves.

A VSD is usually easier to cross from the left to the right ventricle, rather than vice versa, because of the smooth left ventricular surface and the left-to-right shunt present in most defects. The left ventricle can be entered retrograde from the aorta or transseptally from the venous side and across the mitral valve. The choice depends on patient size and VSD location. Right- and left-sided hemodynamics are measured, and a left ventriculogram is performed in a projection most likely to profile the VSD. The decision must then be made as to what venous access to use for device delivery. A middle or apical muscular VSD is easiest to close via the internal jugular vein or via the transseptal approach from the femoral vein, because the course is straighter and the sheath is less likely to kink. On the other hand, an anterior muscular VSD is easiest to close from the right ventricular side via the femoral vein. The VSD is crossed from left to right. An exchange wire is then advanced out of that catheter, snared, and drawn out through the skin at the venous site to be used for closure. It is important to avoid getting the wire entangled in the tricuspid valve apparatus. This wire now runs from either the femoral vein or artery through the heart, across the VSD and out (e.g., internal jugular vein). Traction on this wire can damage the heart or induce aortic or mitral regurgitation depending on its course. This wire is used to take selective pictures in the VSD using a pigtail catheter and Y-arm adaptor and for balloon sizing of the defect, although balloon-sizing is not as important for VSDs as for ASDs. Gentle traction on the through-and-through guidewire facilitates positioning of the long sheath across the defect.

For double umbrellas, the device is chosen to be 1.6 to 2 times the diameter of the defect. For the Amplatzer device, the waist of the device is chosen to equal the diameter of the defect. Device delivery is similar to that described for ASDs.

Results

Between February 1989 and July 1998, 148 VSDs were closed at Boston Children's Hospital with no deaths or late morbidity resulting from the procedure. Echocardiographic follow-up studies showed that 83% of the defects either were closed or had trivial residual leaks. Because of the presence of multiple defects, many patients had multiple devices placed. As a result the complexity and extent of the catheter manipulation involved, transient arrhythmias and hemodynamic compromise were not uncommon during these procedures (82). Other complications included asymptomatic hemothorax and a case in which the umbrella compromised the septal leaflet of the tricuspid valve. There is very limited experience with the recently released Amplatzer VSD device.

Patent Ductus Arteriosus Occlusion

As noted previously, coils are now used to close the most common small PDAs. PDAs larger than 3 mm usually require multiple coils. While this may be a reasonable option in many patients, there are other devices that can be used for larger PDAs. Currently, the only approved device is the Grifka bag (Cook) (83). This device is similar in concept to a detachable balloon, but instead of being fluid filled it is a nylon bag filled with a coil. It requires an 8F sheath and is usually delivered from the venous side, as are most devices. The fact that secure positioning requires a PDA with some length has limited its use. The Amplatzer device comes in a PDA design and is in clinical trials in this country. The clamshell has been used successfully to close large PDAs, and the CardioSEAL has been used occasionally to close large PDAs in patients who are at increased surgical risk as part of a high-risk protocol.

INTRAVASCULAR STENTS

Since 1989, when intravascular stents were first implanted in a patient with branch pulmonary artery stenosis, they have become an integral part of the management of congenital heart disease (84,85,86 and 87) (Fig. 28.7). In the last 10 years, 477 patients have undergone stent implantation at Children's Hospital, Boston. The most common lesions were branch pulmonary arteries in 246 patients, obstructed right ventricular-to-pulmonary artery conduits or homografts in 108 patients, and coarctation of aorta in 32 patients. Other sites included obstructed Fontan baffles or conduits in 21 patients, stenotic pulmonary veins in 18 patients, systemic ventricular outflow tract obstructions in 14 patients, stenotic aortopulmonary collaterals in 12 patients, and systemic venous obstructions in 16 patients. Uncommon, although often successful, uses of stents have included peripheral arterial obstructions, the creation and maintenance of ventricular and atrial septal defects and Fontan fenestrations, stenotic or thrombosed Blalock-Taussig shunts, and in patent ductus arteriosus to maintain patency in duct-dependent lesions.

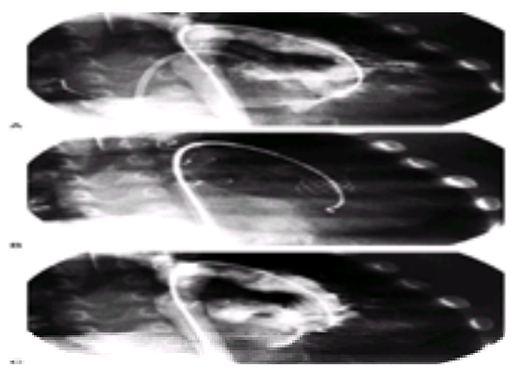

FIG. 28.7. A: Left ventriculogram in a patient with [S,L,L] a single left ventricle demonstrates a restrictive bulboventricular foramen (BVF). **B:** A spot cine film of an 18-mm iliac stent expanded to 12 mm in the BVF. **C:** Repeat ventriculogram taken after stent implantation. The peak systolic ejection gradient was reduced from 70 to 10 mm Hg.

Technique

We have used balloon-expandable Palmaz stents from Johnson and Johnson. The most commonly used sizes are the 10-, 15-, and 20-mm-long biliary stents (predilation diameter, 2.5 mm) and the 12-, 18-, and 30-mm-long iliac stents (predilation diameter, 3.4 mm). The biliary stents can be expanded to approximately 12 mm in diameter and the iliac stents to 18 mm. Because of their design, the Palmaz stents shorten as they expand.

Balloons available for stent implantation continue to improve. In the past, the most common technical problems with stent implantation were the stent's slipping off the balloon during positioning and expansion and balloon rupture during inflation. These problems have been largely overcome with the advent of balloons with surfaces that resist slippage and are scratch resistant. The unique balloon-in-a-balloon (NuMed) has further reduced the technical difficulties of stent implantation.

Stents can be implanted in most patients with the use of routine sedation. General anesthesia is reserved for patients who cannot be controlled with sedation and in those who are likely to be hemodynamically unstable during implantation. Once percutaneous access has been obtained, heparin (100 units/kg body weight) is given, and the activated clotting time is maintained at more than 200 seconds. Prophylactic cefazolin is given before implantation and for 24 hours after implantation.

In most patients, a balloon is inflated in the lesion before stent implantation. This allows determination of the balloon expandability of the lesion and the use of high-pressure balloons, if necessary, before stent implantation. Because it is rarely possible to reposition an expanded Palmaz stent, it is important to position the stent and balloon properly during inflation. Inflating a balloon before stent implantation allows one to determine the optimal balloon position, diameter, and length and to change the guidewire if necessary.

The stent is mounted and crimped onto the appropriate balloon. A long sheath is used to protect the stent as it is advanced to the lesion. One of two techniques can be used. First, the long sheath is positioned across the lesion, and the balloon is advanced over a guidewire through the sheath. The second option is to advance the balloon through the long sheath outside the body. The stent is then mounted on the balloon and retracted into the sheath, leaving the distal tip of the balloon exposed to act as a dilator. The system is then advanced as a unit over the guidewire. The latter technique has two advantages. It eliminates the problem of advancing the stent past kinks that can develop in the sheath with the first technique. It also allows the use of smaller sheaths. The size of the sheath used depends on the balloon and stent size but is most commonly 7F or 8F for biliary stents and 8F to 12F for the iliac stents. An extra-stiff exchange-length guidewire with a short, floppy tip facilitates positioning of the stent and stabilizes the balloon during inflation. With either technique, a side-arm adaptor at the proximal end of the sheath prevents blood loss and allows injections of contrast material to ensure proper positioning of the stent before inflation. When the stent is in position, the long sheath is retracted and the balloon is inflated. Angiograms and hemodynamic measurements are repeated after implantation.

Anticoagulation during the catheterization is achieved with heparin. Patients who have pulsatile flow through the stent are given heparin for at least 12 hours and aspirin for at least 6 months. For stents with nonpulsatile flow, patients are given warfarin for 6 months and heparin until the prothrombin time is elevated.

Results

The most common indication for stent implantation remains branch pulmonary artery stenosis (88). The majority have been implanted in the proximal left or right pulmonary artery. Implantation more distally in the lung is limited by the multiple branches, so that stenting of one branch open covers others; such covered branches, however, are not necessarily occluded by the stent. In the first 77 patients at our institution, the diameter of the stenosis was increased from an average of 3.8 to 8.3 mm, or an average of 120%. The gradient was reduced from 53 to 20 mm Hg, and the right ventricular pressure as a percentage of systemic pressure was reduced from 88% to 62%. These are significantly better results than those achieved with conventional dilation. Follow-up analyses have demonstrated a very low incidence of restenosis.

The second most commonly stented lesion has been right ventricular-to-pulmonary artery homografts and conduits (89). In our first 50 patients, the diameter of the narrowest area was almost doubled and the gradient was reduced by approximately 50%. Stenting has prolonged the life of homografts, on average, by 2.5 years. Stents have proved very useful in systemic venous obstructions, including baffle obstructions occurring after Mustard or Senning repairs of D-transposition of the great arteries. We have implanted stents inside the heart in seven patients with left ventricular outflow obstruction. The sites of obstruction have included restrictive VSDs in patients who have undergone a Rastelli-type repair, tunnel subaortic stenosis, and an obstructed left ventricular-to-descending aorta conduit.

The fastest growing indication for stents in patients with congenital heart disease over the last few years has been coarctation (90). Initially, stents were implanted primarily in patients with recoarctations who were at increased surgical risk and for whom conventional dilation had failed. Their success in that group led to their evaluation for other indications. These include the use of primary stenting for native and postoperative coarctations in adults. This approach, which avoids conventional dilation, reduces the size of the balloons used and may decrease the incidence of aneurysms, dissections, and rupture. Another group comprises those with relative mild stenoses and gradients less than 20 mm Hg who may nonetheless develop left ventricular dysfunction, systolic and/or diastolic. Neither conventional surgery nor balloon dilation has much to offer this group, but stents can reduce or eliminate the gradient in most patients. The ultimate indications in patients with coarctations await further study.

Significant nontransient complications during implantation are rare. The most common remains stent malposition, which occurs in approximately 1% of cases. The most common reason is balloon rupture during inflation. Although most malpositioned stents can be left, occasionally a patient is sent to the operating room for removal. Stent fracture during follow-up has been seen, and the incidence varies with the lesion stented. We have not seen it in pulmonary artery stents, but approximately 10% of homograft stents fracture. The only complication of fracture has been recurrence of the gradient.

At present, neither the indications nor the contraindications to stent implantation are absolute, and the continue to change as experience is gained. For example, stent implantation in small infants should be avoided because the stents do not grow and the ability to redilate stents is somewhat limited. However, we have now implanted stents in many infants who, at the time, had no good medical or surgical options. The stents were implanted in locations accessible to the surgeon (e.g., not in the distal pulmonary arteries), and many of the patients have subsequently gone to surgery, where stent removal has not been a problem. The indications also will change with the availability of new stent designs, including covered stents (91), biodegradable stents, and stents that allow dilation of side branches that have been covered by stents.

CHAPTER REFERENCES

1. Rashkind WJ, Miller WW. Creation of an atrial septal defect without thoracotomy: palliative approach to complete transposition of the great arteries. *JAMA* 1996;196:991.
2. Park SC, Zuberbuhler JR, Neches WH, et al. A new atrial septostomy technique. *Cathet Cardiovasc Diagn* 1975;1:195.
3. Edwards BS, Lucas RV, Lock JE, et al. Morphologic changes in the pulmonary arteries after percutaneous balloon angioplasty for pulmonary arterial stenosis. *Circulation* 1985;71:195.
4. Ring JC, Kulik TJ, Burke BA, et al. Morphologic changes induced by dilation of the pulmonary valve annulus with overlarge balloons in normal newborn lambs. *Am J Cardiol* 1984;55:210.
5. Yeager S. Letter. *J Am Coll Cardiol* 1987;9:467.
6. Rubio-Alvarez V, Limon RL, Soni J. Valvulotomias intracardiacas por medio de un cateter. *Arch Inst Cardiol Mex* 1953;23:183.
7. Semb BKH, Tjonneland S, Stake G, et al. Balloon valvulotomy of congenital pulmonary valve stenosis with tricuspid valve insufficiency. *Cardiovasc Radiol* 1979;2:239.
8. Kan JS, White RI Jr, Jitchell SE, et al. Percutaneous balloon valvuloplasty: a new method for treating congenital pulmonary valve stenosis. *N Engl J Med* 1982;307:540.
9. Radkte W, Keane JF, Fellows KE, et al. Percutaneous balloon valvotomy of congenital pulmonary stenosis using oversized balloons. *J Am Coll Cardiol* 1986;8:909.
10. Ali Khan MA, Yousef SA, Mullins CE. Percutaneous transluminal balloon pulmonary valvuloplasty for the relief of pulmonary valve stenosis with special reference to double-balloon technique. *Am Heart J* 1986;112:158.
11. Stanger P, Cassidy SC, Girod DA, et al. Balloon pulmonary valvuloplasty: results of the valvuloplasty and angioplasty of congenital anomalies registry. *Am J Cardiol* 1990;65:775.
12. Perry SB, Keane JF, Lock JE. Interventional catheterization in pediatric congenital and acquired heart disease. *Am J Cardiol* 1988;61:109G.
13. Lababidi Z. Aortic balloon valvuloplasty. *Am Heart J* 1983;106:751.
14. Sholler GF, Keane JF, Perry SB, et al. Balloon dilation of aortic stenosis: results and influence of technical and morphological features on outcome. *Circulation* 1988;78:351.
15. Rocchini AP, Beekman RH, Schachar GB, et al. Balloon aortic valvuloplasty: results of the valvuloplasty and angioplasty of congenital anomalies registry. *Am J Cardiol* 1990;65:784.
16. Cribier A, Savin T, Berland J, et al. Percutaneous transluminal balloon valvuloplasty of adult aortic stenosis: report of 92 cases. *J Am Coll Cardiol* 1987;9:381.
17. Rosenfeld HM, Landzberg MJ, Perry SB, et al. Balloon aortic valvuloplasty in the young adult with congenital aortic stenosis. *Am J Cardiol* 1994;73:1112.
18. Moore P, Egito E, Mowrey BS, et al. Midterm results of balloon dilation of congenital aortic stenosis: predictors of success. *J Am Coll Cardiol* 1996;27:1257.
19. Helgason H, Keane JF, Fellows KE, et al. Balloon dilation of the aortic valve: studies in normal lambs and in children with aortic stenosis. *J Am Coll Cardiol* 1987;9:816.
20. Waller BF, Girod DA, Dillon JC. Transverse aortic wall tears in infants after balloon angioplasty for aortic valve stenosis: relation of aortic wall damage to diameter of inflated angioplasty balloon and aortic lumen in 7 necropsy cases. *J Am Coll Cardiol* 1984;4:1235.
21. Egito ES, Moore P, O'Sullivan J, et al. Transvascular balloon dilation for neonatal critical aortic stenosis: early and midterm results. *J Am Coll Cardiol* 1997;29:442.
22. Rhodes LA, Colan SD, Perry SB, et al. Predictors of survival in neonates with critical aortic stenosis. *Circulation* 1991;84:2325.
23. Singer MI, Rowen M, Dorsey TJ. Transluminal aortic balloon angioplasty for coarctation of the aorta in the newborn. *Am Heart J* 1982;103:131.

24. Saul JP, Keane JF, Fellows KE, et al. Balloon dilation angioplasty of postoperative aortic obstructions. *Am J Cardiol* 1987;59:943.
25. Morrow WR, Vick GW, Nihil MR, et al. Balloon dilation of unoperated coarctation of the aorta: short- and intermediate-term results. *J Am Coll Cardiol* 1988;11:133.
26. Beekman RH, Rocchini AP, Dick M. Percutaneous balloon angioplasty for native coarctation of the aorta. *J Am Coll Cardiol* 1987;10:1078.
27. Tynan M, Finley JP, Fontes V, et al. Balloon angioplasty for the treatment of native coarctation: results of the valvuloplasty and angioplasty of congenital anomalies registry. *Am J Cardiol* 1990;65:790.
28. Hellenbrand WE, Allen HD, Golinko RJ, et al: Balloon angioplasty for aortic recoarctation: results of the valvuloplasty and angioplasty of congenital anomalies registry. *Am J Cardiol* 1990;65:793.
29. Rao PS, Galal O, Smith PA, et al. Five to nine year follow up results of balloon angioplasty of native aortic coarctation in infants and children. *J Am Coll Cardiol* 1996;27:462.
30. Shaddy RE, Boucek MM, Sturtevant JE, et al. Comparison of angioplasty and surgery for unoperated coarctation of the aorta. *Circulation* 1993;87:793.
31. McCrindle BW, Jones TK, Morrow WR, et al. Acute results of balloon angioplasty of native coarctation versus recurrent aortic obstruction are equivalent. *J Am Coll Cardiol* 1996;28:1810.
32. De Giovanni JV, Lip GYH, Osman K, et al. Percutaneous balloon dilatation of aortic coarctation in adults. *Am J Cardiol* 1996;77:435.
33. Fletcher SE, Nihill MR, Grifka RG, et al. Balloon angioplasty of native coarctation of the aorta: midterm follow-up and prognostic factors. *J Am Coll Cardiol* 1995;25:730.
34. Lock JE, Niemi T, Burke B, et al. Transcutaneous angioplasty of experimental aortic coarctation. *Circulation* 1982;66:1280.
35. Perry SB, Zeevi B, Keane JF, et al. Interventional catheterization of left heart lesions, including aortic and mitral valve stenosis and coarctation of the aorta. *Cardiol Clin* 1989;7:341.
36. Rothman A, Perry SB, Keane JF, et al. Early results and follow-up of balloon angioplasty for branch pulmonary artery stenosis. *J Am Coll Cardiol* 1990;15:1109.
37. Kan JS, Marvin WJ, Bass JL, et al. Balloon angioplasty—Branch pulmonary artery stenosis: results from the valvuloplasty and angioplasty of congenital anomalies registry. *Am J Cardiol* 1990;65:798.
38. Gentles TL, Lock JE, Perry SB. High pressure balloon angioplasty for branch pulmonary artery stenosis: early experience. *J Am Coll Cardiol* 1993;22:867.
39. Zuberbuhler JR, Anker E, Zoltun R, et al. Tissue adhesive closure of aortic-pulmonary communications. *Am Heart J* 1974;88:41.
40. Barth KH, White RI, Kaufman SL, et al. Embolotherapy of pulmonary arteriovenous malformations with detachable balloons. *Radiology* 1982;142:599.
41. Perry SB, Radtke W, Fellows KE, et al. Coil embolization to occlude aortopulmonary collateral vessels and shunts in patients with congenital heart disease. *J Am Coll Cardiol* 1989;13:100.
42. Perry SB, Rome J, Keane JF, et al. Transcatheter closure of coronary artery fistulas. *J Am Coll Cardiol* 1992;20:205.
43. Cambier PA, Kirby WC, Wortham DC, et al. Percutaneous closure of small (<2.5 mm) patent ductus arteriosus using coil embolization. *Am J Cardiol* 1992;69:815.
44. Lloyd TR, Raymond F, Mendelsohn AM, et al. Transcatheter occlusion of patent ductus arteriosus with Gianturco coils. *Circulation* 1993;88:1412.
45. Gianturco C, Anderson JH, Wallace S. Mechanical devices for arterial occlusion. *AJR Am J Roentgenol* 1975;124:428.
46. Anderson JH, Wallace S, Gianturco C, et al. “Mini” Gianturco stainless steel coils for transcatheter vascular occlusion. *Radiology* 1979;132:301.
47. Porstmann W, Wierny L, Warnke H, et al. Catheter closure of patent ductus arteriosus: 62 cases treated without thoracotomy. *Radiol Clin North Am* 1971;9:203.
48. Sato K, Fujino M, Kozuka T, et al. Transfemoral plug closure of patent ductus arteriosus. *Circulation* 1975;51:337.
49. King TD, Mills NL. Secundum atrial septal defects: nonoperative closure during cardiac catheterization. *JAMA* 1976;235:2506.
50. Rashkind WJ. Transcatheter treatment of congenital heart disease. *Circulation* 1983;67:711.
51. Rashkind WJ, Mullins CE, Hellenbrand WE, et al. Nonsurgical closure of patent ductus arteriosus: clinical application of the Rashkind PDA occluder system. *Circulation* 1987;75:583.
52. Lock JE, Rome JJ, Davis R, et al. Transcatheter closure of atrial septal defects: experimental studies. *Circulation* 1989;79:1091.
53. Lock JE, Block PC, McKay RG, et al. Transcatheter closure of ventricular septal defects. *Circulation* 1988;78:361.
54. Bridges ND, Perry SB, Keane JF, et al. Preoperative transcatheter closure of congenital muscular ventricular septal defects. *N Engl J Med* 1991;324:1312.
55. Lock JE, Cockerham JT, Keane JF, et al. Transcatheter umbrella closure of congenital heart defects. *Circulation* 1987;75:593.
56. Hourihan M, Perry SB, Mandell VS, et al. Transcatheter umbrella closure of valvular and paravalvular leaks. *J Am Coll Cardiol* 1992;20:1371.
57. Perry S, van der Velde M, Bridges N, et al. Transcatheter closure of atrial and ventricular septal defects. *Herz* 1993;18:135.
58. Rome J, Keane J, Perry S, et al. Double-umbrella closure of atrial defects: initial clinical applications. *Circulation* 1990;82:751.
59. Sideris E, Sideris S, Fowlkes J, et al. Transvenous atrial septal occlusion in piglets using a “buttoned” double disc device. *Circulation* 1990;81:312.
60. Rao P, Wilson A, Levy J, et al. Role of “buttoned” double disc device in the management of atrial septal defects. *Am Heart J* 1992;123:191.
61. Rao R, Chandar J, Sideris E. Role of inverted buttoned device in transcatheter occlusion of atrial septal defects or patent foramen ovale with right-to-left shunting associated with previously operated complex congenital cardiac anomalies. *Am J Cardiol* 1997;80:914.
62. Sharafuddin M, Gu X, Titus J, et al. Transvenous closure of secundum atrial septal defects: preliminary results with a new self-expanding nitinol prosthesis in a swine model. *Circulation* 1997;95:2162.
63. Babic U, Grujicic S, Popovic Z, et al. Double-umbrella device for transvenous closure of patent ductus arteriosus atrial septal defect: first experience. *J Interven Cardiol* 1991;4:283.
64. Sievert H, Babic U, Ensslen R, et al. Transcatheter closure of large atrial septal defects with the Babic system. *Cathet Cardiovasc Diagn* 1995;36:232.
65. Das G, Voss G, Jarvis G, et al. Experimental atrial septal defect closure with a new, transcatheter, self-centering device. *Circulation* 1993;88:I-754.
66. Agarwal S, Ghosh P, Mittal P. Failure of devices used for closure of atrial septal defects: mechanisms and management. *J Thorac Cardiovasc Surg* 1996;1112:21.
67. Das G, Hijazi Z, O'Laughlin M, et al. Initial results of the VSD/PFO/ASD closure trial. *J Am Coll Cardiol* 1996;27:119A.
68. Hansdorf G, Schneider M, Franzbach B. Transcatheter closure of secundum atrial septal defects with the atrial septal occlusion system (ASDOS): initial experience in children. *Heart* 1996;75:83.
69. Hellenbrand W, Fahey J, McGowan F, et al. Transesophageal echocardiographic guidance of transcatheter closure of atrial septal defect. *Am J Cardiol* 1990;66:207.
70. Latson L, Benson L, Hellenbrand W, et al. Transcatheter closure of ASD-early results of multicenter trial of the Bard Clamshell Septal Occluder. *Circulation* 1991;84[Suppl II]:II-544.
71. Prieto L, Foreman C, Cheatham J, et al. Intermediate-term outcome of transcatheter secundum atrial septal defect closure using the Bard Clamshell Septal Umbrella. *Am J Cardiol* 1996;78:1310.
72. Lloyd T, Rao R, RH Beekman, et al. Atrial septal defect occlusion with the buttoned device (a multi-instutional U.S. trial). *Am J Cardiol* 1994;73:286.
73. Magni G, Hijazi Z, Pandian N, et al. Two- and three-dimensional transesophageal echocardiography in patient selection and assessment of atrial septal defect closure by the new DAS-Angel Wings device. *Circulation* 1997;96:1722.
74. Masura J, Gavora P, Formanek A, et al. Transcatheter closure of secundum atrial septal defects using the new self-centering Amplatzer Septal Occluder: initial human experience. *Cathet Cardiovasc Diagn* 1997;42:388.
75. Prewitt K, Gaither N, Frab A, et al. Transient ischemic attacks after long-term clamshell occluder implantation for closure of atrial septal defect. *Am Heart J* 1992;124:1394.
76. Rao P, Sideris E, Hausdort G, et al. International experience with secundum atrial septal defect occlusion by the buttoned device. *Am Heart J* 1998;128:1022.
77. Sievert H, Babic U, Ensslen R, et al. Occlusion of atrial septal defect with a new occlusive device. *Zeitschrift fur Kardiologie* 1996;85:97.
78. Zamora R, Rao P, Lloyd T, et al. Intermediate-term results of phase I Food and Drug Administration Trials of Buttoned Device occlusion of secundum atrial septal defects. *J Am Coll Cardiol* 1998;31:674.
79. Masura J, Lange PE, Wilkinson JL: US/International multicenter trial of atrial septal catheter closure using the Amplatzer Septal Occluder: initial results. *J Am Coll Cardiol* 1998;31[Suppl A]:57A.
80. Bridges N, Perry S, Keane J, et al. Preoperative transcatheter closure of congenital muscular ventricular septal defects. *N Engl J Med* 1991;324:1312.
81. Amin Z, Gu I, Berry J, et al. A new device for closure of muscular ventricular septal defects in a canine model. *Circulation* 1997;96:I-373.
82. Laussen P, Hansen D, Perry S, et al. Transcatheter closure of ventricular septal defects: hemodynamic instability and anesthetic management. *Anesth Analg* 1995;80:1076.
83. Grifka RG, Miller MW, Frischmeyer KJ, et al. Transcatheter occlusion of a patent ductus arteriosus in a Newfoundland puppy using the Gianturco-Grifka vascular occlusion device. *J Vet Intern Med* 1996;10:42.
84. O'Laughlin MP, Perry SB, Lock JE, et al. Use of endovascular stents in congenital heart disease. *Circulation* 1991;83:1923.
85. O'Laughlin MP, Slack MC, Grifka RG, et al. Implantation and intermediate-term follow-up of stents in congenital heart disease. *Circulation* 1993;88:605.
86. Fogelman R, Nykanen D, Smallhorn JF. Endovascular stents in the pulmonary circulation: clinical impact on management and medium term follow-up. *Circulation* 1995;92:88.
87. Mc Leold K, Blackburn M, Gibbs J. Stenting of stenosed aortopulmonary collaterals: a new approach to palliation in pulmonary atresia with multifocal aortopulmonary blood supply. *Br Heart J* 1994;71:487.
88. Shaffer KM, Mullins CE, Grifka RG, et al. Intravascular stents in congenital heart disease: short and long term results from a large single-center. *J Am Coll Cardiol* 1998;311:661.
89. Powell AJ, Lock JE, Keane JF, et al. Prolongation of RV-PA conduit life-span by percutaneous stent implantation: intermediate term results. *Circulation* 1995;92:3282.
90. Suarez de Lezo J, Pan M, Romero M, et al. Balloon-expandable stent repair of severe coarctation of the aorta. *Am Heart J* 1995;129:1002.
91. Preminger TJ, Lock JE, Perry SB. Traumatic aortopulmonary window as a complication of pulmonary artery balloon angioplasty: transcatheter occlusion with a covered stent. A case report. *Cathet Cardiovasc Diagn* 1994;31:286.

29
Profiles in Valvular Heart Disease

William Grossman

University of California, San Francisco, School of Medicine; Division of Cardiology, University of California, San Francisco Medical Center, San Francisco, California 94143

The cardiac valves have as their function the maintenance of unidirectional flow, to ensure that the energy released during myocardial contraction is transformed efficiently into the circulation of blood around the body. When the valves become diseased, compensatory mechanisms are brought into play to maintain the circulation commensurate with the metabolic needs of the body. These mechanisms, chief among which are dilatation and hypertrophy, are not without clinical costs, and it is these costs that are responsible for the major manifestations of valvular heart disease.

Valvular disease results in either incompetence of the valve with regard to its function of maintaining unidirectional flow (i.e., valvular insufficiency and regurgitation) or obstruction to the forward and natural course of the circulation (i.e., stenosis). Although mixed stenosis and insufficiency, both of moderate degree, frequently coexist in a particular valve, severe stenosis and severe insufficiency are almost never both present in the same valve. For example, the 0.5-cm ^{2} valvular orifice of a patient with severe calcific aortic stenosis may barely allow 50 to 60 mL to be ejected from the left ventricle during systole, and this only at a left ventricular systolic pressure of 200 to 300 mm Hg. The tiny fixed orifice cannot be expected to permit more than mild regurgitation in the subsequent diastole, where the driving force is an aortic diastolic pressure of 80 mm Hg.

I have seen an exception to this general rule in a middle-aged woman with rheumatic aortic stenosis and insufficiency. Aortography demonstrated severe aortic regurgitation; nevertheless, there was a resting transaortic systolic gradient of approximately 60 mm Hg. The explanation was apparent on close examination of the aortic valve during cineaortography: Although two leaflets were heavily calcified and immobile, the third was thickened but mobile. During diastole this leaflet prolapsed freely into the left ventricular cavity, whereas during systole its opening motion was limited or checked by apparent abutment against the free edges of the other two calcific, immobile leaflets. Another example of mixed, severe stenosis and aortic insufficiency is described later in this chapter and illustrated in Fig. 29.9.

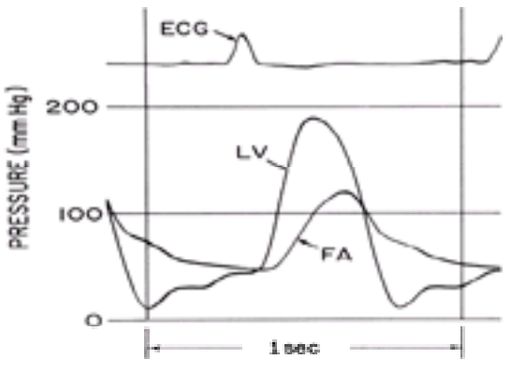

FIG. 29.9. Left ventricular (LV) and femoral artery (FA) pressure tracings in a 78-year-old man with increasing dyspnea on exertion and one episode of pulmonary edema. In this case, femoral artery and central aortic pressures were almost superimposable. There is a 70-mm Hg peak-to-peak systolic gradient, but there is also unusually rapid aortic diastolic runoff with equilibration (diastasis) of end-diastolic LV and FA pressures. This latter finding suggested significant aortic regurgitation, which was confirmed by aortography.

Valvular heart disease may be considered to impose two different types of stress on the cardiac chamber proximal to the lesion—either pressure overload (increased afterload) or volume overload (increased preload). The former is generally the result of valvular stenosis and the latter of valvular insufficiency. Both pressure overload and volume overload serve as stimuli for the heart to call on compensatory mechanisms. As mentioned, chief among these mechanisms are hypertrophy (which allows the generation of greater systolic force and at the same time tends to normalize wall stress by increasing wall thickness) and dilatation (which enables increased strength and extent of shortening by the Frank-Starling mechanism). These mechanisms preserve the circulation at the cost of increased myocardial oxygen needs and elevated ventricular filling pressures, leading to clinical evidence of ischemia and congestive heart failure.

This chapter illustrates the hemodynamic and angiographic findings seen in patients with valvular heart disease. It is useful to apply the general physiologic principles just discussed to the interpretation of catheterization data obtained from patients with disordered valve function, and this approach generally enables the physician to unravel even the most complicated problems.

MITRAL STENOSIS

The orifice area of the normal mitral valve is about 4.5 cm ^{2}. As a result of chronic rheumatic heart disease, the orifice becomes progressively smaller, and this leads to at least two distinct and important circulatory changes (1). The first is the development of a pressure gradient across the mitral valve, the left ventricular mean diastolic pressure remaining at its normal level of about 5 mm Hg and the left atrial mean pressure rising progressively, reaching about 25 mm Hg when the orifice of the mitral valve is reduced to approximately 1.0 cm^2(Fig. 29.1). A second major circulatory change is reduction of blood flow across the mitral valve (i.e., reduction of

the cardiac output). The normal resting cardiac output of 3.0 L/min/m^2 usually falls to about 2.5 L/min/m^2 when the valve size is 1.0 cm^2. A rise in left atrial pressure necessitates a similar rise in pressure in pulmonary veins and capillaries, and pulmonary edema occurs when the pulmonary capillary pressure exceeds the oncotic pressure of normal plasma, which is about 25 mm Hg.

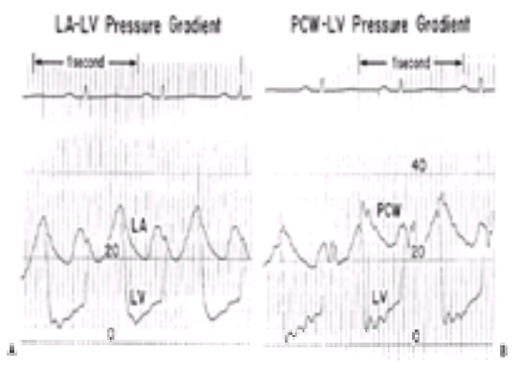

FIG. 29.1. Simultaneous left atrial (LA) and left ventricular (LV) pressures **(A)** and pulmonary capillary wedge (PCW) and LV pressures **(B)** in a patient with tight mitral stenosis and a mean PCW pressure of approximately 25 mm Hg. LV end-diastolic pressure is normal at 10 mm Hg. Note the presence of *a* waves in the LA and PCW trace which are not transmitted to the LV because of the damping effect of the stenotic mitral valve. (Reproduced from Lange RA, et al. Use of pulmonary capillary wedge pressure to assess severity of mitral stenosis: is true left atrial pressure needed in this condition? *J Am Coll Cardiol* 1989;13:825, with permission.)

Reactive pulmonary hypertension practically never occurs in mitral stenosis until the mitral valve area approaches 1.0 cm^2 (i.e., when the resting left atrial pressure approaches 25 mm Hg). After this point, reactive changes in the pulmonary arteriolar bed develop frequently, resulting in progressive obstruction to blood flow through the lungs.

As pulmonary vascular obstruction becomes increasingly severe, the pulmonary arterial pressure rises and occasionally may exceed the systemic arterial pressure. In the extreme, the pulmonary vascular resistance can rise to 25 or 30 times normal. Despite substantial hypertrophy, the right ventricle cannot cope with the enormous pressure load imposed on it, and it dilates and fails.

Thus, in mitral stenosis, two “stenoses” eventuate—first at the mitral valve and second in the arterioles of the lung. The hemodynamic findings in patients with tight mitral stenoses with and without major pulmonary vascular disease are illustrated in Fig. 29.2. As can be seen, the second stenosis (bottom panel) has resulted in a 70-mm Hg mean pressure gradient across the lungs, giving a pulmonary vascular resistance of 1866 dyn·sec·cm^{-5}. Workup of the patient with mitral stenosis should include an assessment of both of these obstructions.

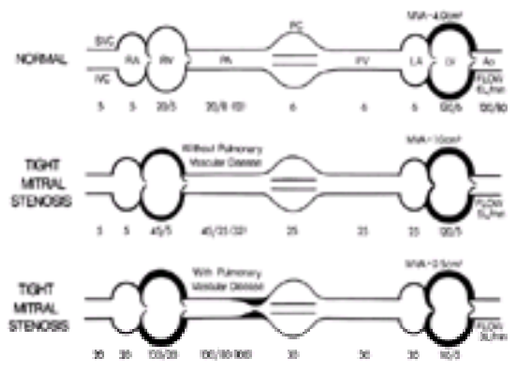

FIG. 29.2. Diagrammatic representation of the circulation in patients with normal hemodynamics *(top)*, tight mitral stenosis *(center)*, and tight mitral stenosis with pulmonary vascular disease and the development of a second stenosis at the pulmonary arteriolar level *(below)*. (See text for discussion.)

Catheterization Protocol

The usual indication for cardiac catheterization in patients with mitral stenosis is that the patient is being considered for either balloon mitral valvuloplasty or corrective surgery. Catheterization should be a combined right- and left-sided heart procedure in which the following measurements and calculations are made:

1. Simultaneous left ventricular diastolic pressure, left atrial (or pulmonary capillary wedge [PCW]) diastolic pressure, heart rate, diastolic filling period, and cardiac output. From these, the size of the mitral valve orifice may be calculated (see Chapter 10 for details of the orifice area calculation).
2. If the transmitral pressure gradient is less than 5 mm Hg, the error in calculation of the mitral valve orifice area is appreciable. The circulatory measurements should be repeated under circumstances of stress (exercise, reversible increase in preload resulting from passive elevation of the patient's legs, tachycardia induced by pacing) to increase the pressure gradient across the mitral valve.
3. Simultaneously, or in close order, pulmonary arterial mean pressure, left atrial (or PCW) mean pressure, and cardiac output for the calculation of pulmonary vascular resistance.
4. Right ventricular systolic and diastolic pressures for assessment of right ventricular function.
5. If other lesions are suspected (e.g., mitral regurgitation, ortic valve disease, left atrial myxoma), they too must be evaluated. Certain lesions tend to occur in combination with mitral stenosis. Many (if not most) patients with severe mitral stenosis have some degree of aortic regurgitation. Also, although it is rare, tricuspid stenosis always should be looked for in the patient with severe mitral stenosis, because it is seen only in association with this condition. Another condition that may be associated with mitral stenosis is atrial septal defect with left-to-right shunt. The combination of mitral stenosis and atrial septal defect is known as Lutembacher's syndrome. Therefore, as with standard right-sided heart catheterization, described in Chapter 4, Chapter 5 and Chapter 6, the operator should obtain screening blood samples from the superior vena cava and pulmonary artery for oximetry determination. This has taken on added importance in the present era when balloon mitral valvuloplasty (see Chapter 26) has become a standard treatment for mitral stenosis. Balloon mitral valvuloplasty usually requires transseptal catheterization and involves limited dilatation of the interatrial septum; the procedure may create an atrial septal defect, thereby producing iatrogenic Lutembacher's syndrome (2).

The following case studies illustrate the clinical and hemodynamic syndromes seen in patients with mitral stenosis. The first is a typical example of a symptomatic patient with “tight” mitral stenosis, normal pulmonary vascular resistance, and a normal-sized heart (stage II in Fig. 29.3). The second is an example of a relatively asymptomatic patient with more severe mitral stenosis, a 5- to 10-fold increase of pulmonary vascular resistance, and an enlarged heart caused principally by enlargement of the right ventricle (stage III). The third represents terminal mitral stenosis with an extreme degree of pulmonary vascular resistance, pulmonary hypertension, and right ventricular failure (stage IV).

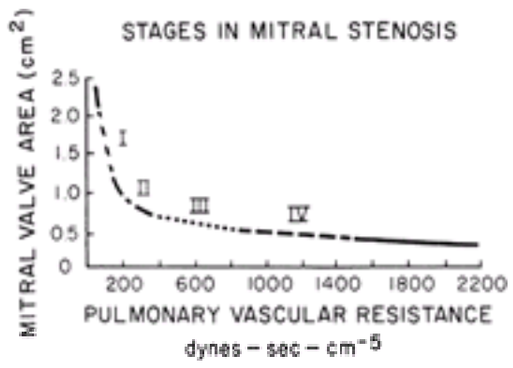

FIG. 29.3. Stages in the natural history of mitral stenosis. As the mitral orifice progressively narrows, pulmonary vascular resistance increases. The increase is slow at first, but when the mitral valve area becomes "critical" (less than 1 cm^2), the increase is rapid, reflecting the development of a second stenosis at the level of the precapillary pulmonary arterioles. Clinical correlations are discussed in the text.

Case 1: Tight Mitral Stenosis with Normal Pulmonary Vascular Resistance. A.R., a 35-year-old woman, had chorea as a child and was asymptomatic thereafter until age 33 years, when she noted the onset of exertional dyspnea. This progressed to the point of her having to stop after climbing one flight of stairs slowly. She had had one recent episode of hemoptysis. Her most troublesome symptom at the time of presentation had been paroxysmal atrial fibrillation over a period of several months. She had had orthopnea and one episode of paroxysmal nocturnal dyspnea.

On physical examination, she was in no apparent distress. Blood pressure was 130/70 mm Hg, and pulse rate was 80 beats per minute (bpm) and regular. There was no jugular venous distention, the lungs were normal, and the point of maximal impulse was in the fifth interspace in the midclavicular line. The first heart sound (S_1) was accentuated. At the apex, there was a grade 1/6 holosystolic murmur, an opening snap, and a grade 2 diastolic rumble with presystolic accentuation. The liver edge was at the costal margin, and there was no edema. The electrocardiogram (ECG) was within normal limits. The chest roentgenogram showed a normal-sized heart, an enlarged left atrium, a mild degree of pulmonary vascular redistribution, and no calcification in the region of the mitral valve, and was otherwise normal.

Cardiac catheterization revealed the following:

Body surface area, m^2	1.78
O_2 consumption, mL/min	180
A-V O_2 difference, mL/L	40
Cardiac output, L/min	4.5
Heart rate, bpm	76, NSR
Pressures, mm Hg	
Brachial artery	130/70, $\overline{90}$
Left ventricle	130/8
Diastolic mean	6
Diastolic filling period, sec/beat	0.42
Pulmonary capillary wedge	
Mean	24
Diastolic mean	20
Pulmonary artery	40/22, $\overline{28}$
Right ventricle	40/6
Right atrium, mean	4
Pulmonary vascular resistance, dyn · sec · cm^{-5}	71
Calculated mitral valve area, cm^2	1.0

Cineangiography of the left ventricle revealed no mitral regurgitation.

Interpretation. This patient was symptomatic because of her increased left atrial pressure and atrial arrhythmia. She had not yet developed the "second stenosis" at the precapillary pulmonary arteriolar level discussed previously. Therefore her pulmonary artery pressure elevation was purely a consequence of the increased left atrial and pulmonary venous pressures, and the pulmonary vascular resistance was normal (less than 120 dyn·sec·cm^{-5}). In the spectrum of patients with mitral stenosis, she would fall into stage II (Fig. 29.3). Appropriate therapy might be balloon mitral valvuloplasty or surgical mitral commissurotomy. Without relief of the mitral stenosis, her paroxysmal atrial fibrillation is likely to become continuous.

Case 2: Severe Mitral Stenosis, Moderately Elevated Pulmonary Vascular Resistance, Few Symptoms, Fatigue Syndrome. E.C., a 42-year-old woman, had no history of acute rheumatic fever. She was asymptomatic until she was 19 years old, when, during the last month of her first pregnancy, at which time she was quite anemic, she developed pulmonary congestion. She responded well to therapy and remained asymptomatic thereafter, even during three subsequent pregnancies. However, during her fifth pregnancy at age 37 years, dyspnea, orthopnea, paroxysmal nocturnal dyspnea, and one episode of hemoptysis of pure red blood occurred at the seventh month, necessitating hospitalization through term. Thereafter she improved but became progressively tired with loss of energy and drive. She became less thorough in her housework and in her attention to the children's clothes and lost her previous meticulousness. If she pushed herself, she would become somewhat short of breath on a flight of stairs, but it was fatigue more than breathlessness that bothered her.

On examination, she was well nourished and had a malar flush. Her blood pressure was 115/70 mm Hg; her pulse was 90 bpm and irregularly irregular. Respirations were 15 per minute. There was no pulmonary or peripheral congestion. The neck veins were just visible at the clavicles with the patient sitting upright. The point of maximal impulse was in the fifth interspace just outside the midclavicular line. The impulse was normal. A prominent parasternal heave was present. S_1 was accentuated. No apical systolic murmur was present. There was an opening snap and a grade 2 apical diastolic rumble. The ECG showed right ventricular hypertrophy and atrial fibrillation. Chest radiographs showed the heart to be moderately enlarged because of enlargement of the left atrium and right ventricle. The pulmonary arteries were prominent, and there was a moderate degree of pulmonary vascular redistribution.

The findings at cardiac catheterization were as follows:

Body surface area, m^2	1.41
O_2 consumption, mL/min	188
A-V O_2 difference, mL/L	51
Cardiac output, L/min	3.7
Heart rate, bpm	85, AF
Pressures, mm Hg	
Brachial artery	120/62, $\overline{84}$
Left ventricle	120/7
Diastolic mean	5
Diastolic filling period, sec/beat	0.38
Pulmonary capillary wedge	
Mean	27
Diastolic mean	23
Pulmonary artery	82/32, $\overline{51}$
Right ventricle	82/10

Right atrium, mean	8
Pulmonary vascular resistance, dyn · sec · cm^{-5}	520
Calculated mitral valve area, cm^2	0.7

Interpretation. This patient's symptoms were caused initially by elevated left atrial pressure when, during her fifth pregnancy, she developed hemoptysis, orthopnea, and paroxysmal nocturnal dyspnea. Subsequently, however, her major symptom was fatigue, associated with a reduced cardiac output and an increased arteriovenous oxygen difference (A-V O_2 difference). The orthopnea and paroxysmal dyspnea had receded somewhat despite the fact that her pulmonary capillary pressure was at the pulmonary edema level. This is a common, although poorly understood, phenomenon in patients with mitral stenosis when pulmonary vascular disease begins to occur. Therefore, this patient was beginning to develop the “second stenosis” discussed previously, and this is apparent from the elevated pulmonary vascular resistance (520 dyn·sec·cm^{-5}). In the spectrum of patients with mitral stenosis, she would be representative of stage III (Fig. 29.3). As was true for the patient in case 1, appropriate therapy would be either balloon mitral valvuloplasty or surgical commissurotomy.

Case 3: Terminal Mitral Stenosis with Severe Pulmonary Hypertension. C.A., a 47-year-old woman, had had acute rheumatic fever at 8 years of age and a murmur ever since. She did well until age 42 years, when she noticed exertional dyspnea and paroxysmal nocturnal dyspnea. At age 43, these symptoms worsened. Orthopnea and ankle edema appeared. Her symptoms then improved for almost 2 years, only to return 2 months before admission. Since then, despite a good cardiac regimen, she had had to lead a bed-chair-bathroom existence.

On examination, she was cachectic, dyspneic, and orthopneic. Acrocyanosis was evident. Blood pressure was 96/72 mm Hg; pulse rate was 90 bpm and irregularly irregular; respirations were 32 per minute. Neck veins were distended to the angle of the jaw, *v* waves were prominent, and there were bibasilar rales over the lung fields. The point of maximal impulse was in the anterior axillary line. The apex impulse was normal, but a parasternal heave was present. S_1 was loud. Systole was silent. An opening snap was present, and there was a barely audible mitral diastolic murmur with appreciable presystolic accentuation. The pulmonary component of S_2 was loud. The liver was palpable, two fingerbreadths below the right costal margin and was tender. There was considerable pitting edema to the knees. The ECG showed atrial fibrillation, right-axis deviation, and right ventricular hypertrophy. Chest roentgenogram showed a large heart with prominent left atrium, right ventricle, pulmonary arteries, pulmonary vasculature, and Kerley B lines.

Cardiac catheterization revealed the following:

Body surface area, m^2	1.4
O_2 consumption, mL/min	201
A-V O_2 difference, mL/L	110
Cardiac output, L/min	1.8
Heart rate, bpm	92, AF
Pressures, mm Hg	
Brachial artery	108/70
Left ventricle	108/12
Diastolic mean	10
Diastolic filling period, sec/beat	0.36
Pulmonary capillary wedge	
Mean	33
Diastolic mean	31
Pulmonary artery	125/65, $\overline{75}$
Right ventricle	125/20
Right atrium, mean	19
Pulmonary vascular resistance, dyn · sec · cm^{-5}	1838
Calculated mitral valve area, cm^2	0.3

Interpretation. This patient had symptoms of left atrial hypertension 5 years before her catheterization, suggesting that she was in stage II (Fig. 29.3) of mitral stenosis at that time. At the time of presentation to us, she had evidence of advanced right-sided heart failure and pulmonary hypertension. This woman had “two stenoses,” and both were severe: The mitral orifice area was less than one-tenth normal at 0.3 cm^2, and the pulmonary vascular resistance was approximately 18 times normal at 1838 dyn·sec·cm^{-5}. She was in late stage IV of mitral stenosis (Fig. 29.3). Even at this stage in their course, patients can respond dramatically to correction of their mitral stenosis. As pointed out in Chapter 8, pulmonary vascular resistance gradually returns toward normal in patients with advanced mitral stenosis (stage III or IV) after successful balloon valvuloplasty or surgical commissurotomy/valve replacement.

MITRAL REGURGITATION

Mitral incompetence, failure of the valve to prevent regurgitation of blood from the left ventricle to the left atrium during ventricular systole, may be caused by functional or anatomic inadequacy of any one of the components of the mitral valve apparatus, which consists of two valve leaflets, two papillary muscles with their chordae tendineae, and the valve ring or annulus.

Mitral regurgitation may occur when there is destruction or deformation of the valve leaflets as a result of *rheumatic fever* or *bacterial endocarditis*. In patients with mitral regurgitation resulting from either of these conditions, mitral regurgitation begins during “isometric” ventricular contraction and continues throughout systole, giving rise to a holosystolic murmur. A fibromyxomatous process in the mitral valve leaflets and chordae tendineae may give rise to *mitral prolapse* and the “floppy valve syndrome.” In such patients, regurgitation usually does not begin until ventricular ejection has led to a reduction in left ventricular chamber size, so that the regurgitation and accompanying murmur occur in middle or late systole. There may or may not be evidence of Marfan's syndrome in these patients. The papillary muscles are usually normal, but there is a marked redundancy of the valve leaflets and chordae with resulting prolapse into the left atrium during systole and accompanying regurgitation.

The papillary muscles are particularly vulnerable to ischemia from coronary artery disease and damage from viral myocarditis. The posterior papillary muscle derives its blood supply from the right coronary and left circumflex arteries. Ischemic dysfunction of this muscle may occur in association with either an inferior or posterolateral myocardial infarction. Less frequently, ischemic involvement of the anterior papillary muscle in an anterior or anterolateral infarction produces mitral regurgitation. Papillary-chordal integrity is maintained to a point when the left ventricle dilates. The common occurrence of a mitral regurgitant murmur in patients with large left ventricles, however, may reflect a simple anatomic loss of this integrity, an involvement of the papillary muscle with the same disease that causes the left ventricle to dilate, or an abnormality of contraction of the mitral annulus.

Physiology

Mitral regurgitation from whatever cause implies a double outlet to the left ventricle: During systole, blood exits the left ventricle through both aortic and mitral valves. Although total left ventricular output rises, that going into the aorta may fall. The left ventricular “output” regurgitated through the mitral valve depends on at least five factors: the size of the regurgitant orifice, left atrial compliance, the systolic mean pressure difference between the left ventricle and the left atrium, the duration of systole, and the resistance to forward ejection of blood through the aortic valve and into the aorta (e.g., aortic stenosis or peripheral vasoconstriction exacerbates mitral regurgitation). Although hypertension aggravates and lowering of blood pressure lessens mitral regurgitation, the most important factor is probably the size of the regurgitant orifice.

In patients with mitral regurgitation, cardiac catheterization is important to provide a complete hemodynamic and angiographic assessment of the severity of the valvular lesion.

Hemodynamic Assessment

First, it is important to assess the hemodynamic consequences of the mitral regurgitation by measuring cardiac output and right and left heart pressures (3,4,5,6,7 and

8).

Interpretation of V Waves in the Pulmonary Capillary Wedge Tracing

With acute mitral regurgitation (e.g., ruptured chordae tendineae), giant u waves are seen in the left atrial or pulmonary artery pressure tracing (Fig. 29.4). In this regard, our Fellows and Residents have often asked, “How large must a u wave be in order to be diagnostic of severe mitral regurgitation?” In my experience, u waves up to twice the mean left atrial pressure can be seen in the absence of any mitral regurgitation. The patient with left ventricular failure from any cause may have a distended, noncompliant left atrium, and the normal u wave (which is caused by left atrial filling from the pulmonary veins during left ventricular systole) will be prominent in this circumstance (7). When pulmonary blood flow is increased, the normal u wave increases in prominence correspondingly; this is particularly striking in cases of acute ventricular septal defect complicating myocardial infarction, in which enormous u waves (more than 50 mm Hg) can be seen in the absence of any mitral regurgitation.

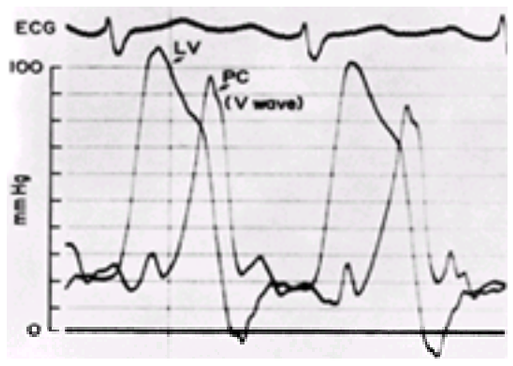

FIG. 29.4. Left ventricular (LV) and pulmonary capillary wedge (PC) pressure tracings from a patient with ruptured chordae tendineae and acute mitral insufficiency. The giant *v* wave results from regurgitation of blood into a relatively small and noncompliant left atrium. The electrocardiogram (ECG) tracing illustrates the timing of the PC *v* wave; its peak follows ventricular repolarization, as manifested by the T wave of the ECG.

V waves greater than twice the mean left atrial (or PCW) pressure are suggestive of severe mitral regurgitation, and when the height of the u wave is three times higher, a diagnosis of severe mitral regurgitation is virtually certain (Fig. 29.4). However, the absence of a prominent u wave by no means rules out severe mitral regurgitation. Slowly developing chronic mitral regurgitation commonly leads to marked left atrial enlargement, and the dilated left atrium can accept an enormous regurgitant volume per beat without any increase in mean pressure or height of the u wave (9). Also, the level of afterload, as determined by systemic vascular resistance, may greatly affect the height of the regurgitant or u wave in patients with mitral regurgitation (4). As seen in Fig. 29.5, a patient with severe mitral regurgitation had a u wave of 48 mm Hg at a time when left ventricular systolic pressure was approximately 140 mm Hg. With sodium nitroprusside (right-hand panel), the left ventricular systolic pressure came down to 120 mm Hg, and the u wave was essentially abolished (10). Although this patient's regurgitant fraction was reduced with sodium nitroprusside (from 80% to 64%), it still remained in the range of severe mitral regurgitation (see later discussion). As summarized in a study by Snyder et al. (11), prominent u waves in the PCW tracing are insensitive and have a poor positive predictive value for identifying moderate or severe mitral regurgitation.

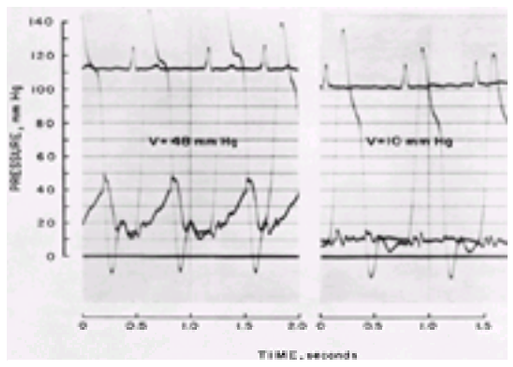

FIG. 29.5. Left ventricular and pulmonary capillary wedge pressures before *(left)* and during *(right)* an infusion of sodium nitroprusside in a patient with severe mitral regurgitation and atrial fibrillation. These tracings illustrate the sensitivity of the *v* wave height to left ventricular afterload in patients with mitral regurgitation. (See text for discussion.) (From Harshaw CW, et al. Reduced systemic vascular resistance as therapy for severe mitral regurgitation of valvular origin. *Ann Intern Med* 1975;83:312.)

Exercise Hemodynamics

Another important hemodynamic parameter in the assessment of mitral regurgitation is the forward cardiac output. Low cardiac output is common in advanced mitral regurgitation and may account for much of the clinical picture. If resting cardiac output is near normal, and if the patient's primary symptoms are related to exertion (i.e., easy fatigability and dyspnea on exertion), dynamic exercise during cardiac catheterization may be revealing. If the symptoms are cardiac in origin, the patient usually fails to increase cardiac output appropriately with exercise; that is, the increase in cardiac output is less than 80% of predicted (see formula for prediction of cardiac output increase with exercise in Chapter 15). In addition, PCW or left atrial mean pressure rises with exercise, commonly reaching levels greater than 35 mm Hg by 4 to 5 minutes of supine bicycle exercise, even if the control value was almost normal.

Angiographic Assessment

The second objective of cardiac catheterization in patients with mitral regurgitation is the angiographic assessment of the severity of the regurgitation by left ventriculography. The assessment may be qualitative, by noting the degree of opacification of the left atrium caused by regurgitation back through the incompetent valve, using a scale of 1 + (mild), 2 + (moderate), 3 + (moderately severe), and 4 + (severe) regurgitation. Although these grades are subjective, certain criteria can be used to enhance consistency of their use. Regurgitation that is 1 + essentially clears with each beat and never opacifies the entire left atrium. When regurgitation is 2 + (moderate), it does not clear with one beat and generally does opacify the entire left atrium (albeit faintly) after several beats; however, opacification of the left atrium does not equal that of the left ventricle. In 3 + regurgitation (moderately severe), the left atrium is completely opacified and achieves equal opacification with the left ventricle. In 4 + regurgitation (severe), opacification of the entire left atrium occurs within one beat, opacification becomes progressively more dense with each beat, and contrast material can be seen refluxing into the pulmonary veins during left ventricular systole.

Regurgitant Fraction

The angiographic assessment of severity of mitral regurgitation also may be made more quantitative by calculation of the regurgitant fraction. This entails measurement of total left ventricular stroke volume (TSV) from the left ventriculogram and the amount that goes forward by way of the aorta to the body (the forward stroke volume, FSV) by Fick or indicator-dilution technique. The TSV is calculated as the difference between end-diastolic and end-systolic left ventricular volumes (EDV – ms ESV = TSV), as described in Chapter 16. Regurgitant stroke volume (RSV, regurgitant volume per beat) is given as RSV = TSV – ms FSV. Regurgitant fraction (RF) is then calculated as RF = RSV/TSV.

The accuracy of these calculations depends on many factors. Because FSV is calculated by dividing the cardiac output by the heart rate at the time of Fick (or other) cardiac output determination, it is an average stroke volume. The particular beat chosen from the left ventriculogram for volume determination must therefore be an

“average” or representative beat; alternatively, volumes from multiple beats may be calculated and averaged. In patients with atrial fibrillation or extrasystoles during ventriculography, the regurgitant stroke volume and regurgitant fraction may be highly inaccurate, and they should not be calculated in such patients. It also should be obvious that the accuracy of the regurgitant fraction depends on a similar physiologic state's prevailing between the cardiac output and angiographic phases of the catheterization procedure. An increase in arterial blood pressure may substantially increase the mitral regurgitation and decrease forward output. Therefore, if blood pressure or other hemodynamic variables change significantly between the time of cardiac output determination and left ventriculography, it is pointless to calculate regurgitant fraction. Finally, the regurgitant fraction quantifies, at best, the total amount of regurgitation. Therefore, if a patient has both mitral and aortic regurgitation, the regurgitant fraction gives an assessment of the regurgitation resulting from both lesions combined.

A study from the Mayo Clinic used left ventricular cineangiography to calibrate Doppler echocardiographic techniques for quantification of mitral regurgitation in 180 patients with isolated, pure mitral regurgitation (12). Patients had left ventricular cineangiography to quantify mitral regurgitation, using a grading scale of I to IV, much as just described. The researchers found that grade I angiographic mitral regurgitation corresponded to a Doppler-measured regurgitant fraction of 28% ± 9%, grade II to 38% ± 9%, grade III to 44% ± 10%, and grade IV to 59% ± 12%. The finding for grade I is surprising and probably reflects the sensitivity of the Doppler technique in detecting mitral regurgitation. Using angiographic methods for quantifying left ventricular volumes and regurgitant fraction, grade I (mild) angiographic mitral regurgitation probably corresponds to a regurgitant fraction of less than 20%, grade II (moderate) to 20% to 40%, grade III (moderately severe) to 41% to 60%, and grade IV (severe) to more than 60%.

Assessment of Left Ventricular Function

A third objective of cardiac catheterization in patients with mitral regurgitation is the assessment of left ventricular function by measurement of the left ventricular diastolic pressure and, more importantly, the left ventricular ejection fraction (LVEF) and end-systolic volume. As others have emphasized, the nearer the preoperative ejection fraction is to normal, the greater is the degree of postoperative restoration to full activity. Specific parameters of left ventricular function are discussed in Chapter 16 and Chapter 17.

Catheterization Protocol

1. Right-sided heart catheterization for evaluation of right atrial pressure (to detect possible tricuspid valve disease or right ventricular failure), pulmonary artery pressure (degree of pulmonary hypertension), and PCW pressure (u wave height). In severe, acute mitral regurgitation, a u wave may actually be seen in the pulmonary artery as a second or late systolic hump in the pressure waveform (8).
2. Left-sided heart catheterization for measurement of left ventricular end-diastolic pressure (LVEDP) and assessment of gradients (if any) across mitral or aortic valves. A characteristic of severe mitral regurgitation is that the LVEDP is usually much lower than the left atrial or PCW mean pressure. In contrast, in left ventricular failure due to cardiomyopathy or coronary artery disease, LVEDP is usually equal or approximately equal to the PCW mean pressure, and in aortic regurgitation or left ventricular aneurysm, LVEDP is usually much higher than the PCW mean pressure.
3. Cardiac output by Fick or indicator-dilution technique. This measures the fraction of blood going out by way of the aorta to the body and by itself yields no information about regurgitant flow. The response of forward cardiac output to dynamic exercise may provide useful information, however, because patients with severe mitral regurgitation are usually incapable of increasing forward output commensurate with the needs of the body, as estimated by the increased oxygen consumption (see Chapter 15).
4. Left ventriculography is the definitive method for evaluating mitral regurgitation. By this method, it is possible to measure left ventricular volumes and regurgitant fraction, as discussed previously. Coronary angiography usually is carried out as well, to assess the need for revascularization at the time of valve repair or replacement surgery, should that prove necessary.
5. Pharmacologic intervention. An infusion of sodium nitroprusside (Fig. 29.5) often has a dramatic and salutary effect on the hemodynamic abnormalities in mitral regurgitation and may have both diagnostic and therapeutic value. Although TSV may not change, RSV decreases and FSV increases, leading to increased cardiac output.

Case 4: Mitral Regurgitation. G.A. was a 59-year-old woman with no history of rheumatic fever in childhood. She was healthy and active until 6 months before admission, when she noticed both dyspnea and lower chest discomfort on mild exertion but no other symptoms of heart failure. There was no past history of bacterial endocarditis.

On physical examination, she had normal body habitus. Blood pressure was 130/70 mm Hg; pulse was 80 bpm and regular. The jugular veins were not distended, the carotid pulsations were normal, and the lungs were clear. The apical impulse was diffuse; S_1 was diminished. There was a grade 3/6 apical pansystolic murmur transmitted to the axilla. No opening snap, S_3, or diastolic murmur was heard. There were no aortic murmurs. The ECG showed normal sinus rhythm, complete right bundle branch block, and left-axis deviation. Chest roentgenogram showed enlargement of the left ventricle and left atrium. No valvular calcification was seen.

Cardiac catheterization, left ventriculography, and coronary angiography were performed with the following findings:

Body surface area, m^2	1.95
O_2 consumption, mL/min	200
A-V O_2 difference, mL/L	52
Cardiac output, L/min	
Total left ventricular output (angiographic)	10.4
Forward flow (Fick)	3.9
Regurgitant flow	6.5
Heart rate, bpm	67
Stroke volume, mL/beat	
End-diastolic LV volume, mL (angiography)	197
End-systolic LV volume, mL (angiography)	42
Total LV stroke volume, mL (angiography)	155
Forward stroke volume, mL (Fick)	58
Regurgitant stroke volume, mL	97
Ejection fraction (155 ¸197)	0.79
Regurgitant fraction (97 ¸ 155)	0.63
Pressures, mm Hg	
Brachial artery	140/84, 105
Left ventricle	140/14
Systolic mean	112
Systolic ejection period, sec/beat	0.28
Pulmonary capillary wedge	
Mean	12
V wave	24
Pulmonary artery	30/14, 19
Right ventricle	30/6
Right atrium, mean	4
Pulmonary vascular resistance	143
Pulmonary vascular resistance, dyn · sec · cm^{-5}	2071

Left ventriculography showed excellent and uniform contraction of the left ventricle and a large regurgitant jet into the left atrium, which was filled completely within one beat. The mitral valve did not prolapse into the left atrium.

Coronary angiography revealed normal epicardial vasculature, no irregularities or narrowings, and normal runoff.

Interpretation. Mitral regurgitation was identified and quantified. There were no other valvular lesions. Although the LVEDP and left ventricular end-diastolic volume were above normal, the left ventricle contracted uniformly and vigorously, as judged by cineangiography. The ejection fraction of 0.79 and the end-systolic volume

were normal. The slight elevation of pulmonary vascular resistance was mainly related to the low pulmonary blood flow (forward cardiac output) of 3.9 L/min (cardiac index = 2.0 L/min/m^2).

Systemic vascular resistance was substantially increased, perhaps representing excessive vasoconstriction in response to the decreased forward cardiac output. The increased systemic vascular resistance presented an augmented afterload to the left ventricle, worsening this patient's mitral regurgitation. Reduced systemic vascular resistance, induced by vasodilator therapy with a converting-enzyme inhibitor, an angiotensin receptor antagonist, an a-adrenergic blocker, or hydralazine would probably improve this patient's cardiac output and her symptoms of dyspnea on exertion.

AORTIC STENOSIS

Aortic stenosis may be valvular, subvalvular, or supravalvular. Valvular aortic stenosis is most often of the acquired calcific type, which develops on the substrate of a congenitally deformed (e.g., bicuspid) aortic valve. Valvular aortic stenosis also may be present from birth (congenital aortic stenosis), or it may develop as a consequence of rheumatic fever. Subaortic stenosis is of various types. Supravalvular stenosis is rare. All types of aortic stenosis can result in a significant systolic pressure difference between the left ventricle and the aorta. In subaortic stenosis, the gradient is between the main portion of the left ventricle and its outflow tract, although in “tunnel” subaortic stenosis there may be no discrete subvalvular chamber. In supravalvular stenosis, the gradient is just beyond the aortic valve, between the initial segment of the proximal aorta and the main segment of the ascending aorta. To facilitate surgical intervention, it is important to identify the site and nature of the obstruction in each instance. This is determined by both hemodynamics and angiography. In addition, left ventricular function and the presence or absence of aortic and mitral regurgitation should be evaluated. The left ventricle becomes progressively hypertrophied in aortic stenosis. The cardiac output is well maintained until the left ventricle dilates and fails; it then becomes progressively reduced. The following discussion focuses on valvular aortic stenosis in the adult.

The cardinal indications for cardiac catheterization in anticipation of surgery for all three types of aortic stenosis are left ventricular failure, angina pectoris, or syncope. Coronary angiography should be performed in essentially all adults being studied for evaluation of hemodynamically significant aortic stenosis.

Hemodynamic Assessment

In the hemodynamic assessment of valvular aortic stenosis, primary importance should be placed on obtaining simultaneous measurement of pressure and flow across the aortic valve. As discussed in Chapter 10, this permits calculation of the aortic orifice or valve area. In the typical adult with symptomatic aortic stenosis, the aortic valve area is reduced to 0.7 cm^2 or less. Occasionally, a valve of 0.8 to 0.9 cm^2 results in a symptomatic presentation, especially when there is concomitant coronary artery disease or hypertension or when the absolute value of cardiac output is high (e.g., a large patient, anemia, fever, thyrotoxicosis). When the aortic valve area is 0.5 cm^2 or less, severe aortic stenosis is present and cardiac reserve is minimal or absent.

For the typical adult patient with acquired aortic stenosis, the correlation between clinical severity and aortic valve area calculated by the Gorlin equation (see Chapter 10) is summarized in Table 29.1. If other cardiac disease is present (e.g., coronary disease, other valve disease, cardiomyopathy), the correlations listed in Table 29.1 are not applicable.

Aortic valve area	Clinical severity
≥1.0 cm^2	Mild: symptoms rare in absence of other heart disease (coronary disease, other valve lesions)
0.7 to 1.0 cm^2	Moderate: symptoms with unusual stress, such as vigorous exercise, rapid atrial fibrillation, influenza
0.5 to 0.7 cm^2	Moderately severe: symptoms with ordinary activities of daily living
≤0.5 cm^2	Severe: symptoms at rest or minimal exertion, biventricular failure

TABLE 29.1. *Correlation between clinical severity of acquired aortic stenosis in adults and aortic valve area*

Most patients with aortic stenosis, particularly those with the clinical presentation of angina and/or syncope, have a normal cardiac output/index, normal right heart and PCW mean pressures, and normal LVEF. The LVEDP is usually increased, reflecting a stiff left ventricle, and there is a prominent A wave in PCW, left atrial, and left ventricular pressure tracings (Fig. 29.6). In more advanced cases, LVEF and cardiac output are depressed, and right heart and PCW mean pressures are elevated. Severe pulmonary hypertension with right-sided heart failure, ascites, and edema may come to dominate the picture. In these patients, the low-output state may lead to a reduction in the intensity of the characteristic systolic murmur, obscuring the diagnosis.

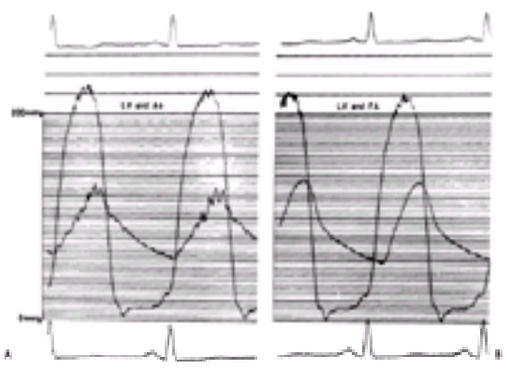

FIG. 29.6. Pressure recordings in a patient with aortic stenosis. **A:** Left ventricular (LV) and central aortic (Ao) pressures recorded simultaneously. **B:** LV and femoral arterial (FA) pressures. The FA pressure is out of phase and exhibits distortion (higher systolic peak and lower end-diastolic pressure) characteristic of peripheral arterial pressures. (Reproduced with permission from Blitz LR, Kolansky DM, Hirshfeld JW Jr. Valve function: stenosis and insufficiency. In: Pepine CJ, Hill JA, Lambert CR, eds. *Diagnostic and therapeutic cardiac catheterization,* 3rd ed. Baltimore: Williams & Wilkins, 1998.)

Carabello's Sign

An interesting hemodynamic finding, described by Carabello and coworkers (13), is a rise in arterial blood pressure during left heart catheter pullback in patients with severe aortic stenosis (Fig. 29.7). Pressure tracings from 42 patients with aortic stenosis who underwent continuous arterial pressure recording during left heart catheter pullback (withdrawal from the left ventricle to the central aorta of a catheter that had been placed in the left ventricle by retrograde technique) were examined. Increases in *peripheral arterial pressure* of 5 mm Hg or more were noted during withdrawal in 15 of the 42 patients. Fifteen (75%) of 20 patients with aortic valve area of 0.6 cm^2 or less demonstrated this phenomenon, but none of 22 patients with aortic valve area of 0.7 cm^2 or more showed such an increase. It was concluded that a rise in peak arterial pressure during left ventricular catheter withdrawal is an ancillary hemodynamic finding of critical aortic stenosis (Fig. 29.7). The mechanism of this phenomenon is most likely related to partial obstruction of an already narrowed aortic orifice by the retrograde catheter and relief of this obstruction when the catheter is withdrawn.

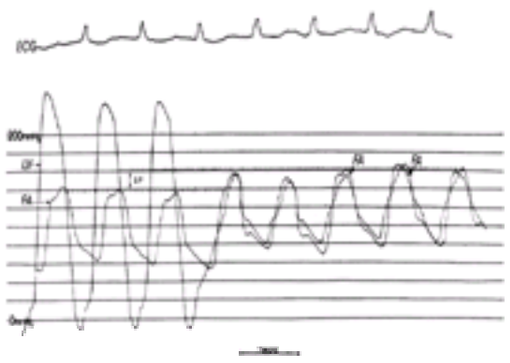

FIG. 29.7. Left ventricular (LV) and femoral artery (FA) pressure tracings in a patient with severe aortic stenosis (aortic valve area, 0.4 cm^2). During pullback of the retrograde catheter from LV to ascending aorta, the peak systolic femoral artery pressure increased (ΔP) by approximately 20 mm Hg. This sign is seen only in patients with aortic valve areas less than 0.6 cm^2. The mechanism of this phenomenon is believed to be partial obstruction of an already narrowed aortic orifice by the retrograde catheter and relief of this obstruction with catheter withdrawal. (From Carabello BA, et al. Changes in arterial pressure during left heart pull-back in patients with aortic stenosis. *Am J Cardiol* 1979;44:424.)

Angiographic Assessment

In patients with aortic stenosis, left ventriculography can yield important information, and I believe that it generally should be part of the catheterization procedure. It must be emphasized, however, that patients with left ventricular failure and high PCW pressure due to aortic stenosis may not tolerate the radiographic contrast load of left ventriculography. Adequate preventriculography preparation (e.g., intravenous furosemide, morphine, or oxygen) and use of nonionic or low-osmolality contrast agents are mandatory in such patients, and ventriculography should not be done without careful consideration of risk versus benefit. The value to be obtained from left ventriculography includes assessment of the mitral valve (whether there is significant mitral regurgitation), detection of regional wall motion abnormalities or left ventricular aneurysm indicative of major coronary disease, and overall assessment of left ventricular function. In addition, wall thickness and left ventricular mass may be measured from the ventriculogram. Often this information can be obtained from echocardiography, and contrast left ventriculography can be avoided.

Aortography is generally not required in the patient with aortic stenosis unless the gradient is small and the aortic pulse pressure is wide. Selective coronary arteriography should be done in most patients with acquired calcific aortic stenosis, especially if chest pain is present.

Catheterization Protocol

1. Right-sided heart catheterization for measurement of right heart pressures and cardiac output.
2. Left-sided heart catheterization for measurement of the pressure gradient across the aortic valve and the LVEDP and for assessment of the presence or absence of a transmitral gradient (concomitant mitral stenosis). Retrograde crossing of a tight aortic valve may be difficult. From the brachial approach, many operators have been successful in crossing a tight aortic valve using a Sones catheter (Cordis Corporation, Miami Lakes, FL). The Cordis polyurethane Sones catheter has high torque control and tapers to a 5.5F tip, which often can be negotiated across a stenotic aortic valve without the aid of a guidewire. When a guidewire is required, a 0.35-inch-diameter straight wire passes easily through the Sones catheter and can help in crossing the aortic valve.

   With a femoral approach, a pigtail catheter together with a straight guidewire protruded a short distance beyond the catheter tip is a widely used first approach to retrograde catheterization of the left ventricle in the patient with aortic stenosis; this method is illustrated in Chapter 4. On occasion, a right or left Judkins coronary catheter used together with a straight guidewire is successful in crossing a tight aortic valve in a patient with aortic stenosis. In one patient with calcific aortic stenosis and a very eccentric aortic valve orifice for whom all these approaches had failed, a left L2 Amplatz catheter with a straight guidewire was introduced successfully in retrograde catheterization of the left ventricle.

   An improved catheter design for crossing stenosed aortic valves has been developed by Feldman and coworkers (14) at the University of Chicago. Using this catheter (Feldman A catheter, Cook, Inc., Bloomington, IN), the authors found that the median time to cross the aortic valve retrograde was 30 to 40 sec in a group of 17 patients with a mean aortic valve area of 0.75 cm^2.

   If these approaches are not successful (or are not desirable in a particular patient), a transseptal approach may be used. In some laboratories, the transseptal approach is the primary technique for patients with aortic stenosis.

   In patients with aortic stenosis, it is highly desirable to measure transvalvular gradients as near as possible to the site of obstruction. Therefore, as seen in Fig. 29.6, the transaortic gradient measured with a catheter in the left ventricle and another catheter in the central aorta may differ from that obtained when arterial pressure is measured in the femoral artery. This problem is discussed in greater detail in Chapter 10. Newer double-lumen pigtail catheters (e.g., Cook Instruments) make it possible to measure left ventricular and central aortic pressures with a single catheter, avoiding the need for a separate arterial entry site.

   Another potentially important source of error in pressure measurement in patients with aortic stenosis can result from incomplete entry of a multiple side-hole catheter into the left ventricular chamber. Figure 29.8 illustrates this problem, with a pigtail catheter partially (*A*) or completely (*B*) within the left ventricular chamber. The partial entry pressures lead to a gross underestimation of the severity of the aortic stenosis.

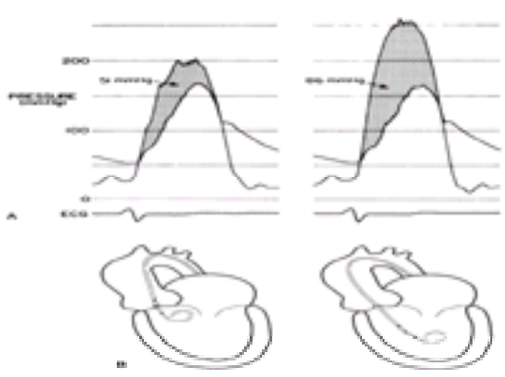

FIG. 29.8. Pressure recordings in a patient with aortic stenosis, illustrating the artifacts that can result when a multiple side-hole pigtail catheter is incompletely advanced into the left ventricular chamber (**A**). (See text for details.) (Reproduced with permission from Blitz LR, Kolansky DM, Hirshfeld JW Jr. Valve function: stenosis and insufficiency. In: Pepine CJ, Hill JA, Lambert CR, eds. *Diagnostic and therapeutic cardiac catheterization,* 3rd ed. Baltimore: Williams & Wilkins, 1998.)

3. Angiography according to the guidelines just discussed.

   Left ventriculography demonstrates the stenotic orifice of the valve during systole as outlined by a jet of contrast material ejected into the aorta. The valve cusps may appear irregular, their mobility may be reduced, and often the number of cusps can be identified. In congenital aortic stenosis, the valve may form a funnel during systole. The ascending aorta is dilated (poststenotic dilatation), but the subvalvular area is widely patent. A subaortic membrane, with a small central orifice, or a subvalvular muscular ring may be seen. The characteristic changes of idiopathic hypertrophic subaortic stenosis may be observed. In supravalvular stenosis, the narrowing of the proximal aorta can be seen.

Aortography also can be helpful in evaluation of the patient with aortic stenosis. In “pure” aortic stenosis (no concomitant aortic regurgitation), aortography often demonstrates a negative jet of radiolucent blood exiting focally from the left ventricle. In congenital aortic stenosis, there may be upward doming of the aortic valve leaflets which, together with the central negative jet, gives the so-called Prussian helmet sign. In the patient with aortic stenosis who also has some aortic regurgitation, aortography permits a rough quantitation of the severity of the regurgitation. If interventional catheter techniques (e.g., balloon aortic valvuloplasty) are under consideration, determination of the extent of associated aortic regurgitation may become important in clinical decision making.

Hemodynamic assessment often can detect the presence of mixed significant aortic stenosis and regurgitation, as illustrated by the patient whose pressure tracings are shown in Fig. 29.9. This 78-year-old man had the unusual combination of hemodynamically significant aortic stenosis (70 mm Hg gradient) and significant aortic regurgitation (grade 3 +, regurgitant fraction 48%).

Case 5: Aortic Stenosis Without Appreciable Cardiomegaly. L.C. was a 48-year-old married woman with a history of rheumatic fever in childhood. Six months before admission, she noted increasing exertional dyspnea and decreased effort tolerance. She had had dizziness but no syncope or angina.

Physical examination was normal except for the heart. There was a forceful apex impulse in the midclavicular line in the fifth interspace. Rhythm was regular. S_1 and S_2 were normal. The only murmur was a grade 2/6 ejection-type systolic murmur, maximal along the left sternal border and transmitted to the apex and into the carotids. No thrill was detected. The carotid pulsations exhibited a slow upstroke but were of normal amplitude. The ECG revealed left ventricular hypertrophy and strain. Chest radiographs showed a heart of normal overall size. There was a little rounding in the region of the left ventricle. The other cardiac chambers appeared normal, as did the lungs. At fluoroscopy, calcification was observed in the region of the aortic valve.

The findings at cardiac catheterization were as follows:

Body surface area, m^2	1.87
O_2 consumption, mL/min	225
A-V O_2 difference, mL/L	40
Cardiac output, L/min	5.6
Heart rate, bpm	70
Pressures, mm Hg	
Brachial artery	100/66
Systolic mean	84
Left ventricle	176/16
Systolic mean	140
Systolic ejection period, sec/beat	0.35
Pulmonary capillary wedge, mean	10
Pulmonary artery	25/11, $\overline{15}$
Right ventricle	25/5
Right atrium, mean	5
Pulmonary vascular resistance, dyn · sec · cm^{-5}	72
Calculated aortic valve area, cm^2	0.7
Ejection fraction	0.69

Left ventriculography showed a vigorously contracting, normal-sized left ventricle and a calcified aortic valve with three cusps. The valve leaflets were almost immobile. A jet was seen passing through the valve that almost immediately became obscured by the radiopacity of the aorta. There was a rather discrete poststenotic dilation of the[iu9] ascending aorta just above the aortic valve.

Interpretation. The moderately severe calcific aortic stenosis in this woman was probably rheumatic in origin. The left ventricle contracted well, as indicated by an LVEF of 0.69 and a normal cardiac output. The elevated LVEDP at rest was compatible with a decreased chamber distensibility from hypertrophy.

Case 6: Aortic Stenosis with Appreciable Cardiomegaly. A.H., a 77-year-old man, was well until 3 years before admission, when exertional dyspnea, orthopnea, fatigue, and peripheral edema appeared. Despite therapy, these symptoms increased progressively to the point of invalidism. He had mild angina and had had two syncopal episodes.

On physical examination, the blood pressure was 110/80 mm Hg; the pulse was 78 beats per minute and regular; respirations were 24 per minute. The carotids were of small volume with slow upstroke. Neck veins were moderately distended. There were basilar rales audible over both lungs. The point of maximal impulse was in the sixth interspace 2 cm within the anterior axillary line, diffuse and forceful. There was no parasternal heave. A grade 2/6 aortic systolic ejection murmur was heard all along the left sternal border and over both carotid arteries. The liver was two palpable fingerbreadths below the right costal margin. There was slight pitting edema of both lower legs. The ECG showed left ventricular hypertrophy and strain pattern. Chest roentgenogram showed enlargement of the left ventricle, calcification in the region of the aortic valve, moderate redistribution of vascular markings to the upper lobes of the lungs, and a small amount of pleural fluid on the right.

Cardiac catheterization yielded the following results:

Body surface area, m^2	1.76
O_2 consumption, mL/min	218
A-V O_2 difference, mL/L	81
Cardiac output, L/min	2.7
Heart rate, bpm	90
Pressures, mm Hg	
Brachial artery	135/78
Systolic mean	100
Left ventricle	184/35
Systolic mean	140
Systolic ejection period, sec/beat	0.27
Pulmonary capillary wedge, mean	29
Pulmonary artery	75/40, $\overline{52}$
Right ventricle	75/12
Right atrium, mean	10
Pulmonary vascular resistance, dyn · sec · cm^{-5}	683
Calculated aortic valve area, cm^2	0.4
Ejection fraction	0.30

Left ventriculography was performed only after pretreatment with intravenous furosemide and showed a large dilated left ventricle with uniformly poor contractions in systole. There was no mitral or aortic regurgitation. The aortic valve had two leaflets that appeared ragged and were heavily calcified. There was considerable dilation of the ascending aorta. Left ventriculography was tolerated well, and coronary angiography (two injections of the left coronary artery and one injection of the right coronary artery) revealed the absence of significant coronary artery obstruction.

Interpretation. There was severe calcific aortic stenosis, as indicated by a calculated valve area of 0.4 cm^2. Severe left ventricular failure was present, as indicated by left ventricular dilatation, high LVEDP (35 mm Hg), uniformly poor contraction by cineangiography, an LVEF of only 0.30, and a very low cardiac output. The aortic obstruction was severe. The left ventricle was so decompensated that it generated a peak systolic pressure of only 184 mm Hg (instead of 250 to 300 mm Hg, as

would be expected with a normal cardiac output), and the mean transaortic pressure gradient was only 40 mm Hg.

The PCW pressure of 29 mm Hg explained the rales heard at both lung bases as well as the patient's shortness of breath. The pulmonary hypertension was caused in part by the elevated left ventricular diastolic pressure (passive rise) and in part by reactive pulmonary hypertension, as revealed by the finding of a pulmonary vascular resistance of 683 dyn·sec·cm^{-5}, more than five times normal.

The pressure load on the right ventricle resulted in its decompensation, as indicated by a mild elevation of the right ventricular diastolic and right atrial pressures. The clinical counterpart was slight distention of the neck veins, an enlarged liver, and peripheral edema.

AORTIC REGURGITATION

The dynamic effects of aortic regurgitation are caused by regurgitation of blood from the aorta to the left ventricle in diastole. The magnitude of the regurgitation depends on the size of the regurgitant orifice, the pressure difference between the aorta and the left ventricle in diastole, and the duration of diastole. The regurgitant aperture may be as large as 1.0 cm^2, but regurgitation is generally severe when the aperture is more than 0.5 cm^2. The total left ventricular stroke volume increases and equals that which supplies the body (forward flow) plus that which is regurgitated. The amount of blood regurgitated may be as much as 60% or more of the systolic discharge. The regurgitation usually occurs in early diastole.

Hemodynamic Assessment

The large stroke volume entering the aorta with systole produces an elevated systolic pressure, whereas the regurgitation produces a lowered aortic diastolic pressure (Fig. 29.10). Left ventricular workload increases progressively with the magnitude of regurgitation. This is a result not only of the raised stroke volume and the rise of systolic pressure but also of the high left ventricular wall stress that develops when a dilated left ventricle contracts to produce a given pressure (LaPlace's law). Dilatation and hypertrophy of the left ventricle are invariable consequences of aortic regurgitation. The heart may become the largest encountered in cardiac pathology—the so-called *cor bovinum*. Up to a point, the forward cardiac output is well maintained. The addition of blood regurgitated to the normal inflow from the left atrium increases the diastolic volume of the left ventricle, leading to a more forceful contraction (Starling's law). With time, the fraction of end-diastolic volume ejected per beat (LVEF) becomes diminished, reflecting impaired myocardial function. Furthermore, the left ventricle may operate with an excessive end-systolic volume—another index of left ventricular dysfunction.

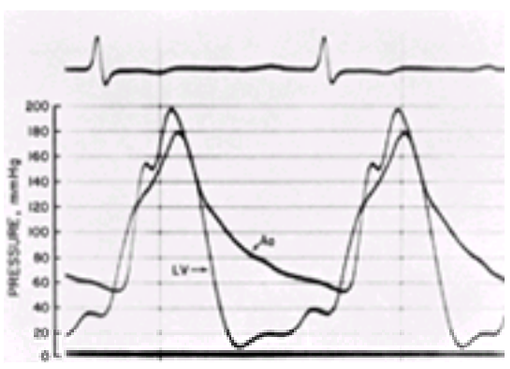

FIG. 29.10. Left ventricular (LV) and aortic (Ao) pressure tracings in a patient with severe aortic insufficiency, secondary to rheumatic heart disease. In this condition, the aortic and left ventricular pressures may equalize in late diastole, a phenomenon occasionally termed diastasis.

Premature Mitral Valve Closure

The reflux of blood from the aorta into the left ventricle in diastole, added to the blood streaming through the mitral valve from the left atrium, results in a rapid rise in left ventricular pressure early in diastole. The mitral valve may close prematurely because the regurgitating blood may raise the left ventricular diastolic pressure to exceed that in the left atrium. This is particularly common in acute aortic regurgitation, where the sudden onset of severe regurgitation into a normal-sized left ventricle leads to striking elevations in left ventricular diastolic pressure. In the case illustrated in Fig. 29.11, LVEDP approaches 50 mm Hg, and left ventricular diastolic pressure exceeds left atrial (or PCW) pressure for almost half of diastole. This reversal of pressures is associated with premature mitral valve closure, which may be seen on the echocardiogram.

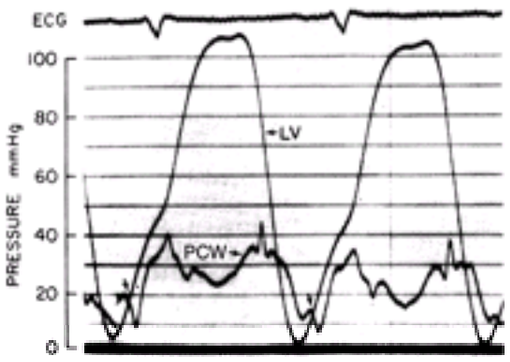

FIG. 29.11. Left ventricular (LV) and pulmonary capillary wedge (PCW) pressures in a patient with acute aortic regurgitation due to infective endocarditis. Note the unusual waveform of the LV pressure with its striking late diastolic rise, loss of clear *a* wave, and high elevation of LVEDP (approximately 45 to 50 mm Hg). LV diastolic pressure rises in late diastole to exceed left atrial and pulmonary wedge pressures *(downward arrows)*, forcing premature closure of the mitral valve. (From Mann T, et al. Assessing the hemodynamic severity of acute aortic regurgitation due to infective endocarditis. *N Engl J Med* 1975;293:108.)

Another example of premature closure of the mitral valve in association with severe aortic regurgitation is shown in Fig. 29.12. These tracings were recorded during cardiac catheterization in a 71-year-old man who had previously undergone aortic valve replacement for aortic stenosis. After doing extremely well for more than 5 years, he suddenly developed marked shortness of breath and a new murmur of aortic regurgitation. Pressure recordings show that the left ventricular diastolic pressure exceeds left atrial (PCW) pressure by the end of the first third of the diastolic filling period. Also, complete diastasis of aortic and left ventricular pressures occurs by mid-diastole, at which point aortic regurgitation ceases because there is no longer any gradient driving the regurgitant flow. As expected, this patient's diastolic murmur was blowing in quality, decrescendo, and ended by mid-diastole.

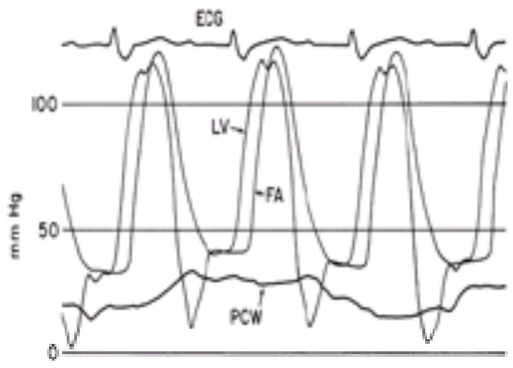

FIG. 29.12. Severe aortic regurgitation in a 71-year-old man with a prosthetic aortic valve. There is diastasis between left ventricle (LV) and aorta. Also, LV diastolic pressure exceeds pulmonary capillary wedge (PCW) pressure early in diastole. ECG, electrocardiogram; FA, femoral artery. (See text for details.)

Acute Versus Chronic Aortic Regurgitation

The typical hemodynamic findings in acute versus chronic aortic regurgitation have been reported by Mann et al. (15) and are presented in Table 29.2. As can be seen, widened pulse pressure is characteristic only of chronic aortic regurgitation, reflecting both the enormous stroke volume associated with this condition and the tachycardia commonly seen in patients with acute aortic regurgitation. This may give rise to a situation in which a high LVEDP exists in the noncompliant left ventricle in the presence of little if any elevation of the mean pressure in the left atrium. With time and with the severity of the leak, the mean diastolic pressure of the left ventricle rises, and when this happens, left atrial and PCW pressures rise.

Parameter	Acute AR	Chronic AR	*P* Value
Age (yr)	33 ± 14	40 ± 15	NS
Regurgitant fraction	0.6 ± 0.1	0.7 ± 0.1	NS
LVEDP (mm Hg)	41 ± 12	36 ± 13	NS
Ejection fraction	0.6 ± 0.1	0.6 ± 0.1	NS
Heart rate (bpm)	108 ± 15	71 ± 14	<0.01
LV volumes (mL/m²)			
EDV	146 ± 28	264 ± 64	<0.01
ESV	57 ± 23	101 ± 42	<0.02
TSV	89 ± 22	163 ± 57	<0.01
Aortic pressure (mm Hg)			
Systolic	110 ± 14	155 ± 26	<0.01
Diastolic	56 ± 11	53 ± 6	NS
Mean	76 ± 12	90 ± 8	<0.02
Pulse pressure (mm Hg)	55 ± 7	105 ± 22	<0.01
Systemic vascular resistance (dyn · sec · cm⁻⁵)	1326 ± 372	1341 ± 481	NS

EDV, ESV, and TSV, left ventricular end-diastolic, end-systolic and total stroke volumes, respectively; AR, aortic regurgitation; LVEDP, left ventricular end-diastolic pressure; NS, not significant.
(Modified from Mann JT, et al. Assessing the hemodynamic severity of acute aortic regurgitation due to infective endocarditis. *N Engl J Med* 1985;312:30.)

TABLE 29.2. *Comparison of hemodynamic and angiographic findings in acute and chronic aortic regurgitation (mean ± SD)*

Another hemodynamic finding in aortic regurgitation is the amplification of peak systolic pressure in peripheral arteries (especially the femoral and popliteal arteries), so that peak systolic femoral artery pressure may exceed central aortic pressure by 20 to 50 mm Hg. This is essentially an exaggeration of a normal phenomenon (see Chapter 7), but it emphasizes the importance of central aortic pressure measurement in aortic regurgitation.

Angiographic Assessment

Aortic cineangiography (aortography) yields a graphic demonstration of the severity and dynamics of the regurgitation. Qualitative assessment is subjective, as for mitral regurgitation. A scale of 1 + to 4 + may be used, employing the following definitions to aid discrimination of these four degrees of regurgitation. In 1 + regurgitation (mild), a small amount of contrast material enters the left ventricle in diastole; it is essentially cleared with each beat and never fills the ventricular chamber. More contrast material enters with each diastole in 2 + (moderate) regurgitation, and faint opacification of the entire chamber occurs. With moderately severe (3 +) regurgitation, the left ventricular chamber is well opacified and equal in density with the ascending aorta. Severe (4 +) aortic regurgitation is characterized by complete, dense opacification of the left ventricular chamber in one beat, and there is the appearance that the left ventricle is more densely opacified than the ascending aorta.

Quantitative assessment of aortic regurgitation involves calculation of the regurgitant fraction (RF), as described in Chapter 16. The same scale of interpretation holds as for mitral regurgitation, with RF less than 20% corresponding to mild regurgitation; 20% to 40%, moderate; 40% to 60%, moderately severe; and more than 60%, severe aortic regurgitation.

Part of the angiographic assessment of aortic regurgitation involves assessment of the aortic valve leaflets (mobility, calcification, number of leaflets), the ascending aorta (extent and type of dilatation), and possible associated abnormalities (e.g., coronary lesions, sinus of Valsalva aneurysm, dissecting aneurysm of the aorta, ventricular septal defect). All these aspects are best evaluated in the left anterior oblique view.

Catheterization Protocol

1. Right-sided heart catheterization for measurement of right heart pressures and cardiac output.
2. Left-sided heart catheterization for measurement of central aortic pulse pressure and detection of transvalvular gradients (if any), of diastasis between left ventricle and aorta (if present, Fig. 29.12), and of relative height of LVEDP compared with PCW or left atrial mean pressure.
3. Angiography, including left ventriculography, aortography, and possibly coronary angiography (if indicated clinically).
4. If resting hemodynamics are normal, consider stress intervention, such as dynamic exercise.

TRICUSPID REGURGITATION

Tricuspid regurgitation can be functional or organic. Functional tricuspid regurgitation is thought to be caused by right ventricular dilatation and failure as a result of excessive right ventricular afterload. Most commonly, this is caused by pulmonary hypertension from mitral stenosis, cardiomyopathy, primary pulmonary hypertension, cor pulmonale, or pulmonary embolism.

“Organic” tricuspid regurgitation implies disease of the tricuspid valve or its supporting apparatus and is seen most commonly with bacterial endocarditis, rheumatic heart disease, or right ventricular infarction.

Hemodynamic Assessment

In tricuspid regurgitation, either organic or functional, the primary hemodynamic finding is a large systolic wave in the right atrial pressure tracing. Tracings of jugular venous pulsations show *a*, *c*, and *v* waves in the normal subject; in the patient with moderate tricuspid regurgitation, there is a fourth pulsation, the *s* wave. This systolic wave precedes and blends with the normal venous filling (*v*) wave, and in severe tricuspid regurgitation the *s* and *v* waves form a single regurgitant systolic wave. As can be seen in Fig. 29.13, the right atrial pressure tracing in severe tricuspid regurgitation resembles the right ventricular pressure tracing. In the most extreme cases, the right atrial and ventricular pressure tracings are virtually superimposable, which is to be expected because the right atrium and ventricle are physiologically a common chamber in such cases.

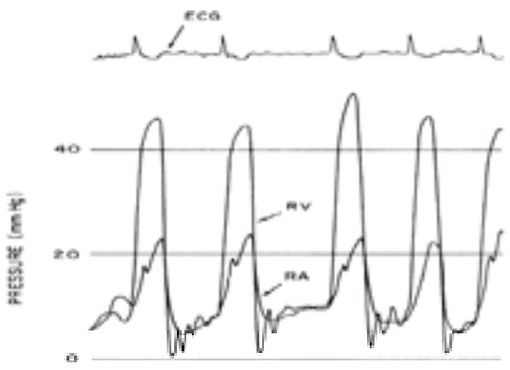

FIG. 29.13. Right atrial (RA) and ventricular (RV) pressure tracings in a 75-year-old woman with rheumatic heart disease. There is severe organic tricuspid regurgitation, with the RA waveform resembling the RV pressure.

The hemodynamic distinction between *organic* and *functional* tricuspid regurgitation is difficult. Generally, if the patient with severe tricuspid regurgitation has a right ventricular systolic pressure greater than 60 mm Hg, the tricuspid regurgitation is functional, whereas if the right ventricular systolic pressure is 40 mm Hg or less, there is a substantial organic component. This distinction is of practical importance in terms of surgical correction, because *functional tricuspid regurgitation* improves substantially solely with correction of the right ventricular hypertension (e.g., after balloon valvuloplasty or corrective surgery for mitral stenosis), whereas the patient with major organic tricuspid regurgitation may not survive cardiac surgery unless the operation includes tricuspid valve replacement or tricuspid annuloplasty.

Angiographic Assessment

The angiographic demonstration of tricuspid regurgitation is usually accomplished by right ventricular cineangiography in the right anterior oblique projection, as discussed in Chapter 12. Some artificial tricuspid regurgitation is seen because of the presence of the catheter across the tricuspid valve, but this is usually minor. It is important to choose a catheter type, position, and injection rate that avoid extrasystoles, because a run of ventricular tachycardia makes it impossible to evaluate the degree of tricuspid regurgitation; these considerations are discussed in Chapter 12. There has been much experience with the Grollman, pigtail, and Eppendorf catheters situated in the middle right ventricle or right ventricle outflow tract, with injection rates of 12 to 18 mL/sec depending on right ventricle size and irritability. A scale of 1 + to 4 + is used to grade the severity of tricuspid regurgitation, with the criteria of definition being similar to those described for mitral regurgitation. In some circumstances, a right atrial cineangiogram in the right anterior oblique projection can be used for assessment of tricuspid regurgitation; in this instance, a negative jet (unopacified blood) from right ventricle to right atrium shows the regurgitation.

The cardiac catheterization protocol depends on the associated conditions.

TRICUSPID STENOSIS

Previously, this rare condition was seen only in patients with rheumatic heart disease and mitral stenosis. Today, stenosis of a prosthetic tricuspid valve (placed originally as treatment for tricuspid regurgitation) accounts for the majority of the cases seen in most major medical centers. The clinical diagnosis may be difficult, especially if the patient is in atrial fibrillation. Diagnosis is aided by the characteristic finding of an increased jugular venous pressure with blunting or absence of the *y* descent. One patient seen by me had severe stenosis of her native mitral, aortic, and tricuspid valves. This was a 43-year-old woman with a history of repeated bouts of rheumatic fever in childhood, whose major complaint was fatigue and “blackouts.”

Hemodynamic Assessment

The *sine qua non* of tricuspid stenosis is a pandiastolic gradient across the tricuspid valve. The gradient is usually small (4 to 8 mm Hg) and may be missed unless a careful assessment is made. Two catheters (or a single catheter with a double lumen) and simultaneous measurement of right atrial and right ventricular pressures should be used if there is any doubt about the presence of this condition. However, a careful right ventricle-to-right atrial pullback using a standard catheter serves to confirm or eliminate this diagnosis with reliability in most cases. The tricuspid valve area is calculated by the formula given in Chapter 10. Tricuspid stenosis is usually of clinical and hemodynamic significance when the tricuspid valve area is less than 1.3 cm^2.

Angiographic Assessment

The valve is usually calcified and shows decreased mobility. There may be associated right atrial dilatation and some tricuspid regurgitation.

The cardiac catheterization protocol depends on the associated lesions.

PULMONIC STENOSIS AND REGURGITATION

Pulmonic stenosis is essentially a congenital condition. Pulmonic regurgitation is usually functional and a consequence of severe pulmonary hypertension. When the pulmonary artery pressure exceeds 100 mm Hg systolic, there is usually some pulmonic regurgitation. This may lead to widening of the pulmonary artery pulse pressure and an increase in right ventricular end-diastolic pressure. Angiographic assessment of pulmonic regurgitation is difficult because the angiographic catheter lying across the pulmonic valve may cause artifactual regurgitation. Echocardiography is far superior to angiography in assessing pulmonic regurgitation.

The cardiac catheterization protocol depends on associated conditions.

RELATIVE STENOSIS OF PROSTHETIC VALVES

An unusual case of relative tricuspid stenosis, mitral stenosis, and aortic stenosis in a 60-year-old man is shown in Fig. 29.14 and illustrates an important point concerning function of prosthetic cardiac valves.[iu14] This man had mitral valve replacement with a Harken disc valve in 1969 for rheumatic mitral regurgitation. He did well until 1980, when he presented with left- and right-sided heart failure and was found at cardiac catheterization to have severe aortic and tricuspid regurgitation but normal function of the mitral prosthetic valve. Aortic valve replacement (Starr-Edwards prosthesis) and tricuspid valve replacement (porcine prosthesis) led to improvement, but over the following years he required large amounts of diuretic therapy to remain free of edema and pulmonary congestion. Echocardiographic assessment of his prosthetic valves demonstrated apparently normal function, and left ventricular contraction was vigorous.

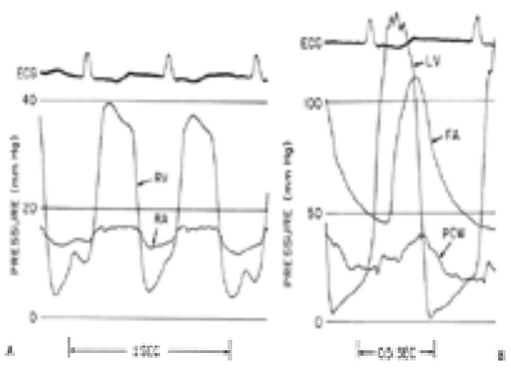

FIG. 29.14. Pressure tracings in a 60-year-old man with high cardiac output and significant pressure gradients across normally functioning tricuspid, mitral, and aortic

valve prostheses—**(A)** from the right ventricle (RV) and right atrium (RA); **(B)** from the left ventricle (LV), femoral artery (FA), and pulmonary capillary wedge position (PCW). ECG, electrocardiogram.

Because of persistent left- and right-sided heart failure, cardiac catheterization was undertaken in 1985. The porcine tricuspid valve was crossed antegrade with a Swan-Ganz catheter, and the Starr-Edwards aortic prosthesis was crossed retrograde with a Sones catheter to obtain the pressure measurements shown in Fig. 29.14. As can be seen, significant pressure gradients were present across tricuspid, mitral, and aortic prostheses. A surprising finding was an elevated cardiac output, measured by both Fick and thermodilution methods. The oxygen consumption index was 148 mL/min/m^2 and the arteriovenous oxygen difference was 29 mL O_2/L, giving a Fick cardiac index of 5 L/min/m^2 and a cardiac output of 10 L/min. Using the Gorlin formula (Chapter 10), aortic valve area was calculated to be 1.3 cm^2, mitral valve area 1.6 cm^2, and tricuspid valve area 2.4 cm^2; these values were all consistent with the known effective orifice areas of the particular prosthetic valves implanted and did not signify prosthetic valve dysfunction or stenosis. Therefore, a *high cardiac output state* caused substantial pressure gradients to occur across the patient's three prosthetic valves, resulting in the clinical picture of biventricular failure. Thyroid function tests were normal, and a search for other causes of high output state (e.g., arteriovenous fistula, Paget's disease) was unrevealing. This patient responded to thiamine supplementation, b-blockade, and diuretic therapy with spironolactone and furosemide; evidence of high-output state receded and a vigorous diuresis ensued.

Catheter Passage across Prosthetic Valves

As illustrated in the case just described, it has become routine to cross prosthetic valves with catheters in an attempt to assess their function or the function of other valves. Published reports have documented the safety of this procedure in a large number of patients (16,17) with a variety of prosthetic valves. Based on my own experience and anecdotal experience reported to me by many others, I offer the following guidelines. First, porcine valves may be crossed retrograde or antegrade safely with a variety of catheters. For retrograde crossing of a porcine prosthetic valve in the aortic position, a pigtail catheter is usually highly effective. The pigtail catheter tip is rested on top of the valve's leaflets as they protrude into the aorta, high above the sewing ring, and is gently advanced until it prolapses into the left ventricular chamber. Antegrade crossing of a porcine tricuspid prosthesis is accomplished easily with the use of a balloon-flotation catheter, as described in the preceding section. Retrograde crossing of a ball-valve (e.g., Starr-Edwards) prosthesis in the aortic position may be accomplished easily by a 7F or 8F Sones catheter with or without guidewire assistance. The pigtail catheter also may be advanced into the left ventricle over a guidewire across a ball-valve prosthesis, but the wire should be reinserted for catheter withdrawal to avoid hooking the pigtail on the metal cage. Although some operators have crossed low-profile disc-valve prostheses (e.g., Bjork-Shiley valve) retrograde without complications, instances of catheter entrapment with such crossings have been reported (18). Also, Dr. Viking Bjork has stated specifically that the Bjork-Shiley valve must not be crossed retrograde, based on his own large experience. When restudy has been required in his patients, a transseptal approach has been used. Accordingly, one should not attempt to cross a Bjork-Shiley valve or any low-profile disc valve prosthesis retrograde.

ACKNOWLEDGMENT

Some material in this chapter has been retained from the first and second editions, to which Dr. Lewis Dexter had contributed.

CHAPTER REFERENCES

1. Abbo KM, Carroll JD. Hemodynamics of mitral stenosis: a review. *Cathet Cardiovasc Diagn* 1994;[Suppl 2]:16.
2. Cequier A, Bonan R, Serra R, et al. Left-to-right atrial shunting after percutaneous mitral valvuloplasty: incidence and long-term hemodynamic follow-up. *Circulation* 1990;81:1190.
3. Braunwald E. Mitral regurgitation: physiologic, clinical and surgical considerations. *N Engl J Med* 1969;281:425.
4. Braunwald E, Welch GH Jr, Morrow AG. The effects of acutely increased systemic resistance on the left atrial pressure pulse: a method for the clinical detection of mitral insufficiency. *J Clin Invest* 1958;37:35.
5. Brody W, Criley JM. Intermittent severe mitral regurgitation: hemodynamic studies in a patient with recurrent acute left-sided heart failure. *N Engl J Med* 1970;183:673.
6. Baxley WA, Kennedy JW, Feild B, et al. Hemodynamics in ruptured chordae tendineae and chronic rheumatic mitral regurgitation. *Circulation* 1973;48:1288.
7. Pichard AD, Kay R, Smith H, et al. Large *v* waves in the pulmonary wedge pressure tracing in the absence of mitral regurgitation. *Am J Cardiol* 1982;50:1044.
8. Grose R, Strain J, Cohen MV. Pulmonary arterial *v* waves in mitral regurgitation: clinical and experimental observations. *Circulation* 1984;69:214.
9. Fuchs RM, Heuser RP, Yin FCP, et al. Limitations of pulmonary wedge *v* waves in diagnosing mitral regurgitation. *Am J Cardiol* 1982;49:849.
10. Grossman W, Harshaw CW, Munro AB, et al. Lowered aortic impedance as therapy for severe mitral regurgitation. *JAMA* 1974;230:1011.
11. Snyder RW, Glamnn DB, Lange RA, et al. Predictive value of prominent pulmonary arterial wedge *v* waves in assessing the presence and severity of mitral regurgitation. *Am J Cardiol* 1994;73:568.
12. Dujardin KS, Enriquez-Sarano M, Bailey KR, et al. Grading of mitral regurgitation by quantitative Doppler echocardiography: calibration by left ventricular angiography in routine clinical practice. *Circulation* 1997;96:3409.
13. Carabello BA, Barry WH, Grossman W. Changes in arterial pressure during left heart pullback in patients with aortic stenosis: a sign of severe aortic stenosis. *Am J Cardiol* 1979;44:424.
14. Feldman T, Carroll JD, Chin YC. An improved catheter design for crossing stenosed aortic valves. *Cathet Cardiovasc Diagn* 1989;16:279.
15. Mann T, McLaurin LP, Grossman W, et al. Assessing the hemodynamic severity of acute aortic regurgitation due to infective endocarditis. *N Engl J Med* 1975;293:108.
16. Kosinski EJ, Cohn PF, Grossman W, et al. Severe stenosis occurring in antibiotic sterilised homograft valves. *Br Heart J* 1978;40:194.
17. Rigaud M, Dubourg O, Luwaert R, et al. Retrograde catheterization of left ventricle through mechanical aortic prostheses. *Eur Heart J* 1987;8:689.
18. Kober G, Hilgermann R. Catheter entrapment in a Bjork-Shiley prosthesis in aortic position. *Cathet Cardiovasc Diagn* 1987;13:262.

30
Profiles in Coronary Artery Disease

C. Michael Gibson

University of California San Francisco, School of Medicine, San Francisco, California 94118

Today's cardiologist is faced with a rapidly expanding selection of diagnostic and therapeutic modalities in the management of coronary artery disease. The purpose of this chapter is to place these evolving diagnostic and therapeutic strategies into a clinical context through the use of case histories. The discussion of the cases is largely evidence-based and draws on data from randomized, prospective trials.

ATYPICAL CHEST PAIN WITH NORMAL CORONARY ARTERIES

The most common clinical manifestation of coronary artery disease is chest pain, but this symptom is nonspecific and there is a broad differential diagnosis of the noncardiac causes of chest pain. An abbreviated list of the most common causes of noncardiac chest pain includes musculoskeletal disorders (costochondritis), neurologic disorders (cervical disc disease, thoracic outlet syndrome, zoster), mediastinal disorders (neoplastic and inflammatory), pulmonary disorders (pneumonia, pleuritic processes, pulmonary embolism, neoplasia, and other parenchymal processes), and gastrointestinal disorders (esophageal spasm, esophagitis, peptic ulcer disease, cholecystitis, and pancreatitis). The fairly common condition of esophageal spasm presents a particular diagnostic dilemma because both ischemic coronary artery disease and esophageal spasm may respond to nitrates. Esophageal spasm may even result in radiation of the discomfort into the left arm.

A variety of cardiac conditions may also mimic the symptoms of obstructive coronary artery disease, including myocarditis, pericarditis, aortic and subaortic valvular disease, aortic dissection, thoracic aortic aneurysm, intramyocardial compression (“bridging”) of a coronary artery segment, primary pulmonary hypertension, cardiomyopathies, mitral valve prolapse, and a ruptured sinus of Valsalva aneurysm.

The frequency of finding “normal” or “nonobstructive” coronary anatomy at the time of cardiac catheterization is approximately 20%, according to registry data from the Society of Cardiac Angiography (1). This frequency varies depending on local practice patterns, including the use of noninvasive tests. Female gender is associated with a more than four-fold higher incidence of false-positive exercise tolerance tests (2). The cause of atypical chest pain with documented ischemia, but in the absence of obstructive epicardial disease, is not clear. One potential cause is impaired coronary vasodilator reserve. Data suggest that 50 mg of imipramine daily may reduce the frequency of these patients' symptoms by 52%, possibly through a visceral analgesic effect (3). The prognosis of patients with chest pain and angiographically normal coronary arteries is quite good (4).

Another cause of ischemic chest pain in the presence of coronary arteries that appear normal or near-normal is epicardial coronary spasm. Although Prinzmetal originally described a syndrome of focal coronary spasm that occurred at the site of fixed atherosclerotic narrowing (5), it has become appreciated that spasm can also occur at sites that are minimally diseased or are angiographically completely free of obstructive disease.

Case 1. A 45-year-old man presented with chest discomfort. He had a 30 pack-year history of cigarette smoking and mild systolic hypertension treated with an angiotensin-converting enzyme inhibitor. The chest discomfort occurred predominantly at rest, often during emotional upset, but also on occasion with exertion. He exercised for 9 minutes on a standard Bruce protocol and had neither chest pain nor diagnostic electrocardiographic (ECG) changes. He was compliant with a smoking cessation program and was prescribed aspirin. However, he continued to experience substernal chest pain for the next 6 months, which prompted a diagnostic cardiac catheterization.

On cardiac catheterization, coronary angiography initially showed a mild lesion in the proximal circumflex artery (Fig. 30.1*A*). The left anterior descending (LAD) and the right coronary arteries were free of disease. However, after the initial injections contrast agent, the patient developed chest pain and a very brief episode of total occlusion of the circumflex artery, which was followed by a marked and sustained reduction in the caliber of the circumflex artery (Fig. 30.1*B*). His pulmonary capillary wedge (PCW) pressure rose to 30 mm Hg. He was treated with 10 mg of sublingual nifedipine, with resolution of the chest pain and relief of coronary spasm on angiography. He was prescribed a calcium channel blocker and experienced resolution of both his rest and exertional symptoms.

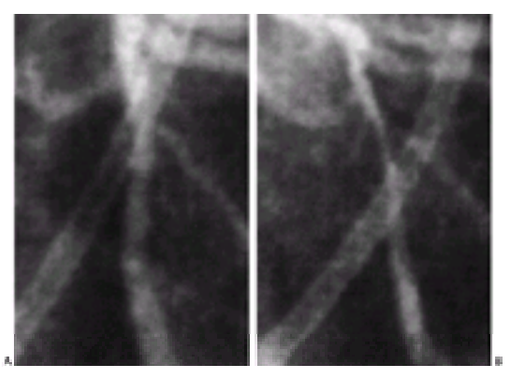

FIG. 30.1. Example of coronary spasm. **A:** A diffuse mild lesion is present in the proximal circumflex on initial angiography. **B:** After several injections, the patient developed chest pain and the artery narrowed. The symptoms and narrowing were relieved with sublingual nifedipine.

Illustrative points. Coronary spasm can be observed during the performance of coronary angiography and is often caused by catheter-induced spasm at the ostium of the coronary artery (particularly the right coronary artery). The narrowing observed here was not induced by the catheter tip, and the patient's presenting symptoms were reproduced. This patient most likely had *Prinzmetal's variant angina*. He may have also had exercise-induced coronary spasm. Although coronary spasm occurred spontaneously during the course of cardiac catheterization in this patient, provocative testing with ergonovine maleate is usually required to document this syndrome. Normal coronary arteries narrow diffusely in response to this agent, but patients with variant angina respond with focal spasm that totally occludes the coronary artery. If coronary spasm is suspected based on the clinical history (nocturnal or temporally reproducible symptoms, intermittent ST-segment elevation), then calcium channel blockers and nitrates should be discontinued for at least 24 hours before coronary angiography so that provocative maneuvers do not result in a false-negative study.

The vast majority of patients respond well to nitrates plus a single calcium channel blocker, but approximately 10% require a combination of calcium channel blockers. Patients with drug-resistant coronary spasm often have multivessel coronary spasm, which can be associated with fatal arrhythmias (6). If percutaneous transluminal coronary angioplasty (PTCA) is performed in a patient with variant angina, the risk of restenosis is higher than in a patient with a fixed obstruction (35% vs. 22%) (7).

STABLE ANGINA

Chronic ischemic heart disease is a common disorder in developed Western countries. Conventional medical management of this syndrome consists of b-blockers, aspirin, and nitrates as needed to reduce symptoms. In patients with hypercholesterolemia, there is clear evidence that the risk of cardiac events and all-cause

mortality can be reduced with aggressive lipid lowering (8,9,10). Furthermore, prospective randomized data from angiographic trials have shown that atherosclerotic disease progression can be halted or even reversed in patients with hyperlipidemia (11). Examples of disease regression from the Familial Atherosclerosis Treatment Study (FATS), in which patients with hyperlipoproteinemia were treated with lovastatin and cholestipol or niacin and cholestipol, are shown in Fig. 30.2 (11). Compared with control patients, percent stenosis in treated patients typically improved by approximately 1 percentage point for each of the 2.5 years of follow-up in regression trials (11). Of interest, each of the arterial segments has been shown to respond at an independent rate to lipid-lowering therapy (12), and it has been demonstrated that, in addition to systemic risk factors, local mechanical factors such as shear stress may play a role in mediating disease progression (13).

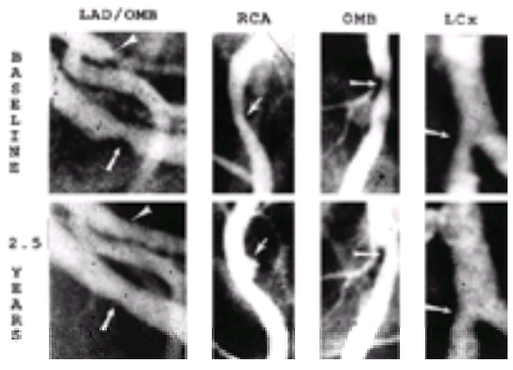

FIG. 30.2. Examples of lesion regression taken from the Familial Atherosclerosis Treatment Study (FATS) study. The top row of images were obtained before lipid-lowering therapy, and the bottom row were obtained 2.5 years later. The left anterior descending coronary artery (LAD) improved from 100% to 28% (*arrowheads*), the left-panel obtuse marginal branch (OMB) from 39% to 18% (left-panel, lower arrows), the right coronary artery (RCA) from 48% to 30%, a second OMB from 69% to 37%, and the left circumflex (LCx) from 44% to 30%. (From Brown BG, Albers JJ, Fisher LD, et al. Regression of coronary artery disease as a result of intensive lipid-lowering therapy in men with high levels of apolipoprotein B. *N Engl J Med* 1990;323:1289. Reprinted by permission of *The New England Journal of Medicine*. Copyright 1990, *Massachusetts Medical Society*. All rights reserved.)

Despite the small numbers of patients in these trials and the minimal changes in percent diameter narrowing of the arteries, a significant reduction in clinical events has been observed (11). Although lipid-lowering may not alter or may only minimally alter the extent of *fixed* structural lesions, it may instead improve the *dynamic* function of arteries, such as stabilizing the plaque against plaque rupture (14) or improving the vasomotor responsiveness of the artery to endothelial-derived relaxing factor (15). Statins may also reduce inflammation and thereby reduce reperfusion injury (16).

Despite these preventive strategies and aggressive medical management, patients sometimes have persistent and/or intolerable symptoms that require cardiac catheterization to define coronary anatomy with an eye toward possible intervention. The most appropriate intervention depends on the findings at coronary arteriography.

Case 2. A 55-year-old woman complained of chest discomfort that occurred with exertion in a stable pattern over the course of 2 years. Her risk factors for coronary artery disease included a total cholesterol level of 280 mg/dL and a high-density lipoprotein (HDL) level of 30 mg/dL, giving a cholesterol/HDL ratio of 7.3. The family history was notable for a myocardial infarction in her father at 50 years of age. The patient had been taking a b-blocker for the past year, which helped but did not eliminate her symptoms of exertional angina. She was following an American Heart Association Diet and wanted to engage in an exercise program to improve her HDL level. An exercise tolerance test showed 2 mm of ST depression in the inferior leads after 3 minutes. She was referred for cardiac catheterization, which showed normal LAD and circumflex arteries but an 80% eccentric right coronary artery lesion (Fig. 30.3*A*). The patient was treated with directional atherectomy with excellent angiographic results (Fig. 30.3*B*) and resolution of exercise-induced ischemia.

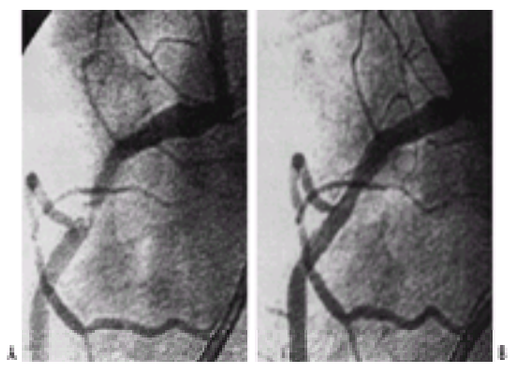

FIG. 30.3. Example of a single-vessel intervention in a patient with stable angina. An 80% eccentric right coronary artery lesion **(A)** was treated with directional atherectomy with an excellent angiographic result **(B)**.

Illustrative points. This woman had single-vessel disease, a clinical syndrome for which the benefits of PTCA have been compared with those of medical therapy in a randomized, prospective fashion in the Veterans Affairs Angioplasty Compared to Medicine (ACME) trial (17). In that study of 212 patients with single-vessel disease, PTCA resulted in a reduction of anginal symptoms compared with medical therapy at 1 month (50% vs. 24% angina free, respectively). However, although the benefit of PTCA was still significant at 6 months, the magnitude of this benefit was reduced (64% vs. 45% angina free, respectively). Patients treated with PTCA also had an improvement of 2.1 ± 3.1 minutes in exercise duration, which was significantly greater than the 0.5 ± 2.2 minutes observed in the medical therapy group. The Atorvastatin Versus Revascularization Therapy (AVERT) study demonstrated that, among patients with stable angina and minimal ischemia, aggressive lipid lowering to a low-density lipoprotein (LDL) level of 78 mg/dL can be associated with a greater reduction in hospitalization for recurrent ischemia compared with PTCA (18). Despite the lower frequency of events in the medical therapy arm of AVERT, there was still a higher frequency of angina among medical therapy patients. This eccentric lesion was not treated with conventional PTCA but rather with atherectomy, which has been shown to result in a lower rate of restenosis at 6 months (19).

Case 3. A 63-year-old man presented with 1 year of substernal chest pain with exertion. His risk factors for coronary artery disease included a positive family history and a history of hypertension. He did not have diabetes. On exercise tolerance testing, he was found to have anterior ST-segment depression at 4 minutes on a standard Bruce protocol. His medications included a b-blocker, aspirin, and nitrates, but he continued to experience chest pain with approximately one block of exertion.

His symptoms limited his lifestyle, and he elected to undergo cardiac catheterization, which showed an 80% proximal right coronary artery lesion and a 90% mid-LAD artery lesion. His PCW pressure was 10 mm Hg, and his left ventricular ejection fraction (LVEF) was 55%. The patient had diffuse disease of the coronary arteries, with small vessels that were less than 3.0 mm in diameter. He was treated with a multivessel PTCA, leaving a 10% to 20% residual stenosis at both sites. His chest discomfort resolved after the procedure.

Illustrative points. The role of percutaneous strategies in the patient with multivessel disease continues to evolve. It is difficult to interpret nonrandomized data comparing the efficacy of multivessel PTCA with that of coronary artery bypass grafting (CABG) because most multivessel PTCA series involve patients, such as this one, with two-vessel disease and a preserved LVEF. In contrast, many CABG series involve patients with three-vessel disease or left main disease and a higher proportion of patients with reduced LVEF (20). A number of randomized, prospective trials have now been completed (e.g., EAST, RITA, GABI, ERACI) (21,22,23,24) comparing percutaneous and surgical approaches to multivessel disease. These studies have shown that the incidence of death and recurrent myocardial infarction is similar after these two strategies. Although CABG has been associated with a higher incidence of myocardial infarction and longer hospitalizations, patients treated with PTCA usually require more antianginal medications and require repeat revascularization more frequently (21,22,23,24). This observation may be explained by two

phenomena: first, patients treated with CABG have a higher incidence of postoperative infarction, and consequently they may experience less angina postoperatively in the infarcted territory on this basis; second, patients treated with PTCA may have been less completely revascularized. In many patients, chronic total occlusions limit the ability of a percutaneous procedure to provide complete revascularization; indeed, approximately half the patients screened in the EAST trial were not deemed suitable for PTCA on this basis.

Although CABG surgery is a well established and characterized technique, new percutaneous techniques and adjunctive medical strategies to prevent restenosis continue to evolve. This difference renders comparisons between these two strategies very difficult. It must also be realized that restenosis occurs relatively *early* after PTCA, and that vein graft degeneration occurs *late* after CABG. Consequently, if the duration of follow-up is short, then angioplasty will appear less efficacious, whereas long-term follow-up over many years provides a more valuable comparison of these two strategies. The corollary is that PTCA patients may cross over to a strategy of CABG early on, but patients treated with CABG may crossover to PTCA later in the course of a trial. A high rate of crossover in both directions can confound the results of these trials if they are analyzed on a conventional intention-to-treat basis.

UNSTABLE ANGINA

The management of unstable angina continues to evolve rapidly. A variety of new adjunctive antiplatelet agents such as clopidogrel (25) and glycoprotein IIb/IIIa inhibitors (26), as well as low-molecular-weight heparin compounds (27), have been demonstrated to be efficacious.

The term *unstable angina* actually encompasses a variety of clinical syndromes that are of differing severity and carry differing prognoses (28). Stable angina that has begun to increase in frequency or severity (Braunwald class IB [28]) has the most benign course and may respond in many cases to medical therapy alone. These patients have a complication rate after PTCA which is comparable to that of patients with stable angina, but one that is lower than that of patients with angina at rest or postinfarction unstable angina (28). Patients with angina at rest associated with T-wave inversions or ST-segment depression (Braunwald class IIB and IIIB [28]), and particularly those with chest pain that is refractory to medical therapy, have a poorer prognosis than do patients with progressive angina. Finally, patients with postinfarction angina (Braunwald class IIC and IIIC [28]) also have a poorer prognosis than patients with progressive angina. The mainstay of medical therapy at this time remains aspirin, heparin, nitrates, and b-blockers. Thrombolytic agents were not shown to offer any clinical benefit in the Thrombolysis in Myocardial Infarction (TIMI III) trial, possibly because of the exposure of fibrin-bound thrombin and the procoagulant effects after thrombolysis, as well as the platelet-rich composition of thrombi in patients with unstable angina, which are more resistant to thrombolytics (29).

In patients with acute coronary syndromes, glycoprotein IIb/IIIa inhibitors have been shown to reduce the composite end point of death, recurrent myocardial infarction, and urgent revascularization by approximately 30% (26). The metaanalysis of Kong and coworkers did show an early mortality benefit for this class of agents, and a mortality benefit was observed when abciximab was combined with intracoronary stenting in the EPISTENT trial (30). The subgroups of patients who derive the greatest benefits appear to be those with ST-segment depression (not just flipped T waves), those with elevated serum troponin levels, and those for whom aspirin has failed (31). The majority of the benefit occurs in the first days after the intervention.

Case 4. A 72-year-old man had undergone CABG surgery 13 years previously, with saphenous vein grafts placed to the two obtuse marginals and the LAD artery. He underwent reoperation 8 years ago, with a left internal mammary artery graft being placed to the LAD artery and saphenous vein grafts being placed to the obtuse marginal and to the posterior descending artery. He now presented with chest pain at rest and associated inferolateral ST-segment depression. Myocardial infarction was ruled out by creatine kinase enzymes, but troponin was positive. His medications on admission included oral nitrates, a b-blocker, a calcium channel blocker, aspirin, and furosemide. Despite heparinization, intravenous nitroglycerin, and maximal medical therapy for 4 days, he continued to have chest pain at rest with inferolateral ST-segment depression.

He was prescribed a glycoprotein IIb/IIIa inhibitor and was later brought to the cardiac catheterization laboratory, where he was found to have total occlusion of all his native vessels proximally, a patent left internal mammary artery graft to his LAD artery, a 90% lesion in the midcourse of the saphenous vein graft to the posterior descending artery (Fig. 30.4), and a proximal 70% lesion of the saphenous vein graft to the first obtuse marginal artery. The LVEF was moderately reduced at 40%.

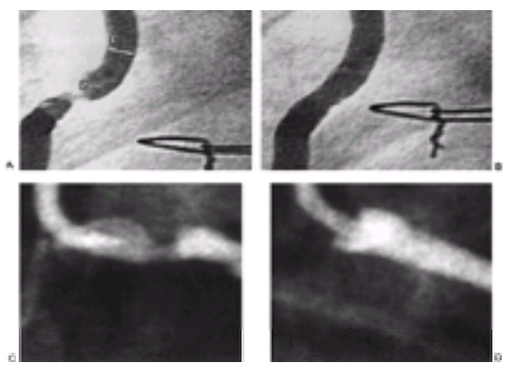

FIG. 30.4. Example of multivessel stenting in the setting of unstable angina. A 90% lesion in the midcourse of the saphenous vein graft to the posterior descending artery **(A)** was treated with a 3.5-mm Palmaz-Schatz stent, leaving a 0% to 10% residual stenosis **(B)**. A 70% lesion at the origin of the saphenous vein graft to the obtuse marginal **(C)** was treated with a 3.0-mm Palmaz-Schatz stent, again leaving a 0% to 10% residual stenosis **(D)**.

The patient had a 3.5-mm Palmaz-Schatz stent placed in the saphenous vein graft to the posterior descending artery, leaving a 0% to 10% residual stenosis (Fig. 30.4*A*,Fig. 30.4*B*). He was given a loading dose of clopidogrel. An exercise tolerance test with thallium imaging performed 10 days after the procedure showed persistent lateral wall ischemia. Therefore, a second 3.0-mm Palmaz-Schatz stent was placed in the saphenous vein graft to the obtuse marginal, again leaving a 0% to 10% residual stenosis (Fig. 30.4*C*,Fig. 30.4*D*). He continued to receive clopidogrel for 1 month after the procedure and experienced full resolution of his symptoms.

Illustrative points. This patient had an uncomplicated postintervention course, as has become common since the introduction of glycoprotein IIb/IIIa inhibitors, intracoronary stenting, and clopidogrel. Glycoprotein IIb/IIIa inhibitors have been shown to reduce the incidence of myocardial infarction before intervention, and this patient was given a glycoprotein IIb/IIIa inhibitor before the intervention. As discussed previously for patients with stable angina, the choice of revascularization strategies in the patient with unstable angina and multivessel disease is complex. This patient would have required a third CABG operation, which carries a mortality rate two to three times greater than that of the second operation and much higher than that of the initial operation (32). Some authors have advocated dilating only the culprit lesion in the setting of unstable angina (33). However, this patient demonstrates that multiple lesions may require dilation to eliminate exercise-induced ischemia. There are conflicting results in the literature as to whether patients with unstable angina have a higher restenosis rate than those with stable angina. Although conventional angioplasty of bypass grafts has been associated with a high rate of restenosis, the results of stent placement in bypass grafts have been more favorable (34). In addition, intracoronary stenting of native coronary vessels larger than 3.0 mm has been shown to reduce restenosis rates at 6 months when compared with conventional angioplasty in randomized trials (35,36).

ACUTE MYOCARDIAL INFARCTION

Although thrombolysis has been the primary mode of therapy for acute myocardial infarction, thrombolytic strategies have been limited by the fact that approximately 20% of patients fail to achieve reperfusion, 10% to 15% experience reocclusion, and approximately 1% have a risk of intracranial bleeding (37). Since the last edition of this textbook, more potent and fibrin-specific thrombolytic agents have been evaluated (38,39), and they have now been combined with glycoprotein IIb/IIIa inhibitors to accelerate the rate of thrombolysis (40). At the same time that improvements have been developed for thrombolytic strategies, newer interventional techniques have been introduced that present a formidable challenge to thrombolytic agents because they may achieve a higher incidence of TIMI grade 3 flow and a lower rate of reocclusion and are associated with a low rate of intracranial hemorrhage (37,41).

Case 5. A 70-year-old woman was admitted to the hospital with chest pain at rest and nonspecific ECG changes. Her risk factors for coronary artery disease included hypercholesterolemia and hypertension. After admission, she was treated with aspirin and heparin, and the dosing of her b-blocker was increased. On the second day of hospitalization, she developed chest pain that was refractory to intravenous nitrates, heparin, aspirin, and b-blockers. An ECG showed 1 to 2 mm of new

ST-segment elevation in leads I, L, and V_6, as well as 1 to 2 mm of ST depression in leads $V_{1\text{-}V2}$. She received an additional bolus of heparin for a subtherapeutic partial thromboplastin time and was given 5 mg of metoprolol intravenously.

The patient developed chest pain in the afternoon, at a time when the cardiac catheterization laboratory staff was present in the hospital and a cardiac catheterization suite was immediately accessible. She was rushed to the cardiac catheterization suite, where she was found to have single-vessel disease with a totally occluded circumflex obtuse marginal branch (Fig. 30.5*A*). The patient underwent primary PTCA with restoration of normal TIMI grade 3 flow and a minimal residual stenosis (Fig. 30.5*B*). She was discharged to home 3 days later, after a negative submaximal exercise tolerance test.

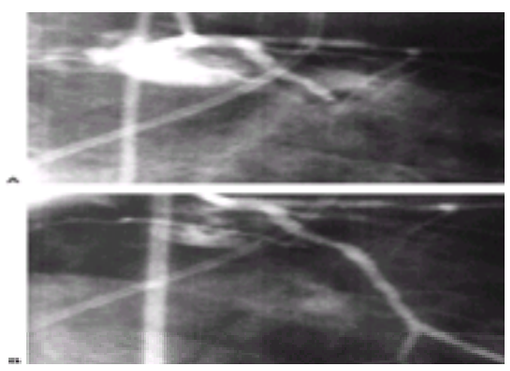

FIG. 30.5. Example of primary angioplasty for acute myocardial infarction. The patient developed chest pain and ST-segment elevation and was found to have a totally occluded obtuse marginal branch **(A)**. The patient underwent primary percutaneous transluminal coronary angioplasty, with restoration of TIMI grade 3 flow and a minimal residual stenosis **(B)**.

Illustrative points. There are several prospective randomized trials comparing the efficacy of primary PTCA with that of thrombolytic therapy (41). This patient was in many ways an ideal candidate for primary PTCA, both because immediate access to cardiac catheterization was available and because she was an elderly woman, a subgroup that has been shown to derive particular benefit from primary PTCA (42). In the Primary Angioplasty in Myocardial Infarction trial (PAMI), primaryPTCA was associated with a lower rate of intracranial hemorrhage and a lower rate of reinfarction or death compared with thrombolytic therapy (42). This patient is part of a small subgroup of patients with a circumflex lesion, the natural history of which is not well characterized in thrombolytic trials because such lesions represent less than 15% of lesions in these trials.

Case 6. A 56-year-old man presented with chest discomfort that awoke him from sleep 1 hour before admission. On presentation to the emergency room, he had a blood pressure of 92/54 mm Hg. His ECG showed sinus bradycardia at a rate of 52 beats per minute (bpm), with 2 mm of ST-segment elevation in leads II, III and avF. He was given a bolus of heparin intravenously and treated with 100 mg of tissue-type plasminogen activator (tPA) over 90 minutes. Initially, he was treated with intravenous nitroglycerin, which resulted in a further drop in blood pressure. Right-sided leads were obtained, which showed 1 mm of ST-segment elevation in the right precordial leads. He was treated aggressively with intravenous fluids, resulting in a rise in his blood pressure, but he also began to develop rales on examination. His chest pain persisted for the first 60 minutes after thrombolysis.

Given the patient's hemodynamic instability and persistent chest pain, he was taken to the cardiac catheterization laboratory. Shortly after vascular access was obtained, his chest pain resolved and his ST-segment elevation improved. On angiography, he was found to have an ulcerated eccentric 90% stenosis in the mid-right coronary artery (Fig. 30.6), with TIMI grade 2 flow that was collateralized by the LAD artery. Given that the vessel was open and the patient's pain had resolved, it was elected not to intervene. However, 6 hours later the patient developed recurrent chest pain, and repeat cardiac catheterization showed a total occlusion of the right coronary artery, which was treated with PTCA, resulting in restoration of TIMI grade 3 flow and a 30% residual stenosis.

FIG. 30.6. Example of a lesion with a high risk of reocclusion after thrombolysis. The lesion is an ulcerated, eccentric plaque in the right coronary artery with TIMI grade 2 flow that was collateralized by the left anterior descending coronary artery.

Illustrative points. This patient had several angiographic features on early catheterization that have been associated with reocclusion 1 day later (43). In descending order of importance, these angiographic features are the presence of an ulceration, the presence of TIMI grade 2 (slow) flow, the presence of thrombus, the presence of an eccentric lesion, increased lesion severity, and the presence of collaterals. The management of a patent artery with slow flow is poorly defined. Despite an intuitive belief that *routine* adjunctive angioplasty should improve clinical outcomes in patients with a patent (normal and slow flow combined) but narrowed artery after successful thrombolysis, several large trials have shown no benefit for PTCA in this setting (44).

Currently, there is an impetus toward improving the flow in patent arteries after thrombolysis based on the finding that better TIMI flow grades and better TIMI frame counts are associated with improved outcomes (45,46). However, it remains unclear whether TIMI grade 2 flow is just a *marker* of larger infarcts or a *cause* of more extensive necrosis. Indeed, it has been shown that the magnitude of slow flow is proportional to the extent of myocardial necrosis (47), and Kloner et al. demonstrated repeatedly that this may be mediated by the microvasculature (48). Furthermore, we showed that perfusion at the level of the myocardium (the myocardial perfusion grade or blush) is a predictor of mortality in acute myocardial infarction, independent of flow in the epicardial artery (49). It appears that flow in all three arteries (not just the “culprit” artery) may be abnormal, and that global flow abnormalities are related to a higher mortality rate in acute myocardial infarction (50). Therefore, there is an increased emphasis on treating the microvasculature in addition to treating the stenosis in patients with TIMI 2 flow. Treatment of the stenosis may confer benefits above and beyond those of improved flow, such as potential reduction in the risk of reocclusion.

Case 7. A 69-year-old woman presented to the emergency room of a local community hospital with 5 hours of substernal chest discomfort radiating to the left arm, and 2 mm of ST-segment elevation in the anterior precordial leads. She had a blood pressure of 90/60 mm Hg, a pulse rate of 90 bpm, and rales one-half way up her lung fields bilaterally. She was treated immediately with aspirin, intravenous heparin, and 1.5 million units of streptokinase. After 60 minutes of persistent chest pain and ST-segment elevation, she was transferred for cardiac catheterization. She was found to have a totally occluded LAD artery, which was treated with rescue PTCA, resulting in restoration of TIMI grade 3 flow and a minimal residual stenosis.

Illustrative points. There has been only one randomized, prospective trial assessing the efficacy of rescue angioplasty for failed thrombolysis. There is an inherent belief among angioplasty operators that restoring perfusion would certainly be beneficial, and this bias is reflected by the fact that almost 80% of operators approached to participate in the Randomized Evaluation of Salvage Angioplasty with Combined Utilization of Endpoints (RESCUE) study (51) declined, because they believed that it would be unethical to withhold attempted revascularization for an occluded vessel immediately after failed thrombolysis.

The RESCUE trial involved 150 patients from 20 centers with TIMI grade 0 or 1 flow 1.5 to 8 hours after myocardial infarction. Generalization of results from this trial are limited because enrollment was restricted to patients with their first myocardial infarction and to those patients with an anterior infarction. There was no difference in outcome for the prespecified primary end point of the trial, the resting LVEF at 30 days after myocardial infarction (40% with PTCA vs. 39% without PTCA). The incidence of death in patients treated with rescue angioplasty was 5.2%, which did not differ significantly from the 9.9% for those not treated with rescue angioplasty. As a secondary end point, death and congestive heart failure were analyzed together, and there was a trend for a reduced incidence in the group treated with rescue PTCA (6.5% vs. 16.4%, $p = .055$). The magnitude of benefit in this trial and in others may be small because thrombolysis must first fail over the course of the first 90 minutes, and time must then be taken to bring the patient to the cardiac catheterization suite. Because of the inherent time delays in performing rescue angioplasty, the benefits of *early* restoration of patency may not be realized.

Several other trials have evaluated the strategy of rescue PTCA in a nonrandomized, retrospective fashion (52). In keeping with the fact that the *early and full* reperfusion paradigm of thrombolytic success is only partially fulfilled in cases of successful rescue PTCA, the *delayed* and often *full* reperfusion achieved in these patients in the TIMI 4 trial resulted in an overall rate of adverse events (death, severe congestive heart failure, cardiogenic shock, or LVEF less than 40%), 28.8%, that was intermediate between that of patients with immediate thrombolytic success (22.8%) and that of patients treated with no rescue PTCA for an occluded vessel (35.1%), who frequently achieved reperfusion even later (52). Overall success rates have varied (71% to 100%) and on the whole have been lower than those reported for primary PTCA, probably because of either a larger or a more pharmacologically resistant thrombus burden (53). Similarly, mortality rates have been high (10% to 17%), and in particular the mortality rates of patients with a failed procedure have been very high (33% to 39%) (53). Pooled data have shown no improvement in left ventricular function between the time of the rescue procedure and 7 days later and suggest that the rate of reocclusion is higher in patients treated with tPA (24%) compared with nonspecific plasminogen activators (14%) (53). A potential problem with a strategy of rescue PTCA lies in identifying patients who would be appropriate candidates for intervention, because reliable clinical and noninvasive markers of reperfusion have not been validated for widespread use. The utility of new device interventions in this setting has not been evaluated.

The management of acute myocardial infarction continues to evolve rapidly. Throughout all of the clinical trial data, one paradigm that consistently emerges is the importance of early restoration of patency regardless of the thrombolytic agent or mechanical strategy used to open the artery. In keeping with the time-dependent nature of the open-vessel hypothesis, the choice of a revascularization strategy should be guided by the clinician's assessment of the most expeditious method by which patency can be achieved in a given patient, at a given time of the day, at a given institution, by a given operator (37).

CHAPTER REFERENCES

1. Johnson LW, Lozner EC, Johnson S, et al. Coronary arteriography 1984–1987. A report of the registry of the Society for Cardiac Angiography and Interventions: I. Results and complications. *Cathet Cardiovasc Diagn* 1989;17:5.
2. Weiner DA, Ryan TJ, McCabe CH, et al. Correlations among history of angina: ST-segment response and prevalence of coronary artery disease in the Coronary Artery Surgery Study (CASS). *N Engl J Med* 1979;301:230.
3. Cannon RO, Quyyumi AA, Mincemoyer R, et al. Imipramine in patients with chest pain despite normal coronary angiograms. *N Engl J Med* 1994;330:1411.
4. Pasternak RC, Thibault GE, Savoia M, et al. Chest pain with angiographically insignificant coronary arterial obstruction: clinical presentation and long-term follow-up. *Am J Med* 1980;68:813.
5. Prinzmetal M. Angina pectoris: I. A variant form of angina pectoris. *Am J Med* 1959;27:375.
6. Fujii H, Yasue H, Okumura K, et al. Hyperventilation-induced simultaneous multivessel coronary spasm in patients with variant angina: an echocardiographic and arteriographic study. *J Am Coll Cardiol* 1988;12:1184.
7. Bertrand ME, LaBlanche JM, Thieuleux FA, et al. Comparative results of percutaneous transluminal coronary angioplasty in patients with dynamic versus fixed coronary stenosis. *J Am Coll Cardiol* 1986;8:504.
8. Scandinavian Simvastatin Survival Study Group. Randomised trial of cholesterol lowering in 4444 patients with coronary heart disease: the Scandinavian Simvastatin Survival Study (4S). *Lancet* 1994;344:1383.
9. Sacks FM, Pfeffer MA, Moye LA, et al. The effect of pravastatin on coronary events after myocardial infarction in patients with average cholesterol levels. *N Engl J Med* 1996;335:1001.
10. West of Scotland Coronary Prevention Study Group. Influence of pravastatin and plasma lipids on clinical events in the West of Scotland Coronary Prevention Study (WOSCOPS). *Circulation* 1998;97:1440.
11. Brown BG, Albers JJ, Fisher LD, et al. Regression of coronary artery disease as a result of intensive lipid-lowering therapy in men with high levels of apolipoprotein B. *N Engl J Med* 1990;323:1289.
12. Gibson CM, Sandor T, Stone PH, et al. Quantitative angiographic and statistical methods to assess serial changes in coronary luminal diameter and implications for atherosclerosis regression trials. *Am J Cardiol* 1992;69:1286.
13. Gibson CM, Diaz L, Kandarpa K, et al. The relationship of vessel wall shear stress to atherosclerosis progression. *Arterioscler Thromb* 1993;13:310.
14. Fuster V, Badimon L, Badimon JJ, et al. The pathogenesis of coronary artery disease and the acute coronary syndromes. *N Engl J Med* 1992;326:242.
15. Treasure CB, Klein JL, Weintraub WS, et al. Beneficial effects of cholesterol-lowering therapy on the coronary endothelium in patients with coronary artery disease. *N Engl J Med* 1995;332:481.
16. Lefer AM, Campbell B, Shin YK, et al. Simvastatin preserves the ischemic-reperfused myocardium in normocholesterolemic rat hearts. *Circulation* 1999;100:178.
17. Parisi AF, Folland ED, Hartigan P, for the Veterans Affairs ACME Investigators. A comparison of angioplasty with medical therapy in the treatment of single-vessel coronary artery disease. *N Engl J Med* 1992;326:56.
18. Pitt B, Waters D, Brown WV, et al., for the Atorvastatin Versus Revascularization Treatment (AVERT) Investigators. Aggressive lipid-lowering therapy compared with angioplasty in stable coronary artery disease. *N Engl J Med* 1999;341:70.
19. Topol EJ, Leya F, Pinkerton CA, et al., for the CAVEAT study group. A comparison of directional atherectomy with coronary angioplasty in patients with coronary artery disease. *N Engl J Med* 1993;329:221.
20. Mark DB, Nelson CL, Harrell FE, et al. Medical, surgical, and angioplasty survival outcomes in 7655 coronary disease patients. *J Am Coll Cardiol* 1992;19[Suppl A]:209A.
21. King SB III, Lembo NJ, Weintraub WS, et al. A randomized trial comparing coronary angioplasty with coronary bypass surgery. *N Engl J Med* 1994;331:1044.
22. RITA Trial Participants. Coronary angioplasty versus coronary artery bypass surgery: the randomized intervention treatment of angina (RITA) trial. *Lancet* 1993;341:573.
23. Hamm CW, Reimers J, Ischinger T, et al. A randomized study of coronary angioplasty compared with bypass surgery in patients with symptomatic multivessel coronary disease. *N Engl J Med* 1994;331:1037.
24. Rodriguez A, Boullon F, Perez-Balino N, et al. Argentine randomized trial of percutaneous transluminal coronary angioplasty versus coronary artery bypass surgery in multivessel disease (ERACI): in-hospital results and 1-year follow-up. *J Am Coll Cardiol* 1993;22:1060.
25. CAPRIE Steering Committee. A randomised, blinded, trial of clopidogrel versus aspirin in patients at risk of ischaemic events (CAPRIE). *Lancet* 1996;348:1329.
26. Kong DF, Califf RM, Miller DP, et al. Clinical outcomes of therapeutic agents that block the platelet glycoprotein IIb/IIIa integrin in ischemic heart disease. *Circulation* 1998;98:2829.
27. Cohen M, Demers C, Gurfinkel EP, et al. A comparison of low-molecular-weight heparin with unfractionated heparin for unstable coronary artery disease: Efficacy and Safety of Subcutaneous Enoxaparin in Non-Q-Wave Coronary Events Study Group. *N Engl J Med* 1997;337:447.
28. Braunwald E. Unstable angina: a classification. *Circulation* 1989;80:410.
29. The TIMI IIIB Investigators. Effects of tissue plasminogen activator and a comparison of early invasive and conservative strategies in unstable angina and non-Q-wave myocardial infarction: results of the TIMI IIIB trial. *Circulation* 1994;89:1545.
30. Lincoff AM, Califf RM, Moliterno DJ, et al. Complementary clinical benefits of coronary-artery stenting and blockade of platelet glycoprotein IIb/IIIa receptors: Evaluation of Platelet GP IIb/IIIa Inhibition in Stenting. *N Engl J Med* 1999;341:319.
31. c7E3 Fab Antiplatelet Therapy in Unstable Refractory Angina (CAPTURE) Study Investigators. Benefit of abciximab in patients with refractory unstable angina in relation to serum troponin T levels. *N Engl J Med* 1999;340:1623.
32. Loop FD. The value and conduct of reoperations for coronary atherosclerosis. *Semin Thorac Cardiovasc Surg* 1994;6:116.
33. Wohlgelernter D, Cleman M, Highman HA, et al. Percutaneous transluminal coronary angioplasty of the “culprit lesion” for management of unstable angina pectoris in patients with multivessel coronary artery disease. *Am J Cardiol* 1986;58:460.
34. Carrozza JP, Kuntz RE, Levine MJ, et al. Angiographic and clinical outcome of intracoronary stenting: acute and long-term results from a large single-center experience. *J Am Coll Cardiol* 1992;20:328.
35. Serruys PW, DeJaegere P, Kiemeneij F, et al. A comparison of balloon-expandable-stent implantation with balloon angioplasty in patients with coronary artery disease. *N Engl J Med* 1994;331:489.
36. Fishman DL, Leon MB, Baim DS, et al. A randomized comparison of coronary stent placement and balloon angioplasty in the treatment of coronary artery disease. *N Engl J Med* 1994;331:496.
37. Gibson CM. Primary angioplasty versus thrombolysis: new issues in the era of glycoprotein IIb/IIIa inhibition and stenting. *Ann Intern Med* 1999;130:841.
38. Cannon CP, Gibson CM, McCabe CH, et al., for the TIMI 10B Investigators. TNK-Tissue Plasminogen Activator compared with front-loaded alteplase in acute myocardial infarction: results of the TIMI 10B trial. *Circulation* 1998;98:2805.
39. Gibson CM, Cannon CP, Murphy SA, et al. Weight adjusted dosing of TNK-tissue plasminogen activator and its relationship to angiographic outcomes in the TIMI 10B trial. *Am J Cardiol* 1999;84:976.
40. Antman EM, Giugliano RP, Gibson CM, et al., for the Thrombolysis in Myocardial Infarction (TIMI) 14 investigators. Abciximab facilitates the rate and the extent of thrombolysis: results of TIMI 14 trial. *Circulation* 1999;99:2720.
41. Weaver WD, Simes RJ, Betriu A, et al. Comparison of primary coronary angioplasty and intravenous thrombolytic therapy for acute myocardial infarction: a quantitative view. *JAMA* 1997;278:2093.
42. Grines CL, Browne KF, Marco J, et al., for the Primary Angioplasty in Myocardial Infarction Study Group: A comparison of immediate angioplasty with thrombolytic therapy for acute myocardial infarction. *N Engl J Med* 1993;328:673.
43. Gibson CM, Cannon CP, Piana RN, et al. Angiographic predictors of early reocclusion in the TIMI 4 trial. *J Am Coll Cardiol* 1995;25:582.
44. The TIMI Research Group. Immediate versus delayed catheterization and angioplasty following thrombolytic therapy for acute myocardial infarction. *JAMA* 1988;260:2849.
45. The GUSTO Angiographic Investigators. The effects of tissue plasminogen activator, streptokinase, or both on coronary artery patency, ventricular function, and survival after acute myocardial infarction. *N Engl J Med* 1993;329:1615.
46. Gibson CM, Murphy SA, Rizzo MJ, et al. The relationship between the TIMI frame count and clinical outcomes after thrombolytic administration. *Circulation* 1999;99:1945.
47. Gibson CM, Murphy SA, Menown I, et al., for the TIMI Study Group. Determinants of coronary blood flow following thrombolytic administration. *J Am Coll Cardiol* 1999;34:1403.
48. Kloner RA, Alker KJ. The effect of streptokinase on intramyocardial hemorrhage, infarct size, and the no-reflow phenomenon during coronary reperfusion. *Circulation* 1984;70:513.
49. Gibson CM, Cannon CP, Murphy SA, et al., for the TIMI Study Group. The relationship of the TIMI myocardial perfusion grade to mortality following thrombolytic administration. *Circulation* 2000;101:125.

50. Gibson CM, Ryan KA, Murphy SA, et al. Impaired coronary blood flow in non-culprit arteries in the setting of acute myocardial infarction. *J Am Coll Cardiol* 1999;34:974.
51. Ellis SG, Ribeiro da Silva E, Heyndrickx GR, et al., for the RESCUE Investigators: Randomized comparison of rescue angioplasty with conservative management of patients with early failure of thrombolysis for acute anterior myocardial infarction. *Circulation* 1994;90:2280.
52. Gibson CM, Cannon CP, Greene RM, et al., for the TIMI 4 study group. Rescue angioplasty in the TIMI 4 trial. *Am J Cardiol* 1997;80:21.
53. Gibson CM. Primary and rescue angioplasty in the setting of acute myocardial infarction in randomized trials in cardiovascular disease [published as a companion to *Braunwald's Heart Disease*], 1st ed. Philadelphia: WB Saunders, 1999.

31
Profiles in Pulmonary Embolism

Samuel Z. Goldhaber

Harvard Medical School, Division of Cardiovascular, Brigham and Women's Hospital, Boston, Massachusetts 02115

As fewer pulmonary angiograms are required to solve diagnostic dilemmas, more are undertaken as the necessary prelude to mechanical intervention. Contemporary noninvasive diagnostic evaluation can be integrated by judicious use of the plasma D-dimer ELISA blood test, transthoracic or transesophageal echocardiography, and spiral chest computed tomography (CT) scanning with contrast, in addition to traditional ventilation-perfusion lung scanning. Therefore, the diagnosis of pulmonary embolism can usually be established or excluded without resorting to pulmonary angiography. In the new millennium, we have devised algorithms in which diagnostic pulmonary angiography is undertaken only after a series of noninvasive tests are deemed unhelpful (Fig. 31.1). Since lung scanning only occasionally provides a definitive “high probability” or “normal” result, chest CT scanning with contrast is increasingly utilized as the initial imaging test.

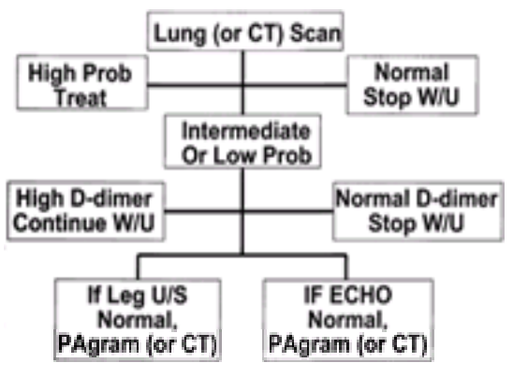

FIG. 31.1. Proposed diagnostic strategy that integrates lung and chest CT scanning, plasma D-dimer ELISA, echocardiography, leg ultrasonography, and pulmonary angiography.

Techniques for fragmentation, rheolytic, and aspiration thrombectomy (Table 31.1) are improving, and these procedures are being utilized with increasing frequency among patients with right ventricular dysfunction due to pulmonary embolism. We also carry out pulmonary angiography as part of the preoperative evaluation for patients with chronic pulmonary embolism and pulmonary hypertension who are being considered for pulmonary thromboendarterectomy (Fig. 31.2).

I. Fragmentation thrombectomy
A. Pigtail (bimanual) rotation catheter
B. “Clot Buster” Amplatz thrombectomy device (Microvena Corp., White Bear Lake , MN)—8F catheter with enclosed impeller, driven at 150,000 rpm by an air turbine
II. Rheolytic Thrombectomy
A. AngioJet Rapid Thrombectomy System (Possis Medical Inc., Minneapolis, MN)—a high-velocity saline jet from a dedicated expensive drive unit creates a strong Venturi effect at the tip of a 5F catheter
B. Hydrolyser-Cordis Thrombectomy Catheter—uses a standard contrast medium-power injection to create a saline jet
III. Aspiration thrombectomy
A. Meyerovitz technique: 8F or 9F coronary guiding catheter (without side-holes) is placed through a 10F Arrow sheath; aspirate with a 60 mL-syringe
B. Greenfield embolectomy catheter

TABLE 31.1. Contemporary catheter thrombectomy

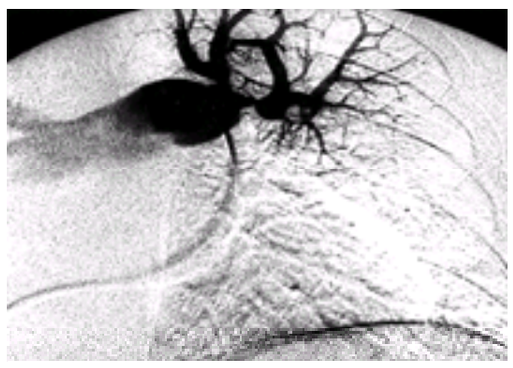

FIG. 31.2. Pulmonary angiogram of chronic pulmonary embolism. A 31-year-old man with progressive dyspnea and clinical evidence of pulmonary hypertension had right heart pressures as follows: right atrium, 12; right ventricle, = 98/18; pulmonary artery, 90/40; mean, 65; and pulmonary capillary wedge, 8 mm Hg. The contrast pulmonary angiogram shows occlusion of the descending left pulmonary artery and 80% stenosis of the anterior segmental pulmonary artery of the left upper lobe.

Our concept of hemodynamic impairment has undergone an important evolution. We used to define *hemodynamic instability* rather simplistically as persistent systemic arterial hypotension requiring fluid resuscitation or pressors. We currently judge patients with pulmonary embolism to be hemodynamically unstable if they present with right ventricular hypokinesis, usually documented on echocardiogram, even in the presence of a normal systemic arterial pressure (1,2). Such patients may initially appear deceptively stable based on the clinical evaluation alone. However, despite adequate heparin anticoagulation, patients with right ventricular hypokinesis are at high risk of recurrent pulmonary embolism and clinical deterioration, even if they are normotensive initially (3,4 and 5). Such patients, therefore, are prime candidates for more aggressive treatment with thrombolytic therapy or mechanical intervention.

DIAGNOSIS

Maintaining a high degree of clinical suspicion for possible pulmonary embolism is of paramount importance. The onset of symptoms may be sudden, gradual, or

intermittent. The most common symptoms and signs are nonspecific: dyspnea, chest pain, tachypnea, and tachycardia. Usually, pulmonary embolism patients with severe chest pain or hemoptysis have anatomically small emboli near the periphery of the lung, where nerve innervation is greatest and where pulmonary infarction is most likely to occur due to poor collateral circulation. Ironically, patients with life-threatening pulmonary embolism often have a painless presentation characterized by dyspnea, syncope, or cyanosis.

Pulmonary embolism should be suspected in hypotensive patients when (a) there is evidence of, or there are predisposing factors for, venous thrombosis and (b) there is clinical evidence of acute cor pulmonale (acute right ventricular failure) such as distended neck veins, an S3 gallop, a right ventricular heave, tachycardia, or tachypnea, especially if (c) there is electrocardiographic evidence of acute cor pulmonale manifested by a new S1—Q3—T3 pattern, new incomplete right bundle branch block, or right ventricular ischemia. Under such circumstances, a bedside echocardiogram is especially helpful.

Laboratory and Imaging Tests

Chest x-ray abnormalities include focal oligemia (Westermark's sign), indicating massive central embolic occlusion, or a peripheral wedge-shaped density above the diaphragm (Hampton's hump), indicating pulmonary infarction. An enlarged right descending (6) pulmonary artery (Palla's sign) is also a useful clue. Furthermore, the chest radiograph can help identify patients with other diseases, such as lobar pneumonia or pneumothorax, that can mimic pulmonary embolism. However, patients with these illnesses can also have concomitant pulmonary embolism.

The *electrocardiogram* helps to exclude acute myocardial infarction and to identify electrocardiographic manifestations of right heart strain. The finding of T-wave inversion in leads V1 to V4 is surprisingly common in pulmonary embolism (7). The differential diagnosis of new right heart strain includes acute pulmonary embolism, acute asthma, or exacerbation of chronic bronchitis in patients with chronic obstructive pulmonary disease. Unfortunately, the time-honored screening test of abnormal room-air *arterial blood gases* is not helpful in triaging the population of patients suspected of pulmonary embolism (8). Although arterial blood gases are inexpensive and readily available, extensive analyses of the large Prospective Investigation of Pulmonary Embolism Diagnosis (PIOPED) database indicate that even sophisticated calculations of the alveolar/arterial oxygen difference do not accurately differentiate patients with pulmonary embolism from those without pulmonary embolism (9). Therefore, arterial blood gases should not be obtained as a screening test in patients suspected of pulmonary embolism. An abnormally elevated level of *ELISA-determined plasma D-dimer* (>500 ng/mL) has a more than 90% sensitivity for identifying patients with pulmonary embolism proven by lung scan (10) or by angiogram (11). This test relies on the principle that most patients with pulmonary embolism have ongoing endogenous fibrinolysis that is not effective enough to prevent pulmonary embolism, but that does break down some of the fibrin clot to D-dimers (Fig. 31.3). These D-dimers can be assayed by monoclonal antibodies that are commercially available.

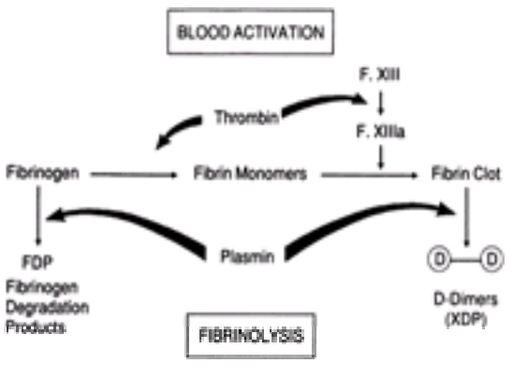

FIG. 31.3. Plasma D-dimer is generated exclusively from plasmin breakdown of fibrin clot. The D-dimers can be measured by commercially available ELISA kits. Plasma D-dimer ELISA is an excellent screening test for pulmonary embolism. Elevated levels are sensitive and normal levels have a high negative predictive value for pulmonary embolism at angiography.

Although elevated plasma concentrations of D-dimers are sensitive for the presence of pulmonary embolism, they are not specific. Levels will be elevated in patients for at least 1 week postoperatively and will also be abnormally high in patients with myocardial infarction, sepsis or almost any other systemic illness. Therefore, the plasma D-dimer ELISA is best used in patients without coexisting acute systemic illness. *A normal plasma D-dimer ELISA has a greater than 90% probability of excluding PE.*

Ventilation-perfusion (V-Q) lung scanning has traditionally served as the principal diagnostic imaging test when the clinical suspicion for pulmonary embolism is high. The V-Q scan is most useful if it is clearly normal or if it demonstrates a pattern indicating a high probability for pulmonary embolism. Intermediate-probability scans or low-probability scans with high clinical suspicion do not exclude pulmonary embolism (12). Patients in these latter categories may require chest CT scanning with contrast or pulmonary angiography, particularly if the plasma D-dimer level is elevated in the presence of normal leg ultrasonography and echocardiography.

Spiral chest CT scanning with contrast is beginning to replace lung scanning as the initial imaging test and is often viewed as a noninvasive alternative to conventional diagnostic pulmonary angiography. This technique is superb for the identification of proximal lesions. Its success rate for detection of clinically important distal pulmonary embolism is controversial (13).

In the future, gadolinium-enhanced *magnetic resonance pulmonary angiography* will be especially useful (14). This technique can combine detled anatomy with cine loops of right ventricular wall motion.

Ultrasonography of the leg veins is usually accurate in diagnosing proximal leg deep venous thrombosis in *symptomatic outpatients* (15) and may serve as a useful surrogate for pulmonary embolism. However, about one-third of pulmonary embolism patients have no venographic evidence of leg deep venous thrombosis (16). Therefore, if clinical suspicion of pulmonary embolism is high, patients without clinical or imaging evidence of deep venous thrombosis should still be worked up for pulmonary embolism.

Echocardiography is most useful among hemodynamically unstable patients who appear to be too ill to be transported for lung scanning or pulmonary angiography. If transthoracic echocardiographic images are technically inadequate, then transesophageal echocardiography should be considered. Rarely, echocardiography demonstrates a thrombus in the main pulmonary artery or at its proximal bifurcation. More often, bedside echocardiography will suggest pulmonary embolism if a constellation of findings indicates right heart failure, especially with sparing of the right ventricular apex (McConnell's sign) (Table 31.2). Echocardiography in this setting can also help exclude other life-threatening conditions, such as ventricular septal rupture, aortic dissection, and pericardial tamponade. Nevertheless, patients can have a normal echocardiogram despite anatomically extensive pulmonary embolism. Therefore, except for clinically unstable patients, echocardiography should be considered an ancillary rather than a principal diagnostic test.

Right ventricular dilatation
Right ventricular hypokinesis
Persistent normal motion of right ventricular apex (McConnell's sign)
Bowing of the interventricular septum into the left ventricle
Tricuspid regurgitation
Preserved left ventricular function

TABLE 31.2. Echocardiographic findings in pulmonary embolism

Before undertaking diagnostic *pulmonary angiography*, it is of paramount importance to obtain accurate and high-quality recordings of right heart pressures and waveforms. Before injection of the contrast agent, a carefully performed right heart catheterization may provide important clues to alternative diagnoses not suspected by the referring physicians. For example, the cause of unexplained shortness of breath might be cardiac tamponade or left ventricular failure rather than pulmonary embolism. Patients with dyspnea and pulmonary hypertension might have intracardiac shunting, which can be defined most precisely by an oxygen saturation run. Therefore, information gleaned from catheterization may be more valuable than angiography and may occasionally make angiography unnecessary.

If the pressure tracing “dampens” or “wedges” in the proximal pulmonary artery without balloon expansion, anatomically massive pulmonary embolism should be suspected before injection of the contrast agent. Even when the angiographic diagnosis is, in fact, pulmonary embolism, a carefully performed right heart catheterization can provide clues about the age of the thrombus, based on the degree of elevation of the pulmonary artery systolic pressure. In general, if the pulmonary artery systolic pressure exceeds approximately 50 mm Hg, the differential diagnosis should include chronic pulmonary embolism or acute superimposed on chronic pulmonary embolism.

Among patients undergoing pulmonary angiography, an intraluminal filling defect seen in more than one projection is the most reliable feature to diagnose pulmonary embolism. Secondary signs of pulmonary embolism reflect decreased perfusion and consist of abrupt occlusion (“cutoff”) of vessels, oligemia or avascularity of a segment, a prolonged arterial phase with slow filling and emptying of veins, and tortuous tapering peripheral vessels. Standard-contrast pulmonary angiography can detect emboli accurately in peripheral vessels as small as 1 or 2 mm. Neither spiral CT nor magnetic resonance (MR) have achieved comparable imaging resolution of small vessels.

Pulmonary angiography may also help diagnose chronic pulmonary embolism (Fig. 31.2). Arteries may appear “pouched,” and thrombus appears organized, with a concave edge. Bandlike defects called webs may be present, in addition to intimal irregularities and abrupt narrowing or occlusion of lobar vessels (17).

Pulmonary angiography can almost always be accomplished safely if (a) selective angiography is performed, with the perfusion lung scan or chest CT serving as a road map to the angiographer; (b) soft, flexible catheters with side-holes are employed, rather than stiff catheters with end-holes; and (c) a low-osmolar contrast agent is utilized to minimize the transient hypotension, heat, and coughing sensation that often occurs with conventional radiocontrast agents. In general, pulmonary angiography is exceedingly safe and uncomplicated (18). Nevertheless, if the diagnosis of pulmonary embolism (PE) is reliably established noninvasively, pulmonary angiography is not necessary, even if thrombolysis is planned.

Case Presentation: Diagnostic Dilemma in a 21-Year-Old Woman Who Is 8 Weeks Pregnant.A 21-year-old woman, 8 weeks pregnant and nulliparous, was hospitalized with suspicion of pulmonary embolism. She had complained of pleuritic chest and back discomfort for 1 week. A ventilation-perfusion lung scan was interpreted as demonstrating intermediate probability for pulmonary embolism. Leg ultrasonography and echocardiography were both normal. A plasma D-dimer ELISA was 2,003 ng/mL (normal less than 500 ng/mL).

Her physician estimated the overall likelihood of pulmonary embolism to be 50%. With an intermediate clinical suspicion and intermediate-probability lung scan, the PIOPED estimate of her likelihood of pulmonary embolism was 29% (13). However, the presence of a markedly elevated plasma D-dimer level in the setting of pregnancy increased the overall likelihood estimate to 50%. The dilemma was whether to treat her empirically as having a pulmonary embolism or to undertake pulmonary angiography, despite her being pregnant.

If she did *not* have pulmonary embolism, she would be exposed needlessly to the immediate risk of heparin-associated osteopenia. She would also suffer the unnecessary burden of continued hospitalization and prolonged outpatient treatment with anticoagulation. She would subsequently be prohibited from taking oral contraceptives during child-bearing years and hormone replacement therapy after menopause. In contrast, if pulmonary angiography were normal, she could be discharged as “healthy” within several hours of completing the procedure.

The fetal exposure to radiation during pulmonary angiography is well below the recommended maximum for pregnancy (19). After considerable discussion, the patient and her physician agreed to proceed with cardiac catheterization and pulmonary angiography. Appropriate lead-shielding of the abdomen was employed, and fluoroscopy time was kept to a minimum. Right heart pressures were entirely normal (RA = 5 mm Hg, PA = 25/9 mm Hg), but angiography demonstrated a large right lower lobar pulmonary embolism (Fig. 31.4). Therefore, she was maintained on therapeutic levels of heparin for her entire pregnancy and was anticoagulated postpartum with warfarin.

FIG. 31.4. Pulmonary angiography with digital subtraction (left anterior oblique projection) demonstrates a large, acute embolus in the right lower lobar pulmonary artery (*arrowhead*).

PATHOPHYSIOLOGY: IMPORTANCE OF RIGHT VENTRICULAR FUNCTION

The hemodynamic response to pulmonary embolism depends on the size of the embolus, coexistent cardiopulmonary disease, and neurohumoral activation. Pulmonary artery obstruction and circulating neurohumoral substances reduce the pulmonary vascular bed and cause an increase in right ventricular afterload. As right ventricular and pulmonary artery pressures rise, the right ventricle dilates, becomes hypokinetic, and ultimately fails. Progressive right heart failure leads to reduced forward cardiac output and is usually the cause of death from acute pulmonary embolism.

Sudden increases in right ventricular pressure adversely affect left ventricular function because of the anatomic juxtaposition of the two ventricles and “ventricular interdependence.” Moderate right ventricular hypertension can displace the interventricular septum toward the left ventricle, resulting in decreased left ventricular diastolic filling and end-diastolic volume (Fig. 31.5). The subsequent reduction in coronary artery perfusion pressure to the overloaded right ventricle may cause progressive right ventricular ischemia and failure. Ultimately, right ventricular infarction, circulatory arrest, and death may ensue.

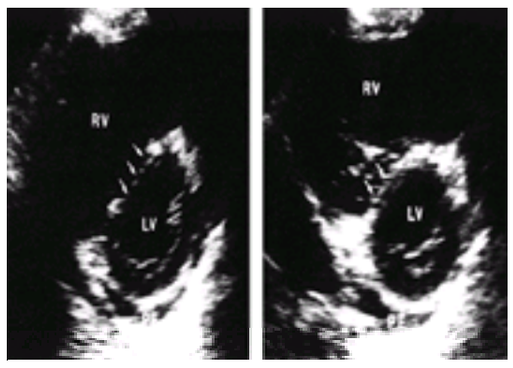

FIG. 31.5. Parasternal short-axis views of the right ventricle (RV) and left ventricle (LV) in diastole (left) and systole (right). There is diastolic and systolic bowing of the interventricular septum (*arrows*) into the left ventricle compatible with right ventricular volume and pressure overloads, respectively. The right ventricle is appreciably dilated and markedly hypokinetic, with little change in apparent right ventricular area from diastole to systole. PE, small pericardial effusion. (Reprinted with permission from Come PC. Echocardiographic evaluation of pulmonary embolism and its response to therapeutic interventions. *Chest* 1992;101:151S.)

Thrombolysis, mechanical interventions (e.g., suction embolectomy, pulverization, or fragmentation and distal embolization of clot), or open surgical embolectomy can relieve obstruction to major pulmonary artery blood flow, thereby rapidly lowering the abnormally elevated pulmonary artery pressure. As a result, right ventricular function usually improves quickly. Because of ventricular interdependence, improved right ventricular function leads to better left ventricular function, which helps reverse cardiogenic shock. The use of thrombolysis or mechanical intervention in patients at high risk for adverse outcomes with anticoagulation alone might reduce the mortality rate from pulmonary embolism by quickly restoring normotensive pulmonary artery and right ventricular pressures and by normalizing right ventricular wall motion.

THROMBOLYSIS, MECHANICAL INTERVENTION, AND SURGICAL EMBOLECTOMY

In the past, a normal blood pressure and heart rate too often engendered a sense of complacency among physicians caring for pulmonary embolism patients. Typically, clinically undetected right heart failure worsened, caused pressor dependence, and led to unremitting cardiogenic shock. As rapid overt deterioration ensued, desperate clinicians considered employing thrombolysis or surgical embolectomy as a last resort, often with poor results. After high-risk PE patients are identified with moderate or severe right ventricular dysfunction, adequate anticoagulation with heparin should be followed by screening to determine suitability for pharmacologic thrombolysis or other aggressive treatment modalities.

Thrombolysis (Fig. 31.6) (20), mechanical catheter interventions (21), and open surgical embolectomy debulk clot and provide primary treatment of pulmonary embolism, whereas intensive anticoagulation is critical for prevention of recurrent pulmonary embolism. These aggressive approaches to pulmonary embolism management are almost always successful if undertaken before the onset of cardiogenic shock. Echocardiography showing moderate or severe right ventricular dysfunction should serve as a trigger for consideration of aggressive intervention. However, patients with normal right ventricular function on echocardiography can be treated conservatively and have an excellent prognosis when managed with anticoagulation alone (3).

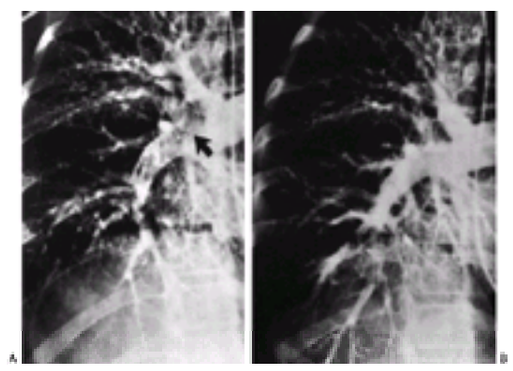

FIG. 31.6. A: A large embolus is present in the right pulmonary artery (*arrow*). **B:** After a 2-hour infusion of rt-PA through a peripheral vein, there is pronounced resolution, with only a small amount of residual thrombus in segmental branches. (Reprinted with permission from Goldhaber SZ et al. Acute pulmonary embolism treated with tissue plasminogen activator. *Lancet* 1986;2:886.)

Over the past decade, the administration of thrombolysis to pulmonary embolism patients has been streamlined so that it is safer, less expensive, and less time-consuming than previously. There is a wide 14-day “window” for effective use of thrombolysis (22). Increasing age, catheterization for pulmonary angiography, and obesity are risk factors for major hemorrhage after thrombolysis (23). At least half of high-risk PE patients will be relatively unsuitable candidates for thrombolysis.

An inferior vena caval (IVC) filter does not treat an established pulmonary embolism directly, nor does it halt the thrombotic process. Accepted indications for filter insertion to prevent pulmonary embolism include (a) *established venous thrombosis* with active, clinically important *bleeding* that prohibits the use of heparin, or (b) *recurrent pulmonary embolism* despite adequate anticoagulation. An IVC filter may also be used adjunctively to prevent recurrent pulmonary embolism among hemodynamically compromised patients in whom pulmonary embolism cannot be treated with thrombolytic therapy. Whenever possible, anticoagulation should be utilized in combination with a filter to prevent further thrombosis (24).

There has been a resurgence of interest in catheter-based embolectomy, including fragmentation (25), rheolytic (26), and aspiration (27) thrombectomy (Table 31.1). Other interventional techniques are under development (28,29 and 30). At times, thrombolysis and mechanical intervention can be combined (31). If catheter-based strategies fail, emergent surgical embolectomy with cardiopulmonary bypass can be undertaken (32,33).

Case Presentation: Combined Approach of Suction Catheter Embolectomy and Thrombolysis in a 78-Year-Old Woman with Massive Pulmonary Embolism and Hemodynamic Instability. 78-year-old woman presented with marked shortness of breath, persistent hypotension (systemic arterial pressure 78/51 mm Hg), and right ventricular dilatation and hypokinesis on echocardiogram. Pulmonary angiogram showed a massive right pulmonary artery embolism, as well as a small left lung volume because of a prior thoracoplasty to treat tuberculosis (Fig. 31.7*A*). She received heparin and placement of a Greenfield filter. Hypoxemia persisted despite ventilatory support. She developed melena on heparin. Cardiac surgeons felt she would not survive surgical embolectomy because of the prior left lung thoracoplasty.

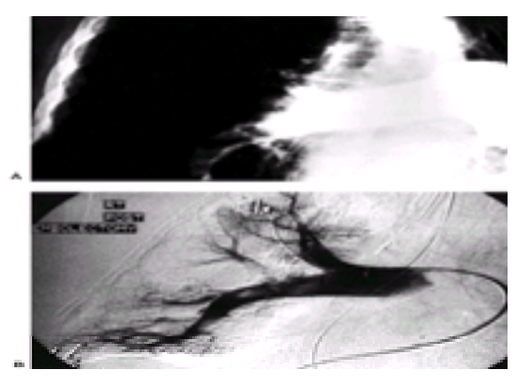

FIG. 31.7. A: Massive right main pulmonary artery embolism in the presence of markedly diminished left lung volume due to prior thoracoplasty. Cardiopulmonary diseases and cardiac tumors. Philadelphia: Current Medicine, 1995:3.1.) **B:** Digital subtraction pulmonary angiography immediately following combined suction catheter embolectomy and thrombolysis. There is an approximately 30% reduction in overall clot burden compared with the baseline angiogram (**A**). (Reprinted with permission from Goldhaber SZ. Treatment of acute pulmonary embolism. In: Goldhaber SZ, ed. *Cardiopulmonary diseases and cardiac tumors.* Philadelphia: Current Medicine, 1995:3.1.)

Because of her hemodynamic compromise, with melena on heparin and surgical inoperability, aspiration thrombectomy was undertaken in the catheterization laboratory by Michael F. Meyerovitz using the Meyerovitz technique. The right common femoral vein was accessed with a single wall puncture needle. A guidewire was advanced across the Greenfield filter. A 7F pigtail catheter was used with a tip-deflecting guidewire to enter the pulmonary artery. The catheter was exchanged for a 9F multipurpose coronary guiding catheter. Pressures were 18 mm Hg (mean) in the right atrium, 90/18 mm Hg in the right ventricle, and 90/40 mm Hg in the pulmonary artery. Suction catheter embolectomy removed both fresh and old clot from the pulmonary artery branches of the upper and lower right lobar arteries.

Systemic arterial hypotension persisted and therefore 50 mg of rt-PA was administered over 15 minutes through the pulmonary artery catheter. Pulmonary angiography then showed an approximately 30% reduction in the overall clot burden (Fig. 31.7*B*).

The procedure was complicated by a retroperitoneal bleed that was corrected with 12 units (U) of packed red blood cells. She also developed pneumonia and acute respiratory distress syndrome. Nonetheless, her clinical picture gradually improved. She was successfully weaned from the ventilator and was transferred to a rehabilitation facility. Two years later, she wrote to me and stated, “I am able to get around with a walker and portable cannister of oxygen. I celebrated my 80th birthday last May, so I guess I'm a tough old bird.”

Case Presentation: Failed Aspiration Thrombectomy Followed by Open Surgical Embolectomy. A 65-year-old dentist underwent right frontal craniotomy for resection of a malignant astrocytoma. He received venous thromboembolism prophylaxis with heparin 5,000 U subcutaneously twice daily and intermittent pneumatic compression boots. Nevertheless, on postoperative day 11, he developed pulmonary embolism with a systolic blood pressure of 100 mm Hg and severe right ventricular dysfunction on echocardiogram. A right (Fig. 31.8*A*) and left (Fig. 31.8*B*) pulmonary angiogram was done as a prelude to catheter aspiration embolectomy, which yielded only a small amount of thrombus (Fig. 31.8*C*) and did not improve his clinical condition. A Bird's nest filter (Cook, Bloomington, IN) was then placed (Fig. 31.8*D*) and he was taken to the operating room, where a large volume of thrombus was removed from the right (Fig. 31.8*E*) and left pulmonary artery (Fig. 31.8*F*). He subsequently recuperated uneventfully and is clinically stable more than 2 years postoperatively. In his case, cardiac surgical backup during interventional angiography was crucial to ensure a successful outcome.

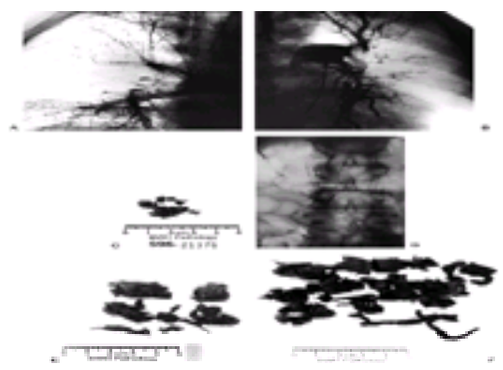

FIG. 31.8. A: Massive right main pulmonary artery embolism. **B:** Massive left main pulmonary artery embolism. **C:** Several centimeters of thrombus removed in the Interventional Laboratory. **D:** Placement below the renal veins of a bird's nest filter. **E,F:** Large amount of thrombus surgically extracted from the right and left pulmonary arteries, respectively.

CHRONIC PULMONARY EMBOLISM

Patients with chronic pulmonary hypertension due to prior pulmonary embolism may be virtually bedridden with breathlessness due to high pulmonary arterial pressures. They should be considered for pulmonary thromboendarterectomy, which, if successful, can reduce and at times even cure pulmonary hypertension (34).

The operation involves a median sternotomy, institution of cardiopulmonary bypass, and deep hypothermia with circulatory arrest periods. Incisions are made in both pulmonary arteries. The surgeon who performs thromboendarterectomy creates an endarterectomy plane and then dissects endothelialized thrombus from as many involved pulmonary vessels as possible.

At the University of California at San Diego Medical Center, the operative mortality rate is approximately 6%. The two major causes of postoperative mortality are (a) inability to remove sufficient thrombotic material at the time of operation, resulting in persistent postoperative pulmonary hypertension and right ventricular dysfunction, and (b) severe reperfusion lung injury (35). Thus, at selected centers, pulmonary thromboendarterectomy can be performed with good results and at an acceptable risk among patients debilitated from chronic pulmonary hypertension due to pulmonary embolism.

Case Presentation: Pulmonary Thromboendarterectomy for Treatment of Chronic Pulmonary Embolism in a 53-Year-Old Man with Pulmonary Hypertension and Right Ventricular Dysfunction. 53-year-old man presented with gradually worsening dyspnea on exertion. He complained of fatigue and inability to work and pursue leisure activities without marked shortness of breath. Echocardiography showed a severely enlarged and somewhat hypertrophied right ventricle with moderately reduced systolic function. The left ventricle was relatively small with marked septal flattening and abnormal septal motion but preserved systolic function.

At age 25, he had suffered bilateral deep venous thrombosis of the legs but did not receive a prolonged course of anticoagulation due to a duodenal ulcer 3 years previously. At age 36, he presented with syncope accompanied by tachycardia and diaphoresis. His electrocardiogram was notable for atrial fibrillation and inverted T waves in leads V1 through V3. Five years later, he complained of exertional dyspnea. A lung scan showed perfusion defects that were of high probability for pulmonary embolism. At that time, his mean pulmonary artery pressure was 32 mm Hg, and a pulmonary angiogram was reportedly positive for pulmonary embolism. He was placed on warfarin.

Despite 12 years of anticoagulation, his dyspnea worsened to the point where he could not pursue the active lifestyle that he desired. Chronic pulmonary embolism was suspected, and he was referred for possible pulmonary thromboendarterectomy. Therefore, right heart catheterization and pulmonary angiography were repeated.

Catheterization demonstrated a right atrial pressure of 10 mm Hg, right ventricular pressure of 55/10 mm Hg, and pulmonary artery pressure of 55/28 mm Hg, with a mean pulmonary artery pressure of 35 mm Hg. Pulmonary angiography (Fig. 31.9*A*) revealed total occlusion of his left lower lobe pulmonary arteries. He underwent pulmonary thromboendarterectomy at Brigham and Women's Hospital. The surgeon endarterectomized multiple large thrombi that were chronic and laminated (Fig. 31.9*B*). The patient has subsequently done well and is no longer incapacitated in any way. He runs a factory and hunts and fishes in his leisure time.

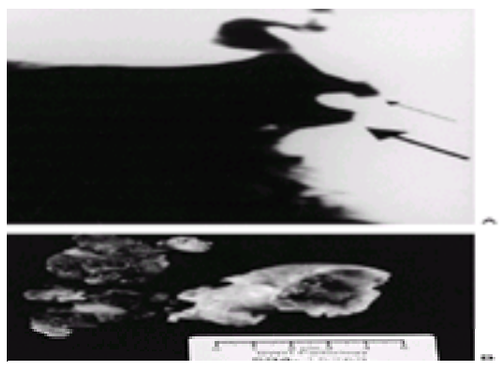

FIG. 31.9. A: Left pulmonary arteriogram of a 53-year-old man with chronic pulmonary embolism causing total occlusion of left lower lobar pulmonary arteries. **B:** This patient underwent pulmonary thromboendarterectomy at Brigham and Women's Hospital, where large and extensive thrombi were surgically removed. The specimen contains laminated thrombus that is adherent to the endothelial wall of the endarterectomy.

CHAPTER REFERENCES

1. McConnell MV, Solomon SD, Rayan ME, Come PC, Goldhaber SZ, Lee RT. Regional right ventricular dysfunction detected by echocardiography in acute pulmonary embolism. *Am J Cardiol* 1996;78:469.
2. Nass N, McConnell MV, Goldhaber SZ, Chyu S, Solomon SD. Recovery of regional right ventricular function following thrombolysis for pulmonary embolism. *Am J Cardiol* 1999;83:804.
3. Goldhaber SZ, Haire WD, Feldstein ML, et al. Alteplase versus heparin in acute pulmonary embolism: randomised trial assessing right ventricular function and pulmonary perfusion. *Lancet* 1993;341:507.
4. Konstantinides S, Geibel A, Olschewski M, et al. Association between thrombolytic treatment and the prognosis of hemodynamically stable patients with major pulmonary embolism: results of a multicenter registry. *Circulation* 1997;96:882.
5. Goldhaber SZ, Visani L, De Rosa M. Acute pulmonary embolism: clinical outcomes in the International Cooperative Pulmonary Embolism Registry (ICOPER). *Lancet* 1999;353:1386.
6. Palla A, Donnamaria V, Petruzzelli S, Rossi G, Riccetti G, Giuntini C. Enlargement of the right descending pulmonary artery in pulmonary embolism. *Am J Roentgenol* 1983;141:513.
7. Ferrari E, Imbert A, Chevalier T, Mihoubi A, Morand P, Baudouy M. The ECG in pulmonary embolism: predictive value of negative T waves in precordial leads--80 case reports. *Chest* 1997;111:537.
8. Stein PD, Goldhaber SZ, Henry JW, Miller AC. Arterial blood gas analysis in the assessment of suspected acute pulmonary embolism. *Chest* 1996;109:78.
9. Stein PD, Goldhaber SZ, Henry JW. Alveolar-arterial oxygen gradient in the assessment of acute pulmonary embolism. *Chest* 1995;107:139.
10. Bounameaux H, de Moerloose P, Perrier A, Reber G. Plasma measurement of D-dimer as diagnostic aid in suspected venous thromboembolism: an overview. *Thromb Haemostas* 1994;71:1.
11. Goldhaber SZ, Simons GR, Elliott CG, et al. Quantitative plasma D-dimer levels among patients undergoing pulmonary angiography for suspected pulmonary embolism. *JAMA* 1993;270:2819.
12. The PIOPED Investigators. Value of the ventilation/perfusion scan in acute pulmonary embolism: results of the Prospective Investigation of Pulmonary Embolism Diagnosis (PIOPED). *JAMA* 1990;263:2753.
13. Remy-Jardin M, Remy J, Deschildre F, et al. Diagnosis of pulmonary embolism with spiral CT: comparison with pulmonary angiography and scintigraphy. *Radiology* 1997:200:699.
14. Meaney JFM, Weg JG, Chenevert TL, Stafford-Johnson D, Hamilton BH, Prince MR. Diagnosis of pulmonary embolism with magnetic resonance angiography. *N Engl J Med* 1997;336:1422.
15. Lensing AWA, Prandoni P, Brandjes D, et al. Detection of deep-vein thrombosis by B-mode real-time ultrasonography. *N Engl J Med* 1989;320:342.
16. Hull RD, Hirsh J, Carter CJ, et al. Pulmonary angiography, ventilation lung scanning, and venography for clinically suspected pulmonary embolism with abnormal perfusion lung scan. *Ann Intern Med* 1983;98:891.
17. Auger WR, Fedullo PF, Moser KM, et al. Chronic major-vessel thromboembolic pulmonary artery obstruction: appearance at angiography. *Radiology* 1992;182:393.
18. Stein PD, Athanasoulis C, Alavi A, et al. Complications and validity of pulmonary angiography in acute pulmonary embolism. *Circulation* 1992;85:462.
19. Toglia MR, Weg JG. Venous thromboembolism during pregnancy. *N Engl J Med* 1996;335:108.
20. Goldhaber SZ, Vaughan DE, Markis JE, et al. Acute pulmonary embolism treated with tissue plasminogen activator. *Lancet* 1986;2:886.
21. Goldhaber SZ. Integration of catheter thrombectomy into our armamentarium to treat acute pulmonary embolism. *Chest* 1998;114:1237.
22. Daniels LB, Parker JA, Patel SR, Grodstein F, Goldhaber SZ. Relation of duration of symptoms with response to thrombolytic therapy in pulmonary embolism. *Am J Cardiol* 1997;80:184.
23. Mikkola KM, Patel SR, Parker JA, Grodstein F, Goldhaber SZ. Increasing age is a major risk factor for hemorrhagic complications after pulmonary embolism thrombolysis. *Am Heart J* 1997;134:69.
24. Decousus H, Leizorovicz A, Parent F, et al. A clinical trial of vena caval filters in the prevention of pulmonary embolism in patients with proximal deep-vein thrombosis. *N Engl J Med* 1998;338:409.
25. Schmitz-Rode T, Janssens U, Schild HH, et al. Fragmentation of massive pulmonary embolism using a pigtail rotation catheter. *Chest* 1998;114:1427.
26. Koning R, Cribier A, Gerber L, et al. A new treatment for severe pulmonary embolism. Percutaneous rheolytic thrombectomy. *Circulation* 1997;96:2498.
27. Greenfield LJ, Proctor MC, Williams DM, et al. Long-term experience with transvenous catheter pulmonary embolectomy. *J Vasc Surg* 1993;18:450.
28. Sharafuddin MJA, Hicks ME. Current status of percutaneous mechanical thrombectomy. Part I. General principles. *J Vasc Interv Radiol* 1997;8:911.
29. Sharafuddin MJA, Hicks ME. Current status of percutaneous mechanical thrombectomy. Part II. Devices and mechanisms of action. *J Vasc Interv Radiol* 1998;9:15.
30. Sharafuddin MJA, Hicks ME. Current status of percutaneous mechanical thrombectomy. Part III. Present and future applications. *J Vasc Interv Radiol* 1998;9:209.
31. Fava M, Loyola S, Flores P, Huete I. Mechanical fragmentation and pharmacologic thrombolysis in massive pulmonary embolism. *J Vasc Interv Radiol* 1997;8:261.
32. Gulba DC, Schmid C, Borst H-G, Lichtlen P, Dietz R, Luft FC. Medical compared with surgical treatment for massive pulmonary embolism. *Lancet* 1994;343:565.
33. Meyer G, Tamiser D, Reynaud P, Sors H. Acute pulmonary embolectomy. In: Goldhaber SZ, ed. *Cardiopulmonary diseases and cardiac tumors*. Philadelphia: Current Medicine, 1995:7.1.
34. Moser KM, Auger WR, Fedullo PF. Chronic major-vessel thromboembolic pulmonary hypertension. *Circulation* 1990;81:1735.
35. Fedullo PF, Auger WR, Channick RN, Jamieson SW, Moser KM. A multidisciplinary approach to chronic thromboembolic pulmonary hypertension. In: Goldhaber SZ, ed. *Cardiopulmonary diseases and cardiac tumors.* Philadelphia: Current Medicine, 1995: 7.1.

32
Profiles in Dilated (Congestive) and Hypertrophic Cardiomyopathies

William Grossman

University of California, San Francisco, School of Medicine; Division of Cardiology, University of California, San Francisco Medical Center, San Francisco, California 94143

Cardiomyopathies are primary disorders of heart muscle. Although the term *cardiomyopathy* is sometimes restricted to refer to cardiac muscle disorders of unknown etiology, most cardiologists include disorders of both unknown and known etiology. For example, the cardiac muscle disorder associated with long-standing ingestion of excessive quantities of ethanol is generally termed *alcoholic cardiomyopathy,* and the disorder resulting from high-dose doxorubicin therapy for malignancy is called doxorubicin or Adriamycin cardiomyopathy.

In general, cardiomyopathies are classified descriptively, as listed in Table 32.1. This chapter discusses only the first two types of cardiomyopathy listed in Table 32.1. Restrictive cardiomyopathy is discussed in Chapter 33, along with constrictive pericarditis, with which it is often confused. Obliterative cardiomyopathy is extremely rare in the United States and is beyond the scope of this book.

I. Dilated (congestive) cardiomyopathy: dilated ventricular chambers with increased end-diastolic and end-systolic volumes and decreased ventricular ejection fraction
A. Idiopathic
B. Postmyocarditis
C. Toxic: 2° to ethanol, doxorubicin, uremia
D. Peripartum
E. Chronic overload (e.g., long-standing severe volume overload, untreated hypertension)
F. Congenital
G. Miscellaneous (diabetes, autoimmune disease, sarcoid)
II. Hypertrophic cardiomyopathy: hypertrophic ventricular chambers with normal volumes and generally normal contractile function
A. Asymmetric septal hypertrophy
B. Apical hypertrophic cardiomyopathy
C. Diffuse symmetric hypertrophy
III. Restrictive cardiomyopathy: normal ventricular volumes and contractile function, but increased resistance to diastolic filling
A. Infiltrative type: amyloidosis, hemochromatosis, Fabry's disease
B. Idiopathic
C. Diffuse fibrosis (e.g., postmyocarditis, diffuse nontransmural myocardial infarction)
IV. Obliterative cardiomyopathy: eosinophilic endomyocardial fibroelastosis

TABLE 32.1. *Descriptive classification of cardiomyopathies*

DILATED (CONGESTIVE) CARDIOMYOPATHY

The clinical syndrome of dilated cardiomyopathy represents a collection of disorders and is also called congestive cardiomyopathy. The term *congestive cardiomyopathy* was used previously to refer to this syndrome because the clinical presentation is marked primarily by peripheral and pulmonary edema. Currently, the term *dilated cardiomyopathy* is preferred because with modern noninvasive techniques (echocardiography, radionuclide ventriculography) it has become possible to diagnose this syndrome before the onset of clinical signs and symptoms of congestion. Also, with effective diuretic and vasodilator management, the congestive component can be eliminated and ventricular filling pressures returned to normal. The ventricular chambers remain dilated, however, with increased end-systolic and end-diastolic volumes and reduced ventricular ejection fraction. Dilated cardiomyopathy is a syndrome that can develop in the setting of a variety of specific cardiac disorders (1), and the hemodynamic profile may vary, depending on the etiology.

CARDIAC CATHETERIZATION PROTOCOL

Study of the patient who is suspected of having dilated cardiomyopathy should include right and left heart catheterization with measurement of pressures, cardiac output, and resistances. As discussed in Chapter 4 and Chapter 5, during right heart catheterization the routine measurement of oxygen saturation in blood taken from the superior vena cava and pulmonary artery is essential to detect unsuspected right-to-left shunting. In one elderly patient referred to the author for evaluation of advanced left heart failure, stretching of a patent foramen ovale by high left atrial pressures had led to left-to-right shunting and a Q_p/Q_s of 2.0. Surgical closure of this patent foramen ovale resulted in marked clinical improvement. Angiographic studies will need to be tailored to the individual case, but left ventriculography and coronary angiography are commonly done as a part of the diagnostic study in patients with dilated cardiomyopathy.

Hemodynamic Findings

In the symptomatic patient with dilated cardiomyopathy referred for cardiac catheterization, *left and right ventricular filling pressures usually are elevated*. As mentioned, however, it is possible that the ventricular filling pressures at rest may be normal; this finding is particularly likely in the asymptomatic patient detected early in the course of his or her disease by noninvasive screening. Also, the patient who has been treated intensively with diuretics (e.g., furosemide and spironolactone) and who is receiving a potent vasodilator (e.g., enalapril) may show little or no elevation in ventricular filling pressures at rest. In general, increases in left and right ventricular filling pressures can be induced easily in such patients by supine bicycle exercise, performed as outlined in Chapter 15. With 6 minutes of supine bicycle exercise, pulmonary capillary wedge pressure commonly rises from 10 to between 25 and 40 mm Hg, and right atrial pressure increases from 6 to between 15 and 20 mm Hg. Supine bicycle exercise places an acute volume and pressure load on the ventricular myocardium and easily brings out underlying loss of contractile reserve.

Cardiac output is generally reduced in the patient with dilated cardiomyopathy. In milder cases, the cardiac index may be normal or only slightly reduced and may range from 2.4 to 3.0 L/min/m^2. In patients with New York Heart Association (NYHA) class III or IV symptoms from dilated cardiomyopathy, it is common to find the cardiac index depressed more severely. Thus a cardiac index of 1.6 to 2.3 L/min/m^2 can be expected in the usual symptomatic patient presenting with dilated cardiomyopathy, and a cardiac index of 1.5 L/min/m^2 or less indicates an advanced depression of myocardial function and a poor prognosis.

The *left ventricular pressure waveform* is typically abnormal in patients with dilated cardiomyopathy. Both the rate of rise and the rate of fall of left ventricular pressure are slow, and this is usually visible to the naked eye (Fig. 32.1). Slowing of both the rate of rise and the rate of fall of left ventricular pressure gives a *triangular appearance* to the pressure waveform, with the peak systolic pressure representing the apex of the triangle; end-diastolic and minimal (early) diastolic left ventricular pressures define the triangle's base. This deformity accounts for the brief duration of systolic ejection in dilated cardiomyopathy and contrasts with the trapezoidal, almost square-wave appearance of left ventricular pressure in a normal, vigorous heart. A corollary of the triangular waveform of left ventricular pressure in dilated cardiomyopathy is a normal or low peak systolic pressure. The triangular waveform is associated with reduced values for both the rate of rise (+ *dP*/*dt*) and the rate of decline (– *dP*/*dt*) of left ventricular isovolumic pressure. The marked reductions in + *dP*/*dt* seen in dilated cardiomyopathy reflect impaired inotropy and are not increased in response to pacing-induced increases in heart rate, as seen in normal hearts (2,3). Thus a flat “force/frequency” relation may be demonstrated in the

cardiac catheterization laboratory in such patients, paralleling observations in isolated heart muscle (2).

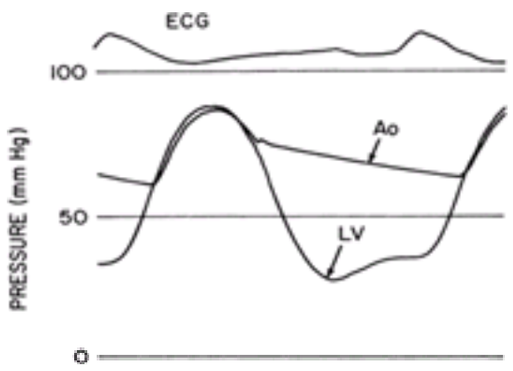

FIG. 32.1. Left ventricular (LV) micromanometer and aortic (Ao) pressure tracings in a 68-year-old woman with advanced dilated cardiomyopathy. Marked slowing of the rates of left ventricular pressure rise and fall give the LV pressure tracing a triangular appearance. Also, the minimal value for left ventricular diastolic pressure is markedly elevated.

A second abnormality of the left ventricular pressure tracing in dilated cardiomyopathy is elevation in the value for left ventricular *minimal* diastolic pressure (Fig. 32.1). Normally, the left ventricular pressure declines briskly after aortic valve closure, reaching a nadir close to 0 mm Hg shortly after mitral valve opening. This reflects the normal pattern of rapid myocardial relaxation, acting together with *restoring forces* generated by a vigorous systolic contraction, with end-systolic elastic compression and torsion forces being released during early diastolic filling. In the experimental laboratory under conditions of extremely vigorous contraction (e.g., isoproterenol infusion) or hypovolemia (e.g., hemorrhage), the left ventricular diastolic pressure actually may become negative early in diastole, a phenomenon known as *diastolic suction*. In dilated cardiomyopathy, diastolic relaxation is generally slow and incomplete (3), and restoring forces produced by the weakened systolic contraction are minimal. These factors militate against a normal low value for left ventricular minimal diastolic pressure. In addition, end-systolic volume is increased in patients with dilated cardiomyopathy, and this abnormality tends to elevate diastolic volume and pressure above normal.

To appreciate these abnormalities in the left ventricular pressure waveform in dilated cardiomyopathy, one must have pressure tracings of good quality with careful attention to the details discussed in Chapter 7. Micromanometer catheters are not necessary to achieve such high-quality tracings, as can be seen in Fig. 32.2, where fluid-filled and micromanometer tracings are superimposed.

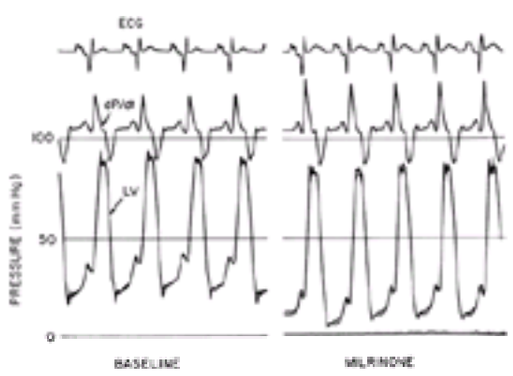

FIG. 32.2. Left ventricular (LV) micromanometer pressure and its first derivative (*dP*/*dt*) in a patient with dilated cardiomyopathy before (left) and after (right) intravenous infusion of milrinone. Positive and negative dP/dt have increased without increase in arterial pressure and with a decline in preload, suggesting increased myocardial contractility and relaxation. Left ventricular minimal diastolic pressure is now closer to zero, as is normal. Fluid-filled and micromanometer pressures are displayed simultaneously, indicating the excellent fidelity that can be achieved with fluid-filled systems using the principles described in Chapter 7. (Reproduced with permission from Baim DS et al. Evaluation of a new bipyridine inotropic agent—milrinone—in patients with severe congestive heart failure. *N Engl J Med* 1983;309:748.)

The left ventricular pressure tracing abnormalities just described can be corrected substantially by acute administration of an inotropic drug (4,5 and 6). Figure 32.2 and Figure 32.3 illustrate the effects of a phosphodiesterase inhibitor (milrinone) and a beta-adrenergic agonist (prenalterol) on the left ventricular pressure contour in patients with dilated cardiomyopathy. As can be seen, early diastolic relaxation is more rapid and more complete after administration of these drugs, as reflected by the steep decline in left ventricular pressure to a value near zero in early diastole.

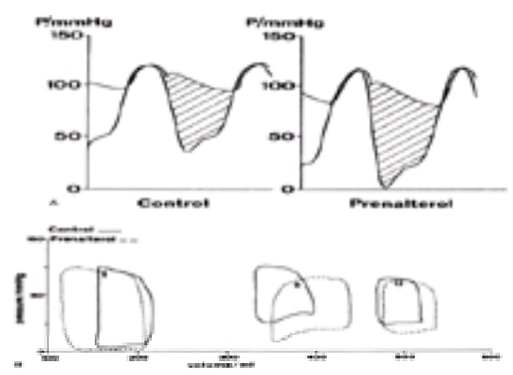

FIG. 32.3. Effects of the beta agonist prenalterol on left ventricular and aortic pressure (**A**) and left ventricular pressure-volume plots (**B**) in patients with idiopathic dilated cardiomyopathy. The tracings illustrate the restoration of a normal low value for the left ventricular diastolic pressure nadir, as well as a downward shift in the diastolic pressure volume relationship. (Reproduced with permission from Erbel R, et al. Hemodynamic effects of prenalterol in patients with ischemic heart disease and congestive cardiomyopathy. *Circulation* 1982;66:361.)

Patients with dilated cardiomyopathy often have elevations in pulmonary and systemic vascular resistance. It is common to find pulmonary vascular resistance increased to 150 to 300 dyn-sec-cm^{-5}, and patients with values 400 dyn-sec-cm^{-5} or more are not rare. These increases in pulmonary vascular resistance result in pulmonary hypertension with mean pulmonary artery pressure commonly of 30 to 50 mm Hg. Systemic vascular resistance is usually 1,500 dyn-sec-cm^{-5} or more in untreated patients with advanced dilated cardiomyopathy, probably representing a response to combined elevations in serum levels of angiotensin, vasopressin, and norepinephrine. Because cardiac output is reduced, modest increases in systemic vascular resistance do not result in actual elevation of arterial blood pressure but rather tend to preserve arterial pressure at a normal or only slightly reduced level.

Reduction of systemic and pulmonary vascular resistances to normal by administration of vasodilator agents often results in a striking increase in cardiac output and a simultaneous reduction in left and right ventricular filling pressures. As shown in Fig. 32.4, acute administration of sodium nitroprusside (7,8) or captopril (9,10) results in an upward and leftward displacement of the left ventricular filling pressure/stroke volume relationship, since heart rate is affected minimally by these agents in the

setting of chronic heart failure.

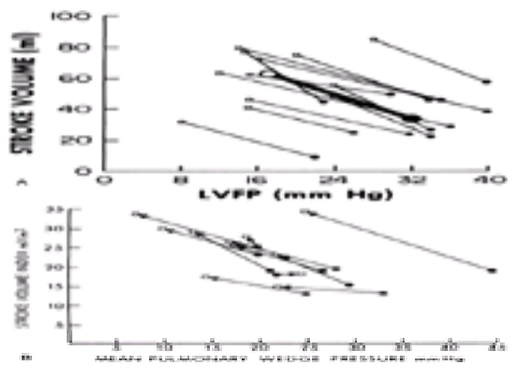

FIG. 32.4. Effects of acute administration of sodium nitroprusside (**A**) and captopril (**B**) on left ventricular filling pressure-stroke volume relationships in patients with advanced heart failure. Some of these patients had heart failure on the basis of idiopathic dilated cardiomyopathy, and some had ischemic heart disease. Responses were similar and appeared to be independent of etiology. (See text for discussion.) (Reproduced with permission from (A) Guiha NH, et al. Treatment of refractory heart failure with infusion of nitroprusside. *N Engl J Med* 1974;291:587; and (B) Davis R, et al. Treatment of chronic congestive heart failure with captopril, an oral inhibitor of angiotensin-converting enzyme. *N Engl J Med* 1979;301:117.)

During cardiac catheterization in patients with dilated cardiomyopathy, it is often wise to test responsiveness to a vasodilator in the laboratory. This can be done routinely using the following protocol. After measurement of cardiac output and resting hemodynamics and before angiography, if filling pressures are elevated significantly (e.g., pulmonary capillary wedge pressure ³ 16 mm Hg) and cardiac output is depressed (e.g., pulmonary artery blood oxygen saturation £ 65%), begin an infusion of sodium nitroprusside as long as arterial systolic pressure is 90 mm Hg or more and has been stable. The starting dose is 15 µg/min through a secure, free-flowing intravenous line, and the infusion rate is increased every 3 to 5 minutes to doses of 25, 50, 75, 100, 150, 200, and 300 µg/min, if needed, until arterial mean pressure has fallen 10 to 20 mm Hg or wedge pressure has fallen by 50% or more or pulmonary artery oxygen saturation has increased to 75% or more. Usually, one of these three end points is achieved at a dose of sodium nitroprusside of 200 µ/min or less; however, there are occasional patients in whom 300 µ/min or more is required. If the patient is feeling well during the vasodilator infusion (as is generally the case), continue the infusion during left ventriculography and coronary angiography as a prophylactic measure to protect against pulmonary edema. The dose should be reduced if the arterial systolic pressure is 85 mm Hg or less. A favorable response to sodium nitroprusside in the cardiac catheterization laboratory is not only an aid to the safety of the procedure but also a predictor of a favorable response to an oral vasodilator in the patient's long-term management.

Angiographic Studies

The hallmark of dilated cardiomyopathy as seen on left ventriculography is left ventricular enlargement (increased end-diastolic and end-systolic volumes) with a reduced ejection fraction. Left ventriculography in patients with dilated cardiomyopathy classically reveals extensive hypokinesis, which, although usually diffuse in nature, is commonly associated with regional wall motion abnormalities that suggest a heterogeneity of the myocardial injury and mimic coronary artery disease. This may represent the consequence of asymmetric injury initially, and in this regard it is of interest that myocarditis may be focal in its inflammatory effects. We have seen several patients in whom biopsy-proven acute myocarditis mimicked regional ischemia and infarction, with left ventriculography showing discrete areas of akinesis or even focal aneurysm formation. These areas of regional dysfunction also could represent the result of coronary emboli from mural thrombus because the occurrence of left ventricular mural thrombus is increased in patients with dilated cardiomyopathy.

Angiographic abnormalities associated with dilated cardiomyopathy include dilatation and loss of the normal eccentric shape of the left ventricle. Normally, the ratio of long axis *L* to the minor axis *M* is 2:1 for the left ventricular chamber at end-diastole. In dilated cardiomyopathy, *L*/*M* approaches 1:1. This change tends to increase meridional wall stress (see Chapter 16) but has an unpredictable effect on longitudinal wall stress, depending on the extent of associated ventricular hypertrophy. In this regard, left ventricular hypertrophy is common in patients with dilated cardiomyopathy (11). Some authors have reported a substantial beneficial effect of hypertrophy on survival in patients with dilated cardiomyopathy and have suggested that protection against increasing wall stress might have a protective role for these patients (11).

Endomyocardial Biopsy

Enthusiasm for obtaining endomyocardial biopsy as a part of the diagnostic workup in patients with suspected dilated cardiomyopathy often reflects the experience of a particular laboratory in performing the procedure. Endomyocardial biopsy is done almost routinely in many laboratories as part of the diagnostic study in patients with advanced heart failure. In more than 100 endomyocardial biopsies in nontransplant patients with advanced heart failure at Beth Israel Hospital in Boston, specific heart muscle disorders (inflammatory myocarditis, amyloidosis, hemochromatosis) were found in approximately 15% of cases.

Viral myocarditis is widely regarded as a precursor and etiologic agent for many patients with dilated cardiomyopathy, although evidence confirming this hypothesis definitively remains elusive (12). Endomyocardial biopsy early in the course of viral myocarditis shows a characteristic inflammatory cell infiltrate. (See Chapter 20 for details.) However, in the chronic phase (days 15 to 90 in experimental studies) the cellular infiltrate largely disappears, followed by the appearance of myocardial fibrosis. Special studies can detect persistent viral DNA in this stage. There is also evidence that apoptosis is found in the chronic stage, accounting for the ongoing loss of myocytes in the absence of cell necrosis (12).

The technique of endomyocardial biopsy and additional specific diseases it can detect are described in detail in Chapter 20. In one study of 100 consecutive endomyocardial biopsies carried out to evaluate heart failure of uncertain etiology (13), the pathologic information obtained was judged to be clinically useful in 54 patients and not useful in 46 patients. Specific diagnoses that could be made from histologic examination of the biopsy material included inflammatory myocarditis, amyloidosis, sarcoidosis, scleroderma, endomyocardial fibrosis with eosinophilia, doxorubicin cardiomyopathy, radiation-induced cardiomyopathy, and vasculitis (13).

In summary, a variety of hemodynamic, angiographic, and histologic features can be defined precisely in the course of a single diagnostic cardiac catheterization procedure in patients with suspected dilated cardiomyopathy. Findings from such a diagnostic study yield valuable information about prognosis (11,13,14 and 15) and help direct appropriate therapy.

HYPERTROPHIC CARDIOMYOPATHY

Cardiac hypertrophy develops to some extent in a wide variety of cardiac diseases. In hypertrophic cardiomyopathy, however, the development of cardiac hypertrophy proceeds without an obvious inciting stimulus, or develops out of proportion to the magnitude of the stimulus or stimuli that can be identified. Hypertrophic cardiomyopathy was noted early on to be familial in most cases (16) and is transmitted as an autosomal-dominant trait; nevertheless, in clinical practice many cases appear to be sporadic. Studies of molecular genetics have shown that mutations in any of at least seven different genes can cause hypertrophic cardiomyopathy; each of these “culprit” genes encodes for proteins essential for the formation of the normal cardiac sarcomere (17). Expression of some of these genes in transgenic mice has duplicated some of the features of hypertrophic cardiomyopathy. However, we are still at an early point in this research, and it is not yet possible to link a particular genetic mutation with a specific hemodynamic/anatomic phenotype. Most authors distinguish between obstructive and nonobstructive forms of the disorder based on the presence or absence of a resting (unprovoked) systolic pressure gradient within the left ventricle (16), and the presence of a gradient has caused this disorder to be called *idiopathic hypertrophic subaortic stenosis* (IHSS) or hypertrophic obstructive cardiomyopathy (HOCM). There remains controversy as to whether true “obstruction” occurs in this condition (1,18) because there is some evidence that most of the left ventricular stroke volume has been ejected before development of a significant gradient. There is general agreement, however, that the pressure gradient, when present, has several adverse consequences, including increased systolic wall stress (in cardiac muscle proximal to the site of septal/mitral leaflet contact) and increased myocardial oxygen consumption.

Hypertrophic cardiomyopathy may be diffuse and symmetric, involving all regions of the left ventricle equally, or it may be *asymmetric*. Asymmetric hypertrophic cardiomyopathy commonly involves the high interventricular septum, which is disproportionately hypertrophied so that the ratio of thickness of the diastolic septal wall

to that of the free (lateral or posterior) left ventricular wall is 1.3 or more. Another form of asymmetric hypertrophic cardiomyopathy, which has been reported from Japan (19), involves massive apical hypertrophy of the left ventricle. A characteristic electrocardiographic feature is the presence of giant negative T waves in the precordial leads. The apical form of hypertrophic cardiomyopathy has now been recognized to occur in Europe and North America (20,21).

Hemodynamic Findings

As in the patient with suspected dilated cardiomyopathy, cardiac catheterization in the patient being evaluated for hypertrophic cardiomyopathy should include right and left heart study. Right atrial and right ventricular pressures usually are normal in patients with hypertrophic cardiomyopathy. Rarely, involvement of the right ventricle is said to result in a systolic gradient within the right ventricular chamber, although I have never seen such a case personally. If the hypertrophic process involves the right ventricle or if the pulmonary capillary wedge pressure is substantially elevated, right ventricular diastolic pressures may be elevated.

Left ventricular end-diastolic pressure may be normal in patients with hypertrophic cardiomyopathy but is usually elevated (16,18,19), reflecting decreased left ventricular diastolic distensibility. The decreased diastolic distensibility in hypertrophic cardiomyopathy is caused by both increased passive stiffness of the thick-walled left ventricular chamber and decreased rate and extent of myocardial relaxation (1,22,23,24,25 and 26). Pulmonary capillary wedge pressure may be elevated, particularly if there is mitral regurgitation, a common finding in patients with hypertrophic cardiomyopathy (27).

Cardiac output is usually normal or increased in patients with hypertrophic cardiomyopathy, except in the late stages of the disease, when contractility decreases.

The most dramatic hemodynamic features of hypertrophic cardiomyopathy are those related to the systolic intraventricular pressure gradient. As seen in Fig. 32.5, the pressure gradient is present between the body and the outflow tract of the left ventricle. A key feature of this systolic gradient and of most of the associated findings is their variability. Most patients with hypertrophic cardiomyopathy do not have a systolic pressure gradient at rest but may develop one with appropriate provocative maneuvers as listed in Table 32.2.

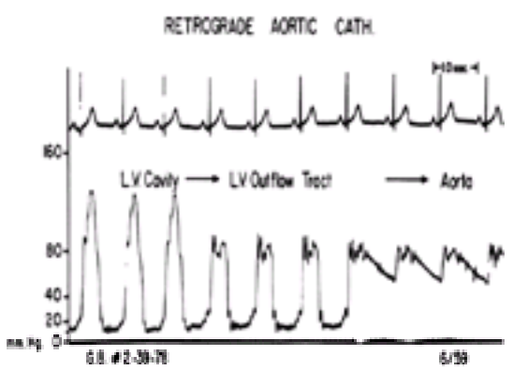

FIG. 32.5. Left ventricular (LV) catheter pullback to the aorta in a patient with hypertrophic cardiomyopathy. There is a significant systolic gradient within the left ventricular cavity, and the LV outflow tract and aortic pressure waveforms exhibit a spike-and-dome contour. (Reproduced with permission from Braunwald E, et al. Idiopathic hypertrophic subaortic stenosis: a description based on an analysis of 65 patients. *Circulation* 1964;30[Suppl 4]:3.)

1. Valsalva maneuver
2. Amyl nitrite inhalation
3. Postextrasystolic potentiation
4. Isoproterenol
5. Exercise

TABLE 32.2. *Provocative maneuvers for development of systolic pressure gradient in hypertrophic cardiomyopathy*

It should be emphasized that the presence of a systolic gradient at rest or following provocation is a hallmark of only one variety of hypertrophic cardiomyopathy: that form with asymmetric septal hypertrophy. The diffuse hypertrophic variety and the variety associated with massive apical hypertrophy do not exhibit true left ventricular outflow tract gradients at rest or with provocation (19,21). However, catheter entrapment can develop easily in patients with apical as well as symmetric forms of hypertrophic cardiomyopathy, giving the false impression of an outflow gradient (21).

An interesting aspect of the systolic gradient is an associated deformity that develops in the aortic pressure waveform. This deformity consists of an initial rapid rise in aortic pressure to give a spike early in ejection, followed by a dip in pressure and a secondary rounded or dome-shaped tidal wave before the dicrotic notch. This spike-and-dome configuration is seen in the central aortic pressure and is transmitted to the carotid pulse and peripheral arterial tracings. It is most evident following an extrasystolic contraction (Fig. 32.6) but is also seen during Valsalva maneuver (Fig. 32.7) and at other times (Fig. 32.8). The mechanism for this spike-and-dome configuration may be related to blending of an initial hyperdynamic ejection velocity leading to the development of a Venturi effect that sucks the anterior mitral leaflet into the outflow tract, thereby impeding middle and late systolic ejection velocity.

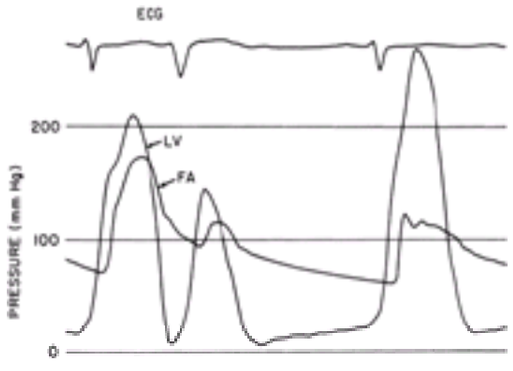

FIG. 32.6. Left ventricular (LV) and femoral artery (FA) pressure tracings in a woman with hypertrophic cardiomyopathy and asymmetric septal hypertrophy illustrating the increase in gradient and development of a spike-and-dome configuration in the arterial pressure waveform following an extrasystolic beat. Also, arterial pulse pressure clearly narrows in the postextrasystolic beat compared with the control value in the beat before the extrasystole. This narrowing of pulse pressure is known as the Brockenbrough-Braunwald sign.

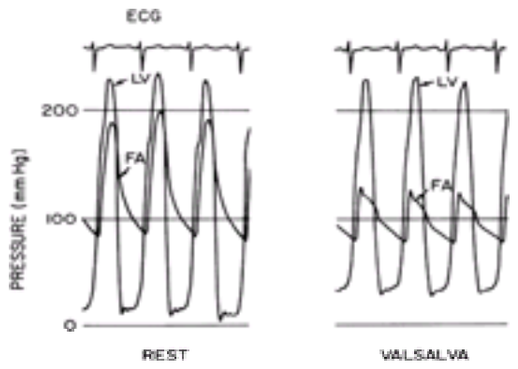

FIG. 32.7. Left ventricular (LV) and femoral artery (FA) pressure tracings in the patient illustrated in Fig. 32.6. Valsalva maneuver produces a marked increase in the gradient, as well as a change in the femoral arterial pressure waveform to a spike-and-dome configuration.

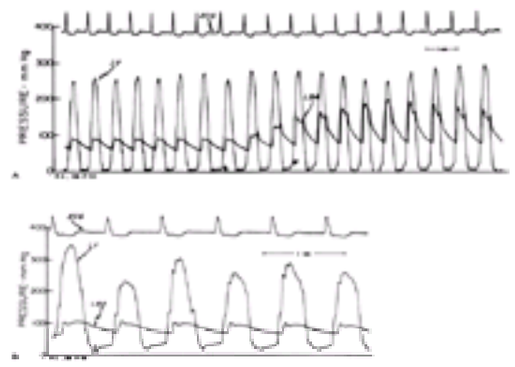

FIG. 32.8. Left ventricular (LV) and left brachial artery (LBA) pressure tracings in a 64-year-old woman with hypertrophic cardiomyopathy. **A:** The effect of a spontaneous change from nodal rhythm to sinus rhythm. The short *arrows* show LV end-diastolic pressure. With restoration of sinus rhythm and a presumed decrease in the obstruction, LV stroke volume increases as reflected in the improved LBA pulse pressure. Also, the loss of atrial kick in patients with a stiff ventricle leads to an acute reduction in cardiac output. **B:** Following a premature contraction (not shown) there is LV pulsus alternans. A spike-and-dome pattern is clearly seen in the LBA tracing. (Reproduced with permission from Glancy L, et al. The dynamic nature of left ventricular outflow obstruction in idiopathic hypertrophic subaortic stenosis. *Ann Intern Med* 1971;75:589.)

In addition to developing a spike-and-dome pattern, the aortic pulse pressure fails to widen in a postextrasystolic potentiated beat (16). Normally, a potentiated left ventricular contraction has a larger stroke volume than the preceding sinus beats, and this increased stroke volume results in an increased aortic pulse pressure.

Patients with hypertrophic cardiomyopathy, however, develop a spike-and-dome onfiguration in which pulse pressure is unchanged or actually reduced following an extrasystolic beat (Fig. 32.6). This sign, which was described by Brockenbrough et al. (28) in 1961, is known as the Brockenbrough-Braunwald sign and is believed to reflect worsening of obstruction of the left ventricular outflow tract during the potentiated beat, with diminished stroke volume and aortic pulse pressure.

The impaired left ventricular diastolic relaxation seen in hypertrophic cardiomyopathy (22,23,24,25 and 26) can be dramatic and can affect the contour of the left ventricular diastolic pressure tracing (Fig. 32.9). The patient illustrated in Fig. 32.9 was a 55-year-old woman with a family history of hypertrophic cardiomyopathy who presented with advanced congestive heart failure manifested by paroxysmal nocturnal dyspnea, marked fatigue, and peripheral edema. An echocardiogram showed asymmetric septal hypertrophy. At cardiac catheterization, there was no outflow tract gradient at rest or with provocation. Right atrial mean pressure was increased (11 mm Hg), reflecting pulmonary hypertension (60/30, 40 mm Hg), which in turn reflected a markedly increased mean pulmonary capillary wedge pressure (32 mm Hg). Arteriovenous oxygen difference was wide (71 mL O_2/L), and cardiac index was depressed (2.0 L/min/m^2). Left ventricular ejection fraction was reduced at 41%, a finding sometimes seen in late-stage hypertrophic cardiomyopathy. As seen in Fig. 32.9, the left ventricular diastolic pressure did not exhibit its normal rapid decline to a nadir near zero. Instead, early left ventricular diastolic pressure was increased at approximately 35 mm Hg and continued to decline after mitral valve opening until atrial systole produced a diastolic pressure rise coincident with the *a* wave. The diastolic abnormalities of hypertrophic cardiomyopathy are improved by calcium channel blockade (22,23,29,30 and 31), although occasional serious adverse effects have been seen with verapamil (32). Combined treatment with beta blockade and verapamil is currently regarded as the pharmacologic treatment of choice. However, disopyramide has been reported to have beneficial hemodynamic effects in some patients.

FIG. 32.9. Left ventricular (LV) and aortic (Ao) pressure tracings and rate of LV pressure rise (*dP*/*dt*) in a 55-year-old woman with hypertrophic cardiomyopathy. There is no resting pressure gradient. LV diastolic pressure waveform is very abnormal, suggesting marked impairment in myocardial relaxation. Fluid-filled and micromanometer LV tracings are both shown.

Diastolic dysfunction is also prominent in *hypertensive hypertrophic cardiomyopathy of the elderly*, a syndrome described by Topol et al. (33). This condition represents a form of hypertrophic cardiomyopathy seen in elderly patients with mild to moderate hypertension who exhibit severe concentric hypertrophy, a small left ventricular cavity, supernormal systolic function characterized by excessive left ventricular emptying, and marked abnormality of diastolic relaxation. In describing this syndrome, Topol and coworkers (33) observed that several of their patients with this condition improved when treatment with digoxin and diuretics was stopped. In contrast, beta-adrenergic blocking agents often were effective in relieving dyspnea and chest pain. Left ventriculography in such patients shows a severely hypertrophied ventricular chamber, which demonstrates cavity obliteration at end-systole.

Although I will not discuss restrictive cardiomyopathy in this chapter, it is perhaps of value to point out that some unusual forms of infiltrative cardiomyopathy may present with features of both restrictive and hypertrophic cardiomyopathy. Miller et al. (34) reported a patient with eosinophilic heart disease who had a left ventricular subaortic gradient of 90 mm Hg, a spike-and-dome pattern in the central aortic pressure tracing, and a systolic murmur that increased with either amyl nitrate inhalation or Valsalva maneuver. Left and right ventricular end-diastolic pressures were elevated at 28 and 16 mm Hg, respectively, and left ventricular ejection fraction was markedly increased at 94%. Treatment with prednisone and warfarin resulted in substantial improvement over a 4-month period (34).

Angiographic Findings

The angiographic findings in hypertrophic cardiomyopathy are rather unique and help to explain some (but not all) of the unusual hemodynamic features just described. In hypertrophic cardiomyopathy with asymmetric septal hypertrophy, left ventriculography shows a thickened intraventricular septum bulging into the left ventricular outflow tract in diastole and systole. In addition to this abnormality, patients with hypertrophic cardiomyopathy in whom a systolic gradient is present within the left ventricular chamber generally show *systolic anterior movement* (SAM) of the mitral valve's anterior leaflet (Fig. 32.10).

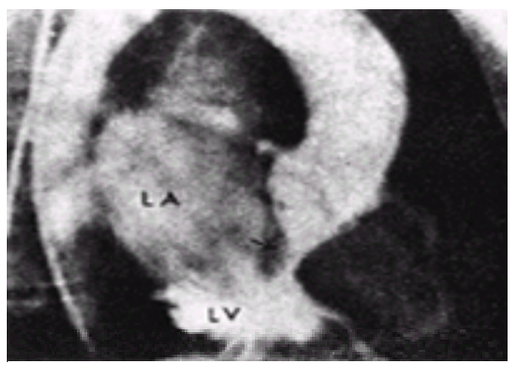

FIG. 32.10. Left ventricular (LV) angiogram in the lateral position in a patient with hypertrophic cardiomyopathy with obstruction. The anterior leaflet of the mitral valve moves toward the interventricular septum in systole (*arrow*), producing marked narrowing of the LV outflow tract. Mitral regurgitation into the left atrium (LA) is present. (Reproduced with permission from Braunwald E, et al. Idiopathic hypertrophic subaortic stenosis: a description based on an analysis of 65 patients. *Circulation* 1964;30[Suppl 4]:3.)

In contrast to hypertrophic cardiomyopathy with asymmetric septal hypertrophy, the patient with asymmetric apical hypertrophy does not show systolic anterior motion of the mitral leaflet. In patients with apical hypertrophic cardiomyopathy, the left ventricle shows marked thickening of its anteroapical wall, giving the ventricle a *spade-shaped appearance* (Fig. 32.11).

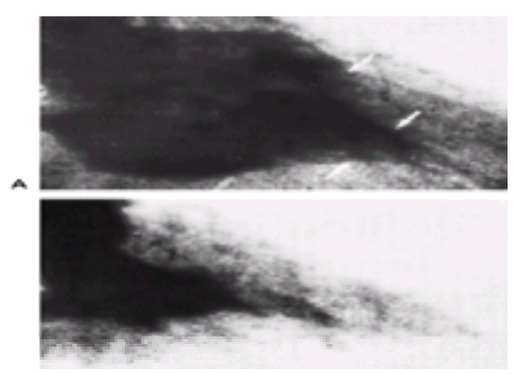

FIG. 32.11. Left ventriculogram at end-diastole (**A**) and end-systole (**B**) in a patient with apical hypertrophic cardiomyopathy. There is a spadelike configuration at end-diastole with a marked increase in free wall thickness and an extremely vigorous contraction with almost total cavity obliteration at end-systole. (Reproduced with permission from Yamaguchi H, et al. Hypertrophic non-obstructive cardiomyopathy with giant negative T waves (apical hypertrophy): ventriculographic and echocardiographic features in 30 patients. *Am J Cardiol* 1979;44:401.)

Patients with asymmetric septal hypertrophy have a distortion of the left ventricle that in the right anterior oblique view often resembles a *banana*, partly because of the large papillary muscles, which appear as filling defects.

In addition to exhibiting abnormal shapes (spade, banana) and systolic anterior movement of the mitral valve, patients with hypertrophic cardiomyopathy often exhibit mitral regurgitation on left ventriculography. This is usually mild but may progress to become hemodynamically significant. Coronary angiography may show characteristic abnormalities in hypertrophic cardiomyopathy, with marked systolic compression of septal branches of the left anterior descending artery (35). In addition, a “sawfish” systolic narrowing of the left anterior descending artery has been reported by Brugada et al. (36) and is illustrated in Fig. 32.12. The indentations of the left anterior descending artery associated with systolic narrowing of the vessel may represent the effect of contracting hypertrophied and disorganized muscle fiber bundles in the vicinity of the coronary artery.

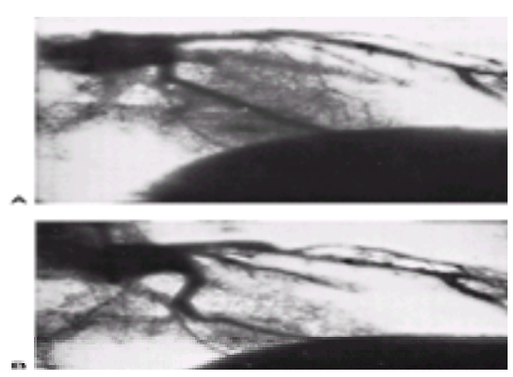

FIG. 32.12. Left coronary angiogram in right anterior oblique projection with caudocranial angulation. Diastolic (**A**) and systolic (**B**) frames are shown. A “sawfish” appearance of the left anterior descending artery is seen in association with systolic compression of septal branches in this patient with hypertrophic cardiomyopathy. (Reproduced with permission from Brugada P, et al. “Sawfish” narrowing of the left anterior descending coronary artery: an angiographic sign of hypertrophic cardiomyopathy. *Circulation* 1982;66:800.)

Catheter-Based Therapy for Hypertrophic Cardiomyopathy

Surgical resection of part of the interventricular septum (myotomy/myectomy) was one of the first treatments developed for patients with idiopathic hypertrophic cardiomyopathy, and this operation is widely regarded as a last-resort therapy for patients with refractory symptoms. Based on the concept that the hypertrophied, hypercontractile interventricular septum may be playing an important role in the pathophysiology of this condition, a catheter-based therapy was developed (37) in which ethanol is infused into the septal artery(ies) supplying the hypertrophic myocardium. In one report (38) of 33 symptomatic patients with hypertrophic obstructive cardiomyopathy and a resting gradient of 40 mm Hg, 2 to 5 mL of absolute ethanol infused into the septal artery distal to a local septal artery balloon occlusion induced a focal myocardial infarction with creatine kinase elevations to nearly 2,000 U. Complete heart block developed in 11 patients, who required permanent pacemaker placement. All patients were improved symptomatically, with NYHA class decreasing from 3.0 ± 0.5 to 0.9 ± 0.6. This promising therapy requires further

study but may be an effective substitute for surgical myotomy/myectomy in the patient with refractory symptoms.

CHAPTER REFERENCES

1. Dec GW, Fuster V. Idiopathic dilated cardiomyopathy. *N Engl J Med* 1994;331:1564.
2. Hasenfuss G, Holubarsch C, Hermann HP, Astheimer K, Pieske B, Just H. Influence of the force-frequency relationship on hemodymanics and left ventricular function in patients with non-failing hearts and in patients with dilated cardiomyopathy. *Eur Heart J* 1994;15:164.
3. Feldman MD, Alderman JD, Aroesty JM, et al. Depression of systolic and diastolic myocardial reserve during atrial pacing tachycardia in patients with dilated cardiomyopathy. *J Clin Invest* 1988;82:1661.
4. Baim DS, et al. Evaluation of a new bipyridine inotropic agent—milrinone—in patients with severe congestive heart failure. *N Engl J Med* 1983;309:748.
5. Monrad ES, et al. Improvement in indices of diastolic performance in patients with congestive heart failure treated with milrinone. *Circulation* 1984;70:1030.
6. Erbel R, et al. Hemodynamic effects of prenalterol in patients with ischemic heart disease and congestive cardiomyopathy. *Circulation* 1982;66:361.
7. Harshaw CW, Munro AB, McLaurin LP, Grossman W. Reduced systemic vascular resistance as therapy for severe mitral regurgitation of valvular origin. *Ann Intern Med* 1975;83:312.
8. Guiha NH, et al. Treatment of refractory heart failure with infusion of nitroprusside. *N Engl J Med* 1974;291:587.
9. Davis R, et al. Treatment of chronic congestive heart failure with captopril, an oral inhibitor of angiotensin-converting enzyme. *N Engl J Med* 1979;301:117.
10. Dzau VJ, et al. Sustained effectiveness of converting-enzyme inhibition in patients with severe congestive heart failure. *N Engl J Med* 1980;302:1373.
11. Benjamin HJ, Schuster EH, Bulkley BH. Cardiac hypertrophy in idiopathic dilated congestive cardiomyopathy: a clinicopathologic study. *Circulation* 1981;64:442.
12. Kawai C. From myocarditis to cardiomyopathy: mechanisms of inflammation and cell death. *Circulation* 1999;99:1091.
13. Parrillo JE, et al. The results of transvenous endomyocardial biopsy can frequently be used to diagnose myocardial disease in patients with idiopathic heart failure. *Circulation* 1984;69:93.
14. Unverferth DV, et al. Factors influencing the one-year mortality of dilated cardiomyopathy. *Am J Cardiol* 1984;54:147.
15. Fuster V, et al. The natural history of idiopathic dilated cardiomyopathy. *Am J Cardiol* 1981;54:525.
16. Braunwald E, et al. Idiopathic hypertrophic subaortic stenosis: a description based on an analysis of 65 patients. *Circulation* 1964;30[Suppl 4]:3.
17. Bonne G, Carrier L, Richard P, Hainque B, Schwartz K. Familial hypertrophic cardiomyopathy: from mutations to functional defects. *Circ Res* 1998;83:580.
18. Murgo JP, et al. Dynamics of left ventricular ejection in obstructive and nonobstructive hypertrophic cardiomyopathy. *J Clin Invest* 1980;66:1369.
19. Yamaguchi H, et al. Hypertrophic nonobstructive cardiomyopathy with giant negative T waves (apical hypertrophy): ventriculographic and echocardiographic features in 30 patients. *Am J Cardiol* 1979;44:401.
20. Webb JG, Sasson Z, Rakowski H, Liu P, Wigle D. Apical hypertrophic cardiomyopathy: clinical follow-up and diagnostic correlates. *J Am Coll Cardiol* 1990;15:83.
21. Maron BJ. Apical hypertrophic cardiomyopathy: the continuing saga. *J Am Coll Cardiol* 1990;15:91.
22. Lorell BH, et al. Improved diastolic function and systolic performance in hypertrophic cardiomyopathy after nifedipine. *N Engl J Med* 1980;303:801.
23. Lorell BH, et al. Modification of abnormal left ventricular diastolic properties by nifedipine in patients with hypertrophic cardiomyopathy. *Circulation* 1982;64:499.
24. St John Sutton MG, et al. Echocardiographic assessment of left ventricular filling and septal and posterior wall dynamics in idiopathic hypertrophic subaortic stenosis. *Circulation* 1978;57:512.
25. Hanrath P, Mathey DG, Siegert R, Bleifeld W. Left ventricular relaxation and filling pattern in different forms of left ventricular hypertrophy: an echocardiographic study. *Am J Cardiol* 1980;45:15.
26. Stewart S, Mason DT, Braunwald E. Impaired rate of left ventricular filling in IHSS and valvular aortic stenosis. *Circulation* 1968;37:8.
27. Dinsmore RE, Sanders CA, Harthorne JW. Mitral regurgitation in idiopathic hypertrophic subaortic stenosis. *N Engl J Med* 1966;275:1225.
28. Brockenbrough EC, Braunwald E, Morrow AG. A hemodynamic technic for the detection of hypertrophic subaortic stenosis. *Circulation* 1961;23:189.
29. Paulus WJ, et al. Comparison of the effects of nitroprusside and nifedipine on diastolic properties in patients with hypertrophic cardiomyopathy: altered left ventricular loading or improved muscle inactivation? *J Am Coll Cardiol* 1983;2:879.
30. Lorell BH. Use of calcium channel blockers in hypertrophic cardiomyopathy. *Am J Med* 1985;78[Suppl 2B]:43.
31. Bonow RO, et al. Effects of verapamil on left ventricular systolic function and diastolic filling in patients with hypertrophic cardiomyopathy. *Circulation* 1981;64:787.
32. Epstein SE, Rosing DR. Verapamil: its potential for causing serious complications in patients with hypertrophic cardiomyopathy. *Circulation* 1981;64:437.
33. Topol EJ, Traill FA, Fortuin NJ. Hypertensive hypertrophic cardiomyopathy of the elderly. *N Engl J Med* 1985;312:277.
34. Miller W, Walsh RA, McCall D. Eosinophilic heart disease presenting with features suggesting hypertrophic obstructive cardiomyopathy. *Cathet Cardiovasc Diagn* 1987;13:185.
35. Pichard AD, et al. Septal perforation compression (narrowing) in idiopathic hypertrophic subaortic stenosis. *Am J Cardiol* 1977;40:310.
36. Brugada P, et al. “Sawfish” systolic narrowing of the left anterior descending artery: an angiographic sign of hypertrophic cardiomyopathy. *Circulation* 1982;66:800.
37. Sigwart U. Nonsurgical myocardial reduction for hypertrophic obstructive cardiomyopathy. *Lancet* 1995;346:211.
38. Lakkis NM, Nagueh SF, Kleiman NS, et al. Echocardiography-guided ethanol septal reduction for hypertrophic obstructive cardiomyopathy. *Circulation* 1998;98:1750.

33
Profiles in Constrictive Pericarditis, Restrictive Cardiomyopathy, and Cardiac Tamponade

Beverly H. Lorell and William Grossman

BHL: Harvard Medical School, Hemodynamic and Molecular Physiology Research Laboratory and Cardiac Catheterization Laboratory, Beth Israel Deaconess Medical Center, Boston, Massachusetts 02215.
WG: University of California, San Francisco, School of Medicine; Division of Cardiology, University of California, San Francisco Medical Center, San Francisco, California 94143

Pericarditis from any cause can be followed by three hemodynamic complications: a pericardial effusion under pressure, resulting in cardiac tamponade; progressive pericardial fibrosis and thickening, causing constrictive physiology; or a combination of both. A common feature of each is the presence of external compression of the heart, which prevents adequate diastolic filling, elevates right and left heart diastolic pressures, and results ultimately in reduced stroke volume because of inadequate preload. The diastolic filling pattern during each cardiac cycle and the response to respiration differ in constrictive pericarditis and tamponade, so that distinctive hemodynamic profiles usually can be recognized in the Cardiac Catheterization Laboratory. The hemodynamic evaluation also must include consideration of the presence of restrictive cardiomyopathy, in which features of impaired diastolic filling with preserved systolic contractile function may simulate constrictive pericarditis.

CONSTRICTIVE PERICARDITIS

Clinical Features

Constrictive pericarditis is a symmetric process in which scarring of both the parietal and visceral pericardial layers affects all chambers of the heart. Localized constriction, which may produce external stenosis of the mitral and tricuspid valves, is rare (1). In the chronic stage, pericardial calcification may develop, but it may be absent in earlier stages despite severe hemodynamic compromise. Tuberculosis was previously the most important cause of constrictive pericarditis. Today the most common causes of constrictive pericarditis are recurrent idiopathic or viral pericarditis, delayed constriction after mediastinal radiation therapy, and pericarditis after open heart surgery (2,3 and 4). After open heart surgery, large organizing hematomas may cause constrictive physiology. Less common causes include neoplastic pericardial involvement; septic pericarditis, including opportunistic AIDS-related infections; chronic renal failure; and connective-tissue disorders such as rheumatoid arthritis and progressive systemic sclerosis. It is important for cardiologists to appreciate that mediastinal irradiation may cause constrictive pericarditis many years after therapy; in this regard it is not yet known if intracoronary irradiation therapy as an adjunct to coronary stent placement will be associated with late risk of localized pericardial constriction. Regardless of the cause of pericardial injury, some patients with acute pericarditis may develop transient mild pericardial constriction that resolves spontaneously within a few months of the initial illness (5).

The clinical features of constrictive pericarditis reflect the gradual development of systemic and pulmonary venous hypertension, and later reduction of cardiac output. In patients in whom right and left atrial pressures are modestly elevated in the range of 10 to 18 mm Hg, symptoms and signs of systemic venous congestion predominate. These include leg edema, postprandial discomfort, hepatic congestion, and ascites. As right and left heart filling pressures become elevated to a level of 18 to 30 mm Hg, exertional dyspnea and orthopnea appear, and pleural effusions may develop. As stroke volume falls, compensatory increases in systemic resistance and sinus tachycardia develop that initially maintain cardiac output and systemic blood pressure. The impairment of diastolic filling initially impairs the ability to augment cardiac output during exercise, resulting in exertional fatigue. As resting cardiac output falls, severe lethargy and cardiac cachexia supervene. The electrocardiogram usually shows reduced voltage and diffuse ST–T-wave abnormalities that may be mistaken for ischemia due to coronary artery disease. Atrial fibrillation is present in about 10% of patients. The chest roentgenogram may show a small, normal, or modestly enlarged cardiac silhouette with redistribution of pulmonary flow or pleural effusions. The finding of pericardial calcification on the lateral projection is present in about 50% of cases. In summary, constrictive pericarditis should be considered in any patient with unexplained jugular venous distension, systemic edema, and hepatic congestion. It should also be considered in the postoperative heart surgery patient who has unexplained tachycardia, low cardiac output, and venous congestion in the first months after surgery.

Echocardiography and other noninvasive imaging techniques are an essential component of evaluation of patients with suspected constrictive pericarditis. Echocardiographic evaluation strongly suggests the diagnosis if it demonstrates pericardial thickening, dilatation of the superior and inferior vena cavae, diastolic flattening of the posterior ventricular wall, and abrupt cessation of ventricular dimension change in early diastole. Doppler flow velocity studies typically show exaggerated inspiratory increase in tricuspid flow velocity and reduction in mitral flow velocity (>25% inspiratory reduction in mitral flow velocity). Accurate measurement of pericardial thickening can be achieved by transesophageal echocardiography or by computed tomographic or magnetic resonance imaging (MRI) measurements. In adults, the mean normal pericardial thickness is 1.2 ± 0.8 mm (2 SD), and a pericardial thickness of 3 mm or more distinguishes a pathologically thickened from a normal pericardium (6). The finding of a pathologic increase in pericardial thickening supports the diagnosis but does not demonstrate that the constrictive physiology is present; conversely, hemodynamically significant constriction can be present with a minimally thickened pericardium.

In addition to noninvasive imaging, right and left heart catheterization and angiography should be performed in every patient with this potentially curable disease to (a) confirm the presence of constrictive physiology and assess its severity before consideration of pericardiectomy; (b) assist in differentiating pericardial disease from restrictive cardiomyopathy; (c) exclude major coexisting causes of right atrial hypertension, such as severe pulmonary hypertension; and (d) exclude rare instances of localized constriction causing external valvular constriction or pinching of the epicardial coronary arteries.

Hemodynamic and Angiographic Profile

Both pericardial constriction and cardiac tamponade increase *ventricular interdependence*, in which filling of one ventricle limits simultaneous filling of the other, which is mediated by both the mechanical constraint of the pericardium and the shared interventricular septum. A key contemporary model characterizes the nature of pericardial constraint in cardiac tamponade as “coupled” constraint exerted by uniform liquid pressure on the heart, versus “uncoupled” constraint exerted by regional surface pressure in pericardial constriction (7). Coupled constraint (tamponade) produces greater gains in ventricular interdependence than constriction, so that increased inspiratory filling of the right ventricle results in highly coupled reduction in filling of the left ventricle and the occurrence of pulsus paradoxus, whereas uncoupled constraint (constriction) has a more modest effect on ventricular interdependence but greatly modifies the effective elastance of the thin-walled right ventricle, increasing the occurrence of Kussmaul's sign (7). This provides a framework for understanding the steady-state and respiratory-related events that are

detected by complementary echo-Doppler and hemodynamic evaluations in constrictive pericarditis and cardiac tamponade.

In constrictive pericarditis, both right and left heart catheterization should be performed, and right and left ventricular pressures should be measured simultaneously at equisensitive gains with meticulous attention to calibration and elimination of waveform damping. The symmetric surface pressure of the constricting pericardium usually impairs diastolic filling and “entrains” diastolic pressures of all chambers of the heart. Right and left ventricular diastolic pressures are *elevated* and usually equal within 5 mm Hg or less. Although right and left *ventricular* diastolic pressures are equal, right and left atrial (pulmonary capillary wedge) pressures may differ if coexisting mitral or tricuspid regurgitation is present associated with a large *a* or *v* wave in either atrium. Because the strength of atrial contraction may differ, right and left ventricular diastolic pressures may also differ at end-diastole during the *a* wave. Hypovolemia may lower these pressures, and it is important to avoid excessive diuresis before catheterization. In the hypovolemic patient, a rapid volume challenge of 1,000 mL normal saline solution may be useful to unmask the hemodynamics of constrictive pericarditis. However, in the absence of characteristic symptoms and signs of constrictive pericarditis, including characteristic noninvasive echo-Doppler findings, we have found that performance of a volume challenge to detect “occult” pericardial constriction is not valuable.

Pulmonary artery and right ventricular systolic pressures are usually between 35 and 45 mm Hg. Pulmonary artery systolic pressure may be low (reflecting reduced right ventricular stroke volume and pulse pressure) or mildly elevated if chronic left atrial hypertension has caused a secondary increase in pulmonary vascular resistance. Severe pulmonary hypertension is not a feature of constrictive pericarditis and is indicative of coexisting heart or pulmonary disease.

In constrictive pericarditis, in which the heart is encased in a rigid and adherent fibrotic shell, the end-systolic volume of the heart is usually less than that defined by the rigid pericardium. Therefore in the setting of elevated atrial pressures, early diastolic filling of the ventricles is unimpeded and abnormally rapid, but early diastolic filling is abbreviated and halts abruptly when total cardiac volume expands to the volume set by the stiff pericardium. The physical finding of a *pericardial knock* is the loud acoustic marker of the abrupt cessation of early diastolic filling (8) and corresponds to the peak of the *e* wave of Doppler atrioventricular valve flow velocity signals. In constrictive pericarditis, virtually all ventricular filling occurs in early diastole, which is reflected in the early diastolic dip-and-plateau pattern in the right and left ventricular waveforms. The right atrial waveform typically shows a prominent and rapid diastolic *y* descent, which indicates that right atrial emptying after tricuspid valve opening is rapid and initially unimpeded. (As discussed later, this pattern differs from cardiac tamponade in which the diastolic *y* descent is blunted or absent.) The diastolic *y* descent is followed by a steep *a* wave and systolic *x* descent because the atrium is attempting to eject blood into a right ventricle that is already filled to capacity. The steep *x* and *y* descents impart to the right atrial pressure waveform its characteristic M or W configuration (Fig. 33.1). This characteristic waveform is also present in the left atrial pressure tracing but may be obscured in the pulmonary capillary wedge pressure waveform. The presence of tachycardia partially obscures these atrial and ventricular pressure waveforms, and underdamping of the ventricular pressure transducer system may confuse recognition of diastolic equilibration of pressures (Fig. 33.2).

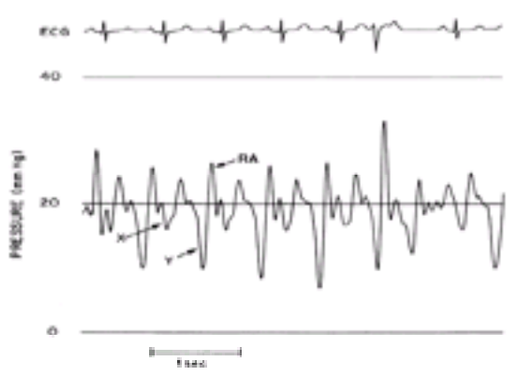

FIG. 33.1. Right atrial (RA) pressure recording from a patient with constrictive pericarditis. Note the prominent *y* descent in the right atrial waveform, which indicates that the right atrial emptying is rapid and unimpeded in early diastole. The nadir of the *y* descent corresponds with the abrupt cessation of early diastolic ventricular filling. The prominent *x* and *y* descents give the right atrial waveform its characteristic M- or W-shaped appearance in constrictive pericarditis. The mean value of the right atrial pressure is more than twice normal, at 18 to 20 mm Hg.

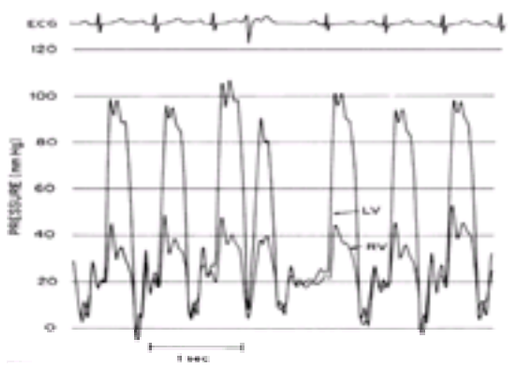

FIG. 33.2. Left ventricular (LV) and right ventricular (RV) pressures recorded simultaneously in the patient with constrictive pericarditis shown in Fig. 33.1 illustrate technical pitfalls in evaluation of pressure tracings. The resence of resting tachycardia partially obscures evaluation of the diastolic waveforms, and underdamping of the left ventricular pressure-transducer system accentuates an undershoot of left ventricular pressure in early diastole and an overshoot during atrial contraction. A long diastole following a premature beat permits the recognition of equilibration of left and right ventricular diastolic pressures and the appreciation of a dip-and-plateau configuration of the ventricular waveforms.

Examination of respiratory fluctuations in hemodynamics is an important component of the cardiac catheterization. In severe pericardial constriction, negative intrathoracic pressure during inspiration is not communicated to the intrapericardial space and the right heart. This contrasts with both normal subjects and patients with cardiac tamponade who demonstrate a fall in systemic venous and right atrial pressures during inspiration. As illustrated in Fig. 33.3, in extreme cases systemic venous pressure increases during inspiration (Kussmaul's sign) (9). The occurrence of pulsus paradoxus in constrictive pericarditis is variable and sometimes absent, and depends on the presence of inspiratory variation of right and left ventricular filling and the magnitude of ventricular interdependence. This contrasts with cardiac tamponade, in which severely exaggerated inspiratory filling of the right ventricle occurs at the expense of left ventricular filling, and pulsus paradoxus is a striking hemodynamic finding in almost all patients. In constrictive pericarditis, the magnitude of dynamic respiratory changes of increased ventricular interdependence, when present, can be appreciated during meticulous simultaneous measurement of right and left ventricular pressures. Using micromanometer pressure measurements, Hurrell et al. (10) reported that *discordance of right and left ventricular pressures during respiration is an indicator of increased ventricular interdependence in constrictive pericarditis*. As illustrated in Fig. 33.4, the inspiratory augmentation of right ventricular systolic pressure simultaneous with a fall in left ventricular systolic pressure distinguished patients with surgically proven constrictive pericarditis from patients with other causes of heart failure. These findings are attributed to an inspiratory fall in intrathoracic and pulmonary venous pressures that results in a reduction of left heart filling and stroke volume that is accompanied by an increase in right heart filling and stroke volume. In patients with these findings, some degree of pulsus paradoxus should also be present.

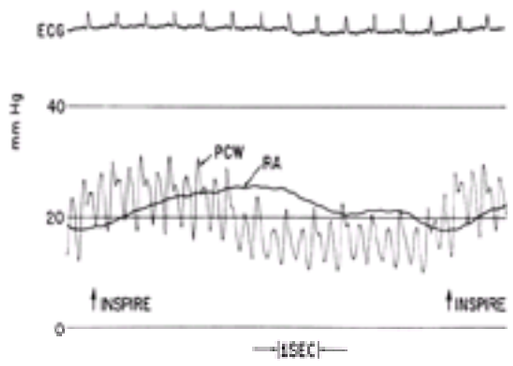

FIG. 33.3. Right atrial (mean, RA) and pulmonary capillary wedge (phasic, PCW) pressure tracings from a patient with constrictive pericarditis. An *arrow* marks the beginning of the inspiratory phase of each respiratory cycle. Note that the mean right atrial pressure increases during inspiration (Kussmaul's sign). The pulmonary capillary wedge pressure is out of phase with right atrial pressure and begins to fall during inspiration as right atrial pressure is rising.

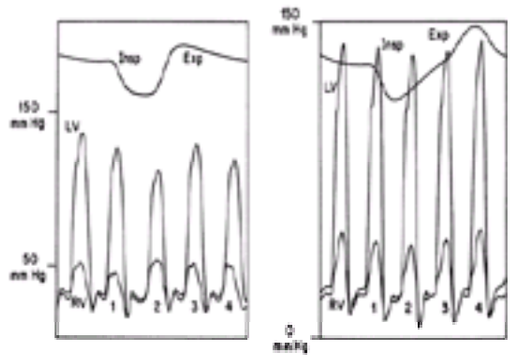

FIG. 33.4. Respiratory changes in left ventricular (LV) and right ventricular (RV) pressures measured with micromanometer catheters in a patient with constrictive pericarditis (left panel) and in a patient with restrictive cardiomyopathy (right panel). Peak inspiration is indicated in beat 2 in each cardiac cycle. In the patient with constrictive pericarditis (left panel), there is a discordant change in left and right ventricular systolic pressures during respiration: Left ventricular systolic pressure falls to its minimum value during peak inspiration simultaneous with an increase in right ventricular systolic pressure to its highest value in the cardiac cycle. These findings indicate the presence of ventricular interdependence caused by the constricting pericardium and suggest that as left ventricular filling and stroke volume decreases, there is a corresponding increase in right ventricular filling and stroke volume. In contrast, in the patient with restrictive cardiomyopathy (right panel), there are concordant changes in left and right ventricular pressures during respiration. (Adapted from Hurrell DG, Nishimura RA, Higano ST, et al. Value of dynamic respiratory changes in left and right ventricular pressures for the diagnosis of constrictive pericarditis. *Circulation* 1996;93:2007.)

Stroke volume is almost always reduced in patients with constrictive pericarditis, but resting cardiac output may be preserved because of tachycardia. Studies of atrial pacing in patients with constrictive pericarditis showed that increases in heart rate up to about 140 beats per minute increased cardiac output in the presence of unchanged stroke volume and ventricular filling pressure (11). After pericardiectomy, when ventricular filling was no longer confined to early diastole, atrial pacing caused a normal pattern of impairment of cardiac output at higher heart rates. Dynamic exercise usually causes only a slight rise in cardiac filling pressures since diastolic volume is relatively fixed, but cardiac output fails to increase appropriately relative to the increase in systemic oxygen consumption. In these patients, enhanced oxygen demand is met almost entirely by increased oxygen extraction and widening of the arteriovenous oxygen differences. In advanced constrictive pericarditis, resting cardiac index is depressed in association with systemic arterial vasoconstriction and arterial hypotension. In patients with constrictive pericarditis, the depression of stroke volume is predominantly related to reduced diastolic filling rather than to the depression of myocardial contractile function. In the absence of extensive coexisting myocardial fibrosis, left ventricular ejection fraction is usually normal or increased, and both isovolumic and ejection phase indices of contractile function (e.g., peak *dP*/*dt*) are preserved (10,12). The important exception to this is patients with extensive coexisting myocardial fibrosis, which is a complication of radiation-induced pericardial constriction, or with infiltrative processes such as amyloid that may involve both the pericardium and the myocardium (13). Left ventriculography may not be required during cardiac catheterization if a current high-quality imaging study (echocardiography, gated computed tomography, or MRI) has defined global and regional left ventricular ejection fraction and volumes, and excluded significant coexisting valvular heart disease.

Coronary angiography should be performed as part of the cardiac catheterization evaluation of constrictive pericarditis. In addition to defining significant occult atherosclerotic coronary artery disease, the angiogram can detect the rare problem of external pinching or compression of the coronary arteries by the constricting pericardium prior to pericardiectomy (14). Recent studies indicate that pericardial constriction limits coronary flow reserve measured by adenosine-induced hyperemia, and causes abrupt cessation and rapid deceleration of the normal pattern of early diastolic flow velocity (15).

Fibroelastic Pericardial Constriction: The Contemporary Presentation

The hemodynamic and angiographic findings may differ in patients with subacute noncalcific pericarditis, in whom the pericardium is characterized by an adherent fluid-fibrin layer in the process of organization rather than by a rigid, scarred shell. In the classic paper defining this clinical entity, Hancock (16) compared this relatively *elastic form of constrictive pericarditis* with encircling the heart tightly with rubber bands. In this fibroelastic form of pericardial disease, cardiac compression is present throughout the cardiac cycle, and the pattern of ventricular filling and the pressure waveforms are more like those of cardiac tamponade. In terms of contemporary conceptual framework, it is likely that this results in a highly “coupled” pericardial constraint in which ventricular interdependence is increased. In this setting, inspiratory reduction in left heart filling and stroke volume resulting from the effects of negative intrathoracic pressure on the pulmonary veins is accompanied by augmented right ventricular filling and stroke volume. In comparison with earlier studies of classic constrictive pericarditis in which the pericardium was composed of a rigid calcified shell, we speculate that many contemporary studies of patients with constrictive pericarditis, in whom respiratory cardiac filling patterns share features of cardiac tamponade, are comprised of patients with the fibroelastic form of constrictive pericarditis.

Intervention

The definitive treatment of constrictive pericarditis is pericardiectomy. Constrictive pericarditis in symptomatic patients, in whom there are typical noninvasive imaging findings, including a thickened pericardium as well as characteristic hemodynamic findings described earlier, should be managed by an experienced cardiovascular surgical team with complete visceral and parietal pericardiectomy with the ability to mobilize the heart via cardiopulmonary bypass. In contemporary practice, in which the operation is performed early in the disease before development of end-stage depression of rest cardiac output and poor organ perfusion, outcome is excellent. For example, a surgical series of 21 patients from a major tertiary center reported no perioperative mortality, mean postoperative hospital stay of 7 days, and return to functional New York Heart Association (NYHA) class I in all patients (17). However, Mayo Clinic studies of 58 patients showed that abnormalities of diastolic filling detected by Doppler mitral flow velocity signals were present in about 40% of patients after pericardiectomy (18). Increases in myocardial collagen content, changes in the proportion of types I and III collagen, and alterations in collagen network architecture occur in patients with constrictive pericarditis cause by prior irradiation and other forms of pericardial disease (19). In patients with constrictive pericarditis, changes in both myocardial collagen content and the thickness of fibrous trabeculae appear to contribute to depression of ejection fraction and persistent diastolic dysfunction after pericardiectomy (19). Because alteration in collagen architecture predominantly involves the epicardial myocardium, endocardial myocardial biopsy may not detect these changes.

RESTRICTIVE CARDIOMYOPATHY

Clinical Features

The differentiation between constrictive pericarditis and restrictive cardiomyopathy is often difficult. In restrictive cardiomyopathy, the restrictive element resides in the

myocardium itself so that the ventricular walls resist and stretch abnormally during cardiac filling. Therefore, the clinical features of restrictive cardiomyopathy caused by idiopathic etiology, radiation-induced fibrosis, metabolic storage diseases, hemochromatosis, and cardiac amyloidosis are often similar to those of constrictive pericarditis (20). In both disorders, ventricular diastolic filling is impaired and diastolic pressures are elevated, resulting in symptoms of congestive heart failure. Stroke volume is fixed or reduced in both conditions, resulting in fatigue and poor exercise tolerance, and systolic contractile function is essentially normal. In both disorders, patients may complain of chest and neck discomfort during exertion, which may be related to impaired coronary reserve and/or neck vein distension. In both disorders, the electrocardiogram commonly shows abnormal low voltage, ST–T-wave abnormalities, and atrial fibrillation may occur.

Hemodynamic and Angiographic Profile

Noninvasive imaging helps to discriminate findings indicative of constrictive pericarditis rather than restrictive cardiomyopathy. Documentation of pericardial thickening, obtained by transesophageal echocardiography or gated computed tomography, supports a diagnosis of constrictive pericarditis. Findings suggestive of *ventricular interdependence*, including exaggerated and opposite respiratory fluctuations in simultaneous tricuspid and mitral valve flow velocity signals, are usually more prominent in constrictive pericarditis than in restrictive cardiomyopathy. As described earlier, the “restrictive” pattern of the Doppler mitral flow velocity signal, which is characterized by a steep early diastolic *e* wave, abbreviation of early diastolic transmitral flow, and rapid *e* wave deceleration with reduced *a* wave, can be observed in both disorders. The echocardiographic findings of a “sparkling” appearance of the myocardium and the presence of thickened ventricular walls with reduced electrocardiographic R-wave voltage suggest the presence of an infiltrative process such as amyloid, but their absence does not exclude the presence of restrictive cardiomyopathy resulting from amyloid or other etiologies.

In most cases, careful attention to hemodynamics does permit identification of the patient whose symptoms of congestive failure are due to restrictive cardiomyopathy. Right and left ventricular diastolic pressures should be recorded simultaneously at equisensitive gains. Left ventricular diastolic pressure is usually higher than right ventricular diastolic pressure, and supine exercise usually causes elevation of left greater than right ventricular diastolic pressures. In constrictive pericarditis, left and right ventricular diastolic pressures are elevated and equal at baseline with minimal change during supine dynamic exercise because ventricular volumes are fixed. Pulmonary hypertension is usually more severe in restrictive cardiomyopathy than in constrictive pericarditis, and pulmonary systolic pressures in excess of 45 to 50 mm Hg are common. Isovolumic and ejection phase indices, including ejection fraction, are usually normal or mildly impaired. For example, in a reported series of nine symptomatic patients with restrictive cardiomyopathy (20), left ventricular ejection fraction was 63 ± 8%, left ventricular diastolic pressure (23 ± 6 mm Hg) was higher than right ventricular diastolic pressure (16 ± 5 mm Hg), and pulmonary artery systolic pressure was elevated (49 ± 21 mm Hg). However, in cohorts of patients with constrictive pericarditis versus restrictive cardiomyopathy, there is frequently overlap between individuals in each group (10). As illustrated in Fig. 33.4, Hurrell and coworkers observed that constrictive pericarditis is usually characterized by increased ventricular interaction such that right ventricular systolic pressure reaches its maximum value during inspiration simultaneous with a fall in left ventricular systolic pressure. In contrast, inspiration is usually accompanied by a concordant inspiratory fall in both left and right ventricular systolic pressures in restrictive and other cardiomyopathies (10). These promising observations need to be corroborated by prospective comparative studies.

In some but not all patients with restrictive cardiomyopathy, the diastolic filling pattern differs from that of constrictive pericarditis. Using either frame-by-frame angiographic or radionuclide analysis of ventricular filling, one pattern in restrictive cardiomyopathy is a very slow early diastolic filling rate compared with normal. This sluggish “molasses-like” pattern of early diastolic filling sharply contrasts with the explosively rapid but abbreviated early diastolic filling pattern in constrictive pericarditis (21,22). However, other patients with restrictive cardiomyopathy exhibit an excessively rapid and abbreviated early diastolic filling pattern similar to constrictive pericarditis. In such patients, a dip-and-plateau ventricular pressure waveform itself suggests that early diastolic filling is excessively rapid and abruptly attenuated. Although extensive cross-correlation observations describing simultaneous ventricular hemodynamic measurements and Doppler flow velocity measurements in restrictive cardiomyopathy are lacking, it is likely that the “restrictive” Doppler mitral flow velocity pattern (23) of steep early diastolic *e* wave and abbreviation of early diastolic transmitral flow is accompanied by a dip-and-plateau pattern in the ventricular pressure waveforms in patients with restrictive cardiomyopathy. It is important to realize that insights from noninvasive studies have shown that this “restrictive” pattern of atrioventricular valve inflow and diastolic filling is *not* specific for restrictive cardiomyopathy. It can be observed in other forms of cardiomyopathy besides restrictive cardiomyopathy in the setting of high left atrial pressure and can be modified or abolished by reduction in preload (23,24). Thus the diagnosis of restrictive cardiomyopathy requires careful clinical judgment and integration of both noninvasive imaging data and hemodynamic analyses.

Endomyocardial Biopsy

Although endomyocardial biopsy is not routinely indicated in the evaluation of patients with dilated cardiomyopathy, we believe that it plays an important role in the evaluation of the symptomatic patient with restrictive cardiomyopathy. Endomyocardial biopsy is also an adjunctive diagnostic tool in confusing situations where discrimination of constrictive pericarditis versus restrictive cardiomyopathy is needed or where the disease process may involve both tissues, such as cardiac amyloidosis. Myocardial biopsy is valuable in making a definitive diagnosis in patients with restrictive cardiomyopathy due to amyloid and other specific causes (myocarditis, metabolic storage disease, hemachromatosis) (25). In patients with cardiac irradiation injury in which both pericardium and myocardium may be involved, the documentation of extensive myocardial fibrosis and myocyte dropout should be included in the decision to proceed to surgical pericardiectomy. As discussed earlier, constrictive pericarditis of multiple etiologies is often accompanied by changes in collagen deposition and architecture involving predominantly the epicardial myocardium, and a “normal” endomyocardial biopsy does not exclude this remodeling.

OTHER CONDITIONS ASSOCIATED WITH CONSTRICTIVE PHYSIOLOGY

The normal pericardium restrains cardiac dilatation and couples the function of both ventricles in conditions in which the pericardium has not grown or stretched to accommodate an increase in cardiac volume. In the presence of normal cardiac volumes and low filling pressures, cardiac volumes dynamically fluctuate during respiration and changes in posture within the loose, lubricated pericardial sac with minimal pericardial constraint and ventricular interaction. However, as right ventricular volume increases to a level associated with a diastolic pressure of about 10 to 12 mm Hg, pericardial constraint appears and ventricular interdependence (coupling) increases strikingly. Ventricular interdependence can be recognized when increments in ventricular diastolic pressure cause a similar gain in diastolic pressure of the opposite ventricle and when respiratory filling of one ventricle causes marked reduction of filling of the opposite chamber. This phenomenon has recently been shown to be important in dilated cardiomyopathy, in which reductions in elevated right heart filling result in the augmentation of left ventricular filling via ventricular interaction (24).

Pericardial constraint is also important during acute and severe right ventricular infarction with secondary right ventricular dilatation. Acute right ventricular infarction in humans (26) and experimental animal models may cause constrictive physiology with elevation and equilibration of right and left ventricular pressures, a dip-and-plateau ventricular waveform, and reduced right ventricular pulse pressure. Volume overload due to subacute tricuspid regurgitation with an intact pericardium can also cause increased pericardial constraint and ventricular interaction, as illustrated in Fig. 33.5. In a classic paper, Bartle and Hermann (27) reported that acute and subacute mitral regurgitation can cause a striking hemodynamic pattern suggestive of pericardial constriction. In this condition, pulmonary hypertension is an obligatory part of the hemodynamic pattern. Acute pulmonary embolism, with secondary right ventricular dilatation and moderate pulmonary hypertension in the setting of a nonhypertrophied right ventricle, can also cause constrictive physiology due to pericardial constraint.

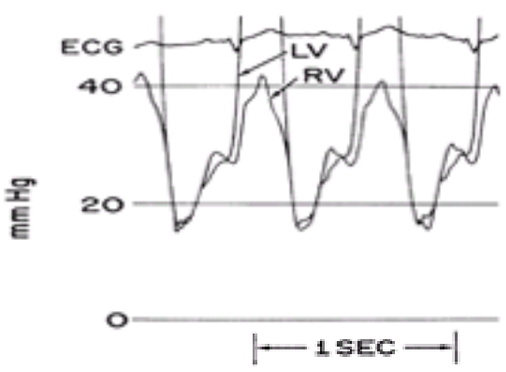

FIG. 33.5. Simultaneous right ventricular (RV) and left ventricular (LV) pressure tracings recorded in a patient with several-week history of severe tricuspid insufficiency. Note that right and left ventricular end-diastolic pressures are markedly elevated (approximately 28 mm Hg) with virtual identity of pressures throughout diastole. Right ventricular systolic pressure is minimally increased, an indication that the elevation of right ventricular diastolic pressure is not caused primarily by pulmonary hypertension. These findings suggest a restraining effect of the intact normal pericardium with increased ventricular interdependence in the presence of

subacute volume overload of the right ventricle.

CARDIAC TAMPONADE

Clinical Features

The development of an increase in intrapericardial pressure and the restriction of cardiac filling depends on (a) the rate of fluid accumulation, (b) the volume of fluid, (c) the distensibility of the pericardium, and (d) the underlying distensibility of the cardiac chambers. The normal unstretched pericardium usually contains less than 50 mL of fluid and can accommodate respiratory and postural changes in cardiac volume with little change in the intrapericardial pressure and minimal coupling of ventricular function. Studies using special flat balloon catheters suggest that *constraint pressure* exerted by the normal pericardium is nearly equal to right atrial pressure, whereas normal intrapericardial pressure measured by a standard fluid-filled open-end catheter is zero or negative relative to atmosphere, and virtually equal to intrathoracic pressure. This controversy does not detract from the utility of using fluid-filled catheters in patients undergoing pericardiocentesis, since intrapericardial pressure can be measured accurately by either method once more than about 50 mL fluid is present (28).

The rapid accumulation of more than about 150 mL of pericardial fluid results in a steep rise in intrapericardial pressure, which equilibrates with right atrial pressure such that both pressures then rise together. The classic echocardiographic finding of partial collapse of the right atrial and right ventricular free walls in patients with cardiac tamponade is a marker of this equilibration of pressures during part of each cardiac cycle, and loss of normal transmural distending pressure that mediates right heart filling during diastole. Further increases in intrapericardial volume cause equilibration of pericardial and right heart filling pressures with left atrial and left ventricular diastolic pressures. In patients with coexisting left ventricular disease that has caused basal elevation of left heart filling pressures, cardiac tamponade with impaired right heart filling and reduction in stroke volume occurs *before* pericardial pressure equilibrates with left-sided filling pressures. For this reason, diagnosis of cardiac tamponade cannot be made by isolated bedside right heart catheterization and examination of mean right atrial and pulmonary capillary wedge pressures. Cardiac output and blood pressure are maintained initially by the compensatory mechanisms of sympathetically mediated vasoconstriction and tachycardia, a period sometimes labeled as “compensated cardiac tamponade.” As impairment of filling becomes more severe, hypotension and shock ensue and are often accompanied by profound vagally mediated bradycardia and loss of baroreceptor-mediated vasomotor control.

Patients with acute intrapericardial hemorrhage due to cardiac trauma manifest the classic clinical triad described by Beck (29): (a) elevation of systemic venous pressure, (b) severe arterial hypotension, and (c) small quiet heart. In contemporary medical patients, the most common etiologies of pericardial tamponade are idiopathic (viral) pericarditis, malignant involvement of the pericardium, irradiation-induced injury, collagen-vascular disease, uremia, hypothyroidism, anticoagulant-induced hemorrhage, and infection (including AIDS-related tuberculosis and other opportunistic infections) (30,31 and 32). In patients with subacute or chronic pericardial inflammation and fluid accumulation, the pericardium may accumulate large volumes of fluid (500 mL to more than 1 L) before tamponade develops. In patients with dehydration, “low-pressure tamponade” can develop when intrapericardial pressure rises slightly and equilibrates with an abnormally low right atrial pressure (33).

The most common symptoms include dyspnea or air hunger during exertion, restlessness, and fatigue; in addition, peripheral edema and gastrointestinal symptoms may develop, including abdominal fullness due to hepatomegaly or ascites, early satiety, and weight loss. In medical patients with subacute development of tamponade, physical findings usually include jugular venous distension (which is commonly missed unless carefully sought), moderate tachycardia, mild tachypnea, and pulsus paradoxus if sinus rhythm is present. Pulmonary rales, indicative of severe pulmonary congestion, are rare. Frank hypotension is usually absent, and elevated arterial blood pressure may be present in patients with prior systemic hypertension; this elevated arterial blood pressure may fall to normal after pericardiocentesis (34). Hypoxemia is *not* a feature of cardiac tamponade; if found, it suggests a coexisting pulmonary process such as large pleural effusion or pulmonary microvascular spread of tumor. The electrocardiogram may show only sinus tachycardia; in severe cardiac tamponade, low voltage as well as electrical alternans of the QRS complex may be indicative of periodic pendular swinging of the heart within the pericardium. The chest roentgenogram typically shows an enlarged, flask-shaped cardiac silhouette; although small pleural effusions may be present, overt infiltrates of pulmonary edema are rare.

Two-dimensional echocardiography is an essential aid in all patients with suspected cardiac tamponade. Characteristic findings include an echo-free space around the heart, partial invagination of the right atrial and right ventricular free walls, enhanced inspiratory right ventricular filling with reduction in left ventricular filling, and plethora of the vena cavae. If the echocardiographic study is technically inadequate or if regional tamponade is suspected, additional computed tomographic or gated MRI studies should be obtained.

Tamponade Complicating Catheter-Based Procedures

In the Cardiac Catheterization Laboratory, all operators should know and recognize the signs that indicate development of acute hemorrhagic tamponade due to cardiac perforation (35,36). Although it occurs rarely during diagnostic catheterization, cardiac tamponade is a known hazard of mitral and aortic valvuloplasty, invasive electrophysiologic intervention procedures, and angioplasty-based interventional procedures complicated by overt coronary perforation. It can also occur shortly after the procedure following technically uneventful interventions, including rotational atherectomy, directional coronary atherectomy, and stenting.

In a recent series of 960 consecutive pericardiocenteses performed at the Mayo Clinic (37), 9.6% were performed for cardiac perforation complicating catheter-based procedures. Utilizing echocardiographically guided pericardiocentesis, tamponade was relieved in 99% and further pericardial drainage was required in only 18% (37).

Hemodynamic Profile

Although both cardiac tamponade and constrictive pericarditis cause the elevation and equalization of intracardiac filling pressures, there are several important differences. First, cardiac tamponade causes continuous compression of the heart throughout the cardiac cycle. The ventricles are compressed at end-systole and early diastole. This prevents rapid atrial emptying and rapid ventricular filling in early diastole, in contrast with constrictive pericarditis in which early diastolic ventricular filling is explosively rapid and abruptly abbreviated. For this reason, the right atrial waveform shows attenuation or loss of the diastolic *y* descent, as illustrated in Fig. 33.6. The right ventricular waveform shows elevation of diastolic pressure throughout diastole and the absence of the dip-and-plateau pattern seen in cardiac tamponade. Because stroke volume is depressed, right ventricular pulse pressure is reduced, and right ventricular and pulmonary artery systolic pressures are normal or reduced.

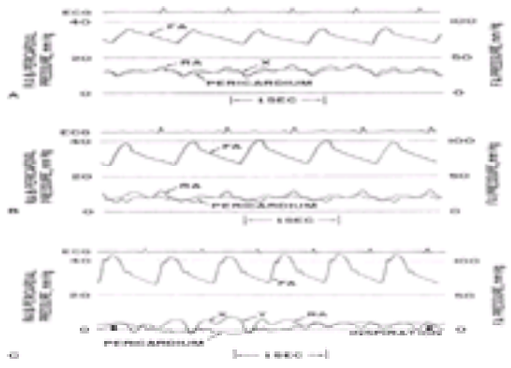

FIG. 33.6. Simultaneous right atrial (RA) and intrapericardial pressure (scale 0 to 40 mm Hg) and femoral artery (FA) pressure (scale 0 to 100 mm Hg) recorded in a patient with cardiac tamponade. **A:** Recordings before pericardiocentesis show the presence of systemic hypotension and the elevation and equalization of the right atrial and intrapericardial pressures. Note that a systolic *x* descent is present, but the diastolic *y* descent is absent, suggesting that right atrial emptying in early diastole is impeded because of cardiac compression by the pericardial effusion. **B:** After aspiration of 100 mL of pericardial fluid, right atrial and intrapericardial pressures have fallen and are beginning to separate, and systolic arterial hypertension has improved compared with baseline. **C:** After aspiration of a total of about 300 mL of pericardial fluid, tamponade physiology is relieved, as evidenced by (a) restoration of intrapericardial pressure to zero, (b) restoration of right atrial pressure to a normal level, and (c) reappearance of the diastolic *y* descent in the right atrial waveform, indicative of the relief of cardiac compression in early diastole. Note the negative fluctuation in intrapericardial pressure during inspiration, accompanied by an increased steepness in the fall of right atrial pressure during the *x* and

y descents. Although this degree of fluid aspiration completely relieved tamponade physiology, an additional 1,500 mL of fluid was removed from the pericardial space.

Second, *negative inspiratory pressure is communicated to both the fluid-filled pericardial space and the intracardiac chambers, in contrast with pericardial constriction.* This results in two major hemodynamic hallmarks of tamponade: (a) *Kussmaul's sign* is not a feature of cardiac tamponade. Even though pericardial and right atrial pressures are elevated, both fall during inspiration. (b) *Pulsus paradoxus* describes an inspiratory fall in arterial systolic pressure and pulse pressure of more than 15 to 20 mm Hg, which is an exaggeration of the normal slight inspiratory fall in arterial systolic pressure of less than 10 mm Hg. In its most formal use, the term *pulsus paradoxus* describes the truly paradoxical transient loss of a palpable arterial pulse during inspiration in each cardiac cycle. *Pulsus paradoxus is a striking feature of cardiac tamponade, if sinus rhythm is present*. In the presence of "coupled" constraint on the heart exerted by pressurized fluid, ventricular interdependence is increased. In cardiac tamponade, the normal pattern of increased inspiratory filling of the right ventricle with bowing of the septum and reduced filling of the left ventricle is exaggerated, resulting in marked inspiratory filling of the right ventricle and augmentation of right ventricular stroke volume at the expense of reduced left ventricular filling and stroke volume. Classic experimental studies of cardiac tamponade in dogs by Shabetai and coworkers (38) showed unequivocally that the predominant mechanism is inspiratory expansion of right heart volume at the expense of left heart volume in the heart compressed by fluid. Other mechanisms that contribute to the inspiratory fall in arterial systolic pressure include operation of the underfilled left ventricle on the steep ascending limb of the Starling curve so that any inspiratory fall in volume elicits a large fall in stroke volume, and loss of the septal contractile contribution to left ventricular work when inspiratory bowing and deformation of the septum occur (39).

These important effects of respiration on highly coupled ventricular filling that cause pulsus paradoxus may be absent in atrial fibrillation and during severe hypotension. Pulsus paradoxus will not be present in patients with atrial septal defect and cardiac tamponade, in which the intracardiac shunt modifies filling of the ventricles and respiratory variations in filling are absent (40). Pulsus paradoxus may also be absent when respiratory changes in ventricular filling are modified by conditions such as aortic regurgitation due to aortic dissection or severe pulmonary hypertension, and when tamponade is due to localized compression by blood or thrombus.

Combined Cardiac Catheterization and Pericardiocentesis

For nearly two decades, we have employed a combined procedure of cardiac catheterization and catheter pericardiocentesis. We have reported use of this technique in two separate consecutive series of symptomatic patients with cardiac tamponade and demonstrated that this approach successfully relieves tamponade in 99% of patients with no major complications (31,41). A recent series of 51 patients managed with catheter pericardiocentesis at another institution also demonstrated that this approach successfully relieved tamponade in 96% of cases with no major complications, and 80% of patients required no further treatment (42). We recommend this approach because (a) it is the only reliable way to determine the hemodynamic significance of a pericardial effusion, (b) it permits very complete and rapid drainage of nonloculated pericardial fluid, (c) it allows assessment of adequacy or inadequacy of relief of tamponade physiology, (d) it excludes coexisting causes of right atrial hypertension that may be present in as many as 40% of medical patients with tamponade (43), and (e) hemodynamic monitoring and fluoroscopic guidance enhance the safety of the procedure.

At our centers, a *two-dimensional echocardiogram is always obtained the day of the procedure*, even if prior studies have been done, to document the presence and size of the effusion and to exclude the presence of loculated and/or posterior localization of effusion or significant stranding suggesting rapid organization. The safety and success of percutaneous pericardiocentesis are related to size of the effusion, and our experience has confirmed the observation that the procedure is likely to be uncomplicated if both anterior and posterior echo-free spaces are at least 10 mm). In addition, we believe that pericardiocentesis usually should not be performed in minimally symptomatic patients with incidental effusions in whom echocardiographic evidence of hemodynamic compromise is absent. Although some groups routinely and successfully utilize echocardiographically guided pericardiocentesis for all procedures (37), we have not found it necessary and reserve echocardiographically guided pericardiocentesis for small or regional effusions. In patients who are anticoagulated with warfarin, pericardiocentesis should be deferred until the INR is within normal range. If pericardiocentesis must be done urgently in the anticoagulated patient with elevated INR, fresh-frozen plasma should be administered in the catheterization suite immediately after catheter access to the pericardium is achieved by an expert operator, and drainage is initiated to avoid conversion of a free hemorrhagic effusion into mixture of fluid and gelatinous clot.

The combined procedure of cardiac catheterization and percutaneous catheter pericardiocentesis is performed in the Cardiac Catheterization Laboratory with hemodynamic and fluoroscopic monitoring. The pressure transducers used to measure arterial pressure, right heart pressure, and pericardial pressure are prepared to avoid underdamping and ensure equisensitive pressure measurements (see Chapter 7). First, systemic arterial pressure is recorded with a small radial artery cannula or 5F sheath with sidearm in the femoral artery, and displayed throughout the procedure for continuous monitoring of blood pressure and heart rate. Right heart catheterization is then performed with a balloon-tipped flow-directed catheter via the right femoral vein: phasic and mean pressures in the right atrium, right ventricle, pulmonary artery, and pulmonary capillary wedge position are recorded. Arterial and mixed venous (pulmonary artery) oxygen saturations are measured for estimation of cardiac output. Left heart catheterization is not routinely performed. The right heart catheter tip is then positioned in the right atrium. The *patient is then propped up to a level of about 45° using a bolster or other mechanism* , and the zero reference height of the transducers is quickly readjusted to the level of the heart. These procedures usually require less than 5 to 8 minutes.

For pericardiocentesis and pericardial pressure measurement, the transducer used to record intrapericardial pressure is connected by a short piece of fluid-filled tubing to the side of a three-way stopcock (Fig. 33.7). (We find it convenient and quick to simply use the standard manifold-transducer system that is routinely used for left heart catheterization and coronary angiography.) The male end of the stopcock is attached to a long (8-inch), thin-walled hollow-pointed pericardiocentesis needle. We currently use the 18-gauge hollow needle with 30° bevel supplied in a standard, commercially available pericardiocentesis kit. The needle with its stopcock is then attached to a handheld syringe labeled and filled with 1% or 2% lidocaine. The metal needle hub can be attached via sterile connector to the V lead of the physiologic recorder.

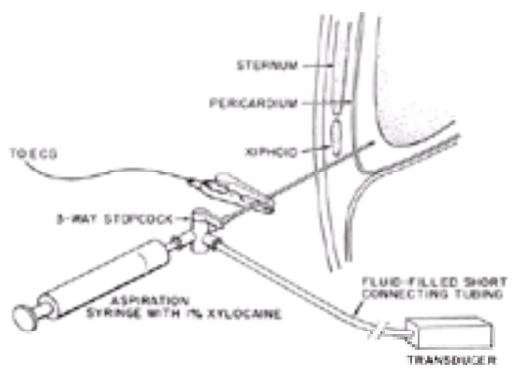

FIG. 33.7. Diagram showing the subxiphoid approach to pericardiocentesis. A hollow, thin-walled, 18-gauge needle is connected via a three-way stopcock to an aspiration syringe filled with 1% xylocaine and to a short length of fluid-filled tubing connected to a pressure transducer. A sterile V lead of an electrocardiographic recorder is attached to the metal needle hub. The needle is advanced until pericardial fluid is aspirated or an injury current appears on the V-lead electrocardiographic recording. Once fluid is aspirated, the stopcock is turned so that needle-tip pressure is displayed against simultaneously measured right atrial pressure from a right heart catheter. When needle-tip position within the pericardial space is confirmed, a J-tipped guidewire is passed through the needle into the pericardial space, the needle is removed, and a catheter with end and side-holes is advanced over the guidewire and subsequently connected via the three-way stopcock to both its transducer and the syringe. This permits thorough drainage of the pericardial effusion using a catheter rather than a sharp needle, and documentation that tamponade physiology is relieved when right atrial pressure falls and intrapericardial pressure is restored to a level at or below zero.

With the patient's head and chest propped up at a 45° angle to the horizontal, the skin and subcutaneous tissues are anesthetized about 0.5 cm below the xiphoid process, and the skin is pierced with a no. 11 blade and the subcutaneous tissues are spread with a mosquito clamp. The operator confirms that phasic arterial pressure and phasic right atrial pressure are displayed continuously. Using the needle that is attached via the stopcock to both a syringe and via fluid-filled tubing to

the transducer (Fig. 33.7), the needle is advanced, aspirated, and a small amount of lidocaine injected if there is no fluid return. If no fluid is aspirated, the needle is advanced until an injury current of ST elevation is observed on the needle's electrocardiographic lead; the needle is then slowly withdrawn. The needle may then be redirected and advanced again, if needed. When fluid is aspirated, the stopcock is turned to display intrapericardial pressure. The pericardium and right atrial transducers are quickly “zeroed” to atmosphere and both phasic and mean pericardial and right atrial pressures are simultaneously displayed and recorded. (If the pericardial needle tip displays a right ventricular waveform, the tip is quickly but smoothly withdrawn under continuous hemodynamic monitoring until the adjacent pericardial space is entered.) *If cardiac tamponade is present, both pericardial pressure and right atrial pressures will be virtually equal, with nearly identical waveforms.* As illustrated in Fig. 33.6, the pressure waveforms also show blunting or absence of the diastolic *y* descent.

When the needle tip's position with the pericardial space is confirmed, a floppy-tip 0.038-inch guidewire is passed and “wrapped” around the heart, as confirmed by fluoroscopy. The needle is removed, and a soft, tapered, large-bore lumen 6F or 7F catheter with end- and side-holes is advanced over the guidewire, and the guidewire is removed. Catheter tip pressure is recorded to confirm position in the pericardial space. Fluid is then aspirated and sent for chemical, bacteriologic, and cytologic examination, including appropriate processing of samples for culture for acid-fast bacilli and fungi. It is our practice then to completely evacuate the pericardial space by attachment of the catheter to a sealed vacuum bottle . *This permits rapid and complete evacuation of pericardial contents using the pericardial catheter but should never be attempted using a sharp needle in the pericardial space.* If this container is heparinized, it serves as a large, excellent-quality sample for cytology examination. In patients with HIV infection and AIDS, meticulous attention should be paid to bacteriologic and cytologic examination of pericardial fluid, since pericardial effusion may be related to pericardial involvement by Kaposi's sarcoma, atypical lymphoma, tuberculosis, and other opportunistic infections (32). The detection of tuberculosis by fluid culture varies widely in reported series, and there is enthusiasm that molecular analysis using polymerase chain reaction (PCR) would enhance diagnostic accuracy. In a recent series of patients with tuberculous pericarditis, fluid culture was diagnostic in more than 90%, whereas histologic tissue examination was diagnostic in about 87%. Disappointingly, the sensitivity of PCR in pericardial fluid was low (44).

Complete drainage has usually been accomplished when no more fluid can be aspirated. At this point we usually obtain a limited two-dimensional echocardiographic evaluation in the catheterization laboratory to confirm that the pericardial effusion has been eliminated and that there are no regional loculated pockets of fluid. Pericardial pressure and right heart pressures, as well as systemic arterial pressure, are recorded again. Repeat samples of arterial and mixed venous (pulmonary artery) blood are obtained for measurement of oxygen saturation and subsequent calculation of cardiac output. As shown in Fig. 33.6, cardiac tamponade physiology is relieved if (a) pericardial pressure falls to a level at or below 0 mm Hg; (b) right atrial pressure separates from pericardial pressure and falls to normal range with restoration of the diastolic *y* descent, which indicates that normal atrial emptying and early ventricular diastolic filling are restored; and (c) pulsus paradoxus is relieved. In hypotensive patients, systemic arterial pressure usually rises in association with an increase in mixed venous oxygen content, indicative of an increase in cardiac output. Failure of pericardial pressure to fall to a level of 0 to –2 mm Hg indicates that the reference height of the transducers is incorrect or that pericardial fluid under pressure (free or loculated) is still present.

Effusive-Constrictive Pericarditis

Failure of right atrial pressure to fall to normal levels suggests that a coexisting cause of right atrial hypertension is present. *Persistent elevation of right atrial pressure with appearance of a prominent* y *descent and a dip-and-plateau pattern in the right ventricular waveform suggest the presence of effusive-constrictive pericarditis*. In this condition, relief of cardiac tamponade unmasks significant residual visceral pericardial constriction (45,46). Effusive-constrictive pericarditis is important to recognize and diagnose, since definitive treatment requires extensive pericardiectomy (not pericardial window or repeat pericardiocentesis) (47). The jugular veins should also be examined. In patients with malignant effusion, persistent jugular venous pressure elevation despite relief of right atrial hypertension and restoration of pericardial pressure to a level near 0 mm Hg mandates exclusion of coexisting superior vena caval obstruction (43). In patients with suspected malignant effusion and hypoxemia, which is not a feature of cardiac tamponade, a pulmonary wedge aspirate for cytologic examination can be obtained to evaluate pulmonary microvascular spread of tumor (48).

After pericardiocentesis, the pericardial catheter may be left in place safely for about 24 hours and attached securely to a closed, sterile system using gravity, not active suction, for drainage. Ordinarily, it should not be left in place for longer periods due to risk of iatrogenic infection. In contemporary practice, there is usually no indication for infusion of air or carbon dioxide into the pericardial space. Two-dimensional echocardiography is readily available and more accurate in assessing reaccumulation of fluid or presence of intracardiac masses. After pericardiocentesis, most patients should be observed for about 24 hours in an intensive-care setting until rapid fluid reaccumulation is excluded and the pericardial catheter is removed. Patients with underlying left ventricular dysfunction or respiratory distress syndrome should be monitored closely for the development of pulmonary edema that is due to the abrupt increase in pulmonary blood flow and left heart filling after decompression of cardiac tamponade (49).

PERCUTANEOUS PERICARDIOSCOPY AND PERICARDIOTOMY

In patients with large recurrent pericardial effusions, and in patients in whom there is a strong clinical suspicion of malignant pericarditis or tuberculous pericarditis, several small uncontrolled series of pericardioscopy and pericardial biopsy suggest that this approach may increase the likelihood of obtaining a definitive diagnosis. In a recent prospective series of 142 patients with unexplained pericardial effusions who underwent surgical pericardioscopy including cytologic fluid analysis, visualization of the pericardium, and guided biopsy, a specific cause (neoplastic, infected purulent, or sterile radiation-induced effusion) was identified in 49%, whereas 51% were considered idiopathic. Of note, an unrecognized cause not detected by pericardioscopy-biopsy was subsequently discovered in 4% (50). In this series, no death was attributable to pericardioscopy but in-hospital mortality was 5.6% related to underlying disease. Maisch et al. (51) recently reported a series of 14 patients with idiopathic pericarditis and 15 patients with malignant pericarditis who underwent percutaneous pericardioscopy with both pericardial and epicardial biopsy from a registry of 136 patients undergoing pericardiocentesis. In this experience, subxiphoid pericardiocentesis and sampling of fluid for cytologic study, immunologic examination, and culture were performed first, followed by evacuation of pericardial fluid; replacement of warmed, clear, sterile saline in the pericardial sac; and introduction of both rigid and flexible pericardioscopes. Both epicardial biopsies and pericardial biopsies were obtained with a resterilizable bioptome, after site selection by both pericardioscopy and biplane fluoroscopy. Sterile saline was then evacuated. In patients with neoplastic disease, there was a trend that epicardial biopsy was more sensitive than fluid cytology, whereas pericardial biopsy did not contribute additional information. In this series of patients with proven malignant pericarditis, fluid cytology was diagnostic in 71% and epicardial biopsy was diagnostic in 80%. In our experience and in several series of pericardiocentesis in patients with malignant effusion, cytologic examination is positive in about 80% to 85% of cases. In malignant effusion, false-negative cytologic analysis is rare in carcinomatous pericarditis, whereas false-negative cytologic examinations tend to occur in pericardial malignant involvement by lymphoma or mesothelioma (52). Thus a clear role for diagnosis by fluid cytology versus pericardioscopy and directed pericardial and/or epicardial biopsy is not yet defined.

It is also controversial whether evacuation of pericardial fluid by pericardiocentesis or surgical drainage is justified for therapeutic or diagnostic reasons in patients with large pericardial effusions without tamponade or strong clinical suspicion of purulent pericarditis. Merce et al. (53) recently reported 71 such consecutive patients with large pericardial effusions evident as echo-free pericardial space greater than 20 mm. In this cohort, 26 underwent pericardial drainage and examination of pericardial fluid and 45 were managed conservatively. Only 2 of the 26 pericardiocenteses yielded a definitive diagnosis. Among the 45 patients who did not undergo pericardial drainage, moderate or large effusions persisted in only two patients and no patient developed cardiac tamponade or died as a result of pericardial disease. *These data suggest that pericardiocentesis in patients with large asymptomatic pericardial effusions has a very low diagnostic yield and no clear therapeutic benefit*.

Percutaneous Balloon Pericardiotomy

Percutaneous balloon pericardiotomy is an alternative approach to the treatment of cardiac tamponade that may be especially valuable in patients with recurrent large malignant effusions (54). The incidence of recurrent tamponade appears to be higher in patients who undergo pericardiocentesis for malignant effusion than in those with other etiologies. For example, in our experience 62% of patients with malignant effusion managed by complete pericardiocentesis drainage redeveloped cardiac tamponade after a median of 7 days (41). In comparison, in most series of cardiac tamponade that is unrelated to malignant effusion, pericardiocentesis is effective and requires no further intervention in more than 80% of patients. The technique involves pericardiocentesis by the subxiphoid approach using an approach similar to that described earlier. Approximately 100 to 200 mL of fluid is left or that amount of sterile saline is reintroduced, and 20 mL of dilute contrast is injected to aid visualization of the pericardial space. A 0.038-inch J-tip guidewire is then introduced, the pericardiocentesis catheter is withdrawn, the tract is dilated with a 10F dilator, and a 20-mm-diameter, 3-cm-long dilating balloon (e.g., Mansfield) containing dilute contrast is advanced over the guidewire. The balloon is positioned to “straddle” the pericardial border and is inflated slightly to define a waist at the parietal pericardial border, as illustrated in Fig. 33.8. The balloon is then fully expanded to create a rent in the pericardium. The guidewire is reintroduced, the balloon is removed, the pericardial catheter is reintroduced, and about 10 mL of contrast is injected to confirm free exit of fluid through the rent in the pericardium. Any remaining fluid is evacuated. Sometimes more than one site must be dilated to ensure rapid emptying of the pericardial space. Both echocardiography and chest roentgenography must be performed within 24 hours to evaluate any reaccumulation of pericardial effusion or development of left pleural effusion or pneumothorax. Ziskind et al. (54) reported an experience in 50 patients in which balloon pericardiotomy was effective in preventing recurrent tamponade in 46 patients during a 3.6-month follow-up. In this experience, pneumothorax developed in 20%, two patients

required postpericardiotomy operation for pericardial hemorrhage, and two additional patients required late operation for recurrent tamponade.

FIG. 33.8. Illustration of the percutaneous balloon pericardiotomy technique. After partial drainage of the pericardium using a pericardial catheter, a 0.038-inch stiff J-tip wire is introduced into the pericardial space. A 3-cm-long dilating balloon is then advanced over the guidewire to “straddle” the parietal pericardial membrane and is manually inflated to create a rent in the pericardium. (From Ziskind AA, Pearce AC, Lemmon CC, et al. Percutaneous balloon pericardiotomy for the treatment of cardiac tamponade and large pericardial effusions: description of technique and report of the first 50 cases. *J Am Coll Cardiol* 1993;21:1.)

Recent modifications of the procedure include use of an Inoue balloon catheter. The procedure was successful in 10 of 11 (91%) patients who underwent Inoue balloon pericardiotomy for treatment of recurrent large effusion, with all 10 remaining free of recurrent effusion for a follow-up period of 4 months (55). It has now been established that balloon pericardiotomy causes drainage and absorption of most fluid within the peritoneal cavity rather than the pleura (56). This consideration is important in patients with malignancy potentially confined to the thorax, in whom there is the potential for peritoneal dissemination of malignant cells by balloon pericardiotomy.

At present, balloon pericardiotomy is a potential alternative to repeat catheter pericardiocentesis in patients with recurrent pericardial effusions and cardiac tamponade. We do not recommend it as the index procedure because percutaneous catheter pericardiocentesis with vacuum-assisted complete drainage is effective in relieving tamponade, and the complications and morbidity are lower than balloon pericardiotomy. Surgical subxiphoid pericardiotomy, a “pericardial window” that can often be done under local anesthesia, is also a treatment option. In a recent series of 94 patients treated with subxiphoid pericardiotomy for cardiac tamponade of which 64% were malignant effusions, the procedure was successful in all patients, with no operative deaths. The procedure was associated with a rate of recurrent tamponade of 1.1% in comparison with a recurrence rate of 30% in a nonrandomized concurrent series of 23 patients managed with percutaneous catheter pericardiocentesis (57). In patients with recurrent malignant effusion, multiple small series discuss the use of intrapericardial sclerosing agents, but there are no prospective randomized series that compares the risks and benefits of catheter pericardiocentesis with and without instillation of sclerosing agents.

CARDIAC COMPRESSION AFTER CARDIAC SURGERY

Acute compression of the heart after cardiac surgery by localized cardiac tamponade or an organizing hematoma is an important cause of hypotension and “failure to thrive” in postoperative patients, even when the pericardium is left partially open (58,59). It has recently been reported as a cause of delayed postoperative death after minimally invasive direct coronary artery bypass surgery (60). The recognition of postoperative tamponade, which occurs in about 2% of patients after cardiac surgery, is challenging because both the clinical and echocardiographic presentations are atypical (58). In a series of 29 patients with postsurgical tamponade reported by Chuttani et al. (59), pulsus paradoxus was present in less than half of the patients and 66% had a localized posterior effusion or hematoma that was associated with isolated left ventricular diastolic collapse and rarely with right ventricular diastolic collapse. Despite these atypical features, elevated diastolic pressures with equalization was observed at cardiac catheterization in more than 80%. In such patients, fibrotic constrictive pericarditis may develop, but its incidence is not known. Techniques for reliable and safe percutaneous echocardiographically guided pericardiocentesis are not yet available to treat posterior effusion causing localized left ventricular tamponade.

INTRAPERICARDIAL THERAPEUTIC INTERVENTIONS

The pericardial mesothelium actively secretes and metabolizes multiple molecules—including prostaglandins, nitric oxide, atrial natriuretic peptide, and endothelin-1—that have the potential to both modulate cardiac performance via paracrine signaling (61,62). In addition, growth factors with the potential to modify underlying myocyte and smooth muscle cell growth appear to be diffusible between cardiac tissue and the pericardial space and concentrated in pericardial fluid. Fujita and coworkers (63) demonstrated that concentrations of basic fibroblast growth factor (bFGF) are about 10-fold higher in the pericardial fluid of patients with unstable angina than in patients with nonischemic heart disease, raising the possibility that growth factors concentrated in the pericardial space may mediate collateral blood vessel growth in humans. Laham and coworkers (64) demonstrated that a single intrapericardial bolus of bFGF in pigs with coronary constriction promoted growth of collaterals, and there is now growing evidence from multiple experimental animal studies that supports the potential for therapeutic myocardial angiogenesis using percutaneous intrapericardial drug delivery. For these reasons, there is interest in developing techniques for minimally invasive access of the pericardial space in patients without pericardial effusions for sampling of pericardial fluid, intrapericardial drug delivery of growth factors and drugs that may modify arrhythmias, and gene transfer via adenovirus and other vectors. As illustrated in Fig. 33.9, Verrier and coworkers (65) have reported the development of access to the normal pericardial space via percutaneous catheterization of the right femoral vein and puncture of the right atrial appendage for diagnostic sampling and therapeutic interventions. March and coworkers (66) recently reported successful gene transfer using adenoviral vectors introduced via catheter-based pericardial gene delivery in dogs. Their approach utilized percutaneous puncture of the apex of the right ventricle with a hollow, helical-shaped catheter during fluoroscopic visualization to achieve access to the normal pericardial space. These experimental studies suggest the feasibility of percutaneous pericardial drug and gene delivery in humans, and rapid development of techniques for safe and reliable access of the normal human pericardium is anticipated.

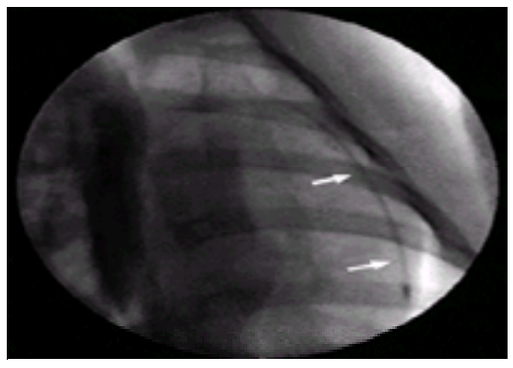

FIG. 33.9. Fluoroscopic image illustrating transatrial pericardial access to the normal pericardial space for drug or gene delivery in an experimental pig model. Via an 8F catheter, a needle catheter was advanced from the right atrial appendage into the pericardial space, a guidewire was introduced, the needle was removed, and a 4F delivery catheter (*arrows*) was advanced through the appendage wall and positioned in the pericardial space. (Adapted from Waxman S, Moreno R, Rowe KA, Verrier RA. Persistent primary coronary dilation induced by transatrial delivery of nitroglycerin into the pericardial space: A novel approach for local cardiac drug delivery. *J Am Coll Cardiol* 1999;33:2073.)

ANOMALIES OF THE PERICARDIUM

Anomalies of the pericardium may cause confusion during cardiac catheterization and angiography unless their characteristic features are recognized. Pericardial

cysts, which are filled with clear fluid, are usually located at the right costophrenic angle and come to attention as unexplained protrusion of the right heart border on the chest roentgenogram or during fluoroscopy at cardiac catheterization. Rarely, cysts may cause chest pain or right ventricular outflow obstruction (67). Although most can be managed conservatively, large pericardial cysts located at the costophrenic angle can be decompressed by percutaneous aspiration under fluoroscopic guidance (68). Total absence of the pericardium is extremely rare and usually not associated with symptoms. *Absence of the left side of the pericardium is more common*, and patients may be referred to cardiac catheterization because of chest pain, palpitations, or dyspnea (69). These patients have widened splitting of the second heart sound, a systolic murmur at the upper left sternal border, electrocardiographic findings of right axis deviation and clockwise displacement of the precordial transition zone, and chest roentgenogram findings of a leftward displacement of the heart and prominent pulmonary artery. This anomaly may be confused with pulmonic stenosis or atrial septal defect. Although cardiac angiography with diagnostic left pneumothorax was previously used to outline the pericardium, this is rarely indicated today if typical clinical and radiologic features are present. In patients with *partial left-sided pericardial defects*, however, cardiac catheterization and angiography can be helpful. These patients frequently complain of chest pain and are at risk for sudden death due to herniation and strangulation of the heart through the defect. A definitive diagnosis can be made by pulmonary artery angiography with follow-through to the left heart, which usually demonstrates herniation of the left atrium or its appendage or part of the left ventricle beyond the heart border (70). Partial right-sided pericardial defect can also be complicated by severe chest pain related to inspiratory herniation of the right atrium (71). In this condition, right atrial contrast angiography in the left anterior oblique position demonstrates herniation of the right atrium through the pericardial defect.

CHAPTER REFERENCES

1. Pi RG, Tarazi R, Wong S. Constrictive pericarditis causing extrinsic mitral stenosis and a left heart mass. *Clin Cardiol* 1996;19:517.
2. Cameron J, Oesterle SN, Baldwin JC, Hancock EW. The etiologic spectrum of constrictive pericarditis. *Am Heart J* 1987;113:354.
3. Mehta A, Mehta M, Jain AC. Constrictive pericarditis. *Clin Cardiol* 1999;22:334.
4. Tuna IC, Danielson GK. Surgical management of pericardial diseases. *Cardiol Clin* 1990;84:683.
5. Sagrista-Sauleda J, Permanger-Miralda G, Candell-Riera J, Angel J, Soler-Soler J. Transient cardiac constriction: an unrecognized pattern of evolution in effusive acute idiopathic pericarditis. *Am J Cardiol* 1987;59:961.
6. Ling LH, et al. Pericardial thickness measured with transesophageal echocardiography: feasibility and potential clinical usefulness. *J Am Coll Cardiol* 1997;29:1317.
7. Takata M, Harasawa Y, Beloucif S, Robotham JL. Coupled vs uncoupled pericardial constraint: effects on cardiac chamber interactions. *J Appl Physiol* 1997;83:1799.
8. Tyberg TI, Goodyer AVN, Oangou RA. Genesis of pericardial knock in constrictive pericarditis. *Am J Cardiol* 1980;46:570.
9. Shabetai R, Fowler NO, Guntheroth WG. The hemodynamics of cardiac tamponade and constrictive pericarditis. *Am J Cardiol* 1970;26:480.
10. Hurrell DG, et al. Value of dynamic respiratory changes in left and right ventricular pressures for the diagnosis of constrictive pericarditis. *Circulation* 1996;93:2007.
11. Chandrashekhar Y, Anand IS, Kalra GS, Wander GS. Rate-dependent hemodynamic responses during atrial pacing on chronic constrictive pericarditis before and after surgery. *Am J Cardiol* 1993;72:615.
12. Gaasch WH, Peterson KL, Shabetai R. Left ventricular function in chronic constrictive pericarditis. *Am J Cardiol* 1974;34:107.
13. Kern MJ, Lorell BH, Grossman W. Cardiac amyloidosis masquerading as constrictive pericarditis. *Cathet Cardiovasc Diagn* 1982;8:629.
14. Goldberg E, Stein J, Berger M, Berdoff RL. Diastolic segmental coronary artery obliteration in constrictive pericarditis. *Cathet Cardiovasc Diagn* 1981;7:197.
15. Akasaka T, et al. Phasic coronary flow characteristics in patients with constrictive pericarditis: comparison with restrictive cardiomyopathy. *Circulation* 1997;96:1874.
16. Hancock EW. On the elastic and rigid forms of constrictive pericarditis. *Am Heart J* 1980;100:917.
17. Trotter MC, Chung KC, Ochsner JL, McFadden PM. Pericardiectomy for pericardial constriction. *Am Surg* 1996;62:304.
18. Senni M, et al. Left ventricular systolic and diastolic function after pericardiectomy in patients with constrictive pericarditis: Doppler echocardiographic findings and correlation with clinical status. *J Am Coll Cardiol* 1999;33:1182.
19. Chello M, et al. Collagen network remodeling and left ventricular function in constrictive pericarditis. *Heart* 1996;75:184.
20. Benotti JR, Grossman W, Cohn PF. The clinical profile of restrictive cardiomyopathy. *Circulation* 1980;61:1206.
21. Tyberg TI, et al. Left ventricular filling in differentiating restrictive amyloid cardiomyopathy and constrictive pericarditis. *Am J Cardiol* 1981;47:791.
22. Aroney CN, et al. Differentiation of restrictive cardiomyopathy from pericardial constriction: Assessment of diastolic function of radionuclide angiography. *J Am Coll Cardiol* 1989;13:1007.
23. Little WC, et al. Evaluation of left ventricular diastolic function from the pattern of left ventricular filling. *Clin Cardiol* 1998;21:5.
24. Atherton JJ, Moore TD, Thomson HL, Frenneaux MP. Restrictive left ventricular filling patterns are predictive of diastolic ventricular interaction in chronic heart failure. *J Am Coll Cardiol* 1998;31:413.
25. Schoenfield MH, et al. Restrictive cardiomyopathy versus constrictive pericarditis: role of endomyocardial biopsy in avoiding unnecessary thoracotomy. *Circulation* 1987;75:1012.
26. Lorell BH, et al. Right ventricular infarction. *Am J Cardiol* 1979;43:465.
27. Bartle SH, Hermann HJ. Acute mitral regurgitation in man. Hemodynamic evidence and observations indicating an early role for the pericardium. *Circulation* 1967;36:839.
28. Smiseth OA, et al. Assessment of pericardial constraint in dogs. *Circulation* 1985;71:158.
29. Beck CS. Two cardiac compression triads. *JAMA* 1935;104:714.
30. Guberman BA, et al. Cardiac tamponade in medical patients. *Circulation* 1981;64:633.
31. Levine MJ, Lorell BH, Diver DJ, Come PC. Implications of echocardiographically assisted diagnosis of pericardial tamponade in contemporary medical patients: detection prior to hemodynamic embarrassment. *J Am Coll Cardiol* 1991;17:59.
32. Silva-Cardoso J, et al. Pericardial involvement in human immunodeficiency virus infection. *Chest* 1999;115:418.
33. Antman EM, Cargill V, Grossman W. Low-pressure cardiac tamponade. *Ann Intern Med* 1979;91:403.
34. Brown J, MacKinnon D, King A, Vanderbush E. Elevated arterial blood pressure in cardiac tamponade. *N Engl J Med* 1992;327:463.
35. Friedrich SP, Berman AD, Baim DS, Diver DJ. Myocardial perforation in the cardiac catheterization laboratory: incidence, presentation, diagnosis, and management. *Cathet Cardiovasc Diagn* 1994;32:99.
36. Bottner RK, Hardigan KR. Cardiac tamponade following stent implantation with adjuvant platelet IIb/IIIa receptor inhibitor administration. *Cathet Cardiovasc Diagn* 1997;40:380.
37. Tsang TSM, et al. Rescue echocardiographically guided pericardiocentesis for cardiac perforation complicating catheter-based procedures. *J Am Coll Cardiol* 1998;32:1345.
38. Shabetai R, Fowler NO, Fenton JC, Massangkay M. Pulsus paradoxus. *J Clin Invest* 1965;44:1882.
39. Savitt MA, Tyson GS, Elbeery JR, et al. Physiology of cardiac tamponade and paradoxical pulse in conscious dogs. *Am J Physiol* 1993;265:H1996.
40. Joffe II, Douglas PS. Cardiac tamponade in association with an atrial septal defect: echocardiographic Doppler and hemodynamic observations. *J Am Soc Echocardiogr* 1996;9:909.
41. Laham RJ, Cohen DJ, Kuntz RE, Baim DS, Lorell BH, Simons M. Pericardial effusion in patients with cancer: outcome with contemporary management strategies. *Heart* 1996;75:67.
42. Ball JB, Morrison WL. Cardiac tamponade. *Postgrad Med J* 1997;73:141.
43. Krikorian JG, Hancock EW. Pericardiocentesis. *Am J Med* 1978;65:808.
44. Cegielski JP, et al. Comparison of PCR, culture, and histopathology for diagnosis of tuberculous pericarditis. *J Clin Microbiol* 1997;35:3254.
45. Hancock EW. Subacute effusive-constrictive pericarditis. *Circulation* 1971;43:183.
46. Mann T, Brodie BR, Grossman W, McLaurin LP. Effusive-constrictive hemodynamic pattern due to neoplastic involvement of the pericardium. *Am J Cardiol* 1978;41:781.
47. Walsh TJ, Baughman KL, Gardener TJ, Bulkley BH. Constrictive epicarditis as a cause of delayed or absent response to pericardiectomy. *J Thorac Cardiovasc Surg* 1982;83:126.
48. Safian RD, Come SE, Kadin M, Lorell BH. Use of pulmonary capillary wedge aspirates for the ante-mortem diagnosis of pulmonary microvascular tumor. *Cathet Cardiovasc Diagn* 1989;17:112.
49. Vandyke WH, Cure J, Chakko CS, Gheorghiode M. Pulmonary edema after pericardiocentesis for cardiac tamponade. *N Engl J Med* 1983;309:595.
50. Nugue O, et al. Pericardioscopy in the etiologic diagnosis of pericardial effusion in 141 consecutive patients. *Circulation* 1996;94:1625.
51. Maisch B, et al. Intrapericardial treatment of inflammatory and neoplastic pericarditis guided by pericardioscopy and epicardial biopsy—results from a pilot study. *Clin Cardiol* 1999;22[Suppl I]:17.
52. Lorell BH, Braunwald E. Pericardial disease. In: Braunwald E, ed. *Heart disease,* 5th ed. Philadelphia: WB Saunders, 1997:1513.
53. Merce J, Sagrista-Sauleda J, Permanyer-Miralda G, Soler-Soler J. Should pericardial drainage be performed routinely in patients who have a large pericardial effusion without tamponade? *Am J Med* 1998;105:106.
54. Ziskind AA, Pearce AC, Lemmon CC, et al. Percutaneous balloon pericardiotomy for the treatment of cardiac tamponade and large pericardial effusions: description of technique and report of the first 50 cases. *J Am Coll Cardiol* 1993;21:1.
55. Chow WH, Chow TC, Yip AS, Cheung KL. Inoue balloon pericardiotomy for patients with recurrent pericardial effusion. *Angiology* 1996;47:57.
56. Bertrand O, Legrand V, Kulburtus H. Percutaneous balloon pericardiotomy: a case report and analysis of mechanism of action. *Cathet Cardiovasc Diagn* 1996;38:180.
57. Allen KB, Faber LP, Warren WH, Shaar CJ. Pericardial effusion: subxiphoid pericardiotomy versus percutaneous catheter drainage. *Ann Thorac Surg* 1999;67:437.
58. Russo AM, O'Connor WH, Wasman HL. Atypical presentations and echocardiographic findings in patients with cardiac tamponade occurring early and late after cardiac surgery. *Chest* 1993;104:71.
59. Chuttani K, Tischler MD, Pandian NG, Lee RT, Mohanty PK. Diagnosis of cardiac tamponade after cardiac surgery: relative value of clinical, echocardiographic, and hemodynamic signs. *Am Heart J* 1994;127:913.
60. Lazzara RR, et al. Cardiac tamponade following minimally invasive direct coronary artery bypass. *Chest* 1997;112:1112.
61. Mebazaa A, et al. Potential paracrine role of the pericardium in the regulation of cardiac function. *Cardiovasc Res* 1998;40:332.
62. Horkay F, et al. Presence of immunoreactive endothelin-1 and atrial natriuretic peptide in human pericardial fluid. *Life Sci* 1998;62:267.
63. Fujita M, et al. Elevated basic fibroblast growth factor in pericardial fluid of patients with unstable angina. *Circulation* 1996;94:610.
64. Laham RJ, Hung D, Simons M. Therapeutic myocardial angiogenesis using percutaneous intrapericardial drug delivery. *Clin Cardiol* 1999;22[Suppl I]:6.
65. Verrier RL, et al. Transatrial access to the normal pericardial space: a novel approach for diagnostic sampling, pericardiocentesis, and therapeutic interventions. *Circulation* 1998;98:2331.
66. March KL, et al. Efficient *in vivo* catheter-based pericardial gene transfer mediated by adenoviral vectors. *Clin Cardiol* 1999;22[Suppl. I]:23.
67. Ng AF, Olak J. Pericardial cyst causing right ventricular outflow tract obstruction. *Ann Thorac Surg* 1997;63:1147.
68. Peterson DR, Zatz LM, Popp RL. Pericardial cyst ten years after acute pericarditis. *Chest* 1975;67:719.
69. Nasser WK. Congenital absence of the left pericardium. *Am J Cardiol* 1970;26:466.
70. Bernal JM, et al. Angiographic demonstration of a partial defect of the pericardium with herniation of the left atrium and ventricle. *J Cardiovasc Surg* 1986;27:344.
71. Minocha GK, Falicov RE, Nijensohn E. Partial right-sided congenital pericardial defect with herniation of right atrium and right ventricle. *Chest* 1979;76:484.

34
Profiles in Congenital Heart Disease

John F. Keane, Stanton B. Perry, and James E. Lock

Harvard Medical School and Department of Cardiology, Children's Hospital, Boston, Massachusetts 02115

In 1938 the first successful surgical management of a congenital heart lesion, a patent ductus arteriosus (PDA), was reported by Gross, and this was followed several years later by aortic coarctation surgical repair. During the subsequent two decades, intracardiac repair of atrial septal defect (ASD), ventricular septal defect (VSD), valvar pulmonary and aortic stenoses, and more complex lesions such as tetralogy of Fallot (TOF) became commonplace. Cardiac catheterization techniques developed in parallel with these advances, and, indeed, preoperative catheterizations preceded essentially all operations and helped considerably in improving surgical outcomes. In 1966, Rashkind and Miller introduced the first widely used catheter-based interventional technique, namely balloon atrial septostomy (BAS) for transposition. In 1982 Kan et al. described static balloon pulmonary valvotomy for pulmonary stenosis, which heralded the current surge of interventional procedures in the management of congenital heart diseases. From a pediatric perspective, now more than a half century after the pioneering report of Gross and together with the remarkable advances in ultrasound technology and surgery, most of the complex lesions, particularly in neonates and infants, are repaired surgically without catheterization. The catheterization laboratory patient population now consists primarily of those with residual lesions or simple unoperated lesions who come for interventional management.

Table 34.1 compares the incidence of the more commonly studied lesions in adults (older than 21 years of age) catheterized at our hospital during the periods 1973–1978 and 1993–1998. This chapter attempts to reflect these changes. The techniques involved in each instance are described briefly and illustrated by case histories where appropriate. Some information from the increasing number of patients with Fontan-repaired single ventricles is included. More detailed descriptions of the interventional techniques used are presented in Chapter 28 and are also available elsewhere (1).

Lesion	1973–1979 (N = 156)	1993–1998 (N = 312)
Atrial septal defect	23	65[a]
Ventricular septal defect	25	26
Patent ductus arteriosus	3	13
Valvar aortic stenosis	27	26
Valvar pulmonary stenosis	9	16
Coarctation of aorta	8	15
Tetralogy of Fallot	45	87
DTGA	3	19
Single ventricle	13	45
Postop Fontan	0	33

DTGA = D transposition of great arteries; Postop Fontan = Postoperative Fontan procedure (many of these included in single ventricle category).
[a] Includes patent foramen ovale.

TABLE 34.1. *Selected congenital heart lesions catheterized in adults (>21 yr), comparing two 5-year periods at Children's Hospital, Boston*

ATRIAL SEPTAL DEFECTS

In the past, all patients with an ASD were catheterized before cardiac surgical correction. It is now clear that virtually all such defects can be diagnosed by physical examination, electrocardiography (ECG), chest radiography, and, in particular, echocardiography (transthoracic, transesophageal, three-dimensional). Therefore, surgery is undertaken without catheterization at most institutions. However, improving success with an increasing variety of umbrella devices for transcatheter closure of centrally located defects of small or moderate size has resulted in an increase in the number of such patients being catheterized at selected institutions (2,3,4 and 5) (Table 34.1).

Anatomic Types

There are three main types of ASD; namely, ostium secundum, ostium primum, and sinus venosus defects. At our institution, the frequencies of these defects have been 68%, 18%, and 6%, respectively (6). Secundum defects are located in the fossa ovalis below the limbic band; they are usually single and central and are often amenable to device closure. Sinus venosus defects occur in the posterior part of the interatrial septum, near the entrance of the superior vena cava (SVC) or, rarely, the inferior vena cava (IVC) and at this time are not amenable to device closure, largely because of the proximity of nearby right pulmonary veins.

Physiology

The size and direction of shunting through an ASD depend on both the size of the hole and the relative compliances of the right and left ventricles. Factors that lead to right ventricular (RV) hypertrophy, thereby decreasing RV compliance (e.g., pulmonary stenosis, pulmonary hypertension) induce a smaller left-to-right shunt or a larger right-to-left shunt, whereas factors that reduce left ventricular (LV) compliance (e.g., systemic hypertension, LV infarction) produce a larger left-to-right shunt. In infancy, the RV is normally hypertrophied as a result of intrauterine circulation, and there is little net shunt across an ASD. With increasing age, however, RV hypertrophy recedes, and a substantial left-to-right shunt develops, resulting in clinical detection of ASDs in childhood and early adulthood. The tendency for left-to-right shunting to increase throughout adult life (as systemic arterial blood pressure rises and LV compliance falls) has prompted many authors to advocate a policy of closing all ASDs at the time of diagnosis (6).

Catheterization Technique

As the catheter is advanced from the femoral vein, it frequently passes from right atrium (RA) to left atrium (LA). An alternate approach is to withdraw the catheter from the SVC to the RA with the tip positioned posteromedially, so that it drops beneath the limbic band into the fossa ovalis (as in a Brockenbrough transseptal puncture) and then to the LA. Primum defects are located more inferiorly, and sinus venosus defects are located more superiorly. Difficulty in crossing a known ASD usually implies the presence of the latter type of defect.

Crossing the atrial septum with a catheter does not confirm the presence of an ASD, because a probe-patent foramen ovale (in which the septum primum and septum secundum overlap but can be separated by a catheter or by a marked rise in RA pressure) is a normal finding in many children and in 10% to 15% of adults.

Oximetry Data

ASDs with left-to-right shunts are characterized by an increase, or step-up, in the oxygen content (or saturation) of blood in the RA (Fig. 34.1).

In children, an increase of 10% or more in oxygen saturation between the high SVC and the RA indicates an abnormal increase at the RA level (6). In adults (see Chapter 9), samples from both the SVC and IVC have been used to quantitate the degree of shunting. IVC blood is poorly mixed because of the streaming of renal vein blood, and multiple IVC samples have proved helpful in this regard.

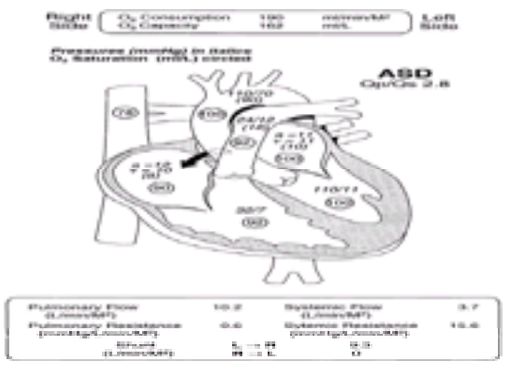

FIG. 34.1. Cardiac catheterization findings in a 6-year-old girl with an atrial septal defect; note the left-to-right shunt at the atrial level and the small flow gradient across the pulmonary valve.

A significant step-up at the RA level does not guarantee the presence of an ASD; patients who have a VSD and associated tricuspid regurgitation can have identical oximetric data, as can those with a so-called “LV-RA” VSD. Associated abnormalities such as partial anomalous pulmonary venous return can be difficult to diagnose from oximetry data alone, although they are suggested by saturations greater than 85% in the SVC or IVC. Oximetry data are used to calculate pulmonary blood flows and shunts, but because oximetry values can vary by 3% to 6% on a random basis, shunts in which the pulmonary-to-systemic flow ratio is less than 1.5:1 cannot be detected reliably by oximetry (7). Obviously, the absence of a measured shunt does not exclude an important ASD; with the development of pulmonary vascular disease and progressive RV hypertension, RV compliance may fall, with the left-to-right shunt becoming negligible. Further decreases in RV compliance may then result in right-to-left shunting and cyanosis.

Pressure Data

The hallmark of a moderate or large ASD is the equalization of atrial pressures; previous workers documented that right and left atrial pressures are equal within 1 to 2 mm Hg and that *a* and *v* wave peaks are within 3 to 4 mm Hg in a good-sized ASD (8). Obviously, the *a* and *v* waves tend to become similar in both atria with a large defect. We frequently use the pressure gradient across the atrial septum to differentiate a patent foramen ovale (PFO) from a moderate or large ASD. Conversely, the

absence of a transatrial gradient does not make the diagnosis of an ASD; pericardial tamponade, restrictive physiology, and diseases that raise RA pressures all tend to reduce the normal gradient across the atrial septum.

Angiography

Until recently, angiography was an unimportant part of catheterization in a patient with an ASD; pressure equalization across the atria, catheter course, and a step-up at the atrial level together make a compelling diagnosis. Many cardiologists do a pulmonary artery (PA) angiogram to visualize pulmonary venous return. With the advent of transcatheter closure of ASDs, both angiography and balloon sizing of atrial defects are carried out to assess whether transcatheter closure is feasible (see Chapter 28); this is nowadays the main reason for catheterizing these patients. Whenever we suspect the presence of an ostium primum ASD in a patient undergoing cardiac catheterization, we perform an LV angiogram in a so-called hepatoclavicular view (40° cranial, 40° left anterior oblique [LAO]) to outline the integrity of the most posterior part of the interventricular septum (9).

Interventional Catheterization

Although sinus venosus and ostium primum defects are not amenable to transcatheter double-umbrella closure, about 50% to 60% of patients with secundum ASDs appear to be good candidates (2,10). In those lesions suitable for closure (less than 24 mm stretched diameter), balloon sizing of the defect with a soft, deformable balloon and angiography precede device placement (see Chapter 28). All other ASDs are surgically closed, with a ministernotomy technique for most secundum defects.

Case History 1. A 6-year-old asymptomatic girl was evaluated for a heart murmur. A grade 2/6 systolic ejection murmur was detected at the left upper sternal border, and a diastolic flow rumble of similar intensity was noted inferiorly. Her second heart sound was widely split and fixed. On ECG, right axis deviation and some RV hypertrophy were present, and echocardiographically a central 12-mm ASD secundum was identified. At catheterization (Fig. 34.1), an ASD of moderate size was confirmed, with a small transatrial mean gradient of 2 mm Hg and a pulmonary-to-systemic flow ratio of 2.8. The ASD was then closed with a 33-mm double umbrella device.

VENTRICULAR SEPTAL DEFECTS

It is increasingly rare for patients with VSDs to be referred for initial diagnosis during adulthood. Loud murmurs permit diagnosis of the patient with a VSD at an early age; large defects produce symptoms early in life and demand early closure; and small defects tend to get smaller (and often close completely) with advancing age. Pediatric cardiologists tend to “fish or cut bait” in patients with VSDs by 2 years of age, or certainly by age 5; defects unclosed by that age will probably never require surgical attention. Although today most single, clinically significant VSDs are repaired surgically without catheterization, particularly in infancy, there are patients with congenital, postoperative, posttraumatic, or postinfarction VSD who require diagnostic or interventional cardiac catheterization, or both.

Anatomic Types

Most congenital VSDs are defects in or about the membranous septum (“perimembranous”) and are located just underneath the aortic valve. Atrioventricular canal–type VSDs are less common, are developmentally related to ostiumprimum defects, and occur in the posterior interventricular septum adjacent to the atrioventricular valves. Like ostium primum defects, they tend to be associated with a counterclockwise superior QRS in the ECG frontal plane and are seen more commonly in patients with Down syndrome. Subpulmonary VSDs result from deficiency of the conal septum, occur more commonly in Asian patients, and are frequently associated with prolapse of the right coronary cusp and aortic regurgitation. In Caucasian patients aortic regurgitation also occurs, but it is more commonly associated with membranous defects and often with prolapse of the noncoronary cusp alone or in conjunction with the right cusp (11).

Muscular VSDs can occur anywhere in the interventricular septum. Most are “midmuscular,” located just below the moderator band in the RV, although defects can occur in the apical, anterior, or posterior septum. Finally, some defects, termed Swiss-cheese VSDs, have large openings on the LV side of the septum but then are divided into a myriad of channels by muscle bundles on the RV side.

Physiology

Because shunting through a VSD occurs primarily in systole, the size and direction of shunting are determined mostly by the afterload that each ventricle faces. Therefore, factors that increase LV afterload (e.g., hypertension, coarctation) or decrease RV afterload (e.g., the fall in pulmonary resistance that occurs normally in early infancy) increase the left-to-right shunt, and factors that decrease LV afterload (e.g., vasodilator therapy) or increase RV afterload (e.g., the development of pulmonary stenosis or pulmonary vascular disease) decrease the left-to-right shunt or even produce a right-to-left shunt and cyanosis.

There is a strong natural tendency for VSDs to close with advancing age; most muscular defects close or become small by 5 years of age, and perimembranous defects may close by aneurysm formation or by adherence of the septal leaflet of the tricuspid valve to the edges of the defect. Therefore, medical and not surgical management is generally advised initially for any restrictive VSD in an asymptomatic patient.

Catheterization Technique

Until recently, catheter passage through a VSD was avoided for the most part, because it was unnecessary in making the diagnosis or estimating the size of the shunt. With increasingly successful efforts to close certain VSDs using a transcatheter umbrella approach (see Chapter 28), it is important to emphasize the catheter courses in these defects. For perimembranous defects near the tricuspid valve, the catheter is advanced into the RV and turned posteriorly (clockwise) to cross the VSD into the LV outflow tract. Midmuscular and apical VSDs are most easily crossed with balloon flotation catheters from the LV, whereas anterior muscular VSDs are best crossed from RV to LV with precurved stiff catheters and soft torque-control wires. Right-sided heart pressures and oximetry measurements from the wedge position, distal PAs, main PA, RV, RA, and SVC define the pulmonary vascular resistance and the shunt size (Fig. 34.2).

In patients with elevated PA pressure and pulmonary vascular resistance, previous authors have advanced the notion of a “reactive” pulmonary vascular bed; if the pulmonary vascular resistance falls in response to a vasodilator agent (nitric oxide), it is more likely to fall after corrective surgery (12).

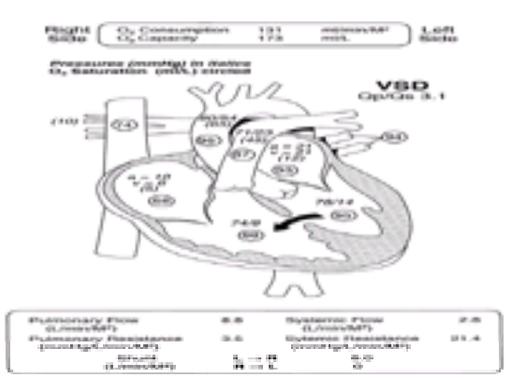

FIG. 34.2. Cardiac catheterization findings in 2-year-old patient with large, perimembranous ventricular septal defect; note the left-to-right shunt at the ventricular level, pulmonary artery mean pressure at two thirds of the systemic level with mildly elevated pulmonary vascular resistance, and elevated left ventricular filling pressure.

Pressure Data

Patients with small VSDs have a large pressure gradient across the interventricular septum. Equalization of ventricular pressures always occurs with a large VSD but does not prove the presence of a large defect; small defects with associated pulmonary hypertension may mimic the pressure findings in a large defect. Therefore, the size and location of a VSD must be determined by an imaging technique.

Angiography

Optimal angiography of VSDs utilizes the long axial view technique introduced by Bargeron et al. (13). Because the interventricular septum may be regarded as having the surface of a cone that points from right back to left front, any chest radiographic view that is a left anterior view with cranial angulation tends to put the septal surface in its longest (least foreshortened) projection. In general, the membranous, conoventricular (Fig. 34.3), middle and apical portions of the interventricular septum (Fig. 34.4) are best seen in a long axial oblique view.

The anterior portion of the septum is best seen with a straight anteroposterior (or even a right anterior oblique) view, and the posterior portion of the septum (the location of atrioventricular canal defects and posterior muscular defects) is best seen with a four-chambered view (see Chapter 6). As usual, injection of contrast material into the high-pressure chamber (LV) is required; because anatomic definition is needed rather than extrasystole-free function evaluation, in children we inject nonionic contrast volumes (1 to 1.5 mL/kg) at rapid rates (less than 1-second injection times) to outline the defects.

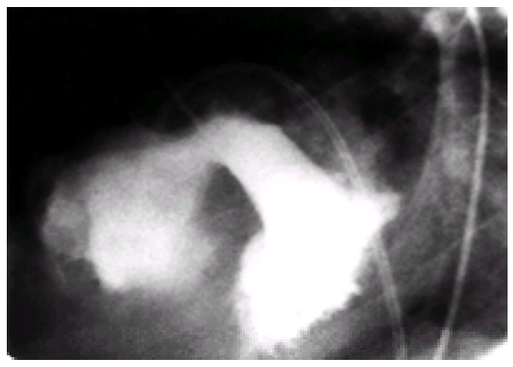

FIG. 34.3. Left ventriculogram in the long axial oblique view, demonstrating a conoventricular ventricular septal defect in tetralogy of Fallot.

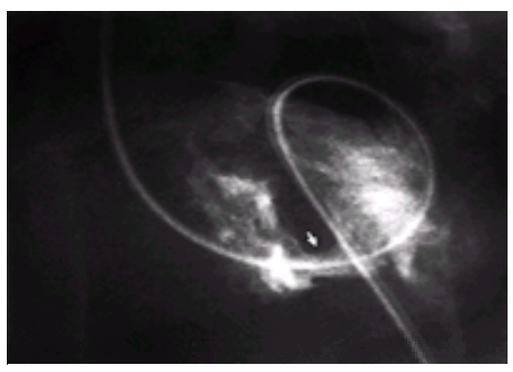

FIG. 34.4. Left ventriculogram in long axial oblique view demonstrating apical muscular ventricular septal defect *(arrow)*.

Interventional Cardiology

Our earlier experience with transcatheter closure of selected VSDs using a double umbrella (14) has now been expanded to some 200 cases, and results continue to improve. Such transcatheter closure (see Chapter 28) is our treatment of choice for apical and anterior muscular defects and for most residual postoperative defects. Evaluation of this technique in the management of postinfarction defects continues. Considering that the aortic and tricuspid valves are close to the edges of most perimembranous VSDs, surgery currently remains the mainstay of management for these patients.

Case History 2. A 2-year-old patient presented with a large perimembranous VSD and continued to exhibit congestive heart failure and failure to thrive despite medical treatment. At catheterization (Fig. 34.2), a large left-to-right shunt at the ventricular level (pulmonary-to-systemic flow ratio, 3.1) was identified, with PA mean pressure at two thirds of the systemic level, mildly elevated pulmonary resistance (3.5 Wood units), and mildly elevated left ventricular end-diastolic pressure (LVEDP) at 14 mm Hg. Angiographically, a perimembranous VSD was identified. The defect was successfully closed surgically with a patch via a transatrial approach, with return of PA pressure to normal.

Case History 3. A 3-year-old patient who had had surgical repair of both a membranous VSD and coarctation of the aorta in infancy was catheterized because of an unsuspected additional VSD. A large, muscular apical VSD was identified and closed at that study with a 28-mm double-umbrella device.

PATENT DUCTUS ARTERIOSUS

One of the more common forms of congenital heart disease, PDA is usually diagnosed in childhood and corrected at the time of diagnosis. Patency of the ductus is maintained before birth by the production of prostaglandin E (PGE). Premature babies may have an incidence of PDA as high as 40%; these are readily closed by administration of the cyclooxygenase inhibitor indomethacin in most cases.

In the past, the diagnosis of a PDA was made on the basis of physical examination and echocardiography and then the lesion was closed surgically. Catheterization was reserved for those patients with unusual findings or suspected pulmonary hypertension. The development of safe, reliable methods for transcatheter PDA occlusion (15,16,17,18 and 19) has reestablished the importance of catheter techniques in this lesion and brought many more patients, including adults with PDA (Table 34.1), to the catheterization laboratory. Alternatively, the PDA can be closed surgically by the video-assisted thoroscopy (VATS) technique.

PDAs are almost always located off the underside of the aortic arch just distal to the origin of the left subclavian artery, left of the trachea, and proximal to the left main stem bronchus. Most commonly, they have an hourglass shape with a prominent aortic diverticulum and a narrowing near the PA end. Some are cone shaped or arise from an anomalous left subclavian artery in a patient with a right aortic arch.

Physiology

PDAs are rarely large, except perhaps in patients with Down syndrome and those who live at high altitude. The usual “restrictive” PDA is characterized by a measurable step-up in PA blood oxygen saturation, perhaps some pulmonary hypertension, and no change in aortic or RV blood oxygen saturation (Fig. 34.5).

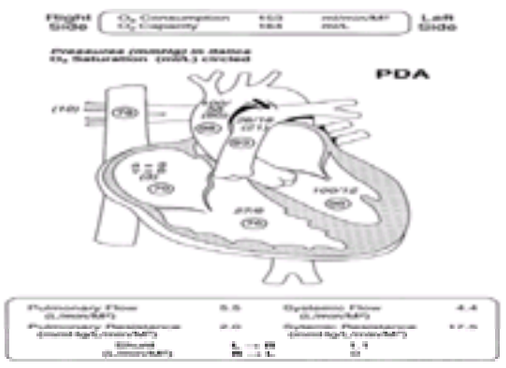

FIG. 34.5. Cardiac catheterization findings in a 2-year-old child with a small patent ductus arteriosus; note the left-to-right shunt at the great vessel level.

The size of the shunt usually does not change much with the passage of time, although the elderly patient with a PDA may tolerate a relatively small shunt poorly. In our experience, patients with small PDAs remain asymptomatic throughout childhood and most of adulthood but are likely to become symptomatic in their sixties and seventies.

Catheterization Technique

The techniques of a standard right-sided heart catheter study estimate the hemodynamic effects of a PDA. Because *in utero* the ductus arteriosus is merely an extension of the main PA, any soft, straight catheter usually passes from the main PA into the descending aorta across the PDA or in the opposite direction from an aortic approach. Transcatheter closure is accomplished either from a venous approach for double-umbrella or coil occlusion or from a retrograde arterial route for coil occlusion.

Oximetry Data

Although it is seemingly straightforward, calculation of the shunt in a patient with a PDA is technically difficult. Because aortic blood crosses into the PA without passing through a mixing chamber, there is considerable streaming in the PAs. Blood sampled from the cephalad portion of the main PA is often fully saturated; left PA blood usually has a higher oxygen saturation than that from the right PA; and a “mixed” PA value cannot be defined accurately. Similarly, in the presence of a right-to-left shunt, descending aortic blood is bluer than ascending aortic blood. Therefore, shunt sizes are estimates at best and do not allow accurate calculation of resistances. If it is necessary to determine (in a patient with a hypertensive PDA) whether closing of the PDA will result in a fall (or a rise) in PA pressure, one must temporarily balloon-occlude the duct and remeasure saturations and pressures.

Pressure Data

Most PDAs do not alter right- or left-sided heart pressures unless they are large. In the face of any left-sided heart abnormalities (e.g., poor LV function, aortic stenosis), a PDA increases LV systolic pressure, LV diastolic pressure, or both.

Angiography

Needed to provide an accurate landmark for transcatheter closure, angiographic definition of PDA is best done in a straight lateral view with contrast material injected distal to the PDA so that it is outlined before the transverse aortic arch (Fig. 34.6).

FIG. 34.6. Lateral aortogram showing a small (2 mm diameter) patent ductus arteriosus (PDA) *(arrow)* in a 2-year-old child. Contrast material has been injected distal to the PDA so that the PDA is outlined before the transverse aortic arch.

Interventional Catheterization

Although a plug and long-wire technique had been used to close PDAs in the catheterization laboratory for more than 20 years by Porstmann and colleagues (20), most workers use coils in small PDAs and a modification of the double-umbrella technique of Rashkind (21) or a Grifka coil and bag (19) in larger ones (see Chapter 28).

Case History 4. A symptomatic 2-year-old girl was seen for evaluation of a loud, continuous murmur in the left infraclavicular area. Her ECG and chest radiograph were normal, and a constrictive PDA was confirmed echocardiographically. At catheterization, a small left-to-right shunt and normal pulmonary resistance were measured (Fig. 34.5), and a small PDA was visualized angiographically (Fig. 34.6). Using a single Gianturco coil delivered in retrograde fashion, the PDA was closed completely with concomitant elimination of the murmur.

AORTIC STENOSIS

Aortic stenosis, the great majority of which occurs at valvar level, remains a common form of congenital heart disease in both children and adults. The advent of Doppler echocardiography has markedly improved the noninvasive assessment of obstruction severity, and therefore the need for frequent diagnostic cardiac catheterizations in patients with this lesion has largely disappeared. In general, catheterization in the patient with valvar aortic stenosis is undertaken for balloon valvotomy, which we recommend whenever cardiac dysfunction appears in the neonate or whenever the peak-to-peak transvalvar gradient (at normal cardiac output) is higher than 50 mm Hg and associated with mild (at most) aortic regurgitation in older children. Rarely, patients have symptoms or ECG changes out of proportion to their estimated transvalvar gradient, prompting a diagnostic catheterization.

Anatomic Types

More than 75% of children with valvar aortic stenosis have a bicommissural valve (rarely, uncommissural) with leaflet fusion. In these cases, absence of the intercoronary commissure is more common than absence of that between the right and noncoronary cusps. Absence of the commissure between the left and noncoronary cusps is extremely rare. If only one commissure is affected, there is little fusion between the cusp edges, and the valve is not thickened, then there may be little gradient or murmur, with the only finding being a constant aortic ejection click at the cardiac apex. Progression of obstruction occurs in one third of those with

valvar aortic stenosis, making careful follow-up mandatory (22).

In a small proportion of patients with congenital aortic stenosis, the obstruction is subvalvar owing to either a thin fibrous ridge or fibromuscular dysplasia of the LV outflow tract. These lesions are progressively obstructive in a large proportion of cases and are known to cause deterioration of the otherwise normal aortic valve, producing aortic regurgitation. Surgery is generally indicated for significant stenosis or symptoms in order to protect the aortic valve, but it is probably best delayed until after the first decade of life to reduce the risk of recurrence.

Finally, some children have an hourglass deformity above the aortic valve, so-called supravalvar aortic stenosis. Caused at least partly by thickening of the supracoronary ridge, supravalvar aortic stenosis is often seen in association with Williams syndrome and with branch PA stenosis.

Physiology

The clinical findings in all three lesions are similar in these patients with uncompromized LV function, except for the absence of an ejection click in subvalvar and supravalvar aortic stenosis. In addition, although patients with supravalvar aortic stenosis usually have large coronary vessels with unobstructed flow, a few have stenosis of a coronary ostium or even occlusion of the orifice by an adherent cusp, with evidence of ischemia.

Catheterization Technique

Most of what has been written about catheterization technique in adults with aortic stenosis (see Chapter 4 and Chapter 5) applies to children with congenital aortic stenosis as well. In addition, congenitally narrowed valves tend to have an opening in the posterior part of the valve, between the left and noncoronary cusps. As a result, once the catheter crosses the valve it tends to pass posterior among the chordae of the mitral valve. Because crossing congenitally stenotic aortic valves can be difficult, we sometimes use a side-arm arterial sheath that is one size larger than the catheter; simultaneous pressures are measured from the catheter and the sheath with the catheter in the ascending aorta to directly measure the amount of pulse delay and pulse amplification. Then, once the catheter is advanced across the valve, a simultaneous measurement of LV and femoral artery pressures allows accurate assessment of the transvalvar gradient and valve area. Beyond infancy, we usually place a second arterial catheter in the ascending aorta via the contralateral femoral artery.

Oximetry Data

There are no oxygen saturation changes in the left or right heart blood in these patients. Indeed, the normal variation in right-sided heart oximetry values was established primarily from children with mild valvar aortic or pulmonary stenosis (7).

Pressure Data

In addition to the simultaneous pressure tracings from the LV and aorta, a pullback tracing across the aortic valve always should be obtained as an internal control. Multihole pigtail catheters are used to enter the LV; a pullback tracing with these catheters may not localize the presence of subvalvar or supravalvar stenosis, making use of an end-hole catheter necessary for this purpose.

Angiography

Both aortography and left ventriculography should be obtained in patients with aortic stenosis. Aortography (usually in anteroposterior and lateral views) assesses the degree of aortic regurgitation, as well as anatomy and mobility of the leaflets and coronary arteries grossly. Ventriculography (LAO with cranial angulation) is used to measure the annulus diameter, to estimate ventricular function, to identify subvalvar pathology, and to further outline valvar and supravalvar anatomy. Multiple views may be required to best outline the subvalvar region, including a right anterior oblique view with caudal angulation.

Interventional Catheterization

Balloon valvotomy (see Chapter 28) has become the treatment of choice for valvar aortic stenosis at our institution. The results are roughly equivalent to those of surgical valvotomy, even in some of our older patients in the fourth decade of life. Although balloon valvotomy may reduce the gradient in some cases of membranous subaortic stenosis, it has been ineffective in most cases in our experience.

Case History 5. An 11-day-old infant was seen with critical valvar aortic stenosis. He was intubated, ventilated, and given PGE_1 to reopen his PDA and improve cardiac output. He was catheterized via an umbilical artery and femoral vein. The hemodynamic data included an elevated LVEDP of 25 mm Hg, a peak systolic ejection gradient of 90 mm Hg across the aortic valve, moderate mitral regurgitation, and a left-to-right atrial shunt. A balloon valvotomy was carried out via the umbilical artery; the peak transvalvular gradient reduced to 37 mm Hg and the LVEDP to 11 mm Hg. Some 5 years later, a second balloon valvotomy was carried out for recurrent obstruction, with reduction of the gradient from 80 to 30 mm Hg via a femoral artery approach with only mild aortic regurgitation resulting. Both the atrial shunt and mitral regurgitation had resolved spontaneously after the initial valvotomy.

PULMONARY STENOSIS

Obstructions to the RV outflow tract usually are seen in association with other congenital lesions, such as TOF, transposition of the great arteries, or single ventricle. Isolated valvar pulmonary stenosis is nonetheless common, although it is frequently an asymptomatic lesion beyond the neonatal period. Noninvasive diagnosis and severity assessment are now accurate in almost all circumstances, and catheterization is reserved for those who require balloon valvotomy, at any age.

Anatomic Types

Valvar obstruction accounts for more than 80% of isolated pulmonic stenosis. In typical valvar pulmonary stenosis the annulus is of normal size, the leaflets are thin, the commissures are fused, and there is marked poststenotic dilation. Dysplastic pulmonary valves exhibit a different pathology: the annulus is small, the leaflets are markedly thickened (usually thicker than they are long), they do not move during systole, and they are fused. In addition, the main PA is short and narrow. A spectrum of anatomic variants exists between these extremes, and all but the most dysplastic valves can be dilated successfully.

RV muscle bundles occur as anomalously thickened bundles of muscle within the RV cavity and are usually associated with other lesions such as VSD or subvalvar aortic stenosis. The pulmonary valve and annulus are generally normal. Unlike other forms of pulmonary stenosis, muscle bundles frequently become progressively more obstructive.

The rarest form of pulmonary stenosis is branch PA stenosis. It is often associated with both supravalvar aortic stenosis and Williams syndrome.

Physiology

Except for anomalous muscle bundles, pulmonary stenosis rarely increases in severity after the first year of life. Severe forms of stenosis in the neonate generally lead to markedly reduced RV compliance with increasing RA pressure and then right-to-left shunting across a PFO. Therefore, critical valvar pulmonary stenosis commonly manifests with cyanosis and sometimes with heart failure. Moderate degrees of stenosis (e.g., gradients of 40 to 80 mm Hg) rarely cause symptoms. However, several studies have shown that patients with moderate pulmonary stenosis have decreased exercise performance at cardiac catheterization, even in childhood (23). On the basis of these studies and because balloon valvotomy is both safe and successful, most cardiologists now recommend dilation in any patient with more than mild stenosis (Fig. 34.7), on an elective basis, before 5 years of age.

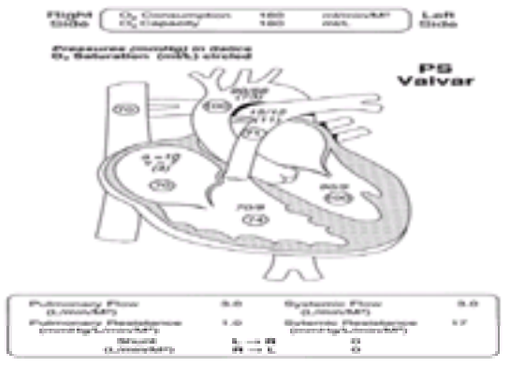

FIG. 34.7. Catheterization data in 5-year-old patient with moderate valvar pulmonary stenosis, with a peak systolic pressure gradient of 55 mm Hg.

Catheterization Technique

The foramen ovale is usually open, allowing catheter access to the left side of the heart from a femoral venous approach. Arterial catheters usually are required only in ill neonates and those with severe or more obstruction. The opening in the pulmonary valve of an infant with severe pulmonary stenosis may be extremely small (less than 1 to 2 mm in diameter) (Fig. 34.8).

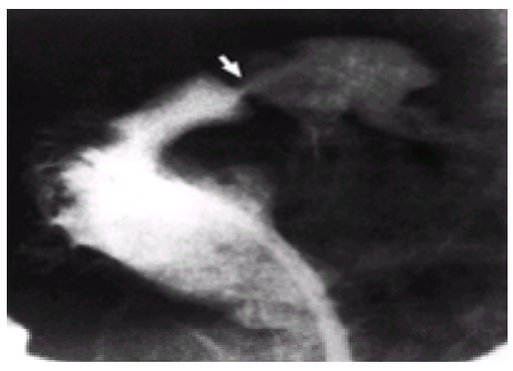

FIG. 34.8. Lateral right ventricular angiogram in a neonate with critical valvar pulmonary stenosis showing contrast jet *(arrow)* through stenotic orifice and poststenotic dilation of main pulmonary artery.

Passage of a standard 5F or 6F catheter across such a valve essentially occludes the orifice, stops pulmonary blood flow, and may result in hemodynamic collapse in less than 1 minute. For this reason, we do not routinely measure PA pressure directly in infants with critical valvar pulmonary stenosis. Rather, we use preformed 4F catheters and a 0.018-inch torque wire to cross the valve, followed by rapid balloon dilation.

Oximetry Data

Most of these patients have neither a right-to-left nor a left-to-right shunt. In critical severe valvar pulmonary stenosis, however, a right-to-left shunt occurs at the atrial level, producing cyanosis. In these patients, the pressure gradient underestimates the severity of the stenosis (because less than a full cardiac output is crossing the pulmonary valve), and the pulmonary venous blood is fully saturated with oxygen (Fig. 34.7). Rarely, one encounters a patient with both mild pulmonary stenosis and an ASD. With a large left-to-right shunt at the atrial level, the gradient across the pulmonary valve is “falsely” elevated. Closing the ASD reduces the RV pressure as well as the gradient across the pulmonic valve.

Pressure Data

In mild pulmonary valve stenosis, the RV pressure is normal. As the degree of stenosis increases, the RA *a* wave increases. With severe pulmonary stenosis, RV systolic pressure approaches or exceeds LV pressure, main PA pressure falls, and the PA pulse pressure dampens. Marked hypertrophy of the RV may cause the infundibular os to close during late systole, resulting in further obstruction.

Angiography

Right ventriculography in a straight lateral view outlines both the pulmonary valve and the subvalvar region (Fig. 34.8).

Although a straight anteroposterior view with cranial angulation also may outline the pulmonary valve, poststenotic dilation of the main PA often obscures the PA branch origins. Following the contrast material temporally until it appears in the LA allows one to rule out an associated ASD. Further angiography is rarely required.

Interventional Catheterization

As noted in Chapter 26 and Chapter 28, balloon dilation, safe and effective at all ages, has become the treatment of choice for this lesion.

COARCTATION OF THE AORTA

Catheterization of the patient with isolated coarctation for diagnostic purposes is rarely required before surgery, because improved noninvasive imaging, including magnetic resonance imaging, allows precise anatomic definition of the lesion. However, the continued incidence of recurrent coarctation after surgical repair, the common association of coarctation with other forms of congenital heart disease (especially VSD, valvar or subvalvar aortic stenosis, and mitral stenosis), and increasing use of balloon dilation in discrete nonoperated coarctation make this a common lesion studied in the laboratory.

Anatomic Types

Virtually all forms of coarctation occur at or just distal to the left subclavian artery, at or near the level of the old ductus arteriosus. Coarctations have discrete “curtains” of tissue indenting the posterior wall of the aorta, although they may be associated with hypoplasia of the transverse aortic arch. Rarely, a coarctation involves a long segment of thoracic or abdominal aorta.

Physiology

The gradient across a coarctation is influenced not only by the degree of obstruction but also by the degree of collateral flow around the obstruction. Collateral flow is carried most commonly by the internal mammary, the intercostal (whose enlargement may eventually produce rib notching), the scapular, and the epigastric arteries. Rarely, an obstruction in the transverse aortic arch produces a cerebral steal from the carotids, through the circle of Willis and down the left vertebral artery.

Upper-extremity hypertension, the primary sequela of a coarctation, usually resolves after surgical correction. In some children, however, hypertension persists despite adequate anatomic repair. This persistent hypertension is more common when repair occurs late in childhood, prompting the general recommendation that

coarctation should be diagnosed and corrected before the child reaches 3 years of age.

Catheterization Technique

Crossing a coarctation is usually straightforward and not hazardous. Occasionally, when catheterizing an older patient with coarctation, one may enter an enlarged collateral vessel thinking it to be the aorta. Complex catheter manipulation in this confined space may prove difficult and even hazardous.

Oximetry Data

Patients with isolated coarctation have no abnormalities in their intracardiac oxygen saturations. Those with associated intracardiac defects (ASD, VSD) have the size of their left-to-right shunt augmented by the coarctation-induced increase in LV afterload.

Pressure Data

Even mild coarctations have a systolic pressure gradient across the coarctation site, although only a minimal diastolic gradient is found. As obstruction increases, a gradient is present throughout the cardiac cycle. The gradient measured by pullback in the catheterization laboratory is frequently smaller than the gradient measured by sphygmomanometer in clinic; although the normal pulse amplification persists in the arms in patients with coarctation, it is frequently absent in the legs, contributing further to the classic finding of diminished femoral pulses on physical examination.

Angiography

A straight lateral aortogram usually provides excellent visualization of the coarctation. If the contrast injection also opacifies the head and neck vessels, an estimate of collateral flow can be obtained. Such estimates are not precise; if the coarctation site is balloon-occluded and pressures are measured in the descending aorta, a more precise estimate of collateral adequacy is available. After surgery has distorted the coarctation site, a lateral aortogram may not define the anatomy well, and various oblique views with cranial or caudal angulation may be needed to define the narrowest site.

Interventional Catheterization

Although balloon dilation frequently reduces the gradient across an unoperated coarctation site, the results (particularly in babies) are not generally as good as those seen with surgical management. However, in thin membranous obstructions beyond infancy, the use of this technique, with care, is increasing and appears effective. Balloon dilation of recurrent coarctation has, however, proved clinically invaluable with or without stent placement.

TETRALOGY OF FALLOT

The association of a malalignment VSD, infundibular and valvar pulmonary stenosis with resultant aortic overriding, and cyanosis is referred to as TOF complex. It remains a difficult and important surgical challenge. Catheterization of infants with this lesion, especially if they are cyanotic, may be hazardous. Therefore, if echocardiographic information is adequate in this age group, surgery is undertaken without catheterization. However, if anatomic details are uncertain, these babies may be studied with great care and with particular emphasis on *not* traversing the RV outflow tract. Beyond infancy, many patients with TOF are still catheterized preoperatively, particularly if pulmonary atresia with aortopulmonary collaterals is present.

Anatomic Types

In addition to the lesions already mentioned, common additional defects include (a) branch PA stenosis (5% to 10%), (b) pulmonary atresia with PDA-dependent pulmonary blood flow (5% to 10%), (c) additional muscular VSDs (5% to 10%), (d) aortopulmonary collateral arteries supplying blood flow to the lungs (5% to 10%), and (e) coronary arterial anomalies, especially the left anterior descending arising from the right coronary artery (1% to 2%). Each of these variables must be assessed accurately and considered before an attempt at operative repair is made.

Physiology

The combination of pulmonary obstruction and a VSD produces a right-to-left shunt at the ventricular level. The size of this shunt is unrelated to the size of the VSD, which in TOF is almost always large and unrestrictive. Rather, the right-to-left shunt and degree of cyanosis are determined primarily by the degree of pulmonary obstruction and less by the level of systemic vascular resistance. So called “tetrad spells” (characterized by hyperventilation, acidosis, extreme desaturation, and unconsciousness) or hypercyanotic episodes may be provoked by increased pulmonary obstruction or decreased systemic resistance, or both; they are best treated by sedation (which may decrease catecholamine tone and lower the level of muscular pulmonary obstruction), intravenous volume infusions, and increasing the systemic vascular resistance.

In general, the anatomic obstruction to pulmonary blood flow tends to increase with time in these patients, thereby increasing the degree of right-to-left shunting. Previously, aortopulmonary shunts such as the Blalock-Taussig shunt were created surgically to increase pulmonary blood flow. Currently, so-called complete cardiac correction, relieving the pulmonary stenosis and closing the VSD, is usually undertaken in infancy or early childhood.

Catheterization Technique

Because a PFO is the rule in these patients, one can enter the left side of the heart from the RA without difficulty. Similarly, one can generally pass the catheter from the RV both to the aorta and into the PA. Catheter passage into the PA, however, often provokes a hypercyanotic spell, and catheter passage from the RV to the aorta often produces transient heart block. Both are to be avoided.

Oximetry Data

Because the VSD is just below the aortic valve in patients with TOF, there are usually no abnormalities in oxygen saturation at the atrial level or the ventricular level. The right-to-left shunt is documented only in the aorta.

Small changes in the degree of RV outflow obstruction or level of systemic resistance have major effects on the arterial blood oxygen saturation measured at catheterization. The latter number may have little relation to day-to-day arterial oxygen saturation, which is often best reflected by the patient's level of blood hemoglobin. If the cyanosis (and hence the degree of RV obstruction) is severe, a right-to-left shunt may be present at the atrial level as well, across a PFO. These atrial shunts are signs of substantially decreased RV compliance and suggest long-standing RV hypertension.

Pressure Data

Almost by definition, RV and LV pressures are equal in patients with TOF. Both atrial pressures are usually normal, as are LV and aortic values. PA pressures (when measured) are decreased in cyanotic patients without prior surgery; in the presence of the surgically created Waterston or Potts aortopulmonary shunts, the PA is often distorted and pressures are elevated even to the level of advanced pulmonary vascular disease, but this is rarely so after Blalock-Taussig shunts.

Angiography

Angiographic definition of anatomic detail (Fig. 34.9) is the key element in the cardiac catheterization of patients with TOF.

FIG. 34.9. Right ventriculogram in tetralogy of Fallot demonstrates subpulmonary valvar stenosis *(open arrow)*, small main pulmonary artery *(white arrow)*, and early filling of the aorta through right-to-left shunting via the ventricular septal defect.

A biplane RV angiogram (with cranial angulation of the anteroposterior camera) establishes the diagnosis, defines the anatomy of the pulmonary valve and subpulmonary region, and identifies the main PA and proximal PA branches. A left ventriculogram in the so-called long axial oblique view but with less LAO, because the ventricular septum runs more straight right to left, outlines the VSD and may identify the coronary artery pattern. An ascending aortogram may be necessary to further delineate coronary artery anatomy, and in particular to identify the origin of the left anterior descending artery. Aortography (especially of the descending aorta) is also often necessary to see whether any aortopulmonary collaterals are present.

Interventional Catheterization

Interventional procedures are rarely required before definitive surgical correction in patients with uncomplicated TOF. However, in infants with TOF, pulmonary atresia, and diminutive PAs, dilation of hypoplastic PAs and coil embolization of aortopulmonary arteries make up an essential component of management. Similar interventional procedures together with PA stent placement are often required postoperatively.

Case History 7. A 36-year-old woman with TOF was seen for evaluation. She had undergone a classic left Blalock-Taussig shunt for cyanosis at 5 years of age and had been lost to cardiology follow-up since that time. She was married, had had three miscarriages but no live children, and worked full-time. On examination she had marked generalized cyanosis and clubbing, a grade 3/6 continuous murmur at the left upper sternal border, and a single second heart sound. Her ECG showed right axis deviation, and both RA and RV hypertrophy were evident. Her hematocrit was 70% and her platelet count 96,000/mm ^{3}. Echocardiographic information was limited because of patient size and poor windows, but a VSD was visualized with predominant right-to-left shunting.

She underwent repeated red cell phereses and then had cardiac catheterization (Fig. 34.10).

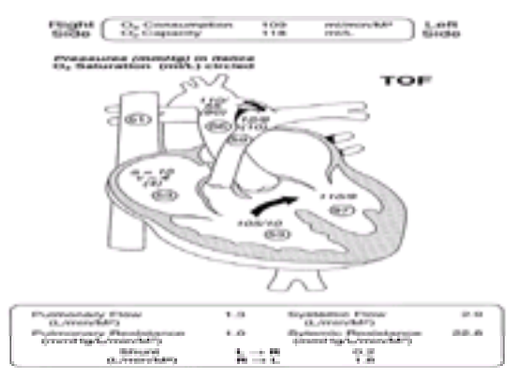

FIG. 34.10. Catheterization findings in a 36-year-old woman with tetralogy of Fallot showing right-to-left shunting at the ventricular level *(larger arrow)*, with aortic saturation lower than the left ventricular value due to streaming, equal ventricular pressures, a 93 mm Hg peak gradient across the pulmonary outflow tract and a left Blalock-Taussig shunt *(smaller arrow)*.

There was right-to-left shunting at the ventricular level via the VSD and a small left-to-right shunt at the PA level due to the Blalock-Taussig shunt. The RV pressure was at the systemic level, a peak gradient of 93 mm Hg was measured across the stenotic RV infundibulum and pulmonary valve, and the PA pressure was low. The Blalock-Taussig shunt was dilated with an 8-mm balloon, resulting in a 5% rise in aortic saturation. TOF was confirmed angiographically, with a single VSD, marked infundibular and valvar pulmonary stenosis, adequate PA size, and normal coronary arteries. Two months later, the TOF was repaired surgically, and at follow-up 1 year later the patient was asymptomatic. There had been a dramatic improvement in her activity level, cyanosis was absent, and a substantial reduction in the degree of digit clubbing had occurred.

TRANSPOSITION OF THE GREAT ARTERIES

In transposition of the great arteries (TGA), the great arteries arise from the wrong ventricles (i.e., the aorta from the RV and the PA from the LV). There are two main types. By far the more common variety is known as dextro-TGA (DTGA); the ventricle position is normal (i.e., the RV is right-sided and the LV left-sided, with the RV giving rise to a right-sided anterior aorta and the LV to a left-sided posterior PA). In the most common form of DTGA, there are no other major anomalies; a smaller number of patients have a VSD in addition, and in the least common variation subpulmonary stenosis is present in addition to the VSD. BAS (24), PGE_1, and, in particular, the introduction of the remarkable arterial switch operation in the first few days of life have made DTGA, with or without VSD, a correctable lesion and no longer a lethal one. The other type of TGA, referred to as levo-TGA (LTGA) or corrected transposition, is much less common. In this anomaly the ventricles are inverted (the so-called L-loop), so that the LV is right-sided and the RV left-sided, with the LV giving rise to a right-sided PA and the RV to a left-sided aorta. This type of transposition is almost always accompanied by a VSD and subpulmonary stenosis, is often by tricuspid regurgitation and atrioventricular conduction abnormalities, and is a very difficult lesion to deal with. The following brief comments are confined to the more common DTGA variety.

Physiology

Unlike the normal circulation, in which blood travels to the lungs and then to the body in sequential fashion, the pulmonary and systemic circulations in TGA run in parallel: Red blood coming back from the lungs returns to the lungs, and blue blood coming back from the body returns to the body. Without a defect in the circulation (e.g., ASD, PDA, VSD) to allow mixing between the two circuits, the patient would die a few minutes after birth. Therefore, the early goal of therapy is to promote mixing between the circulations by making a hole in the atrial septum (BAS) or between the great arteries (using prostaglandins to open the PDA). These measures may stabilize the patient and relieve acidosis, but they relieve the severe associated cyanosis only partially and must be followed within days by an arterial switch operation, together with VSD closure if the VSD is more than tiny in size.

Catheterization Technique

Because echocardiographic definition is so precise, the only reasons to catheterize such neonates are to do a BAS and, in a few, to outline coronary artery anatomy. The umbilical vessels provide the necessary access routes in the majority. The almost invariable presence of an ASD in TGA makes the entire heart accessible to a venous catheter. Nonetheless, catheter entry into the PA, usually unnecessary in the newborn, may be difficult; after the catheter enters the LV from the LA, it must

take a 180° turn, over a short distance, to enter the PA. The use of a tip deflector wire to bend the catheter at the apex of the LV reliably allows PA cannulation.

Oximetry Data

As noted previously, the well-being of the infant before surgical repair is determined primarily by the degree of mixing that occurs between the two parallel circuits. Although the mixing can take place at the atrial, ventricular, or great artery level, its net effect is reflected in the aortic and PA blood oxygen saturations. With perfect mixing, the aortic and PA blood oxygen saturations are equal (at perhaps 82%). As mixing becomes progressively less adequate, the aortic blood oxygen saturation falls and the PA saturation rises (Fig. 34.11).

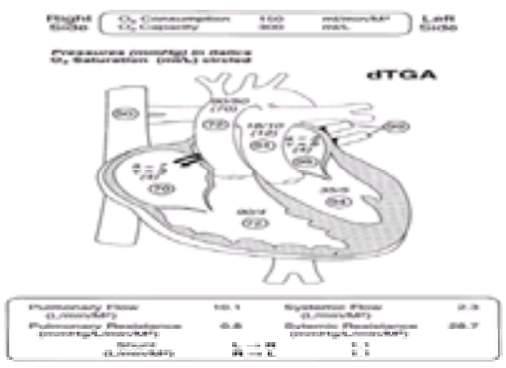

FIG. 34.11. Catheterization findings in an infant with transposition of the great arteries and a small atrial septal defect. There is bidirectional shunting at the atrial level *(arrows)*, arterial desaturation, poor mixing, and a small systolic pressure gradient across the left ventricular outflow tract.

Pressure Data

Because the aorta arises from the RV, the RV systolic pressure is always at least at aortic level. In the early neonatal period, a persistent PDA in many (especially if PGE_1 is being administered) causes the PA pressure (and hence LV pressure) to be elevated. Over the first few weeks of life, both PA and LV pressures fall as the PDA closes, unless there is an associated VSD or pulmonary stenosis. Of note, pulmonary stenosis may be masked if a PDA is present, with a pressure gradient developing only when the PDA closes. LA pressure varies with the degree of LV pressure elevation, the amount of pulmonary blood flow returning to the LA, and the size of the ASD; it commonly exceeds that the RA pressure when the ASD is very small.

Angiography

RV angiography in standard anteroposterior and lateral views establishes the diagnosis, assesses RV function, determines the presence of a VSD or a PDA, and assesses tricuspid regurgitation. An LV angiogram in the long axial oblique view demonstrates the presence and nature of LV outflow tract lesions and demonstrates the location of a VSD.

With the neonatal arterial switch operation now the surgical procedure of choice, the precise definition of coronary arterial anatomy in TGA is mandatory. We use the “laid-back” balloon occlusion aortogram (25) as the angiographic procedure that best outlines coronary arterial anatomy. With the 45° of caudal angulation inherent in this view, the coronary anatomy is displayed in a transverse section, identifying both the cusp origins and branching patterns of these vessels.

Interventional Catheterization

Even though an arterial switch operation is performed electively in the first 10 days of life, we continue to perform a BAS in the early neonatal period (see Chapter 6). Creation of an ASD remains the optimal method for stabilization of these cyanotic infants during the days before surgical repair. Postoperatively, the majority have at most trivial obstruction in the region of the RV outflow–main PA anastomosis, but in some this may be significant together with right PA–and left PA–origin stenosis, this being amenable to balloon dilation/stent placement in some. Significant lesions involving the left heart outflow or coronary arteries are very rare in our experience.

SINGLE VENTRICLE

The term “single ventricle” refers to a family of lesions, often complex and with highly variable anatomy, in which there is only one functional ventricular chamber. All these lesions have the features of a single effective pumping chamber with one or two atrioventricular or semilunar valves. Since the introduction of the Fontan procedure and other preceding palliative procedures such as the Norwood stage 1 and bidirectional Glenn operations, it is clear that this patient population with its evolving problems is rapidly increasing (Table 34.1), as are vascular anomalies as a consequence of these operations.

Anatomic Types

The most common form of single ventricle is the highly lethal hypoplastic left heart syndrome (HLHS), which is usually caused by aortic or mitral atresia. In this syndrome, the LV is diminutive, much too small to sustain life. Although in the past neonates with HLHS uniformly died when the PDA closed, the pioneering efforts of Norwood et al. (26) to create a new aorta surgically, using the RV as a single ventricle, have improved the survival of these children dramatically. A less common but similar condition is tricuspid atresia, in which the right side of the heart is hypoplastic and blood flow to the lungs occurs through a VSD into a small RV. Patients with asplenia and polysplenia syndromes also frequently have single ventricles. Nowadays, after a Norwood stage 1 procedure in babies with HLHS and others palliated with a shunt, a second-stage bidirectional Glenn shunt surgical procedure is performed in the latter half of the first year of life. Subsequently, usually 1 or 2 years later, the Fontan procedure is completed, often leaving a fenestration in the atrial baffle. A year or so later this fenestration, if still patent, is closed with the use of a clamshell double umbrella (27). Therefore, most of these patients are catheterized at least twice electively—between the stage 1 and bidirectional Glenn procedures and between the latter and the Fontan operation—and many a third time after the Fontan surgery. In 1971, Fontan demonstrated that atrial pressure alone was enough to maintain a full cardiac output through the lungs, allowing separation of the systemic and pulmonary circulations in children with single ventricle, which eliminates both the volume load on the heart and the deleterious effects of longstanding cyanosis. The resulting RA pressures are elevated in patients so treated, to 12 to 18 mm Hg, and are generally well tolerated.

Catheterization Techniques

Between the Stage 1 and Bidirectional Glenn Procedures

These patients have in common a pulmonary blood flow supplied by an aortopulmonary shunt, usually a Blalock-Taussig shunt, and the mandatory catheterization information consists of measurement of PA pressure and resistance, intracardiac and aortic pressures, and PA and systemic venous anatomic details. Measurement of PA pressure through the shunt is best accomplished by modifying the tip of a pigtail catheter to a 180° bend. This catheter is advanced from the descending aorta into the mouth of the (usually right) subclavian artery. The soft end of an 0.018-inch torque guidewire is passed from the tip of the pigtail to the distal PA via the shunt; once it is securely in the PA, the catheter is advanced over the guidewire to allow both pressure measurement and angiography. An alternative method of PA pressure estimation is to measure the pulmonary venous wedge value, but this is a reliable approximation only when the PA mean is less than 20 mm Hg. Additional angiography is necessary in the left innominate vein to exclude a persistent left SVC-to-coronary sinus which, if present, must be coil-occluded. This vessel, if present and left patent, will enlarge after a bidirectional Glenn procedure because of the increased SVC pressure, resulting in significant right-to-left flow with subsequent further decrease in systemic arterial saturation.

After the Bidirectional Glenn Procedure and Just Before the Modified Fontan Procedure

Because the SVC has been disconnected from the RA and anastomosed to the PA, another venous line from the left subclavian vein is required in the catheterization of these patients, in addition to femoral venous and arterial lines. As before, the basic information required includes, from all sites, measurement of saturations and pressures together with PA resistance and anatomy. In addition, because SVC pressure has been elevated for some time, venovenous channels may have appeared in many cases, such as left innominate to left and/or right pulmonary vein (Fig. 34.12).

FIG. 34.12. Angiographic demonstration of venous channels from left innominate vein *(black arrow)* to right and left pulmonary veins *(white arrows)* resulting in right-to-left shunting, after a bidirectional Glenn procedure.

There are many variations in the types of such vessels encountered (28), and all require occlusion (usually by coils) when identified. The development of pulmonary arteriovenous fistulas in these patients is increasingly recognized (29) and is considered to be a consequence of the exclusion of hepatic venous blood from the pulmonary circulation by the bidirectional Glenn procedure (Fig. 34.13).

FIG. 34.13. Angiographic demonstration of diffuse punctate arteriovenous fistulas in right lung after a bidirectional Glenn procedure, resulting in dramatic decreases in right pulmonary venous and systemic arterial oxygen saturations.

These are angiographically recognized by their punctate appearance and by the rapid transit (less than three cardiac cycles) of contrast agent through the affected lung to the left PA; they are verified by direct sampling of blood from the appropriate pulmonary veins (29). These lesions are usually too diffuse to attempt coil occlusion, and many appear to regress with time after surgical incorporation of hepatic flow into the pulmonary circuit.

After the Fontan Procedure

Many patients after a Fontan procedure who have not had a fenestration placed in the baffle at the time of surgery and who are doing well are not electively catheterized. There are, however, a significant number who had a fenestration placed who later come to have this communication electively closed with a double-umbrella device (27). There are also others who have cyanosis for some other reason or evidence of congestive heart failure/venous hypertension who require catheterization for diagnostic and interventional purposes. Many of the latter have had earlier types of baffling procedures, such as direct RA-to-PA anastomosis or interposition of valved conduits between RA and RV or RA and PA, these being done before the more recent intraatrial lateral tunnel procedures. In those with a simple fenestration, the studies are straightforward and basically require hemodynamic evaluation (saturation, pressure, and cardiac output measurements) with and without balloon occlusion of the fenestration. If such temporary occlusion is hemodynamically tolerated, the fenestration is occluded with a double-umbrella device. In the others, the catheterizations tend to be very long and complex, and meticulous evaluation of a large and growing list of possible abnormalities with appropriate interventional procedures is necessary. For example, in those with cyanosis, sites of right-to-left shunting may be encountered that result from an ASD, a baffle leak, or a coronary sinus-to-LA shunt, alone or in combination. In those with congestive heart failure/systemic venous hypertension, obstruction may be present in a conduit (Fig. 34.14) or in a branch PA (a 2-mm gradient is very significant), and the latter requires balloon dilation and stent therapy.

In those with the earlier RA-RV or RA-PA anastomoses, the RA may be of enormous size and may compress the right pulmonary veins (30). This is best visualized by magnetic resonance imaging and may require surgical conversion to an atrial tunnel channel. Excessive aortopulmonary collaterals may be present; they may lead to ventricular failure and require coil occlusion. Aortic arch obstructions similarly cause ventricular failure and require dilation and stenting even if gradients are small (e.g., 10 mm Hg). In addition, a few patients have significant subaortic stenosis, a complication that is best managed surgically.

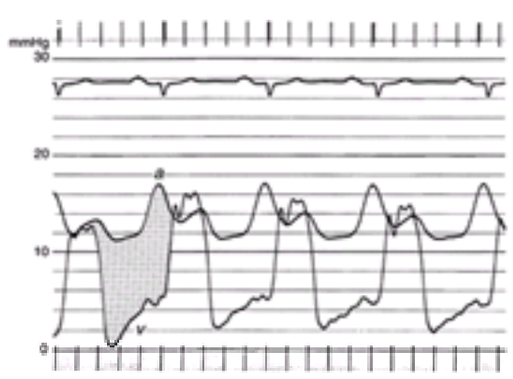

FIG. 34.14. Simultaneous right atrial (*a*)–right ventricular (*v*) pressure tracings across a valved RA-RV conduit placed as part of modified Fontan procedure for tricuspid atresia. Significant obstruction *(shaded area)* is present across conduit.

CHAPTER REFERENCES

1. Lock JE, Keane JF, Fellows KE. *Diagnostic and interventional catheterization in congenital heart disease.* Boston: Martinus Nijhoff, 1987.
2. Rome JJ, Keane JF, Perry SB, et al. Double umbrella closure of atrial defects: initial clinical applications. *Circulation* 1990;82:752.

3. Masura J, Gavora P, Formanek A. Transcatheter closure of secundum atrial septal defects using the new self-centering Amplatzer Septal Occluder: initial human experience. *Cathet Cardiovasc Diagn* 1997;42:388.
4. Rao P, Sideris E, Hausdort G, et al. Interventional experience with secundum atrial septal defect occlusion by the buttoned device. *Am Heart J* 1994;128:1022.
5. Sievert H, Babic UU, Hausdort G, et al. Transcatheter closure of atrial septal defect and patent foramen ovale with the ASDOS device (a multi-institutional European trial). *Am J Cardiol* 1998;82;1405.
6. Nadas AS, Fyler DC. *Nadas' pediatric cardiology.* Philadelphia: Hanley and Belfus, 1992:518.
7. Freed MD, Miettinen OS, Nadas AS. Oximetric detection of intracardiac left-to-right shunts. *Br Heart J* 1979;42:690.
8. Levin AR, Spach MS, Boineau JP, et al. Atrial pressure-flow dynamics in atrial septal defects (secundum type). *Circulation* 1968;37:476.
9. Elliot LP, Bargeron LM Jr, Bream PR, et al. Axial cineangiography in congenital heart disease: II. Specific lesions. *Circulation* 1977;56:1084.
10. Lock JE, Rome JJ, Davis R, et al. Transcatheter closure of atrial septal defects: experimental studies. *Circulation* 1989;79:1091.
11. Rhodes LA, Keane JF, Keane JP, et al. Long follow-up (to 43 years) of ventricular septal defect with audible aortic regurgitation. *Am J Cardiol* 1990;66:340.
12. Roberts JD, Lang P, Bigatello LM, et al. Inhaled nitric oxide in congenital heart disease. *Circulation* 1993;87:447.
13. Bargeron LM Jr, Elliot LP, Soto B, et al. Axial cineangiography in congenital heart disease: I. Technical and anatomic considerations. *Circulation* 1977;56:1056.
14. Bridges ND, Perry SB, Keane JF, et al. Preoperative transcatheter closure of congenital muscular ventricular septal defects. *N Engl J Med* 1991;324:1312.
15. Rashkind WJ, Cuaso CC. Transcatheter closure of patent ductus arteriosus. *Pediatr Cardiol* 1979;1:3.
16. Wessel DL, Keane JF, Parness I, et al. Outpatient closure of the patent ductus arteriosus. *Circulation* 1988;77:1068.
17. Bermudez-Canete R, Giuseppe Santoro G, Bialkowsky J, et al. Patent ductus arteriosus occlusion using detachable coils. *Am J Cardiol* 1998;82:1547.
18. Rothman A, Lucas VW, Sklansky MS, et al. Percutaneous coil occlusion of patent ductus arteriosus. *J Pediatr* 1997;130:447.
19. Grifka RG, Vincent JA, Nihill MR, et al. Transcatheter patent ductus arteriosus closure in an infant using the Gianturco-Grifka vascular occlusion device. *Am J Cardiol* 1996;78:721.
20. Porstmann W, Wierny L, Warnke H, et al. Catheter closure of patent ductus arteriosus: 62 cases treated without thoracotomy. *Radiol Clin North Am* 1971;9:203.
21. Raskind WJ. Transcatheter treatment of congenital heart disease. *Circulation* 1983;67:711.
22. Wagner HR, Ellison RC, Keane JF, et al. Clinical course in aortic stenosis. *Circulation* 1977;56:1.
23. Stone FM, Bessinger FB, Lucas RV, et al. Pre and postoperative rest and exercise hemodynamics in children with pulmonary stenosis. *Circulation* 1974;49:1102.
24. Raskind WJ, Miller WW. Creation of atrial septal defect without thoracotomy. *JAMA* 196;1966;991.
25. Mandell VS, Lock JE, Mayer JE, et al. The “laid-back” aortogram: a new angiographic view for demonstration of coronary arteries in transposition of the great arteries. *J Am Coll Cardiol* 1990;65:1379.
26. Norwood WI, Lang P, Hansen D. Physiologic repair of aortic atresia-hypoplastic left heart syndrome. *N Engl J Med* 1983;308:23.
27. Bridges ND, Lock JE, Castaneda AR. Baffle fenestration with subsequent transcatheter closure: modification of the Fontan operation for patients at increased risk. *Circulation* 1990;82:1681.
28. Magee AG, McCrindle BW, Mawson J, et al. Systemic venous collateral development after the bidirectional cavopulmonary anastomosis: prevalence and predictors. *J Am Coll Cardiol* 1998;32:502.
29. Srivastava D, Preminger T, Lock JE, et al. Hepatic venous blood and the development of pulmonary arteriovenous malformations in congenital heart disease. *Circulation* 1995;92:1217.
30. Kreutzer J, Keane JF, Lock, JE, et al. Conversion of modified Fontan procedure to lateral atrial tunnel cavopulmonary anastomosis. *J Thorac Cardiovasc Surg* 1996;111:1169.

35
Profiles in Aortic and Peripheral Vascular Disease

Stephen R. Ramee, Jose A. Silva, and Christopher J. White

Ochsner Foundation Hospital, New Orleans, Louisiana 70121

The anatomy and interventional approaches to aortic and peripheral vascular disease have been reviewed in Chapter 14 and Chapter 27, respectively. In this chapter, we again take a regional approach to reviewing these diseases, using a series of actual case examples to integrate clinical, noninvasive, angiographic, and therapeutic issues.

AORTIC ARCH AND CAROTID ARTERY ANGIOPLASTY

Vertebral Artery Angioplasty

The indications for revascularization of the vertebral arteries are symptoms of vertebrobasilar insufficiency, namely, dizziness, visual disturbances, and confusion or coma. There is a great deal of variation from patient to patient in the severity of lesions causing symptoms (1). In some patients the degree of stenosis may be severe yet the patient may experience minimal or no symptoms; in others there appears to be adequate flow but profound symptoms are present. The lack of correlation between the degree of stenosis and the clinical manifestations is due to variations in collateral blood supply. The posterior fossa receives blood supply from the contralateral vertebral artery and from the carotid artery system through the posterior communicating arteries. Consequently, when assessing a patient with significant stenosis of a vertebral artery, the interventionist should determine the patency of the contralateral vertebral artery, whether the diseased vertebral artery is dominant, and the amount of blood supplied to the vertebrobasilar system by the carotid arteries.

Depending on the location of the stenosis, treatment options to revascularize the vertebral arteries may include balloon angioplasty with or without stenting (2,3,4,5 and 6), and surgery with transplantation of the vertebral arteries onto the carotid artery, or bypass grafting from the subclavian artery to the vertebral artery (7).

Lesions located in the ostium or the proximal portion of the vertebral artery can be approached percutaneously (2,3,4,5 and 6). As is the case for other aortoostial lesions (saphenous vein grafts, right coronary arteries, or renal arteries), a strategy of endovascular stenting should be strongly considered for ostial vertebral stenoses to minimize the otherwise substantial degree of elastic recoil. Lesions located more distally may be treated with balloon angioplasty with provisional stenting, depending on the angiographic results and the tortuosity of the vessel. Distal vertebral artery lesions are much more difficult to access and more prone to dissection. Lesions proximal to the basilar artery are readily treatable, but those at the vertebrobasilar junction and in the basilar artery have a higher complication rate and are the most prone to dissection, occlusion, and perforation and stroke (8,9 and 10).

In a prospective study from our institution (6), 16 patients and 20 lesions (18 ostial, one in the proximal, and one in the middle portion of the vertebral artery) were treated with 22 stents (8 Palmaz, 5 Crown, 2 NIR, 5 Multi-link, 1 GFX, and 1 Wallstent). The indications for the procedure were as follows: diplopia ($n = 1$), dizziness ($n = 10$), transient ischemic attack of the vertebrobasilar system ($n = 3$), and angiographic stenosis ($n = 2$). Angiographic success (<20% residual diameter stenosis and freedom from in-hospital death, stroke, or emergent surgery) was achieved in 100%. One patient had a transient ischemic attack 1 hour after the procedure that lasted for 5 minutes. Repeated angiography in this patient revealed a widely patent stent without evidence of embolization. At a mean follow-up of 491 ± 387 days, all patients were alive, and 15 of 16 patients (94%) were free of recurrent symptoms. One patient developed symptomatic in-stent restenosis 6 months after the procedure that was successfully treated with balloon angioplasty.

Case 1. A 49-year-old woman presented with six transient episodes of left superior homonymous hemianopsia over a 2-month period. She also complained of episodic dizziness that was orthostatic in nature, without lightheadedness or syncope. Her history was pertinent for hyperlipidemia, systemic atherosclerosis, prior myocardial infarction, coronary artery bypass surgery, and aortobifemoral bypass surgery. Her physical examination revealed a right carotid bruit and a left supraclavicular bruit. Her neurologic examination was normal. A color-flow Doppler examination of the carotid and vertebral vessels revealed no significant carotid stenosis and high velocities at the origin of both vertebral arteries consistent with antegrade flow through a stenosis. She was referred for aortic arch, cerebral, and vertebral angiography and possible intervention.

After pretreatment with clopidogrel and aspirin, diagnostic digital subtraction angiography was performed using a 6F pigtail catheter for arch angiography and a JR4 diagnostic catheter for selective subclavian and carotid angiography. This revealed 80% stenosis of the right vertebral artery, 90% stenosis of the left vertebral artery (Fig. 35.1*A*), and noncritical carotid artery stenosis. There were no significant intracranial stenoses. Left vertebral artery angioplasty was performed using a 6F multipurpose guiding catheter introduced over a 0.035-inch Wholey wire. A 4.0- × 16-mm NIR stent was deployed at 16 atmospheres (atm) over a 300-cm 0.014-inch Extra Support wire. Poststent angiography (Fig. 35.1*B*) revealed no residual stenosis or dissection. The patient had complete resolution of her symptoms at 1-year follow-up.

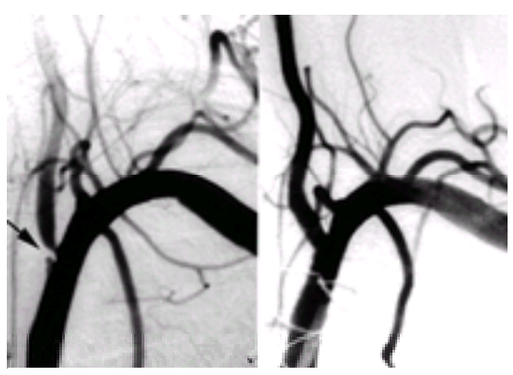

FIG. 35.1. A: Digital subtraction angiography of the subclavian artery through a guiding catheter demonstrating that the left vertebral artery origin (*large arrow*) has a high-grade stenosis with very faint filling of the distal vertebral artery. Notice the location of the left IMA (*small arrow*) just distal and inferior to the origin of the left vertebral artery. **B:** After stenting there is very good filling of the vertebral artery and no residual stenosis.

Illustrative points. The vertebral arteries arise from the right and left subclavian artery just proximal and contralateral to the internal mammary arteries. They converge to the basilar artery, which supplies the brainstem (pons, medulla, and midbrain), cerebellum, and posterior cerebral arteries (supplying the visual cortex). Via the posterior communicating arteries, they may also supply collaterals to the middle and anterior cerebral arteries in patients with critical carotid artery stenosis. For a patient to have intracranial symptomatic ischemia from vertebral or subclavian stenosis, *both* vertebral arteries or the basilar artery itself must be involved. Because the posterior circulation is a dual system, only one artery needs to be treated to relieve the vertebral ischemia. The surgical treatment of symptomatic vertebral artery stenosis has a high complication and failure rate, requires excision and reimplantation of the vertebral artery, and is feasible only for ostial lesions. Angioplasty and more recently, stenting of the vertebral artery can be accomplished using low-profile coronary artery systems that minimize the risk of complications. The acute success approaches 100% and the restenosis rate in our series is less than 10% (6).

Carotid Angioplasty

Most patients with internal carotid atherosclerotic are asymptomatic (11,12). However, even asymptomatic patients with 75% or greater stenoses have a 2% to 5% risk of stroke during the first year. If there is concomitant plaque ulceration, the risk of stroke increases to 7.5% per year (13).

Several large cooperative randomized trials have shown that surgical intervention with carotid endarterectomy (CEA) changes the natural history of this disease when compared with aspirin alone. The North American Carotid Endarterectomy Trial (NASCET) suggested that patients with symptomatic internal carotid artery (ICA) of 50% or greater will benefit from CEA (14). In this trial, the risk of stroke was 26.0% at 2 years (13% per year) for patients with symptomatic stenoses from 70% to 99% treated medically, compared with a 9% risk of stroke in the surgical group during this 2-year period (4.5% per year). This translates into a relative risk reduction of 65% for the surgically treated patients. The Asymptomatic Carotid Atherosclerosis Study (ACAS) found that endarterectomy in patients with an asymptomatic stenosis of 60% or greater resulted in a 5.8% absolute risk reduction of fatal or nonfatal ipsilateral stroke (15) in asymptomatic patients.

A major criticism of the preceding trials is that the inclusion criteria were too rigid, leading to exclusion of most of the patients screened and a failure of the results to represent the “real world.” There are thus a large number of patients with high-risk carotid lesions who would not meet the criteria established for enrollment in those studies and for whom the indications and risks of CEA are not established. In general, these “exclusion” patients have a greater risk from surgery, as evidenced by comparing the published mortality in the NASCET trial (0.6%) with the mortality (3%) among Medicare patients undergoing CEA during the same period (16).

Although the widespread use of balloon angioplasty and stenting is not indicated or recommended for the entire spectrum of carotid occlusive disease, certain subgroups may benefit from this technique. Several studies have been published in which stenting was carried out with a very acceptable degree of safety and with excellent acute and 6-month outcomes (17,18,19,20,21,22,23,24 and 25). This group of patients represents a cohort at high risk for complications with endarterectomy and for whom the efficacy of surgery has not been unequivocally demonstrated (Table 35.1) (22,23,24 and 25).

1. Significant medical comorbidity
2. Recurrent stenosis after carotid endarterectomy
3. Contralateral carotid artery occlusion
4. Radiation-induced stenosis
5. Surgically difficult-to-access, high-cervical stenosis
6. Aorto-ostial lesions
7. Tracheostomy

TABLE 35.1. *Patients at high risk for endarterectomy who are potential candidates for angioplasty and stenting*

Case 2. A 79-year-old man presented with episodic orthostatic lightheadedness without focal neurologic symptoms. He had a history of hyperlipidemia, ischemic cardiomyopathy, coronary artery bypass surgery, chronic atrial fibrillation, a permanent pacemaker, coronary angioplasty, renal artery stenting, and bilateral superficial femoral artery angioplasty. At the time of evaluation he had stable New York Heart Association (NYHA) class II heart failure but no angina. His physical examination was unremarkable, with a normal neurologic examination. Carotid duplex examination revealed 80% to 99% stenosis of the right ICA and 40% to 59% stenosis of the left ICA. Carotid angiography revealed 90% right internal carotid stenosis, 70% right external carotid stenosis, and 50% left internal carotid stenosis. He was referred for carotid angioplasty and stenting.

After pretreatment with aspirin and clopidogrel, and 5,000 units (U) of intraarterial heparin, carotid stenting was performed under a protocol for patients at high risk for carotid endarterectomy. A 9F multipurpose guiding catheter was advanced to the right common carotid over a 300-cm Wholey wire and 125-cm Vitek catheter. Angiography was performed using digital subtraction, in anteroposterior (AP) and lateral views to image the common carotid bifurcation and the cerebral circulation. The right ICA had a 90% stenosis just after the common carotid bifurcation (Fig. 35.2*A*). Some plaque was present in the common carotid and external carotid artery as well. The lesion was crossed with a 0.018 Road Runner (Cook, Indianapolis, IN) wire and dilated with a 4.0-mm × 4.0-cm Cobra balloon. An 8-mm × 2-cm Wallstent was then deployed across the carotid bifurcation. The stent was postdilated to 8 atm using a 5.0-mm × 2-cm Opta-5 balloon (Cordis). Final angiography was performed, including AP and lateral views of the cerebral circulation. There was 10% to 20% residual stenosis at the angioplasty site (Fig. 35.2*B*). The patient's lightheaded spells were no longer present at 6-month follow-up and the stent had no evidence of restenosis by carotid duplex examination.

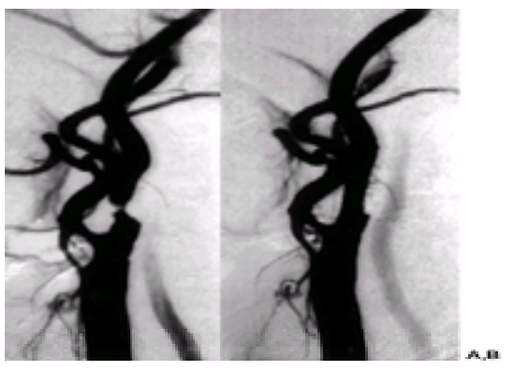

FIG. 35.2. A: A lateral digital subtraction angiogram of the common carotid artery and its branches demonstrates minor plaquing in the common carotid just before the bifurcation and critical stenosis of the right internal carotid artery 1.0 cm beyond the bifurcation. **B:** After stenting there is still 10% to 20% residual stenosis in the internal carotid artery. Overdilating and trying to achieve a perfect result is not recommended because of the risk of distal embolization and stroke. Notice the external carotid artery has minor plaquing and remains patent after stenting across the bifurcation. Note also that it is important to label the films because lateral views of the right and left carotid artery are identical.

Illustrative points. Treatment of both symptomatic and asymptomatic carotid artery stenosis remains an experimental technique. It is already clear, however, from more than 2,000 cases that have been performed in a worldwide registry, that this therapy has an acceptable morbidity and mortality in high-risk surgical patients, with less than 5% major stroke and mortality (25). Unlike coronary artery stenting, the goal is not a perfect angiographic result after carotid stenting. The main risk of this carotid intervention is distal embolization (not abrupt closure or restenosis), so great care is taken to avoid unnecessary manipulation of the carotid artery. Using this technique of underdilation of self-expanding stents, a restenosis rate of less than 10% can be expected (20). There are no reports of complications from covering the

ostium of the external carotid artery using the technique shown. This procedure has also been found to relieve nonfocal neurologic symptoms, such as the dizziness and decreased mentation (i.e., “brain angina”) in a large number of patients at our institution. This suggests that chronic cerebral ischemia can have manifestations other than the classic focal embolic symptoms of transient ischemic attacks and stroke.

Case 3. A 77-year-old man suffered a stroke 4 months previously, with residual left hemiparesis. He has stable angina, prior myocardial infarction, and hyperlipidemia. He previously had radiation therapy to his neck for inoperable laryngeal carcinoma with resultant radiation fibrosis. On physical examination, he continues to have weakness of his left hand, but his leg strength has returned to normal. Carotid duplex examination revealed subtotal occlusion of the right ICA. Angiography revealed 95% stenosis of the right ICA above the bifurcation (Fig. 35.3*A*).

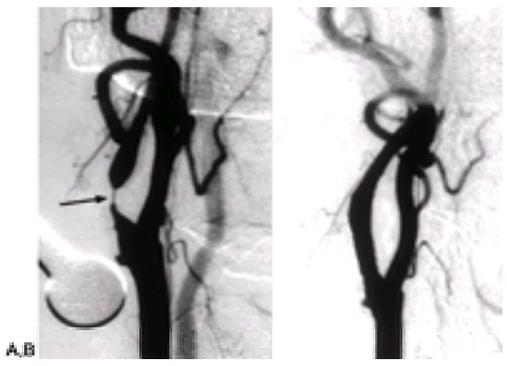

FIG. 35.3. A: Critical stenosis (*arrow*) of the right internal carotid artery demonstrated by digital subtraction technique. The spherical structure in the lower left is a reference ball used for quantitative angiography. **B:** After placement of a self-expanding nitinol stent there is no significant residual stenosis. A slightly irregular appearance is noted at the site of stenting, characteristic of the first-generation nitinol stents. Notice also that because this stent does not shorten appreciably, the lesion can be treated without stenting the carotid bifurcation.

Carotid stenting was performed after pretreatment with aspirin, clopidogrel, and heparin using a 90-cm 7F Cook sheath inserted over a 125-cm 6F JR4 and a 300-cm extra-stiff Glidewire. After advancing the sheath into the common carotid artery, the lesion was crossed with a Road Runner wire and dilated with a 4.0-mm × 4.0-cm Cobra balloon. An 8- × 20-mm self-expanding Smart stent was then deployed at the site of stenosis and dilated with a 5- × 20-mm Opta-5 balloon. Final angiography of the common carotid bifurcation and cerebral vessels was then performed (Fig. 35.3*B*). After the procedure, the patient developed transient hypotension that responded to volume expansion and transient administration of an alpha agonist.

Illustrative points. Patients considered to be at high risk for carotid endarterectomy include those with inaccessible carotid lesions (high internal carotid or aortoostial common carotid), contralateral carotid occlusion, prior ipsilateral endarterectomy, permanent tracheostomy, radiation fibrosis, or high medical comorbidity. These patients are candidates for endovascular therapy using stents. Self-expanding stents are preferred for the carotid bifurcation because of the risk of crushing balloon-expandable stents. The Smart stent is one of a new generation of self-expanding nitinol stents that show great promise in experimental trials. These stents can be delivered through either a 7F sheath or a 9F guiding catheter. The choice of delivery depends on the operator's preference. The nonkinking 7F sheaths have an outer diameter that is approximately the same as a 9F guiding catheter, so the size of the access site is similar. Hypotension after carotid endarterectomy may signify bleeding from the access site but may also result from stretching of the carotid sinus by the stent. This generally responds to volume expansion, although atropine and alpha agonists are employed when volume expansion alone is not sufficient.

Intracranial Angioplasty

Several studies have shown that intracranial disease can be viewed as a marker of extensive cerebrovascular and systemic atherosclerotic disease, particularly coronary artery disease (26). Although the traditional risk factors for development of atherosclerotic disease, particularly tobacco abuse and hypertension, also affect the intracranial circulation (27), some authors have suggested that intracranial atherosclerosis is especially prevalent in African Americans and Asians (28,29).

The incidence of stenotic lesions located in the intracranial ICA, the intracranial vertebrobasilar system, and the proximal middle cerebral artery is less than that of extracranial carotid and vertebral atherosclerosis. In one study from the Mayo Clinic, of 1,000 consecutive patients undergoing angiography, 19% had moderate to severe intracranial ICA stenosis and 29% had mild intracranial ICA stenosis (26). The most common location is the intracranial portion of the ICA (49%) (particularly the intracavernous portion), followed by the middle cerebral artery (20%), posterior cerebral artery (11%), distal vertebral and basilar arteries (11%), and anterior cerebral artery (9%) (30). These lesions are responsible for 5% to 10% of all ischemic strokes (31).

The prognosis of symptomatic patients with intracranial stenosis is well characterized, particularly for lesions involving the ICA and middle cerebral artery. In one study (32), 58 patients with intracranial ICA stenosis were followed for 30 months. Forty-three percent of the patients suffered a cerebrovascular incident or had died at follow-up. Most deaths were due to a cardiac event or stroke. In another study (33), 72 patients with stenosis or occlusion involving the anterior circulation were randomized to medical treatment or extracranial/intracranial bypass surgery. The stroke rate was 36% in the patients randomized to medical treatment and 38% in the patients randomized to surgery. A comparable fate has been observed in patients with symptomatic intracranial lesions of the posterior circulation (34).

Because of the current technical limitations of angioplasty for intracranial stenosis, this form of treatment should be reserved only for patients who have failed medical treatment (10,35,36 and 37). The best medical treatment for this kind of atherosclerotic disease has not been assessed in controlled prospective studies. Based on retrospective data, warfarin appears to be superior to aspirin (34).

Compared with angioplasty of the extracranial carotid and vertebral arteries, angioplasty of the intracranial portion of these vessels is technically more difficult and carries a higher complication rate. Clark et al. (10) reported their results of intracranial angioplasty in 17 patients and 22 vessels. Their procedural success was 82%. There were two strokes during angioplasty, for a 30-day morbidity rate of 9.1% per treated vessel and 11.7% per case. The average preangioplasty stenosis was 72 ± 8% and postangioplasty stenosis was 43 ± 24%. Interestingly, at 6-month angiographic follow-up, further angiographic improvement was observed (37 ± 21%), in eight patients and 12 vessels, suggesting a process of “positive” remodeling. In another study of 12 patients, Terada et al. (8) reported successful results without complications in eight patients (67%). Two patients suffered thromboembolism and two had acute dissection resulting in permanent neurologic deficit in two patients and transient neurologic deficit in the other two patients. At 11 months follow-up none of the 11 surviving patients had experienced a new neurologic event. Stenting of the intracranial carotid has also been reported with encouraging results (38,39 and 40). Whether the new, more flexible coronary stents (Chapter 24) will improve the outcome of angioplasty in the intracranial circulation and change the natural history of the disease will have to be determined in large controlled studies.

Case 4. An 86-year-old man was referred for angiography because of recurrent episodes of lightheadedness and transient ischemic attacks involving weakness of his right upper and lower extremity. On physical examination, he had inability to dorsiflex his right foot and had a remote traumatic amputation of his right arm. Color flow Doppler examination revealed no significant carotid artery lesions. Angiography with cranial angulation revealed 80% stenosis of the left ICA at the siphon with no significant cervical carotid stenosis (Fig. 35.4*A*). Angioplasty was performed on this lesion using coronary equipment (see Chapter 23). A 6F multipurpose coronary guiding catheter was advanced to the ICA just below the first 90° bend. The lesion was crossed with a 0.014-inch hydrophilic wire over which a Transit catheter was advanced to the middle cerebral artery. The wire was exchanged for an Extra Support coronary wire and the lesion was dilated with a 3.5- × 15-mm monorail coronary balloon. Final angiography was performed revealing less than 30% residual stenosis (Fig. 35.4*B*). An abciximab infusion was begun after completion of a successful procedure. The patient had resolution of his transient ischemic attacks (TIAs) and was enrolled in a stroke rehabilitation program.

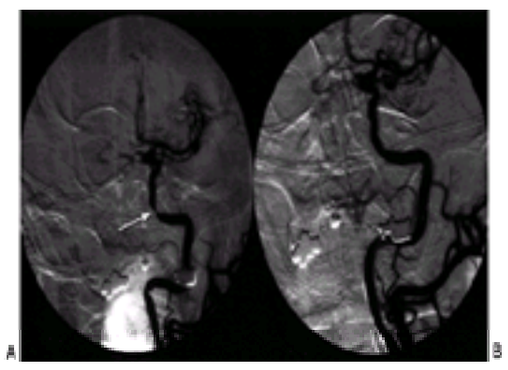

FIG. 35.4. A: Intracranial angioplasty. Left internal carotid artery siphon stenosis before intervention (*arrow*). Notice the artifact in the proximal internal carotid artery caused by a dental prosthesis. **B:** The same vessel after balloon angioplasty with a coronary system showing no significant stenosis.

Illustrative points. Intracranial angioplasty is a field in its infancy where collaboration between neurology, neuroradiology, and the cardiovascular interventionist is important. This case illustrates how patients with recurrent focal symptoms in the same vascular distribution should be referred for angiography even if the duplex examination shows no cervical carotid stenosis. Lesions of the aortoostial common carotid artery and the high internal carotid, including intracranial carotid artery, can be missed by carotid duplex examination. The role of platelet glycoprotein IIb/IIIa receptor inhibitors has some theoretic basis but has not been established in this patient population.

Subclavian and Brachiocephalic Artery Angioplasty

The prevalence of brachiocephalic or subclavian artery stenosis ranges between 12% to 15% of patients undergoing angiography for cerebrovascular symptoms (41). It is usually located in the proximal portion of the vessel before the origin of the vertebral and internal mammary artery and tends to be relatively focal. The left subclavian artery is involved three to four times more frequently than the right. Although atherosclerotic disease is by far the most common cause of subclavian artery stenosis, unusual conditions such as Takayasus's arteritis, fibromuscular dysplasia, giant cell arteritis, radiation-induced occlusive disease, and thoracic outlet syndrome may affect this vessel and cause significant stenosis (42,43,44,45,46 and 47).

The clinical manifestations of subclavian artery stenosis include upper extremity ischemic symptoms with arm claudication related to exercise or resulting from embolization to the digits (48). Subclavian steal syndrome occurs as a result of flow reversal in the vertebral artery, leading to symptoms of vertebrobasilar insufficiency (49,50). In coronary/subclavian steal syndrome, there is reversal of flow in an internal mammary graft as a result of a proximal subclavian stenosis that may cause symptoms of myocardial ischemia (51,52).

Before the advent of percutaneous revascularization techniques, surgery was considered the standard treatment for this condition. Several surgical techniques were used, including transthoracic procedures, carotid/subclavian bypass, and axilloaxillary bypass. However, they all carry significant risk of morbidity and mortality. Hadjipetru et al. (53) recently reviewed the outcomes of 52 surgical studies with 2,496 patients. The technical success was 96% (range, 75% to 100%) and the complication rate was 16 ± 11% (range, 0 to 43%), with a mortality rate of 2 ± 2% (range, 0 to 11%) and a stroke rate of 3 ± 4% (range, 0 to 14%). At a mean follow-up of 51 ± 25 months, recurrence of symptoms occurred in 16 ± 14%.

Balloon angioplasty for subclavian artery stenosis can be carried out with considerable technical success and has been described as a feasible alternative to surgery (54,55,56 and 57). Yet there has been uncertainty regarding distal embolization and patency rates due to inadequate long-term follow-up. When stenting is used in addition to balloon dilation, it may reduce the risk of embolization and achieve anatomically and physiologically superior results. The previously mentioned study of Hadjipetru et al. (53) also summarized the published series of patients treated with stents. Of 108 patients treated with these devices, technical success was obtained in 97 ± 4%. Adverse events were reported in 6 ± 5%. In a multicenter registry involving eight centers, stenting of the subclavian artery was successful in 98.5% of patients and a TIA occurred in only one (0.5%) patient (57).

Based on the current available data, percutaneous revascularization with balloon angioplasty followed by stenting appears to yield superior results with fewer complications than surgery. Until a large prospective randomized trial is carried out, stenting should be considered the treatment of choice with these lesions.

Case 5. A 66-year-old woman presented with a chief complaint of left arm claudication. She stated that she had a history of progressive pain and weakness in her left arm that was associated with the symptom of the room “spinning around her” during left arm exertion. Symptoms were especially prominent while washing the dishes, folding laundry, and using the “butterfly” machine at the gym. She had a history of hypertension, hyperlipidemia, and diabetes. Her blood pressure was 180/90 in the right arm and 130/60 in the left arm. Her left radial pulse was weak. Duplex scanning revealed reversal of flow in the left vertebral artery. Coronary angiography by the referring physician revealed nonobstructive coronary disease. Angiography of the left subclavian artery revealed 90% stenosis of the left subclavian artery proximal to the left internal mammary artery (Fig. 35.5*A*). The vertebral vessel filled in a retrograde manner.

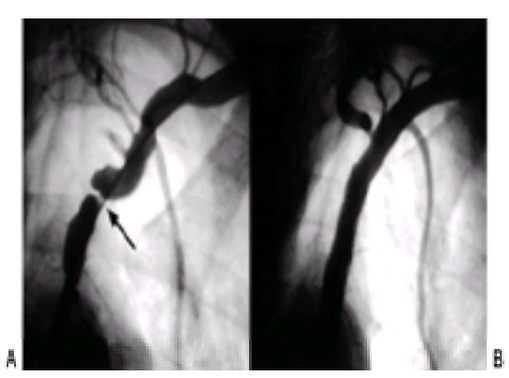

FIG. 35.5. A: Critical stenosis in the left subclavian artery (*arrow*), which supplies both the left vertebral (underfilled) and left internal mammary artery as well as the axillary artery. There is ostial disease in the subclavian artery as well. **B:** After placing tandem balloon-expandable Palmaz stents in the left subclavian artery, there is normalization of flow to the left vertebral and left axillary arteries. The left vertebral has a 50% ostial stenosis that was not treated.

The patient underwent percutaneous intervention using a 9F multipurpose guiding catheter inserted over a 0.035 Road Runner PC wire and a 125-cm long 6F diagnostic multipurpose catheter. The peak translesional gradient was measured to be 50 mm Hg. The lesion was predilated using a 6- × 20-mm Opta-5 balloon. A P204 Palmaz stent mounted on a 7- × 20-mm Opta-5 balloon was then advanced across the lesion and deployed. A second P154 stent was deployed proximal to the first stent using 12 atm inflation. Final angiography was performed revealing restoration of antegrade flow into the left vertebral artery (Fig. 35.5*B*). The pressure gradient across the lesion was abolished.

Illustrative points. Subclavian artery stenosis can present with claudication, critical limb ischemia, or subclavian steal syndrome. This patient's symptoms and examination were classic for the lesion that was found. In patients with prior left internal mammary artery (LIMA) to coronary artery bypass surgery, angina may be the presenting symptom. The surgical treatment of this lesion by carotid to subclavian bypass has a mortality of 5% and a major morbidity (mainly cardiac) of approximately 25%. In a multicenter registry (57) the treatment of these patients with stents has a major morbidity of less than 1% and a restenosis rate of 10%. The same technique is used to perform aortoostial stenting of the carotid and innominate arteries. Balloon-expandable stents are preferred in this location because of the ability to position them precisely at the ostium without compromise of important side branches.

THORACIC AORTIC INTERVENTION

Coarctation of the Aorta

Patients with long-standing coarctation of the aorta have an increased risk for development of coronary artery disease, aortic dissection, and pseudoaneurysm (58). The treatment of native coarctation of the aorta has traditionally been surgical. Although this procedure is effective in obliterating the pressure gradient and relieving symptoms, the incidence of restenosis and aneurysm formation is not negligible, ranging from 5% to as high as 50% (59,63). Percutaneous catheter-based procedures have emerged as a feasible option to surgical treatment in selected patients (see also Chapter 28). Several studies have shown that balloon angioplasty can be carried out with high technical success and few complications (64,65,66,67,68 and 69). Whether balloon angioplasty or surgery is the treatment of choice for native coarctation of the aorta remains controversial, but many investigators agree that balloon angioplasty is a better treatment for postoperative coarctation (70,71).

Most of the published studies found that angioplasty was highly effective in reducing the pressure gradient (64,65,66,67,68,69,70 and 71). In one study of 43 patients in native coarctation of the aorta, pressure gradient was reduced from 69 ± 24 mm Hg before angioplasty to 12 ± 8 mm Hg after angioplasty (65). In three patients (7%) the pressure gradient remained more than 20 mm Hg after the procedure. There were no procedural deaths but 7% developed a local aneurysm at follow-up (range, 1 to 10 years). Recurrence coarctation developed in 7% at 12-month angiographic follow-up. In another study of 90 patients with recurrent coarctation, pressure gradient was reduced from 31 ± 21 mm Hg to 8 ± 9 mm Hg (68). There were two neurologic events and one death. In 11 patients (12%), the procedure did not reduce the pressure gradient to less than 20 mm Hg (procedure failure). At 12-month follow-up, 72% remained free from the need for reintervention. Other investigators have not found significant differences in treating native or recurrent coarctation with balloon angioplasty (69).

The use of endoluminal stents to minimize the elastic recoil, improve the immediate hemodynamic results, and possibly decrease the recurrence of coarctation has been investigated, although the experience is still limited (72,73). In one study (73), nine patients were treated with stenting. (Seven patients had had previous operation or balloon dilation.) Reduction in gradient across the coarctation and increase in diameter of the narrow segment occurred immediately after stent implantation. At a median follow-up of 13 months, residual gradient across the stented segment remained low in 8 patients. One patient required redilation of the stent.

Indications for the use of endoluminal stents in coarctation of the aorta are yet to be determined, but on the basis of this limited but encouraging experience it has been suggested that potential indications for these devices include hypoplasia of the isthmus or transverse aortic arch; tortuous coarctation with misalignment of the proximal with distal aortic segment, which are difficult to treat surgically; and recurrent aortic coarctation or small aneurysm after previous surgical or balloon therapy (74).

Case 6. A 41-year-old woman who had undergone coarctation repair at the age of 2 years now presents with hypertension, congestive heart failure, and decreasing ejection fraction over time. Despite treatment with digitalis, diuretics, and ACE inhibitors she continues to have NYHA class II heart failure. Her examination was remarkable for a systolic bruit between her scapulae, a gradient of 40 mm Hg between her arm and leg blood pressure, and weak but symmetric pulses in her lower extremities. Catheterization revealed a 70% stenosis in the aorta just distal to the left subclavian artery with poststenotic dilatation (Fig. 35.6*A*) and 35-mm peak systolic gradient across the coarctation. Intravascular ultrasound demonstrated the aorta to measure 17 mm in diameter proximal to the coarctation and 25 mm in diameter distal to the coarctation. The coarctation was dilated with a 16 mm × 4.0 cm XXL balloon with a 0.035-inch Amplatz extra stiff exchange wire advanced through a 90-cm-long 10F sheath. Intravascular ultrasound (IVUS) demonstrated significant recoil with dissection and persistent gradient of 18 mm Hg, so that a P308 stent was deployed at 8 atm using the same balloon. Angiography (Fig. 35.6*B*), IVUS, and pressure gradients all confirmed correction of the coarctation.

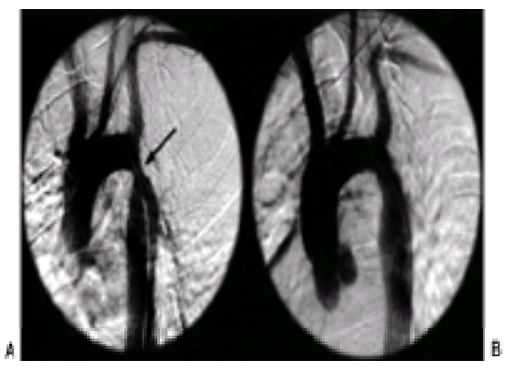

FIG. 35.6. A: A typical coarctation just distal to the left subclavian artery seen by digital subtraction angiography with a pigtail catheter located in the aortic arch. **B:** After stenting with a balloon-expandable P308 Palmaz stent there is no residual stenosis compared with the isthmus (proximal part) of the coarctation. It is important to size the balloon by measuring the vessel proximal to the coarctation rather than distal to reduce the risk of the serious complications of dissection and rupture.

Illustrative points. Coarctation of the aorta usually presents with hypertension proximal to the coarctation and symptoms related to hypertension. In this patient with long-standing coarctation, congestive heart failure had resulted from chronic pressure overload. When treating coarctation of the aorta with endovascular techniques, IVUS is recommended to size the vessel and to avoid overdilation of the aorta, which can lead to serious dissection, rupture, or even death. Self-expanding stents tend to migrate into the distal ectatic aorta rather than remain in the narrowed coarctation, so balloon-expandable stents are recommended. The maximum diameter that a P308 stent can be expanded to is 16 mm, and considerable shortening occurs at this diameter, so careful positioning is important. Postsurgical correction coarctations are less likely to develop dissection and rupture with balloon angioplasty than virgin coarctations.

Endoluminal Thoracic Aneurysm Repair

The prevalence of thoracic aneurysms in the United States is difficult to determine because of underreporting of these aneurysms in mortality statistics. In Sweden, in a stable urban population with an autopsy rate of 83%, the incidence of thoracic aortic aneurysm between 1958 and 1985 was 489 per 100,000 autopsies in men 65 years of age and 670 per 100,000 autopsies in 80-year-olds (75).

The prognosis of patients with untreated thoracic aneurysms is poor. In three large studies that included 264 patients with thoracic aneurysms who did not undergo surgery at the time of diagnosis, rupture of the aneurysm was the most common cause of death, ranging from 42% to 70% of the patients (76,77 and 78). In these series of patients, the 5-year survival rate ranged from 13% to 39%.

In general terms, patients with aneurysms larger than 5.0 to 5.5 cm in the ascending aorta, larger than 5.5 to 6.0 cm in the aortic arch, or larger than 5.0 to 6.0 cm in the descending aorta should undergo surgical intervention (79).

Because of the high prevalence on cardiovascular disease and the age of this patient population, surgical treatment carries a significant mortality, which can be as high as 12% when the procedure is performed electively or as high as 50% when the procedure is performed emergently (76,80). Similarly, brain infarction and spinal cord injury are not infrequent complications of surgical treatment (79).

Endovascular stent-grafts have been described as an alternative to surgical treatment for descending aortic aneurysms in selected patients (81,82). Dake et al. (82) reported their experience in 13 patients with descending thoracic aortic aneurysm with a mean diameter of 6.1 cm (range, 5 to 8 cm). Technical success was obtained in all 13 patients. There were no deaths, paraplegia, or stroke at 11.6 months of follow-up. There was complete thrombosis of the thoracic aortic aneurysm surrounding the stent-graft in 12 patients, and one patient with extensive chronic dissection required open surgical graft replacement because of progressive dilation of the arch. The authors added that since the time of the submission of their paper until the time of its publication, 20 additional patients with 23 thoracic aneurysms underwent endovascular stent-grafts. In 21 cases, the procedure was successful. Two patients died of multiorgan failure, and one of the deaths was preceded by paraplegia.

Although the experience is still limited, endovascular stent-grafts appear a promising alternative to surgery for the treatment of thoracic aortic aneurysms in selected patients.

Case 7. A 58-year-old man was referred with an asymptomatic 6-cm saccular descending thoracic aneurysm (Fig. 35.7*A*). He was treated by endovascular means using a femoral cutdown and a self-expanding nitinol endoluminal graft during a procedure that lasted under on hour. Following deployment of the graft, there was still a bulge of graft material into the aneurysm due to a lack of external support on the graft; however, there was no evidence of leaking (Fig 35.7*B*).

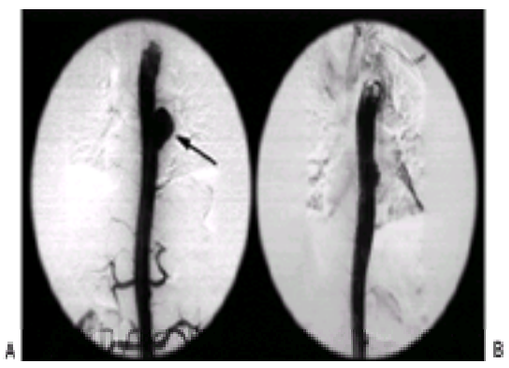

FIG. 35.7. A: Digital subtraction aortography of the descending thoracic aorta demonstrates a saccular aneurysm (*arrow*). **B:** After placement of an oversized, self-expanding endoluminal graft, there is no evidence of graft leaking. There is ectasia at the site of the aneurysm caused by expansion of the prosthesis into the aneurysm. This appearance is expected. Oversizing is necessary with self-expanding stents and endoluminal grafts to ensure good appostition of the stent or graft to the vessel wall.

Illustrative points. Although this is a very promising and exciting area for endovascular intervention, the nonsurgical treatment of these aneurysms is still in its infancy. Because standard surgical repair carries with it a high morbidity and mortality, as stated earlier, investigators are anxiously awaiting the development of an endovascular solution to this problem. Of note, the most likely cause of this type of saccular aneurysm of the thoracic aorta is infection, especially salmonellosis, not atherosclerosis.

CELIAC AND MESENTERIC ARTERY ANGIOPLASTY

Chronic mesenteric ischemia has been recognized as an uncommon but unequivocal cause of chronic abdominal pain. Although its prevalence is approximately one case in 100,000 (83), its lethal nature requires vigilance and a high clinical suspicion. The mesenteric circulation includes three arteries: the celiac trunk, the superior mesenteric artery (SMA), and the inferior mesenteric artery (IMA). The stomach and upper half of the duodenum comprise the foregut and are supplied by the celiac trunk. The lower half of the duodenum, jejunum, ileum, cecum appendix, ascending colon, and proximal two-thirds of the transverse colon comprise the midgut and are supplied by the SMA. The distal third of the transverse colon, sigmoid colon, descending colon, sigmoid colon, rectum, and the upper part of the anal canal comprise the hindgut and are supplied by the IMA.

There is significant communication among these three vessels and significant collateral flow to the mesenteric circulation from other aortic branches (such as the lumbar intercostal, middle sacral, mammary, and internal iliac arteries). Because of this, the clinical syndrome of chronic mesenteric ischemia usually develops as a result of critical stenosis or occlusion of more than two of the celiac artery, SMA, or IMA. More than 90% of the cases of chronic mesenteric ischemia are due to atherosclerosis, usually extensions of aortic atheroma rather than intrinsic disease of the mesenteric branches.

Abdominal pain is the most frequent symptom, with some series reporting this manifestation in up to 100% of the patients (84,85 and 86). Other symptoms include weight loss, diarrhea, nausea, vomiting, and constipation. The abdominal pain is usually crampy, localized in the epigastrium or middle abdomen. More than 80% of the patients note the relationship of pain with caloric intake (85,86). A significant percentage of patients may have concomitant coronary or peripheral vascular disease, which may make the clinical presentation confusing (87).

The traditional treatment for chronic mesenteric ischemia has been surgical. Because stenosis of the mesenteric branches is frequently focal, limited to the ostium and/or the very proximal portion of the vessel, percutaneous, catheter-based techniques of revascularization have been explored and appear to be an alternative to surgery in selected patients. An analysis of 11 published studies with 126 patients treated with balloon angioplasty (88) revealed a mean initial technical success of 86% (range, 38% to 100%). After exclusion of technical failures, the clinical success rate (resolution of symptoms) was 90%. At a mean follow-up of up to 101 months the primary and secondary clinical success was 76% and 92%. Major complications occurred in 6% of the patients, and the 30-day mortality was 3%.

Endovascular stenting of the mesenteric branches has rarely been reported but appears to be safe and effective in selective patients. In a study from our institution (89), 11 vessels (five SMA and six celiac arteries) of eight patients with chronic mesenteric ischemia were treated with Palmaz-Schatz stents. Clinical success (<30% diameter stenosis and relief of symptoms without in-hospital need for surgical revascularization or death) was obtained in 100% of the patients. There were no significant procedural complications. Two patients died of cardiovascular causes after discharge. At a mean follow-up of 11.5 ± 7.6 months, all survivors (six patients) were asymptomatic. Although experience is still limited, catheter-based techniques of revascularization such as balloon angioplasty with or without stenting appears a promising alternative to surgical intervention in selective patients with chronic mesenteric ischemia.

Case 8. A 69-year-old man presented with a 9-month history of postprandial midepigastric pain with a 50-pound weight loss. He denied anorexia but had essentially stopped eating to avoid the recurrence of the pain. On examination, he was cachectic, weighed only 120 pounds, and appeared chronically ill. He had bilateral carotid bruits, an epigastric bruit, and diminished tibial and dorsalis pedis pulses bilaterally. An extensive gastrointestinal workup was negative, including upper and lower endoscopy; small bowel follow-through; computed tomographic scan of the abdomen; ultrasound of the gallbladder, liver, and spleen; complete blood count; and serum chemistries. He denied cardiac symptoms and had quit smoking 10 years earlier. He was referred for abdominal aortography and selective celiac and mesenteric angiography, which was performed via percutaneous brachial artery entry. The superior mesenteric artery and inferior mesenteric artery were occluded.

Figure 35.8*A* demonstrates high-grade stenosis of the celiac trunk, engaged with a 6F multipurpose catheter. This lesion was crossed with a Wholey wire, and a 6 × 20 Opta-5 balloon was advanced through a multipurpose guiding catheter and used to predilate the lesion. A P154 Palmaz stent was then deployed mounted on this same balloon. After deployment, the stent was postdilated with a 7- × 20-mm Opta-5 balloon at 12 atm. Final angiography (Fig. 35.8*B*) demonstrated no residual stenosis. The gradient was reduced from 60 mm Hg to less than 5 mm Hg. The patient's symptoms were immediately relieved, and by 2 months later he had regained 20 pounds.

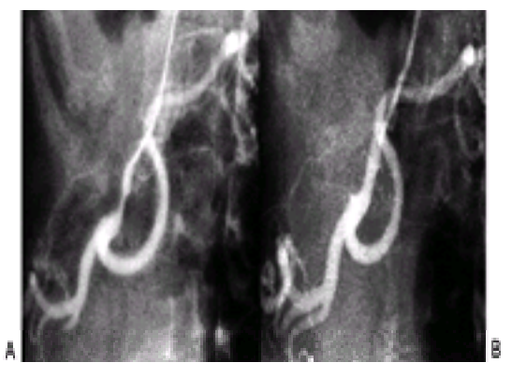

FIG. 35.8. A: Angiography of the celiac artery demonstrating high-grade stenosis at the origin (*arrow*) before intervention. **B:** After stenting, there is no residual

stenosis. The stent is placed so that several millimeters of stent extend into the aorta, because this is an ostial lesion.

Illustrative points. This is a classic case of chronic mesenteric ischemia. The diagnosis is usually missed in the early stages because of the myriad causes of abdominal pain. Profound weight loss with postprandial abdominal pain is the hallmark of this condition. Symptoms do not usually occur unless there is stenosis or occlusion of two or more of the three vessels (celiac, SMA, IMA). The traditional management of this condition has been surgical; however, mesenteric ischemia lends itself very nicely to an endovascular approach, because the lesions are usually ostial and ideal for balloon-expandable stents. Furthermore, by the time the diagnosis is made, the patients are usually cachectic and not ideal surgical candidates. Because of the high flow in these vessels, the poststent medical regimen consists of aspirin alone.

RENAL ARTERY ANGIOPLASTY

Renal artery stenosis is common in patients with known coronary or peripheral atherosclerotic disease (90,91). In one study of 196 patients undergoing cardiac catheterization for presumptive coronary artery disease, the prevalence of significant (>50%) renal artery disease was 18%, and when coronary artery disease was confirmed in 152 patients, the prevalence was 22% (90). Some investigators have reported a prevalence of renal artery stenosis of more than 60% in patients with concomitant peripheral vascular disease and hypertension (92). For this reason in many cardiac catheterization laboratories, including ours, screening renal angiography is routinely performed in patients undergoing cardiac catheterization for atherosclerotic coronary disease.

Significant hemodynamic obstruction of the renal blood flow causes renovascular hypertension. This activates the renin angiotensin system leading to excessive production of angiotensin II, which in turn causes systemic hypertension and fluid retention. The diagnosis of renovascular hypertension should be suspected in patients with onset of hypertension at the ages of less than 35 years and more than 55 years, malignant or refractory hypertension, renal failure, resistant hypertension, coronary or peripheral atherosclerosis, an abdominal bruit, and a unilateral small kidney, and in patients who develop azotemia with ACE inhibitor therapy (93). These groups should undergo a noninvasive screening test to rule out this entity. The noninvasive test of choice for making the diagnosis of renal artery stenosis is the renal duplex ultrasound examination (94). Although captopril renal artery scintigraphy is a sensitive and specific test to demonstrate unilateral renal artery stenosis (95), the incidence of a false-negative test is substantial in patients with parenchymal disease or bilateral renal artery stenosis, which occurs in approximately one-third of the patients. Renal vein renin assays have been used in the past, and because many antihypertensive medications such as beta blockers may interfere with the release of renin, the need to withhold these medications prior to the test makes it impractical as a routine examination (96).

Surgical revascularization of atherosclerotic renal artery stenosis is an effective treatment for renovascular hypertension (97). Nevertheless, it carries an operative mortality of up to 3% as well as complications such as bypass graft thrombosis and nephrectomy in up to 4% of the cases (98,99). Percutaneous transluminal renal angioplasty is the treatment of choice for fibromuscular dysplasia (100,101 and 102) and is an accepted treatment for selected patients in whom renal artery stenosis is causing renovascular hypertension and/or renal insufficiency (100,103). However, atherosclerotic aortoostial renal artery lesions are particularly difficult to treat with balloon angioplasty alone because they are prone to significant vascular recoil, leading to a restenosis rate of approximately 50% over 6 months (104). On the other hand, endovascular stents have the capacity to scaffold dilated lesions and minimize the elastic recoil. Several studies have shown a significantly greater acute gain in luminal diameter and better angiographic results with renal artery stenting than with balloon angioplasty alone (105,106 and 107). In a study of 76 patients and 92 renal arteries treated with primary stenting, technical success was obtained in 100%, with a restenosis rate at 6 months of 25% (106). Blum et al. (108) treated 74 renal artery stenosis with endovascular stents. Technical success was achieved in 100% of the vessels, and the restenosis rate at 12-month follow-up was 11%. The renal function remained unchanged in all patients, but 62% of the patients had significant improvement of blood pressure, including 16% in whom the blood pressure normalized. In another study, balloon-expandable stents were placed in 100 patients and 133 renal arteries (109). Angiographic success was obtained in 132 of 133 (99%) of the lesions. At 6-month follow-up the systolic blood pressure was reduced from 173 ± 25 to 147 ± 12 mm Hg ($p < 0.001$) and the diastolic blood pressure was reduced from 88 ± 17 to 76 ± 12 mm Hg ($p < 0.001$). At a mean angiographic follow-up of 8.7 ± 5.0 months, the restenosis rate was 19%. Renal function after stent placement showed a small but statistically significant decline in blood urea nitrogen but no significant change in serum creatinine.

Stenting for renal artery stenosis also appears to have a beneficial effect in patients with refractory unstable angina and congestive heart failure (110). In 48 patients with unstable angina ($n = 23$) or congestive heart failure ($n = 25$) who had hypertension refractory to medical therapy and significant unilateral ($n = 30$) or bilateral ($n = 18$) renal artery stenosis, stenting significantly improved the blood pressure and functional class at 24-hour and 6-month follow-up. The dramatic improvement seen in this very sick group of patients was independent of a coronary angioplasty procedure.

In conclusion, the incidence of renal artery stenosis in patients with poorly controlled hypertension and atherosclerotic cardiovascular disease ranges from 20% to 30%. These patients should be identified at the time of diagnostic cardiac catheterization. The treatment of renal artery stenosis has a dramatic impact in the hypertension control and appears to have a beneficial effect in the treatment of refractory unstable angina and congestive heart failure. Considering the treatment alternatives for atherosclerotic renal artery stenosis causing medically refractory hypertension and/or renal insufficiency, stent placement is the current treatment of choice.

Case 9. A 68-year-old man underwent diagnostic coronary and renal angiography because of hypertension and congestive heart failure. His blood pressure was 185/90 on three antihypertensive medications and his blood urea nitrogen (BUN) and creatinine were normal. Renal color flow duplex examination demonstrated unilateral left renal artery stenosis. Angiography demonstrated moderate three-vessel coronary disease, an ejection fraction of 45% with global hypokinesis, and elevated left ventricular end diastolic pressure. Selective renal angiography performed at the time of coronary angiography with a 6F IMA catheter revealed high-grade unilateral left renal artery ostial stenosis (Fig. 35.9*A*). Renal angioplasty and stenting were performed using a soft, steerable 0.035-inch wire, an Opta-5 balloon, an 8F hockey stick guiding catheter, and a P154 Palmaz stent. The wire was positioned through the diagnostic catheter; then the balloon and guiding catheter were advanced to the lesion as a unit. The lesion was predilated with the balloon and the guiding catheter was carefully advanced into the renal artery to facilitate stenting. The balloon was withdrawn and the stent was mounted between the balloon markers. The stent was then advanced across the lesion and the guiding catheter was withdrawn into the aorta before stent deployment (Fig 35.9*B*). The sheath was removed 2 hours later and the patient was discharged the following morning.

FIG. 35.9. A: Typical appearance of an aortoostial renal artery plaque (*arrow*) causing renovascular hypertension. An internal mammary artery, Cobra 1, or Simmons 1 catheter will usually engage the renal ostium for angiography and guidewire passage without causing atheroemboli. Use of a guiding catheter to engage the renal artery is discouraged. **B:** After stenting there is no residual stenosis.

Illustrative points. Unilateral renal artery stenosis may cause hypertensive heart disease and heart failure because of diastolic dysfunction. In the elective patient, renal color flow Doppler examination is recommended before angiography in institutions that can perform high-quality diagnostic studies. The management of diastolic dysfunction and congestive heart failure is facilitated by treatment of the renal artery stenosis. Currently, an 8F guiding catheter is required to place balloon-expandable renal stents. The average diameter of a single renal artery is 5 to 6 mm, but vessels as large as 8.0 mm and as small as 3.0 mm can be found. Patients with dual or triple renal arteries on one side often have vessels that are less than 3.0 mm in diameter. Although predilatation is always recommended for

these ostial lesions, atherectomy is rarely required.

Case 10. A 77-year-old female with known coronary artery disease and angina has a history of long-standing hypertension and diastolic dysfunction. Despite three antihypertensive medications, her blood pressure was 200/95. Her physical examination and laboratory data were normal. A color flow duplex Doppler examination suggested unilateral right renal artery stenosis. At the time of diagnostic coronary angiography, renal angiography was also performed; this revealed fibromuscular dysplasia of the middle right renal artery and ostial atherosclerosis (Fig. 35.10*A*). Balloon angioplasty was performed on the area of fibromuscular dysplasia with a 5.0-mm balloon and 0.035-inch Wholey wire. The ostium was treated with a balloon-expandable stent (Fig. 35.10*B*). She was discharged the next morning on only one antihypertensive medication with a blood pressure of 145/70 mm Hg.

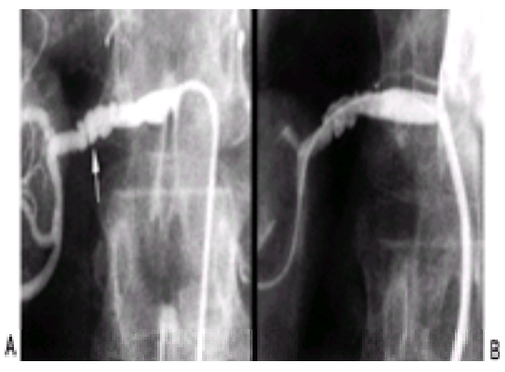

FIG. 35.10. A: This patient has both atherosclerotic ostial stenosis and fibromuscular dysplasia. The typical appearance of fibromuscular dysplasia (*arrow*) is a corrugation of the vessel. This is diagnostic of fibromuscular dysplasia but not of renovascular hypertension (see text). **B:** The corrugated appearance of the vessel does not change after balloon angioplasty; however, the ostial lesion has been successfully stented. Stenting of the fibromuscular disease is reserved for persistent hypertension after balloon angioplasty.

Illustrative points. Fibromuscular dysplasia (FMD) is commonly found in young adults, especially women, but the condition can persist into later life. This interesting case illustrates the combination of two classic lesions: atherosclerotic renal artery ostial stenosis and FMD of the middle renal artery. The angiographic appearance of a corrugated vessel is diagnostic of FMD, and the renal artery is the most common location for this abnormality. The finding of fibromuscular dysplasia is not diagnostic of renovascular hypertension, but the noninvasive screening tests and selective renal vein renin analysis also lack sensitivity and specificity for this condition. In a patient with FMD who is hypertensive despite medical therapy, balloon angioplasty is indicated and the lesion usually responds to balloon angioplasty without the need for stenting. Ostial renal artery stenosis due to atherosclerosis does not respond to balloon angioplasty and does require stenting. In this hypertensive patient, both treatments were utilized to treat the specific lesions that were found with clinical success.

Case 11. A 77-year-old man who had had coronary bypass surgery was referred for coronary angiography because of unstable angina. He was noted to have hypertension with recent onset, so renal angiography was also performed at the time of coronary angiography. His renal function was normal. He was found to have critical stenosis in the LIMA to left anterior descending (LAD) coronary artery and critical right renal artery stenosis (Fig. 35.11A). Combined coronary and renal angioplasty was performed. The LIMA to LAD was dilated and stented using coronary equipment. The left renal artery was predilated with a 6- × 20-cm Opta-5 balloon, advanced through an 8F hockey stick guiding catheter over a Wholey wire. The guiding catheter was positioned across the lesion, and a P154 Palmaz balloon-expandable stent was introduced. After pulling the guiding catheter back into the aorta and careful positioning of the stent at the renal artery ostium, it was deployed at 12 atm (Fig. 35.11B). The patient was discharged the following morning without angina and with control of his hypertension on no medications.

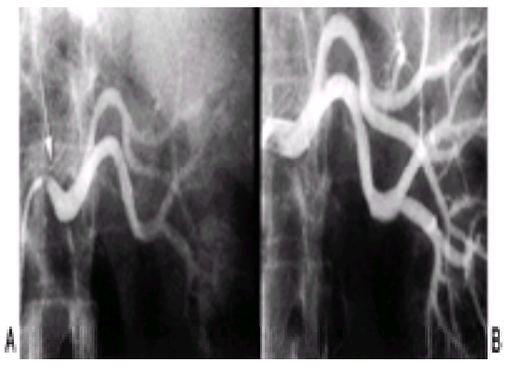

FIG. 35.11. A: Atherosclerotic left renal artery stenosis (*arrow*) before intervention. **B:** After stenting there is no residual stenosis. Note that the preangioplasty angiogram is performed through the diagnostic catheter before passing the Wholey wire. The poststent angiogram is performed through the 8F guiding catheter.

Illustrative points. Renal stenting can facilitate the management of angina pectoris by controlling hypertension. In patients with combined coronary and renal atherosclerosis and normal renal function, both coronary and renal lesions can be treated at one time. In patients with renal dysfunction, selective renal angiography and stenting are performed first. The patient then returns for staged coronary intervention in 24 to 48 hours after the renal function has improved or normalized. Unilateral renal artery stenosis does not cause renal dysfunction, because the contralateral kidney can still function normally. In patients with hypertension and renal insufficiency, either bilateral renal artery stenosis or parenchymal disease (i.e., nephrosclerosis) is usually present.

Case 12. A 73-year-old man was referred for evaluation and treatment of uncontrolled hypertension and ischemic cardiomyopathy with congestive heart failure. His blood pressure was 179/96 on four antihypertensive medications: diltiazem, 300 mg qd; metoprolol, 200 mg qd; Cardura, 2 mg qd; and Dyazide. He had undergone coronary artery bypass surgery 12 years previously. There were no audible abdominal bruits. His BUN was 23 mg/dL and creatinine 1.4 mg/dL. Because he was unstable, noninvasive studies were deferred and he underwent cardiac catheterization and renal angiography. Nonselective renal angiography was obtained with an AP abdominal aortogram (Fig. 35.12*A*).

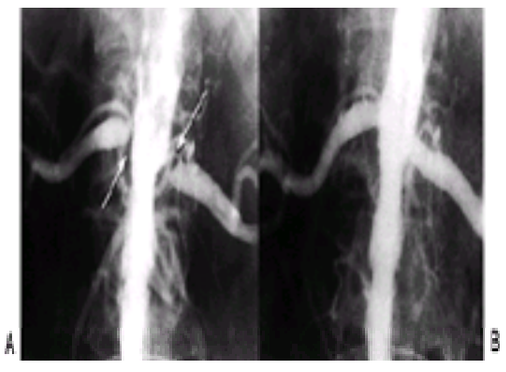

FIG. 35.12. A: Bilateral aortoostial renal artery stenosis (*arrows*) as demonstrated by cineangiograpy at the time of cardiac catheterization. Notice the diffuse atherosclerotic involvement of the infrarenal aorta. **B:** Aortogram of the same patient immediately after bilateral stent implantation.

This demonstrated bilateral severe, aortoostial renal artery stenosis and no significant coronary artery stenoses. The left renal artery was engaged with a 5F IMA catheter and selective angiography was performed. Renal artery stenting was performed using peripheral balloons and biliary stents. The right renal stent was dilated with a 7.0-mm balloon, and the left renal stent with an 8.0-mm balloon. Final angiography revealed no significant stenosis (Fig. 35.12*B*). The patient remains asymptomatic without recurrent hospitalizations on dyazide and metoprolol 50 mg qd 5 years after renal stenting.

Illustrative points. As this case illustrates, not all patients with bilateral, severe renal artery stenosis have renal insufficiency. It also illustrates how the lesions of renal artery stenosis are often aortic plaque that encroaches on the renal ostia rather than plaque originating in the renal arteries themselves. Notice how diseased the abdominal aorta is in this patient. For this reason these authors strongly recommend selective cannulation of the renal arteries using a diagnostic 5F or 6F catheter rather than an 8F guiding catheter to avoid the risk of distal atheroembolism. Furthermore, as this case also illustrates, bilateral renal artery stenosis can be easily treated at one session using the same catheters and balloons. The enduring effects of renal stenting on control of hypertension and congestive heart failure is very gratifying. With the controversy that exists in many medical communities over providing credentials for peripheral procedures, the patient may get lost in the shuffle. Given the fact that we have an excellent, low-risk treatment for atherosclerotic renovascular hypertension, study of the renal arteries in patients with atherosclerosis and hypertension during otherwise-indicated cardiac catheterization would appear to be good medical practice.

AORTOILIAC ANGIOPLASTY

Angioplasty has proved to be an effective technique for the treatment of aortoiliac occlusive atherosclerotic disease. Nevertheless, angioplasty should be performed only in symptomatic patients, despite the fact that the procedural complication rate is low (111) or in patients who have severe aortoiliac arterial occlusive disease and who require insertion of an intraaortic balloon pump for high-risk coronary revascularization procedures or cardiogenic shock (112). The ideal candidates for aortoiliac angioplasty are patients with discrete stenosis. The technical success and 5-year patency rate of iliac angioplasty are related to many factors, including lesion length, adequacy of distal runoff, presence of occlusion or stenosis, and presence of diabetes (113,114 and 115). Based on this, the American Heart Association, in the Guidelines for Peripheral Percutaneous Transluminal Angioplasty of the Abdominal Aorta and Lower Extremity Vessels (111), stratified lesions according to the degree of complexity. Category 1 iliac lesions are concentric uncalcified stenoses less than 3 cm in length. Category 2 lesions are calcified stenoses 3 to 5 cm in length or eccentric stenoses less than 3 cm in length. Category 3 lesions are stenoses 5 to 10 cm in length or occlusions less than 5 cm in length after thrombolytic therapy. Category 4 lesions are stenoses more than 10 cm in length, occlusions longer than 5 cm, extensive bilateral disease, iliac stenoses in patients with abdominal aortic aneurysms, or other lesions requiring aortoiliac surgery.

Category 4 lesions should be treated surgically, whereas categories 1 to 3 can be treated with angioplasty. The overall technical success for categories 1 and 2 lesions is 95%. The 5-year patency rate is 80% to 85% for categories 1 to 2 lesions compared with a patency of 65% to 75% for category 3 lesions. A very similar classification applies for aortic lesions with a technical success of aortic angioplasty of 90% for category 1 (less than 2 cm [111]).

Endovascular stents have been introduced in the treatment of aortoiliac atherosclerotic disease in an attempt to overcome the acute procedural complications such as abrupt occlusion and long-term restenosis rate. Several studies have suggested that the procedural success with these devices is as high (or higher) and the restenosis rate lower than balloon angioplasty alone (106,107,108,109,110,111,112,113,114,115,116,117,118 and 119). However, comparative studies between these two catheter-based approaches are scarce in the literature. Bosh et al. (120) performed a metaanalysis of 6 percutaneous transluminal angioplasty (PTA) studies (1,300 patients) with eight stent placement studies (816 patients). The technical success was higher for the stent patients (96% vs. 91%, $p < .05$). The complication and mortality rates were similar for the two groups. The 4-year primary patency rate for stenosis (77% vs. 65%) and occlusions (61% vs. 54%) in patients with claudication was statistically higher in the stent-treated group. The 4-year primary patency rate for stenosis (67% vs. 53%) and occlusions (53% vs. 44%) in patients with critical ischemia was also statistically higher in patients treated with endovascular stents.

Until large prospective randomized trials comparing PTA with stenting are available, stenting when possible should be the treatment of choice for aortoiliac arterial occlusive disease.

Case 13. A 73-year-old woman was referred for global revascularization. She complained of severe dizziness and intermittent left arm weakness, left arm claudication and exaggerated dizziness with use of her left arm, poorly controlled hypertension, and long-standing bilateral buttock, thigh, and lower extremity claudication at less than 100 yards (Fontaine IIB). She had no cardiac symptoms. On examination, she had diminished blood pressure in her left arm, bilateral carotid and subclavian bruits, and femoral and tibial pulses that could only be detected on Doppler examination. Her ankle–brachial index (ABI) was 0.5 bilaterally; BUN and creatinine were normal. Color flow Doppler examination revealed reversal of flow in the left vertebral artery, antegrade flow in the right vertebral with a high-velocity jet at the ostium consistent with ostial stenosis, and critical left carotid stenosis. A dobutamine echo demonstrated inferior ischemia. The left subclavian artery ostium was not visualized; however, there was evidence of left subclavian stenosis by the presence of reversal of flow in the left vertebral artery. Global angiography was performed using digital subtraction and cineangiographic techniques. This confirmed the presence of left carotid, right vertebral, left subclavian, left renal, and bilateral common iliac artery stenoses. The right coronary artery was occluded with good collaterals.

The abdominal aortogram (Fig. 35.13*A*) demonstrates the presence of stenosis at the terminal aorta involving the common iliac artery bifurcation. Note the presence of a small abdominal aortic aneurysm and the presence of diffuse atherosclerosis in the aorta and both common iliac arteries. A staged approach to global revascularization was planned in this patient with severe, symptomatic, systemic atherosclerosis. The first step, to secure and preserve access for future procedures and relieve her claudication, was aortoiliac bifurcation stenting.

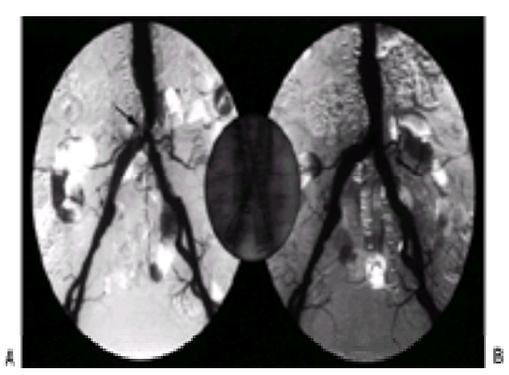

FIG. 35.13. A: Severe atherosclerotic involvement of the terminal aorta and common iliac artery origins (*arrow*) with a small infrarenal aortic aneurysm. Bifurcation Palmaz stents (insert). **B:** Angiographic appearance after stenting the aortoiliac bifurcation.

Right common femoral access was obtained by fluoroscopic visualization of calcium in the common femoral artery, since there was no palpable pulse. A 30-cm-long 7F sheath was inserted and advanced into the right external iliac artery. Using a steerable 0.035-inch guidewire, a pigtail catheter was advanced into the abdominal aorta. There was a 60-mm gradient across the common iliac bifurcation. Aortography was performed that visualized the left common femoral artery, into which a second long 6F sheath was inserted. A second steerable wire was positioned through this sheath, terminating in the aorta. After documenting the diameter of the infrarenal aorta (16 mm) and both common iliac arteries (9 mm) two 8- × 40-mm balloons were advanced across the aortoiliac bifurcation (one balloon through each femoral sheath) and inflated simultaneously to 8 atm. The sheaths were then advanced across the stenosis over the partially deflated balloons. Two Palmaz balloon-expandable stents (P294) were mounted on the balloons and positioned across the aortic bifurcation using bony landmarks and roadmapping techniques. After withdrawing the sheaths and confirming correct stent position with contrast injections through the sheaths, the stents were deployed simultaneously at 8 atm. The right common iliac stent appeared underdeployed angiographically, so a second simultaneous inflation was performed across the bifurcation using a 9-mm balloon on the right and an 8-mm balloon on the left. The stents were then fully expanded (Fig 35.13, insert), with no residual gradient across the bifurcation and an excellent angiographic result without residual stenosis or dissection (Fig 35.13*B*). Her ABI was 0.9 bilaterally and her claudication was relieved. The patient was discharged 8 hours later and was scheduled to return for endovascular revascularization of the other vascular beds in a staged manner.

Illustrative points. This case is an example of the systemic nature of atherosclerosis and how a global approach to the diagnosis and management of these patients is important for providing optimal care. Although this patient had no coronary symptoms, the primary cause of death in patients with claudication is cardiac, so coronary angiography is indicated to rule out life-threatening coronary lesions. The staging of procedures in this patient is necessary because too much contrast is required for each intervention to allow global revascularization as one procedure. The iliac arteries are treated first to preserve vascular access for the other procedures. The carotid, vertebral, and subclavian lesions will be stented next because of their importance in causing the patient symptoms. It has not been established whether treating asymptomatic patients with aortic arch and carotid stenoses by endovascular means has any value in preventing stroke or prolonging life, so treating symptomatic lesions remains the benchmark. The renal artery stenosis will be treated last because this will likely lead to relative hypotension, which could exacerbate symptoms in the presence of symptomatic aortic arch and carotid stenoses.

Case 14. A 74-year-old gentleman with unstable angina was referred for complex coronary intervention. He had an ischemic cardiomyopathy with an ejection fraction of 15% and had severe stenosis of the saphenous vein graft to the left anterior descending, which supplied all the collaterals to the inferior wall. To accomplish the coronary intervention safely, intraaortic balloon counterpulsation was desirable, but the patient had severe peripheral vascular disease with a long history of bilateral lower extremity claudication. His femoral pulses were present only on Doppler examination, and his ABI was 0.4 bilaterally. Common femoral access was obtained on the right, but the right common iliac artery was found to be occluded. Left common femoral access was obtained, followed by retrograde aortoiliac angiography using cineangiographic technique by injection through the sheath (Fig. 35.14*A*). This demonstrated subtotal occlusion of the left common iliac artery and occlusion of the right common iliac artery. A gradient of 60 mm Hg was documented across the stenosis. This common iliac lesion was crossed with a steerable 0.035-inch guidewire and balloon angioplasty was performed using a 7- × 40-mm balloon. Because of persistent stenosis, a Palmaz P295 (iliac) stent was deployed at 8 atm and dilated again to 10 atm with the same balloon through a 30-cm-long 7F sheath. Angiography was performed again through the sheath, demonstrating a widely patent left common iliac artery and a large lumbar collateral to the right internal iliac artery (Fig. 35.14*B*). There was no residual gradient across the common iliac artery. An intraaortic balloon pump was passed through the stent and advanced to the descending aorta, where counterpulsation was initiated. Coronary intervention was successfully performed via the brachial artery without hemodynamic embarrassment. The intraaortic balloon was removed at the end of the coronary intervention replaced with a 9F sheath. Both the brachial and femoral sheaths were removed when the anticoagulation was sufficiently attenuated. There were no complications.

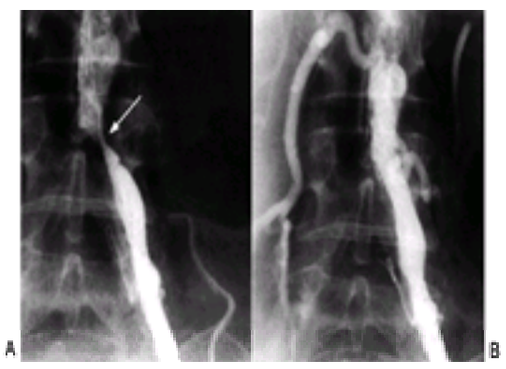

FIG. 35.14. A: Right common iliac occlusion and left common iliac stenosis in a patient with severe bilateral claudication who needs an intraaortic balloon pump. **B:** After stenting with a balloon-expandable stent. Notice the persistence of a large right lumbar collateral supplying the right lower extremity via the internal iliac artery.

Illustrative points. This case demonstrates how valuable it is for cardiologists to possess the knowledge and skill to perform iliac intervention to prevent iliofemoral complications and to preserve access for coronary intervention. Without treatment of the left common iliac stenosis, potentially life-saving intraaortic balloon counterpulsation would not have been feasible in this patient without jeopardizing his left lower extremity. Iliac stenting can be performed safely in patients undergoing intraaortic balloon counterpulsation during coronary intervention (112). It is important that the stent be well expanded to prevent the balloon pump catheter from catching on the stent. In this case, the balloon pump catheter was removed immediately under direct visualization, although such visualization is not required after proper stent deployment. In patients who need prolonged counterpulsation, the balloon pump catheter can be removed in the critical care setting.

FEMOROPOPLITEAL AND PROFUNDA FEMORIS ANGIOPLASTY

Femoropopliteal Angioplasty

Atherosclerotic occlusive disease is three to five times more common in the femoropopliteal artery than in the iliac artery. Among the femoropopliteal artery, occlusions are three times more frequent than stenosis, a distribution that is the opposite of the aortoiliac system (121,122). Furthermore, most occlusions are long, which often precludes the use of angioplasty in many of these patients (121).

Only symptomatic patients should be considered for percutaneous revascularization of the femoropopliteal artery (111). As is the case for the aortoiliac system, the technical success and the long-term patency rate vary according to the lesion characteristics. Treatment of short (<5 cm) and/or stenosed lesions yield better results than treatment of long (>10 cm) and/or occluded lesions (111). The presence of patent runoff vessels correlates with long-term benefits, reflected in the improved outcome in patients with milder symptoms (114,123,124). Significant residual stenosis after angioplasty correlates with a poor long-term outcome (124), and low residual stenosis and the absence of diabetes correlates with an improved patency rate (111).

In a study of 236 patients who underwent conventional balloon angioplasty in 254 femoral or popliteal arteries, procedural success was obtained in 96% (123,125). At 1-month follow-up, 88.8% of the procedures were considered successful (determined by an improved clinical grade and noninvasive vascular laboratory measurements). The success rate was 62.5% at 1-year follow-up and only 38% at 4-year follow-up. In this study, the most important independent predictors of long-term success, using multivariate analysis, were adequate distal runoff and lesion stenosis (rather than occlusion). Adar et al. (126) reviewed several published studies and found an early patency rate of 89% with a 3-year patency rate of 62% for patients with intermittent claudication compared with an early patency rate of 77% and a 3-year patency rate of 43% for limb salvage.

Although the long-term patency rate of femoropopliteal angioplasty is not as favorable as in PTA of the aortoiliac system, particularly when treating long or occluded lesions, percutaneous revascularization is an alternative to surgery in selected patients or may complement surgical treatment in patients with more extensive disease.

In contrast with the favorable impact of endovascular stents in patency rate in the aortoiliac system, these devices have not been shown to improve the late patency rate when implanted in the femoropopliteal system. A European prospective study (127) showed that conventional femoropopliteal PTA has a 1-year primary patency rate (65%) equivalent to that of femoropopliteal Wallstent's secondary patency rate (69%). In this study, early clinically significant restenosis was 38% and early thrombosis was 19% in the stent group. Another large prospective U.S. study showed similar lack of benefits with stents (128).

Because there is no advantage of stenting over conventional balloon angioplasty in the femoropopliteal system, these devices should be used in cases of suboptimal results, flow-limiting dissection, or abrupt occlusions after balloon angioplasty.

Case 15. A 67-year-old man with an orthotopic heart transplant 10 years earlier presented with a 1-month history of progressive claudication that was symptom-limiting (Fontaine 2A). He was no longer able to participate in his cardiac rehabilitation walking program. His femoral pulses were normal; however, he had absent left lower extremity pulses and an ABI of 0.6. He was referred for angiography and possible intervention for symptom-limiting claudication. Diagnostic angiography was performed via the right common femoral artery and demonstrated proximal occlusion of the left superficial femoral artery with mild stenosis in the profunda femoris (Fig. 35.15*A*). There was three-vessel runoff below the knee, visualized by late collateral filling. The SFA occlusion was recanalized with a contralateral 6F sheath, a glidewire, and a 16-hour coaxial infusion of urokinase that was initiated through a multiple-side-hole catheter at 2,000 U/min (Fig. 35.15*B*). Following successful lysis (Fig 35.15*C*), balloon angioplasty was performed on the culprit lesion in the mid-SFA (Fig 35.15*D*). The patient was discharged the following morning and remains asymptomatic 1 year after angioplasty.

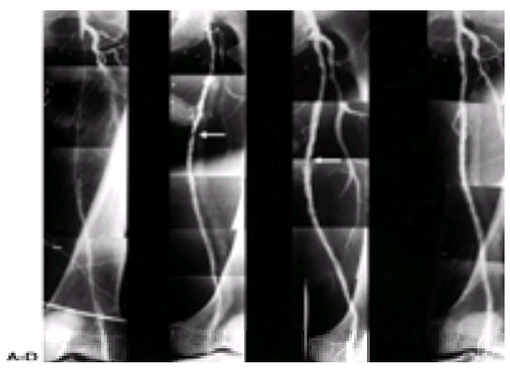

FIG. 35.15. A: Long occlusion of the left superficial femoral artery (baseline). **B:** After 4 hours of thrombolysis there is recanalization but persistence of thrombus. **C:** After 16 hours of urokinase there is no residual thrombus, but a focal mid-SFA stenosis is present. **D:** Following balloon angioplasty of the mid-SFA stenosis there is no residual stenosis.

Illustrative points. In patients with recent onset of symptoms and occluded vessels, thrombus is likely to be present. Direct angioplasty in this setting carries with it a high risk of distal embolization, which can convert a stable claudicator into a patient with limb-threatening ischemia in a matter of minutes. In the setting of acute thrombus, treatment of the thrombus by thombolysis (or more recently by mechanical thrombectomy [see Chapter 25]) will help to avoid distal embolization and its consequences. Another advantage of thrombolysis or thrombectomy is the ability to convert a long occlusion that is not ideal for balloon angioplasty into a simple, focal stenosis. Simple, focal stenoses such as the one that was the culprit lesion in this patient (Fig 35.14*C*) generally respond well to balloon angioplasty with an excellent acute and acceptable long-term result. Stenting of the SFA is only recommended if done in a provisional manner unless it is under protocol. At this time, there are no FDA-approved stents for the SFA, and the reported restenosis rates and reocclusion rates are unacceptably high.

Case 16. This 62-year-old man was referred for SFA angioplasty because of symptom-limiting claudication and serial high-grade stenoses in the left SFA. He was enrolled in a protocol testing the efficacy of a new endoluminal graft. The lesion (Fig. 35.16*A*) was initially dilated with a 5.0- × 80-mm balloon; then an endoluminal graft was deployed (Fig. 35.16*B*). The patient's ABI improved from 0.7 to 1.0 after the procedure and he was rendered asymptomatic. He was discharged on aspirin and clopidogrel.

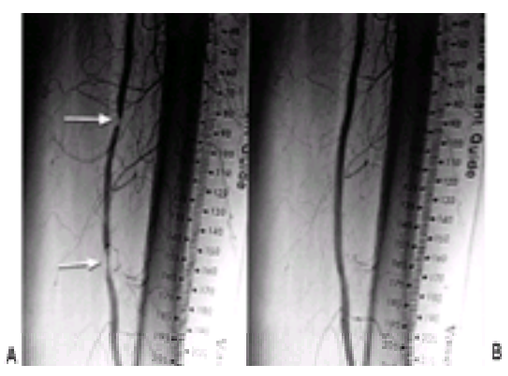

FIG. 35.16. A: Serial focal SFA stenoses in a patient with claudication. **B:** Same patient after placement of a Hemobond self-expanding endoluminal graft.

Illustrative points. A number of investigational therapies, including brachytherapy, self-expanding stents, and endoluminal grafts are being tested in randomized trials to see if they will offer an advantage over simple balloon angioplasty. Although the early registry data are very promising, there are no randomized trials indicating a restenosis benefit from any of these therapies. This case illustrated how a simple, focal stenosis can become occluded and lead to a long occlusion. It is certainly safer and easier to intervene on the simple stenoses; however, without the presence of symptoms this is not justified.

Profunda Femoris Artery Angioplasty

The profunda femoris artery (PFA) becomes an essential vessel for maintaining limb viability when occlusive atherosclerotic disease affects other vascular territories of the same limb. The profunda femoris artery not only provides the primary blood supply to the tissues of the thigh, but also is the most important vessel for collateralizing an obstructed or occluded superficial femoral artery (129,130,131 and 132). Historically, significant occlusive disease of the PFA has been treated surgically. However, atherosclerosis of the PFA is usually focal, preferentially involving the origin and the very proximal portion of the vessel in most limbs (133), which makes a percutaneous catheter-based approach an attractive alternative to surgical profundoplasty.

There are a handful of studies in the literature that have suggested that balloon angioplasty is a feasible alternative to surgery in selected patients (134,135,136 and 137). In a study from our institution (138), PFA balloon angioplasty was performed in 31 patients and 32 limbs with severe ischemia (41% had Fontaine class 2B and 59% had Fontaine class 3 or 4). The superficial femoral artery was occluded in 20 limbs (62%). In 22 limbs (69%) an additional vessel was treated. Procedural success was attained in 91% of the limbs. The ABI increased from 0.5 ± 0.2 at baseline to 0.73 ± 0.2 after intervention ($p < .01$). In-hospital limb salvage in 30 survivors was 94% and the in-hospital amputation- and revascularization-free survival was 90%. At a mean follow-up of 34 ± 20 months, no patients underwent amputation and five additional patients died. Freedom from revascularization of the 25 survivors was 88%. At follow-up, 88% had Fontaine class 1 or 2A, and only 12% had Fontaine class 2B or 3 ($p < .001$ compared with baseline).

Based on our results as well as previous studies, we conclude that percutaneous revascularization of the profunda femoris artery is a safe and effective alternative to surgical treatment.

Case 17. A 65-year-old woman with coronary artery disease, bilateral carotid endarterectomy, and bilateral renal artery stenting presented with a 1-year history of progressive, Fontaine class 2B claudication in both lower extremities, which was worse on the left. She has known chronic bilateral SFA occlusion. The femoral pulses were normal but the tibial pulses were weak and monophasic on the right and absent on the left. The ABI was 0.3 on the right and not obtainable on the left. Angiography performed at the referring institution revealed occlusion of the proximal SFA and serial high-grade stenoses of the left profunda femoris (Fig 35.17*A*). Using contralateral retrograde femoral access, a 7F contralateral sheath was advanced to the left external iliac artery. Baseline angiography was performed and the lesion was crossed with a 0.035-inch Wholey wire. When the lesion could not be crossed with a 4- × 20-mm balloon, the wire was exchanged for a floppy Rotawire and rotational atherectomy (see Chapter 25) was performed on all three profunda femoris lesions using a 1.75- followed by a 2.25-mm burr. The lesions were then dilated with the 4- × 20-mm balloon at 6 atm. Postangioplasty angiography demonstrated a widely patent profunda femoris and the ABI increased to 0.4 on the left (Fig. 35.17*B*). The patient was discharged the following morning with relief of his claudication.

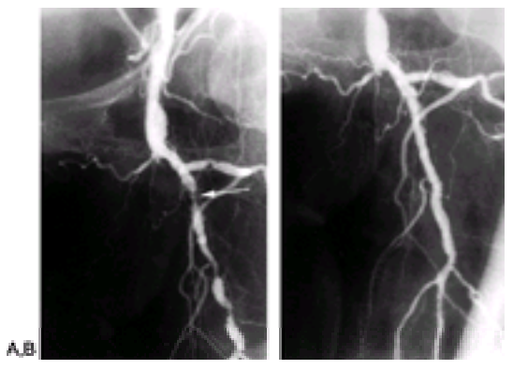

FIG. 35.17. A: Severe, diffuse atherosclerotic involvement of the infrainguinal vessels. The SFA is occluded and the profunda femoris is diffusely diseased. Involvement of the profunda femoris is typical in patients with long-standing diabetes. **B:** After rotational atherectomy and balloon angioplasty, an excellent angiographic result.

Illustrative points. The two most important arteries for maintaining a viable leg are the common femoral artery and the profunda femoris. The SFA is often occluded; however, in the presence of a patent profunda, the limb usually remains viable. In patients with chronic SFA occlusion and lesions of the common femoral or profunda, revascularization of these vessels can restore the patient to his previous mild level of symptoms even without revascularizing the chronically occluded SFA. This case also demonstrates that the use of coronary equipment and techniques can permit peripheral angioplasty success in otherwise undilatable lesions. Another option in this patient would have been to use coronary wires and balloons to cross and dilate the lesions; however, by debulking the lesions with rotablator in patients with lower extremity ischemia, it is easier to achieve an acceptable balloon result with lower pressure and less risk of dissection. The acute clinical success and limb salvage rate using the rotablator for undilatable lesions exceeds 90%.

INFRAPOPLITEAL ANGIOPLASTY

The traditional indications for infrapopliteal angioplasty have been ischemic rest pain, ischemic ulceration, or gangrene (111). However, severe claudication that prevents minimal ambulation, and infrapopliteal angioplasty for use in patients with moderate to severe claudication to increase the durability and effectiveness of femoropopliteal PTA has been advocated by some investigators as acceptable indications (139). It is possible that with the advent of small-profile balloons, improvement in technique, and increased operator experience, the use of tibial angioplasty will not be limited to the previously mentioned indications, as it has been proposed (140).

Some centers have reported tibial angioplasty to be an integral component in the treatment of limb salvage, which has led to a dramatic decrease in the amputation rate (141,142). Dorros et al. (140) reported their results of below-knee angioplasty in 111 patients and 168 tibioperoneal vessels. The indications were claudication (42%), nonhealing ulcer/gangrene (27%), and rest pain (26%). The procedural success was 90% (99% in stenoses and 65% in occlusions). Significant complications (death, emergent bypass surgery, or distal embolization) occurred in 3%. At discharge 95% of the patients were clinically improved. At a mean follow-up of 9 ± 6 months, 40% needed a second PTA; however, only a third of those that required a second PTA showed lesion recurrence, with the rest showing progression of disease. Hanna et al. (143) reported their results of infrapopliteal PTA for limb salvage in 29 diabetic patients. Technical success (<20% residual stenosis) was achieved in 26 patients (90%), and clinical success (avoidance of amputation and achievement of wound healing) at 12-month follow-up was obtained in 23 patients (79%).

Balloon angioplasty of the infrapopliteal vessels is an effective technique for treating patients with distal atherosclerotic occlusive disease. It has been utilized mainly in patients with limb-threatening ischemia and multisegment disease. Appropriate anatomic selection is a key factor to maximize the benefit of the technique.

Case 18. A 68-year-old man with a 100-pack-per-year smoking history presented with a nonhealing ulcer of the second digit on his right lower extremity. He denied trauma to this extremity. He had a history of severe coronary artery disease and peripheral vascular disease, and had undergone bilateral SFA angioplasty 7 years earlier for symptom-limiting claudication. At that time, he had an 80% stenosis of his right tibioperoneal trunk, but this was not treated because his claudication was relieved by treatment of the SFA lesions alone. His ABI was 0.4 on the right, 0.8 on the left. Left common femoral access was obtained and a pigtail catheter was used to perform bilateral aortography and runoff using digital subtraction and a stepping table. Selective right lower extremity angiography was performed from the contralateral access using an IMA catheter and a glidewire, demonstrating critical stenosis in the tibioperoneal trunk and severe stenosis in the right posterior tibial artery with occlusion of the peroneal and anterior tibial vessels (Fig. 35.18*A*). The IMA catheter was exchanged over an extra-stiff wire for a 6F multipurpose coronary guiding catheter that was advanced to the midpopliteal artery. The lesions were crossed and dilated using a 0.014-inch extra-support wire and a 3.0- × 40-mm coronary balloon. Provisional stenting was performed on the lesion at the tibioperoneal trunk because of a suboptimal balloon result (Fig. 35.18*B*). The posterior tibial vessel was treated with angioplasty alone. The patient was discharged on aspirin, clopidogrel, and ciprofloxicillin and follow-up at weekly intervals until he had complete healing of his ulcer. His ABI improved to 0.9 on the right.

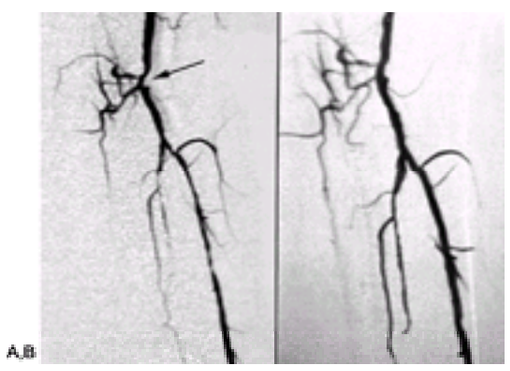

FIG. 35.18. A: Critical stenosis in the right tibioperoneal trunk (*arrow*) and posterior tibial artery in a patient with critical limb ischemia. The anterior tibial and peroneal vessels are occluded. **B:** After stenting of the tibioperoneal trunk and balloon angioplasty of the posterior tibial artery there is straight-line flow to the foot with a palpable pulse.

Illustrative points. The primary indication for tibial angioplasty in chronic lower extremity ischemia is critical limb ischemia, defined as rest pain, nonhealing ulcers, or gangrene. As this case demonstrates, critical limb ischemia requires stenosis or occlusion of all three infrapopliteal vessels, unlike coronary artery disease, where single-vessel involvement can cause severe symptoms or even death. In some centers with excellent results, tibial intervention is also offered to patients with severe claudication, but this is not the norm. Typically, claudication improves with treatment of the proximal stenoses (i.e., iliac and femoral) even in the presence of untreated severe tibial disease, as was illustrated by this man's course 7 years earlier. Once critical limb ischemia is present, the interventionist and surgeon both attempt to provide pulsatile flow to the extremity since the chances of healing are very low in the absence of pulsatile flow. The introduction of low-profile coronary systems into the periphery has greatly improved the success rate of infrapopliteal intervention. Stenting is not performed routinely in these lesions, but a prudent strategy of provisional stenting with antiplatelet therapy appears beneficial in cases such as this one. The surgical procedure of choice for critical limb ischemia is a distal vein bypass, which has a limb salvage rate of 70%, but a 5-year patency of less that 50%. The important goal here is to heal the ulcer; restenosis, if it occurs, may in fact be asymptomatic and may not require treatment.

CHAPTER REFERENCES

1. Connors JJ, III. Other extracranial locations amenable to angioplasty and stenting. In: Connors JJ III, Wojak JC, eds. *Interventional neuroradiology: strategies and practical techniques.* Philadelphia: WB Saunders, 1999:484.

2. Schutz H, Yeung HP, Chiu MC, et al. Dilation of vertebral-artery stenosis. *N Engl J Med* 1981;304:732.
3. Motarjeme A, Keifer JW, Zuska AJ. Percutaneous transluminal angioplasty of the vertebral arteries. *Radiology* 1981;139:715.
4. Storey GS, Marks MP, Dake M, et al. Vertebral artery stenting following percutaneous transluminal angioplasty. Technical note. *J Neurosurg* 1996;84:883.
5. Feldman RL, Rubin JJ, Kuykendall RC. Use of coronary Palmaz-Schatz stent in the percutaneous treatment of vertebral artery stenoses. *Cathet Cardiovasc Diagn* 1996;38:312.
6. Jenkins JS, Zhang S, Jain SP, Collins TJ, White CJ, Ramee SR. Acute and long-term results of vertebral artery stenting. *Circulation* 1999. (Submitted.)
7. Smith RB III. The surgical treatment of peripheral vascular disease. In: Hurst JW, Schlant RC, Rackley CZ, Sonnenblick EH, Wenger NK, eds. *The Heart*, 7th ed. New York: McGraw-Hill, 1992:2235.
8. Terada T, Higashida R, Halbach VV, et al. Transluminal angioplasty for atherosclerotic disease of the distal vertebral and and basilar arteries. *J Neurol Neurosurg Psychiatry* 1996;60:377.
9. Takis C, Kwan ES, Pessin MS, Jacobs DH, Caplan LR. Intracranial angioplasty: experience and complications. *Am J Neuroradiol* 1997;18:1661.
10. Clark WM, Barnwell SL, Nesbit G, et al. Safety and efficacy of percutaneous transluminal angioplasty for intracranial atherosclerotic stenosis. *Stroke* 1995;26:1200.
11. Norris JW, Zhu CZ, Bornstein NM, et al. Stroke risk of asymptomatic carotid stenosis. *Stroke* 1991;22:1485.
12. O'Holleran LW, Kennelly MM, McClurken M, et al. Natural history of asymptomatic carotid plaque: five-year follow-up study. *Am J Surg* 1987;154:659.
13. Autret A, Pourcelot L, Saudeau D, et al. Stroke risk in patients with carotid stenosis. *Lancet* 1987;1:888.
14. North American Carotid Endarterectomy Trial Collaborators. Beneficial effect of carotid endarterectomy in symptomatic patients with high-grade carotid stenosis. *N Engl J Med* 1991;325:445.
15. Executive Committee for the Asymptomatic Carotid Atherosclerosis Study. *JAMA* 1995;237:1421.
16. Hsai DC, Krushat M, Mosoe LM. Epidemiology of carotid endarterectomies among Medicare beneficiaries. *J Vasc Surg* 1992;16:201.
17. Roubin GS, Yadav S, Iyer SS, Vitek J. Carotid stent-supported angioplasty: a neurovascular intervention to prevent stroke. *Am J Cardiol* 1996;78[Suppl 3A]:8.
18. Diethrich EB, Ndiaye M, Reid DB. Stenting in the carotid artery: initial experience in 110 patients. *J Endovasc Surg* 1996;3:76.
19. Dorros G. Complications associated with extracranial carotid artery interventions. *J Endovasc Surg* 1996;3:166.
20. Yadav, Roubin GS, Vitek J, et al. Elective stenting of extracranial arteries. *Circulation* 1997;376.
21. Yadav, Roubin GS, Vitek J, et al. Late outcome after carotid angioplasty and stenting. *Circulation* 1996;94[suppl I]:I.
22. Bergeron P. Carotid angioplasty and stenting: is endovascular treatment for cerebrovascular disease justified? *J Endovasc Surg* 1996;3:129.
23. Diethrich EB.Indications for carotid artery stenting: a previous of the potential derived from early clinical experience. *J Endovasc Surg* 1996;3:132.
24. Joint Officers of the Congress of Neurological Surgeons and the American Association of Neurological Surgeons. Carotid angioplasty and stents: an alternative to carotid endarterectomy. *Neurosurgery* 1997;40:344.
25. Wholey, MH, Wholey M, Bergeron P, et al. Current global status of carotid artery stent placement. *Cathet Cardiovasc Diagn* 1998;44:1.
26. Marzewski DJ, Furlan AJ, Louis PS, et al. Intracranial internal carotid artery stenosis: long-term prognosis. *Stroke* 1982;13:821.
27. Ingall TJ, Hormer D, Baker HL, et al. Predictors of intracranial carotid artery arteriosclerosis: duration of cigarette smoking and hypertension are more more powerful than serum lipid levels. *Arch Neurol* 1991;48:687.
28. Caplan LR, Gorelick PB, Hier DB. Race, sex and occlusive cerebrovascular disease: a review. *Stroke* 1986;17:648.
29. Leung SY, Ng THK, Yuen ST, et al. Patterns of cerebral atherosclerosis in Hong Kong Chinese: severity in intracranial and extracranial vessels. *Stroke* 1993;24:779.
30. Akins PT, Pilgram TK, Cross DT, Moran CJ. Natural history of stenosis from intracranial atherosclerosis by serial angiography. *Stroke* 1998;29:433.
31. Sacco RL, Kargman DE, Gu Q, et al. Race-ethnicity and determinants of intracranial atherosclerotic cerebral infarction: the Northern Manhattan Stroke Study. *Stroke* 1996;26:14.
32. Craig DR, Meguro K, Watridge C, et al. Intracranial carotid artery stenosis. *Stroke* 1980;13:825.
33. The EC/IC Bypass Study Group. Failure of extracranial/intracranial arterial bypass to reduce the risk of ischemic stroke: results of an international randomized trial. *N Engl J Med* 1985;313:1191.
34. Chimowitz MI, Kokkinos J, Strong J, et al. The warfarin-aspirin symptomatic intracranial disease study. *Neurology* 1995;45:1488.
35. Higashida RT, Tsai FY, Halbach VV, et al. Interventional neurovascular techniques in the treatment of stroke: state of the art therapy. *J Intern Med* 1995;237:105.
36. Higashida RT, Tsai FY, Halbach VV, et al. Transluminal angioplasty for atherosclerotic disease of the vertebral and basilar arteries. *J Neurosurg* 1993;78;192.
37. Higashida RT, Tsai FY, Halbach VV, et al. Cerebral percutaneous transluminal angioplasty. *Heart Dis Stroke* 1993;2:497.
38. Dorros G, Cohn JM, Palmer LE. Stent deployment resolves a petrous carotid artery angioplasty dissection. *Am J Neurovasc Radiol* 1998;19:392.
39. Feldman RL, Trigg L, Gaudier J, Galat J. Use of coronary Palmaz-Schatz stent in percutaneous treatment of an intracranial carotid stenosis. *Cathet Cardiovasc Diagn* 1996;38:316.
40. Gomez CR, Vitek JJ, Roubin GS. Stenting of intracranial carotid artery. *J Endovasc Surg* 1998;5[Suppl 1]:I.
41. Zelenock GB, Cronenwett JL, Graham LM, et al. Brachiocephalic arterial occlusive and stenosis: manifestations and management of complex lesions. *Arch Surg* 1985;120:370.
42. Perace WM, Yao JST. Upper extremity ischemia: overview. *Semin Vasc Surg* 1990;3:207.
43. Pokrowsky AV. Nonspecific aortoarteritis. In: Rutherford RB, ed. *Vascular surgery,* 3rd ed. Philadelphia: WB Saunders, 1989.
44. Iwai T, Konno S, Hiejima K, et al. Fibromuscular dysplasia in the extremities. *J Cardiovasc Surg* 1985;26:496.
45. Joyce JW. The giant cell arteritides: diagnosis and the role of surgery. *J Vasc Surg* 1986;3:827.
46. Kretschmer G, Niederle B, Polterauer P, et al. Irradiation-induced changes in the subclavian and axillary arteries after radiotherapy for carcinoma of the breast. *Surgery* 1986;99:658.
47. Scher LA, Veith FJ, Samson RM, et al. Vascular complications of the thoracic outlet syndrome. *J Vasc Surg* 1986;3:565.
48. Bryan AJ, Hicks E, Lewis MH. Unilateral digital ischemia secondary to embolization from subclavian atheroma. *Ann Coll Surg Eng* 1989;71:140.
49. Reivich M, Holling HE, Roberts B, Toole JF. Reversal of blood flow through the vertebral artery and its effects on the cerebral circulation. *N Engl J Med* 1961;265:878.
50. Fields WS, Lemak NA. Joint study of extracranial arterial occlusion. Subclavian steal: A review of 168 cases. *JAMA* 1972;222:1139.
51. Granke K, Van Meter CH Jr, White CJ, Ochsner JL, Hollier LH. Myocardial ischemia caused by postoperative malfunction of an internal mammary coronary artery graft. *J Vasc Surg* 1990;11:659.
52. Olsen CO, Dunton RF, Maggs PR, Lahey SJ. Review of coronary-subclavian steal following internal mammary artery-coronary artery bypass surgery. *Ann Thorac Surg* 1988;46:675.
53. Hadjipetru P, Cox S, Piemonte T, Eisenhauer A. Percutaneous revascularization of atherosclerotic obstruction of aortic arch vessels. *J Am Coll Cardiol* 1999;33:1238.
54. Bachman DM, Kim RM. Transluminal dilation for subclavian steal syndrome. *Am J Roentgenol* 1980;135:995.
55. Burke DR, Gordon RL, Mishkin JD, et al. Percutaneous transluminal angioplasty of subclavian arteries. *Radiology* 1987;164:699.
56. Insall RL, Lambert D, Chamberlain J, et al. Percutaneous transluminal angioplasty of the innominate, subclavian and axillary arteries. *Eur J Vasc Surg* 1990;4:591.
57. Jain SP, Ramee SR, Ansel GM, et al. Endoluminal stenting of subclavian and innominate artery: acute and long term results from a multicenter stent registry. *Circulation* 1998;98:I-484(abst).
58. Ralph-Edwars AC, Williams WG, Coles JC, et al. Reoperation for recurrent aortic coarctation. *Ann Thorac Surg* 1995;60:1303.
59. Johnson MC, Canter CE, Strauss AW, Spray TL. Repair of coarctation of the aorta in infancy: comparison of surgical and balloon angioplasty. *Am Heart J* 1993;125:464.
60. Kron IL, Flanagan TL, Rheuban KS, et al. Incidence and risk of reintervention after coarctation repair. *Ann Thorac Surg* 1990:49;920.
61. Beekman RH, Rocchini AP, Behrendt DM, Rosenthal A. Reoperation for coarctation of the aorta. *Am J Cardiol* 1981;48:1108.
62. Bromberg BI, Beekman RH, Rocchini AP, et al. Aortic aneurysm after patch aortoplasty repair of coarctation: prospective analysis of prevalence, screening tests and risks. *J Am Coll Cardiol* 1989;14:734.
63. Beekman RH, Rocchini AP, Behrendt DM, et al. Long-term outcome after repair of coarctation in infancy: subclavian angioplasty does not reduce the need for reoperation. *J Am Coll Cardiol* 1986;8:1406.
64. Giovanni JV, Lip GYH, Osman K, et al. Percutaneous balloon dilation of aortic coarctation in adults. *Am J Cardiol* 1996;77:435.
65. Fawzy ME, Sivanandam V, Galal O, et al. One- to ten-year follow-up results of balloon angioplasty of native coarctation of the aorta in adolescents and adults. *J Am Coll Cardiol* 1997;30:1542.
66. Lababidi Z. Percutaneous balloon coarctation angioplasty: long-term results. *J Intervent Cardiol* 1992;5:57.
67. Beekman RH, Rocchini AP, Dick M, et al. Percutaneous balloon angioplasty for native coarctation of the aorta. *J Am Coll Cardiol* 1987;10:1078.
68. Yetman AT, Nykanen D, McCrindle BW, et al. Balloon angioplasty of recurrent coarctation: a 12-year review. *J Am Coll Cardiol* 1997;30:811.
69. McCrindle BW, Jones TK, Morrow WR, et al. Acute results of balloon angioplasty of native coarctation versus recurrent aortic obstruction are equivalent. *J Am Coll Cardiol* 1996;28:1810.
70. Anjos R, Quershi SA, Rosenthal E, et al. Determinants of hemodynamic results of balloon dilation of aortic recoarctation. *Am J Cardiol* 1992;69:665.
71. Rao PS, Wilsson AD, Chopra PS. Immediate and follow-up results of balloon angioplasty of postoperative recoarctation in infants and children. *Am Heart J* 1990;120:1315.
72. Suarez de Lezo J, Pan M, Romero M, et al. Balloon expandable stent repair of severe coarctation of the aorta. *Am Heart J* 1995;129:1002.
73. Ebeid RE, Prieto LR, Latson LA. Use of balloon-expandable stents for coarctation of the aorta: initial results and intermediate-term follow-up. *J Am Coll Cardiol* 1997;30:1847.
74. Rao PS. Stents in treatment of aortic coarctation. *J Am Coll Cardiol* 1997;30:1853.
75. Svensjo S, Bengtsson H, Bergqvist D. Thoracic and thoracoabdominal aortic aneurysm and dissection: an investigation based on autopsy. *Br J Surg* 1996;83:68.
76. Pressler V, McNamara JJ. Thoracic aortic aneurysm: natural history and treatment. *J Thorac Cardiovasc Surg* 1980;79:489.
77. Bickerstaff LK, Pairolero PC, Hollier LH, et al. Thoracic aortic aneurysms: a population-based study. *Surgery* 1982;92:1103.
78. Perko MJ, Norgaard M, Herzog TM, Olsen PS, Schroeder TV, Pettersson G. Unoperated aortic aneurysms: a survey of 170 patients. *Ann Thorac Surg* 1995;59:1204.
79. Kouchoukos NT, Dougenis D. Surgery of the thoracic aorta. *N Engl J Med* 1997;336:1876.
80. Moreno-Cabral CE, Miller DC, Mitchell RS, et al. Degenerative and atherosclerotic aneurysms of the thoracic aorta: determinants of early and late surgical outcome. *J Thorac Cardiovasc Surg* 1984;88:1020.
81. Mitchell RS, Dake MD, Sembra CP, et al. Endovascular stent graft repair of thoracic aneurysm. *J Thorac Cardiovasc Surg* 1996;11:1054.
82. Dake M, Miller C, et al. Transluminal placement of endovascular stent-graphs for the treatment of descending thoracic aortic aneurysms. *N Engl J Med* 1994;331:1729.
83. Martson A. Diagnosis and management of intestinal ischemia. *Ann R Coll Surg Engl* 1972;50:29.
84. Mc Millan WD, McCarthy WJ, Bresticker MR, et al. Mesenteric artery bypass: objective patency determination. *J Vasc Surg* 1995;21:729.
85. Harward TR, Brooks DL, Flynn TC, Seeger JM. Multiple organ dysfunction after mesenteric artery revascularization. *J Vasc Surg* 1993;18:459.
86. Calderon M, Reul GJ, Gregoric ID, et al. Long-term results of the surgical management of symptomatic chronic intestinal ischemia. *J Cardiovasc Surg* 1992;33:723.
87. Schwartz LB, Gewertz BL. Chronic mesenteric arterial occlusive disease: clinical presentation and diagnostic evaluation. In: Perler BA, Becker GJ, ed. *Vascular intervention: a clinical approach.* New York: Thieme, 1998:517.
88. Matsumoto AH, Angle JF, Tegtmeyer CJ. Mesenteric angioplasty and stenting for chronic mesenteric ischemia. In: Perler BA, Becker GJ, ed. *Vascular intervention: a clinical approach.* New York: Thieme, 1998:545.
89. Khosla S, Zhang SY, Jenkins JS, Collins TJ, White CJ, Ramee SR. Endovascular stent revascularization of mesenteric and celiac arteries for the management of chronic mesenteric ischemia. *Circulation* 1997;96[Suppl I]:I.
90. Jean WJ, Al-Bittar I, Xwicke DL, et al. High incidence of renal artery stenosis in patients with coronary artery disease. *Cathet Cardiovasc Diagn* 1994;32:8.
91. Olin JW, Melia M, Young JR, Graor RA, Risius B. Prevalence of atherosclerosis renal artery stenosis in patients with atherosclerosis elsewhere. *Am J Med* 1990;88:1.
92. Eyler WR, Clark GJ, Rian RL, Menninger DE. Angiography of the renal areas including a comparative study of renal arterial stenosis with and without hypertension. *Radiology* 1962;78:879.
93. White CJ, Ramee SR, Collins TJ, Jenkins JS. Renal artery stent placement. *J Endovasc Surg* 1998;5:71.
94. Olin JW, Young JR, DeAnna S, Grubb M, Childs MB. The utility of duplex ultrasound scanning of the renal arteries for diagnosing significant renal artery stenosis. *Ann Intern Med* 1995;122:833.
95. Meir GH, Sumpio B, Black HR, Gusberg RJ. Captopril renal scintigraphy: an advance in the detection and treatment of renovascular hypertension. *J Vasc Surg* 1990;11:770.
96. Working Group on Renovascular Hypertension. Detection, evaluation, and treatment of renovascular hypertension. Final report. *Arch Intern Med* 1987;145:820.
97. Weibull H, Bergqvist D, Bergentz SE, et al. Percutaneous transluminal angioplasty versus reconstruction of atherosclerotic renal artery stenosis: a prospective randomized study. *J Vasc Surg* 1993;18:841.
98. Hansen KJ, Starr SM, Sands RE, et al. Contemporary surgical management of renovascular disease. *J Vasc Surg* 1992;16:319.
99. Novick AC, Ziegelbaum M, Vidt DG, et al. Trends in surgical revascularization for renal artery disease. *JAMA* 1987;257:498.

100. Derkx F, Schalekamp M. Renal artery stenosis and hypertension. *Lancet* 1994;344:237.
101. Archibald GR, Beckmann CF, Libertino JA. Focal renal artery stenosis caused by fibromuscular dysplasia: treatment by percutaneous transluminal angioplasty. *Am J Radiol* 1988;151:593.
102. Cluzel P, Raygnaud A, Beyssen B, Pagny JV, Gaux JC. Stenosis of renal branch arteries in fibromuscular dysplasia: results of percutaneous transluminal angioplasty. *Radiology* 1994;193:227.
103. Losinno F, Zuccala A, Busato F, Zucchelli P. Renal artery angioplasty for renovascular hypertension and preservation of renal function: long-term angiographic and clinical follow-up. *Am J Radiol* 1994;162:853.
104. Weibull H, Bergqvist D, Jonsson K, Hulthen L, et al. Long-term results after percutaneous transluminal angioplasty of atherosclerotic renal artery stenosis: the importance of intensive follow-up. *Eur J Vasc Surg* 1991;291.
105. Dorros G, Prince C, Mathiak L. Stenting of a renal artery stenosis achieves better relief of the obstructive lesion than balloon angioplasty. *Cathet Cardiovasc Diagn* 1993;29:191.
106. Dorros G, Jaff M, Jain A, Dufek C, Mathiak L. Follow-up of primary Palmaz-Schatz stent placement for atherosclerotic renal artery stenosis. *Am J Cardiol* 1995;75:1051.
107. Rees CR, Palmaz JC, Becker GJ, Ehrman KO, et al. Palmaz stent in atherosclerotic stenoses involving the ostia of the renal arteries: preliminary report of a multicenter study. *Radiology* 1991;181:507.
108. Blum U, Krumme B, Flugel P, et al. Treatment of ostial renal-artery stenoses with vascular endoprostheses after unsuccessful balloon angioplasty. *N Engl J Med* 1997;336:459.
109. White CJ, Ramee SR, Collins TJ, Jenkins JS, Escobar A, Shaw D. Renal artery stent placement: utility in lesions difficult to treat with balloon angioplasty. *J Am Coll Cardiol* 1997;30:1445.
110. Khosla S, White CJ, Collins TJ, Jenkins JS, Shaw D, Ramee SR. Effects of renal artery stent implantation in patients with renovascular hypertension presenting with unstable angina or congestive heart failure. *Am J Cardiol* 1997;80:363.
111. Pentecost MJ, Criqui MH, Dorros G, et al. Guidelines for peripheral percutaneous transluminal angioplasty of the abdominal aorta and lower extremity vessels. *Circulation* 1994;89:511.
112. Cooper CJ, Moore JA, Burket MW, et al. Intraaortic balloon pump insertion after percutaneous revascularization in patients with aortoiliac stenosis. *Circulation* 1998;98 [Suppl I]:I.
113. Kwasnik EM, Siouffi SY, Jay ME, Khuri SF. Comparative results of angioplasty and aortofemoral bypass in patients with symptomatic iliac disease. *Arch Surg* 1987;122:288.
114. Cambria RP, Faust G, Gusberg R, et al. Percutaneous angioplasty for peripheral arterial occlusive disease: correlates of clinical success. *Arch Surg* 1987;122:283.
115. Stokes KR, Strunk HM, Campbell DR, et al. Five-year results of iliac and femoropopliteal angioplasty in diabetic patients. *Radiology* 1990;174:977.
116. Vorwerk D, Gunther RW, Schurman K, Wendt G. Aortic and iliac stenoses: follow-up results of stent placement after insufficient balloon angioplasty in 118 cases. *Radiology* 1996;45.
117. Vorwerk D, Gunther RW, Schurman K, et al. Primary stent placement for chronic iliac artery occlusions: follow-up results in 103 patients. *Radiology* 1995;194:745.
118. Strecker EPK, Hagen B, Liermenn D, et al. Iliac and femoropopliteal vascular occlusive disease treated with flexible tantalum stents. *Cardiovasc Intervent Radiol* 1993;16:158.
119. Spijkerboer AM. Peripheral angiography and angioplasty. *Curr Opin Radiol* 1992;4:81.
120. Bosch JL, Hunink MGM. Meta-analysis of the results of percutaneous transluminal angioplasty and stent placement for aortoiliac occlusive disease. *Radiology* 1997;204:87.
121. Martin EC. Transcatheter therapies in peripheral and noncoronary vascular disease. *Circulation* 1991;[Suppl I]:I1.
122. Martin EC. The impact of angioplasty: a perspective. *J Vasc Interv Radiol* 1992;3:511.
123. Johnston KW, Rae M, Hogg-Johnston SA, et al. Five-year results of a prospective study of percutaneous transluminal angioplasty. *Ann Surg* 1987;206:403.
124. Capek P, McLean GK, Berkowitz HD. Femoropopliteal angioplasty: factors influencing long-term success. *Circulation* 1991;83[Suppl I]:I-70.
125. Johnston KW. Femoral and popliteal arteries: reanalysis of results of balloon angioplasty. *Radiology* 1992;183:767.
126. Adar R, Critchfield GC, Eddie DM. A confidence profile analysis of the results of femoropopliteal percutaneous transluminal angioplasty in the treatment of lower-extremity ischemia. *J Vasc Surg* 1989;10:57.
127. Do D, Triller J, Walpoth BH, et al. A comparison study of self-expandable stents vs balloon angioplasty alone in femoropopliteal artery occlusions. *Cardiovasc Intervent Radiol* 1992;15:306.
128. Martin EC, Katzen BT, Benenati JF, et al. Multicenter trial of the wallstent in the iliac and femoral arteries. *J Vasc Interv Radiol* 1995;6:843.
129. Leeds FH, Gilfillan RS. Importance of the profunda femoris artery in the revascularization of the ischemic limb. *Arch Surg* 1961;82:25.
130. Morris GC Jr, Edwards E, Cooley DA, Crawford ES, De Bakey ME. Surgical importance of the profunda femoris artery. *Arch Surg* 1961;82:32.
131. Waibel PP, Wolf G. The collateral circulation in occlusions of the femoral artery. *Surgery* 1966;4:912.
132. Bernhard VM, Ray LI, Millitello JP. The role of angioplasty of the profunda femoris artery in revascularization of the ischemic limb. *Surg Gynecol Obstet* 1976;142:840.
133. Beales JSM, Adcock FA, Frawley JS, et al. The radiological assessment of disease of the profunda femoris artery. *Br J Radiol* 1971;44:854.
134. Motarjeme A, Keifer JW, Zuska AJ. Percutaneous transluminal angioplasty of the deep femoral artery. *Radiology* 1980;135:613.
135. Waltman AC. Percutaneous transluminal angioplasty: iliac and deep femoral arteries. *Am J Roentgenol* 1980;135:921.
136. Dacie JE, Daniell SJN. The value of percutaneous transluminal angioplasty of the profunda femoris artery in threatened limb loss and intermittent claudication. *Clin Radiol* 1991;44:311.
137. Varty K, London NJM, Ratliff DA, Bell PRF, Bolia A. Percutaneous angioplasty of the profunda femoris artery: a safe and effective endovascular technique. *Eur J Vasc Surg* 1993;7:483.
138. Silva JA, White CJ, Ramee SR. Percutaneous profundoplasty in the treatment of severe lower extremity ischemia: immediate results and clinical follow-up. *J Endovasc Surg* (in press).
139. Horvath W, Oertl M, Haidinger D. Percutaneous transluminal angioplasty of crural arteries. *Radiology* 1990;177:565.
140. Dorros G, Lewin RF, Jamnadas P, Mathiak LM. Below knee angioplasty: tibioperoneal vessels, the acute outcome. *Cathet Cardiovasc Diagn* 1990;19:170.
141. Veith FJ, Gupta SK, Wengerten KR, et al. Changing arteriosclerotic disease patterns and management strategies in lower-limb-threatening ischemia. *Ann Surg* 1990;212:402.
142. Veith FJ, Gupta SK, Samson RH, et al. Progress in limb salvage by reconstructive arterial surgery combined with new or improved adjunctive procedures. *Ann Surg* 1981;194:386.
143. Hanna GP, Fujise K, Kjellgren O, et al. Infrapopliteal transcatheter interventions for limb salvage in diabetic patients: importance of aggressive interventional approach and role of transcutaneous oximetry. *J Am Coll Cardiol* 1997;30:664.